SUSTAINABLE AVIATION FUELS

EDITED BY: Michael P. Wolcott, Nathan Brown, William Goldner, Zia Haq, Season Hoard, Johnathan Holladay and Kristin C. Lewis

PUBLISHED IN: Frontiers in Energy Research

frontiers Research Topics

ISSN 1664-8714
ISBN 978-2-83250-436-9
DOI 10.3389/978-2-83250-436-9

About Frontiers

Frontiers is more than just an open-access publisher of scholarly articles: it is a pioneering approach to the world of academia, radically improving the way scholarly research is managed. The grand vision of Frontiers is a world where all people have an equal opportunity to seek, share and generate knowledge. Frontiers provides immediate and permanent online open access to all its publications, but this alone is not enough to realize our grand goals.

Frontiers Journal Series

The Frontiers Journal Series is a multi-tier and interdisciplinary set of open-access, online journals, promising a paradigm shift from the current review, selection and dissemination processes in academic publishing. All Frontiers journals are driven by researchers for researchers; therefore, they constitute a service to the scholarly community. At the same time, the Frontiers Journal Series operates on a revolutionary invention, the tiered publishing system, initially addressing specific communities of scholars, and gradually climbing up to broader public understanding, thus serving the interests of the lay society, too.

Dedication to Quality

Each Frontiers article is a landmark of the highest quality, thanks to genuinely collaborative interactions between authors and review editors, who include some of the world's best academicians. Research must be certified by peers before entering a stream of knowledge that may eventually reach the public - and shape society; therefore, Frontiers only applies the most rigorous and unbiased reviews.
Frontiers revolutionizes research publishing by freely delivering the most outstanding research, evaluated with no bias from both the academic and social point of view. By applying the most advanced information technologies, Frontiers is catapulting scholarly publishing into a new generation.

What are Frontiers Research Topics?

Frontiers Research Topics are very popular trademarks of the Frontiers Journals Series: they are collections of at least ten articles, all centered on a particular subject. With their unique mix of varied contributions from Original Research to Review Articles, Frontiers Research Topics unify the most influential researchers, the latest key findings and historical advances in a hot research area! Find out more on how to host your own Frontiers Research Topic or contribute to one as an author by contacting the Frontiers Editorial Office: frontiersin.org/about/contact

SUSTAINABLE AVIATION FUELS

Topic Editors:
Michael P. Wolcott, Washington State University, United States
Nathan Brown, Federal Aviation Administration, United States
William Goldner, United States Department of Agriculture (USDA), United States
Zia Haq, United States Department of Energy (DOE), United States
Season Hoard, Washington State University, United States
Johnathan Holladay, LanzaTech, United States
Kristin C. Lewis, Volpe National Transportation Systems Center, United States

Citation: Wolcott, M. P., Brown, N., Goldner, W., Haq, Z., Hoard, S., Holladay, J., Lewis, K. C., eds. (2022). Sustainable Aviation Fuels. Lausanne: Frontiers Media SA. doi: 10.3389/978-2-83250-436-9

Table of Contents

06 ***Editorial: The Motivations for and the Value Proposition of Sustainable Aviation Fuels***
Kristin C. Lewis, Nathan L. Brown, William R. Goldner, Zia Haq, Season Hoard, Johnathan E. Holladay and Michael P. Wolcott

14 ***Comparing Alternative Jet Fuel Dependencies Between Combustors of Different Size and Mixing Approaches***
Randall C. Boehm, Jennifer G. Colborn and Joshua S. Heyne

26 ***Recycled Paper as a Source of Renewable Jet Fuel in the United States***
William L. Kubic Jr., Cameron M. Moore, Troy A. Semelsberger and Andrew D. Sutton

42 ***Production of Sustainable Aviation Fuels in Petroleum Refineries: Evaluation of New Bio-Refinery Concepts***
Abid H Tanzil, Kristin Brandt, Xiao Zhang, Michael Wolcott, Claudio Stockle and Manuel Garcia-Perez

56 ***Qualification of Alternative Jet Fuels***
Mark A. Rumizen

64 ***Regulatory and Policy Analysis of Production, Development and Use of Sustainable Aviation Fuels in the United States***
Ekrem Korkut and Lara B. Fowler

82 ***Construction and Demolition Waste-Derived Feedstock: Fuel Characterization of a Potential Resource for Sustainable Aviation Fuels Production***
Quang-Vu Bach, Jinxia Fu and Scott Turn

102 ***Estimating the Reduction in Future Fleet-Level CO_2 Emissions From Sustainable Aviation Fuel***
Samarth Jain, Hsun Chao, Muharrem Mane, William A. Crossley and Daniel A. DeLaurentis

116 ***Quantitative Policy Analysis for Sustainable Aviation Fuel Production Technologies***
Z. Juju Wang, Mark D. Staples, Wallace E. Tyner, Xin Zhao, Robert Malina, Hakan Olcay, Florian Allroggen and Steven R. H. Barrett

126 ***Economic Analysis of Developing a Sustainable Aviation Fuel Supply Chain Incorporating With Carbon Credits: A Case Study of the Memphis International Airport***
Bijay P Sharma, T. Edward Yu, Burton C. English and Christopher N. Boyer

141 ***Biofuel Discount Rates and Stochastic Techno-Economic Analysis for a Prospective Pennycress (Thlaspi arvense L.) Sustainable Aviation Fuel Supply Chain***
Carlos Omar Trejo-Pech, James A. Larson, Burton C. English and T. Edward Yu

156 ***The U.S. Energy System and the Production of Sustainable Aviation Fuel From Clean Electricity***
Jonathan L. Male, Michael C. W. Kintner-Meyer and Robert S. Weber

168 ***Determining the Adsorption Energetics of 2,3-Butanediol on RuO_2(110): Coupling First-Principles Calculations With Global Optimizers***
Carrington Moore, Difan Zhang, Roger Rousseau, Vassiliki-Alexandra Glezakou and Jean-Sabin McEwen

180 ***Pilot-Scale Pelleting Tests on High-Moisture Pine, Switchgrass, and Their Blends: Impact on Pellet Physical Properties, Chemical Composition, and Heating Values***
Jaya Shankar Tumuluru, Kalavathy Rajan, Choo Hamilton, Conner Pope, Timothy G. Rials, Jessica McCord, Nicole Labbé and Nicolas O. André

197 ***Oilseed Cover Crops for Sustainable Aviation Fuels Production and Reduction in Greenhouse Gas Emissions Through Land Use Savings***
Farzad Taheripour, Ehsanreza Sajedinia and Omid Karami

207 ***Searching for Culture in "Cultural Capital": The Case for a Mixed Methods Approach to Production Facility Siting***
Marc Boglioli, Daniel W. Mueller, Sarah Strauss, Season Hoard, Tyler A Beeton and Rachael Budowle

221 ***Perspectives on Fully Synthesized Sustainable Aviation Fuels: Direction and Opportunities***
Stephen Kramer, Gurhan Andac, Joshua Heyne, Joseph Ellsworth, Peter Herzig and Kristin C. Lewis

228 ***Social Science Applications in Sustainable Aviation Biofuels Research: Opportunities, Challenges, and Advancements***
Brian J. Anderson, Daniel W. Mueller, Season A. Hoard, Christina M. Sanders and Sanne A. M. Rijkhoff

243 ***Building Structure-Property Relationships of Cycloalkanes in Support of Their Use in Sustainable Aviation Fuels***
Alexander Landera, Ray P. Bambha, Naijia Hao, Sai Puneet Desai, Cameron M. Moore, Andrew D. Sutton and Anthe George

256 ***Understanding the Compositional Effects of SAFs on Combustion Intermediates***
M. Mehl, M. Pelucchi and P. Osswald

273 ***Economic Impacts of the U.S. Renewable Fuel Standard: An* Ex-Post *Evaluation***
Farzad Taheripour, Harry Baumes and Wallace E. Tyner

290 ***Cumulative Impact of Federal and State Policy on Minimum Selling Price of Sustainable Aviation Fuel***
Kristin L. Brandt, Lina Martinez-Valencia and Michael P. Wolcott

303 ***Advanced Fuel Property Data Platform: Overview and Potential Applications***
Simon Blakey, Bastian Rauch, Anna Oldani and Tonghun Lee

314 ***Modeling Yield, Biogenic Emissions, and Carbon Sequestration in Southeastern Cropping Systems With Winter Carinata***
John L. Field, Yao Zhang, Ernie Marx, Kenneth J. Boote, Mark Easter, Sheeja George, Nahal Hoghooghi, Glenn Johnston, Farhad Hossain Masum, Michael J. Mulvaney, Keith Paustian, Ramdeo Seepaul, Amy Swan, Steve Williams, David Wright and Puneet Dwivedi

328 *The Economic Impact of a Renewable Biofuels/Energy Industry Supply Chain Using the Renewable Energy Economic Analysis Layers Modeling System*
Burton C. English, R. Jamey Menard and Bradly Wilson

342 *From Farm to Flight: CoverCress as a Low Carbon Intensity Cash Cover Crop for Sustainable Aviation Fuel Production. A Review of Progress Towards Commercialization*
Winthrop B. Phippen, Rob Rhykerd, John C. Sedbrook, Cristine Handel and Steve Csonka

frontiers | Frontiers in Energy Research

TYPE Editorial
PUBLISHED 26 September 2022
DOI 10.3389/fenrg.2022.1005493

OPEN ACCESS

EDITED BY
Haiping Yang,
Huazhong University of Science and Technology, China

REVIEWED BY
Fernano Israel Gómez-Castro,
University of Guanajuato, Mexico
Luis Cortez,
State University of Campinas, Brazil

*CORRESPONDENCE
Kristin C. Lewis,
kristin.lewis@dot.gov

SPECIALTY SECTION
This article was submitted to Smart Grids,
a section of the journal
Frontiers in Energy Research

RECEIVED 28 July 2022
ACCEPTED 05 September 2022
PUBLISHED 26 September 2022

CITATION
Lewis KC, Brown NL, Goldner WR, Haq Z, Hoard S, Holladay JE and Wolcott MP (2022), Editorial: The motivations for and the value proposition of sustainable aviation fuels. *Front. Energy Res.* 10:1005493. doi: 10.3389/fenrg.2022.1005493

Editorial: The motivations for and the value proposition of sustainable aviation fuels

Kristin C. Lewis[1]*, Nathan L. Brown[2], William R. Goldner[3], Zia Haq[4], Season Hoard[5], Johnathan E. Holladay[6] and Michael P. Wolcott[5]

[1]Volpe National Transportation Systems Center, Cambridge, MA, United States, [2]Federal Aviation Administration, Washington, DC, United States, [3]National Institute of Food and Agriculture (USDA), Washington, DC, United States, [4]Bioenergy Technologies Office (DOE), Washington, DC, United States, [5]Washington State University, Pullman, WA, United States, [6]LanzaTech, Skokie, IL, United States

KEYWORDS

decarbonization, drop-in fuel, sustainable aviation fuel, SAF, sustainability, aviation, carbon-neutral aviation

Editorial on the Research Topic
The motivations for and the value proposition of sustainable aviation fuels

Drivers of aviation sector interest in sustainable aviation fuels

All forecasts for aviation expect continued growth in the sector over time. It will take some time for the aviation sector to return to pre-pandemic levels of activity, with some estimates putting this recovery to 2024 and beyond (Airlines for America, 2021a), and this recovery will likely be affected by traveler willingness, workforce availability, and other factors. Nevertheless, the long-term perspective suggests that aviation will continue to grow based on its value proposition to society of safe, efficient, high-speed movement of goods and people. This growth in traffic and locations of service will result in accompanying increases in fuel demand (Fleming & de Lépinay, 2019). Under current practices, this expansion of traffic would lead to increased carbon emissions. However, the aviation sector has made several commitments to addressing carbon-dioxide emissions.

The first of these was the first industrial-sector-wide commitment to carbon-neutral growth, in which increases in aviation activity must be de-coupled from increases in greenhouse gas emissions. Meeting these emissions goals relies on what the International Civil Aviation Organization (ICAO) refers to as a "basket of measures" for reducing carbon emissions associated with aviation (ICAO Secretariat, 2019), including improved operations, new technology, alternative fuels, and other market-based measures (see

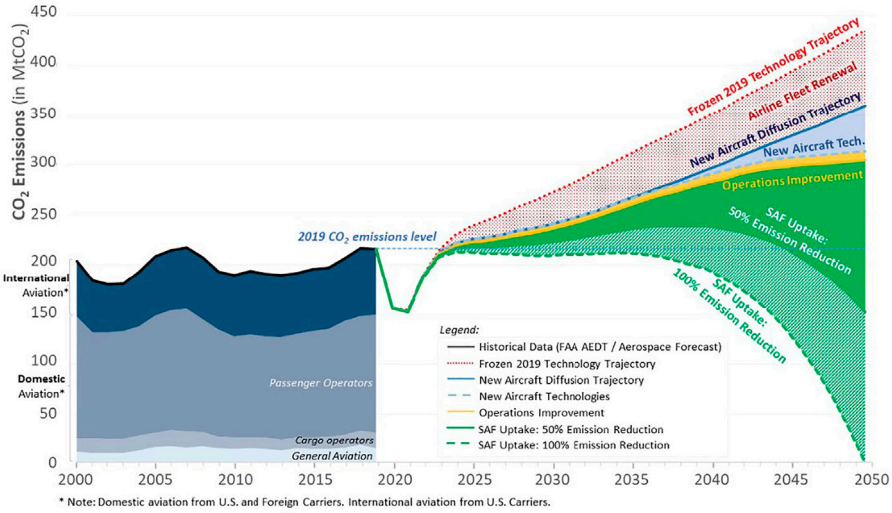

FIGURE 1
Projection of future annual emissions of aviation out to 2050 with and without the application of the "basket of measures" of operational and technological advancements and SAF deployment. Without SAF, the aviation sector will not meet the net-zero emissions goals they have set. Source (United States, 2021) used with permission.

Figure 1). The ICAO Carbon Offsetting and Reduction Scheme for International Aviation (CORSIA) caps carbon emissions from international aviation at 2019 levels out to 2035. Airline operators of participating countries must report their emissions each year and, if emissions exceed the baseline, offset those emissions (ICAO, 2021a). The emissions obligation associated with fuel burn can be reduced by replacing standard petroleum-based jet fuel with low carbon CORSIA-eligible fuel, including SAF or fossil-based "lower carbon aviation fuels." The aviation sector is currently in the pilot phase of CORSIA, which is expected to continue to drive interest in carbon-beneficial alternatives to standard petroleum-based jet fuel.

Additionally, in March 2021, Airlines for America (A4A), a trade association of U.S. airlines, announced that all its members have committed to net zero carbon emissions by 2050, a commitment that can be achieved with the successful deployment of the full basket of measures (Airlines for America, 2021b). At the 77th Annual General Meeting of the International Air Transport Association (IATA) in Boston, United States, on 4 October 2021, a resolution was passed by IATA member airlines committing them to achieving net-zero carbon emissions from their operations by 2050. This pledge brings air transport in line with the objectives of the Paris agreement to limit global warming to 1.5°C. In November 2021, the U.S. federal government released the 2021 Aviation Climate Action Plan (United States, 2021) committing to net zero carbon emissions for the U.S. aviation sector by 2050 and detailing the strategy to achieve this goal. In the U.S., the White House's SAF Grand Challenge is a new effort to facilitate the deployment of SAF, setting U.S. SAF production goals of three billion gallons by 2030 and 100% of U.S. aviation fuel need (or 35 billion gallons) by 2050. A federal agency roadmapping effort is underway to identify key governmental actions to facilitate coordinated support for industry-led SAF production expansion (U.S. White House, 2021).

The aviation sector has made tremendous strides in technology and operational efficiency since the inception of jet-powered air travel, increasing fuel efficiency of aircraft by 85% since the 1950s and operational efficiency by 55% (Air Transport Action Group, 2020). Recent efforts to integrate real-time satellite and geospatial information into flight routing and operational controls in the U.S. through the NextGen program has led to improvements of 17%, reduction in fuel burn and 21% reductions in aircraft operating costs (FAA, 2021). Many of the easiest efficiency gains may have already been made, and future improvements to operations and infrastructure will be more challenging. ICAO estimates that even in an optimistic scenario, fuel burn improvements from technology and operations will be 0.98 and 0.39%, respectively per annum out to 2050 (Fleming & de Lépinay, 2019). Therefore, to achieve greater decarbonization, other measures from the basket will be needed. The expanded use of SAF is one lever the aviation sector can use to start decarbonization immediately and will be an important contributor in the future (Jain et al.).

The pursuit of drop-in sustainable aviation fuels

The unique power requirements for flight and longevity of the commercial fleets, as well as the global infrastructure compatibility requirements of aircraft and airports means that drop-in, low carbon fuel that can leverage the existing global aircraft fleet and fueling system infrastructure to improve environmental performance, while maintaining energy security and price certainty, can facilitate near-term and lowest cost decarbonization of aviation. Drop-in SAFs have essentially identical composition, performance, and safety to existing petroleum-based kerosene fuels and are fungible with existing fuels and in existing fueling systems.

Fuel suitability and safety is assured through detailed production specifications, handling procedures, and certification testing protocols established by the aviation industry. These specifications and operating practices are published by specification bodies such as ASTM International and recognized by national regulatory authorities as well as original equipment manufacturers and academic institutions (Rumizen).

Until 2009, jet fuel used for turbine powered aircraft was produced from petroleum. Furthermore, aircraft and other equipment are certified for use with petroleum-based jet fuel, so to avoid recertifying all equipment, the alternative fuels must be considered interchangeable with standard jet fuel. The commonly used specification of conventional aviation turbine fuel is ASTM D1655 (Standard Specification for Aviation Turbine Fuels (ASTM International, 2020)) although there are similar, equivalent standards used internationally (e.g., DEF STAN 91-091 (MODUK, 2020)). Alternative fuels (non-petroleum origination) with comparable properties that have been approved for use are defined in a specification under the ASTM D7566. If testing demonstrates that a fuel has the required physical and fit-for-purpose characteristics to be considered usable as jet fuel, the specification body will issue an annex to ASTM D7566 that outlines the characteristics of the novel fuel type including feedstock, conversion process parameters, and fuel characteristics. Once a fuel is qualified under D7566 and blended at specified levels with petroleum-based jet fuel, it is redesignated as jet fuel under D1655. This fungibility is a critical aspect of the ASTM qualification that allows new fuels to be brought into the marketplace without the recertification of equipment and aircraft. Further information about the specification of synthetic aviation fuels can be found in (Rumizen). Drop-in, synthesized fuel production also has the potential to meet environmental, social, and economic sustainability criteria (such as those required by voluntary and/or regulatory frameworks, as described in Section 5), resulting in SAF.

Short overview of the range of fuels available

There are many ways to make alternative fuels from resources other than petroleum. Most of these processes produce, not only alternative jet fuel (C7 to C17 hydrocarbons), but also renewable diesel (C12 hydrocarbons and above) and naphtha or reformate blending components for gasoline (C12 and below). First-generation biofuels such as ethanol and biodiesel still contain oxygen from the original biomass, whereas advanced alternative fuels are strictly hydrocarbons and therefore chemically like the petroleum counterparts they seek to replace.

Biomass can be converted into fuels using thermochemical or biochemical processes, or combinations of the two. The thermochemical processes utilize heat, pressure, catalysts, and a reactor to decompose the biomass to varying degrees (e.g., gasification, pyrolysis, or hydrothermal liquefaction), and then recompose the constituent molecules (syngas or bio-oil intermediates) into pure hydrocarbons in the jet fuel range. In contrast, biochemical processes use microbial processing (e.g., enzymatic hydrolysis, fermentation, anaerobic digestion) to produce a primarily hydrocarbon intermediate. In either process, the liquid hydrocarbon intermediate is catalytically converted to hydrocarbons which may require subsequent upgrading steps to produce fuel distillates (Huber, Iborra, & Corma, 2006). Wastes, such as used cooking oil, and purpose-grown lipids can be directly upgraded to hydrocarbons using commercially available hydro-treatment and upgrading processes. The most cost-effective sources of these lipids include waste fats, oils, and greases (FOGs); however, vegetable oils from corn or oil-seed crops, and even oil derived from algae can be converted into SAF using this same technology.

As of August 2022, seven alternative aviation fuel production pathways were defined in specifications under Annexes of ASTM D7566-20c (CAAFI, 2021a; ASTM International, 2021). Furthermore, an annex has been added to D1655 to allow for the coprocessing of either fatty acids, fatty acid esters, or Fischer-Tropsch (FT) biocrude within a traditional petroleum refinery at up to 5% by volume.

As of this time, additional fuel pathways to produce aromatics and more diversified fuel molecules are also undergoing evaluation and testing in the ASTM specification development process (CAAFI, 2021b). These include pyrolysis, hydrothermal liquefaction and additional alcohol-to-jet pathways, and biomass-based pathways similar to those already included in D7566. Task force groups are in place to progress these fuels through the ASTM specification development and approval process. Additional research is being performed to better understand both the potential for conversion pathway optimization and the chemical and combustion characteristics of the products of various

pathways (e.g., (Boehm et al.; Landera et al.; Mehl et al.; Moore et al.) and to effectively leverage these data and make them available to facilitate ASTM prescreening and fuel testing (Blakey et al.). An additional Task Force is currently active at ASTM to define how to enable higher blend levels up to 100% SAF to be used in aircraft, including what technical and performance characteristics are needed and to what extent backward compatibility with existing aircraft will be required (Kramer et al.).

Additional SAF production pathways that have received significant attention and potential investment, particularly in Europe, include "power-to-liquids" or "e-fuel" technologies. These approaches utilize renewable electricity to power electrocatalysis processes to produce a liquid intermediate which is subsequently converted into a hydrocarbon. One common approach is to electrolyze water to produce renewable hydrogen and convert waste or atmospheric carbon dioxide (CO_2) into syngas (carbon monoxide + hydrogen gas). The syngas can then be converted to hydrocarbons using the FT process or to alcohols to be used in an alcohol-to-jet process (Schmidt, Weindorf, Roth, Batteiger, & Riegel, 2016). However, the supply of these fuels is dependent on a significant ramp up in production and availability of low cost, low carbon renewable energy (Holladay, Male, Rousseau, & Weber, 2020; Male et al.) to achieve the targeted very low fuel carbon intensities. These e-fuels, outside of those that might be produced via FT conversion of syngas, are not yet being evaluated as part of the ASTM qualification process.

There is currently no mechanism for incorporating non-drop-in fuels into the aviation sector by ASTM or other specification processes. Hydrogen fuel cells or direct combustion of hydrogen are possible long-term options for aviation but would require significant redesign of aircraft, engines, ground equipment, airports, fueling infrastructure, and safety procedures to be accommodated. The Air Transport Action Group (ATAG) estimates that hydrogen-fuel cell regional aircraft could enter the market in 2030 and that some hydrogen-combustion powered short haul flights could happen by the 2040 timeframe, but medium- and long-haul flights are unlikely to be powered by hydrogen until 2050 or beyond (Air Transport Action Group, 2020). On the other hand, renewable hydrogen could be immediately used to significantly reduce the life-cycle carbon footprint of alternative fuels if used in place of fossil-based hydrogen in SAF production processes. In the near term, this may be the best use for hydrogen in aviation.

Another alternative energy source that has received significant recent attention for aviation is electrification. However, electrification is challenging for aviation due to the size and weight of batteries, as even the best lithium-ion batteries have a lower mass-specific energy density by a factor of 60 compared to standard kerosene (Hepperle, 2012). It is currently anticipated that only small aircraft and flights under 200 nautical miles would be feasible with current technology, and future envisioned technologies necessary for extending range and passengers.

Sustainability is a key value proposition for SAF

ASTM specifications are focused on the physical and fit-for-performance characteristics of turbine fuels, but do not provide any evaluation of environmental, social, or economic impacts. However, the drivers outlined above have motivated airlines and other end users to see sustainability as a key component of the value proposition of non-petroleum aviation fuels. Given their cost, many of these fuels would not be competitive with standard petroleum-based jet fuel without the added value of verifiable environmental and social outcomes.

Three key issues previously raised regarding first generation biofuels continue to challenge advanced biofuels options: 1) concerns about induced land use change in which production of feedstocks for biofuels leads to displacement of another crop, followed by conversion of land from forest or other natural, carbon sequestering systems to agriculture or forestry to compensate, 2) potential impacts on food prices associated with reallocation of land to alternative fuels and 3) resource availability or how much SAF can be produced given sustainability constraints. Airline fuel purchasers are sensitive to these concerns and seek assurance that the SAF they purchase will not lead to sustainability issues. On the other hand, sustainable aviation fuel production—including from biomass—has the potential to contribute positively to economic and social sustainability outcomes such as rural economic development, creation of skilled jobs, and energy security.

Therefore, to be successful, SAF must:

1) Be economically viable.
2) Avoid environmental damage and/or improve environmental sustainability.
3) Meet social sustainability goals (e.g., land-use change, food security, local economic sustainability, energy security etc.).

Existing regulatory schemes that provide requirements and incentives for renewable/low carbon fuels, such as the European Union's Renewable Energy Directive (EU RED), the U.S. Renewable Fuel Standard (RFS2), and California Low Carbon Fuel Standard (CA LCFS), include criteria for one or more of these sustainability pillars. Under the E.U. RED fuels are certified by voluntary and national certification schemes to meet the requirements for carbon reduction, reducing carbon stock depletion, and avoiding highly biodiverse lands. Other

sustainability criteria may also be included in the future (European Commission, 2020). Under RFS as defined in the Energy Independence and Security Act (U.S. Public Law 110-140, 2007), fuels that are produced according to a process defined and accepted by the Environmental Protection Agency (EPA) are assigned a carbon reduction level based on their category. EPA is responsible for determining fuel volume requirements under RFS based on impacts on "air quality, climate change, conversion of wetlands, ecosystems, wildlife habitat, water quality, and water supply," as well as "job creation, the price and supply of agricultural commodities, rural economic development, and food prices." EPA is responsible for periodically assessing the impact of the program on "soil conservation, water availability, and ecosystem health and biodiversity, including impacts on forests, grasslands, and wetlands," "hypoxia, pesticides, sediment, nutrient and pathogen levels in waters, acreage and function of waters, and soil environmental quality" as well as potential "growth and use of cultivated invasive or noxious plants." Producers have to meet a limited number of specific criteria regarding their pathway definition and restriction of land use conversion after 19 December 2007.

In the context of ICAO, SAF are a "renewable or waste-derived aviation fuel that meets the CORSIA Sustainability Criteria under [Annex 16, Volume IV of the Convention on International Civil Aviation]" (ICAO, 2018). In the pilot phase (2021-2023) there are only two themes and three criteria approved that define SAF: lifecycle greenhouse gas emissions (including a 10% reduction threshold) and carbon stock (safeguarding high carbon stock lands and providing requirements for land conversion after a threshold date of 1 January 2008) (ICAO, 2021b). An expanded set of sustainability criteria will be used under CORSIA during the "Voluntary" phase from 1 January 2024 to 31 December 2026 (ICAO Council, 2021). These criteria include environmental, social, and economic indicators and principles addressing greenhouse gases, carbon stock/land use change, water, soil, air, conservation, wastes and chemicals, human and labor rights, land use rights and land use, water use rights, local and social development, and food security (ICAO, 2021c). The expanded CORSIA Sustainability Criteria were developed by drawing upon existing voluntary sustainability certification scheme themes, principles, and criteria. ICAO relies on approved sustainability certification schemes to execute the certification of SAF under CORSIA (ICAO, 2020).

The interest in SAF from airlines and other fuel purchasers (e.g., business aviation, air framers) as well as existing and emerging regulatory requirements and mandates indicates that sustainability improvements will continue to be a critical component of the value proposition of alternative aviation fuels.

Tools for evaluating SAF and SAF supply chains—Reducing costs and enabling supply

While technical opportunities remain and new pathways are constantly emerging, the key challenges for commercial scale SAF deployment include cost, supply chain development and risk management, and demonstration of sustainability.

While selling prices for produced SAF are not disclosed, SAF currently appears to cost more than conventional petroleum-based jet fuel. Absorbing this cost differential is a significant challenge for airlines seeking to reduce their carbon footprint, as many airlines are unwilling or unable to pay extra for SAF given their existing expenses and competitive environment. However, while the energy content of SAF is completely fungible with conventional fuels, the environmental services of carbon reduction overcome problems from its conventional counterpart and must be considered as part of its value.

Technoeconomic analysis (TEA) can be a useful tool to evaluate the economic factors affecting fuel selling price and identify opportunities to reduce costs within the supply chain. To compare among fuel production pathways, consistent TEAs for a range of options are extremely valuable. The U.S. Dept of Energy has developed one set of biofuel TEAs that focus on potential to drive down costs based on DOE targets (Kinchin, 2020). Another set of harmonized TEAs for the seven certified SAF pathways have been developed with consistent approaches to economic, finance, feedstock preparation, and support system (Brandt et al.). These models have been used to evaluate the influence of federal and state policies that evaluate environmental services provided by SAF. For real world costs as currently understood, researchers are implementing stochastic and deterministic TEA analysis assuming various policies and technology maturation rates to aid in thinking about uncertain future conditions (Tanzil, et al.; Trejo-Pech et al.). Other researchers are analyzing the influence of technoeconomics, technology maturation rates, and policies on deployment potential for SAF and other fuels (Newes, Han, & Peterson, 2017; Lewis, et al., 2018).

Life cycle analysis (LCA) of greenhouse gas emissions is critical for ensuring that the SAF that is commercially produced are carbon-beneficial. Highly rigorous and reviewed tools such as the Argonne National Laboratory's GREET model (ANL, 2021) provide reliable and transparent GHG accounting that demonstrates emissions reductions for SAF. ICAO publishes a standard set of GHG LCA values for SAF used under CORSIA (ICAO, 2021d) as well as a standardized methodology for calculating core GHG LCA values for SAF (ICAO, 2021a). The California Air Resources Board similarly has a set of default carbon intensities published for fuels under the Low Carbon Fuel Standard (CARB, 2022).

Because new supply chains must be established to support SAF deployment, risk management is a critical issue for supply chain participants and investors. The Commercial Aviation

Alternative Fuels Initiative's Feedstock Readiness Level, Fuel Readiness Level, and Environmental Progression frameworks provide consistent scoring and communication approach and clearly identify stages of development for feedstocks and fuels (CAAFI, 2021a) to facilitate communication about technical performance of SAF.

Understanding potential and probable availability of SAF feedstock is another critical aspect of supply chain development that requires detailed analyses of different potential species or feedstock opportunities by location and potential economic performance (e.g., Bach et al.; Kubic et al.; Sharma et al.; Trejo-Pech et al.; Field et al.; Tumuluru, et al.). SAF feedstock performance must also be characterized to ensure that both feedstocks and preparatory processes are suitable for fuel production (Bach et al.; Tumuluru, et al.). Waste feedstocks (e.g., municipal solid waste, waste fats, oils, and greases, wet wastes, or waste gases from industrial processes) are often less expensive than dedicated energy crops and considered advantageous for SAF production. Cover crops are also seen as a potentially beneficial feedstock type, with the potential to be integrated into existing crop rotations and provide benefits in the form of reduced erosion and disruption of pathogen and pest cycles and reduced land use demand (Taheripour et al.; Field et al.). Integrated analyses of potential supply chains based on agricultural and forestry products have been established through the US Dept. of Agriculture's Coordinated Agriculture projects, which focus on convening regional stakeholders to "facilitate the development of regionally-based industries producing advanced biofuels, industrial chemicals, and other biobased products," (National Institute of Food and Agriculture, 2021). SAF-relevant projects include the Southeast Partnership for Advanced Renewables from Carinata (Field et al.), the Integrated Pennycress Research Enabling Farm and Energy Resilience (IPREFER) project (Phippen et al.) and eight other projects so far.

Other tools have been developed to identify supply chain development and deployment opportunities, including tools for siting biorefineries based on geographic variation in capital and operational costs and resource availability (e.g., (English et al.) and how geography and transportation scenarios and disruptions influence supply chain performance (Lewis, et al., 2018). Social criteria, including social capital and cultural capital, should be considered when identifying the potential suitability of biorefinery candidate locations (Anderson et al.). These criteria should be assessed through mixed methods approaches, especially ongoing outcomes of biofuel development, as quantitative assessment does not adequately measure many of these impacts, especially at a more local level (Anderson et al.).

Policy can be a critical enabler for the development of new industries and the establishment of supply chains Nevertheless, for sound policy to be developed and implemented, it is crucial to develop an understanding of how past policies have worked and their impact on this and similar industries. This issue contains several papers that provide insight into the benefits and hurdles posed by various alternative fuel- and SAF-related policies (Korkut and Fowler; Brandt et al.; Taheripour et al.; Wang, et al.).

Given the key role of sustainability in the value proposition of SAF, reliable and consistent ways to measure the environmental, social, and economic outcomes of SAF are needed to build confidence in the marketplace. Compliance with CORSIA sustainability criteria is one definition of sustainability (ICAO, 2021b). Only three sustainability criteria are currently required for SAF under CORSIA, which most airlines and stakeholders would deem incomplete; however, as indicated above, ICAO has established additional sustainability criteria for the post-pilot phase. Whether under CORSIA or separately, voluntary certification by an independent sustainability certification scheme (e.g,. RSB, ISCC) can provide assurance of environmental, social, and economic sustainability. Compliance with regulatory schemes such as the U.S. Renewable Fuel Standard, California's Low Carbon Fuel Standard, and others can also provide both sustainability assurance and economic benefits (e.g., sellable Renewable Identification Numbers). Enhancement of ecosystem services are another way to demonstrate environmental benefits and potentially add revenue for feedstock producers (Gasparatos, et al., 2018; Brandt et al.).

This special issue in Frontiers in Energy Research

Sustainable aviation fuels are a key component of the basket of measures being pursued by the aviation sector to meet environmental, social, and economic goals, particularly to address climate change. A broad array of fuel production pathways are currently in development that need to be assessed for their technical production, performance, supply chain viability, and sustainability. Stakeholders from across the aviation and alternative fuels sectors, including government, academic, and private entities, have been researching, developing, and deploying a wide range of potential alternative jet fuel options, and along the way have also developed tools, data, and models to help with alternative jet fuel assessment and supply chain development. In this special topic, the contributors highlight some of the key research tools, models, and outcomes to provide a better overall understanding of the current state of play for alternative jet fuels. We have highlighted these papers in the preceding sections. Each paper provides an important perspective on the technologies and feedstocks to produce SAF, development of specifications to ensure safety and performance of SAF, the development and deployment of SAF supply chains, and sustainability. Future directions for SAF research include reducing the cost of SAF

production via innovative biochemical, thermochemical, and hybrid approaches, the development of a specification for high blend levels/100% synthetic fuels that would enable simplified logistics and greater deployment, and enhanced understanding of the non-CO_2 impacts of aviation (e.g., contrails) and the potential for SAF to address these issues.

Author contributions

The authors served as co-editors of the Research Topic on Sustainable Aviation Fuels, led by MW. KL led the drafting of the paper, and all authors contributed to the development and revision of the paper to reflect the state of SAF development and deployment.

Funding

FAA supported this work by KL under contract 693KA9-20-N-00013, and by MW and SH through the ASCENT Center of Excellence under FAA Award #13-C-AJFE-WaSU-013. Any opinions, findings, conclusions, or recommendations expressed in this material are those of the authors and do not necessarily reflect the views of the FAA nor other agencies of the U.S. Government.

Acknowledgments

The authors thank S. Csonka of CAAFI for reviewing this paper before submission.

Conflict of interest

The authors declare that the research was conducted in the absence of any commercial or financial relationships that could be construed as a potential conflict of interest.

Publisher's note

All claims expressed in this article are solely those of the authors and do not necessarily represent those of their affiliated organizations, or those of the publisher, the editors and the reviewers. Any product that may be evaluated in this article, or claim that may be made by its manufacturer, is not guaranteed or endorsed by the publisher.

References

Air Transport Action Group (2020). *Waypoint 2050*. Available at: https://aviationbenefits.org/media/167187/w2050_full.pdf.

Airlines for America (2021b). *Letter to secretary-designate buttigieg, january 19, 2021*. Washington, DC: Bloomberg News. Available at: https://www.bloomberg.com/news/articles/2021-01-19/wave-of-senate-confirmation-hearings-begins-inaugural-update (January 20, 2021).

Airlines for America (2021a). *A4A climate change commitment and flight path: Innovative industry and government action to achieve net zero carbon emissions*. Washington, DC, USA. Available at: https://www.airlines.org/wp-content/uploads/2021/03/A4A-Climate-Change-Commitment-Flight-Path-to-Net-Zero-FINAL-3-30-21.pdf.

ANL (2021). *GREET model*. Argonne, IL. Available at: https://greet.es.anl.gov/index.php (April 29, 2022).

ASTM International (2020). *D1655-20d: Standard specification for aviation turbine fuels*. West Conshohocken, PA, USA: ASTM International.

ASTM International (2021). *D7566-20c: Standard specification for aviation turbine fuel containing synthesized hydrocarbons*. West Conshohocken, PA, USA. doi:10.1520/D7566-20C

CAAFI (2021a). *Commercial aviation alternative fuels initiative*. Path to Alternative Jet Fuel Readiness:Available at: https://www.caafi.org/tools/Path_to_Alternative_Jet_Fuel_Readiness.html.

CAAFI (2021b). *Current fuels in the D4054 qualification process*. Available at: https://www.caafi.org/focus_areas/fuel_qualification.html#qualification (April 1, 2021).

CARB (2022). *LCFS pathway certified carbon intensities. State of CA*. Available at: https://ww2.arb.ca.gov/resources/documents/lcfs-pathway-certified-carbon-intensities (April 29, 2022).

English, B. C., Menard, R. J., and Wilson, B. (2022). The economic impact of a renewable biofuels/energy industry supply chain using the renewable energy economic analysis layers modeling system. *Front. Energy Res.* 10. doi:10.3389/fenrg.2022.780795

European Commission (2020). *Voluntary schemes*. Available at: https://ec.europa.eu/energy/topics/renewable-energy/biofuels/voluntary-schemes_en (April 05, 2021).

FAA (2021). *NextGen benefits*. from Federal Aviation Administration:,Available at: https://www.faa.gov/nextgen/benefits/ (July 20, 2022).

Fleming, G. G., and de Lépinay, I. (2019). "Environmental trends in aviation to 2050," in *Environmental report*. Editor I. C. Organization (Montreal, Canada: International Civil Aviation Organization).

Gasparatos, A., Romeu-Dalmau, C., von Maltitz, G., Johnson, F. X., Jumbe, C. B., Stromberg, P., et al. (2018). Using an ecosystem services perspective to assess biofuel sustainability. *Biomass Bioenergy*. doi:10.1016/j.biombioe.2018.01.025

Hepperle, M. (2012). *Electric flight – potential and limitations. AVT-209 workshop on energy efficient technologies and concepts operation*. Lisbon, Portugal. (pp. STO-MP-AVT-209) Available at: https://www.mh-aerotools.de/company/paper_14/MP-AVT-209-09.pdf.

Holladay, J. E., Male, J. L., Rousseau, R., and Weber, R. S. (2020). Synthesizing clean transportation fuels from CO2 will at least quintuple the demand for non-carbogenic electricity in the United States. *Energy fuels.* 34, 15433–15442. doi:10.1021/acs.energyfuels.0c02595

Huber, G. W., Iborra, S., and Corma, A. (2006). Synthesis of transportation fuels from biomass: Chemistry, catalysts, and engineering. *Chem. Rev.* 106, 4044–4098. doi:10.1021/cr068360d

ICAO (2018). *Annex 16 to the convention on international Civil aviation: Environmental protection - volume IV. Carbon offsetting and reduction scheme for international aviation (CORSIA). Montreal, ontario, Canada*. Available at: https://elibrary.icao.int/home/product-details/229739.

ICAO (2021c). *Carbon offsetting and reduction scheme for international aviation (CORSIA). Montreal, quebec, Canada*. Available at: https://www.icao.int/environmental-protection/CORSIA/Pages/default.aspx.

ICAO (2020). *CORSIA approved sustainability certification schemes*. Montreal, Ontario, Canada: ICAO. Available at: https://www.icao.int/environmental-protection/CORSIA/Documents/ICAO%20document%2004%20-%20Approved%20SCSs.pdf.

ICAO (2021d). *CORSIA sustainability criteria for CORSIA eligible fuels*. Montreal, ON, Canada. Available at: https://www.icao.int/environmental-protection/CORSIA/Documents/ICAO%20document%2005%20-%20Sustainability%20Criteria%20-%20November%202021.pdf.

ICAO Council (2021). *Council 222nd session, twelfth meeting summary of decisions. C-DEC 222/12*. Montreal, Canada: ICAO. Available at: https://www.

icao.int/about-icao/Council/Council%20Documentation/222/C-DECs/C.222.DEC.12.EN.pdf.

ICAO Secretariat (2019). "Introduction to the ICAO basket of measures to mitigate climate change," in *ICAO, ICAO environmental report 2019* (Montreal: ICAO), 111–115. Available at: https://www.icao.int/environmental-protection/Documents/EnvironmentalReports/2019/ENVReport2019_pg111-115.pdf.

ICAO (2021a). *CORSIA default life cycle emissions values for CORSIA eligible fuels*. Montreal, ON, Canada. Available at: https://www.icao.int/environmental-protection/CORSIA/Pages/CORSIA-Eligible-Fuels.aspx.

ICAO (2021b). *CORSIA methodology for calculating actual life cycle emissions values*. Montreal, ON, Canada. Available at: https://www.icao.int/environmental-protection/CORSIA/Pages/CORSIA-Eligible-Fuels.aspx.

Kinchin, C. (2020). *BETO biofuels TEA database*. Washington, DC: Dept. of Energy. Available at: https://bioenergykdf.net/content/beto-biofuels-tea-database (April 29, 2022).

Lewis, K. C., Newes, E. K., Peterson, S. O., Pearlson, M. N., Lawless, E. A., Brandt, K., et al. (2018). December 7) US alternative jet fuel deployment scenario analyses identifying key drivers and geospatial patterns for the first billion gallons. *BioFPR*. doi:10.1002/bbb.1951|

MODUK (2020). *DEF STAN 91-091 revision I12*. Glasgow, UK: MODUK British Defense Standards.

National Institute of Food and Agriculture (2021). *AFRI Regional Bioenergy System Coordinated Agricultural Projects*. Washington, DC: US Department of Agriculture. Available at: https://nifa.usda.gov/afri-regional-bioenergy-system-coordinated-agricultural-projects.

Newes, E., Han, J., and Peterson, S. (2017). "NREL/TP-6A20-67482: Potential avenues for significant biofuels penetration in the U.S. Aviation market," in *Golden, CO: Nrel*. Available at: https://www.nrel.gov/docs/fy17osti/67482.pdf.

Schmidt, P., Weindorf, W., Roth, A., Batteiger, V., and Riegel, F. (2016). *Background/september 2016 - power-to-liquids: Potentials and perspectives for the future supply of renewable aviation fuel*. Munich: German Environment Agency.

United States (2021). *United States 2021 aviation climate action plan*. Washington, D.C.: United States Government. Available at: https://www.faa.gov/sites/faa.gov/files/2021-11/Aviation_Climate_Action_Plan.pdf.

U.S. Public Law 110-140 (2007). *Energy independence and security Act of 2007*. USA. Available at: https://www.govinfo.gov/content/pkg/BILLS-110hr6enr/pdf/BILLS-110hr6enr.pdf.

White House, U. S. (2021). *Fact sheet: Biden administration advances the future of sustainable fuels in American aviation*. Washington, DC, USA. Available at: https://www.whitehouse.gov/briefing-room/statements-releases/2021/09/09/fact-sheet-biden-administration-advances-the-future-of-sustainable-fuels-in-american-aviation/ (December 07, 2021).

frontiers in Energy Research

ORIGINAL RESEARCH
published: 13 August 2021
doi: 10.3389/fenrg.2021.701901

Comparing Alternative Jet Fuel Dependencies Between Combustors of Different Size and Mixing Approaches

Randall C. Boehm, Jennifer G. Colborn and Joshua S. Heyne*

Department of Mechanical and Aerospace Engineering, University of Dayton, Dayton, OH, United States

Analyses used to reveal fuel dependencies on lean blow out and ignition at specific operating conditions in specific combustors show inconsistent trends with each other. Such variety is however consistent with the occurrence of transitions between the governing physical phenomena as the ratios between evaporation, mixing, or chemical time scales with their respective residence times also vary with specific operating conditions and combustor geometry. It is demonstrated here that the fuel dependencies on LBO in a large, single-cup, swirl-stabilized, rich-quench-lean combustor varies with operating conditions such that a feature importance match is attained to fuel dependencies observed in a much smaller combustor at one end of the tested range, while a qualitative match to fuel dependencies observed in a lean, premixed, swirler-stabilized combustor of comparable size at the other end of the tested range. The same reference combustor, when tested at cold conditions, is shown to exhibit similar fuel dependencies on ignition performance as the much smaller combustor, when tested at both cold and warm conditions. The practical significance of these findings is that a reference rig, such as the Referee Rig, can capture fuel performance trends of proprietary industry combustors by tailoring the inlet air and fuel temperatures of the tests. It is, therefore, a trustworthy surrogate for screening and evaluating sustainable aviation fuel candidates, reducing the dependency on proprietary industrial combustors for this purpose, thereby increasing transparency within the evaluation process while also expediting the process and reducing cost and fuel volume.

Keywords: lean blowout, ignition, fuel dependencies, sustainable aviation fuel, jet fuel, rig to engine correlation

OPEN ACCESS

Edited by:
Nathan Brown,
Federal Aviation Administration,
United States

Reviewed by:
Muhammad Farooq,
University of Engineering and Technology, Lahore, Pakistan
Sen Li,
Institute of Mechanics (CAS), China

****Correspondence:***
Randall C. Boehm
rboehm1@udayton.edu

Specialty section:
This article was submitted to Bioenergy and Biofuels, a section of the journal Frontiers in Energy Research

Received: *28 April 2021*
Accepted: *29 July 2021*
Published: *13 August 2021*

Citation:
Boehm RC, Colborn JG and Heyne JS (2021) Comparing Alternative Jet Fuel Dependencies Between Combustors of Different Size and Mixing Approaches. Front. Energy Res. 9:701901. doi: 10.3389/fenrg.2021.701901

INTRODUCTION

As global fuel demand increases environmental, economic, and security interests have led to the investigation of sustainable aviation fuels (SAF) for wider use. Due to the differences in composition between SAF and petroleum-derived fuels, qualification of these fuels is required before implementation. The current process in place for the qualification of SAF, ASTM D4054, focuses on developing "drop-in" hydrocarbon fuels, meaning no changes need to be made to engine, aircraft, and airport infrastructure for a fuel to be compatible. Unless a candidate fuel qualifies for fast track approval, this evaluation is an extensive process that takes years to complete, millions of dollars and thousands of gallons of fuel (Oldani, 2020). As shown in **Figure 1**, the approval process for non-fast track jet fuel qualification involves four levels of testing as well as two stages of reports with

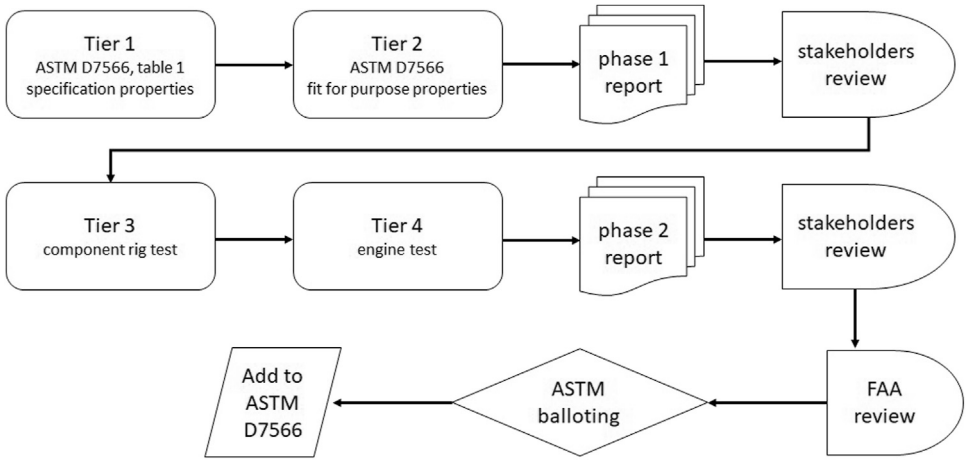

FIGURE 1 | ASTM D4054 fuel evaluation process.

comprehensive stakeholder review. Fuel is first tested for general specifications and fit-for-purpose properties before the phase 1 report is released to the stakeholders who complete a technical review of the data before it can proceed to tier 3 and tier 4 testing. Here, both rig and engine testing are completed. The amount of fuel required for testing increases about 10-fold with every tier in the qualification process.

Recently, a renewable jet fuel produced through catalytic hydrothermolysis referred to as RediJet was submitted to ASTM subcommittee J for aviation fuels for approval. As reported by Coppola (2018), approximately 72,000 gallons of SAF was required to complete the test plan. Component and rig tests were performed by three different engine manufacturers over nine different test conditions. Engine testing was completed by two engine manufacturers, including a flight test with a twin-engine Falcon 20. Three fuel mixtures were used for each test condition: neat Jet A as a baseline, neat RediJet, and a 50:50 blend. A total of 144,000 gallons of jet fuel was used for full qualification of the new "drop-in" SAF. Reducing the volume of fuel required for qualification would be advantageous for both fuel manufacturers and the sponsors who have a vested interest in SAF. The aim of the National Jet Fuel Combustion Program (NJFCP) was to shorten and redirect the process for jet fuel qualification (Colket et al., 2017). By developing predictive models for fuel behavior and adding some tailored, low-volume testing prior to the phase I research report, additional feedback to the ATSM evaluation committee and to fuel manufacturers would be provided to guide early fuel development. The work scope of tier 3 and tier 4 testing could then be directed toward a narrower range of potential concerns thereby reducing total fuel required. Alternatively, the candidate fuel might be reformulated into product that has a higher probability of achieving qualification. Importantly, there is a need to understand how fuel effects in small-scale rigs compare with engine observations. Validation of small-scale rigs against full-scale engines is essential for developing predictive models and testing methodology.

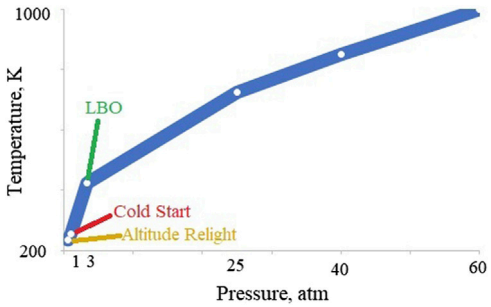

FIGURE 2 | Visual representation of operating conditions relevant to combustion figures of merit.

At the program level, a range of operating conditions were identified where lean blowout (LBO) or ignition is most likely to be impacted by differences in fuel composition and properties (Colket and Heyne, 2021). The most sensitive LBO conditions involve a throttle-chop at cruise to flight idle, and the start transient where the increase in fuel flow rate may not sufficiently keep up with the increase in airflow rate if the control schedule is improperly set for the fuel being used. Fuel impacts on ignition center on cold conditions, namely a cold-soaked auxiliary power unit (APU) at altitude or a cold-soaked main engine on the ground. The operating conditions are shown pictorially in **Figure 2** for the typical temperatures (T_{cmb}) and pressures (P_{cmb}) entering the combustion chamber. Here, altitude relight and cold start both refer to ignition cases. These conditions were selected because they are some of the most extreme conditions that will be seen within an engine and are consistent with the tests required by ASTM D4054 (Colket et al., 2017; Coppola, 2018). Similar fuel dependencies have been noted for cold ground start, and altitude relight (Hendershott et al., 2018; Stouffer et al., 2020).

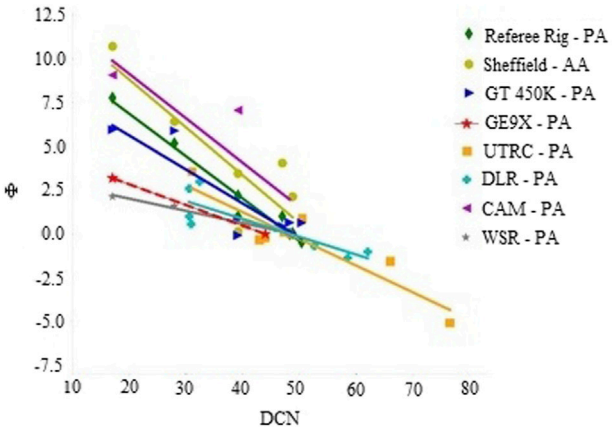

FIGURE 3 | LBO limit as a function of DCN for eight different rigs used within the NJFCP.

Nine experimental rigs within the NJFCP, featuring a wide range of geometries and time scales were used to observe fuel effects (Colket and Heyne, 2021). As shown in **Figure 3**, eight of the nine rigs showed correlation between derived cetane number (DCN) and relative equivalence ratio at LBO (Φ_i), which is defined in **Equation 1**. The parameter, Φ_i is read as, the LBO performance of fuel i relative to the LBO performance of the reference fuel (A2), and it is expressed as a percentage in plots shown throughout this report. The only rig used within the program that did not show a correlation to DCN was the Honeywell 131-9 APU combustor rig (APU-CR), one of the two industry combustors used in the program. On its face, this result is incongruent with the goal of the NJFCP; to reduce tier 3 or tier 4 testing. However, closer examination of results in both the Referee Rig (RR) and a GE9X full annular combustor rig (GE9X-FAR) showed that fuel dependencies vary with operating conditions.

$$\Phi_i = \frac{\phi_i - \phi_{A2}}{\phi_{A2}} \quad (1)$$

Colborn et al. (2020) showed that the relative LBO at 65°C and 107 kPa air temperature and pressure in the RR is dominated by the Ohnesorge number (Oh) at 2% ΔP/P, while at 6% ΔP/P the DCN dominates, with a smooth transition from one extreme to the other. Also, at 3.5% ΔP/P and 107 kPa, the fuel with the lowest DCN and most favorable atomization properties (labeled as C1) showed no sensitivity to air temperature between 65°C and 83°C. Complementary to this data, Boehm et al. (2020) found this same fuel (C1) had measurably worse LBO performance in a GE9X combustor than the other three fuels tested at three of four test conditions. At a lower air temperature, C1 showed the same LBO performance as the reference petroleum-derived fuel when each were heated to 60°C, which was the reference fuel temperature for this set of tests. A summary of these results is presented in **Figure 4**. The data suggest that fuel physical and chemical properties are both important near the low temperature boundary of the GE9X engine operating range at conditions important to aircraft engine LBO margin, while only chemical properties are important at higher air temperature and loading.

In this report the results introduced above are shown to be consistent with LBO theory (Plee and Mellor, 1979; Mellor, 1980), and the RR, in concert with a well-thought-out test plan, is capable of showing the same fuel dependencies as the APU-CR and the GE9X-FAR. The timescales of evaporation and chemical reactions are impacted significantly by fuel and air temperature, suggesting the tested range of operating conditions is critical to a thorough investigation of fuel dependencies. We assert that it is not necessary to match commercial combustor geometry and operating conditions provided the test combustor is tested over a sufficiently wide range of operating conditions to sweep through the range of timescale ratios that are relevant to commercial combustor operability.

BACKGROUND

Previous Work

Several investigations relating to fuel effects on LBO have been completed. Rock et al. (2019) measured the LBO threshold in an un-cooled flame tube of 18 different fuels and 3 different inlet air temperatures and noted correlation to DCN, T10, T90, or surface tension dependent on inlet air temperature. Casselberry et al. (2019) demonstrated correlation between pyrolysis products at 625°C and the LBO threshold in the RR when operated at chop-like (warm) conditions, using the same set of 18 fuels as Rock et al. An investigation into the role of preferential vaporization was conducted by Won et al. (2019), suggesting that DCN of the front end of the distillation may be a better indicator of LBO than DCN of the fully vaporized fuel, and they also observed that fuel physical properties are more strongly correlated with LBO than fuel chemistry at low temperature operation. Similarly, Grohmann et al. (2018) observed that both physical and chemical fuel properties influence combustor LBO. While focusing on the effects of atomization, Muthuselvan et al. (2020) related atomization quality with timescales relevant to LBO.

Many experiments and analyses of ignition characteristics of hydrocarbon fuels have focused on pre-vaporized and

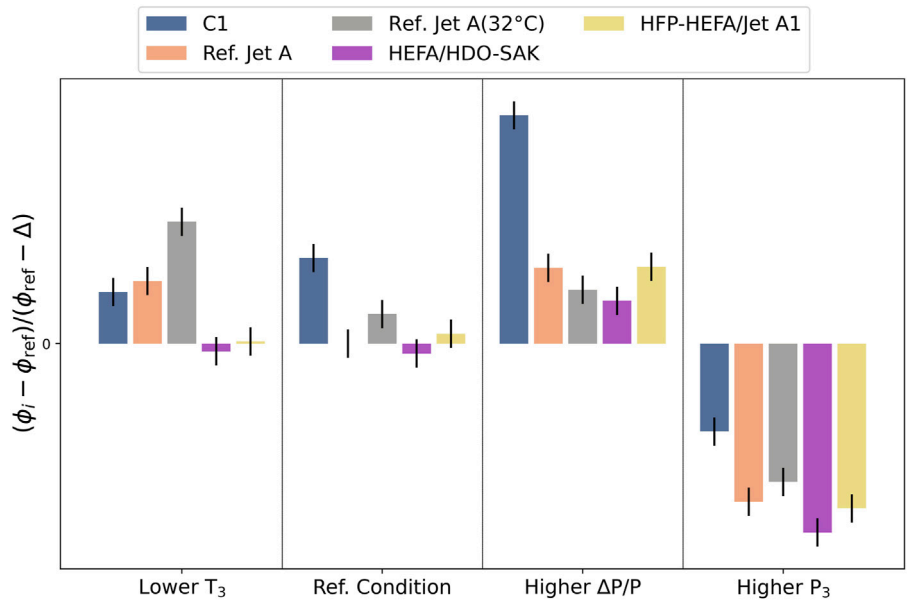

FIGURE 4 | Relative LBO at four operating conditions in GE9X-FAR: Figure redrawn using digitally extracted data from GE report to FAA as part of the CLEEN II Consortium Program Update–Public Plenary.

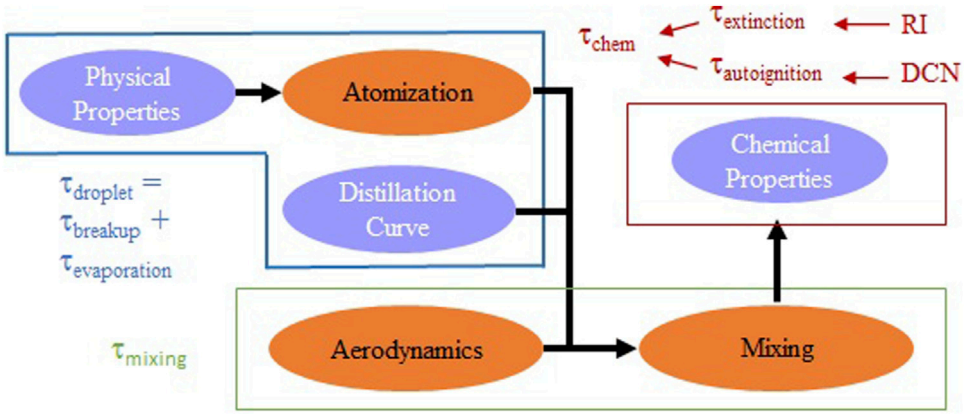

FIGURE 5 | Available LBO pathways. Orange ovals represent combustor-specific characteristics and purple ovals show any fuel-dependent properties that can impact LBO limits.

premixed fuel or other fuels and conditions that depart significantly from the most extreme start-up requirements for gas turbines used in aviation. Excellent reviews on the topic have been published by Aggarwal (1998) and more recently by Colket et al. (Colket and Heyne, 2021). Mayhew (2018) observed correlation between ignition probabilities at cold altitude relight conditions in a derivative of the RR and each of four fuel properties: viscosity, surface tension, T_{20}, and flash point. Opacich et al. (2019) observed similar correlations within datasets derived from both the RR and the APU-CR, although vapor pressure and heat capacity were chosen instead of T_{20} and flash point to represent volatile properties. Part of this work is a direct follow-up of work introduced by Opacich et al.

LBO Theory

A common theme discussed implicitly or explicitly in several of the works cited above is that LBO performance can be evaluated by considering three timescales that impact LBO limits as shown in **Equation 2**: chemical, mixing and evaporative timescales (Plee and Mellor, 1979; Mellor, 1980). This theory is further illustrated in **Figure 5**.

$$\frac{1}{\phi_{LBO}} \sim \left(\frac{1}{\tau_{chem}} + \frac{1}{\tau_{mix}} + \frac{1}{\tau_{evap}} \right)^{-1} \tag{2}$$

Fuel physical properties along with aerodynamic shear forces, flow field, fuel nozzle design, and fuel pressure all impact fuel spray atomization: droplet size distribution and spray

distribution. While combustor design and operating conditions are important to atomization, fuel properties are also an important factor for some commercial combustors at relevant, in-service operating conditions.

Fuel vapor pressure (and/or thermal conductivity), spray characteristics, and combustor aerodynamics all influence the evaporation timescale. From the perspective of fuel dependencies on LBO, it is important to note the evaporation timescale of some commercial combustors will be impacted significantly by vapor pressure, which varies not only with droplet surface temperature but also with the time-varying composition of the liquid fuel throughout the evaporation process. For systems that are evaporation limited, it is expected that fuels with a higher vapor pressure at a given temperature would ignite more readily than a fuel with lower vapor pressure.

The mixing of fuel vapor with air depends on the flow field, turbulence intensity, and the spatial relationship between the fuel spray, the eddies within the flow field, and the flame. Because turbulence is overwhelmingly more important than laminar diffusion in most industry combustors, there is ample technical justification for neglecting this term when considering fuel effects. Moreover, the characteristic mixing time of a given commercial combustor at any well-defined operating condition is likely to be held as proprietary by the engine companies.

The details around fuel-air mixing influence the gaseous mixture residence time and reactant concentration which, along with species reactivity, determine the fuel chemistry of combustion and blowout. The chemical timescale is relevant to this physics and may be comprised of different pieces such as autoignition and extinction.

Cold Ignition Overview

At extreme low fuel temperatures, fuel vapor pressure is low and with equally low inlet air temperature, no heating of droplets occurs until they reach a heat source, which could be a plasma discharge or the kernel of a previously ignited fuel/air mixture. At the extreme cold condition, the size and spatial distribution of the liquid fuel droplets within the combustor flow field is expected to be critical for most if not all combustors in aviation service. Very little evaporation occurs outside of the domain of the plasma discharge (spark), therefore it must supply enough energy to both evaporate the fuel and overcome the critical kernel radius (Kim et al., 2013). The heat released by each kernel must be high enough to both sustain the flame and sufficiently evaporate enough surrounding liquid fuel droplets to replenish the fuel consumed by the combustion that is occurring inside it. Only then can the flame kernel grow and potentially propagate upstream to an anchor point, transitioning to a self-sustaining flame. This process can be influenced significantly by fuel volatility, thermal properties and the physical properties that influence atomization.

Atomization Overview

Atomization will be affected by the viscosity, density, and surface tension (Guildenbecher et al., 2009; Lefebvre and McDonell, 2017). Increasing the surface tension will inhibit fuel breakup, while increasing the viscosity will dampen instabilities that allow for breakup, and increased density drives lower flow velocities in engines that are controlled to deliver a scheduled enthalpy flux or equivalence ratio. This in turn reduces the gage pressure that supplies the energy driving atomization.

EXPERIMENTS, DATA AND METHODS

Referee Rig Experiments

Experiments performed in the RR were completed at the Air Force Research Laboratory located at Wright-Patterson Air Force Base, and have been published elsewhere (Hendershott et al., 2018; Colborn et al., 2020). The Referee Rig is a non-proprietarty, single-cup, swirl-stabilized combustor designed by GE (this article's correspondance author) with input from four other leading engine manufacturers to simulate representative aerodynamic characteristics of both legacy and emerging, swirl-stabilized, combustors (Colket and Heyne, 2021). It is a classic rich-quench-lean, combustor with effusion cooled liners, a flat dome protected by an impingement-cooled heat shield, primary dilution holes located ½ dome height downstream from the dome and seconday dilution holes located just aft of the primary reaction zone. It features a modular construction to facilitate swapping of fuel injectors and swirlers to allow for evalation of different swiler effective areas, swirl numbers, spray angles and flow numbers. However, most of the data collected off this combustor so far has been with just one design configuration. Modification from it's original 4-cup design to a single cup design was completed by AFRL, and UDRI custom-buillt a thryatron-based exciter to achieve better control over spark energy and frequency relative to jet engine exciters. Readers interested in fabricating a copy of this combustor should contact the author for leads on where to find a copy of the drawings.

The four operating conditions analyzed in this work are as listed in **Table 1**. Fuel and air temperature were matched in each case, and LBO was determined after each successful ignition at $\frac{\Delta P}{P} = 2\%$. For all test conditions, the normalization described by **Equation 1** was reset so its value corresponding to the fuel sample designated as A2 was always zero. By this normalization, the dependencies on operating conditions are reduced, and fuel dependencies are highlighted.

APU-CR Experiments

The APU-CR experiments were performed at Honeywell Aerospace, in their combustor component test facility, and was operated at simulated engine conditions (Culbertson and Williams, 2017). APUs are small gas turbine engines that are used to provide power to spool-up the main engine during starter-assisted air starts. APUs are particularly sensitive to the physical properties that influence atomization and vaporization (Peiffer et al., 2019) because of their small volume, and corresponding low combustor residence time ($\tau_{cmb} = \rho_{air} V_{cmb} / W_{air}$). The 131-9 combustor is swirl-stabilized and relies on a rich-quench-lean combustion process, like many of the much-larger, main engine combustors. A standard 131-9 ignition system was used with the igniter located at approximately the eight o'clock position of the combustor (Culbertson and Williams, 2017).

TABLE 1 | APU-CR and RR operating conditions.

Rig	Operating condition	Fuel temperature [°C]	Air temperature [°C]	Pressure [atm]	$\Delta P/P_{cmb}$ [%]
RR	Cold lean blowout Colborn et al. (2020)	−30, 5	−30, 5	1.02	2%
	Cold start Hendershott et al. (2018)	−30, 5	−30, 5	1.02	2%, 3.5%
APU-CR	Lean blowout Culbertson and Williams (2017)	15	51 to 314	1.02, to 5.72	
	Cold ignition Culbertson and Williams (2017)	−37	−44, −35, 15	1.05, 0.2, 0.3	
	Warm ignition Culbertson and Williams (2017)	15	−38, 15	1.05, 0.2	

TABLE 2 | Property data of fuels used in GE9X-FAR testing.

Property	Jet A	C1	HFP-HEFA/Jet A1	HEFA/HDO-SAK
Density@15.6°C (g/ml)	0.809	0.758	0.786	0.789
LHV (MJ/kg)	43.3	44.0	43.4	43.2
Hydrogen (wt%)	13.91	15.25	14.23	13.90
Viscosity@37.8°C (cSt)	1.49	1.53	1.16	1.21
Viscosity@−20°C (cSt)	5.02	4.99	3.15	
Viscosity@15.6°C (cSt)		2.41 (curve fit)		1.66
DCN	~48	17.1		

Readers who wish to reproduce any of the data presented in the noted publications should contact Honeywell Aerospace.

The warm ignition (T_{fuel} = 15°C) light off boundary was determined at a baseline air temperature (−35°C) and pressure (1.05 atm) along with single point derivatives to higher temperature or lower pressure, as listed in **Table 1**. The cold ignition (T_{fuel} = −37°C) light off boundary was determined at each of the conditions used for warm ignition plus two additional points at a somewhat colder air temperature and low pressure, also listed in **Table 1**, and the lean blowout dataset included six operating conditions. For all test conditions, the analyzed equivalence ratios were normalized by **Equation 1**, just as was done with the RR data.

GE9X-FAR Experiments

The GE9X-FAR experiments were performed at GE, in their combustor component test facility, and was operated at simulated engine conditions, which are proprietary. However, a public release of sanitized data is available through reference (Boehm et al., 2020), and readers who wish to reproduce this data should contact GE. Quite unlike the RR and the APU-CR, the GE9X is a large combustor which achieves lean combustion for low NOx emissions with its twin annular premixing swirler. Limited details about the this combustor design have been published by Dhanuka et al. (2011). The understandable restrictions around sharing test data, procedures, and combustor design relating to fuel evaluation tests such as these was and is one of the prime motivators behind the development of the RR.

The GE data was not presented in a format that could be included in the statistical analyses that are reported in this work. The LBO data shown in **Figure 4** was normalized at the baseline operating condition by an equation like Equation 4, but it was not reset at each operating condition because dependence on operating condition was part of the story GE communicated. The un-disclosed constant denoted by 'Δ' in the axis label of **Figure 4** is the difference between the actual and displayed equivalence ratio at the reference condition, which disguises engine-proprietary LBO performance. However, the original source does indicate the tested points track along a reference velocity which scales as the log of air flow times air temperature squared, in the same order as they are presented in **Figure 4** and with roughly equal spacing.

Fuel Property Data

The RR and APU-CR experiments were directly or indirectly part of the NJFCP and used fuels that were distributed to affiliated labs by a control center, led by Tim Edwards at the Air Force Research Laboratory, who was also responsible for acquiring and publishing fuel property data (Edwards, 2017). This data is also available through the National Alternative Jet Fuels Test Database (Home | AJF:TD | U of I, 2021). The fuel samples designated as A1, A2, A3, C1, C2, and C5 were tested in both rigs. Additionally, the samples designated as C3, C4, and C7 were also tested in the RR. The GE9X experiments occurred under a different program but did include one fuel (C1) which was provided by Tim Edwards. Documentation of the property data of the fuels used by GE is provided in **Table 2**.

The fuel densities used in the analyses of the LBO datasets were as measured at 15°C. For analyses of the ignition datasets, all fuel properties were transformed into their respective values at the tested fuel temperature by the approach previously described by Opacich et al. (2019). Fuel properties that were measured over a range of temperatures that bounded the tested fuel temperature were interpolated to the test temperature (e.g., density). Temperature-dependent fuel properties that were not measured over a sufficient range to warrant interpolation (e.g., vapor pressure) were determined as outlined here. First, a surrogate fuel composition was derived by match to measured fuel property data and GCxGC-determined hydrocarbon class concentration data, using published blending rules (Flora et al.,

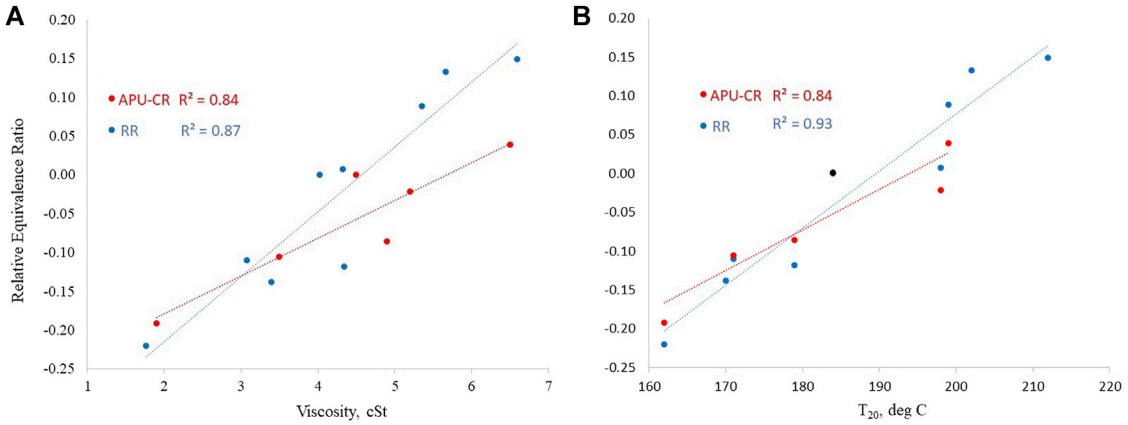

FIGURE 6 | APU-CR & RR LBO performance correlation with **(A)** viscosity (***v***), and **(B)** 20% recovered temperature (T_{20}). Data is from Colborn et al. (2020).

2019) to relate molecular properties and compositions to mixture properties. Next the molecular properties over a range of temperatures were calculated based on the models provided in the molecular properties database published by the National Institute of Standards and Technology (Kroenlein et al., 2012), and the blending rules applied at each modeled temperature. The resulting temperature-dependent mixture properties were then curve-fitted and those models were used to estimate the fuel properties at each, tested fuel temperature.

Analysis

The random forest statistical analysis approach used in this work has been described previously (Peiffer et al., 2019; Colborn et al., 2020). In summary, the method employs random sampling and replacement to decrease overfitting and allows for one dependent variable (e.g., LBO or ignition performance) to be evaluated against multiple independent variables (e.g., fuel properties) (Hastie et al., 2008). Standard Monte Carlo methods were used to simulate uncertainties in each independent variable based on measurement reproducibility as quoted in the relevant ASTM standard with an assumed Gaussian distribution, and these distributions represent the uncertainty domain within the random forest method. The regression approach taken was the same as that described by Opacich et al. (2019) and Peiffer et al. (2019). The simulation includes many trials to capture the full distribution of possible values within the reproducibility domain of each measured value. Each time, the relative importance values of each independent variable is recorded. In this way confidence bands around each relative importance value are estimated.

One set of random forest analyses was used here to assess the relative importance of atomization, evaporation rate, autoignition and extinction in each of two LBO datasets. Since none of these fundamental processes were clearly known or regress-able for all the fuels used in both test articles, it was necessary to choose a set of four independent/orthogonal properties that are known to correlate strongly with each of these four fundamental processes. Primary and secondary droplet breakup at incipient LBO conditions was represented by density at 15°C. T_{20} was selected to represent evaporation rate. Extinction was represented by radical index (RI), and autoignition was represented by derived cetane number. The idea was to use a comparison of these two analyses to assess how well one dataset, LBO in the RR at cold conditions, represents another dataset, LBO in the APU-CR at normal operating conditions.

Another set of random forest analyses was used to assess the relative importance of three independent variables in each of three cold ignition datasets. The Ohnesorge Number, which combines dynamic viscosity (μ), density, surface tension (σ), and the nozzle diameter, D, into one dimensionless parameter as shown in **Equation 3**, was used to

$$Oh = \frac{\mu(T)}{\left[\rho(T)\sigma(T)D\right]^{0.5}} \tag{3}$$

represent the atomization dependencies. The fuel dependency on evaporation rate was represented by vapor pressure, and specific heat was used to represent the fuel dependency on droplet heating. The definition of the dependent variable, representing ignition performance is somewhat different between the RR dataset and the APU-CR datasets. For the APU-CR datasets the ignition variable was defined by the minimum equivalence ratio required to achieve ignition within a Honeywell-standard duration of time during which the ignitor is firing periodically as it would in a commercial APU. For the RR dataset the ignition variable was defined by the equivalence ratio corresponding to 10% ignition probability per spark along a binomial regression fitted curve to the equivalence ratio and light/no-light data corresponding to each spark. Details of the binomial regression have been published by Hendershot et al. (2018).

RESULTS

LBO Results

While several laboratory rigs show a strong correlation between LBO and DCN (**Figure 3**), the APU-CR does not. Instead, it

shows a strong correlation to physical and volatility properties such as viscosity (ν), and 20% recovered temperature (T_{20}) as shown in **Figure 6**. At cold conditions, in contrast to the results at warm conditions, the RR also shows a correlation to physical and volatility properties, but not DCN. Due to the relatively low fuel temperatures at cold start, temperature-dependent physical properties such as density, viscosity, and surface tension trend higher which is detrimental to fuel atomization, and vapor pressure trends lower which is detrimental to evaporation so it is not surprising that the effects of such properties would be more observable at these conditions. In essence, the cold temperature in the cold LBO experiments with the RR serves to prolong the time scale of the physical processes necessary for combustion (namely, evaporation), driving it closer to the combustor residence time.

Main effects plots of Φ versus fuel property, as represented by **Figure 6**, suggest that both rigs show a correlation to fuel physical properties when the time scale of evaporation is on the same order as the combustor residence time. To further analyze this property dependency, a random forest statistical analysis was performed 1000 times, and a summary of these results is shown in **Figure 7**.

One important result of this analysis is that each rig shows nearly the same relative importance of T_{20} (representing evaporation rate) and density (representing atomization) on LBO, which suggests that the RR, when operated at cold conditions, does represent the relevant physics that largely determine LBO performance in the APU-CR operating at representative engine conditions. Another important result is that fuel properties that influence evaporation rate are clearly more important than those that correlate strongly with chemical reactivity. This result suggests that the LBO performance of these two rigs, as operated in these tests, is affected by evaporation more than chemical reactivity, so the data collected in this way should be used to evaluate the impact of fuel physical property variation on LBO. The third important result is that the relative importance of the radical index in the RR at these conditions does not match those of the APU-CR, suggesting that the RR is not a good surrogate for the APU-CR in this context. However, that may not be a requirement since radical index has less impact on LBO than the other properties considered. In contrast, the LBO performance of the GE9X-FAR is more strongly determined by the fuel chemistry properties so a useful surrogate laboratory combustor and test condition for it should reproduce similar values of the chemical property influence factors.

Turning now to the data from the GE9X-FAR, the notable differences, documented in **Table 2**, between the reference petroleum-derived fuel and the SAF blend component, designated as C1, are as follows. Sample C1 is 6.3% lighter, has 1.7% higher specific energy and has a much lower DCN. The lower density and higher specific energy of C1 are expected to affect LBO toward a lower (more favorable) ϕ_{C1} because lower density leads to a higher volumetric flow rate which leads to higher fuel pressure and therefore finer atomization and the higher LHV leads to a higher flame temperature for a given equivalence ratio. Conversely, the lower DCN of C1 is expected to lead to a higher (less favorable) ϕ_{C1} based on the empirical trends

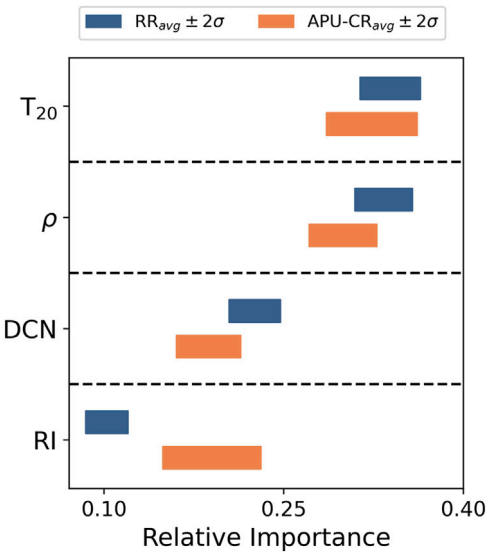

FIGURE 7 | LBO determinants importance values for the RR at cold conditions and the APU-CR at normal operating conditions. On average, 98.6% of the LBO performance variance in the RR is explained by the chosen independent variables, while 91.8% of the LBO performance variance in the APU-CR is explained. RR results are shown above APU-CR results in each block.

shown in **Figure 3**. The data shows higher ϕ_{C1} at three of the four test conditions, which is consistent with the much lower DCN of C1 relative to the reference fuel. At the lowest air temperature condition, however there is essentially no difference between ϕ_{C1} and ϕ_{ref} which is likely the result of the favorable density and specific energy of C1 compensating for its unfavorable DCN. GE also provided LBO data for Jet A fuel at two different temperatures. While this is not the same fuel, it is from the same supplier, and it is reasonable to assume that the properties of each are comparable, if not similar. The colder fuel will have higher density, viscosity, and surface tension and lower initial vapor pressure, but the chemical properties of the fuel vapor are the same. These property differences are reflected in the data: at the lowest air temperature condition the $\phi_{ref,@32C}$ is higher than $\phi_{ref,@60C}$. At each of the three conditions where C1 shows measurably worse LBO performance than the reference fuel, the colder reference fuel shows no clear difference compared to the warmer reference fuel. Together, these trends suggest that the LBO phenomenon in the GE9X-FAR is governed by chemistry at three of the four test conditions, but when the air temperature is reduced, evaporation becomes important as well. The two SAF fuels that are derived in part from hydrogenated esters and fatty acid (HEFA) show similar results to each other at all conditions, and an improvement relative to the reference fuel at the lowest temperature test condition, as expected based on their lower viscosity and lower density relative to the reference fuel.

Ignition Results

Main effects plots of Φ versus fuel property, as represented by **Figure 8**, suggest that both rigs show a correlation to fuel physical

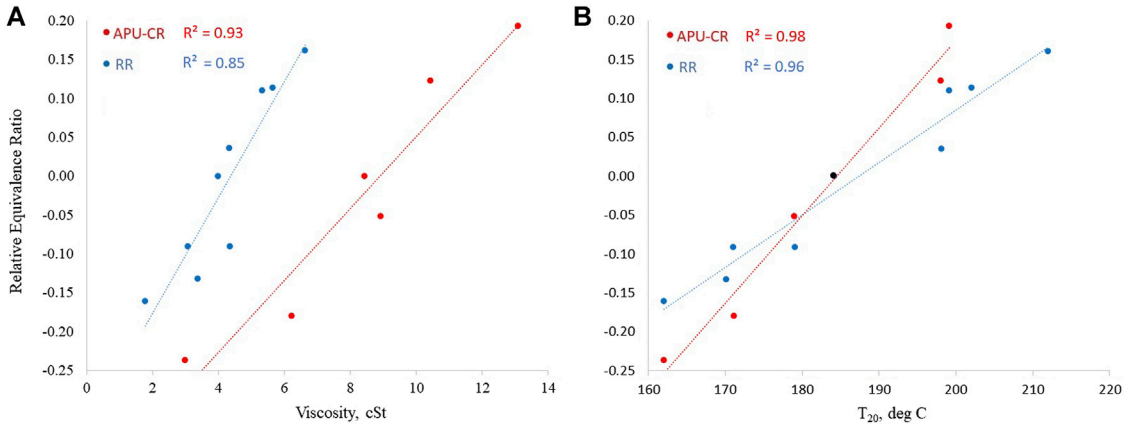

FIGURE 8 | RR and APU-CR ignition equivalence ratio as a function of **(A)** Viscosity and **(B)** 20% recovered temperature (T_{20}). Data is from Hendershot et al. (2018).

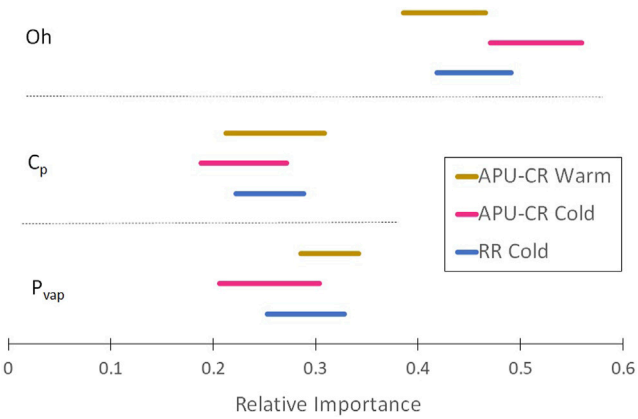

FIGURE 9 | Ignition determinants importance values for the RR at cold conditions and the APU-CR at both cold and warm conditions. On average, 94% of the ignition performance variance in the RR is explained by the chosen independent variables, 96% of the ignition performance variance in the APU-CR at cold conditions is explained, and 95% of the ignition performance variance in the APU-CR at warm conditions is explained. The display order from top to bottom in each block is the same as is shown in the legend.

properties (viscosity) and volatile properties (T_{20}). To further analyze this property dependency, a random forest statistical analysis was performed 1,000 times, and a summary of these results is shown in **Figure 9**. As noted in *Referee Rig Experiments* section, $Oh(T_{fuel})$, $C_p(T_{fuel})$ and $P_{vap}(T_{fuel})$ were used to represent atomization, droplet heating, and droplet evaporation rate, respectively, in these analyses. It should be noted here as well that several other count and combinations of independent variables were evaluated and the down-select to the three that are reported here was based on their connection to theory and goodness of fit (R^2). Inclusion of air temperature or pressure did not improve the fit but did proportionately impact the relative importance of each fuel property as additional variables were available to correlate with the variation in the ignition performance.

Each of the three selected fuel properties were shown be of similar importance in all three datasets: the RR at cold conditions and in the APU-CR at both cold and warm conditions. The Ohnesorge number accounts for about 46% of the observed variation in ignition performance, while vapor pressure accounts for 29% and specific heat accounts for 25%. In each dataset, these 3 variables alone explain 94–96% of the variation across the whole dataset which is especially interesting given the range of air temperature, pressure, or velocities that were tested. A small disconnect between the relative importance of the Ohnesorge number on ignition performance in the APU-CR with cold fuel relative to warm fuel is consistent with expectations based on visual observation of sprays at similar conditions in a benchtop inspection, where the cold fuel produces visually observable coarser spray.

The main point illuminated by this analysis is that the fuel property dependencies within each of the three datasets are nearly the same, which suggests that it is possible to use a small, standardized set of test articles to characterize fuel dependencies on ignition within the industry-wide fleet of combustors, which has important practical implication for the evaluation of potential SAF's. From a more fundamental perspective it is an interesting observation that two fuel properties are required to account for the evaporation timescale. This observation suggests that more detailed data relating to fundamental heat and mass transfer processes within the intersecting region of cold fuel droplets and plasmas or pre-existing flame kernels could lead to an even better understanding of the fundamental processes that govern fuel property dependencies on kernel initiation and growth.

CONCLUSION

In this work it has been suggested that combustor operating conditions can be used to vary the relative

importance of the evaporation, chemical, and mixing timescales that are characteristics of combustion phenomenon. By adjusting the operating conditions of the LBO experiments the ratio of the evaporation time scale to residence time can be matched between to combustors with vastly different length scales, the so-called Referee Rig and the Honeywell 131-9 APU combustor rig (APU-CR). It has been demonstrated that the RR, when operated at cold fuel and air conditions, exhibits the same fuel property dependencies (density and the temperature corresponding to 20% distilled) on lean blowout as the APU-CR at normal operating conditions. Further, when operated at representative flight idle conditions, the RR exhibits the same LBO dependencies on fuel properties (derived cetane number) as the GE9X full annular rig (GE9X-FAR) at similar operating conditions. Moreover, it has been observed that when the GE9X-FAR is operated at lower temperature, the LBO phenomenon is not governed primarily by derived cetane number, but rather by a combination of chemical and physical fuel properties, consistent with previous work (Colborn et al., 2020) probing the transition in operating conditions space, between evaporation-governed LBO and chemistry-governed LBO in the RR.

Analysis of data pertaining to the fuel dependencies on cold ignition in the RR as well as both standard-day and cold ignition in the APU-CR shows that atomization and evaporation are equally important to ignition performance. The atomization time scale is represented well by the Ohnesorge number, while the evaporation timescale is represented well by specific heat and vapor pressure. The correlations suggest that evaporation rate, under the conditions of the three sets of experiments, is determined by heat absorption (represented by specific heat) and the response to heat absorption (represented by the initial vapor pressure) with equal weighting. Most importantly, from a practical perspective, such fuel dependencies are shown to be common across a large difference in combustor cup volume or the operating environment.

Together these results indicate that the RR shows a great deal of correlation to real engines with respect to gaging the fuel dependencies of combustor operability, and thus shows potential as a standard, laboratory-scale test article to represent swirl-stabilized combustors in the ASTM fuel evaluation process for sustainable aviation fuels.

DATA AVAILABILITY STATEMENT

The raw data supporting the conclusions of this article are provided in the supplementary material or should be requested from the original source, as cited.

AUTHOR CONTRIBUTIONS

RB rewrote the original draft, brought in data and discussion around **Figure 4** and **Table 2**, added about 20 references and cleaned up the rest. RB also provided conceptualization. JC wrote the original draft, brought in the data around **Table 1** and **Figures 3**, **6**, **8**, and performed the statistical analyses JH provided conceptualization, funding and manuscript review and editing.

FUNDING

This research was funded by the U.S. Federal Aviation Administration Office of Environment and Energy through ASCENT, the FAA Center of Excellence for Alternative Jet Fuels and the Environment, project 34 through FAA Award Number 13-C-AJFE-UD-024 under the supervision of Anna Oldani. Any opinions, findings, conclusions or recommendations expressed in this material are those of the authors and do not necessarily reflect the views of the FAA. Open access publication fees are provided by the University of Dayton.

ACKNOWLEDGMENTS

The authors acknowledge support and helpful technical discussions with Tim Edwards and Edwin Corporan of the Air Force Research Laboratory as well as Scott Stouffer and Tyler Hendershott of the University of Dayton Research Institute.

SUPPLEMENTARY MATERIAL

The Supplementary Material for this article can be found online at: https://www.frontiersin.org/articles/10.3389/fenrg.2021.701901/full#supplementary-material

REFERENCES

Aggarwal, S. K. (1998). A Review of spray Ignition Phenomena: Present Status and Future Research. *Prog. Energ. Combustion Sci.* 24 (6), 565–600. doi:10.1016/S0360-1285(98)00016-1

Boehm, R., Thomsen, D. D., and Andac, M. G. (2020). *GE-aviation Program Update - Public Plenary*. Cincinnati, OH: FAA CLEEN II Consortium.

Casselberry, R. Q., Corporan, E., and DeWitt, M. J. (2019). Correlation of Combustor Lean Blowout Performance to Supercritical Pyrolysis Products. *Fuel* 252, 504–511. doi:10.1016/j.fuel.2019.04.128

Colborn, J. G., Heyne, J. S., Stouffer, S. D., Hendershott, T. H., and Corporan, E. (2020). Chemical and Physical Effects on Lean Blowout in a Swirl-Stabilized Single-Cup Combustor. *Proceedings of the Combustion Institute* 38 (4): 6309-6316. doi:10.1016/j.proci.2020.06.119

Colket, M., and Heyne, J. (2021). Fuel Effects on Operability of Aircraft Gas Turbine Combustors. *AIAA, Prog. Astronautics Aeronautics* 262, 2021 submitted in proofing. doi:10.2514/4.106040

Colket, M., Heyne, J., Rumizen, M., Gupta, M., Edwards, T., Roquemore, W. M., et al. (2017). Overview of the National Jet Fuels Combustion Program. *AIAA J.* 55 (4), 1087–1104. doi:10.2514/1.J055361

Coppola, E. N. (2018). *CHJ Pathway ReadiJet Renewable Jet Fuel Produced by Catalytic Hydrothermolysis (CH). ASTM Committee D02 on Petroleum Products and Lubricants, Subcommittee D02.J0.06 on Emerging Turbine Fuels.*

Culbertson, B., and Williams, R. (2017), *Alternative Aviation Fuels for Use in Military APUs and Engines, Versitile Affordable Advanced Turbine Engine (VAATE), Phase II and III, Delivery Order 0007 : AFRL-RQ-WP-TR-2017-0047.*

Dhanuka, S. K., Temme, J. E., and Driscoll, J. F. (2011). Unsteady Aspects of Lean Premixed Prevaporized Gas Turbine Combustors: Flame-Flame Interactions. *J. Propulsion Power* 27 (3), 631–641. doi:10.2514/1.B34001

Edwards, J. T. (2017). Reference Jet Fuels for Combustion Testing. In:*55th AIAA Aerospace Sciences Meeting*. Grapevine, TX, Reston, VA: AIAA. doi:10.2514/6.2017-0146

Flora, G., Kosir, S. T., Behnke, L., Stachler, R. D., Heyne, J. S., Zabarnick, S., et al. (2019). Properties Calculator and Optimization for Drop-In Alternative Jet Fuel Blends, *AIAA Scitech 2019 Forum*. doi:10.2514/6.2019-2368

Grohmann, J., Rauch, B., Kathrotia, T., Meier, W., and Aigner, M. (2018). Influence of Single-Component Fuels on Gas-Turbine Model Combustor Lean Blowout. *J. Propulsion Power* 34 (1), 97–107. doi:10.2514/1.B36456

Guildenbecher, D. R., López-Rivera, C., and Sojka, P. E. (2009). Secondary Atomization. *Exp. Fluids* 46, 371–402. doi:10.1007/s00348-008-0593-2

Hastie, T., Tibshirani, R., and Friedman, J. (2008). *The Elements of Statistical Learning, Data Mining, Inference, and Prediction*. 2nd Editio. Stanford, California: Springer.

Hendershott, T. H., Stouffer, S., Monfort, J. R., Diemer, J., Busby, K., Corporan, E., et al. (2018). Ignition of Conventional and Alternative Fuel at Low Temperatures in a Single-Cup Swirl-Stabilized Combustor. In: *AIAA Aerospace Sciences Meeting*. Kissimmee, Florida: American Institute of Aeronautics and Astronautics, Inc. doi:10.2514/6.2018-1422

Home | AJF:TD | U of I n.D. (2021) Available at: https://altjetfuels.illinois.edu/. (Accessed Jul 5, 2021).

Kim, H. H., Won, S. H., Santner, J., Chen, Z., and Ju, Y. (2013). Measurements of the Critical Initiation Radius and Unsteady Propagation of N-Decane/air Premixed Flames. *Proc. Combustion Inst.* 34 (1), 929–936. doi:10.1016/j.proci.2012.07.035

Kroenlein, K., Muzny, C., Kazakov, A., Diky, V., Chirico, R., and Magee, J. (2012). *NIST Standard Reference 203: TRC Web Thermo Tables (WTT) [Internet]*. Gaithersburg. MD: National Institutes of Standards and Technology n. d., 1.

Lefebvre, A. H., and McDonell, V. G. (2017). *Atomization and Sprays*. 2nd ed. Boca Raton, Florida: CRC Press Taylor & Francis Group.

Mayhew, E. K. (2018). Impact of Alternative Jet Fuels on Gas Turbine Combustion Systems. *Dissertation for the Doctoral Degree*. Urbana-Champaign: University of Illinois at.

Mellor, A. M. (1980). Semi-empirical Correlations for Gas Turbine Emissions, Ignition, and Flame Stabilization. *Prog. Energ. Combustion Sci.* 6 (4), 347–358. doi:10.1016/0360-1285(80)90010-6

Muthuselvan, G., Suryanarayana Rao, M., Iyengar, V. S., Pulumathi, M., Thirumalachari, S., and K, S. (2020). Effect of Atomization Quality on Lean Blow-Out Limits and Acoustic Oscillations in a Swirl Stabilized Burner. *Combustion Sci. Techn.* 192 (6), 1028–1052. doi:10.1080/00102202.2019.1607846

Oldani, A. (2020). FAA ASCENT & Clearinghouse Programs. In: *PNNL HTL Workshop* Richland, WA: PNNL.

Opacich, K. C., Heyne, J. S., Peiffer, E., and Stouffer, S. D. (2019). Analyzing the Relative Impact of Spray and Volatile Fuel Properties on Gas Turbine Combustor Ignition in Multiple Rig Geometries. In: *AIAA Scitech 2019 Forum*. San Diego: California. doi:10.2514/6.2019-1434

Peiffer, E. E., Heyne, J. S., and Colket, M. (2019). Sustainable Aviation Fuels Approval Streamlining: Auxiliary Power Unit Lean Blowout Testing. *AIAA J.* 57 (11), 4854–4862. doi:10.2514/1.j058348

Plee, S., and Mellor, A. (1979). Characteristic Time Correlation for Lean Blowoff of bluff-body-stabilized Flames☆. *Combustion and Flame* 35, 61–80. doi:10.1016/0010-2180(79)90007-5

Rock, N., Chterev, I., Emerson, B., Won, S. H., Seitzman, J., and Lieuwen, T. (2019). Liquid Fuel Property Effects on Lean Blowout in an Aircraft Relevant Combustor. *J. Eng. Gas Turbines Power* 141 (7), 071005–071017. doi:10.1115/1.4042010

Stouffer, S. D., Hendershott, T. H., Colborn, J., Monfort, J. R., Corporan, E., Wrzesinski, P., et al. (2020). Fuel Effects on Altitude Relight Performance of a Swirl Cup Combustor. In: *AIAA Scitech 2020 Forum*. Reston, VA: AIAA. doi:10.2514/6.2020-1882

Won, S. H., Rock, N., Lim, S. J., Nates, S., Carpenter, D., Emerson, B., et al. (2019). Preferential Vaporization Impacts on Lean Blow-Out of Liquid Fueled Combustors. *Combustion and Flame* 205, 295–304. doi:10.1016/j.combustflame.2019.04.008

Conflict of Interest: The authors declare that the research was conducted in the absence of any commercial or financial relationships that could be construed as a potential conflict of interest.

Publisher's Note: All claims expressed in this article are solely those of the authors and do not necessarily represent those of their affiliated organizations, or those of the publisher, the editors and the reviewers. Any product that may be evaluated in this article, or claim that may be made by its manufacturer, is not guaranteed or endorsed by the publisher.

NOMENCLATURE

C_p = **specific heat**

$\boldsymbol{D}$ = characteristic diameter

$\boldsymbol{Oh}$ = Ohnesorge number

P_{cmb} = **combustor pressure**

P_{vap} = **vapor pressure**

T_{cmb} = **combustor temperature**

$\boldsymbol{T_{20}}$ = 20% recovered temperature

$\boldsymbol{T_{fuel}}$ = fuel temperature

V_{cmb} = **combustor volume**

$\boldsymbol{W}$ = mass flow rate

ΔP = **pressure drop across combustor dome**

ϕ = **equivalence ratio**

Φ = **relative equivalence ratio**

μ = **dynamic viscosity**

ν = **kinematic viscosity**

ρ = **density**

σ = **surface tension or standard deviation**

$\boldsymbol{\tau_{cmb}}$ = combustor residence time

APU = auxiliary power unit

APU-CR = honeywell 131-9 APU combustor rig

ASTM = ASTM international

A2 = reference fuel, single source

C1 = jet fuel blend component, ASTM D7755, annex A5

DCN = derived cetane number

FAA = federal aviation administration

GE9X-FAR = GE9X full annular combustor rig

LBO = lean blowout

NJFCP = national jet fuel combustion program

RI = radical index

RR = referee rig

SAF = sustainable aviation fuel

frontiers in Energy Research

ORIGINAL RESEARCH
published: 12 October 2021
doi: 10.3389/fenrg.2021.728682

Recycled Paper as a Source of Renewable Jet Fuel in the United States

William L. Kubic Jr.[1]*, *Cameron M. Moore*[2], *Troy A. Semelsberger*[3] and *Andrew D. Sutton*[4]

[1]Process Modeling and Analysis Group, Los Alamos National Laboratory, Los Alamos, NM, United States, [2]Inorganic, Isotope, and Actinide Chemistry Group, Los Alamos National Laboratory, Los Alamos, NM, United States, [3]Material Synthesis and Integrated Devices Group, Los Alamos National Laboratory, Los Alamos, NM, United States, [4]Chemical Process Scale-Up Group, Oak Ridge National Laboratory, Oak Ridge, TN, United States

Converting biomass into jet fuel involves more than the core chemical process. The overall process includes the logistics of harvesting and transporting the biomass, handling and preparing the material for processing, and processing and disposal of waste. All of these activities contribute to cost. Controlling cost involves more than developing efficient process chemistry. Choice of feedstock also has a significant impact on process economics. We consider chemical conversion of paper from municipal solid waste as a feedstock for the production of jet fuel and diesel. Paper has a significantly higher cellulose content than raw lignocellulosic biomass such as corn stover, so it requires less pretreatment to convert it into hydrocarbons than lignocellulosic biomass. Our techno-economic analysis showed that the cost of converting paper waste into jet fuel is about $1.00/gal less than jet fuel produced from corn stover. Although the cost of recycling paper into jet fuel is less than producing it from corn stover, the process is not competitive with petroleum. We estimated a minimum selling price of $3.97/gal for paper-derived jet fuel. Our sensitivity studies indicated that the biggest economic obstacle is the cost of cellulose hydrolysis. Direct hydrogenation of paper to sugar alcohols combined with increased economy of scale could make recycling paper jet fuel competitive.

Keywords: recycled paper, municipal solid waste, cellulosic biomass, renewable jet fuel, renewable hydrocarbons, techno-economic analysis

OPEN ACCESS

Edited by:
Jalel Labidi,
University of the Basque Country, Spain

Reviewed by:
Jianguo Zhang,
University of Shanghai for Science and Technology, China
David B. Hodge,
Montana State University, United States

***Correspondence:**
William L. Kubic Jr.
wkubic@lanl.gov

Specialty section:
This article was submitted to Bioenergy and Biofuels, a section of the journal Frontiers in Energy Research

Received: *21 June 2021*
Accepted: *23 September 2021*
Published: *12 October 2021*

Citation:
Kubic Jr WL, Moore CM, Semelsberger TA and Sutton AD (2021) Recycled Paper as a Source of Renewable Jet Fuel in the United States. Front. Energy Res. 9:728682. doi: 10.3389/fenrg.2021.728682

INTRODUCTION

In 2019, the US aviation industry consumed 636 million barrels or 3.8 EJ of fuel (US Energy Information Agency, 2021a). Air travel accounts for about 12% of the fuel consumed by the US transportation sector and about 13% of the carbon dioxide emissions (US Energy Information Agency, 2021a). The International Air Transport Association is committed to carbon-neutral growth of their industry (Stalnaker et al., 2016). This goal will limit carbon dioxide emissions from air transportation to 2020 levels (International Air Transport Association, 2015). Strategies for meeting this goal include efficiency improvements, but efficiency improvements alone are not sufficient. A bio-based hydrocarbon fuel with low life-cycle carbon dioxide emissions is also needed.

Sustainability encompasses economic and social impacts as well as environmental impact. Use of lignocellulosic biomass addresses, in part, economic and social impacts by avoiding competition with food crops and the social impact of higher food prices. However, a sustainable fuel also must be cost competitive. The average US jet fuel price in 2019 was $1.97/gal (US Energy Information Agency, 2021a).

TABLE 1 | Typical compositions of raw corn stover and recycle paper.

Component	Composition (wt%)		
	Corn stover	Recyclable paper	Unrecyclable paper
Water	20.0	5.6	4.6
Cellulose	28.0	63.2	52.5
Hemicellulose	15.6	13.0	10.8
Starches	3.5	—	—
Lignin	12.6	6.5	5.4
Lipids	—	1.0	15.7
Protein	2.5	—	—
Other Organic Material	13.9	—	—
Ink	—	5.2	3.3
Inorganic Material	3.9	3.0	3.9
Metal	—	2.6	3.7

The US Energy Information Agency projects only a moderate increase in price to $2.04/gal by 2030 (US Energy Information Agency, 2021b). The National Renewable Energy Laboratory (NREL) estimated the cost of producing hydrocarbon fuels from lignocellulosic biomass to be $4.05/gal in 2011 US dollars (USD) (Davis et al., 2015). Wang et al. (2016) report the cost of converting lignocellulosic biomass into jet fuel to be $4.00–$23.30/gal. Currently, producing jet fuel from lignocellulosic biomass is not sustainable because it is not economically competitive.

Producing jet fuel from biomass involves more than the chemistry. It includes the logistics of obtaining the biomass, preparation and pretreatment of the biomass, and processing and disposal of waste. All of these associated processing steps contribute to the overall capital investment and operating costs of the plant. Controlling cost requires more than efficient process chemistry. Choice of feedstock with its associated costs, availability, and logistics has a significant impact on process economics.

FIGURE 1 | A simple diagram of the carbon cycle for the production of jet fuel from recycle paper.

We investigated other sources of sustainable jet fuel and concluded that recycle paper is a promising alternative to raw lignocellulosic biomass. Paper is a refined product with significantly higher cellulose content than raw biomass (see **Table 1**); so it requires less handling and pretreatment. It also contains less waste materials than raw biomass. Therefore, producing hydrocarbon fuels from recycle paper instead of raw biomass reduces the capital investment and the operating costs. Cultivated forest biomass, such as the loblolly pine in the Southeastern US, is an important source of wood pulp (Gonzalez et al., 2011) and a possible source of lignocellulosic biomass for fuel production (US Department of Energy, 2016). **Figure 1** shows that producing jet fuel from recycled paper is part of a closed carbon cycle similar to other biofuels. The biomass to paper to jet fuel cycle differs from other biofuel cycles in that it involves reuse of a commercially valuable intermediate product.

We considered whether using recycle paper to produce fuels has any economic advantages over processes based on raw lignocellulosic biomass. Therefore, we performed a techno-economic analysis of a process for converting recycle paper into jet fuel. Our conceptual design is based on a process that

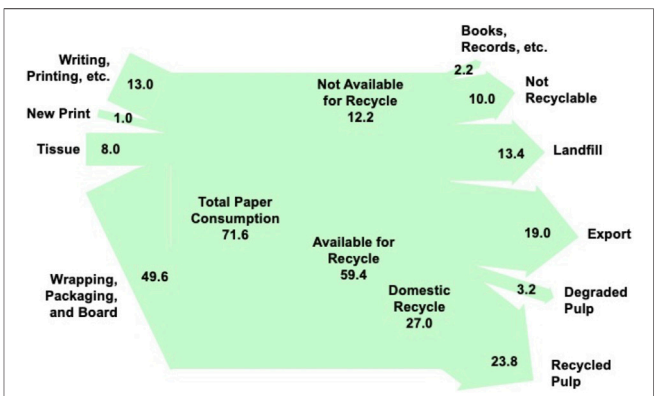

FIGURE 2 | 2017 US paper consumption and ultimate disposition in million annual tonnes. The diagram is based on information from (European Integrated Pollution Prevention and Control Bureau, 2001), (Food and Agriculture Organization of the United Nations, 2015), and (US Environmental Protection Agency, 2020).

Blommel and Price (2017) patented for converting sugars into hydrocarbon fuels. The evaluation included the availability of paper for recycling, costs, and lifecycle carbon dioxide emissions and solid waste generation. The time needed to commercialize a new process for a commodity chemical is on the order of 10 years (Vogel 2005), so we have set our target production cost to the projected 2030 jet fuel price of $2.04/gal.

The goal is not to argue that recycling paper to jet fuel is the solution to sustainable air transportation. Instead, we want to show that using recycled paper as a feedstock could be a first step in commercializing technology for producing fuels from cellulosic materials.

VIABILITY OF RECYCLED PAPER AS A SOURCE OF JET FUEL

Figure 2 shows US paper consumption for 2017 and its ultimate disposition. Overall paper usage in the US is decreasing; but wrapping, packaging, and board, which is the major use of paper products, is increasing as a result of increased e-commerce (Food and Agricultural Organization of the UN, 2015). About 83% of the paper consumed is suitable or available for recycling into paper products. The remaining 17% is used for books and other permanent records or it is contaminated with food and materials that make it unsuitable as a source of paper products. Currently, about 64% of the paper used in the US is collected for recycling (US Environmental Protection Agency, 2020). Of the paper collected, domestic recyclers use 59% and the remainder is exported. When paper is recycled, an average of 12% of the cellulose fibers are rejected because of degradation (European Integrated Pollution Prevention and Control Bureau, 2001).

Scrap paper currently being exported, paper currently discarded to landfills, and degraded pulp from recycling plants could be used for jet fuel production without any impact on current domestic recyclers. Thus, the minimum amount of scrap paper available for fuel product would be 36 million tonnes/yr. We estimated that 1 tonne of mixed paper waste could produce about 2.4 bbl of jet fuel. (We will discuss the basis of this estimate in subsequent sections.) The minimum amount scrap paper available for fuel production could yield about 76–83 million bbl of jet fuel per year, which is 13–14% of the annual US demand. The maximum amount of paper that could be converted to jet fuel is the total amount of paper available for recycling plus part of the paper that is currently not recyclable, or 59 million tonne/yr. The maximum jet fuel production would be about 124–136 million bbl/yr or 21–22% of the US demand. We estimated that up to 3 million tonnes/yr of food contaminated waste that is currently considered not recyclable may be suitable for producing an additional 7 million bbl/yr of jet fuel. Although recycle paper cannot be used to replace all US jet fuel needs, the amount of fuel that could be produced from this raw material is not trivial.

Recyclable paper has some logistical advantages over lignocellulosic biomass. First, paper is not a seasonal crop. It is available continually throughout the year, which reduces storage requirements and costs. Second, the largest sources of recyclable paper are large metropolitan areas where the amount of paper available per hectare is much greater than lignocellulosic biomass derived from agricultural waste. If 75% of the rural land in a Midwestern state is available for corn production, and corn stover are harvested from 50% of the available land, the concentration of biomass would be 1.9 tonne/ha which yields 1.0 tonne/ha of sugar (Aden et al., 2002). Based on average US paper consumption per capita, average recycling rates, and population density, we estimated the concentration of recyclable paper in New York City to be 19 tonne/ha, which yields 16 tonne/ha of sugar. New York City is the most concentrated source of recyclable paper, but the concentration of recyclable paper in less densely populated cities is still greater than the concentration of corn stover in a Midwestern farming area (European Integrated Pollution Prevention and Control Bureau 2001). The amount of recyclable paper available in the 10 largest US metropolitan areas is sufficient to produce about 10% of the fuel consumed by the domestic air transport industry. Because of the high concentration of recyclable paper in cities, collection cost per tonne for recycle paper are less than harvesting agricultural waste. Also, plants for converting recycled paper into jet fuels would be best located near large cities serviced by one or more large airports. Thus, jet fuel production would be located near the largest consumers, which would reduce distribution costs.

PROCESS DESCRIPTIONS

Blommel and Price (2017) patented a process for converting corn syrup into a hydrocarbon mixture encompassing the boiling range of jet fuel and diesel. The National Renewable Energy Laboratory (NREL) developed conceptual design of a process for converting lignocellulosic biomass into naphtha and diesel fuel based on Blommel and Price's patent and enzymatic hydrolysis of cellulose. We developed two concepts based on Blommel and Price's patent for converting recycle paper into jet fuel. The first concept is an adaptation of NREL's process with enzymatic hydrolysis of cellulose. The second concept uses acid hydrolysis to produce the sugar syrup. Both processes require hydrogen, which is assumed to be supplied by an on-site steam reforming planted located on site.

Summary of Process With Enzymatic Hydrolysis

Figure 3 is a simplified block diagram showing the major steps of the paper to jet fuel process with enzymatic hydrolysis. This process is a version of the process developed by Davis et al. (2015) that has been modified to accept paper as the feedstock rather than corn stover. The process consists of eight major steps plus storage and utilities.

- *Mechanical Repulping* uses technology from the paper recycling industry to convert the recycled paper into a cellulose fiber slurry. The step includes creation of the fiber slurry, removal of filler materials, and deinking.

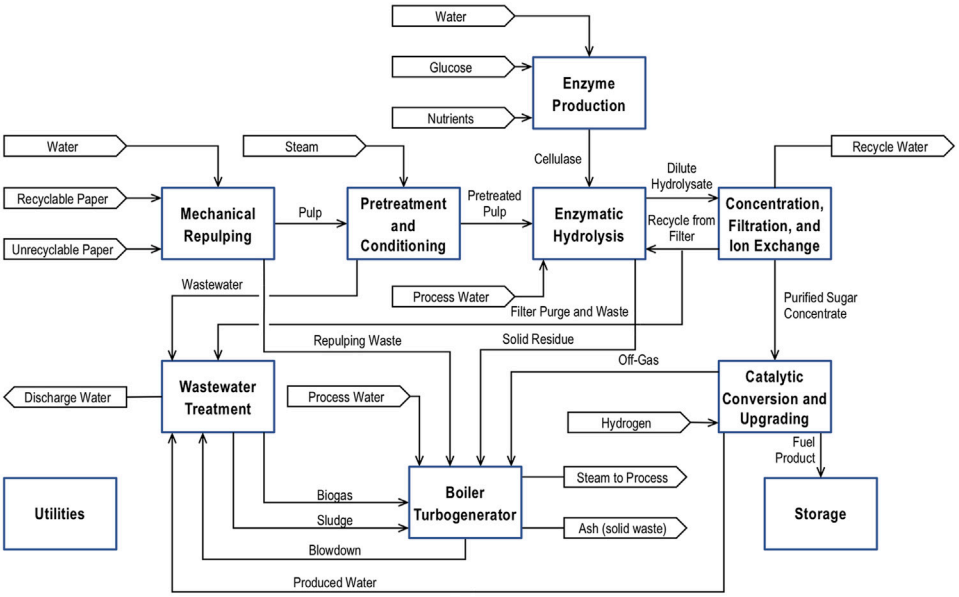

FIGURE 3 | A block diagram of a process for converting recycle paper into jet fuel with enzymatic hydrolysis.

Calcium carbonate is the major component of the filler, and it must be removed to reduce sulfuric acid consumption. The process differs from paper recycling because it does not include fractionation of the fibers or extensive dewatering steps. Because fiber quality is irrelevant, the process can accept paper contaiminate with food and other materials that make it unsuitable for paper products. The process is purely mechanical and uses no heat or chemicals.

- *Pretreatment and Conditioning* uses a dilute sulfuric acid to hydrolyze hemicellulose into its component sugars and organic acids. The sulfuric acid is neutralized with sodium hydroxide prior to Enzymatic Hydrolysis.
- *Enzyme Production* is a fermentation for production of the cellulase used for enzymatic hydrolysis of the cellulose fibers.
- *Enzymatic Hydrolysis* first converts the cellulose to dissolved glucose via an enzymatic hydrolysis. The hydrolysate is filtered to separate lignin and other solids from the aqueous solution.
- *Concentration, Filtration, Ion Exchange* evaporates excess water from the hydrolysate, it filters out any remaining solids, and it removes dissolved ionic species in a series of ion exchange columns. The product of this step is an aqueous solution that is nearly 50 wt% soluble sugars.
- *Catalytic Conversion and Upgrading* is based on (Blommel and Price, 2017) process chemistry. The sugars are first hydrogenated to produce sugar alcohols. A sequence of dehydration, hydrogenation, and condensation reactions to covert sugar alcohols into C_1–C_{24+} hydrocarbons. This process step includes distillation to separate a light of hydrocarbons from the heavier distillate product.
- *Wastewater Treatment* is a combination of anaerobic and aerobic digestion to remove organic materials from the water. Anaerobic digestion produces a CH_4/CO_2 biogas that can be used as fuel in the boiler. Sludge for aerobic digestion is dewatered and used as fuel. The wastewater treatment process also removes dissolved solids making the treated water suitable for reuse in the process.
- *Boiler/Turbogenerator* burns biogas, off gas from Catalytic Conversion and Upgrading, solid waste and organic materials from Mechanical Repulping, dewatered sludge for Wastewater Treatment, lignin, and other combustible solids to produce steam. Steam is used for process heat and generating electricity.

Our Catalytic Conversion and Upgrading process is nearly identical to NREL's (Davis et al., 2015) realization of (Blommel and Price, 2017) process. This process consists of four reaction steps and a distillation. We used the same catalysts and operating conditions for the reactor in our design, but we modified the distillation to produce an off gas (C_1–C_7) and a fraction with the boiling range of jet fuel (C_{8+}). Davis et al. (2015) give the details of the catalysts and operating conditions used for Catalytic Conversion and Upgrading process.

The first step is catalytic hydrogenation to reduce the sugars to sugar alcohols (e.g., sorbitol) or other polyols. The sugar alcohols then undergo catalytic aqueous-phase reforming (APR), which is a complex set of reactions that produce hydrogen, carbon dioxide, light alkanes, oxygenated compounds (Cortright et al., 2002). APRs tend to cleave C-C bonds and C-O bonds. Oxygenated products include alcohols, ketones, aldehydes, furans, diols, triols, and organic acids. Cleavage of aldehyde groups form hydrogen, carbon monoxide, and smaller polyols. In the water rich environment, carbon monoxide undergoes the water-gas shift reaction to form hydrogen and carbon dioxide.

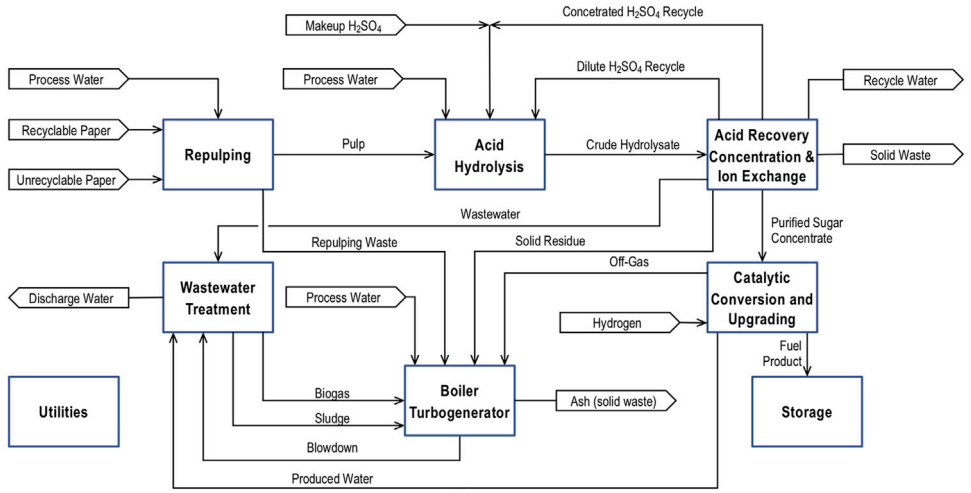

FIGURE 4 | A block diagram of a process for converting recycle paper into jet fuel with acid hydrolysis.

Carbon monoxide can also participate in the methanation and Fischer-Tropsch reactions to for light hydrocarbons.

The organic compounds in the APR product stream have an average carbon number less than six. In the condensation reactor, chain length increase to C_8–C_{24}. Multiple reactions occur in this step including dehydration, oligomerization, cyclization, aromatization, and hydrogenation producing normal and iso-paraffins, olefins, ketones, aromatics, and cycloparaffins (Blommel and Price, 2017; Cortright and Blommel, 2013) The organic products, which are insoluble in water, are separated from the aqueous phase and fed to hydrotreating reactor where hydrodeoxygenation reactions remove oxygen from condensation products while leaving the carbon chains intact.

Summary of Process With Acid Hydrolysis

Figure 4 is a block diagram of the process with acid hydrolysis. The process is similar in structure to the process with enzymatic hydrolysis. Acid hydrolysis performs the same function as the combined function Pretreatment and Conditioning, Enzyme Production, and Enzymatic Hydrolysis. The processing step takes the repulped fibers and hydrolyzes the cellulose and hemicellulose into simple sugars. Acid Recovery, Concentration, and Ion Exchange removes the sulfuric acid for the hydrolysate and concentrates it for recycling. This step also includes filtering out residual solids, concentrating the hydrolysate, and removing dissolved ionic species from the hydrolysate. The product of these two steps is a syrup containing about 50 wt% dissolve sugars. The sugar solution is converted into jet fuel using the same method as the process with enzymatic hydrolysis.

Acid hydrolysis is based on what the technical literature refers to as the two-step process. It is called the two-step process because it consists of two hydrolysis steps–a dilute acid hydrolysis of hemicellulose followed by a concentrated acid hydrolysis of cellulose (Kosaric et al., 2011). The complete process includes the hydrolysis steps plus separation processes. The process begins with the dilute acid hydrolysis. Sulfuric acid is added to the pulp slurry creating a mixture containing 4.4 wt% sulfuric acid. Dilute acid hydrolysis occurs at 100°C. This step results in complete hydrolysis of the hemicellulose in the paper. The mild operating conditions minimize the conversion of pentoses into furfural and the production furfural oligomers and polymers. After dilute hydrolysis, the remaining solids are filtered out of the slurry, dried, and combined with 85 wt% sulfuric acid. After the solids are mixed with the acid, water is added to reduce the sulfuric acid concentration to 8 wt%. Concentrated acid hydrolysis occurs at 110°C and results in a 90% cellulose conversion. Residual solids are removed from the hydrolysate, and the hydrolysate is combined with the dilute acid hydrolysate.

The first step in purifying and concentrating the hydrolysate is removing the sulfuric acid using resin wafer electrodeionization (RW-EDI) (Datta et al., 2013). RW-EDI is a modified version of electrodialysis that incorporates ion exchange resin beads within the electrodialysis stack. RW-EDI removes 99% of the sulfuric acid from the hydrolysate and concentrates it to 25 wt%. The hydrolysate passes through an ultrafilter prior to RW-EDI to ensure that it contains no fine particles that could foul the membrane. Part of the sulfuric acid is distilled to produce 85 wt% sulfuric acid for concentrated acid hydrolysis. The remainder is recycled to dilute acid hydrolysis. After the sulfuric acid has been removed, the hydrolysate is concentrated using the same process as in the process with enzymatic hydrolysis, and dissolved anionic species are removed in an ion exchange column. The hydrolysate contains no cationic species other than hydrogen ions.

MATERIAL AND ENERGY BALANCES

We determined the material balances for a 3,900 bbl/day jet fuel plant. We included a corn stover to jet fuel process based on the biomass to hydrocarbon process of Davis et al. (2015). The

TABLE 2 | Overall material and energy balances for corn stover to jet fuel, recycle paper to jet fuel with enzymatic hydrolysis, and recycle paper to jet fuel with acid hydrolysis.

Quantity	Corn stover to jet	Paper to jet with enzymatic hydrolysis	Paper to jet with acid hydrolysis
Feedstock			
Corn Stover (kg/h)	104,200	—	—
Recyclable Paper (kg/h)	—	54,211	54,980
Unrecyclable Paper (kg/h)	—	13,826	14,021
Process Chemicals			
sulfuric acid (kg/h)	2,240	2,038	1,420
ammonia (kg/h)	368	495	—
Hydrochloric Acid (kg/h)	1,120	1,790	—
Caustic (kg/h)	950	690	—
Glucose (kg/h)	1,210	1,690	—
Corn Steep Liquor (kg/h)	83	116	—
Corn Oil (kg/h)	7	10	—
Host Nutrients (kg/h)	34	47	—
Sulfur Dioxide (kg/h)	8	11	—
Hydrogen (kg/h)	3,890	3,870	3,890
Wastewater Treatment			
ammonia (kg/h)	109	15.3	16.4
Polymer (kg/h)	2	0.30	0.30
Boiler/Turbogenetator			
Electricity Generated (MW)	46	31.8	11.3
Boiler Chemicals (kg/h)	0.2	0.13	0.13
FGD Lime (kg/h)	180	—	—
Cooling Towers			
Cooling Water (m^3/h)	520	248	355
Cooling Water Chemicals (kg/h)	3	1.4	2
Makeup Water (m^3/h)	157	75	107
Utilities			
Process Water (m^3/h)	377	91	127
Steam (MW)	46	45	81
Electricity Consumed (MW)	35	34	69
Plant Air (Nm^3/h)	181,000	181,000	181,000
Products			
Jet Fuel Yield (bbl/tonne feed)	1.56	2.40	2.36
Jet Fuel (bbl/hr)	163	163	163
Electricity Exported (MW)	11	—	—
Waste			
Water Discharge (m^3/h)	182	122	128
Ash (kg/hr)	9,940	3,320	3,610

process was modified to produce a distillate consisting of hydrocarbons with chain-lengths in the jet fuel range. The corn stover composition for this process is given in **Table 1**. Material and energy balances for this process were obtained directly from Davis et al. (2015) with slight modifications. **Table 2** contains a summary of the material and energy balances for the corn stover to jet fuel process.

The feedstock for the recycle paper to jet fuel process consists of 80% recyclable paper and 20% unrecyclable paper, which approximates typical municipal solid waste. **Table 1** gives the composition of recyclable and unrecyclable paper. Food contamination of unrecyclable paper is represented by a high lipids content. The inorganic content of paper consists of whitening agents and filler. Calcium carbonate and talc constitute the vast majority of these inorganic materials. The metal content consists of staples, fastener, foil, and other metals that were not removed when the paper was discarded or segregated for recycling.

To calculated the material and energy balances for the paper to jet fuel process with enzymatic hydrolysis, we used the same assumptions and models used by Davis et al. (2015) for their biomass to hydrocarbon process. Most of the ink, inorganic filler materials, and metal are removed from the paper during the repulping process using a series of settling and flotation operations. Repulping consumed electricity to drive the mechanical repulping and physical separation processes. We obtained an estimate of the power consumption from an International Energy Agency publication (Börjessen and

Ahlgren, 2015). **Table 2** contains a summary of the material and energy for the paper to jet fuel process with enzymatic hydrolysis.

For the paper to jet fuel process with acid hydrolysis, we used a ChemCAD model to determine the material and energy balances for acid hydrolysis, acid recovery, hydrolysate concentration, and ion exchange. Power needed for the RW-EDI process was estimated from the current cell, voltage, and cell efficiency (Patel et al., 2020). The paper to jet fuel process with acid hydrolysis produces a concentrated hydrolysate containing about 50 wt% sugars, which is fed to Catalytic Conversion and Upgrading. Assumptions and models used for Chemical Conversion and Upgrading are the same as those used for the process with enzymatic hydrolysis. The assumptions and models for wastewater treatment and the boiler/turbogenerator are the same as used in the process based on corn stover (Davis et al., 2015). **Table 2** contains a summary of the material and energy for the paper to jet fuel process with acid hydrolysis.

A key difference among the three processes is yield per tonne of feedstock. The yields of all three processes are about 80% of the theoretical maximum based on carbohydrate content (i.e. cellulose, hemicellulose, and starches), but the carbon hydrate content of corn stover is significantly less than paper. Corn stover contains about 47 wt% carbohydrates while paper contains 63–76 wt% carbohydrates. The lower carbohydrate content means that 1.4–1.5 tonnes of corns stover is required to produce the same volume of jet fuel as 1.0 tonne of recycle paper.

Another key difference is the fuel produced per tonne of feedstock. Corn stover contains more lignin and other organic matter that can be used as fuel than paper. The additional fuel means that the corn stover process is net producer of electricity while recycle paper processes are net electric consumers. Because of the greater volume processed and the chemical form of the inorganic material, burning the corn stover residue produces approximately 3 times the solid waste than burning the residue of a paper to jet fuel process.

A third key difference is the ratio of cellulose to hemicellulose. Paper is a refined bioproduct that contains nearly 5 times more cellulose than hemicellulose. The cellulose to hemicellulose ratio in corn stover is about 1.8. Because the glucose from cellulose constitutes a greater fraction of the total sugars produced, a jet fuel process with enzymatic hydrolysis of paper requires more cellulase than a process based on corn stover as well as the more if the chemical feedstocks needed to produce cellulase.

The hydrolysis process has a significant impact on material and energy balances for the paper to jet fuel processes. The overall yields of both processes are about the same. However, recovery and recycling of sulfuric acid is also energy intensive. A process with acid hydrolysis consumes about twice as much steam as a process with enzymatic hydrolysis. Increased process steam consumption in the process using acid hydrolysis result in approximately 64% less electrical power generation than a process with enzymatic hydrolysis. Use of RW-EDI in for sulfuric acid production results in a process that consumes about twice as much electricity as the process with enzymatic hydrolysis. As a consequence of lower power generation and higher power demand, the net electrical power consumption is about 12 times greater for the process with acid hydrolysis than the process with enzymatic hydrolysis.

TECHNO-ECONOMIC ANALYSIS

Techno-economic analysis consists of three major parts–capital cost estimation to determine the investment required to build the process; operating costs estimate to determine the annual expenses of operating the plant; and a cash flow analysis, which combines capital and operating costs to determine the overall production costs. We use a methodology and assumptions that have been benchmarked against cellulosic ethanol production for the analysis (Kubic, 2019). Cost estimates are based on a US Midwest location. Estimates are in 2020 USD.

Capital Cost Estimates

Capital cost estimates for the recycle paper to jet fuel were based on conceptual designs with a low level of maturity. Given the low level of process definition, the appropriate estimation method should be consistent with an Association for the Advancement of Cost Engineering International Class 5 (AACE International, 2011) estimate with an accuracy range of -20/+30% to 50/+100% or an American National Standards Institute order-of-magnitude estimate (Institute of Industrial Engineers, 2000) with an accuracy of −30/+50%. We used a factor method (Woods, 2007) to determine fixed capital investment (FCI) and total capital investment (TCI) from purchased equipment cost (FOB cost).

We determined FOB costs and installation factors from correlations in Woods (2007) and data in Davis et al. (2015). FOB costs were converted to 2020 USD using Chemical Engineering Plant Cost Index. Assumptions for estimating additional direct costs, indirect costs, and additional capital costs were based on the recommendations of (Kubic et al., 2019). Contingencies are added to the cost estimate to account for judgment errors in accumulation of the project scope (Page 1996). Contingencies can range from 10 to 80% of direct costs depending on the degree of project definition (Garrett, 1989; Woods, 2007). Cost estimates in this study are based on a conceptual design, so large contingencies are appropriate. We assumed a contingency of 30% of direct costs based on (US Department of Energy, 1997) guidance.

Table 3 is a summary of the capital cost estimates. The FCI for the corn stover to jet fuel is 5% greater than the paper to jet fuel with enzymatic hydrolysis. This difference is well withing the estimation errors for a Class 5 estimate. The FCI for the paper to jet fuel process with enzymatic hydrolysis is 10% greater than the process with acid hydrolysis. About 80% of this difference can be attributed to differences in the cost of the hydrolysis process. The installed equipment cost for enzymatic hydrolysis is more than 40% greater than the installed equipment cost for acid hydrolysis. Although the differences in FCI and installed equipment costs of hydrolysis equipment are within the uncertainty of Class 5 estimate, the count of major operations suggest that the difference may be real. Correlations for order-of-magnitude cost estimates have been developed that give FCI as a function

TABLE 3 | Capital cost estimates for corn stover to jet fuel, recycle paper to jet fuel with enzymatic hydrolysis, and recycle paper to jet fuel with acid hydrolysis in million USD (2020).

Capital expense (basis)	Corn stover to jet		Paper to jet with enzymatic hydrolysis		Paper to jet With acid Hydrolysis	
	FOB	Installed	FOB	Installed	FOB	Installed
ISBL equipment costs						
Feedstock Handling	$13.2	$28.7	—	—	—	—
Repulping	—	—	$19.3	$49.0	$16.2	$40.5
Pretreatment	$29.7	$55.9	$27.3	$53.3	—	—
Enzymatic Hydrolysis[a]	$44.7	$71.3	$30.1	$67.7	—	—
Enzyme Production	$6.2	$13.9	$8.5	$18.6	—	—
Acid Hydrolysis[b]	—	—	—	—	$40.3	$95.8
Catalytic Conversion	$33.6	$85.7	$33.6	$88.6	$33.6	$87.1
Total ISBL Equipment Cost	$127.4	$255.5	$118.7	$277.1	$90.1	$223.4
OSBL Equipment Costs						
Wastewater Treatment	$29.2	$49.8	$18.8	$35.2	$21.5	$40.1
Boiler/Turbogenerator	$35.8	$79.0	$1.7	$3.7	$24.4	$55.5
Storage	$2.4	$6.2	$28.1	$63.8	$4.2	$8.3
Utilities	$3.4	$8.4	$2.7	$5.8	$1.8	$4.0
Total OSBL Equipment Cost	$70.7	$143.5	$51.3	$108.5	$51.9	$107.9
Additional Direct Costs						
Fire Protection (0.7% of ISBL)	$1.8		$1.9		$1.6	
Auxiliary Buildings (5% of ISBL)	$12.8		$13.9		$11.2	
Additional Piping (4.5% of FOB)	$8.9		$7.6		$6.4	
Site Development (9% of FOB)	$17.8		$15.3		$12.8	
Engineering Services (10% of ISBL)	$15.8		$12.4		$12.1	
Construction Services (5% of ISBL)	$7.9		$6.2		$6.0	
Project Management (5% of ISBL)	$7.9		$6.2		$6.0	
Total Direct Costs	$471.8		$449.1		$387.3	
Indirect Costs						
Contractor Fee (5% of direct costs)	$23.6		$22.5		$19.4	
Continencies (30% of direct costs)	$141.5		$134.7		$116.2	
Total Indirect Costs	$165.1		$157.2		$135.8	
Fixed Capital Investment	$637.0		$606.4		$552.9	
Additional Capital Expenses						
Land (2% of FCI)	$12.7		$12.1		$10.5	
Spare Parts (2% of FCI)	$12.7		$12.1		$10.5	
Legal Fees (1% of FCI)	$6.4		$6.1		$5.2	
Working Capital (25% of mfg. costs)	$39.7		$25.6		$31.7	
Startup Expenses (15% of FCI)	$95.5		$91.0		$78.4	
Total Additional Capital Expenses	$167.1		$146.9		$136.3	
Total Capital Investment	$804.1		$753.3		$659.2	

[a]*Includes enzymatic hydrolysis and concentration, filtration, and ion exchange in* ***Figure 3****.*
[b]*Includes acid hydrolysis and acid recovery, concentration, and Ion exchange in* ***Figure 4****.*

TABLE 4 | Prices of recycle paper in the US Midwest in USD (2020) (Recycling Today, 2020).

Recycle paper classification	Fraction of recyclable paper	Price range ($/tonne)
Mixed Paper	34%	$22.00–$27.50
Old Cardboard	7%	$55.00–$60.50
Sorted Residential Paper	36%	$49.50–$55.00
Sorted Office Paper	23%	$104.50–$115.50
Unrecyclable Paper (landfill)	—	-$52.64

TABLE 5 | Prices for feedstocks, chemicals, catalysts, utilities, and waste disposal in USD (2020).

Quantity	Price	Quantity	Price
Feedstocks		Catalysts	
Corn Stover ($/tonne)	$80.00	APR-1 Catalyst ($/tonne)	$120,000
Recyclable Paper ($/tonne)	40.45	APR-2 Catalyst ($/tonne)	$16,500
Unrecyclable Paper ($/tonne)	-$52.64	Condensation Catalyst ($/tonne)	$43,000
Process Chemicals		Wastewater Treatment Chemicals	
Sulfuric Acid ($/tonne)	$53.80	Boiler Chemicals ($/tonne)	$6,200
Caustic ($/tonne)	$250	FGD Lime ($/tonne)	$28
Ammonia ($/tonne)	$480	Cooling Tower Chemicals	
Hydrochloric Acid ($/tonne)	$35	Cooling Tower Chemicals ($/tonne)	$3,700
Glucose ($/tonne)	$700	Makeup Water ($/m^3)	$1.08
Corn Steep Liquor ($/tonne)	$970	Electricity	
Host Nutrients ($/tonne)	$1,000	Industrial Rate ($/MWh)	$52.64
Sulfur Dioxide ($/tonne)	$250	Wholesale Price ($/MWh)	$30.00
Hydrogen ($/tonne)	$894	Waste Disposal	
		Ash ($/tonne)	$52.64

of number of processing steps and plant capacity (Zhang and El-Halwagi, 2017). Enzymatic hydrolysis requires 12 processing steps while acid hydrolysis requires 9. Fewer processing steps suggest that the FCI for acid hydrolysis should be less than the FCI for enzymatic hydrolysis.

Operating Cost Estimates

Operating costs are generally divided into two categories–variable costs, which depend on production volume, and fixed costs, which are independent of production volume. Variable costs include feedstock costs, chemicals, utilities, and waste disposal. We obtained the price of delivered corn stover from Thompson and Tyner (2011). Price was adjusted for moisture content and converted to a 2020 price using the producer price index for hay from the US Bureau of Labor Statistics. The price of recycle paper depends on its classification, as shown in **Table 4**. We used a weighted average of mixed paper, old cardboard, and sorted residential paper for the price of recyclable paper for our cost estimates. Unrecyclable paper is currently sent to landfills for disposal. We assumed a credit for unrecyclable paper equal to the average landfill charge in the US Midwest.

We determined 2020 prices for chemicals, catalysts, and utilities from advertised prices, trade journals (e.g., *ICIS Chemical Business*), technical journals and reports, commodity trading data, and the US Energy Information Agency. If data was available, we used annual average values. If multiple sources of data were available, we used the median value. If prices for 2020 were not available, we estimated the price using the available data and the appropriate producer price index from the US Bureau of Labor Statistics. We assumed that an onsite natural gas steam reforming plant provides hydrogen, and we estimated the hydrogen prices based on the 2020 industrial natural gas price of $3.29/Mscf. Electricity is purchased at the average 2020 price for the industrial users in the Midwest, which is $66.60/MWh. Excess electricity is exported at the average wholesale price for the Midwest. Makeup water price is based on the 2020 price for the City of Chicago. The only waste produced is ash from the boiler. **Table 5** lists the prices for chemicals, catalysts, utilities, and waste disposal.

To determine variable costs on an annual basis, we assumed a 90% process availability. Repulping is established and reliable technology, so an assumed availability of 90% is reasonable for the paper to jet fuel processes. Current technology for preprocessing corn stover is unreliable and, therefore, has a low availability. To determine the inherent price advantage of recycle paper as a feedstock, we assumed that reliable technology for preprocessing corn stover already exists; and the corn stover to jet fuel process also has a 90% availability.

The number of operators required per shift using Brown's method (Brown, 2000). We assume that the plant employs five complete crews. Five complete crews provide a sufficient number of operators to ensure process is completely staffed at all times

TABLE 6 | Annual Operating Cost in million USD (2020).

Operating cost	Corn stover to jet	Paper to jet with enzymatic hydrolysis	Paper to jet with acid Hydrolysis
Feedstock and chemicals			
Feedstock	$65.7	$11.55	$11.71
Hydrogen	$27.43	$27.90	$27.43
Chemicals and Catalysts	$18.02	$19.60	$8.01
Waste Disposal	$4.12	$1.38	$1.50
Subtotal	$115.27	$60.43	$48.65
Utilities			
Electricity	—	$3.34	$36.29
Water	$1.35	$0.38	$0.74
Other	$0.64	$0.11	$0.14
Subtotal	$1.99	$3.83	$37.17
Total Variable Operating Costs	$117.26	$67.73	$85.82
Direct Production Costs			
Operators	95	85	75
Operator Salary ($26.50/hr)	$5.24	$4.69	$4.13
Payroll Overhead (50% of labor)	$2.62	$2.34	$2.07
Supervision (10% of labor)	$0.52	$0.47	$0.41
Laboratory Charges (10% of labor)	$0.52	$0.47	$0.41
Maintenance (3.6–4.5% of FCI)	$22.98	$21.53	$23.68
Royalties (2% of sales)	$5.90	$4.28	$4.71
Subtotal	$39.00	$33.78	$37.92
Fixed Charges			
Property Taxes (1.5% of land + equipment)	$6.53	$6.32	$5.41
Insurance (0.7% of FCI)	$0.21	$0.21	$0.21
Plant Overhead (15% of total wages)	$0.94	$0.84	$0.74
Subtotal	$7.68	$7.37	$6.37
General Expenses			
Administrative Costs (2% of sales)	$5.90	$4.28	$4.71
Distribution and Sales (2.5% of sales)	$7.37	$5.35	$5.88
Research and Development (1% of sales)	$2.95	$2.14	$2.35
Subtotal	$16.22	$11.77	$12.94
Total Fixed Cost	$61.67	$52.92	$54.73
Total Operating Cost	$178.93	$120.65	$140.55

without the need for operators to work overtime. We assumed an operator wage of $26.50 per hour based on the average reported by the US Bureau of Labor Statistics for the Midwest in 2020.

The average maintenance cost for ethanol plants and biotechnology companies is less than the average for the chemical industry because materials tend to be less corrosive and operating conditions are milder than the chemical industry. Based on data from the ethanol industry and biotechnology companies, we estimated the average maintenance cost for a biorefinery to be 2.4% of FCI per year, which is less than average value of 6% for the chemical industry (Garrett, 1989). Corn stover to jet fuel and paper to jet fuel process have characteristics of biorefineries and ordinary chemical plants. For example, enzyme production is a biorefinery-like operation, which should have maintenance costs typical of a biorefinery. Catalytic conversion is petrochemical-like and should have maintenance costs typical of the chemical industry. To account for the mixed nature of the processes, we used a cost weight average to estimate maintenance cost.

We used the cost factors and methods recommended by Kubic et al. (2019) to estimate the remaining fixed operating costs.

TABLE 7 | Financial parameters for discount cash flow analysis.

Plant life	30 years
Depreciation Time	7 years
Equity Financing	60%
Loan Interest Rate	5.5%
Loan Term	7
Federal Corporate Tax Rate	21%
State Corporate Tax Rate	4.8%

Table 6 contains a summary of variable and fixed operating cost estimates.

Inspection of **Table 6** reveals three important differences among the three processes. First, the cost of corn stover is substantially higher than recycle paper. The cost of corn stover per tonne is greater than paper and more corn stover must be processed to produce volume of product because of its lower carbohydrate content. Second, chemical costs for the paper to jet fuel process with acid hydrolysis are less than the other two processes because acid hydrolysis requires no chemicals and nutrients for cellulase production. Electric costs for the paper to

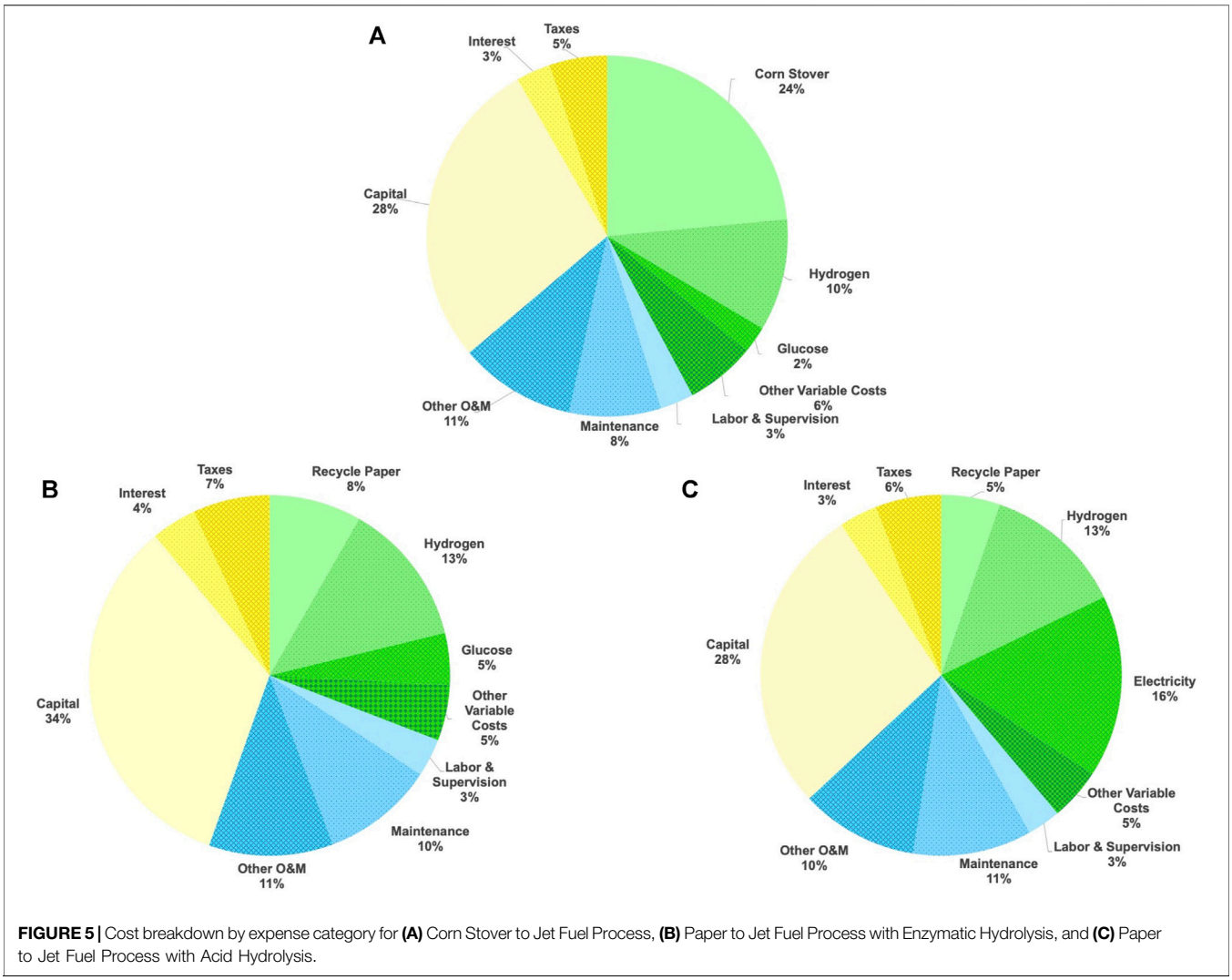

FIGURE 5 | Cost breakdown by expense category for **(A)** Corn Stover to Jet Fuel Process, **(B)** Paper to Jet Fuel Process with Enzymatic Hydrolysis, and **(C)** Paper to Jet Fuel Process with Acid Hydrolysis.

jet fuel process with acid hydrolysis are much greater than the other two processes because of the power consumption of RW-EDI.

Cash Flow Analysis

We use a discount cash flow analysis to evaluate the minimum selling price for jet fuel. Minimum selling price is the product price needed to give a 10% real internal rate of return after taxes. The cash flow analysis begins with construction of the plant and continues through the life of the plant. Construction time can be estimated using the following correlation. (Kubic, 2014).

$$\theta = \alpha . TCI^{0.25},$$

where θ is the construction time in years, α is a constant that depends on the type of project, and *TCI* is the total capital investment. For a chemical plant with TCI computed in million 2020 USD, α is 0.53. Construction spending as a function of time is approximated by a beta distribution. Working capital and start-up expenses are accrued during the final year of construction. Startup, which is the time from the introduction of feedstock until the process achieves some degree of steady operations, is assumed to be 3 months (Myers et al., 1986). Production is assumed to be zero during the startup period and 80% of nameplate capacity during the first year of operations.

Table 7 summarizes the financial parameters for the discount cash flow analysis. Plant life is measured from the end of start-up. It is not a true measure of plant life. Rather, it is a time horizon for the cash flow analysis. Depreciation in the analysis is only used to estimate corporate profit taxes. We use a modified accelerated cost recovery system with a 7 years depreciation time. The method and depreciation time are dictated by the US tax code. Both federal and state corporate taxes are included in the analysis. We use a state tax rate of 4.8%, which is the average state tax rate in the US.

The minimum selling prices for the three processes that we considered in this study are $5.14/gal for the corn stover to jet fuel process, $3.97/gal for the paper to jet fuel process with enzymatic hydrolysis, and $4.13/gal for the paper to jet fuel process based in acid hydrolysis. **Figure 5** shows the cost breakdown for the three processes by expense category. The minimum selling price for jet fuel produced from corn stover is more than $1.00 higher than jet

TABLE 8 | Impact of possible process improvements on minimum selling price.

Process improvement	Cumulative impact ($/gal)			Cost reduction ($/gal)		
	Acid hydrolysis	Enzymatic hydrolysis	Enzymatic hydrolysis	Acid hydrolysis	Enzymatic hydrolysis	Enzymatic hydrolysis
Nominal	$4.13	$3.97	$3.97	—	—	—
Improve RW-EDI Efficiency	$4.01	(a)	(a)	$0.12	—	—
Hydrogenation of Pulp	$3.01	$3.01	$3.01	$1.00	$1.09	$1.09
Hydrogenation of Paper	$2.32	$2.32	(b)	$0.69	$0.69	—
Double Capacity	$1.72	$1.72	$2.44	$0.60	$0.60	$0.57
Reducing Catalyst Cost	$1.60	$1.60	$2.32	$0.12	$0.12	$0.12
Decreasing Excess hydrogen	$1.58	$1.58	$2.30	$0.02	$0.02	$0.02

(a) RW-EDI is not used with enzymatic hydrolysis. (b) Hydrogenation of paper not included in this series of sensitivity studies.

fuel produced from recycle paper. This difference is the result of the high cost of corn stover relative to recycle paper. The minimum selling price for the paper to jet fuel processes within the uncertainty limits of the analysis. Although the total capital investment is less for the process with acid hydrolysis, the operating cost are higher as a result of the high electrical power consumption by RW-EDI.

Meeting the Cost Goal

The proposed paper to jet fuel processes do not meet the target production cost of $2.04/gal. Therefore, it is reasonable to consider possible technological improvements that could make the process competitive with petroleum-derived fuels. We identified six engineering improvements and technological advances that could improve process economics and determined their impact on cost.

- *Increase Efficiency of RW-EDI*–**Figure 5** shows that electricity account for 16% of the cost for the paper to jet fuel process with acid hydrolysis, and RW-EDI accounts for over 60% of the energy consumption. Reducing RW-EDI power consumption and increasing the sulfuric acid concentration in the permeate would reduce power consumption and steam consumption as well as reduce capital costs. These savings would reduce the cost of producing jet fuel with the process with acid hydrolysis.
- *Hydrogenation of Cellulose and Hemicellulose in Pulp*–Pretreatment and hydrolysis account for over 25% of production costs for both paper to jet fuel processes. Direct hydrogenation of the pulp to produce sugar alcohols would eliminate the capital and operating costs associated with hydrolysis and reduce overall production costs.
- *Hydrogenation of Cellulose and Hemicellulose in Paper*–The cost of sorting paper in municipal solid waste is estimated to be about $75/tonne and the cost of repulping the paper is not negligible. Hydrogenating unsorted paper to produce sugar alcohols would reduce repulping costs and eliminate hydrolysis costs. By eliminating or substantially reducing sorting costs it could turn recycle paper costs into a credit.
- *Increase Plant Capacity*–**Figure 5** shows that capital costs are the largest single factor in the overall cost of jet fuel. The paper to jet fuel processes scale with capacity to the 0.66 power. Doubling capacity will reduce capital costs relative to operating cost resulting in a reduction in product cost.
- *Reduce Catalyst Cost*–The catalysts for Catalytic Conversion and Upgrading are expensive. Reducing catalyst cost by a factor of 10 by finding less expensive options and improving catalyst life will reduce operating costs.
- *Reduce Excess Hydrogen*–In the current process design, about 22% more hydrogen is fed to Catalytic Conversion and Upgrading than is consumed by the process. Reducing excess hydrogen to less than 5%would reduce production costs.

We evaluated the possible cost saving for each of these scenarios considering reductions in capital costs as a result of eliminating processing steps, reduction in variable capital costs as a result of eliminating or reducing chemical feeds, and reducing the required number of operators. Only two of the perturbations could change overall process yields–direct hydrogenation of pulp and paper. For these two perturbations, we assumed yields were equal to those of the process based on acid hydrolysis.

Table 8 contains a summary of the results. The results show that no single innovation reduces the cost of converting recycled paper into jet fuel to the target value of $2.04/gal. The gains from incremental process improvements (i.e., increasing efficiency of RW-EDI, reducing catalyst cost, reducing excess hydrogen, and increasing plant capacity) are not large enough to meet the target price. A major technical innovation is needed.

Pretreatment and hydrolysis account for over 25% of production costs. Direct hydrogenation of cellulose is the subject of current research activities (Kobayashi et al., 2011; Jiang, 2014; Liao et al., 2014; Negoi et al., 2014). Using direct hydrogenation of cellulose and hemicellulose would eliminate the capital and operating costs associated with pretreatment and hydrolysis reducing production costs by $1.09/gal. Direct hydrogenation of pulp combined with a doubling of process capacity reduces costs to $2.44/gal, which still exceeds the target value of $2.04/gal. Additional cost savings could be achieved by developing a process for direct hydrogenation of unsorted paper. This innovation would eliminate repulping costs and sorting costs. Direct hydrogenation of unsorted paper would reduce production costs to $2.31/per gal, which is $1.80/gal reduction

TABLE 9 | Carbon dioxide emissions and solid waste production for corn stover to jet fuel and paper to jet fuel processes.

Waste product	Petroleum	Corn stover	Paper with enzymatic hydrolysis	Paper with acid Hydrolysis
Carbon Dioxide Emissions (kg CO_2/bbl)	517	102	133	318
Net Solid Waste Generation (kg/bbl)	0.5	61	–63	–64

TABLE 10 | Results for the lifecycle analysis of jet fuel and paper production and use. The analysis is based on the paper to jet fuel process with enzymatic hydrolysis.

Scenario	CO_2 emissions (million tonne/yr)	Solid waste (million tonne/yr)
Baseline	421	38
1	383	13
2	366	16
3	359	16
4	352	47

from the nominal value. Hydrogenation of unsorted paper combined with increased plant capacity could bring production costs down to $1.71.

ENVIRONMENTAL IMPACT

We performed a lifecycle analysis to determine net carbon dioxide emissions and solid waste generation. The analysis was limited to the combined emissions from jet fuel and paper production assuming current levels of use. We based the analysis on the Greenhouse Gases, Regulated Emissions, and Energy Use in Transportation (GREET) model (Energy Systems Division, 2014). Pathways not related to jet fuel production and use were eliminated from the GREET model; and pathways for paper production, use, and disposal were added. GREET was the primary data source supplemented with additional data for emissions and solid waste generation for the paper pathways (Suhr et al., 2010; Bajpai, 2014; US Environmental Protection Agency, 2018; Kinstrey and White, 2006) and solid waste from biomass (Lizotte et al., 2015). Emissions and solid waste associated with the conversion of biomass and recycled paper to jet fuel were based on the material and energy balances discussed in the previous section. Estimates of net solid waste production for the paper to jet processes account the reduction in paper waste currently been disposed of in landfills.

Table 9 gives the carbon dioxide emitted and solid waste generated from the three jet fuel processes evaluated in this study. The paper to jet fuel process with acid hydrolysis emits 2.4 times as much carbon dioxide as the process with enzymatic hydrolysis. The difference is the result of the high electrical power consumption of RW-EDI in the process with acid hydrolysis to recover and recycle sulfuric acid. Because the paper to jet fuel processes consume paper from municipal solid waste, net solid waste generation is negative.

We analyzed four scenarios to determine the combined carbon dioxide emissions and solid waste generation of commercial air transportation and the paper industry in the US.

- *Baseline*–The baseline scenario was the current case in which jet fuel is produced from petroleum and paper is produced from a combination of virgin and recycled pulp.
- *Scenario 1*–All recyclable paper not currently recycled domestically and degraded pulp from recycling plants are converted into jet fuel and the balance of the US jet fuel demand is obtained from petroleum. Paper is produced from the current combination of virgin paper and recycled pulp.
- *Scenario 2*–All discarded paper available for recycle is converted into jet fuel and the balance of the jet fuel demand is obtained from petroleum. All paper is produced in the US from virgin pulp.
- *Scenario 3*–The same volume of renewable jet fuel produced in this scenario as produced in Scenario 2, but only paper not recycled domestically is converted into jet fuel. The additional renewable jet fuel is produced from corn stover. The balance of the US jet fuel demand is obtained from petroleum. Paper is produced from the current combination of virgin paper and recycled pulp.
- *Scenario 4*–The same volume of renewable jet fuel produced in Scenario 2 is produced from the corn stover biomass. The balance of jet fuel needed domestic demand is obtained from petroleum. Paper is produced from the current combination of virgin and recycled pulp.

The results of the lifecycle analysis for these scenarios are summarized in **Table 10**. Because of the high carbon dioxide emissions from the paper to jet fuel process with acid hydrolysis, we only present results from the process with enzymatic hydrolysis. Scenario 4, in which all renewable jet fuel is produced from corn stover, results in the lowest level carbon dioxide emissions. As shown in **Table 9**, lifecycle carbon dioxide emissions jet fuel produced from corn stover are less than for jet fuel produced from recycle paper. US paper recycled in other countries also contributes to the reduction in emissions. However, considering the uncertainty in the analysis, carbon dioxide emissions for Scenarios 2, 3, and 4 are not significantly different. Scenario 1, in which domestic paper recycle is maintained at current levels, produces the minimum amount of solid waste. Producing virgin pulp generates significantly more solid waste than repulping recycled paper, and producing jet fuel from corn stover produces more solid waste than recycling paper into jet fuel. Scenarios 2 and 3 also produce significantly less solid waste than the baseline scenario.

Scenario 3, in which jet fuel is produced from recycled paper and corn stover, is probably the best from an environmental and social perspective. It reduces net carbon dioxide emissions from the US air transportation industry by 15% without increasing logging for virgin paper production or disrupting the domestic paper recycling industry. It also eliminates paper destined for landfills reducing total solid waste destine for landfills by 6%.

CONCLUSION

Recycle paper has advantages over agricultural residue, such as corn stover, as a cellulosic feedstock for fuel production. Efficient and reliable technology exists in the recycle paper industry for converting paper into fibers suitable for chemical conversion. Unlike equipment for handling and preprocessing of corn stover, industrial experience demonstrates that repulping equipment has high availability. The combination of proven repulping technology, the high cellulose content of paper, and existing supply network gives recycle paper a significant economic advantage over corn stover and other sources of lignocellulosic biomass. Net lifecycle carbon dioxide emissions of paper derived fuels are comparable to corn stover derived fuels, and paper generated significantly less solid waste.

A key disadvantage of producing jet fuel from paper is its limited supply, so it can only satisfy a fraction of the total demand. More importantly, the cost of producing jet fuel from recycle paper is not competitive with petroleum using current technology.

Our sensitivity studies have shown that the key to a competitive paper to jet fuel process is direct hydrogenation of cellulose and hemicellulose to sugar alcohols. Direct hydrogenation of cellulose would reduce capital and operating costs. Several researchers have explored direct catalytic hydrogenation of cellulose, but considerably more work is needed convert this idea into a practical industrial process. Direct hydrogenation of cellulose and hemicellulose combined with greater economy of scale could make paper to jet fuel comparative. In this study we have only considered the paper to jet fuel via sugar alcohols as an intermediate. Another possibility is a process with furfural and 5-methylfurfural or levulinic acid as intermediates. Such a process would eliminate hydrolysis as a separate processing step and reduce hydrogen consumption. This alternative route warrants consideration.

Perhaps the biggest value of developing a process to convert recycle paper into hydrocarbons is its use as a method of jumpstarting a cellulosic biofuels industry. The process chemistry for producing fuels from paper is the same as lignocellulosic biomass. Developing a paper to jet fuel process would provide an opportunity for demonstrating the process chemistry at an industrial scale without the need to develop a new supply chain for lignocellulosic biomass or solve all the current problems involved with handling and preprocessing lignocellulosic biomass. The process would also be useful for reducing municipal solid waste.

DATA AVAILABILITY STATEMENT

The original contributions presented in the study are included in the article/Supplementary Material, further inquiries can be directed to the corresponding author.

AUTHOR CONTRIBUTIONS

The concept of converting recycle paper into jet fuel and the technical approach to the problem were the result of discussions among WK, CM, TS, and AS. WK developed idea and executed the analysis including the material and energy balances, the techno-economic analysis, and the life cycle analysis.

FUNDING

This work was supported by the U.S. Department of Energy Office of Energy Efficiency and Renewable Energy Bioenergy Technologies Office (program Award Number NL0033622). Los Alamos National Laboratory is operated by Triad National Security, LLC, for the National Nuclear Security Administration of U.S. Department of Energy (Contract No. 89233218CNA000001).

ACKNOWLEDGMENTS

The authors thank members of the Los Alamos National Laboratory Biomass Conversion Team for their review and suggestion. The author also thanks Travis Moulton of the Process Modeling and Analysis Group at Los Alamos for his review of this manuscript.

REFERENCES

AACE International (2011). *AACE International Certified Cost Technician Primer*. Morgantown, WV: Association for the Advancement of Cost Engineering International.

Aden, M. R., Ibsen, K., Jechura, J., Neeves, K., Sheehan, J., Wallace, B. et al. (2002). *Lignocellulosic Biomass to Ethanol Process Design and Economic Utilization Co-current Dilute Acid Prehydrolysis and Enzymatic Hydrolysis for Corn Stover*. Report No. NREL/TP-510-32438. Golden, CO: National Renewable Energy Laboratory.

Bajpai, P. (2014). *Management of Pulp and Paper Mill Waste*. Heidelberg, Germany: Springer International Publishing.

Blommel, P., and Price, R. (2017). *Production of Alternative Gasoline Fuels. US Patent Application No. US 2017/0044443 A1*. Washington, DC: US Patent and Trademark Office.

Börnjesson, M. H., and Ahlgren, E. O. (2015). *Energy Technology Systems Analysis Programme*. Paris, France: International Energy Agency.Pulp and Paper Industry. Technical Brief 107.

Brown, T. R. (2000). Estimating Product Costs. *Chem. Eng.* 107 (8), 86–89.

Cortright, R. D., and Blommel, P. G. (2013). *Synthesis of Liquid Fuels and Chemicals from Oxygenated Hydrocarbons*. Washington, DC: U.S. Patent No.US Patent and Trademark Office, 455.

Cortright, R. D., Davda, R. R., and Dumesic, J. A. (2002). Hydrogen from Catalytic Reforming of Biomass-Derived Hydrocarbons in Liquid Water. *Nature* 418 (6901), 964–967. doi:10.1038/nature01009

DattaLin, S. Y., Lin, Y. J., Schell, D. J., Millard, C. S., Ahmad, S. F., Henry, M. P. et al. (2013). Removal of Acidic Impurities from Corn Stover Hydrolysate Liquor by Resin Wafer Based Electrodeionization. *Ind. Eng. Chem. Res.* 52, 13777–13784. doi:10.1021/ie4017754

Davis, R., Tao, L., Scarlats, C., Tan, E., Ross, J., Lukas, J. et al. (2015). *Process Design and Economics for Conversion of Lignocellulosic Biomass to Hydrocarbons: Dilute Acid and Enzymatic Deconstruction of Biomass to Sugars and Catalytic Conversion of Sugars to Hydrocarbons*. Report No. NREL/TP-5100-62498. Golden, CO: National Renewable Energy Laboratory.

Energy Systems Division (2014). *GREET Life-Cycle Model: Model*. Lemont, IL: Argonne National Laboratory.

European Integrated Pollution Prevention and Control Bureau (2001). *Best Available Techniques in the Pulp and Paper Industry. Reference Document*. Luxembourg, Luxembourg: European Commission, Integrated Pollution Prevention and Control Bureau.

Food and Agriculture Organization of the United Nations (2015). Rome: Food and Agriculture Organization of the United Nations.Pulp and Paper Capacities.

Garrett, D. E. (1989). *Chemical Engineering Economics*. New York, NY: Van Nostrand Reinhold.

Gonzalez, R., Phillips, R., Saloni, D., Jameel, H., Abt, R., Pirraglia, A. et al. (2011). Biomass to Energy in Sothern United States: Supply Chain and Delivered Cost. *Bioresources* 6, 2954–2976.

Institute of Industrial Engineers (2000). *Industrial Engineering Terminology: A Revision of ANSI Z94.0-1989*. Norcross, GA: Engineering and Management Press.

International Air Transport Association (2015). *IATA Sustainable Aviation Fuel Roadmap*. Montreal-Geneva: International Air Transport Association.

Jiang, C. (2014). Hydrolytic Hydrogenation of Cellulose to Sugar Alcohols by Nickel Salts. *Cellulose Chem. Tech.* 48, 75–78.

Kinstrey, R., and White, D. (2006). *Pulp and Paper Industry – Energy Bandwidth Study*. Greenville, SC: Jacobs: Project No. 16CX8700.

Kobayashi, H., Matsuhashi, H., Komanoya, T., Hara, K., and Fukuoka, A. (2011). Transfer Hydrogenation of Cellulose to Sugar Alcohols over Supported Ruthenium Catalysts. *Chem. Commun.* 47, 2366–2368. doi:10.1039/c0cc04311g

Kosaric, N., Duvnjak, Z., Farkas, A., Sahm, H., Bringer-Meyer, S., Goebel, O. et al. (2011). "Ethanol," in *Ullmann's Encyclopedia of Chemical Technology* (Weinheim: Wiley-VCH Verlag GmbH & Co), 1–72. doi:10.1002/14356007.a09_587.pub2

Kubic, W., Booth, S., Suton, A., and Moore, C. (2019). *Evaluation and Benchmarking of Economic Analysis Methods for Biofuels. Report No. LA-UR-10-30785*. Los Alamos, NM: Los Alamos National Laboratory.

Kubic, W. (2014). *Construction Cost Growth for New Department of Energy Nuclear Facilities, Report No. LA-UR-14-23698*. Los Alamos, NM: Los Alamos National Laboratory.

Liao, Y., Liu, Q., Wang, T., Long, J., Zhang, Q., Ma, L. et al. (2014). Promoting Hydrolytic Hydrogenation of Cellulose to Sugar Alcohols by Mixed Ball Milling of Cellulose and Solid Acid Catalyst. *Energy Fuels* 28, 5778–5784. doi:10.1021/ef500717p

Lizotte, P-L., Savoie, P., and de Champlain, A. (2015). Ash Content and Calorific Energy of Corn Stover Components in Eastern Canada. *Energies* 8, 3827–4838. doi:10.3390/en8064827

Myers, C. W., Shangraw, R. F., Devey, M. R., and Hayashi, T. (1986). *Understanding Process Plant Schedule Slippage and Startup Costs. Report No. R-3215-PSSP/RC*. Santa Monica, CA: Rand Corporation.

Negoi, A., Triantafyllidis, K., Parvulescu, V. I., and Coman, S. M. (2014). The Hydrolytic Hydrogenation of Cellulose to Sorbitol over M (Ru, Ir, Pd, Rh)-BEA-Zeolite Catalysts. *Catal. Today* 223, 122–128. doi:10.1016/j.cattod.2013.07.007

Page, J. S. (1996). *Conceptual Cost Estimating Manual*. 2nd Ed. Burlington, MA: Elsevier, 326.

Patel, S. K., Qin, M., Walker, W. S., and Elimelech, M. (2020). Energy Efficiency of Electro-Driven Brackish Water Desalination: Electrodialysis Significantly Outperforms Membrane Capacitive Deionization. *Environ. Sci. Technol.* 54, 3663–3677. doi:10.1021/acs.est.9b07482

Recycling Today (2020). Weird Times for Recovered Paper. Recycling Today. Available at: https://www.recyclingtoday.com/article/recovered-paper-market-report-september-2020/(Accessed June 3, 2021).

Stalnaker, T., Usman, K., and Taylor, A. (2016). *Airline Economic Analysis for the Raymond James Global Airline Book*. New York: Oliver Wyman.

Suhr, M., Klein, G., Kourti, I., Rodrigo Gonzalo, M., Giner Santonjia, G., Roudier, S. et al. (2010). *Best Available Techniques (BAT) Reference Document for Production of Pulp, Paper, and Board*. Luxembourg: Publications Office of the European Union.

Thompson, S., and Tyner, W. (2011). *Purdue Extension*. West Layfayette, IN: Purdue University.Corn Stover for Bioenergy Production: Cost Estimates and Farmer Supply Response. Report No. RE-3-W.

US Department of Energy (1997). *Cost Estimating Guide. Report No. DOE G430.1-1*. Washington, DC: US Department of Energy.

US Energy Information Agency (2021b). *Annual Energy Outlook 2021 with Projections to 2050*. Washington, DC: US Department of Energy.

US Energy Information Agency (2021a). *May 2021 Monthly Energy Review*. Report No DOE/EIA-0035(2021/5). Washington, DC: US Department of Energy.

US Environmental Protection Agency (2018). 2011 – 2016 Greenhouse Gas Reporting Program Industrial Profile: Pulp and Paper. Available at: https://www.epa.gov/sites/production/files/2018-10/documents/pulp_and_paper_2016_industrial_profile.pdf (Accessed June 11, 2021).

US Environmental Protection Agency (2020). *Facts and Figures about Materials, Waste and Recycling*. Paper and Paperboard: Material-Specific Data. Available at: https://www.epa.gov/facts-and-figures-about-materials-waste-and-recycling/paper-and-paperboard-material-specific-data (Accessed May 28, 2021).

U.S. Department of Energy (2016). *2016 Billion-Ton Report: Advancing Domestic Resources for a Thriving Bioeconomy*, 1. Oak Ridge, TN: Economic Availability of FeedstocksOak Ridge National Laboratory. Report No. ORNL/TM-2016/160. doi:10.2172/1271651

Vogel, G. H. (2005). *Process Development*. Weinheim, Germany: Wiley-VCH Verlag GmbH & Co.

Wang, W-C., Tao, L., Markham, J., Zhang, Y., Tan, E., Batan, L. et al. (2016). *Review of Biojet Fuel Conversion Technologies*. Report No. NREL/TP-5100-66291. Golden CO: National Renewable Energy Laboratory.

Woods, D. R. (2007). *Rules of Thumb in Engineering Practice*. Weinheim, Germany: Wiley-VCH Verlag GmbH & Co.

Zhang, C., and El-Halwagi, M. (2017). Estimating the Capital Cost of Shale-Gas Monetization Projects. *Chem. Eng. Prog.* 113 (120), 28–32.

Conflict of Interest: The authors declare that the research was conducted in the absence of any commercial or financial relationships that could be construed as a potential conflict of interest.

Publisher's Note: All claims expressed in this article are solely those of the authors and do not necessarily represent those of their affiliated organizations, or those of the publisher, the editors and the reviewers. Any product that may be evaluated in this article, or claim that may be made by its manufacturer, is not guaranteed or endorsed by the publisher.

NOMENCLATURE

APR Aqueous-phase reforming

FCI Fixed capital investment

FOB Cost Purchased equipment cost–freight on board

GREET Greenhouse Gases, Regulated Emissions, and Energy Use in Transportation

NREL National Renewable Energy Laboratory

RW-EDI Resin Wafer Electrodeionization

TCI Total Capital Investment.

frontiers in Energy Research

ORIGINAL RESEARCH
published: 20 October 2021
doi: 10.3389/fenrg.2021.735661

Production of Sustainable Aviation Fuels in Petroleum Refineries: Evaluation of New Bio-Refinery Concepts

*Abid H Tanzil[1], Kristin Brandt[2], Xiao Zhang[3], Michael Wolcott[2], Claudio Stockle[1] and Manuel Garcia-Perez[1,4]**

[1]*Department of Biological Systems Engineering, Washington State University, Pullman, WA, United States,* [2]*Institute for Sustainable Design, Civil and Environmental Engineering Department, Washington State University, Pullman, WA, United States,* [3]*The Voiland School of Chemical Engineering and Bioengineering, Washington State University, Richland, WA, United States,* [4]*Bioproducts Sciences and Engineering Laboratory, Richland, WA, United States*

OPEN ACCESS

Edited by:
Peer Schenk,
The University of Queensland, Australia

Reviewed by:
Bheru Lal Salvi,
Maharana Pratap University of Agriculture and Technology, India
Halil Durak,
Yüzüncü Yıl University, Turkey

***Correspondence:**
Manuel Garcia-Perez
mgarcia-perez@wsu.edu

Specialty section:
This article was submitted to Bioenergy and Biofuels, a section of the journal Frontiers in Energy Research

Received: *03 July 2021*
Accepted: *30 September 2021*
Published: *20 October 2021*

Citation:
Tanzil AH, Brandt K, Zhang X, Wolcott M, Stockle C and Garcia-Perez M (2021) Production of Sustainable Aviation Fuels in Petroleum Refineries: Evaluation of New Bio-Refinery Concepts. Front. Energy Res. 9:735661. doi: 10.3389/fenrg.2021.735661

The potential for petroleum refineries (PRs) to integrate sustainable aviation fuel (SAF) technologies is manifold, unlike with other existing industrial infrastructures that lack such technical similarities. A midsize PR with a crude oil capacity of 120,000 barrels per day was analyzed in this study to determine the feasibility of integrating five well-known lignocellulosic SAF technologies, namely, Virent's BioForming (VB), alcohol to jet (ATJ), direct sugar to hydrocarbon (DSHC), fast pyrolysis (FP), and gasification and Fischer–Tropsch (GFT) methods, as well as one novel concept referred to as integrated carbonization-gasification-Fischer–Tropsch (ICGFT). The following three integrated scenarios were studied to derive the costs and environmental impact reductions: sharing of infrastructures from outside battery limits (OSBL), co-processing of SAF technology-derived intermediates with PR-derived gas oil inside battery limits (ISBL) and repurposing of an idle or shutdown PR. Sharing OSBL infrastructures resulted in reductions of the minimum fuel selling price (MFSP) by 3–14% relative to the corresponding standalone cases. Co-processing of intermediate products such as VB-derived long chain hydrocarbons, ATJ-derived ethanol, DSHC-derived farnesene, pyrolysis-derived bio-oil, and GFT-derived FT products reduced the MFSP by 10–19% from corresponding standalone cases. Moreover, repurposing scenarios reduced the costs by 16–34%. Greenhouse gas (GHG) estimations showed that 17 of 21 integrated scenarios resulted in GHG savings (7–92%). Lignocellulosic SAF technologies are limited by low fuel yields, which are governed by the high oxygen content of the feedstock. However, ICGFT was found to be advantageous in terms of fuel production at a maximized fuel yield.

Keywords: sustainable aviation fuel, MFSP, co-location, repurposing, co-processing, sustainable aviation fuel (SAF), GHG (green house gas) emission, co-processing

INTRODUCTION

The contributions of fossil fuel-based energy throughout the world have been high over the past century (US Energy Information Administration, 2021). However, in the last 30 years, gradual increases in the use of renewable energy forms such as wind, solar, biomass, and hydroelectric power have occurred [US Energy Information Administration, 2021; British Petroleum (2021)., 2021]. In recent years, United States.-based petroleum refineries (PRs) have become a focal point of biomass-based renewable energy expansion strategies (Freeman et al., 2013; Gas Technology Institute, 2015; van Dyk et al., 2019; Giorgi, 2021). Declines in quality reservoirs, increases in environmental awareness, and advancement of biomass-based renewable energy technologies are some of the major drivers that have led PRs to seek out technical opportunities to incorporate renewable energy technologies (Keyrilainen and Koskinen, 2011; Ericson et al., 2019). Large corporations such as Phillips 66, Exxon Mobil, and World Energy are evaluating plans to repurpose their respective existing refineries to produce renewable fuels [Lane, 2019; City of Paramount (2020)., 2020; Elliott, 2020; Sanicola, 2021; Global Clean Energy Holdi, 2020]. Additionally, the United States Federal Aviation Administration (FAA) is collaborating with academic researchers and private organizations to develop biomass-based sustainable aviation fuel (SAF) supply chains to reduce carbon dioxide emissions (Hileman et al., 2013; Gas Technology Institute, 2015; Brown, 2016). However, even with recent advancements in biorefinery concepts, the majority of lignocellulosic biorefineries are still in either the demonstration or pilot phase (Mawhood et al., 2016) due to the high capital costs and low product yields (Swanson et al., 2010; Jones et al., 2013; Davis et al., 2015).

The downstream processing for most SAF concepts, according to current studies (Huber et al., 2006; Swanson et al., 2010; Jones et al., 2013; Pearlson et al., 2013; Davis et al., 2015), has technical similarities to conventional PR manufacturing operations such as hydrotreatment, hydrocracking, isomerization, steam methane reforming, and the final product distribution (Gary et al., 2010). Importantly, each of these manufacturing operations has the potential to be leveraged to improve the economics of SAFs. Depending on the initial feedstock type, several SAF technologies can be integrated at various stages of an existing refinery operation. For example, triglyceride feed can be readily fed into the hydrotreatment or fluid catalytic cracking (FCC) unit with heavy vacuum gas oil (HVGO) or light vacuum gas oil (LVGO) (Lappas et al., 2009; Sági et al., 2016; Bezergianni et al., 2018; De Paz Carmona et al., 2018; van Dyk et al., 2019), but it cannot be added into an atmospheric distillation unit (van Dyk et al., 2019). Lignocellulosic sugar streams, consisting of five- and 6-carbon components, require preprocessing (West et al., 2008; Olcay et al., 2013; Davis et al., 2015), before these materials can be co-processed with HVGO or LVGO. Another promising lignocellulosic intermediate, pyrolysis oil or bio-oil, can be co-processed with LVGO or HVGO (Zacher et al., 2014; Pinho et al., 2015; Pinho et al., 2017; Bezergianni et al., 2018; Stefanidis et al., 2018; Pinheiro Pires et al., 2019). However, the high oxygen content of bio-oil makes this intermediate unstable (Elliott, 2007; Bridgwater, 2012), and thus, it requires stabilization (Jones et al., 2013; Zacher et al., 2014) before co-processing. Co-processing-based integration scenarios have been conceptualized throughout the literature; however, detailed technoeconomic analyses of such scenarios are limited (Ali et al., 2018; Wu et al., 2019).

In this study, a framework developed by Martinkus et al. (Martinkus and Wolcott, 2017) was adopted to study the integration of lignocellulosic SAF technologies within existing PRs under various scenarios with the aim of achieving improvements in the cost structure as well as reductions in the environmental impacts. This framework of utilizing existing infrastructures was used to derive the following three types of integrated scenarios: 1) scenarios that use outside battery limits (OSBL) infrastructures, which are non-conversion units; 2) scenarios that co-process SAF-derived intermediates with PR-derived intermediates using both OSBL and inside battery limits assets (ISBL), and 3) scenarios that use an idle or shutdown PR infrastructure. Three sugar-based SAF technologies—Virent's BioForming (VB) (Davis et al., 2015), alcohol to jet (ATJ) (Geleynse et al., 2018), direct sugar to hydrocarbon (DSHC) (Klein-Marcuschamer et al., 2013; Tanzil et al., 2021a) and two thermochemical SAF technologies—fast pyrolysis (Jones et al., 2013) and gasification and Fischer–Tropsch (GFT) (Swanson et al., 2010)—were studied in this work. In addition to these technologies, a new conceptual pathway (Tanzil et al., 2021a) referred to as integrated carbonization-gasification-Fischer–Tropsch (ICGFT) technology was also studied.

MATERIALS AND METHODS

Methodology for the Evaluation of Biorefinery Concepts

To evaluate biorefinery concepts, Excel based standalone process models that include mass and energy balances, technoeconomic analyses (TEA) and greenhouse gas (GHG) emission analyses are built by following the methodology described in previous work (Garcia-Nunez et al., 2016). Data needed to build standalone process models of a PR and six SAF technologies are described in detail in *Petroleum Refineries* and *Sustainable Aviation Fuel Scenario*. Integration concepts of co-location and repurposing were applied to generate alternative scenarios for the evaluations of costs and environmental impact reductions.

Petroleum Refineries

Unlike a corn ethanol mill or sugarcane mill, the existing PRs are not concentrated in a specific region in the United States (US Energy Information Administration, 2016). For this work, it was assumed that the existing PRs were located within the Midwest (PADD 2) (US Energy Information Administration, 2016), which allowed us to take advantage of corn stover-based SAF technologies that have been developed in previous work (Tanzil et al., 2021b). A PR with an atmospheric distillation capacity of 120,000 BPD (barrels per day) was used as the existing baseline capacity (Sun et al., 2018). This refinery accommodates an atmospheric distillation column that produces gas, light naphtha, heavy naphtha, gas oil, and heavy bottoms (Gary

TABLE 1 | Processing capacities of major equipment in the PR scenario and utility consumption; all values were taken from (Sun et al., 2018).

Parameter	Value
Capacity (BPD)	
Crude distillation unit	120,000
Vacuum distillation unit	59,858
Naphtha hydrotreater	22,671
Catalytic reformer	22,444
Isomerization NHT	2,400
Diesel hydrotreater	35,191
Hydrocracker	31,110
Delayed coker	33,720
Gas oil hydrotreater	20,529
Fluid catalytic cracking	24,749
Alkylation unit (Alky)	4,792
Sulfur plant (MTD)[a]	391
Amine regeneration	12
Utility consumption	
Electricity (MW/barrel crude)	13.7
Water (L/barrel crude)	74.7
Steam (MJ/barrel crude)	88.6
Hydrogen (kg/barrel crude)	1.7

[a]*metric ton per day.*

et al., 2010; Sun et al., 2018). Light naphtha, heavy naphtha, and gas oil are further processed (hydrotreatment, hydrocracking, isomerization, and catalytic reforming) in the refinery to produce jet/kerosene, diesel, and gasoline (Gary et al., 2010; Sun et al., 2018). The historic significance of heavy bottoms or residuals as direct fuel for other industries has dwindled over the past few decades in response to new environmental regulations (Gary et al., 2010). Therefore, further sequential processing of bottoms via vacuum distillation, fluid catalytic cracking (FCC), coking, and hydrotreatment must be completed (Sun et al., 2018). A schematic of this complicated process is included in the Supplemental Information. **Table 1** shows the capacity of the major processing units for the PR scale used in this study, as well as utility consumption (Sun et al., 2018).

Sustainable Aviation Fuel Scenario

The PR facility was assumed to be located in the Midwest, so the most abundant lignocellulosic feedstock (corn stover) in that region (National Corn Growers Ass, 2016) was chosen as the feedstock for the SAF technologies. The standalone SAF technologies were termed VB_A, ATJ_A, DSHC_A, FP_A, and GFT_A, where A denotes the respective standalone technology. The conceptualized novel process, ICGFT, which has been described in detail in previous work (Tanzil et al., 2021a) was also modeled as a standalone scenario (ICGFT_A). This work investigated the integration opportunities offered for lignocellulosic processes. Although triglyceride-based HEFA (hydroprocessed esters and fatty acids) processes are readily available for integration as intermediates because of the low oxygen content (Starck et al., 2016), HEFA-based integration is only under construction by World Energy on a commercial scale (Lane, 2019) at a California site [City of Paramount (2020)., 2020]. This study focused on lignocellulosic SAF processes, which pose challenges as a result of their high oxygen content in both the feedstock and intermediates. These challenges are addressed on a case-by-case basis.

In two previous studies (Tanzil et al., 2021b; Tanzil et al., 2021c) integration scenarios were formulated based on the existing facilities capital structure. However, an existing PR facility has both a larger capacity and higher capital costs (Gary et al., 2010) than an existing corn ethanol mill (Wallace et al., 2005; Kwiatkowski et al., 2006) or sugarcane mill (Tanzil et al., 2021c). The capacity of standalone SAF scenarios was determined by the co-processing capacity of a PR, which typically ranges between 5 wt% to 15 wt% of the co-processing material (Gary et al., 2010; Pinho et al., 2015). In this work, this range was used to calculate the SAF capacity of each technology so that the corresponding feedstock capacity (corn stover) was maintained at under 2,000 metric tons per day (MTD). This can be regarded as a viable commercial-scale feedstock capacity (Swanson et al., 2010; Humbird et al., 2011; Jones et al., 2013; Quinn and Davis, 2015). Therefore, the co-processing ratio differed from 6 to 15%. For example, GFT_A-derived Fischer–Tropsch (FT) products were co-processed at a co-processing ratio of 7% to maintain the initial feedstock capacity under 2000 MTD. DSHC_A-derived farnesene was co-processed at a ratio of 6% in the hydrocracker. Farnesene is a C-15 unsaturated hydrocarbon molecule that is hydrogenated and cracked in the hydrocracker. Both VB_A and ATJ_A had a 10% co-processing ratio. For FP_A, a 15% co-processing ratio was used to limit the feedstock capacity to 1274 MTD. Because of the proposed high fuel yield (Tanzil et al., 2021a), ICGFT_A had a significantly lower feedstock capacity.

Table 2 shows the calculated SAF capacities [million liters per year (MLY)], corn stover capacity, and fixed capital investment (FCI). Capacities and FCIs of these standalone facilities were scaled from process models built in previous studies (Tanzil et al., 2021a; Tanzil et al., 2021b).

TABLE 2 | SAF capacities, feedstock capacities, and scaled FCI; corn stover was the feedstock.

Technology	Co-processing material	Insertion point to PR	Corn stover capacity, MTD	SAF capacity, MLY	FCI, MM$
VB_A	Condensation product	Hydrotreater	1,527	105	823
ATJ_A	Oligomerized product	Fluid catalytic cracking	1,995	89	754
DSHC_A	Farnesene	Hydrocracker	1,980	41	793
FP_A	Pyrolysis oil	Fluid catalytic cracking	1,274	48	347
GFT_A	FT products	Hydrocracker	1,988	77	507
ICGFT_A	FT products	Hydrocracker	354	162	349

TABLE 3 | Defined features of integrated scenarios–co-located; corn stover was the feedstock.

Scenario	Power use	Integration scenario	Shared costs with PR
VB_B1	Self-generation	OSBL	OSBL: service facilities, buildings, yard improvements; management
VB_B2	Purchase		
VB_B3	Purchase	Co-processing	OSBL: service facilities, buildings, yard improvements; ISBL-hydrocracker; management
ATJ_B1	Self-generation	OSBL	OSBL: service facilities, buildings, yard improvements; management
ATJ_B2	Purchase		
ATJ_B3	Purchase	Co-processing	OSBL: service facilities, buildings, yard improvements; ISBL: hydrotreater; management
DSHC_B1	Self-generation	OSBL	OSBL: service facilities, buildings, yard improvements; management
DSHC_B2	Purchase		
DSHC_B3	Purchase	Co-processing	OSBL: service facilities, buildings, yard improvements; ISBL: hydrotreater; management
FP_B1	Purchase	OSBL	OSBL: service facilities, buildings, yard improvements; management
FP_B2	Purchase	Co-processing	OSBL: service facilities, buildings, yard improvements; ISBL: hydrotreater; management
GFT_B1	Self-generation	OSBL	OSBL: service facilities, buildings, yard improvements; management
GFT_B2	Purchase		
GFT_B3	Purchase	Co-processing	OSBL: service facilities, buildings, yard improvements; ISBL: hydrotreater; management
ICGFT_B	Purchase	OSBL	OSBL: service facilities, buildings, yard improvements; management

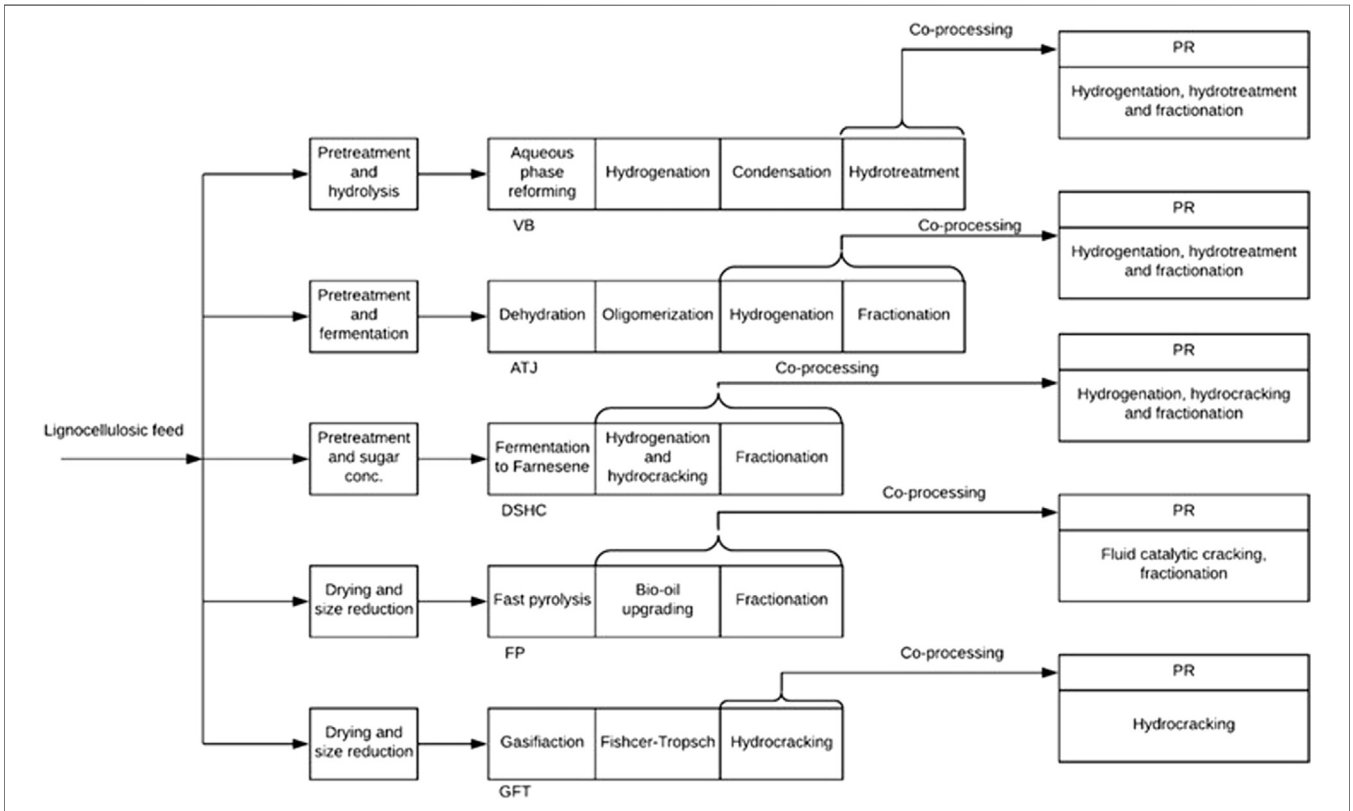

FIGURE 1 | Schematic of the proposed co-processing scenarios between an existing PR and emerging SAF processes.

Depending on the SAF process pathway, the biomass-derived intermediates were co-processed with heavy gas oil (HGO) in the following upgrading units: hydrotreater, hydrocracker, and FCC.

Integrated SAF Concepts

Two types of integration strategies were included in the analysis (de Jong et al., 2015; Tanzil et al., 2019; Tanzil et al., 2021b), namely, co-location and repurposing. Co-location strategies explored the infrastructure of an existing PR without interruption of the production of petroleum products (de Jong et al., 2015). In this work, co-located scenarios were divided into two categories. In the first category, scenarios that utilized only OSBL infrastructures were defined (**Table 3**).

TABLE 4 | Defined features of integrated scenarios–repurposed; corn stover was the feedstock.

Scenario	Power use	Repurposed infrastructure (from PR)	
		OSBL	ISBL
VB_C ATJ_C DSHC_C FP_C GFT_C ICGFT_C	Self-power generation Power purchase	Buildings; yard improvements; service facilities: steam generation and distribution, power substation and distribution, water distribution, raw material and final product storage, sanitary and process waste disposal, communication	Hydrotreater; hydrocracker; fluid catalytic cracker; steam methane reformer; power generation

These were not directly involved in the conversion process of crude oil to various fuel products, e.g., buildings, yard improvements, and some of the service facilities. The capacities of the five components of service facilities—steam generation, power substation, power distribution, water distribution, and product storage capacity—were subject to co-located integration strategies. Due to the high capacity of PR infrastructure and well-established technological identities, a 20% cutoff margin was assumed for these service facilities to share with any of the SAF technologies. The core management group of plant managers and engineers was also considered to be shared.

In the second category of co-located scenarios, the co-processing capabilities of a PR were utilized, and these are detailed in *Sustainable Aviation Fuel Scenario*. Therefore, scenarios involving co-processing of compatible intermediates were generated (**Figure 1**). In addition to the OSBL component of the first category, these scenarios represent the conversion process equipment located ISBL.

Table 3 lists the integrated scenarios, which utilize existing infrastructure for either co-location or co-processing as well as defining each scenario as either purchasing or self-generating electricity.

Because of the feedstock limitations, the crude oil capacity of 120,000 BPD chosen for co-location was too large for the repurposing scenarios. Therefore, the SAF capacity for the repurposed scenarios (**Table 4**) remained the same as that in the co-located scenarios. Lignocellulosic SAF technology requires additional equipment not included in a PR. However, two large advantages for repurposing a PR are the avoidance of power generation module costs and not having to purchase hydrogen from an external source; note that these are required for co-located scenarios. However, a repurposed PR needs to be valued and added as an FCI component in the repurposed scenarios. In this work, this component was calculated to be $72 MM$ from the literature (Lane, 2019) assuming the six-tenth rule of scaling.

Mass and Energy Flow

The technical data that were required to build the material and energy flows of the studied processes are given in the Supplemental Information (**Supplementary Tables S1A–S1E**; **Supplementary Tables S2A–S2F**); these data were used to build the material and energy flows of both the standalone and integrated scenarios.

Technoeconomic Analysis

TEA included capital and operational cost estimations, followed by a financial analysis to determine the minimum fuel selling price (MFSP) of each scenario. In this work, the MFSP was

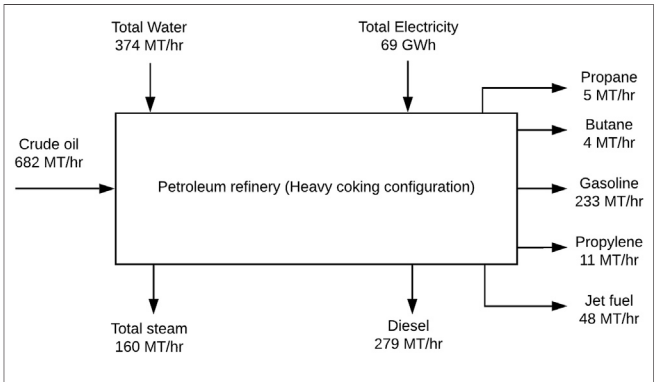

FIGURE 2 | Process flow diagram for a 120,000 BPD or 682 MT/hr petroleum refinery; The entities that were essential to determine the extent of integration strategies were reported in this flow diagram.

estimated for the SAF. Other fuel prices were determined based on the correlation between historic price data for the SAF and other fuels, which was carried out in previous work (Tanzil et al., 2021b). The methodology to conduct the TEA has been well documented in two previous studies (Tanzil et al., 2021a; Tanzil et al., 2021b). The set of assumptions for the financial analysis are given in **Supplementary Tables S4 and S5**. Reference equipment costs were taken from various sources (Davis et al., 2015; Jones et al., 2013; Swanson et al., 2010; Klein-Marcuschamer et al., 2013; Humbird et al., 2011) and were used to calculate fixed capital costs using ratio factors (Peters et al., 2004). The modified cost ratio factors for this work are given in **Supplementary Table S3** in the Supplemental Information. A corn stover price of $70/dry metric ton (20% initial moisture) was taken from the literature (Edwards, 2014). Electricity sales price ($0.038/kWh) and purchase price ($0.069/kWh) were taken as 5 year averages (2013–2017) from the Energy Information Administration (EIA) (EIA. US, 2018; US EIA, 2020a). The 5 year average (2013–2017) of natural gas ($4.20/MMBtu) was also taken from the EIA (US EIA, 2018). Other raw material prices are given in the Supplemental Information (**Supplementary Table S6**). A levelized hydrogen price of $1.77/kg was taken from a United States Department of Energy (DOE) estimation that included capital and operational costs to produce hydrogen (Dillich et al., 2012). The reference salary structure was taken from the literature (Jones et al., 2013) (**Supplementary Table S9**). The methodology to determine the adjusted salary structure has

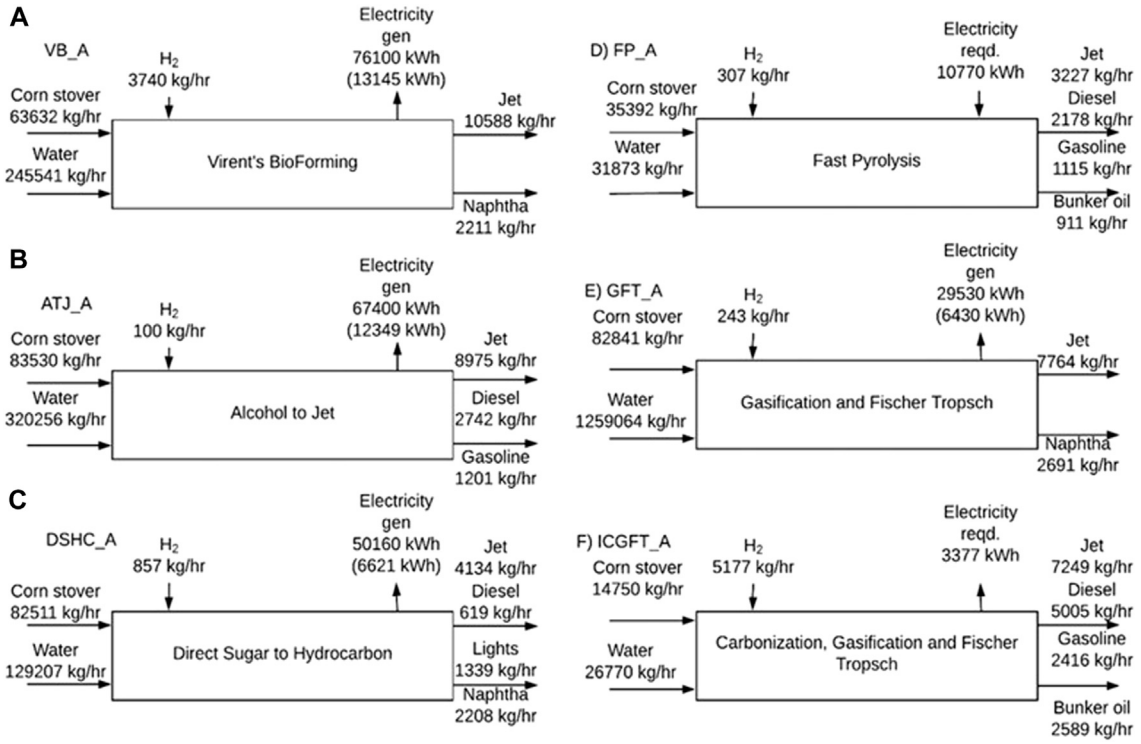

FIGURE 3 | Mass and energy flow in the corn stover-based SAF standalone scenarios.

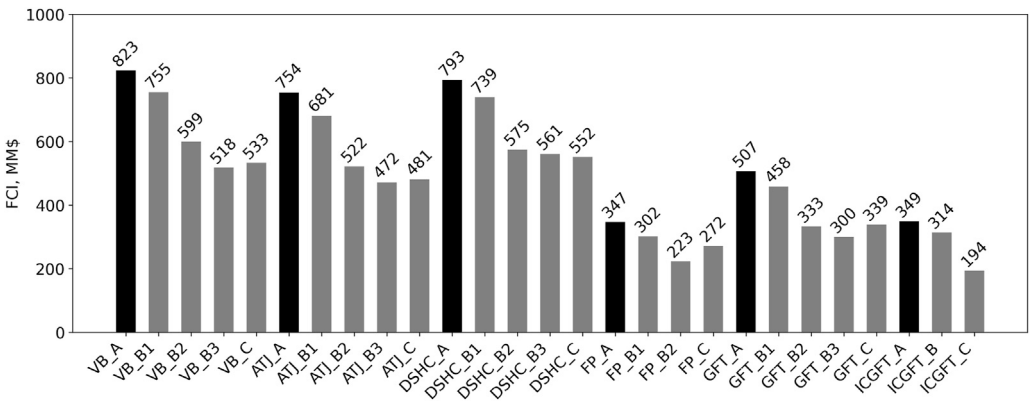

FIGURE 4 | FCI reductions of integrated scenarios (grey), in comparison with their respective standalone scenarios (black).

been outlined in previous work (Tanzil et al., 2021b). All of the analyses were carried out for the cost year of 2017.

Greenhouse Gas Emissions

GHG emission profiles were developed for the integrated scenarios between the PR and SAF processes following an attributional life cycle assessment (ALCA) approach. A cradle-to-gate system boundary was established as in previous work (Tanzil et al., 2021b). The material and energy flow data are given in **Supplementary Tables S7A–S7F**. A list of emission factors is also given in the Supplemental Information (**Supplementary Table S8**). The functional unit selected was 1 MJ of the total fuel product.

RESULTS AND DISCUSSION

Overall Mass and Energy Flowrate

For this study, a medium-sized PR with a heavy coking configuration that processes 120,000 BPD was analyzed (Sun

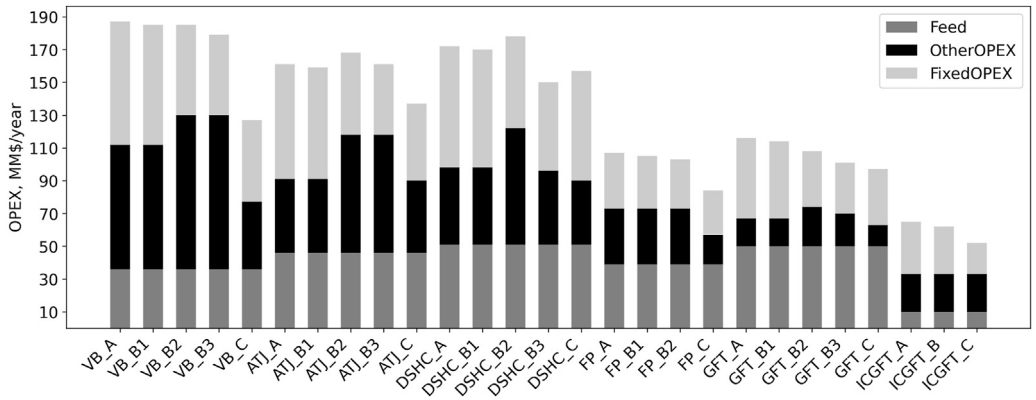

FIGURE 5 | Comparison of OPEX components of integrated scenarios with their respective standalone scenarios (VB_A/ATJ_A/DSHC_A/FP_A/GFT_A/ICGFT_A).

et al., 2018). **Figure 2** shows a flow diagram of the overall material and energy flow. The hydrogen flow represents a steam methane reforming facility inside the refinery that produces 8.5 MT H_2/hr as required. This configuration processes heavy fuel oil via further hydrotreatment and cracking (FCC) to produce gasoline and diesel.

Fig. shows the overall material and energy flow for the Midwest-based SAF standalone scenarios. The high co-processing capacity of the PR enabled the studied SAF technologies to increase the fuel capacity beyond that in previous work (Tanzil et al., 2021a; Tanzil et al., 2021b). The high H_2 consumption by ICGFT_A was caused by the steam methane reforming (SMR) facility that provided CO_2 for gasification to increase the fuel yield (Tanzil et al., 2021a). The material and energy flows in **Figure 2** and **Figure 3** were used to determine whether the OSBL-based co-located scenarios matched the 20% cutoff sharing infrastructures.

The large capacity of the PR (**Figure 2**) allowed the integrated SAF processes to utilize service facilities without surpassing the 20% cutoff requirement for the steam generation, power substation, distribution, and product storage. The water distribution facility was only utilized by two co-located scenarios, namely, FP_B1 and FP_B2, because of the lower water consumption in these two scenarios. Thus, the portion of the ratio factor that covered the service facilities was modified to be in the range of 27–29.5% for all co-located scenarios (**Supplementary Table S3**). The ratio factor was also reduced for buildings to 29% (Peters et al., 2004). However, for repurposed scenarios, this decreased to 7% for buildings (Peters et al., 2004). In addition, the yard improvement cost was assumed to be zero for all scenarios. More service facilities would be available for a repurposed scenario, and hence, a much lower ratio factor of 8.5% was needed. Details are given in **Supplementary Table S3**.

CAPEX, OPEX, and MFSPs

Unlike corn ethanol mills (Tanzil et al., 2021b) and sugarcane mill-based integration (Tanzil et al., 2021c), PR-based integration scenarios have higher capital and operational costs as a result of the higher production capacities (**Table 2**). **Figure 4** demonstrates the FCI reduction opportunities for each integrated scenario from their respective standalone scenario. Sharing the cost of the OSBL infrastructure (VB_B1, ATJ_B1, DSHC_B1, FP_B1, GFT_B1, and ICGFT_B) reduced the costs by 6–10%. In addition to OSBL cost sharing, replacement of the power generation module with power purchases (VB_B2, ATJ_B2, DSHC_B2, and GFT_B2) reduced the costs by 26–33% compared with the standalone scenarios. The capital costs were reduced by 28–39% if co-processing was adopted (VB_B3, ATJ_B3, DSHC_B3, FP_B2,

TABLE 5 | MFSPs of all studied scenarios.

Scenario	MFSP ($/liter SAF)	% Reduction
VB_A	2.35	
VB_B1	2.27	3
VB_B2	2.08	11
VB_B3	1.97	16
VB_C	1.56	34
ATJ_A	2.04	
ATJ_B1	1.95	4
ATJ_B2	1.86	9
ATJ_B3	1.76	14
ATJ_C	1.57	23
DSHC_A	3.56	
DSHC_B1	3.45	3
DSHC_B2	3.28	8
DSHC_B3	2.89	19
DSHC_C	2.98	16
FP_A	1.43	
FP_B1	1.37	4
FP_B2	1.26	12
FP_C	1.12	22
GFT_A	1.78	
GFT_B1	1.70	4
GFT_B2	1.52	15
GFT_B3	1.44	19
GFT_C	1.43	20
ICGFT_A	0.69	
ICGFT_B	0.65	6
ICGFT_C	0.50	28

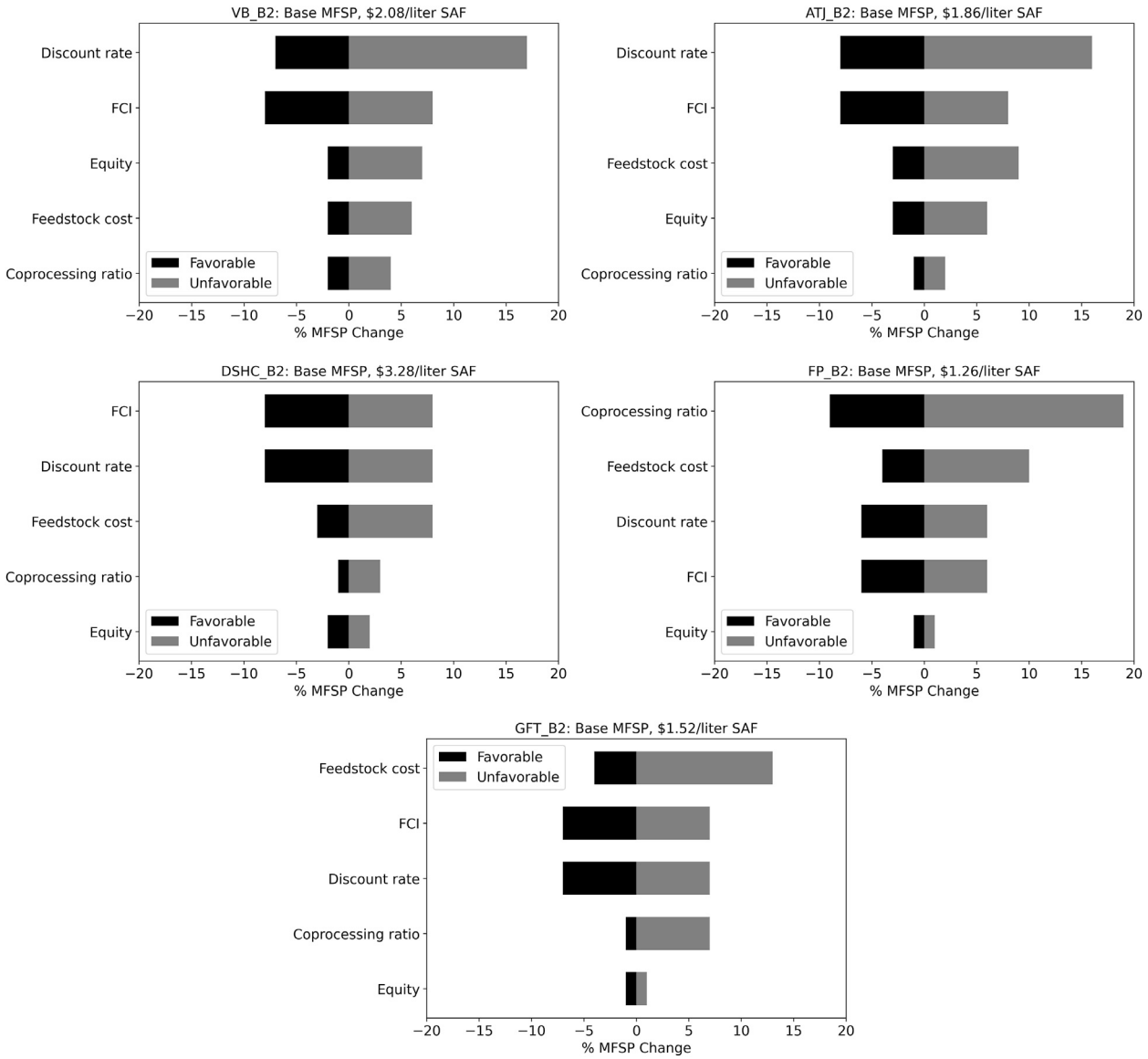

FIGURE 6 | Examples of the sensitivity analyses of integrated scenarios for OSBL sharing.

and GFT_B3). Repurposing strategies reduced the capital costs by 12–44% in comparison with the standalone scenarios (VB_C, ATJ_C, DSHC_C, FP_C, and GFT_C). In all repurposed scenarios, the cost of the PR (72 MM$) was added as the FCI component.

Although CAPEX reductions were realized, OPEX did not always decrease as shown in **Figure 5**. Four scenarios, namely, VB_B2, VB_B3, ATJ_B2, and DSHC_B2, had OPEXs that increased by 3–9% because of the purchase of electricity. Six scenarios that only utilized OSBL infrastructures from the PR (VB_B1, ATJ_B1, DSHC_B1, FP_B1, GFT_B1, and ICGFT_B) reduced OPEX slightly by 1–2% from the respective standalone scenarios due to salary reductions of 10%. For these scenarios, the maintenance cost (**Supplementary Table S5**) did not change from the corresponding standalone scenarios because these integrated scenarios did not have cost reductions from ISBL.

For the other scenarios, fixed OPEX was reduced by 3–41% from the corresponding standalone scenarios because of cost reductions from ISBL. Therefore, three co-processing scenarios (DSHC_B3, FP_B2, and GFT_B3) reduced the total OPEX by 10–13% from the respective standalone scenarios, and repurposed scenarios reduced OPEX by 8–32% from the respective standalone scenarios. It is noteworthy that the other OPEX (OPEX of raw materials and energy) of the two repurposed scenarios (VB_C and FP_C) were reduced by 47% because the levelized cost of H_2 was replaced by using already existing steam methane reforming inside the repurposed PR facility. In such a case, the purchase of natural gas (assuming a stoichiometric SMR reaction) nearly halved the other OPEXs.

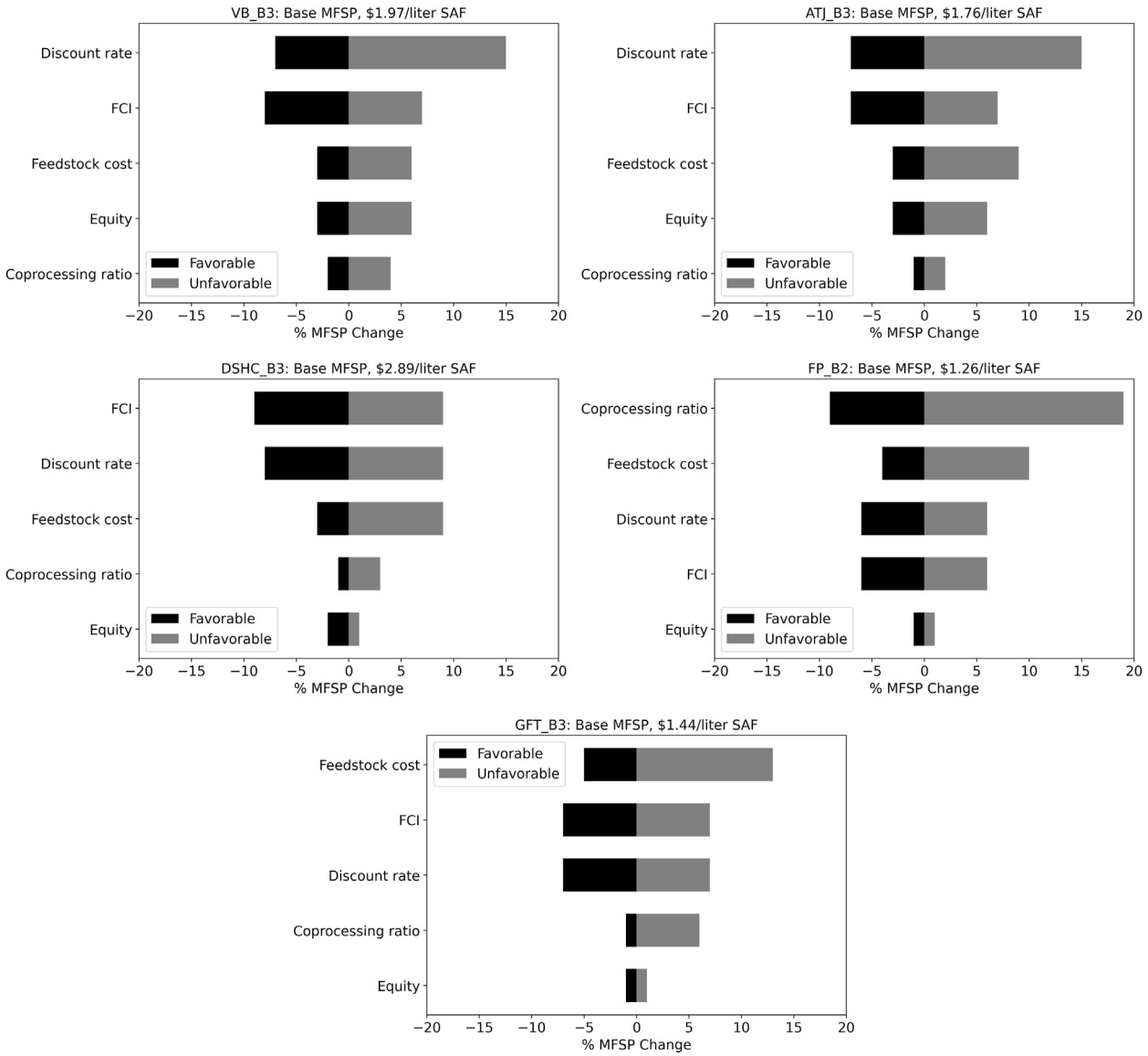

FIGURE 7 | Sensitivity analyses of the co-processing scenarios studied in this work.

The cost profiles of FCI and OPEX were reflected in their respective MFSP estimations (**Table 5**). Sharing only OSBL infrastructures (VB_B1, ATJ_B1, DSHC_B1, FP_B1, GFT_B1, and ICGFT_B) reduced MFSP by 3–6% in comparison with the respective standalone scenarios, while the non-power generating scenarios (VB_B2, ATJ_B2, DSHC_B2, and GFT_B2) reduced the costs by 2–14%. Co-processing scenarios reduced the MFSP by 10–19% compared with the respective standalone scenarios. Repurposed scenarios reduced the MFSP by 16–34%, following contributions from the reduced OPEX and FCI, as discussed above.

Sensitivity Analyses

Single point sensitivity analyses of five parameters—co-processing ratio, feedstock cost, real discount rate, FCI, and equity (Davis et al., 2015)—were carried out in this work. The base values of the equity and real discount rate are taken as 30% of FCI and 10%, respectively (Davis et al., 2015). The rest of the base values are given in *Sustainable Aviation Fuel Scenario*. For favorable and unfavorable values of the equity and discount rate, ±50% of the base value was assigned, as taken from the literature (Humbird et al., 2011; Davis et al., 2015). A favorable value of $60/dry MT and an unfavorable value of $100/dry MT of corn stover was also taken from the literature (Thompson and Tyner, 2014; US Department of Energy, 2011). For the FCI sensitivity calculation, ±30% was used as the percent delivered method considering a ±30% estimation error in estimating the FCI (Peters et al., 2004). Sensitivity analyses for the new concepts ICGFT_B and ICGFT_C were not carried out because their MFSP values were close to conventional jet fuel prices (US EIA, 2020b).

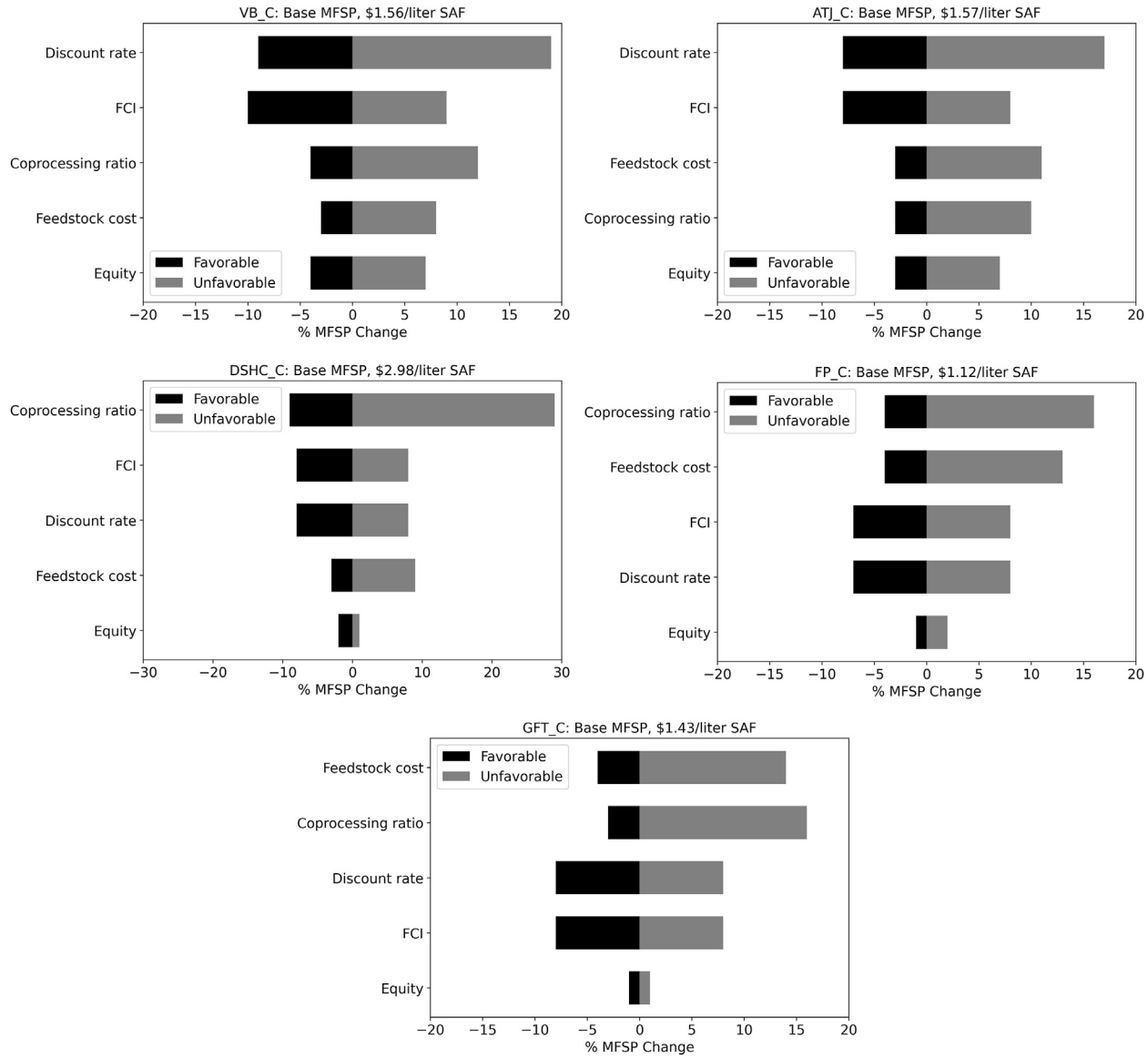

FIGURE 8 | Sensitivity analyses of repurposed scenarios.

Figure 6 shows the sensitivity plot of five integrated scenarios that utilized only the shared infrastructure from an existing PR. The favorable values of these parameters analyzed individually only reduced the MFSP values by 2–16%. In terms of the sensitivity ranking, the impact of the co-processing ratio was consistently among the two bottom parameters except for FP_B1.

The co-processing ratio can be directly correlated to both the fuel capacity and feedstock capacity. As described in *Sensitivity Analyses*, the choice of the base value of the co-processing ratio was dictated by the feedstock processing capacity, which was close to 2,000 MTD, except for FP_B1. Therefore, a ±50% variation indicated a feedstock range between 1,000 and 3,000 MTD (approximately). Previous work suggests (Tanzil et al., 2021a) that MFSP values do not change significantly after 1,000 MTD of feedstock capacity, and values tend to flatten after 2,000 MTD. Similar suggestions also have been made in the case of MFSP vs fuel capacity (Tanzil et al., 2021a). However, it also has been suggested that a high feedstock capacity or fuel capacity can increase the MFSP value (Tanzil et al., 2021a). Because in case of a low fuel yield scenario, high feedstock capacity can significantly increase the capital and operational cost. This explanation can be linked to the fact that DSHC_C (**Figure 8**) had a 30% increase in MFSP for a 50% increase in the co-processing ratio or fuel capacity.

The sensitivity of feedstock cost appears to be among the two top parameters for the majority of the repurposed scenarios (**Figure 8**).

Greenhouse Gas Emission Profiles

Table 6 shows the GHG emission profiles of the integrated scenarios, which were categorized into the following three

TABLE 6 | GHG emission profiles of the studied scenarios.

Scenario	Emission profile, g CO_2-eq/MJ				% GHG savings
	Feedstock	Conversion	Co-product	Total emission	
VB_B1	7.1	98.7	−24.7	81.1	7
VB_B2	7.1	160.1	−47.3	119.8	-
VB_B3	7.1	160.1	−47.3	119.8	-
VB_C	7.1	66.8	−24.7	49.2	43
ATJ_B1	9.0	36.5	−33.3	12.2	86
ATJ_B2	9.0	89.0	−48.8	49.2	43
ATJ_B3	9.0	89.0	−48.8	49.2	43
ATJ_C	9.0	30.4	−33.3	6.1	93
DSHC_B1	14.7	98.4	−46.8	66.4	24
DSHC_B2	14.7	166.8	−70.1	111.5	-
DSHC_B3	14.7	166.8	−70.1	111.5	-
DSHC_C	14.7	86.6	−46.8	54.6	37
FP_B1	6.7	65.6	−39.6	32.7	62
FP_B2	6.7	65.6	−39.6	32.7	62
FP_C	6.7	49.6	−39.6	16.7	81
GFT_B1	11.2	25.8	−25.4	11.7	87
GFT_B2	11.2	42.7	−17.7	36.2	58
GFT_B3	11.2	42.7	−17.7	36.2	58
GFT_C	11.2	25.8	−25.4	11.7	87
ICGFT_A	3.9	42.6	−39.6	6.9	92
ICGFT_B	3.9	42.6	−39.6	6.9	92

segments: feedstock usage, conversion site, and co-product credits. Greenhouse gas (GHG) estimations showed that 17 of 21 integrated scenarios resulted in GHG savings (7–92%).

Corn stover usage resulted in GHG emissions in the range of 4–15 g $CO_{2\text{-eq}}$/MJ of total fuel. The emissions from the conversion site were dominated by the energy consumption as well as hydrogen consumption. VB_B2, VB_B3, DSHC_B2, and DSHC_B3 showed higher emissions as a result of the high hydrogen consumption and fossil fuel-based electricity. The repurposed scenarios yielded lower emissions than co-located scenarios because the former took advantage of the onsite SMR plant to produce hydrogen, thus avoiding the high emission factor of purchased hydrogen. The co-product credit includes lignin sales, the electricity credit, and the displaced emission profile by hydrocarbon fuels other than SAF. Dry lignin fuel was assumed to replace the emissions caused by coal.

A displacement factor of 10 kg coal/kg lignin (Pourhashem et al., 2013) was used to calculate the emission credit by lignin fuel sales. Seventeen integrated scenarios resulted in GHG savings (**Table 6**) compared with the GHG emission value of 87.3 g$CO_{2\text{-eq}}$/MJ of conventional fossil fuel (GREET, 2018).

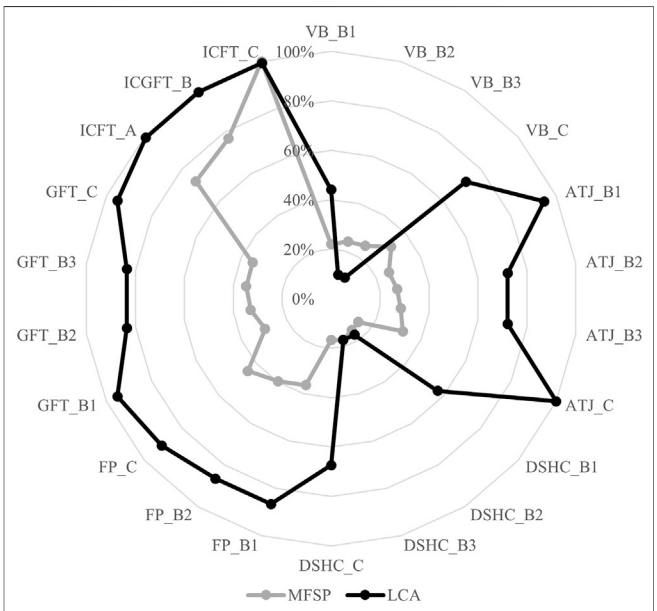

FIGURE 9 | Spider plot of economic and environmental performances for all integrated scenarios.

Selection Matrix

The estimated MFSPs (**Table 5**) and GHG emissions (**Table 6**) are two performance criteria used to evaluate the integrated scenarios. Economic performance largely relies on the cost structure (lower MFSP is desired), while environmental performance relies on process improvements in terms of less energy consumption and on the method of emission estimation (lower GHG emission is desired). Scores from 0% (highest MFSP/GHG emission) to 100% (lowest MFSP/GFG emission) were assigned to each of the estimated MFSP and GHG emission values.

The detailed methodology for depicting both types of performance (**Figure 9**) is adopted from elsewhere (Garcia-Nunez et al., 2016; Tanzil et al., 2021b) and outlined in the Supplemental Information (**Supplementary Tables S10, S11**). The spider plot in **Figure 9** shows that the repurposed scenario

(ICGFT_C) of the proposed novel technology ICGFT had the best performance in terms of both economic and environmental impacts. Although each of the integrated scenarios reduced the MFSP, only one scenario (ICGFT_C) from the proposed novel concept had an MFSP lower than that of conventional jet fuel ($0.54/L) (US EIA, 2020b).

CONCLUSION

The technical compatibility and higher capacities of petroleum refineries allow for larger SAF capacities compared with existing corn ethanol (Tanzil et al., 2021b) and sugarcane mills (Tanzil et al., 2021c). The high processing capacity of petroleum refineries offers significant cost reduction opportunities. Co-processing offers ISBL cost savings downstream, particularly during hydroprocessing. On the other hand, repurposing enables cost savings by not only the hydroprocessing unit, but also by the SMR unit. Although the cost of using a shutdown PR facility is added, repurposed scenarios also offer significant OPEX reduction opportunities because of the cheaper natural gas consumption compared with the direct consumption of expensive hydrogen. The overall capital cost reduction ranged from 7 to 44% in this study. The overall MFSP reduction ranged from 3 to 28%. Only the repurposed scenarios reduced the GHG emissions from the corresponding base cases. However, 14 out of the 21 scenarios resulted in GHG savings of 16–92% from the known emission of 87 $gCO_{2\text{-}eq}$/MJ for fossil fuel (GREET, 2018). The results from this research indicated that the high yielding novel concept of ICGFT could have both economic and environmental advantages by providing a pathway to maximize the fuel yield, which needs to be further investigated. In the case of sensitivity analyses, almost every scenario showed a distinguishable trend (ranking) in terms of the sensitivity of the MFSP according to the five parameters mentioned above. This finding indicated that all five parameters may play an important role in further reductions of the MFSP.

DATA AVAILABILITY STATEMENT

The original contributions presented in the study are included in the article/**Supplementary Material**, further inquiries can be directed to the corresponding author.

AUTHOR CONTRIBUTIONS

All authors contributed to the concept design and development. AT collected the data and completed the model analysis with intellectual input from KB, MW, and MG-P. The first draft was written by AT and all other authors provided their suggestions on previous versions. The final version of the manuscript was read and approved by all authors.

FUNDING

We will use funds from our FAA project to pay for this paper (13C-AJFE-WaSu-013). Dr. Garcia-Perez is very thankful to the USDA/NIFA for financial support through Hatch Project #WNP00701.

SUPPLEMENTARY MATERIAL

The Supplementary Material for this article can be found online at: https://www.frontiersin.org/articles/10.3389/fenrg.2021.735661/full#supplementary-material

REFERENCES

Ali, A. A. M., Mustafa, M. A., and Yassin, K. E. (2018). A Techno-Economic Evaluation of Bio-Oil Co-processing within a Petroleum Refinery. *Biofuels* 12, 645–653. doi:10.1080/17597269.2018.1519758

Bezergianni, S., Dimitriadis, A., Kikhtyanin, O., and Kubička, D. (2018). Refinery Co-processing of Renewable Feeds. *Prog. Energ. Combustion Sci.* 68, 29–64. doi:10.1016/j.pecs.2018.04.002

Bridgwater, A. V. (2012). Review of Fast Pyrolysis of Biomass and Product Upgrading. *Biomass and Bioenergy* 38, 68–94. doi:10.1016/j.biombioe.2011.01.048

British Petroleum (2021). Statistical Review of World Energy 2021. Available at: https://www.bp.com/en/global/corporate/energy-economics/statistical-review-of-world-energy.html.

Brown, N. (2016). Alternative Jet Fuels Research & Development. Available at: https://www.energy.gov/sites/prod/files/2016/11/f34/brown_bioenergy_2016.pdf.

City of Paramount (2020). AltAir/World Energy Refinery Conversion Project under Review. Available at: http://www.paramountcity.com/Home/Components/News/News/1349/16.

Davis, R., Tao, L., Scarlata, C., Tan, E. C. D., Ross, J., Lukas, J., et al. (2015). *Process Design and Economics for the Conversion of Lignocellulosic Biomass to Hydrocarbons:Dilute-Acid and Enzymatic Deconstruction of Biomass to Sugars and Catalytic Conversion of Sugars to Hydrocarbons*. Golden, CO: National Renewable Energy Laboratory.

de Jong, S., Hoefnagels, R., Faaij, A., Slade, R., Mawhood, R., and Junginger, M. (2015). The Feasibility of Short-Term Production Strategies for Renewable Jet Fuels - a Comprehensive Techno-Economic Comparison. *Biofuels, Bioprod. Bioref.* 9 (6), 778–800. doi:10.1002/bbb.1613

De Paz Carmona, H., Horáček, J., Brito Alayón, A., and Macías Hernández, J. J. (2018). Suitability of Used Frying Oil for Co-processing with Atmospheric Gas Oil. *Fuel* 214, 165–173. doi:10.1016/j.fuel.2017.10.133

Dillich, S., Ramsden, T., and Melina, M. (2012). "Hydrogen Cost Using Low Cost Natural Gas,". DOE Hydrogen and Fuel Cells Program Record # 12024 (Washington, DC: Office of Energy Efficiency and Renewable Energy).

Edwards, W. (2014). *Estimating a Value for Corn Stover*. Ames, IA: Iowa State University Extension and Outreach. Available at: https://store.extension.iastate.edu/product/14061.

EIA. US (2018). *Average Annual Industrial Electricity Price*. Washington, DC: Energy Information Administration. Available at: https://www.eia.gov/electricity/.

Elliott, D. C. (2007). Historical Developments in Hydroprocessing Bio-Oils. *Energy Fuels* 21 (3), 1792–1815. doi:10.1021/ef070044u

Elliott, R. (2020). US Oil Refiners Accelerate Shift to Renewables in Downturn. Available at: https://www.wsj.com/.

Ericson, S., Engel-Cox, J., and Arent, D. (2019). "Approaches for Integrating Renewable Energy Technologies in Oil and Gas Operations,". NREL/TP-6A50-72842 (Golden, CO: Joint Institute for Strategic Energy Analysis (JISEA) at the National Renewable Energy Laboratory (NREL)).

Freeman, C. J., Jones, S. B., Padmaperuma, A. B., Valkenburg, C., and Shinn, J. (2013). *Initial Assessment of U.S. Refineries for Purposes of Potential Bio-Based Oil Insertions, PNNL-22432*. Richland, WA: Pacific Northwest National Laboratory.

Garcia-Nunez, J. A., Rodriguez, D. T., Fontanilla, C. A., Ramirez, N. E., Silva Lora, E. E., Frear, C. S., et al. (2016). Evaluation of Alternatives for the Evolution of palm Oil Mills into Biorefineries. *Biomass and Bioenergy* 95, 310–329. doi:10.1016/j.biombioe.2016.05.020

Gary, J. H., Handwerck, G. E., and Kaiser, M. J. (2010). *Petroleum Refining: Technology and Economics*. 5th ed. NYC, NY: CRC Press, Taylor & Francis Group.

Gas Technology Institute (2015). Refinery Upgrading of Hydropyrolysis Oil from Biomass. Available at: https://www.osti.gov/servlets/purl/1221922.

Geleynse, S., Brandt, K., Garcia-Perez, M., Wolcott, M., and Zhang, X. (2018). The Alcohol-To-Jet Conversion Pathway for Drop-In Biofuels: Techno-Economic Evaluation. *ChemSusChem* 11 (21), 3728–3741. doi:10.1002/cssc.201801690

Giorgi, P. (2021). Reinventing the Refinery through the Energy Transition and Refining Petrochemical Integration. Available at: https://ihsmarkit.com/research-analysis/energy-transition-and-petchem-integration.html.

Global Clean Energy Holdings Inc (2020). California Refinery to Be Converted to Produce Renewable Diesel. Available at: http://biomassmagazine.com/articles/17036/california-refinery-to-be-converted-to-produce-renewable-diesel.

GREET (2018). *Greenhouse Gases, Regulated Emissions, and Energy Use in Transportation (GREET) Model Argonne*. Lemont, IL: National Laboratory.

Hileman, J. I., De la Rosa Blanco, E., Bonnefoy, P. A., and Carter, N. A. (2013). The Carbon Dioxide challenge Facing Aviation. *Prog. Aerospace Sci.* 63, 84–95. doi:10.1016/j.paerosci.2013.07.003

Huber, G. W., Iborra, S., and Corma, A. (2006). Synthesis of Transportation Fuels from Biomass: Chemistry, Catalysts, and Engineering. *Chem. Rev.* 106 (9), 4044–4098. doi:10.1021/cr068360d

Humbird, D., Davis, R., Tao, L., Kinchin, C., Hsu, D., Aden, D., et al. (2011). "Process Design and Economics for Biochemical Conversion of Lignocellulosic Biomass to Ethanol: Dilute-Acid Pretreatment and Enzymatic Hydrolysis of Corn Stover,". NREL/TP-5100-47764 (Golden, CO: National Renewable Energy Laboratory).

Jones, S., Meyer, P., Snowden-Swan, L., Padmaperuma, A., Tan, E., Dutta, A., et al. (2013). "Process Design and Economics for the Conversion of Lignocellulosic Biomass to Hydrocarbon Fuels: Fast Pyrolysis and Hydrotreating Bio-Oil Pathway,". PNNL-23053, NREL/TP-5100-61178 (Golden, CO: Pacific Northwest National Laboratory, Richland, WA and National Renewable Energy Laboratory).

Keyrilainen, J., and Koskinen, M. (2011). Renewable Fuels and Biofuels in Petroleum Refinery. Available at: https://www.digitalrefining.com/article/1000424/renewable-fuels-and-biofuels-in-a-petroleum-refinery#.YUIwFJ1KhPY.

Klein-Marcuschamer, D., Turner, C., Allen, M., Gray, P., Dietzgen, R. G., Gresshoff, P. M., et al. (2013). Technoeconomic Analysis of Renewable Aviation Fuel from microalgae,Pongamia Pinnata, and Sugarcane. *Biofuels, Bioprod. Bioref.* 7 (4), 416–428. doi:10.1002/bbb.1404

Kwiatkowski, J. R., McAloon, A. J., Taylor, F., and Johnston, D. B. (2006). Modeling the Process and Costs of Fuel Ethanol Production by the Corn Dry-Grind Process. *Ind. Crops Prod.* 23 (3), 288–296. doi:10.1016/j.indcrop.2005.08.004

Lane, J. (2019). The Paramount Deal: World Energy Takes off with Audacious $72M Acquisition of Alt Air and the Paramount Oil Refinery November 12. Available at: http://www.biofuelsdigest.com/.

Lappas, A. A., Bezergianni, S., and Vasalos, I. A. (2009). Production of Biofuels via Co-processing in Conventional Refining Processes. *Catal. Today* 145 (1-2), 55–62. doi:10.1016/j.cattod.2008.07.001

Martinkus, N., and Wolcott, M. (2017). A Framework for Quantitatively Assessing the Repurpose Potential of Existing Industrial Facilities as a Biorefinery. *Biofuels, Bioprod. Bioref.* 11 (2), 295–306. doi:10.1002/bbb.1742

Mawhood, R., Gazis, E., de Jong, S., Hoefnagels, R., and Slade, R. (2016). Production Pathways for Renewable Jet Fuel: a Review of Commercialization Status and Future Prospects. *Biofuels, Bioprod. Bioref.* 10 (4), 462–484. doi:10.1002/bbb.1644

National Corn Growers Association (2016). World of Corn. Available at: https://www.ncga.com/file/1325/WOC-2016.pdf.

Olcay, H., Subrahmanyam, A. V., Xing, R., Lajoie, J., Dumesic, J. A., and Huber, G. W. (2013). Production of Renewable Petroleum Refinery Diesel and Jet Fuel Feedstocks from Hemicellulose Sugar Streams. *Energy Environ. Sci.* 6 (1), 205–216. doi:10.1039/c2ee23316a

Pearlson, M., Wollersheim, C., and Hileman, J. (2013). A Techno-Economic Review of Hydroprocessed Renewable Esters and Fatty Acids for Jet Fuel Production. *Biofuels, Bioprod. Bioref.* 7 (1), 89–96. doi:10.1002/bbb.1378

Peters, M. S., Timmerhaus, K. D., and West, R. E. (2004). *Plant Design and Economics for Chemical Engineers*. 5th ed. 1221 Avenue of the Americas, New York, NY 10020: McGraw-Hill.

Pinheiro Pires, A. P., Arauzo, J., Fonts, I., Domine, M. E., Fernández Arroyo, A., Garcia-Perez, M. E., et al. (2019). Challenges and Opportunities for Bio-Oil Refining: A Review. *Energy Fuels* 33 (6), 4683–4720. doi:10.1021/acs.energyfuels.9b00039

Pinho, A. d. R., de Almeida, M. B. B., Mendes, F. L., Casavechia, L. C., Talmadge, M. S., Kinchin, C. M., et al. (2017). Fast Pyrolysis Oil from Pinewood Chips Co-processing with Vacuum Gas Oil in an FCC Unit for Second Generation Fuel Production. *Fuel* 188, 462–473. doi:10.1016/j.fuel.2016.10.032

Pinho, A. d. R., de Almeida, M. B. B., Mendes, F. L., Ximenes, V. L., and Casavechia, L. C. (2015). Co-processing Raw Bio-Oil and Gasoil in an FCC Unit. *Fuel Process. Tech.* 131, 159–166. doi:10.1016/j.fuproc.2014.11.008

Pourhashem, G., Adler, P. R., McAloon, A. J., and Spatari, S. (2013). Cost and Greenhouse Gas Emission Tradeoffs of Alternative Uses of Lignin for Second Generation Ethanol. *Environ. Res. Lett.* 8 (2). doi:10.1088/1748-9326/8/2/025021

Quinn, J. C., and Davis, R. (2015). The Potentials and Challenges of Algae Based Biofuels: A Review of the Techno-Economic, Life Cycle, and Resource Assessment Modeling. *Bioresour. Tech.* 184, 444–452. doi:10.1016/j.biortech.2014.10.075

Sági, D., Baladincz, P., Varga, Z., and Hancsók, J. (2016). Co-processing of FCC Light Cycle Oil and Waste Animal Fats with Straight Run Gas Oil Fraction. *J. Clean. Prod.* 111, 34–41. doi:10.1016/j.jclepro.2015.06.059

Sanicola, Laura. (2021). Exxon, Chevron Look to Make Renewable Fuels without Costly Refinery Upgrades. Available at: https://www.reuters.com/world/middle-east/exclusive-exxon-chevron-look-make-renewable-fuels-without-costly-refinery-2021-08-12/.

Starck, L., Pidol, L., Jeuland, N., Chapus, T., Bogers, P., and Bauldreay, J. (2016). Production of Hydroprocessed Esters and Fatty Acids (HEFA) - Optimisation of Process Yield. *Oil Gas Sci. Technology-Revue D Ifp Energies Nouvelles.* 71 (1). doi:10.2516/ogst/2014007

Stefanidis, S. D., Kalogiannis, K. G., and Lappas, A. A. (2018). Co-processing Bio-Oil in the Refinery for Drop-In Biofuels via Fluid Catalytic Cracking. *Wiley Interdiscip. Reviews-Energy Environ.* 7 (3), e281. doi:10.1002/wene.281

Sun, P., Elgowainy, A., Wang, M., Han, J., and Henderson, R. J. (2018). Estimation of U.S. Refinery Water Consumption and Allocation to Refinery Products. *Fuel* 221, 542–557. doi:10.1016/j.fuel.2017.07.089

Swanson, R. M., Satrio, J. A., Brown, R. C., Platon, A., and Hsu, D. D. (2010). "Techno-Economic Analysis of Biofuels Production Based on Gasification,". NREL/TP-6A20-46587 (Golden, CO: National Renewable Energy Laboratory).

Tanzil, A., Brandt, K., Zhang, X., Wolcott, M., and Garcia-Perez, M. (2021). *Evaluation of Bio-Refinery Alternatives to Produce Sustainable Aviation Fuels in Sugarcane Mill*. Submitted to Fuel

Tanzil, A. H., Brandt, K., Zhang, X., Stockle, C., Wolcott, M., Murthy, G., et al. (2019). *Evaluation of Dry Grind Corn Ethanol Bio-Refinery Concepts for the Production of Alternative Jet Fuels*. Submitted to Biomass and Bioenergy.

Tanzil, A. H., Brandt, K., Wolcott, M., Zhang, X., and Garcia-Perez, M. (2021). Strategic Assessment of Sustainable Aviation Fuel Production Technologies: Yield Improvement and Cost Reduction Opportunities. *Biomass and Bioenergy* 145, 105942. doi:10.1016/j.biombioe.2020.105942

Tanzil, A. H., Zhang, X., Wolcott, M., Brandt, K., Stöckle, C., Murthy, G., et al. (2021). Evaluation of Dry Corn Ethanol Bio-Refinery Concepts for the Production of Sustainable Aviation Fuel. *Biomass and Bioenergy* 146, 105937. doi:10.1016/j.biombioe.2020.105937

Thompson, J. L., and Tyner, W. E. (2014). Corn stover for Bioenergy Production: Cost Estimates and Farmer Supply Response. *Biomass and Bioenergy* 62, 166–173. doi:10.1016/j.biombioe.2013.12.020

US Department of Energy (2011). "U.S. Billion-Ton Update: Biomass Supply for a Bioenergy and Bioproducts Industry. R.D. Perlack and B.J. Stokes (Leads),".

ORNL/TM-2011/224 (Oak Ridge, TN: Oak Ridge National Laboratory), 227. Available at: http://www1.eere.energy.gov/bioenergy/pdfs/billion_ton_update.pdf.

US EIA (2018). *US Annual Average Natural Gas Price*

US EIA (2020a). Petroleum & Other Liquids: US Kerosene-type Jet Fuel Wholesale/Resale Price by Refiners. Available at: https://www.eia.gov/dnav/pet/hist/LeafHandler.ashx?n=pet&s=ema_epjk_pwg_nus_dpg&f=a.

US EIA (2020b). Wholesale Electricity and Natural Gas Market Data. Available at: https://www.eia.gov/electricity/wholesale/.

US Energy Information Administration (2021). Monthly Energy Review. Available at: https://www.eia.gov/totalenergy/data/monthly/pdf/mer.pdf.

US Energy Information Administration (2016). Today in Energy: Much of the Country's Refineries Are Concentrated along the Gulf Coast. Available at: https://www.eia.gov/todayinenergy/detail.php?id=7170.

van Dyk, S., Su, J., McMillan, J. D., and Saddler, J. (2019). Potential Synergies of Drop-in Biofuel Production with Further Co-processing at Oil Refineries. *Biofuels, Bioprod. Bioref.* 13 (3), 760–775. doi:10.1002/bbb.1974

Wallace, R., Ibsen, K., McAloon, A., and Yee, W. (2005). *Co-located Corn Stover to Ethanol with Corn Dry Mill; Excel Spreadsheet*. Springfield, VA: National Renewable Energy Laboratory. Available at: https://www.nrel.gov/extranet/biorefinery/aspen-models/.

West, R. M., Liu, Z. Y., Peter, M., Gartner, C. A., and Dumesic, J. A. (2008). Carbon-carbon Bond Formation for Biomass-Derived Furfurals and Ketones by Aldol Condensation in a Biphasic System. *J. Mol. Catal. a-Chemical* 296 (1-2), 18–27. doi:10.1016/j.molcata.2008.09.001

Wu, L., Wang, Y. Q., Zheng, L., Wang, P. Y., and Han, X. L. (2019). Techno-economic Analysis of Bio-Oil Co-processing with Vacuum Gas Oil to Transportation Fuels in an Existing Fluid Catalytic Cracker. *Energ. Convers. Manag.* 197, 111901. doi:10.1016/j.enconman.2019.111901

Zacher, A. H., Olarte, M. V., Santosa, D. M., Elliott, D. C., and Jones, S. B. (2014). A Review and Perspective of Recent Bio-Oil Hydrotreating Research. *Green. Chem.* 16 (2), 491–515. doi:10.1039/c3gc41382a

Conflict of Interest: The authors declare that the research was conducted in the absence of any commercial or financial relationships that could be construed as a potential conflict of interest.

Publisher's Note: All claims expressed in this article are solely those of the authors and do not necessarily represent those of their affiliated organizations, or those of the publisher, the editors and the reviewers. Any product that may be evaluated in this article, or claim that may be made by its manufacturer, is not guaranteed or endorsed by the publisher.

frontiers in Energy Research

POLICY AND PRACTICE REVIEWS
published: 02 November 2021
doi: 10.3389/fenrg.2021.760713

Qualification of Alternative Jet Fuels

Mark A. Rumizen *

Federal Aviation Administration, Aircraft Certification, Senior Technical Experts Program, Burlington, MA, United States

Historically, the commercial aviation industry has relied on a very limited number of well-proven, conventional fuels for certification and operation of aircraft and engines. The vast majority of today's engines and aircraft were designed and certified to operate on one of two basic fuels; kerosene-based fuel for turbine powered aircraft and leaded AVGAS for spark ignition reciprocating engine powered aircraft. These fuels are produced and handled as bulk commodities with multiple producers sending fuel through the distribution system to airports and aircraft. They are defined and controlled by industry consensus-based fuel specifications that, along with the oversight of the ASTM International aviation fuel industry committee, accommodate the need to move the fuel as a commodity. It was therefore expedient to build upon this framework when introducing drop-in jet fuel produced from non-petroleum feed stocks into the supply chain. The process developed by the aviation fuel community utilizes the ASTM International Aviation Fuel Subcommittee (Subcommittee J) to coordinate the evaluation of data and the establishment of specification criteria for new non-petroleum (alternative) drop-in jet fuels. Subcommittee J has issued two standards to facilitate this process; ASTM D4054—"Standard Practice for Qualification and Approval of New Aviation Turbine Fuels and Fuel Additives", and ASTM D7566—"Standard Specification for Aviation Turbine Fuel Containing Synthesized Hydrocarbons". This paper will describe how the aviation fuel community utilizes the ASTM International consensus-based process to evaluate new candidate non-petroleum jet fuels to determine if these new fuels are essentially identical to petroleum derived jet fuel, and, if they are, to issue specifications to control the quality and performance of these fuels.

Keywords: jet fuel, alternative, sustainable, aviation, qualification, certification, sustainable aviation fuels

OPEN ACCESS

Edited by:
Zia Haq,
United States Department of Energy (DOE), United States

Reviewed by:
Ravi Fernandes,
Physikalisch-Technische Bundesanstalt, Germany
Robert L. McCormick,
National Renewable Energy Laboratory (DOE), United States

***Correspondence:**
Mark A. Rumizen
mark.rumizen@faa.gov

Specialty section:
This article was submitted to Bioenergy and Biofuels, a section of the journal Frontiers in Energy Research

Received: *18 August 2021*
Accepted: *05 October 2021*
Published: *02 November 2021*

Citation:
Rumizen MA (2021) Qualification of Alternative Jet Fuels. Front. Energy Res. 9:760713. doi: 10.3389/fenrg.2021.760713

1 INTRODUCTION

Airworthiness standards are regulations established by the national aviation authorities for oversight of the design and operation of aircraft. The airworthiness standards applicable to the oversight of aviation fuel were a key consideration when developing the industry qualification process for alternative jet fuels. These standards compelled the aviation fuel community to focus on drop-in alternative jet fuels as the most expeditious path to supplanting petroleum-derived jet fuels.

1.1 Aviation Fuel Regulatory Overview

The regulations established by the United States' Federal Aviation Administration (FAA) for oversight of the design and operation of aircraft are called "airworthiness standards". The FAA's airworthiness standards applicable to the design of aircraft and engines consider fuel as an operating limitation, as opposed to a physical part of the product. As an operating limitation, the aviation fuels permitted for use are merely identified by the engine and aircraft manufacturer (OEM), rather than

TABLE 1 | D4054 Tier 1 properties.

COMPOSITION		
Total Acidity (mg KOH/g)	0.10	Max
Aromatics (% by Volume)	25	Max
Sulfur Mercaptan (% by Weight)	0.003	Max
Total Sulfur (% by Weight)	0.30	Max
VOLATILITY		
Distillation Temperature (°C)		
•10% Recovered	205	Max
•50% Recovered	Report	
•90% Recovered	Report	
•Final Boiling Point	300	Max
•Residue (% by Volume)	1.5	Max
•Loss (% by Volume)	1.5	Max
Flash Point (°C)	38	Min
Density at 15°C (kg/m^3)	775–840	
Distillation Slope		
•T50-T10, °C	15	Min
•T90-T10, °C	40	Min
FLUIDITY		
Freezing Point (°C)	–40	Max
Viscosity at –20°C (cSt)	8.0	Max
Viscosity –40°C, mm^2/s	12	Max
COMBUSTION		
Net Heat of Combustion, MJ/Kg	42.8	Min
Smoke Point, mm	25	Min
Smoke Point, mm and Naphthalenes (% by Volume)	18	Min
	3	Max
Derived Cetane Number (DCN)	Report	
CORROSION		
Copper Strip (2 h at 100°C)	No. 1	Max
STABILITY		
Jet Fuel Thermal Oxidative Tester 2.5 h at Control Temperature of 260°C		
Filter Pressure Drop (mm Hg)	25	Max
Tube Deposit Rating	<3, No peacock or abnormal color deposits	
CONTAMINANTS		
Existent Gum (mg/100 ml)	7	Max
Water Reaction Interface	1b	Max
ADDITIVES		
Electrical Conductivity (pS/m) with additive	50–600	
LUBRICITY		
Lubricity, mm	0.85	Max

produced under the OEM's quality control system. This facilitates the handling of aviation fuel as a commodity in a fungible supply system where any fuel producer can supply fuel to any aircraft as long as that fuel meets the requirements specified by the OEM (typically an industry fuel specification such as ASTM). In the supply chain, aviation fuel travels in close proximity to other types of fuel where it is exposed to possible mixing and contamination with other non-aviation fuels such as diesel and gasoline. Other sources of contamination exist at all points in the supply chain, requiring periodic spot checking of fuel quality relative to the specification requirements. Also, jet fuel is shipped in very large batches that can be combined with other jet fuel batches from other sources while in transit, thereby losing initial batch identity and associated fuel property data. Because jet fuel is traded as a commodity, ownership of batches of fuel can change hands several times throughout its journey to the airport.

In recognition of this distribution system and the possible changing nature of liquid fuels, FAA regulations are targeted at the end point of the supply chain; the aircraft. The regulations require the aircraft and engine manufacturer to specify the fuel (or fuels) that are permitted for use on the aircraft, and the regulations then require the aircraft operator (or airline) to only use those fuels listed by the manufacturer. How those fuels are produced, transported, or otherwise handled upstream of the wing of the aircraft is beyond the reach of FAA (and other national aviation authorities) regulations.

1.2 Conventional Jet Fuel

The primary aviation fuel specifications used globally to ensure a jet fuel supply with consistent properties and performance include ASTM International D1655 (ASTM International Standard D1655, 1942), UK MOD Defence Standard 91-091 (Defence Standard 91-091, 1138), and the U.S. military MIL-DTL-83133 (Mil-Dtl-83133, 2430), and MIL-DTL-5624 (Mil-Dtl-5624, 1873). Conventional jet fuel defined in these and other specifications is produced from petroleum and was

originally derived from illuminating kerosene. The jet fuel specifications introduced fuel property criteria to accommodate the operational demands of aviation. As aircraft and engine technology advanced and more demands were placed on the performance of jet fuel, additional criteria were introduced to more tightly control the performance and properties of the fuel. Key criteria necessary to support aircraft operations at the cold temperatures experienced at high altitudes include a −40°C freezing point and a viscosity limit of 8 mm^2/s at −20°C. A thermal stability test method was developed and criteria added to the specification to prevent fuel system deposit formation at the high operating temperatures experienced in gas turbine engine fuel systems. The complete list of criteria can be found in **Table 1** of ASTM International D1655 (ASTM International Standard D1655, 1942).

Contemporary jet fuel derived from petroleum and produced in accordance with ASTM International D1655 (ASTM International Standard D1655, 1942) is comprised of a mix of hydrocarbons that typically range from eight to fifteen carbon atoms. These hydrocarbons are comprised of approximately 60% paraffins, 25% cycloparaffins, and 15% aromatics, but note that these concentrations do vary somewhat with each batch of jet fuel. The properties and composition of conventional jet fuel form the basis for comparison when evaluating alternative jet fuels.

1.3 Drop-In Alternative Jet Fuels

Prompted by supply security and environmental concerns with petroleum, the aviation fuel community formed the Commercial Aviation Alternative Fuel Initiative (CAAFI®) coalition in 2006 to promote the development and deployment of alternative aviation fuels. One of the key initial decisions of the organizers was to limit the scope of their effort to drop-in jet fuels. These fuels are defined as have essentially identical properties and composition relative to the existing petroleum-derived jet fuel that is currently used by the today's fleet of commercial and military aircraft. As essentially identical jet fuels, the alternative jet fuels would then be compatible with the existing fleet of aircraft and jet fuel distribution infrastructure. Additionally, because these fuels would be considered the same Jet A/A-1 fuel already approved for use on virtually all commercial aircraft, no special regulatory approval would be required to operate with the fuels. Consequently, CAAFI looked to ASTM International to develop standards to support the evaluation and issuance of specifications for drop-in alternative jet fuels to facilitate the entry into service of these fuels.

ASTM International subcommittee D01. J oversees aviation fuel specifications. The subcommittee is comprised of stakeholders from all elements of the production/distribution/operational supply chain, such as petroleum refining, pipelines, ground handling equipment (such as filtration systems), test instruments, engine/aircraft manufacturers, airlines, military, and government agencies such as the Federal Aviation Administration (FAA). The alternative jet fuel qualification process described below initially relies on the technical review of the engine and aircraft manufactures to determine if the proposed fuel is fit for purpose for aviation. After that hurdle is passed, then the new proposed specification along with supporting data is balloted to the entire ASTM International subcommittee D02. J to assure compatibility with the remainder of the supply chain.

2 OVERVIEW OF THE QUALIFICATION PROCESS

ASTM D4054, "Standard Practice for Evaluation of New Aviation Turbine Fuels and Fuel Additives" (ASTM International Standard D4054, 1942), describes the test and evaluation program created by the members of ASTM's aviation fuel subcommittee to compare the properties and performance of alternative jet fuels to those of petroleum-derived jet fuels. The very rigorous and comprehensive test program defined in D4054 is necessary due to the critical role that jet fuel plays in the safe operation of an aircraft. If, after reviewing the data, the subcommittee members agree that the candidate alternative jet fuel is essentially identical to petroleum-derived jet fuel, then specification criteria for the new alternative jet fuel is incorporated into the drop-in fuel specification; D7566, "Standard Specification for Aviation Turbine Fuel Containing Synthesized Hydrocarbons."

ASTM D4054 is intended to be a guideline, not a prescriptive document. As such, it provides a candidate alternative jet fuel producer with information regarding testing and property targets necessary to evaluate the proposed fuel. D4054 is an iterative process, which requires the candidate fuel developer to test samples of fuel to measure properties, composition, and performance and to then periodically review those results with key aviation fuel industry stakeholders such as engine and aircraft manufacturers. These reviews typically result in questions and comments that in turn might drive the need for additional testing. The testing is divided into four tiers as described in the following sections.

2.1 Tier 1: Basic Specification Properties

The jet fuel specifications described above list fuel property criteria for jet fuel produced from petroleum, shale oil or tar sands, but may also include additional criteria for jet fuel produced from alternative raw materials. The criteria listed in these specifications are not considered sufficient for determining the suitability of jet fuels made from all other raw materials, but they do represent the minimum required performance of a jet fuel. The typical specification properties are summarized in **Table 1**. The Tier 1 testing requirements are relatively inexpensive (approximately $5,000) (ASTM, 2018) and require only small quantities of fuel (less than 10 gallons).

2.2 Tier 2: Fit-For-Purpose Properties

The specification properties tested in Tier 1 represent a subset of the jet fuel properties that must be controlled to ensure safe and proper aircraft and engine operation. There are many other properties that are inherent in petroleum-derived jet fuel and therefore are not listed in the jet fuel specifications. These properties, which are called Fit-For-Purpose (FFP) properties,

do not need to be routinely measured because they are relatively consistent for jet fuels produced from petroleum using conventional, well-understood refining processes. However, it is necessary to measure FFP properties for fuels produced from other materials, such as renewable feedstocks, to determine if the alternative jet fuel is acceptable for use on current or future technology aircraft and engines. These tests cost up to $50,000 (ASTM, 2018) and may require up to 100 gallons of fuel (ASTM, 2018). An overview of the FFP properties is provided below.

2.2.1 Chemical Composition

The concentration of hydrocarbons and trace materials are measured using advanced analytical chemistry methods such as two-dimensional gas chromatography. This test method provides the concentration of each hydrocarbon compound class (isoparaffin, normal paraffin, cycloparaffin, and aromatic) along with the carbon number distribution within each of these classes. The results are then compared to the typical composition petroleum-derived jet fuels. Significant differences to this compositional footprint might drive the need for additional testing. High concentrations of materials that are normally at trace levels in jet fuel (ASTM International Standard D4054, 1942), such as metals or oxygenates, may also be cause for further investigation.

2.2.2 Bulk Physical and Performance Properties

Predictable variation of fuel properties over the operating range of the aircraft and engine is necessary for safe and proper operation of the fuel, combustion, and hydraulic systems. The temperature dependencies of fuel properties such as density, surface tension, viscosity, and permittivity are compared with those of conventional jet fuel. These properties have been found to be linear functions of temperature for pure hydrocarbon fuels, except for isentropic bulk modulus which is influenced by the speed of sound (Heyne, 2021). These properties will be consistent with typical jet fuels if the hydrocarbon composition is similar to conventional jet fuel.

2.2.3 Electrical Properties

Dielectric constant (or permittivity) and conductivity are the electrical properties evaluated under D4054. The dielectric constant of a fuel is the ratio of the electrical capacitance of a fuel to the electrical capacitance of air. This property can influence the accuracy of aircraft fuel quantity indicating systems that rely on fuel tank capacitance probes to measure the fuel level. Dielectric constant is measured relative to density because many of these systems compensate for fuel density (Mil-Hdbk-510A, 2017). The other property, electrical conductivity, is related jet fuel's ability to readily dissipate static electricity which has built up during transportation of the fuel. This is an important safety concern because electrostatic sparks in the proximity of jet fuel can cause explosive response and associated fire. The response of a fuel's electrical conductivity to the addition of Static Dissipator Additive (SDA) is evaluated to ensure the alternative jet fuel responds in the same manner as conventional jet fuel.

2.2.4 Ground Handling Properties and Safety

The fuel's compatibility with existing ground filtration systems is evaluated along with its storage stability, toxicity and flammability. These evaluations are conducted to ensure that the alternative jet fuel can be handled in the same manner as conventional jet fuel.

2.2.5 Compatibility With Approved Additives

The solubility of all currently approved jet fuel additives is evaluated over the operating temperature range of the aircraft to ensure that there are no limitations on use of the additives.

2.2.6 Preliminary Compatibility With Engine and Airframe Seals

Three types of elastomeric seals are soak-tested with the candidate fuel to determine if they respond differently than when soaked in conventional jet fuel. The results of this testing are used to determine if more extensive material compatibility testing is required in Tier 3.

2.3 Tier 3: Engine/Aircraft Systems Rig and Component Testing

The scope of the Tier 3 and Tier 4 testing is based on the evaluation of the Tier 1 and 2 data. The ASTM committee relies on the expertise of the aircraft and engine OEMs to determine this scope due to complexity and advanced technologies of modern gas turbine engines and aircraft, and because Tier 3 and 4 tests typically require the use of OEM specialized equipment, rigs, and facilities. The amount of fuel required for these tests can vary widely from 250 to 15,000 gallons depending on the types of tests required and the cost can be as high as $1.5M. An overview of typical Tier 3 tests is provided below:

2.3.1 Compatibility With Engine and Airframe Seals, Coatings and Metallics

A wide range of materials that represents the current aircraft fleet are soak-tested in the candidate fuel to determine if they respond in the same manner as with conventional Jet A. The list of materials to be tested includes 37 non-metallics and 31 metals (ASTM International Standard D4054, 1942). The scope of this testing will depend on the compositional similarity to conventional Jet A fuel and the results of the preliminary materials compatibility testing.

2.3.2 Turbine Hot Section Testing

Hot section parts such as turbine blades or nozzles are evaluated for corrosive attack by exposure to a high temperature flame from combustion of the candidate alternative fuel on a burner rig.

2.3.3 Fuel System Testing

This includes such tests as fuel component acceptance testing, fuel nozzle (atomizer) spray testing, and atomizer plugging under cold operating conditions.

2.3.4 Combustor Rig Testing

This testing evaluates combustor operability, performance, durability, or emissions when operating with the alternative jet fuel. A full-scale combustor is installed in a test chamber where pressures and temperatures across the engine operating envelope can be simulated. Typical tests include cold starting, lean blowout at high altitude/low power conditions, turbine inlet temperature distribution, and gaseous and smoke emissions.

2.3.5 Auxiliary Power Unit Tests

Ignition tests on full-scale APUs are conducted at cold and altitude conditions in addition to combustor rig tests described above.

2.3.6 Aircraft Fuel System Rig Testing

Tests that have been conducted include ice accretion tests on aircraft fuel system rigs and fuel level measurement accuracy.

2.4 Tier 4: Full-Scale Engine Testing or Aircraft Flight Testing

Full-scale engine tests may be required to evaluate performance, operability, emissions or long-term durability when operating with the candidate alternative jet fuel. Engine tests may require up to 200,000 gallons of fuel and may cost up to $1M (ASTM, 2018). Emissions testing can typically be accomplished concurrently with other engine tests. Aircraft flight tests are typically not required, as it is difficult to cover the critical areas of the flight envelope during a flight test, but in some cases they may be necessary. Aircraft flight testing is typically focused on performance and operability characteristics. Fuel consumption is measured, in-flight restarts and throttle transients are accomplished. The testing may also include aircraft fuel system dedicated tests such as fuel boost pump operation and fuel transfer between fuel tanks.

3 PROCESS IMPROVEMENTS TO THE QUALIFICATION PROCESS

3.1 Pre-Screening of Candidate Alternative Jet Fuels

The D4054 process is a resource intensive process for both the prospective alternative jet fuel producer and the reviewing community. It typically requires a demo-scale production capability to produce the 50 to 100 gallons of fuel required for evaluation and testing, and results in reports that contain up to several hundred pages. Research conducted under the U.S. National Jet Fuel Combustion Program (NJFCP) (Colket et al., 2017) and the European JETSCREEN program (Rauch, 2020) provided the analytical tools to enable very small volumes of candidate alternative jet fuel to be analyzed to determine viability for use in aircraft. While not part of the D4054 process, these Pre-Screening analytical tools and methods that are now available from CAAFI (CAAFI). They enable developers of alternative jet fuel to refine their processes using laboratory-scale equipment and very small fuel volumes to produce products that are more likely to successfully complete the above described qualification process before investing in process scale-up. Pre-Screening utilizes advanced analytical methods such as two-dimensional gas chromatography, mid-infrared absorption, and nuclear magnetic resonance, along with testing of physical properties such as viscosity, distillation curve, mass density, flash point, derived cetane number (DCN), and surface tension.

3.2 ASTM D4054 Fast Track Process

The ASTM D4054 process described above includes extensive test and evaluation requirements and therefore requires a significant level of resources to accomplish. This was necessary to ensure the fit for purpose of the candidate alternative jet fuel for use on aircraft and engines. The ASTM International subcommittee J, in close cooperation with the engine and aircraft manufactures, reviewed past data accumulated from testing and evaluation of the approved alternative jet fuels. It was agreed that reduced testing requirements could be made available to producers of new alternative jet fuel blending components that fell within compositional and performance range of a typical conventional jet fuel. These reduced testing requirements were incorporated as Annex A4 of D4054 in September 2020 and called the Fast Track process. The annex specifies target values as a guideline and starting point for the evaluation of candidate alternative jet fuels for entry into the fast track process. The target values were established to characterize a nominal jet fuel with mid-range properties and with a typical hydrocarbon composition. For example, maximum and minimum temperature limitations are specified for distillation points across the entire distillation range, and specially developed gas chromatographic methods are specified for detailed identification of hydrocarbon molecular classes and distribution and polar molecules. The Fast Track annex imposes a 10% maximum blending limit as a tradeoff with the reduced testing requirements.

4 THE PRODUCT OF THE EVALUATION PROCESS; A NEW SPECIFICATION ANNEX

4.1 ASTM D7566: The Drop-In Fuel Specification

ASTM D7566—"Standard Specification for Aviation Turbine Fuel Containing Synthesized Hydrocarbons" (ASTM International Standard D7566, 1942) is a stand-alone specification that is separate and distinct from the petroleum-derived (or conventional) jet fuel specification D1655. The decision to issue a separate specification was driven by the need to incorporate more stringent criteria for these new fuels that were lacking any demonstrable service experience, and by the concern from petroleum producers of this more stringent criteria being applied to their mature, well understood fuels. D7566 also includes a provision to allow "re-designation" of D7566 jet fuel

batches to D1655 fuel to enable these new fuels to fit within the existing jet fuel supply and operational infrastructure which based on the D1655 conventional jet fuel specification. This resulted in a stand-alone specification that provided more stringent criteria for production, yet enabled seamless integration into the existing infrastructure including meeting existing certification requirements.

The initial conversion processes considered for incorporation into D7566 produced hydrocarbon products that were compositional subsets of a typical conventional jet fuel. For example, both the Fischer-Tropsch process (see *A1: Fischer-Tropsch Hydroprocessed Synthesized Paraffinic Kerosene* below) and the HEFA process (see *A2: Synthesized Paraffinic Kerosene From Hydroprocessed Esters and Fatty Acids* below) result in a pure paraffinic fuel, lacking the 8–20% aromatic concentration found in conventional jet fuel. Therefore, blending with conventional jet fuel was necessary to create a jet fuel composition with an aromatics concentration and density that was within the experience base of conventional jet fuel. For those alternative jet fuels that had a composition that was consistent with conventional jet fuel, such as Annex A4 Fischer-Tropsch Synthesized Paraffinic Kerosene with Aromatics (FT-SPK/A) (see *A4: Synthesized Kerosine With Aromatics Derived by Alkylation of Light Aromatics From Non-petroleum Sources* below) and Annex A6 Catalytic Hydrothermolysis Jet (CHJ) (see *A6: Synthesized Kerosene From Hydrothermal Conversion of Fatty Acid Esters and Fatty Acids* below), a 50% maximum blending limit was imposed as a conservative approach to entry into service. To accommodate the need for blending, a two-step approach was implemented where first the alternative jet fuel must meet criteria specified in an annex unique to that fuel, then after blending with conventional jet to below a prescribed limit, the finished jet fuel is again tested to criteria specified in the main body of the specification.

The property tables in each annex also are a key, unique characteristic of D7566. Each annex contains two of these tables, the first of which specifies primarily physical properties such as density, freezing point, distillation and thermal stability, which must be measured for each batch of fuel. The second table specifies compositional criteria intended to support management of change events such as the start of production, significant changes to the process, or as necessary to support continued production of a consistent, high quality product. However, currently all of the annexes except Annex A1 require measurement of these properties for each batch of alternative fuel blend component. As more experience is gained with fuel produced to the other annexes, the testing requirements for the second tables will be moved from batch frequency to a management of change frequency (ASTM International Standard D7566, 1942).

4.2 Overview of the D7566 Annexes

There are currently seven annexes in D7566 that have been periodically added since the initial issuance of the specification in 2009. The issuance of each annex followed a rigorous testing program conducted in accordance with D4054 as described above and balloting to the ASTM membership. Each annex includes a description of the conversion process, feedstock, and composition of the resulting alternative fuel along with property requirements that the alternative fuel must meet.

4.2.1 A1: Fischer-Tropsch Hydroprocessed Synthesized Paraffinic Kerosene

The FT-SPK process specifies a feed stock of carbon monoxide and hydrogen synthesis gas. This synthesis gas is produced from the gasification of coal or biomass, reforming of natural gas, or other means of producing hydrogen and carbon. The synthesis gas is converted to a liquid hydrocarbon product in the FT reactor that is comprised primarily of isoparaffins. Typical refinery processing techniques such as hydroprocessing or isomerization are then used to produce a jet fuel blending component primarily composed iso-paraffins distributed across the jet fuel carbon number range. The Annex allows blending up to 50% by volume FT SPK with Jet A, subject to property limitations such as density and aromatics concentration on the final blended jet fuel. Blending is required to add the normal paraffins, cycloparaffins and aromatics that are absent from the FT-SPK.

4.2.2 A2: Synthesized Paraffinic Kerosene From Hydroprocessed Esters and Fatty Acids

The annex defines the feed stocks as mono-, di-, and tri-glycerides, free fatty acids and fatty acid esters. Typical tri-glyceride feed stocks are soybean, algae, other plant oils, or tallow. The HEFA conversion process consists of a catalytic deoxygenation step followed by hydroprocessing. Similar to FT, HEFA consists of primarily iso-paraffins in the jet fuel carbon number range and exhibits similar properties, and may be blended up to 50% by volume with Jet A due to similar property limitations. Similar to FT-SPK, blending is required to add the normal paraffins, cycloparaffins, and aromatics that are absent from the HEFA.

4.2.3 A3: Synthesized Iso-paraffins From Hydroprocessed Fermented Sugars

The alternative jet fuel blending component specified in this annex is a single hydrocarbon compound called farnesane (2,6,10-Trimethyldodecane). An intermediate hydrocarbon product (an olefin) is produced from the fermentation of sugars using a genetically engineered microorganism. This is followed by hydroprocessing to produce the farnesane iso-paraffin final product. Petroleum-derived jet fuel consists of a range of hydrocarbons containing from 8 to 16 carbon atoms that supports stable combustion across the wide range of gas turbine engine operating conditions, but farnesane is a single hydrocarbon molecule containing 15 carbon atoms. To avoid overloading the blended jet fuel with hydrocarbons in one slice of the compositional distribution, SIP is limited to a 10% blend concentration.

4.2.4 A4: Synthesized Kerosine With Aromatics Derived by Alkylation of Light Aromatics From Non-petroleum Sources

This conversion process is an adaptation of the FT-SPK process specified in Annex A1 that produces a similar alternative jet fuel

blend component, but with aromatics. It co-processes a benzene-rich stream that is a by-product of coal gasification with the C3 and C4 olefins produced by the FT reactor during the downstream polymerization process step to produce alkylated aromatics along with isoparaffinic kerosene. The result is FT-SPK plus 15–20% aromatics and is called FT-SPK/A. The feed stocks, property limitations and blending limits are all similar to Annex A1. Because FT-SPK/A is compositionally identical to petroleum-derived Jet A fuel, there are not any property limitations that necessitate blending of FT-SPK/A with conventional jet fuel. However, a maximum 50% blending limit was specified to allow the accumulation of service experience prior to permitting its use unblended.

4.2.5 A5: Alcohol-To-Jet Synthetic Paraffinic Kerosene

The conversion process described in this annex converts alcohol to an alternative jet fuel blending component. The process first dehydrates the alcohol to remove oxygen resulting in hydrocarbon olefins. Next, the olefins are oligomerized into higher molecular weight olefins (or unsaturated oligomers). The unsaturated oligomers that have molecular weights within the jet fuel range are separated and hydroprocessed to saturate the olefins into paraffins, resulting in the final ATJ-SPK jet fuel for blending purposes. ATJ-SPK is comprised primarily of isoparaffins and may currently be blended with conventional jet fuel at a 50% concentration to attain the other hydrocarbon molecular classes and to meet jet fuel property limits.

4.2.6 A6: Synthesized Kerosene From Hydrothermal Conversion of Fatty Acid Esters and Fatty Acids

The Annex A6 conversion process is called Catalytic Hydrothermolysis Jet (CHJ). The CHJ process consists of hydrothermal conversion and hydrotreating of the same feed stock that HEFA uses resulting in a fully-formulated alternative jet fuel (including aromatics) with a similar distribution of hydrocarbon molecular classes and carbon number distribution. Because CHJ is compositionally identical to petroleum-derived Jet A fuel, there are not any property limitations that necessitate blending of CHJ with conventional jet fuel. However, a maximum 50% blending limit was specified to allow the accumulation of service experience prior to permitting its use unblended.

4.2.7 A7: Synthesized Paraffinic Kerosene From Hydroprocessed Hydrocarbons, Esters and Fatty Acids (HC-HEFA)

The process is the same as the Annex A2 HEFA conversion process and produces a mix of isoparaffins, normal paraffins, and cycloparaffins in the jet fuel carbon number range. However, this process specifies a different feed stock which is comprised of hydrocarbons in addition to free fatty acids and fatty acid esters. The Botryococcus braunii algae produces this feed stock, which is an oil containing a high percentage of unsaturated hydrocarbons known as botryococcenes, instead of triglycerides or fatty acids that other species of algae produce. This annex was the first to be approved under theD4054 Fast Track. As discussed earlier, the blend ratio of HC-HEFA with conventional jet fuel is limited to 10% maximum as required under the Fast Track process.

5 REGULATORY BASIS FOR USE OF ASTM D7566 DROP-IN ALTERNATIVE JET FUELS

Successful completion of the ASTM D4054 evaluation program that culminates in the issuance of an ASTM D7566 annex is aligned with the existing jet fuel approval basis for virtually all gas turbine powered aircraft operating around the globe. This in turn, enables use of D7566 fuels on these aircraft. This regulatory basis has been confirmed by the FAA and is documented in SAIB NE-11-56 (FAA Special Airworthiness Information Bulletin, 1956) and described below.

5.1 Existing Jet Fuel Approval Basis

Jet A or Jet A-1 fuel is the fuel specified for use on most turbine engine-powered aircraft currently in use or entering into service. Globally, many different specifications are used to define and control Jet A/A-1 fuel, but all are based on two primary specifications; ASTM D1655 or DEF STAN 91-091. As discussed earlier in this paper, this fuel definition is a regulatory requirement for each aircraft and engine manufacturer and any fuel that meets the Jet A/A-1 specification can be used on these aircraft.

5.2 Jet A/A-1 Comparison

As described previously, ASTM has issued standard practice D4054 that defines the testing required to compare the physical properties, chemical composition, and materials compatibility of candidate alternative jet fuels to typical petroleum-derived Jet A/A-1 fuels. If the test data indicates that the candidate alternative jet fuel is essentially identical to petroleum-derived jet fuel, then the ASTM subcommittee will take action to designate it as Jet A/A-1 fuel.

5.3 Incorporation Into the Drop-In Fuel Specification

If the candidate alternative jet fuel is concluded to be essentially identical to Jet A/A-1, the ASTM subcommittee will approve a ballot to add it to ASTM D7566, the drop-in jet fuel specification, as a new annex. The annex will include all of the necessary information to describe and control the new alternative fuel, such as descriptive criteria for the feed stock, conversion process, and composition, along with prescriptive criteria for the physical properties and composition. As described in the previous section, all of the fuels defined in the D7566 annexes currently specify a maximum blending percentage for blending with conventional jet fuel. D7566 is structured to require two testing steps when producing the annex fuel. First, each batch of alternative fuel must be tested to the annex criteria. In the second step, testing of the finished jet fuel after blending with the annex fuel to the criteria in the main body of the specification is required.

5.4 Re-Designation as ASTM D1655 Jet A/A-1 Fuel

Both ASTM D7566 and ASTM D1655 include language that allows the re-designation of D7566 fuel as D1655 Jet A/A-1 fuel.

This is deemed acceptable because the criteria in D7566 is more stringent than the criteria in D1655, and therefore every batch of D7566 fuel will comply with the D1655 specification requirements.

As a result of the re-designation, the alternative jet fuel is now considered a Jet A/A-1 fuel and therefore meets the certificated aviation fuel operating limitations of virtually all turbine engine-powered aircraft. It now meets the existing certification basis and can be used without any limitations, restrictions, or special handling provisions, effectively meeting the existing approval basis described above. The new fuel can seamlessly enter the jet fuel supply chain without any additional approvals. In summary, the approval to fly with a particular alternative jet fuel annex in D7566 is granted via issuance of that annex in D7566.

6 CONCLUSION

The aviation fuel community has established a collaborative approach to evaluating and approving alternative jet fuels that utilizes the expertise of key stakeholders via the ASTM International consensus-based specification process. The alternative jet fuels that result from this process have essentially identical properties and composition which enables seamless entrance into the existing, well-established jet fuel supply infrastructure without any special handling or accommodations. Additional approvals from the national aviation authorities are not required and these fuels can be used on virtually all existing gas-turbine powered aircraft without any modifications. This process, developed by CAAFI and the FAA, lowers one of the many barriers to entry of sustainable aviation fuels into the aviation fuel supply chain and therefore contributes to reducing aviation's carbon emissions.

AUTHOR CONTRIBUTIONS

The author confirms being the sole contributor of this work and has approved it for publication.

REFERENCES

ASTM (2018). "ASTM D4054 Clearinghouse Guide https://s3.wp.wsu.edu/uploads/sites/192/2018/03/clearinhouse.pdf.

ASTM International Standard D1655 (1942). "*Standard Specification for Aviation Turbine Fuels*.", ASTM International, West Conshohocken, PA, USA: –2959.

ASTM International Standard D7566 (1942). *Standard Specification for Aviation Turbine Fuel Containing Synthesized Hydrocarbons*", ASTM International, West Conshohocken, PA, USA .

ASTM International Standard D4054 (1942). "*Standard Practice for Qualification and Approval of New Aviation Turbine Fuels and Fuel Additives*", ASTM International, West Conshohocken, PA, USA .

CAAFI Prescreening Guidance for Alternative Jet Fuels". Available:https://caafi.org/tools/Prescreening_Guidance.html.

Colket, M. B., Heyne, J. S., Rumizen, M., Edwards, J. T., Gupta, M., Roquemore, W. M., et al. (2017). An Overview of the National Jet Fuels Combustion Program. Reston, VA: *AIAA Journal* 55.

Defence Standard 91-091 *Turbine Fuel, Aviation Kerosine Type, Jet A-1 NATO Code: F-35, Joint Service Designation: AVTUR*", Issued by the United Kingdom (U.K.) Ministry of Defence. Glasglow, UK, https://www.dstan.mod.uk/.

FAA Special Airworthiness Information Bulletin. (1956). *NE-11-56, "Engine Fuel and Control - Semi-Synthetic Jet Fuel*", FFA Aviation Safety, Washington, DC, USA, https://www.faa.gov/aircraft/safety/.

Heyne, J., "*Fuel Effects on Operability of Aircraft Gas Turbine Combustors*", AIAA, Reston, VA, USA, (2021).

Mil-Dtl-5624 (1873). *Detail Specification, Turbine Fuel, Aviation, Grades JP-4 and JP-5*. Lakehurst, NJ: Naval Air Warfare Center, Aircraft Division. https://assist.dla.mil.

Mil-Dtl-83133 (2430). *Detail Specification, Turbine Fuel, Aviation, Kerosene Type*, AFPET/PTPS, Dayton, OH, USA. https://assist.dla.mil.

Mil-Hdbk-510A, (2017). *Aerospace Fuels Certification*, AFLCMC/EN-EZ, Dayton, OH, USA. Standards@us.af.mil https://assist.dla.mil.

Rauch, B. "Jetscreen" Available:.

Conflict of Interest: The author declares that the research was conducted in the absence of any commercial or financial relationships that could be construed as a potential conflict of interest.

frontiers in Energy Research

POLICY AND PRACTICE REVIEWS
published: 15 November 2021
doi: 10.3389/fenrg.2021.750514

Regulatory and Policy Analysis of Production, Development and Use of Sustainable Aviation Fuels in the United States

Ekrem Korkut[1] *and Lara B. Fowler*[2]*

[1]Penn State Law, Penn State University, University Park, PA, United States, [2]Penn State Institutes of Energy and the Environment, Penn State Law, Penn State University, University Park, PA, United States

OPEN ACCESS

Edited by:
Kristin C. Lewis,
Volpe National Transportation Systems Center, United States

Reviewed by:
Jon Strand,
World Bank Group, United States
Colin Murphy,
University of California, Davis, United States

***Correspondence:**
Lara B. Fowler
lbf10@psu.edu

Specialty section:
This article was submitted to Bioenergy and Biofuels, a section of the journal Frontiers in Energy Research

Received: *30 July 2021*
Accepted: *22 October 2021*
Published: *15 November 2021*

Citation:
Korkut E and Fowler LB (2021) Regulatory and Policy Analysis of Production, Development and Use of Sustainable Aviation Fuels in the United States. Front. Energy Res. 9:750514. doi: 10.3389/fenrg.2021.750514

The United States, spurred in part by international developments, is expanding its law and policy to incentivize the use of sustainable aviation fuels. While the U.S. has agreed to participate in the International Civil Aviation Organization's (ICAO's) Carbon Offsetting and Reduction Scheme for International Aviation (CORSIA), it has only recently adopted federal rules that define greenhouse gas emission reduction standards for certain classes of airplanes (effective January 2021). However, such standards focus on engine efficiency rather than the fuel burned. For sustainable aviation fuels, the U.S. continues to rely on voluntary programs at a federal, state, and regional level. The federal Renewable Fuel Standard program allows producers to opt in. In addition, states have started to allow sustainable aviation fuel producers to "opt in" to their programs; this includes California's Low Carbon Fuel Standard, Oregon's Clean Fuels Program, and Washington's newly adopted Clean Fuels Program. Other states are also starting to consider such programs. Elsewhere, states like Hawaii are starting to support SAF production in other ways, including through tax mechanisms. In addition, regional and private efforts to adopt and/or promote sustainable aviation fuels are underway. This piecemeal approach—due in part to the lack of cohesive U.S. federal policy—stands in contrast to the European Union's Renewable Energy Directive and Emissions Trading System, and adoption of policies by European countries. Because of aviation's international nature, tracking what is happening in Europe matters greatly for U.S. carriers. As the U.S. works to meet its international obligations through CORSIA, finding a way forward with sustainable aviation fuel in the United States may depend on a more defined federal policy. Actions taken by both the EU and European countries offers some guidance for actions that could be taken by the U.S. Even in the absence of more defined measures, better tracking of voluntary measures is a critical step.

Keywords: aviation emissions, sustainable aviation fuel (SAF), SAF mandate, renewable jet fuel, Low Carbon Fuel Standard (LCFS), corsia

INTRODUCTION

Consistent law and policy guidance for sustainable aviation fuel (SAF) is critical to ensure emission reductions from aviation, both for U.S. carriers flying domestically and internationally. Although airline miles flown decreased temporarily due to COVID-19, airline travel had been increasing significantly and is expected to do so again. As the largest emitter of CO_2 from aviation, the U.S. has up until now depended on voluntary activities related to SAF to reduce such emissions.

As part of the International Civil Aviation Organization (ICAO), the U.S. has agreed to legal regulation of greenhouse gas (GHG) emissions from aircraft. The U.S. is starting to do so by implementing ICAO standards and recommended practices. During the last decade, this includes the development and implementation of CO_2 emission standards and the Carbon Offsetting and Reduction Scheme for International Aviation (CORSIA). While U.S. federal policy is starting to adapt to these international commitments, state, regional and private initiatives for reducing aviation-related GHG emissions by increasing the use of SAF may be the driver necessary to support more aggressive federal action.

According to the Intergovernmental Panel on Climate Change (IPCC), aviation is estimated to generate 2% of anthropogenic CO_2 emissions. According to a study published by the International Council on Clean Transportation, the United States was the biggest CO_2 emitter from the aviation sector in 2018, followed by China (Graver et al., 2019, p. 6). China is expected to replace the U.S. as the world's largest passenger market by 2029 (IATA, 2015). Aviation emissions also include nitrogen oxide, water vapor, particulate matter, and other pollutants. In the U.S., aircraft emissions constituted about 2.7% of total GHG emissions in 2019 (EPA, 2021, at 2–37). Although greenhouse gas emissions in the U.S. from the aviation sector overall decreased by 4% (7.9 MMT CO_2) between 1990 and 2019, which includes a 66% (23.1 MMT CO_2) decrease in GHG emissions from domestic military operations, GHG emissions from the domestic operation of commercial aircrafts increased by 22% (24.3 MMT CO_2) from 1990 to 2019 (**Figure 1**; EPA, 2021, at 3–24). From 2003 to 2017, revenue passenger miles in the U.S. increased from 657.3 billion to 964.3 billion, and people taking flights increased from 647.5 million passengers to 849.3 million passengers (Bureau of Transportation Statistics, 2018). While there were 1,054.79 billion revenue passenger miles in 2019, this decreased to 377.99 billion in 2020 due to the COVID-19 pandemic (Mazareanu, 2021).

Despite the increase in passengers around the world on average of 5% percent each year prior to the coronavirus outbreak, aviation has decoupled its emissions growth to around 3% due to advancements in new technology and coordinated action to implement new operating procedures (Air Transport Action Group, 2017, p. 2). Consistent law and policy incentives would continue this advancement.

Although the use of sustainable aviation fuel is considered an important element for further reducing aviation's impacts on the climate change and improving air quality (ICAO, 2016a, p. 153), not all SAF produce less emissions than the petroleum displaced. For example, biodiesel produced from the first rotation cycle of palm produces 98% more emission than the fossil fuel (Meijide et al., 2020, p. 4). A life cycle assessment of each type of SAF is beyond the scope of this review.

What counts as "sustainable aviation fuel" in turn depends on a number of definitions. In general, SAF is fuel produced from renewable and waste resources—such as biological and non-biological resources—that help provide an ecological balance by avoiding depletion of natural resources and reducing climate change impacts (Air Transport Action Group, 2017, p. 4). CORSIA specifically defines sustainable aviation fuel as "a renewable or waste-derived aviation fuel that meets the CORSIA Sustainability Criteria" under Volume IV, Annex 16 of the

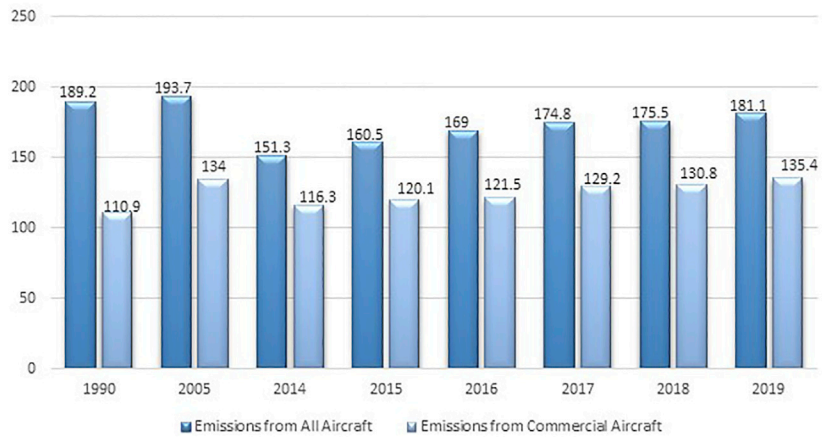

FIGURE 1 | GHG Emissions from domestic aircraft operation in the U.S. (EPA, 2021, at 3–24; prepared based on data from EPA Inventory of U.S. Greenhouse Gas Emissions and Sinks: 1990–2019).

Convention on the International Civil Aviation (ICAO, 2018). There are two criteria for CORSIA sustainable aviation fuels: 1) "CORSIA eligible fuel should generate lower carbon emissions on a life cycle basis," at least 10% compared to the aviation fuel on a life cycle basis; 2) "CORSIA eligible fuel should not be made from biomass obtained from land with high carbon stock" (ICAO, 2019). Sustainable aviation fuel is considered an alternative to fossil fuel sources because it includes any materials or substances that can be used as fuels, other than conventional fossil sources (CAAFI, n.d.a). Drop-in fuels can be used "as is" in engines that operate with only conventional fuel and do not require adaptation of the fuel distribution network or the engine fuel systems. The term "drop-in" refers to alternative jet fuels that are entirely compatible with a conventional jet fuel in terms of materials, safety, and composition (CAAFI, n.d.b).[1]

ASTM International has certified seven SAF production pathways; additional pathways are being evaluated. In 2009, ASTM International approved the FT-SPK method (Fischer-Tropsch Synthetic Paraffinic Kerosene), which allows for biomass converted to synthesis gas and then into the aviation fuel. In 2011, HEFA-SPK pathway (Hydroprocessed Esters and Fatty Acids), hydroprocessing of oil and fats, was approved under D7566-11. In 2014, HFS-SIP method (Hydroprocessed Fermented Sugars to Synthesized Iso-Paraffinic) was approved; this is the microbial conversion of sugars to a hydrocarbon. In 2016, ATJ-SPK (Alcohol to Jet Synthetic Paraffinic Kerosene) was certified; this involves upgrading of alcohols from sugars or cellulose to jet fuels. In 2018, FT-SPK/A, a variation of FT-SPK "where alkylation of light aromatics creates a hydrocarbon blend that includes aromatic compounds" was approved (European Union Aviation Safety Agency et al., 2019, p. 42). Catalytic Hydrothermolysis Jet (CHJ) was approved on December 15, 2019, and published as ASTM D766 Annex A6. The biofuel is produced using the isoconversion process which converts waste fats, oils, and greases into jet fuel (Biofuels International, 2020). The seventh pathway for SAF production, HC-HEFA, was approved in May 2020 as Annex 7 to ASTM's SAF specification D7566, which establishes criteria for the production of a type of synthesized paraffinic kerosene from hydrocarbon-hydroprocessed esters and fatty acids (Green Car Congress, 2020).

The International Civil Aviation Organization (ICAO) indicated that if enough alternative fuels were produced in 2050 to substitute for conventional jet fuel, projected CO_2 emissions could be decreased by 63% from international flights (ICAO, 2016a, p. 19). Certification of seven different types of sustainable jet fuel makes this at least possible (CAAFI, n.d.b). The certification process allows a maximum blend of 50% (SAF with conventional jet fuel) for some technologies. ICAO is leading the efforts to prepare international agreements and aspirational targets on how to achieve such reductions.

In the U.S., SAF use by airlines has been largely voluntary to date. This policy review paper explores the legal framework for the reduction of greenhouse gas emissions from domestic operation of aircraft in the U.S. and how international changes are affecting the United States. Part 2 briefly lays out overall regulation of the aviation industry, starting with ICAO's role. Part 3 outlines regulation of sustainable jet fuel at the U.S. federal level. It first examines the federal endangerment finding, the U.S. Renewable Fuel Standard, and implementation for aviation. Part 4 examines state, regional, and private efforts to promote sustainable jet fuels. Finally, Part 5 returns to the international arena by examining the European Union efforts to decrease aviation-related greenhouse gas emissions and how those might inform U.S. efforts.

INTERNATIONAL FRAMEWORK FOR SUSTAINABLE JET FUEL

The need for predictable and enforceable U.S. law and policy directly relates to international aviation agreements. The framework for sustainable jet fuel in international flights has been led by the International Civil Aviation Organization under the Carbon Offsetting and Reduction Scheme for International Aviation (CORSIA).

Role of the International Civil Aviation Organization (ICAO)

The International Civil Aviation Organization (ICAO) was established by the Convention on International Civil Aviation, known as the Chicago Convention, signed on December 7, 1944.[2] According to Article 44, ICAO's aims and objectives are to develop the principles and techniques of international air navigation and to foster the planning and development of international air transport. ICAO does not have regulatory authority. Once it adopts a guidance or standard, it is up to member states (countries) to adopt and enforce them.

ICAO has multiple layers of governance. The General Assembly, which meets every 3 years, considers major policy issues in the economic, legal, technical cooperation, and environmental fields brought to its attention by the Council or states. ICAO's executive body, the Council, convenes the Assembly, submits annual reports to the Assembly, and appoints and defines committee duties. The Committee on Aviation Environmental Protection (CAEP) assists the Council in formulating new policies and adopting Standards and Recommended Practices (SARPs) related to aviation environmental activities. It has 25 members, including the U.S., and 17 observers (ICAO, 2016b).

Carbon Offsetting and Reduction Scheme for International Aviation (CORSIA)

In 2013, the 38th General Assembly unanimously agreed to develop a global market-based measure (MBM) scheme to

[1]There are alternative fuels that are not SAF. For example, coal-based FT (Fischer-Tropsch) fuels are from an alternative/non-traditional jet fuel but they are not SAF.

[2]Convention on International Civil Aviation, Dec. 7, 1944, 15 UNTS 295.

reduce greenhouse gas emissions from international aviation. How to effectuate this scheme took some time to develop. In its October 2016 meeting, ICAO's 39th General Assembly adopted Resolution A39-3, an agreement to implement a global MBM scheme known as the "Carbon Offsetting and Reduction Scheme for International Aviation" (CORSIA) as part of a set of measures, which also include aircraft technologies, operational improvements, and sustainable aviation fuels (ICAO, 2016c). In 2018, the ICAO Council formally adopted CORSIA to offset international civil aviation's CO_2 emissions above 2020 levels.[3] The 2019 General Assembly then adopted Resolution A40-19 (Consolidated Statement of continuing ICAO policies and practices related to environmental protection—CORSIA), which replaced the previous Assembly's Resolution A39-3. It requested the ICAO Council to develop and update the CORSIA documents but mostly reiterated Resolution A39-3's objectives (ICAO, n.d.a). The 2019 Assembly also urged states to assess ICAO's taxation policies in their related national objectives and "to conduct appropriate cost-benefit analyses before the introduction of taxes on air transport" (ICAO, n.d.b).

By adopting CORSIA, the ICAO General Assembly sought to use offsets or to promote use of CORSIA-eligible fuels to enable reductions in greenhouse gas emissions (European Union Aviation Safety Agency et al., 2019, p. 78). CORSIA-eligible fuels can be a CORSIA-defined sustainable aviation fuel or a CORSIA lower carbon aviation fuel (ICAO, 2018). In the pilot phase (2021–2023) and first phase (2024–2026), CORSIA applies only to international flights between voluntarily participating states.[4] Eighty-eight states, including the U.S., pledged to participate in the initial phases (ICAO, 2020). Regardless of their participation, all member states whose aircraft operators undertake international flights must monitor, report and verify emissions from international flights during 2019 and 2020.[5] The average yearly emissions reported during this period will be used as baseline for the carbon neutral growth from 2020.

An eligible emission unit arises from emissions reduction achieved by the implementation of a project elsewhere from various sectors, including domestic aviation (ICAO Secretariat, 2017). On March 13, 2020, the ICAO Council approved a set of eligible emissions units during the pilot phase from eight emissions programs: the American Carbon Registry, Architecture for REDD + Transactions (ART), China GHG Voluntary Emission Reduction Program, Clean Development Mechanism, Climate Action Reserve, Global Carbon Council (GCC), the Gold Standard, and Verified Carbon Standard (ICAO, 2021). The emission units are issued for activities between 2016 and 2020 and will be published on the ICAO CORSIA website (ICAO, 2021).

The second phase (2027–2035) is mandatory. It will apply to "all States that have an individual share of international aviation activities in RTKs (Revenue Ton Kilometers) in year 2018 above 0.5 percent of total RTKs or whose cumulative share in the list of states from the highest to the lowest amount of RTKs reaches 90 per cent of total RTKs, except Least Developed Countries (LDCs), Small Island Developing States (SIDS) and Landlocked Developing Countries (LLDCs)."[6] Revenue Ton Kilometers or RTKs is the measure of capacity used for passengers and cargo expressed in metric tons, multiplied by the distance flown. In other words, it corresponds to the volume of air transport activity.[7] The scheme does not cover aircraft operators emitting less than 10,000 tons of CO_2 emissions from international aviation per year; aircraft with less than 5,700 kg of Maximum Take Off Mass (MTOM); or humanitarian, medical and firefighting operations.[8] The amount of CO_2 emissions required to be offset by an aircraft operator in given year would be defined by combining the operator's emissions growth with a sector-wide growth factor.[9] Each airline operator must meet its offsetting requirements for international flights on a 3-years compliance basis period.

In February 2019, ICAO's Committee on Aviation Environmental Protection (CAEP) agreed to the "means to calculate and claim the benefits accrued from the use of sustainable aviation fuels within the context of CORSIA." (ICAO, 2019a). The CAEP approved "default values and the methodologies for calculating actual values needed to calculate the life-cycle CO2 emissions reduction benefits of different feedstocks" (ICAO, 2019a). An airline operator will be able to satisfy their CORSIA offset requirements by claiming emissions reductions from the use of CORSIA eligible fuels; if they use CORSIA eligible fuels, they can reduce or eliminate their offset requirements. The ICAO Council released sustainability criteria for CORSIA eligible fuels in June 2019 (ICAO, 2019b) and requirements for Sustainability Certification Schemes in November 2019 (ICAO, 2019c).

[3]The Council adopted CORSIA on June 27, 2018 as Annex 16, Volume IV to the Chicago Convention.

[4]In this instance, states mean countries.

[5]Because the COVID-19 pandemic has caused a sharp decline in aviation activity, the ICAO Council changed the CORSIA baseline to 2019 emissions only and voted to remove 2020 emission from two other baseline calculation in the scheme. "ICAO Council Agrees CORSIA Baseline Change to Protect Covid-Stricken Airline Sector from Higher Carbon Costs," *GreenAir Archives*, July 1, 2020, https://www.greenaironline.com/news.php?viewStory=2715. This was criticized by EDF which said that paragraph 11(e) (1) (i) of the 2016 General Assembly Resolution A39-3, re-affirmed by ICAO in 2019, already allows airlines to calculate their offset obligation for 2021, 2022, and 2023 based on their 2020 emissions rather than their emissions in those years and there was no need to change baselines. Pedro Piris-Cabezas and Annie Petsonk, "Coronavirus and CORSIA," *EDF,* March 2020, https://www.edf.org/sites/default/files/documents/Coronavirus_and_CORSIA_analysis.pdf.

[6]Resolution A39-3, para. 9(e). "A State's individual RTK share is calculated by dividing the State's RTKs by the total RKTs of all States. Those State who have an individual RTK share below 0.5 percent of the total RTK, will be exempt from offsetting requirements, unless the cumulative RTK share is less than 90 percent. The cumulative RTK share is calculated by sorting the individual RTK shares from the highest to lowest, then successively increasing the value by summing the RTK shares from highest to lowest until the value reaches 90%. The values of all States are considered for this calculation, regardless if a State might be exempted from offsetting requirements in CORSIA afterwards." ICAO, What is CORSIA and How Does It Work? *Environment*, https://www.icao.int/environmental-protection/Pages/A39_CORSIA_FAQ2.aspx (accessed June 6, 2019).

[7]Ibid.

[8]Resolution A39-3, para. 13.

[9]Resolution A39-3, para. 11.

The U.S. has started down the path of direct CORSIA compliance. On March 14, 2019, the Federal Aviation Administration (FAA) published a notice in the Federal Register announcing the availability of the CORSIA Monitoring, Reporting and Verification (MRV) Program.[10] The MRV Program has enabled the U.S. to implement the CORSIA standards and recommended practices and monitor, report and verify CO_2 emissions from international flights. The program required U.S. air carriers, commercial, and general aviation operators to submit to the FAA certain airplane CO_2 emissions data for 2019 and 2020.[11] Under the MRV Program, each country's reported data was used for the calculation of CORSIA's baselines. While the U.S. is making other federal law and policy changes that help support the use of SAF, the 2027 deadline for the Phase II mandates will likely require more coordinated action by the U.S. to address its international aviation footprint.

U.S. FEDERAL REGULATIONS AND INITIATIVES

While U.S. reduction of emissions through the use of sustainable aviation fuels has been voluntary to date, recent legal changes at a federal level have started to recognize the importance of reducing aviation-related greenhouse gas emissions. In 2016, the U.S. Environmental Protection Agency issued an "endangerment finding" that greenhouse gas emissions from aviation contributed to air pollution under the Clean Air Act. On December 28, 2020, EPA published its first greenhouse gas emissions regulations for airplanes. Further, the U.S. Renewable Fuel Standard (RFS) program, originally enacted in 2005 and amended in 2007, allows renewable jet fuel to generate credits and creates an incentive for SAF; however, these are not requirements. In addition to voluntary opportunities under the RFS, agreements at ICAO are resulting in changes in U.S. policy as mentioned above. More details on each of these dynamics is addressed in further detail below, followed by a review of state and regional/industry initiatives in Part 4.

EPA's 2016 Endangerment Finding for Aviation Emissions

In 2016, the U.S. Environmental Protection Agency issued an endangerment finding, determining that emissions from certain aircraft, defined below, were endangering the public health and welfare.[12] The 2016 rule was based on the 2009 endangerment finding for light duty vehicles under Section 202(a) of the Clean Air Act (CAA).[13]

EPA issued the endangerment finding for the U.S. aviation sector under CAA Section 231(a) (2) (A). This requires the EPA Administrator to issue "proposed emission standards applicable to the emission of any air pollutant from. . . aircraft engines which in his judgment causes, or contributes to, air pollution which may reasonably be anticipated to endanger public health or welfare." In its final finding on July 25, 2016, EPA determined that CO_2 and nitrous oxide emissions from certain classes of engines in certain aircraft were contributing to the mix of GHGs in the atmosphere that were endangering the public health and welfare.[14] Covered aircraft include subsonic jet aircraft with a maximum takeoff mass (MTOM) greater than 5,700 kg and subsonic propeller-driven aircraft with a MTOM greater than 8,618 kg.[15] Examples of covered aircraft include the Cessna Citation CJ3+, the Embraer E170, Airbus 380, Boeing 747, ATR 72 and the Bombardier Q400.

By issuing an endangerment finding, EPA must define emission standards applicable to GHG emissions from the aircraft engine classes listed under CAA Section 231. FAA then must issue regulations to ensure compliance with EPA's standards. On December 28, 2020, EPA published the first GHG emissions regulations for new airplanes to be used in commercial aviation and large business jets. Although the rule will not reduce emissions more because U.S. airplanes producers have already begun working to meet the ICAO standards, it will give EPA oversight authority. Because noncompliant aircraft will likely be out of production or seek an exemption by 2028, EPA indicated that it is not expecting the regulations to reduce GHG emissions as they only apply to new type design airplanes after the effective date of the rule and to in-production airplanes on or after January 1, 2028 (Sobczyk, 2020). The standards address subsonic jet aircraft with a MTOM greater than 5,700 kg and subsonic propeller driven airplanes with a MTOM greater than 8,618 kg (EPA, 2020).

EPA promulgated the regulation without the 30-day waiting period for publication, which is normally required by the Administrative Procedure Act (APA) Section 53. EPA invoked the good cause exception to the 30-day waiting period which allows a rule to become effective upon promulgation. The immediate effective date of the rule prevented the new administration from quickly replacing or repealing the rule (Sobczyk, 2020). However, the Biden Administration issued an Executive Order on January 20, 2021 ordering, among other things, EPA to review the regulations about aviation emissions (Ahn, 2021). This remains pending.

Opportunities for Voluntary Credits Under the U.S. Renewable Fuel Standard Program

Although the 2016 Endangerment Finding sets out a not-yet realized regulatory approach for greenhouse gas emissions, there is also a voluntary way for aviation fuel producers to earn credits under the U.S. Renewable Fuel Standard (RFS) program. The U.S. Energy Policy Act of 2005[16] established the RFS program and added requirements for renewable fuel production as a new section to

[10]FAA's CORSIA Monitoring, Reporting and Verification Program, 84 Fed. Reg. 9,412 (Mar. 14, 2019).
[11]Ibid.
[12]40 C.F.R. §§ 87 and 1,068.
[13]Ibid.
[14]Finding That Greenhouse Gas Emissions from Aircraft Cause or Contribute to Air Pollution that May Reasonably Anticipated to Endanger Public Health and Welfare, 81 Fed. Reg. 54,421 (Aug. 15, 2016).
[15]Ibid. at 54,423.
[16]EPAct 2005, Pub. L. No. 109–58, § 1,501.

the Clean Air Act: CAA Section 211(o).[17] The program's goal is to designate "a certain volume of renewable fuel to replace or reduce the quantity of petroleum-based transportation fuel, heating oil or jet fuel" (EPA, n.d.a). The Energy Independence and Security Act of 2007 (EISA) increased the mandatory use of renewable fuel to 36 billion gallons of U.S. biofuels in use by 2022.[18] It further specified that 21 billion gallons of the 2022 goal must be derived from second generation feedstocks: non-food-based sources such as cellulosic biofuels.[19] However, volume requirements for both total renewable fuel and total advanced biofuel have not been met since 2013; this has been authorized through the use of annual waivers (Bracmort, 2020, p. 1).

The RFS requires "obligated" parties to produce or purchase renewable fuels for blending. An obligated party is any "any refiner that produces gasoline or diesel fuel within the 48 contiguous states or Hawaii, or any importers that import gasoline or diesel fuel into the 48 contiguous states or Hawaii during a compliance period."[20] The definition of "obligated parties" does not include aviation fuel producers. Although federal law does not mandate production or use of renewable jet fuel, producers or importers of renewable jet fuels can generate credits under the RFS program if their fuels meet the definition of renewable fuel in 40 CFR Section 80.1401.

This definition includes four categories of renewable fuels: biomass-based diesel, cellulosic biofuel, advanced biofuel and total renewable fuel. Renewable fuels must achieve a reduction in GHG emissions compared to a 2005 petroleum baseline to qualify as a renewable fuel under the RFS program. EISA defines advanced biofuel (code "D-5") as a renewable fuel, other than corn ethanol, that reduces greenhouse gas emissions by at least 50% when compared to petroleum diesel.[21] Cellulosic biofuel (D-3, D-7) is a renewable fuel derived from cellulose, hemicellulose, or lignin derived from renewable biomass and provide a 60% reduction in emissions from baseline gasoline and diesel.[22] Biomass-based diesel (D-4) must have a 50% lifecycle GHG reduction.[23] Finally, renewable fuels (D-6) is produced from renewable biomass and must achieve at least a 20% reduction in lifecycle GHG emissions.[24] Renewable jet fuels can qualify for RINs mostly under the D-4 code. Depending on the production process, they may also qualify for D3, D-5, and D-7.

EPA has approved renewable fuel pathways under the RFS program for all four categories of renewable fuels (EPA, n.d.b). For example, the advanced biofuel pathways already include ethanol derived from sugarcane, cellulosic ethanol made from corn stover, and sustainable jet fuel made from camelina (EPA, n.d.c).

Based on a petition by a renewable fuel producer, EPA periodically approves new pathways for alternative fuels based on feedstock and processes, codified at 40 C.F.R. Section 80.1,426. For example, on September 23, 2019, EPA approved a pathway request from Texmark Chemicals for the production of biomass-based diesel (D-4) for renewable jet fuel (EPA, 2019).[25]

Credits under the RFS program are tracked using "Renewable Identification Numbers" or RINs. At their simplest, RINs are the "currency" of the RFS program. They serve as the accounting mechanism and trading currency used by obligated parties to satisfy the RFS. All obligated parties must acquire enough RINs to satisfy the RFS. They can do so either by buying renewable fuels and their associated RINs or buying RINs on the open market. Each gallon of renewable fuel is directly associated with an individual RIN. The number of RINs generated per gallon of biofuel depends on which type of biofuel is produced. When that RIN travels with that fuel from one party to another, it is called an "assigned RIN." Sometimes RINs originally assigned to a batch of fuel become unassigned. Such "separated RINs" may be purchased separately. Market participants trade these RINs; **Figure 2** includes annual sales reports of total RINs from 2015–2019, while **Figure 3** includes the amount of renewable jet fuel produced over time and number of RINs gained with it. ASTM International-approved SAF pathways (see above) have been recognized to generate RINs.

EPA has defined different renewable fuels to have different RIN equivalence values based on the energy density of each fuel. For instance, corn ethanol has an equivalence value of 1, so that 1 gallon of corn ethanol is associated with one RIN. Biodiesel generates 1.5 RINs, because it is more energy dense. Renewable jet fuel has an equivalence value of 1.6, so 1 gallon of renewable jet fuel is associated with 1.6 RINs. These RINs are created by renewable fuel producers or importers, and generally sold along with the renewable fuel to gasoline refiners or importers. RIN production for renewable jet fuel has been modest compared to other renewable fuel types. In 2019, fuel producers introduced 2,428,369 gallons of renewable jet fuel (EV 1.6), which generated 3,885,392 RINs. Despite the COVID-19 pandemic, this number almost doubled at the end of 2020, where producers introduced 4,608,379 gallons of renewable jet fuel (EV 1.6), which generated 7,373,408 RINs (EPA, n.d.c).

Although renewable jet fuels have one of the highest equivalence values (1.6), it still has an equivalence value smaller than renewable diesel (1.7). Because the production of renewable jet fuel generally costs more than renewable diesel, fuel producers prefer to produce renewable diesel rather than renewable jet fuel. One potential medication to incentivize SAF production would be to increase SAF's equivalence value to 1.7 (Ghatala, 2020).

In addition, a report published by the Atlantic Council proposes extension of application of various tax credit programs to SAF production and development to reduce the price gap between SAF and conventional jet fuel (Ghatala, 2020,

[17]Clean Air Act, 42 U.S.C. § 7,545 (o) (2010).
[18]Energy Independence and Security Act of 2007, Pub. L 110–140.
[19]CAA § 211(o) (2)(B) (i) (I).
[20]40 CFR § 80.1406.
[21]CAA § 211(o) (1) (B).
[22]CAA § 211 (o) (1) (E).
[23]CAA § 211(o) (1) (D).
[24]CAA § 211(o) (1) (J); 40 CFR § 80.1401.
[25]Renewable Fuel Standard Program: Grain Sorghum Oil Pathway, 83 Fed. Reg. 37,735 (Envtl. Prot. Agency, Aug. 2, 2018).

FIGURE 2 | Annual RIN sales reports (includes all RINs, not just renewable jet fuel) (EPA, n.d.b).

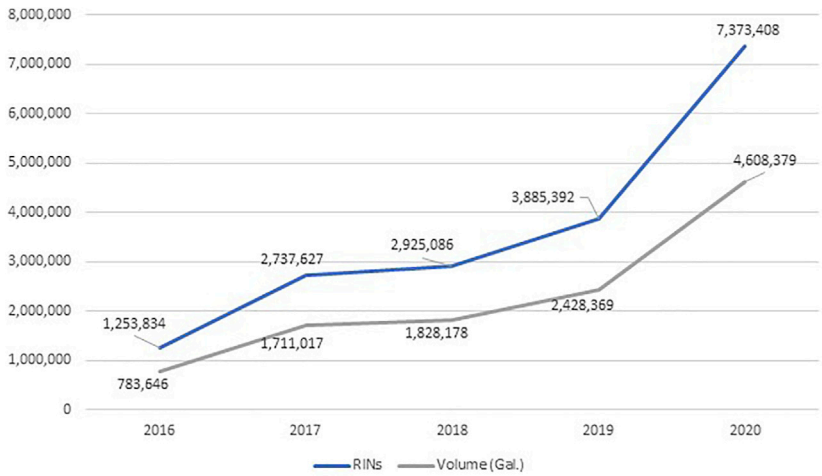

FIGURE 3 | Renewable jet fuel production under the RFS program (EPA, n.d.c).

p. 39). Possible programs include an investment tax credit program for SAF production facilities, a performance tax credit similar to the IRS section 45Q, which provides a tax credit on a per ton basis for CO_2 that is sequestered or CO_2 used in enhanced oil or natural gas recovery, and a SAF-focused production tax credit (Ghatala, 2020, p. 16). In addition, existing programs can be modified. For example, the Biodiesel and Renewable Diesel Blender Tax Credit (BTC) is paid to the fuel blenders that place renewable fuels into the market (Ghatala, 2020, p. 21).[26] SAF qualifies as a renewable diesel under the BTC, thereby decreasing production cost relative to fossil jet fuel but not against renewable diesel (Ghatala, 2020, p. 21).[27] The program provides $1.00 per gallon of biodiesel or renewable diesel used in the blending process. Because this program expires in December 2022, the report proposes extending the program for SAF for a longer term.[28]

The opportunity to implement or extend such tax credits exists. Congress introduced the Sustainable Skies Act in May 2021, which would create a blender's tax credit for SAF. The bill would provide a long-term blender's tax credit between $1.50/gallon up and $2.00/gallon for fuels that achieve a 100% GHG emissions reductions (Hubbard, 2021). However, this has not yet passed.

Despite the 2016 Endangerment Finding and subsequent federal laws related to regulating aviation emissions, U.S. federal law and policy remains based on voluntary measures

[26]26 U.S. Code § 40A.
[27]Ibid. § 40A(f).
[28]Ibid.

driven by the Renewable Fuel Standard. Individual states have also been working to incentivize reductions in aviation-related emissions, again through voluntary measures so far. Finally, regional airports and individual airlines have also been adopting SAF in their operations.

REGULATION AND INITIATIVES BY U.S. STATES AND REGIONAL/INDUSTRY EFFORTS

Absent a comprehensive federal program mandating the use of sustainable aviation fuel, states have been working to promote use of sustainable aviation fuels through incentives at the state level. California's Low Carbon Fuel Standard has provided a model now adopted in Oregon and Washington and being considered in other states. Hawaii has taken a different approach mainly through tax incentives.

At the same time, regional airports, airlines, and private industry are moving forward with developing, supplying and using SAF to reduce aviation-related GHG emissions.

California's Low Carbon Fuel Standard

California's Low Carbon Fuel Standard (LCFS) may pave the way for a functional opt-in credit system to incentivize production and use of sustainable aviation fuel, important because California accounts for one-fifth of U.S. jet fuel use (U.S. Energy Information Administration, 2021a). The LCFS, created by California Executive Order S-1-07 in 2007 and approved by the California Air Resources Board (CARB) in 2009, calls for a reduction of at least 10% in the carbon intensity of California's transportation fuels by 2020 compared to conventional petroleum fuels (CARB, n.d.a). A 2018 amendment to the LCFS requires a 20% reduction in carbon intensity by 2030 (CARB, n.d.a). In addition to reducing greenhouse gas emissions, the secondary goals of the LCFS program are to diversify the fuel portfolio of California, reduce petroleum dependence, and reduce emissions of other air pollutants.

The program, administered by CARB, requires regulated producers of petroleum-based fuels to reduce the carbon intensity of their fuels by either developing low carbon fuel products, or by buying LCFS credits from other producers who develop and sell low carbon alternative fuels. Regulated parties under the LCFS include providers of most petroleum and biofuel products in California. Alternative fuel providers already achieving the 2020 reduction goals are exempt, but they may "opt in" to the program to generate credits they can sell on the LCFS marketplace (CARB, 2021a).

Under the LCFS, each fuel is given a carbon intensity rating which accounts for GHG emissions associated with the production, transportation, and use of a given fuel (CARB, n.d.c).

Fuels that have lower carbon intensity than the target established by CARB generate credits. Fuels with higher carbon intensities than the target generate deficits (CARB, n.d.c). Fuel producers with deficits must have enough credits, through generation or acquisition, to be in annual compliance with the standard (CARB, n.d.c). Carbon credit generating fuels include bio-based natural gas, fossil-based natural gas, electricity, hydrogen, ethanol, biomass-based diesel and renewable diesel fuels. Carbon deficit generating fuels include conventional gasoline and diesel fuels. The LCFS program uses CARB-accredited verifiers to provide additional verification of reported reductions in carbon intensity. This process is substantially similar to the existing verification standards for emissions reductions in California's cap and trade program.

The LCFS is a performance-based standard allowing the market to determine how the carbon intensity of California's transportation fuels will be reduced. It does not favor one fuel over another (California Delivers, n.d.). In other words, "because the standard is technology-neutral, companies can earn LCFS "credits" any number of ways, including improving their processes or through switching to renewable feedstocks and inputs" (PROMOTUM, 2015, p. 3). The program incentivizes adoption of low-carbon transportation fuels, based on the fuel's carbon intensity. While the average price for a credit under the program was $31, $101, and $160 for 2014, 2016, and 2018, respectively, the average price per credit was $192 for 2019 and $199 for 2020 (**Figure 4**; CARB, 2021b). The average price of credits increased over the years, peaking in 2020.

CARB sets a maximum price for selling a credit each year (CARB, 2020),[29] which was $200.00 for 2016, $205.40 for 2017, $209.92 for 2018, $213.07 for 2019, $217.97 for 2020, and $221.67 for 2021 (**Figure 5**; CARB, n.d.b).

One concern with the LCFS is the potential impact on indirect land use change. While direct effects of the production and use of the fuel is calculated via the California Greenhouse Gases, Regulated Emissions, and Energy Use in Transportation (CA-GREET) and Oil Production Greenhouse Gas Emissions Estimator (OPGEE) models, indirect land use change (ILUC) is calculated via Global Trade Analysis Project (GTAP) and Agro-Ecological Zone Emissions Factor (AEZ-EF) models, which are the strongest approach against ILUC risk, although not a perfect protection (CARB, n.d.a, p. 16).

In September 2018, CARB voted to add SAF producers to the list of entities that may voluntarily opt-in to the LCFS program. As of January 1, 2019, alternative jet fuels can generate credits under California's LCFS. Currently, aircraft, military vehicles, ocean vessels, and locomotives are exempt from LCFS regulation. Some SAF related credits are being generated under this opt-in.

On November 5, 2020, the average incentive per gallon for SAF in a given year was $1.0516/gal, a decrease from $1.4250/gal (Pedrick, 2020); additional information on SAF consumed versus credits is included in **Table 1**. However, SAF production in California is sputtering compared to production of renewable

[29]17 Cal. Code of Regulations Section 95,487 (a) (2) reads as follows: A regulated entity may not (D) Sell or transfer credits at a price that exceeds the Maximum Price set by the following formulate: 1) $200 ($MTCO_2e$) in 2016. 2) The per credit price shall be adjusted annually by the rate of inflation as measured by the most recently available 12 months of the Consumer Price Index for All Urban Consumers. "Consumer Price Index for All Urban Consumers" means a measure that examines the changes in the price of a basket of goods and services purchased by urban consumers, and is published by the U.S. Bureau of Labor Statistics. 3) The Maximum Price will be published on the first Monday of April and go into effect on June 1st.

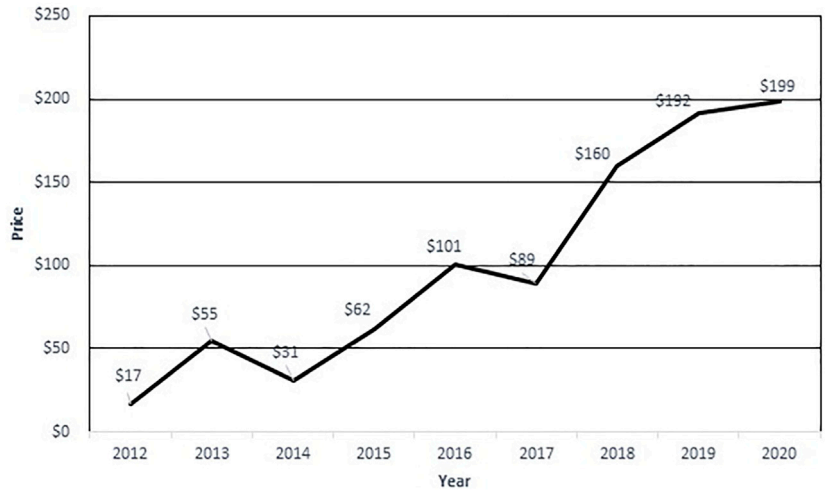

FIGURE 4 | Average price for a credit under California LCFS (CARB, 2021b).

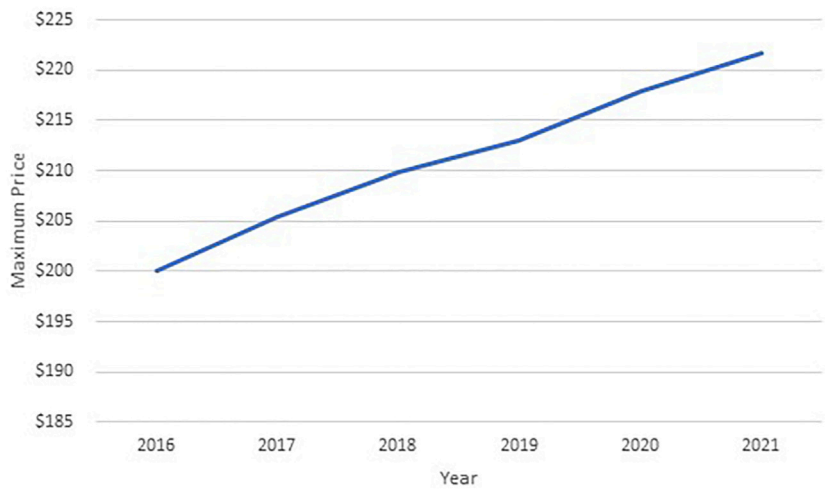

FIGURE 5 | Maximum price for selling a credit each year under LCFS program (CARB, n.d.b).

TABLE 1 | SAF consumed in California (Pedrick, 2020).

Time period	Q2 2019	Q1 2020	Q2 2020
SAF Consumed (gal)	753,532	248,190	1.32 million
SAF Credits (mt)	3,600	2,028	7,042

diesel. Why? The main reason is that renewable diesel allows an obligated party to avoid generating deficits that would have resulted from the use of conventional diesel. However, conventional jet fuel or aviation gasoline is exempt under the LCFS and does not generate deficits. Second, a fuel with a low carbon intensity (e.g. produced from used cooking oil or tallow) will generate more revenue than a fuel with a high carbon intensity (e.g. produced from soybean oil) (Mazzone et al., 2021, p. 13). Renewal diesel and SAF are produced by using similar feedstocks and process. However, SAF requires an additional fractionation step which adds cost to the production of SAF. Because the LCFS program assigns renewable diesel a higher energy density, obligated parties prefer to produce renewable diesel compared to SAF (Mladenik, 2020).

Although the LCFS has been subject to several legal challenges both at the federal and state level, it has been upheld in a complicated set of legal decisions. On September 19, 2013, the Ninth Circuit Court of Appeals upheld the California LCFS in a federal case known as *Rocky Mountain I*, reversing the district court decision holding that the California's LCFS violated the dormant Commerce Clause of the U.S. Constitution.[30] The Ninth

[30]Rocky Mountain Farmers Union v. Corey, 730 F.3d 1,070 (9th Cir. 2013).

Circuit held that the California LCFS did not facially discriminate against out-of-state commerce because the carbon intensity measurement is based on scientific data (e.g., transportation emissions, electricity supplies) rather than the fuel's state of origin.[31] Further, the Court held that California was not imposing its regulations on other jurisdictions.[32]

After the *Rocky Mountain I* decision, a California state court issued a decision in 2013 requiring CARB to reconsider the LCFS based on procedural administrative law requirements.[33] The court said that CARB failed to comply with the procedural requirements required under the California's Administrative Procedure Act (APA) and California Environmental Quality Act (CEQA) i.e., to complete an environmental analysis before approving the LCFS.[34] That led CARB to adopt the 2015 LCFS which repealed the 2011 LCFS and the 2012 amendments. The 2015 LCFS was identical to the 2011 LCFS and kept the same carbon intensity and lifecycle analysis. After the re-adoption of the LCFS in 2015, plaintiffs appealed again alleging that the environmental analysis "still did not adequately analyze the potential for increase NOx emissions" (Hecht, 2019). The Court of Appeal ruled in favor of plaintiffs, ordering CARB to complete another environmental analysis (Hecht, 2019). As a result of the order, CARB amended the LCFS in 2018 (CARB, 2018).

After CARB's 2015 updates, plaintiffs in the federal case amended their complaint—which had challenged the 2012 amendments to the LCFS's crude oil provisions—to challenge the 2015 version of the LCFS. After losing at the U.S. District Court, plaintiffs appealed to the Ninth Circuit again, alleging that all three versions of the LCFS violate the Commerce Clause for two reasons. The first was by facially and purposefully discriminating against interstate commerce in their treatment of crude oil and ethanol; the second was by regulating extra territorially.[35] On January 28, 2019, the Ninth Circuit held that challenges to the 2011 LCFS and the 2012 amendment were moot because CARB repealed these amendments.[36] It also dismissed plaintiffs' claim of extraterritoriality because it was precluded in *Rocky Mountain I*,[37] and said that "plaintiffs do not and cannot explain how their extraterritoriality claims under the Commerce Clause function differently against the new version of the regulation."[38] After the plaintiffs' request for review by the U.S. Supreme Court in *Rocky Mountain I* was denied, plaintiffs did not file a petition with the Supreme Court.

Having withstood these legal challenges, California's LCFS is becoming more operational day by day and serves as a model for other states, particularly given that as of January 1, 2019, alternative jet fuel producers can generate credits under the LCFS. California's LCFS is critical as a template for other states, and for the U.S. as a whole.

Oregon's Clean Fuels Program

Oregon's Clean Fuels Program is modeled on California's LCFS; like in California, the aviation sector is not required to but may generate credits. In 2009, the Oregon Legislature passed HB 2186, authorizing the Oregon Environmental Quality Commission to reduce the average carbon intensity of Oregon's transportation fuels by 10% over a 10-year period. In 2015, the Legislature passed SB 324, directing the Oregon Department of Environmental Quality (DEQ) to implement the Clean Fuels Program.[39] Effective in 2016, the Clean Fuels Program is part of Oregon's overall plan to reduce greenhouse gas emissions including methane emissions from the transportation sector by reducing reduce carbon intensity for gasoline and diesel fuels used in-state by 10% from 2015 levels by 2025.

Each year, the Oregon DEQ establishes Clean Fuel Standards, which is the annual average carbon intensity with which a regulated party must comply. This allows the State to update its annual targets until the 10% reduction by 2025 is met.[40] The State set baseline carbon intensity levels—94.63 (gCO_2/MJ) for gasoline, 95.29 for diesel and 90.8 for alternative jet fuel-for compliance in 2021 (Oregon DEQ, n.d.a). Clean fuels are those that have a lower carbon intensity level than the fuel replaced. Most types of ethanol, biodiesel, renewable diesel, renewable natural gas, biogas, electricity, and hydrogen qualify (Oregon DEQ, n.d.b).

Like California's LCFS, deficits are generated when the carbon intensity of a certain fuel exceeds the Clean Fuel Standard in a given year and credits are generated if the carbon intensity is below the Clean Fuel Standard. Credit generators can voluntarily register with the program if they would like to generate and sell credits. Regulated parties are importers of gasoline, diesel, ethanol, and biodiesel. Producers of ethanol and biodiesel within the State of Oregon are also regulated parties. These regulated parties must comply with the Clean Fuels Program regulations, including purchasing credits from generators through the state's marketplace when necessary.

Fuels used for aviation, construction equipment, farm vehicles, locomotives, logging vehicles, military vehicles, racing vehicles and watercrafts are exempt from the carbon intensity reduction requirements. However, as of January 1, 2019, renewable aviation fuels are now an "opt in" fuel for generating credits, which may spur further development (Lipson, 2019).[41]

As in California, Oregon was sued for these standards. In March 2015, the American Fuel and Petrochemical Manufacturers, American Trucking Associations, and Consumer Energy Alliance challenged the Oregon Program before the U.S. District Court in Oregon. Plaintiffs alleged that the Program violated the Commerce Clause and was preempted by the Clean Air Act (CAA) Section 211(c).[42] The District Court dismissed the case.[43] The Ninth Circuit said that the Oregon

[31]*Rocky Mountain*, 730 F. 3d at 1,089.
[32]Ibid. at 1,101.
[33]POET, LLC v. CARB, 218 Cal. App. 4th 681, 766-67.
[34]Ibid.
[35]Rocky Mountain Farmers v. Corey (9th Cir. Jan. 18, 2019) (No. 17-16881), p. 16.
[36]Ibid., at 19.
[37]Ibid. at 20.
[38]Ibid. at 21.
[39]ORS 468A.275.
[40]OAR 340-253-8,010.
[41]OAR 340-253-320, 330 and 350.
[42]Am. Fuel and Petrochemical Mfrs. v. O′ Keeffe, 134 F. Supp. 3d 1,270 (D. Or. Sept. 23, 2015).
[43]Am. Fuel and Petrochemical Mfrs. v. O'Keeffe, 903 F.3d 903 (9th Cir. Or. Sept. 7, 2018).

Program did not infringe on the Commerce Clause as it had also held for the California LCFS in *Rocky Mountain I*,[44] also dismissing plaintiffs' preemption claim under Article IV, paragraph 2 of the U.S. Constitution, commonly known as the Supremacy Clause. CAA Section 211(c)(4)(A) prohibits states from adopting rules to control and prohibit emissions from motor vehicles related to a fuel or additive if the EPA has decided to regulate a particular fuel, or if the EPA has found that no such regulation is necessary and publishes this decision in the Federal Register. Although the EPA excluded methane under the 1994 Reformulated Gasoline Rule (RFGR) indicating that it did not present a sufficient threat to the public health or welfare, it did not find that regulating methane's contributions to greenhouse gas emissions was unnecessary nor published it as required under CAA Section 211(c) (4)(i).[45] Therefore, the Ninth Circuit denied the plaintiff's preemption argument. Plaintiffs then petitioned to the U.S. Supreme Court for review; this was denied on May 13, 2019. This cleared any challenges against the constitutionality of the Oregon Clean Fuels Program.

At this point, Oregon's Clean Fuels Program is starting to generate credits. Overall, the Clean Fuels Program reduced 5,300,000 metric tons of GHG between 2016–2020 (Oregon DEQ, n.d.a). However, the state's quarterly data summaries do not provide the SAF consumption amount or credits based on SAF (Oregon DEQ, n.d.c). Being able see this kind of data would be critical.

The Oregon Clean Fuels Program has been strengthened by an Oregon Executive Order on climate change. On March 10, 2020, Oregon Governor Kate Brown issued an executive order that aims to limit GHG emissions to 45% below 1990 levels by 2035, and an 80% reduction by 2050 with the help of 18 state agencies (VanderHart, 2020). The move came after the Oregon Senate killed a bill about a cap and trade program 1 week earlier. The order requires agencies to amend building codes to prioritize energy efficiency and decrease the carbon intensity of gasoline (VanderHart, 2020). It directed the Environmental Quality Commission and the Department of Environmental Quality to amend the Clean Fuels Program to reduce emissions by 20% below 2015 levels, and 25% by 2035 (VanderHart, 2020). How this plays out remains to be seen, particularly for SAF.

Washington's Clean Fuels Program

The State of Washington followed the path taken by California and Oregon by adopting a Clean Fuels Program which allows SAF producers to generate credits. This is critical as Washington has several large U.S. Air Force and Navy installations and is among the top-10 jet fuel consuming states (U.S. Energy Information Administration, 2021b). It is also home to Boeing, one of the world's largest aircraft manufacturers.

Setting the stage was Washington's Renewable Fuel Standard (WRFS), effective in 2013, which requires that at least 2% of all of the diesel fuel sold within the state be biodiesel or renewable diesel.[46] This statute was a legislative response to the "public interest (in) establish (ing) a market for alternative fuels in Washington." Goals for the WRFS include reducing "dependence on foreign oil," improving "the health and quality of life for Washingtonians" and stimulating "the creation of a new industry in Washington that benefits farmers and rural communities."[47] The required percentage of biodiesel or renewable diesel sold within the state is supposed to increase from 2 to 5% 180 days after the Washington State Department of Agriculture determines that in-state feedstock and oil seed crushing capacity can meet a 3% sales requirement.[48]

Washington increased its focus on renewable transportation fuels through very recent legislation. On April 25, 2021, Washington adopted, and on May 17, 2021, Governor Inslee signed the legislation for its Clean Fuels Program that will reduce GHG emissions from transportation fuels sold in the state by 20% below 2017 levels by 2038 (Christensen et al., 2021).[49] The bill ordered the Washington Department of Ecology to develop rules to implement the program which must become effective no later than January 1, 2023.[50] The bill exempts fuels used for aircraft, vessels, railroad locomotives, military tactical vehicles, and until January 1, 2028, logging, off-road, agriculture and mining vehicles (Hopkins et al., 2021).[51] However, like in California and Oregon, these industries can voluntarily opt in to the program in order to generate credits. The Clean Fuels Program will be linked to low carbon fuel standard programs in Oregon and California, creating a robust market for carbon reduction credits (Christensen et al., 2021). How this regional approach affects aviation-related credits also remains to be seen.

Other State Efforts on LCFS-Type Laws

Other states are starting to consider LCFS-type laws. For example, Colorado released a roadmap on pollution reduction and a clean energy transition (Colorado Energy Office, 2021). In 2021, New Mexico proposed a LCFS, which, if adopted, would have allowed aviation industry to generate credits (New Mexico Environment Department, 2021). In addition, New York tried to introduce bills relating to LCFS both in 2020 and 2021, however, neither proposal advanced to a vote (Argus Media, 2021). Finally, Minnesota proposed a LCFS program but did not pass it during the 2021 legislative session (Orenstein, 2021). The effort of these states highlights the potential for more of a national standard or approach and merit watching.

Hawaii's Tax Incentives

In contrast, Hawaii has focused more on tax incentives. While not yet allowing for the same LCFS type program, Hawaii presents an interesting opportunity given the major role that aviation plays in Hawaii's economy, energy balance, and CO2 inventory. Hawaii

[44]Am. Fuel and Petrochemical Mfrs., 903 F.3d 903, 911.

[45]Am. Fuel and Petrochemical Mfrs. v. O′ Keeffe, 134 F. Supp. 3d at 1,285.

[46]RCW 19.112.110.

[47]Washington State Legislature, RCW 19.112.110, Notes: Findings—Intent—2006 c 338, https://app.leg.wa.gov/RCW/default.aspx?cite=19.112.110.

[48]RCW 19.112.110.

[49]HB 1091, Chapter 317, Law of 2021, 67th Legislature, 2021 Regular Session, Effective Date July 25, 2021.

[50]Ibid., Sec. 3.

[51]Ibid., Sec. 4 (5), Sec. 5 (1) (b) and (2).

consumes over 700 million gallons of jet fuel per year, excluding the jet fuel consumption of the U.S. military (Hawaii Natural Energy Institute, 2020). All jet fuel used is petroleum-based. The transportation sector uses almost two-thirds of all petroleum consumed in Hawaii; of this, jet fuels constitutes half of all transportation fuel consumed in the state because of significant demand from military installations and commercial airlines (U.S. Energy Information Administration, 2021c).

Hawaii is beginning to develop an incentive system for SAF, mainly through tax credits. This is bolstered by Hawaii's determination to "achieve its goal of 100 percent of renewable energy generation by 2045" (Hawaii State Energy Office, N.D.). Although this is currently focused on generation of electricity, Hawaii's focus on renewable energy sources may provide the policy support needed to grow the biofuels industry for transportation, including for aviation.

There are a number of laws in place that support renewable fuels. For example, Hawaii enacted the Hawaii Environmental Response, Energy, and Food Security Tax (aka the "Barrel Tax") in 1993. The Barrel Tax, originally set at $0.05 per barrel, increased to $1.05 per barrel on July 1, 2010 with the passage of Act 73, Session Laws of Hawaii 2010.[52] In theory, the tax discourages the importation and use of petroleum-based fuels, incentivizing the use of alternative or biofuels. Its major impact, however, has been to create a funding source for energy and food security initiatives. Of the proceeds generated, a portion of the tax collected provides support for four funds: the Environmental Response Revolving Fund, the Energy Security Special Fund, the Energy Systems Development Special Fund, and the Agricultural Development and Food Security Fund. The tax also provides support for the Hawaii Clean Energy Initiative and the Hawaii Natural Energy Institute. The Barrel Tax on petroleum products specifically excludes aviation fuels and any fuel sold to a refiner. Despite these exemptions, the Barrel Tax applies to roughly 2/3 of the barrels of fossil fuels imported into Hawaii each year and provides more than $25 million in revenue to the state annually (Department of Taxation, State of Hawaii, 2016, p. 21). Set to sunset in 2015, the tax was extended for 15 more years in 2014, so now sunsets in 2030.[53]

A direct avenue to support aviation and implementation of SAF may come through a production tax credit. A renewable fuels production tax credit provides an income tax credit equal to $0.20 per 76,000 BTUs (or about $0.29 per gallon) of renewable fuels including renewable jet fuel sold for distribution in Hawaii beginning after December 31, 2016.[54] The facility must produce at least 2.5 billion BTUs annually to receive the tax credit and may claim the tax credit for up to 5 years, not to exceed $3 million per calendar year.[55] After 1 year of production, the taxpayer must complete and submit an independent, third-party certified statement to the Department of Business, Economic Development, and Tourism.[56] The statement must include, among other things, the type, quantity, and British thermal unit value of each qualified renewable fuel, the feedstock used for each type of qualified renewable fuel, and the proposed total amount of credit to which the taxpayer is entitled for each calendar year.[57] However, this tax credit program expires on December 31, 2021; [58] if it is renewed, it may be a vehicle to support production of SAF.

Financial incentives and a voluntary market may also help. In 2021, Hawaii passed House Bill 683, which has established a SAF program to provide matching grants to Hawaii small businesses developing and producing SAF (Burnett, 2021).[59] The bill set baseline carbon intensity for jet fuel at 89 g of CO_2 per megajoule.[60] Therefore, a SAF production which has carbon intensity below 89 g of CO_2 per megajoule would be eligible to receive matching grants.

Other proposed incentives might help bolster local SAF production. For example, in March 2020, the Hawaii legislation proposed to replace the existing barrel tax with a carbon emission tax on each fossil fuel, including jet fuel. If enacted, the tax on jet fuel would be $0.0598 per gallon.[61] Hawaiian Senator Karl Rhoads said that "aviation fuel and electricity are taxed relatively lightly if you look at the per-carbon content" (Dalzell, 2019). While the bill did not advance to the House floor, it does signify that aviation fuel is a topic of concern.

An alternative pathway may also come through a statewide alternative fuel standard. In 2006, the Hawaiian legislature passed Act 240, creating the Hawaii Alternative Fuel Standard (AFS). This Act required 20 percent of highway fuel to come from alternative fuel by 2020, increasing to 30 percent by 2030.[62] It includes biomass crops and municipal solid waste as eligible renewable energy sources. Ethanol produced from cellulosic materials is considered the equivalent of 2.5 gallons of non-cellulosic ethanol under the AFS.[63] While aviation is currently not a regulated under Hawaii's AFS, which currently focuses only on highway fuel standards, it could be modified or updated like Washington State did to allow for SAF.

Aviation offers Hawaii an opportunity to meet its GHG reduction goals, with a number of legal and policy pieces already in place to support SAF development and others proposed. Whether these come to fruition or not remains to be seen. Even as the federal government and states figure out how to support SAF, regional and airline initiatives are moving forward anyway.

[52]HB 2421, Act 73 (2010), available online at https://www.capitol.hawaii.gov/session2010/bills/HB2421_ACT73_.pdf.
[53]Act 107, Session Laws of Hawaii 2014.
[54]HI Rev. Stat. § 235–110.31.
[55]Ibid.
[56]Ibid.
[57]Ibid.
[58]Ibid.
[59]Hawaii House Bill 683 (2021), Regular Session.
[60]Ibid., Section 2.
[61]S.B. No. 1463, "A Bill for an Act Relating to Taxation," (2019), https://www.capitol.hawaii.gov/session2020/bills/SB1463_SD2_.HTM.
[62]HI Rev. Stat. § 196-42.
[63]Ibid.

Regional and Industry Initiatives

Because of the different developments at the federal and state level—in part in response to CORSIA—some airports and airlines are adopting infrastructure for SAF with private industry is scaling up to meet these demands. For example, the Port Authority of New York and New Jersey and the company NESTE signed a MOU on June 6, 2019 to work together to facilitate the use of SAF at Port Authority facilities (Aviation Benefits Beyond Borders, 2019). On June 18, 2018, NESTE announced a partnership with Dallas Fort Worth International Airport to reduce air pollution from activities at the airport. The solutions include use of NESTE MY Renewable Jet Fuel at Dallas Fort Worth International Airport, along with renewable de-icing fluid, paints and plastics (Tisheva, 2018).

Airlines are also taking steps toward sustainable aviation fuel. United Airlines conducted the first commercial flight based on biofuel using algae derived aviation fuel on November 7, 2011 (Ayres, 2011). This was followed by the world's first commercial flight based on forest residuals-based fuels from Seattle to Washington, D.C. conducted by Alaskan Airlines on November 14, 2016 (Alaska Airlines Newsroom, 2016). Alaska Airlines also signed a Memorandum of Understanding (MOU) with NESTE to work closely to "design, create and implement solutions that lay the groundwork for the wider adoption of renewable fuels within the airline industry" (Alaska Airlines Newsroom, 2018). On September 17, 2019, Delta Air Lines announced a $2 million investment to partner with Northwest Advanced Bio-fuels for study of a potential facility to produce biofuel from wood residues and wood slash. The facility is expected to be established in Washington State to provide fuel for Delta operations in Seattle, Portland, San Francisco, and Los Angeles (Delta News Hub, 2019a). That same year, Delta concluded a long-term offtake agreement to purchase 10 million gallons per year of advanced renewable biofuels from Gevo (Delta News Hub, 2019b). Similarly, on May 22, 2019, United Airlines agreed to purchase up to 10 million gallons of cost-competitive sustainable aviation fuel from World Energy over the next 2 years. United Airlines is the first airline in the world to use sustainable aviation biofuel on continuous basis (United Airlines, 2019).

Other private companies are also working to meet demand for SAF. For example, Fulcrum Bioenergy constructed a biorefinery in Storey County, Nevada, to convert municipal solid waste (MSW) into renewable jet fuel (Fulcrum BioEnergy, 2021). The facility is expected to process about 175,000 tons of MSW annually creating 11 million gallons per year of renewable synthetic crude oil which will then be upgraded to transportation fuels including SAF (Fulcrum BioEnergy, 2021). On April 15, 2018, the Oregon DEQ approved construction of a bio-jet and biodiesel production plant to be built in Oregon. The plant will convert 166,000 tons of woody biomass into 16.1 million gallons/year of renewable fuel (Red Rock Biofuels, n.d.). World Energy aims to increase SAF production from 25 million gallons per year to 150 million gallon per year while NESTE aims to increase its production from 34 million gallons per year to 500 gallons per year after 2023.

While voluntary now, these airport, airline, and industry initiatives tie back into the global emphasis on reducing greenhouse gas emissions from aviation. Such actions are ramping up in the European Union, which is critical for U.S.-based aviation. The push of EU-based regulation is also an important factor that will continue to shape U.S. law and policy for SAF.

EUROPEAN UNION LAW AND POLICY DRIVERS

While the U.S. federal and state governments are working on potential incentives for renewable jet fuel, the aviation industry is global and responding to international pressures as well. In 2009, the European Union adopted a Renewable Energy Directive which required fuel suppliers to produce at least 14% of their transportation fuel from renewable fuels. Although the RED targets do not apply to aviation fuel, SAF counts as a renewable source to meet the RED targets (European Union Aviation Safety Agency et al., 2019, p. 48). Along with EU wide policies, country-specific laws are driving change.

The EU Renewable Energy Directive (RED)

In 2009, the EU adopted the Renewable Energy Directive (RED), which sets out an overall policy for the production of energy from renewable sources in the EU.[64] First, the RED required EU countries to fulfill at least 20% of their energy needs and at least 10% of their transportation fuels from renewable sources by 2020 (European Commission, n.d.a). A revision to the RED entered into force in December 2018 and stipulates a new binding target of at least 32% for energy by 2030 (European Commission, n.d.a). Fuel suppliers are required to ensure that at least 14% of their transportation fuel comes from renewable energy by 2030.

The RED provides multipliers which count use of biofuel by a factor greater than 1 to encourage the use of advanced biofuels, while limiting the contribution of bio-based biofuel derived from food and feed crops (European Union Aviation Safety Agency et al., 2019, p. 48). Advanced biofuels are defined as biofuels produced from the feedstock listed in the RED, Annex IX; this includes algae, municipal waste, industry waste not fit for use in the food or feed chain, straw, animal manure and sewage sludge, tall oil pitch, forestry biomass, and other non-food cellulosic material. A multiplier inflates the contribution of certain renewables; this includes a 1.2 multiplier for sustainable aviation fuels compared to fuels used in transportation and rail sectors. In other words, "the contribution of non-food renewable fuels supplied to these sectors count 1.2 times their energy content" (European Commission, 2019). This contrasts to the 1.6 multiplier provided by the U.S. Renewable Fuel Standard (RFS).

While the RED targets do not apply to aviation fuel, a 2015 amendment introduced a way that countries can voluntarily opt in through their own legislation (European Union Aviation Safety

[64]Directive 2009/28/EC of the European Parliament and of the Council of 23 April 2009 on the Promotion of the Use of Energy from Renewable Sources and Amending and Subsequently Repealing Directives 2001/77/EC and 2003/30/EC, adopted April 23, 2009, *O J L* 140 (June 5, 2009), https://eur-lex.europa.eu/legal-content/EN/ALL/?uri=CELEX:32009L0028.

Agency et al., 2019, p. 48). A number of countries are starting to pursue this; see below.

EU Emissions Trading System (EU ETS)

In the meantime, emissions for airline flights in Europe are also regulated under the EU Emissions Trading System (ETS). The EU ETS is a cap and trade system which limits the overall level of CO_2 emissions allowed from certain sectors but authorizes participants to buy and sell allowances as they require (European Commission, n.d.b). Launched on January 1, 2005, the EU ETS helps EU countries achieve their commitments to cap greenhouse gas emissions in a cost-effective way (European Commission, n.d.b). In addition to CO_2 emissions from commercial aviation within the European Economic Area, it covers the power and heat sector, energy-intensive industry sectors including oil refineries, steel works and production of iron, aluminum, metals, cement, lime, glass, ceramics, pulp, paper, cardboard, acids and bulk organic chemicals, nitrous oxide (N_2O) emissions from production of nitric, adipic and glyoxylic acids and glyoxal, and perfluorocarbons (PFCs) from aluminum production (European Commission, n.d.b). In addition to EU countries, the program applies to Norway, Iceland and Liechtenstein, which are other members of the European Economic Area (European Commission, n.d.b).

In July 2008, the EU issued a directive including aviation activities in the EU ETS beginning on January 1, 2012.[65] EU ETS for aviation applies to emissions from flights from, to, and within the EU plus Iceland, Liechtenstein and Norway. The U.S. aviation industry then challenged the ETS directive for aviation.[66] Ultimately, the European Court of Justice dismissed the plaintiffs' claims in 2011.[67] However, the EU limited application of the EU-ETS to only intra-Europe flights, known as the "stop the clock" decision because of non-European airlines and partners pushback.[68] At this point, flights to and from an airport beyond these countries have been excluded until 2023 to facilitate negotiation of a global agreement at ICAO (European Union Aviation Safety Agency et al., 2019, p. 75). Also excluded are military aviation, search and rescue flights, state flights transporting third countries' heads of state, government and government ministers, and police flights.

Aircraft operators receive some free allowances for their emissions from member states. They may emit up to the limit but must offset the remaining emissions. At the end of each year, each emission source must submit allowances at least equal to its emissions in the preceding year. Every ton of CO_2 emitted require one allowance. An operator with more allowances than needed may sell the extra to another entity needing credit (Leggett et al., 2012, p. 10). If the operator does not have enough allowances to satisfy its previous year's emissions, it can buy additional allowances at auction or from other companies having a surplus (Transport and Environment, n.d.). During the period from January 1, 2012 to December 31, 2012, the total quantity of allowances allocated to aircraft operators was 97% of the average historic aviation emissions between 2004 and 2006 (Leggett et al., 2012, p. 12). Eighty-five percent of the allowances were distributed for free, and 15% of the total allowances were auctioned with a bidding process. The allowances for phase of 2013–2020 was set to 95% of historical aviation emissions (European Union Aviation Safety Agency et al., 2019, p. 76). While 82% of the allowances are allocated freely, 15% are auctioned, and 3% of them are allocated free to new entrants and fast-growing operators (European Union Aviation Safety Agency et al., 2019, p. 76). In other words, if their emissions are over 95%, they have to purchase allowances from other sectors. If there is still 15% available from the auction, they can purchase from there as well.

In addition to aviation allowances, aircraft operators may benefit from allowances from stationary sources but not vice versa. For example, while an airline operator can use allowances from a stationary source, e.g. a steel production company, the company is not allowed to use allowances from the aviation sector. Aircraft operators can also use international credits up to 15% of their emissions in 2012. Between 2013 and 2020, each aircraft operator could use certain international credits up to a maximum of 1.5% of its verified emissions during that phase (European Union Aviation Safety Agency et al., 2019, p. 76). During the fourth phase of EU ETS, from 2021 to 2030, each annual limit will be further reduced by 2.2% each year from the aviation cap. Emission reductions will have to be exclusively domestic, meaning no international credits may be used (European Union Aviation Safety Agency et al., 2019, p. 78). EU ETS provides an incentive to use SAF attributing zero emissions to SAF under the EU ETS (European Union Aviation Safety Agency et al., 2019, p. 48), although almost all SAF have an actual life-cycle carbon intensity greater than zero. Therefore, the use of SAF reduces an airlines' emissions, and the number of allowances it has to purchase. That, in turn, provides a financial incentive for airlines to use more SAF instead of conventional jet fuels (European Union Aviation Safety Agency et al., 2019, p. 48).

"Fit for 55"

On July 14, 2021, the European Commission adopted a package of proposals called "Fit for 55," which would provide a GHG emissions reduction of 55% by 2030 compared to 1990 levels (European Commission, 2021a). The proposals include "application of emissions trading to new sectors and a

[65]Directive 2008/101/EC of the European Parliament and of the Council of 19 November 2008 amending Directive 2003/87/EC so as to include aviation activities in the Scheme for Greenhouse Gas Emission Allowance Trading within the Community, https://eur-lex.europa.eu/legal-content/EN/TXT/?uri=celex%3A32008L0101.

[66]*See* Case C-366/10, Air Trans. Assoc. of America v. Sec. of State for Energy and Climate Change, 2011, http://curia.europa.eu/juris/document/document.jsf?text=&docid=117193&pageIndex=0&doclang=EN&mode=lst.

[67]Court of Justice of the European Union, Press Release No 139/11, The Directive Including Aviation Activities in the EU's Emissions Trading Scheme is Valid, December 21, 2011, https://curia.europa.eu/jcms/upload/docs/application/pdf/2011-12/cp110139en.pdf.

[68]Decision No 377/2013/EU of the European Parliament and of the Council of 24 April 2013, derogation temporarily from Directive 2003/87/EC establishing a scheme for greenhouse gas emission allowance trading within the Community, https://eur-lex.europa.eu/legal-content/EN/TXT/PDF/?uri=CELEX:32013D0377&from=EN.

TABLE 2 | Example laws and regulations relating SAF that are pending or failed. (Sources: European Commission, 2021a; Burnett, 2021; New Mexico Environment Department, 2021; Argus Media, 2021; Orenstein, 2021.)

Proposal at/by	Title	Date	Status
U.S. Congress	Sustainable Skies Act	May 20, 2021	Introduced in House
New Mexico	Clean Fuel Standard Act	March 11, 2021	Failed
New York	An act to amend the environmental conservation law, in relation to establishing the "clean fuel standard of 2021"	January 26, 2021	Failed
Minnesota	Future Fuels Act	March 10, 2021	Failed
Hawaii	A Bill for an Act Relating to Taxation	March 2020	Failed
European Commission	Proposal for a Regulation of the European Parliament and of the Council on Ensuring a Level Playing Field for Sustainable Air Transport	July 14, 2021	Being considered by the Council and the European Parliament
France	French Eco Tax	2019	Entry is delayed until air traffic returns to the 2019 levels

tightening of the existing EU ETS; greater energy efficiency; a faster roll-out of low emission transport modes and the infrastructure to support them; measures to prevent carbon leakage; and tools to preserve and grow natural carbon sinks" (European Commission, 2021a).

As a part of the package, the European Commission proposed a revision of the RED in July 2021, which raises renewable targets by at least 40% in 2030 (European Commission, 2021b). Another proposal provides blending mandates for SAF on aviation fuel suppliers via the Refuel EU Aviation initiative. The blending mandates are proposed for 5-year periods beginning in 2025: a minimum of 2% from 2025; a minimum of 5% from 2030, of which a minimum share is of 0.7% of synthetic aviation fuels, while in 2050 reaching to 63% of SAF, with a minimum share of 28% of synthetic aviation fuels.[69]

Another proposal under the package aims to gradually single out free emission allowances for aviation and to transition to full auctioning of allowances by 2027 (Campi, 2021). Finally, another proposal would terminate the tax exemption for kerosene used as fuel in the aviation industry and heavy oil used in the maritime industry (Campi, 2021). Although it is not clear when the proposal would enter into force, all of them have to be approved by the Council of the EU and the European Parliament in order to take effect (Buyck, 2021). Even as further EU mandates are considered, individual countries within the EU are taking action.

European Country Level Actions

In addition to EU-wide action, different countries are also enacting legislation. For example, the Netherlands has enacted national legislation which allowed SAF producers to generate biofuel certificates (called Hernieuwbare Energie Eenheid-HBEs), when supplying SAF to the Dutch Market. These HBEs can be sold to the road transport obligated parties (Meijerink, 2016, p. 6). The SAF must be produced in the Netherlands (Meijerink, 2016, p. 19).

Germany increased its aviation tax which entered into force in April 2020 (Ash, 2019). The aim of the tax is to reduce CO_2 emissions from the aviation sector and incentivize people to use less air travel and more railway transportation. The tax increase will raise airfares by around 28% overall (Ash, 2019). The tax is charged per passenger at the following rates: domestic and Europe flights, €12.88; mid-haul, €32.62; and long haul (which is more than 6,000 km), €58.73 (FCC Aviation, n.d.a).

France adopted the French Eco Tax but delayed its entry until air traffic returns to 2019 levels (Mitchell, 2021; FCC Aviation, n.d.b). It will be applied with the solidarity tax. Passengers traveling to airports in the European Economic Area and Switzerland will be charged at €2.63 (lower rate) or €20.27 (higher rate) depends on traveling in lowest class or higher classes. Passengers traveling to all other destination will be charged between €7.51 or €63.07 (Mitchell, 2021; FCC Aviation, n.d.b). The French government also announced a roadmap to replace jet fuel with 2% of SAF from 2025, 5% by 2030 and 50% by 2050 (GreenAir, 2020).

Since January 2020, Norway requires aviation fuel suppliers to blend 0.5% biofuel into their jet fuel (Norwegian Ministry of Climate and Environment, 2018). The country aims to have a 30% share of biofuels in the aviation sector by 2030 (Gevo Inc., 2020).

In contrast, the United Kingdom Renewable Transport Fuel Obligation (RTFO) requires suppliers of transport and non-road mobile machinery fuel in the United Kingdom to show that at least 9.75% of the fuel they supply after 2020 (which will increase to 12.4% in 2032) comes from renewable and sustainable sources (Department of Transport, 2018). Although aviation fossil fuels are not covered under the RTFO program, the changes in 2018 to the RTFO have allowed renewable jet producers to opt into the program (Department of Transport, 2018). After the withdrawal of the United Kingdom from the EU, the United Kingdom adopted the United Kingdom Emission Trading Scheme replacing the EU ETS. The United Kingdom ETS will apply to energy intensive industries including aviation (UK Department for Business, Energy and Industrial Strategy, 2021). Specifically, covered aviation routes include United Kingdom domestic flights, flights between the United Kingdom and Gibraltar, and flights departing the United Kingdom to European Economic Area countries operated by all aircraft operators, regardless of

[69]Annex I (Volume Shares), Proposal for a Regulation of the European Parliament and of the Council on Ensuring a Level Playing Field for Sustainable Air Transport," Brussels, July 14, 2021, https://ec.europa.eu/info/sites/default/files/refueleu_aviation_-_sustainable_aviation_fuels.pdf.

nationality (UK Department for Business, Energy and Industrial Strategy, 2021). Free allocation of allowance in the United Kingdom ETS will be similar to Phase IV of the EU ETS (UK Department for Business, Energy and Industrial Strategy, 2021). It is possible that EU and the United Kingdom will decide to form a new partnership for the EU ETS (European Union Aviation Safety Agency, n.d.).

Each of these actions potentially affects U.S. companies that fly internationally while also providing examples of what could be pursued in the U.S. as it works to comply with international commitments. **Table 2** also highlights proposed actions.

CONCLUSION

As discussed above, the international nature of aviation is driving efforts to reduce greenhouse gas emissions and increase SAF through international agreements and country-by-country implementation. As the U.S. works to meet its current voluntary but soon to be mandatory reductions in aviation-related GHG emissions, it could learn from actions taken by various U.S states, the European Union (EU), and individual European countries. These actions include, but are not limited to, adopting a SAF blending mandate, a federal low carbon fuel standard program, various tax credits, and/or a cap and trade program. As discussed in this review, there are multiple ways to refine existing programs or develop new programs. For any changes, analysis of how such changes might affect the supply chain and/or economics should be considered; however, such analyses are outside the scope of this review. Providing further law and policy support for GHG reductions from aviation—provided any source of SAF indeed reduces GHG emissions—is critical for the U.S. in meeting its commitments and obligations under CORSIA and as an opportunity to step into a leadership role as countries around the worlds works to reduce GHG emissions.

AUTHOR CONTRIBUTIONS

All authors listed have made a substantial, direct, and intellectual contribution to the work and approved it for publication.

FUNDING

This research was funded by the U.S. Federal Aviation Administration Office of Environment and Energy through ASCENT, the FAA Center of Excellence for Alternative Jet Fuels and the Environment, project 001 through FAA Award Number 13-C-AJFE-PSU under the supervision of Nate Brown (U.S. FAA). Any opinions, findings, conclusions or recommendations expressed in this material are those of the authors and do not necessarily reflect the views of the FAA.

ACKNOWLEDGMENTS

The authors would like to thank KL (U.S. DOT Volpe Center), Nate Brown (U.S. FAA) and Michael P. Wolcott (WSU) for their critical review and comments as well as Season Ashley Hoard, Carol Sim and Christina M. Sanders from the WSU. Any errors are those of the authors.

REFERENCES

Ahn, S. (2021). EPA's New Aviation Emissions Standard: Why It's Already Obsolete. Harvard Environmental & Energy Law Program. Available at: https://eelp.law.harvard.edu/2021/02/epas-aviation-emissions-standard/ (Accessed July 25, 2021).

Air Transport Action Group (ATAG) (2017). *Beginner's Guide to Sustainable Aviation Fuel*.

Alaska Airlines Newsroom (2018). Alaska Airline and Neste Grow Innovative Partnership to Fly More Sustainably. Available at: https://newsroom.alaskaair.com/2018-09-10-Alaska-Airlines-and-Neste-grow-innovative-partnership-to-fly-more-sustainably.

Alaska Airlines Newsroom (2016). Alaska Airlines Flies First Commercial Flight with New Biofuel Made from Forest Residuals. Available at: https://blog.alaskaair.com/alaska-airlines/company-news/nara-flight/.

Argus Media (2021). New York LCFS Supporters Look to Next Year. Available at: https://www.argusmedia.com/en/news/2224308-new-york-lcfs-supporters-look-to-next-year.

Ash, L. (2019). Germany's Increased Aviation Taxes Are Set to Come into Force in April 2020. Simple Flying. Available at: https://simpleflying.com/germany-aviation-tax-april-2020/.

Aviation Benefits Beyond Borders (2019). Neste and NY & NJ Port Authority Collaborate to Facilitate Use of Sustainable Transportation Fuels. Available at: https://aviationbenefits.org/newswire/2019/06/neste-and-ny-nj-port-authority-collaborate-to-facilitate-use-of-sustainable-transportation-fuels/.

Ayres, A. S. (2011). First Commercial U.S. Biofuel Flight Takes off. National Geographic. Available at: https://www.nationalgeographic.com/environment/article/first-commerical-biofuel-flight-eu-cap-and-trade.

Biofuels International (2020). Sustainable Aviation Fuel Production Pathway Approved by ASTM. Available at: https://biofuels-news.com/news/sustainable-aviation-fuel-production-pathway-approved-by-astm/.

Bracmort, K. (2020). *The Renewable Fuel Standard (RFS): An Overview*. Washington, D.C., U.S.: Congressional Research Service.

Bureau of Transportation Statistics (2018). 2017 Annual and December U.S. Airline Traffic Data. Available at: https://www.bts.dot.gov/newsroom/2017-annual-and-december-us-airline-traffic-data (Accessed July 24, 2021).

Burnett, J. (2021). New Laws Bolster Sustainability. Hawaii Tribune Herald. Available at: https://www.hawaiitribune-herald.com/2021/07/03/hawaii-news/new-laws-bolster-sustainability/.

Buyck, C. (2021). SAF Central to Europe's ReFuelEU Plans. AIN Online. Available at: https://www.ainonline.com/aviation-news/air-transport/2021-06-01/saf-central-europes-refueleu-plans.

CAAFI (n.d.b). Fuel Qualification. Available at: https://www.caafi.org/focus_areas/fuel_qualification.html (Accessed May 17, 2021).

CAAFI (n.d.a). What Is a Drop-In Alternative Jet Fuel? FAQ. Available at: http://caafi.org/resources/faq.html (Accessed April 3, 2020).

California Delivers (n.d.). California's Low Carbon Fuel Standard. Available at: http://www.cadelivers.org/low-carbon-fuel-standard (Accessed July 21, 2021).

Campi, G. (2021). European Commission Proposes to Adapt its Legislative Framework in Various Policy Areas to Make it 'Fit for 55.' National Law Review. Available at: https://www.natlawreview.com/article/european-commission-proposes-to-adapt-its-legislative-framework-various-policy-areas.

CARB (2018). CARB Amends Low Carbon Fuel Standard for Wider Impact. Available at: https://ww2.arb.ca.gov/index.php/news/carb-amends-low-carbon-fuel-standard-wider-impact (Accessed July 26, 2021).

CARB (n.d.a). LCFS Basics. Available at: https://ww2.arb.ca.gov/resources/documents/lcfs-basics.

CARB (n.d.b). LCFS Credit Clearance Market. Available at: https://ww2.arb.ca.gov/resources/documents/lcfs-credit-clearance-market#:~:text=The%20LCFS%20regulation%20established%20the,all%20years%20subsequent%20to%202016 (Accessed May 24, 2021).

CARB (2020). "Low Carbon Fuel Standard Amendments 2019," Proposed Amendments to the Low Carbon Fuel Standard Regulation. Available at: https://ww2.arb.ca.gov/rulemaking/2019/lcfs2019 (Accessed July 26, 2021).

CARB (2021a). LCFS Pathway Certified Carbon Intensities. Available at: https://www.arb.ca.gov/fuels/lcfs/fuelpathways/pathwaytable.htm (Accessed July 26, 2021).

CARB (n.d.c). Low Carbon Fuel Standard. about. Available at: https://ww2.arb.ca.gov/our-work/programs/low-carbon-fuel-standard/about (Accessed July 21, 2021).

CARB (2021b). Monthly LCFS Credit Transfer Activity Reports. Available at: https://ww3.arb.ca.gov/fuels/lcfs/credit/lrtmonthlycreditreports.htm (Accessed July 26, 2021).

Christensen, E. L., Detterman, B. J., Weber, D. C., and Winkes, A. E. (2021). Fourth Time's the Charm: Washington Enacts Clean Fuels Program, Creating West Coast Market for Law-Carbon Transportation Fuels. *National L. Rev.* XI, 158, 2021 . Available at: https://www.natlawreview.com/article/fourth-time-s-charm-washington-enacts-clean-fuels-program-creating-west-coast-market.

Colorado Energy Office (2021). *Colorado Greenhouse Gas Pollution Reduction Roadmap*.

Dalzell, N. (2019). Hawaii's Carbon Pricing Bill Passes Senate with Unanimous Support. Climate XChange. Available at: https://climate-xchange.org/2019/03/14/hawaiis-carbon-pricing-bill-passes-senate-unanimous-support/.

Delta News Hub (2019b). Delta Enters Offtake Agreement with Gevo for 10M Gallons Per Year of Sustainable Aviation Fuel, Creates Long-Term Carbon Solution-1. Available at: https://news.delta.com/delta-enters-offtake-agreement-gevo-10m-gallons-year-sustainable-aviation-fuel-creates-long-term.

Delta News Hub (2019a). Delta Invests $2 Million for Study of Potential Facility to Produce Biofuel from Forest Floor Debris. Available at: https://news.delta.com/delta-invests-2-million-study-potential-facility-produce-biofuel-forest-floor-debris.

Department of Taxation, State of Hawaii (2016). Annual Report (2015-2016). Available at: http://files.hawaii.gov/tax/stats/stats/annual/16annrpt.pdf.

Department of Transport (2018). New Regulations to Double the Use of Sustainable Renewable Fuels by 2020. Available at: https://www.gov.uk/government/news/new-regulations-to-double-the-use-of-sustainable-renewable-fuels-by-2020.

EPA (2020). EPA Finalizes Airplane Greenhouse Gas Emission Standards. Office of Transportation and Air Quality. Available at: https://www.epa.gov/sites/production/files/2020-12/documents/420f20057.pdf (Accessed July 25, 2021).

EPA (2021). Inventory of U.S. Greenhouse Gas Emissions and Sinks: 1990-2019. Available at: https://www.epa.gov/sites/production/files/2021-04/documents/us-ghg-inventory-2021-main-text.pdf.

EPA (n.d.a). Renewable Fuel Standard Program. Available at: https://www.epa.gov/renewable-fuel-standard-program/overview-renewable-fuel-standard (Accessed July 26, 2021).

EPA (n.d.b). RIN Trades and Price Information. Available at: https://www.epa.gov/fuels-registration-reporting-and-compliance-help/rin-trades-and-price-information (Accessed July 15, 2021).

EPA (n.d.c). RINs Generated Transactions. Fuels Registration, Reporting, and Compliance Help. Available at: https://www.epa.gov/fuels-registration-reporting-and-compliance-help/rins-generated-transactions (Accessed April 5, 2021).

EPA (2019). Texmark-Neste Pathway. Available at: https://www.epa.gov/sites/production/files/2019-10/documents/texmark-chem-neste-us-deter-ltr-2019-09-23.pdf (Accessed July 21, 2021).

European Commission (n.d.b). EU Emissions Trading System (EU ETS). Available at: https://ec.europa.eu/clima/policies/ets_en#tab-0-2 (Accessed June 28, 2021).

European Commission (2021a). Press Release. European Green Deal: Commission Proposes Transformation of EU Economy and Society to Meet Climate Ambitions. Available at: https://ec.europa.eu/commission/presscorner/detail/en/ip_21_3541 (Accessed July 26, 2021).

European Commission (n.d.a). Renewable Energy Directive. Available at: https://ec.europa.eu/energy/en/topics/renewable-energy/renewable-energy-directive (Accessed June 15, 2021).

European Commission (2021b). Renewable Energy Directive, 2021 Revision of the Directive. Available at: https://ec.europa.eu/energy/topics/renewable-energy/directive-targets-and-rules/renewable-energy-directive_en (Accessed July 18, 2021).

European Commission (2019). Renewable Energy- Recast to 2030 (RED II). Available at: https://ec.europa.eu/jrc/en/jec/renewable-energy-recast-2030-red-ii.

European Union Aviation Safety Agency (n.d.). Brexit. Available at: https://www.easa.europa.eu/brexit (Accessed July 27, 2021).

European Union Aviation Safety Agency; the European Environment Agency; EUROCONTROL (2019). *European Aviation Environmental Report*.

FCC Aviation (n.d.b). French Eco Tax. Available at: https://www.fccaviation.com/regulation/france/eco-tax (Accessed July 27, 2021).

FCC Aviation (n.d.a). German Aviation Tax. Available at: https://www.fccaviation.com/regulation/germany/aviation-tax (Accessed July 26, 2021).

Fulcrum BioEnergy (2021). Fulcrum BioEnergy Completes Construction of the Sierra Biofuels Plant. Available at: https://fulcrum-bioenergy.com/wp-content/uploads/2021/07/2021-07-06-Sierra-Construction-Completion-Press-Release-FINAL.pdf.

Gevo Inc (2020). Gevo: Sweden and Norway Target Increased Use of SAF. Biomass Magazine. Available at: http://biomassmagazine.com/articles/17378/gevo-sweden-and-norway-target-increased-use-of-saf.

Ghatala, F. (2020). *Sustainable Aviation Fuel Policy in the United States: A Pragmatic Way Forward*. Washington, D.C: Atlantic Council.

Graver, B., Zhang, K., and Rutherford, D. (2019). *CO2 Emissions from Commercial Aviation, 2019*. Washington, D.C: ICCT.

Green Car Congress (2020). ASTM Approves 7th Annex to D7566 Sustainable Jet Fuel Specification: HC-HEFA. Available at: https://www.greencarcongress.com/2020/05/20200514-ihi.html.

GreenAir (2020). French Government Announces Launch of Roadmap and Deployment Targets for A National Sustainable Aviation Fuel Industry. Available at: https://www.greenaironline.com/news.php?viewStory=2659.

Hawaii Natural Energy Institute (2020). Sustainable Aviation Production. Available at: https://www.hnei.hawaii.edu/projects/sustainable-aviation-fuel-production.

Hawaii State Energy Office (N.D). Energy Policy. Available at: https://energy.hawaii.gov/energypolicy (Accessed June 9, 2021).

Hecht, S. B. (2019). U.S. Supreme Court Declines to Revive Challenge to Oregon Clean Fuels Program. Legal Planet. Available at: https://legal-planet.org/2019/05/16/u-s-supreme-court-declines-to-revive-challenge-to-oregon-clean-fuels-program/.

Hopkins, C., Comeskey, R., and Rondinelli, K. (2021). Wash. Clean Fuel Standard Hinges on Regs, Likely Litigation. Law360. Available at: https://www.law360.com/environmental/articles/1393465/wash-clean-fuel-standard-hinges-on-regs-likely-litigation?nl_pk=9a987e74-8a65-413c-8f7c-78ea540d3d7c&utm_source=newsletter&utm_medium=email&utm_campaign=environmental.

Hubbard, D. (2021). *NBAA Welcomes News Legislation to Incentivize SAF Production*. Washington, DC, United States: National Business Aviation Association. Available at: https://nbaa.org/press-releases/nbaa-welcomes-new-legislation-to-incentivize-saf-production/ (Accessed July 26, 2021).

IATA (2015). IATA Air Passenger Forecast Shows Dip in Long-Term Demand. Available at: https://www.iata.org/en/pressroom/pr/2015-11-26-01 (Accessed July 24, 2021).

ICAO (n.d.b). 40th ICAO Assembly Drives New Progress toward Key Economic Development Priorities for Air Transport. Available at: https://www.icao.int/Newsroom/Pages/40th-ICAO-Assembly-drives-new-progress-toward-key-economic-development-priorities-for-air-transport.aspx (Accessed July 27, 2021).

ICAO (2016b). Committee on Aviation Environmental Protection (CAEP). Available at: https://www.icao.int/publications/Pages/Caep.aspx (Accessed July 27, 2021).

ICAO (2019b). CORSIA Eligibility Framework and Requirements for Sustainability Certification Schemes. Available at: https://www.icao.int/environmental-protection/CORSIA/Documents/ICAO%20document%2003%20-%20Eligibility%20Framework%20and%20Requirements%20for%20SCS.pdf.

ICAO (2021). CORSIA Eligible Emissions Units. *CORSIA Newsl.*

ICAO (2020). CORSIA States for Chapter 3 State Pairs. Available at: https://www.icao.int/environmental-protection/CORSIA/Documents/CORSIA_States_for_Chapter3_State_Pairs_Jul2020.pdf (Accessed April 5, 2021).

ICAO (2019c). CORSIA Sustainability Criteria for CORSIA Eligible Fuel. Available at: https://www.icao.int/environmental-protection/CORSIA/Documents/ICAO%20document%2005%20-%20Sustainability%20Criteria.pdf.

ICAO (2019). CORSIA Sustainability Criteria for CORSIA Eligible Fuels. Available at: https://www.icao.int/environmental-protection/CORSIA/Documents/ICAO%20document%2005%20-%20Sustainability%20Criteria.pdf.

ICAO (2016a). Environmental Report 2016, Aviation and Climate Change. Available at: https://www.icao.int/environmental-protection/Documents/ICAO%20Environmental%20Report%202016.pdf.

ICAO (2016c). Resolution A39-3: Consolidated Statement of Continuing ICAO Policies and Practices Related to Environmental Protection – Global Market-Based Measure (MBM) Scheme. Available at: https://www.icao.int/environmental-protection/documents/resolution_a39_3.pdf.

ICAO Secretariat (2017). 5. Emissions Units and Registries. Available at: https://www.verifavia.com/bases/ressource_pdf/376/CORSIA-Seminar-5.-Emissions-Units-ver09.pdf (Accessed July 14, 2021).

ICAO (2018). Volume IV, Carbon Offsetting and Reduction Scheme for International Aviation (CORSIA). Annex 16 to the Convention on International Civil Aviation. Available at: https://www.unitingaviation.com/publications/Annex-16-Vol-04/#page=3.

ICAO (2019a). Sustainable Aviation Takes Significant Step Forward at ICAO. Available at: https://www.icao.int/Newsroom/Pages/Sustainable-aviation-takes-significant-step-forward-at-ICAO.aspx.

ICAO (n.d.a). What ICAO Process Was Followed to Develop CORSIA? Available at: https://www.icao.int/environmental-protection/CORSIA/Pages/CORSIA-FAQs.aspx (Accessed July 27, 2021).

Leggett, J. A., Elias, B., and Shedd, D. T. (2012). *Aviation and the European Union's Emission Trading Scheme*. Washington, D.C: Congressional Research Service.

Lipson, J. (2019). Clean Fuels Program Comparison Chart: California, Oregon, and Proposed Washington Programs. Available at: https://app.leg.wa.gov/committeeschedules/Home/Document/194104.

Mazareanu, E. (2021). *Total Revenue Passenger Miles of U.S. Airlines from 2004 to 2020 (In Billions)*. Hamburg: Statista. Available at: https://www.statista.com/statistics/690466/total-us-airline-revenue-passenger-miles/.

Mazzone, D., Witcover, J., and Murphy, C. (2021). Multijurisdictional Status Review of Low Carbon Fuel Standards, 2010-2020 Q2: California, Oregon, and British Columbia. *UC Davis Res. Rep.* Available at: https://escholarship.org/uc/item/080390x8.

Meijerink, O. (2016). *The Voluntary RED Opt-In for Aviation Biofuels: Identifying Opportunities within the 28 EU Member States. [Internship Report]*. Amsterdam: Universiteit Utrecht.

Meijide, A., de la Rua, C., Guillaume, T., Röll, A., Hassler, E., Stiegler, C., et al. (2020). Measured Greenhouse Gas Budgets Challenge Emission Savings from Palm-Oil Biodiesel. *Nat. Commun.* 11, 1089. doi:10.1038/s41467-020-14852-6

Mitchell, R. (2021). *France Climate Bill Would Postpone Higher Air Ticket Taxes*. New York: Bloomberg Law.

Mladenik, J. (2020). *Airlines Want Renewable Jet Fuel, but Renewable Diesel Is Stealing Their Thunder. Stillwater Associates. Available at: https://stillwaterassociates.com/airlines-want-renewable-jet-fuel-but-renewable-diesel-is-stealing-their-thunder/*.

New Mexico Environment Department (2021). Clean Fuel Standard Act Passes New Mexico Senate. Available at: https://www.env.nm.gov/wp-content/uploads/2021/03/2021-03-11-SB11-passes-Senate-002.pdf.

Norwegian Ministry of Climate and Environment (2018). Aviation Will Use 0.5 Percent Advanced Biofuel from 2020. Available at: https://www.regjeringen.no/no/aktuelt/biodrivstoff-i-luftfarten/id2613122/.

Oregon DEQ (n.d.a). Annual Cost of the Clean Fuels Program. Available at: https://www.oregon.gov/deq/ghgp/cfp/Pages/Annual-Cost.aspx (Accessed June 3, 2021).

Oregon DEQ (n.d.b). Oregon Clean Fuels Program Overview. Available at: https://www.oregon.gov/deq/ghgp/cfp/Pages/CFP-Overview.aspx (Accessed June 9, 2021).

Oregon DEQ (n.d.c). Quarterly Data Summaries, Oregon Clean Fuels Program. Available at: https://www.oregon.gov/deq/ghgp/cfp/Pages/Quarterly-Data-Summaries.aspx (Accessed July 16, 2021).

Orenstein, W. (2021). Minnesota Lawmakers Look to Low-Carbon Fuel Standards as a Way to Address Transportation Emissions. Available at: https://www.minnpost.com/greater-minnesota/2021/08/minnesota-lawmakers-look-to-low-carbon-fuel-standards-as-a-way-to-address-transportation-emissions/.

Pedrick, J. (2020). SAF's California LCFS Credit Value Tumbles as Average Carbon Score Climbs. Available at: https://www.spglobal.com/platts/en/market-insights/latest-news/coal/110620-safs-california-lcfs-credit-value-tumbles-as-average-carbon-score-climbs.

PROMOTUM (2015). California's Low Carbon Fuel Standard: Evaluation of the Potential to Meet and Exceed the Standards. Available at: https://www.ucsusa.org/sites/default/files/attach/2015/02/California-LCFS-Study.pdf.

Red Rock Biofuels (n.d.). Red Rock Biofuels. Available at: https://www.redrockbio.com/lakeview-site/(Accessed June 3, 2021).

Sobczyk, N. (2020). *EPA Finalizes First-Ever Airplane Greenhouse Gas Regulations*. Washington, D.C., US: E&E News. Available at: https://www.eenews.net/greenwire/2020/12/28/stories/1063721505?utm_campaign=edition&utm_medium=email&utm_source=eenews%3Agreenwire (Accessed July 25, 2021).

Tisheva, P. (2018). Neste to Help Texas Airport Cut Emissions. Renewables Now. Available at: https://renewablesnow.com/news/neste-to-help-texas-airport-cut-emissions-616898/.

Transport and Environment (n.d.). Aviation in the ETS. Available at: https://www.transportenvironment.org/what-we-do/flying-and-climate-change/aviation-ets (Accessed July 26, 2021).

UK Department for BusinessEnergy and Industrial Strategy (2021). Participating in the UK ETS. Available at: https://www.gov.uk/government/publications/participating-in-the-uk-ets/participating-in-the-uk-ets.

United Airlines (2019). Expanding Our Commitment to Powering More Flight with Biofuel. Available at: https://hub.united.com/united-biofuel-commitment-world-energy-2635867299.html.

U.S. Energy Information Administration (2021a). California, State Profile and Energy Estimates. Available at: https://www.eia.gov/state/analysis.php?sid=CA (Accessed July 26, 2021).

U.S. Energy Information Administration (2021c). Hawaii, State Profile and Energy Estimates. Available at: https://www.eia.gov/state/analysis.php?sid=HI (Accessed July 26, 2021).

U.S. Energy Information Administration (2021b). Washington: State Profile and Energy Estimates. Available at: https://www.eia.gov/state/analysis.php?sid=WA (Accessed July 26, 2021).

VanderHart, D. (2020). *Gov. Kate Brown Orders State Action on Climate Change*. Portland, Oregon, United States: OPB. Available at: https://www.opb.org/news/article/oregon-governor-kate-brown-climate-change-executive-order-cap-and-trade-bill/?fbclid=IwAR1EigG6E_fPhBq38V-6BVfvizLVnAgVa18RlFQip1dLpdtOfOU0yxjcKg4.

Conflict of Interest: The authors declare that the research was conducted in the absence of any commercial or financial relationships that could be construed as a potential conflict of interest.

frontiers in Energy Research

ORIGINAL RESEARCH
published: 16 November 2021
doi: 10.3389/fenrg.2021.711808

Construction and Demolition Waste-Derived Feedstock: Fuel Characterization of a Potential Resource for Sustainable Aviation Fuels Production

Quang-Vu Bach, Jinxia Fu and Scott Turn*

Hawai'i Natural Energy Institute, University of Hawai'i, Honolulu, HI, United States

Detailed characterization of physical and fuel properties of construction and demolition waste (CDW) can support research and commercial efforts to develop sustainable aviation fuels. The current study reports time-series data for bulk density, mineral composition, reactivity, and fuel properties (proximate analysis, ultimate analysis, heating value and ash fusibility) of the combustible material fraction of samples mined from an active CDW landfill on the island of O'ahu, Hawai'i. The fuel properties are in ranges comparable to other reference solid wastes such as demolition wood, municipal solid wastes, and landfilled materials. Ash fusion temperatures (from initial deformation to fluid deformation) among the samples were found to lie in a narrow range from 1,117 to 1,247°C. Despite higher ash contents, the CDW derived feedstock samples had comparable heating values to reference biomass and construction wood samples, indicating the presence of higher energy content materials (e.g., plastics, roofing material, etc.) in addition to wood. The waste samples show lower reactivity peaks in the devolatilization stage, but higher reactivity peaks (located at lower temperatures) in the gasification and combustion stage, compared with those of reference biomass and construction woods. Mineral elemental analysis revealed that materials from various sources (gypsum, plastic, rust, paint, paint additives, and soils) were present in the samples. Soil recovered from the landfill contained higher Ca, Cu, Fe, K, Mn, Pb, and Zn levels than soil samples from elsewhere on the island. Results from this study can provide insight on variations in the physical and fuel properties of the CDW derived feedstocks, and support the design of conversion systems.

Keywords: construction and demolition waste (C & D waste), sustainable aviation fuels (SAF), fuel properties, proximate analysis, ultimate analysis, heating value, mineral composition

OPEN ACCESS

Edited by:
Zia Haq,
United States Department of Energy (DOE), United States

Reviewed by:
Jean-Henry Ferrasse,
Aix-Marseille Université, France
Salmiaton Ali,
Universiti Putra Malaysia, Malaysia

****Correspondence:***
Quang-Vu Bach
qvbach@hawaii.edu

Specialty section:
This article was submitted to Bioenergy and Biofuels, a section of the journal Frontiers in Energy Research

Received: *19 May 2021*
Accepted: *25 October 2021*
Published: *16 November 2021*

Citation:
Bach Q-V, Fu J and Turn S (2021) Construction and Demolition Waste-Derived Feedstock: Fuel Characterization of a Potential Resource for Sustainable Aviation Fuels Production. Front. Energy Res. 9:711808. doi: 10.3389/fenrg.2021.711808

INTRODUCTION

Construction and demolition waste (CDW), one of the major wastes associated with population growth and rapid industrial development, is generated during the construction, renovation, and demolition of buildings and civil-engineering structures. In the United States, about 569 million tons of CDW materials were generated in 2017 (US EPA, 2017). More than 90% of CDW is generated by

demolition and renovation activities, while construction waste accounts for the rest (US EPA, 2017). In the European Union, CDW is the most voluminous component, accounting for 25–30% of the total waste (Cristelo et al., 2018). The composition of CDW strongly depends on the activities and the sources that generate the debris. Depending on location, CDW may also be mixed with other municipal wastes and/or hazardous materials. Concrete, asphalt, bricks, metals (ferrous and non-ferrous), wood, gypsum, glass, plastics, fibers, and soils are major components of CDW. They may also contain potentially hazardous elements and chemicals at trace concentration levels (Clark et al., 2006), e.g., arsenic (in termite treated wood), cadmium (in paints and batteries), lead (in paints and batteries), mercury (in electrical switches and thermostats), asbestos insulations, polycyclic aromatic hydrocarbons (PAHs), and polychlorinated biphenyls (PCBs). While some inert materials (concrete, asphalt) are believed to have minimal environmental impacts (Wu et al., 2014) and may be beneficial for reuse, e.g., recycled concrete production (Sadek, 2012; Safiuddin et al., 2013), the other fractions of CDW are normally disposed in landfills. Improper disposal or management of CDW may cause negative impacts on human health and the surrounding environment, therefore, regulations and standards have been promulgated and enforced to reduce unsafe management and utilization (Clark et al., 2006).

To reduce the disposal of wastes in landfills and dependency on fossil fuels, organic fractions (construction wood, tree parts, paper, cardboard, and plastics) of CDW can be utilized for sustainable aviation fuel (SAF) production (Shahabuddin et al., 2020). Implementation, however, requires insight and management of the variability in composition and fuel properties resulting from the inherent heterogeneity of CDW streams (Edo et al., 2018). Varied composition and fuel properties of CDW are known to contribute to conversion facility operating problems and require additional attention placed on emission controls and ash disposal.

Recently, SAF from waste materials, such as municipal solid waste (MSW) and CDW (Yilmaz and Atmanli, 2017; Shahabuddin et al., 2020), has received great interest. By May 2021, seven conversion pathways have been approved by ASTM for incorporation into ASTM D7566-20c (ASTM, 2020). Detailed fuel properties of CDW feedstocks are required to select appropriate technologies and system designs for these thermochemical conversion processes (Ragland et al., 1991; Bosmans et al., 2013). CDW can be extremely heterogeneous with composition that varies from sample to sample, making fuel characterization more challenging. Although some researchers investigated the composition of the CDW or similar wastes (e.g., MSW), these works mainly focused on the classification and characterization of individual components/materials (Rodríguez-Robles et al., 2015; Ansah et al., 2016; Nordi et al., 2017) rather than composite CDW materials. In addition, most of the studies considered CDW as debris rather than fuel-production feedstock, so their findings were helpful for waste management (Douglas et al., 2001; Roussat et al., 2008; Wu et al., 2014; Song et al., 2017; Bassani et al., 2019) but may not be useful for utilization of CDW as feedstock. Attention has been also paid to landfill-mined materials (van der Zee et al., 2004; Krook et al., 2012; Jain et al., 2013; Powell et al., 2016; Jagodzińska et al., 2021). Reclamation, material recycling, pollution control, and market opportunities of landfill mining have been discussed in recent publications (van der Zee et al., 2004; Krook et al., 2012; Jain et al., 2013; Jagodzińska et al., 2021). In addition, Powell et al. (Powell et al., 2016) estimated that a gross energy of 338 billion MJ per year can be produced from a total municipal waste stock of 8.5 billion Mg available in 1,232 landfills in U.S. from 1960 to 2013. Currently, there are only a few studies (Littlejohns et al., 2020; Passos et al., 2020; Peres et al., 2020) examining the fuel properties of CDW or landfilled materials and their potential for energy conversion via gasification. However, none of these works characterized the composite CDW materials in detail. Peres et al. (Peres et al., 2020) classified the biomass at a construction site into four sub-groups: mixed wood, pine (*Pinus elliotti*), plastic-coated plywood, and resin-coated plywood. Littlejohns et al. (Littlejohns et al., 2020) subdivided landfill diverted wood waste into CDW, discarded pallets and oriented strand board (OSB). García-López et al. (García-López et al., 2019) segregated waste directly excavated from a landfill into several types of materials including glass, inert, non-ferric metals, ferric metals, plastics, textile, paper, wood and fine particles. In addition, these studies employed single sampling events, which may not reflect the compositional variation of the CDW materials.

The present study characterizes the fuel properties of the combustible fraction of CDW derived feedstock necessary for its use for SAF production via thermochemical pathways. The analyses include non-combustible fraction, bulk density, proximate analysis, ultimate analysis, heating value, mineral composition, ash fusion temperatures, and reactivity. The CDW derived feedstock (CDWDF) samples reported in this study were collected from a construction and demolition landfill on the island of Oʻahu (Hawaiʻi) over the course of several months to characterize the variation in composition and fuel properties. Material collection, preparation, and analysis were guided by ASTM standards. For perspective, three different types of construction timbers and two woody biomass samples were also characterized.

MATERIAL COLLECTION AND CHARACTERIZATION METHODS

Material Collection and Preparation

The CDWDF samples were collected at the PVT Land Company Ltd. (approximate location: 21°24′07.9″N, 158°08′39.3″W), located in Nānākuli in the Waiʻanae district of Oʻahu (Hawaiʻi). Climate characteristics relevant to landfill conditions include the mean annual rainfall 667 mm (Giambelluca et al., 2013), mean annual temperature 23.64°C (Giambelluca et al., 2014), and mean annual Priestley-Taylor potential evapotranspiration of 1,625 mm. CDWDF material was generated either directly from trucks entering the landfill or from material mined from the landfill. CDWDF (**Figure 1A** and blue arrow in **Figure 1B**) was processed by PVT to remove

FIGURE 1 | CDWDF materials **(A)** mining and **(B)** processing at PVT Land Company (blue arrow: CDWDF intake, red arrow: CDWDF sampling position).

recyclable material and noncombustible material. Feedstock for energy conversion exited the process line from an outfall conveyor (red arrow in **Figure 1B**) and was collected and stored in a dedicated cell in the landfill to be reclaimed for future use. One sample was collected from processed material that originated from incoming trucks in 2018. All the other samples were collected from processed material that had been mined from the existing landfill (11 samples). These materials were landfilled for ~25 years. During the 2019 sampling campaign, the process line operated exclusively on mined material. The samples were identified by processing day, i.e., #yymmdd. The total amount of collected materials ranged from 35 to 55 kg per batch. It is worth noting that big inert objects, such as concrete and stones, were removed by the company prior to the sample collection in this study. The CDWDF samples obtained from the outfall conveyor were further hand sorted into combustible and non-combustible fractions. The non-combustible fraction includes small stones, ceramic, glass, and metal pieces (e.g., nails extracted from wood). After the removal of the non-combustible fraction, the weight of remaining combustible material ranged from 24 to 46 kg. These materials were primarily composed of construction wood, tree parts, plastics, rubber, paper, textiles, and roofing material. Of these, wood-based materials were abundant. This remaining combustible fraction of CDWDF, which can be employed as feedstock for energy and fuel production, is termed "combustible construction and demolition waste derived feedstock" (CCDWDF). The entire CCDWDF sample was ground to pass a 6 mm screen (SM400 XL Cutting Mill, Retsch, Haan, Germany). Subsequently, the 6 mm CCDWDF samples were riffled repeatedly, following ASTM E1757 (ASTM, 2015b), until four riffled subsamples of 200–400 g remained. To confirm the reproducibility of the characterization and analyses, one sample batch (#190213) was subdivided from the initial 25+ kg CCDWDF sample to a nominal 200 g sample four times. After producing a 200 g sample, the remaining material (~25 kg) was remixed and the riffling process repeated to produce four identical sub-samples (~200 g each) for analysis and comparison. This reproducibility assessment was conducted early in the sampling campaign to provide an estimate of error.

Three construction wood and two woody biomass samples were included in this study and serve as reference woods for comparison with the CCDWDF materials. Two Douglas Fir construction wood samples purchased from local stores were not termite treated and were labeled "Constr. Wood 1" and "Constr. Wood 2." The third sample (labeled "CCA Wood") was removed from a home constructed in Honolulu in 1973 when construction wood was commonly treated with chromated copper arsenate (CCA) as a termite preventative. The two woody biomass are Douglas Fir and Eucalyptus. These reference woods were also ground to pass a 6 mm screen. However, they were not riffled due to their high homogeneity.

Characterization Methods

After riffling and subsampling were complete, the bulk density of the CCDWDF materials reduced to <6 mm particle size was determined according to ASTM E873 (ASTM, 2013b). Moisture

content of the CCDWDF subsamples was determined using ASTM E871 (ASTM, 2013a). After measuring the moisture content, the remainder of the ~250 g CCDWDF sample was dried at 105 ± 1°C (Lindberg MO-1440A Blue M Mechanical Oven, Asheville, NC, United States) for 16 h prior to size reduction. The dried CCDWDF materials were ground using a ball mill (Retsch PM100, Düsseldorf, Germany). Milled material was hand screened to pass a 70-mesh sieve (opening size of 0.21 mm). A small fraction of the CCDWDF material could not be adequately pulverized to pass the 70-mesh sieve after repeated ball milling and typically consisted of flexible polymeric materials, such as plastics, rubbers, and textiles. A cryogenic ball mill (Retsch Cryomill, Düsseldorf, Germany) using liquid nitrogen was employed to grind the recalcitrant materials to pass a 70-mesh sieve. The cryogenic and ambient ball milled materials were recombined and thoroughly mixed by a shaker and stored in a sealed bag for further analyses.

Proximate analysis of the ~0.2 mm particle size CCDWDF samples was conducted using a LECO Macro TGA-801 (LECO Corporation, St. Joseph, MI, United States) according to ASTM D7582 (ASTM, 2015a). The moisture content reflected the moisture that CCDWDF materials adsorbed during fine grinding, handling, and storage. The moisture and ash contents from this test were used to convert subsequent measured quantities to dry basis (db) or dry and ash-free basis (daf), following the calculations provided in ASTM E791 (ASTM, 2016b).

Ultimate analysis (including C, H, N, and S contents) of the CCDWDF samples was measured using a LECO CHN-628 with a sulfur module S-628 (LECO Corporation, St. Joseph, MI, United States) according to ASTM D5373 (ASTM, 2016a) and ASTM D4239 (ASTM, 2018a), respectively. Higher heating values (HHVs) of the CCDWDF samples were measured using a Parr 6200 bomb calorimeter (Parr Instrument Company, Moline, IL, United States), according to the ASTM D4809 (ASTM, 2018b). Mineral compositions of CCDWDF materials were determined by X-ray fluorescence (XRF) (Bruker S8 Tiger, Bruker Corporation, Karlsruhe, Germany). The elemental concentration determined by XRF was calculated using a $C_6H_{10}O_5$ matrix representing lignocellulosic biomass. The detailed XRF sample preparation and measurement procedure were described by Morgan et al. (Morgan et al., 2017).

Because most CCDWDF samples were mined from the landfill and were in contact with soil present in the landfill, analysis of soil samples was included in the study to provide context. Samples were collected from 1) screened soil recovered as part of PVT landfill mining operations and used internally on site (sample identification PVT); 2) an undisturbed land parcel upwind and upslope from the PVT landfill and across Lualualei Naval Road from the PVT landfill site (sample identification AR); and 3) screened recycled soil product offered for sale by the West Oʻahu Aggregate Co. Inc., located on an adjacent land parcel ~1 km from the landfill mining activities (sample identification WOA). The PVT soil sample is representative of material adherent upon the CCDWDF samples. The AR soil sample serves as a reference soil indicative of the environment surrounding the landfill. West Oʻahu Aggregate's recycling services takes in material from across Oʻahu and the WOA soil sample represents a composite for the island. At each of the three locations, five sub-samples were collected. The soil samples were sent to the Agricultural Diagnostic Service Center (ADSC) at the University of Hawaiʻi at Mānoa to analyze their loss-on-ignition and metal content following ASTM D7348 (ASTM, 2008) and EPA Method 3050B (US EPA, 1996), respectively.

Selected CCDWDF samples (#181227, #190116, #190213, #19312, #190405, #190718, and #19815) were also sent to a commercial laboratory (Hazen Research Inc., Golden, CO, United States) for additional analyses. The analyses, including proximate analysis, ultimate analysis, heating value, and elemental composition, were performed to provide comparative data to University of Hawaiʻi (UH) measurements. Hazen employed an inductively coupled plasma, optical emission spectrometry (ICP-OES) for determination of CCDWDF mineral composition, while the UH analysis employed XRF. Prior to ICP analysis, the samples were oxidized at 600°C and the resulting ash was microwave digested in a mixture of four acids. For the volatile elements As, Br, Hg, and Se, a parallel ICP-OES analysis was performed that acid digested fuel samples directly (i.e., no ashing step). The acid HF was not used in this parallel analysis to allow F quantification. Ash fusion temperatures of the selected samples were determined by Hazen according to ASTM E953 (ASTM, 2016c) to characterize ash deformation behavior.

Reactivity of the CCDWDF samples in reducing and oxidizing atmospheres was determined using a thermogravimetric analyzer Mettler Toledo TGA/SDTA851e (Schwerzenbach, Switzerland). The CCDWDF sample was loaded into a crucible, which was heated from room temperature to a final temperature set point at a heating rate of 10°C/min under a gas flow rate of 100 ml/min. For reducing reactivity tests, a ~10 mg sample was heated to 1,100°C under a CO_2 atmosphere, whereas a ~1 mg sample and final temperature of 900°C was used for oxidizing reactivity tests in synthetic air. An initial 30 min isothermal period was performed at 105°C for all tests to remove moisture absorbed during storage and handling.

Similar sample preparation processes and fuel analyses were applied to the reference wood samples. However, non-combustible fraction, bulk density, and ash fusion temperatures of the reference wood samples were not determined due to limited sample amounts. In addition, at least three replicates were conducted for all measurements to provide an error estimate for the experimental data (i.e., measurement uncertainties). Data variations in the four sub-samples from the batch #190213 are reported as sampling uncertainties. A list of characterizations conducted in the current study is presented in **Supplementary Table S1**.

RESULTS AND DISCUSSION

The following section presents the analytical results from the sampling campaign and the reference materials.

Material Fractions of CDWDF

Figure 2 illustrates the material fractions of CDWDF samples. Note that the mined samples were normally coupled with soil, dust and adventitious materials; some materials were also

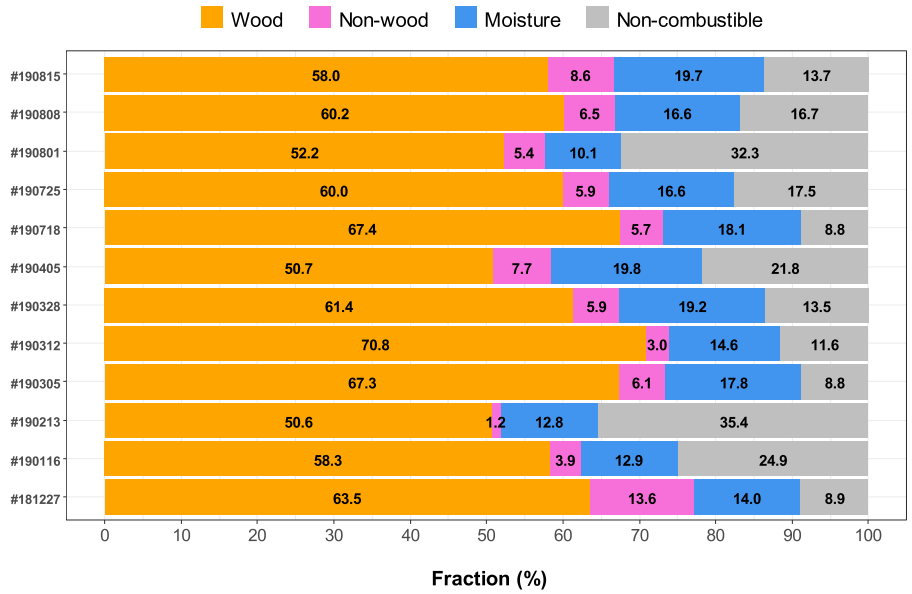

FIGURE 2 | Material fractions of CDWDF from PVT Land Co.

degraded or deformed, making material separation and identification more challenging. The CDWDF samples at PVT were classified into four general fractions: non-combustible material, moisture, combustible non-wood material and woody material. Non-combustible material, combustible non-wood material and woody material were hand sorted and weighed. Moisture content was calculated after drying at 105°C until constant weight. The non-combustible fraction of CDWDF spans a wide range from 8.8 to 35.4 wt% across sampling events and reflects the effectiveness of the PVT processing line. Moisture accounts for 10.1–19.8 wt% of the CDWDF materials. The lowest fraction (1.2–13.6 wt%) in CDWDF belongs to the non-wood material, which may include rubber, plastics, paper, and textile. Woody material is the largest fraction with 50.6–70.8 wt%. The CDWDF in this study contains more woody materials (>50 wt%) than García-López et al. (García-López et al., 2019) reported for material excavated from a landfill and directly characterized (<4.1 wt%). Removal of non-combustible and recyclable materials by the PVT Land Co. processing line prior to the sample collection point was largely responsible for this difference. The fraction of mined material removed by the process line was not quantified. García-López et al. characterized all the mined materials (García-López et al., 2019). In addition, the landfill studied by García-López et al. (García-López et al., 2019) accepted MSW, which would result in a lower wood fraction than CDWDF.

Moisture Content and Bulk Density of CCDWDF Materials

From this point forward, the results pertain only to the combustible fraction of construction and demolition waste derived feedstock (CCDWDF).

Table 1 presents data for the wet bulk density, moisture content and dry bulk density for the <6 mm CCDWDF materials. The wet bulk density of seven batches of the CCDWDF materials (<6 mm) ranged from 220 to 269 kg/m^3, with an average of 241 kg/m^3 and a standard deviation of ±18 kg/m^3. The range of moisture content of the <6 mm CCDWDF materials was 14.88–25.35 wt%, and was higher than the reference wood samples (10.12–14.21 wt%); the latter indicative of equilibrium moisture content at ambient conditions. The mean annual rainfall, temperature, and evapotranspiration rates at the site contribute to the relatively low moisture content of samples; wood recovered in samples was notably well preserved. Apart from the inherent moisture of the CCDWDF materials, water was actively sprayed on the CDWDF materials for dust control by PVT personnel during mining operations and at the inlet and outlet of the processing line (**Figure 1B**). This added water contributed to the moisture content of the CCDWDF materials, partially explaining their elevated moisture content compared to the reference wood samples. The moisture data in this study are in good agreement with that of Littlejohns (Littlejohns et al., 2020), a CDWDF moisture content (as-received) of 20 wt%, and in a common moisture content range (6.16–38.70 wt%) of other solid waste samples (**Table 2**). The dry bulk density, calculated from the wet bulk density and moisture content, varied from 171 to 229 kg/m^3. The bulk densities (both wet and dry) are relatively consistent across sampling days and are close to the bulk densities of other wood chips reported in the literature (Eisenbies et al., 2019), indicating that the handling, transporting, and feeding requirements for CCDWDF and wood chip fuels may be similar. It is worth noting that the particle size of the CCDWDFs in this study is less than 6 mm, but data for the wood chips in (Eisenbies et al., 2019) were not reported.

TABLE 1 | Physical properties of CCDWDF materials (<6 mm) and reference woods.

Sample	Wet bulk density (kg/m³)	Moisture content (wt%)	Dry bulk density (kg/m³)
#181227	NA	15.34 ± 0.22	NA
#190116	NA	17.14 ± 0.31	NA
#190213	NA	19.07 ± 1.24	NA
#190305	NA	19.49 ± 0.23	NA
#190312	NA	16.51 ± 0.14	NA
#190328	220 ± 13	22.19 ± 0.36	171
#190405	240 ± 2	25.35 ± 0.48	179
#190718	223 ± 4	19.88 ± 0.10	179
#190725	241 ± 3	20.13 ± 0.14	192
#190801	269 ± 5	14.88 ± 0.12	229
#190808	261 ± 3	19.96 ± 0.12	209
#190815	232 ± 7	22.88 ± 0.11	179
Constr. wood 1	NA	10.12 ± 0.04	NA
Constr. wood 2	NA	14.21 ± 0.06	NA
CCA wood	NA	10.74 ± 0.06	NA
Doug Fir	NA	13.81 ± 0.04	NA
Eucalyptus	NA	NA	NA

NA: not available.

TABLE 2 | Summary of higher heating values, proximate and ultimate analyses of solid waste samples from the literature.

Solid wastes	Proximate analysis (wt%, db except moisture)				Ultimate analysis (wt%, db)						HHV (MJ/kg, db)	Ref.
	Moisture	Volatile matter	Fixed carbon	Ash	Carbon	Hydrogen	Nitrogen	Oxygen	Sulfur	Chlorine		
CDW	20	74.5	18.9	0.8	42.0	7.2	0.08	50.8	0.03	–	18.3	Littlejohns et al. (2020)
Discarded pallets	17	75.3	16.0	0.8	42.4	6.7	0.04	50.8	0.09	–	18.8	Littlejohns et al. (2020)
OSB	7	74.8	17.6	0.6	41.7	7.3	0.26	50.7	0.04	–	18.5	Littlejohns et al. (2020)
Demolition wood	11.60	79.83	16.18	3.99	54.15	8.60	0.69	32.55	0.02	–	19.21[a]	Dunnu et al. (2010)
MSW (Germany)	6.16	72.60	10.57	16.83	49.23	8.15	1.82	23.72	0.25	–	20.30[a]	Dunnu et al. (2010)
Plastic and paper	6.83	67.74	5.62	26.64	49.03	8.25	0.87	15.09	0.12	–	20.36[a]	Dunnu et al. (2010)
RDF (Sweden)	38.7	–	–	16.4	43.1	5.7	0.7	33.9	–	–	17.90[b]	Skrifvars et al. (1999)
RDF Fall (United States)	–	78.45	10.91	10.64	46.95	6.55	–	34.86	0.26	0.24	20.93	Canova and Bushnell (1992)
RDF Winter (United States)	–	66.40	10.19	23.41	39.99	5.55	0.52	29.77	0.33	0.43	17.75	Canova and Bushnell (1992)
RDF Spring (United States)	–	65.96	10.29	23.75	39.23	5.33	0.79	30.11	0.27	0.52	17.73	Canova and Bushnell (1992)
RDF Summer (United States)	–	62.93	9.35	27.72	38.69	5.61	0.70	26.03	0.71	0.54	17.67	Canova and Bushnell (1992)
RDF mix (United States)	–	68.44	10.18	21.38	41.22	5.76	0.50	30.32	0.39	0.43	18.52	Canova and Bushnell (1992)

[a]*Calculated from LHV.*
[b]*Calculated from ultimate analysis.*

Proximate Analysis

The proximate analysis results of the CCDWDF materials and the reference woods are listed in **Table 3**. The ash content of the CCDWDF varies in a wide range from 6.20 to 18.21 wt% because of the heterogeneity of these materials, collected from different sources and containing varied components. Compared with the ash contents of the reference wood samples (0.05–0.89 wt%), those of the CCDWDF are significantly higher, implying that the CCDWDF includes materials with elevated ash content that may include wood adulterated with inorganic material such as wood treatment chemicals, wall plaster, paint additives, rust, soil, and dust particles. Cardboard, paper, PVC, low density polyethylene, rubber, textiles and roofing materials, present in varying amounts in the CCDWDF samples, each has higher ash content (Cui and

TABLE 3 | Proximate analysis of CCDWDF materials and reference woods (on dry basis).

Sample	Volatile matter (wt%)	Fixed carbon (wt%)	Ash (wt%)
#181227	69.41 ± 0.61	12.38 ± 0.27	18.21 ± 0.60
#190116	74.13 ± 0.42	17.67 ± 0.53	8.20 ± 0.11
#190213	73.74 ± 0.54	19.80 ± 0.66	6.46 ± 0.14
#190305	72.52 ± 0.11	19.28 ± 0.26	8.20 ± 0.16
#190312	73.65 ± 0.23	20.16 ± 0.21	6.20 ± 0.14
#190328	69.69 ± 0.33	17.74 ± 0.31	12.57 ± 0.18
#190405	67.77 ± 0.42	17.36 ± 0.19	14.87 ± 0.42
#190718	72.82 ± 0.08	18.56 ± 0.07	8.61 ± 0.01
#190725	69.75 ± 0.15	19.80 ± 0.12	10.45 ± 0.03
#190801	69.91 ± 0.25	21.11 ± 0.24	8.98 ± 0.01
#190808	70.65 ± 0.08	19.43 ± 0.12	9.91 ± 0.04
#190815	70.37 ± 0.21	18.44 ± 0.21	11.19 ± 0.08
Constr. wood 1	77.82 ± 0.15	21.90 ± 0.13	0.28 ± 0.03
Constr. wood 2	76.41 ± 0.09	23.07 ± 0.07	0.52 ± 0.02
CCA wood	80.00 ± 0.22	19.12 ± 0.24	0.89 ± 0.03
Doug Fir	82.07 ± 0.13	17.88 ± 0.15	0.05 ± 0.03
Eucalyptus	82.11 ± 0.02	17.29 ± 0.01	0.60 ± 0.01

Sampling uncertainties: volatile matter (±0.57 wt%), fixed carbon (±0.71 wt%), ash (±0.15 wt%).

Turn, 2018) and would contribute to elevated ash in the composite sample. Management of high ash fuels is often necessary in thermochemical energy conversion facilities to mitigate negative impacts on operations, working surface materials, and emissions.

The volatile matter contents of the CCDWDF materials (67.77–74.13 wt%) are all lower than those of the reference wood samples (76.41–82.11 wt%). The fixed carbon contents of the CCDWDF samples vary from 12.38 to 21.11 wt%, which are lower than those of the two construction wood samples (21.90 and 23.07 wt%). The fixed carbon contents of the CCA wood (19.12 wt%) and two woody biomass (17.88 and 17.29 wt%) are in the bottom range of the CCDWDF values. These data indicate that the more labile components of the CCDWDF materials that are measured as volatile matter have been preferentially degraded during their time in the landfill. The PVT landfill opened in 1985 and the portion under active mining during the project period was estimated to date to the mid to late 1990s. PVT's location falls between 525 and 800 mm annual rainfall isohyets (Giambelluca et al., 2013) so low degradation rates are not unexpected.

Proximate analysis values reported from other high-ash biomass such as rice husk (Ma et al., 2015) and macroalgae (Bach et al., 2014), are comparable to the CCDWDF materials. The volatile matter contents of the CCDWDF materials (67.77–74.13 wt%) are in the range spanned by those summarized in **Table 2** (62.93–78.83 wt%), while the CCDWDF materials fixed carbon (12.38–21.11 wt%) and the ash (6.20–18.21 wt%) contents trend higher (5.62–18.90 wt%) and lower (3.99–27.72 wt%, except value in Littlejohns et al., 2020) respectively, than those in the literature. The ash content of CCDWDF measured in this study is much higher than the 0.8 wt % (air dry basis) value reported by Littlejohns et al. (Littlejohns et al., 2020). Although they did not clearly describe the location and processing of the CDW, it appears that the waste was relatively clean. The sample unloaded from incoming trucks (#181227) has higher ash content but lower fixed carbon content than the samples mined from the landfill. Nevertheless, more data are needed for material from incoming trucks to establish trends.

Ultimate Analysis

Results from the ultimate analysis (i.e., average C, H, N, S and O contents) of the CCDWDF materials and reference woods on dry basis are tabulated in **Table 4**. Carbon and hydrogen contents of the CCDWDF materials are similar to those of the reference woods. The carbon contents of the CCDWDF materials and reference wood samples are respectively 42.77–49.85 wt% and 49.12–53.21 wt%, while the hydrogen contents of the CCDWDF materials and reference woods are 5.16–5.81 wt% and 5.88–6.06 wt%, respectively. Conversely, the nitrogen contents of the CCDWDF materials (0.25–0.41 wt%) are higher than those of the reference wood samples (0.13–0.19 wt%). The sulfur contents of the CCDWDF materials vary from 0.33 to 2.04 wt %, while those of the reference woods are below the detection limits. Consequently, the oxygen contents (calculated by difference) of the CCDWDF materials (31.41–38.52 wt%) are lower than those of the reference woods (40.26–44.04 wt%).

Compare with other solid wastes in **Table 2**, the carbon, nitrogen and oxygen contents of the CCDWDF materials are well-fitted in the ranges of those of the solid wastes. The hydrogen contents of the CCDWDF materials are in the lower range but the sulfur contents of the CCDWDF materials are in the higher range, compared with those of the solid wastes. Overall, the ultimate analysis data of the CCDWDF materials are in good agreement with those of the solid wastes.

The atomic H/C and O/C ratios were calculated based on the ultimate analysis data and plotted in a van Krevelen diagram (**Figure 3**). The diagram show that the positions of the CCDWDF materials and the construction woods (Constr. Wood 1, Constr. Wood 2, and CCA Wood) are all in the biomass area. The O/C and H/C ratios of these materials are in the range of 0.56–0.72 and 1.47–1.70, respectively, whereas those of the woody biomass (Douglas fir and Eucalyptus) are 0.72–0.80 and 1.61–1.74.

TABLE 4 | Ultimate analysis of CCDWDF materials and reference woods (on dry basis).

Sample	Carbon (wt%)	Hydrogen (wt%)	Nitrogen (wt%)	Sulfur (wt%)	Oxygen[a] (wt%)
#181227	42.77 ± 0.35	5.16 ± 0.24	0.41 ± 0.01	2.04 ± 0.08	31.41
#190116	49.30 ± 0.51	5.53 ± 0.14	0.30 ± 0.00	0.60 ± 0.01	36.07
#190213	49.85 ± 0.60	5.60 ± 0.04	0.29 ± 0.01	0.33 ± 0.02	37.47
#190305	48.45 ± 0.53	5.79 ± 0.21	0.36 ± 0.01	0.64 ± 0.02	36.56
#190312	48.70 ± 0.77	5.81 ± 0.19	0.25 ± 0.01	0.52 ± 0.02	38.52
#190328	47.72 ± 0.56	5.58 ± 0.13	0.40 ± 0.03	0.95 ± 0.02	32.78
#190405	46.67 ± 0.34	5.50 ± 0.08	0.34 ± 0.01	0.95 ± 0.03	31.67
#190718	47.74 ± 0.14	5.77 ± 0.09	0.29 ± 0.01	0.61 ± 0.01	36.98
#190725	46.32 ± 0.23	5.62 ± 0.03	0.28 ± 0.00	0.76 ± 0.01	36.57
#190801	47.33 ± 0.10	5.64 ± 0.02	0.28 ± 0.01	0.78 ± 0.01	36.99
#190808	47.15 ± 0.05	5.59 ± 0.02	0.30 ± 0.01	0.74 ± 0.01	36.31
#190815	46.87 ± 0.11	5.66 ± 0.01	0.36 ± 0.02	0.75 ± 0.02	35.17
Constr. wood 1	52.62 ± 0.20	5.98 ± 0.02	0.13 ± 0.01	<LoD	40.99
Constr. wood 2	53.21 ± 0.18	5.88 ± 0.03	0.13 ± 0.01	<LoD	40.26
CCA wood	51.34 ± 0.22	5.92 ± 0.02	0.13 ± 0.00	<LoD	41.72
Doug Fir	51.35 ± 0.11	6.06 ± 0.04	0.18 ± 0.01	<LoD	42.36
Eucalyptus	49.12 ± 0.20	6.05 ± 0.07	0.19 ± 0.00	<LoD	44.04

Sampling uncertainties: C (±0.25 wt%), H (±0.02 wt%), N (±0.01 wt%), S (±0.01 wt%).
[a]*Calculated by difference.*

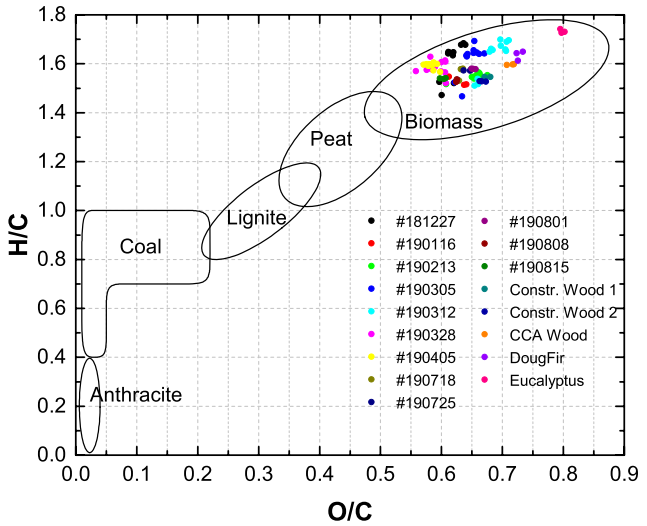

FIGURE 3 | Van Krevelen diagram for CCDWDF materials and reference woods.

Higher Heating Value

Higher heating values (HHVs) of the CCDWDF materials and reference woods on dry basis are presented in **Figure 4**. Sampling uncertainty of this analysis is ±0.35 MJ/kg as determined from the #190213 replicates. On dry basis, the HHV averages of the CCDWDF materials vary from 17.22 to 20.22 MJ/kg, and are similar to those of the CCA treated wood (19.87 MJ/kg) and the two woody biomass (18.74 and 18.88 MJ/kg). However, the CCDWDF materials have lower HHVs than the untreated construction woods (21.04–21.08 MJ/kg). The CCDWDF sample having the highest ash contents (#181227) also possessed the lowest HHV whereas the CCDWDF sample with the lowest ash contents (#190312) has the highest HHV. Nevertheless, there is no correlation between the ash content and the HHV of the CCDWDF materials. The HHVs of the CCDWDF materials in this study are in good agreement with the reported values for other solid wastes (17.67–20.93 MJ/kg) in **Table 2** (Canova and Bushnell, 1992; Skrifvars et al., 1999; Dunnu et al., 2010; Littlejohns et al., 2020).

Mineral Analysis

This section presents results from the mineral analysis of all CCDWDF materials by XRF and selected samples by ICP-OES. Soil sample analyses by ICP-OES are also presented.

Soil Analysis

The composition of the soil samples serves as background data useful in tracing the origin of the mineral elements present in CCDWDF materials. **Figure 5** shows that the AR and WOA soils have comparable concentrations of K, Zn, Mn, Cu, V, Ca, and Fe. The PVT sample has significantly higher contents of K, Zn, Cu, Pb, As, Cd, Ca and Na than the AR and WOA soils, indicating that these elements originated from the CCDWDF materials. Naturally occurring As concentration in Hawai'i soils are <20 ppmw (USDA-NRCS, 2011).

The loss on ignition data (12.44, 23.22 and 13.39 wt% for AR, PVT, and WOA samples, respectively) indicates that the samples from PVT had higher organic matter than the other locations and that the PVT sample was a mixture of soil and CCDWDF. Certain elements (i.e., Mn, Cr, Ni, and V) are present at lower concentrations in the PVT soil, compared with the AR soils, indicating that the soil contributions have been diluted by inorganic matter originating from the PVT CDW. Fe in the three soil samples is the second highest in abundance and has comparable concentrations among the samples. This is expected as Hawai'i's volcanic soils are normally high in Fe (Thompson et al., 2011). Most trace

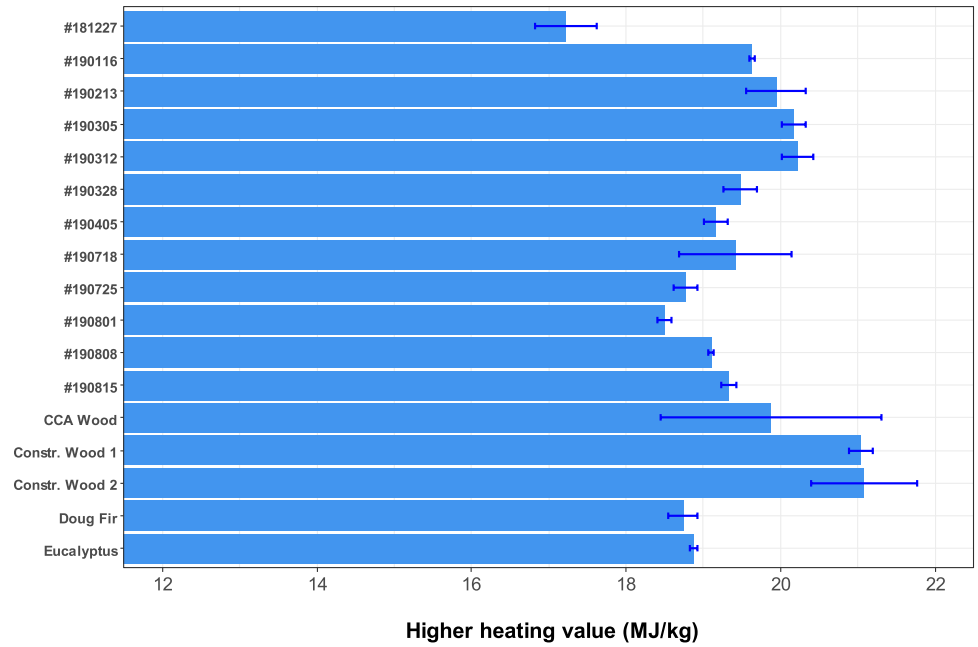

FIGURE 4 | Higher heating values of CCDWDF materials and reference woods.

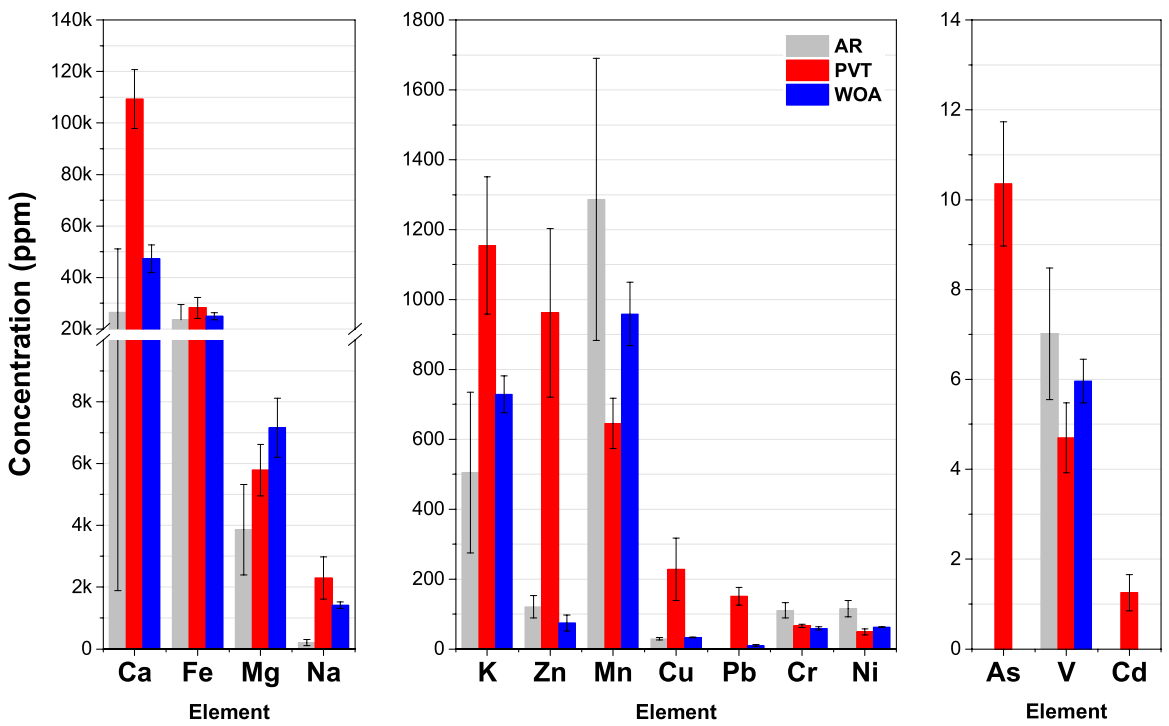

FIGURE 5 | Element concentrations in different soil samples.

element concentrations are in typical ranges for soils (Pais and Jones, 1997), with the exception of Zn levels in the PVT sample.

CCDWDF Analysis

The values reported are the average of 6 measurement (3 pellets and 2 sides for batches with a single sub-sample) or 24

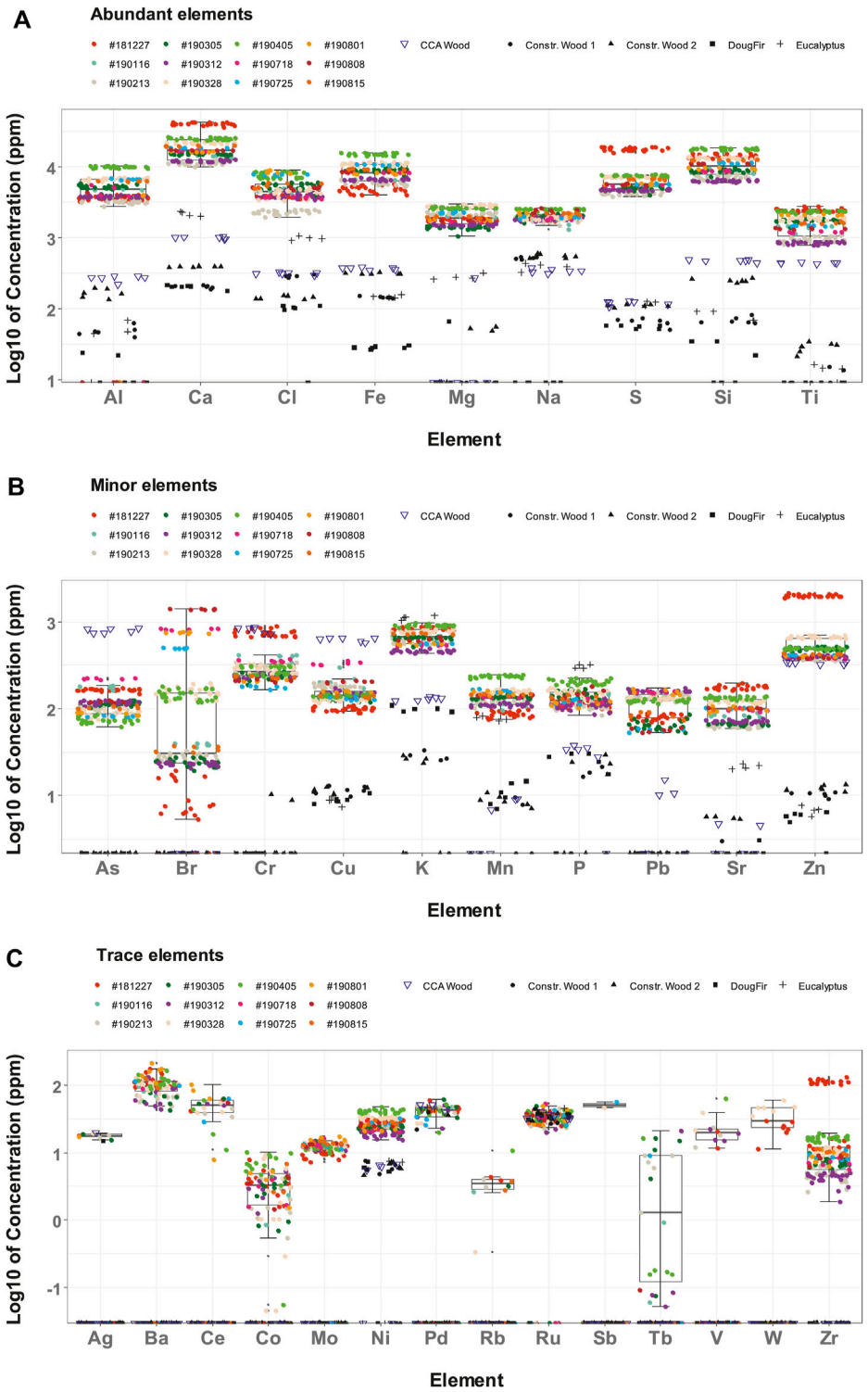

FIGURE 6 | Concentration of elements from individual measurements in CCDWDF materials and reference woods for **(A)** abundant elements, **(B)** minor elements, and **(C)** trace elements.

measurements (3 pellets and 2 sides for batches with 4 sub-samples). Detected elements divided into three ranges are presented in **Figures 6A–C**, based on their average concentrations: >1,000 ppm, 100–1,000 ppm, and <100 ppm, respectively. In total, 68 elements were scanned by the XRF. Elements concentrations below the detection limits were excluded from **Figure 6**.

The limit of detection (LoD) for each element slightly varies due to differences in element concentration from sample to sample. The reported LoDs, tabulated in **Supplementary Table S2**, for the CCDWDF materials and the reference wood samples are the maximum individual LoD values for each element in the two material groups. In addition, a full list of all scanned elements is tabulated in **Supplementary Table S3** for the CCDWDF materials and **Supplementary Table S4** for the reference wood samples.

CCDWDF Analysis: Abundant Elements (>1,000 ppm)

Figure 6A presents the measured concentrations of the major elements (>1,000 ppm) in the CCDWDF materials, including Ca, Si, Fe, S, Al, Cl, Mg, Na, and Ti, listed here in order of generally decreasing concentration. The concentrations of these elements in the CCDWDF materials are much higher than those in all reference wood samples, indicating that the wood fraction of CCDWDF would not be expected to be their source.

The most abundant mineral element in the CCDWDF materials is calcium (12,078–42,485 ppm) Samples with higher calcium content also have higher sulfur and silicon contents, and vice versa. Although construction wood, the main component of CCDWDFs, also contains calcium, its concentration is much lower. The potential sources of calcium in the CCDWDF samples are from gypsum ($CaSO_4{\cdot}2H_2O$) as wall plaster and surrounding soils (e.g., in form of calcite $CaCO_3$). It is easy to understand the presence of gypsum in the CCDWDF materials because sheetrock or drywall is one of the most common substances for house construction. The second highest concentration is silicon (6,790–19,010 ppm), which may originate as caulking present as a material of construction or be present as adherent soil from activities prior to landfill entry or within the landfill after delivery. Iron, in third highest concentration (5,053–15,960 ppm), may originate from corroded fasteners, steel, and other iron-based materials. Adherent soil may also contribute to high concentrations of iron in CCDWDF samples (**Figure 5**). The range of concentration of sulfur in the CCDWDF materials, 4,501–18,837 ppm, is associated with the presence of calcium. This is supported by the Ca to S molar ratios ranging from 1.64 to 2.94 (**Supplementary Table S5**), indicating a positive correlation between the two elements. The fifth most abundant element is aluminum (1,384–10,590 ppm) that may be derived from household aluminum-based materials, paint additives, and soil. The next most abundant element is chlorine (2,477–8,879 ppm), commonly found in polyvinyl chloride (PVC), one of the most widely produced polymer in the world, and other chlorine-containing polymers such as polychloroprene (Neoprene) and chlorinated butyl rubber. Magnesium (1,489–2,978 ppm) and sodium (1,780–2,680 ppm) concentrations are slightly lower than chlorine. They are present at much higher concentrations in the CCDWDF materials in comparison with the reference woods. Presumably the source of the two elements are soil impurities although only magnesium was detected in the soil analysis in the previous section. The lowest concentration in this group is titanium (917–2,595 ppm). Considering lower titanium concentrations in the reference woods, this elements might be derived from TiO_2 present in soils and additives for surface coating materials and paints.

Note that the CCDWDF sample from trucks (#181227) has significantly higher concentrations of calcium and sulfur than other CCDWDF samples, indicating that the sample from trucks may have much higher amount of gypsum than the others. Another possible explanation is that the gypsum ($CaSO_4{\cdot}2H_2O$) in landfilled samples was leached and mobilized in the landfill over time (Palha et al., 2012; Aldaood et al., 2015), resulting in lower concentrations of calcium and sulfur in the landfilled CCDWDF samples and higher calcium concentration in the soil.

CCDWDF Analysis: Minor Elements (100–1,000 ppm)

Figure 6B presents the concentrations of minor elements in the CCDWDF materials, including As, Br, Cr, Cu, K, Mn, P, Pb, Sr, and Zn. Among the reference wood samples, the CCA wood has much higher concentrations of chromium, copper, and arsenic. Also, the concentrations of these three elements in the CCA wood are higher than those in the CCDWDF materials, with the exception of the chromium content of sample #181227. The higher Cr, Cu, and As concentrations in the CCA wood sample resulted from the CCA treatment used as a wood preservative and to repel termites. The lower concentrations of the three elements in the CCDWDF materials may be because the wood-based materials in the CCDWDFs were not all CCA treated, or were treated at lower concentrations. Mobilization of CCA within the landfill over time could also result in reduced concentrations.

Concentrations of potassium and phosphorus in eucalyptus are higher than the other wood and CCDWDF materials. These two elements are plant macronutrients and it might be presumed that eucalyptus absorbed them from fertilizers applied to the plantation or from the surrounding soils during growth. The potassium and phosphorus concentrations of the CCDWDF materials are much higher than those of other reference woods (noting the exception of eucalyptus). Referring to the soil analysis, the PVT soil has significantly higher potassium content than the other soils indicating that potassium was present in the CCDWDF materials and mixed with surrounding soil at PVT. On the other hand, the source of phosphorus in the CCDWDF materials appears to be from the soil impurities.

For the remaining elements, Br, Mn, Pb, Sr, and Zn, the CCDWDF materials overall have higher concentrations than the reference wood samples. In addition, the concentrations of chromium and zinc in the CCDWDF sample from trucks (#181227) was significantly higher than the other CCDWDF samples. These elements were likely present in paint additives rather than in woody materials. This observation is coupled with the highest concentrations of calcium and sulfur in this sample. Because paints were used to cover the surface of gypsum, the sample with a higher amount of gypsum is also associated with more elements present in paint additives. Zinc is also used to galvanize metal that may be present in water pipes and roofing materials of older homes in Hawai‘i. Among the elements, bromine in the CCDWDF materials varies in a very wide range from 45 to 1,437 ppm, and was not detected in any reference wood samples. These concentrations are consistent with its presence in plastics and its use as a flame retardant in

consumer products and building materials (Vainikka and Hupa, 2012). Bromine stands at the fourth position in average concentration in this group, the top three concentrations are potassium (493–9,580 ppm), zinc (394–2,096 ppm), and chromium (184–784 ppm). The following elements are copper (104–345 ppm), manganese (92–250 ppm), phosphorous (115–215), and lead (81–171 ppm).

These elements (except lead) are present in the reference woods at lower concentrations, which indicate that their main sources were not from wood-based materials. Among those, copper may come from electric wires and water pipes besides wood treated chemicals; manganese can be found at a small concentration in steel and aluminum household items, phosphorous might be present in soil impurities, while lead is normally used in paints. Arsenic (81–229 ppm) and strontium (68–185 ppm) have the lowest concentrations among the minor elements. The former is likely from CCA treated wood and the latter can occasionally be found in Hawai'i soil (Chadwick et al., 2009).

CCDWDF Analysis: Trace Elements (<100 ppm)

Elements that were detected by the XRF in individual scans of CCDWDF samples are presented in **Figure 6C** and include Ag, Ba, Ce, Co, Mo, Ni, Pd, Rb, Ru, Sb, Tb, V, W, and Zr. However, most of these elements have the average concentrations lower than the LoDs, except nickel and molybdenum, indicating that the presences of these elements in the CCDWDF materials have high uncertainties. Moreover, most of these elements were not detected in the reference woods, recognizing that their LoDs for the reference woods were lower than those of the CCDWDF materials as indicated in **Supplementary Table S1**. With the exception of nickel, most of the trace elements in the CCDWDF materials do not appear to be derived from wood components and thus are sourced from adherent soil or other construction materials.

Comparison of XRF and ICP-OES Data

Seven CCDWDF samples were sent to an external commercial laboratory for independent analyses to provide comparative measurements. For the proximate, ultimate, and heating value analyses, both the UH and Hazen teams followed the same ASTM standards and their results are in good agreement, see **Supplementary Figure S1**. The XRF and ICP-OES datasets are presented in **Supplementary Tables S3, S6**, respectively, and compared in **Figure 7**. Note that the concentrations of elements S and Cl in **Figure 7** used the total chlorine and sulfur contents from the Hazen analysis result rather than ICP-OES data. Overall, the elemental concentrations acquired from the two techniques are consistent with a few exceptions. The elements fluorine, mercury, bismuth, cadmium, lanthanum, rhenium, antimony, and yttrium were detected only by ICP-OES (see **Supplementary Table S5** for values). Cobalt and molybdenum were identified only by XRF. The ICP-OES data show higher concentrations in vanadium, zirconium, and barium than the XRF data, whereas the XRF analysis report higher content of nickel, bromine, lead, zinc, chlorine, and calcium.

The comparison in **Figure 7** reveals that the ICP-OES may be more sensitive and can detect more elements at low concentrations, while the element concentrations from the XRF are mostly greater than those from the ICP-OES for elements present in higher concentrations. Lower LoDs for ICP-OES compared to XRF have been reported elsewhere (McComb et al., 2014; Chojnacka et al., 2018). The differences may come from the principles of the analytical methods. In the XRF method, the X-ray scans the surface of the sample pellets within a few micrometers to millimeters depth, depending on the matrix. This scanning principle makes trace elements at low concentrations difficult to detect. Sample preparation to produce a homogeneous mixture in the pellet thus plays an important role for XRF. For ICP-OES, acid digestion is employed to prepare the sample prior to detection by the ICP-OES. Elements such as silicon may resist acid digestion resulting in measured element concentrations lower than actual. Samples subjected to either ICP or XRF were dried and ground (<0.2 mm) prior to analysis, but the ICP samples were ashed and acid digested. These additional steps provide opportunities for loss of elemental mass prior to analysis and could contribute to the generally lower values determined by ICP-OES. In addition, spectral interferences and matrix effects may occur and reduce the precision of the ICP-OES method in detecting elements with high concentration (Olesik, 1991).

Comparison With Other Data

Table 5 compares heavy metal concentrations in other MSW and landfilled materials (Esakku et al., 2005; Jain et al., 2005; García-López et al., 2018; Littlejohns et al., 2020) reported in common with CCDWDF data. Among the elements, the CCDWDF materials have higher Al, As, and Ba levels than other wastes. Cr, Cu, Fe, Mn, Ni, Pb, and Zn contents in the CCDWDF materials are comparable. Cd, Co, Hg, Se, and V concentrations in the CCDWDF materials were lower than their LoDs, but were occasionally detected in the samples from the literature.

The mineral composition in the CCDWDF samples (from both XRF and ICP measurements) are calculated and illustrated in **Figure 8** in the chemical classification system of inorganic matter in biomass adopted from (Vassilev et al., 2012), note that Si content from XRF was also used for ICP data because the ICP analysis did not report it. Data for other solid wastes (in **Tables 2**, **8**) are also included for comparison. The ternary diagram shows that the CCDWDF materials are located in the shaded biomass area and surrounded by MB (mixture of biomass), AVB (all varieties biomass) and HAS (herbaceous and agricultural straw). The variation between XRF and ICP analyses is visible but not unexpected, because the ICP measured the element concentrations in the ashes prepared at 600°C while the XRF was employed without an ashing step. In both analysis methods, the truck sample (#181227) is located lower in the diagram and distant from the other samples due to its significantly high calcium content. On the other hand, most referenced solid wastes are positioned in the coal area, except the demolition wood (Dunnu et al.,

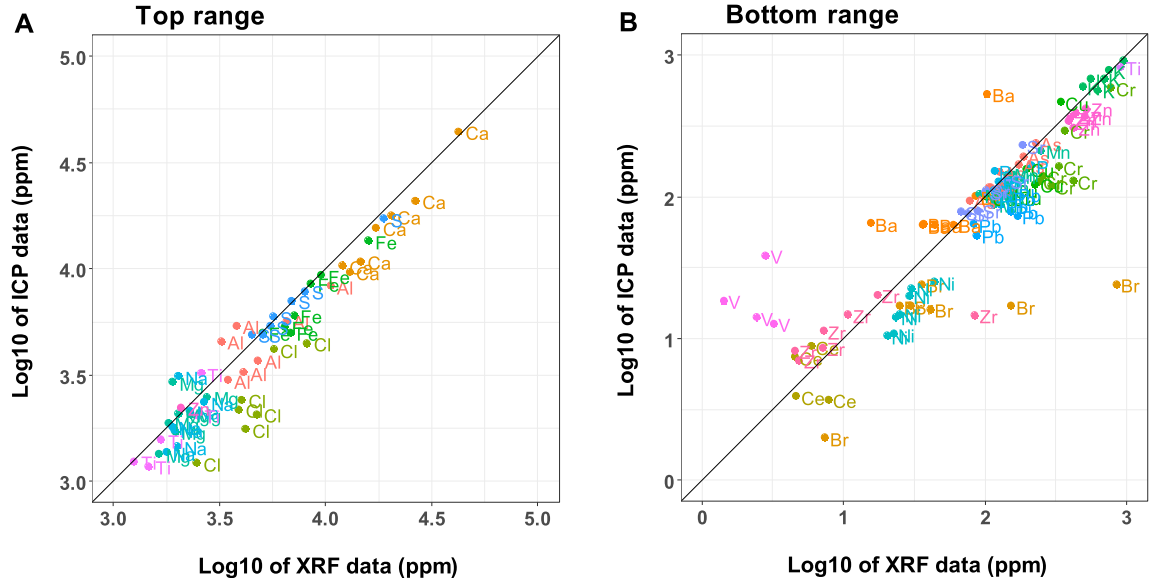

FIGURE 7 | Comparison of mineral element data from UH XRF and Hazen ICP analyses across two concentration ranges, **(A)** >1,000 ppm and **(B)** <1,000 ppm (ICP data do not include chlorine and sulfur).

TABLE 5 | Heavy metal contents in other MSW and landfill materials (in ppm).

Element	Reclaimed MSW, Florida, United States (3–8 year old) Jain et al. (2005)	Reclaimed MSW, Chennai, India (10 year old) Esakku et al. (2005)	Excavated landfill material, Halbenrain, Austria (>15 year old) García-López et al. (2018)	Landfill material, Ottawa, Canada (unknown age) Littlejohns et al. (2020)	CCDW Hawai'i, United States (20–25 year old) current study
Al	6.6 ± 0.0	NA	NA	NA	1,384–10,590
As	2.7 ± 1.6	NA	60.5 ± 0.0	0–0.2	81–229
Ba	29.0 ± 1.3	NA	NA	11.5–20.9	<92–171
Cd	0.9 ± 2.4	1.14 ± 0.08	31.9 ± 0.0	0.11–0.35	<LoD
Co	1.3 ± 0.6	NA	NA	0.04–0.09	<LoD
Cr	19.1 ± 1.5	394.7 ± 22.1	1,911 ± 26	0–0.3	184–784
Cu	40.9 ± 2.1	466.8 ± 31.4	5,564 ± 2424	0.8–1.3	104–345
Fe	5.9 ± 0.0	20,239 ± 883		28–87	5,053–15,960
Hg	0.2 ± 2.0	NA	NA	NA	<LoD
Mn	86.1 ± 2.0	361.7 ± 5.5	NA	44.1–81.8	92–250
Ni	9.4 ± 1.9	144.2 ± 6.1	390.9 ± 13.2	0.13–0.54	20–44
Pb	13.2 ± 2.4	196.9 ± 12.0	1,357 ± 649	0.38–0.48	81–171
Se	3.0 ± 0.0	NA	NA	NA	<LoD
V	4.9 ± 1.1	NA	NA	NA	<LoD
Zn	246.2 ± 1.9	487.0 ± 23.4	5,978 ± 689	15–27	394–2,096

NA: not available in the reference.

2010), locating outside of either coal or biomass area. This may result from its very high Mg and Ca in ash.

Ash Fusion Temperature

Table 6 presents ash fusion temperatures of selected CCDWDF materials under reducing and oxidizing atmospheres. After initial fuel characterization (proximate, ultimate, and XRF analyses), samples were chosen to represent a range of collection dates and variation in ash contents and compositions. The CCDWDF ash samples started their initial deformation at 1,117–1,245 and 1,184–1,205°C in reducing and oxidizing atmospheres, respectively. Fluid deformation occurred at temperatures ranging from 1,138 to 1,248°C in a reducing atmosphere and 1,191–1,210°C in an oxidizing atmosphere. Although the elemental and mineral compositions of the CCDWDF materials are varied, their ash fusion temperatures show marginal variation among these samples. In addition, the temperature ranges from the initial deformation to fluid temperature of most samples are relatively narrow, only 3–9°C, with a few exceptions for the samples #190116, #190405, #190815 in the reducing atmosphere, in which the differences between the initial deformation and fluid temperatures are 21–38°C.

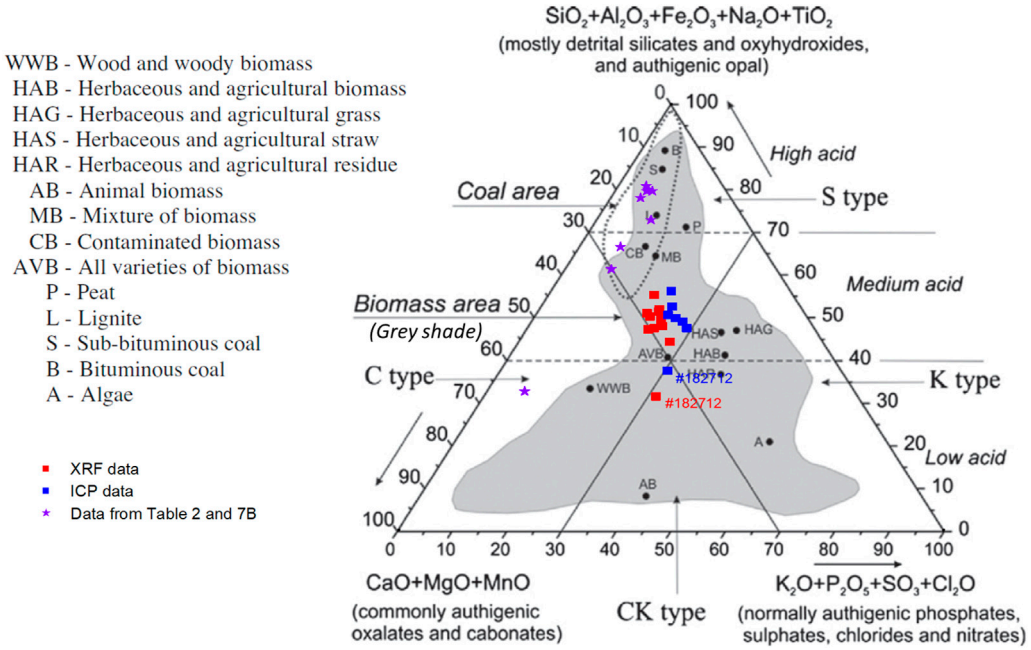

FIGURE 8 | Position areas of CCDWDF samples and referenced solid wastes in the chemical classification system of inorganic matter in biomass based on (Vassilev et al., 2012). Reprinted from *Fuel*, 94, Vassilev, S. V., D. Baxter, L. K. Andersen, C. G. Vassileva, and T. J. Morgan. An overview of the organic and inorganic phase composition of biomass. pp 1-33, Copyright 2012, with permission from Elsevier.

TABLE 6 | Ash fusion temperature of selected CCDWDF materials.

Ash fusion temperature	Sample						
	#181227	#190116	#190213	#190312	#190405	#190718	#190815
Reducing atmosphere							
T_I (°C)	1,244.44	1,175.56	1,188.33	1,215.56	1,117.78	1,210.00	1,156.11
T_S (°C)	1,246.11	1,186.11	1,189.44	1,217.78	1,133.33	1,212.22	1,159.44
T_H (°C)	1,247.22	1,195.00	1,191.11	1,219.44	1,137.78	1,213.33	1,177.22
T_F (°C)	1,247.78	1,208.33	1,192.22	1,221.11	1,138.89	1,215.00	1,193.89
Oxidizing atmosphere							
T_I (°C)	1,198.89	1,185.00	1,195.56	1,204.44	1,200.00	1,205.00	1,184.44
T_S (°C)	1,201.67	1,187.78	1,197.78	1,206.11	1,204.44	1,206.11	1,188.89
T_H (°C)	1,204.44	1,189.44	1,199.44	1,207.78	1,206.11	1,207.22	1,191.11
T_F (°C)	1,206.67	1,191.67	1,201.67	1,210.00	1,208.33	1,207.78	1,193.33

T_I: initial temperature; T_S: softening temperature; T_H: hemispherical temperature; T_F: fluid temperature.

Table 7 presents ash composition and deformation (oxidizing atmosphere) data for biomass with ash fusion temperature ranges comparable to the CCDWDF materials (Fernández Llorente and Carrasco García, 2005; Skrifvars et al., 2005; Du et al., 2014; Chen et al., 2015). Their initial and fluid deformation temperatures ranged from 1,088 to 1,200 and 1,206–1,280°C, respectively. The data reveal that the ash initial deformation temperatures of the CCDWDF are in the higher range of those of the selected biomass, while the fluid temperature of the CCDWDF ashes are in the lower range of those of the selected biomass ashes. In addition, the temperature ranges from the initial deformation to fluid temperature of the biomass samples are 70–118°C, which is much wider than those of the CCDWDF materials. Although full ash composition data of **Table 7** biomass samples were not reported, their ash tended to have significantly higher concentrations of CaO (13–52 wt%) and SiO_2 (26–52 wt%, excluding eucalyptus bark in (Skrifvars et al., 2005), only 0.1 wt%) than other oxides, indicating higher concentrations of Ca and Si than other elements. These two elements are also the most abundant in CCDWDF materials in this study.

Ash composition and deformation (oxidizing atmosphere) data from demolition wood, waste plastic and paper, MSW, and refuse derived fuel (RDF) are presented in **Table 8**. Initial and fluid deformation temperatures of these wastes ranged from 1,090 to 1,180 and from 1,210 to 1,277°C, respectively. The demolition wood (Dunnu et al., 2010) has exceptional high

TABLE 7 | Ash composition and fusibility of a selection of biomass comparable to CCDWDF materials.

Biomass	Ash content (wt%)	Ash composition (wt%)												Ash deformation, oxidizing atmosphere (°C)				Ref.
		Al_2O_3	CaO	Fe_2O_3	K_2O	MgO	MnO	Na_2O	P_2O_5	SiO_2	SO_3	TiO_2	Cl	T_I	T_S	T_H	T_F	
Poplar	1.3	6.9	34.8	3.8	8.2	4.1	NA	0.7	7	26.8	5.5	NA	1.5	1,088	1,184	1,194	1,206	Du et al. (2014)
Eucalyptus bark	3.6	9.75	13.20	6.82	11.20	9.63	NA	2.01	NA	40.50	NA	0.67	NA	1,181	1,201	1,225	1,236	Chen et al. (2015)
Pine	3.1	NA	13	NA	7.9	4.5	NA	1.9	NA	52	NA	NA	NA	1,190	1,200	1,220	1,280	Fernández Llorente and Carrasco García (2005)
Eucalyptus I	4.3	NA	18	NA	8.7	4.2	NA	1.9	NA	41	NA	NA	NA	1,160	1,170	1,190	1,230	Fernández Llorente and Carrasco García (2005)
Eucalyptus II	8.1	NA	22	NA	4.7	2.9	NA	1.2	NA	41	NA	NA	NA	1,150	1,230	1,240	1,260	Fernández Llorente and Carrasco García (2005)
Cork	4.5	NA	35	NA	5.1	1.4	NA	0.7	NA	20	NA	NA	NA	1,190	1,200	1,220	1,280	Fernández Llorente and Carrasco García (2005)
Eucalyptus bark	13	0.2	52.4	0.3	6.0	3.0	1.6	0.5	1.5	0.1	NA	NA	NA	1,200	–	1,250	1,275	Skrifvars et al. (2005)
Mined CCDWF, min	6.20	4.93[a]	21.00[a]	3.47[a]	0.76[a]	2.37[a]	0.06[a]	2.04[a]	0.17[a]	17.74[b]	13.72[b]	2.35[a]	0.64[a]	1,184	1,188	1,189	1,192	Current study
Mined CCDWF, average	9.26	9.30[a]	24.03[a]	11.45[a]	1.00[a]	3.73[a]	0.18[a]	2.82[a]	0.33[a]	28.25[b]	18.14[b]	2.53[a]	1.41[a]	1,196	1,199	1,200	1,202	Current study
Mined CCDWF, max	14.87	11.28[a]	29.96[a]	15.00[a]	1.25[a]	5.35[a]	0.24[a]	3.77[a]	0.44[a]	49.68[b]	24.42[b]	2.92[a]	2.19[a]	1,205	1,206	1,208	1,210	Current study

T_I: initial temperature; T_S: softening temperature; T_H: hemispherical temperature; T_F: fluid temperature.

NA: not available in the reference.

[a]*Calculate from ICP data.*

[b]*Calculated from XRF data.*

TABLE 8 | Ash composition and fusibility of selected solid wastes.

Solid wastes	Ash content (wt%)	Ash composition (wt%)											Ash deformation, oxidizing atmosphere (°C)				Ref.
		Al_2O_3	CaO	Fe_2O_3	K_2O	MgO	MnO	Na_2O	P_2O_5	SiO_2	SO_3	TiO_2	Cl	T_I	T_S	T_H	T_F	
Demolition wood	3.99	4.98	12.65	2.05	2.20	45.88	NA	1.97	0.65	18.55	3.75	3.98	NA	1,335	1,340	>1,500	>1,500	Dunnu et al. (2010)
MSW (Germany)	16.83	11.18	25.41	2.88	2.34	3.68	NA	4.18	1.18	38.12	4.50	2.33	NA	1,180	1,180	1,195	1,210	Dunnu et al. (2010)
Plastic and paper	26.64	16.18	21.80	3.94	2.82	2.59	NA	4.80	1.70	36.07	2.50	1.31	NA	1,170	1,130	1,190	1,220	Dunnu et al. (2010)
RDF (Sweden)	16.4	20.2	13.1	4.4	2.5	1.6	NA	2.7	2.1	34.7	1.0	NA	2.8	1,090	1,190	1,220	1,240	Skrifvars et al. (1999)
RDF Fall (United States)	10.64	21.51	14.51	3.77	0.96	1.85	NA	6.70	1.17	42.12	3.23	2.92	NA	1,143	1,171	1,182	1,260	Canova and Bushnell (1992)
RDF Winter (United States)	23.41	13.57	11.23	9.98	1.81	1.76	NA	0.20	1.39	49.86	3.22	1.93	NA	1,138	1,171	1,182	1,260	Canova and Bushnell (1992)
RDF Spring (United States)	23.75	14.61	12.42	4.28	2.42	1.81	NA	5.00	1.62	54.55	1.80	1.48	NA	1,154	1,204	1,221	1,277	Canova and Bushnell (1992)
RDF Summer (United States)	27.72	11.23	12.57	2.49	1.77	1.52	NA	7.92	1.28	57.11	1.96	1.52	NA	1,154	1,204	1,221	1,277	Canova and Bushnell (1992)
RDF mix (United States)	21.38	15.23	12.68	5.13	1.74	1.74	NA	4.96	1.37	50.91	2.55	1.96	NA	1,138	1,166	1,182	1,260	Canova and Bushnell (1992)
Mined CCDWF, min	6.20	4.93[a]	21.00[a]	3.47[a]	0.76[a]	2.37[a]	0.06[a]	2.04[a]	0.17[a]	17.74[b]	13.72[b]	2.35[a]	0.64[a]	1,184	1,188	1,189	1,192	Current study
Mined CCDWF, average	9.26	9.30[a]	24.03[a]	11.45[a]	1.00[a]	3.73[a]	0.18[a]	2.82[a]	0.33[a]	28.25[b]	18.14[b]	2.53[a]	1.41[a]	1,196	1,199	1,200	1,202	Current study
Mined CCDWF, max	14.87	11.28[a]	29.96[a]	15.00[a]	1.25[a]	5.35[a]	0.24[a]	3.77[a]	0.44[a]	49.68[b]	24.42[b]	2.92[a]	2.19[a]	1,205	1,206	1,208	1,210	Current study

T_I: initial temperature; T_S: softening temperature; T_H: hemispherical temperature; T_F: fluid temperature.

NA: not available in the reference.

[a]*Calculate from ICP data.*

[b]*Calculated from XRF data.*

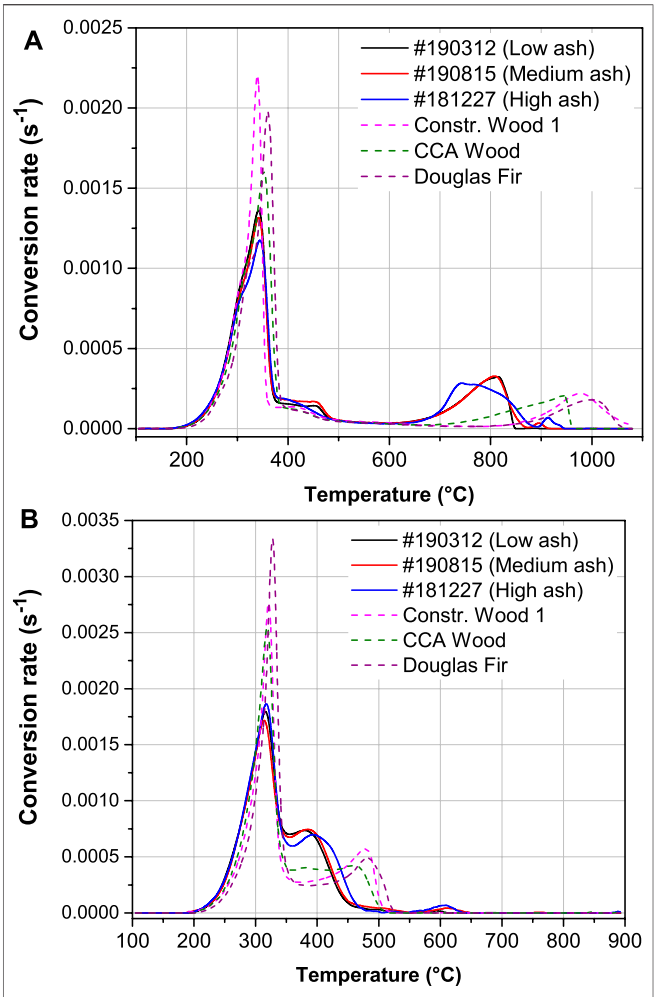

FIGURE 9 | Reactivity of CCDWDF materials in **(A)** reducing and **(B)** oxidizing atmospheres.

initial and fluid deformation temperatures of 1,335 and >1,500°C, respectively, noting that this material does not belong to either coal or biomass in the ternary inorganic matter plot (**Figure 8**). The data indicate that the CCDWDF materials in this study have ash fusion temperatures in the range of other solid wastes reported in the literature.

Reactivity

Thermogravimetric data were differentiated, smoothed, and normalized by the reactive sample mass to produce comparable conversion rates. **Figure 9** shows the conversion rate curves of three CCDWDF samples, one construction wood, CCA wood, and Douglas fir under reducing (**Figure 9A**) and oxidizing (**Figure 9B**) atmospheres (isothermal drying at 105°C is not included in the figure). The CCDWDF samples selected in this experiment are #190312, #190815, and #181227, which have the lowest, medium, and highest ash contents, respectively.

The initial devolatilization of the samples peaked at 340–360°C in reducing atmosphere and 315–330°C in oxidizing atmosphere. Note the reactivity of the sample groups are different in this stage: the CCDWDF materials always have lower reactivity than the reference woods in both atmospheres, stemming from their lower volatile matter contents (see **Table 3**). As expected, the conversion rates of the samples in reducing atmosphere are lower than those in oxidizing atmosphere.

The conversion at 400–500°C in **Figure 9A** shows a broader and protracted peak for the CCDWDF materials that may indicate higher lignin content resulting from biodegradation while landfilled or the presence of non-biomass polymer content.

The char gasification of the CCDWDFs occurred earlier (initiated at approximately 600°C, peaking at 740–810°C, and ending at ~950°C) than that of the reference wood samples (initiated at approximately 700°C, peaking at 950–1,010°C, ending at ~1,080°C) (**Figure 9A**). The reactivity of the CCDWDF samples during the gasification stage is higher than that of reference wood samples.

The conversion of the CCDWDF samples immediately following devolatilization, peaked at 380–390°C, and ended at ~550°C. The combustion of the reference woods occurred at higher temperatures than that of the CCDWDFs, peaked at 450–480°C, and also ended at ~550°C. The lower reaction temperatures and higher combustion rates of the CCDWDFs compared to those of reference wood samples may indicate catalytic activity of the elements (e.g., K) present in the elevated ash content.

Besides the main gasification and combustion peaks, the CCDWDFs also have small peaks at 895–915°C (in reducing atmosphere) and 595–615°C (in oxidizing atmosphere), which do not exist in the curves of the reference woods. These peaks likely result from reactions of ash elements at high temperatures, considering the significantly high ash contents of CCDWDF samples.

The thermogravimetric analysis reveals that the CCDWDFs are not reactive at temperatures higher than 950°C in reducing atmosphere and 650°C in oxidizing atmosphere because only ash remains at this temperature. Initial ash deformation temperatures for all CCDWDF samples are higher than 1,100°C (**Table 6**) under both reducing and oxidizing environments indicating that ash-related problems (e.g., agglomeration and slagging) associated with the thermochemical conversions of CCDWDFs may be reduced.

CONCLUSION

Results from the fuel analyses indicate that the CDWDF materials have a wide range of non-combustible fractions that should be removed prior to thermochemical applications. The appearance of the CCDWDF materials and their physical properties are similar to those of woody biomass and wood chip fuels. The bulk density of CCDWDF materials are in the same common range as other wood chips. Similarly, the CCDWDF materials have the proximate and ultimate compositions comparable to other reference woods. However, the ash contents of the CCDWDFs are significantly higher than those of the reference woods. On the van Krevelen diagram, the CCDWDF materials lie closer to the coal region than Douglas fir and eucalyptus. The HHVs (on dry basis) of CCDWDFs are comparable to woody

biomass (Douglas fir and eucalyptus) but lower than those of the reference construction wood samples.

The ash fusion temperatures of the selected CCDWDF materials show a marginal variation among the samples. The CCDWDFs have lower reactivity than the reference woods in the devolatilization stage (in both reducing and oxidizing atmospheres), but higher reactivity in the gasification and combustion stages. In addition, the gasification and combustion of the CCDWDF samples occurred earlier, at lower temperatures, than the reference wood samples. The thermogravimetric analysis shows that the CCDWDF materials are reduced to ash and have virtually no reactivity at temperatures higher than 950°C in reducing atmosphere and 650°C in oxidizing atmosphere. Ash melting begins at temperatures higher than 1,100°C. These characteristics may reduce the ash-related problems of these CCDWDFs in thermochemical conversion systems.

Mineral elemental analysis reveals that the CCDWDF includes material from various sources; gypsum, plastic, rust, paint, paint additives, and soils. In addition, the CCDWDF sample collected from trucks had much higher concentrations of calcium, sulfur, chromium, and zinc which may come from gypsum, paint, and paint additives. Analysis reveals that certain elements (Ca, Cu, Fe, K, Mn, Pb, and Zn) were present in soil recovered from the landfill. A comparison of elemental data confirms that the ICP-OES can quantify trace elements at lower concentrations than the XRF. Measured concentrations of abundant elements in the XRF data are higher (with few exceptions) than those from the ICP-OES measurement. The reduced sample preparation required for XRF analysis compared to ICP can reduce analysis time making XRF a potential screening tool for fuels management.

In summary, CCDWDF has potential use in the production of SAF, other bio-based fuels, or electric power. Nevertheless, more study is recommended to understand the fates of mineral elements during thermochemical conversion of CCDWDF materials. In addition, a better understanding of the relationship between the mineral composition and the ash fusion temperatures of the CCDWDF materials warrant further analysis.

DATA AVAILABILITY STATEMENT

The original contributions presented in the study are included in the article/**Supplementary Material**, further inquiries can be directed to the corresponding author.

AUTHOR CONTRIBUTIONS

Q-VB and ST collected and pre-processed the materials. Q-VB and JF characterized the fuels. Q-VB prepared the first draft of the manuscript, ST and JF revised and improved the manuscript. ST acquired funding and supervised this work.

FUNDING

This research was funded in part by the U.S. Federal Aviation Administration Office of Environment and Energy through ASCENT, the FAA Center of Excellence for Alternative Jet Fuels and the Environment, Project 001 through FAA Award Number 13-C-AJFE-UH under the supervision of James Hileman and Nathan Brown. Funding was also provided by Hawaii's Environmental Response, Energy, and Food Security Tax (HRS Section 243-3.5 "Barrel Tax") through the Hawaii Natural Energy Institute's Energy Systems Development Special Fund and the Office of Naval Research, Asia Pacific Regional Energy System Assessment Program, (Award No. N0014-17-1-2923). Any opinions, findings, conclusions or recommendations expressed in this material are those of the authors and do not necessarily reflect the views of the FAA.

ACKNOWLEDGMENTS

The authors would like to thank: Dr. Kristin C. Lewis (U.S. Dept. of Transportation, Volpe Center) for her thorough review of the manuscript prior to submission and her suggestions for improvement; Sohrab Haghighi Mood (Washington State University) for his help with thermogravimetric analyses of CCDWDF and reference wood samples; Steve Joseph, Billy Lyon, and the management of PVT Land Company Ltd. for guidance, access, and support.

SUPPLEMENTARY MATERIAL

The Supplementary Material for this article can be found online at: https://www.frontiersin.org/articles/10.3389/fenrg.2021.711808/full#supplementary-material

REFERENCES

Aldaood, A., Bouasker, M., and Al-Mukhtar, M. (2015). Effect of Long-Term Soaking and Leaching on the Behaviour of Lime-Stabilised Gypseous Soil. *Int. J. Pavement Eng.* 16 (1), 11–26. doi:10.1080/10298436.2014.893329

Ansah, E., Wang, L., and Shahbazi, A. (2016). Thermogravimetric and Calorimetric Characteristics during Co-pyrolysis of Municipal Solid Waste Components. *Waste Management* 56, 196–206. doi:10.1016/j.wasman.2016.06.015

ASTM (2018a). *ASTM D4239-18e1, Standard Test Method for Sulfur in the Analysis Sample of Coal and Coke Using High-Temperature Tube Furnace Combustion*. West Conshohocken, PA: ASTM International. Available at: www.astm.org.

ASTM (2016a). *ASTM D5373-16, Standard Test Methods for Determination of Carbon, Hydrogen and Nitrogen in Analysis Samples of Coal and Carbon in Analysis Samples of Coal and Coke*. West Conshohocken, PA: ASTM International. Available at: www.astm.org.

ASTM (2008). *ASTM D7348-08, Standard Test Methods for Loss on Ignition (LOI) of Solid Combustion Residues*. West Conshohocken, PA: ASTM International. Available at: www.astm.org.

ASTM (2020). *ASTM D7566-20c, Standard Specification for Aviation Turbine Fuel Containing Synthesized Hydrocarbons*. West Conshohocken, PA: ASTM International. Available at: www.astm.org.

ASTM (2015a). *ASTM D7582-15, Standard Test Methods for Proximate Analysis of Coal and Coke by Macro Thermogravimetric Analysis*. West Conshohocken, PA: ASTM International. Available at: www.astm.org.

ASTM (2016c). *Practice for Fusibility of Refuse-Derived Fuel (RDF) Ash*. West Conshohocken, PA: ASTM International. Available at: www.astm.org.

ASTM (2015b). *Standard Practice for Preparation of Biomass for Compositional Analysis*. West Conshohocken, PA: ASTM International. Available at: www.astm.org.

ASTM (2013b). *Standard Test Method for Bulk Density of Densified Particulate Biomass Fuels*. West Conshohocken, PA: ASTM International. Available at: www.astm.org.

ASTM (2016b). *Standard Test Method for Calculating Refuse-Derived Fuel Analysis Data from As-Determined to Different Bases*. West Conshohocken, PA: ASTM International. Available at: www.astm.org.

ASTM (2018b). *Standard Test Method for Heat of Combustion of Liquid Hydrocarbon Fuels by Bomb Calorimeter (Precision Method)*. West Conshohocken, PA: ASTM International. Available at: www.astm.org.

ASTM (2013a). *Standard Test Method for Moisture Analysis of Particulate Wood Fuels*. West Conshohocken, PA: ASTM International. Available at: www.astm.org.

Bach, Q.-V., Sillero, M. V., Tran, K.-Q., and Skjermo, J. (2014). Fast Hydrothermal Liquefaction of a Norwegian Macro-Alga: Screening Tests. *Algal Res.* 6 (0), 271–276. doi:10.1016/j.algal.2014.05.009

Bassani, M., Tefa, L., Russo, A., and Palmero, P. (2019). Alkali-activation of Recycled Construction and Demolition Waste Aggregate with No Added Binder. *Construction Building Mater.* 205, 398–413. doi:10.1016/j.conbuildmat.2019.02.031

Bosmans, A., Vanderreydt, I., Geysen, D., and Helsen, L. (2013). The Crucial Role of Waste-To-Energy Technologies in Enhanced Landfill Mining: a Technology Review. *J. Clean. Prod.* 55, 10–23. doi:10.1016/j.jclepro.2012.05.032

Canova, J. H., and Bushnell, D. J. (1992). "Testing and Evaluating the Combustion Characterictics of Densified RDF and Mixed Paper," in *Energy from Biomass and Wastes XVI. Institite of Gas Technology)*. Editor D. L. Klass.

Chadwick, O. A., Derry, L. A., Bern, C. R., and Vitousek, P. M. (2009). Changing Sources of Strontium to Soils and Ecosystems across the Hawaiian Islands. *Chem. Geology.* 267 (1), 64–76. doi:10.1016/j.chemgeo.2009.01.009

Chen, M., Yu, D., and Wei, Y. (2015). Evaluation on Ash Fusion Behavior of eucalyptus Bark/lignite Blends. *Powder Technology* 286, 39–47. doi:10.1016/j.powtec.2015.07.043

Chojnacka, K., Samoraj, M., Tuhy, Ł., Michalak, I., Mironiuk, M., and Mikulewicz, M. (2018). Using XRF and ICP-OES in Biosorption Studies. *Molecules* 23 (8), 2076. doi:10.3390/molecules23082076

Clark, C., Jambeck, J., and Townsend, T. (2006). A Review of Construction and Demolition Debris Regulations in the United States. *Crit. Rev. Environ. Sci. Technology* 36 (2), 141–186. doi:10.1080/10643380500531197

Cristelo, N., Fernández-Jiménez, A., Vieira, C., Miranda, T., and Palomo, Á. (2018). Stabilisation of Construction and Demolition Waste with a High Fines Content Using Alkali Activated Fly Ash. *Construction Building Mater.* 170, 26–39. doi:10.1016/j.conbuildmat.2018.03.057

Cui, H., and Turn, S. (2018). Fuel Properties and Steam Reactivity of Solid Waste Streams from Contingency Bases. *Waste Management* 78, 16–30. doi:10.1016/j.wasman.2018.05.023

Du, S., Yang, H., Qian, K., Wang, X., and Chen, H. (2014). Fusion and Transformation Properties of the Inorganic Components in Biomass Ash. *Fuel* 117, 1281–1287. doi:10.1016/j.fuel.2013.07.085

Dunnu, G., Maier, J., and Scheffknecht, G. (2010). Ash Fusibility and Compositional Data of Solid Recovered Fuels. *Fuel* 89 (7), 1534–1540. doi:10.1016/j.fuel.2009.09.008

Edo, M., Ortuño, N., Persson, P.-E., Conesa, J. A., and Jansson, S. (2018). Emissions of Toxic Pollutants from Co-combustion of Demolition and Construction wood and Household Waste Fuel Blends. *Chemosphere* 203, 506–513. doi:10.1016/j.chemosphere.2018.03.203

Eisenbies, M. H., Volk, T. A., Therasme, O., and Hallen, K. (2019). Three Bulk Density Measurement Methods Provide Different Results for Commercial Scale Harvests of Willow Biomass Chips. *Biomass and Bioenergy* 124, 64–73. doi:10.1016/j.biombioe.2019.03.015

Esakku, S., Selvam, A., Joseph, K., and Palanivelu, K. (2005). Assessment of Heavy Metal Species in Decomposed Municipal Solid Waste. *Chem. Speciation Bioavailability* 17 (3), 95–102. doi:10.3184/095422905782774883

Fernández Llorente, M. J., and Carrasco García, J. E. (2005). Comparing Methods for Predicting the Sintering of Biomass Ash in Combustion. *Fuel* 84 (14), 1893–1900. doi:10.1016/j.fuel.2005.04.010

García López, C., Küppers, B., Clausen, A., and Pretz, T. (2018). Landfill Mining: A Case Study Regarding Sampling, Processing and Characterization of Excavated Waste from an Austrian Landfill. *Detritus* 2, 29–45. doi:10.31025/2611-4135/2018.13664

García-López, C., Ni, A., Parrodi, J. C. H., Küppers, B., Raulf, K., and Pretz, T. (2019). Characterization of Landfill Mining Material after Ballistic Separation to Evaluate Material and Energy Potential. *Detritus* 8, 5–23.

Giambelluca, T. W., Chen, Q., Frazier, A. G., Price, J. P., Chen, Y.-L., Chu, P.-S., et al. (2013). Online Rainfall Atlas of Hawai'i. *Bull. Amer. Meteorol. Soc.* 94 (3), 313–316. doi:10.1175/BAMS-D-11-00228.1

Giambelluca, T. W., Shuai, X., Barnes, M. L., Alliss, R. J., Longman, R. J., Miura, T., et al. (2014). *Evapotranspiration of Hawai'i. Final Report Submitted to the U.S. Army Corps of Engineers—Honolulu District, and the Commission on Water Resource Management, State of Hawai'i.*

Jagodzińska, K., Garcia Lopez, C., Yang, W., Jönsson, P. G., Pretz, T., and Raulf, K. (2021). Characterisation of Excavated Landfill Waste Fractions to Evaluate the Energy Recovery Potential Using Py-GC/MS and ICP Techniques. *Resour. Conservation Recycling* 168, 105446. doi:10.1016/j.resconrec.2021.105446

Jain, P., Kim, H., and Townsend, T. G. (2005). Heavy Metal Content in Soil Reclaimed from a Municipal Solid Waste Landfill. *Waste Management* 25 (1), 25–35. doi:10.1016/j.wasman.2004.08.009

Jain, P., Townsend, T. G., and Johnson, P. (2013). Case Study of Landfill Reclamation at a Florida Landfill Site. *Waste Management* 33 (1), 109–116. doi:10.1016/j.wasman.2012.09.011

Krook, J., Svensson, N., and Eklund, M. (2012). Landfill Mining: A Critical Review of Two Decades of Research. *Waste Management* 32 (3), 513–520. doi:10.1016/j.wasman.2011.10.015

Lawson, N., Douglas, I., Garvin, S., McGrath, C., Manning, D., and Vetterlein, J. (2001). Recycling Construction and Demolition Wastes - a UK Perspective. *Env Mgtt and Health* 12 (2), 146–157. doi:10.1108/09566160110389898

Littlejohns, J. V., Butler, J., Luque, L., and Austin, K. (2020). Experimental Investigation of Bioenergy Production from Small-Scale Gasification of Landfill-Diverted Wood Wastes. *Waste Biomass Valor.* 11 (12), 6885–6901. doi:10.1007/s12649-020-00940-7

Ma, Z., Ye, J., Zhao, C., and Zhang, Q. (2015). Gasification of rice Husk in a Downdraft Gasifier: The Effect of Equivalence Ratio on the Gasification Performance, Properties, and Utilization Analysis of Byproducts of Char and Tar. *BioResorces* 10 (2), 2888–2902. doi:10.15376/biores.10.2.2888-2902

McComb, J. Q., Rogers, C., Han, F. X., and Tchounwou, P. B. (2014). Rapid Screening of Heavy Metals and Trace Elements in Environmental Samples Using Portable X-Ray Fluorescence Spectrometer, A Comparative Study. *Water Air Soil Pollut.* 225 (12), 2169. doi:10.1007/s11270-014-2169-5

Morgan, T. J., Andersen, L. K., Turn, S. Q., Cui, H., and Li, D. (2017). XRF Analysis of Water Pretreated/Leached Banagrass to Determine the Effect of Temperature, Time, and Particle Size on the Removal of Inorganic Elements. *Energy Fuels* 31 (8), 8245–8255. doi:10.1021/acs.energyfuels.7b01135

Nordi, G. H., Palacios-Bereche, R., Gallego, A. G., and Nebra, S. A. (2017). Electricity Production from Municipal Solid Waste in Brazil. *Waste Manag. Res.* 35 (7), 709–720. doi:10.1177/0734242X17705721

Olesik, J. W. (1991). Elemental Analysis Using ICP-OES and ICP/MS. *Anal. Chem.* 63 (1), 12A–21A. doi:10.1021/ac00001a00110.1021/ac00001a711

Pais, I., and Jones, J. B. (1997). *The Handbook of Trace Elements*. Boca Raton: FL. CRC Press.

Palha, F., Pereira, A., de Brito, J., and Silvestre, J. D. (2012). Effect of Water on the Degradation of Gypsum Plaster Coatings: Inspection, Diagnosis, and Repair. *J. Perform. Constr. Facil.* 26 (4), 424–432. doi:10.1061/(ASCE)CF.1943-5509.0000258

Passos, J., Alves, O., and Brito, P. (2020). Management of Municipal and Construction and Demolition Wastes in Portugal: Future Perspectives through Gasification for Energetic Valorisation. *Int. J. Environ. Sci. Technol.* 17 (5), 2907–2926. doi:10.1007/s13762-020-02656-6

Peres, S., Loureiro, E., Santos, H., Vanderley e Silva, F., and Gusmao, A. (2020). The Production of Gaseous Biofuels Using Biomass Waste from Construction Sites in Recife, Brazil. *Processes* 8 (4), 457. doi:10.3390/pr8040457

Powell, J. T., Pons, J. C., and Chertow, M. (2016). Waste Informatics: Establishing Characteristics of Contemporary U.S. Landfill Quantities and Practices. *Environ. Sci. Technol.* 50 (20), 10877–10884. doi:10.1021/acs.est.6b02848

Ragland, K. W., Aerts, D. J., and Baker, A. J. (1991). Properties of wood for Combustion Analysis. *Bioresour. Technology* 37 (2), 161–168. doi:10.1016/0960-8524(91)90205-X

Rodríguez-Robles, D., García-González, J., Juan-Valdés, A., Morán-del Pozo, J. M., and Guerra-Romero, M. I. (2015). Overview Regarding Construction and Demolition Waste in Spain. *Environ. Technology* 36 (23), 3060–3070. doi:10.1080/09593330.2014.957247

Roussat, N., Méhu, J., Abdelghafour, M., and Brula, P. (2008). Leaching Behaviour of Hazardous Demolition Waste. *Waste Management* 28 (11), 2032–2040. doi:10.1016/j.wasman.2007.10.019

Sadek, D. M. (2012). Physico-mechanical Properties of Solid Cement Bricks Containing Recycled Aggregates. *J. Adv. Res.* 3 (3), 253–260. doi:10.1016/j.jare.2011.08.001

Safiuddin, M., Alengaram, U. J., Rahman, M. M., Salam, M. A., and Jumaat, M. Z. (2013). Use of Recycled concrete Aggregate in concrete: a Review. *J. Civil Eng. Management* 19 (6), 796–810. doi:10.3846/13923730.2013.799093

Shahabuddin, M., Alam, M. T., Krishna, B. B., Bhaskar, T., and Perkins, G. (2020). A Review on the Production of Renewable Aviation Fuels from the Gasification of Biomass and Residual Wastes. *Bioresour. Technology* 312, 123596. doi:10.1016/j.biortech.2020.123596

Skrifvars, B.-J., Öhman, M., Nordin, A., and Hupa, M. (1999). Predicting Bed Agglomeration Tendencies for Biomass Fuels Fired in FBC Boilers: A Comparison of Three Different Prediction Methods. *Energy Fuels* 13 (2), 359–363. doi:10.1021/ef980045+

Skrifvars, B.-J., Yrjas, P., Kinni, J., Siefen, P., and Hupa, M. (2005). The Fouling Behavior of Rice Husk Ash in Fluidized-Bed Combustion. 1. Fuel Characteristics. *Energy Fuels* 19 (4), 1503–1511. doi:10.1021/ef049714b

Song, Y., Wang, Y., Liu, F., and Zhang, Y. (2017). Development of a Hybrid Model to Predict Construction and Demolition Waste: China as a Case Study. *Waste Management* 59, 350–361. doi:10.1016/j.wasman.2016.10.009

Thompson, A., Rancourt, D. G., Chadwick, O. A., and Chorover, J. (2011). Iron Solid-phase Differentiation along a Redox Gradient in Basaltic Soils. *Geochimica et Cosmochimica Acta* 75 (1), 119–133. doi:10.1016/j.gca.2010.10.005

US EPA (2017). *Advancing Sustainable Materials Management*. Washington, DC: U.S. Environmental Protection Agency: 2017 Fact Sheet.

US EPA (1996). *Method 3050B: Acid Digestion of Sediments, Sludges, and Soils, Revision 2*. Washington, DC.

Usda-Nrcs (2011). *National Cooperative Soil Survey Soil Characterization Database. Soil Survey Laboratory, National Soil Survey Center. U.S Department of Agriculture (USDA)*. Lincoln, Nebraska: Natural Resources Conservation Services NRCS. Available at: http://ssldata.srsc.usda.gov/.

Vainikka, P., and Hupa, M. (2012). Review on Bromine in Solid Fuels - Part 2: Anthropogenic Occurrence. *Fuel* 94, 34–51. doi:10.1016/j.fuel.2011.11.021

van der Zee, D. J., Achterkamp, M. C., and de Visser, B. J. (2004). Assessing the Market Opportunities of Landfill Mining. *Waste Management* 24 (8), 795–804. doi:10.1016/j.wasman.2004.05.004

Vassilev, S. V., Baxter, D., Andersen, L. K., Vassileva, C. G., and Morgan, T. J. (2012). An Overview of the Organic and Inorganic Phase Composition of Biomass. *Fuel* 94, 1–33. doi:10.1016/j.fuel.2011.09.030

Wu, Z., Yu, A. T. W., Shen, L., and Liu, G. (2014). Quantifying Construction and Demolition Waste: An Analytical Review. *Waste Management* 34 (9), 1683–1692. doi:10.1016/j.wasman.2014.05.010

Yilmaz, N., and Atmanli, A. (2017). Sustainable Alternative Fuels in Aviation. *Energy* 140, 1378–1386. doi:10.1016/j.energy.2017.07.077

Conflict of Interest: The authors declare that the research was conducted in the absence of any commercial or financial relationships that could be construed as a potential conflict of interest.

Publisher's Note: All claims expressed in this article are solely those of the authors and do not necessarily represent those of their affiliated organizations, or those of the publisher, the editors and the reviewers. Any product that may be evaluated in this article, or claim that may be made by its manufacturer, is not guaranteed or endorsed by the publisher.

frontiers in Energy Research

ORIGINAL RESEARCH
published: 29 November 2021
doi: 10.3389/fenrg.2021.771705

Estimating the Reduction in Future Fleet-Level CO_2 Emissions From Sustainable Aviation Fuel

Samarth Jain[1], *Hsun Chao*[2], *Muharrem Mane*[1], *William A. Crossley*[1]* *and Daniel A. DeLaurentis*[2]

[1]Aerospace Systems Design, Analysis, and Optimization Lab, School of Aeronautics & Astronautics, Purdue University, West Lafayette, IN, United States, [2]Center of Integrated Systems in Airspace (System-of-Systems Lab), School of Aeronautics & Astronautics, Purdue University, West Lafayette, IN, United States

With rising concerns over commercial aviation's contribution to global carbon emissions, the aviation industry faces tremendous pressure to adopt advanced solutions for reducing its share of CO_2 emissions. One near-term potential solution to mitigate this global emissions situation is to operate existing aircraft with sustainable aviation fuel (SAF); this solution requires almost no modification to current aircraft, making it the "quickest" approach to reduce aviation carbon emissions, albeit the actual impact will be determined by the degree to which airlines adopt and use SAF, the ticket price impact of SAF, and the future growth of travel demand. This article presents results that estimate the expected fleet-wide emissions of future airline operations using SAF considering various projected traveler demand and biofuel penetration/utilization levels. The work demonstrates an approach to make these predictions by modeling the behavior of a profit-seeking airline using the Fleet-Level Environmental Evaluation Tool (FLEET). Considering five future SAF scenarios and two future passenger demand projection scenarios, FLEET estimates future fleet-level CO_2 emissions, showcasing the possible upper and lower bounds on future aviation emissions when SAF is introduced for use in airline fleets. Results show that the future fleet-level CO_2 emissions for all scenarios with SAF are lower than the baseline scenario with no SAF, for all demand projection scenarios. The passenger demand served and the trips flown for a given SAF scenario depends on the SAF price and the biofuel penetration levels. This shows that even if airlines serve a higher passenger demand for some future scenarios, the carbon emissions could still be lower than the current baseline scenario where airlines only use conventional jet fuel.

Keywords: commercial aviation CO_2 emissions, sustainable aviation fuels (SAF), airline fleet-level predictions, future aviation CO_2 scenarios, model-based prediction method

OPEN ACCESS

Edited by:
Kristin C. Lewis,
Volpe National Transportation Systems Center, United States

Reviewed by:
Huaping Sun,
Jiangsu University, China
Mohammed Hassan,
Georgia Institute of Technology, United States

***Correspondence:**
William A. Crossley
crossley@purdue.edu

Specialty section:
This article was submitted to Sustainable Energy Systems and Policies, a section of the journal Frontiers in Energy Research

Received: *06 September 2021*
Accepted: *29 October 2021*
Published: *29 November 2021*

Citation:
Jain S, Chao H, Mane M, Crossley WA and DeLaurentis DA (2021) Estimating the Reduction in Future Fleet-Level CO_2 Emissions From Sustainable Aviation Fuel. Front. Energy Res. 9:771705. doi: 10.3389/fenrg.2021.771705

1 INTRODUCTION

The Paris Agreement, a multinational treaty that intends to confine the temperature growth to 2°C from pre-industrial levels by the year 2050 (United Nations Framework Convention on Climate Change, 2021), impacts all industries. The United States recently re-signed the Paris Agreement (U.S. Department of State, Office of the Spokesperson, 2021) and set 2030 emission reduction targets to accomplish its goals (The White House, 2021). The aviation industry is responsible for about 2.5% of global carbon emissions (Ritchie, 2020). Although this figure is relatively low, it is reasonable to

assume that aviation will have to do its part to meet the agreement's goals. In Europe, the "Destination 2050" report outlines a vision for European Aviation to attain net-zero CO_2 emissions by the year 2050 (van der Sman et al., 2021). Additionally, the International Civil Aviation Organization (ICAO) (International Civil Aviation Organization, 2016) launched the Carbon Offsetting and Reduction Scheme for International Aviation (CORSIA) in 2021. The ICAO CORSIA monetizes the carbon emissions from international routes and it creates incentives for airline operators to use SAF with a premium price (Chao et al., 2019a; Chao et al., 2019b) to confine the carbon emissions from the aviation sector to the 2020 level (IATA, 2016; International Civil Aviation Organization, 2016; Chao et al., 2019c).

Achieving these goals will require technological improvements as well as policy changes. Sustainable Aviation Fuel (SAF) is one technology that has been under development for several years and that has been used in operation by some airlines (Csonka, 2016; United Airlines, 2021). SAF is a mixture of biofuels and conventionally petroleum-derived jet fuel (CJF) that has a lower life-cycle carbon footprint than conventional jet fuel. Because biofuels, commonly made from crops, absorb carbon dioxide when crops are grown, they can have reduced net carbon emissions; i.e. life-cycle emissions. Although biofuels tend to be priced higher than CJF, adopting SAF is one of the most straightforward actions commercial aviation could take to reduce carbon emissions and meet the emission reduction targets (The White House, 2021). Moolchandani et al. (Moolchandani et al., 2011) show that the use of SAF can potentially reduce 2050 emissions in the U.S. by 55–92% of a 2005 baseline level. The resulting variation in CO_2 reduction levels is governed by the sensitivity of the SAF adoption rate to the CJF prices. The Destination 2050 report (van der Sman et al., 2021) attributes a 34% reduction in future CO_2 emissions for European Aviation from the use of SAF and an additional 12% reduction from the "effect of SAF on demand."

Studies into the feasibility of SAF to achieve these emission goals include analysis of SAF production pathways, fleet penetration of leading aircraft technologies, and economic interactions between SAF and commercial aviation industries. Winchester et al. show the economic and environmental impacts of Hydro-processed Ester and Fatty Acids (HEFA) biofuels on U.S. commercial aviation (Winchester et al., 2013). Haller defined and explored future aircraft technologies for environmental improvement under NASA's Subsonic Fixed Wing project (Haller, 2012). In the Renewable Fuel Standard Program (RFS2) Regulatory Impact Analysis from EPA, Sissine showed the properties of biofuels from different pathways in different regions (Sissine, 2010). Sun et al. (2020) and Sun et al. (2021) already showed that stringent environmental policies can enhance domestic innovation and improve energy efficiency however, the impacts of the environmental policies on the aviation industry are still unclear.

The aviation trade organization, Airlines for America, the U.S. Department of Agriculture, and the aircraft manufacturer, Boeing, established the Farm to Fly initiatives to help develop the U.S. SAF industry. Farm to Fly was later extended with the addition of the Department of Transportation's Federal Aviation Administration (FAA) and major private partners such as the Commercial Aviation Alternative Fuels Initiative (CAAFI), as well as the Department of Energy and the Department of Defense. The new initiative, which is called Farm to Fly 2.0 (F2F2), set a goal to supply about 1 billion gallons of SAF as drop-in aviation biofuels in 2018. CAAFI kept fostering supply chain development activities in several states of the U.S. through the F2F2 Public-Private-Partnership efforts. Therefore, the industry is growing towards a sustainable commercial industry.

The year 2016 was the first year for commercial scale biofuel production; the U.S. aviation sector used over a million gallons of biofuel. The AltAir facility dominated the delivery of tallow HEFA fuel to Los Angeles Airport (LAX) for that year. There exist about 19 biofuel production facilities in the U.S., including those that are already producing biofuel for commercial usage and those that have plans to begin commercial operations soon, with an expected combined production capacity of about 1 billion gallons per year (CAAFI, 2018).

With this backdrop, airlines are looking at SAF as a feasible option for meeting the Paris Agreement and ICAO CORSIA emission goals. United Airlines started using SAF on a trial-basis for outbound flights from Los Angeles in 2016 (United Airlines, 2021), while Southwest Airlines and Alaska Airlines have established agreements with SAF producers (Csonka, 2016). However, because SAF have a higher production cost than CJF (Doliente et al., 2020) and their production capacity is still to be determined, the degree of utilization of SAF by commercial airlines and their ability to meet the emission goals is uncertain. Fuel demands of airlines may dwarf SAF production capacity and its higher production cost could increase ticket prices, which–in turn–could reduce the passenger demand and potentially hurt their bottom line, albeit lower travel demand would reduce emissions. Hence, there is a need to assess the effectiveness of introducing and utilizing SAF across commercial air transportation in achieving the carbon reduction emissions. This is relevant because the pricing of SAF, the level of introduction across the fleet of aircraft, and the fleet-level life-cycle emissions all work together to influence the utilization of SAF as an aviation fuel and aviation emissions.

Several studies using different models and analytical approaches have ventured to estimate the environmental impact of commercial aviation and the impact of potential mitigation strategies. For example, Kim et al. (Kim et al., 2007) and Lee et al. (Lee et al., 2007) used the system tool for assessing aviation's global emission (SAGE)—commissioned by the FAA—to assess global commercial aviation fuel usages and emissions. Li et al. (2016) studied 22 airlines over the 2008–2012 period and found that European airlines have higher efficiency than non-European ones due to higher operational and business efficiency, similar to the results of European Union Emission Trading Scheme. Implementing aviation emission taxes could reduce emissions due to higher ticket fares and lower passenger demands; however, Hofer et al. (2010) show that these emission reductions can be offset as people divert to other modes of transportation. Hassan et al. (2018) provide a modeling

framework that accounts for biofuel availability, fuel price, and inverse demand effects, and provide a probabilistic assessment of the achievability of CO_2 targets in the US; however, the assessments date the pre-COVID era and do not take into account the sharp dip in demand in 2020.

The work summarized in this paper presents an approach that uses a more realistic operations-based model where an aircraft allocation problem is solved while satisfying passenger demand and fleet-level operational constraints for different future scenarios. The research assesses the expected fleet-wide emissions of future airline operations for various projected demand, levels of penetration/utilization of biofuels, and the price of biofuels and its impact on ticket prices. Projected demand is based on assumptions about future demand growth in an existing network of operations; levels of penetration of biofuels in airline operations are based on estimated biofuel production capacity; and prices of biofuels are based on estimations of potential future cost reductions, either through technology advancements, production capacity improvements, or competition with conventional fuels. Note that higher fuel prices are likely to affect air travel demand and reduce airline profits. We assume that new policies to either encourage or to force airlines to achieve the aforementioned emission goals will be in affect and proceed to assess the potential reduction in emissions that can be achieved if airlines abide by these regulations. The authors assess the impact of using SAF (starting in year 2020) on airline emissions using the Fleet-Level Environmental Evaluation Tool (FLEET) (Moolchandani et al., 2017), in which the biofuel and the CJF have the emission intensity 2.31 and 3.67 lb CO_2-equivalent per lb consumed fuel, respectively. FLEET simulates the behavior of a profit-seeking airline and uniquely combines an airline fleet operations model with the assessment of the environmental impacts of US-touching commercial aviation. By exploring different future scenarios of SAF utilisation and travel demand, the results provide bounds on potential future fleet-level emissions and the ability of airlines to reduce emissions by the year 2050.

2 SUSTAINABLE AVIATION FUEL

Sustainable Aviation Fuel (SAF) is a mixture of biofuels and CJF and has different properties depending on the type biofuel. The SAFs from different production pathways and feedstocks have different production costs and life-cycle carbon emission intensities. According to the American Society for Testing and Materials (ASTM) International Specification D7566 (Sissine, 2010), the SAF is a mixture between biomass-derived synthesized paraffinic kerosene (SPK) and the CJF. SPK usually includes biofuels based on biomass feedstocks. Although aircraft emit similar amounts of carbon emissions by using both CJF or SAFs (Stratton et al., 2010), the biomass feedstocks from SPK production pathways can capture carbon dioxide from the atmosphere. Hence, SAFs have lower carbon emission intensity than CJF when considering the life cycle of both types of fuels, which include the net carbon emissions from "well to wake" in CJF and "seed to wake" in SAF. Similarly, to assess SAF economic competitiveness, different SPK production pathways can result in various compositions of production costs, e.g. feedstock acquisition cost, feedstock transportation cost, fuel transportation cost, and bio-refinery operational cost, etc.

TABLE 1 | Types of HEFA biofuel and their emission intensities.

Type of HEFA biofuel	Emission intensity (lb CO2-equivalent per lb fuel)
Tallow	0.970
Used Cooking Oil	0.600
Palm Fatty Acid Distillate	0.893
Corn Oil	0.742
Soybean Oil	1.743
Rapeseed Oil	2.045
Camelina Oil	1.812
Palm Oil	1.613
Brassica Carinata	1.484

The blending ratio of SPKs should also be lower than 50% (Sissine, 2010). Then, the SAF production costs and life-cycle emission intensities depend on the types of SPK and the blending ratios. Doliente et al. (2020) thoroughly reviewed production costs and life-cycle emission intensities of SPKs from the HEFA, the Fischer-Tropsch production pathway (FT), and the alcohol-to-jet production pathway (ATJ). These production pathways convert different feedstocks to the SPKs for SAF production. For example, HEFA uses oils, like vegetable oil, as the feedstock; while the FT uses lignocellulosic feedstocks.

The common feedstocks for HEFA production pathways are camelina, algae, and used cooking oil (UCO). Even though camelina is not the most popular oilseed grown in the U.S., commercial airlines have used SJF developed from this feedstock (Hileman et al., 2009). For algae, the open pond approach and the photo-bio-reactor are the two most common ways to cultivate algae. The open pound approach is more attractive to the photo-bio-reactor for biofuel productions, because it requires less capital investments, operation costs, and life-cycle carbon emissions (Jorquera et al., 2010; Stephenson et al., 2010). Finally, Doliente et al. (2020) mention that the UCO has relatively low feedstock acquisition cost and will not create land competition with edible feedstock. However, the uncertainty and variability of UCO waste stream are current challenges for SAF.

At the time of this paper, HEFA-based SAF is the only SAF reaching commercial production; the AltAir facility delivered a million gallons of tallow HEFA fuel in 2019 to Los Angeles Airport (LAX) for U.S. airline operations (CAAFI, 2018). Doliente et al. (2020) also reveal that the HEFA fuels have the lowest production cost (68.70 ¢/lb), which includes the feedstock costs, among the other studied SAFs. Additionally, the HEFA fuels based on conventional oil crops have the emission intensity of 2.312 lb CO2-equivalent per lb consumed fuel (Doliente et al., 2020). For the comparison, the production cost of CJF is 26.42 ¢/lb (Doliente et al., 2020) with emission intensity of 3.775 lb CO2-equivalent per lb consumed fuel (de Jong et al., 2017). The ICAO CORSIA supporting document shows the slightly lower carbon emission intensity of conventional oil crops (Soybean, Rapeseed,

TABLE 2 | Future SAF scenarios.

Scenario	Biofuel price	Penetration level
1	Reference	Reference
2	Reference	High
3	Reference	Low
4	Constant	High
5	Special	High

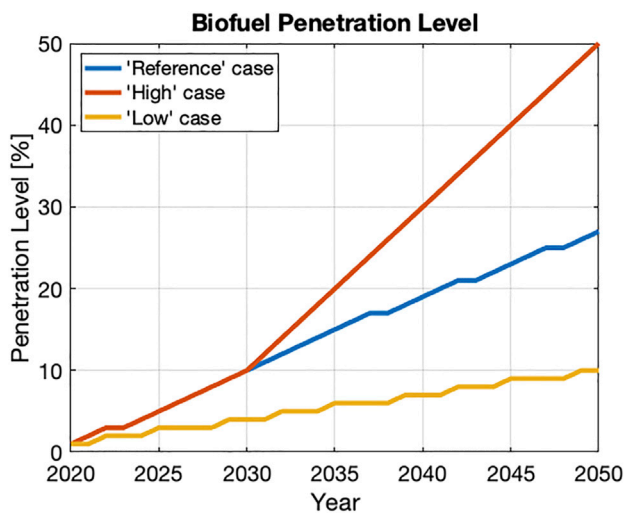

FIGURE 1 | Different biofuel penetration level cases considered in this study.

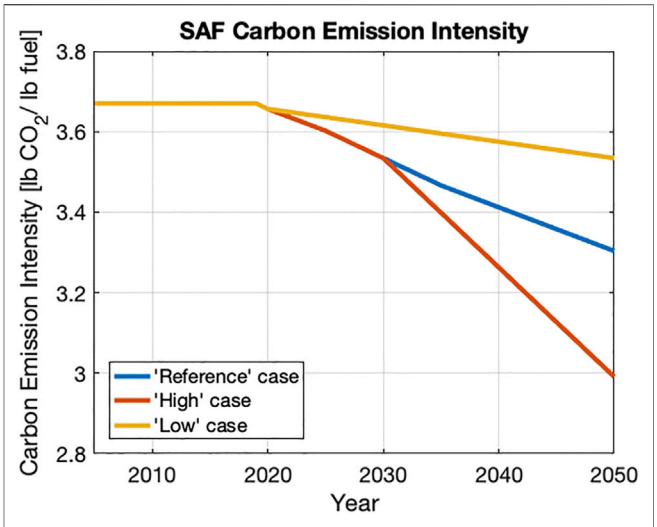

FIGURE 2 | SAF carbon emission intensities for different biofuel penetration levels considered in this study.

and Camelina in **Table 1**) (ICAO, 2019). Hence, the authors also include a study to identify how the different carbon emission intensity settings might affect the evolution of future fleet-level emissions.

2.1 Future Scenarios

The work presented in this article considers multiple possibilities for biofuel market penetration levels, biofuel price, and future travel demand to create five possible scenarios of biofuel utilization (**Table 2**). The HEFA fuel market penetration level affects the SAF price and the carbon emission intensities. Because the biofuel industry is in its infancy, the high risk and high production costs depress the initial penetration level (Chao et al., 2019a). Additionally, due to the ASTM regulations, the penetration level of biofuel is confined to 50%. Feuvre (Le Feuvre, 2019) estimates that the SPK penetration level will be about 19% in 2040. Based on the available biofuel penetration level information, the authors consider three potential penetration level scenarios. The "Reference" penetration level case follows the prediction of Feuvre (Le Feuvre, 2019). The "Low" penetration level case assumes that the biofuel penetration increases linearly to 10% by 2050. Finally, the "High" penetration level case assumes that the penetration level follows prediction of Feuvre (Le Feuvre, 2019) until year 2030, increasing linearly to 50% by year 2050. **Figure 1** shows the different biofuel penetration levels—the blue line shows the "Reference" penetration case, the grey line shows the "Low" penetration level, and the "High" penetration level is depicted by the orange line; the stair-step looking line shape represents the discrete leaps in production facilities. The 2016 Billion-Ton report conservatively estimates that the U.S. biomass can produce biofuel meeting more than 30% of 2005 U.S. petroleum consumption (Langholtz et al., 2016). Considering that the US petroleum consumption in 2019 was 61% of petroleum consumed in 2005 (Administration, 2021a), this means that using the Longholtz et al. estimates, the U.Ss biomass can produce biofuel meeting 49% of U.S. petroleum needs (30%/61% = 49%) of 2019. Because the U.S. aviation sector is responsible for about 6.5% of U.S. petroleum fuel consumption, according to U.S. Energy Information Administration (EIA) estimates for 2020 (Administration, 2021b,c), this means that there is sufficient biomass to supply the SAF needs of aviation, even at 2020 levels.

These different penetration levels lead to lower carbon emission intensities for SAF compared to CJF. The carbon emission intensity for each penetration level is calculated using **Eq. 1**, where the CJF emission intensity is 3.67 lb CO2-equivalent per lb consumed fuel, and the biofuel emission intensity is 2.312 lb CO2-equivalent per lb consumed fuel (Doliente et al., 2020). **Figure 2** shows the SAF carbon emission intensity for the "Reference," "High," and "Low" penetration level cases.

$$SAF_{emission_{intensity}} = (1 - penetration_{level}) * CJF_{emission_{intensity}} + penetration_{level} * biofuel_{emission_{intensity}} \quad (1)$$

For biofuel price, the authors consider three different pricing levels—"Reference," "Constant," and "Special." The "Reference" biofuel price case assumes that the price difference between biofuel and CJF reduces linearly from the current differential to zero from years 2019–2050. The decreasing price difference

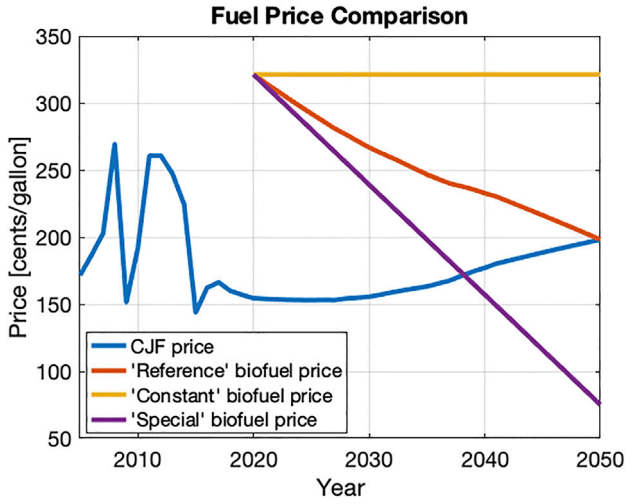

FIGURE 3 | Comparison of Conventional Jet Fuel (CJF) price in FLEET with "Reference," "Constant," and "Special" biofuel price (in 2005 U.S. Dollars).

reflects that the potential technology improvements and the scale of the economy reduce the biofuel production costs. The "Constant" biofuel price case assumes that the biofuel price stays constant at the 2020 value. In the "Special" biofuel price case, the authors assume that the biofuel price reduces linearly to 75¢/gallon. **Figure 3** shows the CJF cost, "Reference" biofuel cost, "High" biofuel cost, and "Low" biofuel cost values in fixed 2005 U.S. dollars; the simulation used in the studies for this paper uses 2005 as the initial year. The CJF fuel price is based on U. S. Energy Information Administration, 2011 Annual Energy Outlook (U. S. Energy Information Administration, 2011).

The authors construct a set of five scenarios using different combinations of the three biofuel price cases and the three biofuel penetration level cases (as listed in **Table 2**). The first three scenarios consider all possible combinations of the "Reference" biofuel price with the different biofuel penetration levels. The last two scenarios consider only the "High" penetration level, combined with "Constant" and "Special" biofuel price cases.

For each scenario, the SAF price calculation considers the biofuel price and the biofuel penetration level. **Eq. (2)** depicts the SAF price calculation, where the CJF price and biofuel price are adapted from **Figure 3** and the penetration levels are adapted from **Figure 1** based on the scenario under consideration. For example, the SAF price for scenario 1 ("Reference" biofuel price + "Reference" penetration level) in the year 2040 is given by *(1–0.19)x177.12 + 0.19 × 232.7 = 187.7¢/gallon*. **Figure 4** shows the SAF price for all the scenarios. The SAF price for all scenarios follows the CJF price trend shown in **Figure 3** for years 2005–2019 because there is no biofuel present in the fuel mix. After 2019, the SAF price deviates from CJF price trends due to the addition of biofuels in the fuel mix. Scenarios 4 and 5 lead to the highest and the lowest SAF prices in the year 2050, respectively, with the 2050 SAF prices for scenarios 1, 2, and 3 matching the 2050 CJF prices.

$$SAF_{price} = (1 - penetration_{level}) * CJF_{price} + penetration_{level} * biofuel_{price} \quad (2)$$

3 MODELING TOOL—FLEET

To analyze the environmental impact of SAF on commercial airline travel, there is a need to—1) model airline operations, 2) model and project passenger demand into the future, and 3) model the introduction and use of different aircraft types into the future. Fleet-Level Environmental Evaluation Tool (FLEET) is a system dynamics-inspired simulation that combines all these models into a single tool; **Figure 5** provides a representation of FLEET (Moolchandani et al., 2017).

FLEET simulation enables the prediction of the environmental impacts of commercial aviation by evolving a mix of aircraft in a notional airline's fleet and passenger demand over time (Moolchandani et al., 2017); the primary environmental impact considered here is CO_2 emissions. At the heart of FLEET is an optimization algorithm that solves an allocation problem to maximize airline profit while satisfying passenger demand and operational constraints over its route network. The tool can reflect the performance of new technology aircraft that are predicted to consume less fuel and generate less noise than current aircraft; with these aircraft models, FLEET simulates how an airline would use these new aircraft to meet passenger demand on a route network. The predicted usage of these new aircraft drives the fleet-level environmental impacts. Many studies exist that discuss the various studies conducted with FLEET considering only subsonic aircraft operations (Moolchandani et al., 2011; Moolchandani et al., 2012; Moolchandani et al., 2013; Chao, 2016; Chao et al., 2016; Chao et al., 2017; Moolchandani et al., 2017; Ogunsina et al., 2017; Ogunsina et al., 2018; Jain and Crossley, 2020; Jain et al., 2021a). Recent

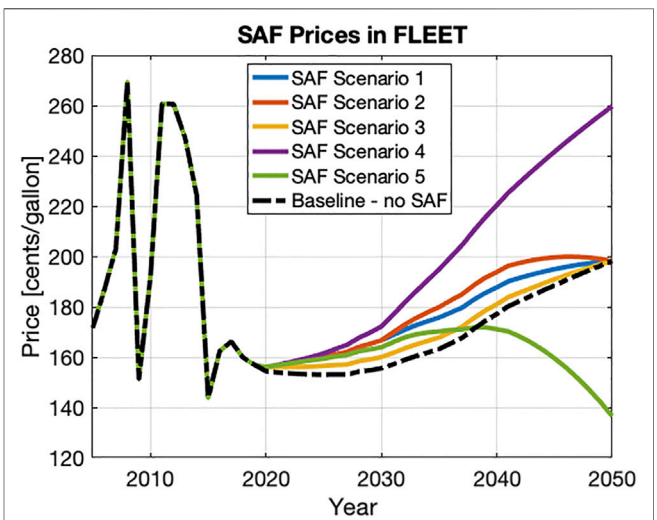

FIGURE 4 | SAF prices in FLEET for all future scenarios.

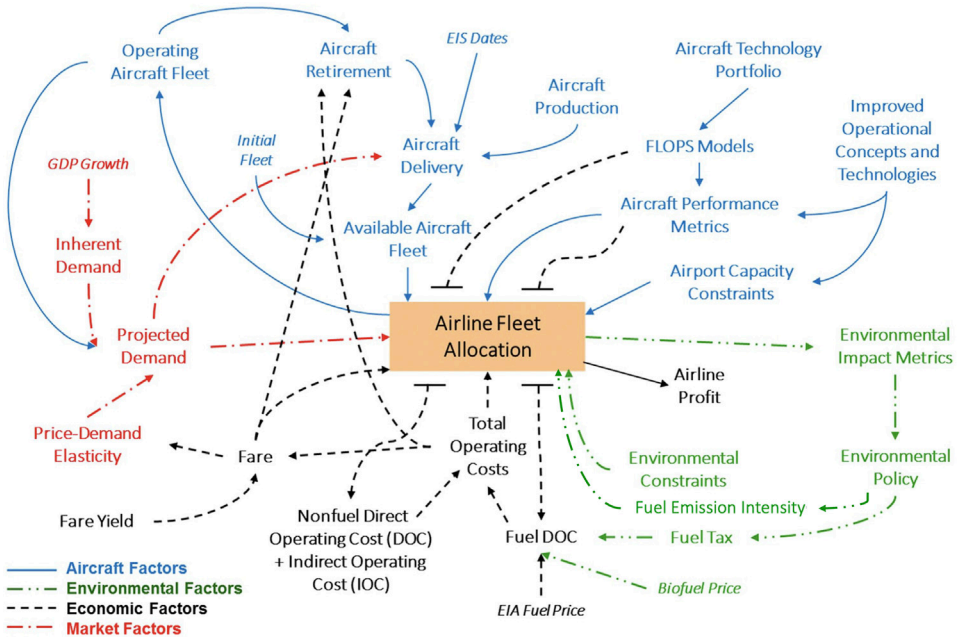

FIGURE 5 | System-dynamics-inspired representation of FLEET [adapted with permission from (Moolchandani et al., 2017)].

TABLE 3 | Aircraft types in study with [Label] and (EIS).

	Representative-in-class	Best-in-class	New-in-class	Future-in-class
Class 1	Canadair RJ200/RJ440 [SRJ]	Embraer ERJ145 [SRJ]		
Class 2	Canadair RJ700 [RJ]	Canadair RJ900 [RJ]	Gen1 DD RJ (2020)	Gen2 DD RJ (2030)
Class 3	Boeing 737-300 [SA]	Boeing 737-700 [SA]	Gen1 DD SA (2017)	Gen2 DD SA (2035)
Class 4	Boeing 757-200 [STA]	Boeing 737-800 [STA]	Gen1 DD STA (2025)	Gen2 DD STA (2040)
Class 5	Boeing 767-300ER [LTA]	Airbus A330-200 [LTA]	Gen1 DD LTA (2020)	Gen2 DD LTA (2030)
Class 6	Boeing 747-400 [VLA]	Boeing 777-200LR [VLA]	Gen1 DD VLA (2025)	Gen2 DD VLA (2040)

EIS, entry into service; LTA, large twin aisle; RJ, regional jet; SRJ, small regional jet; SA, single aisle; STA, small twin aisle; VLA, very large aircraft.

FLEET studies considering a mixture of supersonic and subsonic commercial aircraft in airline fleet also exist (Jain et al., 2020; Jain et al., 2021b; Mane et al., 2021).

As discussed by the authors in (Jain et al., 2021b, Jain et al., 2021a; Moolchandani et al., 2017), FLEET represents aircraft by class (based on number of seats) and by technology age. There are six different classes of subsonic aircraft in FLEET—1) Small Regional Jet (up to 50 seats), 2) Regional Jet, 3) Small Single Aisle, 4) Large Single Aisle, 5) Small Twin Aisle, and 6) Large Twin Aisle. There are four different technology ages in FLEET—1) Representative-in-class (most flown aircraft in 2005), 2) Best-in-class (aircraft with most recent entry into service dates as of 2005), 3) New-in-class (aircraft currently under development that will enter service in near future), and 4) Future-in-class (aircraft that will enter into service after new-in-class aircraft). FLEET uses year 2005 as the first year of simulation because many future goals for aviation CO_2 emissions use 2005 as a reference year. **Table 3** lists the subsonic aircraft available in FLEET; Mavris et al. (Mavris et al., 2017) provide details about these aircraft. These different classes and technology of aircraft are modeled using the Flight Optimization Software (FLOPS) (McCullers, 2016) and represent the mix of aircraft sizes and technologies in the airline fleet.

In the FLEET allocation problem, the notional airline could best be thought of as an aggregate airline representing all US flag carrier airlines. Jain et al. (2021a) discuss that FLEET predictions for routes and passenger demand build upon reported data from the Bureau of Transportation Statistics (BTS) (U.S Dept. of Transportation, Bureau of Transportation Statistics, 2017). For historical years, FLEET uses a dynamic route network that follows how US flag carrier airlines updated their route networks from 2005 to 2018—as reported in the BTS data. This is followed by a static route network from 2018 and beyond (i.e., FLEET does not predict the addition or deletion of routes in the future). FLEET also uses BTS reported values of historical passengers carried as the passenger demand from 2005 to 2018, followed by passenger demand predictors using economic and price factors for years 2019 and beyond. In 2018 (and all the subsequent years), there are 1,974 routes in the FLEET network that connect a subset of

TABLE 4 | Future demand projection scenarios; the ones marked in red font are considered in this study (Jain et al., 2021a).

Scenario #	Description	Passenger demand (% of pre-COVID-19 levels)					GDP growth rate (As % of 'nominal')
		2020	2021	2022	2023	2024	
1	2023 recovery	34%	52%	88%	100%	—	No change
2	2023 recovery + GDP slowdown to 75% until 2030	34%	52%	88%	100%	—	75% (–25%)
3	2023 recovery + GDP inflation to 125% until 2030	34%	52%	88%	100%	—	125% (+25%)
4	2024 recovery	34%	38%	50%	75%	100%	No change
5	2024 recovery + GDP slowdown to 75% until 2030	34%	38%	50%	75%	100%	75% (–25%)
6	2024 recovery + GDP inflation to 125% until 2030	34%	38%	50%	75%	100%	125% (+25%)

WWLMINET 257 airports (Kim et al., 2005). All these routes are either US domestic routes or international routes with direct flights originating or ending at a US airport, because these are the only routes that appear in the BTS database.

The FLEET simulation output provides information about the type(s) of and number of aircraft allocated to routes to meet passenger demand based on a number of scenarios. The scenarios are essentially a combination of low, nominal, and high values for aircraft technology, economic growth rate, and energy price. More details about the subsonic-only FLEET scenarios are available in (Mavris et al., 2017; Ogunsina et al., 2018). This work considers only the "Current Trends Best Guess (CTBG)" scenario of technology development and economic conditions from the previous work; this scenario comprises nominal aircraft technology development, nominal economic growth, and nominal energy price evolution.

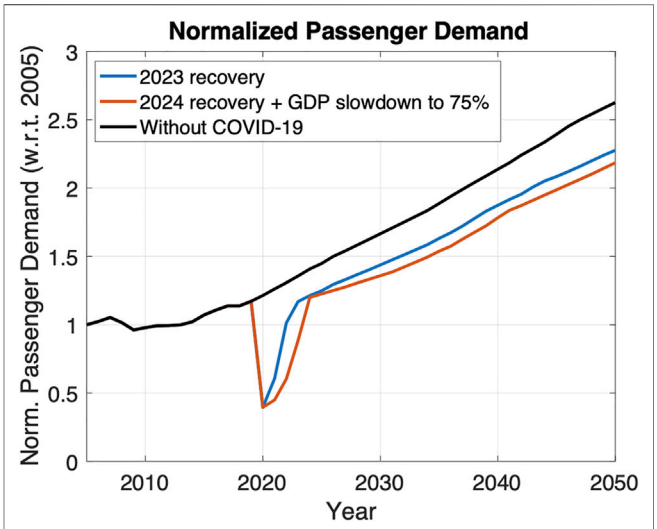

FIGURE 6 | Passenger demand in FLEET considering different demand recovery scenarios.

4 FUTURE PASSENGER DEMAND PROJECTIONS

The passenger demand forecast in FLEET is modeled is a function of two factors: the demand changes due to broad economic factors, referred to here as the "inherent demand growth," and the demand change due to passenger response to changes in ticket prices charged by the airlines, called the "elastic growth." In the inherent demand growth model, the demand growth is a function of GDP growth, while the elastic growth model incorporates the effects of range and availability of alternative modes of transport into its calculation to determine whether demand might increase or decrease on a given route as airline ticket prices change. More information about passenger demand modeling in FLEET is available in (Moolchandani et al., 2017).

The novel coronavirus (COVID-19) pandemic has induced one of the sharpest declines in air travel demand in aviation history; full-year global passenger traffic results from both the International Air Transport Association (IATA) and the International Civil Aviation Organization (ICAO) indicate that 2020 was the worst year in the history for air travel demand (IATA, 2021a; Hasegawa, 2021). There is an uncertainty about how the air travel demand recovery will look like in the near future, with complete demand recovery to pre-COVID-19 levels (2019) expected by year 2023 or 2024 (IATA, 2021b; Pearce, 2021), depending on the continuation of travel restrictions imposed world-wide due to the spread of more contagious COVID-19 variants.

To account for the impact of the COVID-19 pandemic on future passenger demand, the authors consider two different future demand projection scenarios for this article. These demand projection scenarios assume airline operations recovery to pre-COVID-19 (2019) levels in year 2023 and 2024, along with variations in the GDP growth rates–starting from the year of passenger demand recovery to 2019 levels to the year 2030. The two demand projection scenarios considered here are a subset of the six scenarios identified by the authors in (Jain et al., 2021a). **Table 4** summarizes all six future demand scenarios; the authors only consider two scenarios marked with red font in this article—scenario 1 ("2023 recovery") and scenario 5 ("2024 recovery + GDP slowdown to 75% until 2030"). In the table, the passenger demand for different years is listed as a percentage of pre-COVID-19 levels (2019) and the GDP growth rate is listed as a percentage of the "Nominal" GDP growth rate in FLEET (Moolchandani et al., 2017; Mavris et al., 2017). The total passenger demand in 2020 for all scenarios is set to be 34% of the passenger demand levels in 2019, signifying a 66% drop in total passenger demand (IATA, 2021b; Jain et al., 2021a). **Figure 6**

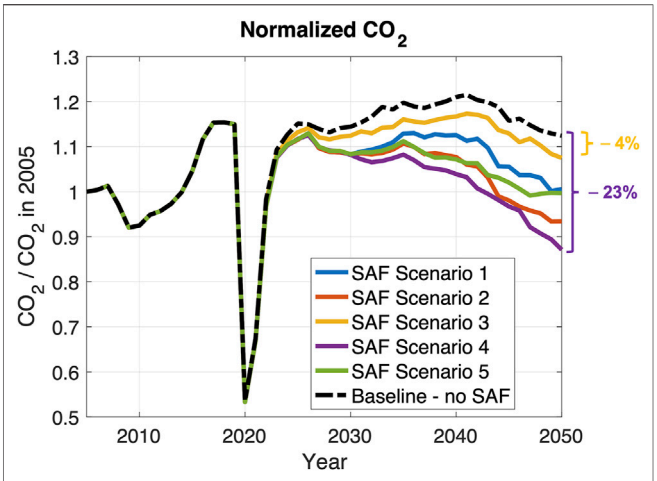

FIGURE 7 | Normalized fleet-level CO_2 emissions for SAF scenarios (considering passenger demand recovery to pre-COVID-19 levels by 2023); biofuel emission intensity: 2.312 lb CO2-equivalent per lb consumed fuel; CJF emission intensity: 3.67 lb CO2-equivalent per lb consumed fuel.

shows the historical and projected demand in FLEET for the two projected demand scenarios in consideration (Jain et al., 2021a).

The "2023 recovery" scenario is the primary scenario for this work; this represents an optimistic view that the airline operations will recover to pre-COVID-19 (2019) levels by 2023, with minimal impact on GDP growth. The total passenger demand is set to recover to 52% of pre-COVID-19 levels by 2021, 88% of pre-COVID-19 levels by 2022, and 100% of pre-COVID-19 levels by 2023 (Jain et al., 2021a; IATA, 2021b), along with the assumption that the passenger demand in FLEET continues to grow based on FLEET's GDP growth rate beyond 2023. The "2024 recovery + GDP slowdown to 75% until 2030" acts as an additional scenario for this work, taking into account the possibility of lower passenger demand recovery due to the spread of new COVID-19 variants. Also, this scenario assumes that the passenger demand grows at 75% of FLEET's GDP growth rate until year 2030, representing the worst case scenario for future passenger demand growth. The total passenger demand is set to recover to 38% of pre-COVID-19 levels by 2021 (IATA, 2021a), 50% of pre-COVID-19 levels by 2022, 75% of pre-COVID-19 levels by 2023, and to pre-COVID-19 levels by 2024 (Jain et al., 2021a).

5 RESULTS

The FLEET simulation is run from years 2005–2050. The results presented here use the previously developed "Current Trends Best Guess (CTBG)" scenario (Mavris et al., 2017) as the baseline scenario, using the subsonic CTBG results (with no SAF) for comparing the current results. The five future SAF scenarios (discussed in **Section 2.1**) are input into FLEET to estimate the changes in fleet-level CO_2 emissions and airline operations with the introduction of SAF to the airline fleet in year 2020. As mentioned above, this article considers two future passenger demand projection scenarios—"2023 recovery" and "2024 recovery + GDP slowdown to 75% until 2030"—this leads to a total of ten scenarios. The authors consider the "2023 recovery" scenario to be the primary simulation scenario, with the "2024 recovery + GDP slowdown to 75% until 2030" scenario acting as an additional scenario that simulates changes in CO_2 emissions when SAF are introduced considering the worst case passenger demand growth.

5.1 Primary Simulation Scenario (2023 Passenger Demand Recovery)

This subsection presents FLEET simulation results considering the "2023 recovery" passenger demand projection—recovery to pre-COVID-19 (2019) levels by 2023, with no impact on GDP growth. **Figure 7** shows the normalized CO_2 emissions predicted by FLEET for the SAF scenarios along with the no SAF baseline scenario. As visible in the figure, there is a slump in fleet-level CO_2 emissions in the year 2020 due to the COVID-19 pandemic-related travel restrictions. The fleet-level emissions for all five SAF scenarios are always lower than the no-SAF baseline scenario. The minimum reduction in 2050 fleet-level CO_2 emissions is 4.4% (for scenario 3) and the maximum reduction is 22.5% (for scenario 4). With the current modeling, FLEET simulation results

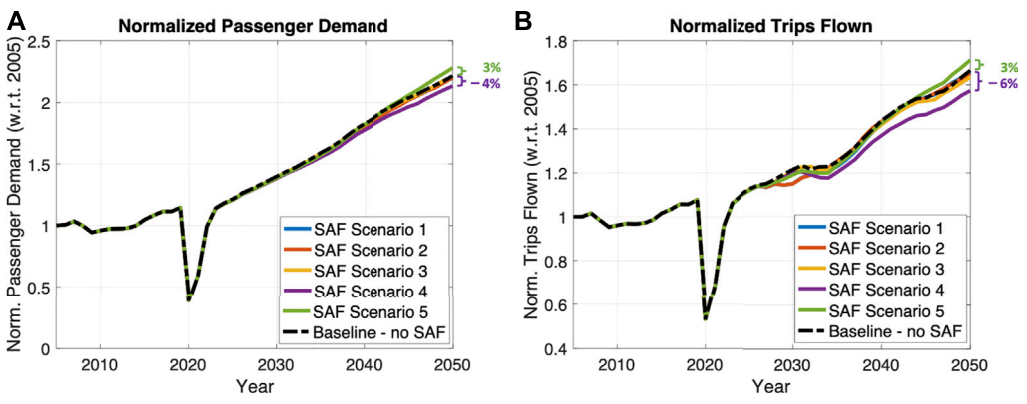

FIGURE 8 | (A) Normalized passenger demand, **(B)** Normalized trips flown, for SAF scenarios (considering passenger demand recovery to pre-COVID-19 levels by 2023).

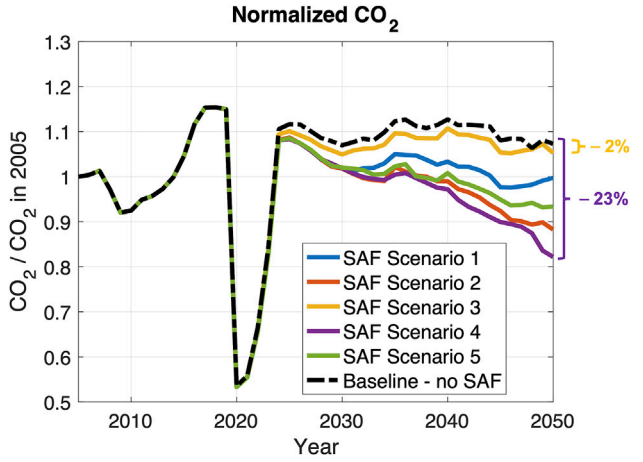

FIGURE 9 | Normalized fleet-level CO_2 emissions for SAF scenarios (considering passenger demand recovery to pre-COVID-19 levels by 2024 and GDP slowdown to 75% until 2030); biofuel emission intensity: 2.312 lb CO2-equivalent per lb consumed fuel; CJF emission intensity: 3.67 lb CO2-equivalent per lb consumed fuel.

show that the fleet-level CO_2 emissions could go below 2005 levels if scenario 2 ("Reference" biofuel price + "High" penetration level), scenario 4 ("Constant" biofuel price + "High" penetration level), or scenario 5 ("Special" biofuel price + "High" penetration level) were to materialize in reality; these are depicted by green, red, and purple color solid lines, respectively, in **Figure 7** (and in all subsequent figures in this section).

Perhaps not surprisingly, FLEET predictions show that the scenario with the highest SAF price (refer to **Figure 4**)—scenario 4 ("Constant" biofuel price + "High" penetration level)—leads to the lowest CO_2 emissions. This reduction in emissions can be explained by looking at the passenger demand served and the trips flown in scenario 4. The high SAF price leads to an increase in the airline ticket prices, which causes the air travel demand to shrink, leading to lesser trips and subsequently lesser emissions. **Figures 8A,B** show the normalized passenger demand and trips flown, respectively, for the SAF scenarios along with the baseline scenario. There is a 3.7% reduction in the 2050 passenger demand for scenario 4 and a 5.5% reduction in the 2050 trips flown compared to the baseline scenario (depicted by purple solid line in **Figures 8A,B**), indicating that the reduced emissions are a combination of using SAF and the consequent reduction in the number of passengers and trips flown by the airline.

Similarly, the scenario with the lowest SAF price—scenario 5 ("Special" biofuel price + "High" penetration level)—leads to CO_2 emissions that are higher than the other scenarios with "High" biofuel penetration levels, i.e., scenarios 2 and 4. The reason for this behavior can be traced back to the increased passenger demand (3.0%) and trips flown (2.9%) by the airline for scenario 5 (depicted by green solid line in **Figures 8A,B**); the reduced SAF prices lead to lower ticket prices, causing a surge in air travel demand, leading to more trips and, subsequently, more emissions.

The authors note that scenarios with 'High' biofuel penetration levels lead to a higher reduction in the fleet-level CO_2 emissions, followed by scenarios with "Reference" and "Low" biofuel penetration levels. This indicates that higher biofuel penetration levels could lead to lower fleet-level CO_2 emissions, even if the airline ends up serving higher passenger demand. The FLEET-predicted maximum 22.5% CO_2 reduction by 2050 relative to the non-SAF baseline from introducing SAF and the price-elastic demand effects of SAF, while for the US-touching based network and airlines discussed above, is notably lower than the cumulative 46% predicted for European Aviation by (van der Sman et al., 2021).

5.2 Additional Simulation Scenario (2024 Passenger Demand Recovery With GDP Slowdown to 75%)

This subsection talks about FLEET simulation results considering the "2024 recovery + GDP slowdown to 75% until 2030" passenger demand projection—recovery to pre-COVID-19 (2019) levels by 2024 (a year later than previous demand projection), with GDP slowdown to 75% until year 2030.

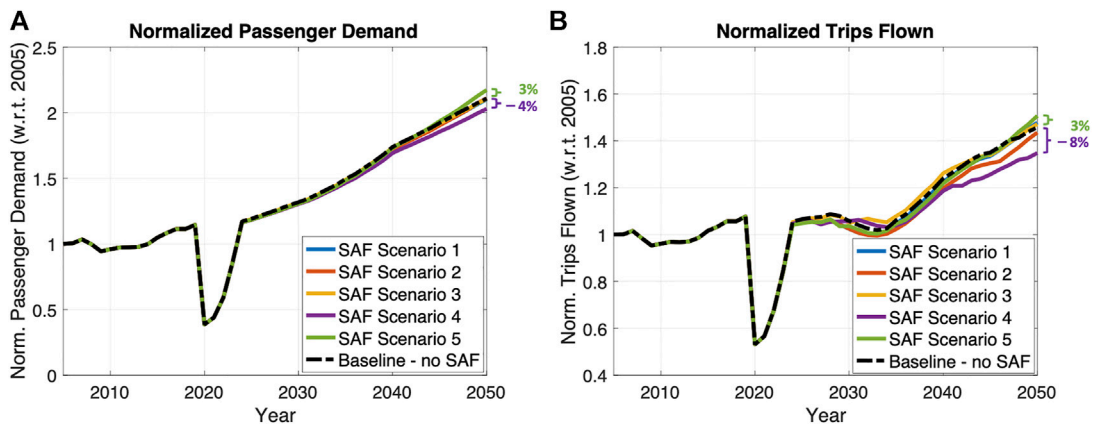

FIGURE 10 | (A) Normalized passenger demand, **(B)** Normalized trips flown, for SAF scenarios (considering passenger demand recovery to pre-COVID-19 levels by 2024 and GDP slowdown to 75% until 2030).

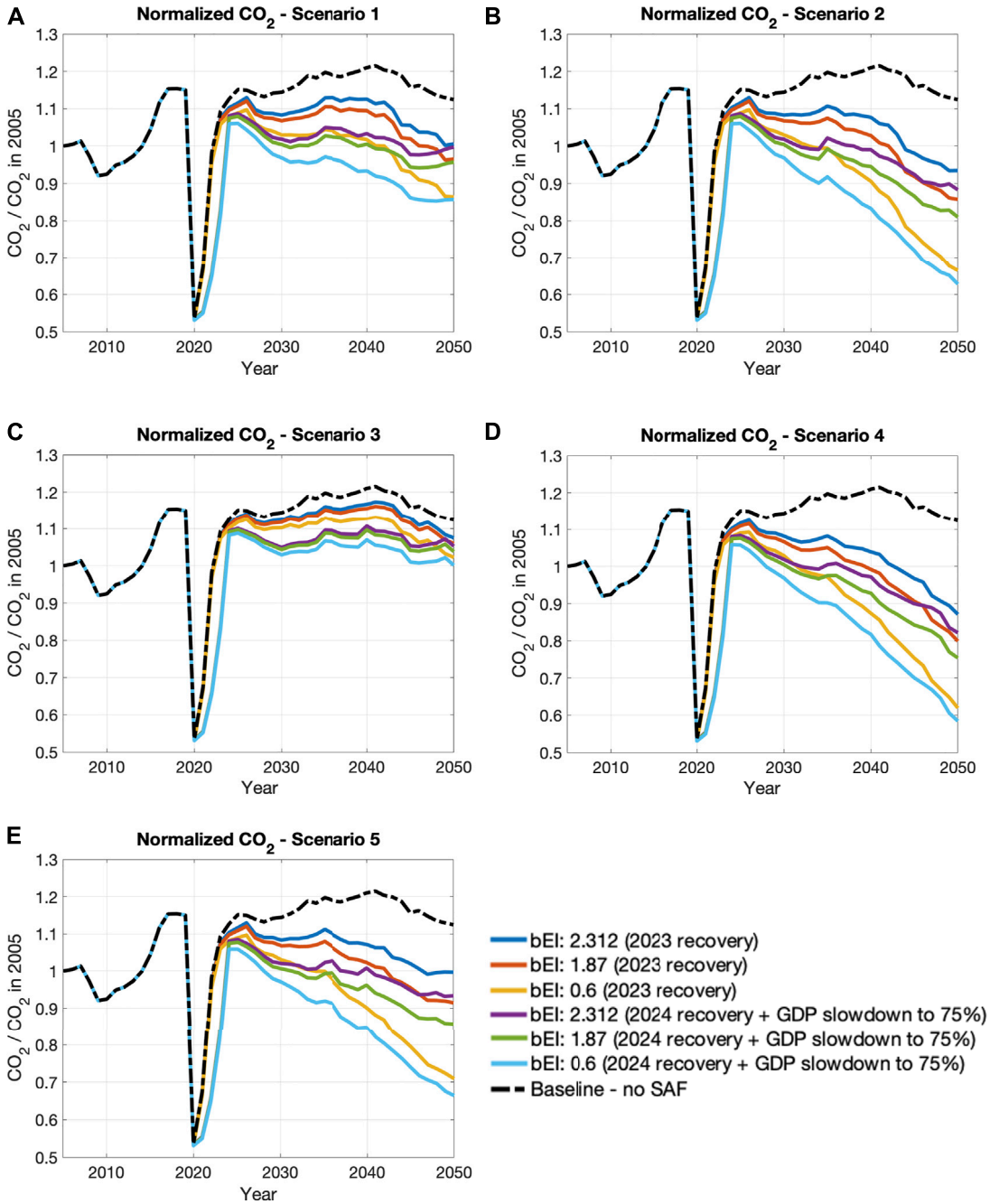

FIGURE 11 | Normalized fleet-level CO_2 emissions for different SAF scenarios considering multiple biofuel emission intensities and future demand growth projections – **(A)** Scenario 1: reference biofuel price, reference penetration level, **(B)** Scenario 2: reference biofuel price, high penetration level, **(C)** Scenario 3: reference biofuel price, low penetration level, **(D)** Scenario 4: constant biofuel price, high penetration level, **(E)** Scenario 5: special biofuel price, high penetration level; 'bEI' refers to 'biofuel emission intensity' (in lb CO2-equivalent per lb consumed fuel.

Figure 9 shows the normalized CO_2 emissions for the SAF scenarios along with the no SAF baseline scenario in FLEET. As with the previous set of results, the emissions from all five scenarios are always lower than the baseline scenario, with a minimum reduction of 1.9% (for scenario 3) and a maximum reduction of 23.4% (for scenario 4) in 2050 fleet-level CO_2 emissions.

With the current modeling, FLEET simulation results show that the fleet-level CO_2 emissions could go below 2005 levels if

four out of the five SAF scenarios were to materialize in reality (compared to the only three for the demand projections considered in **Section 5.1**)—scenario 1 ("Reference" biofuel price + "Reference" penetration level), scenario 2 ("Reference" biofuel price + "High" penetration level), scenario 4 ("Constant" biofuel price + "High" penetration level), and scenario 5 ("Special" biofuel price + "High" penetration level). For the current demand projection scenario, the authors note that 2005 emission levels (or lower) could be achieved for "High" and "Reference" biofuel penetration levels. For the previous demand projection case, these levels could only be obtained using the "high" biofuel penetration level.

Similar to the previous set of results, the airline ends up serving the highest demand for the SAF scenario with lowest SAF price (scenario 5), leading to CO_2 emissions that are higher than the other scenarios with "High" biofuel penetration levels, i.e., scenarios 2 and 4. **Figure 10** shows the normalized passenger demand and trips flown for the SAF scenarios along with the baseline scenario. For scenario 5, there is a 3.1% increase in 2050 passenger demand and a 3.4% increase in trips flown by the airline compared to the baseline scenario. Scenario 4 leads to the lowest fleet-level CO_2 emissions due a combination of using SAF and a 3.7% reduction in the passenger demand served (along with a 7.5% reduction in trips flown), depicted the purple solid lines in **Figure 10**.

Interestingly, the predictions show that a delay in the passenger demand recovery from COVID-19 (recovery in 2024) due to extended travel restrictions and a GDP slowdown until 2030 could lead to lower overall fleet-level emissions (comparing **Figures 7**, **9**). The widened gap in passenger demand recovery after the demand slump in 2020—visible when comparing **Figure 10A** with **Figure 8A**—contributes positively to CO_2 emission reductions, and the usage of SAF instead of CJF helps to pull down emissions even further.

5.3 Biofuel Alternatives

The results presented in **Sections 5.1, 5.2** are based on a biofuel emission intensity of 2.312 lb CO2-equivalent per lb consumed fuel (based on HEFA oil crops in (Doliente et al., 2020)) and a CJF emission intensity of 3.67 lb CO2-equivalent per lb consumed fuel. The authors note that the biofuel and CJF emission intensities vary from study to study, making it a good parameter for sensitivity analysis. For this sensitivity study, two biofuel emission intensity values are considered—) 1.87 lb CO2-equivalent per lb consumed fuel—this is an average value for HEFA oil crops (Soybean, Rapeseed, and Camelina; shown in **Table 1**) based on (ICAO, 2019), and 2) 0.60 lb CO2-equivalent per lb consumed fuel—value for used cooking oil based on (ICAO, 2019). These emission intensities are chosen so that they can help us set bounds on future fleet-level CO_2 emissions, with the assumption that the biofuel cost evolution stays the same for all the different biofuels considered here. The CJF emission intensity is also updated to 3.775 lb CO2-equivalent per lb consumed fuel based on (de Jong et al., 2017).

Figure 11 shows the normalized CO_2 emissions for all five SAF scenarios while considering different biofuel emission intensities (2.312, 1.87, and 0.6 lb CO2-equivalent per lb consumed fuel) and different future demand growth projections ("2023 recovery" and "2024 recovery + GDP slowdown to 75% until 2030"). The figure clearly shows the impact of biofuel selection and demand projection on future aviation emissions. As expected, reductions in biofuel emission intensity and future passenger demand could lead to lower emissions. Scenario 4 ("Constant" biofuel price + "High" penetration level)—shown in **Figure 11D**—leads to the lowest emissions among all scenarios, with a maximum possible reduction of 48% for the case with biofuel emission intensity of 0.6 lb CO2-equivalent per lb consumed fuel (used cooking oil used as biofuel) and passenger demand recovery in 2024 (with GDP slowdown to 75% until 2030).

6 CONCLUSION

This article discusses the possible impact of using SAF on fleet-level CO_2 emissions and airline operations, while taking into account the air travel demand disruption due to the COVID-19 pandemic and various possibilities of the introduction and use of biofuels by airlines. The authors consider five SAF scenarios (listed in **Table 2**) along with two COVID-19-related demand projection scenarios (listed using red font in **Table 4**). The SAF scenarios are based on a combination of different biofuel prices and different biofuel penetration levels; the future demand projection scenarios use a combination of different passenger demand recovery possibilities and different GDP growth rates. The authors used FLEET to model the behavior of a profit-seeking airline for different SAF and projected demand scenarios and estimate changes in future fleet-level CO_2 emissions, along with predicting the future passenger demand and trips flown. In addition, because of the numerous sources of biofuel, the study explores the potential future emission levels if any of these biofuels were used by airlines at the assumed penetration levels and prices.

The results indicate that the introduction SAF for use in airline fleets and the projected demand scenarios could notably impact the future fleet-level aviation CO_2 emissions. Considering a biofuel emission intensity of 2.312 lb CO2-equivalent per lb consumed fuel, the total CO_2 emissions from all five SAF scenarios are always lower than the no-SAF baseline scenario, for both the COVID-19-related projected demand scenarios. For the "2023 recovery" scenario, a minimum of 4.4% reduction (for scenario 3) and a maximum of 22.5% reduction (for scenario 4) is possible in the 2050 fleet-level emissions. For the "2024 recovery + GDP slowdown to 75% until 2030" scenario, the maximum possible reduction in fleet-level emissions is higher—23.4%, but the minimum possible reduction is lower—1.9%; the late recovery of passenger demand to pre-COVID-19 levels along with a GDP slowdown until year 2030 causes the emissions from the no-SAF baseline case to decrease, diminishing the benefits of using SAF with "Low" biofuel penetration levels. However, when FLEET evaluates SAF usage with "Reference" and "High" biofuel penetration levels, the predicted benefits of SAF are

amplified, leading to even lower future emissions when compared to the "2023 recovery" scenario.

The authors note that the SAF scenarios with low SAF price lead to higher fleet-level emissions for both future demand projections scenarios; this happens because low fuel prices lead to low ticket prices, which causes a surge in demand, and the airline ends up flying more trips—leading to higher emissions. For SAF scenarios with high SAF price, the opposite occurs—high fuel prices push ticket prices up, shrinking demand, causing the airline to fly lesser number of trips, leading to lower fleet-level emissions.

Looking at the biofuel penetration levels, current modeling suggests that the "High" penetration level leads to 2050 emissions that are lower than the 2005 emissions levels, for both future demand projections scenarios. For the "2024 recovery + GDP slowdown to 75% until 2030" scenario, the 2050 emissions from the "Reference" penetration level are also lower than the 2005 emission levels. These results show that the reason for the reduction in fleet-level emissions for the SAF scenarios is a combination of the reduced overall CO_2 emissions from using SAF and reduced passenger demand (and hindered demand growth for one of the COVID-19-related demand scenarios).

Additionally, the type of biofuel selected (and subsequently its carbon emission intensity) also impacts the future aviation emissions; biofuels with lower carbon emission intensities lead to lower emissions. The reduction in emissions could be as high as 48% compared to the baseline scenario with no SAF, when using a biofuel with an emission intensity of 0.6 lb CO2-equivalent per lb consumed fuel (used cooking oil used as biofuel) along with passenger demand recovery in 2024 (with GDP slowdown to 75% until 2030).

The CO_2 emission predictions presented in this work—considering five scenarios combining different biofuel prices and biofuel penetration levels—show that future emissions can decrease when SAF with high biofuel penetration levels are introduced for use in airline fleets. The results do not intend to show the exact CO_2 emission levels, but provide upper and lower bounds on possible future aviation emissions. As expected, not introducing SAF will lead to the highest CO_2 emissions possible, followed by introducing SAF with "Low" penetration levels; these scenarios could act as the upper bounds for without SAF and with SAF future aviation emission predictions, respectively. With the current modeling, introducing SAF with "High" penetration levels could lead to the lowest possible emissions, serving as the "best case scenario" for future aviation CO_2 emissions.

DATA AVAILABILITY STATEMENT

The raw data supporting the conclusion of this article will be made available by the authors upon request, without undue reservation.

AUTHOR CONTRIBUTIONS

SJ was the lead author, providing the overall outline for the article and conducting most of the FLEET simulations. HC provided inputs for the paper and for FLEET regarding SAF costs and penetration rates. MM provided major revisions and editing oversight for the article and developed demand scenarios reflecting COVID-19 impacts. WC provided final revisions to the article and oversight of the FLEET simulation tool. DD also provided reviews of the article and oversight of the FLEET simulation tool.

FUNDING

The open access publication fees are provided from discretionary funds of the authors generated at Purdue University.

REFERENCES

Administration, T. U. E. I. (2021a). *Adjusted Distillate Fuel Oil Sales for Residential Use*. Dataset.

Administration, T. U. E. I. (2021c). *Use of Energy for Transportation - U.S. Energy Information Administration*. EIA. Dataset.

Administration, T. U. E. I. (2021b). *U.S. Fossil Fuel Consumption Fell by 9nearly 30 Years - Today in Energy - U.S. Energy Information Administration*. EIA. Dataset.

CAAFI (2018). Alternative Jet Fuel Production Facilities Status. Commercial Aviation Alternative Fuels Initiative (CAAFI), Available at: http://www.caafi.org/focus_areas/docs/Alternative_Jet_Fuel_Production_Facilities_Status.pdf (Accessed June 2018).

Chao, H., Agusdinata, D. B., and DeLaurentis, D. A. (2019a). The Potential Impacts of Emissions Trading Scheme and Biofuel Options to Carbon Emissions of U.S. Airlines. *Energy Policy* 134, 110993. doi:10.1016/j.enpol.2019.110993

Chao, H., Agusdinata, D. B., and DeLaurentis, D. A. (2019c). The Potential Impacts of Emissions Trading Scheme and Biofuel Options to Carbon Emissions of U.S. Airlines. *Energy Policy* 134, 110993. doi:10.1016/J.ENPOL.2019.110993

Chao, H., Agusdinata, D. B., DeLaurentis, D., and Stechel, E. B. (2019b). Carbon Offsetting and Reduction Scheme with Sustainable Aviation Fuel Options: Fleet-Level Carbon Emissions Impacts for U.S. Airlines. *Transportation Res. D: Transport Environ.* 75, 42–56. doi:10.1016/j.trd.2019.08.015

Chao, H., DeLaurentis, D., and Agusdinata, B. (2017). "Sensitivity Analysis of Fleet-Level Life Cycle Carbon Emissions to Biofuel Options and Emission Policy Schemes for the U.S. Commercial Airlines," in 17th AIAA Aviation Technology, Integration, and Operations Conference. doi:10.2514/6.2017-3768

Chao, H. (2016). *Fleet Level Environmental Evaluation of Emission Taxing Scheme and Biofuel: A Combined Optimization and Multi-Actor ApproachMaster's Thesis*. West Lafayette, Indiana: Purdue University, School of Aeronautics and Astronautics. URL: https://docs.lib.purdue.edu/open_access_theses/932.

Chao, H., Kolencherry, N., Ogunsina, K., Moolchandani, K., Crossley, W. A., and DeLaurentis, D. A. (2017). "A Model of Aircraft Retirement and Acquisition Decisions Based on Net Present Value Calculations," in 17th AIAA Aviation Technology, Integration, and Operations Conference. doi:10.2514/6.2017-3600

Chao, H., Ogunsina, K. E., Moolchandani, K., DeLaurentis, D. A., and Crossley, W. A. (2016). "Airline Competition in Duopoly Market and its Impact on Environmental Emissions: A Game Theory Approach," in 16th AIAA Aviation Technology, Integration, and Operations Conference, Reston, Virginia (American Institute of Aeronautics and Astronautics). doi:10.2514/6.2016-3759

Csonka, S. (2016). "CAAFI: Ten Years and Growing! (Opening Remarks)," in 5th CAAFI Biennial General Meeting, October 25, 2016. Washington, DC:

Commercial Aviation Alternative Fuels Initiative. URL: https://caafi.org/information/pdf/Biennial_Meeting_Oct252016_Opening_Remarks.pdf.

de Jong, S., Antonissen, K., Hoefnagels, R., Lonza, L., Wang, M., Faaij, A., et al. (20172017). Life-cycle Analysis of Greenhouse Gas Emissions from Renewable Jet Fuel Production. *Biotechnol. Biofuels* 10 (1 10), 1–18. doi:10.1186/S13068-017-0739-7

Doliente, S. S., Narayan, A., Tapia, J. F. D., Samsatli, N. J., Zhao, Y., and Samsatli, S. (2020). Bio-aviation Fuel: A Comprehensive Review and Analysis of the Supply Chain Components. *Front. Energ. Res.* 8, 110. doi:10.3389/fenrg.2020.00110

Haller, B. (2012). Overview of Subsonic Fixed Wing Project: Technical Challenges for Energy Efficient, Environmentally Compatible Subsonic Transport Aircraft. *Tech. Lead Syst. Anal.* 1–23.

Hasegawa, T. (2021). Effects of Novel Coronavirus (Covid-19) on Civil Aviation: Economic Impact Analysis. ICAO Economic Impacts of COVID-19 on Civil Aviation. Available at: https://www.icao.int/sustainability/Documents/COVID-19/ICAO COVID 2021 06 23 Economic Impact TH Toru.pdf (Accessed 22-June-2021).

Hassan, M., Pfaender, H., and Mavris, D. (2018). Probabilistic Assessment of Aviation Co2 Emission Targets. *Transportation Res. Part D: Transport Environ.* 63, 362–376. doi:10.1016/j.trd.2018.06.006

Hileman, J. I., Wong, H. M., Waitz, I. A., Ortiz, D. S., Bartis, J. T., Weiss, M. A., et al. (2009). *Near-Term Feasibility of Alternative Jet Fuels*. Santa Monica: Aviation.

Hofer, C., Dresner, M. E., and Windle, R. J. (2010). The Environmental Effects of Airline Carbon Emissions Taxation in the US. *Transportation Res. Part D: Transport Environ.*, 15, 37–45. doi:10.1016/j.trd.2009.07.001

IATA (2021a). 2020 Worst Year in History for Air Travel Demand. Geneva: IATA Press Release. Available at: https://www.iata.org/en/pressroom/pr/2021-02-03-02/(Accessed February 3, 2021).

IATA (2016). Offsetting CO2 Emissions with Corsia. International Air Transport Association. Geneva: IATA. Available at: https://www.iata.org/en/programs/environment/corsia/(accessed Aug, 2021).

IATA (2021b). Optimism when Borders Reopen, 33. Geneva: IATA Press Release. Available at: https://www.iata.org/en/pressroom/pr/2021-05-26-01/(Accessed May 26, 2021).

ICAO (2019). *CORSIA SUPPORTING DOCUMENT, CORSIA Eligible Fuels-Life Cycle Assessment Methodology*. Tech. rep. Montreal: ICAO.

International Civil Aviation Organization (2016). *Online CORSIA Tutorial*. Dataset.

Jain, S., and Crossley, W. (2020). "Predicting Fleet-Level Carbon Emission Reductions from Future Single-Aisle Hybrid Electric Aircraft," in *AIAA Propulsion and Energy 2020 Forum*. doi:10.2514/6.2020-3554

Jain, S., Mane, M., Chao, H., Crossley, W. A., and DeLaurentis, D. A. (2021a). "Estimating the Impact of Novel Coronavirus (Covid-19) on Future Fleet-Level Co_2 Emissions and Airline Operations," in 21st AIAA Aviation Technology, Integration, and Operations Conference (Reston: AIAA AVIATION).

Jain, S., Mane, M., Crossley, W. A., and DeLaurentis, D. A. (2021b). "Investigating How Commercial Supersonic Aircraft Operations Might Impact Subsonic Operations and Total Co_2 Emissions," in 21st AIAA Aviation Technology, Integration, and Operations Conference (Reston: AIAA AVIATION).

Jain, S., Ogunsina, K. E., Chao, H., Crossley, W. A., and DeLaurentis, D. A. (2020). Predicting Routes for, Number of Operations of, and Fleet-Level Impacts of Future Commercial Supersonic Aircraft on Routes Touching the United States. doi:10.2514/6.2020-2878

Jorquera, O., Kiperstok, A., Sales, E. A., Embiruçu, M., and Ghirardi, M. L. (2010). Comparative Energy Life-Cycle Analyses of Microalgal Biomass Production in Open Ponds and Photobioreactors. *Bioresour. Tech.* 101, 1406–1413. doi:10.1016/J.BIORTECH.2009.09.038

Kim, B., Fleming, G. G., Balasubramanian, S. N., Malwitz, A., Lee, J., Waitz, I. A., et al. (2005). *System for Assessing Aviation's Global Emissions*. version 1.5. Washington, DC: SAGE. technical manual. Tech. Rep. DOT-VNTSC-FAA-05-14. URL: https://rosap.ntl.bts.gov/view/dot/8909.

Kim, B. Y., Fleming, G. G., Lee, J. J., Waitz, I. A., Clarke, J.-P., Balasubramanian, S., et al. (2007). System for Assessing Aviation's Global Emissions (SAGE), Part 1: Model Description and Inventory Results. *Transportation Res. Part D: Transport Environ.* 12, 325–346. doi:10.1016/J.TRD.2007.03.007

Langholtz, M. H., Stokes, B. J., and Eaton, L. M. (2016). *BILLION-TON REPORT Advancing Domestic Resources for a Thriving Bioeconomy*, 1160. Washington, DC: Oak Ridge National Laboratory, 2016.

Le Feuvre, P. (2019). Are Aviation Biofuels Ready for Take off? International Energy Agency. Commentary. Paris: IEA. Available at: https://www.iea.org/commentaries/are-aviation-biofuels-ready-for-take-off (Accessed March 18, 2019).

Lee, J. J., Waitz, I. A., Kim, B. Y., Fleming, G. G., Maurice, L., and Holsclaw, C. A. (2007). System for Assessing Aviation's Global Emissions (SAGE), Part 2: Uncertainty Assessment. *Transportation Res. Part D: Transport Environ.* 12, 381–395. doi:10.1016/J.TRD.2007.03.006

Li, Y., Wang, Y.-z., and Cui, Q. (2016). Has Airline Efficiency Affected by the Inclusion of Aviation into European Union Emission Trading Scheme? Evidences from 22 Airlines during 2008-2012. *Energy*, 96, 8–22. doi:10.1016/j.energy.2015.12.039

Mane, M., Jain, S., Crossley, W. A., and DeLaurentis, D. A. (2021). "Speed and Cost Impact on Market success of Supersonic Passenger Transport Aircraft," in 21st AIAA Aviation Technology, Integration, and Operations Conference (Reston: AIAA AVIATION).

Mane, M., Tetzloff, I., Crossley, W., Agusdinata, D., and DeLaurentis, D. (2011). "Impact of Development Rates of Future Aircraft Technologies on Fleet-wide Environmental Emissions," in 11th AIAA Aviation Technology, Integration, and Operations (ATIO) Conference, 1–13. doi:10.2514/6.2011-6843

Mavris, D., Delaurentis, D., Crossley, W., and Alonso, J. J. (2017). *Project 10 Aircraft Technology Modeling and Assessment: Phase I Report*.

McCullers, L. (2016). *Flight Optimization Software FLOPS v.9, Software Package*. NASA Langley Research Center, Hampton, VA, release 9.0.0 edn. URL: https://software.nasa.gov/software/LAR-18934-1.

Moolchandani, K. A., Agusdinata, D. B., DeLaurentis, D. A., and Crossley, W. A. (2012). "Airline Competition in Duopoly Market and its Impact on Environmental Emissions," in 12th AIAA Aviation Technology, Integration, and Operations (ATIO) Conference, 1–11. doi:10.2514/6.2012-5466

Moolchandani, K., Agusdinata, D. B., Mane, M., DeLaurentis, D., and Crossley, W. (2013). "Assessment of the Effect of Aircraft Technological Advancement on Aviation Environmental Impacts," in 51st AIAA Aerospace Sciences Meeting including the New Horizons Forum and Aerospace Exposition, Reston, Virigina (American Institute of Aeronautics and Astronautics). 13. doi:10.2514/6.2013-652

Moolchandani, K., Govindaraju, P., Roy, S., Crossley, W. A., and DeLaurentis, D. A. (2017). Assessing Effects of Aircraft and Fuel Technology Advancement on Select Aviation Environmental Impacts. *J. Aircraft* 54, 857–869. doi:10.2514/1.C033861

Ogunsina, K., Chao, H., Kolencherry, N., Jain, S., Moolchandani, K., Crossley, W. A., et al. (2018). "Fleet-level Environmental Assessments for Feasibility of Aviation Emission Reduction Goals," in Proceedings of CESUN Global Conference, Tokyo, Japan.

Pearce, B. (2021).Covid-19: An Almost Full Recovery of Air Travel in prospect. IATA Economic Reports, Available at: https://www.iata.org/en/iata-repository/publications/economic-reports/an-almost-full-recovery-of-air-travel-in-prospect/(Accessed May 26, 2021).

Ritchie, H. (2020). Climate Change and Flying: what Share of Global CO2 Emissions Come from Aviation? Published online at OurWorldInData.org. Available at: https://ourworldindata.org/co2-emissions-from-aviation.

Sissine, F. (2010). *Renewable Fuel Standard Program (RFS2) Regulatory Impact Analysis*.Tech. rep.. Washington, DC.

Stephenson, A. L., Kazamia, E., Dennis, J. S., Howe, C. J., Scott, S. A., and Smith, A. G. (2010). Life-Cycle Assessment of Potential Algal Biodiesel Production in the United Kingdom: A Comparison of Raceways and Air-Lift Tubular Bioreactors. *Energy Fuels* 24, 4062–4077. doi:10.1021/ef1003123

Stratton, R. W., Min Wong, H., and Hileman, J. I. (2010). Life Cycle Greenhouse Gas Emissions from Alternative. *Jet Fuels* 571, 1–133. PARTNER-COE-2010-001.

Sun, H., Edziah, B. K., Kporsu, A. K., Sarkodie, S. A., and Taghizadeh-Hesary, F. (2021). Energy Efficiency: The Role of Technological Innovation and Knowledge Spillover. *Technol. Forecast. Soc. Change* 167, 120659. doi:10.1016/j.techfore.2021.120659

Sun, H., Kporsu, A. K., Taghizadeh-Hesary, F., and Edziah, B. K. (2020). Estimating Environmental Efficiency and Convergence: 1980 to 2016. *Energy* 208, 118224. doi:10.1016/j.energy.2020.118224

The White House (2021). FACT SHEET: President Biden Sets 2030 Greenhouse Gas Pollution Reduction Target Aimed at Creating Good-Paying Union Jobs

and Securing U.S. Leadership on Clean Energy Technologies. The White House Statements and Releases, Available at: https://www.whitehouse.gov/briefing-room/statements-releases/2021/04/22/fact-sheet-president-biden-sets-2030-greenhouse-gas-pollution-reduction-target-aimed-at-creating-good-paying-union-jobs-and-securing-u-s-leadership-on-clean-energy-technologies/(Accessed April 22, 2021).

United Airlines (2021). Sustainable Fuel Sources. Available at: https://www.united.com/ual/en/us/fly/company/global-citizenship/environment/sustainable-fuel-sources.html.

United Nations Framework Convention on Climate Change (2021). The Paris Agreement. Available at: https://unfccc.int/process-and-meetings/the-paris-agreement/the-paris-agreement.

U.S Dept. of Transportation, Bureau of Transportation Statistics (2017). Airline Origin and Destination Survey (DB1B) Available at: http://www.transtats.bts.gov/DatabaseInfo.asp?DB_ID=125&Link=0, Accessed Dec. 2017. [Dataset].

U.S. Department of State, Office of the Spokesperson (2021). U.S.-China Joint Statement Addressing the Climate Crisis - United States Department of State. Media Note Available at: https://www.state.gov/u-s-china-joint-statement-addressing-the-climate-crisis/(Accessed April 17, 2021).

U. S. Energy Information Administration (2011). Annual Energy Outlook 2011. Available at: www.eia.gov/forecasts/aeo/, Accessed Oct, 2016. [Dataset].

van der Sman, E., Peerlings, B., Kos, J., Lieshout, R., and Boonekamp, T. (2021). Destination 2050–A Route to Net Zero European Aviation. Tech. Rep. NLR-CR-2020-510, Netherlands Aerospace Centre NLR. Available at: https://reports.nlr.nl/handle/10921/1555/.

Winchester, N., McConnachie, D., Wollersheim, C., and Waitz, I. A. (2013). Economic and Emissions Impacts of Renewable Fuel Goals for Aviation in the US. *Transportation Res. A: Pol. Pract.* 58, 116–128. doi:10.1016/j.tra.2013.10.001

Conflict of Interest: The authors declare that the research was conducted in the absence of any commercial or financial relationships that could be construed as a potential conflict of interest.

Publisher's Note: All claims expressed in this article are solely those of the authors and do not necessarily represent those of their affiliated organizations, or those of the publisher, the editors and the reviewers. Any product that may be evaluated in this article, or claim that may be made by its manufacturer, is not guaranteed or endorsed by the publisher.

frontiers in Energy Research

ORIGINAL RESEARCH
published: 08 December 2021
doi: 10.3389/fenrg.2021.751722

Quantitative Policy Analysis for Sustainable Aviation Fuel Production Technologies

Z. Juju Wang[1], Mark D. Staples[1], Wallace E. Tyner[2], Xin Zhao[2], Robert Malina[3], Hakan Olcay[3], Florian Allroggen[1] and Steven R. H. Barrett[1]*

[1]Laboratory for Aviation and the Environment, Massachusetts Institute of Technology, Cambridge, MA, United States, [2]Department of Agricultural Economics, Purdue University, West Lafayette, IN, United States, [3]Centre for Environmental Sciences, Hasselt University Campus Diepenbeek, Diepenbeek, Belgium

This paper quantifies the impact of different policy options on the economic viability of sustainable aviation fuel (SAF) production technologies. The pathways considered include isobutanol to jet from corn grain, hydroprocessed esters and fatty acids (HEFA) from inedible fats and oils, HEFA from palm fatty acid distillate, synthesized iso-paraffins from sugarcane, Fischer-Tropsch (FT) gasification and synthesis from municipal solid waste, and micro FT from wood residues. The policies considered include feedstock subsidies, capital grants, output based incentives, and two policies intended to reduce project risk. Stochastic techno-economic analysis models are used to quantify the policies' impact on project net present value and minimum selling price of the middle distillate fuel products. None of the technology pathways studied are found to be financially viable without policy aid. The median total policy costs required for economic viability range from 35 to 337 million USD per production facility, or 0.07–0.71 USD/liter. Our results indicate that the cumulative impact of multiple policies, similar in magnitude to analogous real-world fuel policies, could result in economically viable SAF production.

Keywords: sustainable aviation fuel, monte-carlo simulation, environmental policy, biofuels, techno-economic analysis

OPEN ACCESS

Edited by:
Season Hoard, Washington State University, United States

Reviewed by:
Christopher Michael Saffron, Michigan State University, United States
Benyamin Khoshnevisan, Chinese Academy of Agricultural Sciences (CAAS), China

****Correspondence:***
Mark D. Staples
mstaples@alum.mit.edu

Specialty section:
This article was submitted to Bioenergy and Biofuels, a section of the journal Frontiers in Energy Research

Received: *01 August 2021*
Accepted: *05 November 2021*
Published: *08 December 2021*

Citation:
Wang ZJ, Staples MD, Tyner WE, Zhao X, Malina R, Olcay H, Allroggen F and Barrett SRH (2021) Quantitative Policy Analysis for Sustainable Aviation Fuel Production Technologies. Front. Energy Res. 9:751722. doi: 10.3389/fenrg.2021.751722

1 INTRODUCTION

Prior to the COVID-19 pandemic, commercial aviation accounted for approximately 2% of total anthropogenic greenhouse gas (GHG) emissions. Assuming a recovery in the sector, and in the absence of mitigation measures, this is expected to grow to 5% by 2035 due to air traffic growth. At the same time, regional, national, and international policies are taking shape to address the challenge of mitigating the climate impacts of aviation (Seber et al., 2014). For example, the International Civil Aviation Organization (ICAO) Carbon Offset and Reduction Scheme for International Aviation (CORSIA) policy aims to have carbon neutral growth of international aviation from 2020 onwards. CORSIA includes mechanisms to enable sustainable aviation fuels (SAF) to play a role in achieving the goals of the policy.

SAF, with lower life cycle GHG emissions than conventional petroleum derived jet, can be produced from a variety of biomass and waste feedstocks. At the time of writing, five technology pathways for sustainable aviation fuel production have been certified by the American Society for Testing and Materials International (ASTM) for use in aviation turbine engines (Christensen et al., 2014). These fuels have been approved as drop-in fuels, which can be used at blends up to 50%

without any changes made to commercial aircraft (Staples et al., 2014). A number of private firms are targeting commercial-scale production and delivery of SAF such as AirBP and Neste. In addition, many airlines are investing in SAF, for example United Airlines, who entered an offtake agreement with Fulcrum BioEnergy in 2015.

However, the production cost premium of these fuels remains a significant barrier to large scale SAF uptake. Consequently, a number of policy incentives exist to economically support the production of SAF. Examples include the US Renewable Fuels Standard 2 (RFS2), the California Low Carbon Fuel Standard (LCFS), and CORSIA.

In this analysis, we quantify the economic impacts of various policy options on a set of SAF production pathways (Zhao et al., 2016). Six pathways, isobutanol to jet (ATJ) from corn grain, hydroprocessed esters and fatty acids (HEFA) from inedible fats and oils (IFO), HEFA from palm fatty acid distillate (PFAD), synthesized iso-paraffins (SIP) from sugarcane, Fischer-Tropsch (FT) gasification and synthesis from municipal solid waste (MSW), and micro FT from wood residues, are modeled as individual refineries using harmonized financial assumptions. The economic performance of these facilities is quantified in terms of their project net present value (NPV) and the fuel product minimum selling price (MSP). The MSP is calculated as the breakeven output price at which NPV reaches zero. The analysis is carried out stochastically to quantify uncertainty. Next, the impact of policy options including output based incentives, feedstock subsidies, capital grants, loan guarantees, and off-take agreements, on MSP and NPV are quantified. While previous studies have performed techno-economic analysis (TEA) on SAF pathways and take into account policy considerations, individual pathway studies have mostly been carried out in isolation. Differing financial, operational, and policy assumptions have meant that the findings are not directly comparable between studies and pathways. Although a number of previous analyses have quantified the MSP or production costs of various SAF pathways, few have addressed the impact of various policy supports on economic viability in a consistent manner across a number of SAF pathways (Weibel, 2018). To the best of our knowledge at the time of publication, this analysis is the first quantitative, stochastic assessment of the impacts of various policy instruments on this scope of SAF production pathways, using a harmonized set of assumptions to enable consistent and meaningful comparison of results.

2 MATERIALS AND METHODS

2.1 Sustainable Aviation Fuel Pathways

Six techno-economic models of SAF refineries are developed for the following pathways: corn grain ATJ (*via* iso-butanol), IFO HEFA, PFAD HEFA, sugarcane SIP, MSW FT, and forestry residue micro FT. All pathways produce a slate of drop-in hydrocarbon fuels, including fuels suitable for use in aviation. We have selected this scope of analysis because these pathways represent relatively mature technologies in the nascent SAF industry, and they represent all of the fuel production pathways currently certified by ASTM to produce fuels suitable for use in aircraft engines. All facilities are assumed to be commercial-scale "nth-of-a-kind" plants, as opposed to demonstration scale or first-of-a-kind. Although minor differences in the physical properties of the SAF produced from these facilities would exist in practice, for the purposes of this analysis we assume each of these pathways produce an identical SAF product. Furthermore, we compare the costs of SAF to petroleum jet fuel on a per liter fuel basis, neglecting small differences in the density and specific energy of these fuels, in order to stay consistent with units commonly used to describe fuel volumes and costs. The pathway mass and energy balances and techno-economics are modeled stochastically using MATLAB 2017b. We take a calculated NPV greater than zero to indicate that a project is financially viable. The MSP is defined in this study as the minimum price at which the middle distillate fuel fractions - diesel and jet - must be sold in order to achieve a project NPV of zero.

Table 1 shows the mass and energy balances associated with each pathway. All of the technologies considered in this analysis are nascent and there is uncertainty associated with the mass and energy balances used to represent their performance. As a result, material quantities for inputs of natural gas, hydrogen, and electricity, as well as output fuel yield are modeled as stochastic distributions. Common inputs such as natural gas, electricity, and water have consistent costs across pathways. Inputs such as catalysts and other treatment chemicals are not listed but are included in the financial model. The input feedstock quantity is set to a constant value for each pathway, such that average total fuel yield is 2,000 bpd (111.3 million liters/year). Note that while total average fuel yield is equivalent across the different pathways considered here, the SAF proportion of fuel yield varies between production technologies. 2,000 bpd of total fuel yield is considered here in keeping with previously published analyses, such as (Pearlson et al., 2013), (Staples et al., 2018), and Bann et al. (2017).

2.1.1 Financial Assumptions

Each SAF production pathway is modeled as a refinery with a 20-years operating lifetime, and an average total fuel production capacity of 2000 bpd. The fixed capital investment (FCI) of each plant is modeled employing the same method used in Bann et al. (2017). A positively skewed beta pert distribution is drawn around the deterministic FCI that varied between 80 and 150% of the deterministic FCI, based on the work of Brown, 2015.

The financial modeling assumptions in Bann et al. (2017) and Zhao et al. (2015) are used to guide assumptions in this study. Capital financing is assumed to be 40% equity and the remainder is financed through a 10-years loan with 8% interest. The cost of equity is set at 15%. It is assumed that the refinery takes 3 years to build, and startup costs are split among the first 3 years by 8, 60 and 32%, respectively. Depreciation is assumed to take place on a 10-years schedule, using a double declining balance, and then switching to straight line in year 10 until the asset value is zero. Working capital is 5% of the FCI and direct operating costs such as maintenance and overhead are assumed to be 7.7% of the FCI. Each year is assumed to include 350 operational days, with the

TABLE 1 | Pathway average input and outputs.

Pathway	Inputs				Outputs					
	Feedstock (million kg/yr)	Power (million kWh/yr)	Natural Gas (MT/yr)	Hydrogen (MT/yr)	Jet Fuel (million liters/yr)	Diesel (million liters/yr)	Lightends (million liters/yr)	Gasoline (million liters/yr)	Other	Deterministic Capex (millions USD)
ATJ (Corn)	531	0.65	255	1,400	111	0	0	0	146 million kgs/year DDGS	140
FT (MSW)	228	0	0	0	15.1	89.3	0	14.0	64,600 MWh/year	264
HEFA (PFAD)	484	8.2	5,490	2,660	15.6	82.3	2.8	2.4	7.3 million liters/yr propane	63
HEFA (IFO)	484	8.2	5,490	2,660	15.6	82.3	2.8	2.4	7.3 million liters/yr propane	63
SIP (Sugarcane)	537	0	0	4,070	111	0	0	0	3,080 MWh/yr	197
Micro FT (Wood Residue)	459	69	0	0	33	32	23	25	0	317

first year at 75% capacity. The income tax rate is set at 16.9% which was the average effective US tax rate prior to the 2018 tax law, and inflation is set to 2%. All costs are calculated in 2018 dollars. The NPV of the facility is calculated using a discounted cash flow rate of return (DCFROR) analysis, and the MSP for middle distillates is calculated by iteratively adding a price premium for both jet and diesel fuels until the NPV of the facility is zero.

2.1.2 Time Series Data

A time series of future prices for natural gas, electricity, gasoline and various feedstocks are estimated using an autoregressive integrated moving average (ARIMA) model. Historical pricing data is gathered for natural gas, electricity, gasoline, corn grain, yellow grease, PFAD, and sugarcane, and an ARIMA model is generated for each commodity price trend. Commodity prices are limited to be no greater than 125%, and no less than 75%, of the highest and lowest historically observed values for that commodity. This is an approach taken from previous TEA studies to avoid historically unprecedented or unrealistic results. Aside from fuel products, all commodity prices are assumed to vary independently. This means that, all else being equal, the contribution of commodity price to variance in the results may be over-represented in this analysis.

2.2 Policy Types

Four different policy types have been identified to be considered in this study, based on biofuel policies implemented in different jurisdications around the world. The way each policy is modeled is noted in the following sections, along with real-world examples of these policy types' implementation. It is important to note that a number of the example policies discussed here are applicable to biofuels in general, and not necessarily SAF specifically.

2.2.1 Output Based Incentives

For the purposes of this study, an output based incentive is a policy for which the fuel producer receives some monetary benefit tied to the quantity or type of fuels produced and sold. For example, the value of the benefit could be a function of production volumes, which is the case for Renewable Identification Numbers (RINs) generated under the US RFS2. It could also depend on the life cycle emissions reductions compared to a petroleum fuel, which is the case for the California LCFS and ICAO CORSIA policies. We model both of these types of output based incentives. In the case of the GHG-reduction dependent incentive, emissions reductions are estimated based on the default core life cycle analysis values agreed upon for use under CORSIA.

In reality, incentives of this kind may be uncertain, as the size of the credit depends on the market or mandate for sustainable fuels or emissions reductions. However, the magnitude of the credit is assumed here to be deterministic and constant. In the DCFROR model, the monetary value of this incentive is modeled as annual revenue that is not taxed, and is only applicable to middle distillate products. The total cost of the policy can be evaluated using the DCFROR model.

2.2.2 Feedstock Subsidies

A feedstock subsidy is a monetary benefit to reduce a facility's operating costs for feedstock. It may also have the benefit of supporting feedstock producers, by providing agricultural incentives to establish the supply chain. A feedstock subsidy could also take the form of a monetary credit or avoided cost for using waste products such as MSW that would otherwise take up landfill capacity. Some examples of feedstock subsidies include the Brazil Social Fuel Seal and the 2014 US Biomass Crop Assistance Program (BCAP). The Brazil Social Fuel Seal gives fuel producers tax breaks when using fuel produced in rural farming regions, and the US BCAP program, provides a 1:1 matching subsidy for eligible feedstocks, up to 20 $/short ton.

In this analysis, we model feedstock subsidies as a reduction in feedstock costs. The reduced feedstock cost is then used in the DCFROR model to obtain MSP and NPV. To calculate the total cost of the policy, the subsidy per quantity of feedstock is multiplied by feedstock quantity per year. The total cost over the lifetime of the facility is then found using a DCFROR calculation for the 20 years of refinery operation.

2.2.3 Capital Grants

A capital grant is typically a one-time monetary benefit, granted by the government to cover or reduce facility construction costs.

Two examples of implemented capital grant policies are the 2018 Calrecylce Organics recycling projects and the Rural Energy for America Program (REAP). The Calrecycle program distributed $25 million to organics recycling projects, including biofuel refineries. REAP started in 2003 and in 2018 had a budget of $600 million for FY2018 for both grants and loans. We model capital grants policies as a lump sum received in the first year of refinery construction.

2.2.4 Risk Reduction Policies

Two additional policies, loan guarantees and offtake agreements, are modeled to quantify the impact of risk reduction policies on project economics. A loan guarantee is an agreement between the guarantor and the bank, that states if a refinery defaults on a loan, the guarantor will pay the bank in its stead. This results in a lower cost of debt, as some risk associated with the project has been borne by the guarantor (usually the government), rather than the bank. REAP also provides loan guarantees up to $25 million. A loan guarantee is modeled here as a reduction in the cost of debt.

An offtake agreement occurs when a fuel purchaser agrees to purchase fuel quantities at a pre-negotiated price at some future date rather than the prevailing market price. A number of airlines have established offtake agreements with SAF producers, such as Lufthansa and Gevo, and United Airlines and Fulcrum bioenergy. This is modeled as a percentage of total fuel production (subject to the agreement), and a fixed price for the lifetime of the agreement.

Note that, in this study we do not calculate the cost of the loan guarantee or the offtake agreement policies, as the primary purpose of these policies are to reduce risk, rather than a monetary transfer. The valuation of risk or risk reduction is beyond the scope of this analysis, but has been covered previously by Bittner et al., 2015.

2.3 Policy Simulation

The policy types described above are analyzed in three different ways. First, a "breakeven" analysis is carried out to quantify the magnitude of each policy type required, in isolation, to achieve a project NPV of zero. The total policy cost of each of the policy alternatives is also calculated.

Next, we assess the impact of policies of the magnitude of examples seen in the real world on the pathways' economic viability. We consider a feedstock subsidy of $20/short ton, with a maximum value of $12.5 million per year, based on BCAP. An output subsidy of $0.25/L is assumed which is similar in magnitude to 2018 RIN values from the US RFS2. A capital grant of $5 million is assumed, similar to grants given to biofuel refineries under the Calrecycle program. Finally, CO_2 offset costs expected under the CORSIA policy are used to estimate a GHG emission reduction-defined output incentive, ranging from 20–47 $ per metric tonne of CO_2 equivalent ($/t$CO_2$e) abated.

In addition to analyzing the impact of individual policies on various pathways, we also compare the differing impacts of equal-cost policies (policies with equal total monetary cost to the funder of the policy, typically the government) on economic viability. To do this, the total cost of the policy to the government is calculated for a single output based incentive value. Using that total cost, the magnitudes of equal-cost policies are calculated for the feedstock subsidy, GHG emissions based reduction subsidy, and capital grant policies. These equal-cost policy cases are then assessed to determine their impact on median NPV and MSP, as well as the distribution of these indicators. This is done for a range of output-based incentive values from 0.01–0.75$/L.

Finally, we model a number of policies to reduce financial risk. The loan guarantee is modeled as a decrease in cost of debt from 8 to 3%, and the offtake agreement is modeled as a percentage of fuel produced and purchased at the MSP varying from 0 to 100%. We also model the feedstock subsidy as a percentage reduction in feedstock cost rather than a fixed $/short ton, for consistency across disparate feedstock types.

3 RESULTS AND DISCUSSION

3.1 Baseline, "No Policy" Results

Figure 1 shows NPV and MSP results for each of the six pathways, in the absence of policy support. In both plots, the red line indicates the median value, the box indicates the 25th and 75th percentile, and the black dotted lines indicate the entire range of values. The MSP of middle distillate fuel products (jet and diesel) from each pathway are shown on the right. For reference, the market price of jet fuel at the time of writing is 0.50 $/L shown by the blue dotted line. The MSW FT and IFO HEFA pathways have the lowest median MSP at 0.60 and 0.90 $/L, respectively, while the corn grain ATJ and forestry residue micro FT pathways have the highest median MSPs at 1.16 and 1.33 $/L, respectively. The differences in MSP variance between pathways is due, in large part, to uncertainty and variance in the costs of different feedstock types.

The NPV of each pathway is shown on the left of **Figure 1**, and the dotted line represents an NPV of zero, meaning that the region to the right of the line indicates financial viability. The median NPV for each pathway is below zero indicating that at the mean level, none of these pathways are financially viable in the absence of policy support. All pathways do have some fraction of stochastic results where the NPV goes above zero. In particular, the FT from MSW and IFO HEFA cases have the greatest probability of a positive NPV, at 40 and 11% with no policy support, respectively. The differences in variance between pathways is smaller for the NPV results than it is for MSP. This is because variance in NPV, while still correlated to feedstock cost, is attributable in large part to fuel price variability. In contrast, fuel price uncertainty is not factored in MSP distributions as it represents an estimate of levelized cost in our study. Therefore, although a higher MSP is generally correlated to a lower NPV, this is not always the case. The micro FT from forestry residue pathway has a higher MSP, but lower NPV relative to ATJ from corn grain. This is due to differences in middle distillate output quantities, relative to non-middle distillate fuel quantities.

In the FT MSW pathway, the median MSP value is lower than previous findings in (Suresh et al., 2018) and Bann et al. (2017), which estimated the MSP of MSW-derived FT fuels to be

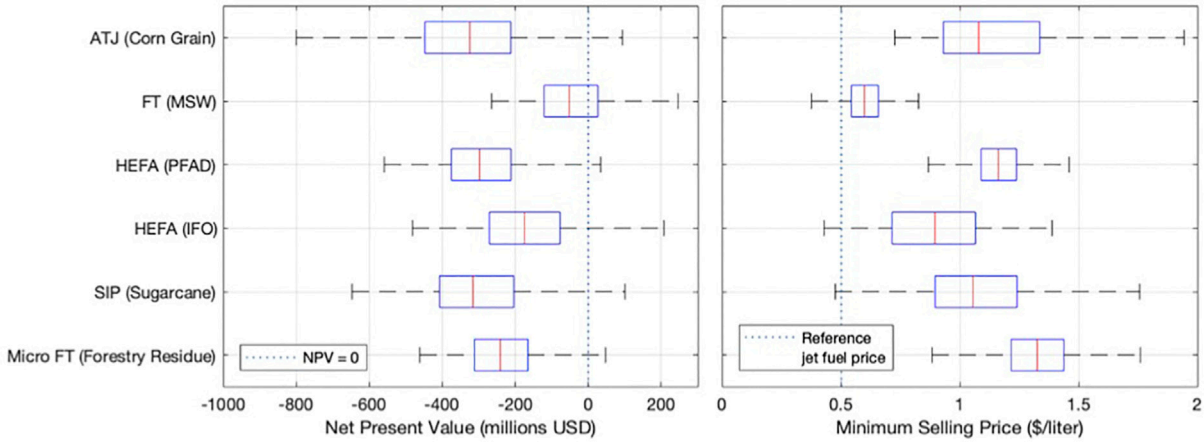

FIGURE 1 | Box and whisker plots of NPV and MSP values for all pathways with no policy added. Dotted lines indicate either an NPV of zero, or the current market price of jet fuel (March 2019).

approximately 1.10 $/L. However, our findings agree with work by Niziolek et al., 2015 with a median MSP of approximately 0.60 $/L. It is important to note that this result is contingent on the assumption of a zero-cost MSW feedstock, delivered to the plant gate.

3.2 Breakeven Results

Table 2 shows the median breakeven policy values required for an NPV of zero for each pathway, as well as the total cost of the policy. The 25th and 75th percentile values are included in the brackets.

The results in columns 2 and 3 show that the magnitude and total cost of a quantity-based output subsidy for breakeven is proportional to the MSP for each pathway. However, the variance of the magnitude of the required policy reflects the differences in fuel yield between pathways. For example, in the no-policy case shown in **Figure 1**, variance in MSP for the forestry residue micro FT pathway is less than that of sugarcane SIP. However, column 2 of **Table 2** shows that the variance of forestry residue micro FT under the volume-based output subsidy is greater than that of sugarcane SIP. This is because the forestry residue micro FT pathway produces a smaller proportion of middle distillates that benefit from this policy, relative to the other pathways. Therefore, variance in the breakeven policy increases, reflecting the smaller quantity of qualifying fuel. The breakeven output subsidies required for the MSW FT and IFO HEFA pathways are 0.09 and 0.35 $/L respectively, which is within the 0.01–2.00 range of available RFS2 RIN prices at the time of writing. Column 3 in **Table 2** shows the total policy costs for a breakeven output subsidy. As anticipated, the total policy cost is equivalent to the negative NPV of each pathway in the absence of policy support.

Column 4 shows the values for a breakeven feedstock subsidy. These range from 17 $/short ton for sugarcane SIP to 1,619 $/short ton for MSW FT pathways. This discrepancy exists due to the variation in feedstock input quantities. FT from MSW has a high $/short ton value because of a relatively lower quantity of feedstock input required, and SIP has a low $/short ton value because of a relatively larger quantity of feedstock required.

The total policy cost for feedstock subsidies (column 5) is proportional to the no-policy NPV of each pathway, although greater than that of the output-based incentives. This is a result of how feedstock subsidies are modeled in this analysis, as a reduction in feedstock cost, which increases the cash flow that is taxed.

Column 6 of **Table 2** shows the magnitude of a capital grant required to achieve a NPV of zero for each pathway. The size of the capital grant is equivalent to the negative NPV of each pathway in the absence of any policy, as expected. The smallest capital grants needed for financial viability are for the FT MSW and HEFA pathways, with values of 43 and 174 million USD, respectively. Note that the manner in which the capital grant is modeled does not account for changes in the project capital structure, such as a decrease in the loan amount, which could also impact project NPV. A change in financial structure could change debt and equity costs, and in this case the cost of a breakeven policy required would no longer be equal in absolute value to the NPV of the pathway.

The last four columns show the magnitude of life cycle emissions reduction-based output subsidies, in US$/tCO$_2$e, in order to achieve a project NPV of zero. Column 8 gives the results when the policy is applied to all fuels in the product slate, and column 10 gives results if the policy were applicable only to the SAF fraction. The magnitude of the subsidy for the corn grain ATJ and sugarcane SIP pathways are the same in both columns, as both pathways are assumed to produce 100% SAF. These results can be compared to the size of the incentive anticipated under CORSIA, of 20–47 $/tCO$_2$e, which is applied only to the jet fuel fraction. CORSIA values are up to 277 $/tCO$_2$e, lower than what is required for a project NPV of zero, if this policy is considered in isolation. However, similar incentives are available under other policy schemes, such as California LCFS, and would apply to all fuel products. The LCFS credit is 180 $/tCO$_2$e abated (April 2019) which is above the policy values required for breakeven for MSW FT, IFO HEFA, and forestry residue micro FT. The total policy cost for GHG emission reduction based incentive and capital grants are equal.

TABLE 2 | Median breakeven policies values and total policy cost required for a pathway NPV of zero. 25th and 75th percentile values are included within brackets.

Policy	Output Subsidy		Feedstock Subsidy		Capital Grant		GHGe Reduction Credit (all)		GHGe Reduction Credit (jet)	
Pathway	Policy ($/L)	Total policy cost (mil USD)	Policy ($/ton)	Total policy cost (mil USD)	Policy (mil USD)	Total policy cost (mil USD)	Policy ($/tonne CO2 abated)	Total policy cost (mil USD)	Policy ($/tonne CO2 abated)	Total policy cost (mil USD)
ATJ (Corn Grain)	0.55 [0.36, 0.76]	324 [212, 448]	130 [85, 179]	390 [255, 539]	324 [212, 448]	324 [212, 448]	1,172 [760, 1,615]	324 [212, 448]	1,172 [760, 1,615]	324 [212, 448]
FT (MSW)	0.09 [-0.07, 0.22]	43 [-34, 109]	1,619 [-1253,4086]	46 [-36, 117]	43 [-34, 109]	43 [-34, 109]	53 [-41, 135]	43 [-34, 109]	420 [-326, 1,064]	43 [-34, 109]
HEFA (PFAD)	0.59 [0.42, 0.75]	297 [211, 375]	635 [452, 801]	319 [227,402]	297 [211, 375]	297 [211, 375]	233 [165, 295]	297 [211, 375]	1,622 [1,150, 2054]	297 [211,375]
HEFA (IFO)	0.35 [0.16, 0.54]	174 [79, 271]	371 [169, 579]	187 [85,291]	174 [79, 271]	174 [79, 271]	140 [64, 219]	174 [79, 271]	977 [442, 1,427]	174 [79, 271]
SIP (Sugarcane)	0.50 [0.31, 0.54]	316 [204, 408]	17 [11, 22]	339 [219, 437]	316 [204, 408]	316 [204, 408]	387 [241, 538]	316 [204, 408]	387 [241, 538]	316 [204, 408]
Micro FT (Forestry Residue)	0.72 [0.50, 0.93]	240 [165, 312]	123 [85, 159]	258 [177, 335]	240 [165, 312]	240 [165, 312]	165 [113, 213]	240 [165, 312]	530 [364, 686]	240 [165, 312]

Determining the breakeven value of policies is helpful for current policymakers and producers to better understand the effectiveness of current policies. We show here that the magnitude of a policy required for breakeven is greater than what can be expected from similar existing policy schemes. This means that it is unlikely a single policy, in isolation, will push the pathways assessed to financial viability.

3.3 Real-World Policy Case Results

Figure 2 shows the MSP for each pathway, and the no-policy case is represented by the right-most extent of the bar for each pathway. The colored bars indicate the cumulative decrease in MSP due to each real-world policy. The blue bar represents MSP remaining when all policies are applied to the pathway in combination. The results show that the cumulative impact of the policies reduce the mean MSP of MSW FT below the current market price of petroleum jet fuel. The sugarcane SIP and IFO HEFA pathway are also within 0.10$/L to the current selling price of conventional jet fuel.

Although the same policies are applied to all pathways, their impacts for each pathway vary. For example, the output subsidy has a smaller impact on forestry residue micro FT than any of the other pathways considered. This is because the subsidy is only applied to middle distillates, and although each facility produces 2000 bpd of total product, middle distillates only account for 62% of the micro-FT refinery production. In contrast, middle distillates account for at least 91% of total fuel products from all other pathways.

The feedstock subsidy also has different impacts between pathways. Each pathway requires a different feedstock type and quantity, and at different market prices. For the MSW FT pathway, feedstock costs are assumed to be zero (as a waste feedstock) and the input subsidy has no effect, whereas the corn grain ATJ, sugarcane SIP, and forestry residue micro FT pathways were able to take full advantage of the input subsidy up to the $12.5 million per year limit of the BCAP program.

Similarly, the life cycle GHG emissions of each pathway are unique. Therefore, the pathways with greater reduction potential relative to petroleum fuels, such as forestry residue micro FT and sugarcane SIP, benefit more from the GHG subsidy policy.

Two conclusions may be drawn from this analysis. First, when considering the cumulative impacts of policies of the magnitude that can be found today, a number of pathways, such as MSW FT and IFO HEFA, have MSPs approaching parity with current market prices for petroleum fuels. Second, the results show that the impacts of the policies considered are independent of one another, and that the cumulative impact of the policies is equal the sum of their impacts in isolation.

3.4 Equal Policy Results

We also quantified the impact of equal-cost policies of each policy type, equivalent to volume-based output subsidies of 0.01, 0.02, 0.05, 0.10, 0.25, 0.50 and 0.75 $/L.

Figure 3 shows the NPV change of each pathway as a function of the total policy cost for different policies. This shows that the total cost of the policy has a linear relationship with the NPV. With the exception of the feedstock subsidy case, there is a 1:1

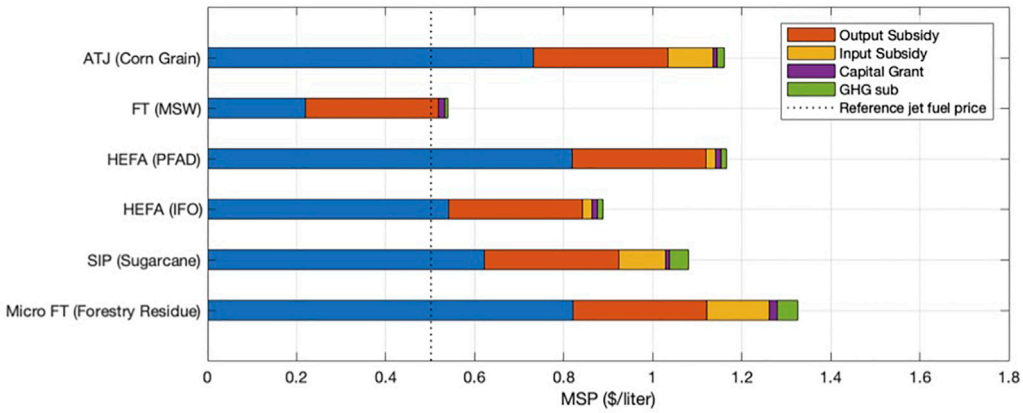

FIGURE 2 | Real-world policy effects on MSPs for pathways. Details on the individual policies are listed in the Methods and Materials Section.

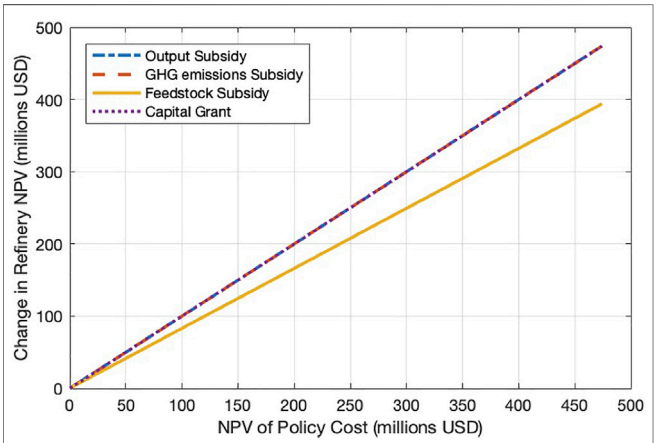

FIGURE 3 | Change in refinery NPV vs. total cost of policy for all pathways (lines for output subsidy, GHG emissions subsidy, and capital grant overlap).

correspondence between the increase in NPV and the total policy cost. The feedstock subsidy is unique from the other policy types, because the benefit of the feedstock subsidy is taxed in our model. The ratio between the increase in refinery NPV to total policy cost is 0.831:1 which correlates with the 16.9% tax rate. Therefore, the feedstock subsidy has a smaller impact on NPV than an output subsidy of the same total cost.

3.5 Policies to Reduce Risk

The loan guarantee policy decreases the MSP, and increases NPV of the all of the pathways considered as seen in **Table 3**. The magnitude change in NPV correlates directly with the FCI of each facility. The forestry residue micro FT pathway has the highest deterministic FCI cost of 318 million USD which results in a 36 million USD increase in mean NPV. The PFAD HEFA pathway, with an FCI of 62 million USD, shows an NPV increase of 9 million USD. The results of a loan guarantee change when combined with a capital grant, as the capital structure of the refinery may change.

TABLE 3 | Changes in NPV and MSP values and variances due to a loan guarantee debt reduction from 8 to 3%.

Pathway (feedstock)	NPV [change from baseline NPV] (millions USD)	MSP [change from baseline MSP] ($/L)
ATJ (Corn grain)	−316 [21]	1.12 [0.04]
FT (MSW)	−22 [22]	0.54 [0.06]
HEFA (PFAD)	−280 [9]	1.14 [0.02]
HEFA (IFO)	−161 [9]	0.87 [0.02]
SIP (sugarcane)	−258 [41]	1.00 [0.08]
Micro FT (Wood residue)	−199 [36]	1.19 [0.13]

To quantify the impact of an offtake agreement, we present only the corn grain ATJ pathway here. This is because the impact of offtake agreements and feedstock subsidies on variance in the results follow the same trends across all pathways considered. The results in **Table 4** show that the offtake agreement has different impacts on the variance of MSP and NPV. Variance in NPV decreases because the price for the fuel in the offtake agreement is static. However, variance in the MSP of fuel volumes not included in the offtake agreement increases, because the non-offtake volumes bare all of the variance required to achieve an NPV of zero.

3.5.1 Alternative Policy Implementations

Results were also generated for the case where feedstock subsidies were defined as a percentage of feedstock cost, rather than a fixed monetary amount. With this assumption, risk associated with commodity price uncertainty is shifted from the project developer on to the entity paying for the policy (e.g., the government). This is also true if output subsidy and capital grant type policies are defined in terms of percentage of costs or revenues.

Figure 4 shows feedstock subsidies at 0, 25, 50, 75, and 100 percent of feedstock cost for the corn grain ATJ pathway in blue, along with the equivalent average total cost (in $/short ton) feedstock subsidy in red. The average increase in NPV and decrease in MSP remains the same for both cases. However, in the percentage reduction case, the variance in MSP decreases as

TABLE 4 | Changes in NPV and MSP values and standard deviations due to offtake agreements.

Offtake percentage (%)	MSP ($/L)		NPV (millions USD)	
	Average	Standard deviation	Average	Standard deviation
0	1.16	0.29	−448	235
25	1.16	0.38	−356	214
50	1.16	0.57	−224	198
75	1.16	1.14	−111	188
100	N/A	N/A	0	185

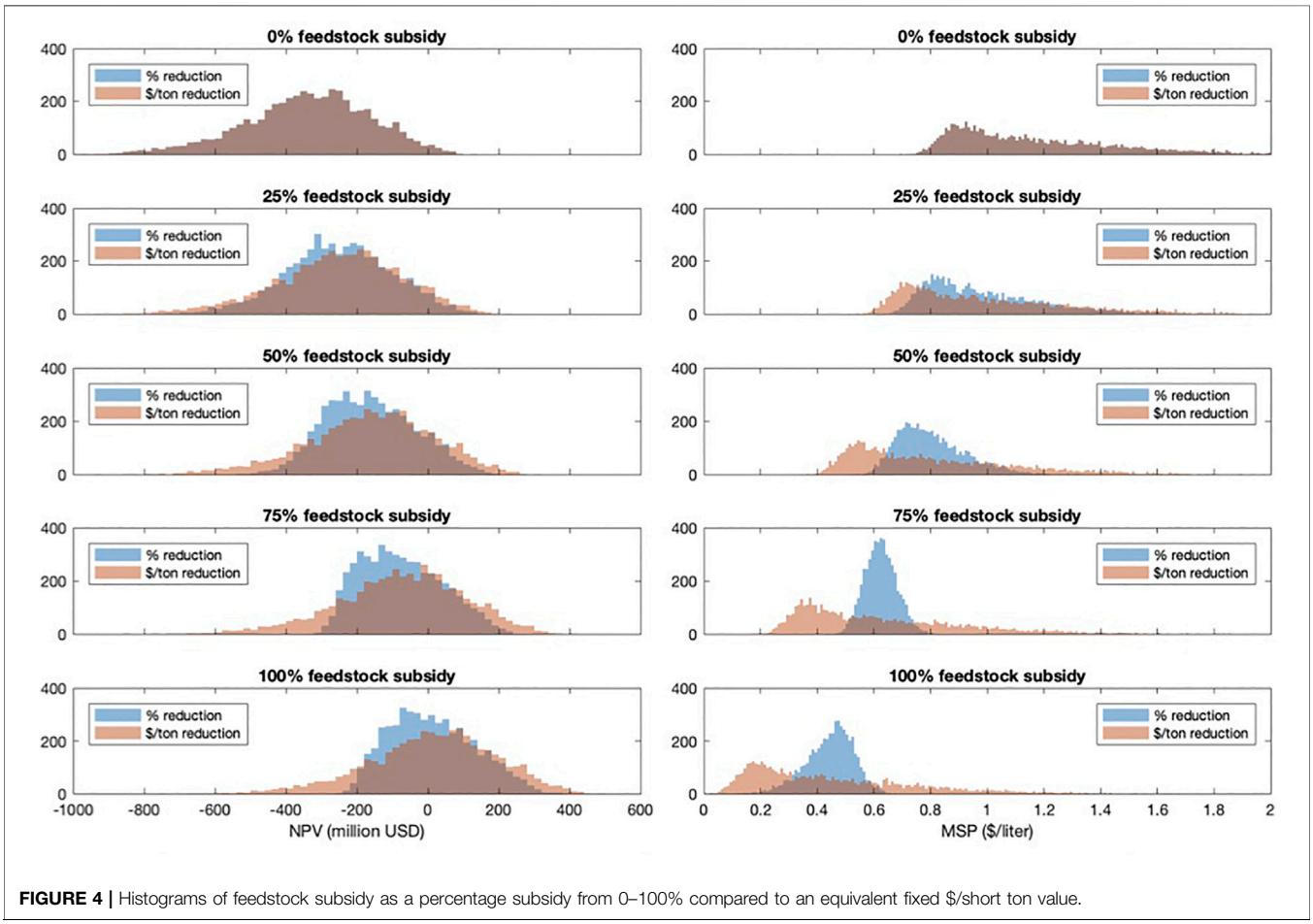

FIGURE 4 | Histograms of feedstock subsidy as a percentage subsidy from 0–100% compared to an equivalent fixed $/short ton value.

the magnitude of the policy increases. Similarly for NPV, as feedstock subsidy increases, NPV variance decreases. At 100%, feedstock cost is zero and does not contribute to variance.

The variance increases at the highest percentages here in the corn grain ATJ case as we shift from a 75–100% feedstock subsidy. A co-product of this pathway is distillers dried grain with solubles (DDGS), the market price of which is modeled as a percentage of corn grain prices. Because DDGS sales prices and feedstock costs are directly correlated, variance in the two stochastic variables (one a cost, the other a source of revenue) have a mitigating impact on overall variance in the results. When corn grain feedstock costs are reduced to zero, we see variance increase from DDGS sales. Note that, while variance is decreasing, the number of stochastic runs that are above an NPV of zero is decreasing, decreasing the probability of financial viability.

3.6 Limitations and Areas for Future Work

A number of limitations of the analysis and results presented here warrant discussion. Although this study is an "*n*th" plant analysis, the technologies assessed are relatively nascent at a commercial scale. This means significant uncertainty exists around the technology performance represented here. The mass and energy balances and distributions used for each pathway are based on the best data available to the authors at the time of writing, however higher fidelity empirical data for these fuel production pathways would improve the accuracy of our

results. Another significant source of uncertainty lies in the prediction of future costs for inputs and fuels. Further work could focus on augmenting the future cost estimates of commodity inputs, and the associated uncertainty.

In addition, our analysis assumes that all of the modeled facilities are located in the US, and uses US-centric financial assumptions. Refinery siting and location is not accounted for in terms of the costs of permitting, or feedstock availability and pricing. We consider only a single scale bio-refinery (2000 bpd) for ease of comparison across pathways. In reality, we recognize that facility scale would likely be optimized to improve financial performance according to the specific fuel production pathway and local context. These also represent interesting areas for further study.

Finally, this analysis does not account for uncertainty in the policies themselves, such as volatility in the value of output subsidies (RIN values, CORSIA carbon credits). We assume that policies are in place for the entire operating lifetime of a facility which may not be the case. In addition, the policy types assessed here may interact with the financial structure and taxation of a given project, but this feedback is not represented in our models.

4 CONCLUSION

This study compares the impact of five different policy types on six SAF pathways. In all the pathways modeled, the median NPV is below zero, indicating the need of policy support for financial viability. The breakeven analysis shows that a pathway is unlikely to achieve financial viability through the impact of a single policy. However, the cumulative impact of multiple policies, similar in magnitude to policies operating today, brings all pathways to financial viability. In addition, impacts on pathways for the policies modeled are independent. Finally, policies can be implemented in a way to impact variance of pathway NPV and MSP, effectively reducing investment risk.

DATA AVAILABILITY STATEMENT

The original contributions presented in the study are included in the article/**Supplementary Material**, further inquiries can be directed to the corresponding author.

AUTHOR CONTRIBUTIONS

ZJW collected data, created and ran simulations, analyzed results, and wrote the first draft of the manuscript. MDS guided the methodology of the work and revised the manuscript for the final version. WET, XZ, RM, HO, FA, SRHB supported the research technically, provided data, and made edits to the manuscript.

FUNDING

This research was funded by the U.S. Federal Aviation Administration Office of Environment and Energy through ASCENT, the FAA Center of Excellence for Alternative Jet Fuels and the Environment, project 1 through FAA Award Number 13-C-AJFE-MIT under the supervision of James Hileman and Daniel Williams. Any opinions, findings, conclusions or recommendations expressed in this material are those of the authors and do not necessarily reflect the views of the FAA.

SUPPLEMENTARY MATERIAL

The Supplementary Material for this article can be found online at: https://www.frontiersin.org/articles/10.3389/fenrg.2021.751722/full#supplementary-material

REFERENCES

Bann, S. J., Malina, R., Staples, M. D., Suresh, P., Pearlson, M., Tyner, W. E., et al. (2017). The Costs of Production of Alternative Jet Fuel: A Harmonized Stochastic Assessment. *Bioresour. Tech.* 227, 179–187. doi:10.1016/j.biortech.2016.12.032

Bittner, A., Tyner, W. E., and Zhao, X. (2015). Field to Flight: A Techno-Economic Analysis of the Corn stover to Aviation Biofuels Supply Chain. *Biofuels, Bioprod. Bioref.* 9, 201–210. doi:10.1002/bbb.1536

Brown, T. R. (2015). A Critical Analysis of Thermochemical Cellulosic Biorefinery Capital Cost Estimates. *Biofuels, Bioprod. Bioref.* 9, 412–421. doi:10.1002/bbb.1546

Christensen, A., Searle, S., and Malins, C. (2014). A Conversational Guide to Renewable Identification Numbers (RINs) in the U.S. Renewable Fuel Standard (Accessed: : 2019-05-26).

Niziolek, A. M., Onel, O., Hasan, M. M. F., and Floudas, C. A. (2015). Municipal Solid Waste to Liquid Transportation Fuels - Part II: Process Synthesis and Global Optimization Strategies. *Comput. Chem. Eng.* 74, 184–203. doi:10.1016/j.compchemeng.2014.10.007

Pearlson, M., Wollersheim, C., and Hileman, J. (2013). A Techno-Economic Review of Hydroprocessed Renewable Esters and Fatty Acids for Jet Fuel Production. *Biofuels, Bioprod. Bioref.* 7, 89–96. doi:10.1002/bbb.1378

Seber, G., Malina, R., Pearlson, M. N., Olcay, H., Hileman, J. I., and Barrett, S. R. H. (2014). Environmental and Economic Assessment of Producing Hydroprocessed Jet and Diesel Fuel from Waste Oils and Tallow. *Biomass and Bioenergy* 67, 108–118. doi:10.1016/j.biombioe.2014.04.024

Staples, M. D., Malina, R., Olcay, H., Pearlson, M. N., Hileman, J. I., Boies, A., et al. (2014). Lifecycle Greenhouse Gas Footprint and Minimum Selling price of Renewable Diesel and Jet Fuel from Fermentation and Advanced Fermentation Production Technologies. *Energy Environ. Sci.* 7, 1545–1554. doi:10.1039/c3ee43655a

Staples, M. D., Malina, R., Suresh, P., Hileman, J. I., and Barrett, S. R. H. (2018). Aviation Co2 Emissions Reductions from the Use of Alternative Jet Fuels. *Energy Policy* 114, 342–354. doi:10.1016/j.enpol.2017.12.007

Suresh, P., Malina, R., Staples, M. D., Lizin, S., Olcay, H., Blazy, D., et al. (2018). Life Cycle Greenhouse Gas Emissions and Costs of Production of Diesel and Jet Fuel from Municipal Solid Waste. *Environ. Sci. Technol.* 52, 12055–12065. doi:10.1021/acs.est.7b04277

Weibel, D. (2018). *Techno-economic Assessment of Jet Fuel Naphthalene Removal to Reduce Non-volatile Particulate Matter Emissions*. Cambridge, MA: Master's thesis, Massachusetts Institute of Technology.

Zhao, X., Brown, T. R., and Tyner, W. E. (2015). Stochastic Techno-Economic Evaluation of Cellulosic Biofuel Pathways. *Bioresour. Tech.* 198, 755–763. doi:10.1016/j.biortech.2015.09.056

Zhao, X., Yao, G., and Tyner, W. E. (2016). Quantifying Breakeven price Distributions in Stochastic Techno-Economic Analysis. *Appl. Energ.* 183, 318–326. doi:10.1016/j.apenergy.2016.08.184

Conflict of Interest: The authors declare that the research was conducted in the absence of any commercial or financial relationships that could be construed as a potential conflict of interest.

Publisher's Note: All claims expressed in this article are solely those of the authors and do not necessarily represent those of their affiliated organizations, or those of the publisher, the editors and the reviewers. Any product that may be evaluated in this article, or claim that may be made by its manufacturer, is not guaranteed or endorsed by the publisher.

frontiers in Energy Research

ORIGINAL RESEARCH
published: 09 December 2021
doi: 10.3389/fenrg.2021.775389

Economic Analysis of Developing a Sustainable Aviation Fuel Supply Chain Incorporating With Carbon Credits: A Case Study of the Memphis International Airport

Bijay P Sharma[1], T. Edward Yu[2], Burton C. English[2] and Christopher N. Boyer[2]*

[1]Institute for Sustainability, Energy and Environment, University of Illinois, Urbana-Champaign, IL, United States, [2]Department of Agricultural and Resource Economics, University of Tennessee, Knoxville, TN, United States

Sustainable aviation fuel (SAF) has been considered as a potential means to mitigate greenhouse gas (GHG) emissions from the aviation sector, which is projected to continuously expand. This study examines the impact of developing a SAF sector along with carbon credits on carbon equivalent emissions from aviation using a Stackelberg leader-follower model that accounts for economic interaction between SAF processor and feedstock producers. The modeling framework is applied to an *ex-ante* optimization of commercial scale SAF production for the Memphis International Airport from the switchgrass-based alcohol-to-jet pathway. Results suggest that supplying 136 million gallons of SAF to the Memphis International Airport annually could reduce 62.5% of GHG emissions compared to conventional jet fuel (CJF). Incorporating with carbon credits, SAF could lower GHG emissions by about 65% in total from displacing CJF and generate additional welfare gains ranging between $12 and $51 million annually compared to the case without carbon credits. In addition, sensitivity analysis suggests advancing SAF conversion rate from biomass could lower the SAF break-even considerably and enhance the competitiveness of SAF over CJF.

Keywords: sustainable aviation fuel (SAF), stackelberg model, carbon credit, land use, land cover change, GHG emissions

OPEN ACCESS

Edited by:
Kristin C. Lewis,
Volpe National Transportation Systems Center, United States

Reviewed by:
Bheru Lal Salvi,
Maharana Pratap University of Agriculture and Technology, India
Denny K. S. NG,
Heriot-Watt University Malaysia, Malaysia

****Correspondence:***
T. Edward Yu
tyu1@utk.edu

Specialty section:
This article was submitted to Bioenergy and Biofuels, a section of the journal Frontiers in Energy Research

Received: *13 September 2021*
Accepted: *08 November 2021*
Published: *09 December 2021*

Citation:
Sharma BP, Yu TE, English BC and Boyer CN (2021) Economic Analysis of Developing a Sustainable Aviation Fuel Supply Chain Incorporating With Carbon Credits: A Case Study of the Memphis International Airport. Front. Energy Res. 9:775389. doi: 10.3389/fenrg.2021.775389

INTRODUCTION

There is mounting evidence that has documented the negative impacts of increasing cumulative anthropogenic greenhouse gas (GHG) emissions on human and environmental health [United States Environmental Protection Agency (EPA) 2017; Intergovernmental Panel on Climate Change Intergovernmental Panel on Climate Change (IPCC) 2014; Intergovernmental Panel on Climate Change (IPCC) 2018]. Lowering the atmospheric GHG concentration calls for actions that stabilize the atmospheric carbon content, which has been endorsed by numerous governments and private sectors across the world. One such action that has been a primary focus of researchers is lowering GHG emissions from the aviation sector (Grote et al., 2014). The International Air Transport Association (IATA) established goals of carbon neutral growth by 2020 and 50% GHG emissions reduction relative to the 2005 level by 2050 (IATA, 2015). Among various potential approaches to mitigate GHG emissions, utilizing renewable jet fuels (RJF) or sustainable aviation fuels (SAF)

produced from agricultural and forestry residues, energy crops, or municipal wastes could have a crucial role in meeting the GHG emissions reduction goal (Fellet, 2016). As a "drop-in" fuel, SAF can be used in existing aircrafts without modifying engine designs or other engineering aspects (IATA, 2017).

The volume of SAF purchased by the U.S. aviation sector has increased from nearly zero in 2015 [U.S. Federal Aviation Administration (FAA), 2017] to about 4.5 million gallons in 2020 based on U.S. EPA's Renewable Jet Fuel renewable identification numbers (RINs) data (Brown, 2021). In September 2021, the U.S. government announced a SAF Grand Challenge with the proposed goals to reach 3 billion gallons of SAF domestic production annually by 2030, and 35 billion gallons $year^{-1}$ by 2050. Provision of tradable carbon credits could be a means to promote the use of SAF (Luo and Miller, 2013). Those carbon credits could be structured like RIN credits that are bought by registered blenders to ensure the compliance of a target or mandate. For example, the federal agency may issue GHG emission permits to the SAF processors and those permits can be traded in carbon market for credits.

Economic feasibility is considered as a key factor to expedite SAF production, thus studies related to SAF/RJF have primarily focused on the holistic economic assessment of various conversion technologies of SAF. Those studies estimated the break-even or minimum selling price (MSP) of SAF subject to conversion technologies and feedstock choices. Zhao et al. (2015) applied stochastic dominance rank study to identify the MSP for SAF at \$3.11 $gallon^{-1}$ of gasoline equivalent. Using stochastic dominance approach, Yao et al. (2017) found the mean break-even prices of \$3.65 to 5.21 $gallon^{-1}$ from various feedstock using the alcohol-to-jet (ATJ) pathway; whereas (Tao et al., 2017) estimated the MSP of \$4.20 to \$6.14 $gallon^{-1}$ of SAF associated with the ethanol-to-jet (ETJ) upgrading technique. Bann et al. (2017) calculated the MSPs of Hydro-processed Esters and Fatty Acids (HEFA) and Fischer-Tropsch (FT) conversion pathways, and determined the MSP price ranging between \$2.50 and 5.38 $gallon^{-1}$ of SAF.

In addition to economic evaluations, a number of studies have examined the life cycle GHG emissions of SAF or RJF and indicated that replacing conventional jet fuel (CJF) with SAF/RJF could lower GHG emissions by 16–73% subject to feedstock choice and conversion pathways (Han et al., 2017). Specifically, Staples et al. (2018) indicated that SAF have the potential to reduce life cycle GHG emissions from aviation industry up to 68% in 2050 only if the policies were introduced to incentivize using bioenergy and waste feedstocks for SAF production over other alternative uses. The pathways of generating the SAF have substantial impacts on the GHG savings (O'Connell et al., 2019). Few studies have integrated carbon life cycle analysis (LCA) with economic analysis for SAF. Staples et al. (2014) calculated GHG footprint of SAF produced from Advanced Fermentation (AF) pathway and suggested RJF's GHG emissions in the range of −27.0 to 89.8 $gCO_2e\ MJ^{-1}$ given the MSPs of \$0.61 to \$6.30 $liter^{-1}$ (\$2.31 to \$23.85 $gallon^{-1}$) from different feedstocks, compared to 90.0 $gCO_2e\ MJ^{-1}$ of CJF. Winchester et al. (2013) assessed the implicit subsidy required for SAF production from oilseed rotation crops *via* HEFA pathway, the cost of abating CO_2 $tonne^{-1}$ from the aviation from adopting SAF ranges between \$50 and \$400. Similarly, Winchester et al. (2015) evaluated the implicit subside for SAF produced via the AF pathway from perennial energy crops, and suggested the cost of abating CO_2 equivalent could be from \$42 to \$652 $tonne^{-1}$.

Despite the numerous studies on the economic assessment and LCA related to SAF, one key element generally neglected in these economic analyses of SAF is the potential interaction between feedstock producers and SAF processors. The biomass feedstock, such as perennial grass, cover crops, or forest residues, are not currently traded in the market. Therefore, it is important to incorporate feedstock producers' decision process in allocating their scarce resources, such as land, when assessing the potential feasibility of SAF. Feedstock producers make decisions primarily based on their profit margins that account for a large portion of processors' variable costs of SAF production (Agusdinata et al., 2011). As a result, the market price of SAF produced from a given feedstock-based conversion technology is a consequence to competition among the supply chain participants. Such interaction between the participants is influential to the optimization of bioethanol supply chains (Bai et al., 2012).

Another missing piece in the research on SAF production is the welfare analysis of SAF production and the probable policy mechanism. In order to achieve the determined target of the SAF Grand Challenge (3 billion gallons by 2030, 35 billion gallons by 2050) from the current level (~4.5 million gallons in 2020), understanding the welfare implications to the related entities in the SAF supply chain could encourage more SAF production. In addition, how a GHG emissions policy or provision, such as carbon credits, may affect the optimization of SAF supply chain, net GHG emissions, and associated welfare for SAF processors and feedstock producers will provide important insights of policy mechanism on aviation GHG emissions reduction.

This study thus aims to contribute to the literature of SAF in two dimensions: first, the competitive interaction among the feedstock producers and the SAF processor is incorporated to determine the impacts of commercial-scale SAF production on farmland allocation, processing facility configuration, and GHG emissions using high resolution spatial data. Second, the impact of tradable carbon credits, a policy instrument for incentivizing the GHG emission reductions, on the welfare of the SAF processor and feedstock producers is assessed while addressing the economic interaction in the supply chain.

A Stackelberg leader-follower model is applied to capture the interaction of the SAF processor and feedstock producers and their location decision for biorefinery and feedstock draw area. As the follower, the feedstock producers are assumed to maximize their individual profits competing amongst each other in land use decision to fulfill the derived demand. The SAF processor, on the other hand, is the leader that maximizes its profit nesting the profit maximizing behavior of the individual feedstock producers. Under this circumstance, multiple decision makers from

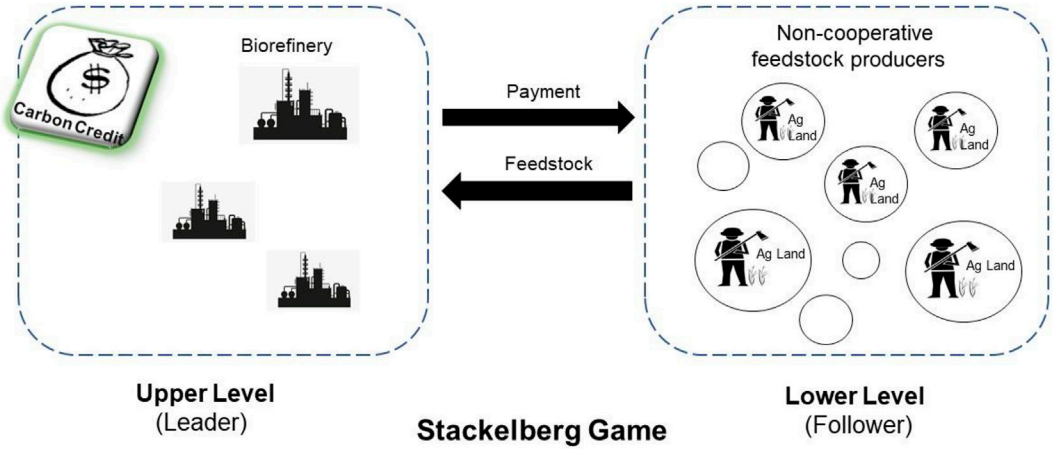

FIGURE 1 | The Stackelberg leader-follower game of the SAF feedstock supply chain. Note: Figure is adapted from **Figure 2** in Yao et al. (2019).

upstream to downstream of the supply chain are involved in the decisions of resource (farmland) allocation and site selection. Such sequential decision process can be formulated as a bi-level optimization problem (Lim and Ouyang, 2016), which indicates that the leader (SAF processor) considers the follower's (feedstock producer) optimization outcome when optimizing its goals (Sinha et al., 2018).

The modeling framework is applied to an *ex-ante* optimization of supplying switchgrass as feedstock for SAF production to meet 50% of the aviation fuel use in the Memphis International Airport (MEM). Switchgrass is selected as the feedstock given its suitability to the soil and weather condition in the southeastern region (Wright and Turhollow, 2010). Given the selected biomass feedstock, the ATJ pathway is selected for the analysis since it is one of the technical feasible technologies to convert biomass to SAF (Yao et al., 2017). The findings from this study should provide researchers, the industry, and policy makers more insights of the potential economic and environmental impacts of developing a commercial scale SAF for the aviation industry. The modeling framework can be applied to alternative feedstock and the associated SAF pathways in different regions.

ANALYTICAL METHODS

A supply chain framework entailing game-theoretic competition between the feedstock producers and the SAF processor is implemented to analyze the economic and environmental metrics of the SAF supply chain. Following (Bai et al., 2012), the interactive decision process is modeled as a Stackelberg leader-follower game with farmland use and facility location decisions. Illustrated in **Figure 1**, the SAF processor (leader) select farmers for contracts based on the types of lands with a predetermined payment under the situation with carbon credit (the Baseline) and without the credit (alternative scenarios), and farmers (follower) choose to accept or decline the offer price for converting their current land use to supply feedstock. Farmers compete for the contracts without cooperative arrangements. Since there is no well-established market for large volume switchgrass transaction, land use changes are the primary decisions that go into the profit maximization problem of the feedstock producers. The "take it or leave it" feedstock price is exogenously determined by the processor based on the quantity of SAF to be produced. Since the SAF price is exogenously determined as a contractual agreement between the processor and the airlines rather than a market clearing mechanism, the processor's profit maximization is essentially a cost minimization problem.

The model assumes that the SAF processor determines the break-even price for the SAF before accepting the airlines' offered price leading to an offtake agreement[1]. The SAF processor then decides the feedstock price and offers an identical price to all feedstock producers in the region. An individual feedstock producer's decision to accept the offered price for producing biomass feedstock is determined by whether the offered price meets the producer's minimal profits expectation or not. Essentially, the processor chooses a processing capacity for the potential plant with its spatial configuration along with a price offered to the feedstock producers that minimizes its feedstock procurement and the SAF processing costs. Finally, a premium above the break-even price obtained from the processor's bi-level optimization is assumed as the contract price between airlines and the SAF processor to satisfy the profit of the processor.

Feedstock Producer's Profit Maximization

Feedstock producers decide on biomass supply quantities to maximize their profits based on the exogenous feedstock price offered from the processing facility subject to land availability and SAF demand. Feedstock producers' objective is generalized as:

[1]Offtake agreements are contracts between fuel consumers and producers specifying the procurement of specified fuel volumes for a period and have recently been agreed upon with several airlines [Commercial Aviation Alternative Fuels Initiative (CAAFI), 2016].

$$\underset{\substack{X_i=[X_{ih}]_{h\in H}\\ XQ_i=[XQ_{mij}]_{m\in M,j\in J}}}{\overbrace{Maximize}} \pi_i = \sum_{j\in J}\sum_{m\in M_{on}}\left(P-\theta_{ij}\right)\times XQ_{mij} + \sum_{j\in J}\sum_{m\in M_{off}}\left(P-\gamma-\theta_{ij}\right)\times XQ_{mij} - \sum_{h\in H}\left(\alpha+\omega+AM+\beta_{ih}\right)\times X_{ih}, \quad (1)$$

where M_{on} denotes harvest season whereas M_{off} denotes off-harvest season, P denotes the feedstock price (\$ ton^{-1}) offered by processing facility, θ_{ij} denotes feedstock transportation cost from site i to j (\$ ton^{-1}), XQ_{mij} denotes feedstock supply quantity (tons) from site i to j at season m, γ denotes feedstock storage cost (\$ ton^{-1}), α denotes annualized feedstock establishment cost (\$ acre^{-1}), ω denotes annual feedstock harvest cost (\$ acre^{-1}), AM denotes annual maintenance cost (\$ acre^{-1}) of feedstock field, β_{ih} denotes opportunity cost (\$ acre^{-1}) at site i for existing crop h, and X_{ih} denotes acreage of harvested feedstock at site i replacing existing crop h.

The first summation term in **Eq. 1** presents the revenues from feedstock supply subtracting transportation costs during harvest season, while the second summation term represents the revenues after deducting feedstock transportation and storage costs during the off-harvest season. The third component sums up annualized feedstock establishment, harvest, maintenance, and the opportunity costs of land use change. Opportunity cost is defined as either net return from existing land use or land rent, whichever is higher (Yu et al., 2016), given by:

$$\beta_{ih} = \left\{ \begin{array}{ll} p_{ih}\times Y_{ih} - C_{ih} & if\ \left(p_{ih}\times Y_{ih}-C_{ih}\right)\geq R_{ih} \\ R_{ih} & if\ \left(p_{ih}\times Y_{ih}-C_{ih}\right)< R_{ih} \end{array} \right\},$$

where p_{ih} denotes price (\$ acre^{-1}) at site i for crop h, Y_{ih} denotes yield (ton acre^{-1}) at site i for crop h, C_{ih} denotes production cost (\$ acre^{-1}) at site i for crop h, and R_{ih} land rent (\$ acre^{-1}) at site i for crop h.

The profit maximization problem is subject to certain constraints presented in **Eqs. 2–8** below. **Eq. 2** limits feedstock production area to the available agricultural land. **Eq. 3** assures that total harvested biomass equals the total biomass production. **Eq. 4** models the competitive relationship between the individual feedstock producers and assures that biomass supplied by profit maximizing feedstock producers together does not exceed the production capacity of the processing facility. **Eqs 5**, **6** are mass balance/flow constraints. **Eqs 7**, **8** are the non-negativity constraints imposed on the continuous decision variables.

$$X_{ih} \leq A_{ih} \forall\ i,h, \quad (2)$$

$$\sum_{j\in J}\left(XNS_{ij}+XS_{ij}\right) = Y_{ix}\times\sum_{h\in H}X_{ih}\forall i, \quad (3)$$

$$\sigma\times\left(XQ_{mij}+\sum\nolimits_{-i}XQ_{mij}\right)\leq\Delta_{mjg}\times z_{jg}\forall m,j, \quad (4)$$

$$XNS_{ij} = \sum_{m\in M_{on}}\frac{XQ_{mij}}{(1-DT)}\forall i,j, \quad (5)$$

$$XS_{ij} = \sum_{m\in M_{off}}\frac{XQ_{mij}}{(1-DS)\times(1-DT)}\forall i,j, \quad (6)$$

$$X_{ih}\in\mathbb{R}^{+}\forall i,h, \quad (7)$$

$$XQ_{mij}\in\mathbb{R}^{+}\forall m,i,j, \quad (8)$$

where A_{ih} denotes available acreage at site i under existing crop h, Y_{ix} denotes spatial switchgrass (x) yield (ton acre^{-1}) at site i, XNS_{ij} denotes switchgrass not stored at the harvest site i for facility j after harvest (tons), XS_{ij} denotes switchgrass stored at the harvest site i for facility at site j after harvest (tons), σ denotes the feedstock-SAF conversion efficiency (gallon ton^{-1}), Δ_{mjg} denotes seasonal production capacity (gallons) of the facility at j with annual capacity g, z_{jg} denotes binary variable for locating facility at j with annual capacity g, DT denotes dry matter loss during transportation (%), and DS denotes dry matter loss during storage (%).

Processor's Bi-level Optimization Problem

The SAF processor also aims to maximize profit assuming the final SAF price is a contract between the processor and the airlines once the processor determines its break-even level and its profit margins. Thus, the processor needs to decide on biomass procurement price and the configuration of facilities to minimize its costs as its break-even level subject to the anticipated optimal behavior of the feedstock producers. The processor's profit maximization objective is thus converted to a cost minimization objective as:

$$\underset{\substack{XO=[XO_{mj}]_{m\in M,j\in J}\\ Z=[z_{jg}]_{j\in J,g\in G}}}{\overbrace{Minimize}} \eta = \sum_{j\in J}\sum_{m\in M}\left(\rho+\delta_{jd}\right)\times XO_{mj} + \sum_{j\in J}\sum_{g\in G}\left(\mu_g\times z_{jg}\right)+\sum_{j\in J}\sum_{m\in M}\left(P\times\sum_{i\in I}XQ_{mij}\right), \quad (9)$$

where XO_{mj} denotes SAF transported at season m from facility j to the airport d, ρ denotes facility operation cost (\$ gallon^{-1}), δ_{jd} denotes SAF transportation cost (\$ gallon^{-1}), μ_g denotes amortized facility investment cost (\$ facility^{-1}) with annual capacity g, and D_m denotes seasonal SAF demand at the airport. The first component in **Eq. 9** denotes the total of feedstock-to-SAF conversion and SAF transportation costs. The second term presents the annualized investment costs of processing facilities, while the last component sums the feedstock procurement costs of the SAF processor.

Eqs 10–15 below define the constraints imposed on the cost minimization problem. **Eq. 10** ensures that the amount of biomass transported during each season is all converted into SAF by processing facility. **Eq. 11** guarantees SAF sent to airport in each season meets the seasonal demand of SAF by the airlines. **Eq. 12** limits the number of processing plants at each site. **Eqs 13**, **14** denote the domains of the binary and continuous decision variables. **Eq. 15** assures that profit of individual feedstock producers to be at least r_1 % higher than the net returns from current use at their land (i.e., opportunity cost). **Eq. 15** incorporates feedstock producers' objective in SAF processors' decision process. A minimum margin of 10% is assumed in this study to fulfill the profitability expectations of the potential feedstock producers.

$$XO_{mj} = \sigma\times\sum_{i\in I}XQ_{mij}\ \forall\ m,j, \quad (10)$$

$$\sum_{j\in J} XO_{mj} = D_m \,\forall m, \tag{11}$$

$$\sum_{g\in G} z_{jg} \le 1 \,\forall\, j, \tag{12}$$

$$z_{jg} \in \{0,\ 1\} \,\forall\, j, g, \tag{13}$$

$$XO_{mj} \in \mathbb{R}^{+} \,\forall m, j, \tag{14}$$

$$\pi_i \ge r_1 \times \sum_{h\in H} \beta_{ih} \times X_{ih}, \tag{15}$$

Solution Approach to Bi-level Optimization

Since the profit maximization problem of the feedstock producers (lower-level problem) is linear, the typical approach to solving the bi-level optimization is to convert it into a single-level optimization by replacing the original constraints of the lower-level including the objective function by its corresponding Karush-Kuhn-Tucker (KKT) conditions. The KKT conditions guarantee the objective function and all the constraints corresponding to individual feedstock producer's profit maximization problem are satisfied. The KKT transformation is a non-convex non-linear problem which is often difficult to solve (Gümüş and Floudas, 2005). These KKT constraints are thus reformulated as disjunctions with the introduction of slack variables, and converted into mixed-integer constraints using the Big-M and binary variables (Gümüş and Floudas, 2005). The resulting problem then becomes linear and is solved using the CPLEX solver of the General Algebraic Modeling System (GAMS) 24.2 (Rosenthal, 2008).

GHG Emissions, SAF Co-products and RIN Credits

The LCA-based GHG emissions from SAF[2] is estimated to evaluate the environmental impact of SAF. The estimated total supply-chain GHG emissions include GHG emissions from land use change into switchgrass; energy use emissions from switchgrass production, harvest, and storage; emissions from energy use during transportation of biomass and SAF; and the emissions related with feedstock grinding and conversion.

As the ATJ pathway produces other hydrocarbon fuels as co-products in addition to the SAF, estimation of LCA-based GHG emissions for the main-product should account for the contribution of its co-products (Wang et al., 2011). GHG emissions from the co-products are calculated using an allocation method based on their approximately equal energy contents (Han et al., 2017). In addition, the revenue generated from the co-products by displacing the fossil fuels is estimated using the displacement method at the market prices of fossil fuels. In particular, the environmental benefit of SAF and its co-products is assessed by estimating changes in GHG emissions between the energy products from the ATJ-pathway (SAF, cellulosic-diesel, and cellulosic-gasoline) and the displaced fossil fuels (CJF, diesel, and gasoline).

The Renewable Fuel Standard program established in the Energy Policy Act of 2005 is a market-based compliance system that utilizes RIN credits as a mechanism to trace if biofuel refiners or terminal operators produce the mandated level of biofuels under the Energy Act. Two different RIN credits for cellulosic biofuel based on average price for 2016 (2016-A), and 2017 (2017-A) are considered to examine its impacts on economic feasibility of SAF. The impact of revenues from ATJ co-products as well RIN credits is exogenous since they are taken as additional economic incentives for supporting SAF production. Thus, RIN credits, revenues, and GHG emission reductions from co-products are included in estimating the cost, environmental, and welfare impacts of SAF.

Welfare Analysis of the SAF Sector

Given the price assumptions used in satisfying the economic objectives of the supply-chain participants, surpluses for feedstock producers (PS_{FS}) and the SAF processor (PS_{SAF}) are set equal to the total feedstock producer profit and processor's profit, respectively. Also assumed, the processing facility produces SAF only if the price received from the airlines includes a premium at least \$ r_2 above break-even. A \$0.10 gallon^{-1} as the markup[3] is used as the premium assuming that it satisfies the profitability requirements of the SAF processor. The consumers surplus in the SAF market (CS_{SAF}) is calculated using CJF price (p_{CJF}) as the maximum willingness to pay. Finally, the net welfare associated with SAF market is assessed while internalizing the environmental (social) costs of aviation emissions based on the social cost of carbon as follows:

$$Welfare = PS_{FS} + PS_{SAF} + CS_{SAF} - c_e E_{LCA}, \tag{16}$$

$$PS_{FS} = \sum_{i\in I} \pi_i, \tag{17}$$

$$PS_{SAF} = r_2 \times \sum_{m\in M} D_m, \tag{18}$$

$$CS_{SAF} = \left\{p_{CJF} - \left(p_k^{BE} + r_2\right)\right\} \times \sum_{m\in M} D_m, \tag{19}$$

where c_e is the environmental cost of emission in \$ tonCO_2e^{-1}, and E_{LCA} denotes total feedstock production to combustion (field-to-wake) GHG emissions from SAF in tonCO_2e.

Carbon Credits Analysis

For a processor, the choice for the processing facility location and the contracted feedstock producers could vary considerably whether carbon credits are available or not at the investment stage. The presence of tradable carbon credits incentivizes the SAF processor to reduce the total field-to-wake GHG emissions since the total value of carbon credits is proportional to the difference in energy equivalent well-to-wake (fuel extraction to

[2]The GHG emissions from feedstock production through SAF delivery to the airport is considered as the LCA-based emission because GHG emissions from burning biomass-based renewable fuel nearly equal the amount of CO_2 sequestered by the biomass during its growth, i.e. biogenic carbon (Elgowainy et al., 2012; Wang et al., 2012).

[3]The profit margin is approximated based on the percentage of refining costs and profits of average retail price paid for gasoline in the U.S for 2008–2017 (U.S. Energy Information Administration (EIA), 2017), and the average retail price for CJF in the year 2017 [Bureau of Transportation Statistics (BTS), 2016a].

combustion) GHG emissions from CJF and field-to-wake GHG emissions from SAF. The reduction in GHG emissions for the SAF processor is achieved either through contracting feedstock producers for crop land conversion to switchgrass because of net carbon sequestration or by reducing feedstock and SAF transportation GHG emissions through optimal facility location. To estimate the economic, environmental and welfare implication of the hypothetical carbon credits on the SAF supply-chain, the system is defined in **Eqs. 1–15** as the Baseline in which SAF processor and feedstock producers make their decisions without carbon credits. In contrast, under the alternative scenarios of having carbon credit, the augmented objective function of SAF processor in **Eq. 9** is defined as follows:

$$\begin{aligned} &\underbrace{Minimize}_{XO=\left[XO_{mj}\right]_{m\,\epsilon\,M,j\,\epsilon\,J}} \eta\colon \sum_{j\in J}\sum_{m\in M}\left(\rho+\delta_{jd}\right)\times XO_{mj}+\sum_{j\in J}\sum_{g\in G}\left(\mu_g\times z_{jg}\right)\\ &Z=\left[z_{jg}\right]_{j\in J,g\,\epsilon\,G}\\ &+\sum_{j\in J}\sum_{m\in M}\left(P\times\sum_{i\in I}XQ_{mij}\right)\\ &-p_e\left(\Phi_{LCA}\times\left(\sum_{j\in J}\sum_{m\in M}XO_{mj}\right)-\mathrm{E}_{\mathrm{LCA}}^{\mathrm{CC}}\right) \end{aligned} \tag{20}$$

where p_e is the carbon credits in \$ tonCO_2e^{-1}, Φ_{LCA} denotes well-to-wake emission from energy-equivalent CJF in tonCO_2e gallon^{-1}, and E_{LCA}^{CC} denotes total field-to-wake emission from SAF in tonCO_2e as a result of processor's optimal decisions under carbon credit scenarios.

Three different carbon credit scenarios corresponding to historical low and high carbon prices in the California Cap-and-Trade program (CalCaT-L and CalCaT-H, respectively), and historical high carbon price in the European Union Emission Trading System (EUETS-H) are used to evaluate the impact of potential carbon markets in GHG emissions reduction and supply-chain welfare. These scenarios are selected to reflect the ranges of the U.S. as well as the global carbon prices in the emission trading market. In each scenario, a share of the total carbon credits per gallon of SAF (r_3 %) is used as an additional margin in determining the SAF contract price.

The leader-follower nature merits the processor in a way that impacts the optimal land use decisions of the feedstock producers through its facility location decisions under carbon credits. The processor is able to simultaneously lower the break-even SAF price and GHG emissions since the total carbon credits is proportional to the GHG emissions reduction compared to equivalent CJF. This decision process changes net welfare primarily through changes in the surpluses for feedstock producers, the processor, and the airlines as follows:

$$Welfare^{CC}=PS_{FS}^{CC}+PS_{SAF}^{CC}+CS_{SAF}^{CC}-c_eE_{LCA}^{CC}, \tag{21}$$

$$PS_{FS}^{CC}=\sum_{i\in I}\pi_i^{CC}, \tag{22}$$

$$PS_{SAF}^{CC}=\left(r_2+r_3\times\frac{p_e\left(\Phi_{LCA}\sum_{m\in M}D_m-E_{LCA}^{CC}\right)}{\sum_{m\in M}D_m}\right)\times\sum_{m\in M}D_m, \tag{23}$$

$$CS_{SAF}^{CC}=\left\{p_{CJF}-\left(p_k^{BE^{CC}}+r_2+r_3\times\frac{p_e\left(\Phi_{LCA}\sum_{m\in M}D_m-E_{LCA}^{CC}\right)}{\sum_{m\in M}D_m}\right)\right\}\times\sum_{m\in M}D_m, \tag{24}$$

where $p_k^{BE^{CC}}$ is the break-even price for processor delivering SAF to airport k with carbon credits.

DATA

The data used for cellulosic ATJ conversion pathway is categorized into two groups: feedstock-based ethanol production data, and the data on potential conversion technology of ethanol to SAF. The parameters used to calculate costs and GHG emissions of feedstock-based ethanol production are from (Yu et al., 2016); whereas the parameters used for calculating costs, yields including co-products, and GHG emissions of ethanol-to-SAF conversion are primarily based on recent techno-economic analysis of feedstock-based ATJ or ETJ conversion pathways (Elgowainy et al., 2012; Han et al., 2017; Tao et al., 2017; Yao et al., 2017). The ethanol-to-SAF conversion parameters are augmented with relevant feedstock-based ethanol production data in estimating the feedstock-to-SAF conversion parameters.

Data from switchgrass field trials between 2006 and 2011 at west Tennessee (Boyer et al., 2012; Boyer et al., 2013) is used to simulate feedstock yields across 5 sq. mile spatial units on existing agricultural lands. Mean yields obtained from normally distributed simulations are matched to the number of potential feedstock producers supplying feedstock. Spatial yield variation is determined following the simulated spatial variation in switchgrass yields in the region (Jager et al., 2010). A total of 18 industrial parks are identified as candidates for establishing processing facilities. Each location can have at most one facility with the capacity of either 50 million gallons year^{-1} (MGY) or 100 MGY. Similarly, a total of 1936 hexagon-shaped spatial units (5 mile^2 per unit) are taken as potential feedstock producers opting to cultivate switchgrass replacing current crops. An annual SAF demand of 136 million gallons for the MEM is assumed which replaces one-third of the total jet fuel consumption for flights departing from the MEM airport in 2016[4]. The price feedstock producers received at the processing facility gate in the study region is \$75 ton^{-1} derived from the estimated average plant gate cost of switchgrass delivered to an ethanol plant in west Tennessee in Yu et al. (2016).

Table 1 presents key conversion parameters used in the analysis including co-products i.e. cellulosic-gasoline and cellulosic-diesel. Conversion cost and GHG emissions in the table refer to the parameters associated with feedstock-to-SAF conversion excluding feedstock grinding. The cost and GHG emission parameters on feedstock grinding are taken into account separately based on (Yu et al., 2016). The LCA-based GHG emissions of displaced

[4]Total fuel consumption at the Memphis airport (MEM) was estimated around 410 million gallons in 2016 (Pearlson, 2020). The assumed SAF demand is close to 33% of the total jet fuel consumption, which is under the current statutory blending limit (50%) for the ATJ pathway

TABLE 1 | Parametric assumptions for cellulosic alcohol-to-jet (ATJ) conversion pathway.

ATJ product	Conversion yield	Unit	Source
SAF	26.72	gallon ton^{-1}	Han et al. (2017), Yao et al. (2017)
Cellulosic-gasoline	5.65	gallon ton^{-1}	Han et al. (2017), Yao et al. (2017)
Cellulosic-diesel	2.93	gallon ton^{-1}	Han et al. (2017), Yao et al. (2017)
ATJ product	**Conversion cost[a]**	**Unit**	**Source**
SAF	1.89	\$ $gallon^{-1}$	Tao et al. (2017), Yao et al. (2017), Yu et al. (2016)
ATJ product	**Conversion GHG**	**Unit**	**Source**
SAF	2.80	$kgCO_2e$ $gallon^{-1}$	Argone National Laboratory (2017), Yao et al. (2017), Yu et al. (2016)

[a]*All the monetary terms are in 2015 U.S., dollar values.*
Note: The parameters for ATJ pathway originally available in energy (mega joule-MJ) units, are converted into volumetric (gallon) units based on energy-equivalence. One liter of Gasoline, Diesel and CJF releases around 34.2, 35.8 and 34.1 MJ of energy, respectively.

TABLE 2 | Parameters on energy-equivalent substitutes to ATJ products.

LCA-based GHG			
Fossil fuel	Emission	Unit	Source
CJF	11.289	$kgCO_2e$ $gallon^{-1}$	Wang et al. (2016)
Gasoline	12.258	$kgCO_2e$ $gallon^{-1}$	Elgowainy et al. (2012)
Diesel	12.496	$kgCO_2e$ $gallon^{-1}$	Elgowainy et al. (2012)
Market price			
Fossil fuel	Price[a]	Unit	Source
CJF	1.759	\$ $gallon^{-1}$	BTS (2016a)
Gasoline	2.408	\$ $gallon^{-1}$	AFDC (2017)
Diesel	2.669	\$ $gallon^{-1}$	AFDC (2017)

[a]*All the monetary terms are in 2015 U.S. dollar values.*

TABLE 3 | RIN credits and parameters for carbon credit scenarios.

RIN price[a]	Unit	Level	Source
2016-A	\$ RIN^{-1}	1.85	RFA (2017)
2017-A	\$ RIN^{-1}	2.69	RFA (2017)
Carbon credit[a]	**Unit**	**Level**	**Source**
CalCaT-L	\$ $tonCO_2e^{-1}$	11.58	California Carbon Dashboard (2018)
CalCaT-H	\$ $tonCO_2e^{-1}$	22.85	California Carbon Dashboard (2018)
EUETS-H	\$ $tonCO_2e^{-1}$	42.56	Luo and Miller (2013)

[a]*All the monetary terms are in 2015 U.S., dollar values.*
Note: 2016-A and 2017-A denote RIN credits for cellulosic biofuel based on average price for 2016 and 2017, respectively. CalCaT-L, CalCaT-H and EUETS-H denote lowest carbon price in the California Cap-and-Trade program, highest carbon price in the California Cap-and-Trade program and highest carbon price in the European Union Emission Trading System, respectively.

conventional energy products (fossil fuels) are shown in **Table 2**. The market prices of fossil fuels displaced by corresponding ATJ products are also included in **Table 2**. **Table 3** shows the levels of RIN credits[5] used and carbon credits considered for specific carbon credit scenarios. The social cost of carbon, \$33.70 $tonCO_2e^{-1}$, is adapted from (Nordhaus, 2017).

RESULTS AND DISCUSSION

The Baseline Solutions of the Stackelberg Model

Supply-Chain Economic and GHG Emissions Outputs

Under the Baseline, the overall cost accrued by the SAF processor from the optimal game-theoretic model is \$1,155 million $year^{-1}$, while the aggregate profit of feedstock producers is \$16.88 million. The optimal location of processing facility and the contracted individual feedstock producers are shown in **Figure 2**. An important factor in producers' decision on converting their land to a new operation is the opportunity cost of land use change. Selection of land for food crops had higher opportunity costs than pasture land. Additionally, spatial variation in switchgrass yields across west Tennessee creates comparative advantage to some of the potential feedstock producers. A total of 657,000 acres of farmland are selected for feedstock cultivation with more than 58% converting from pasture land. Crop land use changes occur with soybean and corn acreages shifting to switchgrass production.

The processor's facility configuration decisions are influenced by the spatial distribution of the potential feedstock producers, their opportunity costs of supplying feedstock, and the spatial yield variability. The processor decides to locate a larger processing facility (100 MGY capacity) at a site surrounded by feedstock producers farming agricultural lands with lower opportunity costs. On the other hand, feedstock producers with higher yields are pivotal in determining the location for the 50 MGY facility simultaneously securing their profit margins.

The margin over the opportunity cost gained by feedstock producers from supplying feedstock is shown in the **Figure 3**. Most of the feedstock producing areas (more than 57%) received a margin ranging from 10 to 47% over their opportunity cost of converting the land, whereas a few feedstock producing areas obtained substantial margins of up to 658%. The observed gains are primarily dictated by the types of land used for feedstock cultivation. In general, the margin is higher for feedstock producers converting pasture land. Because of the higher

[5]Advanced biofuels such as biomass-based biodiesel (BBD) counts as 1.5 or 1.7 RINS (depending on fuel type) to reflect its higher energy content compared to ethanol (Congressional Research Service, 2013). The available RIN prices on cellulosic ethanol are multiplied by a factor of 1.7 for generating cellulosic SAF-based RIN credits

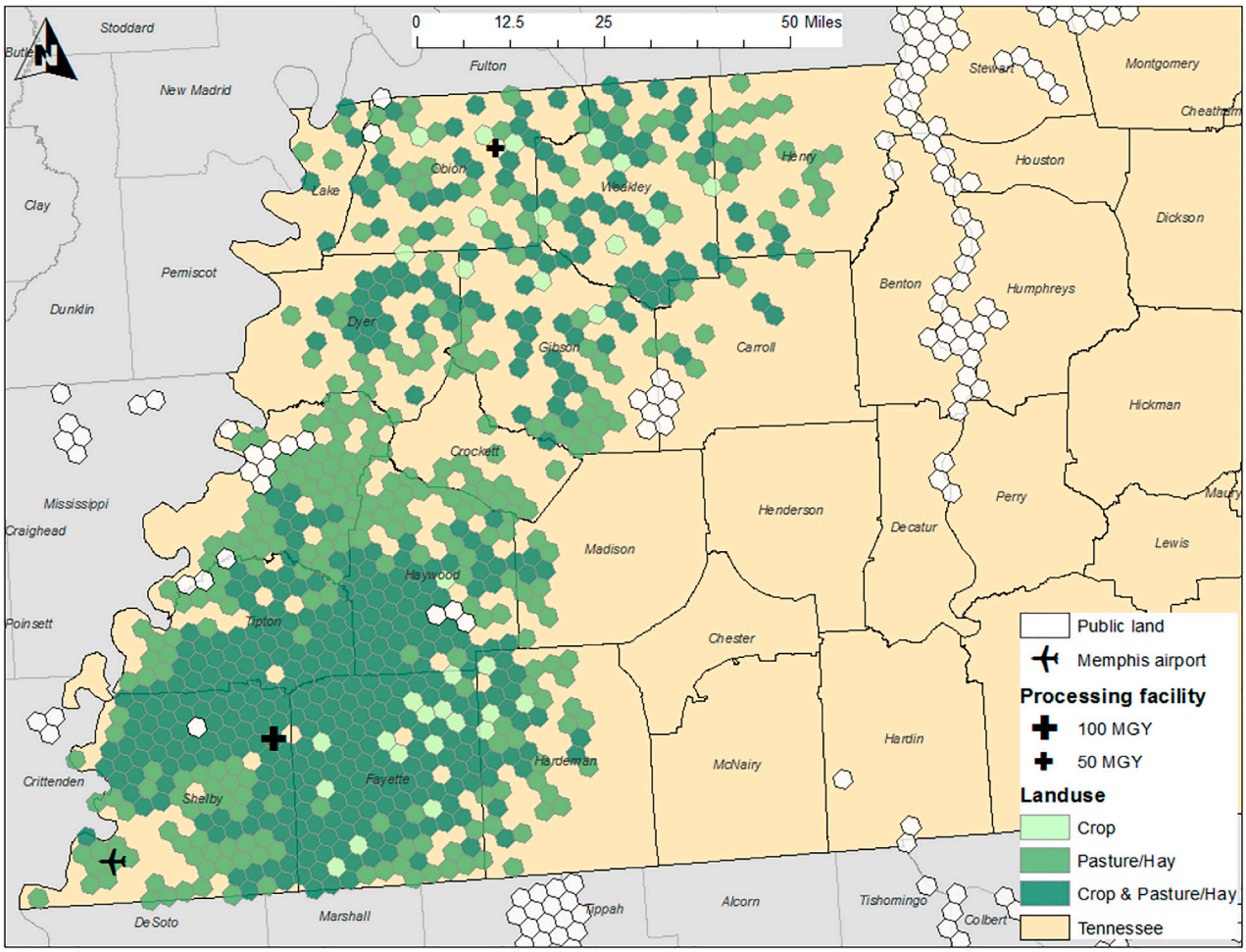

FIGURE 2 | Optimal land use and facility locations under the Baseline.

opportunity costs of cropland, less margin is acquired in areas with significantly more cropland when compared to pastureland, resulting conversion of either crop land alone or a mix of the pasture and crop land.

The annualized costs and GHG emissions of each operation in the bi-level supply-chain optimization for the Baseline are summarized in **Table 4**. The largest component of the processor's cost is related to SAF conversion, around \$515 million year^{-1}. Similarly, feedstock procurement (approximately \$382 million) consists of a sizeable portion of the processor's cost. With a conversion factor of 26.72 gallons ton^{-1}, a total of 5.09 million tons of feedstock are procured for fulfilling the SAF demand at the MEM airport. Feedstock harvest cost of nearly \$114 million are the highest costs incurred in aggregate, followed by feedstock transportation cost of around \$107 million.

The conversion process produces the highest GHG emissions, above 380,000 tons of CO_2e with feedstock harvest producing around 265,000 tons of CO_2e emissions annually. Land use change results in sequestration of around 57,000 tons of CO_2e emissions, primarily through crop lands conversion to switchgrass because of net carbon sequestration in the soil. More than 777,000 tons year^{-1} of CO_2e emissions are generated from this switchgrass-based SAF supply chain. The total LCA-based GHG emission reduction through displacement of the fossil fuels with the ATJ-pathway is 62.5% under the Baseline, which lies within the range of 16–80% estimated in Han et al. (2017) for various feedstock conversion pathways.

Supply-Chain Welfare Analysis

In this study, the producer surpluses for feedstock producers (denoted as PS-FS) are equal to the total feedstock producer profit, while and the SAF processor surpluses (denoted as PS-SAF) and the processor's profit. The feedstock producers' economic surplus is about \$16.9 million, while the SAF processor secures a surplus of \$13.6 million. The consumer surpluses for the SAF (denoted by CS-SAF) are -\$256.8 million and \$158 thousand with 2016-A and 2017-A RIN credits, respectively, for the Baseline. Internalized environmental costs of aviation GHG emissions of around \$26.2 million result in net supply-chain welfares -- around -\$252.5 million and \$4.44 million with 2016-A and 2017-A RIN credits, respectively, for the Baseline.

The large negative values in the estimated social welfare is mainly related to prohibitively expensive production and

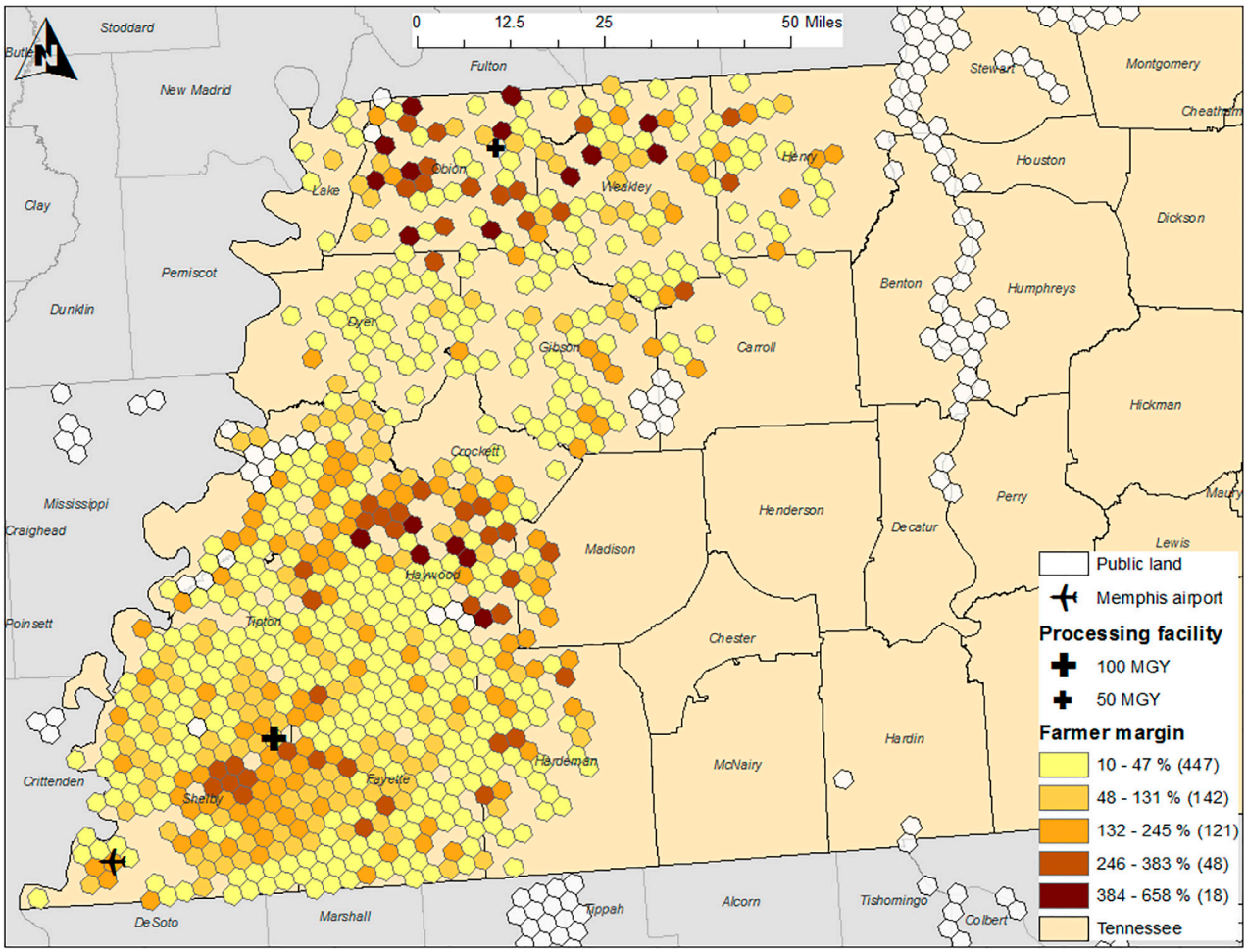

FIGURE 3 | Margins of individual feedstock producers under the Baseline. Note: Number in the parenthesis refers the amount of feedstock producers.

processing costs of switchgrass-based SAF. This is in line with the prior studies indicating cellulosic biofuel mandates with the blending credits may have large negative welfare estimates because of heightened production costs and burden to taxpayers (Chen et al., 2011). Even though there are no explicit SAF mandates and subsidies in place, a recent analysis of SAF produced from *Camelina sativa* shows that a combination of 9% subsidy on the SAF and 9% tax on the CJF would make it at least revenue neutral to the government otherwise society would have to bear a large cost (Reimer and Zheng, 2017).

Comparison Between the Baseline and Carbon Credit Scenarios

Changes in Optimal Solutions for the Bi-level Objectives

Under the scenarios of available carbon credits, the SAF processor decides on facility locations and the contracted feedstock producers in such a way that reduces the total field-to-wake GHG emissions through contracting feedstock producers converting crop lands for switchgrass production or siting facility that reduced feedstock and SAF transportation GHG emissions (see **Supplementary Figures SA1–A3** for the CalCaT-L, CalCaT-H, and EUETS-H scenarios, respectively, in the Appendix). The changes in the annualized costs of related operations in the supply chain from introducing carbon credits is summarized in **Table 5**. Compared to the Baseline, total annual feedstock producer profit declines by $5.88, $5.90, and $10.45 million for the CalCaT-L, CalCaT-H, and EUETS-H scenarios, respectively, as the opportunity costs of land use increased. The crop land use increases by around 98,000 to 151,000 acres for the three scenarios. Meanwhile, there are subsequent reductions in pasture land conversion under all three scenarios.

In addition, the processor locates the facility closer to the MEM airport to reduce SAF transportation GHG emissions in response to carbon credits (see Figs. A1, A2, and A3 for the CalCaT-L, CalCaT-H, and EUETS-H scenarios, respectively, in the Appendix). As a result, the processor's transportation cost also declines. The highest carbon credit scenario, i.e. EUETS-H, triggers major land use changes and facility location, increasing the objective values compared to the no carbon credit case. Similarly, increased cropland use in response to proximity of

TABLE 4 | Annualized variables for the Baseline.

Annualized bi-level cost	Unit	Level
SAF processor cost		
Processing facility investment cost	million $	175.32
Feedstock procurement cost	million $	381.72
Feedstock grinding cost	million $	73.75
SAF conversion cost	million $	514.95
SAF transportation cost	million $	9.60
Feedstock producers cost		
Land use opportunity cost	million $	39.88
Feedstock establishment cost	million $	46.26
Feedstock maintenance cost	million $	34.35
Feedstock harvest cost	million $	113.65
Feedstock storage cost	million $	23.97
Feedstock transportation cost	million $	106.73
Annualized GHG emission	**Unit**	**Level**
SAF processor emission		
Feedstock grinding emission	tonCO_2e	136,298
SAF conversion emission	tonCO_2e	380,297
SAF transportation emission	tonCO_2e	3,374
Feedstock producers emission		
Land use emission	tonCO_2e	(57,299)
Feedstock establishment emission	tonCO_2e	17,773
Feedstock harvest emission	tonCO_2e	265,319
Feedstock storage emission	tonCO_2e	5,086
Feedstock transportation emission	tonCO_2e	26,466

the facility reduced the feedstock transportation costs by $1.72, $1.70, and $2.98 million for the CalCaT-L, CalCaT-H, and EUETS-H scenarios, respectively.

Total annual GHG emissions in the SAF supply chains are reduced between 27.7 to more than 46.6 thousand tonCO_2e under the three carbon credit scenarios compared to the Baseline. As expected, the highest carbon credits (EUETS-H scenario) creates the most impact on GHG emissions reduction from the Baseline, while the changes in GHG emissions for the CalCaT-L and CalCaT-H scenarios are similar. As shown in **Table 5**, major GHG emission reductions from all the carbon credit scenarios are associated with land use change. Reductions in GHG emissions associated with feedstock and SAF transportation are relatively small. With carbon credits, the total GHG emission reductions from using SAF and its co-products range between 64 and 65% among all three scenarios when compared to the displaced CJF and other fuel products.

Change in the Supply Chain Welfare

The changes in net welfare for different carbon credit scenarios against the Baseline is illustrated in **Figure 4**. A subsequent decrease in the SAF processor's break-even price incurs given higher carbon credits. The margin under carbon credits improves the surplus for the SAF processor. Similarly, the surplus for the SAF consumers, i.e., airlines, increases as the SAF price at each carbon credit scenario is lower than the Baseline. However, the surplus for the feedstock producers, i.e. feedstock producers, reduces due to more high opportunity cost crop lands converted for feedstock production driven by the carbon credits acquired by the SAF processor.

Subsequent abatements in the GHG emissions from carbon credits reduce the social cost of emissions compared to the Baseline in each carbon credit scenario. The net welfare increases across all carbon credit scenarios because of the consumer surplus increase toward the airlines. Under the minimum carbon credit (CalCaT-L scenario) scenario,. the SAF processor's surplus increases by $1.53 million and economic surplus of airlines increases by $16.12 million. However, feedstock producers' surplus decreases by $5.88 million due to the selection of higher productive cropland (with higher opportunity cost) that can store more soil carbons after being converted to switchgrass. With $935,000 reduction in the internalized costs of field-to-wake GHG

TABLE 5 | Changes in annualized variables for carbon credit scenarios compared to the Baseline.

Annualized bi-level cost	Unit	CalCaT-L	CalCaT-H	EUETS-H
SAF processor cost				
SAF transportation cost	million $	−2.31	−2.31	−2.34
Feedstock producers cost				
Land use opportunity cost	million $	5.64	5.65	12.20
Feedstock establishment cost	million $	0.90	0.90	0.57
Feedstock maintenance cost	million $	0.67	0.67	0.42
Feedstock harvest cost	million $	0.39	0.39	0.24
Feedstock transportation cost	million $	−1.72	−1.70	−2.98
Annualized GHG emissions	**Unit**	**CalCaT-L**	**CalCaT-H**	**EUETS-H**
SAF processor emissions				
SAF transportation emission	tonCO_2e	−1,200	−1,200	−1,292
Feedstock producers emissions				
Land use change emission	tonCO_2e	−31,145	−31,158	−47,400
Feedstock establishment emission	tonCO_2e	345	345	217
Feedstock harvest emission	tonCO_2e	5,145	5,145	3,242
Feedstock transportation emission	tonCO_2e	−879	−865	−1,369

Note: CalCaT-L, CalCaT-H, and EUETS-H denote lowest carbon price in the California Cap-and-Trade program, highest carbon price in the California Cap-and-Trade program and highest carbon price in the European Union Emission Trading System, respectively.

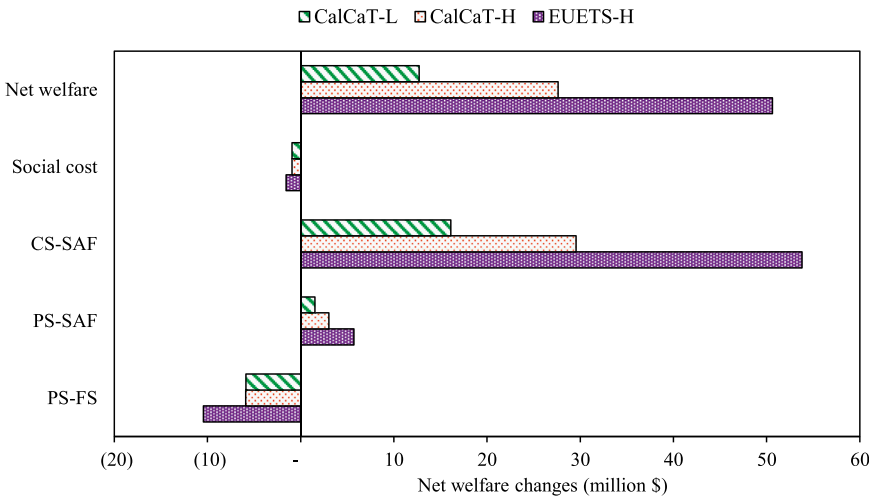

FIGURE 4 | Changes in net welfare for carbon credit scenarios against the Baseline. Note: PS-FS, PS-SAF and CS-SAF denote surplus for feedstock producers, surplus for SAF processor and surplus for SAF consumers, respectively. CalCaT-L, CalCaT-H and EUETS-H denote lowest carbon price in the California Cap-and-Trade program, highest carbon price in the California Cap-and-Trade program and highest carbon price in the European Union Emission Trading System, respectively.

emissions, the net welfare increases by $12.71 for the CalCaT-L scenario compared to the Baseline. Similarly, the net welfare increases by $27.61 and 50.62 million for the CalCaT-H and EUETS-H scenarios, respectively, mainly due to increments in the airlines' surpluses.

In this study, the benefit of a tradable carbon credit is reaped by the SAF processor only even though the reduction in GHG emissions is based on field-to-wake approach. This is because it is assumed that the processor as a leader can reduce field-to-wake GHG emissions indirectly by contracting feedstock producers that convert crop land due to net carbon sequestration, or directly by reducing feedstock and SAF transportation GHG emissions through optimal facility location. If the portion of the carbon credit is allocated to the feedstock producers for soil carbon sequestration, the competition for feedstock and related land use decisions could be different.

Economic Feasibility and GHG Emission Abatement Cost

The inclusion of cellulosic RIN credits has a substantial impact in lowering the break-even SAF price as well as the cost of aviation emission abatement. **Figure 5** depicts the break-even prices[6] for the SAF considering two levels of cellulosic RIN credits (2016-A and 2017-A) along with revenues from the co-products in the Baseline and three carbon credit scenarios. With the 2017-A RIN credit ($2.69 RIN^{-1}), the feedstock processor's break-even for the SAF ($1.65 $gallon^{-1}$) is lower than the market price of the CJF ($1.76 $gallon^{-1}$) regardless of the availability of carbon credits. The SAF remains price-competitive with 2017-A RIN credits after implementing the markup of $0.10 $gallon^{-1}$. If the RIN credit is at the level 2016-A ($1.85 RIN^{-1}), the SAF is not economic competitive with CJF in both the Baseline and the carbon credit scenarios.

Cost associated with the LCA-based GHG emissions reduction using SAF and its co-products from the ATJ-pathway varies across the Baseline and the carbon credit scenarios. With 2017-A RIN credit, the SAF price ($1.75 $gallon^{-1}$) is lower than the market price of the CJF even without the carbon credits, thus no additional cost of GHG emission abatement. However, if the RIN credit remained at 2016-A level, the implicit subsidy from the airlines to the processor is $1.89 $gallon^{-1}$ for the Baseline, which decreases to $1.77, $1.67, and $1.49 $gallon^{-1}$ for the CalCaT-L, CalCaT-H, and EUETS-H scenarios, respectively. Given the 2016-A RIN credit, the implicit cost of abatement for the airlines is $198 $tonCO_2e^{-1}$ for the case of no carbon credits. The estimated abatement cost is within the range of other estimates for SAF produced from oilseed rotation crops and perennial energy crops (Winchester et al., 2013; Winchester et al., 2015). The abatement cost estimates further decreases to $182, $172, and $151 $tonCO_2e^{-1}$ for the CalCaT-L, CalCaT-H, and EUETS-H scenarios, respectively.

To sum up, the findings suggest that the evaluated carbon credits are found influential in reducing aviation GHG emissions while simultaneously improving net welfare of SAF sector. However, the level of RIN credits largely determines the economic feasibility of SAF.

Sensitivity Analysis

As land use competition is critical to the objective of feedstock producers and the SAF processors in this bi-level optimization model (Bai et al., 2012), factors influencing land use choice are further evaluated in the sensitivity analysis. The first key parameter is feedstock procurement price given its directly impact on farmers' profit, and consequently influence on the

[6]The SAF break-even price level without the RIN credits remains above $7.5/gallon which is generally higher compared to the ones estimated in the recent SAF studies (e.g., Tao et al., 2017; Yao et al., 2017) as the minimal profitability expectation of the individual feedstock producers are satisfied given the game-theoretic interaction between the feedstock producers and the processor

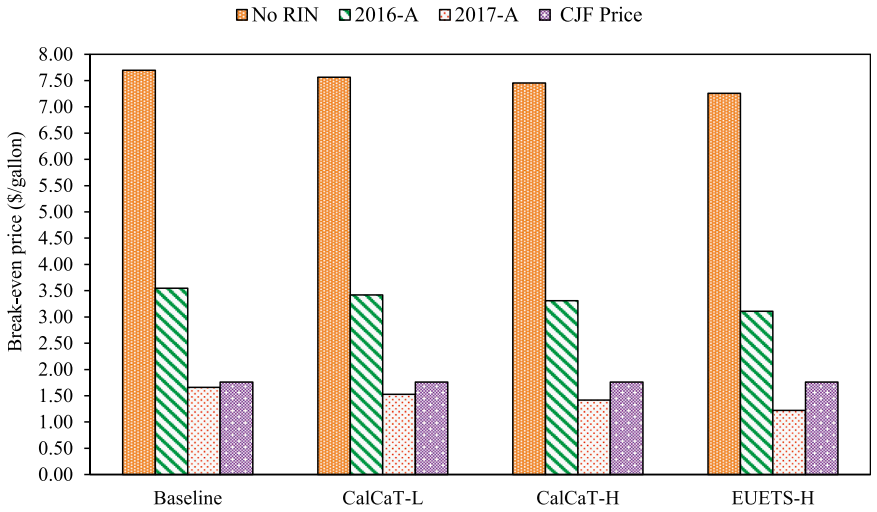

FIGURE 5 | SAF break-even prices with RIN credits and revenues of co-products. Note: 2016-A and 2017-A denote RIN credits for cellulosic biofuel based on average price for 2016 and 2017, respectively. CalCaT-L, CalCaT-H and EUETS-H denote lowest carbon price in the California Cap-and-Trade program, highest carbon price in the California Cap-and-Trade program and highest carbon price in the European Union Emission Trading System, respectively.

location of feedstock supply and the location of biorefineries. The SAF conversion rate is another crucial factor. It determines the required feedstock quantity and resulting land use competition for feedstock supply, and the profit of farmers and SAF producers.

Feedstock Procurement Price Sensitivity Analysis

Two feedstock procurement prices are evaluated in the sensitivity analysis: \$60 ton^{-1} (15% below the baseline feedstock price of \$75 ton^{-1}) and \$90 ton^{-1} (10% above the baseline feedstock price) in presence of cellulosic RIN credits. With a feedstock price of \$60 ton^{-1}, there would not be sufficient number of feedstock producers to supply required feedstock quantity for the SAF demand at the MEM airport. Thus, SAF processor would not operate when offering switchgrass producers \$60 ton^{-1}.

Assuming the feedstock price is offered at \$90 ton^{-1}, the feedstock processor's break-even for SAF is \$4.07 $gallon^{-1}$ with 2016-A RIN credits. With the 2017-A RIN credits, the SAF processor's break-even price is \$2.18 $gallon^{-1}$, making SAF economically infeasible at both RIN credit levels. Considering a \$0.10 $gallon^{-1}$ markup for the SAF processor, the implicit subsidy from the airlines to the processor ranges from \$2.03 to \$2.41 $gallon^{-1}$ in the Baseline and the carbon credit scenarios cases under the provision of 2016-A RIN credits (**Table 6**). Equivalently, the airline's implicit abatement cost is \$251 $tonCO_2e^{-1}$ for the Baseline, which decreases to \$232, \$216, and \$204 $tonCO_2e^{-1}$ for the CalCaT-L, CalCaT-H, and EUETS-H scenarios, respectively. Similarly, under the availability of 2017-A RIN credits, the implicit GHG emissions abatement cost for the airlines is \$54 $tonCO_2e^{-1}$ for the Baseline case and decreases to \$45, \$36, and \$15 $tonCO_2e^{-1}$ for the CalCaT-L, CalCaT-H, and EUETS-H scenarios, respectively.

With the assumed feedstock price of \$90 ton^{-1}, the aggregate net farm income increases and the economic surplus for the feedstock producers is \$59.5 million. Without carbon credits, social cost of aviation GHG emissions is around \$26.0 million and leading to a net supply-chain welfare of approximately -\$280.6 million and -\$23.7 million with 2016-A and 2017-A RIN credits, respectively. Under the availability of CalCaT-L carbon credits, the SAF processor's surplus increases by \$1.6 million, and the airlines' economic surplus increases by \$12 million, while feedstock producers' surplus decreases by \$2.7 million compared to the Baseline. Thus, the net supply-chain welfare for the CalCaT-L scenario increases by \$12.8 with a reduction of \$1.9 million in the internalized costs of aviation GHG emissions relative to the Baseline. Similarly, the net supply-chain welfare increases by \$24.3 and 51.7 million for the CalCaT-H and EUETS-H scenarios, respectively, compared to the Baseline.

Displacing CJF with the ATJ-pathway SAF produced from switchgrass at a price of \$90 ton^{-1} reduces the total LCA-based GHG emissions by 63% under the Baseline. With carbon credits, the total GHG emission reductions from SAF and its co-products reach to 65.5–68% for the three carbon credits scenarios compared to utilizing CJF in the aviation sector.

SAF Conversion Rate Sensitivity Analysis

Sensitivity of SAF conversion rate on economic feasibility of SAF production and associated GHG emission abatement cost is examined with two levels of conversion rate: 24.05 gallons ton^{-1} (10% below the Baseline conversion rate at 26.72 gallons ton^{-1}) and 29.40 gallons ton^{-1} (10% above the Baseline rate) in presence of cellulosic RIN credits. With a conversion rate of 24.05 gallons ton^{-1}, the demand for feedstock increases but there would not be sufficient feedstock producers to supply required feedstock quantity for the SAF demand. Therefore, SAF processor would not be able to operate given the lower conversion rate.

If the conversion rate improves to 29.40 gallons ton^{-1}, the break-even for SAF decreases to \$3.25 $gallon^{-1}$ with 2016-A RIN credits. With a \$0.10 $gallon^{-1}$ markup for the SAF processor, the

TABLE 6 | GHG emission abatement costs with feedstock price at \$90 ton^{-1}.

RIN	Variable	Unit	Baseline	CalCaT-L	CalCaT-H	EUETS-H
2016-A	SAF price	\$ gallon^{-1}	4.17	4.08	3.99	3.80
	Implicit subsidy	\$ gallon^{-1}	2.41	2.32	2.23	2.04
	Abatement cost	\$ tonCO_2e^{-1}	251.4	232.4	216.1	203.7
2017-A	SAF price	\$ gallon^{-1}	2.28	2.19	2.10	1.91
	Implicit subsidy	\$ gallon^{-1}	0.52	0.43	0.34	0.15
	Abatement cost	\$ tonCO_2e^{-1}	54.4	45.2	35.9	15.3

Note: 2016-A and 2017-A denote RIN credits for cellulosic biofuel based on average price for 2016 and 2017, respectively. CalCaT-L, CalCaT-H, and EUETS-H denote lowest carbon price in the California Cap-and-Trade program, highest carbon price in the California Cap-and-Trade program and highest carbon price in the European Union Emission Trading System, respectively.

TABLE 7 | GHG emission abatement costs with conversion yield of 29.40 gallons ton^{-1}.

RIN	Variable	Unit	Baseline	CalCaT-L	CalCaT-H	EUETS-H
2016-A	SAF price	\$ gallon^{-1}	3.35	3.26	3.21	3.11
	Implicit subsidy	\$ gallon^{-1}	1.59	1.50	1.45	1.35
	Abatement cost	\$ tonCO_2e^{-1}	165.03	152.30	144.12	133.78

Note: 2016-A denote RIN credits for cellulosic biofuel based on average price for 2016. CalCaT-L, CalCaT-H, and EUETS-H denote lowest carbon price in the California Cap-and-Trade program, highest carbon price in the California Cap-and-Trade program and highest carbon price in the European Union Emission Trading System, respectively.

implicit subsidy from the airlines to the processor is between \$1.35 and \$1.59 gallon^{-1} in the Baseline and the carbon credit cases under the provision of 2016-A RIN credits (**Table 7**). Equivalently, the implicit GHG emissions abatement cost for the airlines is \$165 tonCO_2e^{-1} under the Baseline, which decreases to \$152, \$144, and \$134 tonCO_2e^{-1} for the CalCaT-L, CalCaT-H, and EUETS-H scenarios, respectively. At the higher conversion rate (29.40 gallons ton^{-1}) and assuming the 2017-A RIN credits, SAF becomes price-competitive to the CJF (\$1.36 vs. \$1.75 gallon^{-1}) even without the carbon credits and does not require additional subsidies for abating GHG emissions. This finding suggests the importance of technology improvement for the commercialization of SAF.

At a 29.40 gallons ton^{-1} conversion rate, the aggregate net farm income decreases given less feedstock demand compared to the Baseline conversion rate, resulting in an economic loss of nearly \$17 million to the feedstock producers. Without carbon credits, social cost of aviation GHG emissions is around \$26.0 million, resulting in a net supply-chain welfare of about -\$211.3 million and \$45.7 million with 2016-A and 2017-A RIN credits, respectively. The net supply-chain welfare under the three carbon credit scenarios increases from \$3.2 million to \$33.4 million compared to the Baseline. Displacing CJF with the ATJ-pathway SAF from switchgrass with a conversion yield of 29.40 gallons ton^{-1} reduces the total LCA-based GHG emissions by 63% under the Baseline. With carbon credits, the total GHG emission reductions from using SAF and its co-products reach to 64.5–66% for the three carbon credits scenarios compared to the CJF usage in the aviation sector.

CONCLUSION

Given the rising interest in reducing GHG emissions from the aviation sector, the implications of costs, GHG emissions, and welfare associated with commercial-scale switchgrass-based SAF under the ATJ-pathway are analyzed. Impacts of SAF production from switchgrass on farmland allocation, processing facility configuration, and GHG emissions are estimated assuming a bi-level Stackelberg model to incorporate possible interaction amongst the participants. Using an *ex-ante* analysis for a case study that targets the MEM, the differences in the optimal decisions of a SAF processor and its contracted feedstock producers are evaluated under a with- and without-hypothetical carbon credit scenarios. The potential impacts of several carbon credit scenarios on the optimal decisions of the feedstock producers and the processor are evaluated in terms of changes in the LCA-based GHG emissions and net supply-chain welfares.

The feedstock producers' annual economic surplus is about \$16.9 million for the no carbon credit case (i.e., Baseline) with the majority of the feedstock producers receiving a margin ranging from 10 to 47% over their opportunity costs of land conversion. Under the case of available carbon credits, the processor's cost decreases by \$17.7 to \$59.5 million annually from the Baseline. Since the SAF processor's optimal decisions includes feedstock producers converting higher opportunity cost crop lands to switchgrass production, a decline of \$5.9 to \$10.5 million annually in the aggregate feedstock producer surplus incures when compared to the Baseline. On the other hand, airlines reduces negative economic surplus because of lower SAF price given carbon and RIN credits. The net supply-chain welfare increases by \$12.7 to \$50.6 million annually under the carbon credit scenarios irrespective of the level of RIN credits.

Replacing the CJF and other fossil fuels with SAF and its co-products from the ATJ-pathway could lead to 62.5–65.0% LCA-based GHG emission reductions. We obtain a range of 31.37–33.37 gCO_2e MJ^{-1} by replacing the CJF and other fossil fuels with SAF and its co-products from the switchgrass-based

ATJ-pathway. The west Tennessee estimates is slightly higher than the values of the International Civil Aviation Organization Carbon Offsetting and Reduction Scheme for International Aviation (2021), which is 28.90 $gCO_2e\ MJ^{-1}$ for LCA-based GHG emission associated with the U.S. switchgrass-based ATJ-pathway.

Utilizing SAF and its co-products is important to achieving IATA's goal of lowering 50% GHG emissions by 2050 relative to the 2005 level. However, the potential environmental benefits would not be achieved without cost. Estimated GHG emission abatement costs, ranging from $151 to 198 $tonCO_2e^{-1}$, imply that the stakeholders of the aviation sector, including policy makers, feedstock and SAF producers, and the airlines, must come together and share the responsibility to help the decarbonization from the sector. In addition, the sensitivity analysis suggests increasing SAF conversion rate from biomass could largely lower the SAF break-even and enhance the competitiveness of SAF over CJF.

DATA AVAILABILITY STATEMENT

The original contributions presented in the study are included in the article/**Supplementary Material**, further inquiries can be directed to the corresponding author.

AUTHOR CONTRIBUTIONS

BS is responsible for the analysis and interpretation of data for the work, and drafting the work; TY initiates the conception of the work and revises the manuscript critically; BE and CB provide approval for publication of the content; all authors agree to be accountable for all aspects of the work.

FUNDING

This work is partially funded by the US Federal Aviation Administration (FAA) Office of Environment and Energy as a part of ASCENT Project 1 under FAA Award Number: 13-C-AJFEUTENN-Amd 5. Any opinions, findings, and conclusions or recommendations expressed in this material are those of the authors and do not necessarily reflect the views of the FAA or other ASCENT sponsor organizations.

SUPPLEMENTARY MATERIAL

The Supplementary Material for this article can be found online at: https://www.frontiersin.org/articles/10.3389/fenrg.2021.775389/full#supplementary-material

REFERENCES

Agusdinata, D. B., Zhao, F., Ileleji, K., and DeLaurentis, D. (2011). Life Cycle Assessment of Potential Biojet Fuel Production in the United States. *Environ. Sci. Technol.* 45 (21), 9133–9143. doi:10.1021/es202148g

Alternative Fuels Data Center (AFDC) (2017). *Alternative Fuel Price Report*. Washington, DC: U.S. Department of Energy. Retrieved from https://www.afdc.energy.gov/uploads/publication/alternative_fuel_price_report_oct_2017.pdf.

Argone National Laboratory (2017). The Greenhouse Gases, Regulated Emissions, and Energy Use in Transportation Model (GREET). Retrieved from http://www.transportation.anl.gov/publications/index.html.

Bai, Y., Ouyang, Y., and Pang, J.-S. (2012). Biofuel Supply Chain Design under Competitive Agricultural Land Use and Feedstock Market Equilibrium. *Energ. Econ.* 34 (5), 1623–1633. doi:10.1016/j.eneco.2012.01.003

Bann, S. J., Malina, R., Staples, M. D., Suresh, P., Pearlson, M., Tyner, W. E., et al. (2017). The Costs of Production of Alternative Jet Fuel: A Harmonized Stochastic Assessment. *Bioresour. Techn.* 227, 179–187. doi:10.1016/j.biortech.2016.12.032

Boyer, C. N., Roberts, R. K., English, B. C., Tyler, D. D., Larson, J. A., and Mooney, D. F. (2013). Effects of Soil Type and Landscape on Yield and Profit Maximizing Nitrogen Rates for Switchgrass Production. *Biomass and Bioenergy* 48, 33–42. doi:10.1016/j.biombioe.2012.11.004

Boyer, C. N., Tyler, D. D., Roberts, R. K., English, B. C., and Larson, J. A. (2012). Switchgrass Yield Response Functions and Profit-Maximizing Nitrogen Rates on Four Landscapes in Tennessee. *Agron.j.* 104 (6), 1579–1588. doi:10.2134/agronj2012.0179

Brown, N. (2021). *SAF Interagency Working Group Updates. CAAFI Virtual Mini-Symposium*. June 1-3.

Bureau of Transportation Statistics (BTS) (2016a). *Airlines and Airports*. Washington, DC: U.S. Department of Transportation. Retrieved from https://www.transtats.bts.gov/NewAirportList.asp?xpage=airports.asp&flag=FACTS.

California Carbon Dashboard (2018). Carbon Price. Retrieved from http://calcarbondash.org/csv/output.csv.

Chen, X., Huang, H., Khanna, M., and Önal, H. (2011). *The Intended and Unintended Effects of US Agricultural and Biotechnology Policies*. University of Chicago Press, 223–267. doi:10.3386/w16697Meeting the Mandate for Biofuels: Implications for Land Use, Food, and Fuel Prices

Commercial Aviation Alternative Fuels Initiative (CAAFI) (2016). 2016 Biennial General Meeting. Retrieved from http://caafi.org/information/pdf/Biennial_Meeting_Oct252016_Opening_Remarks.pdf.

Congressional Research Service (2013). Renewable Fuel Standard: Overview and Issues. Retrieved from https://www.ifdaonline.org/IFDA/media/IFDA/GR/CRS-RFS-Overview-Issues.pdf.

Elgowainy, A., Han, J., Wang, M., Carter, N., Stratton, R., Hileman, J., et al. (2012). *Life-cycle Analysis of Alternative Aviation Fuels in GREET*. Argonne, IL: Argonne National Laboratory (ANL.

Grote, M., Williams, I., and Preston, J. (2014). Direct Carbon Dioxide Emissions from Civil Aircraft. *Atmos. Environ.* 95, 214–224. doi:10.1016/j.atmosenv.2014.06.042

Gümüş, Z. H., and Floudas, C. A. (2005). Global Optimization of Mixed-Integer Bilevel Programming Problems. *Comput. Manage. Sci.* 2 (3), 181–212.

Han, J., Tao, L., and Wang, M. (2017). Well-to-wake Analysis of Ethanol-To-Jet and Sugar-To-Jet Pathways. *Biotechnol. Biofuels* 10 (1), 21. doi:10.1186/s13068-017-0698-z

Intergovernmental Panel on Climate Change. (IPCC) (2014). *synthesis report, contribution of working groups I, II and III to the Fifth assessment report of the intergovernmental panel on climate change*. Editors R. K. Pachauri and L. A. Meyer. Geneva, Switzerland: IPCC. Retrieved from https://www.ipcc.ch/site/assets/uploads/2018/02/AR5_SYR_FINAL_SPM.pdf.

Intergovernmental Panel on Climate Change. (IPCC) (2018). Summary for Policymakers of IPCC Special Report on Global Warming of 1.5°C. Retrieved from https://www.ipcc.ch/2018/10/08/summary-for-policymakers-of-ipcc-special-report-on-global-warming-of-1-5c-approved-by-governments/.

International Air Transport Association (IATA) (2017). Fact Sheet: Alternative Fuels. Retrieved from https://www.iata.org/pressroom/facts_figures/fact_sheets/Documents/fact-sheet-alternative-fuels.pdf.

International Air Transport Association (IATA) (2015). IATA Sustainable Aviation Fuel Roadmap. Retrieved from https://www.iata.org/whatwedo/environment/Documents/safr-1-2015.pdf.

International Civil Aviation Organization (ICAO) (2021). Carbon Offsetting and Reduction Scheme for International Aviation (CORSIA). Retrieved from https://www.icao.int/environmental-protection/CORSIA/Documents/ICAO%20document%2006%20-%20Default%20Life%20Cycle%20Emissions%20-%20March%202021.pdf.

Jager, H. I., Baskaran, L. M., Brandt, C. C., Davis, E. B., Gunderson, C. A., and Wullschleger, S. D. (2010). Empirical Geographic Modeling of Switchgrass Yields in the United States. *GCB Bioenergy* 2 (5), 248–257. doi:10.1111/j.1757-1707.2010.01059.x

Lim, M. K., and Ouyang, Y. (2016). "Biofuel Supply Chain Network Design and Operations," in *Environmentally Responsible Supply Chains*. *Springer Series in Supply Chain Management*. Editor A. Atasu (Cham: Springer), Vol. 3, 143–162. doi:10.1007/978-3-319-30094-8_9

Luo, Y., and Miller, S. (20132013). A Game Theory Analysis of Market Incentives for US Switchgrass Ethanol. *Ecol. Econ.* 93, 42–56. doi:10.1016/j.ecolecon.2013.04.015

Melissae Fellet, M. (2016). Aviation Industry Hopes to Cut Emissions with Jet Biofuel. *C&EN Glob. Enterp* 94 (37), 16–18. doi:10.1021/cen-09437-scitech1

Nordhaus, W. D. (2017). Revisiting the Social Cost of Carbon. *Proc. Natl. Acad. Sci. USA* 114 (7), 1518–1523. doi:10.1073/pnas.1609244114

O'Connell, A., Kousoulidou, M., Lonza, L., and Weindorf, W. (2019). Considerations on GHG Emissions and Energy Balances of Promising Aviation Biofuel Pathway. *Renew. Sust. Energ. Rev* 101, 504–515.

Pearlson, M. (2020). Personal Communication.

Perlack, R. D., Eaton, L. M., Turhollow, A. F., Jr, Langholtz, M. H., Brandt, C. C., Downing, M. E., et al. (2011). US Billion-Ton Update: Biomass Supply for a Bioenergy and Bioproducts Industry.

Reimer, J. J., and Zheng, X. (2017). Economic Analysis of an Aviation Bioenergy Supply Chain. *Renew. Sust. Energ. Rev.* 77, 945–954. doi:10.1016/j.rser.2016.12.036

Renewable Fuels Association (RFA) (2017). Renewable Fuel Standard Program: Standards for 2018 and Biomass-Based Diesel Volume for 2019. Retrieved from http://www.ethanolrfa.org/wp-content/uploads/2017/08/RFA-Comments_2018-RVO-Proposed-Rule_Final.pdf.

Intergovernmental Panel on Climate Change. (IPCC) (2014). in Climate Change 2014: Synthesis Report, Contribution of Working Groups I, II and III to the Fifth Assessment Report of the Intergovernmental Panel on Climate Change *[Core Writing Team*. Editors R. K. Pachauri and L. A. Meyer (Geneva, Switzerland: IPCC). Retrieved from https://www.ipcc.ch/site/assets/uploads/2018/02/AR5_SYR_FINAL_SPM.pdf.

Rosenthal, E. (2008). *GAMS-A User's Guide*. Washington, DC: GAMS Development Corporation.

Sinha, A., Malo, P., and Deb, K. (2018). A Review on Bilevel Optimization: from Classical to Evolutionary Approaches and Applications. *IEEE Trans. Evol. Computat.* 22, 276–295. doi:10.1109/tevc.2017.2712906

Staples, M. D., Malina, R., Olcay, H., Pearlson, M. N., Hileman, J. I., Boies, A., et al. (2014). Lifecycle Greenhouse Gas Footprint and Minimum Selling price of Renewable Diesel and Jet Fuel from Fermentation and Advanced Fermentation Production Technologies. *Energy Environ. Sci.* 7 (5), 1545–1554. doi:10.1039/c3ee43655a

Staples, M. D., Malina, R., Suresh, P., Hileman, J. I., and Barrett, S. R. H. (2018). Aviation CO2 Emissions Reductions from the Use of Alternative Jet Fuels. *Energy Policy* 114, 342–354. doi:10.1016/j.enpol.2017.12.007

Tao, L., Markham, J. N., Haq, Z., and Biddy, M. J. (2017). Techno-economic Analysis for Upgrading the Biomass-Derived Ethanol-To-Jet Blendstocks. *Green. Chem.* 19 (4), 1082–1101. doi:10.1039/c6gc02800d

U.S. Energy Administration System (EIA) (2017). Gasoline and Disesl Fuel Update. https://www.eia.gov/energyexplained/index.php?page=gasoline_factors_affecting_prices.

U.S. Environmental Protection Agency. (EPA) (2017). Climate Change: Basic Information. https://19january2017snapshot.epa.gov/climatechange/climate-change-basic-information_.html.

U.S. Federal Aviation Administration (FAA) (2017). History of Alternative Jet Fuel Use. https://www.faa.gov/nextgen/where_we_are_now/nextgen_update/images/pp_ee_sb1_body1.png.

Wang, M., Han, J., Dunn, J. B., Cai, H., and Elgowainy, A. (2012). Well-to-wheels Energy Use and Greenhouse Gas Emissions of Ethanol from Corn, Sugarcane and Cellulosic Biomass for US Use. *Environ. Res. Lett.* 7 (4), 045905. doi:10.1088/1748-9326/7/4/045905

Wang, M., Huo, H., and Arora, S. (2011). Methods of Dealing with Co-products of Biofuels in Life-Cycle Analysis and Consequent Results within the U.S. Context. *Energy Policy* 39 (10), 5726–5736. doi:10.1016/j.enpol.2010.03.052

Winchester, N., Malina, R., Staples, M. D., and Barrett, S. R. H. (2015). The Impact of Advanced Biofuels on Aviation Emissions and Operations in the U.S. *Energ. Econ.* 49, 482–491. doi:10.1016/j.eneco.2015.03.024

Winchester, N., McConnachie, D., Wollersheim, C., and Waitz, I. A. (2013). Economic and Emissions Impacts of Renewable Fuel Goals for Aviation in the US. *Transportation Res. A: Pol. Pract.* 58, 116–128. doi:10.1016/j.tra.2013.10.001

Wright, L., and Turhollow, A. (2010). Switchgrass Selection as a "model" Bioenergy Crop: A History of the Process. *Biomass and Bioenergy* 34, 851–868. doi:10.1016/j.biombioe.2010.01.030

Yao, G., Staples, M. D., Malina, R., and Tyner, W. E. (2017). Stochastic Techno-Economic Analysis of Alcohol-To-Jet Fuel Production. *Biotechnol. Biofuels* 10 (1), 18. doi:10.1186/s13068-017-0702-7

Yao, H., Mai, T., Wang, J., Ji, Z., Jiang, C., and Qian, Y. (2019). Resource Trading in Blockchain-Based Industrial Internet of Things. *IEEE Trans. Ind. Inf.* 15 (6), 3602–3609. doi:10.1109/tii.2019.2902563

Yu, T. E., English, B. C., He, L., Larson, J. A., Calcagno, J., Fu, J. S., et al. (2016). Analyzing Economic and Environmental Performance of Switchgrass Biofuel Supply Chains. *Bioenerg. Res.* 9 (2), 566–577. doi:10.1007/s12155-015-9699-6

Zhao, X., Brown, T. R., and Tyner, W. E. (2015). Stochastic Techno-Economic Evaluation of Cellulosic Biofuel Pathways. *Bioresour. Techn.* 198, 755–763. doi:10.1016/j.biortech.2015.09.056

Conflict of Interest: The authors declare that the research was conducted in the absence of any commercial or financial relationships that could be construed as a potential conflict of interest.

frontiers in Energy Research

ORIGINAL RESEARCH
published: 10 December 2021
doi: 10.3389/fenrg.2021.770479

Biofuel Discount Rates and Stochastic Techno-Economic Analysis for a Prospective Pennycress (Thlaspi arvense L.) Sustainable Aviation Fuel Supply Chain

Carlos Omar Trejo-Pech, James A. Larson, Burton C. English and T. Edward Yu*

Agricultural and Resource Economics Department, University of Tennessee, Knoxville, TN, United States

OPEN ACCESS

Edited by:
William Goldner, United States Department of Agriculture (USDA), United States

Reviewed by:
Obulisamy Parthiba Karthikeyan, University of Houston, United States
Pau Loke Show, University of Nottingham Malaysia Campus, Malaysia

****Correspondence:***
Carlos Omar Trejo-Pech
ctrejope@utk.edu

Specialty section:
This article was submitted to Bioenergy and Biofuels, a section of the journal Frontiers in Energy Research

Received: *03 September 2021*
Accepted: *22 November 2021*
Published: *10 December 2021*

Citation:
Trejo-Pech CO, Larson JA, English BC and Yu TE (2021) Biofuel Discount Rates and Stochastic Techno-Economic Analysis for a Prospective Pennycress (Thlaspi arvense L.) Sustainable Aviation Fuel Supply Chain. Front. Energy Res. 9:770479. doi: 10.3389/fenrg.2021.770479

The international aviation industry has the goal to gradually reduce carbon emissions mainly by using sustainable aviation fuel (SAF). However, currently SAF cannot be produced at competitive prices relative to petroleum-based jet fuel. Pennycress is a crop whose oilseed could be used as a relatively low-cost feedstock to produce SAF, potentially benefiting farmers and the environment. This stochastic techno-economic analysis (TEA) studies an enterprise buying pennycress oilseed from farmers, extracting the bio-oil and selling it to a biorefinery that converts bio-oil into SAF. Maximum buying prices (MBP)—prices that yield a zero net present value—the crushing enterprise could pay farmers for pennycress oilseed are estimated. To conduct the analysis, discount rates are estimated based on financial data of biofuel firms, thus providing a realistic benchmark to evaluate profitability and feedstock buying prices. Estimated risk-adjusted discount rates vary between 12 and 17%, above rates typically used in similar valuations. Estimated stochastic MBP range between 10.18 and 11.73 ¢ pound^{-1}, which is below the price at which farmers are willing to plant pennycress, according to recent research. By considering the crushing facility's inherent cash flow structure and risk, the distributions of stochastic modified internal rate of return suggest the crushing enterprise could be economically attractive at a 14% discount rate, our most likely estimate. However, between 11 and 17% times the cash flow model is simulated, the firm falls under financial distress. Overall, the findings suggest potential barriers for deployment of a SAF supply chain without governmental incentives or related policies.

Keywords: sustainable aviation fuel supply, profitability and risk, investment hurdle rates, stochastic techno-economic analysis, pennycress supply chain, biofuel discount rates

Abbreviations: ~, Indicates a stochastic variable; CAPEX, Capital expenditures; CAPM, Capital asset pricing model; DCF, Discounted cash flow; DDGS, Distillers' dried grain with solubles; FCF, Free cash flow; HEFA, Hydroprocessed esters and fatty acids; MBP, Maximum buying price; MIRR, Modified internal rate of return; MSP, Minimum selling price; NPV, Net present value; PERT, Program evaluation and review technique; TEA, Techno-economic analysis; USDA, United States Department of Agriculture; WACC, Weighted average cost of capital.

HIGHLIGHTS

- o This study estimates discount rates to apply in biofuel valuations based on actual financial data from publicly traded US biofuel firms.
- o Most likely, lower bound, and upper bound discount rates are estimated at 14, 12, and 17%, respectively.
- o The study also estimates maximum buying prices a prospective crushing enterprise could pay farmers for pennycress oilseed feedstock
- o Stochastic maximum buying prices range between 10.18 and 11.73 ¢ pound^{-1}, which is below the price at which farmers are willing to plant pennycress, according to recent research
- o By considering the crushing facility's inherent cash flow structure and risk, the distributions of stochastic modified internal rate of return suggest the crushing enterprise could be economically attractive at a 14% discount rate. However, between 11 and 17% the times the cash flow model is simulated, the firm falls under financial distress.
- o Challenges for the establishment of a crushing facility, and in consequence deployment of the SAF supply chain in Southern US, are discussed in this article.

1 INTRODUCTION

The international aviation industry is motivated to reduce their greenhouse gas footprint over the next few decades. Policies such as the United Nations International Civil Aviation Organization's Carbon Offsetting and Reduction Scheme for International Aviation are mandating reductions in carbon emissions for commercial aviation (ICAO, 2021). Taking 2005 as the baseline, the industry is expected to reduce 50% of carbon emissions by 2050 (Hileman et al., 2013; Khanal and Shah, 2021; Tanzil et al., 2021). Factors such as improved fuel consumption and infrastructure are important, but the use of biomass derived, or sustainable aviation fuel (SAF) is projected to be the most important factor driving carbon reduction in aviation (Wang et al., 2019; Khanal and Shah, 2021). SAF is a substitute or complementary product for fossil jet fuels, produced from a variety of feedstocks including waste organics, agricultural residues, and crops cultivated for human food consumption (Air BP, 2021; Eswaran et al., 2021; SkyNRG, 2021). Currently available SAF production technologies in the US have been evaluated. Tanzil et al. (2021) found that hydroprocessed esters and fatty acids (HEFA) is the most competitive current technology for SAF production compared to five lignocellulose-based technologies evaluated. While SAF production volume in the US is still limited, several biorefineries are producing it at demonstration, pilot, and commercial scale (Trejo-Pech et al., 2019; Khanal and Shah, 2021; Tanzil et al., 2021). One of the current challenges is to produce SAF at prices competitive with fossil-based jet fuel. SAF cost of production is estimated around three times higher than conventional jet fuel cost (Khanal and Shah, 2021), particularly high when crops that are demanded in food markets are used as feedstock to produce SAF. Promising conversion technologies and the use of dedicated energy crops—low production cost crops grown for energy production purposes mainly and not for food—as feedstock are likely to reduce the SAF vs. fossil jet fuel price gap and accelerate SAF adoption. This study analyzes Pennycress (*Thlaspi arvense L.*), an emerging dedicated energy crop whose oilseed has the potential to be a relatively low-cost feedstock to produce SAF.

Pennycress has the potential to provide both economic benefits to farmers and ecosystem benefits. Planting pennycress does not require additional land because it could be incorporated as a winter cover crop in corn-soybean rotations. Typically, pennycress would be grown during the fall-to-spring after harvesting corn in year one, and it would be harvested in year two before cultivating soybean. This production system would result in three, rather than two, cash crops in 2 years, economically benefiting farmers.[1] The use of pennycress as a cover crop potentially reduces land nutrients losses, suppresses weed, reduces soil erosion, and provides collateral ecosystem benefits such as producing spring early-season nectar and pollen for beneficial insects (Eberle et al., 2015; Thomas et al., 2017; Marks et al., 2021). Marks et al. (2021) highlight the importance of incorporating pennycress in farmland remaining fallow during the fall noting that in US Midwest corn-soybean rotations are planted on around 175 million acres but winter cover crops are incorporated in less than 5% of those lands because traditional cover crops are not highly profitable and the environmental benefits are not obvious to farmers. Regarding the potential of pennycress as a bioenergy crop, oilseed from pennycress has the chemical and physical properties to be converted into SAF meeting the quality specifications by the United States American Society for Testing and Materials (Moser et al., 2009; Fan et al., 2013; Moser et al., 2015). Furthermore, pennycress' oil yield, from oilseed to reactor-ready feedstock, has been estimated to be comparable to other oilseeds such as canola and camelina (Mousavi-Avval and Shah, 2020). However, deploying a pennycress oilseed to SAF supply chain presents some challenges such as high oil yield variability (Mousavi-Avval and Shah, 2020), moderate to low willingness of farmers to plant pennycress (Zhou et al., 2021), and appropriate farmers-biorefinery agreements to incentivize oilseed production for SAF (McCollum et al., 2021). Despite these challenges, pennycress is a very promising feedstock for the establishment of a SAF supply chain potentially yielding economic benefits and ecosystem services and this is the reason we selected this crop to conduct a techno-economic analysis (TEA).

Recently published TEA studying the economic viability of SAF focusing on promising feedstocks other than pennycress include Eswaran et al. (2021), Kubic et al. (2021), and McCollum et al. (2021). Eswaran et al. (2021) estimated the minimum selling price (MSP) of SAF produced with carinata oil, soybean oil, yellow grease, and brown grease at $1.32, $1.50, $1.19, and

[1]Given the relatively low level of inputs required to produce pennycress under the corn-pennycress-soybean rotation, growing pennycress is likely to produce marginal profits to farmers (Markel et al., 2018; Mousavi-Avval and Shah, 2020). Prospective farmers adopting pennycress have reported risks and challenges though (Mousavi-Avval and Shah, 2020; Zhou et al., 2021).

$1.00 L^{-1} respectively; all these prices above the average price of petroleum-based jet fuel from 2008 to 2018, at $0.60 L^{-1}. Similarly, Kubic et al. (2021) estimated that the MSP of SAF produced with paper from municipal solid waste is lower than SAF produced with corn stover, but still not competitive with petroleum-based jet fuel. They estimated paper to SAF process with enzymatic hydrolysis' MSP at $1.05 L^{-1} compared to a $0.54 L^{-1} petroleum-based jet fuel target price. McCollum et al. (2021) TEA inquiries how contractual conditions between farmers and biorefineries, in 11 states in western US, may impact farmers' willingness to supply canola, another promising feedstock, for sustainable SAF production. They find that the likelihood of a biorefinery obtaining sufficient supply of canola is most feasible in Kansas and North Dakota, but across all states, canola prices need to considerably increase from typical levels—which may not be realistic in some cases—to induce enough supply. Their findings suggest that biorefineries may need to consider compensating farmers for a share of the variable cost of production to ensure sufficient oilseed feedstock supply (e.g., offer favorable contract prices above what market prices may suggest). The aforementioned articles and previous research highlight the relevance of feedstocks in general for SAF production, either in terms of 1) the high portion of feedstock cost relative to total cost of SAF production, 2) the high sensitivity of SAF MSP to feedstock cost, or 3) the barriers of obtaining enough feedstock supply at competitive prices to deploy a viable SAF supply chain.

TEA specific to pennycress for SAF production include Trejo-Pech et al. (2019), Stevens and Taheripour (2020), Mousavi-Avval and Shah (2020), and Mousavi-Avval and Shah (2021). Trejo-Pech et al. (2019) evaluate enterprise budgets for prospective farmers and processors converting pennycress oilseed to bio-oil and meal cake (e.g., crushers), and identify potential locations for crushing and biorefineries facilities supplying SAF to Nashville, Tennessee international airport. Their analysis compares MSP for pennycress oilseed at the farm level and maximum buying price (MBP) at the crushing facility to make both enterprises economically viable. Stevens and Taheripour (2020) analyze a prospective SAF biorefinery located in US Midwest. Stevens and Taheripour (2020) use crushing facility parameters from Trejo-Pech et al. (2019) to estimate the crushing facility's MSP in comparison with MBP the biorefinery could offer. In other words, while Trejo-Pech et al. (2019) focuses the analysis on the interconnection between farmers and processors, Stevens and Taheripour (2020) analyze the price relationship between processors and biorefineries. Stevens and Taheripour (2020) also provide scenarios that may make pennycress SAF production economically viable. Mousavi-Avval and Shah (2020) focus their TEA on the production, harvest, and post-harvest logistics of pennycress supplying a SAF biorefinery, providing anticipated production resources needed for one prospective biorefinery at commercial scale located in Ohio. Mousavi-Avval and Shah (2021) extend Mousavi-Avval and Shah (2020) considering pennycress oilseed handling and conditioning, oil extraction and hydroprocessing SAF conversion, estimating SAF's MSP at $1.20 L^{-1} in Ohio, a price comparable to other promising oilseeds but still below the price of petroleum-based jet fuel.

Our study builds on the crushing facility model of Trejo-Pech et al. (2019) by incorporating risk components in the analysis, as explained next. In Trejo-Pech et al. (2019) pennycress supply chain model, farmers produce pennycress oilseed as a winter crop incorporated into corn-pennycress-soybean rotation at an estimated cost of 8.0 ¢ pound^{-1} at the crushing facility plant gate. The crushing facility purchases pennycress oilseed and converts it to bio-oil and pennycress meal cake providing capital investors an assumed 12.5% expected rate of return over investment if the crushing facility pays farmers 10.8 ¢ pound^{-1} for oilseed the year operations start and sells reactor-ready feedstock at soybean forecast prices by the USDA and meal cake at distillers' dried grain with solubles historical prices (partial cash flow projections are provided in the **Appendix**, with the 10.8 ¢ pound^{-1} cost of feedstock shown in line 3). Buying oilseed above 10.8 ¢ pound^{-1}, the MBP, would yield on average returns on investment below the crushing facility capital investors' expectation and would discourage reactor-ready feedstock supply. Three crushing facilities are projected to supply bio-oil to one Aviation Sustainability Center's HEFA hypothetical biorefinery as designed by Tanzil et al. (2021), which would in turn supply SAF to the Nashville International Airport. Further analysis of the MBP of pennycress oilseed is relevant particularly because pennycress is currently not planted for commercial purposes and the actual cost of production at deployment time may differ from current budgets. To illustrate this, Mousavi-Avval and Shah (2020) estimated that MSP of field pennycress in Ohio varies from 8.5 to 11.5 ¢ pound^{-1}; at the high-end of this budget, prospective investors may not invest in the pennycress crushing enterprise. In addition, the analysis in Trejo-Pech et al. (2019) is based on deterministic parameters and an assumed discount rate. In this study the work in Trejo-Pech et al. (2019) is extended by incorporating two relevant risk components into the analysis: 1) estimating the discount rate to value the crushing facility investment (i.e., estimating a rate of return based on investors' expectations instead of assuming a 12.5% discount rate), and 2) performing stochastic simulation of selected sensitive parameters affecting expected profitability of the crushing facility. Our study focuses on the crushing facility and considers field pennycress oilseed production cost and HEFA biorefinery demand as exogenous to the crushing enterprise. Our analysis provides additional insights regarding potential MBPs for oilseed pennycress and permits to compare these values with recent survey data on willingness to plant pennycress in Southern US. In addition, this is the first study that estimates the discount rate based on actual financial data from established biofuel firms.

According to finance theory, the discount rate is a hurdle rate for investment decisions, meaning that it provides a clear-cut decision rule: entrepreneurs would not establish the abovementioned crushing facility if they had to pay farmers more than 10.8 ¢ pound^{-1} for oilseed because their expected annual return would be lower than 12.5% given assumed projected output prices. However, in practice, the discount rate is used more as a reference for investment decision making than as a rigid hurdle for investment. This is because

the estimation of a discount rate involves several inputs that require projections based on historical values and rely on models intended to capture capital investors' *expectations* according to the degree of risk borne. Thus, the first objective of this paper is to determine the impacts of risk-adjusted discount rates on the financial performance—particularly through MBP of field pennycress—of the prospective crushing facility featured in Trejo-Pech et al. (2019). For this objective, methods used by financial practitioners (Graham and Harvey, 2001; Jacobs and Shivdasani, 2012; Brotherson et al., 2013; Graham and Harvey, 2018) and financial data from companies operating in bioenergy-related industries are employed.

It is common practice in bioenergy TEA studies to not disclose assumptions and/or frameworks applied to estimate the discount rates used in valuations.[2] Yet, the importance of the discount rate in prospective bioenergy investment has been suggested in previous research. For instance, Lamers et al. (2015) argue that biorefineries are highly risky investments due to variability of feed stock supply and show that the minimum selling price of fuel produced is highly sensitive to the discount rate employed in biorefinery valuations. The framework employed in this paper to estimate the discount rate allows for a more insightful sensitivity analysis than analysis conducted on an assumed point-estimate discount rate value. Moreover, the discount rates estimated in this paper could be used in other TEAs evaluating prospective bio-energy investment, given that estimations are done for a variety of biofuel companies.

The second objective of this study is to evaluate the effects of stochastic cash flows on the financial performance of the crushing facility. Like with to the first objective, we focus the analysis on breakeven or MBPs. Trejo-Pech et al. (2019) analysis relies on deterministic production and price parameters and on one-way sensitivity analysis, whereas in this study selected parameters at which the crushing facility's financial performance metrics are highly sensitive to, vary stochastically. Pennycress bio-oil prices, pennycress meal prices, and feedstock to bio-oil conversion rate are modeled with stochastic distribution dynamics applied in previous bioenergy studies (Petter and Tyner, 2014; Zhao et al., 2015; Zhao et al., 2016). Outcomes of the stochastic analysis include distributions of crushing facility's expected return on investment given alternative estimated discount rates, potential maximum oilseed buying prices for the crushing facility to financially breakeven, and stochastic sensitivity analysis of selected variables. Overall, our analysis combining estimated discount rates and stochastic simulation provide a more robust assessment of profitability and risk for a prospective crushing facility within a potential SAF supply chain.

[2]While most TEA studies provide detailed operating cost budgets, the discount rate at which projected cash flows are discounted is generally assumed to be exogenous to the firm or project under evaluation and no details on the assumptions for its estimation are provided

2 BACKGROUND AND LITERATURE REVIEW

2.1 Discounted Cash Flow, the Weighted Average Cost of Capital, and Hurdle Rates

The finance literature seems to concur that most US firms employ a discounted cash flow (DCF) framework when evaluating potential long-term investments. Jagannathan et al. (2016) report that over 90% of surveyed chief financial officers selected a DCF-related financial metric—net present value, adjusted present value, internal rate of return or profitability index—as one of their top two metrics used for investment evaluation. Another study report that between 80 and 90% of surveyed members of the Association for Financial Professionals employ DCF to analyze prospective investment (Jacobs and Shivdasani, 2012). Earlier studies also show that most financial managers rely on DCF as the analytical tool to support their investment decisions (Baker et al., 2010). Unsurprisingly, DCF is widely applied in bioenergy TEAs as well (Campbell et al., 2018).

DCF-related metrics compare investment and projected free cash flow (FCF) values, both expressed in present value terms. To account not only for inflation but also for capital investors' expected returns, projected FCFs are discounted by a risk-adjusted opportunity cost of capital. Most of the abovementioned survey-based studies report that financial managers use the firm's estimated weighted average cost of capital (WACC) as a reference or baseline to define the discount rate used for investment evaluations. The WACC considers the mix of capital debt (D) and capital equity (E), expected rates of return by debt and equity capital providers (Rd and Re), and an income tax rate (t) that accounts for the fact that interest payments are tax deductible:

$$WACC = \frac{D}{D+E} \times Rd \times (1-t) + \frac{E}{D+E} \times Re. \quad (1)$$

Further, most surveyed managers indicate they apply the capital asset pricing model (CAPM), by Sharpe (1964), to estimate equity holders' expected rate of return, Re in **Eq. 1**, or opportunity cost of equity. For instance, Graham and Harvey (2001) report that more than 70% of financial managers responding a survey indicate applying CAPM to estimate Re. CAPM is specified by:

$$Re = rf + \beta \times MRP, \quad (2)$$

where rf is the risk-free rate, proxied by a US government issued free of default security, and MRP is the market risk premium, defined as the expected return by a market portfolio minus the risk-free rate. The firm's beta (β) is obtained by regressing the firm's historical stock or equity returns on the corresponding market risk premia. According to the CAPM, risk of an individual firm's equity is measured by its beta, which estimates the firm stock price's sensitivity to overall price movements in the market, the latter represented by a diversified market portfolio (Sharpe, 1964; Blume and Friend, 1973).

Estimating a risk-adjusted discount rate presents a couple of challenges. First, no consensus exists among financial practitioners regarding the specific proxies or inputs to use

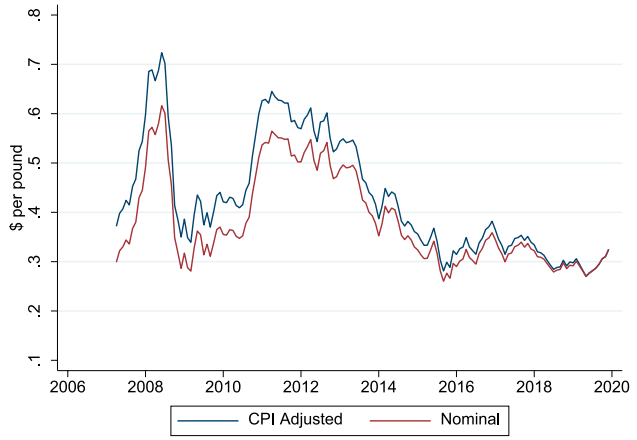

FIGURE 1 | Soybean oil prices, April 2007 to December 2019. Note: **Figure 1** provides nominal and consumer price index (CPI) adjusted prices expressed as of the end of 2019.

when estimating WACC and CAPM. Second, practitioners appear to apply a discount rate that is higher than their estimated WACC. In other words, even though some financial managers estimate the firm's WACC, they use it as a reference and systematically chose a higher hurdle rate to evaluate prospective investments (Jagannathan et al., 2016; Graham and Harvey, 2018). Particular to the energy industry, the anomalous use of high discount rates in the evaluation of energy efficient projects has also been raised in previous research (Howarth and Sanstad, 1995; Thompson, 1997). This is puzzling behavior by financial practitioners because, as **Eqs 1**, **2** show, WACC captures the cost of each capital or financing component according to its risk level and corresponding expected return. This may also be problematic for firm decision making since managers may forgo economically attractive positive net present value (NPV) projects by choosing artificially high discount rates. Challenges of estimating the WACC through CAPM for the prospective pennycress crushing facility are explained in the methods section of this paper.

To recap, a framework including DCF financial metrics that considers WACC and CAPM is well known and applied by financial practitioners. In this study we estimate WACC through CAPM and propose discount rates to use when valuing biofuel investments. As an example, we apply these discount rates to the prospective crushing facility presented in Trejo-Pech et al. (2019), a firm purchasing pennycress oilseed and converting it to bio-oil and pennycress meal cake.

2.2 Stochastic Simulation

Most biofuel TEA studies are conducted with deterministic models. While deterministic TEAs are usually analyzed by providing an array of relevant scenarios on which selected variables are changed while the rest of variables in the model are kept constant, stochastic models have the potential to better capture and model risk inherent on historical data. This is because instead of using only point-estimates for relevant variables, stochastic models simulate potential values drawn from a series of historical data, according to a statistical distribution and iterate the model thousands of times to provide expected values or values at other percentile of the distribution.

Stochastic simulation becomes particularly important in models relying on highly uncertain variables. As an example, deployment of the pennycress-based SAF supply chain of interest in this study assumes that pennycress bio-oil will be sold at soybean oil prices given the similarities between the oils extracted from these two crops (Moser et al., 2009; Fan et al., 2013) and because a market for pennycress bio-oil is not developed yet. **Figure 1** shows that while soybean oil prices have been relatively stable lately, they have been highly volatile from a mid-term and long-term perspective. In this study, this uncertainty is incorporated into the analysis by projecting stochastic bio-oil prices (and other variables) to the crushing facility DCF model supplying bio-oil to the SAF supply chain. The stochastic simulation approach taken in this study is similar to other biofuel stochastic TEAs including Jeong et al. (2020), Lan et al. (2020), McGarvey and Tyner (2018), Yao et al. (2017), and Zhao et al. (2015).

3 METHODS

Coupling the estimation of WACC with CAPM is most suitable for publicly traded companies. CAPM was conceived for publicly traded firms because it requires firm's market stock prices as inputs to estimate the firm's beta risk factor. However, private firms such as the prospective crushing facility analyzed in this study can use estimated WACC of comparable publicly traded firms as a proxy for their own WACC. Brotherson et al. (2013) for instance, document that 68% of surveyed financial managers directly or indirectly benchmark and adjust their estimated market betas (and by extension their WACC given the connection between **Eqs 1**, **2**) with betas of comparable firms, companies operating in the same industry. In this study, we estimate the WACC of publicly traded biofuel firms from 2010 to 2020 and use aggregated WACC estimations as a reference to estimate discount rates for the biofuel industry.

Three discount rate values are estimated and incorporated in the analysis: a most likely, a lower bound, and an upper discount rate. To understand how these discount rates affect profitability and risk of a firm converting pennycress oilseed to bio-oil for the production of SAF, we make the 12-year FCF (**Appendix**) projected in Trejo-Pech et al. (2019)[3] stochastic, $\widetilde{FCF}$, and conduct DFC analysis using our estimated discount rates.

[3]The crushing facility, in the **Appendix**, was assumed to sell pennycress bio-oil at soybean oil equivalent prices according to USDA projections. Pennycress meal cake is assumed to be sold at projected prices of distillers' dried grain with solubles, according to USDA projections as well. In this study, those variables are stochastic

3.1 Financial Data and Parameters for the Deterministic Analysis

3.1.1 Firms in the Sample

Companies producing SAF include Alt Air Paramount (acquired by World Energy), Neste Oyj, Gevo Inc., Virent Inc., and Velocys PLC. (Trejo-Pech et al., 2019; Khanal and Shah, 2021; Tanzil et al., 2021). Gevo Inc. is chosen as one of the companies to include in the sample of firms to analyze in this study because, unlike the other aforementioned firms, Gevo is a publicly traded company listed in a US stock exchange market. To identify additional firms for the sample, a list of firms considered Gevo Inc.'s peers in the Standard and Poor's Net Advantage: Capital IQ database, Peer Analysis submodule is used (Standard and Poor's, 2021).

As of June 2021, Standard and Poor's listed 11 firms comparable to Gevo Inc. From this list, we selected firms meeting the following specifications: 1) the firms operated in business segments closely related to the SAF supply chain, 2) the firms had equities traded in a US stock exchange, and 3) the firms had financial accounting and stock prices data available in the two finance databases used in this study to obtain inputs for the WACC and CAPM estimations. Eight firms fulfilled the requirements. The sample includes REX American Resource Corporation (equity ticker REX), Valero Energy Corporation (VLO), Nov Inc. (NOV), Aemetis Inc. (AMTX), Alto Ingredients Inc. (ALTO), Green Plains Inc. (GPRE), Gevo Inc. (GEVO), and Renewable Energy Group (REGI). We estimated the WACC through CAPM for these biofuel firms each quarter from 2010 to 2020.

3.1.2 Financial Databases

Financial data are obtained from databases maintained by Wharton Research Data Services (WRDS, 2021). WRDS is a paid subscription-based finance data provider primarily for researchers. In particular, individual firm financial statement data are obtained from Compustat North America Fundamental Quarterly (Compustat) and Financial Ratios Firm Level by WRDS (Financial Ratios). Firms' betas are estimated in Beta Suite by WRDS (Beta Suite).

3.1.3 WACC and CAPM

Using **Eq. 1**, WACC for individual firms is calculated every quarter given that publicly traded firms report their financial statement to the US Securities and Exchange Commission each quarter. Total debt, D in **Eq. 1**, is computed as short-term debt plus long-term debt, both accounts obtained from COMPUSTAT. For equity, E, the firm's market value is used instead of the firm's book value of equity (Flannery and Rangan, 2006; Trejo-Pech et al., 2015). Market value of equity is calculated by multiplying the firm's number of shares outstanding times its closing stock price by the end of the quarter, as reported in COMPUSTAT. The cost of debt, Rd, is primarily obtained from Financial Ratios by WRDS, defined as total accumulated annual interest expenses divided by average total debt.[4] A 17% income tax rate, t, based on the Aviation Sustainability Center's guidelines for investment evaluation, is assumed (Tyner and Brandt, 2019). Finally, Re, the cost of equity is estimated using CAPM—**Eq. 2**—as explained next.

Firms' systematic risk measures, betas, are estimated using the software Beta Suite by WRDS. Beta Suite estimates the following rolling regression and provides firm beta parameters:

$$r_{i,t} - rf_t = \alpha_i + \beta_{i,t} ER_t + \varepsilon_{i,t} \tag{3}$$

where $r_{i,t}$ is equity or stock return for firm i during period t and ER_t is the Fama and French's excess return on the market during period t (Fama and French, 1993). The latter is defined as the difference between the value-weighted return of a diversified portfolio of all firms with available data trading on the NYSE, AMEX, or NASDAQ stock exchanges minus the corresponding 1-month US Treasury bill rate (the risk-free rate of return in time t or rf_t). Firms' betas are estimated by Beta Suite on a rolling basis from January 2010 to December 2020. The model uses regular monthly rates of return, calculated as $\frac{Price_{month\,t}}{Price_{month\,t-1}} - 1$. We specify betas to be estimated using 60 monthly returns whenever available in Beta Suite. For firms with less than 60 monthly returns, we restricted the model to estimate betas only if the firms had returns for at least 36 months or 3 years. These 3 and 5 years length windows are commonly used in practice (Brotherson et al., 2013).

Betas estimates, $\hat{\beta}_{i,t}$, from **Eq. 3** are used to compute individual firm's equity investors expected rate of return according to CAPM, **Eq. 2**.

For firms/quarters for which no betas could be estimated with **Equation (3)** due to lack of data, we estimated betas using the following relationship (Asquith 1993; Schill 2017):

$$\beta_L = \beta_U \times \left[1 + (1-t) \times \frac{D}{E}\right] \tag{4}$$

where β_L is levered beta, β_U is unlevered beta, t is the tax rate, and D / E is the debt to equity ratio. First, using estimated betas with **Eq. 3**, also known as levered betas $\beta_{L,i,t}$, we estimated unlevered betas (i.e., potential beta values assuming zero debt) per firm/quarter, $\beta_{U,i,t}$, according to **Eq. 4**. Next, we estimated the mean of unlevered betas each year. Finally, we calculated the beta for firms/quarters lacking beta estimates, by re-levering the unlevered beta; that is, estimating β_L in **Eq. 4** the mean of unlevered betas for the corresponding year and the corresponding debt and equity values of firms in the specific quarter the beta estimate was missing. In other words, for firm/quarters on which betas could not be estimated with regression analysis due to lack of market data, betas were estimated using comparable or industry market betas during the year.

Financial analysts and managers use market premia varying between 5 and 8% annual returns (Brotherson et al., 2013). In this study, the mid-point in previous studies, MRP = 6.5%, is assumed. A 2% risk-free rate, rf is applied, which

[4]When this ratio was unavailable in the Financial Ratios database, we calculated it using data from COMPUSTAT. We divided interest expenses during a quarter by average assets and multiplied it by four to have the ratio expressed in annual terms and make this figure comparable to the values in Financial Ratios

approximates the average of the daily annualized rates for the long-term composite rate during the year 2020, according to the US Department of Treasury.[5]

3.1.4 Discount Rates

The WACC estimations are used as a reference to determine hurdle or discount rates for the biofuel industry. The corporate finance literature reports that even though managers estimate their firms' WACC (through CAPM), they use a higher discount rate—relative to their calculated WACC—as the discount rate for DCF analysis and investment decisions. Graham and Harvey (2018) report that firms add 400 basis points to their estimated WACC when setting their discount rates for valuation analysis purposes; i.e., discount rate = WACC + 0.04. We follow this approach, adding 4 percent points to each of the following: 1) the median of our estimated WACC values across biofuel firms (considered the most likely discount rate for the biofuel industry), 2) the first quartile WACC (lower bound), and 3) the third quartile WACC (upper bound).

3.2 Stochastic Discounted Cash Flow Model

Uncertainty is incorporated into the DCF analysis by performing stochastic simulation. Free cash flows (i.e., deterministic FCF in the **Appendix**) are made stochastic, $\widetilde{FCF}$, along with the corresponding financial metrics—$\widetilde{NPV}$ and $\widetilde{MIRR}$— that are function of $\widetilde{FCF}$. Trejo-Pech et al. (2019) assume that crushing facility output prices are deterministic; that is, pennycress bio-oil and pennycress meal cake are sold at soybean oil and distillers' dried grain with solubles (DDGS) prices as projected by the USDA. In this study, pennycress bio-oil prices and pennycress meal prices are modeled to vary stochastically following a Program Evaluation and Review Technique (PERT) distribution. The PERT distribution was chosen for two reasons: 1) previous bioenergy TEAs have modeled prices assuming PERT (Petter and Tyner, 2014; Zhao et al., 2015; Zhao et al., 2016), and 2) the PERT distribution fitted relatively well, according to the Akaike information criterium, the historical price data used to model prices in this study. Pennycress feedstock to bio-oil conversion rates during the oil extraction process are modeled with a PERT distribution as well. Monte Carlo simulations are performed with @RISK® (Palisade, 2018).

Simulated crushing output prices are drawn from a sample of market prices for soybean oil and DDGS obtained from AMS USDA (2019). The sample has monthly prices from April 2007 (the oldest obtainable price series for both products in this database) to December 2019 (the year the crushing facility analyzed by Trejo-Pech et al. (2019) was assumed to start selling pennycress biofuel and meal). The simulations also assume a correlation coefficient = 0.623 for pennycress bio-oil and pennycress meal prices, which is the correlation observed in the price series during the 2007–2019 period. The feedstock to bio-oil conversion rate simulations use a most likely value parameter of 0.329, with the minimum equal to 0.315, and the maximum equal to 0.340, according to reported pennycress oilseed to bio-oil conversion rates in the literature (Evangelista et al., 2012; Fan et al., 2013; Altendorf et al., 2019; Chopra et al., 2019; Metro Ag Energy, 2019).

Simulations, conducted in @RISK®, resulted in stochastic FCF estimates using the deterministic crush facility developed in Trejo-Pech et al. (2019) (**Appendix 1**). The $\widetilde{FCF}$ estimates are discounted at our most likely, lower bound, and upper bound estimated discount rates (discussed in the previous section), to compute $\widetilde{NPV}$ and $\widetilde{MIRR}$ for the crushing enterprise. Output prices and bio-oil crushing conversion rates are simulated every year during the 10-year forecast production period.[6] The simulations are conducted using 10,000 iterations.

Three sets of results are discussed: stochastic breakeven prices or MBPs, distributions of $\widetilde{MIRR}$, and stochastic sensitivity analysis. First, we calculate the *maximum* price the crushing facility could pay farmers for each pound of pennycress oilseed and financially breakeven, also referred as MBP in this study. Breakeven is defined as the condition at which the crushing enterprise is projected to yield $\widetilde{NPV} = 0$, or equivalently, $\widetilde{MIRR}$ = discount rate, holding all other parameters and assumptions of the DCF model constant. Each stochastic breakeven price is estimated separately by discounting $\widetilde{FCF}$ across the three discount rates and applying the Advanced Goal Seek tool of @RISK®.

Second, using our most likely discount rate estimate and its corresponding stochastic expected breakeven price value, we discuss the probabilities of $\widetilde{MIRR}$ for the crushing facility reaching certain thresholds: the most likely estimated discount rate, the minimum rate to service debt, and the likelihood of falling under financial distress. Finally, using the Advanced Sensitivity Analysis tool of @RISK®, we provide results for alternative scenarios, considering deviations from the baseline parameters of capital expenditures (CAPEX), income taxes, and feedstock prices. These variables are selected due to the following reasons. CAPEX represents a high capital amount in this enterprise, i.e., $74.5 million (**Appendix**, line 8), and estimated CAPEX values in biofuel are subject to variability (Bann, 2017; Zhao et al., 2015; Zhao et al., 2016). Income tax rate assumed in Trejo-Pech et al. (2019) is high (at 40%) relative to Aviation Sustainability Center's guidelines for investment evaluation at 17% (Tyner and Brandt, 2019). Finally, feedstock procurement price is widely recognized as one of the most important components in biofuel studies (Tao et al., 2017).

[5]Treasury rates are available at: https://www.treasury.gov/resource-center/data-chart-center/interest-rates/pages/textview.aspx?data=longtermrate. The long-term composite rate is the average rates of US Treasury securities maturing in ten or more years, consistent with the investment horizon of the crushing enterprise (**Appendix**).

[6]While the model uses 12-year projected FCF, the construction of the facility takes place the first 2 years, and production is assumed during 10 years (**Appendix**).

TABLE 1 | Descriptive statistics of WACC and its relevant components for eight biofuel firms from 2010 to 2020.

Variable	n	Mean	S.D.	Min	Q1	Median	Q3	Max
WACC	314	0.11	0.04	0.06	0.08	0.10	0.13	0.31
DtoC	314	0.35	0.24	0.00	0.18	0.33	0.53	0.96
Rd	314	0.09	0.08	0.00	0.05	0.06	0.13	0.51
Re	314	0.13	0.05	0.03	0.10	0.12	0.15	0.33
Beta	314	1.72	0.81	0.17	1.19	1.50	2.04	4.77
Discount rate				0.12	0.14	0.17		

*WACC, is the weighted average cost of capital (**Eq. 1**). DtoC is debt to investment, where debt is short-term debt plus long-term-debt and investment is debt plus market value of equity, the latter calculated by multiplying the firm's stock price as of the end of each quarter times the number of shares outstanding. Rd is the cost of debt, obtained from the Financial Ratios database, which directly provides the actual cost of debt by dividing interest payments over the previous 4 quarters by average debt in the previous 4 quarters. Re is the expected cost of equity, estimated with CAPM (**Eq. 2**). Beta is obtained from regression analysis performed by the Beta Suite software/database, using 60 months when available (minimum 36 months) of firm's stock, market index and US, treasury bill returns. Discount rate = WACC + 0.04. Number of biofuel firms/quarter is denoted by n, standard deviation is S.D., minimum (maximum) value is Min (Max), and Q1 and Q3 indicate first and third quartile.*

4 RESULTS AND DISCUSSION

4.1 The Weighted Average Cost of Capital and Discount Rates for Biofuel Firms

Summary statistics of the weighted average cost of capital, WACC, and WACC-related variables for the eight biofuel firms in the sample are provided in **Table 1**. With the exception of beta and number of observations in the sample (n), results in **Table 1** are presented in annual basis. Variables in **Table 1** were computed every quarter from 2010 to 2020.

Estimated WACC of 314 biofuel firm/quarters is on average 11% annually, with a median value of 10%, a 25th percentile or first quartile (Q1) value of 8%, and third quartile (Q3) value of 13%. As explained below, the median, Q1, and Q3 values are used as references for the determining financial viability analysis of the pennycress crushing facility. Firms in the sample have a debt to capital ratio, *DtoC*, of 35% (average) and 33% (median), indicating that about one third of the capital in these firms is financed with debt and two thirds with equity.[7] Interest rates, *Rd*, represent on average 9% with a median of 6%, and the expected return on equity, *Re*, estimated with CAPM, equals 13% on average with a median of 12%. This is consistent with finance theory indicating that equity capital providers, those that bear the firm's residual risk, are expected to earn a higher rate of return than debt finance capital providers.

Table 1 also provides beta, the firm's systematic risk factor. Biofuel firms in the sample have beta values of 1.72 (mean) and 1.50 (median), indicating that these companies are riskier than the "average" firm in the market.[8] This is consistent with the fact

[7]Following "best practices" reported in the literature, we used the market value of equity, instead of the book value of equity, for all the estimations in this paper (Flannery and Rangan, 2006; Trejo-Pech et al., 2015). Untabulated results indicate that the debt to capital ratio (using book value of equity) for firms in the sample has a 54% mean and 44% median

[8]The beta of a diversified portfolio equals 1.0, with a beta value higher than 1.0 indicating higher risk and vice versa

TABLE 2 | Statistics of WACC and beta across firms in the sample from 2010 to 2020.

Variable	n	Mean	S.D.	Min	Q1	Median	Q3	Max
REX								
WACC	42	0.10	0.03	0.06	0.07	0.09	0.12	0.16
Beta	42	1.31	0.35	0.85	1.01	1.21	1.60	2.16
VLO								
WACC	43	0.10	0.02	0.08	0.08	0.10	0.11	0.14
Beta	43	1.47	0.32	0.92	1.18	1.45	1.75	2.10
NOV								
WACC	43	0.10	0.02	0.07	0.08	0.11	0.12	0.13
Beta	43	1.52	0.31	0.91	1.32	1.60	1.75	2.15
AMTX								
WACC	30	0.15	0.04	0.09	0.11	0.15	0.17	0.25
Beta	30	1.60	1.23	0.17	0.58	1.36	1.91	4.74
ALTO								
WACC	37	0.11	0.02	0.09	0.10	0.11	0.12	0.14
Beta	37	2.13	0.96	1.02	1.43	1.98	2.54	4.77
GPRE								
WACC	43	0.08	0.01	0.06	0.08	0.08	0.09	0.10
Beta	43	1.71	0.40	1.17	1.36	1.57	2.07	2.46
GEVO								
WACC	40	0.18	0.06	0.08	0.12	0.19	0.22	0.31
Beta	40	2.56	1.18	0.82	1.24	2.70	3.42	4.63
REGI								
WACC	36	0.10	0.01	0.08	0.08	0.10	0.11	0.12
Beta	36	1.51	0.45	0.91	1.15	1.44	1.85	2.37

*REX, is the stock ticker of American Resource Corporation; VLO, is the ticker for Valero Energy Corporation; NOV, is the ticker for Nov Inc., AMTX, is the ticker for Aemetis Inc., ALTO, is the ticker for Alto Ingredients Inc., GPRE, is the ticker for Green Plains Inc., GEVO, is the ticker for Gevo Inc., and REGI, is the ticker for Renewable Energy Group. Number of biofuel firms/quarter is denoted by n, standard deviation is S.D., minimum (maximum) value is Min (Max), and Q1 and Q3 indicate first and third quartile. Weighted average cost of capital (WACC) values are expressed on an annual basis. Beta is a normalized metric, with a value of 1.0 representing the risk of a diversified portfolio or a company with an average market risk level. Firm/quarter betas are estimated by rolling regression according to **Eq. 2**. For firm/quarters on which betas could not be estimated with regression analysis due to lack of market data, betas were estimated using comparable or industry market betas during the year, according to **Eq. 4**.*

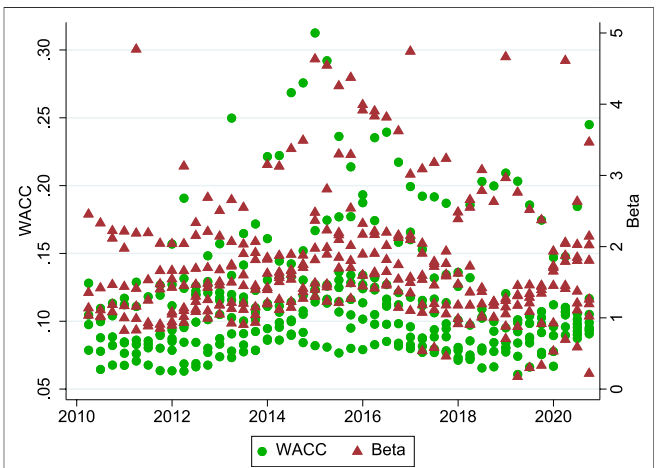

FIGURE 2 | Estimated WACC and beta values per quarter from 2010 to 2020. Note: **Figure 2** provides WACC and beta estimations for each biofuel firm in the sample. Biofuel firms in the sample are indicated in **Table 2**.

that biofuel firms operate in a highly uncertain environment in which the financial impact of using some technologies is yet to be proven successful (Lamers et al., 2015).

The estimates in **Table 1** are relatively stable across bio-oil firms and over time. **Table 2** provides descriptive statistics of WACC and beta for each firm in the sample, and **Figure 2** plots WACC and betas over time. AMTX and GEVO have higher WACCs compared to the rest of firms in the sample, consistent with AMTX having the highest leverage level across firms and GEVO perceived by investors as highly risky given the firm's beta (**Table 2**). However, average WACC for these firms (15 and 18% respectively) are within the range of WACC used in biofuel TEA studies (Tanzil et al., 2021). **Figure 2** shows the majority of estimated WACC values are clustered around 7 and 15% and the majority betas are between 1.00 and 2.50. A few higher WACC and betas seem to concentrate within the 2014–2017 period.

The last row of **Table 1** contains estimated discount rates for the biofuel industry, which are the hurdle rates to use for the analysis of the prospective crushing facility in the SAF supply chain. As explained in the methods section of this paper, these discount rates are calculated by adding 4 percent points (Graham and Harvey, 2018) to our estimated most likely, lower bound, and upper bound WACC values. The discount rates are 14, 12, and 17% respectively. These rates are higher than discount rates used in similar pennycress valuations. For instance, Stevens and Taheripour (2020) and Mousavi-Avval and Shah (2021) assume 10%. Given that the higher the risk and discount rate of any prospective enterprise, the lower is the MBP the firm could pay farmers, this finding implies that previous studies overestimate input MBP, holding other factors constant.

4.2 Stochastic DCF Model

Simulation is incorporated into the analysis by assuming that pennycress bio-oil price, pennycress meal cake price, and pennycress oilseed to bio-oil conversion rate vary stochastically according to a PERT distribution draw from historical prices and conversion rates from previous research. Applying the Distribution Fitting | Fit Manager module in @RISK®, the PERT distribution was consistently ranked among the top distributions (15 or more distributions depending on the stochastic variable) best fitting the data in this study, according to the Akaike information criterium. $\widetilde{FCF}$ were discounted at the estimated discount rates, i.e., 12, 14, and 17%, to compute $\widetilde{NPV}$ and $\widetilde{MIRR}$.

4.2.1 Stochastic Breakeven Prices

Discount rates for the crushing enterprise directly affect oilseed buying prices. We determine the *maximum* price the crushing facility could pay farmers for each pound of oilseed pennycress feedstock and financially breakeven; i.e., $\widetilde{NPV}$ = 0, or equivalently, $\widetilde{MIRR}$ = discount rate. At breakeven, the sum of projected cash inflows during the 12 years equals the value of CAPEX plus working capital investment, all expressed at present values. Stochastic breakeven prices or MBPs, estimated separately by discounting $\widetilde{FCF}$ across alternative discount rates, are provided in **Table 3**. The stochastic breakeven prices in **Table 3** are the *mean* and *median* of simulated breakeven prices. Stochastic breakeven prices, ranging from 10.18 to 11.73 ¢ pound^{-1} are the counterparts of the deterministic 10.80 ¢ pound^{-1} breakeven price point-estimate in Trejo-Pech et al. (2019) (**Appendix**, line 3).

A crushing facility with a 14% discount rate, the most likely discount rate, will breakeven if farmers are paid on average 10.77 ¢ pound^{-1} (mean of simulated prices) or 11.30 ¢ pound^{-1} (median of simulated prices) of pennycress feedstock during the first year of operation. If the crushing facility is less risky than the 'average' firm in this industry and has a 12% discount rate, the breakeven price would be 11.15 ¢ pound^{-1} (mean) or 11.73 ¢ pound^{-1} (median). In contrast, a highly risky crushing facility with a 17% discount rate has an oilseed breakeven price of 10.18 ¢ pound^{-1} (mean) or 10.60 ¢ pound^{-1} (median). The higher the risk and discount rate of the prospective enterprise, the lower is the MBP the firm could pay farmers, and in consequence, the less likely is that farmers will supply feedstock to the prospective SAF supply chain. The next section analyzes the distribution of profitability for the prospective crushing enterprise.

4.2.2 Profitability and Risk for the Most Likely Breakeven Price

Figure 3 provides the distribution of $\widetilde{MIRR}$ for the pennycress crushing facility. For this simulation, the model uses a 14% discount rate—the most likely estimate—and assumes farmers are paid 10.77 ¢ pound^{-1} for oilseed pennycress feedstock, which is the *average* breakeven price (at 14% rate) calculated in the previous section. The distributions indicate that there is approximately 57% probability of this enterprise yielding $\widetilde{MIRR} \geq 14\%$. This is the probability that the firm would have—on average during the life of the project—enough cash inflows to pay interest expenses, principal at the maturity of the loan, and pay back or retain equity owners' capital at or above their expected rate of return. In contrast, there is around 43% probability of this enterprise yielding $\widetilde{MIRR} < 14\%$, or equivalently $\widetilde{NPV} < 0$. Obtaining a negative NPV does not necessarily imply that the crushing facility would experience losses, but rather means that equity capital providers would receive an expected rate of return below their expectations (based on CAPM plus 4 percent points in this application).

Furthermore, as shown in **Figure 3**, a $\widetilde{MIRR}$ equal or higher than 6% but lower than 14% (i.e., 6% is the median cost of debt, *Rd*, in **Table 1**) is 31% likely to occur. Within this range of $\widetilde{MIRR}$, the crushing enterprise produces enough cash to pay back debt capital providers, but equity capital providers obtain a return below their expectations. Finally, there is approximately 11% probability that the crushing enterprise would yield a $\widetilde{MIRR}$ below 6%, which would put the crushing facility under financial distress as the firm would not have enough cash to service its debt unless additional capital were injected into the firm.

The distributions of $\widetilde{MIRR}$ using the *median* breakeven price (11.3 ¢ pound^{-1} at the same 14% rate) calculated in the previous section, are shown in **Figure 4**. Since the median breakeven price the crushing facility would pay farmers is higher than the mean breakeven price, the probability distribution changed a little. The

TABLE 3 | Stochastic oilseed breakeven prices or MBPs a prospective crushing facility could pay farmers for pennycress feedstock across estimated discount rates.

	Most likely (14%)	Lower bound (12%)	Upper bound (17%)
Mean of stochastic breakeven prices (¢ pound^{-1})	10.77	11.15	10.18
Median of stochastic breakeven prices (¢ pound^{-1})	11.30	11.73	10.60

Stochastic breakeven prices are defined as pennycress buying prices yielding a $\widetilde{NPV}$ = 0 or $\widetilde{MIRR}$ = discount rate for the crushing enterprise. The most likely estimated discount rate is 14%, with lower and upper bounds estimated at 12 and 17% respectively. Each stochastic breakeven price is computed separately by discounting $\widetilde{FCF}$ across the three discount rates and applying the Advanced Goal Seek tool of @RISK®.

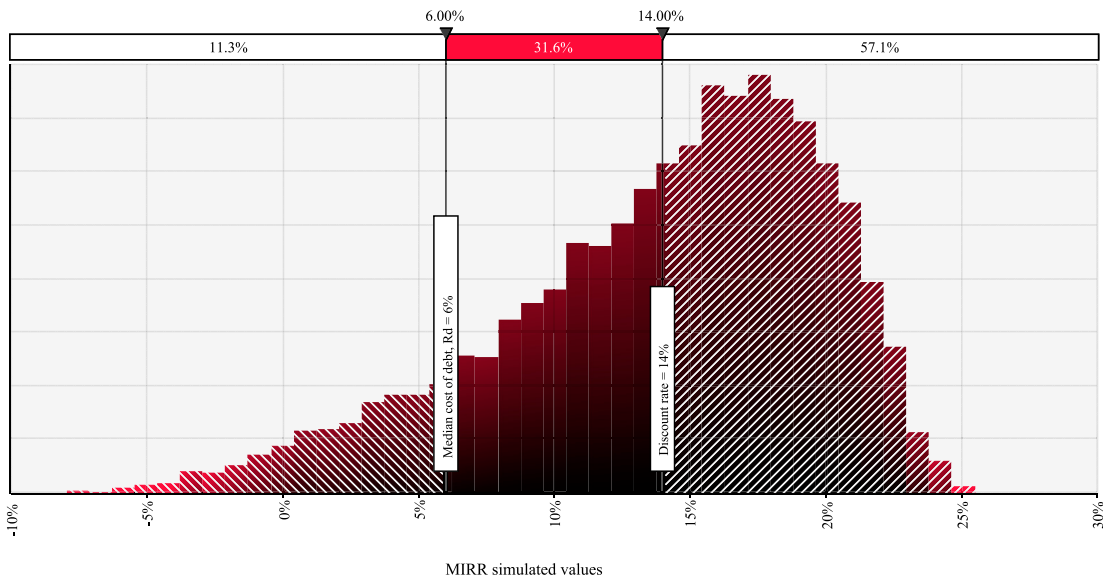

FIGURE 3 | Simulations of MIRR (%) for the pennycress crushing facility (10,000 iterations) using a 14% discount rate, and assuming pennycress feedstock bought at 10.77 ¢ pound^{-1}, which is the *average* stochastic breakeven price.

probability of $\widetilde{MIRR} \geq 14\%$ is approximately 50% and of $\widetilde{MIRR} \geq 6< \widetilde{MIRR} <14\%$, is 17.5%.

4.2.3 Stochastic Sensitivity

Table 4 provides statistics of $\widetilde{MIRR}$ for the prospective crushing facility when CAPEX, income tax rates, and pennycress oilseed buying prices are changed ±3.33% and ±10.00% from the baseline. Simulating the same changes across CAPEX, taxes, and oilseed prices facilitates the visualization of $\widetilde{MIRR}$'s sensitivity to these selected variables, as illustrated in **Figure 5**. As expected, requiring a lower (higher) CAPEX investment would yield a higher (lower) $\widetilde{MIRR}$ relative to the 14.00% baseline. For instance, deviating ±10% would produce mean $\widetilde{MIRR}$ = 13.4% ($\widetilde{MIRR}$ = 14.90%). Similarly, lower (higher) income tax rates and oilseed buying prices yields a higher (lower) $\widetilde{MIRR}$. CAPEX, taxes, and oilseed buying prices are reported as variables biofuel models are highly sensitive to; in particular, oilseed buying price, the focus of this study, has been reported to be the most sensitive variable and represents about 68% of total operating costs of a biorefinery (Tao et al., 2017). Consistently, the slopes of the lines in **Figure 5** and standard deviation values in **Table 4** show that expected profitability of a prospective crushing facility supplying SAF is most sensitive to oilseed buying prices when output prices of bio-oil and meal cake and extraction conversion rates vary stochastically.

4.2.4 Implications

Overall, the distributions of $\widetilde{MIRR}$ suggest the crushing enterprise could be economically attractive when $\widetilde{FCF}$ are discounted at the most likely estimated discount rate of 14%. However, the likelihood of the firm being under financial distress is relatively high at 11 and 17% if the crushing facility pays farmers the mean or median of simulated oilseed prices respectively. In such a situation the firm would not produce enough cash to service debt unless additional capital were raised. This financial implication is an important consideration for potential SAF supply chain stakeholders.

Furthermore, the estimated MBPs in this study may not be sufficient to incentivize farmers to supply pennycress oilseed for SAF production. Zhou et al. (2021) recently surveyed farmers in seven Mid-South US states, finding that farmers ranked "profitability of growing pennycress crops compared with other farming alternatives" and "concern about the market for pennycress as an energy crop" as their top barriers to growing pennycress. In contrast, surveyed farmers reported "additional source of income" as the most important potential benefit of growing pennycress. The potential barriers perceived by farmers shows that the oilseed price crushing

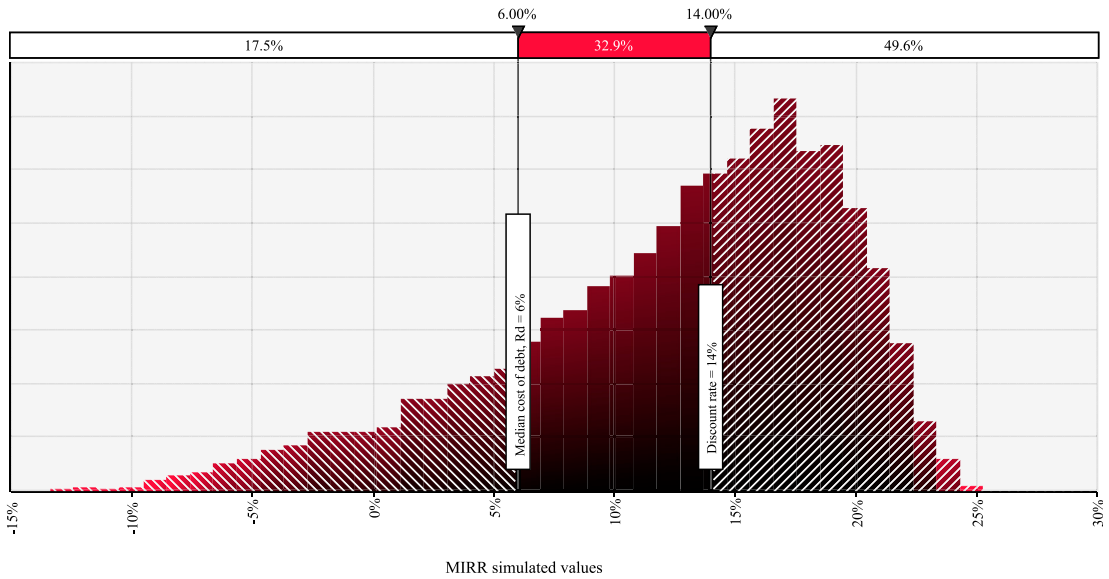

FIGURE 4 | Simulations of MIRR (%) for the pennycress crushing facility (10,000 iterations) using a 14% discount rate, and assuming pennycress feedstock bought at 11.30 ¢ pound^{-1}, which is the *median* stochastic breakeven price.

TABLE 4 | Stochastic sensitivity analysis of $\widetilde{MIRR}$.

Evaluated metrics	Mean	Standard deviation	5% perc	95% perc
CAPEX				
−10.00%	0.149	0.061	0.030	0.228
−3.33%	0.143	0.059	0.028	0.221
+3.33%	0.138	0.057	0.027	0.215
+10.00%	0.134	0.056	0.026	0.209
Income tax rate				
−10.00%	0.144	0.061	0.026	0.223
−3.33%	0.142	0.059	0.027	0.220
+3.33%	0.140	0.057	0.028	0.216
+10.00%	0.137	0.056	0.030	0.212
Feedstock buying price				
−10.00%	0.166	0.043	0.084	0.227
−3.33%	0.150	0.053	0.049	0.221
+3.33%	0.131	0.064	0.004	0.215
+10.00%	0.110	0.078	-0.048	0.208

*$\widetilde{MIRR}$ values estimated applying the Advanced Sensitivity Analysis tool of @RISK®, assuming ±3.33% and ±10.00% from the baseline values. Baseline values are CAPEX = $74.5 million (**Appendix**, line 8), income tax rate = 40%, and feedstock buying price = 10.8 ¢ pound^{-1}, projected during the first year of operation (**Appendix**, line 3).*

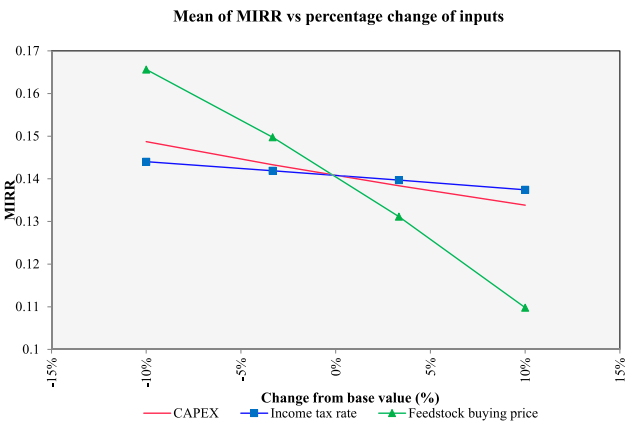

FIGURE 5 | Stochastic sensitivity graph. Notes: Mean of MIRR (vertical axis) vs percentage change of selected inputs (CAPEX, income tax rate, and feedstock buying price) at 14% discount rate, the most likely estimated discount rate. Simulations performed with the Advanced Sensitivity Analysis tool of @RISK®.

facilities could offer farmers is a key determinant of deployment of a SAF supply chain. Zhou et al. (2021) found that among the 58% of farmers who responded indicated interest in growing pennycress. Interested farmers would be willing to plant this crop if the price were set at 12.70 ¢ pound^{-1}, which is higher than the range of estimated MBPs, or breakeven prices, in this study; 10.18 to 11.73 ¢ pound^{-1}. In addition, 88% of farmers interested in planting pennycress would do so under production contracts, given the high risk they perceive for the uncertain market for oilseed to be converted to SAF. This represents another challenge for the prospective crushing facility and deployment of a SAF supply chain. Zhou et al. (2021) findings suggest that efforts to promote pennycress familiarity among farmers, reaching larger farms and more educated farmers, would increase farmers willingness to plant pennycress. Some of these efforts would represent additional costs for stakeholders in this supply chain though. This implication of our findings is similar to McCollum et al. (2021), who analyze canola as a potential SAF feedstock in western US, finding that canola prices need to considerably increase from typical levels to induce enough supply, and suggesting biorefineries to consider compensating farmers for a share of the variable cost of production to ensure sufficient oilseed feedstock supply. Thus, future studies on potential contractual agreements between group of farmers producing feedstock and processors and/or biorefineries are worthwhile. Also, studies

analyzing risks borne by enterprises in a prospective SAF supply chain (e.g., farmers, processors, and biorefineries) may also help to accelerate SAF production. The latter would ultimately help to estimate with more precision input and output prices and expected profit margins for SAF stakeholders. Finally, as shown by the sensitivity analysis in this study, profitability for the prospective crushing facility is most sensitive to pennycress buying price, which reinforces the importance of this TEA focused on pennycress feedstock.

This study does not address the potential impact of government incentives such as Renewable Identification Numbers and other subsidies such as tax credits and loan guarantees since it is assumed that these benefits accrue to the biorefinery. As indicated above, a better understanding of the risk borne by SAF enterprises may provide insights on policies distributing those incentives across supply chain players. Previous research has highlighted the major role played by these incentives on SAF production, but also recognized that the precise nature of the impact on aviation fuel pathways is complex (Eswaran et al., 2021). Thus, those incentives are left outside the scope of this analysis. Related policies that may help SAF deployment are: governmental financing for establishing the market for the by-products of pennycress-based SAF (Mousavi-Avval and Shah, 2020) and tax incentives at the farmer level for production of oilseed feedstock for SAF conversion (McCollum et al., 2021). These recommended policies are in consistency with our findings in this study, as discussed above.

5 CONCLUSION

This stochastic TEA studies the profitability and risk of a pennycress oilseed crushing enterprise buying pennycress oilseed from farmers, extracting the bio-oil (and producing meal cake as a byproduct) and selling bio-oil to a biorefinery that will convert bio-oil into SAF. A crushing enterprise could play an important role on deployment of a SAF supply chain due to its direct contact with farmers growing field pennycress, the feedstock for SAF. Feedstock availability at attractive prices represents the first hurdle for the implementation of this potential supply chain.

Given the relevance of the crushing enterprise within the supply chain, a previous study that projected long-term cash flows for a prospective crushing facility was further analyzed. The deterministic model was converted into a stochastic one by simulating pennycress bio-oil prices, pennycress meal cake prices, and oilseed to bio-oil conversion rates according to a PERT distribution drawing values from a series of historical prices of soybean oil and DDGS as proxies for bio-products prices and conversion rate parameters from previous research. This made the projected cash flows of the crushing facility stochastic.

In addition, we estimated risk-adjusted discount rates appropriate for biofuel investment valuations using financial and market data of a group of biofuel firms publicly trading their stocks in US stock exchange markets. Most likely, lower bound, and upper bound risk-adjusted discount rates were estimated at 14, 12, and 17% respectively. We discounted the stochastic projected cash flows using the risk-adjusted rates and provided an array of outcomes on the profitability and risk of the crushing facility. The primary analysis focus was on stochastic breakeven prices or MBPs the crushing facility could pay farmers for pennycress oilseed; that is, prices that would produce a zero net present value for the crushing enterprise, which would in turn allow the firm to pay both debt capital and equity capital funders their expected rate of return. Breakeven prices ranged between 10.18 and 11.73 ¢ pound^{-1}, depending on the most likely, lower bound and upper bound discount rates. Given the overall results in this study, profitability and risk factors of the crush facility that represent a challenge for the establishment of the crushing facility and in consequence deployment of the SAF supply chain in Southern US were discussed.

Overall, this study finds that while pennycress is a promising feedstock for SAF production providing economic benefits to farmers and ecosystem services, there are still barriers for a viable supply chain deployment. This study focuses on the financial challenges for the prospective processor given the inherent risk in the crushing enterprise and farmers' willingness to plant pennycress given potential prices reported in related research. Previous research also shows that SAF production with pennycress is economically competitive compared to other promising feedstocks, but MSP of biofuel—without considering incentives—is still above the price of petroleum-based jet fuel.

DATA AVAILABILITY STATEMENT

The data analyzed in this study is subject to the following licenses/restrictions: Financial data were obtained mainly from Wharton Research Data Services (WRDS). Particular WRDS databases used are specified in the article. WRDS is accessed thorough library subscription only, and authors are not allowed to post or distribute their data. Other sources of data such as the main discounted cash flow model are included in the article (**Appendix**). Requests to access these datasets should be directed to https://wrds-www.wharton.upenn.edu/.

AUTHOR CONTRIBUTIONS

Conceptualization (CT-P, JL, BE, EY), methodology (CT-P), validation (CT-P, JL, BE, EY), writing—original draft preparation (CT-P), writing—review and editing draft preparation (CT-P, JL, BE, EY), funding acquisition (BE, JL, EY, CT-P).

FUNDING

This work was funded in part by the US Federal Aviation Administration (FAA) Office of Environment and Energy as a part of ASCENT Project 1 under FAA Award Number: 13-C-AJFE-UTENN Amendment No. 15. Funding also was provided by USDA through Hatch Project TN000484 and Hatch Multi-State project 1020537. Any opinions, findings, conclusions, or recommendations expressed in this material are those of the authors and do not necessarily reflect the views of the USDA, FAA or other ASCENT sponsor organizations.

REFERENCES

Air BP (2021). What Is Sustainable Aviation Fuel (SAF) and Why Is it Important? | News and Views. Air Bp. Available at: https://www.bp.com/en/global/air-bp/news-and-views/views/what-is-sustainable-aviation-fuel-saf-and-why-is-it-important.html (Accessed October 24, 2021).

Altendorf, K., Isbell, T., Wyse, D. L., and Anderson, J. A. (2019). Significant Variation for Seed Oil Content, Fatty Acid Profile, and Seed Weight in Natural Populations of Field Pennycress (Thlaspi Arvense L.). *Ind. Crops Prod.* 129, 261–268. doi:10.1016/j.indcrop.2018.11.054

AMS USDA (2019). Feedstuff Corn Distillers Dried Grain Prices. Available at: https://www.marketnews.usda.gov/mnp/ls-report-config?category=Feedstuff. (Accessed July 20, 2021).

Asquith, P. (1993). *Leveraged Betas and the Cost of Equity*. Boston, MA: Harvard Business School Publishing 9-288–036, 1–11.

Baker, H. K., Singleton, J. C., and Veit, E. T. (2010). "Capital Budgeting," in *Survey Research in Corporate Finance* (Oxford, UK: Oxford University Press), 64–138. doi:10.1093/acprof:oso/9780195340372.003.0003

Bann, S. J. (2017). *A Stochastic Techno-Economic Comparison of Alternative Jet Fuel Production Pathways*. Thesis. Boston (MA): Massachusetts Institute of Technology.

Blume, M. E., and Friend, I. (1973). A New Look at the Capital Asset Pricing Model. *J. Finance* 28 (1), 19–34. doi:10.1111/j.1540-6261.1973.tb01342.x

Brotherson, T., Eades, K., Harris, R., and Higgins, R. (2013). Best Practices' in Estimating the Cost of Capital: An Update. *J. Appl. Finance* 23 (1), 1–19.

Campbell, R. M., Anderson, N. M., Daugaard, D. E., and Naughton, H. T. (2018). Financial Viability of Biofuel and Biochar Production from Forest Biomass in the Face of Market Price Volatility and Uncertainty. *Appl. Energ.* 230, 330–343. doi:10.1016/j.apenergy.2018.08.085

Chopra, R., Folstad, N., Lyons, J., Ulmasov, T., Gallaher, C., Sullivan, L., et al. (2019). The Adaptable Use of Brassica NIRS Calibration Equations to Identify Pennycress Variants to Facilitate the Rapid Domestication of a New Winter Oilseed Crop. *Ind. Crops Prod.* 128, 55–61. doi:10.1016/j.indcrop.2018.10.079

Eberle, C. A., Thom, M. D., Nemec, K. T., Forcella, F., Lundgren, J. G., Gesch, R. W., et al. (2015). Using Pennycress, Camelina, and Canola Cash Cover Crops to Provision Pollinators. *Ind. Crops Prod.* 75, 20–25. doi:10.1016/j.indcrop.2015.06.026

Eswaran, S., Subramaniam, S., Geleynse, S., Brandt, K., Wolcott, M., and Zhang, X. (2021). Techno-Economic Analysis of Catalytic Hydrothermolysis Pathway for Jet Fuel Production. *Renew. Sustain. Energ. Rev.* 151, 111516. doi:10.1016/j.rser.2021.111516

Evangelista, R. L., Isbell, T. A., and Cermak, S. C. (2012). Extraction of Pennycress (Thlaspi Arvense L.) Seed Oil by Full Pressing. *Ind. Crops Prod.* 37 (1), 76–81. doi:10.1016/j.indcrop.2011.12.003

Fama, E. F., and French., K. R. (1993). Common Risk Factors in the Returns on Stocks and Bonds. *J. Financial Econ.* 33 (1), 3–56. doi:10.1016/0304-405X(93)90023-5

Fan, J., Shonnard, D. R., Kalnes, T. N., Johnsen, P. B., and Rao, S. (2013). A Life Cycle Assessment of Pennycress (Thlaspi Arvense L.) -Derived Jet Fuel and Diesel. *Biomass and Bioenergy* 55, 87–100. doi:10.1016/j.biombioe.2012.12.040

Flannery, M. J., and Rangan, K. P. (2006). Partial Adjustment toward Target Capital Structures. *J. Financial Econ.* 79 (3), 469–506. doi:10.1016/j.jfineco.2005.03.004

Graham, J. R., and Harvey, C. R. (2018). The Equity Risk Premium in 2018. *SSRN J.*. Rochester, NY: Social Science Research Network. doi:10.2139/ssrn.3151162

Graham, J. R., and Harvey, C. R. (2001). The Theory and Practice of Corporate Finance: Evidence from the Field. *J. Financial Econ.* 60 (2), 187–243. doi:10.1016/S0304-405X(01)00044-7

Hileman, J. I., De la Rosa Blanco, E., Bonnefoy, P. A., and Carter, N. A. (2013). The Carbon Dioxide Challenge Facing Aviation. *Prog. Aerospace Sci.* 63, 84–95. doi:10.1016/j.paerosci.2013.07.003

Howarth, R. B., and Sanstad, A. H. (1995). Discount Rates and Energy Efficiency. *Contemp. Econ. Pol.* 13 (3), 101–109. doi:10.1111/j.1465-7287.1995.tb00726.x

ICAO (2021). Carbon Offsetting and Reduction Scheme for International Aviation (CORSIA). ICAO Environment. Available at: https://www.icao.int/environmental-protection/CORSIA/Pages/default.aspx (Accessed September 3, 2021).

Jacobs, M., and Shivdasani, A. (2012). Do You Know Your Cost of Capital? *Harv. Business Rev.*, 119–124.

Jagannathan, R., Matsa, D. A., Meier, I., and Tarhan, V. (2016). Why Do Firms Use High Discount Rates? *J. Financial Econ.* 120 (3), 445–463. doi:10.1016/j.jfineco.2016.01.012

Jeong, D., Tyner, W. E., Meilan, R., Brown, T. R., and Doering, O. C. (2020). Stochastic Techno-Economic Analysis of Electricity Produced from Poplar Plantations in Indiana. *Renew. Energ.* 149, 189–197. doi:10.1016/j.renene.2019.11.061

Khanal, A., and Shah, A. (2021). Oilseeds to Biodiesel and Renewable Jet Fuel: An Overview of Feedstock Production, Logistics, and Conversion. *Biofuels, Bioprod. Bioref.* 15 (3), 913–930. doi:10.1002/BBB.2198

Kubic, W. L., Moore, C. M., Semelsberger, T. A., and Sutton, A. D. (2021). Recycled Paper as a Source of Renewable Jet Fuel in the United States. *Front. Energ. Res.* 9, 627. doi:10.3389/fenrg.2021.728682

Lamers, P., Tan, E. C. D., Searcy, E. M., Scarlata, C. J., Cafferty, K. G., and Jacobson, J. J. (2015). Strategic Supply System Design - a Holistic Evaluation of Operational and Production Cost for a Biorefinery Supply Chain. *Biofuels, Bioprod. Bioref.* 9 (6), 648–660. doi:10.1002/bbb.1575

Lan, K., Park, S., Kelley, S. S., English, B. C., Yu, T. H. E., Larson, J., et al. (2020). Impacts of Uncertain Feedstock Quality on the Economic Feasibility of Fast Pyrolysis Biorefineries with Blended Feedstocks and Decentralized Preprocessing Sites in the Southeastern United States. *GCB Bioenergy* 12 (11), 1014–1029. doi:10.1111/gcbb.12752

Markel, E., English, B., Hellwinckel, C., and Menard, J. (2018). Potential for Pennycress to Support a Renewable Jet Fuel Industry. *SciEnvironm* 1 (1), 95–102.

Marks, M. D., Chopra, R., and Sedbrook, J. C. (2021). Technologies Enabling Rapid Crop Improvements for Sustainable Agriculture: Example Pennycress (Thlaspi Arvense L.). *Emerging Top. Life Sci.* 5 (2), 325–335. doi:10.1042/ETLS20200330

McCollum, C. J., Ramsey, S. M., Bergtold, J. S., and Andrango, G. (2021). Estimating the Supply of Oilseed Acreage for Sustainable Aviation Fuel Production: Taking Account of Farmers' Willingness to Adopt. *Energ Sustain. Soc.* 11 (1), 33. doi:10.1186/s13705-021-00308-2

McGarvey, E., and Tyner, W. E. (2018). A Stochastic Techno-Economic Analysis of the Catalytic Hydrothermolysis Aviation Biofuel Technology. *Biofuels, Bioprod. Bioref.* 12 (3), 474–484. doi:10.1002/bbb.1863

Metro Ag Energy (2019). Planting PENNYCRESS as a Cover Crop Benefits Farmers. Available at: https://www.metroagenergy.com/farmers-planting-field-pennycress. (Accessed January 9, 2019).

Moser, B. R., Evangelista, R. L., and Isbell, T. A. (2015). Preparation and Fuel Properties of Field Pennycress (Thlaspi Arvense) Seed Oil Ethyl Esters and Blends with Ultralow-Sulfur Diesel Fuel. *Energy Fuels* 30, 473–479. ACS Publications. Available at: https://pubs.acs.org/doi/pdf/10.1021/acs.energyfuels.5b02591 (Accessed October 21, 2021). doi:10.1021/acs.energyfuels.5b02591

Moser, B. R., Knothe, G., Vaughn, S. F., and Isbell, T. A. (2009). Production and Evaluation of Biodiesel from Field Pennycress (Thlaspi arvenseL.) Oil†. *Energy Fuels* 23 (8), 4149–4155. doi:10.1021/ef900337g

Mousavi-Avval, S. H., and Shah, A. (2021). Techno-Economic Analysis of Hydroprocessed Renewable Jet Fuel Production from Pennycress Oilseed. *Renew. Sustain. Energ. Rev.* 149, 111340. doi:10.1016/j.rser.2021.111340

Mousavi-Avval, S. H., and Shah, A. (2020). Techno-Economic Analysis of Pennycress Production, Harvest and Post-Harvest Logistics for Renewable Jet Fuel. *Renew. Sustain. Energ. Rev.* 123, 109764. doi:10.1016/j.rser.2020.109764

Palisade (2018). *@Risk: Risk Analysis and Simulation Add-In for Microsoft Excel*. Ithaca, NY: Palisade Corporation. Available at: https://www.palisade.com/risk/. (Accessed August 20, 2021).

Petter, R., and Tyner, W. E. (2014). Technoeconomic and Policy Analysis for Corn Stover Biofuels. *ISRN Econ.* 2014, 1–13. doi:10.1155/2014/515898

Schill, M. J. (2017). *Business Valuation: Standard Approaches and Applications*. Charlottesville, VA: Darden Business Publishing, University of Virginia UV6586, 1–14. Rev. Nov. 20. doi:10.1108/case.darden.2016.000021

Sharpe, W. F. (1964). Capital Asset Prices: A Theory of Market Equilibrium under Conditions of Risk. *J. Finance* 19, 425–442. doi:10.2307/2977928

SkyNRG (2021). Sustainable Aviation Fuel (SAF). SkyNRG. Available at: https://skynrg.com/sustainable-aviation-fuel/saf/ (Accessed October 24, 2021).

Standard and Poor's (2021). Standard and Poor's Net Advantage. Standard and Poor's Capital IQ. S&P Global Market Intelligence. Available at: www.capitaliq.com (Accessed May 10, 2021).

Stevens, J. H., and Taheripour, F. (2020). *A Stochastic Techno-Economic Analysis of Aviation Biofuel Production from Pennycress Seed Oil*. West Lafayette, IN: Agricultural and Applied Economics Association. 304524.

Tanzil, A. H., Brandt, K., Wolcott, M., Zhang, X., and Garcia-Perez, M. (2021). Strategic Assessment of Sustainable Aviation Fuel Production Technologies: Yield Improvement and Cost Reduction Opportunities. *Biomass and Bioenergy* 145, 105942. doi:10.1016/j.biombioe.2020.105942

Tao, L., Milbrandt, A., Zhang, Y., and Wang, W.-C. (2017). Techno-Economic and Resource Analysis of Hydroprocessed Renewable Jet Fuel. *Biotechnol. Biofuels* 10 (1), 261. doi:10.1186/s13068-017-0945-3

Thomas, J. B., Hampton, M. E., Dorn, K. M., David Marks, M., and Carter, C. J. (2017). The Pennycress (Thlaspi Arvense L.) Nectary: Structural and Transcriptomic Characterization. *BMC Plant Biol.* 17 (1), 201. doi:10.1186/s12870-017-1146-8

Thompson, P. B. (1997). Evaluating Energy Efficiency Investments: Accounting for Risk in the Discounting Process. *Energy Policy* 25 (12), 989–996. doi:10.1016/S0301-4215(97)00125-0

Trejo Pech, C. O., Noguera, M., and White, S. (2015). Financial Ratios Used by Equity Analysts in Mexico and Stock Returns. *Contaduría y Administración* 60 (3), 578–592. doi:10.1016/j.cya.2015.02.001

Trejo-Pech, C. O., Larson, J. A., English, B. C., and Yu, T. E. (2019). Cost and Profitability Analysis of a Prospective Pennycress to Sustainable Aviation Fuel Supply Chain in Southern USA. *Energies* 12 (16), 3055. doi:10.3390/en12163055

Tyner, W., and Brandt, K. (2019). *Techno-Economic Analysis in ASCENT Projects*. NA: The Aviation Sustainability Center.

Wang, M., Dewil, R., Maniatis, K., Wheeldon, J., Tan, T., Baeyens, J., et al. (2019). Biomass-Derived Aviation Fuels: Challenges and Perspective. *Prog. Energ. Combustion Sci.* 74, 31–49. doi:10.1016/j.pecs.2019.04.004

WRDS (2021). Wharton Research Data Services (WRDS). The Global Standard for Business Research. Wharton Research Data Services. CRSP Module. Available at: https://wrds-www.wharton.upenn.edu/ (Accessed May 2, 2021).

Yao, G., Staples, M. D., Malina, R., and Tyner, W. E. (2017). Stochastic Techno-Economic Analysis of Alcohol-To-Jet Fuel Production. *Biotechnol. Biofuels* 10 (1), 18. doi:10.1186/s13068-017-0702-7

Zhao, X., Brown, T. R., and Tyner, W. E. (2015). Stochastic Techno-Economic Evaluation of Cellulosic Biofuel Pathways. *Bioresour. Technol.* 198, 755–763. doi:10.1016/j.biortech.2015.09.056

Zhao, X., Yao, G., and Tyner, W. E. (2016). Quantifying Breakeven Price Distributions in Stochastic Techno-Economic Analysis. *Appl. Energ.* 183, 318–326. doi:10.1016/j.apenergy.2016.08.184

Zhou, X. V., Jensen, K. L., Larson, J. A., and English, B. C. (2021). Farmer Interest in and Willingness to Grow Pennycress as an Energy Feedstock. *Energies* 14 (8), 2066. doi:10.3390/en14082066

Conflict of Interest: The authors declare that the research was conducted in the absence of any commercial or financial relationships that could be construed as a potential conflict of interest.

Publisher's Note: All claims expressed in this article are solely those of the authors and do not necessarily represent those of their affiliated organizations, or those of the publisher, the editors and the reviewers. Any product that may be evaluated in this article, or claim that may be made by its manufacturer, is not guaranteed or endorsed by the publisher.

APPENDIX

Forecast free cash flows yielding NPV = 0 and MIRR = 12.5% with pennycress feedstock buying price = 10.8 ¢ pound^{-1} during the first year of operation

Id	Item\year	1	2	3	4	5	6	7	8	9	10	11	12
1	Revenues			85.33	88.66	90.85	92.20	93.04	94.06	99.91	101.57	103.08	104.95
2	Feedstock cost			57.05	59.28	60.74	61.64	62.20	62.88	66.79	67.90	68.91	70.16
3	Feedstock cost per unit (¢ pound^{-1})			10.8	11.3	11.5	11.7	11.8	11.9	12.7	12.9	13.1	13.3
4	Depreciation			14.87	11.89	9.51	7.61	6.09	4.87	4.87	4.87	4.87	4.87
5	Other costs			9.48	9.64	9.79	9.93	10.07	10.24	10.55	10.75	10.95	11.17
6	Operating income			–6.90	–3.41	–0.73	1.31	2.86	4.11	5.01	5.15	5.25	5.42
7	NOPAT			2.36	4.71	6.49	7.81	8.81	9.64	10.62	10.83	11.01	11.25
8	CAPEX	37.73	37.73	0.00	0.00	0.00	0.00	0.00	0.00	0.00	0.00	0.00	0.00
9	ΔNOWC			14.39	–0.11	–0.14	–0.16	–0.15	–0.07	0.75	0.24	0.22	0.26
10	Residual value												16.35
11	FCF	–37.73	–37.73	2.84	16.71	16.14	15.58	15.04	14.57	14.74	15.46	15.66	32.21

Source: Adapted from Trejo-Pech et al. (2019). Notes: Figures in USD millions, except feedstock cost per unit (item 3). NOPAT is net operating profits after taxes; CAPEX is capital expenditures; ΔNOWC is year-to-year change in net operating working capital; FCF is free cash flow defined as FCF = NOPAT + DEP – CAPEX – ΔNOWC + residual value. and residual value is book value of investment the last year.

frontiers in Energy Research

REVIEW
published: 24 December 2021
doi: 10.3389/fenrg.2021.765360

The U.S. Energy System and the Production of Sustainable Aviation Fuel From Clean Electricity

Jonathan L. Male[1,2], *Michael C. W. Kintner-Meyer*[1] *and Robert S. Weber*[1]*

[1]*Pacific Northwest National Laboratory, Bioproducts Institute, Richland, WA, United States,* [2]*Biological Systems Engineering Department, Washington State University, Pullman, WA, United States*

Jet fuel is relatively small in terms of energy consumption and carbon dioxide emissions (10% of U.S. transportation sector in 2021, expected to increase to 14% by 2050). Still airlines have ambitious goals to reduce their greenhouse footprints from carbon-neutral growth beginning this year to reducing greenhouse gas emission for international flights by 50% by 2050 compared to 2005 levels. The challenge is heightened by the longevity of the current fleet (30–50 years) and by the difficulty in electrifying the future fleet because only 5% of the commercial aviation greenhouse gas footprint is from regional flights that might, conceivably be electrified using foreseeable technology. Therefore, large amounts of sustainable aviation fuel will be needed to reach the aggressive targets set by airlines. Only 3 million gallons (11.4 ML) of sustainable aviation fuel (SAF) (with a heat of combustion totaling about 400 TJ = 0.0004 EJ) was produced in the U.S. in 2019 for a 26 billion gallon per year market (3.6 EJ/year). Fischer-Tropsch and ethanol oligomerization (alcohol-to-jet) are considered for producing SAF, including the use of renewable electricity and carbon dioxide. In sequencing the energy transition, cleaning the U.S. grid is an important first step to have the largest greenhouse gas emissions reduction. While carbon dioxide and clean electricity can potentially provide the SAF in the future, an ethanol oligomerization option will require less energy.

Keywords: jet fuel, fischer-tropsch, ethanol oligomerization, electrofuel, energy storage

OPEN ACCESS

Edited by:
Muhammad Imran Khan, CECOS University of Information Technology and Emerging Sciences, Pakistan

Reviewed by:
Sreedevi Upadhyayula, Indian Institute of Technology Delhi, India
Veera Gnaneswar Gude, Mississippi State University, United States

***Correspondence:**
Robert S. Weber
robert.weber@pnnl.gov

Specialty section:
This article was submitted to Sustainable Energy Systems and Policies, a section of the journal Frontiers in Energy Research

Received: *26 August 2021*
Accepted: *22 November 2021*
Published: *24 December 2021*

Citation:
Male JL, Kintner-Meyer MCW and Weber RS (2021) The U.S. Energy System and the Production of Sustainable Aviation Fuel From Clean Electricity. Front. Energy Res. 9:765360. doi: 10.3389/fenrg.2021.765360

1 INTRODUCTION

Commercial aircraft rely on the combustion of hydrocarbon fuels because they offer high specific energy (energy per unit mass) and high energy density (energy per unit volume). Neither of those flight-critical characteristics can yet be matched by rechargeable power trains consisting of modern batteries or fuel cells and electrical motors in multi-aisle long-haul aircraft. The global aviation sector seeks to reduce greenhouse gas emission for international flights by 50% by 2050 compared to 2005 levels (IATA, 2009). That ambitious goal will require both the continued development of electrical power trains (primarily for regional travel) and drop-in renewable fuels (for long-haul travel). U.S. airlines have committed to net-zero carbon emissions by 2050 and carbon-neutral growth relative to a 2019 baseline for domestic and international flights (Airlines for America, 2021). In March 2021, the member carriers of Airlines for America (A4A) collectively committed to net-zero carbon emissions by 2050. U.S. airlines improved their fuel efficiency by more than 135 percent between 1978 and year-end 2019, saving over five billion metric tons of carbon dioxide (CO_2). However, fuel efficiency improvements with petroleum-based fuels cannot move the industry to net-zero emissions

of CO_2. Sustainable aviation fuel (SAF) is needed. Moreover, about 93% of Global aircraft emissions are from medium- and long-haul flights (International Council on Clean Transportation., 2019). Therefore, addressing the bulk of the emissions requires a long -haul solution, which, from now through 2050, will mean the introduction and use of SAFs.

This paper considers the problem from an energy perspective and does not consider all routes that might contribute to the practical solution of GHG reduction in the transportation sector. The routes that are considered produce fuels that already have ASTM approval for aviation use. The energy analysis provides insights for implementation. The analysis is novel in that it considers the aviation sector in the context of a deliberate pathway to overall reduction in greenhouse gases. In particular, we have included a discussion entitled "Positioning SAF in a sequence of options for making the transportation sector more sustainable."

Here we will consider routes to renewable fuels, starting with renewable or waste sources of carbon and noncarbogenic sources of energy. Noncarbogenic sources include both renewable energy (e.g., biomass, solar, wind), hydropower, and nuclear energy. To compare different sources of energy more easily, it is useful to express supply and demand in a common unit. Here we have chosen to use the SI unit of exajoule (10^{18} J), which is approximately 1 Quad (= 1 quadrillion BTU). As a reference, consider that the U.S. uses about 100 EJ per year, about 3.5% of which serves the airline industry as fuel and 25% serves other modes of transportation (Holladay et al., 2020).

We will express power (energy per time) in Watts (1 W = 1 J/s). Therefore, the roughly 3.6 EJ/year employed by the aviation sector, $P_{aviation}$, averaged across a year, is equivalent to the continuous consumption of more than 100 GW of power:

$$P_{aviation} = \frac{3.6\,\text{EJ}}{\text{year}} \times \frac{1\,\text{year}}{31.5 \times 10^6 \text{s}} = 114\,\text{GW} \quad (1)$$

To further exemplify the units, consider that 1 barrel (159 L) of oil or jet fuel has an enthalpy of combustion of about 6 GJ. Finally, in this litany of conversions, note that the usual unit for expressing electrical energy, the Watt-hour, is equal to 3.6 kJ, so 1 TW-hour (1 trillion Wh) = 0.0036 EJ.

Many countries are considering the use of renewable electricity, coupled with low carbon intensity hydrogen to produce synthetic fuels from CO_2 and other carbon waste streams. Such an approach requires a tremendous amount of renewable electricity that is not yet available. For example, in 2020 the United States generated about 14.5 EJ (3,884 TWh) of electricity of which only 5.4 EJ (1,620 TWh = 0.17 GW) was from renewables or noncarbogenic sources (U.S. Energy Information Administration, 2021a). Waste carbon that contains energy is an important carbon resource. Waste carbon containing energy includes industrial waste gas, municipal solid waste, agricultural and forestry residues, unrecyclable plastic, manures, and municipal wastewater sludge. For this paper, we will focus mainly on the energy requirements for converting CO_2 to jet fuel.

As will be shown below, thermodynamics combined with inefficiencies in the electrochemical conversions mean that every Joule of jet fuel produced electrolytically from CO_2 will require the input of 2–3 J of noncarbogenic electricity. Using waste inputs with negative heats of combustion (e.g., CO, digester methane, manure) would decrease the input of electrical energy but those materials are not available in amounts commensurate with the production of jet fuel. Therefore, on the order of 10 EJ/year (= 317 GW) of new clean electricity generation will be needed to accommodate the generation of current and future levels of demand for aviation fuel.

The mismatch between available, carbon-free electricity and the amount needed for providing clean synthetic fuels reinforces the importance of improving the efficiency of all phases of fuel production, including production of hydrogen. As synthetic fuel technologies scale, in addition to the need for new electric generation, there is a need for additional electric energy storage to buffer momentary, diurnal, and seasonal fluctuations in supply. Finally, if we focus solely on the transportation system, we may miss impacts on reducing CO_2 from the entire system that would be gained by a sequencing of energy transitions.

Because we will be considering the possibility of substituting fossil fuels with fuels produced from environmentally cleaner sources, it is interesting to compare that amount of power with the total installed capacity in the U.S. electricity generating sector, which is about 1100 GW (U.S. Energy Information Administration, 2021a), of which a total of 376 GW (= 12 EJ/year) is produced noncarbogenically from nuclear (92 GW of capacity) plus renewables (284 GW of capacity).

Because we will be considering chemical conversions of different feedstocks into aviation fuel, it is convenient to specify a simplified surrogate for the multicomponent mixture that is actual jet fuel. We have selected to use dodecane, n-$C_{12}H_{26}$, which has molecular weight of 170 g/mol. Its heat of combustion, about 8 MJ/mol = 46.5 MJ/kg, is about 8% higher than that of Jet-A1 (43 MJ/kg). Therefore, the aviation sector's typical consumption of 3.6 EJ/year of primary energy in the U.S. would correspond to the use of 0.46 Tmol/y of a dodecane-like molecule = 26.8 billion gal/year versus 26.7 billion gal/year of actual jet fuel (U.S. Energy Information Administration, 2020). Recall that 1 Teramol = 10^{12} mol; 1 Mt = 1 megaton = 109 kg, and the density of both dodecane and Jet-A1 are about 0.8 kg/L).

Here, we provide estimates for three aspects of producing sustainable aviation fuels: 1) size of the problem, 2) synthetic routes and their material and energy inputs, and 3) a sequence of options that affords significant greenhouse gas savings for the entire economy, including the aviation sector. We discuss the issues from a U.S.-centric perspective, but we note that the underlying science and technology required to address those issues should be generally applicable.

2 SIZE OF THE PROBLEM

Even though the amount of fuel used by U.S. air traffic each year is only 12.5% (3.6 EJ/year) of that consumed by the entire transportation sector in the U.S. (**Figure 1**), replacing the fossil-source energy with renewable resources would impose significant additional demands on the national electric infrastructure, of at least 1,000 TWh/year (= 3.6 EJ/year), which is about 62% of the current

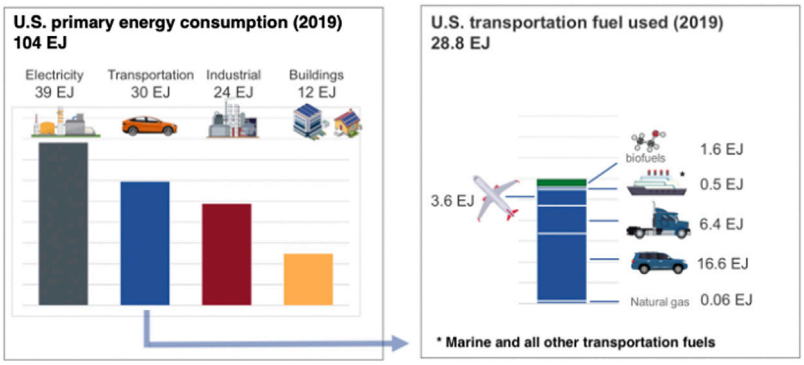

FIGURE 1 | Primary energy input into U.S. sectors (U.S. Energy Information Administration, 2019). Discrepancies in some of the numbers arise from rounding errors.

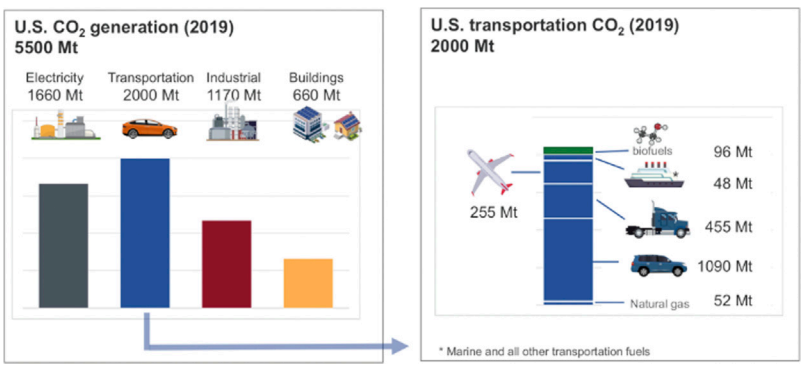

FIGURE 2 | Carbon dioxide emissions from U.S. sectors.

noncarbogenic generation. The fraction of carbon dioxide emitted by the sector is proportional to its use of fuel (~12.8%, **Figure 2**), which is not surprising, given the similarity in heating values, compositions, and energy efficiencies of the conversion of transportation fuels. The inference is that aviation is neither an especially large nor unduly onerous part of the overall problem of reducing carbon emissions from transportation. So, without detracting from the goal of the aviation sector to reduce its emissions of carbon dioxide by 50% over the next 29 years, a rational, global approach to reducing emissions of carbon dioxide should sequence the steps towards ameliorating CO_2 emissions in an order that takes the biggest, cheapest steps as early as possible and that prepares the energy infrastructure for the subsequent changes. We will discuss those points further at the end of this article.

3 SYNTHETIC ROUTES

The thermodynamic constraint on producing renewable fuels—conservation of energy—plus the stoichiometry of a process set lower limits on the amount of renewable energy and renewable material that must be input into the production process to meet the decarbonization goals of the aviation sector. The actual amount of input energy and material will depend on the efficiency and selectivity of the selected process. Here we consider three illustrative routes to Sustainable Aviation Fuel (SAF): 1) Fischer-Tropsch chemistry employing gasification of biomass (de Klerk, 2016); 2) Fischer-Tropsch chemistry employing electrochemically produced synthesis gas, for example (Albert et al., 2016); and 3) oligomerization of ethanol (Brooks et al., 2016). The source of the ethanol in the third case could be either the standard fermentation of sugars (McAloon et al., 2000) or the newer LanzaTech process that ferments CO, CO_2 and H_2 found in industrial waste gas (Handler et al., 2015). Other approaches have been discussed (Brooks et al., 2016; Hannula et al., 2020), but those three serve to illustrate the magnitude of the challenges of accessing sufficient lower carbon intensity energy and renewable carbon. Renewable carbon is defined here as biomass and waste streams, be they solid, liquid, or gas, that are recycled at a molecular level.

3.1 Fischer-Tropsch Process Using Renewable Carbon

The Fischer-Tropsch (FT) process combines synthesis gas, H_2 plus CO, to make mostly straight chain hydrocarbons (Dry,

2004). The oxygen from the CO converts mainly into water but some oxygenated hydrocarbons can be produced as well. The process has been practiced since the Second World War, primarily using fossil fuels (coal, natural gas) as the source of input carbon, and process heat. The synthesis gas is fed to the Fischer-Tropsch reactor at high pressure and high temperature (~500 K, ~25 bar). Production of intermediate synthesis gas decouples the downstream fuel-synthesis process from the feedstock. Therefore, the Fischer-Tropsch reaction can meet ASTM D7566 specification for aviation fuel (ASTM International, 2021) from any source of synthesis gas, including renewable feedstocks (de Klerk, 2016).

The process makes steam and a broad distribution of hydrocarbons that must be separated and upgraded (e.g., hydrocracked) to make jet-range fuel, i.e., our nominal fuel surrogate:

$$12\,CO + 25\,H_2 + \rightarrow C_{12}H_{26} + 12H_2O \qquad \Delta G^0 = -1,684.9\,kJ/mol \qquad \text{Reaction 1}$$

The FT process does make fuel molecules heavier than jet fuel, which might be hydrocracked into the jet range, however, we have ignored them in this first order analysis because their conversion into jet fuel will require additional hydrogen (Ostadi et al., 2019), which will only add to their cost. Selling those products as ultralow sulfur diesel fuel could lower the selling price of the jet fuel but, obviously, would then not directly increase the supply of jet fuel.

The process is approximately 50% carbon efficient (jet-fuel carbon produced/carbon input) (de Klerk, 2016; Gruber et al., 2019) and about 50% energy efficient (heating value of jet-fuel/heating value of biomass input) when the synthesis gas is produced by autothermal gasification of a biomass feedstock (Zhang et al., 2011; Ostadi et al., 2019). The gasification is illustrated simplistically by **Reaction 2**. The feedstock in **Reaction 2** was assumed to have the elemental composition and heat of combustion of a soft wood such as pine; agricultural wastes contain more oxygen and have an enthalpy of combustion value closer to 15 MJ/kg (Hazel and Bardon, 2008)).

$$CH_{4.8}O_{2.1} + 0.55\,O_2 \rightarrow CO + 2.4\,H_2 \qquad \Delta H_{reaction} = -153\,kJ/mol \qquad \text{Reaction 2}$$

The carbon that is not converted to fuel or fuel precursors (e.g., tars that form) can be burned elsewhere in the process to generate heat. In **Reaction 2** as written, the heating value of the "wood" −1,017 kJ/mol is converted into synthesis gas whose heat of combustion is about −860 kJ/mol, so a loss of about 15% of the input energy before consideration of any other sinks for the energy of the feedstock (e.g., compression, reaction selectivity). We note that steam reforming of the wood would produce the CO endothermically and autothermal reforming can be configured to be thermoneutral, but those conversions do not produce synthesis gas with the correct stoichiometry for Fischer Tropsch synthesis.

The process requires about twice the amount of input energy than reports to the fuel. Autothermal gasification of biomass is about 65–75% carbon efficient (Zhang et al., 2011). So, even if the FT process were 70% carbon efficient to making jet range fuels (it is actually closer to 50% carbon efficient (Gruber et al., 2019)), starting with biomass yields no more than a 50% overall carbon efficiency. Heavier (diesel-range, wax products) will require additional processing that will cost money. Selling those products might help offset the price of the SAF but won't directly increase its supply. Because the heating value of lignocellulosic biomass is about 15–20 MJ/kg (Hazel and Bardon, 2008), making a year's supply of jet fuel, 3.6 EJ, would require the input of about 480 Mt of biomass (= 2 × 3.6 EJ ÷ 15 MJ/kg). The long-term base-case of the updated Billion Ton Study (U.S. Department of Energy, 2016) comprises 826 Mt/year of biomass. So, more than half of the potentially available biomass-derived fuel feedstock would need to be devoted to jet fuel if the latter were produced by a process that involved production of the synthesis gas from the biomass.

In one estimate for a plant fed with coal (Reed et al., 2007), the production of 50,000 bbl/day of liquid fuel, was accompanied by an export of 125 MW of electricity. In that case, the net exportable electrical energy amounts to more than 10-times the energy resident in the liquid fuel:

$$\frac{E_{export}}{E_{fuel}} = \frac{125\,MW}{50000\,bbl/day} = \frac{125\,MJ/s}{50000\,bbl/day \times 6.1\,GJ/bbl} \times \frac{31.5 \times 10^6 s}{1\,day} = 12.9 \quad (2)$$

That large ratio reflects the exothermicity of **Reaction 1** plus recovery of process heat generated from the partial oxidation of about half the feedstock to produce the synthesis gas. The estimate is germane also to thermal gasification of biomass (Shahabuddin et al., 2020), where it represents both an opportunity (generation of renewable electricity) and a problem (low carbon yield of fuel) that could be balanced against each other according to higher-level optimization criteria (Tock et al., 2010).

3.2 Fischer-Tropsch Process Using Renewable Carbon and Renewable Energy

If, instead, the energy for producing the synthesis gas could be added directly from renewable sources to renewable materials (Samavati et al., 2018; Gruber et al., 2019; Hannula et al., 2020; Korberg et al., 2021), then the overall process could, in principle, be much more carbon and energy efficient.

For example, concentrated CO_2, perhaps from an ethanol refinery or from the recycle stream in a CO_2-fed Fischer-Tropsch process (Hannula et al., 2020), could be converted into carbon monoxide, CO, using renewable electricity (**Reaction 3**, potentials referenced to the reversible hydrogen electrode (Kortlever et al., 2015)):

$$CO_2 \rightarrow CO + 1/2O_2 \quad E^0 = -1.33\,V,\ \Delta G^0 = 257.1\,kJ/mol \qquad \text{Reaction 3}$$

Similarly, H_2 could be produced by electrolysis of water (**Reaction 4**):

$$H_2O \rightarrow H_2 + 1/2O_2 \quad E^0 = -1.23\,V,\ \Delta G^0 = 237.1\,kJ/mol \qquad \text{Reaction 4}$$

Just making sufficient CO and H_2 from CO_2 and H_2O to synthesize dodecane would require a minimum input energy, ΔG_{min}, that can be calculated from the stoichiometry of **Reaction 1**:

$$\Delta G_{min} = 12 \times 257.1\text{kJ/mol} + 25 \times 237.1\text{kJ/mol} = 9.0\text{MJ/mol}_{\text{dodecane}} \quad (3)$$

To perform the reaction practically, however, that energy must be increased, slightly, by the work required to compress the gas to process conditions (about 20 kJ/mol = RT ln (25 bar/1 bar)) and, significantly, to overcome activation barriers of the constituent reactions. The practical electrochemical overpotentials for **Reactions 3**, **4** are each about 0.6 V (Rakowski-Dubois and Dubois, 2009), so the practical input energies must be increased by about 50% to ~2 V and 1.8 V respectively. The process would still be only about 50% efficient towards the production of jet-range fuel (because of the broad distribution of products in the Fischer Tropsch process. Multiplying ΔG_{min} by 1.5 and doubling M_{min}, the mass of carbon incorporated in the fuel, represent reasonable lower bounds on the renewable energy and renewable carbon required to generate aviation fuel by this route. The inefficient utilization of the feedstock, however, means that the practical energy input, 1.5 × 9.0 MJ/mol = 13.5 MJ/mol, must also be doubled to adjust for the extra feedstock. Therefore, the adjusted, practical energy input, $\Delta G_{practical}$ will be 2 × 13.5 MJ/mol = 27 MJ/mol, which is the reason that we stated above that ≳2 J of input energy is needed for every 1 J of SAF.

The enthalpy of combustion of dodecane (and jet fuel) is about 8 MJ/mol. Therefore, this route would use approximately 27 MJ/mol of energy (from the biomass, electrical power, and other inputs) to make 8 MJ/mol worth of jet fuel. Given that this "electrofuel" would be intended for use in a jet engine whose efficiency would be around 40% (National Academies of Sciences E and Medicine., 2016), the 27 MJ/mol of input energy would result in ~3 MJ/mol of work, a significant degradation that argues for the direct use, where possible of the input electrical energy. As discussed above, however, direct electrification of the propulsion of aircraft cannot yet achieve the desired range of travel. Therefore, we next discuss another route to sustainable aviation fuel that promises to be more energy- and mass-frugal.

3.3 Oligomerization of Ethanol *ex* Cellulose

Both methanol and ethanol can be oligomerized to make fuel range hydrocarbons. The methanol-to-gasoline process invented by ExxonMobil in the 1970s (Chang, 2007; Gogate, 2019) produces, using a small pore zeolite as the conversion catalyst, an unsaturated liquid (olefins, aromatics). The unsaturated intermediate can be hydrogenated to make a liquid fuel fungible with petroleum-derived gasoline. Similarly, ethanol can be converted into gasoline-range molecules through a homologous intermediate. However, ethanol also offers other chemistries (e.g., dehydration to the olefin, Guerbet reaction), that provide effective routes to the heavier molecules that comprise aviation fuel (Brooks et al., 2016).

The source of the ethanol is nearly irrelevant to its downstream conversion into jet fuel (Handler et al., 2015). There are, however, life-cycle differences among the different feedstocks (ethanol from fermentation of sugars derived from biomass, ethanol from waste industrial gas, ethanol from landfill gas). Roughly, the savings in greenhouse gases for each feedstock vary inversely with the cost of the feedstock (**Table 1**).

Those feedstock costs should be compared to the wholesale price of jet fuel, which recently (U.S. Energy Information Administration, 2020) has averaged close to 1.80 USD/gal (= 13.8 USD/GJ). The difference between the feedstock cost and the wholesale price is the amount available for operating costs and amortized capital costs and profit. Despite the low feedstock price of corn stover, it has not played a large role in the production of fuel ethanol, because of the still challenging conversion of cellulose into ethanol (Lamers et al., 2021).

The currently unused amount of potentially available, lignocellulosic feedstocks presented in **Table 1** has been estimated to be 826 Mt/year in the long term (2040), base case scenario of the Billion Ton Study (U.S. Department of Energy, 2016). That material is composed primarily of sugars, e.g., $C_6H_{12}O_6$, which have a molecular weight of 180 g/mol, and lignin (roughly $^2/_3$ of the waste cellulosic feedstock is polysaccharides). The sugar provides the carbon that goes into the growing cells and the product fuel. Usually, the lignin is just burned for process heat (e.g., for distillation). That amount of material would be sufficient to make 0.40 Tmol/year of our surrogate, paraffinic fuel, $C_{12}H_{26}$, if it could be made by fermenting the sugars, $C_6H_{12}O_6$, into ethanol followed by oligomerization of the ethanol (3 sugar molecules per fuel molecule):

$$C_6H_{12}O_6 \rightarrow 2\,C_2H_5OH + 2\,CO_2 \qquad \text{Reaction 5}$$

$$6\,CH_3CH_2OH + H_2 \rightarrow C_{12}H_{26} + 6\,H_2O \qquad \text{Reaction 6}$$

$$826\,\text{MT}_{\text{biomass}}/\text{year} \times \frac{2\,\text{t}_{\text{sugar}}}{3\,\text{t}_{\text{biomass}}} \times \frac{10^9\text{kg}}{\text{Mt}} \times \frac{1\,\text{mol}_{\text{sugar}}}{0.18\,\text{kg}} \frac{1\,\text{mol}_{\text{fuel}}}{3\,\text{mol}_{\text{sugar}}} = 1Tmol_{\text{fuel}}/\text{year} \quad (4)$$

Recall from the introduction that the U.S. uses "only" 0.46 Tmol of jet fuel, therefore, in principle there could be enough feedstock to satisfy this route. However, there are mass inefficiencies in both the fermentation process (72% in one study of making ethanol from wood (Zhu et al., 2010)) and the oligomerization process (~75% carbon efficient to jet fuel and ~90% to jet fuel plus diesel-range fuel in one patent (Lilga et al., 2017). The concatenation of those inefficiencies implies that more than the projected, currently unused supply of lignocellulosic feedstocks would be needed to satisfy the U.S. consumption of jet fuel.

3.4 Oligomerization of Ethanol *ex* Waste Gas

A similar calculation can be made for a route that starts with CO that is produced by the steel industry. In steel making, the U.S. uses about 0.39 EJ worth of metallurgical coke as a reagent (i.e., not as a fuel) (U.S. Energy Information Administration, 2021e). The heating value

TABLE 1 | Comparison of lifecycle analyses and feedstock costs for ethanol-derived SAF.

Source of ethanol	Lifecycle decrease in greenhouse gas emissions (%)	Feedstock cost/ USD GJ^{-1}	Comment and References
CO (steelmaking: $FeO_x + xC \rightarrow Fe + xCO$)	67	2.5	Cost of CO assumed to be $25/ton which makes its energy cost approximately equal to that of natural gas at 2.5$/MMBTU Markets Insider (2021)
Lignocellulosic farm waste (e.g., corn stover)	92	2.3	Graham et al. (2007)
Forestry Lignocellulosics	98	8.5	Averaged ranges (Martinkus et al., 2017) supplied at a rate sufficient to for a biorefinery
Lignocellulosic product/energy crop (e.g., switchgrass)	88	7.5	Agricultural Marketing Resource Center (2018)

of that coke is approximately that of pure carbon, 394 kJ/mol so, in the U.S., the manufacture of steel (110 Mt/year, (U.S. Geological Survey, 2020)) could produce approximately 1 Tmol of CO (**Eq. 5**). A small fraction of the carbon is incorporated into the metal, <0.5 wt% (MIT Department of Civil and Environmental Engineering, 1999) (**Eq. 6**):

$$n_{CO} = \frac{0.39\,\mathrm{EJ}}{394\mathrm{kJ/mol_C}} = 1\,\mathrm{Tmol_C} \times \frac{1\,\mathrm{mol_{CO}}}{\mathrm{mol_C}} \quad (5)$$

$$n_{incorporated} = 0.5\mathrm{wt\%} \times 110\mathrm{Mt/year} \div 0.012\mathrm{kg/mol} = 46\,\mathrm{Gmol} \quad (6)$$

In the LanzaTech process the microbes use CO for energy and as a carbon source in a metabolic process that, formally, is equivalent to water-gas shift. Without suggesting the actual biochemical mechanisms, the overall stoichiometry for converting CO into $C_{12}H_{26}$, our surrogate for jet fuel is, minimally:

$$6\,CO + 3\,H_2O \rightarrow CH_3CH_2OH + 4\,CO_2 \qquad \Delta G_{reaction} = -216\,\mathrm{kJ/mol} \qquad \text{Reaction 7}$$

Combining **Reaction 7** with **Reaction 6** (ethanol oligomerization which, again, is about 75% efficient towards jet range products) implies that the 1 $Tmol_{CO}$ × 1 $mol_{dodecane}/36\ mol_{CO}$ × 0.75 = 21 Gmol of jet fuel and thus satisfy only about 5% of the U.S. demand (0.45 Tmol/year). Gas from a partial combustion fluidized catalytic cracking units in refineries could be a significant source of additional CO (U.S. Environmental Protection Agency, 2010) but we do not have a ready estimate of the available annual flow rates nor of the amenability of refineries to alter their operations to divert such streams away from their usual utility as fuel gas (Babcock and Wilcox Company, 2015).

3.5 Oligomerization of Ethanol *ex* Waste CO_2

Other, carbon-containing waste gases (e.g., from ethanol fermentation, refining, landfill, wastewater treatment) might also be considered as an input to this process. For example, CO and H_2 could be sourced electrochemically as discussed above in **Section 3.2**. In that case, the energy balance and carbon balance will depend on the specific stoichiometry of the inlet synthesis gas (**Table 2**).

Ethanol production, ~16 billion gal/year in the U.S. (U.S. Energy Information Administration, 2021c), produces about 46 Mt/year of CO_2 (≈1.04 $Tmol_{CO_2}$). Consider converting all the carbon dioxide produced by the fermentation of ethanol into a sustainable aviation fuel by a three-step process. In the envisioned process, first, make the synthesis gas electrochemically (**Reaction 3**), then employ fermentation to convert that synthesis gas into ethanol (**Reaction 5**), and finally oligomerize the waste gas-derived ethanol to make jet fuel (**Reaction 6**). The energy input per mol of fuel would be derived from **Reaction 3** (electrolysis of CO_2 to make CO) and the stoichiometries (and carbon efficiencies) of **Reactions 5**, **6**. This route might satisfy 4.7% of the U.S. demand for jet fuel but would require inputting 19 EJ/year of renewable electricity or 3.6 times the amount of noncarbogenic electricity currently produced in the U.S. (see the Excel worksheet in the Supplemental Information for the detailed calculation).

The quantity of fuel produced can be increased and the electrical input can be decreased by adding H_2 to the feed to the CO fermenter. The addition of external H_2 provides a new energy source for the organism, allowing nearly all the carbon to be shunted into ethanol (**Reaction 8**). A minor portion of carbon will go to producing biomass:

$$2\,CO + 4H_2 \rightarrow CH_3CH_2OH + H_2O \qquad \Delta G_{reaction} = -135\,\mathrm{kJ/mol} \qquad \text{Reaction 8}$$

Combining **Reaction 8** with **Reaction 6** (ethanol oligomerization) yields an overall stoichiometric ratio of 12 CO and 24 H_2 per nominal dodecane instead of 12 and 25 respectively. Therefore, the minimum electrical energy required for the electrolysis will be nearly the same as before (**Eq. 3**), which still must be multiplied by 1.5 owing to the overpotentials for the two electrolyses. There will also still be a penalty owing to the selectivity of the oligomerization

TABLE 2 | Summary of inputs for making jet fuel from renewable or waste CO_2.

Feedstock	Notional stoichiometry	Carbon yield	Energy yield (LHV)	J (%)et fuel/U.S. demand (%)	Practical electricity input
CO fermentation from 16 billion $gal_{Ethanol}/year^{-1}$ = fermenter CO_2 (46 Mt/year)[a]	$CO_2 \rightarrow CO + ½O_2$ $6CO + 3H_2O \rightarrow C_2H_5OH + 4CO_2$ $6\ C_2H_5OH \rightarrow C_{12}H_{26} + 6H_2O$	100% 33% 75%	67 73	4.4	19 EJ/year
Fermentation of CO + H_2 from 16 billion $gal_{Ethanol}/year^{-1}$ = (46 Mt_{CO_2}/year)[a]	$3CO_2 \rightarrow 3CO + 1.5O_2$ $3H_2O \rightarrow 3H_2 + 1.5O_2$ $2CO + 4H_2 \rightarrow C_2H_5OH + H_2O$ $6C_2H_5OH + H_2 \rightarrow C_{12}H_{26} + 6H_2O$	100% — 100% 75%	67 67 81	13	17 EJ/year
Fermentation of CO_2 + CO + H_2 fermentation from 180 Mt/year refinery CO_2[b]	$CO_2 \rightarrow CO + ½O_2$ $H_2O \rightarrow H_2 + ½O_2$ $CO_2 + CO + 5H_2 \rightarrow C_2H_5OH + 2H_2O$ $6C_2H_5OH + H_2 \rightarrow C_{12}H_{26} + 6H_2O$	100% 100% 100% 75%	67 67 83	55	53 EJ/year

[a]*Calculated from the U.S., production of 16 billion gallons/year of ethanol; CO, fermentation efficiencies from (Kopke and Simpson, 2020; Green Car Congress, 2021).*
[b]*Amount of CO_2 from (U.S., Environmental Protection Agency, 2020); CO, fermentation efficiencies from (Kopke and Simpson, 2020).*

process (Lilga et al., 2017). However we can now expect a nearly stoichiometric utilization of the carbon in the fermentation process (Kopke and Simpson, 2020). Obviating the reverse water gas shift reaction could also accelerate the kinetics of the overall conversion.

$$\Delta G_{min} = 12 \times 257.1\ \text{kJ/mol} + 24 \times 237.1\ \text{kJ/mol} = 8.8\text{MJ/mol}_{\text{dodecane}} \quad (7)$$

Therefore, the practical energy input will be roughly 17 MJ/$mol_{dodecane}$ = 1.5 ÷ 0.75 × 8.8 MJ/$mol_{dodecane}$ instead of 28 MJ/mol that was employed in less efficient Fischer-Tropsch conversion. Moreover, the process now benefits from reaction conditions that involve near ambient pressures and temperatures instead of the high pressures and temperatures and low carbon utilization of a process that relies on Fischer-Tropsch chemistry. Because of the enhanced utilization of the carbon, this route applied to the CO_2 produced by ethanol fermentation could produce almost 13% of the U.S. demand for jet fuel but would require inputting 17 EJ/year in renewable electricity, which is about 3.2 times the ~5.4 EJ/year of noncarbogenic energy produced in the U.S.

Given a renewable and frugal source of H_2 plus highly competent microorganisms maintained in a well-engineered reactor, one could even imagine using a combination of CO_2 and CO as the source of carbon instead of CO:

$$CO_2 + CO + 5H_2 \rightarrow CH_3CH_2OH + 2H2O \quad \text{Reaction 9}$$
$$\Delta G_{\text{reaction}} = -115\ \text{kJ/mol}$$

In that case the minimum input energy would be smaller because it would, again, be the organisms that would undertake the equivalent of the reverse water gas shift reaction to generate the carbon that reports to the product ethanol The stoichiometric coefficients are derived from **Reaction 9**.

$$\Delta G_{min} = 6 \times 257.1\ \text{kJ/mol} + 30 \times 237.1\ \text{kJ/mol} = 8.7\ \text{MJ/mol}_{\text{dodecane}} \quad (8)$$

However, the practical energy would still be about 2 times larger, $\Delta G_{practical}$ = 16 MJ/mol from the electrochemical overpotential and the penalty arising from the selectivity of the oligomerization process. The process would benefit again from near ambient reaction conditions (temperature, pressure), very effective utilization of the input carbon, and further from the elimination of the electrochemical production of some of the CO. If this process were applied to the roughly 180 Mt/year of CO_2 produced in the refining of petroleum (U.S. Environmental Protection Agency, 2020) then it could satisfy about half the demand for jet fuel but would consume about 10 times the present amount of renewable electricity produced in the U.S. each year (53 EJ/year ÷ 5.4 EJ/year).

4 COMPARISONS WITH AVAILABLE AMOUNTS OF RENEWABLE MATERIAL AND ENERGY

We compare the energy and mass requirements for producing the total U.S. jet fuel consumption in 2020 using the pathways discussed above. Some of the processes just discussed can benefit from direct application of renewable energy and all the processes require direct inputs of either renewable or waste carbon (**Table 3**). The second column of **Table 3** presents the noncarbogenic energy input required to make a year's supply of sustainable aviation fuel for the U.S., either as the heat of combustion of the indicated feedstock or as the amount of renewable electricity needed to make the indicated the starting material from CO_2. The fourth column of the table compares the mass of the indicated, noncarbogenic input required to make the

TABLE 3 | Comparison of minimum and available input energies and masses required by processes that might make 0.45 Tmol/year of sustainable aviation fuel for the U.S. market.

Process	Basis: Required, renewable ΔG_{min}; energy needed to make SAF *Available noncarbogenic energy*	Electric generation and capacity requirements to meet electricity needs	Basis: Required, renewable M_{min}; Mass needed to make SAF *Available noncarbogenic mass*	Comment
Fischer-Tropsch, based on autothermal gasification of sustainably produced biomass	8 $MJ_{th}/mol_{dodecane}$ 14.4 EJ/year as biomass *16.5 EJ/year as biomass* *(=826 Mt/year × 20 MJ/kg)*		12 $mol_{CH_2O}/mol_{dodecane}$ 960 $Mt_{biomass}$/year *826 $Mt_{biomass}$/year*	Assumes 50% energy and C efficiency for production of $C_{12}H_{26}$, biomass = $(-CH_2O-)_n$ available mass from long term, base case of the Billion Ton Study
Fischer-Tropsch, based on electrochemically sourced synthesis gas ex CO_2	9 $MJ_e/mol_{dodecane}$ 12.2 EJ/year as electricity *5.4 EJ/year (U.S. supply of noncarbogenic electricity)*	3,400 TWh of generation 390 GW of firm capacity or 1200 GW of wind (assuming a capacity factor of 33%)	12 $mol_{CO_2}/mol_{dodecane}$ 475 Mt_{CO_2}/year *43 Mt_{CO_2}/year*	CO_2 from production of 16 billion gal/year of ethanol. Assumes 67% energy efficiency and 50% C efficiency for production of $C_{12}H_{26}$
"wood"+ $0.55O_2 \rightarrow CO + 2.4\ H_2$ $2CO + 4\ H_2 \rightarrow C_2H_5OH + H_2O$ $6C_2H_5OH \rightarrow$ jet fuel	8 $MJ_{th}/mol_{dodecane}$ 15 EJ/year as lignocellulosics *16.5 EJ/year as biomass* *(=826 Mt/year × 20 MJ/kg)*		16 $mol_{CO}/mol_{dodecane}$ 770 $Mt_{biomass}$/year *826 $Mt_{biomass}$/year*	Assumes 100% C efficiency in the gasification and fermentation and 75% C efficiency in the oligomerization
Oligomerization of ethanol, *ex* fermentation of starches and sugars	8 $MJ_{th}/mol_{dodecane}$ 7.2 EJ/year as cellulose *12.4 EJ/year as lignocellulose*		3 $mol_{glucose}/mol_{dodecane}$ 360 $Mt_{cellulose}$/year *550 $Mt_{tcellulose}$/year*	Assumes all sugar in lignocellulosic feedstock (2/3 cellulose) is available and does not account for process energy
Oligomerization of ethanol, *ex* waste gas from steel production	8 $MJ_{th}/mol_{dodecane}$ 7.3 EJ as CO *0.4 EJ as CO*		36 $mol_{CO}/mol_{dodecane}$ 650 Mt_{CO}/year *28 Mt_{CO}/year*	CO from use of metallurgical coke; amount from US Energy Information Administration
Oligomerization of ethanol, *ex* electrochemically sourced synthesis gas, *ex* CO_2 and H_2O	8.8 $MJ_e/mol_{dodecane}$ 8.5 EJ as electricity *5.4 EJ/year*	2,400 TWh of generation 270 GW of firm capacity or 810 GW of wind (assuming a capacity factor of 33%)	12 $mol_{CO_2}/mol_{dodecane}$ 340 Mt_{CO_2} *43 Mt_{CO_2}/year*	Amount from 16 billion gal/year of ethanol and fermentation stoichiometry of CO_2/C_2H_5OH = 1

sustainable aviation fuel with its availability. The basis for those inputs derives from the stoichiometries and assumed energy efficiencies described above.

Both types of inputs would require almost all, or more than, the projected availability of those inputs to satisfy the growing demand for renewably-sourced jet fuel in the U.S. For example, the Fischer-Tropsch process based on electrochemically sourced synthesis gas from CO_2 would require on the order of 87% of today's total electricity generation or the addition of 1170 GW of on-shore wind capacity. In 2020, the U.S. has 126 GW installed wind capacity. These are enormous electricity requirements which also require appropriate transmission infrastructure to deliver the electricity from the remote wind-sites to the load centers. While there may be enough production of lignocellulosic feedstock to source a year's consumption of aviation fuel in the U.S., its heating value is not high enough to feed a conventional Fischer-Tropsch process.

Some combination of renewably sourced hydrogen plus carbon dioxide captured from a source less concentrated than the ethanol production of ethanol could supply the requisite material (C and H_2), albeit at a higher capital cost for the equipment needed to capture the CO_2.

To further illustrate the mismatch between the needs of the aviation industry and the availability of noncarbogenic energy and waste or renewable carbon, consider the process discussed in **Section 3.5** at the level of an individual facility (**Figure 3**). An ethanol fermentation plant that makes 100 million gallons per year is near the average size of the facilities in the U.S. (16 billion gallons/year ÷ 200 plants = 80 Mgal/year/plant. By the stoichiometry of **Reaction 5**, such a plant would make 310 kt/year of carbon dioxide. Electrochemically converting that CO_2 and water into a synthesis gas will require a practical input of electrical energy of about 5 PJ_e/year (=160 MW_e) and could make something like 10 million gallons per year of jet fuel. To provide a perspective on the size of existing non-carbon generation capacity it would vary from 14% of a typical nuclear plant or large hydro power plant to about 44% of a large wind farm, to 83% of a large solar farm (**Figure 3**).

Several options described in **Table 3** do not require significant amounts of additional renewable electricity and do match the available resources of renewable carbon: Fischer-Tropsch Synthesis, oligomerization of ethanol produced either from fermenting cellulosic sugar or from synthesis gas made by gasification of biomass. However,

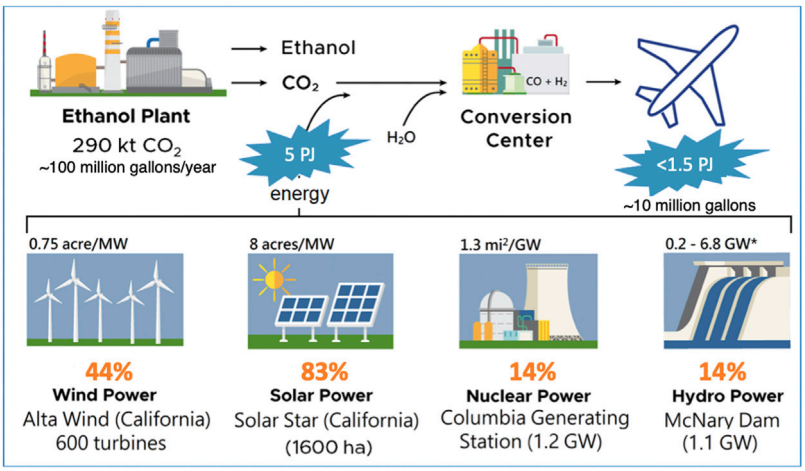

FIGURE 3 | Summary process flow sheet for the example described in **Section 3.5** along with the fraction of a grid scale electricity generating facility needed to power it.

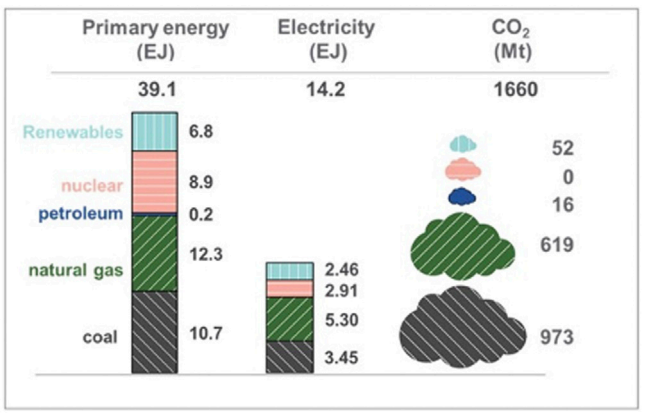

FIGURE 4 | Inputs and outputs of electricity generation by the U.S. grid (U.S. Energy Information Administration, 2021d).

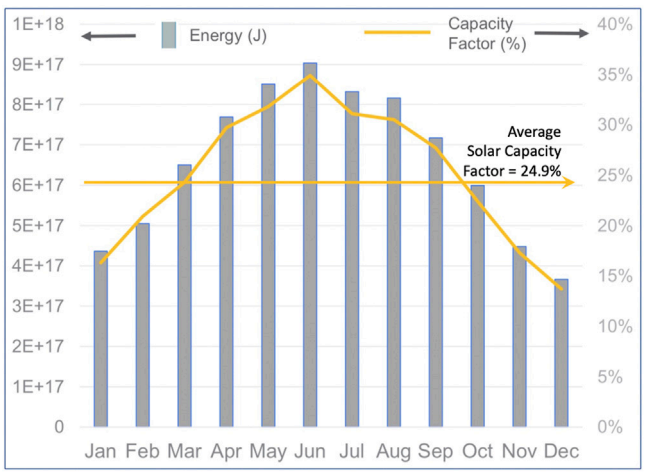

FIGURE 5 | Example of the variability of a renewable resource for generating power that might be used to produce SAF (U.S. Energy Information Administration, 2021b).

each raises a difficulty. We have already mentioned that fermenting cellulosic sugar is problematic. Gasification of biomass can, in principle, produce a synthesis gas whose H_2/CO ratio permits carbon-efficient fermentation (Kopke and Simpson, 2020). In line with our previous assumptions, oligomerizing that ethanol into jet fuel would be 75% carbon efficient. In that case there may be sufficient renewable biomass to produce the 26.8 billion gallons of jet fuel currently employed in the U.S. However, meeting the projected growth in demand for jet fuel would strain the supply of biomass. Moreover, even though gasification is an old, well studied technology, it appears to be difficult to implement robustly at the scale that would be required here. The same issue arises when considering Fischer-Tropsch synthesis starting with biomass-derived synthesis gas. Thus, there is no clear path forward: either there needs to be significant progress in gasifying biomass at scale or the introduction of significant amounts of renewable clean power.

5 POSITIONING SAF IN A SEQUENCE OF OPTIONS FOR MAKING THE TRANSPORTATION SECTOR MORE SUSTAINABLE

The energy inputs listed in the second column of **Table 3** are all near 10 EJ/year. If that delivery rate of fuel or energy were converted to, or employed as, zero-carbon emission grid-supplied power then it could substantially displace the use of coal to generate electrical power and thus remove nearly a Gt/year of CO_2 (**Figure 4**). Therefore, employing renewable or waste resources to first "clean the grid" by eliminating the combustion of fossil fuels for the generation of electricity would offer a larger, more immediate environmental benefit than would employing the resources to produce a noncarbogenic fuel for aviation

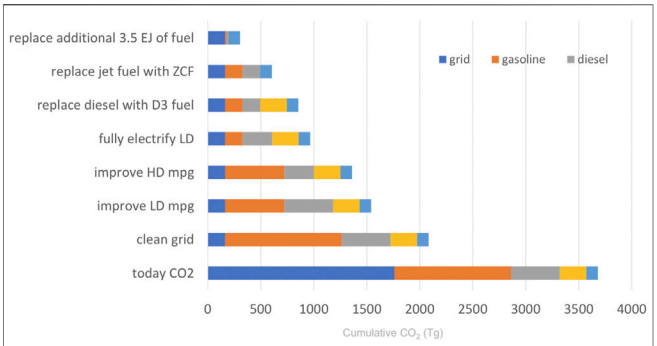

FIGURE 6 | A sequence of technical changes that offers a steady, rapid decrease in the CO_2 footprint of transportation. Abbreviations: ZCF-net zero carbon fuel; D3-diesel fuel derived from a cellulosic feedstock; LD-light duty; HD-heavy duty; mpg-miles per gallon.

(removal of only 255 MT/year (see **Figure 2**). Indeed, given that electricity is nearly fungible, first cleaning the grid is a prerequisite to using grid power for any of the electrochemical step in the production of SAF. Concurrent with dedicating renewable resources to powering the grid, there is a need to implement energy storage to buffer the variability of the resource (e.g., clouds, calm winds) or periodic (diurnal and seasonal) variability (**Figure 5**).

Again, from the perspective of overall efficiency, the first priority should be cleaning the grid by replacing fossil-fueled thermal plants with noncarbogenic generating capacity, followed by a succession of improvements in the utilization of the clean energy (**Figure 6**). The illustrated sequence displaces the dirtiest options as early as possible.

6 CONCLUSION

In the future, feedstocks that are the end products of combustion (e.g., CO_2, H_2O) may be needed as a source of materials to make fuels. First, however, the renewable energy that would be required to upgrade those molecules would be better employed for upgrading carbon-containing feedstocks that do afford enthalpy of combustion (e.g., CO). In comparing systems, we appreciate that examining the energy use, the source of carbon, carbon conversion yields to desired products, and use of hydrogen are important in arriving at an optimal solution. Still, for the systems examined here, very large amounts of energy (more than twice what we have available today) plus energy storage will be needed to generate quantities of fuel that will assist the aviation sector in meeting its environmental targets. Moreover, cleaning and stabilizing the grid must come first. Those improvements will require massive investments in renewable electric generation capacity such as off-shore and on-shore wind and solar, as well as massive amounts of energy storage to balance the daily and seasonal variability of wind and solar resources. We recognize that all the discussed options merit additional analysis and research to order them and to implement them for successful energy transitions and eventual deployment of solutions in the aviation sector that maximize carbon intensity reduction and sustainability. If they are to be deployed, they should be derisked in tandem with building the electrical power energy infrastructure. We believe that a sequencing, like that shown in **Figure 6**, will be critical and represents a novel contribution to this important discussion.

AUTHOR CONTRIBUTIONS

All authors listed have made a substantial, direct, and intellectual contribution to the work and approved it for publication.

FUNDING

This work was funded by the Bioproducts Institute at Pacific Northwest National Laboratory (PNNL) and Washington State University. PNNL is a multiprogram national laboratory operated for DOE by Battelle under Contract DE-AC05-76RL01830.

ACKNOWLEDGMENTS

The analyses and formulation of this paper benefited greatly from the inspiration, insights, and rigor of our colleague, John Holladay.

SUPPLEMENTARY MATERIAL

The Supplementary Material for this article can be found online at: https://www.frontiersin.org/articles/10.3389/fenrg.2021.765360/full#supplementary-material

REFERENCES

Agricultural Marketing Resource Center (2018). Switchgrass. Available at: https://www.agmrc.org/commodities-products/biomass/switchgrass (Accessed July 1, 2021).

Airlines for America (2021). A4A Climate Change Commitment and Flight Path. Available at: https://airlines.org/wp-content/uploads/2021/05/A4A-Climate-Change-Commitment-Flight-Path-to-Net-Zero-FINAL-3-30-21.pdf (Accessed August 16, 2021).

Albert, J., Jess, A., Kern, C., Pöhlmann, F., Glowienka, K., and Wasserscheid, P. (2016). Formic Acid-Based Fischer-Tropsch Synthesis for Green Fuel Production from Wet Waste Biomass and Renewable Excess Energy. *ACS Sustain. Chem. Eng.* 4, 5078–5086. doi:10.1021/acssuschemeng.6b01531

ASTM International (2021). Standard Specification for Aviation Turbine Fuel Containing Synthesized Hydrocarbons, ASTM D7566-21. Available

at: https://www.astm.org/Standards/D7566.htm (Accessed August 4, 2021).

Babcock and Wilcox Company (2015). CO Boilers for the Hydrocarbon Processing Industry. Available at: https://www.babcock.com/resources/learning-center/co-boilers-for-the-hydrocarbon-processing-industry (Accessed August 12, 2021).

Brooks, K. P., Snowden-Swan, L. J., Jones, S. B., Butcher, M. G., Lee, G.-S. J., Anderson, D. M., et al. (2016). "Low-Carbon Aviation Fuel through the Alcohol to Jet Pathway," in *Biofuels for Aviation* (Cambridge: Academic Press), 109–150. doi:10.1016/b978-0-12-804568-8.00006-8

Chang, C. D. (2007). Methanol Conversion to Light Olefins. *Catal. Rev.* 26, 323–345. doi:10.1080/01614948408064716

de Klerk, A. (2016). "Aviation Turbine Fuels through the Fischer-Tropsch Process," in *Biofuels for Aviation* (Cambridge: Academic Press), 241–259. doi:10.1016/b978-0-12-804568-8.00010-x

Dry, M. E. (2004). "Chemical Concepts Used for Engineering Purposes," in *Fischer-Tropsch Technology* (Amsterdam: Elsevier), 196–257. doi:10.1016/s0167-2991(04)80460-9

Gogate, M. R. (2019). Methanol-to-olefins Process Technology: Current Status and Future Prospects. *Pet. Sci. Tech.* 37, 559–565. doi:10.1080/10916466.2018.1555589

Graham, R. L., Nelson, R., Sheehan, J., Perlack, R. D., and Wright, L. L. (2007). Current and Potential U.S. Corn Stover Supplies. *Agron. J.* 99, 1–11. doi:10.2134/agronj2005.0222

Green Car Congress (2021). Shell Invests in LanzaJet; AtJ Sustainable Aviation Fuel. Available at: https://www.greencarcongress.com/2021/04/20210407-lanzajet.html (Accessed November 16, 2021).

Gruber, H., Groß, P., Rauch, R., Reichhold, A., Zweiler, R., Aichernig, C., et al. (2019). Fischer-Tropsch Products from Biomass-Derived Syngas and Renewable Hydrogen. *Biomass Conv. Bioref.* 11, 2281–2292. doi:10.1007/s13399-019-00459-5

Handler, R. M., Shonnard, D. R., Griffing, E. M., Lai, A., and Palou-Rivera, I. (2015). Life Cycle Assessments of Ethanol Production via Gas Fermentation: Anticipated Greenhouse Gas Emissions for Cellulosic and Waste Gas Feedstocks. *Ind. Eng. Chem. Res.* 55, 3253–3261. doi:10.1021/acs.iecr.5b03215

Hannula, I., Kaisalo, N., and Simell, P. (2020). Preparation of Synthesis Gas from CO2 for Fischer-Tropsch Synthesis-Comparison of Alternative Process Configurations. *C* 6, 55–77. doi:10.3390/c6030055

Hazel, D., and Bardon, R. (2008). Conversion Factors for Bioenergy. Available at: https://content.ces.ncsu.edu/conversion-factors-for-bioenergy (Accessed July 15, 2020).

Holladay, J. E., Male, J. L., Rousseau, R., and Weber, R. S. (2020). Synthesizing Clean Transportation Fuels from CO2 Will at Least Quintuple the Demand for Non-carbogenic Electricity in the United States. *Energy Fuels* 34, 15433–15442. doi:10.1021/acs.energyfuels.0c02595

IATA (2009). Working towards Ambitious Targets. Available at: https://www.iata.org/en/programs/environment/climate-change/ (Accessed August 4, 2021).

International Council on Clean Transportation (2019). CO2 Emissions from Commercial Avaition 2018. Available at: https://theicct.org/sites/default/files/publications/ICCT_CO2-commercl-aviation-2018_20190918.pdf.

Köpke, M., and Simpson, S. D. (2020). Pollution to Products: Recycling of 'above Ground' Carbon by Gas Fermentation. *Curr. Opin. Biotechnol.* 65, 180–189. doi:10.1016/j.copbio.2020.02.017

Korberg, A. D., Mathiesen, B. V., Clausen, L. R., and Skov, I. R. (2021). The Role of Biomass Gasification in Low-Carbon Energy and Transport Systems. *Smart Energy* 1, 100006. doi:10.1016/j.segy.2021.100006

Kortlever, R., Shen, J., Schouten, K. J. P., Calle-Vallejo, F., and Koper, M. T. M. (2015). Catalysts and Reaction Pathways for the Electrochemical Reduction of Carbon Dioxide. *J. Phys. Chem. Lett.* 6, 4073–4082. doi:10.1021/acs.jpclett.5b01559

Lamers, P., T. Avelino, A. F., Zhang, Y., D. Tan, E. C., Young, B., Vendries, J., et al. (2021). Potential Socioeconomic and Environmental Effects of an Expanding U.S. Bioeconomy: An Assessment of Near-Commercial Cellulosic Biofuel Pathways. *Environ. Sci. Technol.* 55, 5496–5505. doi:10.1021/acs.est.0c08449

Lilga, M. A., Hallen, R. T., Albrecht, K. O., Cooper, A. R., Frye, J. G., and Ramasamy, K. (2017). *US Pat.* 9, 663416–B2.

Markets Insider (2021). Natural Gas (Henry Hub). Available at: https://markets.businessinsider.com/commodities/natural-gas-price (Accessed July 1, 2021).

Martinkus, N., Latta, G., Morgan, T., and Wolcott, M. (2017). A Comparison of Methodologies for Estimating Delivered forest Residue Volume and Cost to a wood-based Biorefinery. *Biomass and Bioenergy* 106, 83–94. doi:10.1016/j.biombioe.2017.08.023

McAloon, A., Taylor, F., Yee, W., Ibsen, K., and Wooley, R. (2000). Determining the Cost of Producing Ethanol from Corn Starch and Lignocellulosic Feedstocks. Available at: https://www.nrel.gov/docs/fy01osti/28893.pdf.

MIT Department of Civil and Environmental Engineering (1999). Chemical Composition of Structural Steels. Available at: https://web.mit.edu/1.51/www/pdf/chemical.pdf (Accessed July 29, 2021).

National Academies of Sciences and Medicine (2016). *Commercial Aircraft Propulsion and Energy Systems Research*. Available at: https://www.nap.edu/catalog/23490/commercial-aircraft-propulsion-and-energy-systems-research-reducing-global-carbon (Accessed November 29, 2021).

Ostadi, M., Rytter, E., and Hillestad, M. (2019). Boosting Carbon Efficiency of the Biomass to Liquid Process with Hydrogen from Power: The Effect of H2/CO Ratio to the Fischer-Tropsch Reactors on the Production and Power Consumption. *Biomass and Bioenergy* 127, 105282. doi:10.1016/j.biombioe.2019.105282

Rakowski-Dubois, M., and Dubois, D. L. (2009). Development of Molecular Electrocatalysts for CO2 Reduction and H2 Production/Oxidation. *Acc. Chem. Res.* 42, 1974–1982. doi:10.1021/ar900110c

Reed, M., Van Bibber, L., Shuster, E., Haslbeck, J., Olson, S., and Kramer, S. (2007). Baseline Technical and Economic Assessment of a Commercial Scale Fischer-Tropsch Liquids Facility (DOE/NETL-2007/1260). Available at: https://www.netl.doe.gov/sites/default/files/netl-file/Baseline-Technical-and-Economic-Assessment-of-a-Commercial.pdf.

Samavati, M., Santarelli, M., Martin, A., and Nemanova, V. (2018). Production of Synthetic Fischer-Tropsch Diesel from Renewables: Thermoeconomic and Environmental Analysis. *Energy Fuels* 32, 1744–1753. doi:10.1021/acs.energyfuels.7b02465

Shahabuddin, M., Alam, M. T., Krishna, B. B., Bhaskar, T., and Perkins, G. (2020). A Review on the Production of Renewable Aviation Fuels from the Gasification of Biomass and Residual Wastes. *Bioresour. Tech.* 312, 123596. doi:10.1016/j.biortech.2020.123596

Tock, L., Gassner, M., and Maréchal, F. (2010). Thermochemical Production of Liquid Fuels from Biomass: Thermo-Economic Modeling, Process Design and Process Integration Analysis. *Biomass and Bioenergy* 34, 1838–1854. doi:10.1016/j.biombioe.2010.07.018

U.S. Department of Energy (2016). 2016 Billion-Ton Report: Advancing Domestic Resources for a Thriving Bioeconomy, Volume 1: Economic Availability of Feedstocks. Available at: http://energy.gov/eere/bioenergy/2016-billion-ton-report.

U.S. Energy Information Administration (2019). Annual Energy Outlook 2019. Available at: https://www.eia.gov/outlooks/aeo/data/browser/#/?id=12-AEO2019&cases=ref2019&sourcekey=0 (Accessed July 30, 2019).

U.S. Energy Information Administration (2021a). Annual Energy Outlook 2021: Electricity Generating Capacity. Available at: https://www.eia.gov/outlooks/aeo/data/browser/#/?id=9-AEO2021&cases=ref2021&sourcekey=0 (Accessed June 25, 2021).

U.S. Energy Information Administration (2021b). Capacity Factors for Utility Scale Generators Primarily Using Non-fossil Fuels. Available at: https://www.eia.gov/electricity/monthly/epm_table_grapher.php?t=table_6_07_b (Accessed July 29, 2021).

U.S. Energy Information Administration (2021c). Ethanol Plant Production-Fuel Ethanol. Available at: https://www.eia.gov/dnav/pet/pet_sum_sndw_a_EPOOXE_YOP_mbblpd_4.htm (Accessed August 8, 2021).

U.S. Energy Information Administration (20202019). Jet Fuel Consumption, price, and Expenditure Estimates. Available at: https://www.eia.gov/state/

seds/data.php?incfile=/state/seds/sep_fuel/html/fuel_jf.html (Accessed July 2, 2021).

U.S. Energy Information Administration (2021d). July 2021 Monthly Energy Review. Available at: https://www.eia.gov/totalenergy/data/monthly/pdf/mer.pdf (Accessed July 29, 2021).

U.S. Energy Information Administration (2021e). Quarterly Coal Consumption and Quality Report - Coke Plants. Available at: https://www.eia.gov/coal/production/quarterly/pdf/tes2p01p1.pdf (Accessed June 30, 2021).

U.S. Environmental Protection Agency (2010). Available and Emerging Technologies for Reducing Greenhouse Gas Emissions from the Petroleum Refining Industry. Available at: https://www.epa.gov/sites/default/files/2015-12/documents/refineries.pdf (Accessed August 8, 2021).

U.S. Environmental Protection Agency (2020). Greenhouse Gas Reporting Program (GHGRP). Available at: https://www.epa.gov/ghgreporting/ghgrp-refineries#trends-subsector (Accessed August 5, 2021).

U.S. Geological Survey (2020). Iron and Steel. Available at: https://pubs.usgs.gov/periodicals/mcs2020/mcs2020-iron-steel.pdf (Accessed July 29, 2021).

Zhang, Y., Li, B., Li, H., and Liu, H. (2011). Thermodynamic Evaluation of Biomass Gasification with Air in Autothermal Gasifiers. *Thermochim. Acta* 519, 65–71. doi:10.1016/j.tca.2011.03.005

Zhu, J. Y., Zhu, W., Obryan, P., Dien, B. S., Tian, S., Gleisner, R., et al. (2010). Ethanol Production from SPORL-Pretreated lodgepole pine: Preliminary Evaluation of Mass Balance and Process Energy Efficiency. *Appl. Microbiol. Biotechnol.* 86, 1355–1365. doi:10.1007/s00253-009-2408-7

Conflict of Interest: The authors declare that the research was conducted in the absence of any commercial or financial relationships that could be construed as a potential conflict of interest.

Publisher's Note: All claims expressed in this article are solely those of the authors and do not necessarily represent those of their affiliated organizations, or those of the publisher, the editors and the reviewers. Any product that may be evaluated in this article, or claim that may be made by its manufacturer, is not guaranteed or endorsed by the publisher.

frontiers in Energy Research

ORIGINAL RESEARCH
published: 13 January 2022
doi: 10.3389/fenrg.2021.781001

Determining the Adsorption Energetics of 2,3-Butanediol on RuO_2(110): Coupling First-Principles Calculations With Global Optimizers

Carrington Moore[1], Difan Zhang[1,2], Roger Rousseau[2], Vassiliki-Alexandra Glezakou[2]* and Jean-Sabin McEwen[1,2,3,4,5]**

[1]Gene and Linda Voiland School of Chemical Engineering and Bioengineering, Washington State University Pullman, Pullman, WA, United States, [2]Pacific Northwest National Laboratory, Physical Sciences Division, Richland, WA, United States, [3]Department of Physics and Astronomy, Washington State University, Pullman, WA, United States, [4]Department of Chemistry, Washington State University, Pullman, WA, United States, [5]Department of Biological Systems Engineering, Washington State University, Pullman, WA, United States

OPEN ACCESS

Edited by:
Kristin C. Lewis,
Volpe National Transportation Systems Center, United States

Reviewed by:
Yaqiong Su,
Xi'an Jiaotong University, China
Ibukun Oluwoye,
Murdoch University, Australia

***Correspondence:**
Vassiliki-Alexandra Glezakou
vanda.glezakou@pnnl.gov
Roger Rousseau
Roger.Rousseau@pnnl.gov
Jean-Sabin McEwen
js.mcewen@wsu.edu

Specialty section:
This article was submitted to Bioenergy and Biofuels, a section of the journal Frontiers in Energy Research

Received: 22 September 2021
Accepted: 10 November 2021
Published: 13 January 2022

Citation:
Moore C, Zhang D, Rousseau R, Glezakou V-A and McEwen J-S (2022) Determining the Adsorption Energetics of 2,3-Butanediol on RuO_2(110): Coupling First-Principles Calculations With Global Optimizers. Front. Energy Res. 9:781001. doi: 10.3389/fenrg.2021.781001

As climate change continues to pose a threat to the Earth due to the disrupted carbon cycles and fossil fuel resources remain finite, new sources of sustainable hydrocarbons must be explored. 2,3-butanediol is a potential source to produce butene because of its sustainability as a biomass-derived sugar. Butene is an attractive product because it can be used as a precursor to jet fuel, categorizing this work in the alcohol-to-jet pathway. While studies have explored the conversion of 2,3-butanediol to butene, little is understood about the fundamental reaction itself. We quantify the energetics for three pathways that were reported in the literature in the absence of a catalyst. One of these pathways forms a 1,3-butadiene intermediate, which is a highly exothermic process and thus is unlikely to occur since 2,3-butanediol likely gets thermodynamically trapped at this intermediate. We further determined the corresponding energetics of 2,3-butanediol adsorption on an ensemble of predetermined binding sites when it interacts with a defect-free stoichiometric RuO_2(110) surface. Within this ensemble of adsorption sites, the most favorable site has 2,3-butanediol covering a Ru 5–coordinated cation. This approach is compared to that obtained using the global optimization algorithm as implemented in the Northwest Potential Energy Surface Search Engine. When using such a global optimization algorithm, we determined a more favorable ground-state structure that was missed during the manual adsorption site testing, with an adsorption energy of −2.61 eV as compared to −2.34 eV when using the ensemble-based approach. We hypothesize that the dehydration reaction requires a stronger chemical bond, which could necessitate the formation of oxygen vacancies. As such, this study has taken the first step toward the utilization of a global optimization algorithm for the rational design of Ru-based catalysts toward the formation of butene from sustainable resources.

Keywords: energy, butene, RuO2, computational catalysis, butanediol, bio-jet fuel, adsorption analysis

1 INTRODUCTION

The continual use of fossil fuels is contributing to the disruption of the Earth's carbon cycle, resulting in global warming. A contributor to this is aviation fuel—a highly refined and strictly regulated product of the petroleum industry. Bio-jet fuel provides an alternative to petroleum-based aviation fuel as it maintains low weight and high-energy content that is necessary for air travel. The aviation industry recognizes the need for implementing renewable fuels and has committed to halving emissions by 2050. Sustainable aviation fuel has been projected to help in this endeavor as it can offer up to 80% reduction in emissions as compared to petroleum-based fuel, and as such it has been touted as the biggest opportunity in emission abatement within the aviation industry (Interational Air Transport Association, 2020).

One way to upgrade biomass to usable aviation fuel is through the alcohol-to-jet pathway. In this pathway, a biomass-derived alcohol is dehydrated to butene. Butene is then able to undergo additional chemical processes such as oligomerization and hydrogenation to achieve the proper alkane conformation that is specified in the ASTM standards (Wang and Tao, 2016). In producing these alcohols, it is important to be cognizant of the biomass used; specifically, lignocellulosic biomass is considered to be more sustainable as it is indigestible by humans and the most abundant form of biomass on the planet (Zhou et al., 2011). Butanediols have been demonstrated to be produced from fermenting sugars obtained from lignocellulosic biomass, making it an ideal choice as the reactant (Guragain and Vadlani, 2017).

Dehydrating diols, such as 2,3-butanediol (BDO), have been demonstrated to be a more complex process than dehydrating alcohols with only one hydroxyl group. Often research exploring the dehydration of diols yields a mono-alcohol (Aihara et al., 2020; Ohtsuka et al., 2019). A first-principles study on dehydrating diols found that during the multistep process of removing the first hydroxyl, an electron hole is created that migrates along the carbon chain that aids in the removal of the second hydroxyl group. This hole migration is an example of an non-adiabatic charge transfer. The catalyst used for this process was TiO_2 which requires two oxygen vacancies for the adsorption of both hydroxyl groups (Acharya et al., 2013). In a separate study analyzing water's behavior on RuO_2 and TiO_2, it was found that Ru had a higher Lewis acidity than Ti, which results in a strong adsorption energy of water. Therefore, in this research, the chosen catalyst was RuO_2 as it is isostructural compared to the already tested TiO_2 but more reactive with oxygen (Mu et al., 2014).

In this study, the adsorption mechanism of 2,3-butanediol on the RuO_2 surface is tested with two separate methods: an ensemble-based approach with a predetermined set of possible adsorption sites and through a global optimization algorithm using the Northwest Potential Energy Surface Search Engine (NWPEsSe) (Zhang et al., 2020). This comparison highlights the abilities of NWPEsSe software on metal adsorbate calculations—an avenue that has yet to be explored. Demonstrating the capabilities on this system with a defect-free surface provides opportunities to use NWPEsSe software on more complex surfaces, such as those with oxygen vacancies.

2 TIER ONE ARTICLE TYPE

The study presented is an A-type article and original research.

3 MATERIALS AND METHODS

3.1 Quantum Calculations

The calculations presented in this study were carried out using the Vienna *Ab initio* Simulation Package (VASP) (Kresse and Furthmüller, 1996; Kresse and Hafner, 1993), where the latest edition of this software (6.1.2 standard) was used. The core electrons were treated with VASP's projector augmented waves (PAW), 2017 edition (Lejaeghere et al., 2016), to expedite the calculation of the Kohn–Sham equations with an energy cutoff of 500 eV for all calculations. For the surface calculations the energy tolerance was 1×10^{-4} eV, while the force tolerance was set to 0.03 eV/Å with Gaussian smearing and a sigma value of 0.1 eV. The **k**-point mesh was $(2 \times 1 \times 1)$ for the surface calculations and $(7 \times 7 \times 10)$ for the bulk structure. The bulk structure, being hexagonal close-packed, had the lattice constants of $\boldsymbol{a} = \boldsymbol{b} = 4.479$ Å, and $\boldsymbol{c} = 3.113$ Å (see **Supplementary Figure S1** for details) using the Strongly Constrained and Appropriately Normed (SCAN) functional. Electronic exchange and correlation was treated at the generalized gradient approximation level using the Perdew–Burke–Ernzerhof (PBE) functional (Perdew et al., 1996). This level of theory was compared to the more sophisticated *meta*-GGA functional SCAN (Sun et al., 2015) and the van der Waals–DF functional, optB86b-vdW (Becke, 1986) for the BDO molecule in the gas phase. The SCAN functional has been demonstrated to work effectively with spin-polarized metal oxides (Sun et al., 2015) and therefore was used on all surface calculations presented. While RuO_2 has been determined to be antiferromagnetic (Berlijn et al., 2017) as the magnetic ordering of the system delays calculations and is unlikely to significantly affect the adsorption energy calculations presented here. As such, all calculations performed in this study were not spin-polarized.

The rutile structure for RuO_2 was chosen as it is the most stable under standard conditions (Haines et al., 1996), where the bulk structure was cut for the (110) facet where an O_{bridge} termination was determined to be the most stable surface termination. To emulate a semi-infinite surface, four tri-layers (the tri-layers being a function of the rutile stacking) were used with a 13 Å vacuum layer, with dipole layer corrections being applied in the $\hat{z}$-direction (Reuter and Scheffler, 2002). The bottom two layers were fixed with the top two relaxed to allow for the adsorption of BDO. The adsorption energy was calculated as follows:

$$E_{ads} = E_{BDO/RuO_2(110)} - E_{RuO_2(110)} - E_{BDO(g)}, \quad (1)$$

where $E_{BDO/RuO_2(110)}$, $E_{RuO_2(110)}$, and $E_{BDO(g)}$ are the total energies of 2,3-butanediol adsorbed on RuO_2 (110), the clean RuO_2 (110)

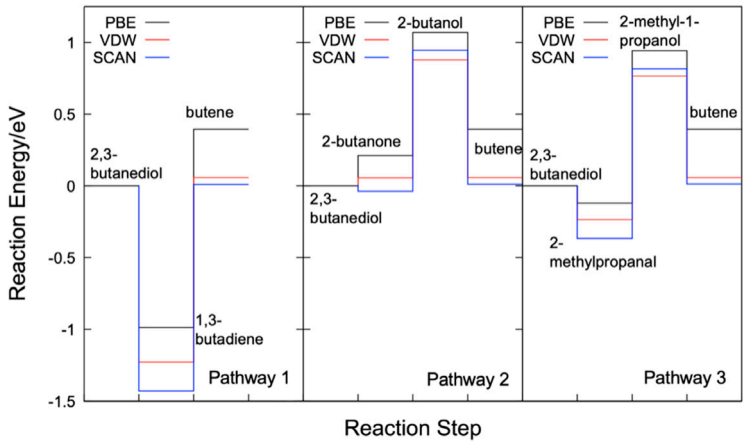

FIGURE 1 | Reaction Pathways 1, 2, and 3 for 2,3-butanediol dehydration to butene at three levels of theory: PBE, van der Waals optB86b functional, and SCAN.

surface, and 2,3-butanediol in the gas phase, respectively. The distortion energy was calculated as follows:

$$E_{\text{dist}} = E_{\text{distorted geometry molecule}} - E_{\text{free gas molecule}}, \quad (2)$$

$E_{\text{free gas molecule}}$ is the total energy of the molecule converged in vacuum space, and $E_{\text{distorted geometry molecule}}$ is calculated from a single-point calculation of the adsorbed molecule on the surface after the surface had been deleted. These two energy calculations have been included to give information about the configuration of the structures and as a comparison point in the adsorption analysis. Additionally, an electronic analysis was carried out, resulting in partial charge density distributions and differential charge density calculations. The differential charge density calculation is based on the following equation:

$$\Delta\rho(\vec{r}) = \rho_{\text{BDO/RuO}_2\,(110)}(\vec{r}) - \rho_{\text{RuO}_2\,(110)}(\vec{r}) - \rho_{\text{BDO}\,(g)}(\vec{r}) \quad (3)$$

where $\rho_{\text{BDO/RuO}_2\,(110)}(\vec{r})$, $\rho_{\text{RuO}_2\,(110)}(\vec{r})$, and $\rho_{\text{BDO}\,(g)}(\vec{r})$ are the ground-state charge distribution for adsorbed system, the clean surface, and the gas-phase molecule that is fixed in its distorted adsorption geometry, respectively. Additionally, a Bader charge analysis (Henkelman et al., 2006) was performed to quantify the atomic interaction during adsorption.

A density of states analysis was carried out such that the Fermi level was set to zero. For the gas-phase BDO the Fermi level was taken to be halfway between the HOMO and LUMO states as was done by (Mittendorfer and Hafner, 2001). In addition to the density of states a *d*-band analysis was performed where the center (**Eq. 4**) and width (**Eq. (5)** were identified by using the following equation (Kitchin et al., 2004) (Hensley et al., 2016):

$$\varepsilon_d = \frac{\int_{-\infty}^{\varepsilon_{\text{Fermi}}} E\rho(E)dE}{\int_{-\infty}^{\varepsilon_{\text{Fermi}}} \rho(E)dE}, \quad (4)$$

$$w_d = \left(\frac{\int_{-\infty}^{\varepsilon_{\text{Fermi}}} E^2\rho(E)dE}{\int_{-\infty}^{\varepsilon_{\text{Fermi}}} \rho(E)dE} \right)^{1/2}, \quad (5)$$

where E is the given energy from the DOS analysis, $\rho(E)$ is the density of the electronic states for E, and $\varepsilon_{\text{Fermi}}$ is the Fermi level.

To determine the most favorable adsorption site with an ensemble of predetermined binding sites, an ensemble-based approach was performed so that "ensemble-based" refers to the process that was conducted without the aid of a global optimization algorithm. As such, it is based on chemical intuition. Within this framework, seven unique possible adsorption sites were determined and tested for two different ways: with the 2,3 C-C bond parallel to the ***a***-axis (horizontal) and with the 2,3 C-C bond parallel to the ***b***-axis (vertical). The conformations of these seven sites are given in **Supplementary Figure S2**.

3.2 Global Optimizer Calculations

We employed the Northwest Potential Energy Surface Search Engine (NWPEsSe) software (Zhang et al., 2020) coupled with the xTB program (Bannwarth et al., 2021) and the VASP program to identify the energetically favorable adsorption configurations of BDO on RuO_2(110). The xTB program provides a semiempirical extended tight-binding package to accurately predict molecular structures and properties without the need to switch to a computationally more expensive model such as the DFT-based method in VASP. In this package, the GFN2-xTB (Bannwarth et al., 2019) method can quickly perform calculations of structures and interactions in molecular structures, and the GFN-FF (Spicher and Grimme, 2020) is a generic force field for even faster evaluation of structures and dynamics for large molecules. Similar to our quantum calculations using VASP, the 110 surface of the rutile structure of RuO_2 was used. The surface of our RuO_2 for the non-periodic boundary conditions (PBC) model (used in GFN-FF and GFN2-xTB) is around 17 × 17 Å^2, and the depth is approximately 12 Å corresponding to four layers of Ru atoms. To accelerate the geometric optimization of the BDO/RuO_2(110) adsorption system, all atoms in the RuO_2 model were fixed using the input files from the ensemble-based adsorption file and their positions were not changed during

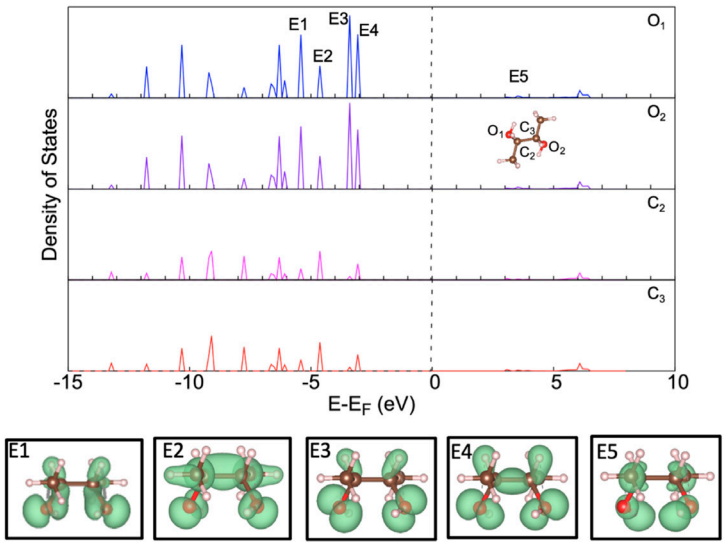

FIGURE 2 | Partial density of states for 2,3-butanediol with accompanying partial charge density images; isosurface of 0.0075 electrons/Bohr^3. The gray, red, brown, and pink spheres are Ru, O, C, and H atoms, respectively.

the optimization. The geometric search of a favorable BDO/RuO_2(110) adsorption configuration was conducted in three steps: 1) BDO was added to the center region of the RuO_2(110) surface and a geometry optimization was carried out using GFN-FF (Spicher and Grimme, 2020) with NWPEsSe. A total of 20,000 structures were generated. The last 1,200 optimized structures with the lowest adsorption energies were kept. 2) The obtained structures in the previous step were further optimized by GFN2-xTB (Bannwarth et al., 2019) to achieve more accurate geometries and energies. The last 10 optimized structures with the lowest adsorption energies were kept. 3) The obtained 10 structures were further optimized using the VASP code, which were used to obtain the corresponding ground-state adsorption energies.

4 RESULTS

4.1 2,3-Butanediol-to-Butene Pathway Analysis

The first step in analyzing the dehydration of BDO is to determine the reaction pathways in the absence of a catalyst based on what is known in the literature. Dehydrating BDO can have a variety of different products such as 3-hydroxy-2-butanone and 2,3-butanedione, but there are three distinct products whose pathways lead to butene (Zheng et al., 2015). These products are 1,3-butadiene, 2-butanone (methyl ethyl ketone), and 2-methylpropanal and are denoted by their respective pathways in **Figure 1** and the accompanying molecular diagrams in **Supplementary Table S1**. Beginning with Pathway 1, BDO undergoes a double dehydration where both hydroxyl groups are removed in one step leaving behind carbon-carbon double bonds in 1,3-butadiene. As this structure is more stable than the final product of butene it is likely for the reaction to get stalled here. For Pathway 2, the step from BDO to 2-butanone is the most dependent on the functional choice with the two extremes being endothermic for PBE and exothermic for SCAN; the van der Waals optB86b-vdW functional is only endothermic by 0.06 eV. The energetic hurdle for this pathway is the transition from 2-butanone to 2-butanol, which is accomplished through hydrogenation. Finally, the transition to butene is favorable with the total process being endothermic to varying degrees depending on the functional choice. In the last pathway, Pathway 3, the dehydration process is very similar to Pathway 2, which accounts for the similarity in their energy diagrams. The difference arises from the placement of the double-bonded oxygen. For 2-butanone, the double-bonded oxygen forms a ketone, whereas for 2-methylpropanal the double-bonded oxygen shifts to an end carbon. In both cases the dehydration of one water molecule occurs. Similarly, as in Pathway 2, 2-methylpropanal is then hydrogenated before the final dehydration to butene—the hydrogenation step requiring the greatest amount of energy input.

Comparing the three pathways, the SCAN functional produced the lowest energies out of the three levels of theory, two exceptions being the intermediary structures in Pathways 2 and 3—2-butanol and 2-methyl-1-propanol. The energetic difference is especially clear when looking at the relative reaction energies for the dehydration process which was 0.395, 0.058, and 0.012 eV for the PBE, VDW, and SCAN functionals, respectively. The SCAN functional improves upon GGA as it has a better capability to distinguish between covalent and metallic bonds, additionally describing them as semi-local (Sun et al., 2015). This distinction should result in less self-interaction error during the DFT calculations.

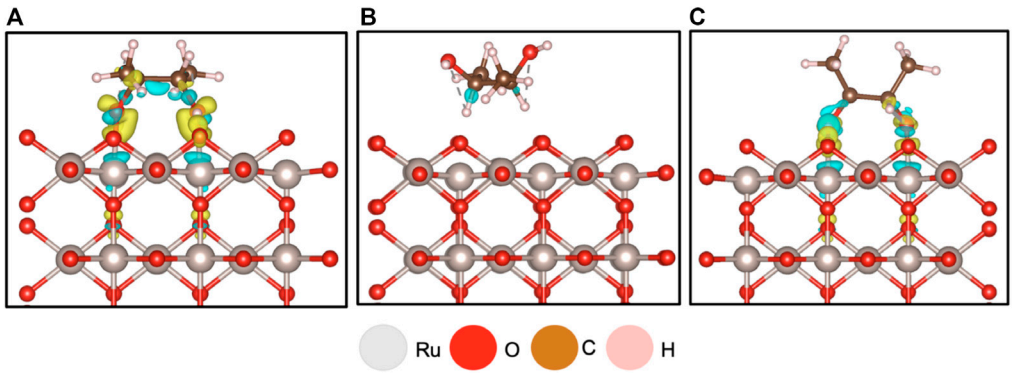

FIGURE 3 | Differential charge density analysis for **(A)** on RuO_2(110) having the oxygen functional groups of 2,3-butanediol facing the surface resulting in an adsorption energy −2.34 eV; **(B)** 2,3-butanediol adsorbed on RuO_2 with its functional groups facing away from the surface resulting in an adsorption energy of −0.3 eV; **(C)** 2,3-butanediol adsorbed on RuO_2, structure generated from NWPEsSe surface adsorption energy −2.61 eV; isosurface level for both figures 0.0075 electrons/$Bohr^3$, yellow indicates charge gain, and blue indicates charge loss.

4.2 Electronic Analysis of 2,3-Butanediol in the Gas Phase

To understand the bonding more accurately between BDO and RuO_2(110), the electronic configuration of the gas phase BDO was analyzed through partial density of states (PDOS). We also analyzed the partial charge density distribution of its four highest occupied molecular orbitals (E1–E4) as well as its lowest unoccupied molecular orbital (E5). This information will later be used in the study to identify changes in the electronic configuration upon adsorption to the surface. The PDOS shown in **Figure 2** was performed for optimized configurations of BDO in the gas phase. The *p*-states of each of the oxygens in the hydroxyl group and their bonded carbons were examined. *s*-states were left out of this plot as they will largely not participate in the bonding to the surface. The partial charge energy intervals that were used for these plots are given in **Supplementary Table S2**. The Fermi level was calculated to be −3.07 eV away from the HOMO level.

Examining the *p*-states shows that the HOMO, identified as E4, is largely occupied by the two oxygens in the hydroxyl groups. The HOMO having the highest magnitude of states with the hydroxyl oxygens suggests that these oxygens are going to be the main participants in the chemisorption of BDO. This is further evidenced with E3 as well as E4 whose partial charge density distribution shows defined p-orbitals surrounding the oxygen species. Moving lower in energy to the E1 and E2 peaks, the charge density is more clearly including the hydrogen species in the hydroxyl group as well as the hydrogen species bonded to each respective carbon. E2 additionally has a very defined σ-cloud around C2 and C3. The LUMO peak at E5 has a significantly smaller peak with the charge density distributing more on the hydrogen species within the hydroxyl group as well as the corresponding bonded carbons.

4.3 2,3-Butanediol Orientation Effects on Adsorption to the Surface

To determine the most favorable adsorption site of 2,3-butanediol, the orientation of the hydroxyl groups relative to the surface—the main interest in the eventual dehydration reaction—needs to be analyzed. Therefore, for 2,3-butanediol, two alternatives were considered: one with hydroxyl groups facing toward the surface (**Figure 3A**) and the other with hydroxyl groups facing away from the surface (**Figure 3B**). As anticipated, the hydroxyl groups facing toward the surface was the more favorable configuration, with an adsorption energy of −2.34 eV, classifying it as chemisorbed to the surface. This is evident in **Figure 3A**, where the charge differential image clearly shows that charge is exchanged from the hydroxyl groups between the oxygen's *p* orbital and the Ru 5-coordinated atom's *d* orbital. The oxygen acts as an electron acceptor that is donated from Ru. Additionally, stabilization from the subsurface Ru species is also evident as charge is donated to the surface. In the case when the hydroxyl group faces away from the surface, virtually no charge exchange occurs (**Figure 3B**). This is consistent with the weak adsorption energy of −0.30 eV, which is indicative of physisorption. Therefore, it can be concluded that the difference between chemisorption and physisorption to the surface depends on the hydroxyl group orientation. This orientation of the hydroxyl groups in the diol is also supported in the literature when one attempts to carry out a dehydration reaction (Acharya et al., 2013).

This differential charge analysis was based on placement at Site 1 in **Supplementary Figure S2** using the ensemble-based approach. Additionally, the configuration chosen was supported by an NWPEsSe-based analysis. The most favorable structure, determined by the NWPEsSe global optimizer, shows that the hydroxyl group orientation faces the surface (**Figure 3C**), where, again, charge transfer is observed between the oxygens in the hydroxyl group and the Ru 5-coordinated atom. This results in a more favorable adsorption energy of −2.61 eV.

4.4 Adsorption Analysis

4.4.1 Ensemble-Based Site Testing

Within the framework of the ensemble-based site testing approach, a horizontal and a vertical site were tested at each of the seven sites can be seen in **Table 1**. As anticipated, the

TABLE 1 | Ensemble-based adsorption site comparison; the site orientation is given in **Supplementary Figure S2**; horizontal parallel to the a axis; and vertical parallel to the b axis.

Site #	1	2	3	4	5	6	7
Horizontal adsorption energy (eV)	−2.34	−0.43	−1.43	−0.46	−2.35	−2.34	−2.30
Vertical adsorption energy (eV)	−1.75	−0.35	−1.71	−0.46	−1.71	−1.97	−2.30

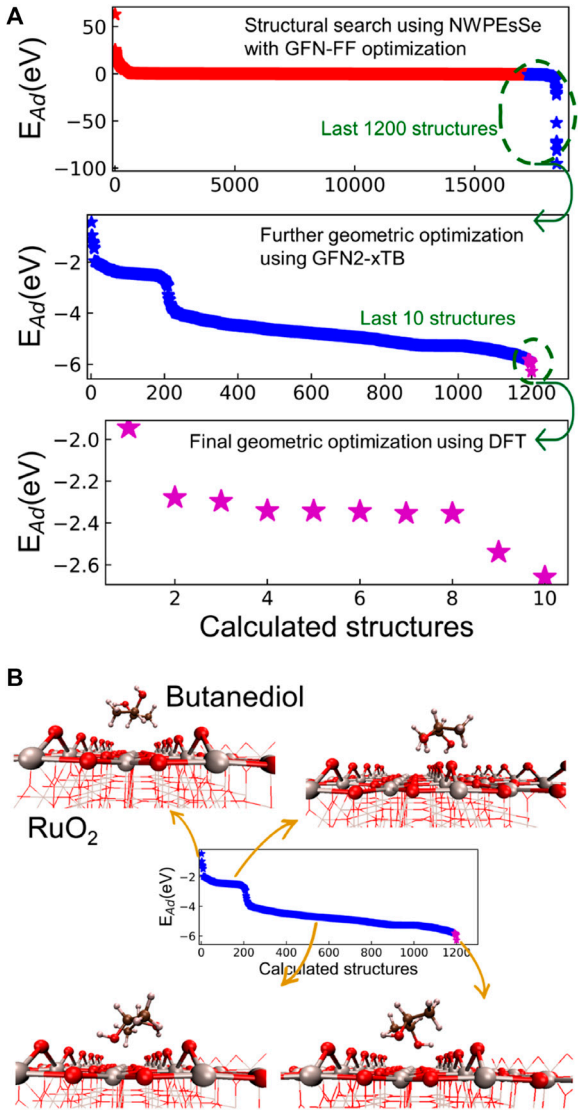

FIGURE 4 | (A) Three steps of searching for BDO/RuO_2(110) adsorption configuration. The calculated structures have been sorted based on their adsorption energies in each plot. **(B)** Examples for snapshots of adsorption configurations obtained in the second step. The gray, red, brown, and pink spheres are Ru, O, C, and H atoms, respectively.

horizontal configurations have lower adsorption energies, attributed to the fact that in the horizontal configuration the hydroxyl groups are parallel to the rows of 5-coordinated Ru (Ru_{5c}) atoms. The most favorable site is above the Ru_{5c} atom, denoted as Site 1 in **Supplementary Figure S2**. Sites 5 and 6 have comparable energies because the converged structure is isostructural to Site 1, meaning that in all three cases both hydroxyl groups are bonded to Ru_{5c} atoms. For the adsorption energies of the vertical adsorption sites, they are generally weaker as in most cases only one hydroxyl group bonds to the surface. The comparably strong adsorption energy seen for Site 7 can be attributed to the fact that the structure converged to a horizontal configuration, mirroring the structure seen for Site 7 in the horizontal set of adsorption energies. This further demonstrates that the horizontal orientation is more energetically favorable as the favorable orientations for the vertical set of tested configurations converged to a horizontal configuration.

4.4.2 Global Optimization Approach

Figure 4A illustrates the three-step approach that we took to search for the most favorable adsorption configuration of BDO on RuO_2(110). The scope of adsorption configurations were successfully narrowed via our approach to ranking these structures based on the adsorption energies. Such an approach enabled us to identify the most energetically favorable adsorption configuration for BDO on RuO_2(110). We note that the absolute adsorption energies calculated by GFN-FF and GFN2-xTB are biased since the system we are considering is not taken especially into account in the parameterization of xTB methods (Bannwarth et al., 2021; Bannwarth et al., 2019; Spicher and Grimme, 2020). However, our focus here is to rank the different adsorption structures based on their adsorption energies. Therefore, the absolute accuracy of the adsorption energy in the first two steps only has a minor impact on our approach.

Furthermore, we analyzed snapshots of the adsorption configurations during our geometric search. The first step using NWPEsSe and GFN-FF generally screened a variety of BDO/RuO_2(110) structures, found a large amount of adsorption configurations, and ruled out unfavorable structures. In the second step involving GFN2-xTB, we were able to refine the obtained structures from the first step and identify several adsorption configurations that were at local minima, as illustrated in **Figure 4B**. When the hydroxyl groups of BDO face the vacuum layer above the RuO_2(110) surface, the adsorption strength is the weakest. When the hydroxyl groups interact with terminal O atoms of RuO_2(110), a weak adsorption is achieved. As the hydroxyl groups get closer to the RuO_2(110) surface and interact with surface Ru atoms, the adsorption of BDO is strengthened, and the most favorable adsorption configuration occurs when both hydroxyl groups interact with surface Ru_{5c} atoms. The last step uses our DFT-based method using the VASP code, which provides a computationally more

TABLE 2 | Comparison of the adsorption energies and specifics of the configurations between ensemble-based approach and the NWPEsSe-based approach in finding the global minimum.

	E_{ads} (eV)	E_{dist} (eV)	$d_{O1\text{-}Ru}$ (Å)	$d_{O2\text{-}Ru}$ (Å)	Dihedral angle O_1 (°)	Dihedral angle O_2 (°)
Manual	−2.34	0.24	2.20	2.20	71.07	70.67
NWPEsSe	−2.61	0.23	2.14	2.16	168.70	166.64

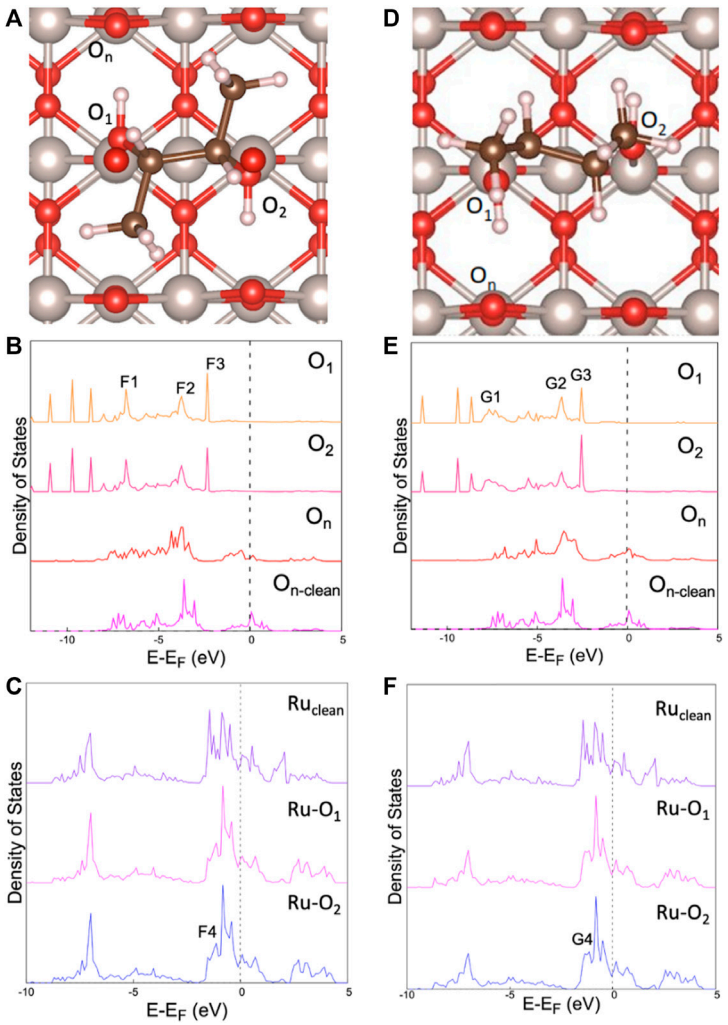

FIGURE 5 | PDOS comparing adsorption of BDO on RuO_2. **(A)** diagram of manual adsorption site; **(B)** *p*-states of manual site testing; **(C)** *d*-states of manual site testing; **(D)** diagram of NWPEsSe adsorption site; **(E)** *p*-states from NWPEsSe generated structure; **(F)** *d*-states from NWPEsSe generated structure; O_1 and O_2 have the same BDO designation shown in **Figure 2**, O_n is in reference to the neighboring oxygen bridge atom to BDO, $O_{n\text{-}clean}$ is the same atom but on the clean surface; Ru-O_1 is referring the ruthenium atom adsorbed to O_1, same case for Ru-O_2; Ru_{clean} is a Ru_{5c} atom without any adsorbates.

expensive but accurate evaluation of several adsorption configurations and their associated adsorption energies.

4.4.3 Comparison of Adsorption Site Testing

Once the final DFT calculations were done on the NWPEsSe-generated structures, we determined which ground-state structure was at the global minimum. **Table 2** compares the ensemble-based site testing to the global minimum that was found using NWPEsSe software. The difference in the dihedral angles can be attributed to the methyl groups being perpendicular to the surface for the NWPEsSe-based structure, whereas in the ensemble-based method they are parallel. As a result, the NWPEsSe-based structure is more strongly bonded to the surface, which correlates well with the shorter bond distance between the oxygen of the hydroxyl functional group and the Ru_{5c} site on the surface. The partial charge analysis shown in **Figure 3A** as

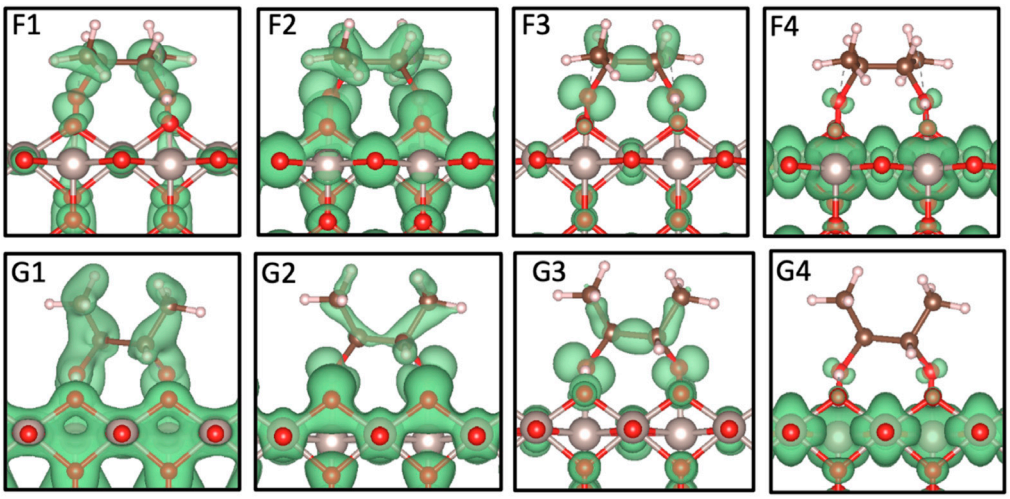

FIGURE 6 | Partial charge density distribution images associated with the PDOS peaks in **Figure 5**; isosurface of 0.0075 electrons/Bohr^3. The gray, red, brown, and pink spheres are Ru, O, C, and H atoms, respectively.

TABLE 3 | *d*-band comparison between the clean Ru_{5c} atom and the Ru_{5c} atoms involved in the adsorption of BDO in the ensemble-based approach and the NWPEsSe-based approach toward obtaining the most favorable ground-state structure.

		Ensemble-based structure		NWPEsSe-based structure	
	Ru_{clean}	Ru-O_1	Ru-O_2	Ru-O_1	Ru-O_2
Center (eV)	−4.10	−4.21	−4.19	−4.26	−4.29
Width (eV)	6.09	6.28	6.25	6.47	6.50

obtained using the ensemble-based approach has its methyl groups in the same plane with the carbon-carbon bond suggesting that this configuration would be more favorable than the one that was generated with NWPEsSe software. That is not the case however as the methyl groups of the ensemble-based structure flatten out and interact with the neighboring oxygens (O_n) causing the bond distance between the hydroxyl functional groups and the surface to elongate, indicating a strain on the surface bonds. On the other hand, the methyl groups in the NWPEsSe-based structure do not interact with the neighboring oxygens, since they are pointing towards the vacuum, allowing for a shorter O-Ru_{5c} bond distance and, as a result, a stronger adsorption energy.

We compare the PDOS analyses of the most favorable adsorption sites resulting from the two methods in **Figure 5**, with the accompanying partial charge density images of select peaks shown in **Figure 6**. The energy intervals analyzed for the partial charge density distribution are available in **Supplementary Table S3**. Comparing **Figures 5B,E** and **Figures 5C,F** shows a strong similarity between the two configurations, which is to be expected. This is further supported by **Figure 6**, which shows almost identical electron cloud distributions around BDO in its respective configurations. The largest difference between the two adsorption configurations is seen in **Figures 5B,E** with the *p*-state analysis of the bonded BDO oxygens to the surface identified by F1 and G1. These lower energy states indicate a more stable bond formation, F1 is more peak-like where G1 has more smearing and has shifted to a lower energy. The smearing and shift to lower energy of G1 as compared to F1 indicates a slight increase in stability for the NWPEsSe-based structure.

The *d*-states of the two systems are given in **Figures 5C,F**; as there is only one significant peak that has interactions with the BDO molecule, the partial charge image for each set is included in **Figure 6** with the *p*-state analysis. The peaks being close to the Fermi level show very little interaction with the surface but the distinct peaks across the Fermi level confirm that the system is metallic, which agrees with the literature (Rogers et al., 1958; Berlijn et al., 2017). This is also likely the reason why the PDOS of the O_n in **Figures 5B,E** has states around the Fermi level as a part of the bonding within the lattice. Analyzing the F4 and G4 peaks, a small *p*-shaped orbital can be seen surrounding the hydroxyl

TABLE 4 | Bader net atomic charge values for the Ru_{5c} atoms and their respective bonded hydroxyl oxygens for the two ground-state structures in the case of the ensemble-based and the NWPEsSe-based site testing approaches with accompanying clean RuO_2(110) surface and gas phase (BDO) Bader net atomic charges for comparison.

	Ensemble-based structure				NWPEsSe-based structure			
	Ru-O_1	Ru-O_2	O_1	O_2	Ru-O_1	Ru-O_2	O_1	O_2
Bader net atomic charge of adsorbed structure (*e*)	1.64	1.64	−1.17	−1.21	1.66	1.68	−1.18	−1.16
Bader net atomic charge of clean surface/gas phase structure (*e*)	1.80	1.80	−1.15	−1.21	1.80	1.80	−1.15	−1.21
Electron behavior	loss	loss	gain	gain	loss	loss	gain	loss

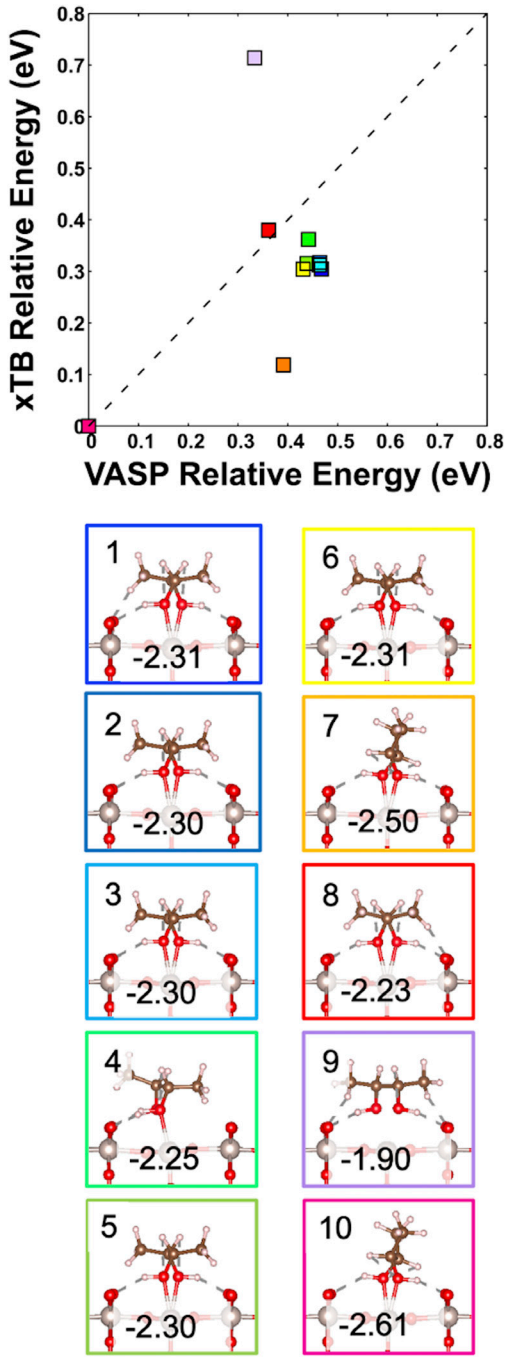

FIGURE 7 | Correlation plot between the relative adsorption energies generated from the 10 lowest structures of GFN2-xTB simulation and their corresponding DFT optimized relative adsorption energies (in eV); the color coding in the plot corresponds to the figure images that have their DFT calculated adsorption energies. The gray, red, brown, and pink spheres are Ru, O, C, and H atoms, respectively.

oxygens and an accompanying charge distribution can be seen for O_n (**Figure 6**); this is likely the result of a very small distribution of states located in the same range. However, most of the charge can clearly be seen in the surface surrounding the Ru cations. The peak isolated by F4 and G4 is more evident in the Ru clean surface PDOS and is noticeably larger in magnitude. The decrease in height for the adsorbed surface is likely the result of the overlap with the hydroxyl oxygen's *p*-states.

Looking at the *d*-band center information seen in **Table 3**, the clean surface has the highest energy value at −4.10 eV, while the centers are lower in energy at ~ −4.20 eV and ~ −4.28 eV for the ensemble-based and NWPEsSe-based structures, respectively. This shift downward is indicative of the surface becoming less reactive once 2,3-butanediol is adsorbed (Kitchin et al., 2004). The *d*-band width leads to similar conclusions as a decrease in the *d*-band center energy typically means a broadening of the *d*-band (Kitchin et al., 2004) as evidenced in **Table 3**. The ensemble-based *d*-band center being slightly higher in energy than that of NWPEsSe-based structure also has a correspondingly narrower width. As both are lower in energy than the clean Ru_{5c} atom, they have a broader width, comparatively. The lower *d*-band center for NWPEsSe-based structure further explains its stronger adsorption energy observed as compared to the ensemble-based structure.

5 DISCUSSION

5.1 2,3-Butanediol in the Gas Phase

Analyzing the three different reaction pathways toward butene formation, as shown in **Figure 1**, makes it clear that Pathway 1 is unlikely as it has the highest potential to get stalled in the intermediary product of 1,3-butadiene. This pathway has been explored in the literature as 1,3-butadiene is an important additive in the production of rubber (Sun et al., 2020); it was found to be hard to produce from BDO as 2-butanone was more favorable (Malcolm Winfield, 1945). This is consistent with the reaction energy pathway comparison as seen in **Figure 1**. Pathways 2 and 3 are more likely as that thermodynamic sink is not present in the same capacity. This has also been found experimentally that both 2-methylpropanal and 2-butanone are the main intermediates in the dehydration of BDO to butene (Zheng et al., 2015).

The HOMO level being primarily occupied by the oxygen *p*-states indicate that they will mainly determine the reactivity with the surface, as shown in **Figure 2**. This is later supported by **Figure 3**, which shows that having the oxygen functional groups face the surface are far more favorable, resulting in chemisorption. This is further supported by the results of the global optimization study. As evidenced by **Figure 4B**, the least favorable structures obtained through a thorough testing of 1,200 structures were the ones where the BDO functional groups are directed toward the vacuum layer. As the BDO surface-facing orientation is required to promote its eventual dehydration, we expect that this adsorption configuration would be more favorable.

5.2 Adsorption Analysis

The adsorption analysis of BDO on RuO_2(110) began by understanding its surface orientation. As is evident by the

differential charge analysis (**Figure 3**) and the global optimization search (**Figure 4**), having the oxygen functional groups face the surface leads to the most favorable adsorption site. This is an expected result, as the PDOS reveals that the HOMO level was mostly occupied by the oxygen *p*-states. Additionally, for an optimal chemisorption configuration, the hydroxyl groups need to be parallel with the Ru_{5c} atoms as evidenced by **Table 1**. While other orientations of the BDO molecule with the surface could have been tested manually, the results from our NWPEsSe-based analysis confirm that the horizontal configuration is the most favorable when BDO adsorbs on a pristine $RuO_2(110)$ surface.

Further confirmation of the differential charge analysis at the surface can be obtained through a Bader charge analysis that is given in **Table 4**, which was completed for both the NWPEsSe-based and ensemble-based determined global minima. In both cases, the Bader charge on the Ru_{5c} atoms decreases with respect to the clean surface indicating a depletion of electrons. On the other hand, the Bader charge analysis of the O_1 species, one of the hydroxyl oxygens, increases upon adsorption of BDO as compared to the clean surface indicating an accumulation of electrons. The hydroxyl oxygens Bader net atomic charge doesn't necessarily indicate a net gain of electrons and that is most likely attributed to how the charge is partitioned in the calculation. Analyzing **Figures 3A–C** it's clear that there is both a charge gain and a charge loss occurring around each oxygen species in BDO's hydroxyl functional groups. Therefore, the Bader analysis is most likely including both in its calculation. Interestingly, in the case of the ensemble-based structure the Bader charge of the O_2 species within the adsorbed BDO molecule is unchanged as compared to its gas phase value, while there is slight loss for the O_2 species in the NWPEsSe-based structure as compared to the gas phase species. However, these changes are minor as compared to those occurring for the Ru_{5c} species. As such, we conclude that the Ru_{5c} species donates electrons to the hydroxyl oxygen to chemisorb BDO to the metal oxide surface.

The electronic configuration of the two different systems is similar. The PDOS of the main species that are involved in the adsorption of BDO (**Figure 5**) and the resulting partial charge density distributions (**Figure 6**) further confirm that both the ensemble-based and the NWPEsSe-based structure chemisorb to the surface. The overlap between the hydroxyl oxygen's *p*-states and Ru_{5c} *d*-states suggest the exchange of electrons. This is evidenced by the distinct partial charge density distributions, specifically between the higher energy peaks shown in **Figure 6** (F3, G3, F4, and G4). In these analyses, a *p*-orbital is clearly seen on the hydroxyl oxygens, and, in the case of F4 and G4, there is significant charge distributed on the Ru cations. The final peak in the *p*-states, G3 and F3, show the most similarity to the E4 HOMO peak found for the BDO molecule in the gas phase (**Figure 2**). The corresponding peaks are shifted 0.6 and 0.4 eV lower than the gas phase values for F3 and G3, respectively. The similarity of the partial charge densities is more clearly seen when comparing the F3 and E4 partial charge distributions as the ensemble-based configuration looks more like the converged gas phase structure. In both cases, F3 and G3, the *p*-orbital cloud is distinct in the hydroxyl oxygens, and the σ cloud is distinct between the C2-C3 bond and the accompanying methyl group attachments to C2 and C3. As these are higher energy peaks, they are less stable and have slight overlap with the Ru cations they are bonded to (**Figure 6**). The chemisorption is also further supported in **Table 3** where the *d*-band center and width decreases and becomes broader as the Ru_{5c} cations exchange electrons with BDO. The *d*-band center value of the NWPEsSe-based structure being slightly more negative indicates a stronger chemical bond as compared to the structure identified by our ensemble-based method.

Between the two analyses, ensemble-based and NWPEsSe-based, the ground-state structure had the same placement on the lattice indicated as Site 1 in **Supplementary Figure S2** of the SI. However, the global minimum of the NWPEsSe-based structure has a lower adsorption energy (−2.61 eV) as compared to the ensemble-based local counterpart (−2.34 eV). The lower energy from the NWPEsSe-based structure is likely attributed to the orientation of the methyl groups. With the NWPEsSe-based structure the methyl groups point toward the vacuum layer, making them perpendicular to the surface, as identified by the large dihedral bond angle with the oxygen functional group. This orientation, while having a comparable distortion energy to the ensemble-based structure from the gas-phase BDO, results in shorter bond lengths. Therefore, we hypothesize that in the ensemble-based structure, the flattening of the methyl groups to become parallel with the surface causes a strain on the hydroxyl bond to the surface and the bond lengthens to accommodate it, resulting in a less favorable adsorption energy. This conjecture is supported by the results from the calculations on the 10 lowest structures from the GFN2-xTB program. Their configuration details and adsorption energies are supplied in **Supplementary Table S4**. Structures 1–3,5, and 6 all have similar dihedral angles, bond lengths, and adsorption energies as compared to the ensemble-based structure. Therefore, we conclude that the ensemble-based structure adsorption site analysis was able to determine one of the lowest energy adsorption configurations but was limited in identifying the global ground-state structure.

We compare the 10 lowest structures from the GFN2-xTB run and their corresponding DFT-based optimizations in **Figure 7**. The relative adsorption energies are shown as the GFN2-xTB program was not specifically parameterized for metal oxide adsorbate systems and therefore provides unrealistic absolute adsorption energies. As such it highlights the need to further optimize these structures using DFT-based calculations to get more accurate adsorption energies. There is good agreement between the two relative energies (although there are two defined outliers seen in orange and purple, Structures 7 and 9, respectively). Structure 7 has a lower energy as it is closest configuration-wise to the ground-state structure seen in pink, Structure 10. Conversely, Structure 9 has the highest relative energy, making it less favorable. As shown in **Figure 7**, Structure 9 did not in fact form a strong bond with the surface and instead is

flattened out by interacting with the neighboring O_n's through hydrogen bonding. The lowest adsorption energy is Structure 10, making it the most favorable conformation and the ground-state structure identified, while Structure 9 is the least favorable. When examining **Supplementary Table S4** it is also clear from the bond lengths, dihedral angles, and adsorption energies that Structure 7 is the structure that has the closest conformation to Structure 10. The agreement between the two systems confirms the accuracy of the calculations in determining the ground-state structure.

6 CONCLUSION

Analyzing the energetic pathways of BDO dehydration to butene (**Figure 1**), it was determined that Pathways 2 and 3 are more favorable since they are less likely to stall in the intermediary phase. By comparing the electronic properties of BDO in the gas phase to when it is adsorbed on the surface, we find that the adsorption of BDO on RuO_2(110) is due to the overlap of the hydroxyl oxygens *p*-states with the Ru_{5c} *d*-states. A differential charge distribution analysis confirmed the adsorption through a noticeable charge exchange between the hydroxyl groups and the surface. Correlation plots between the GFN2-xTB structures generated using the NWPEsSe software and their corresponding DFT-based optimized adsorption energies show agreement between the systems. Comparison between the ensemble-based approach and the NWPEsSe-based approach for adsorption site testing show that the NWPEsSe-based approach was able to find a more favorable ground-state structure with an adsorption energy of −2.61 eV. The success in using the NWPEsSe software in determining the most favorable ground-state structure opens the possibility of using the global optimizer to be used in more complex adsorption systems. This will be especially beneficial with surfaces that have defects and therefore more nuanced adsorption configurations.

NOMENCLATURE

Resource Identification Initiative

To take part in the Resource Identification Initiative, use the corresponding catalog number and RRID in your current article. For more information about the project and for steps on how to search for an RRID, click here.

DATA AVAILABILITY STATEMENT

The raw data supporting the conclusion of this article will be made available by the authors, without undue reservation.

AUTHOR CONTRIBUTIONS

All authors listed have made a substantial, direct, and intellectual contribution to the manuscript and approved it for publication.

FUNDING

This work was funded by the WSU-PNNL Bioproducts Institute, which is a joint research collaboration of Washington State University and the U.S. Department of Energy's Pacific Northwest National Laboratory. V-AG, RR, and DZ acknowledge funding from U.S. Department of Energy, Office of Basic Energy Sciences, Division of Chemical Sciences, Geosciences and Biosciences project number 47319. This work was also partially funded by the Joint Center for Deployment and Research in Earth Abundant Materials (JCDREAM) in Washington State. This research also used resources of the National Energy Research Scientific Computing Center (NERSC), a U.S. Department of Energy Office of Science User Facility operated under Contract No. DE-AC02-05CH11231. The Pacific Northwest National Laboratory is operated by Battelle for the U.S. DOE.

ACKNOWLEDGMENTS

Part of the computational resources was also provided by the Kamiak HPC under the Center for Institutional Research Computing at Washington State University. We also thank Naseeha Cardwell and Nisa Ulumuddin for fruitful discussions.

SUPPLEMENTARY MATERIAL

The Supplementary Material for this article can be found online at: https://www.frontiersin.org/articles/10.3389/fenrg.2021.781001/full#supplementary-material

REFERENCES

Acharya, D. P., Yoon, Y., Li, Z., Zhang, Z., Lin, X., Mu, R., et al. (2013). Site-specific Imaging of Elemental Steps in Dehydration of Diols on TiO_2(110). *ACS Nano* 7, 10414–10423. doi:10.1021/nn404934q

Aihara, T., Asazuma, K., Miura, H., and Shishido, T. (2020). Highly Active and Durable WO_3/Al_2O_3 Catalysts for Gas-phase Dehydration of Polyols. *RSC Adv.* 10, 37538–37544. doi:10.1039/D0RA08340B

Bannwarth, C., Caldeweyher, E., Ehlert, S., Hansen, A., Pracht, P., Seibert, J., et al. (2021). Extended Tight-binding Quantum Chemistry Methods. *WIREs Comput. Mol. Sci.* 11, e1493. doi:10.1002/WCMS.1493

Bannwarth, C., Ehlert, S., and Grimme, S. (2019). GFN2-xTB-An Accurate and Broadly Parametrized Self-Consistent Tight-Binding Quantum Chemical Method with Multipole Electrostatics and Density-dependent Dispersion Contributions. *J. Chem. Theor. Comput.* 15, 1652–1671. doi:10.1021/ACS.JCTC.8B01176

Becke, A. D. (1986). Density Functional Calculations of Molecular Bond Energies. *J. Chem. Phys.* 84, 4524–4529. doi:10.1063/1.450025

Berlijn, T., Snijders, P. C., Delaire, O., Zhou, H.-D., Maier, T. A., Cao, H.-B., et al. (2017). Itinerant Antiferromagnetism in RuO_2. *Phys. Rev. Lett.* 118, 3–8. doi:10.1103/PhysRevLett.118.077201

Guragain, Y. N., and Vadlani, P. V. (2017). 2,3-Butanediol Production Using Klebsiella Oxytoca ATCC 8724: Evaluation of Biomass Derived Sugars and Fed-

Batch Fermentation Process. *Process Biochem.* 58, 25–34. doi:10.1016/J.PROCBIO.2017.05.001

Haines, J., Léger, J. M., and Schulte, O. (1996). Pa3̄ Modified Fluorite-type Structures in Metal Dioxides at High Pressure. *Science* 271, 629–631. doi:10.1126/science.271.5249.629

Henkelman, G., Arnaldsson, A., and Jónsson, H. (2006). A Fast and Robust Algorithm for Bader Decomposition of Charge Density. *Comput. Mater. Sci.* 36, 354–360. doi:10.1016/J.COMMATSCI.2005.04.010

Hensley, A. J. R., Wang, Y., and McEwen, J.-S. (2016). Adsorption of Guaiacol on Fe (110) and Pd (111) from First Principles. *Surf. Sci.* 648, 227–235. doi:10.1016/j.susc.2015.10.030

Interational Air Transport Association (2020). Annual Review, 2020.

Kitchin, J. R., Nørskov, J. K., Barteau, M. A., and Chen, J. G. (2004). Modification of the Surface Electronic and Chemical Properties of Pt(111) by Subsurface 3d Transition Metals. *J. Chem. Phys.* 120, 10240–10246. doi:10.1063/1.1737365

Kresse, G., and Furthmüller, J. (1996). Efficient Iterative Schemes For Ab Initio Total-Energy Calculations Using a Plane-Wave Basis Set. *Phys. Rev. B* 54, 11169–11186. doi:10.1103/PhysRevB.54.11169

Kresse, G., and Hafner, J. (1993). Ab Initio Molecular Dynamics for Liquid Metals. *Phys. Rev. B* 47, 558–561. doi:10.1103/PhysRevB.47.558

Lejaeghere, K., Bihlmayer, G., Björkman, T., Blaha, P., Blügel, S., Blum, V., et al. (2016). Reproducibility in Density Functional Theory Calculations of Solids. *Science* 351, aad3000. doi:10.1126/science.aad3000

Malcolm Winfield, B. E. (1945). The Catalytic Dehydration of 2,3-butanediol to 1,3-butadiene. *J. Counc. Sci. Ind. Res.* 18, 412–423.

Mittendorfer, F., and Hafner, J. (2001). Density-functional Study of the Adsorption of Benzene on the (111), (100) and (110) Surfaces of Nickel. *Surf. Sci.* 472, 133–153. doi:10.1016/S0039-6028(00)00929-8

Mu, R., Cantu, D. C., Lin, X., Glezakou, V.-A., Wang, Z., Lyubinetsky, I., et al. (2014). Dimerization Induced Deprotonation of Water on RuO_2(110). *J. Phys. Chem. Lett.* 5, 3445–3450. doi:10.1021/jz501810g

Ohtsuka, S., Nemoto, T., Yotsumoto, R., Yamada, Y., Sato, F., Takahashi, R., et al. (2019). Vapor-phase Catalytic Dehydration of Butanediols to Unsaturated Alcohols over Yttria-Stabilized Zirconia Catalysts. *Appl. Catal. A: Gen.* 575, 48–57. doi:10.1016/J.APCATA.2019.02.013

Perdew, J. P., Burke, K., and Ernzerhof, M. (1996). Generalized Gradient Approximation Made Simple. *Phys. Rev. Lett.* 77, 3865–3868. doi:10.1103/PhysRevLett.77.3865

Reuter, K., and Scheffler, M. (2002). Composition, Structure, and Stability of RuO_2(110) as a Function of Oxygen Pressure. *Phys. Rev. B* 65, 1–11. doi:10.1103/PhysRevB.65.035406

Rogers, B. D., Shannon, R. D., Sleight, A. W., and Gillson, J. L. (1958). Crystal Chemistry of Metal Dioxides with Rutile-Related Structures. The Chemical Society. Available at: https://pubs.acs.org/sharingguidelines (Accessed April 29, 2021).

Spicher, S., and Grimme, S. (2020). Robust Atomistic Modeling of Materials, Organometallic, and Biochemical Systems. *Angew. Chem. Int. Ed.* 59, 15665–15673. doi:10.1002/ANIE.202004239

Sun, D., Li, Y., Yang, C., Su, Y., Yamada, Y., and Sato, S. (2020). Production of 1,3-butadiene from Biomass-Derived C4 Alcohols. *Fuel Process. Technol.* 197, 106193. doi:10.1016/J.FUPROC.2019.106193

Sun, J., Remsing, R. C., Zhang, Y., Sun, Z., Ruzsinszky, A., Peng, H., et al. (2015). SCAN: An Efficient Density Functional Yielding Accurate Structures and Energies of Diversely-Bonded Materials. Available at: http://arxiv.org/abs/1511.01089 (Accessed October 12, 2020).

Wang, W.-C., and Tao, L. (2016). Bio-jet Fuel Conversion Technologies. *Renew. Sustain. Energ. Rev.* 53, 801–822. doi:10.1016/j.rser.2015.09.016

Zhang, J., Glezakou, V.-A., Rousseau, R., and Nguyen, M.-T. (2020). NWPEsSe: An Adaptive-Learning Global Optimization Algorithm for Nanosized Cluster Systems. *J. Chem. Theor. Comput.* 16, 3947–3958. doi:10.1021/ACS.JCTC.9B01107

Zheng, Q., Wales, M. D., Heidlage, M. G., Rezac, M., Wang, H., Bossmann, S. H., et al. (2015). Conversion of 2,3-butanediol to Butenes over Bifunctional Catalysts in a Single Reactor. *J. Catal.* 330, 222–237. doi:10.1016/j.jcat.2015.07.004

Zhou, C.-H., Xia, X., Lin, C.-X., Tong, D.-S., and Beltramini, J. (2011). Catalytic Conversion of Lignocellulosic Biomass to fine Chemicals and Fuels. *Chem. Soc. Rev.* 40, 5588–5617. doi:10.1039/C1CS15124J

Conflict of Interest: The authors declare that the research was conducted in the absence of any commercial or financial relationships that could be construed as a potential conflict of interest.

Publisher's Note: All claims expressed in this article are solely those of the authors and do not necessarily represent those of their affiliated organizations, or those of the publisher, the editors, and the reviewers. Any product that may be evaluated in this article, or claim that may be made by its manufacturer, is not guaranteed or endorsed by the publisher.

frontiers in Energy Research

ORIGINAL RESEARCH
published: 17 January 2022
doi: 10.3389/fenrg.2021.788284

Pilot-Scale Pelleting Tests on High-Moisture Pine, Switchgrass, and Their Blends: Impact on Pellet Physical Properties, Chemical Composition, and Heating Values

Jaya Shankar Tumuluru[1], Kalavathy Rajan[2], Choo Hamilton[2], Conner Pope[2], Timothy G. Rials[2], Jessica McCord[2], Nicole Labbé[2] and Nicolas O. André[2]*

[1]Mechanical System Design and Control Department, Idaho National Laboratory, Idaho Falls, ID, United States, [2]Center for Renewable Carbon, The University of Tennessee, Knoxville, TN, United States

OPEN ACCESS

Edited by:
Zia Haq,
United States Department of Energy (DOE), United States

Reviewed by:
Macmanus Ndukwu,
Michael Okpara University of Agriculture, Nigeria
Hui Zhou,
Tsinghua University, China

***Correspondence:**
Jaya Shankar Tumuluru
JayaShankar.Tumuluru@inl.gov

Specialty section:
This article was submitted to Bioenergy and Biofuels, a section of the journal Frontiers in Energy Research

Received: 01 October 2021
Accepted: 09 November 2021
Published: 17 January 2022

Citation:
Tumuluru JS, Rajan K, Hamilton C, Pope C, Rials TG, McCord J, Labbé N and André NO (2022) Pilot-Scale Pelleting Tests on High-Moisture Pine, Switchgrass, and Their Blends: Impact on Pellet Physical Properties, Chemical Composition, and Heating Values. Front. Energy Res. 9:788284. doi: 10.3389/fenrg.2021.788284

In this study, we evaluated the pelleting characteristics of southern yellow pine (SYP), switchgrass (SG), and their blends for thermochemical conversion processes, such as pyrolysis and gasification. Using a pilot-scale ring-die pellet mill, we specifically assessed the impact of blend moisture, length-to-diameter (L/D) ratio in the pellet die, and ratio of pine to SG on the physico-chemical properties of the resulting pellets. We found that an increase in pine content by 25–50% marginally affected the bulk density; however, it also led to an increase in calorific value by 7% and a decrease in ash content by 72%. A moisture content of 25% (wet basis) and an L/D ratio of 5 resulted in poor pellet durability at <90% and bulk density values of <500 kg/m^3, but increasing the L/D ratio to 9 and lowering the moisture content to 20% (w.b.) improved the pellet durability to >90% and the bulk density to >500 kg/m^3. Blends with ≥50% pine content resulted in lower energy consumption, while a lower L/D ratio resulted in higher pelleting energy. Based on these findings, we successfully demonstrated the high-moisture pelleting of 2.5 ton of pine top residues blended with SG at 60:40 and 50:50 ratios. The quality of the pellets was monitored off-line and at-line by near infrared (NIR) spectroscopy. Multivariate models constructed by combining the NIR data and the pelleting process variables could successfully predict the pine content (R^2 = 0.99), higher heating value (R^2 = 0.98), ash (R^2 = 0.95), durability (R^2 = 0.94), and bulk density (R^2 = 0.86) of the pellets. Thus, we established how blending and densification of SYP and SG biomass could improve feedstock specifications and that NIR spectroscopy can effectively monitor the pellet properties during the high-moisture pelleting process.

Keywords: southern yellow pine, switchgrass, blends, high moisture pelleting, physical properties, chemical composition, near infrared spectroscopy, multivariate modeling

1 INTRODUCTION

Various woody and herbaceous biomass sources—such as sugarcane, corn stover, dedicated bioenergy crops, forest, and agricultural residues—could be used for biofuels production (National Renewable Energy Laboratory, 2008). According to the United States (U.S.) Department of Energy (DOE) and Department of Agriculture (USDA), it is estimated that more than a billion ton of such lignocellulosic biomass could be made available for energy production (U.S. Department of Energy, 2016). The Renewable Fuel Standard (RFS) mandates that cellulosic biofuel should slowly displace transportation fuels and reach 16 billion gallons by 2022 (U.S. Environmental Protection Agency, 2018), which requires the annual processing of approximately 1,000–1,200 million tons of biomass.

Perennial grasses, such as switchgrass (SG), have the potential to be environmentally beneficial, high-yielding sources of cellulosic feedstock. SG is a dedicated bioenergy crop in North America, which is one of the largest temperate biomes on Earth, as well as being a carbon sink (Risser et al., 1981; Suyker and Verma, 2001). The significant advantages of SG are that it can grow on marginal lands that are not being used currently to grow food crops (Hartman et al., 2011; Feng et al., 2017), it mitigates nutrient pollution from fertilizer, provides flood control, increases yield when used in a crop rotation, creates wildlife habitats, prevents soil erosion, and sequesters carbon with its extensive root system (Blanco-Canqui et al., 2017).

Woody feedstock is essential to meet the U.S. national goal of producing 16 billion gallons of cellulosic ethanol by 2022 (U.S. Environmental Protection Agency, 2018). Besides conventional lumber, residues from forestry operations, urban management, paper, and furniture industries—including sawdust, chips, shrubs, limbs, leaves, tree trimmings, and forest thinning, as well as trees grown for energy—are excellent sources of woody biomass. Southern pine species are an essential component of the forest resources of the U.S. southern region, which is one of the crucial timber-producing regions globally (Prestemon, and Abe, 2002). Out of over 74 million ha of total timberland that are currently available in 11 southern states, excluding Oklahoma and Kentucky, 27.5 million ha are classified as softwood types, while another 8.5 million ha are classified as oak-pine types (Zhang and Polyakov, 2010). Pine plantations account for 15 million ha, more than half of the softwood forest area.

Blending of various biomass feedstocks for biofuel and bioproduct production is gaining momentum. According to Chescheir and Nettles (2017) and Chauhan et al. (2011), there is great interest in planting herbaceous biomass such as SG and other straws with woody biomass, which can make blending of the biomass feasbile in the field. Feedstock cost modeling studies by Idaho National Laboratory (INL) have showed that the blending of woody, herbaceous, and municipal solid waste reduces the grower payment by about 46% (Lane, 2018). Blending or formulation are commonly used in other industries, such as food and feed, to achieve a consistent product with desired quality attributes. In the power industry, coals of different grades are blended to control the SO_x and NO_x emissions (Moroń and Rybak, 2015). Lignocellulosic formulations can be similarly developed by blending multiple woody and herbaceous biomasses to meet the desired chemical composition and specifications for thermochemical and biochemical conversion processes, such as calorific value, volatiles, cellulose, lignin, hemicellulose, carbon, hydrogen, nitrogen, alkaline, and alkali-earth metals contents (Edmunds et al., 2018; Ou et al., 2018). Woody biomasses have a higher lignin and lower ash content, whereas herbaceous biomasses have a lower lignin and higher ash content (Williams et al., 2017). Blending of these biomasses, therefore, has the potential to homogenize their overall chemical composition, as well as improve downstream conversion.

According to Ray et al. (2017), blending helps to overcome the cost and quality limitations of lignocellulosic biomass for biofuels production. Edmunds et al. (2018) indicated that the blending of different biomass sources helps to improve their overall feedstock specifications for thermochemical conversion. Yancey et al. (2013) showed that blending reduces the variability of the physical properties and the chemical compositions in various biomass sources while producing a consistent feedstock. The advantages of biomass blending are increased feedstock availability for biorefineries at a reduced cost and improved quality and preprocessing characteristics. According to Mahadevan et al. (2016), the blending of SG and southern pinewood produced bio-oils with low acidity and viscosity. Despite these advantages, there are significant challenges in blending different biomass types, which could cause issues related to feeding, handling, transportation, and storage (Ray et al., 2017).

The typical challenges in using biomass blends are: 1) variability in density, particle shape and size distribution, and rheological properties, which result in hurdles such as entrainment and classification; 2) segregation of the particles because of variability in density; and 3) low density that creates challenges in feeding and reduces conversion efficiencies (Ray et al., 2017). These challenges can be overcome by densifying the biomass blends. Densification improves the handling and conveyance efficiency of bioenergy in-feed supply systems (Tumuluru et al., 2011). It also provides better control on the particle size distribution of the product stream for improved feedstock uniformity and density, enhancing the deconstruction of biomass structural components and improving biochemical and thermochemical conversions. Pelleting also reduces transportation costs by 43% for distances exceeding 15 miles (Tumuluru and Mwamufiya, 2021). For densification using conventional methods, the lignocellulosic feedstocks are dried to about 10% moisture content on wet basis (w.b.). Woody biomass after harvesting has a moisture content between 30 and 50% (w.b.) and that of SG between 15 and 25% (w.b.). Hence, drying biomass to <10% (w.b.) moisture content using conventional rotary dryers adds to the energy and capital costs (Tumuluru, 2016). Also, high-temperature drying results in volatile organic emissions forming photo-oxidants that are hazardous to human health if inhaled. A high-moisture pelleting process was therefore developed at INL to eliminate the rotary drying step and to reduce energy and capital costs. In this process, the biomass is pelleted at higher moisture levels

>20% (w.b.). We have previously studied the pelleting of corn stover, lodgepole pine, and 2-in. (50.8 mm) pine tops and SG blends in a flat die pellet mill in the moisture range of 20–39% (w.b.) (Tumuluru, 2014, 2016, 2019). The resulting pellets had good quality in terms of density and durability. These results also showed that having a higher pine content (>50%) in the blends resulted in higher quality pellets and lower energy consumption. In their techno-economic analysis (TEA), research conducted by Lamers et al. (2015) indicated that the drying of corn stover to <10% (w.b.) moisture content using conventional rotary dryer added significantly to the pelleting cost, whereas pelleting at high-moisture levels of 30% (w.b.) by eliminating the rotary drying, reduced the pelleting cost by about 40%. Our recent study on municipal solid waste (MSW) also showed that high-moisture pelleting could save about 40–46% of pelleting cost and lower 46% of greenhouse gas emissions (Tumuluru and Mwamufiya, 2021). The resulting MSW pellets exhibited a durability between 90 and 98% and a bulk density of about 450–550 kg/m^3 (Tumuluru and Mwamufiya, 2021). Hence, high-moisture pelleting is a good alternative *in lieu* of conventional pelleting for the densification of pine and SG blends.

In recent years, near infrared (NIR)-based high-throughput spectroscopic techniques have been developed to monitor the output of pelleting and other downstream processing of lignocellulosic biomass (Edmunds et al., 2018; Feng et al., 2018; Li et al., 2018; Li et al., 2021). NIR spectroscopy works based on the absorption, emission, reflection, and diffuse-reflection of light in the region of 800–2,500 nm (e.g., 12,500–4,000 cm^{-1}) (Ozaki et al., 2017). Multivariate prediction models could be built on the basis of on-, at-, or off-line NIR spectroscopic analysis and used for rapid, inexpensive characterization of changes in lignocellulosic feedstocks during thermochemical or physico-chemical conversion processes (Li et al., 2018; Hwang et al., 2021). Principal component analysis of online NIR spectra has been recently used to screen the seasonal variability of cellulose crystallinity and lignin content in sugarcane bagasse (Li et al., 2021). Similarly, off-line NIR spectroscopy was used to monitor regional differences in the composition of cellulose, hemicellulose, lignin, and ash of Jerusalem artichokes (Li et al., 2018). The studies on high-moisture pelleting of southern yellow pine (SYP), switchgrass (SG), and their blends using a pilot-scale pellet mill and data on understanding the quality changes during pelleting using on-, at-, or off-line NIR spectroscopy are not available in the literature. To our knowledge, this will be the first study that tests high moisture pelleting of SYP, SG and their blends using pilot scale pellet mill and uses of at-line and off-line NIR spectroscopy to characterize and predict the properties of blended biomass pellets that are of notable relevance for bioenergy production in the U.S.

The overall objective of this work was to investigate the influence of pellet mill die compression (length to diameter ratio) ratio and moisture content on the pelleting characteristics of different blend ratios of SG and SYP residues. A ring-die pellet mill with one ton/h throughput was used for the pelleting studies. According to Tumuluru et al. (2011), the pelleting process variables—such as die diameter and die compression ratio—and feedstock properties—such as moisture and particle size—impact the quality of the pellet produced. Therefore, the specific objectives of our work were to evaluate the impact of: 1) pellet mill die compression (L/D) ratio between 5 and 9; 2) blend ratios of 6.35 mm ground SG and SYP residues (e.g., 0:100, 25:75, 50:50, 75:25, 100:0); and 3) two different moisture levels of 20 and 25% on resulting pellet properties in terms of moisture, unit, bulk and tapped density, durability, ultimate composition, ash contents, higher heating value (HHV), and specific energy consumption (SEC) of the process. Based on the preliminary studies, we selected the combination of parameters [e.g., blend mositure cotnent of about 20% (w.b.) and a L/D ratio of 9] and demonstrated the pelleting of 2.5 ton of 2-inch (50.8 mm) and 6-inch (152.4 mm) SYP residues blended with SG in the ratio of 60:40 and 50:50. We also demonstrated how off- and at-line NIR spectroscopy could be applied for high-throughput characterization of the pellets and for developing multivariate models to predict physico-chemical properties of blended pellets.

2 MATERIALS AND METHODS

2.1 Feedstock Preparation

Switchgrass (SG) (*Panicum virgatum L.*) cv. Alamo stands were cultivated and harvested in 2017 in Vonore, TN. The SG with leaves and stalks was processed via two-stage grinding; at stage-1, the hammer mill (Bliss Industries LLC, Ponca city, OK) was fitted with a 76.2 mm screen, while at stage-2, it was fitted with a 6.35 mm (1/4-in.) screen. The ground SG biomass was shipped to INL in super-sacks for further pelleting. The chemical composition of the received biomass was 38 ± 1% cellulose, 28 ± 1% hemicellulose, 21 ± 0% lignin, 5 ± 0% extractives, and 5 ± 0% acetyl contents.

Clean southern yellow pine (SYP) (*Pinus* spp.) residues with a 152.4 mm (6-in.) stem diameter were harvested from the mature stands at the School of Forestry and Wildlife Sciences at Auburn University, AL, in 2017. The biomass was chipped, dried to about a 10% (w.b.) moisture content, and then shipped to INL. At INL, the pine chips were further ground using a hammer mill (Bliss Industries LLC, Ponca city, OK) fitted with a 6.35 mm screen. The ground SYP and SG were reconditioned to high moistures (20 and 25%, w.b.) and used to test the high-moisture pelleting process either individually or in blends of 25:75, 50:50, and 75:25, respectively. A pilot-scale ring-die pellet mill was used for conducting the pelleting studies on SG, pine, and their blends. Pioneer pellet mill model number: 35A- 75-80HP, serial number 3193, Bliss Industries, LLC, (Ponca City, OK), was used in the present pelleting studies. According to the manufacturer, the recommended break pressure for operating the pellet mill is 1,000 psi. This mill is designed for overall reliability and maximum efficiency and ease of operation. During the pelleting process, the die and collar assembly were protected by a hydraulic overload system, which stops the main motors when an overload situation occurs.

For the 2.5-ton demonstration of high-moisture pelleting, SYP tops of 50.8 mm (2-in.) and 152.4 mm (6-in.) diameter were

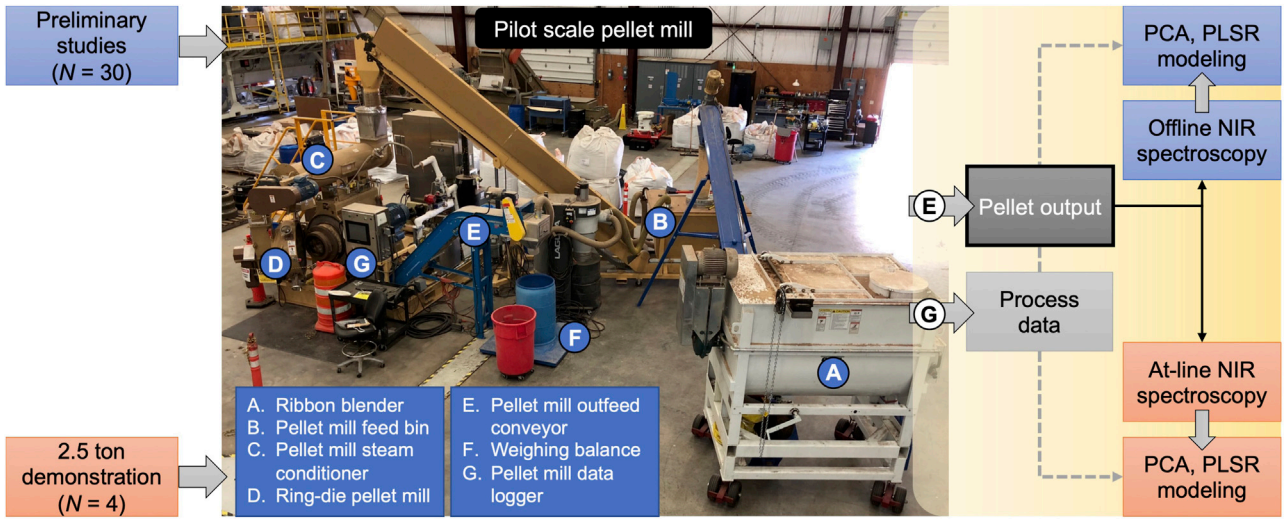

FIGURE 1 | Illustration of high-moisture pelleting of southern yellow pine (SYP) and switchgrass (SG) blends at the pilot-scale set-up (Legend: N–number of treatments; NIR–near infrared spectroscopy; PCA–principal component analysis, PLSR–partial least squares regression).

TABLE 1 | Experimental plan for preliminary and 2.5-ton high-moisture pelleting tests of southern yellow pine (SYP), switchgrass (SG), and their blends.

Sample ID[a]	SYP content (%)[b]	SG content (%)[b]	Moisture content (%)[b]	L/D ratio
Preliminary pelleting tests				
6-in. (152.4 mm) SYP-100	100	0		
6-in. (152.4 mm) SYP-75	75	25		• 5
6-in. (152.4 mm) SYP-50	50	50	• 20	• 7
6-in. (152.4 mm) SYP-25	25	75	• 25	• 9
6-in. (152.4 mm) SYP-0	0	100		
2.5-ton pelleting demonstration				
6-in. (152.4 mm) SYP-50	50	50	20	9
6-in. (152.4 mm) SYP-60	60	40	20	9
2-in. (50.8 mm) SYP-50	50	50	20	9
2-in. (50.8 mm) SYP-60	60	40	20	9

Note: For preliminary pelleting tests, the total number of treatments (N) were 5 blend ratios × 2 moisture levels × 3 L/D ratio = 30.
[a]*SYP, and SG, were ground using a hammer mill fitted with a 6.35 mm (1/4-in.) screen.*
[b]*The percentage pine, SG, and moisture content are provided on a wet weight basis.*

screened and selected. About 50 pine trees were harvested in 2018 from the mature stands of the School of Forestry and Wildlife Sciences at Auburn University, AL, to gather sufficient biomass between 2,000 and 3,000 kg and further dried to about 10% (w.b.) before shipping to INL. These pine residues were ground at INL using a Bliss hammer mill fitted with a 6.35 mm screen size. The ground material was then blended with either 40% or 50% of the previously obtained SG. The chemical composition of the 2-in. (50.8 mm) SYP was 29 ± 0% cellulose, 20 ± 0% hemicellulose, 38 ± 1% lignin, 10 ± 0% extractives, and 1.5 ± 0% acetyl contents, whereas the chemical composition of the 6-in. (152.4 mm) SYP was 36 ± 0% cellulose, 22 ± 0% hemicellulose, 36 ± 1% lignin, 6 ± 0% extractives, and 2 ± 0% acetyl contents.

2.2 High-Moisture Pelleting

A pilot-scale ring-die pellet mill at INL with a throughput capacity of 1 ton/h, as shown in **Figure 1**, was used for both the preliminary testing of SG-SYP blends and for the 2.5-ton high pelleting demonstration. The pellet mill is set-up with a ribbon blender, which pre-conditions the biomass moisture, a steam conditioner that adds moisture and heat during pelleting, and data loggers for recording the pelleting parameters, including conveyor speed, amperage, power, pressure, and steam usage. It also has various pellet dies with different compression (L/D) ratios. During the preliminary pelleting of SYP, SG, and their blends, three L/D ratios (e.g., 5, 7, 9) and two moisture levels (20 and 25% w.b.) were tested for five different biomass blends, as shown in **Table 1**. Based on the preliminary results, we selected an L/D ratio of 9 and a moisture content of 20% (w.b.) for the 2.5-ton pelleting demonstration of 2-in. (50.8 mm) and 6-in. (152.4 mm) SYP blended with SG. During the demonstration, about 1,000 kg of 6-in. (152.4 mm) SYP-50, 227 kg of 6-in. (152.4 mm) SYP-60, 1,000 kg of 2-in. (50.8 mm) SYP-60, and 227 kg of 2-in. (50.8 mm) SYP-50 blends were

pelleted using the parameters listed in **Table 1**. These tests were conducted to understand the impact of blend ratios, L/D ratios, and moisture content on pellet physico-chemical properties, namely ash content, higher heating value (HHV), density (e.g., unit, bulk and tapped), and durability, as well as pelleting energy consumption.

Power consumption data during pelleting were logged using LabVIEW (National Instruments, Austin, TX). An APT power monitor meter (Applied Power Technologies, Inc., San Jose, CA) connected to the pellet mill recorded the power consumption during the high-moisture pelleting in kilowatts. The no-load power was recorded by running the pellet mill empty. The specific energy consumption (SEC) was calculated by subtracting the no-load kW from the full-load power using **Eq. 1**.

$$SEC = \frac{(Full\ load\ power\ (kW) - No\ load\ power\ (kW)) \times time\ (h)}{Weight\ of\ biomass\ processed\ (ton)} \quad (1)$$

2.3 Physico-Chemical Characterization of Pellets

2.3.1 Physical Properties

Pellet moisture content, bulk density, and durability were determined following the American Society of Agricultural and Biological Engineers (ASABE) S269.4 standard (American Society of Agricultural and Biological Engineers (ASABE) Standard S269.4., 2007). Particle size distribution of the ground material was measured using ASABE standard S424.1 (American Society of Agricultural and Biological Engineers (ASABE) Standard S424.1., 1992). The pellets produced were not only analyzed for moisture content; unit, bulk, and tapped density; and durability immediately after pelleting at different moisture levels, but also after drying in an oven at 70°C for 2–3 h to reduce the moisture content to <10% (w.b.). Briefly, moisture content was measured using the oven dry method where the sample was dried at about 105°C for 24 h. The unit density was calculated by measuring the length, diameter, and weight of the individual pellets. The bulk density was measured by pouring the pellets into a cylindrical container and calculated by dividing the weight of the pellets by the container volume. The tapped density was measured by tapping the container on the flat table and filling the container with pellets and measuring the weight again (Tumuluru, 2014; Tumuluru, 2016). A durability tester with four compartments was also used, where 500 g of pellets were placed in each compartment and then rotated at 50 revolutions per minute (RPM) for 10 min (Tumuluru, 2018). Percent durability is given as the ratio of the mass of the intact pellets (after sieving) after tumbling to the total mass of pellets before tumbling. All pellet properties were measured in triplicate.

2.3.2 Ultimate Analysis, Ash, HHV Determination

Biomass materials were ground and screened to a uniform particle size of 0.425 mm (40-mesh) using a Wiley® mini blade mill (Thomas Scientific, Swedesboro, NJ) for ash content and ultimate composition analysis. Total ash content was determined based on the standard laboratory analytical procedure developed by the National Renewable Energy Laboratory (NREL, Golden, CO), where the homogenized biomass was combusted at 575°C, until a constant weight was achieved (Sluiter et al., 2005). The ultimate analysis of carbon (C), hydrogen (H), and nitrogen (N) was performed using a 2,400 Series II CHNS elemental analyzer (PerkinElmer, Shelton, CT), where the oxygen (O) content was calculated by difference [100–(C + H + N)]. For the determination of higher heating value (HHV), about 1.3 g of biomass pellets were loaded into the decomposition vessel of a C 6000 oxygen bomb calorimeter (IKA Works, Inc., Wilmington, NC) and analyzed at 22°C isoperibol mode, with integral oxygen filling/degassing, as well as water recirculation at 3200 RPM. Benzoic acid was used as the calibration standard. All measurements for ash content, CHN, and HHV were conducted in triplicate per sample per biomass blend.

2.4 At- and Off-Line NIR Spectroscopy

Samples from preliminary pelleting tests (N = 30) were characterized off-line using a desktop DA 7250 SD NIR spectrometer (Perten Instruments AB, Hägersten, Sweden). During the 2.5-ton pelleting demonstration, samples of approximately 25 g were manually collected every 2.5 min from the outfeed pellet conveyor and subjected to at-line NIR spectroscopy using the same DA 7250 SD instrument. The at-line NIR scans were meticulously time-stamped and the corresponding pellet temperature was recorded by using a hand-held infrared thermometer. The pellet moisture content was also determined in duplicate by drying at 105°C until constant weight. The pellet samples for both the at- and off-line NIR analysis were packed twice. For each repack, the samples were scanned twice in the range of 950–1,650 nm. The sample temperature and moisture content at the time of NIR analysis are provided in **Supplementary Table S1**.

2.4.1 Multivariate Prediction Modeling

The collected NIR spectra were subjected to detrending and normalization via a standard normal variate (SNV) method prior to mulitivariate analysis using the Unscrambler X v10.4 software (Aspen Technology, Inc., Bedford, MA). Principal component analysis (PCA) was carried out on the preprocessed NIR spectra to identify clusters and/or trends caused by varying the percent of pine and SG, SYP tops diameter, pellet L/D ratio, and moisture content. The non-linear iterative partial least squares (NIPALS) algorithm was used to build the PCA models and the analysis of NIR spectral variability was limited to five principal components. The PCA scores extracted from PC-1, 2, 3, 4, and 5 were then merged with the pellet mill process data to build partial least squares regression (PLSR) models in order to predict a specific pellet property (e.g., moisture, ash, and carbon contents). Process data obtained from the pellet mill data loggers included steam mass flow, steam process pressure, conditioner water flow rate,

TABLE 2 | Ash, ultimate, and calorimetric analyses of the raw material.

Sample ID	[a]Elemental composition (%)				[a]Ash (%)	[a]HHV (J/g)
	Carbon	Hydrogen	Nitrogen	Oxygen		
Preliminary pelleting tests						
SG	46.8 ± 0.2	6.6 ± 0.1	0.3 ± 0.0	46.3 ± 0.2	2.0 ± 0.0	19,335 ± 13
6-in. (152.4 mm) SYP	51.2 ± 0.5	6.4 ± 0.2	0.1 ± 0.0	42.3 ± 0.1	0.9 ± 0.2	20,514 ± 10
2.5-ton pelleting demonstration						
2-in. (50.8 mm) SYP	48.4 ± 0.2	6.6 ± 0.1	0.4 ± 0.0	44.6 ± 0.2	2.3 ± 0.1	20,236 ± 7
6-in. (152.4 mm) SYP	49.0 ± 0.5	6.6 ± 0.1	0.3 ± 0.0	44.1 ± 0.5	1.0 ± 0.0	20,388 ± 19

[a]*Average and standard deviations are provided for* N = *3; Ash and C, H, N, O values are provided on a dry weight basis; HHV–Higher heating value; SG–Switchgrass; SYP–Southern yellow pine tops with the stem diameter provided in paranthesis.*

current, speed, and temperature. Pellet properties, including durability, bulk density, carbon, moisture, ash, HHV, and the amount of pine biomass (%SYP) were used as Y-response factors. The process variables were averaged and the standard deviations for each run were also correlated to the pellet properties. Cross-validation was applied for both the PCA and PLSR models, and up to eight predicting factors were used in the PLSR models. During PLS regression of the preliminary test samples, variables with auto-correlation ($r > 0.9$) and lower coefficient of variation (CV < 1%) were removed from the data set.

3 RESULTS

3.1 Physical and Chemical Properties of Raw Material

The bulk density and geometric mean particle length of switchgrass (SG) after passing through a 6.35 mm screen were 104 kg/m^3 and 1.25 mm, respectively. Determination of particle size distribution indicated that milling of SG in two stages led to more fines in the grind. In the case of 6-in. (152.4 mm) SYP residues used for the preliminary tests, the geometric mean particle length and bulk density were determined to be 0.91 mm and 190 kg/m^3, respectively, at a moisture content of about 10% (w.b.).

The ultimate analysis, ash content, and HHV of the raw material are provided in **Table 2**. Both the 2-in. (50.8 mm) SYP and SG biomass contained twice the amount of ash when compared to the 6-in. (152.4 mm) SYP biomass. Our previous work has also shown that the 2-in. (50.8 mm) SYP biomass (4,595 mg/kg) contained significantly higher amounts of combined alkali and alkaline earth metals (Ca, K, Mg, Na) when compared to SG (2,198 mg/kg) and 6-in. (152.4 mm) SYP (2,472 mg/kg) biomasses (Edmunds et al., 2018). The carbon content of SYP was also appreciably higher than the SG, but the HHV differed by only 5% between these raw materials. Ash could reduce the performance of biomass conversion reactors, whereas alkali and alkaline earth metals can specifically affect the composition and yield of downstream products during thermochemical conversion of lignocellulosic feedstocks (Edmunds et al., 2018; Kim et al., 2018). Hence, blending these raw materials could potentially reduce heterogeneity and improve their downstream conversion properties.

3.2 Preliminary Pelleting of Southern Yellow Pine (SYP) and Switchgrass (SG): Effect of moisture content, L/D, and Blend ratio

In the case of the 100% pine pellets, 5–10% (w.b.) moisture loss was observed during the pelleting process. A higher moisture loss of 10% (w.b.) was observed at a lower L/D ratio of 5 compared to L/D ratios of 7 and 9. The unit, bulk, and tapped densities at different moisture levels and L/D ratios were in the range of 1,096–1,169, 471–569, and 518–616 kg/m^3, respectively. The durability was in the range of 89–95%, where a higher L/D ratio and lower moisture content were found to be beneficial. The physico-chemical properties of all pellet blends are provided in **Table 3**, **Supplementary Tables S2 and S3**, and the appearance of the pellets is depicted in **Figure 2**.

In the case of the 75% pine pellets, there was a moisture loss of 6–8% (w.b.). A higher moisture loss was observed at a higher L/D ratio of 9 and higher blend moisture content of 25% (w.b.). The unit, bulk, and tapped densities were in the range of 799–1,117, 450–573, 499–631 kg/m^3, respectively, and the durability was 85–93%. A higher moisture content and a lower L/D ratio reduced the density and durability of 75% pine pellets.

In the case of the 50% pine pellets, a moisture loss of 6–10% (w.b.) was observed during pelleting and a higher L/D ratio of 9 as well as a higher blend moisture content of 25% (w.b.) resulted in greater losses. The unit, bulk, and tapped densities were in the range of 1,087–1,115, 516–572, 569–623 kg/m^3, respectively, and the maximum durability was observed for a lower blend moisture content and L/D ratio of 9. Overall, the durability values were in the range of 85–95% for the different pelleting parameters.

For the 25% pine pellets, a moisture loss in the range of 5–9% (w.b.) was observed, and a higher blend moisture content of 24% (w.b.) and a L/D ratio of 9 resulted in greater losses. The unit, bulk, and tapped densities were the lowest at an L/D ratio of 5 and a blend moisture content of 19% (w.b.). Overall, the unit, bulk, and tapped densities were in the range of 889–1,146, 465–607, 510–654 kg/m^3, respectively. The lowest durability of 83% was observed at an L/D ratio of 5 and a blend moisture content of 20% (w.b.), whereas a maximum durability of 95% was observed at a L/D ratio of 9 and a moisture content of about 20% (w.b.).

In the case of the 100% SG pellets, the moisture loss was similar to 100% pine pellets (about 5–10%, w. b.), but interestingly, higher moisture losses were recorded at higher L/D ratios of 7 and 9. The unit, bulk, and tapped densities were between 991 and 1,156,

TABLE 3 | Average physical properties of high-moisture pellets produced immediately after pelleting during preliminary tests.

Sample ID	L/D ratio	FMC (%)	PMC (%)	UD (kg/m^3)	BD (kg/m^3)	TD (kg/m^3)	D (%)	SEC (kWh/ton)
6-in. (152.4 mm) SYP-100	7	18.4	13.5 ± 0.7	1,169 ± 34	569 ± 3	616 ± 3	93.5 ± 0.9	119.5
	9	19.5	12.9 ± 0.2	1,188 ± 48	536 ± 5	588 ± 3	95.3 ± 0.3	105.3
	7	24.7	16.2 ± 0.5	1,120 ± 28	473 ± 6	530 ± 5	89.6 ± 0.7	113.6
	9	24.5	17.4 ± 0.5	1,119 ± 49	494 ± 2	547 ± 2	93.6 ± 0.7	142.4
	5	20.2	14.3 ± 0.1	1,096 ± 53	498 ± 5	550 ± 2	89.1 ± 0.6	131.3
	5	26.1	16.2 ± 0.6	1,099 ± 56	471 ± 2	519 ± 6	91.1 ± 0.3	132.2
6-in. (152.4 mm) SYP-75	7	20.4	13.6 ± 0.2	1,093 ± 45	563 ± 1	604 ± 2	93.4 ± 0.4	102.3
	9	19.7	13.2 ± 0.3	1,117 ± 30	534 ± 6	591 ± 5	93.4 ± 0.2	110.6
	5	20.2	14.6 ± 0.2	1,066 ± 50	574 ± 4	631 ± 3	89.2 ± 0.6	127.8
	7	24.3	16.8 ± 0.8	1,110 ± 37	547 ± 3	597 ± 6	91.8 ± 0.7	150.8
	9	24.9	16.8 ± 0.1	1,117 ± 49	478 ± 4	530 ± 3	93.0 ± 0.5	135.6
	5	25.2	17.1 ± 0.8	799 ± 67	450 ± 1	500 ± 3	85.2 ± 1.2	127.1
6-in. (152.4 mm) SYP-50	7	21.1	14.3 ± 0.4	1,151 ± 45	572 ± 3	616 ± 4	90.6 ± 0.5	128.7
	9	18.8	12.6 ± 0.5	1,131 ± 55	561 ± 3	616 ± 3	95.3 ± 0.3	128.6
	5	18.3	13.3 ± 0.2	1,087 ± 41	516 ± 5	567 ± 3	85.8 ± 0.7	124.6
	7	24.7	13.8 ± 0.6	1,135 ± 31	548 ± 3	600 ± 2	92.0 ± 0.3	155.8
	9	24.5	14.2 ± 0.5	1,112 ± 33	536 ± 5	592 ± 2	94.9 ± 0.3	133.9
	5	23.0	15.9 ± 0.0	1,134 ± 66	572 ± 1	623 ± 4	88.7 ± 0.5	151.5
6-in. (152.4 mm) SYP-25	7	19.4	11.8 ± 0.2	1,085 ± 26	608 ± 1	656 ± 1	89.7 ± 0.4	150.8
	9	20.2	14.2 ± 0.2	1,114 ± 32	560 ± 4	621 ± 4	94.9 ± 0.3	125.5
	5	18.8	12.7 ± 0.3	890 ± 32	466 ± 5	510 ± 4	79.8 ± 0.8	128.1
	7	23.9	14.2 ± 0.3	1,107 ± 23	562 ± 1	609 ± 2	91.9 ± 0.4	163.9
	9	24.0	14.8 ± 0.2	1,147 ± 30	550 ± 7	604 ± 7	95.1 ± 0.2	149.4
	5	20.1	14.3 ± 0.2	1,066 ± 38	463 ± 3	521 ± 4	83.1 ± 0.6	122.9
6-in. (152.4 mm) SYP-0	5	17.1	14.1 ± 0.2	963 ± 78	553 ± 4	603 ± 4	85.8 ± 0.2	108.5
	7	20.9	13.1 ± 0.3	1,156 ± 23	565 ± 4	617 ± 3	92.8 ± 0.6	149.0
	9	19.6	13.3 ± 0.3	1,122 ± 34	571 ± 7	621 ± 3	94.6 ± 0.4	123.7
	5	19.8	14.3 ± 0.5	991 ± 35	499 ± 3	547 ± 2	88.3 ± 0.8	142.1
	7	24.5	14.4 ± 0.2	1,145 ± 47	554 ± 5	605 ± 3	93.9 ± 0.3	176.9
	9	24.7	15.0 ± 0.5	1,130 ± 25	555 ± 6	608 ± 4	95.2 ± 0.2	154.2

Note: All physical properties were measured immediately after pellet production, where means and standard deviations are provided for N = 3. L/D ratio–Length-to-diameter ratio; FMC–Feed moisture content in wet basis; PMC–Pellet moisture content in wet basis; UD–Unit density; BD–Bulk density; TD–Tapped density; D–Durability; SEC–Specific energy consumption; SYP–Southern yellow pine tops and switchgrass biomass were ground in a hammer mill fitted with a 6.35 mm screen and blended at 100:0 (SYP-100), 75:25 (SYP-75), 50: 50 (SYP-50), 25:75 (SYP-25), and 0:100 (SYP-0) ratios.

499–552, and 546–621 kg/m^3, respectively, and durability was between 85 and 95%. Overall, higher L/D ratios of 7 and 9 and a lower moisture content of about 20% (w.b.) maximized the durability of 100% SG pellets, as can be seen in **Table 3**.

Drying the pellets at 70°C for 2–3 h was aimed at reducing the moisture content to <10% (w.b.); however, it also affected pellet density and durability. In the case of unit density, a loss of about 40–50 kg/m^3 was observed, whereas the bulk and tapped densities decreased by 20–25 kg/m^3. The pellet durability changed between −4.7% and +1.9%, and most pellet treatments experienced a decrease in durability because of low temperature drying, as observed in **Supplementary Table S2**. The trends observed for blended SYP and SG pellets in terms of bulk density and durability matched our earlier studies with corn stover, lodgepole pine, and municipal solid waste (MSW) (Tumuluru, 2014; Tumuluru et al., 2015; Tumuluru, 2016; Tumuluru and Mwamufiya, 2021), where higher moisture in the biomass reduced the density and higher L/D ratio increased the durability.

Specific energy consumption (SEC) of the pelleting process was determined as per **Eq. 1** and provided in **Table 3**. Based on the results, a higher pelleting moisture and L/D ratio led to an increase in pelleting energy. In the case of 100% pine pellets, the lowest energy consumption was observed at 20% (w.b.) pelleting moisture and an L/D ratio of 9, as can be seen in **Table 3**. Increasing the moisture content increased the pelleting energy to 130–140 kWh/ton for different L/D ratios. Compared to 100% pine, the 100% SG pellets consumed more energy. For example, at an L/D ratio of 9 and 20% (w.b.) moisture content, energy consumption of 100% SG pellet was 123 kWh/ton, whereas the 100% pine only consumed 105 kWh/ton of energy. Further increasing the moisture content and lowering the L/D ratio to 5 increased the pelleting energy to about 176 kWh/ton. In the blended feedstocks, higher amounts of pine (75%) reduced the energy consumption to about 102–110 kWh/ton for the L/D ratios of 7 and 9. In the case of the 50% pine biomass, energy consumption increased to a range of 124–155 kWh/ton for the different L/D ratios (5–9) and moisture contents (20–25%, w. b.). In the case of 75% SG blends, the lowest energy consumption (125 kWh/ton) was observed at a pelleting moisture content of 20% (w.b.) and an L/D ratio of 9.

Multivariate models constructed by combining the NIR data and the pelleting process variables indicated that the L/D ratio (R^2 = 0.72) and bulk density (R^2 = 0.50) had positive correlations with pellet durability, as shown in **Supplementary Figure S1** (Supplementary data), whereas the pine content (R^2 = 0.26)

FIGURE 2 | Raw biomass and pellets made of 6-in. (152.4 mm) southern yellow pine (SYP) tops, switchgrass (SG), and their blends. All pellets were produced at high-moisture content (20% w.b.) and at two different length-to-diameter ratios (7 or 9). **(A)** SYP tops ground to 6.35 mm screen size in a hammer mill; **(B)** SG biomass ground to 6.35 mm screen size in a hammer mill; **(C)** 100% SYP pellets; **(D)** 100% SG pellets; **(E)** 75% SYP and 25% SG pellets; **(F)** 75% SG and 25% SYP pellets; and **(G)** 50% SYP and 50% SG pellets.

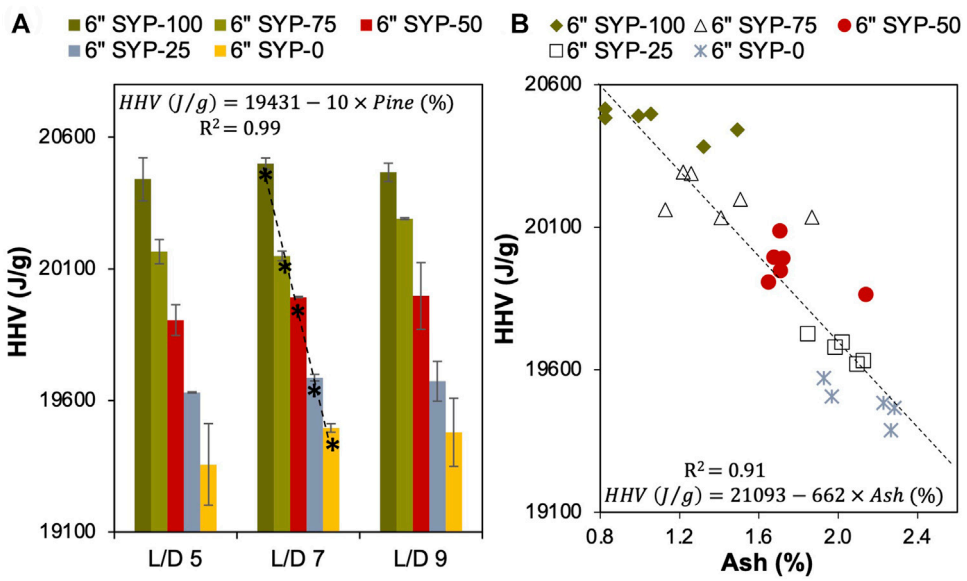

FIGURE 3 | (A) Variations in the higher heating value (HHV) of pellets as a function of biomass blend and length-to-diameter (L/D) ratios. The dotted line represents linear regression between pellet pine content (%) and HHV (J/g) for all L/D ratios, while the corresponding regression equation is provided as an inset; **(B)** Distribution of pellet HHV as a function of ash content. Southern yellow pine (SYP) tops of 6-in. (152.4 mm) stem diameter were ground in a hammer mill fitted with 6.35 mm screen and was blended with similarly ground switchgrass (SG) at 100:0 (SYP-100), 75:25 (SYP-75), 50:50 (SYP-50), 25:75 (SYP-25), and 0:100 (SYP-0) ratios. The linear regression of pellet HHV and ash content is represented as a dotted line, with the corresponding equation provided as an inset.

exhibited a mild negative correlation to the bulk density, and the pelleting moisture content had no correlation to the pellet bulk density (R^2 = 0.09) or durability (R^2 = 0.002). Hence, we determined that an L/D ratio of 9 is desirable to improve pellet durability, whereas the blending of pine residues with SG would improve pelleting energy consumption.

TABLE 4 | Performance of PLSR models for predicting pellet properties based on NIR PCA scores (in 950–1,650 nm region) and pelleting process data.

Output variables	Input = NIR spectra				Input = Process data + NIR PCA scores		
	R_c^2	RMSEC	R_p^2	RMSEP	R_c^2	RMSEC	Significant process variables
Pine content (%)	0.99	2.95	0.97	3.05	1.00	2.84	PC1; PC2; PC3; PC4; PC5; MCC temperature (°*F*); PM1,2 VFD current
Ash content (%)	0.95	0.11	0.93	0.15	0.97	0.12	PC1; PC2; Infeed hopper speed (*Hz*); Steam mass flow (*lb/h*); Conditioner outlet mash temperature (°*F*)
HHV (J/g)	0.98	40.90	0.95	63.80	0.99	69.40	PC1; PC2; PC4; PM1,2 VFD current; MCC temperature (°*F*); Infeed hopper speed (*Hz*)
Bulk density (kg/m^3)	0.77	18.20	0.71	22.30	0.86	21.30	PM1,2 VFD Current; PC1; Infeed hopper speed (*Hz*); PC2; Conditioner outlet mash temperature (°*F*)
Durability (%)	0.64	2.31	0.55	2.50	0.94	0.17	PC1; Infeed hopper speed (*Hz*); PC2; Steam mass flow (*lb/h*)

Note: Partial least squares regression (PLSR) models were built using N *(30 × 2 repacks × 2 scans) = 120 near infrared (NIR) spectra. Pellet properties were determined in triplicate for* N *= 30 treatments. Legend: HHV–Higher heating value; PCA–Principal component analysis; PC–Principal component of NIR spectra; PM–Pellet mill; VFD–Variable frequency drives; MCC–Motor control center.*

3.2.1 Effect of Pelleting Paramters on Ultimate Composition, Ash, and HHV

No significant differences were observed in the carbon (C), hydrogen (H), and oxygen (O) content of the preliminary test pellets as a function of pine blend ratio, blend moisture content, or L/D ratio, as observed in **Supplementary Table S3**. Only the nitrogen (N) content displayed minor variations depending on the pine blend ratio; pellets of 100% SG contained 86% more N than those with 100% SYP, whereas all blended pellets contained even quantities of N. Hence, blending of pine and SG homogenizes the ultimate composition of the resulting pellets. Other physico-chemical properties, namely the ash content and the HHV, were affected by the pelleting parameters. Pine content had a significant positive correlation to the calorific value of the pellets, which can be clearly observed in **Figure 3A**. Similarly, higher pine content and heating values were negatively correlated with the ash content, as shown in **Figure 3B**. However, factors such as L/D ratio (R^2 = 0.02–0.05) and pelleting moisture [(R^2 = 0.05–0.09) did not have any significant impact on pellet ash content or HHV, as observed in **Supplementary Figure S2**]. Hence, modulating the pine content would be essential for controlling the downstream conversion performance of the blended pellets.

3.2.2 Prediction Modeling: Off-Line NIR Spectroscopy Combined With Pelleting Process Data

Partial least squares regression (PLSR) models developed based on off-line NIR spectroscopic data of the 30 preliminary pellet samples showed that the ash content, HHV, and pine ratio could be predicted to a high accuracy, as observed in **Table 4**. We also combined the scores extracted from principal component analysis (PCA) of the pellet NIR spectra with that of the pelleting process information and investigated the effects of PLSR model predictability. As shown in **Table 4**, integration of pelleting process data significantly improved the predictability of pellet bulk density and durability. Input variables of significance to a specific pellet property were obtained from the PLS regression coefficients and provided in **Table 4** as well. Both the NIR PCA scores and process parameters, including in-feed speed, steam mass flow, drive current, and conditioner outlet temperature, were of significance to the pellet properties. We thus showed how PLSR prediction models for lignocellulosic feedstocks could be improved by integrating process data.

3.3 2.5-ton Demonstration of High-Moisture Pelleting

Following the preliminary pilot-scale studies on SYP, SG, and their blends, subsequent demonstration on a 2.5-ton scale were conducted. The L/D ratio of 9 and moisture content of about 20% (w.b.) were selected since these pelleting conditions resulted in higher pellet quality, in terms of bulk density and durability, at lower energy consumption. Pine top residues of 2-in. (50.8 mm) and 6-in. (152.4 mm) diameter were selected to investigate the impact of lower quality feedstock (i.e., 50.8 mm pine tops) on final pellet properties. The grind properties, namely geometric mean particle length and D50 (median particle size) of the 2-in. (50.8 mm) pine residues were 1.22 and 1.30 mm, respectively, and those of 6-in. (152.4 mm) pine residues were 0.99 and 1.06 mm, respectively. The grinding energies for 2-in. (50.8 mm) and 6-in. (152.4 mm) pine residues were 24.3 and 23.3 kWh/ton, respectively. Hence, the pelleting properties were not significantly different for the two types of pine residues tested.

On the other hand, differences in physical properties of the pellets were observed due to the pine blend ratio and pine residue size, as shown in **Table 5**. In the case of 6-in. (152.4 mm) pine residues, the 60% blend resulted in higher unit density, but the bulk and tapped density, as well as the durability, were not significantly different compared to the 50% blend. The energy consumption was slightly higher for the 50% blend of 6-in. (152.4 mm) SYP at 98 kWh/ton when compared to the 60% blend (89 kWh/ton). In the case of 2-in. (50.8 mm) SYP residues, a 60% blend produced pellets with lower unit, bulk, and tapped densities, as well as durability, but the SEC was lower at 87 kWh/ton than that of the 50% blend (95 kWh/ton). Among the four tested blends, 2-in. (50.8 mm) SYP-60 produced lower quality pellets, whereas 6-in. (152.4 mm) SYP-50 produced comparably higher quality pellets. Higher SYP content led to lower pelleting energy consumption. Changes in pine blend ratio and stem diameter had no significant effect on the elemental composition, ash content, and HHV of the pellets, as shown in

TABLE 5 | Average physico-chemical properties of switchgrass (SG) and southern yellow pine (SYP) blended pellets immediately after pelleting produced during 2.5-ton demonstration.

Pellet properties[a]/ Sample ID	6-in. (152.4 mm) SYP-50	6-in. (152.4 mm) SYP-60	2-in. (50.8 mm) SYP-50	2-in. (50.8 mm) SYP-60
Unit density (kg/m^3)	944 ± 84	1,016 ± 37	1,083 ± 48	965 ± 119
Bulk density (kg/m^3)	561 ± 1	557 ± 7	586 ± 1	474 ± 5
Tapped density (kg/m^3)	604 ± 3	599 ± 3	629 ± 3	510 ± 3
Durability (%)	93 ± 0	92 ± 0	91 ± 2	80 ± 2
Carbon (%)	47 ± 0	47 ± 0	47 ± 0	47 ± 0
Hydrogen (%)	7 ± 0	7 ± 0	6 ± 0	6 ± 0
Nitrogen (%)	0 ± 0	0 ± 0	1 ± 0	0 ± 0
Oxygen (%)	46 ± 0	47 ± 0	46 ± 0	47 ± 0
Ash (%)	2 ± 0	2 ± 0	2 ± 0	2 ± 0
HHV (J/g)	19,851 ± 9	19,729 ± 5	19,899 ± 10	19,821 ± 8
SEC (kWh/ton)	98	89	95	87

[a]*Average and standard deviations are provided for* N = *3. The C, H, N, O and ash content are provided on a dry weight basis. Legend: SYP–Southern yellow pine tops; SYP, and SG, were ground to 6.35 mm screen size and blended at 60:40 or 50:50 ratio; SEC–Specific energy consumption; HHV–Higher heating value.*

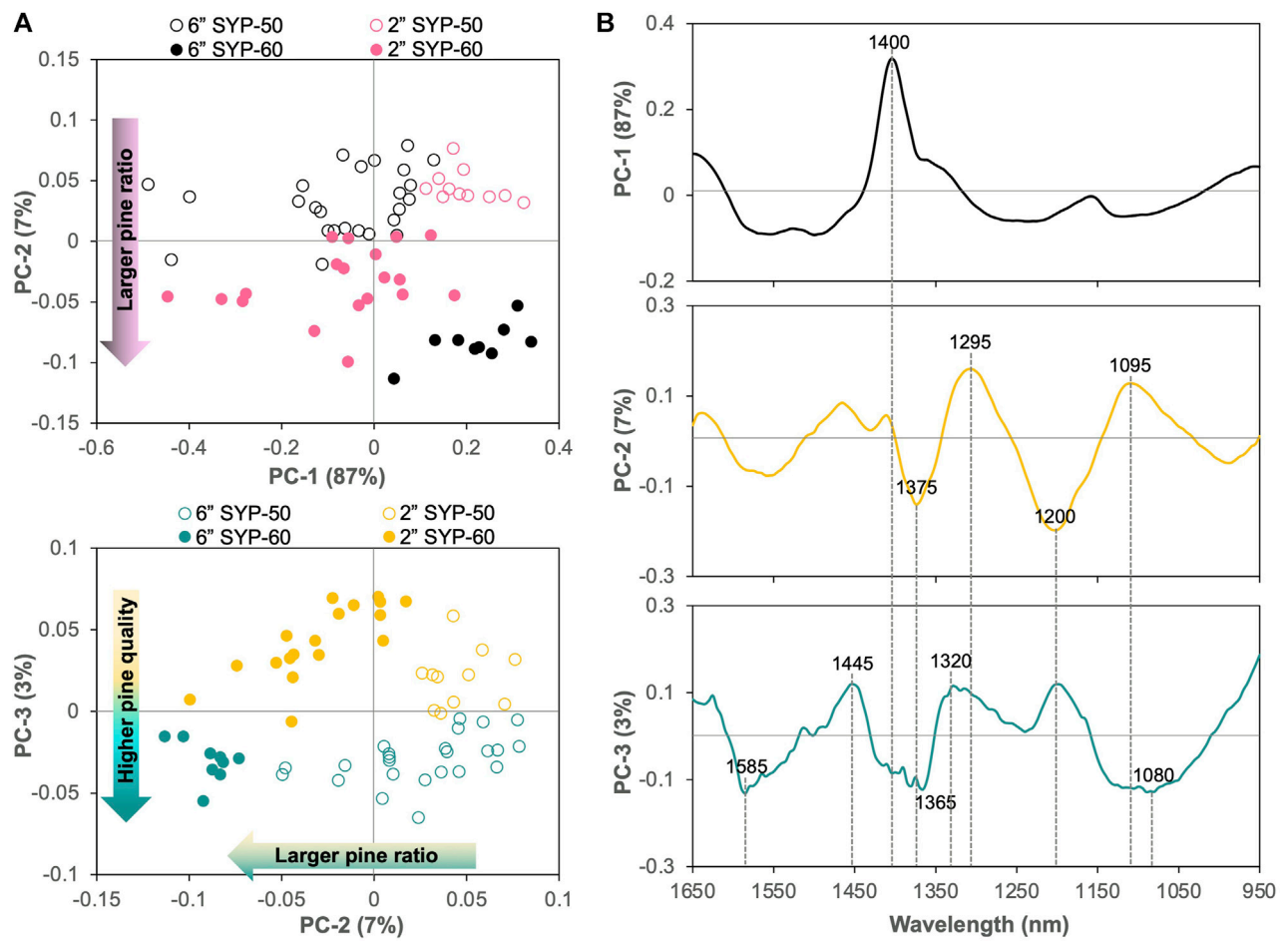

FIGURE 4 | (A) Scatter plots comparing the scores of principal components (PC-) 1, 2, and 3. Principal component analysis (PCA) was conducted with NIR spectra of blended southern yellow pine (SYP) and switchgrass (SG) pellets in the 950–1,650 nm region; **(B)** Line plots of principal component loadings corresponding to PC-1, PC-2, and PC-3. The pellet blends were composed of 6-in. (152.4 mm) or 2-in. (50.8 mm) SYP tops and SG, ground in a hammer mill fitted with a 6.35 mm screen, and mixed at either 60:40 or 50:50 ratio.

TABLE 6 | Performance of PLSR models for predicting pellet properties during 2.5-ton demonstration using at-line NIR spectroscopy (950–1,650 nm region) and pelleting process data.

Output variables	Range	PLSR factors	Calibration		Prediction	
			R_c^2	RMSEC	R_p^2	RMSEP
Ash (%)	1.5–2.2	6	0.96	0.04	0.75	0.10
HHV (J/g)	19,619–20,007	4	0.85	38.50	0.74	54.15
Moisture content (%)	11.3–15.9	7	0.84	0.32	0.72	0.43
Carbon (%)	46.1–47.7	6	0.81	0.16	0.66	0.23

PLSR—Partial least squares regression; R_c^2—Coefficient of determination for calibration; R_c^2—Coefficient of determination for prediction; RMSEC—Root mean square error of calibration; RMSEP—Root mean square error of prediction.

Table 5, which shows that blending of 6-in. (152.4 mm) and 2-in. (50.8 mm) pine tops with SG led to homogenization of chemical properties.

3.3.1 At-Line NIR Spectroscopy of Pellet Outfeed and Multivariate Analysis

The NIR spectra collected at-line on the blended pellets were subjected to PCA and the resulting scores plot showed discernable differences depending on the percentage of SYP content, as well as the size of the SYP tops. As given in **Figure 4A**, principal component 2 (PC-2) accounted for differences in the percentage of pine content, whereas PC-3 accounted for variations due to the pine tops size. Sample spectra belonging to the 60% pine blends, whether 2-in. (50.8 mm) or 6-in. (152.4 mm) in size, were mainly aggregated in the negative quadrant of PC-2, and the 6-in. (152.4 mm) SYP-60 blend displayed significant grouping compared to the other blends. Based on the PC-1 loadings shown in **Figure 4B**, the 6-in. (152.4 mm) SYP-60 blend contained higher O–H stretch (first overtone) for cellulose and hemicellulose corresponding to 1,400 nm (Li et al., 2015). This observation is justified by the fact that 6-in. (152.4 mm) SYP contains more cellulose (36%) than the 2-in. (50.8 mm) SYP (29%). Based on the PC-2 loadings, pellets containing 60% pine registered higher–CH3 deformation and C–H stretching in lignin corresponding to 1,375 nm and 1,200 nm (Jin et al., 2017). The pine biomass contained 36–38% of lignin, as opposed to SG with only 21% of lignin, hence, it is plausible that the 60% pine blends contained detectable lignin signature. The PC-3 accounted for minor (3%) variations between the 2-in. (50.8 mm) and 6-in. (152.4 mm) pine tops content, as observed in **Figure 4A**. According to the PC-3 loadings, shown in **Figure 4B**, these variations could be attributed to higher C–H stretching in cellulose and hemicellulose corresponding to 1,585 nm and 1,365 nm, respectively, and a higher O–H stretch (second overtone in bound forms) in hemicellulose corresponding to 1,080 nm in the 6-in. (152.4 mm) SYP blends (Jin et al., 2017). Thus, at-line NIR spectroscopy was successfully employed to monitor the changes in chemical signatures as a result of changes in pine blend ratio.

PLSR models obtained by combining the pelleting process data with pellet NIR PCA scores showed that, properties, such as ash content, could be predicted to a high coefficient of determination (R^2) of 0.96, as observed in **Table 6**. Other pellet properties namely HHV, moisture content, and carbon content could be predicted to R_c^2 values of 0.85, 0.84, and 0.81, respectively, as shown in **Table 6**. **Figure 5A** depicts the scatter plots of prediction results for pellet ash content using a PLSR model trained with NIR PCA scores. Input variables namely feed hopper current, outfeed current, pellet mill speed, and the NIR bands of 1,030, 1,150, and 1,610 nm were determined to be sensitive to predicting the ash content, as per the regression coefficients given in **Figure 5B**. The signal at 1,610 nm is attributed to the overtone of O–H stretching in bound water (Ma et al., 2020). The regression coefficients for the pellet HHV, moisture, and carbon content are provided in **Supplementary Figures S3–S5**, respectively. Pelleting process parameters namely steam mass flow, in-feed hopper current, pellet mill speed, and conditioner outlet mash temperature had a strong correlation to predicting the pellet HHV, moisture, and carbon content. Similarly, the NIR band at 1,030 nm had a correlation to pellet moisture and carbon content, whereas the bands at 1,310, 1,460, and 1,620 nm were correlated to pellet HHV. Other input variables, including outfeed speed, steam boiler pressure, and the NIR bands at 1,025, 1,155, 1,375, 1,435 and 1,605 nm, were also identified as major contributors to these pellet properties. Thus, fairly robust PLSR models were built for estimating the ash, moisture, carbon, and HHV content of the blended pellets based on at-line NIR spectroscopy combined with the pellet mill process data.

4 DISCUSSION

4.1 Blending Bioenergy Feedstocks

Edmunds et al. (2018) observed that the major advantage of blending woody and herbaceous biomass, such as pine and SG, is the improvement in chemical composition. The limitations of herbaceous biomass for bioenergy production are their lower energy density, issues related to storage, handling, and transportation (Sahoo and Mani, 2016; Sahoo and Mani, 2017). According to Edmunds et al. (2018), Tumuluru et al. (2015), and Sahoo and Mani (2017), herbaceous biomasses typically have a bulk density of 150–160 kg/m^3. Ray et al. (2017) concluded that low density biomasses require more resources for transportation and shipping, which increases cost. These limitations pose a severe challenge to the utilization of herbaceous biomass on a commercial scale. In addition, woody biomasses have higher carbon and lower ash contents, whereas herbaceous biomasses have lower carbon and

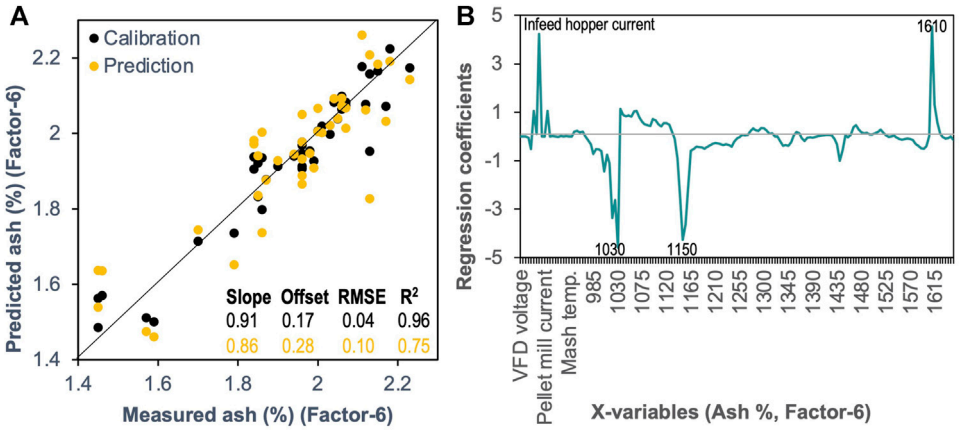

FIGURE 5 | (A) Scatter plots of prediction results for ash content (%) of the blended pellets by a PLSR model trained with NIR principal component scores (in 950–1,650 nm region) and pelleting process data; **(B)** Regression coefficients associated with the PLSR model. The pellet blends were composed of 6-in. (152.4 mm) or 2-in. (50.8 mm) southern yellow pine (SYP) tops and switchgrass (SG), ground in a hammer mill fitted with a 6.35 mm screen and mixed at either 60:40 or 50:50 ratio.

higher ash contents. Blending with woody biomass could therefore help to overcome herbaceous feedstock limitations regarding carbon and ash content and improve their specifications for different conversion scenarios. In thermochemical conversion, desired specifications are high calorific value, and carbon content, but low volatiles, nitrogen, and ash contents. Most herbaceous biomasses, such as corn stover and SG, have higher ash content, lower calorific value, and lower carbon content. Hence, Tumuluru and Fillerup (2020) concluded that blending SG and corn stover with lodgepole pine helped to improve the proximate and ultimate composition and calorific value and made the feedstocks more suitable for preprocessing, such as densification, and for further downstream conversion.

4.2 High-Moisture Pelleting

A major challenge of blending woody and herbaceous biomass is particle segregation during storage, feeding, and handling. One approach to address this challenge is to densify the blended biomass. Tumuluru et al. (2011) suggested that pellet mills, briquette presses, cubers, agglomerators, and tablet presses help to improve the bulk density of biomass feedstocks. Densification not only improves the density, but also avoids particle segregation. Among the various densification systems, pelleting is the most used method for densifying the biomass. But the major challenge in using pellets for biorefinery operations is the cost. Drying biomass to less than 10% (w.b.) moisture content for future pelleting is the major energy consumer in conventional pelleting processes (Lamers et al., 2015). At Idaho National Laboratory we have developed a high-moisture pelleting process that eliminates the high-temperature drying step in pellet production, thus reducing the cost and making pelleting an environment-friendly process. Eliminating high-temperature drying also reduces volatile organic emissions during pelleting. In a techno-economic analysis, Lamers et al. (2015) indicated that a 40% reduction in pellet production costs could be achieved by switching to low temperature dryers, such as grain or belt dryers that operate at a significantly lower cost. In addition, the major advantage of high-moisture pelleting is the versatility of designing pellets with different densities, whereas the conventional method would produce pellets with very high densities (>700 kg/m^3) that are more suitable for long-distance transportation. According to Tumuluru (2016), if pellets are transported by truck, very high bulk densities are not needed to fill the truck to its full capacity. If the pellets are to be transported shorter distances, such as 200–300 miles, they do not need to meet the durability standards set for long-distance transportation. Tumuluru (2016) also suggested that the cost of pellet production using conventional methods cannot be completely offset by saving on transportation costs, especially if the transportation distances are less than 200–300 miles. A recent study conducted by Tumuluru and Mwamufiya (2021) found that transportation costs decreased by about 43% for MSW pellets as compared to non-pelleted material if the transportation distance was >15 miles. Therefore, the high-moisture pelleting tested in this study can make pelleting more cost-effective and environmentally friendly for biorefineries, as it avoids the expensive drying methods commonly used by the industry.

4.3 Impact of Blend Composition on Pelleting Process

Biomass physical and chemical properties significantly affected pellet quality. The lignin component of plant biomass is considered as a natural binding agent and plays an essential role in the densification process in terms of pellet quality and energy consumption. In the present study, SYP residues containing higher lignin required less pelleting energy as compared to SG. Also, blending SYP with SG helped to reduce the SEC and improved pellet properties, such as durability. Studies conducted by Tumuluru and Fillerup (2020) on briquetting blends of lodgepole pine, SG, and corn stover showed that the addition of pine decreased energy consumption and increased the durability of SG briquettes.

Tumuluru et al. (2012) also found that grasses have lower lignin content, require higher pelleting energy, and produce pellets with lower density and durability. This limitation can be overcome by blending grasses with woody biomass. The current study also indicated that, blending SYP with SG improved the chemical composition—especially the lignin and ash contents—and particle size distribution, which helped to produce good quality pellets at lower energy consumption. In addition, blending improved the pelleting characteristics due to better interlocking ability and flowability of the biomass in the pellet die.

4.4 Impact of Process Parameters on Pellet Properties

Tumuluru and Fillerup (2020) studied the briquetting characteristics of woody and herbaceous biomass blends and concluded that the blend moisture content and screen size of the grind affected briquette quality. A smaller hammer mill screen (4.8 mm size) and a lower blend moisture content of 12% (w.b.) resulted in the maximum unit and bulk density values. Our current results indicated that both moisture content and compression ratio of the die (L/D ratio) affected pellet quality. An L/D ratio of 9 and a lower moisture content of 20% maximized the pellet unit, bulk, and tapped densities. Said et al. (2015) studied the pelleting of rice straw in a flat die mill and showed that the bulk density decreased with an increase in moisture content, as observed in the present study. Studies conducted by Jackson et al. (2016) on corn stover at about 20–26% (w.b.) moisture content showed that pellets with bulk densities between 500 and 600 kg/m^3 could be produced. Serrano et al. (2011) used barley straw and came to a similar conclusion that pellet bulk density decreases with an increase in the moisture content of the feedstock. Rhén et al. (2005) investigated the pelleting of Norway spruce at different preheating temperatures and pressures and reported that preheating temperature and moisture content significantly affected the bulk density of the pellets. These observations have been corroborated by the present research findings, whereas higher moisture reduced the bulk density of the SG-SYP pellets.

Studies on rice straw pelleting in a flat die mill by Said et al. (2015) concluded that increasing the moisture content to 17% (w.b.) increased pellet durability. Studies on briquetting the blends of woody and herbaceous biomass by Tumuluru and Fillerup (2020) indicated that durability increased with an increase in hammer mill screen size to 12.7 mm and increasing the moisture content to 15–18% (w.b.). These authors reasoned that increases in briquette durability could be because of the interlocking of larger particles during the compression and extrusion processes. Harun and Afzal (2015) found that higher percentages of woody biomass in the blend of pine and SG increased the pellet strength and durability values. The present research corroborates this observation and supports that the blending SYP with SG produces a good quality pellet in terms of density and durability. Pelleting studies conducted by Tumuluru (2018) using high-moisture woody and herbaceous biomass also determined that woody biomass with higher lignin content produced pellets with higher bulk density and durability. In the present study, pellets produced using pure SYP had higher durability values of >95% at a lower moisture content and higher L/D ratio of the pellet die. For SG, the maximum durability was 95% for a higher L/D ratio of 9 and feedstock moisture content of 20 and 25% (w.b.). The lower durability values of pure SG pellets could be attributed to the lower lignin content. But blending SG with SYP improved the pellet durability at a lower L/D ratio and higher moisture content. Our study also showed that a higher L/D ratio resulted in higher durability of the pellets, which may be because higher residence times of pine and SG particles in the die could induce glass transition of the lignocellulosic components and promote particle binding.

Moisture loss of about 5–10% (w.b.) was observed when SYP and SG blends were pelleted at higher moisture content of 20 and 25% (w.b.). This observation corroborates our earlier works (Tumuluru, 2014; Tumuluru, 2016; Tumuluru, 2019) on corn stover, SG, and lodgepole pine blends, where the loss of moisture depended on the initial moisture content of the feedstock. Higher initial moisture content and larger L/D ratios led to greater moisture losses during pelleting. Moisture losses may occur during pelleting due to flash-off when the pellets are compressed and extruded out of the die. Tumuluru (2016) reasoned that losing moisture during pelleting can be attributed both to frictional heat developed in the die and to further cooling, which can dry most of the pellet surface moisture, resulting in partially dried pellets.

4.5 Application of At-Line and Off-Line NIR Spectroscopy for High-Throughput Prediction of Pellet Properties

Multivariate predictive models constructed based on at-line or in-line NIR spectroscopic analysis could be a valuable resource for high-throughput and inexpensive characterization of chemical and physical changes in lignocellulosic feedstocks during thermochemical or physico-chemical conversion processes (Li et al., 2018; Hwang et al., 2021). Previous research has shown that NIR analysis in the 900–1700 nm region could be coupled with chemometric approaches to predict the cellulose (R^2 = 0.92), hemicellulose (R^2 = 0.84), and lignin (R^2 = 0.71) contents of various types of lignocellulosic pellets like corn stover, rice straw, pine, mahogany, and rubber wood (Feng et al., 2018). PLSR models developed based on NIR spectra have been used to predict HHV (R^2 = 0.92), carbon (R^2 = 0.85), and ash (R^2 = 0.51) content of bamboo culms (Posom and Sirisomboon, 2017). The moisture content (R^2 = 0.99) and calorific value (R^2 = 0.99) of dedicated bioenergy crops like *Miscanthus* and short rotation coppice willow have also been predicted with higher precision using the NIR-PLSR models (Fagan et al., 2011). However, prediction of ash content (R^2 = 0.58) was poor for these lignocellulosic feedstocks (Fagan et al., 2011).

Our previous study has shown that PLSR models developed based on Fourier transform infrared spectra could predict the ash content of hybrid poplar wood and bark, as well as SG biomass, with a higher accuracy (R^2 = 0.98; RMSE = 0.38–0.40%) (Edmunds et al., 2017). In this study, we employed NIR

spectroscopy such that we could collect the pellet samples from the outfeed conveyor and perform rapid "at-line" or "off-line" characterizations. Despite the higher moisture content (11–16%) and temperature (50–55°C) of the pellet samples, at-line NIR spectroscopy provided comparable information to that of off-line NIR spectroscopy. Through the integration of pelleting process parameters, we could build a very good PLSR model (R_c^2 = 0.96; RMSE = 0.04–0.1%) for predicting the pellet ash content based on the at-line NIR spectra. However, the prediction accuracy of moisture, HHV, and carbon content was not comparably significant (R_c^2 = 0.81–0.85). Since PLSR modeling of lignocellulosic feedstocks is affected by the number of samples and the chemical composition range of the calibration and validation set (Kline et al., 2016), there is room for future improvement. Thus, at-line NIR spectroscopy was successfully deployed during the pelleting demonstration and multivariate models were developed for determining the chemical composition of blended feedstocks.

The robustness of PLSR prediction models improved significantly with the use of off-line NIR spectroscopy. Despite the smaller sample size (N = 30), wider variability of the pine and SG blends enhanced the prediction capability. Integration of pelleting process information with the NIR PCA scores improved the predictability of pellet pine ratio, ash content, HHV, bulk density, and durability (R_c^2 improved from 0.64 to 0.94) when compared to only using the NIR spectra. In previous research, integration of process temperature with online NIR spectroscopy enabled the PLS prediction of transesterification efficiency and bio-diesel production from soybean oil (Killner et al., 2011). In the near future, NIR-based sensing and multivariate modeling tools could be applied to develop machine learning techniques that can integrate in-/on-line data directly with process controllers to achieve real-time management of bioproduct manufacturing (Gargalo et al., 2020). Our work also provides the incentive for adapting NIR sensing to monitor industrial scale processing of lignocellulosic feedstocks.

Another important aspect of this study is the utilization of at-line NIR spectroscopy to classify the pellets based on the pine quality and blend ratio. In recent times, blending of feedstocks like that of pine and SG are often recommended to offset the uncertainty of continuous feedstock supply, and to improve the economic feasibility of biorefineries (Ray et al., 2017; Lan et al., 2020). Blending of lignocellulosic feedstocks has the advantage of homogenizing the conversion attributes of pellets, namely the moisture and ash contents (Tumuluru et al., 2012; Edmunds et al., 2018; Lan et al., 2020). Hence, developing a rapid NIR-based screening tool for the "quality control" attributes of blended lignocellulosic feedstocks will ensure successful implementation and operations of biomass conversion facilities. We periodically scanned a 2.5-ton feed of blended pine and SG pellets and developed at-line NIR spectroscopy-based PCA models. Results of PCA showed NIR signals from blended pellets containing higher quality pine residues (152.4 mm tops) and larger percentage of pine (60%) could be isolated based on their chemical signature for cellulose, hemicellulose, and lignin. To our knowledge, this will be the first study that utilizes at-line NIR spectroscopy to classify blended lignocellulosic feedstocks that are of notable relevance for bioenergy production in the U.S.

5 SUMMARY AND CONCLUSION

Based on the high-moisture pelleting studies of southern yellow pine (SYP), switchgrass (SG), and their blends, as well as the subsequent large-scale pelleting demonstration, we could draw the following conclusions:

- High-moisture pelleting resulted in 5–10% (w.b.) moisture loss of the blended pellets. Moreover, a higher initial moisture content resulted in greater moisture loss during pelleting. A higher L/D ratio of 7 and 9 also resulted in higher moisture losses.
- Based on our preliminary pelleting tests, an L/D ratio of 9 and blend moisture content of 20% (w.b.) was determined to produce pellets with >95% durability and >500 kg/m^3 bulk density.
- In the blended pellets, higher SYP content led to an increase in HHV and a reduction in ash content, which is favorable for further thermochemical conversions.
- Drying the pellets at a lower temperature of 70°C reduced the final moisture content to <10% (w.b.), but also adversely affected the pellet durability and density.
- Specific energy consumption of the high-moisture pelleting process was influenced by the type of feedstock; SYP required the lowest and SG required the highest pelleting energy. Blending SYP with SG moderated the energy consumption.
- Demonstration of high-moisture pelleting using 2.5 ton of 2-in. (50.8 mm) and 6-in. (152.4 mm) SYP tops blended with SG at 50:50 and 60:40 ratio successfully produced pellets with a bulk density between 473 and 586 kg/m^3 and durability between 91 and 93%. Energy consumption for the four test blends was between 87 and 98 kWh/ton.
- Partial least square regression models (PLSR), obtained by integrating the pelleting process data with at-line and off-line NIR principal component scores, were successfully developed to predict the pellet pine ratio, ash content, HHV, durability, and bulk density with coefficients of determination (R^2) between 0.86 and 0.997.

DATA AVAILABILITY STATEMENT

The original contributions presented in the study are included in the article/**Supplementary Material**, further inquiries can be directed to the corresponding author.

AUTHOR CONTRIBUTIONS

JST conceived and conducted the preliminary pelleting studies on southern yellow pine, switchgrass, and the blends of the same. JST, TR, NL, JM, and NA conceived and planned the pelleting demonstration using 2- and 6-inch southern yellow pine top blends with switchgrass. JST, KR, CP, CH, JM, and NA conducted the pilot scale pelleting and NIR spectroscopy experiments, as well as the data analysis. All authors contributed to the preparation of the manuscript.

FUNDING

Funding for this research was provided by the U.S. Department of Energy's Logistics for Enhanced-Attribute Feedstocks (LEAF) Project under the Office of Energy Efficiency and Renewable Energy (EERE) Award (#DE-EE0006639).

ACKNOWLEDGMENTS

The authors thank Genera, LLC (Vonore, TN) for providing the switchgrass biomass used in this study.

SUPPLEMENTARY MATERIAL

The Supplementary Material for this article can be found online at: https://www.frontiersin.org/articles/10.3389/fenrg.2021.788284/full#supplementary-material

REFERENCES

American Society of Agricultural and Biological Engineers (ASABE) Standard S424.1. (1992). *Method of Determining and Expressing Particle Size of Chopped Forage Materials by Screening*. MI, USA: American Society of Agricultural and Biological Engineers, St. Joseph.

American Society of Agricultural and Biological Engineers (ASABE) Standard S269.4. (2007). *Cubes, Pellets, and Crumbles – Definitions and Methods for Determining Density, Durability, and Moisture Content*. MI, USA: ASABE, St. Joseph.

Blanco-Canqui, H., Mitchell, R. B., Jin, V. L., Schmer, M. R., and Eskridge, K. M. (2017). Perennial Warm-season Grasses for Producing Biofuel and Enhancing Soil Properties: an Alternative to Corn Residue Removal. *GCB Bioenergy.* 9, 1510–1521. doi:10.1111/gcbb.12436

Chauhan, S. K., Gupta, N., Walia, R., Yadav, S., Chauhan, R., and Mangat, P. S. (2011). Biomass and Carbon Sequestration Potential of Poplar-What Intercropping System in Irrigated Agro-Ecosystem in India. *J. Agric. Sci. Technol. A.* 1, 575–586.

Chescheir, G., and Nettles, J. (2017). *Optimization of Southeastern Forest Biomass Crop Production: Watershed Scale Evaluation of the Sustainability and Productivity of Dedicated Energy Crop and Woody Biomass Operations*. Denver, Colorado: The US, DOE Bioenergy Technologies Office (BETO) Project Peer Review. Available at: https://www.energy.gov/sites/prod/files/2017/05/f34/analysis_and_sustainability_chescheir_1.1.1.101.pdf (Accessed August 15, 2021).

Edmunds, C. W., Hamilton, C., Kim, K., André, N., and Labbé, N. (2017). Rapid Detection of Ash and Inorganics in Bioenergy Feedstocks Using Fourier Transform Infrared Spectroscopy Coupled With Partial Least-Squares Regression. *Energy Fuels.* 31, 6080–6088. doi:10.1021/acs.energyfuels.7b00249

Edmunds, C. W., Reyes Molina, E. A., André, N., Hamilton, C., Park, S., Fasina, O., et al. (2018). Blended Feedstocks for Thermochemical Conversion: Biomass Characterization and Bio-Oil Production From Switchgrass-Pine Residues Blends. *Front. Energ. Res.* 6, 79. doi:10.3389/fenrg.2018.00079

Fagan, C. C., Everard, C. D., and Mcdonnell, K. (2011). Prediction of Moisture, Calorific Value, Ash and Carbon Content of Two Dedicated Bioenergy Crops Using Near-Infrared Spectroscopy. *Bioresour. Technology.* 102, 5200–5206. doi:10.1016/j.biortech.2011.01.087

Feng, Q., Chaubey, I., Engel, B., Cibin, R., Sudheer, K. P., and Volenec, J. (2017). Marginal Land Suitability for Switchgrass, Miscanthus and Hybrid poplar in the Upper Mississippi River Basin (UMRB). *Environ. Model. Softw.* 93, 356–365. doi:10.1016/j.envsoft.2017.03.027

Feng, X., Yu, C., Liu, X., Chen, Y., Zhen, H., Sheng, K., et al. (2018). Nondestructive and Rapid Determination of Lignocellulose Components of Biofuel Pellet Using Online Hyperspectral Imaging System. *Biotechnol. Biofuels.* 11, 88. doi:10.1186/s13068-018-1090-3

Gargalo, C. L., Udugama, I., Pontius, K., Lopez, P. C., Nielsen, R. F., Hasanzadeh, A., et al. (2020). Towards Smart Biomanufacturing: A Perspective on Recent Developments in Industrial Measurement and Monitoring Technologies for Bio-Based Production Processes. *J. Ind. Microbiol. Biotechnol.* 47, 947–964. doi:10.1007/s10295-020-02308-1

Hartman, J. C., Nippert, J. B., Orozco, R. A., and Springer, C. J. (2011). Potential Ecological Impacts of Switchgrass (Panicum Virgatum L.) Biofuel Cultivation in the Central Great plains, USA. *Biomass and Bioenergy.* 35, 3415–3421. doi:10.1016/j.biombioe.2011.04.055

Harun, N. Y., and Afzal, M. T. (2015). Chemical and Mechanical Properties of Pellets Made. *Trans. ASABE.* 58, 921–930. doi:10.13031/trans.58.11027

Hwang, S.-W., Hwang, U. T., Jo, K., Lee, T., Park, J., Kim, J.-C., et al. (2021). NIR-Chemometric Approaches for Evaluating Carbonization Characteristics of Hydrothermally Carbonized Lignin. *Sci. Rep.* 11, 16979. doi:10.1038/s41598-021-96461-x

Jackson, J., Turner, A., Mark, T., and Montross, M. (2016). Densification of Biomass Using a Pilot Scale Flat Ring Roller Pellet Mill. *Fuel Process. Technology.* 148, 43–49. doi:10.1016/j.fuproc.2016.02.024

Jin, X., Chen, X., Shi, C., Li, M., Guan, Y., Yu, C. Y., et al. (2017). Determination of Hemicellulose, Cellulose and Lignin Content Using Visible and Near Infrared Spectroscopy in Miscanthus Sinensis. *Bioresour. Technology.* 241, 603–609. doi:10.1016/j.biortech.2017.05.047

Killner, M. H. M., Rohwedder, J. J. R., and Pasquini, C. (2011). A PLS Regression Model Using NIR Spectroscopy for On-Line Monitoring of the Biodiesel Production Reaction. *Fuel.* 90, 3268–3273. doi:10.1016/j.fuel.2011.06.025

Kim, P., Hamilton, C., Elder, T., and Labbé, N. (2018). Effect of Non-Structural Organics and Inorganics Constituents of Switchgrass During Pyrolysis. *Front. Energ. Res.* 6, 96. doi:10.3389/fenrg.2018.00096

Lamers, P., Roni, M. S., Tumuluru, J. S., Jacobson, J. J., Cafferty, K. G., Hansen, J. K., et al. (2015). Techno-Economic Analysis of Decentralized Biomass Processing Depots. *Bioresour. Technology.* 194, 205–213. doi:10.1016/j.biortech.2015.07.009

Lan, K., Park, S., Kelley, S. S., English, B. C., Yu, T. H. E., Larson, J., et al. (2020). Impacts of Uncertain Feedstock Quality on the Economic Feasibility of Fast Pyrolysis Biorefineries With Blended Feedstocks and Decentralized Preprocessing Sites in the Southeastern United States. *GCB Bioenergy.* 12, 1014–1029. doi:10.1111/gcbb.12752

Lane, J. (2018). The Idaho Team that Looped $1 a Gallon of the Cost of the Fuel and How They Did it. Available at: http://www.biofuelsdigest.com/bdigest/2018/09/09/the-idaho-team-that-lopped-1-a-gallon-off-the-cost-of-fuel-and-how-they-did-it/ (Accessed March 15, 2018).

Li, M., He, S., Wang, J., Liu, Z., and Xie, G. H. (2018). An NIRS-Based Assay of Chemical Composition and Biomass Digestibility for Rapid Selection of

Jerusalem Artichoke Clones. *Biotechnol. Biofuels.* 11, 334. doi:10.1186/s13068-018-1335-1

Li, X., Ma, F., Liang, C., Wang, M., Zhang, Y., Shen, Y., et al. (2021). Precise High-Throughput Online Near-Infrared Spectroscopy Assay to Determine Key Cell wall Features Associated With Sugarcane Bagasse Digestibility. *Biotechnol. Biofuels.* 14, 123. doi:10.1186/s13068-021-01979-x

Li, X., Sun, C., Zhou, B., and He, Y. (2015). Determination of Hemicellulose, Cellulose and Lignin in Moso Bamboo by Near Infrared Spectroscopy. *Sci. Rep.* 5, 17210. doi:10.1038/srep17210

Ma, T., Inagaki, T., and Tsuchikawa, S. (2020). Rapidly Visualizing the Dynamic State of Free, Weakly, and Strongly Hydrogen-Bonded Water with Lignocellulosic Material During Drying by Near-Infrared Hyperspectral Imaging. *Cellulose.* 27, 4857–4869. doi:10.1007/s10570-020-03117-6

Mahadevan, R., Adhikari, S., Shakya, R., Wang, K., Dayton, D., Lehrich, M., et al. (2016). Effect of Alkali and Alkaline Earth Metals on Iin-Ssitu Catalytic Fast Pyrolysis of Lignocellulosic Biomass: A Microreactor Study. *Energy Fuels.* 30, 3045–3056. doi:10.1021/acs.energyfuels.5b02984

M. Kline, L., Labbé, N., Labbé, N., Boyer, C., Edward Yu, T., C. English, B., et al. (2015). Investigating the Impact of Biomass Quality on Near-Infrared Models for Switchgrass Feedstocks. *AIMS Bioeng.* 3, 1–22. doi:10.3934/bioeng.2016.1.1

Moroń, W., and Rybak, W. (2015). NOx and SO2 Emissions of Coals, Biomass and Their Blends Under Different Oxy-Fuel Atmospheres. *Atmos. Environ.* 116, 65–71. doi:10.1016/j.atmosenv.2015.06.013

National Renewable Energy Laboratory (2008). Learning about Renewables. Available at: http://www.nrel.gov/learning (Accessed May 7, 2008).

Ou, L., Luo, G., Ray, A., Li, C., Hu, H., Kelley, S., et al. (2018). Understanding the Impacts of Biomass Blending on the Uncertainty of Hydrolyzed Sugar Yield From a Stochastic Perspective. *ACS Sustainable Chem. Eng.* 6, 10851–10860. doi:10.1021/acssuschemeng.8b02150

Ozaki, Y., Genkawa, T., and Futami, Y. (2017). "Near-infrared Spectroscopy," in *Encyclopedia of Spectroscopy and Spectrometry*. Editors J. Lindon, G. E. Tranter, and D. Koppenall (Cambridge, MA: Academic Press), 40–49. doi:10.1016/b978-0-12-409547-2.12164-x

Posom, J., and Sirisomboon, P. (2017). Evaluation of the Higher Heating Value, Volatile Matter, Fixed Carbon and Ash Content of Ground Bamboo Using Near Infrared Spectroscopy. *J. Near Infrared Spectrosc.* 25, 301–310. doi:10.1177/0967033517728733

Prestemon, J. P., and Abe, R. (2002). "Timber Products Supply and Demand," in " *in Southern Forest Resource Assessment*. Editors D. Wear and J. G. Greis (Asheville, NC: USDA-Forest Service, Southern Research Station), 299–325.

Ray, A. E., Li, C., Thompson, V. S., Daubaras, D. L., Nagle, N., and Hartley, D. S. (2017). "Biomass Blending and Densification: Impacts on Feedstock Supply and Biochemical Conversion Performance," in *Biomass Volume Estimation and Valorization for Energy*. Editor J. S. Tumuluru (Idaho Falls, ID: InTech), 1–22. doi:10.5772/67207

Rhén, C., Gref, R., Sjöström, M., and Wästerlund, I. (2005). Effects of Raw Material Moisture Content, Densification Pressure and Temperature on Some Properties of Norway spruce Pellets. *Fuel Process. Technology* 87, 11–16. doi:10.1016/j.fuproc.2005.03.003

Risser, P. G., Birney, E. C., Blocker, H. D., May, S. W., Parton, W. J., and Wiens, J. A. (1981). *The True Prairie Ecosystem*. Stroudsburg, PA: Hutchinson Ross Publications.

Sahoo, K., and Mani, S. (2016). Engineering Economics of Cotton Stalk Supply Logistics Systems for Bioenergy Applications. *Trans. ASABE.* 59, 737–747. doi:10.13031/trans.59.11533

Sahoo, K., and Mani, S. (2017). Techno-economic Assessment of Biomass Bales Storage Systems for a Large-Scale Biorefinery. *Biofuels, Bioprod. Bioref.* 11, 417–429. doi:10.1002/bbb.1751

Said, N., Abdel Daiem, M. M., García-Maraver, A., and Zamorano, M. (2015). Influence of Densification Parameters on Quality Properties of rice Straw Pellets. *Fuel Process. Technology.* 138, 56–64. doi:10.1016/j.fuproc.2015.05.011

Serrano, C., Monedero, E., Lapuerta, M., and Portero, H. (2011). Effect of Moisture Content, Particle Size and Pine Addition on Quality Parameters of Barley Straw Pellets. *Fuel Process. Technology.* 92, 699–706. doi:10.1016/j.fuproc.2010.11.031

Sluiter, A., Hames, B., Ruiz, R., Scarlata, C., Sluiter, J., and Templeton, D. (2005). "Determination of Ash in Biomass," in *NREL Laboratory Analytical Procedure* (Golden, CO: National Renewable Energy Laboratory), 1–12.

Suyker, A. E., and Verma, S. B. (2001). Year-round Observations of the Net Ecosystem Exchange of Carbon Dioxide in a Native Tallgrass Prairie. *Glob. Change Biol. Bioenergy.* 7, 279–289. doi:10.1046/j.1365-2486.2001.00407.x

Tumuluru, J., Lim, C., Bi, X., Kuang, X., Melin, S., Yazdanpanah, F., et al. (2015). Analysis on Storage Off-Gas Emissions From Woody, Herbaceous, and Torrefied Biomass. *Energies.* 8, 1745–1759. doi:10.3390/en8031745

Tumuluru, J. (2019). Pelleting of pine and Switchgrass Blends: Effect of Process Variables and Blend Ratio on the Pellet Quality and Energy Consumption. *Energies.* 12, 1198. doi:10.3390/en12071198

Tumuluru, J. S. (2018). Effect of Pellet die Diameter on Density and Durability of Pellets Made From High Moisture Woody and Herbaceous Biomass. *Carbon Resour. Convers.* 1, 44–54. doi:10.1016/j.crcon.2018.06.002

Tumuluru, J. S. (2014). Effect of Process Variables on the Density and Durability of the Pellets Made From High Moisture Corn Stover. *Biosyst. Eng.* 119, 44–57. doi:10.1016/j.biosystemseng.2013.11.012

Tumuluru, J. S., and Fillerup, E. (2020). Briquetting Characteristics of Woody and Herbaceous Biomass Blends: Impact on Physical Properties, Chemical Composition, and Calorific Value. *Biofuels, Bioprod. Bioref.* 14, 1105–1124. doi:10.1002/bbb.2121

Tumuluru, J. S., Hess, J. R., Boardman, R. D., Wright, C. T., and Westover, T. L. (2012). Formulation, Pretreatment, and Densification Options to Improve Biomass Specifications for Co-Firing High Percentages With Coal. *Ind. Biotechnol.* 8, 113–132. doi:10.1089/ind.2012.0004

Tumuluru, J. S., and Mwamufiya, M. (2021). FCIC DFO – Moisture Management and Optimization in Municipal Solid Waste Feedstock Through Mechanical Processing. Available at: https://www.energy.gov/sites/default/files/2021-04/beto-12-peer-review-2021-fcic-tumuluru.pdf (Accessed August 15, 2021).

Tumuluru, J. S. (2016). Specific Energy Consumption and Quality of Wood Pellets Produced Using High-Moisture Lodgepole Pine Grind in a Flat die Pellet Mill. *Chem. Eng. Res. Des.* 110, 82–97. doi:10.1016/j.cherd.2016.04.007

Tumuluru, J. S., Wright, C. T., Hess, J. R., and Kenney, K. L. (2011). A Review of Biomass Densification Systems to Develop Uniform Feedstock Commodities for Bioenergy Application. *Biofuels, Bioprod. Bioref.* 5, 683–707. doi:10.1002/bbb.324

U.S. Department of Energy (DOE) (2016). *Billion-ton Report: Advancing Domestic Resources for a Thriving Bioeconomy—Volume 1: Economic Availability of Feedstocks. ORNL/TM-2016/160*. Oak Ridge, TN, USA: Oak Ridge National Laboratory.

U.S. Environmental Protection Agency (EPA) (2018). Overview for Renewable Fuel Standard. Available at: https://www.epa.gov/renewable-fuel-standard-program/overview-renewable-fuel-standard (Accessed October 9, 2018).

Williams, C. L., Emerson, R., and Tumuluru, J. S. (2017). "Biomass Compositional Analysis for Conversion to Renewable Fuels and Chemicals," in *Biomass Volume Estimation and Valorization for Energy*. Editor J. S. Tumuluru, IntechOpen, 251–270. doi:10.5772/65777

Yancey, N. A., Tumuluru, J. S., and Wright, C. T. (2013). Drying, Grinding and Pelletization Studies on Raw and Formulated Biomass Feedstock's for Bioenergy Applications. *J. Biobased Mat Bioenergy.* 7, 549–558. doi:10.1166/jbmb.2013.1390

Zhang, D., and Polyakov, M. (2010). The Geographical Distribution of Plantation Forests and Land Resources Potentially Available for pine Plantations in the U.S. South. *Biomass and Bioenergy.* 34, 1643–1654. doi:10.1016/j.biombioe.2010.05.006

publish or reproduce the published form of this manuscript or allow others to do so for U.S. government purposes.

Conflict of Interest: The authors declare that the research was conducted in the absence of any commercial or financial relationships that could be construed as a potential conflict of interest.

Publisher's Note: All claims expressed in this article are solely those of the authors and do not necessarily represent those of their affiliated organizations, or those of the publisher, the editors and the reviewers. Any product that may be evaluated in this article, or claim that may be made by its manufacturer, is not guaranteed or endorsed by the publisher.

frontiers in Energy Research

ORIGINAL RESEARCH
published: 20 January 2022
doi: 10.3389/fenrg.2021.790421

Oilseed Cover Crops for Sustainable Aviation Fuels Production and Reduction in Greenhouse Gas Emissions Through Land Use Savings

Farzad Taheripour, Ehsanreza Sajedinia and Omid Karami*

Department of Agricultural Economics, Purdue University, West Lafayette, IN, United States

Induced Land Use Changes (ILUCs) can decrease the environmental benefits of Sustainable Aviation Fuels (SAFs) if produced from traditional food crops. The development of oilseed cover crops can eliminate the side effect of ILUCs for biofuel production because they come in rotation with the major crops with some savings in demand for new cropland. This study implemented Life Cycle Analysis (LCA) and GTAP-BIO to estimate ILUC emissions values, the potentially available area, and total possible emissions savings of producing SAFs from carinata, camelina, and pennycress in the United States. The results suggest that: 1) the meals produced in conjunction with increases in Sustainable Aviation Fuel production from carinata, camelina, and pennycress could reduce land use emissions by 12.9, 15.3, and 18.3 gCO_2e/MJ, respectively; 2) the total area of available land for producing these feedstocks could be about 29.3 million ha in 2035; and 3) using this area of land for SAF production, depends on the mix of oilseed cover crops that can be produced in practice, could generate up to 92 million metric tons of savings in GHG emissions per year. The projected emissions savings is about 11% of the current global GHG emissions generated by the aviation industry. Providing incentives to encourage farmers to produce these cover crops and facilitating investment in producing SAF from these cover crops are the most important factors that could help the aviation industry to enhance emissions savings.

Keywords: emissions savings, land use change, multiple cropping, oilseed cover crops, sustainable aviation fuels

OPEN ACCESS

Edited by:
William Goldner, United States Department of Agriculture (USDA), United States

Reviewed by:
Arnaldo Walter, State University of Campinas, Brazil
Benyamin Khoshnevisan, Chinese Academy of Agricultural Sciences (CAAS), China

****Correspondence:***
Farzad Taheripour
tfarzad@purdue.edu

Specialty section:
This article was submitted to Bioenergy and Biofuels, a section of the journal Frontiers in Energy Research

Received: *06 October 2021*
Accepted: *10 December 2021*
Published: *20 January 2022*

Citation:
Taheripour F, Sajedinia E and Karami O (2022) Oilseed Cover Crops for Sustainable Aviation Fuels Production and Reduction in Greenhouse Gas Emissions Through Land Use Savings. Front. Energy Res. 9:790421. doi: 10.3389/fenrg.2021.790421

INTRODUCTION

The use of biofuels has been included in the emissions reduction policies of many countries across the world. However, the effectiveness of this policy is subject to debate as Induced Land Use Changes (ILUCs) and emissions vary across alternative biofuel pathways. Over the past 15 years, many papers have estimated ILUC emissions for various biofuel pathways[1]. The early papers in this field have claimed that producing biofuels from food crops (grains, oilseeds, sugar crops) will not lead to emissions savings due to large ILUC emissions (e.g., Searchinger et al., 2008 and Al-Riffai et al.,

[1]Some of these papers has referred to ILUC as Indirect Land Use Change. However, both terminologies represent the same concept. The first section of the **Supplementary Material** (S.M.) of this paper describes the background of these two terminologies.

2010). However, the subsequent papers have rejected that claim and shown that the early papers in this area overrated the ILUC emissions for the first generation biofuels (Zilberman et al., 2018). On the other hand, several papers have shown that the second-generation biofuels produced from lignocellulosic energy crops cultivated on the available marginal land could make significant emissions savings. For example, Field et al. (2020) have shown that producing biofuels from dedicated energy crops could generate significantly large negative ILUC emissions due to major gains in soil carbon sequestration. The existing literature in this field has been mainly focused on ILUC values for ethanol and biodiesel produced from food crops and lignocellulosic feedstocks. More recently, Zhao et al. (2021) have estimated ILUC values for several aviation biofuel pathways again produced from food crops and lignocellulosic energy crops.

Due to concerns about using food crops for biofuels, since the late 2000s, the biobased industry has made major efforts to develop new biofuel feedstocks to lower the need for cropland and avoid competition between food and biofuel production. Developing new oilseed cover crops that can be used for biofuel production is an outstanding outcome of these efforts. These crops (e.g., camelina, carinata, and pennycress) can be produced on the existing cropland in rotation with other crops in 1 year in a multi cropping system and provide major savings in demand for cropland. It is important to emphasize that these crops could be produced as a second crop on the existing croplands that remain fallow in winter otherwise. While these oilseed cover crops can be used for biodiesel production, many papers have addressed the use of these oilseed cover crops to produce aviation biofuels (Zanetti et al., 2019; Alam and Dwivedi, 2019; Trejo-Pech et al., 2019; Robertson, 2020). Currently, the aviation industry relies on fossil fuels with no other economically affordable fuel alternatives (Prussi et al., 2021). In 2019, the global aviation industry emitted 785 million metric tons of CO_2 (Graver et al., 2020). The United States aviation alone emitted 23% of this amount (Graver et al., 2020). It is about 5% of total energy-related CO_2 emissions nationwide (EIA, 2019). Furthermore, the global aviation demand is expected to increases by 3.7% per year until 2039, regardless of the COVID-19 impact (IATA, 2020). The demand rise will result in around 2.27 billion tonnes of CO_2 emissions, which is 2.31 times greater than the 2021 baseline (Valdés et al., 2021).

IATA members representing 93% of scheduled international air traffic put a cap on aviation net emissions to half the emissions by 2050 compared with the 2005 level (ICAO, 2019a). For this, they implemented a four-pillar policy: investment in technology, more effective operations, more efficient infrastructure, and positive economic measures (ICAO, 2019a). Sustainable Aviation Fuels (SAFs) have been used in many instances to designate fuels produced from non-conventional processes and, consequently, lower environmental impact (ICAO, 2019b). According to the Carbon Offsetting and Reduction Scheme for International Aviation (CORSIA), a SAF lowers carbon aviation fuel which an operator may use to reduce their offsetting requirement (ICAO, 2019b). SAF is becoming popular as one of the most promising ways to mitigate CO_2 emissions from the aviation sector (IBAC, 2019). Some studies focused on SAF from different feedstocks and geographical places. Murphy et al. (2015) focused on the operational and economic factors related to lignocellulosic biomass supply for SAF production in central Queensland, Australia. They concluded that the region has the potential to produce all demand by using 1.1 million hectares of land. Hudson et al. (2016) set up a Roadmap to assess SAF potential production for the United Kingdom in the period up to 2050. They concluded that supports for 12 different biomasses could mitigate up to 24% of the United Kingdom aviation CO_2 and create Gross Added Value up to £265 m. In a similar study in the United States, Chao et al. (2019) concluded that support from the government could reduce aviation emissions by 37.5–50% in 2050.

Besides these papers, and while many papers have examined the extent to which the first and second-generation biofuels provide emissions savings, not much effort has been made to assess the potential emissions savings due to producing biofuels from oilseed cover crops such as pennycress and carinata. However, some other studies analyzed economics (Eswaran et al., 2021; Mousavi-Avval and Shah, 2021) and agronomy (Mohdaly and Ramadan, 2020; Kumar et al., 2020; López et al., 2021) of pennycress and carinata. A typical oilseed cover crop can be produced as a second crop in rotation with other crops in 1 year on the existing croplands that remain fallow in winter otherwise. Many papers have introduced these crops as a proper feedstock for biofuel production (e.g., biodiesel or jet fuel), examined their oils and meals properties, and determined where and under what conditions they can be produced (e.g., Moser et al., 2009 and McGinn et al., 2019). However, to the best of our knowledge, no major effort has been made to quantify the potential emissions savings from using these cover crops for biofuel production. Producing biofuels from these crops will replace their equivalent uses of fossil fuels and generate major emissions savings. On the other hand, producing these oilseeds cover crops as a second crop will not generate additional demands for new cropland. The meal co-products of producing biofuels from these crops could be consumed as animal feed by the livestock industry and provide major savings in demand for cropland. In addition, the cultivation of oilseed cover crops could improve the Soil Organic Carbon (SOC) (Karami, 2021). This paper evaluates the emissions savings due to these effects for various options on cultivating these crops within the United States Midwest Corn Belt and outside this region. It discusses the policy incentives that can be implemented to gain the estimated emissions savings as well.

Finally, it is important to note that within the CORSIA framework, SAF can be produced from various feedstocks. Cultivation of some of these feedstocks could cause land use emissions (e.g., food crops), some could provide savings in land use emissions (e.g., oilseed cover crops or lignocellulosic feedstocks), and some feedstocks may not generate land use emissions (e.g., waste materials). In this paper, we only highlight potential emissions savings that could be gained due to SAF production from oilseed cover crops. Further research is needed to assess potential emissions savings for other SAF pathways.

MATERIALS AND METHODS

To accomplish the goals of this research, we developed the following research activities:

Evaluation of ILUC Values for SAF Produced From Oilseed Cover Crops

Over the past 15 years, a large number of papers have estimated ILUC emissions for various biofuel pathways, including ethanol and biodiesel produced from food crops (grains, sugar crops, and edible vegetable oils) and lignocellulosic feedstocks (some examples are: Searchinger et al., 2008; Al-Riffai et al., 2010; Hertel et al., 2010; Tyner et al., 2010; and Taheripour et al., 2017). However, these papers have exclusively estimated ILUC values for road transportation biofuels. More recently, Zhao et al. (2021) have estimated ILUC values for 17 Sustainable Aviation Fuel (SAF) pathways also produced from food crops and lignocellulosic energy crops. The results of this paper show that ILUC values for aviation biofuels that can be produced from food crops are all positives (e.g., 20, 22.5, 34.6 gCO_2e/MJ for United States soybean oil, Brazilian soybean oil, and palm oil produced in Malaysia and Indonesia, respectively). To the best of our knowledge, no major effort has been made to estimate ILUC values for SAF pathways that can be produced from oilseed cover crops cultivated in rotation with other crops in a double-cropping system. Here, we evaluate ILUC values for three varieties of oilseed cover crops in the United States: carinata, camelina, and pennycress.

We follow Zhao et al. (2021) to assess ILUC values for the cover crops mentioned above. These authors have introduced SAF pathways in the Global Trade Analysis Project-Biofuel (GTAP-BIO) model, which has been frequently used to assess the ILUC emissions due to biofuel production (e.g., Hertel et al., 2010; Tyner et al., 2010; and; Taheripour et al., 2017). GTAP-BIO is a Computable General Equilibrium (CGE) model that tracks production, consumption, and trade of all goods and services produced around the world. In particular, this model is designed to assess the land use consequences of alternative biofuel pathways, while it takes into account interactions between agricultural and energy markets and their links to other economic activities. We further developed this model by introducing SAF pathways for carinata, camelina, and pennycress.

Producing oilseed cover crops in rotation with other crops in a double-cropping system provides an opportunity to produce two products with no additional demand for land: Usable oils that can be converted to biofuels (SAF and biodiesel) and meal that can be used by livestock producers as a source of protein in animal feed diets. For example, the oil and meal contents of carinata are about 40 and 60%, respectively.

While production of an oilseed cover crop in rotation with other crops does not need additional land, its production as the second crop, could generate some savings in land use due to providing meal for the livestock industry. The additional meal produced from expansion in production of oilseed cover crops could help the livestock industry to produce more products using less land. The oilseed cover crops meals can be used as substitute for soybean meal or other oilseeds meals and drop the demand for cropland indirectly. Here we examine the extent to which producing SAF and its biodiesel co-products from oilseed cover crops produced in the United States affect land use changes at the global scale.

To accomplish this task, we added several new sectors into the GTAP-BIO model reported by Zhao et al. (2021) to produce carinata, camelina, and pennycress, their oils, and meals. Following these authors, we also considered the Hydroprocessed Esters Fatty Acids (HEFA) technology to convert the oils of these crops to SAF. This technology has been briefly described in S.M.

The oilseed cover crop sectors use intermediate inputs, including seeds, chemicals, energy, services, and other intermediate inputs. They demand primary inputs, including labor and capital (including profits gained above the operating costs) as well. The cost structures of these crops were determined using the techno-economic analyses used in the lifecycle assessments of these crops (Prussi et al., 2021) and in consultation with experts from CoverCress Inc.

For each new seed sector, a processing sector is included in the model. The new processing sectors purchase seeds, crush the seeds, convert the extracted oils to SAF (and biodiesel co-product), sell the fuels to the blending sector, produce meals, and sell the meals to livestock producers. The livestock industry uses the meal as feed. The cost structures of these industries follow the HEFA cost structure defined in Zhao et al. (2021).

To construct the benchmark database, the conservative yields of 2.4, 1.1, and 1.7 metric tons per hectare were used for carinata, camelina, and pennycress, respectively. In addition, the oil crushing rates of 0.42 for carinata, 0.39 for camelina, and 0.32 for pennycress were assumed. The model database is modified to include small amounts of outputs for each new pathway. Seeding the industry with a small quantity of the product is necessary to permit simulations in GTAP-BIO.

Finally, to assess the ILUC value for each oilseed cover crop pathway (i.e., carinata oil HEFA, camelina oil HEFA, and pennycress oil HEFA) an exogenous shock by 212.9 Million Gallons of Gasoline Equivalent (MGGE) was introduced to the model. For each pathway, the sock consists of 25% SAF and 75% biodiesel co-product. These shares are embedded in the HEFA technology. Following Zhao et al. (2021), a unique set of model parameters has been used across all examined pathways.

Potential Area for Producing Oilseed Cover Crops

Oilseed cover crops can be produced on marginal land or in rotation with other crops as a second crop in one planting year. In this paper, we only concentrate on the second option. Several papers (Sindelar et al., 2017; Akter et al., 2021) have addressed the plantation of oilseed cover crops in a double-cropping system, and some of the papers estimated the areas that these cover crops could be produced in rotation with other crops in the United States (Embaye et al., 2018; Alam and Dwivedi, 2019). Producing these cover crops in the United States Corn-Belt is an

TABLE 1 | Current corn-soybean rotation and proposed corn-second oilseed cover crop-soybean rotation timelines for the United States Corn-Belt.

Description		Crop year 1												Crop year 2											
		Feb	Mar	Apr	May	Jun	Jul	Aug	Sep	Oct	Nov	Dec	Jan	Feb	Mar	Apr	May	Jun	Jul	Aug	Sep	Oct	Nov	Dec	Jan
C-S rotation	First half of land	F	F	F	C	C	C	C	C	C	C	F	F	F	F	F	S	S	S	S	S	S	S	F	F
	Second half of land	F	F	F	S	S	S	S	S	S	S	F	F	F	F	F	C	C	C	C	C	C	C	F	F
C-SC-S Rotation	First half of land	F	F	F	C	C	C	C	C/SC	C/SC	SC	SC	SC	SC	SC	SC	SC/S	S	S	S	S	S	S	F	F
	Second half of land	SC	SC	SC	SC/S	S	S	S	S	S	S	F	F	F	F	F	C	C	C	C	C/SC	C/SC	SC	SC	SC

Notes: C = corn; S = soybean; SC, second oilseed cover crops in rotation with corn and soybeans, F = fallow.

important option. Conventionally, a large portion of cropland in the Corn-Belt has been used to produce corn and soybeans in a 2-year rotation (henceforth: C-S rotation). Therefore, the area that follows this rotation is divided equally between soybean and corn in each crop year. If the land is used for corn production in the first year, that land will be used for soybean production in the second year and vice versa (**Table 1**). In this crop rotation, the whole area of cropland under corn and soybeans remains fallow in about 5 months from February to April at the beginning and then December and January at the end (**Table 1**). As mentioned above, some papers have shown that the oilseed cover crops can be introduced into this rotation in a double-cropping system to produce non-food oilseeds used for SAF production. The rotation of corn, oilseed cover crops, and soybean (henceforth: C-SC-S) is presented in the last two lines of **Table 1**. This table represents a general timeline for the C-SC-S double-cropping rotation. The exact timing of this rotation could vary according to the local agro-ecological conditions, maturity of soybean variety, and the type of cultivated oilseed cover crop. Depending on these conditions, the oilseed cover crops may be cultivated after corn harvest in September or October and harvested in May before soybean cultivation. It is important to note that, as shown in **Table 1**, with the proposed crop rotation, in between corn and soybean, each piece of cropland land will be cultivated for oilseed cover crops every other year. This means that compared with the conventional corn-soybean rotation, the proposed new rotation drops the area of winter fallow land by half.

To determine the potential area of producing oilseed cover crops in the United States, we rely on the work developed by Sindelar et al. (2017). They estimated the potential area for these crops for the United States Corn-Belt based on the common rotations used during 2009–13 in this region. However, Sindelar et al. (2017) missed two important facts: 1) areas of corn and soybean are growing over time while other crops (including Alfalfa) are declining, and 2) multiple cropping is possible outside the Corn-Belt as well. To remove these deficiencies, we considered area expansion for corn and soybean over time. In addition, we included potential areas outside the Corn-Belt. We worked with the average area of 2010–2020 based on USDA and estimated the potential area for producing oilseed cover crops for 2021 to 2035. The S.M. represents details of this estimation.

Finally, it is important to note that carinata, camelina, and pennycress can be produced on marginal cropland or even productive cropland as the main crop in late spring and summer. However, these alternatives may compete with other food crops and cause induced land use changes. The CORSIA framework has not considered these practices in providing feedstock for SAF production. Hence, within the CORSIA framework, oilseed cover crops should not displace other crops. The areas of land that we considered in this paper satisfies this limitation.

Potential Emissions Savings

The annual emission savings due to the use of a given oilseed cover crop (ES_{tj} measured in a million metric tons of CO_2e) for SAF production could be gained from various channels, including:

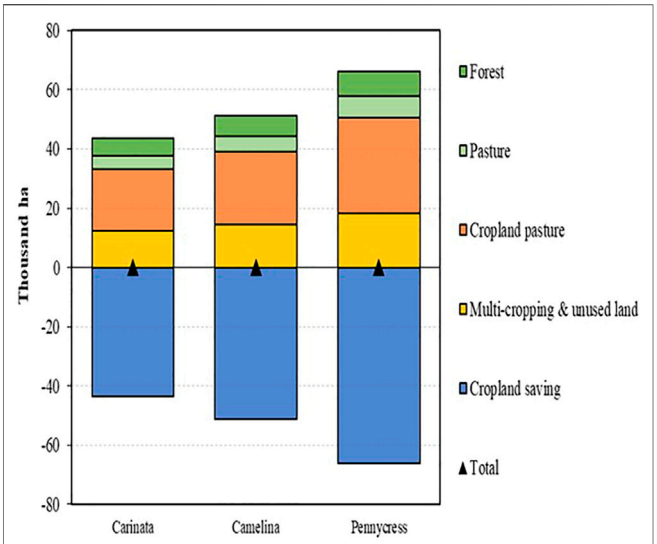

FIGURE 1 | ILUCs due to expansions in SAF from carinata oil, camelina oil, and pennycress (all by HEFA).

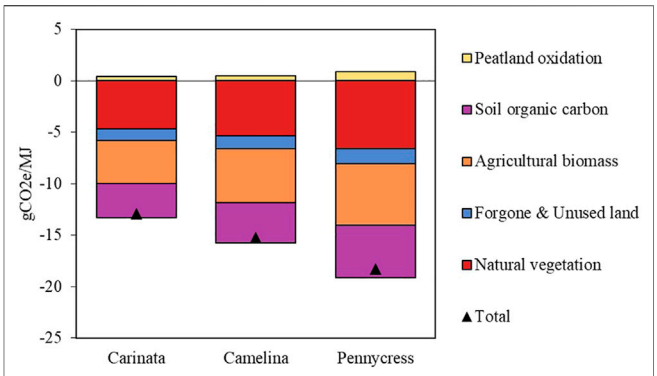

FIGURE 2 | ILUCs for carinata oil, camelina oil, and pennycress in the United States (all by HEFA).

1) Savings in emissions due to replacement of SAF with conventional jet fuel, R_{tj}
2) Savings in ILUC emissions L_{tj},
3) Savings in SOC due to cultivation of the seed, SOC_{tj}

Therefore

$$ES_{tj} = R_{tj} + L_{tj} + SOC_{tj} \quad (1)$$

Where:

$$R_{tj} = (E_{conv} - E_{SAF}) * Q_{tj} \quad (2)$$

$$L_{tj} = -\left(ILUC_j\right) * Q_{tj} \quad (3)$$

$$SOC_{tj} = \theta_j * A_{tj} \quad (4)$$

In these formulas, Q_{tj} represents total energy content of produced SAF and its related energy co-products measured in Mega Joules (MJ), E_{conv} and E_{SAF} show life cycle emissions for conventional jet fuel and SAF, both measured in a million metric tons of CO_2/MJ, $ILUC_j$ measures land-use change emissions due to cultivation of seed j measured in a million metric tons of CO_2e/MJ, θ_j captures improvements in SOC due to cultivation of seed j measured in gCO_2e/ha, and A_{tj} shows hectares of cultivated seed j for SAF production.

The S.M. further describes these formulas and variables and provides sources of the implemented data for each equation.

RESULTS AND DISCUSSION

ILUC Values for Carinata, Camelina, and Pennycress

Unlike biofuels produced from food crops, producing SAF from oilseed cover crops provides savings in cropland demand for two main reasons. First, producing these crops in a double cropping system in rotation with other crops does not increase demand for cropland. Second, converting these crops to SAF produces some meals that can be used by the livestock industry and that leads to savings in demand for cropland and hence less demand for deforestation.

Figure 1 shows the estimated induced land-use changes for the examined pathways. It shows that producing SAF from oilseed cover crops, regardless of the seed type, generates some savings in demand for cropland (blue bars). That leads to savings in land conversion towards active cropland [positive changes in: forest (dark green bars), pasture (light green bars), and marginal land (orange and yellow bars)]. For the same expansion in SAF, among the examined pathways, carinata and pennycress generate the lowest and highest savings in demand for cropland as shown in **Figure 1**. Two factors explain this observation. The first factor is seed yield. Carinata has the highest yield. The higher the yield is, the lower the saving in cropland will be for a given expansion in SAF. The second factor is the meal content of seed. Again, carinata has the lower meal content (or the highest oil content). For these two reasons, for a given shock in production of SAF, carinata provides the lowest and pennycress delivers the largest savings in demand for cropland. However, it is important to note that for a given area of land, carinata delivers more fuels than pennycress, for the same reason (higher seed yield and higher oil content).

Figure 2 shows the calculated ILUC values obtained for the examined pathways and their decompositions across sources of ILUC. The estimated ILUC values for carinata, camelina, and pennycress are -12.9, -15.3, and -18.3 gCO_2e/MJ. These negative ILUC values reflect the fact that producing SAF from oilseed cover crops leads to savings in GHG emissions due to savings in demand for cropland. While carinata provided the lowest savings in land use emissions per MJ of produced fuels, it could provide more emissions savings for a given available area of land, as this crop produces more energy per unit of land. To highlight the importance of these savings, consider the estimated ILUC values for two other SAF pathways that could be produced in the United States: Corn ETJ and soybean oil HEFA. The estimated ILUC values for these two pathways are 24.9 and 20 gCO_2e/MJ (Zhao et al., 2021). Therefore, producing SAF from oilseed cover

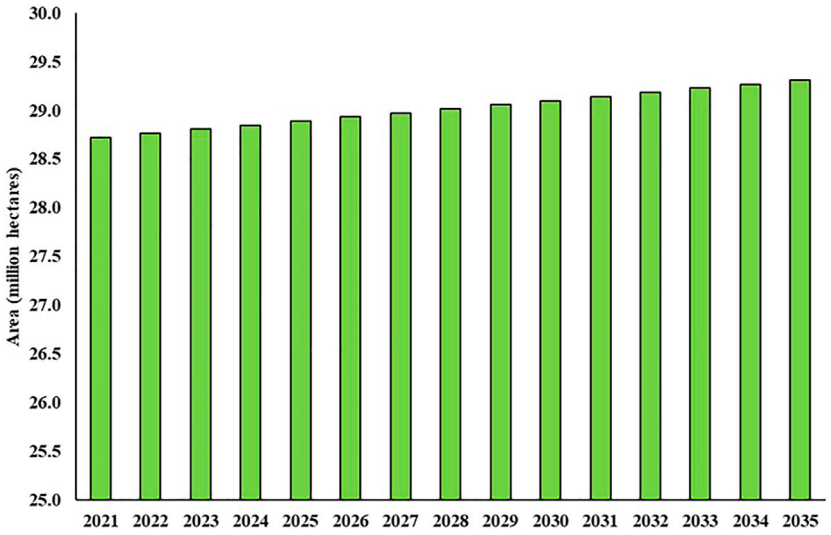

FIGURE 3 | Potential area for oilseed cover crops from 2021 to 2035 in the United States.

crops has an absolute advantage over other SAF pathways that can be produced from food crops.

Figure 2 shows decompositions of the ILUC values for carinata, camelina, and pennycress by the sources of savings in emissions as well. This figure shows that savings in SOC, improvements in agricultural biomass, savings in foregone forest sequestration, and savings in losses of natural vegetation are the main sources of emissions savings for the examined oilseed cover crops; for details, see S.M. From this perspective, carinata, camelina, and pennycress are very similar.

Potential Area

The results show that there is a potential of 28.7 million hectares of land that we can sow oilseed cover crops such as carinata, camelina, and pennycress in 2021 (**Figure 3**). From this area, around 25.3 million hectares are in the United States Corn-Belt, and the other 3.4 million hectares are for the rest of the United States (not shown in the Figure). The potential area is expected to increase to 29.3 million hectares in 2035, as shown in **Figure 3**. Sindelar et al. (2017) also found that there is a potential of 27.1 million ha in the United States Corn Belt for sowing bioenergy crops. They also concluded that several factors affect the adoption rate of the farmers to choose oilseed cover crops in either corn-soybean rotation or corn-corn-soybean rotation.

In practice, the extent to which this area of land will be used for SAF production depends on various factors. The overall national policy and the plan of the United States aviation industry on using SAF are critical factors. A national mitigation policy that supports SAF production (e.g., financial support, mandates, and low carbon fuel standard) could generate major demand for oilseed cover crops encouraging farmers to adopt the C-CS-S rotation in practice. A major commitment to using SAF by the main operators of the aviation industry could cause the same effects. A secure demand for oilseed cover crops, providing educational and logistic supports for the farm industry, will

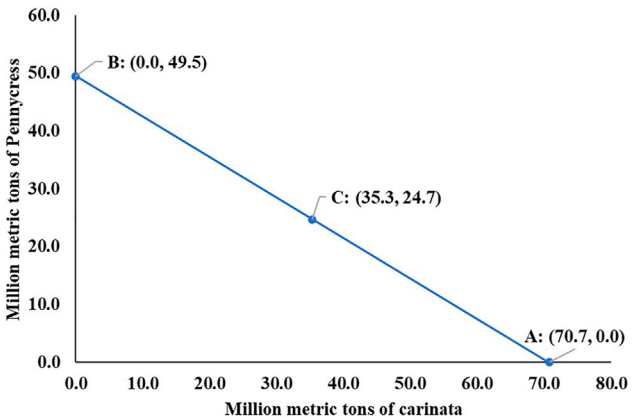

FIGURE 4 | Production possibility Frontier for oilseed cover crops in 2035 in the United States.

encourage farmers to adopt the C-CS-S and other types of rotations better and faster to produce more oilseed cover crops. In practice, it depends on the regional climate and agronomy conditions, the costs of producing each type of oilseed cover crops, and provided policy incentives the farmers are expected to adopt and produce a mix of these crops. These factors jointly will determine the penetration rate for oilseed cover crops in each region.

Production of Oilseed Cover Crops

After knowing the potential area for producing oilseed cover crops, we could assess the potential production of oilseed cover crops. As addressed before, the existing literature mainly shows that carinata, camelina, and pennycress are the main cover crops that can be produced in a double-cropping system in rotation with other crops across the United States. As shown in *Results and*

TABLE 2 | Emission savings for carinata and pennycress from 2021 to 2035.

Year	First scenario (only carinata)	Second scenario (only pennycress)	Third scenario (carinata and pennycress)
2021	90.61	49.82	70.21
2022	90.74	49.89	70.32
2023	90.88	49.96	70.42
2024	91.01	50.03	70.52
2025	91.14	50.10	70.62
2026	91.27	50.18	70.72
2027	91.40	50.25	70.83
2028	91.54	50.32	70.93
2029	91.67	50.40	71.03
2030	91.80	50.47	71.13
2031	91.93	50.54	71.24
2032	92.07	50.62	71.34
2033	92.20	50.69	71.45
2034	92.34	50.76	71.55
2035	92.47	50.84	71.65

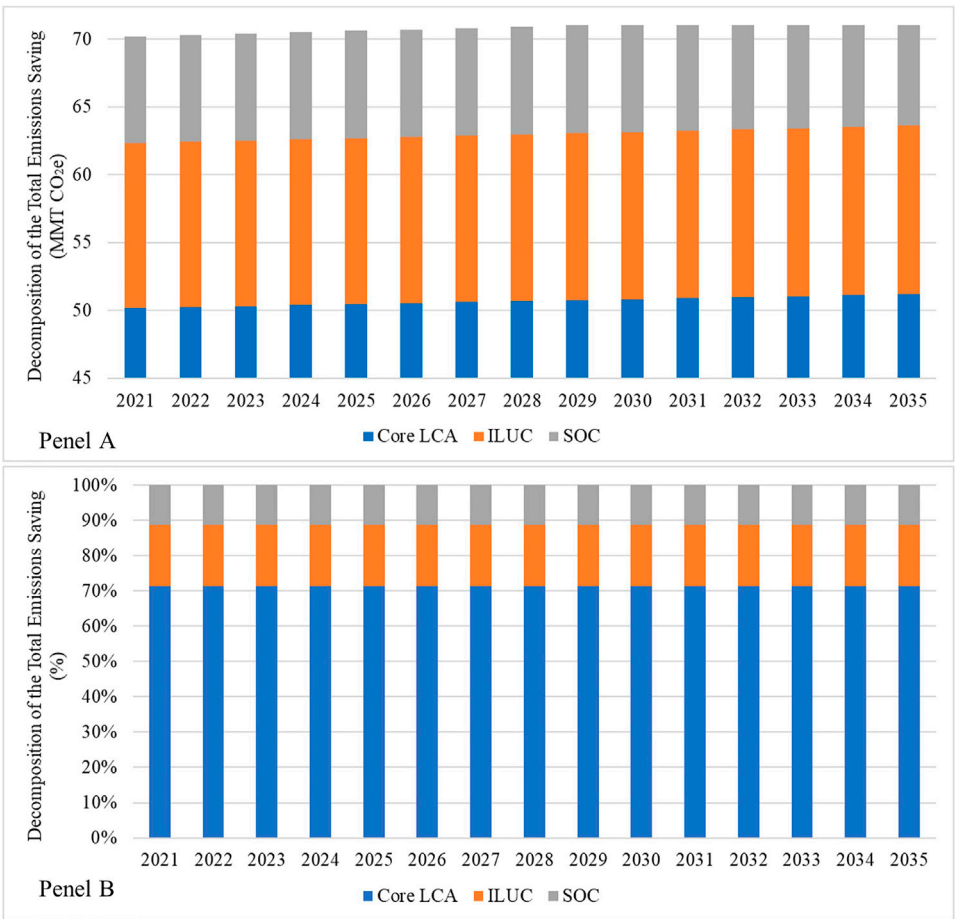

FIGURE 5 | Decomposition of the total emissions savings (third scenario); Panel **(A)** represents total emissions by types of emissions; Pent **(B)** represents emissions shares by types of emissions.

Discussion of the S.M., yields of these crops are not similar and vary by region and location of production. In addition, the extent to which each of these crops will be produced by farmers is uncertain. However, it is straightforward to provide a Production Possibility Frontier (PPF) for producing these crops at a macro level for United States agriculture. To define this PPF, since carinata and camelina are similar crops in terms of productivity and oil content, we concentrate only on carinata and pennycress. Hence, the PPF represents the maximum trade-off between the two selected oilseed cover crops.

To construct the PPF, we considered two extreme scenarios of devoting all available land in winter either to carinata or pennycress. As an example, consider **Figure 4**, which represents the represents the maximum trade-off between the two selected oilseed cover crops for 2035. In this year, as mentioned in the previous section, the total available area for producing oilseed cover crops will be about 29.3 million hectares. This area could be entirely devoted to the production of carinata. In this option, given the assumed carinata yield of 2.4 metric tons per hectare, the total available carinata seed for SAF production will be about 70.7 million metric tons (point A in **Figure 3**). On the other hand, if the entire land is devoted to pennycress in 2035, given the assumed yield of 1.68 metric tons per hectare, the available pennycress seed for SAF production will be about 49.5 million metric tons (point B in **Figure 4**). Any point on or under the PPF for 2035 (line AB in **Figure 4**) shows a possible option for the mix of carinata and pennycress feedstock for SAF production in 2035. For instance, point C shows the mix of the available land divided between carinata and pennycress half by half. Note that the annual PPF lines for 2021 up to 2035 fall below the PPF for 2035. However, the changes are not huge, as the potential area is expected to increase slowly. Indeed, the PPF for 2035 represents the set of potential mixes that might occur in the future in the production of oilseed cover crops for SAF.

Total Emissions Savings

Table 2 provides information about the annual emissions savings that can be achieved for the period of 2021–2035 for the two extreme cases mentioned above. The first scenario devotes the entire potential land for oilseed cover crops to carinata production. The second scenario allocates the entire land to pennycress. For the first scenario, the overall potential emissions savings increase from 91 MMT of CO_2 emissions in 2021 to 92 MMT of CO_2 emissions in 2035. The corresponding figures for pennycress for 2021 and 2035 are 50 and 51 MMT, respectively. Therefore, carinata can make more emissions savings than pennycress if it can be produced all over the potential area for the oilseed cover crops. The higher emission saving for carinata can be due to higher yield per hectare (2.4 versus 1.68 MT) as well as higher oil yield for carinata (43 versus 29%). Finally, **Table 2** shows the potential savings in emissions for a scenario that equally divides the potential area for oilseed cover crops between carinata and pennycress. The estimated potential emissions savings for this case is about 70 MMT for 2021. It could increase to 72 MMT in 2035.

Therefore, the total annual emissions savings from SAF obtained from oilseed cover crops in 2035 could be between 52 and 92 MMT. These emissions savings are about 6–11% of the current annual emissions generated by the aviation industry on a global scale. In other words, if we consider oilseed cover crops in the corn-soybean rotation, we will be able to make enough feedstock to decrease the emissions of the aviation industry at the global scale up to 11%.

To better understand where the total emission savings come from, **Figure 5** shows the decomposition of the total emissions saving for the third scenario mentioned above. The core LCA makes more than 70% of savings which is the highest. In contrast, improving SOC due to the cultivation of oilseed cover crops has the lowest share in total savings, around 11%. Savings due to ILUC stands in the middle by around 17% of total CO_2 savings.

CONCLUSION

Renewable sources can help the United States aviation sector mitigate its emissions, contributing to around 5% of total energy-related CO_2 emissions nationwide (EIA, 2019). Using SAFs can successfully mitigate CO_2 emissions in the aviation sector, particularly if produced from oilseed cover crops.

Oilseed cover crops are suitable feedstocks for SAF production while they can come in rotation with other crops, and there will not be any rise in demand for cropland for fuel production. Moreover, the livestock industry can use the meal that is a co-product in the SAF production process. Therefore, it will induce some savings in demand for cropland. This study estimated the total available land suitable for sowing carinata, camelina, and pennycress to provide feedstock for SAF production. It is possible to fit these oilseed cover crops in either corn-soybean or corn-corn-soybean rotations in the United States Corn Belt and the rest of the country. We also evaluated the total emissions savings due to ILUC, SOC increase, and replacing conventional jet fuel with SAF.

The results showed that producing SAF from carinata, camelina, and pennycress causes reductions in land use emissions by 12.9, 15.3, and 18.3 gCO_2e/MJ, respectively. These ILUC values for oilseed cover crops can be compared with the estimated ILUC values for SAFs produced from corn and soybean, 24.9 and 20 gCO_2e/MJ, respectively (Zhao et al., 2021). As a result, there is a big advantage for producing SAF from oilseed cover crops compared to SAF from food crops.

The estimated potential area for oilseed cover crops planting is 28.7 million hectares in the United States in 2021. From this, 25.3 million hectares will be in the United States Corn-Belt. Therefore, the total available area can reach 29.3 million hectares in 2035. If we sow carinata in all these available lands, we will be able to produce the highest amount of feedstock, 70.7 MMT of carinata. On the other hand, if we sow only pennycress on the available land, we will be able to produce 49.5 MMT of this oilseed cover crop. The total annual emissions savings from SAF obtained from oilseed cover crops in 2035 could be between 52 and 92 MMT, depends on the mix of oilseed cover crops produced. These emissions savings are about 6–11% of the current annual emissions generated by the aviation industry on a global scale.

SAF can mitigate emissions in the aviation sector and provide farmers a chance to improve their profits by including cover crops

in their rotations. A national mitigation policy that supports SAF production (e.g., financial support, mandates, and low carbon fuel standard) could motivate farmers to adopt oilseed cover crops in corn-soybean or corn-corn-soybean rotations. There should also be some incentives for airlines to use SAFs instead of conventional fuels. It is also recommended that the farmers choose better farming practices (promotion of less intensive tillage practices and no-tillage) to improve SOC because SOC has the lowest share in total emissions savings.

The estimated emissions in this paper are subject to various sources of uncertainties. The sources of uncertainties are imbedded in LCAs, ILUC values, and SOC evaluations. The extent to which these cover crops will be produced in practice is uncertain too. However, providing incentives to encourage farmers to produce these cover crops and facilitating investment in producing SAF from these crops are the factors that help farmers to adopt cultivation of these crops faster.

DATA AVAILABILITY STATEMENT

Publicly available datasets were analyzed in this study. This data can be found here: https://quickstats.nass.usda.gov/.

AUTHOR CONTRIBUTIONS

Conceptualization: FT; Methodology: FT, ES, and OK; Data Assembly: FT, ES, and OK; Simulations: FT, ES, and OK; Formal Analysis: FT, ES, and OK; Original Draft: FT; Final Draft: FT and OK; Virtualizations FT, ES, and OK; Supervision: FT.

FUNDING

This study received financial support from: The United States Federal Aviation Administration Office of Environment and Energy through ASCENT, the FAA Center of Excellence for Alternative Jet Fuels and the Environment, ASCENT project (number 107208) through FAA Award (number 13-C-AJFE-PU) under the supervision of A.L. Oldani.

SUPPLEMENTARY MATERIAL

The Supplementary Material for this article can be found online at: https://www.frontiersin.org/articles/10.3389/fenrg.2021.790421/full#supplementary-material

REFERENCES

Abdelazim Mohdaly, A. A., and Ramadan, M. F. (2020). Characteristics, Composition and Functional Properties of Seeds, Seed Cake and Seed Oil from Different Brassica Carinata Genotypes. *Food Biosci.*, 100752. doi:10.1016/j.fbio.2020.100752

Akter, H. A., Dwivedi, P., Anderson, W., Lamb, M., and Lamb, M. (2021). Economics of Intercropping Loblolly Pine and Oilseed Crops for Bio-Jet Fuel Production in the Southern United States. *Agroforest Syst.* 95 (2), 241–255. doi:10.1007/s10457-020-00584-5

Al-Riffai, P., Dimaranan, B., and Laborde, D. (2010). *Global Trade and Environmental Impact Study of the E.* Washington D.C.: U. Biofuels Mandate - Report for the E.C.

Alam, A., and Dwivedi, P. (2019). Modeling Site Suitability and Production Potential of Carinata-Based Sustainable Jet Fuel in the Southeastern United States. *J. Clean. Prod.* 239 (December), 117817. doi:10.1016/J.JCLEPRO.2019.117817

Arnaldo Valdés, R. M., Gómez Comendador, V. F., Comendador, G., and Fernando, V. (2021). The Role of Climate Change Levy Schemes in Aviation Decarbonization by 2050. *IOP Conf. Ser. Mater. Sci. Eng.* 1024 (1), 012114. doi:10.1088/1757-899x/1024/1/012114

Chao, H., Agusdinata, D. B., DeLaurentis, D., and Stechel, E. B.(2019). "Carbon Offsetting and Reduction Scheme with Sustainable Aviation Fuel Options: Fleet-Level Carbon Emissions Impacts for U.S. Airlines. *Transportation Res. D: Transport Environ.* 75: 42–56. doi:10.1016/j.trd.2019.08.015

EIA (2019). *U.S. Energy-Related Carbon Dioxide Emissions*. Washington D.C.: Independent Statistics and Analysis. https://www.eia.gov/environment/emissions/carbon/.

Embaye, W. T., Bergtold, J. S., Archer, D., Flora, C., Andrango, G. C., Odening, M., et al. (2018). Examining Farmers' Willingness to Grow and Allocate Land for Oilseed Crops for Biofuel Production." *Energ. Econ.* 71, 311–320. doi:10.1016/j.eneco.2018.03.005

Eswaran, S., Subramaniam, S., Geleynse, S., Brandt, K., Wolcott, M., and Zhang, X. (2021). Techno-Economic Analysis of Catalytic Hydrothermolysis Pathway for Jet Fuel Production. *Renew. Sustain. Energ. Rev.* 151, 111516. doi:10.1016/j.rser.2021.111516

Field, J. L., Richard, T. L., Smithwick, E. A. H., Cai, H., Laser, M. S., LeBauer, D. S., et al. (2020). Robust Paths to Net Greenhouse Gas Mitigation and Negative Emissions via Advanced Biofuels. *Proc. Natl. Acad. Sci. USA* 117 (36), 21968–21977. doi:10.1073/pnas.1920877117

Graver, B., Rutherford, D., and Zheng, S. (2020). *CO2 Emissions from Commercial Aviation 2013, 2018, and 2019*. Washington D.C.: The International Council On Clean Transportation, no. October.

Hertel, T. W., Golub, A. A., Jones, A. D., O'Hare, M., Plevin, R. J., and Kammen, D. M. (2010). Effects of US Maize Ethanol on Global Land Use and Greenhouse Gas Emissions: Estimating Market-Mediated Responses. *BioScience* 60 (3), 223–231. doi:10.1525/bio.2010.60.3.8

Hudson, L., Jefferson, A. Bauen., Bauen, A., and Nattrass, L. (2016). "Sustainable Aviation." In *Christopher J B T - Biofuels for Aviation Chuck*, 315–37, 315, 337. Academic Press. doi:10.1016/B978-0-12-804568-8.00014-7

IATA (2020). *Pax-Forecast-Infographic-2020-Final*. Montreal, QC: Iata.

IBAC (2019). *Business Aviation and Sustainability: An Industry with a Good Story to Tell*.

ICAO (2019a). ICAO Environment Report. Chapter 4 - Market-Based Measures Available at: https://www.icao.int/Meetings/GLADs-2015/Documents/ENV_Report_MBMs_2010.pdf.

ICAO (2019b). *ICAO Environmental Report 2019_Chapter 6_Climate Change Mitigation*. Montreal, QC: CORSIA.

Karami, O. (2021). *Assessing Environmental and Economic Impacts of Carinata-Based Sustainable Aviation Fuel Production in the S.E. United States*. University of Georgia. Available at: https://www.etdadmin.com/student/mylist?siteId=1003&submissionId=803880.

Kumar, S., Seepaul, R., Mulvaney, M. J., Colvin, B., George, S., Marois, J. J., et al. (2020). Brassica Carinata Genotypes Demonstrate Potential as a Winter Biofuel Crop in South East United States." *Ind. Crops Prod.* 150: 112353. doi:10.1016/j.indcrop.2020.112353

López, M. V., de la Vega, M., Gracia, R., Claver, A., and Alfonso, M. (2021). Agronomic Potential of Two European Pennycress Accessions as a Winter Crop under European Mediterranean Conditions. *Ind. Crops Prod.* 159: 113107. doi:10.1016/j.indcrop.2020.113107

McGinn, M., Phippen, W. B., Chopra, R., Bansal, S., Jarvis, B. A., Phippen, M. E., et al. (2019). Molecular Tools Enabling Pennycress (Thlaspi Arvense) as a

Model Plant and Oilseed Cash Cover Crop. *Plant Biotechnol. J.* 17 (4), 776–788. doi:10.1111/pbi.13014

Moser, B. R., Knothe, G., Vaughn, S. F., and Isbell, T. A. (2009). Production and Evaluation of Biodiesel from Field Pennycress (Thlaspi arvenseL.) Oil†. *Energy Fuels* 23 (8), 4149–4155. doi:10.1021/ef900337g

Mousavi-Avval, S. H., and Shah, A. (2021). "Techno-Economic Analysis of Hydroprocessed Renewable Jet Fuel Production from Pennycress Oilseed." *Renew. Sustain. Energ. Rev.* 149, 111340. doi:10.1016/j.rser.2021.111340

Murphy, H. T., O'Connell, D. A., Raison, R. J., Warden, A. C., Booth, T. H., Herr, A., et al. (2015). "Biomass Production for Sustainable Aviation Fuels: A Regional Case Study in Queensland." *Renew. Sustain. Energ. Rev.* 44, 738–750. doi:10.1016/j.rser.2015.01.012

Prussi, M., Lee, U., Wang, M., Malina, R., Valin, H., Taheripour, F., et al. (2021). CORSIA: The First Internationally Adopted Approach to Calculate Life-Cycle GHG Emissions for Aviation Fuels. *Renew. Sustain. Energ. Rev.* 150 (February), 111398. doi:10.1016/j.rser.2021.111398

Robertson, K. A. (2020). *Biomass Potential in Sustainable Aviation Fuel Development : Switchgrass Production Optimization and Carinata Oilseed Enterprise Viability Analysis*. Knoxville, TN: University of Tennessee.

Searchinger, T., Heimlich, R., Houghton, R. A., Dong, F., Elobeid, A., Fabiosa, J., et al. (2008). Use of U.S. Croplands for Biofuels Increases Greenhouse Gases through Emissions from Land-Use Change. *Science* 319 (5867), 1238–1240. doi:10.1126/science.1151861

Sindelar, A. J., Schmer, M. R., Gesch, R. W., Forcella, F., Eberle, C. A., Thom, M. D., et al. (2017). Winter Oilseed Production for Biofuel in the US Corn Belt: Opportunities and Limitations. *GCB Bioenergy* 9 (3), 508–524. doi:10.1111/gcbb.12297

Taheripour, F., Zhao, X., and Tyner, W. E. (2017). The Impact of Considering Land Intensification and Updated Data on Biofuels Land Use Change and Emissions Estimates. *Biotechnol. Biofuels* 10 (1), 191. doi:10.1186/s13068-017-0877-y

Trejo-Pech, C. O., Larson, J. A., English, B. C., Yu, T. E., and Yu, T. E. (2019). Cost and Profitability Analysis of a Prospective Pennycress to Sustainable Aviation Fuel Supply Chain in Southern USA. *Energies* 12, 3055. doi:10.3390/en12163055

Tyner, W., Taheripour, F., Zhuang, Q., Dileep, K., and Baldos, U. (2010). *Land Use Changes and Consequent CO2 Emissions Due to US Corn Ethanol Production: A Comprehensive Analysis*.

Zanetti, F., Isbell, T. A., Gesch, R. W., Evangelista, R. L., Alexopoulou, E., Moser, B., et al. (2019). "Turning a Burden into an Opportunity: Pennycress (Thlaspi Arvense L.) a New Oilseed Crop for Biofuel Production." *Biomass and Bioenergy* 130: 105354. doi:10.1016/j.biombioe.2019.105354

Zhao, X., Taheripour, F., Malina, R., Staples, M. D., and Tyner, W. E. 2021. "Estimating Induced Land Use Change Emissions for Sustainable Aviation Biofuel Pathways." *Sci. Total Environ.* 779: 146238. doi:10.1016/j.scitotenv.2021.146238

Zilberman, D., Gordon, B., Hochman, G., and Wesseler, J. 2018. "Economics of Sustainable Development and the Bioeconomy." *Appl. Econ. Perspect. Pol.* 40 (1): 22–37. doi:10.1093/aepp/ppx051

Conflict of Interest: The authors declare that the research was conducted in the absence of any commercial or financial relationships that could be construed as a potential conflict of interest.

Publisher's Note: All claims expressed in this article are solely those of the authors and do not necessarily represent those of their affiliated organizations, or those of the publisher, the editors and the reviewers. Any product that may be evaluated in this article, or claim that may be made by its manufacturer, is not guaranteed or endorsed by the publisher.

frontiers in Energy Research

ORIGINAL RESEARCH
published: 21 January 2022
doi: 10.3389/fenrg.2021.772316

Searching for Culture in "Cultural Capital": The Case for a Mixed Methods Approach to Production Facility Siting

Marc Boglioli[1], *Daniel W. Mueller*[2], *Sarah Strauss*[3], *Season Hoard*[4]*, *Tyler A Beeton*[5] *and Rachael Budowle*[6]

[1]Department of Anthropology, Drew University, Madison, NJ, United States, [2]United States Coast Guard Academy, New London, CT, United States, [3]Department of Integrative & Global Studies, Worcester Polytechnic Institute, Worcester, MA, United States, [4]Division of Governmental Studies and Services, School of Politics, Philosophy and Public Affairs, Washington State University, Pullman, WA, United States, [5]Department of Forest and Rangeland Stewardship, Colorado Forest Restoration Institute, Colorado State University, Fort Collins, CO, United States, [6]Haub School of Environment and Natural Resources, University of Wyoming, Laramie, WY, United States

OPEN ACCESS

Edited by:
Sachin Kumar,
Sardar Swaran Singh National Institute of Renewable Energy, India

Reviewed by:
Balendu Shekhar Giri,
Indian Institute of Technology Guwahati, India
Jitendra Kumar Saini,
Central University of Haryana, India

***Correspondence:**
Season Hoard
hoardsa@wsu.edu

Specialty section:
This article was submitted to Bioenergy and Biofuels, a section of the journal Frontiers in Energy Research

Received: *07 September 2021*
Accepted: *24 December 2021*
Published: *21 January 2022*

Citation:
Boglioli M, Mueller DW, Strauss S, Hoard S, Beeton TA and Budowle R (2022) Searching for Culture in "Cultural Capital": The Case for a Mixed Methods Approach to Production Facility Siting. Front. Energy Res. 9:772316. doi: 10.3389/fenrg.2021.772316

Site selection modeling receives much attention in the aviation biofuels literature to ensure sustainability of the aviation biofuel supply chain. These models seek to reflect the multitude of factors and conditions necessary for supply chain success. Social factors impacting that success have received increasingly greater attention but are often excluded due to difficulties in obtaining accurate and standard measures. Some of the most promising work in this arena utilizes a "community capitals approach" to create statistically grounded decision support tools (DSTs) intended to provide rapid assessment of the social characteristics of potential facility locations. Despite the value of the community capitals approach, this methodology is still marked by inconsistent predictivity due to an inability to reliably assess the cultural and historical nuances of local communities that are so vitally important to the long-term viability of these costly projects. This paper more fully examines the Community Assets and Attributes Model (CAAM) that has been developed and applied in the Pacific Northwest to incorporate social assets in site selection modeling. Based on ethnographic fieldwork in Colorado and Wyoming dealing with biomass/bioenergy facility siting, we argue that cultural capital, a key component of the CAAM, is biased to urban locations due to the measurements incorporated. As a result of this bias, current site selection modeling based on the Community Capitals Framework (CCF) does not accurately reflect rural community assets. We assert that the CAAM does not actually measure cultural capital but a product of cultural capital, namely creativity, and innovation Our mixed methods approach that combines quantitative assessment with ethnographic research highlights the limits of the CAAM by revealing that local residents in largely rural counties showed willingness to innovate in some cases but in others referred to history with similar industries that may limit support. The quantitative cultural capital measurements of the CAAM for the four counties we examine, which range in scores from –0.53 to 2, do not capture these dynamics. These scores would generally suggest moderate to high levels of support for

biomass/bioenergy facilities, but the ethnographic research provides nuance for or against support that are not reflected in the quantitative capital scores. This suggests that the quantitative CAAM scores could be misleading without added qualitative context. This work demonstrates that a mixed methods approach, combining ethnographic and historical methodologies with existing quantitative community capital approaches, will produce a more effective predictive methodology for facility siting due to its heightened ability to gather critical data on place-based values, beliefs, and historical legacies relating to natural resource development in general, and the timber industry specifically.

Keywords: aviation biofuels, cultural capital, site selection, mixed methods, sustainability, ethnographic interviews, wood-based biofuels, community assets and attributes model

INTRODUCTION

The ability to select appropriate communities to locate aviation and other similar biofuel supply chain development projects is integral to their long-term sustainability and success. As such, numerous researchers and practitioners have developed methods to optimize site selection to increase the viability of aviation biofuel supply chains. These decision support tools (DSTs) are continuously improving, but most continue to share a glaring omission: the inclusion of social and cultural characteristics that impact the ability, preparedness, and inclination of a given community to support biofuel supply chain development. Rural economic development, while clearly important, does not guarantee that communities will support these projects and inclusion of only economic, natural resources, infrastructure, and other similar resources or criteria, when making decisions renders final conclusion suspect and puts into question the predictions of these models and tools. Unfortunately, this issue is not just prevalent in the site selection literature; it plagues sustainability literature as well, for the simple reason that social sustainability is rarely included in these studies, and social criteria are absent from many certification frameworks.

Fortunately, recent studies and projects have attempted to include social criteria in their frameworks and methods. These include studies that examine relevant, reliable, practical, and important social criteria for sustainability analysis (see Buchholz et al., 2009; Kurka and Blackwood 2013; Kamali et al., 2018) to the addition of social, political, and/or cultural capitals to DSTs for biofuel supply chain development (see Martinkus et al., 2014; Martinkus et al. 2017; Martinkus et al. 2019). These studies attempt to quantify criteria and assets that are often qualitative in nature, relying on quantitative indicators meant to serve as proxies for qualitative concepts. In fact, studies that weight criteria by reliability and practicality lead to the preference for quantitative indicators often collected at the national and potentially at the regional-level, which masks local-level effects and concerns (Anderson et al., Forthcoming 2022). This preference for quantitative indicators and analysis leads not only to incomplete analysis and suspect predictions, but also leads to the relative dearth of qualitative and mixed-methods studies that could provide a more nuanced picture of sustainability and viability of aviation and similar biofuel development.

Nonetheless, recent attempts to include more robust quantitative indicators of the often ignored or limited analysis of social criteria is an important development in both supply chain analysis and broader biofuel sustainability literatures. In particular, the CAAM was developed in the United States to incorporate social criteria more fully in DSTs through the development of county-level capital scores to compare performance in social, capital, political, and human capitals (see Martinkus et al., 2017; Rijkhoff et al., 2017; Mueller et al., 2020; Rijkhoff et al., 2021). This model has been updated and refined over time (adding more capitals and refining indicators) but has only been validated in one study examining biorefineries and similar projects in the Pacific Northwest (see Mueller et al., 2020). CAAM developers have stressed that it should be included in initial support tools, but ground-truthing and mixed-methods analysis is a further step required to ensure accuracy and success due to limits of quantitative measures, especially at a more local-level than a county.

In this study, we take up the call to improve CAAM and other attempts to better measure and include social criteria through mixed-methods research using a case study of woody biomass facilities in the United States Wyoming and Colorado region. Our objective is to compare CAAM model predictions regarding the *social and cultural suitability* of different communities for a new biomass/bioenergy facility with the data obtained though ethnographic interviews with people in those same communities. In doing so, we offer insight on the strengths and limitations of the CAAM approach (in addition to other work based on the CCF) and provide suggestions for improving future industrial siting DSTs. We argue that more comprehensive models, such as the CAAM, should be incorporated in more studies, but mixed methods approaches, especially when assessing cultural capital, are necessary to meet holistic definitions of sustainability, and increase likelihood of aviation biofuels supply chain success.

This paper is organized as follows. First, we discuss DSTs used in biofuels development, followed by the broader literature on capitals which is employed by CAAM. Next, we present an in-depth explanation of the most recent CAAM model and apply this model to make predictions in the Wyoming and Colorado region where woody biomass facilities have been proposed. We

then present the methods section where the ethnographic interview methodology is explained. We conclude with recommendations for not only improving the CAAM but providing recommendations for effective mixed-methods research to better incorporate and examine the social aspects of sustainability which are too often ineffectively incorporated in aviation biofuels research.

LITERATURE REVIEW

Decision support systems (DSS) or DSTs are designed to aid complex decision-making using management information systems (Shim et al., 2002). Gorry et al. (1971) developed an initial framework for assisting managerial decisions within organizations and noted the growth of management information systems but argued that these systems had a limited impact on decision-making within organizations. The development and application of DSTs has grown considerably over the last 30 years, with these tools consisting of three primary components: "a database that can store and manage internal and external information, algorithms necessary for the analysis and an interface for communication with the user" (Perimenis et al., 2011). These tools aid the decision-making process through problem identification and analysis of alternatives which allows decision-makers, through computational modeling, to identify the ideal alternative that optimizes all decision-making criteria to address a problem (Shim et al., 2002).

However, for complex projects and problems, optimizing all decision-making criteria is impossible, and necessitating a compromise solution. Thus, multi-criteria decision analysis (MCDA) which refers to a range of approaches that compare potential solutions through ranking analysis, optimality, or other techniques (Pavan and Todeschini 2009; Wang et al., 2009) is an important component of decision support tools for complex issues (Wang et al., 2009; Perimenis et al., 2011). MCDA-based DSTs involve evaluating alternative solutions to a problem through multiple weighted evaluation criteria with the weighting technique employed impacting results (See Wang et al., 2009). MCDA DSTs have been employed in fields that require balancing areas with conflicting objectives, such as sustainable energy and aviation biofuels, which require balancing across social, economic, and environmental activities (see Afgan and Carvalho, 2002; Jovanovic et al., 2009; Perimenis et al., 2011; Martinkus et al., 2018; Ghose et al., 2019; Xu et al., 2019).

DSTs have been frequently used for facility siting, with much literature in biofuels applying various models to aid biorefinery site selection (see Stewart and Lambert 2011; Zhang et al., 2011; Perimenis et al., 2011; Martinkus et al., 2017; Martinkus et al., 2018; Ghose et al., 2019). A noted issue in the biofuel site selection literature is how to effectively combine social, economic, and environmental criteria in DSTs as many social criteria are qualitative in nature and thus difficult to adapt to quantitative models (Martinkus et al., 2014; Martinkus et al., 2017; Rijkhoff et al., 2017; Martinkus et al., 2019). Noting several limitations in how social criteria were initially incorporated in past studies, Rijkhoff et al. (2017) used Emery and Flora's Community Capitals Framework (CCF) to identify community assets necessary for successful development and implementation of complex projects and developed the Community Assets and Attributes Model (CAAM). The CAAM quantified three social assets—social, cultural, and human capitals—to include in U.S.-based decision support tools. The authors argued that the CAAM model should be incorporated as criteria in decision support tools for aviation biofuel facility-siting or risk the economic sustainability of their projects but left the weighting of criteria to tool developers (Rijkhoff et al., 2017). The CAAM model was further refined by Mueller et al. (2020) through the addition of political capital and exploratory factor analysis to update the indicators used for each of the capitals and to prevent overlap between capital measurements. While Rijkhoff et al. (2017) and Mueller et al. (2020) improved on social asset modeling compared to earlier studies, which often ignored social assets or used unsuitable proxy measures, several limitations of the CAAM model still impact its incorporation into site selection DSTs. Additionally, assessing the ability of the CAAM to adequately predict levels of these assets is important before full scale adoption in United States biorefinery site selection.

DSTs and similar frameworks have an important role to play in sustainable development through informed siting of a variety of different types of energy facilities. An effective DST can help prevent needless expenditures of time, money, and political capital as they, in theory, and increase the likelihood of locating a proposed facility where it would enjoy long-term economic success and community support. Additionally, holistic methods which can examine environmental, economic, and social sustainability are lacking as social sustainability considerations are often excluded from analysis (see Acquaye et al., 2011; Clarens et al., 2011; Collotta et al., 2019) or includes employment as the only "social indicator" (Collotta et al., 2019; Visentin et al., 2020). This exclusion is often due to lack of easily available social metrics that can be included in initial assessments, but also reflects a key issue in aviation biofuels literature broadly and not just site selection: lip service to the importance of social and cultural assets and social sustainability with limited application across sustainability studies.

While more studies have attempted to incorporate social criteria in sustainability research through a variety of techniques (see Buchholz et al., 2009; Kurka and Blackwood 2013; Kamali et al., 2018; Gnansounou and Alves 2019; Mattioda et al., 2020; Mattioda et al., 2020), the indicators included or suggested for inclusion differ depending on the study and often the evaluation of relevance, reliability, practicality, and other metrics used for final selection of indicators. When combined with economic and environmental indicators, social criteria are often rated lower (Buchholz et al., 2009; Kurka and Blackwood, 2013). Additionally, industrialized and non-industrialized countries rate the relevance and importance of social criteria differently (Buchholz et al., 2009). Kamali et al. (2018) argue that the selection of social criteria for evaluation needs to be case-specific and advocate for using case studies to identify appropriate social criteria for evaluation of social performance of biofuel supply chains. Nonetheless, despite

calls for more focus on social sustainability and social evaluation, these studies are still lacking. Thus, the assessment of the CAAM and recommendations for improved analysis of social criteria, assets, and issues, can significantly move research in site selection and sustainability forward.

Community Capitals Framework

The CAAM is based on the CCF (Emory and Flora, 2006) that models community assets using seven capitals: financial, natural, built, political, cultural, human, and social capitals. Rijkhoff et al. (2017) argue that the CCF approach is especially useful for site selection due to its system approach that combines capitals typically used in site selection modeling (natural, financial, and built capitals) and a theoretical base for building models that can incorporate the capitals not systematically included in current site selection models, especially cultural and social capitals. These authors argue that the inclusion of often neglected capitals, social and cultural capitals, are important for ensuring project sustainability, which is rooted in Emery and Flora (2006) claim that cultural capital is an especially important capital for project success, and social capital is an important structural capital that can lead to increases in all other capitals (known as the "spiral up" effect). Thus, Martinkus et al. (2017); Rijkhoff et al. (2017); Mueller et al. (2020) all model their variations of the CAAM on the CCF framework, with each iteration meant to better reflect the CCF capitals as they apply to site selection for aviation biofuels supply chains.

The broad concern we have with models derived from the CCF or other similar capital-based approaches is the extent to which the various capitals are always "valid" and "reliable" measures. This question becomes more pressing when capitals (for example, social capital or cultural capital) are conflated with "proxies" or "indexes" or "indicators" that 1) may or may not have the social significance that researchers think they do; and 2) may have different meanings at different times in history or even in different cultural and social contexts. Simply put, are preconceived assumptions about the importance of certain social practices (for example, going to church) or social statuses (such as having a college degree) influencing the conclusions that emerge from a capitals-based approach? These are important questions, because without valid and reliable data, the ability of a DST to consistently *predict* what people will think and do is seriously compromised. These issues most prominently appear in the quantification of cultural capital, which is acknowledged by each iteration of the CAAM as difficult to quantify and necessitating further research, but also include aspects of social capital, and such as trust. We focus on concerns operationalizing cultural capital and social capital for the rest of this review.

Social Capital

Social capital refers to connections that exist within and across communities and was popularized by Putnam (1993, 1995, 2000) who focused on the importance of civic engagement and community relationships for democratic development and sustainability. Many studies have examined the impact of social capital in a variety of areas. This capital has been linked to economic growth, increased cooperation and collective action, increased trust, better natural resource management, better health, better COVID19 response, and has been used to predict successful environmental policy and sustainability projects in United States cities (See Coleman, 1988; Flora, 1995; Cramb, 2005; Lovrich et al., 2005; Briceno and Stagl 2006; Budd et al., 2008; Erp et al., 2009; Jones et al., 2009; Portney and Berry, 2010; Ehsan et al., 2019; Pitas and Ehmer, 2020). Based on the impact of social capital found in numerous empirical studies, social capital in site selection has been used to narrow the candidate sites for potential biofuel facilities using a stepwise approach (Martinkus et al., 2017; Rijkhoff et al., 2017), as one aspect of a total social component score included in MCDA (Martinkus et al., 2019), and to help develop strategic engagement recommendations to aid in project development and implementation success (Mueller et al., 2020).

While social capital is incorporated in several studies across numerous scholarly literatures, significant disagreement exists on exactly how the concept should be operationalized, such as whether it should or can be measured at the individual-level (Bourdieu 1986; Coleman 1988; Montgomery 2001), or is more appropriate at the community-level through a focus on density of community associations and other measures of engagement, such as voter turnout (Putnam 1993; Rupasingha et al., 2006). Rijkhoff et al. (2017) adopt Putnam's and Rupasignha et al.'s interpretation of social capital, arguing it is a community-level characteristic that can facilitate collective action and cooperation needed for success in highly technical projects. All iterations of the CAAM use data originally developed by Rupasingha et al. (2006), which includes number of associations in a county, types of organizations, voter turnout, and Census response rates. Mueller et al. (2020) update CAAM measurements by ensuring no overlap exists between the capitals, but the indicators of social capital are still derived from Rupasingha et al. (2006) and thus prioritize Putnam (1993); Putnam (2000) interpretation of social capital. Putnam's studies of social capital, however, have been heavily criticized.

Briefly consider Putnam's classic exploration of late 20th century American civic culture, *Bowling Alone: The Collapse and Revival of American Community* (2000). Putnam famously holds up popular 1950s social practices like bowling, community picnics and involvement with civic organizations as strong indicators of civic and political engagement and, most importantly, community-level democratic processes. Since participation in some of these kinds of activities wanes during the 1960s, he concludes that American democracy may be in peril. As many have pointed out, however, Putnam's "anecdotal" claims (Durlauf 2002) and "arbitrary choice of indicators" (Boggs 2001) leave a lot to be desired in terms of empiricism. Issues of correlation and causation are murky, data seem cherry-picked to fit a preconceived narrative (Samuelson, 1996), and, ironically, social capital itself is not well defined. More broadly, his conclusions about the social character of the United States seem a bit blind to the historical realities of the time. As Carl Boggs writes, "Can he be insisting that Americans *after* 1965 became more disengaged, less aware, less politically active than

they were at the height of the placid fifties, when McCarthyism filled the air, when social movements and third parties were nowhere to be seen, when racism, sexism, and homophobia were part of the taken-for-granted ideological discourse?" (2001, 283–84).

To be fair, Martinkus et al. (2017), Rijkhoff et al. (2017) and Mueller et al. (2020) all acknowledge that some aspects of social capital cannot be operationalized quantitatively in the CAAM due to a lack of consistently measured indicators at the community-level, such as the key component of trust. However, these authors do not critique whether existing CAAM indicators for social capital are good proxies for the qualitative phenomena claimed by Putnam and Rupasingha et al. (2006). Whether these are adequate and accurate proxies and relevant to aviation biofuel supply chains needs more thorough investigation, especially through mixed-method analysis that allows researchers to interrogate these relationships more deeply.

Cultural Capital

According to Emery and Flora (2006), "cultural capital reflects the way people 'know the world' and how they act within it, as well as their language and traditions" (21). It influences which voices are heard and prioritized, as well as "how creativity, innovation, and influence emerge and are nurtured" (Emery and Flora 2006). As the elements of cultural capital are difficult to measure quantitively, it seems its inclusion in quantitative frameworks focuses on innovation and creativity, or at least proxies that are meant to reflect creativity and innovation. Thus, as currently conceptualized, these frameworks focus on an effect of cultural capital rather than the concept itself. Relying on the work of Florida (2002), Martinkus et al. (2014), Martinkus et al. (2017) and Rijkhoff et al. (2017) use either elements of the creative vitality index (CVI) or the entire index to measure cultural capital. This index measures the presence of the "creative class" (jobs that require creativity), innovation (patents per capita), high-tech industry and diversity (using the Gay Index created by Florida) as a proxy for community openness and acceptance.

If Putnam's work serves as a cautionary tale about overloading "arbitrary indicators" with broad social significance and not bringing a historical perspective into capitals research, Richard Florida's influential work on the "creative class" also warrants scrutiny for its own reliance on empirically dubious indexes, such as the "Bohemian index" and the "Gay index" to assess the potential economic vitality of urban centers. Importantly, Florida played a vital role in the way that the idea of culture is understood in later "capitals" work. Culture, rather than referring to shared values, beliefs, practices, and traditions in the vein of Emery and Flora (2006), became a shorthand for "creativity" that, in turn, is used as a "proxy" for a community's openness to change and innovation. Academics and cultural critics have pointed out that Florida's notion of the "creative class" is an elitist notion at its core (O'Callaghan, 2010; Bures, 2017; Wainwright, 2017). As cultural geographer, Cian O'Callaghan, put it, "The creative class concept is primarily tailored towards a core audience of urban elites and young high-earning professionals. Thus, the version of "creativity" that is extolled fits neatly with the lifestyles and work practices of this group..." (2010, 1,610). Florida's rather bourgeois understanding of creativity was injected into capitals work largely through the adoption of the CVI (which was created by a non-profit arts preservation organization in Denver called the Western Arts Foundation) to measure "cultural capital" (Florida 2002). In addition, Florida initiated the tendency in capitals work to define "creativity" very narrowly, as having to do with elite cultural practices, such as attending the ballet or the opera.

The work of Martinkus et al. (2014), Martinkus et al. (2017), which should be lauded for striving to bring social dimensions into industrial siting, is a good example of utilizing the idea of culture as, more or less, a synonym for creativity which, in turn, is measured by an index that is then used to indicate a community's openness to change. A community's willingness to try new things, of course, would indicate a community that might be a good candidate for something innovative like a bioenergy facility. As sensible as this chain of logic might seem at first glance (leaving aside the numerous levels of separation from actual communities), when one digs into the details of what counts as "culture," this approach, like Putnam's and Florida's, seems to be weighed down with empirically dubious assumptions about what certain social activities and "indexes" mean. For studies that use the CVI or elements of CVI (Martinkus et al., 2014; Martinkus et al., 2017; Rijkhoff et al., 2017), it is unclear how indicators such as the number of arts related organizations, occupational employment in the arts, and revenues of arts related goods and services might impact which communities would be more open to building bioenergy facilities or which communities would be more creative and adaptable about how and why these facilities should be built.

While Mueller et al. (2020) improve on past efforts by forgoing the use of the CVI, their measure of cultural capital still includes the "creative class" (measured as the proportion of the working population 16 and over employed in management, business, science, and the arts) and education. In fairness, both Mueller et al. (2020); Rijkhoff et al. (2017) argue that lower cultural capital scores may mean that expertise must be imported from other areas to support development and implementation. They also encourage further ground-truthing before final selection of communities. However, whether these measures are valid indicators of cultural capital or even creativity is inadequately addressed. Part of this difficulty is that the very definition of cultural capital is qualitative in nature and points to conditions, culture, and language, which are difficult to quantify and not regularly collected at any level of analysis. Another difficulty is the resources necessary to conduct mixed-methods research and evaluative case studies to more deeply explore these relationships and collect data on the very foundation of cultural capital, history, which has been shown to impact biofuel-related projects (Mueller et al., 2020). *Put simply, there is a need to put culture back into cultural capital and acknowledge at the very least that most frameworks are attempting to measure creativity and not cultural capital.* There is further need to acknowledge that understanding cultural capital and its impact in aviation biofuels requires additional assessment and move the

field towards more integrative mixed-methods research, combining qualitative and quantitative approaches, to better address local-level concerns which are currently lacking.

To achieve these goals, we conduct a mixed-methods study that combines quantitative assessment with ethnographic interviews in southeastern Wyoming and northeastern Colorado. This region has been the focus of woody biomass supply chain development for the past 8 years, with numerous studies conducting supply chain assessment in the region. As such, it provides an ideal opportunity to assess and improve the CAAM and other models that seek to include social measures. Based on the combination of quantitative and qualitative methods, we not only offer suggestions to improve the CAAM for future research, but also provide recommendations to help scholars and practitioners conduct these mixed-methods assessments in the future.

METHODS

This mixed methods analysis combines quantitative analysis of social assets using the most recent version of CAAM (Mueller et al., 2020) and ethnographic interviews conducted in southeastern Wyoming and northeastern Colorado. First, we provide more information on the latest CAAM, including indicators, scores, and interpretation of scores. Next, we provide more information on the thematic analysis and focus of the ethnographic interviews.

Mixed Methods: CAAM

The CAAM dataset provides county-level scores for cultural, social, human, and political capitals. The CAAM itself was created by performing an exploratory factor analysis (EFA) on several different quantitative indicators traditionally associated in the literature with cultural, social, human, and political capitals. After a few iterations of EFA to identify multicollinearity among variables and further simplify the model, a final EFA yielded a four-factor solution, grouping related indicators into each of the four factors, which matched with the four capitals listed above. The final result produces the CAAM in its current version, which measures four capitals using 11 quantitative, county-level indicators. These include income inequality, child poverty, low birth rates, unemployment level, and violent crime rates for human capital, education level and proportion of the population in creative class occupations (see Florida 2019) for cultural capital, turnout levels in the 2012 and 2014 elections for political capital, and data from Rupasingha et al. (2006) for social capital, which includes the number of non-profit organizations per capita, and the aggregated, per capita number of religious, civic, business, political, professional, labor, bowling, recreational, golf, and sports organizations in any given county.

The capital scores in the CAAM are calculated by taking the normalized values for each indicator, multiplying this by each indicator's factor loading as produced by the final EFA, effectively weighting each indicator within each capital, and adding these values together to produce a single score for each capital. Because these scores are not by themselves particularly intuitive, aside from a basic understanding that higher scores reflect higher capital, these scores are further normalized based on the Census Region, Division, or other geographical boundary related to a given study area. This process normalizes the raw scores to the average of a given geography, turning the scores into z-scores that show how many standard deviations a county lies above or below some geographic average. Because the study area of this paper is in Wyoming and Colorado, we use CAAM scores normalized to the Census Mountain Division, which includes the states of Montana, Idaho, Wyoming, Nevada, Utah, Colorado, Arizona, and New Mexico. In other words, all CAAM scores indicate how many standard deviations a county sits above or below the Mountain Division average for each respective capital.

Mixed Methods: Ethnographic Interviews

The second source of data includes 31 ethnographic interviews that were conducted with residents of southeastern Wyoming and northeastern Colorado from the summer of 2015 to the summer of 2019.[1] These 31 interviews represent just a portion of a greater ethnographic data set that was produced by various University of Wyoming faculty and students (both graduate and undergraduate) working on the multi-institution United States Department of Agriculture (USDA) Bioenergy Alliance Network of the Rockies project. Our research participants were loggers, entrepreneurs, small business owners, state and federal foresters, politicians, and other local residents with an interest in forestry and knowledge of land management. Initial interviews were conducted with people with obvious connections to the bioenergy industry. Subsequently we built our sample by using a "snowball" method wherein research participants would recommend other people to interview (Bernard 2018), or we would reach out to people who seemed necessary to contact due to a connection to forestry or forest products. The interviews were coded for relevant themes and analyzed using Atlas ti, versions 8 and 9. Ultimately, the research team delineated 41 different codes.

The interviews focused on gaining an "emic" or an "insider" perspective, which anthropologists have argued should be incorporated in energy studies (Strauss, Rupp, & Love 2013; Chatti et al. 2017). These understandings are gained through cultural data, which refers to information gathered through conversations, interviews, observations, or participation in mundane activities that shed light on the ways that people carry out everyday tasks (whether it be tracking an animal or managing a small business), how they conceptualize their worlds (often referred to as "worldviews" or "ontologies") and the meanings that they attach to social and personal activities. As opposed to "individual attribute data" (age, education, and income, etc.), which can expose illuminating sociological profiles of cohorts of people (say, cross-country skiers or Pennsylvania Republicans), cultural data is extremely effective for providing a more nuanced understanding of what cross-country skiing means to people or why people identify as Republicans. Both sorts of data (cultural and individual

[1]To see a map of this region, please visit https://ngmdb.usgs.gov/topoview/viewer/#9/41.0555/-106.0771.

attribute) and the research methods they require are critical to holistic social science inquiries (Bernard 2018). Ethnographic research is part of larger inductive research project that starts "on the ground" and attempts to find consistent patterns in data that will eventually help researchers understand how people in specific circumstances (a place, a particular social movement, an occupational group, and so forth) conceptualize their worlds, how they think they should act in the world, and what they expect of others. We note that this research took place while the Rocky Mountain region was reeling from a massive mountain pine bark beetle epidemic that left millions of dead trees in the forest. Beyond the obvious waste of a valuable natural resource, people in forest communities were extremely concerned about the possibility of catastrophic forest fires. Also of relevance, during the period of this research, petroleum prices went from extremely high to extremely low, which also colored the ways in which people viewed the value of developing biomass sources for biofuels over time.

While more research would be necessary for us to offer any definitive overarching conclusions on the "worldviews", "ontologies", or "cultural logics" of the communities we visited, we are very confident that our empirical field research provides a more informative data set for understanding the specific perspectives and concerns of our research participants than quantitative county level data. The ethnographic interviews covered a wide range of topics, from pine bark beetles to forest management policies to woody biomass bioenergy facilities. We refer to our interviews as "ethnographic" for the following reasons: First, we asked open-ended questions and invited people to go wherever they wanted to go with their answers. Second, we wanted people to answer questions in their own terms. For example, we never asked what impact global warming was having on the local forest. Instead, we asked people to talk about the various "natural" and "human-caused" impacts on the forest. Third, we were interested in detailed answers, rather than the more general answers that less open-ended interviews elicit. Four, we were interested in the things that people would tell us that we could not have predicted and, therefore, could not have asked about. Any ethnographer would likely admit that it is not uncommon to realize, after conducting months of interviews, that they were not asking "the right questions." There are always aspects of local life that cannot be understood from the comfort of our university offices. There is no proxy for "being there."

The last aspect of our research that is "ethnographic" is the attempt our fieldworkers made to build rapport with community members. The multi-sited (Marcus 1995; Strauss 2004) BANR project engaged with places impacted by pine bark beetle destruction in the Rockies and involved multiple researchers returning to the various communities under study over the course of 6 years. Through this process, BANR researchers gained valuable comparative perspectives shared with the team in succession, as people moved into and out of the project. For example, researchers kept up with local newspapers, and often spent multiple days in towns while conducting research. We attempted to meet in comfortable settings, such as a participant's home or a local restaurant or diner and made it very clear that we valued our participants' unique opinions on these complicated topics. Additionally, because we utilized snowball sampling, we found ourselves more enmeshed in social networks as time passed and through return trips to particular communities. As a result, our meetings with community members often felt more like structured conversations than formal interviews.

The goal of these interviews was to arrive at a better understanding of local perspectives on the feasibility of woody biomass bioenergy facilities. The specific data presented in this paper focus on themes that directly speak to the idea of "cultural capital" as it is used in CCF research. In other words, to what extent are people in Southeastern Wyoming and Northeastern Colorado open to the idea of locating bioenergy facilities in their communities, and to what extent are interview participants willing to innovate or express past instances of innovation? As explained earlier, this paper compares the conclusions reached through our ethnographic analysis with the CAAM predictions (Mueller et al., 2020) for the counties where the ethnographic interviews were conducted. In this way, we can "ground truth" the CAAM predictions and make suggestions for improving DSTs.

Cultural capital is a particularly important aspect of capitals research to interrogate because it seems to be the most difficult capital to define and measure and it is relied upon as an indicator of a community's willingness to change and innovate. As we see in research that attempts to incorporate a mixed-methods approach (Roemer, 2017; Mueller et al., 2020), there seems to be a disconnect between the quantitative cultural capital scores that are based on statistical analysis of county or regional data and the qualitative data that were gathered through interviews with local residents. The reason for this, as alluded to above, is that the statistical indexes and proxies that represent cultural capital are meant to measure the "creativity" (as popularized by Richard Florida) of the local population by analyzing individual attribute data related to topics such as educational attainment and numbers of high-tech employees, but the qualitative interviews, on the other hand, are oriented toward learning about shared values and historical legacies by allowing people to explain their experiences, and share their personal perspectives. In short, the quantitative cultural capital scores and qualitative findings do not always agree, and the fact that they are not even measuring the same things makes the idea of cultural capital difficult to utilize with confidence (Roemer, 2017; Mueller et al., 2020).

RESULTS

The CAAM Predictions

As previously discussed, CCF work relies heavily on cultural capital scores to understand the extent to which communities are willing to adapt, change, and innovate. In the case of industrial siting, the higher the cultural capital z-score the more confidence one would have in a particular community being a good place to locate a facility, since it is more likely such a community would have higher levels of innovation and would not require as much outside expertise to successfully set up a biofuel supply chain. All our Wyoming interviews were conducted in Carbon County. The cultural capital score for

Carbon County (0.56) lands below the regional average. This score would suggest that Carbon County may be a more challenging candidate for a woody biomass energy facility because the community appears to lack the capability for change and innovation that such an endeavor would require. In contrast, the cultural capital scores from the Colorado counties were generally higher than Carbon County, WY: Grand (0.75), Jackson (−0.53), Larimer (2.00), and Routt (1.52). To reiterate, these numbers, which are z-scores, indicate how many standard deviations above or below the Mountain Division average these counties sit. These scores, according to the CAAM, suggest that creativity and innovation may be higher in these counties and thus increase the likelihood of project success. It is important to note that Mueller et al. (2020) would not necessarily rule out Carbon County for biofuel facilities, but "strategically recommend" that outside expertise may be needed in project development and implementation phases.

Ethnographic Interviews

Regardless of state or county, our interviews were noteworthy for their nearly unanimous support of bioenergy as a potential local industry. People across the region were enthusiastic about local jobs that would keep their communities alive; the ability to maintain a natural resource economic tradition; and the long-term economic and environmental sustainability of their communities. This is not to say, however, that all the research participants thought that a bioenergy facility would be economically viable. Indeed, most participants expressed concerns about one or more of the following issues: markets, start-up costs, transportation costs, government policies, and confidence in the sustainability of feedstock supplies. These concerns reflect what researchers have found in other locations (Roos et al., 1999; Upreti and van der Horst 2004; White et al., 2013).

The following quotes are representative responses to interview questions about bioenergy and the potential impacts of a new bioenergy facility on these rural communities. These lengthy ethnographic quotes are not intended to merely provide evidence that people are agreeing (or disagreeing) with each other on a particular topic, but rather to show the wide variety of issues that are taken into consideration by people as they make decisions that will have important consequences for their families, friends, communities, and surrounding landscapes (Strauss and Reeser, 2016; Jensen-Ryan et al., 2019). The complexity of local discourses on bioenergy presented in these quotes illuminates what is missed when "cultural capital," a very general and poorly defined term that has been shown to be an unreliable predictor of behavior (Roemer 2017; Mueller et al., 2020), is relied upon to provide critical insights into the perspectives of people in specific communities at particular moments in history. These statements, then, should disabuse readers of the assumption that residents in small, rural communities are somehow unlikely to embrace change and innovation. On the contrary, they demonstrate that these people are quite capable, in the words of Richard Florida (2019), of being "creative"—regardless of their CVI scores.

Elected Official in Wyoming

"Oh, absolutely it would benefit the community. You know especially if we had some kind of, of a facility. You know other with a value-added thing, fuel would be a really good way, if we had some way of developing a fuel product that could be used in vehicles for example, that value-added would be enough to where the transportation would be a big issue, I don't think. So, yeah, it certainly would benefit the entire community. You know, people here are very proud of their school. It's a very great school. It's named number 19 of the best 50 schools in the United States here just in the last month or so. They want to be able to have enough population here to sustain that school, you have another competing school up the road another 20 miles from ya, it would be real easy to close the high school here and take the high school kids down there. And that would be disastrous to the community. The area where I was raised, they closed the school there and now the town doesn't barely exist, ya know? When you do that it's the center of activity for the whole community, it's a source of pride. So, any kind of any industry that would really help stabilize the population and diversify the income potential, you know, so that you didn't have to just become a bedroom community and commute outta here would certainly be beneficial to us. That's why you know, trying to restart this little sawmill up here would be very beneficial to us. We've got some possibilities of getting that reopened, and it wasn't a good thing for us when it did close, because we did employ people there and it did help the economy. Hopefully we can get it back up and running again. But any kind of a thing, that would do that—and bioenergy sure has a lot of potential for some expansion on that, I just need to find out more about what's going on in the research departments and figure out what we, a program that we can get behind from a state standpoint that we can incentivize, and this would be a perfect place to do it for a pilot program. If it'll work here, it'll work here in more populated areas."

The above quote covers an impressive amount of ground. From concerns about community development to town pride about their school to reminiscing about a long-ago school closing that doomed his hometown to the hope of bolstering the community by getting the local sawmill up and running to an affirmative answer to the only actual question that the interviewer asked: Do you think bioenergy could benefit your community? This is a great example of the "value-added" of an in-depth, open-ended interview and an equally instructive example of the cost of relying on quantitative methods to gather insight into very specific, personal issues. It also shows local resources that could aid the development and implementation of biofuel supply chains that are not necessarily reflected in the quantitative metrics, including willingness to incentivize for development.

Below is the response of a Wyoming resident with family history in the local timber industry when asked about the pros and cons of developing the local bioenergy industry:

"Opportunities is employment, a GOOD employment, not just. . .ya know, manual type, whatever or anything. If you

could get a good industry in here and start keeping some of our youth here. Our youth would like to stay here. They're really, they have to drive a lot of em. Their families live here, and they commute back and forth to the oil fields, the gas fields, wherever they get. And then they come home on weekends or every other week or whanot, ya know. And uh, the community needs a viable economic base. They need an industry. All we have now is tourism, really. That's it. And our ranches."

Interviewer: "Yeah. So, thinking about using the forest for bioenergy. . .um, what are the positives and negatives of that?"

Participant: "I think its. . .um. . .the positives are, you would be using the resources, it wouldn't just be sitting there rotting, dying, going away, burning, whatever. You would use the resource. And we should, we really need to use our resources. Um, so you would be using the resource. There's always a tradeoff. Um, because if you do that, particularly for us locals that view this as our private little playground and whatnot, then there's more people, there's more accessibility, there's more roads, there's more activity in OUR forests. So, it has to be done, I think, in a responsible way."

The response above, like the one before it, provides a textured, and multidimensional snapshot of the thought process of a local resident on the pros and cons of bioenergy. Like the first quote, it expresses concerns about the long-term prospects of the community and the hope that a bioenergy industry could keep some young people at home. The second part of this response delves into concerns about too much industrial use of the forest and points to the affection that people in this community have for their local federal land. Interestingly, this person resides in Carbon County, WY, with its lower (−0.56) CVI score. This quote points to a history with the industry and lands that could lead to more support in this community for biofuel projects and shows a nuanced understanding of the industry and its impact on the community. This suggests that the lower cultural capital score may not reflect the true value of cultural capital in this community as this person, like others we interviewed, is clearly willing to adapt and innovate in the face of changing circumstances.

Wyoming rancher when asked if a biomass facility would benefit local communities:

"Oh, I think so because you know, you've created some jobs. Um, the problem with the tourism industry is there's about 4 months where that's really good. And the rest of the year those people are sitting, local people are going, "well. . .all right I like to go huntin' in ya know October, so I take that month off anyway" but they're unemployed a lot of the year. So yes, if you could provide year-round employment for people, I think it would benefit the community...I think people would be receptive to that, again, as long as it's managed properly and you know, we don't just wipe out a hillside turn it into pellets and ship 'em outta here. And then not care for what you've left behind and not, um ensure that what you've left behind is something sustainable. Or something that will be sustainable."

Again, as with the Wyoming residents in general, we see an interest in bioenergy as a driver of community development, a concern for a sustainable process, and evidence of local residents valuing their local federal land for recreational purposes. It also highlights that bringing employment opportunities is not enough. The impact of this development and what is "left behind" is a concern that will have to be addressed if bioenergy development occurs in this community.

The following two quotes appeared in interviews with two different Colorado foresters. They were commenting on the pros and cons of a local bioenergy facility. These foresters focused their answers more on forestry and less on community development than the previous interview examples. This may have been due to their professions and/or their locations. Their concerns about the viability of bioenergy, however, were commonly held across our research area.

Colorado forester expressing enthusiasm for bioenergy and concerns about supply:

"Well, I really think it's a pro. It would be that it could help us treat some additional forest that's in poor condition and we could do some beneficial treatments there. I would love to see expanded possibilities for some of the value that the biomass can contribute to that processing go back to help offset some of the cost to doing the treatments. Would love to see that."

"I believe our volume per acre is a liability on that because even if there was a high volume per acre right now and we did that treatment and got it down, the productivity is such that we couldn't do that again soon. We would have supply problems unless we had a really big land base which, we've got a pretty big land base but it's in such diverse ownership that it'd be difficult to count on it to be able to access that."

Colorado forester expressing enthusiasm for bioenergy and concerns about cost:

"I think it's a positive thing, probably 100% positive in the situation that we're in strictly because there is so much material that needs to be put to use. There's a way to do it. It takes money to be able to convert your TV in your home to burning wood. By the time you do it, it's far cheaper to do it. You know what I mean? You're not having to pay the gas bills. You're not having to pay the electric bills or whatever that you would to heat your home by simply just burning wood. There's a lot of people out there that do that. I think that's a good thing."

"I think that being able to heat or whatever you can with wood pellets is something that's a good thing. It's just being able to get the wood from the forests to get it processed and then get it into your living room that makes it a viable option. Like I said before, the Forest Service is not cutting up enough forests to let those entities through. If they make it so difficult that you can't get it, then it becomes so expensive that you can't ... If you go through that process, it just makes it more difficult. If that process wasn't so difficult, wasn't so expensive, I think it would be a good thing."

These participants express concerns about feedstock supply and costs that temper their enthusiasm for bioenergy This suggests, if this community were to be selected as a possible location for future development, that these concerns will need to be addressed to help ensure community support despite the relatively high cultural capital scores.

The following is a comparatively "negative" perspective on bioenergy from a land manager in a Colorado tourist community:

Manager: "I think that as a destination community, any type of industrial development, there would be opposition to from

certain camps. When I look at what they had in Walden, that'd be really tough to do here. It's a big industrial plant, you've got big trucks, they've got large amounts of material stored outside, it's not particularly aesthetically attractive and since that's where our bread and butter comes from...we don't have that much land...it would be near someone's home and people aren't going to want to live by that. Depending on the technology, emissions, and odors could be an issue."

Interviewer: "I think you talked a little bit about the pros, but any kind of positive impacts that you can think of for your community specifically?"

Manager: "I think people here are early adopters in some of the environmental things, some people would see it as, just from an ethical point, a better way to go, they'd like to look at alternatives. We've got a lot of people adopting solar and seeing it as an alternative to fossil fuels, so that would be good. I think visitors like to see that kind of thing when they come to an environment like this, to say, 'Hey, we are doing something. We're green. We're using our waste in a positive manner.' I think it's something that could be marketed as well, as part of the culture and lifestyle of living in a place like this."

Interviewer: "So the economics are the major constraint?"

Manager: "I think so. You don't see sawmills ... I've seen sawmills come and go for years in Larimer County because they just can't make it. And you can't be competitive with the mass-marketing and stuff that's coming out of the northwest and Canada. Our trees are just too small and you can't get the product out of them. It has to be more of a specialty market."

This quote is noteworthy because it provides the perspective of a land manager from a community that, unlike the great majority of communities in this study, is not dealing with "rural development" issues and does not have a meaningful connection to a natural resource export economy. The manager's words provide a clear example of a community that does not seem to fall in line with CAAM predictions. Even though Larimer County, Colorado scores well above the regional mean for cultural capital (2.00, as opposed to −0.56 for Carbon County, WY), this land manager suggests that their local community would not necessarily welcome a bioenergy facility with open arms because it would not be "aesthetically attractive." Similarly, the manager speculates that one appealing dimension of bioenergy in this community would be its alignment with "green" lifestyles.

The following comments were made by a forester in Colorado and reflect a common concern about the economic feasibility of bioenergy in a region that currently faces challenges associated with feedstock supplies and transportation costs. An important theme that this forester touches on is the ability of a biomass facility "to stand on its own two legs." Concerns about bioenergy being "propped up" by government subsidies were common in our interviews. Ironically, research participants often held up the fossil fuel industry as an example of an industry that does not need government subsidies. While there were a few participants who offered unsolicited support for government investment in bioenergy, only one person (an employee of a local conservation district) pointed out that fossil fuel receives considerable financial support from the government. This (potential) general misunderstanding of energy economics would seem to be an interesting topic for future investigation.

Colorado Forester

"Whatever biomass I've seen used successfully has had to be done with a higher value product in conjunction. Sawmills using wood waste to drive a kiln, heat a kiln for example. That's an example of a fairly efficient system or produce energy, but when it has to stand on its own two legs I think it's been oversold to the public. To a public that doesn't understand the nuances and the economics. They still think there's a lot of smoke and mirrors going on with biomass. If you take away subsidies, I don't see it as economically viable at this time. It's not that I'm against it. It's just that it doesn't seem sustainable on its own right now. We should not lose sight, any resource would go to highest and best use..."

"I'm sorry to say, but it just doesn't seem like it's being successful right now. Now you're shipping wood all the way to Saratoga. You could cut a tree outside the plant, and we do. A few miles away trees are being harvested, sent to Saratoga, Wyoming and then a byproduct of those trees is then shipped down to the mill. I don't even know if they're making any pellets right now, but in any case, I don't see that as sustainability, good economics. The people who were there were laid off, were told that they may or may not reopen. They bring some people in from time to time. It's not a boom to the local economy and in no way, that I can see, does it help my forest management program at all. I suppose when it was grinding logs and making pellets, when it did take a lot of that lower value wood and allowed us to clean that up rather than burning it in a big pile."

"I think the one lesson is co-locating. When you're shipping wood, you've got to consider co-locating. Creating bio-mass facilities in conjunction with higher use facilities. To ship this wood all over the country makes no sense. The shipping is one of your biggest costs. The economics just don't add up. One set of economics is this: it cost 25 dollars a ton to harvest right now in this economy, it depends, it's variable on the size of the job lots of other things go into this, but as a rule of thumb, 25 dollars a ton to cut a log and stack it onto a log truck. Someone's invested 25 dollars a ton just to put it on a truck, now they need to bring it somewhere. That's going to cost you 4 or 5 dollars round trip mile, loaded mile. Now you've got it to the plant. Well, now what have you got into that? Maybe 28, 30 dollars a ton. Nobody's paying 30 dollars a ton for biomass right now. It doesn't compete with natural gas, so someone has to make up that difference.

This quote again shows considerable concern for viability of the industry. Not only does it reveal concerns that it is not economically viable, but it also speaks to the history of the industry in the area and specifically past failures in the industry. Perhaps even more importantly, it points to concerns that development has not benefited the local community and future bioenergy development in the area will fail to serve the local community. It also points to a willingness to innovate to make future endeavors successful, such as co-

locating, which could reflect the higher cultural capital score found by the CAAM. However, the CAAM cannot capture the perspectives of the industry based on historical experience, or the concern that projects would not benefit the local community.

Again, while all our interviews did touch on the same topics because of the common interview guide, the open-ended structure of the ethnographic interviews allowed for more expansive answers than we could have gathered with a quantitative method or a more streamlined qualitative method. All at once, this approach provided us with basic objective information, such as the number of people who "supported" bioenergy; detailed information about why, for example, people have doubts about the viability of another pellet facility in northern Colorado; and with more subjective reflections that speak to the kinds of activities that people would find ethically or environmentally "acceptable" on their local federal lands. When we assessed the broad sweep of our 31 interviews from this region, it became clear that the CAAM predictions about places with low "cultural capital" did not represent the people we interacted with in various rural communities in Wyoming and Colorado. These individuals showed not only nuanced understandings of the industry and its potential pitfalls and benefits but also reflected a willingness to innovate to meet changing circumstances, something CAAM measures suggest would be difficult for these communities. Part of the limitation of the CAAM may be that the measures are only available at the county level and set to a regional standard (United States Census Region West) for comparison. Thus, these scores are not reflective of more local communities.

Lastly, these interviews highlight an important aspect of cultural capital that the current CAAM score cannot measure quantitatively: history. Many of the interview participants touched on local history and how it impacted perceptions of bioenergy and these perspectives were largely negative. Roemer (2017); Mueller et al. (2020) show that history impacts support for projects and that is something CAAM and similar quantitative models cannot adequately address yet is vital to understanding the culture of a region and local opinions of bioenergy industries.

CONCLUSION AND RECOMMENDATIONS

Clearly, as Roemer (2017); Mueller et al. (2020) suggest, these interviews present a far more nuanced understanding of decision-making processes in these rural Wyoming and Colorado communities than quantitative cultural capital scores can capture. Again, the concerns expressed by our research participants were varied, but these people were certainly not opposed to innovative technological solutions that would allow them to adapt to challenging environmental and economic circumstances. In fact, as we mentioned, participants in the communities with the lower cultural capital z-scores, for a variety of economic and cultural reasons, may be more supportive of a bioenergy facility than communities with higher cultural capital scores.

While there are several potential reasons for this discrepancy between CAAM expectations and the ethnographic data, one in particular stands out. As we have previously discussed, CAAM's cultural capital scores are largely derived from Florida (2019) creative class concept, which already tends to favor larger cities—where the "creative class" tends to be concentrated. If this remains the core of how cultural capital is measured in the CAAM, more rural counties will usually see lower cultural capital scores. Work on the ground, however, clearly shows that these communities do demonstrate a willingness to adapt to change and to support technological innovation. While CAAM is rooted in the CCF, the focus on the "creative class" means that researchers are not assessing cultural capital, but a product of cultural capital in the original conceptualization and should perhaps return to the "creative capital" concept that was used in earlier iterations (Martinkus et al., 2014; Martinkus et al., 2017). Nonetheless, cultural capital is an inherently qualitative concept and the disconnect between quantitative proxies that attempt to measure creativity such as CAAM and the ethnographic interviews reinforces the need, emphasized by Mueller et al. (2020); Boglioli et al. (2019), for qualitative on-the-ground research in communities under consideration for biorefinery projects to understand community contexts that the CAAM alone cannot capture. Mueller et al. (2020) recommend a more strategic application of the CAAM, where capital scores are not used to eliminate potential communities when determining suitability for biofuel projects. They note that CAAM scores should support an initial community assessment that can yield strategies for how to successfully engage with selected communities and potential interventions to help increase support for the projects. However, they emphasize that some critical metrics, like community support for a biofuel project or historic relationships with the industry, can only be ascertained through qualitative research. This paper demonstrates the merits of that recommendation, revealing that the use of the CAAM by itself might have resulted in a community in, for example, Carbon County, WY, getting passed over, and despite potential support for such projects—or at least a willingness to innovate that were only discovered through interviews with community members. Future research is needed to gain a better understanding of this potential trend and develop strategies for using the CAAM as an initial assessment tool supplemented by qualitative research.

Based on our research in Wyoming and Colorado, we suggest developing a mixed-methods DST that would combine the more reliably measured capitals with semi-structured ethnographic interviews and increased attention to local historical legacies. By merging these methodologies, researchers would be capable of producing a DST that is effective at both the general (quantitative) and specific (qualitative) level. Presumably, this would produce a more accurate and less costly technique because it would eliminate the confusions that currently emerge around cultural capital. In this scenario, cultural capital scores, as we presently understand them, would no longer be necessary because cultural issues would be assessed with ethnographic, and historical methods. Instead, future

research could focus on "creative capital" and whether the presence of higher levels of the "creative class" leads to higher levels of innovation on biofuels projects, and additionally, whether the recommendation that additional expertise may be needed for project development and implementation are supported with more case studies. As Mueller et al. (2020) found support that lower "creative class" scores required additional expertise, testing this premise with more cases is especially important.

In a hypothetical search for suitable communities in which to build biorefineries, a set of communities could be chosen based first on whether they meet the biogeophysical requirements for biofuel production. CAAM scores could then uncover a general, quantitative overview of social conditions within these communities, which would provide recommendations about how to engage within them and identify potential challenges to project development. At this point, we would recommend commencing with qualitative ethnographic research in these communities to gain a detailed understanding of local perspectives on bioenergy and what kinds of historical relationships these communities might have with biofuel production or other major industrial projects. This approach would help ascertain whether the community has the innovative capacities to sustain a biofuel supply chain based on local historical considerations that neither biogeophysical nor CAAM data alone can reveal. As these results suggest, a mixed methods approach—incorporating biogeophysical, CAAM, and ethnographic data—provides a more nuanced and comprehensive approach to assessing cultural capital for biofuel site selection and development. By starting with quantitative data and narrowing down community suitability with more qualitative research, we believe projects setting up bioenergy production chains would enjoy higher rates of success and longevity. The key to this approach is the combination of CAAM or similar quantitative approaches with ethnographic approaches to assess cultural capital.

DATA AVAILABILITY STATEMENT

The original contributions presented in the study are included in the article/Supplementary Materials, further inquiries can be directed to the corresponding author.

AUTHOR CONTRIBUTIONS

SS, TAB, and RB contributed to the original conception and ethnographic research design to obtain interview data for the USDA Bioenergy Alliance Network of the Rockies project. RB, TAB, MB, and SS conducted interviews analyzed for this manuscript. DM and SH contributed to the original conception and design of the CAAM model. SH, DM, MB, and SS contributed to the conception and design of mixed method study used in this research. MB and SS analyzed interviews. DM conducted quantitative analysis. MB, SS, SH, and DM wrote sections of the manuscript. MB, SS, SH, and DM contributed to manuscript revision. TAB and RB contributed to manuscript editing and revision.

FUNDING

This research was funded by the U.S. Federal Aviation Administration Office of Environment and Energy through ASCENT, the FAA Center of Excellence for Alternative Jet Fuels and the Environment, project 001(A) through FAA Award Number 13-C-AJFE-WaSU-013 under the supervision of under the supervision of James Hileman and Nathan Brown. Any opinions, findings, conclusions or recommendations expressed in this material are those of the authors and do not necessarily reflect the views of the FAA. This research was funded in part by a grant through the United States Department of Agriculture (AFRI-CAP#2013-3867).

REFERENCES

Acquaye, A. A., Wiedmann, T., Feng, K., Crawford, R. H., Barrett, J., Duffy, K. J., et al. (2011). Identification of 'Carbon Hot-Spots' and Quantification of GHG Intensities in the Biodiesel Supply Chain Using Hybrid LCA and Structural Path Analysis. *Environ. Sci. Technol.* 45 (6), 2471–2478. doi:10.1021/es103410q

Afgan, N. H., and Carvalho, M. G. (2002). Multi-Criteria Assessment of New and Renewable Energy Power Plants. *Energy* 27 (8), 739–755. doi:10.1016/S0360-5442(02)00019-1

Anderson, B. J., Mueller, D. W., Hoard, S. A., Sanders, C. M., and Rijkhoff, S. A. M. (Forthcoming 2022). Social Science Applications in Sustainable Aviation Biofuels Research: Opportunities, Challenges, and Advancements. *Front. Energy Res.*.

Bernard, H. R. (2018). *Research Methods in Anthropology: Qualitative and Quantitative Approaches*. Sixth Edition. Lanham: Rowman & Littlefield.

Boggs, C. (2001). Social Capital and Political Fantasy: Robert Putnam's 'Bowling Alone. *Theor. Soc.* 30 (2), 281–297. doi:10.1023/a:1010875611192

Boglioli, M. A., Strauss, S., Hoard, S., Mueller, D., Budowle, R., Beeton, T. A., et al. (2019). "Searching for Culture in 'Cultural Capital': The Case for a Mixed Methods Approach to Production Facility Siting," in *Presented at the Biochar & Bioenergy Conference* (Fort Collins, CO: Colorado State University)

Bourdieu, P. (1986). "The Forms of Capital," in *In Handbook of Theory and Research for the Sociology of Education* (Westport, CT: Greenwood), 241–258.

Briceno, T., and Stagl, S. (2006). The Role of Social Processes for Sustainable Consumption. *J. Clean. Prod.* 14 (17), 1541–1551. doi:10.1016/j.jclepro.2006.01.027

Buchholz, T., Luzadis, V. A., and Volk, T. A. (2009). Sustainability Criteria for Bioenergy Systems: Results from an Expert Survey. *J. Clean. Prod.* 17 (November), S86–S98. doi:10.1016/j.jclepro.2009.04.015

Budd, W., Lovrich, N., Jr., Pierce, J. C., and Chamberlain., B. (2008). Cultural Sources of Variations in US Urban Sustainability Attributes. *Cities* 25, 257–267. doi:10.1016/j.cities.2008.05.001

Bures, F. (2017). Richard Florida Can't Let Go Of His Creative Class Theory. His Reputation Depends On It. *Belt Magazine*Available at https://beltmag.com/richard-florida-cant-let-go/.

Chatti, D., Archer, M., Lennon, M., and Dove, M. R. (2017). Exploring the Mundane: Towards an Ethnographic Approach to Bioenergy. *Energ. Res. Soc. Sci.* 30 (August), 28–34. doi:10.1016/j.erss.2017.06.024

Clarens, A. F., NassauWhite, H., Resurreccion, E. P., White, M. A., and Colosi, L. M. (2011). Environmental Impacts of Algae-Derived Biodiesel and Bioelectricity for Transportation. *Environ. Sci. Technol.* 45 (17), 7554–7560. doi:10.1021/es200760n

Coleman, J. S. (1988). Social Capital in the Creation of Human Capital. *Am. J. Sociol.* 94, S95–S120. doi:10.1086/228943

Collotta, M., Champagne, P., Tomasoni, G., Alberti, M., Busi, L., and Mabee, W. (2019). Critical Indicators of Sustainability for Biofuels: An Analysis through a Life Cycle Sustainabilty Assessment Perspective. *Renew. Sustain. Energ. Rev.* 115 (November), 109358. doi:10.1016/j.rser.2019.109358

Cramb, R. A. (2005). Social Capital and Soil Conservation: Evidence from the Philippines. *Aust. J. Agric. Res. Econ.* 49 (2), 211–226. doi:10.1111/j.1467-8489.2005.00286.x

Durbin, T. J., Bendixsen, C. G., Jensen-Ryan, D., Molzer, A., and Strauss, S. (2019). The Dangerous Middle: Situational Awareness and Worker Perception of Beetle Kill. *J. Agromedicine* 24 (2), 157–166. doi:10.1080/1059924X.2019.1567424

Durlauf, S. N. (2002). On the Empirics of Social Capital. *Econ. J.* 112 (483), F459–F479. doi:10.1111/1468-0297.00079

Ehsan, A., Klaas, H. S., Bastianen, A., and Spini, D. (2019). Social Capital and Health: A Systematic Review of Systematic Reviews. *SSM - Popul. Health* 8 (August), 100425. doi:10.1016/j.ssmph.2019.100425

Emery, M., and Flora, C. (2006). Spiraling-Up: Mapping Community Transformation with Community Capitals Framework. *Community Develop.* 37 (1), 19–35. doi:10.1080/15575330609490152

Erp, M., Gaffney, M., Goldman, J., Gray, K., and Lovrich, N., Jr. (2009). *WRICOPS – A Decade of Service, 1997-2007: A Brief History, Major Accomplishments, Principal Activities and Prospects for the Future*. Pullman, WA: Division of Governmental Studies and Services, Washington State University.

Flora, C. (1995). Social Capital and Sustainability: Agriculture and Communities in the Great Plains and Corn Belt. *Res. Rural Sociol. Develop.* 6, 227–246.

Florida, R. L. (2002). *The Rise of the Creative Class: And How It's Transforming Work, Leisure, Community and Everyday Life*. New York, NY: Basic Books.

Florida, R. (2019). *The Rise of the Creative Class*. Updated edition. New York, NY: Basic Books.

Ghose, D., Naskar, S., and Uddin, S. (2019). "Q-GIS-MCDA Based Approach to Identify Suitable Biomass Facility Location in Sikkim (India)," in In 2019 Second International Conference on Advanced Computational and Communication Paradigms (ICACCP) (Gangtok, India: IEEE), 1–6. doi:10.1109/ICACCP.2019.8882978

Gnansounou, E., and Alves, C. M. (2019). "Social Assessment of Biofuels," in *Biofuels: Alternative Feedstocks and Conversion Processes for the Production of Liquid and Gaseous Biofuels* (London Wall, London: Academic Press), 123–139. doi:10.1016/b978-0-12-816856-1.00005-1

Gorry, G. A., Michael, S., and Scott, M. (1971). *A Framework for Management Information Systems*. Cambridge, MA: Massachusetts Institute of Technology:

Jensen-Ryan, D., Budowle, R., Strauss, S., Durbin, T. J., Beeton, T. A., and Galvin, K. A. (2019). A Cultural Consensus of Fire and Futility: Harvesting Beetle-Kill for Wood-Based Bioenergy in Wyoming and Colorado. *Energ. Res. Soc. Sci.* 58 (December), 101272. doi:10.1016/j.erss.2019.101272

Jones, N., Sophoulis, C. M., Iosifides, T., Botetzagias, I., and Evangelinos, K. (2009). The Influence of Social Capital on Environmental Policy Instruments. *Environ. Polit.* 18 (4), 595–611. doi:10.1080/09644010903007443

Jovanović, M., Afgan, N., Radovanović, P., and Stevanović, V. (2009). Sustainable Development of the Belgrade Energy System. *Energy* 34 (May), 532–539. doi:10.1016/j.energy.2008.01.013

Kurka, T., and Blackwood, D. (2013). Participatory Selection of Sustainability Criteria and Indicators for Bioenergy Developments. *Renew. Sustain. Energ. Rev.* 24 (August), 92–102. doi:10.1016/j.rser.2013.03.062

Lovrich, N. P., Gaffney, M. J., Weber, E. P., Bireley, R. M., Matthews, D. R., and Bjork, B. (2005). Inter-Agency Collaborative Approaches to Endangered Species Act Compliance and Salmon Recovery in the Pacific Northwest. *Int. J. Organ. Theor. Behav.* 8 (2), 237–273. doi:10.1108/IJOTB-08-02-2005-B005

Marcus, G. E. (1995). Ethnography In/of the World System: The Emergence of Multi-Sited Ethnography. *Annu. Rev. Anthropol.* 24, 95–117. doi:10.1146/annurev.an.24.100195.000523

Martinkus, N., Latta, G., Brandt, K., and Wolcott, M. (2018). A Multi-Criteria Decision Analysis Approach to Facility Siting in a Wood-Based Depot-And-Biorefinery Supply Chain Model. *Front. Energ. Res.* 6 (November). doi:10.3389/fenrg.2018.00124

Martinkus, N., Latta, G., Rijkhoff, S. A. M., Mueller, D., Hoard, S., Sasatani, D., et al. (2019). Season Hoard, Daisuke Sasatani, Francesca Pierobon, and Michael WolcottA Multi-Criteria Decision Support Tool for Biorefinery Siting: Using Economic, Environmental, and Social Metrics for a Refined Siting Analysis. *Biomass and Bioenergy* 128 (September), 105330. doi:10.1016/j.biombioe.2019.105330

Martinkus, N., Rijkhoff, S. A. M., Hoard, S. A., Shi, W., Smith, P., Gaffney, M., et al. (2017). Biorefinery Site Selection Using a Stepwise Biogeophysical and Social Analysis Approach. *Biomass and Bioenergy* 97 (February), 139–148. doi:10.1016/j.biombioe.2016.12.022

Martinkus, N., Shi, W., Lovrich, N., Pierce, J., Smith, P., and Wolcott, M. (2014). Integrating Biogeophysical and Social Assets into Biomass-To-Biofuel Supply Chain Siting Decisions. *Biomass and Bioenergy* 66 (July), 410–418. doi:10.1016/j.biombioe.2014.04.014

Mattioda, R. A., Tavares, D. R., Casela, J. L., and Junior, O. C. (2020). "Social Life Cycle Assessment of Biofuel Production," in *Biofuels for a More Sustainable Future* (Amsterdam, Netherlands: Elsevier), 255–271. doi:10.1016/B978-0-12-815581-3.00009-9

Montgomery, J. D. (2001). "Social Capital as a Policy Resource," in *Social Capital as a Policy Resource*. Editors J D. Montgomery and A Inkeles (Boston, MA: Springer US), 1–17. doi:10.1007/978-1-4757-6531-1_1

Mueller, D., Hoard, S., Roemer, K., Sanders, C., and Rijkhoff, S. A. M. (2020). Quantifying the Community Capitals Framework: Strategic Application of the Community Assets and Attributes Model. *Community Develop.* 51 (5), 535–555. doi:10.1080/15575330.2020.1801785

O'Callaghan, C. (2010). Let's Audit Bohemia: A Review of Richard Florida's 'Creative Class' Thesis and its Impact on Urban Policy. *Geogr. Compass* 4 (11), 1606–1617. doi:10.1111/j.1749-8198.2010.00397.x

Pashaei Kamali, F., Borges, J. A. R., Osseweijer, P., and Posada, J. A. (2018). Towards Social Sustainability: Screening Potential Social and Governance Issues for Biojet Fuel Supply Chains in Brazil. *Renew. Sustain. Energ. Rev.* 92 (September), 50–61. doi:10.1016/j.rser.2018.04.078

Pavan, M., and Todeschini, R (2009). "Multicriteria Decision-Making Methods," in *Comprehensive Chemometrics*. Editors S. D. Brown, R. Tauler, and B. Walczak (Elsevier), 591–629. https://www.sciencedirect.com/science/article/pii/B9780444527011000387.

Perimenis, A., Walimwipi, H., Zinoviev, S., Müller-Langer, F., and Miertus, S. (2011). Development of a Decision Support Tool for the Assessment of Biofuels. *Energy Policy* 39 (3), 1782–1793. doi:10.1016/j.enpol.2011.01.011

Pitas, N., and Ehmer, C. (2020). Social Capital in the Response to COVID-19. *Am. J. Health Promot.* 34 (8), 942–944. doi:10.1177/0890117120924531

Portney, K. E., and Berry, J. M. (2010). Participation and the Pursuit of Sustainability in U.S. Cities. *Urban Aff. Rev.* 46 (1), 119–139. doi:10.1177/1078087410366122

Putnam, R. D. (1993). *Making Democracy Work: Civic Traditions in Modern Italy*. Princeton, NJ: Princeton University Press.

Putnam, R. D. (1995). Bowling Alone: America's Declining Social Capital. *J. Democracy* 6 (1), 65–78. doi:10.1353/jod.1995.0002

Putnam, R. D. (2000). *Bowling Alone: The Collapse and Revival of American Community*. New York, NY, USA: Simon & Schuster [u.a.

Rijkhoff, S. A. M., HoardHoard, S. A., Gaffney, M. J., and Smith, P. M. (2017). Communities Ready for Takeoff. *Polit. Life Sci.* 36 (1), 14–26. doi:10.1017/pls.2017.6

Rijkhoff, S. A. M., Roemer, K., Martinkus, N., Laninga, T. J., and Hoard, S. (2021). "A Capitals Approach to Biorefinery Siting Using an Integrative Model," in *Energy Impacts: A Multidisciplinary Exploration of North American Energy Development*. Editors J B. Jacquet, J H. Haggerty, and G L. Theodori (Boulder, CO: University Press of Colorado), 176–212. http://www.jstor.org/stable/j.ctv19t41pj.10.

Roemer, K. F. (2017). *Exploring the Role of Social Assets in Refinery Implementation: Using Case Study Research to Ground-Truth CAAM.* " Moscow, ID: University of Idaho.

Roos, A., Graham, R. L., Hektor, B., and Rakos, C. (1999). Critical Factors to Bioenergy Implementation. *Biomass and Bioenergy* 17, 113–126. doi:10.1016/s0961-9534(99)00028-8

Samuelson, R. J. (1996). Bowling Alone' is Bunk. *Washington Post*.

Rupasingha, A., Goetz, S. J., and Freshwater, D. (2006). The Production of Social Capital in US Counties. *The J. Socio-Economics* 35 (1), 83–101. doi:10.1016/j.socec.2005.11.001

S. Strauss, S. Rupp, and T. F. Love (Editors) (2013). *Cultures of Energy: Power, Practices, Technologies* (Walnut Creek, CA: Left Coast Press).

Shim, J., Warkentin, M., James, C., Daniel, J. P., Ramesh, S., and Carlsson, C. (2002). Past, Present, and Future of Decision Support Technology. *Decis. Support Syst.* 33 (June), 111–126. doi:10.1016/S0167-9236(01)00139-7

Stewart, L., and Lambert, D. M. (2011). Spatial Heterogeneity of Factors Determining Ethanol Production Site Selection in the U.S., 2000-2007. *Biomass and Bioenergy* 35 (3), 1273–1285. doi:10.1016/j.biombioe.2010.12.020

Strauss, S. (2004). *Positioning Yoga*. Oxford: Berg Publishers, Ltd.

Strauss, S., and Reeser, D. (2016). "Siting, Scale, and Social Capital: Wind Energy Development in Wyoming," in *Cultures of Energy: Power, Practices, Technologies* (Walnut Creek, CA: Left Coast Press), 110–125.

Upreti, B. R., and van der Horst, D. (2004). National Renewable Energy Policy and Local Opposition in the UK: The Failed Development of a Biomass Electricity Plant. *Biomass and Bioenergy* 26 (1), 61–69. doi:10.1016/S0961-9534(03)00099-0

Visentin, C., da Silva Trentin, A. W., Braun, A. B., and Thomé, A. (2020). Life Cycle Sustainability Assessment: A Systematic Literature Review through the Application Perspective, Indicators, and Methodologies. *J. Clean. Prod.* 270, 122509. doi:10.1016/j.jclepro.2020.122509

Wainwright, O. (2017). 'Everything is Gentrification Now': But Richard Florida isn't Sorry. *The Guardian* Available at https://www.theguardian.com/cities/2017/oct/26/gentrification-richard-florida-interview-creative-class-new-urban-crisis.

Wang, J.-J., Jing, Y.-Y., Zhang, C.-F., and Zhao, J.-H. (2009). Review on Multi-Criteria Decision Analysis Aid in Sustainable Energy Decision-Making. *Renew. Sustain. Energ. Rev.* 13 (9), 2263–2278. doi:10.1016/j.rser.2009.06.021

White, W., Lunnan, A., Nybakk, E., and Kulisic, B. (2013). The Role of Governments in Renewable Energy: The Importance of Policy Consistency. *Biomass and Bioenergy* 57 (October), 97–105. doi:10.1016/j.biombioe.2012.12.035

Xu, B., Kolosz, B. W., Andresen, J. M., Ouenniche, J., Greening, P., Chang, T.-S., et al. (2019). Performance Evaluation of Alternative Jet Fuels Using a Hybrid MCDA Method. *Energ. Proced.* 158 (February), 1110–1115. doi:10.1016/j.egypro.2019.01.275

Zhang, F., Johnson, D. M., and Sutherland, J. W. (2011). A GIS-Based Method for Identifying the Optimal Location for a Facility to Convert forest Biomass to Biofuel. *Biomass and Bioenergy* 35 (9), 3951–3961. doi:10.1016/j.biombioe.2011.06.006

Conflict of Interest: The authors declare that the research was conducted in the absence of any commercial or financial relationships that could be construed as a potential conflict of interest.

frontiers in Energy Research

MINI REVIEW
published: 24 January 2022
doi: 10.3389/fenrg.2021.782823

Perspectives on Fully Synthesized Sustainable Aviation Fuels: Direction and Opportunities

Stephen Kramer[1], *Gurhan Andac*[2], *Joshua Heyne*[3], *Joseph Ellsworth*[4], *Peter Herzig*[5] and *Kristin C. Lewis*[5]*

[1]Pratt & Whitney, West Hartford, CT, United States, [2]GE Aviation, Evendale, OH, United States, [3]Department of Mechanical and Aerospace Engineering, University of Dayton, Dayton, OH, United States, [4]Boeing, Chicago, IL, United States, [5]Volpe National Transportation Systems Center, Cambridge, MA, United States

The aviation sector seeks to reduce greenhouse gas (GHG) emissions, with manufacturers and airlines announcing "zero-emission" goals and plans. Reduced carbon aviation fuels are central to meeting these goals. However, current and near-term aircraft, which will remain flying for decades, are designed around the combustion of petroleum-based aviation kerosene (e.g., Jet A/A-1). Therefore, the industry has focused on the qualification and approval of synthesized (e.g., non-petroleum-based) aviation fuel components with maximum blend limit percentages to avoid the blended fuel having properties outside the accepted ranges for Jet A/A-1. The synthesized components approved for blending are not necessarily interchangeable with Jet A/A-1. They may lack certain required chemical components, such as aromatics, or may have other characteristics outside the allowable ranges. To ensure safety, these synthesized aviation fuel components are only qualified to be used in commercial aviation when blended up to approved limits. The sector seeks to move toward the capability of using 100% synthesized aviation fuels that also meet sustainability criteria, known as sustainable aviation fuels, or SAF. However, these fuels must be developed, assessed, and deployed appropriately. This paper explores key questions relating to the introduction of 100% SAF, concluding that:

- Near-term unblended synthesized aviation fuels must be "drop-in," meaning they are compatible with existing aircraft and infrastructure.
- Stand-alone complete fuels could be qualified within 1–2 years, with blends of blending components to reach 100% synthesized fuels to follow.
- Sustainability criteria, while critical to sector acceptance, will continue to be assessed separately from technical performance.

Keywords: ASTM fuel qualification, drop-in, fungible, sustainable aviation fuel, synthesized aviation fuel

OPEN ACCESS

Edited by:
Umakanta Jena,
New Mexico State University,
United States

Reviewed by:
Ibukun Oluwoye,
Murdoch University, Australia
Sgouris Sgouridis,
Masdar Institute of Science and Technology, United Arab Emirates

***Correspondence:**
Kristin C. Lewis
kristin.lewis@dot.gov

Specialty section:
This article was submitted to Bioenergy and Biofuels, a section of the journal Frontiers in Energy Research

Received: *24 September 2021*
Accepted: *31 December 2021*
Published: *24 January 2022*

Citation:
Kramer S, Andac G, Heyne J, Ellsworth J, Herzig P and Lewis KC (2022) Perspectives on Fully Synthesized Sustainable Aviation Fuels: Direction and Opportunities. Front. Energy Res. 9:782823. doi: 10.3389/fenrg.2021.782823

INTRODUCTION

The aviation industry seeks cost-competitive synthesized aviation fuels with a carbon benefit and sustainability performance to counter the effects of price spikes, competition for finite oil supplies, and aviation's high profile as a greenhouse gas (GHG) and particulate emitter. This decarbonization is additionally needed to meet long-term net-zero emissions goals (ATAG, 2021). Current and

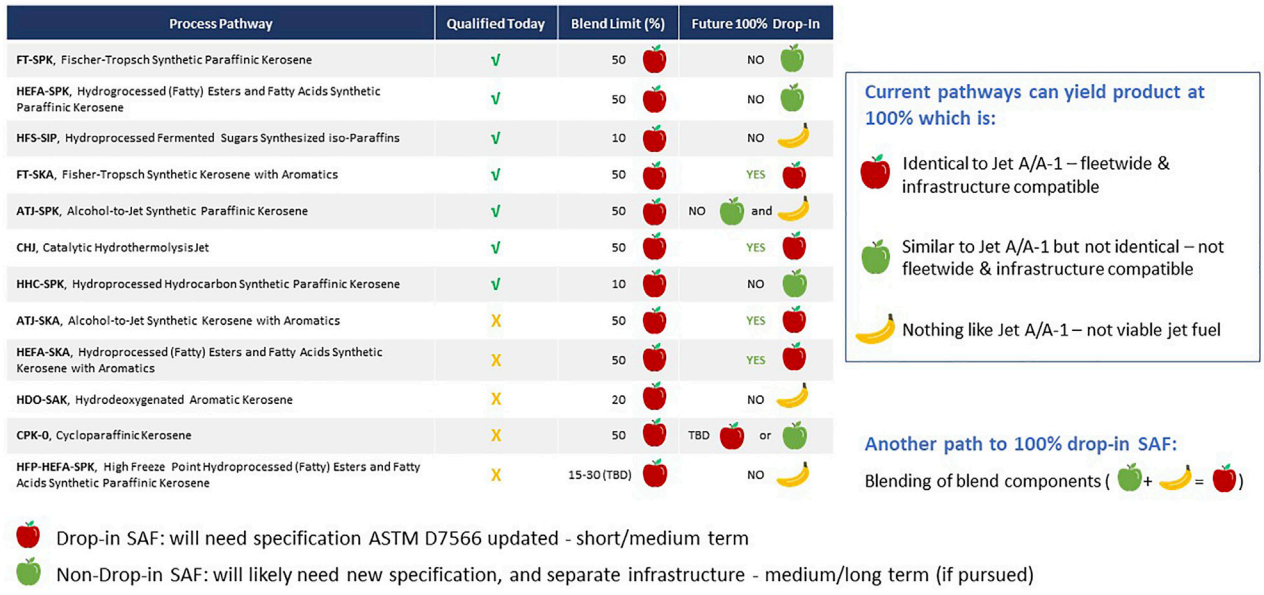

FIGURE 1 | Types of synthesized fuel blendstocks and their ability to be used as drop-in fuels as blendstocks or as stand-alone fuel. The red apples indicate fuels that can be drop-in, green apples are similar to drop-ins and may be usable in some existing aircraft but would require modification of the existing specifications and possibly infrastructure, and bananas indicate fuels that are completely different from petroleum-based kerosene and could not be used as stand-alone jet fuel in current infrastructure or equipment.

near-term (10–20 years) aircraft will remain in operation for decades and are designed around aviation kerosene (e.g., Jet A/A-1). Technologies to increase the efficiency of new aircraft by a fleet average of 1–2% each year are offset by a 4–5% compound average annual travel growth rate (Fleming and de Lepinay, 2019) leading to projected emissions increases (IATA, 2019). Proposed "zero emissions" options, such as batteries (Hepperle, 2012; Schäfer, et al., 2019) or cryogenic fuels, are of low technology readiness, have restricted range, and require new energy supply networks (McKinsey and Co., 2020). However, reducing the carbon footprint of jet fuel reduces aviation's impact on the environment now and in the long-term.

Since 2006, the Commercial Aviation Alternative Fuels Initiative (CAAFI®), a public-private partnership including United States government, aviation sector stakeholders, and aviation fuel supply chain participants, has worked to enhance energy security and environmental sustainability for aviation with alternative jet fuels by facilitating their deployment in the marketplace (CAAFI, 2021). Initially, due to safety and compatibility concerns, CAAFI and the industry focused on qualification of *synthesized fuel blending components* that come from sources other than petroleum to be added to conventional aviation fuel sourced from petroleum, which are qualified by ASTM D4054 for use in ASTM D7566 (ASTM International, 2021) (see **Figure 1**). These blending components are limited to a maximum blend percentage to ensure that all blended fuels properties are within accepted ranges for Jet A/A-1 (particularly aromatic content) (Zschocke et al., 2012). Thus, the resultant blended fuels are interchangeable with unblended Jet A/A-1 regarding handling, operability, and safety and referred to as "drop-in" aviation fuels (Colket., et al., 2016). The blended fuel is re-identified as Jet A/A-1 for transport, storage, purchase, and use under the ASTM D1655 petroleum-based jet fuel specification (ASTM International, 2020).

The existing synthesized blending components are not necessarily sustainable, as environmental, social, and economic performance requirements are not part of ASTM qualification. To address sustainability goals, aviation stakeholders and International Civil Aviation Organization (ICAO) member States put a process in place to evaluate production, feedstock, land-use, social impact, and life-cycle carbon footprint of various possible paths, and consider relevant environmental, social, and economic risks, formalized *via* the ICAO Carbon Off-setting and Reduction Scheme for International Aviation (CORSIA) (ICAO, 2021a). Fuels certified as sustainable under this, and similar approaches, are called sustainable aviation fuels (SAF). The synthesized blending components complying with ASTM D7566 can be made according to sustainability criteria to become SAF.

The current production of SAF globally is much less than 1% (Csonka, 2020). However, the United States has set a target of producing 3 billion gallons of SAF per year by 2030, totaling about 10% of anticipated annual jet fuel consumption, and targets complete replacement of petroleum-based jet fuel by 2050 (U.S. White House, 2021), and SAF mandates are in place or are under consideration globally (Malicier, 2021). While overall SAF availability is currently low, 100% SAF may be available at particular locations very soon. Airfields could provide limited amounts of 100% SAF to those willing to pay for that distinction, such as private jet owners. Or a particular airport or nation could set goals to fuel a certain number of flights with 100% SAF, possibly within the decade. Aircraft manufacturers have made

commitments to compatibility with 100% SAF by 2030 even in the absence of an agreed upon definition for 100% SAF (Boeing, 2021). Furthermore, the qualification of 100% SAF would eliminate the need for controlled blending of that SAF into the fuel pool, reducing supply chain complexity. Thus, the 100% synthesized fuel definition and qualification process should happen now to prepare for these future needs.

The ability to use neat SAF (without blending with conventional fuel), or "100% SAF" could further reduce aviation's global GHG generation and human health impacts. Additionally, 100% SAFs containing reduced or no aromatics reduce non-volatile particulate matter (nvPM) emissions, which are linked to contrail formation (Voigt, et al., 2021), and contrails are suggested to contribute more to aviation radiative forcing than CO_2 emissions (Lee, et al., 2021). Finally, 100% SAF has very low levels of sulfur, which leads to low levels of sulfur oxide (SOx) emissions (Moore, et al., 2015). Thus 100% SAF would reduce aviation's GHG production, contrails, and SOx emissions, all significant environmental benefits.

However, the synthesized blending components approved to date are not by themselves necessarily drop-in or interchangeable with Jet A/A-1, and so cannot be used as 100% synthesized fuels alone (**Figure 1**). They may lack aromatics required in legacy aircraft and aircraft engines for seal compatibility (Anuar et al., 2021). Properties such as freeze point or mass density may be near the limits for the accepted Jet A/A-1 range (Edwards, 2017; Colket and Heyne, 2021). They may contain a restricted number of chemical species or have limited carbon number range and not meet the Jet A/A-1 distillation curve requirements (Bell et al., 2018; Won et al., 2019). These differences may impact the performance, operability, and/or safety of some aircraft models and engines currently flying (Bell et al., 2018; Won et al., 2019).

The challenge is to achieve 100% SAF that meets all the safety and operability requirements of the ASTM qualification process, as well as the affordability and sustainability goals of the industry. In this paper, we explain the importance of the "drop-in" requirement, highlight potential approaches to achieve fully synthesized aviation fuels and provide perspectives on the viability of those approaches, and discuss how sustainability criteria can be layered onto fully synthesized jet fuels to create complete sustainable aviation fuels.

IMPORTANCE OF "DROP-IN" AS A REQUIREMENT

Jet A/A-1s are unique mixtures of hydrocarbons that cannot be simply defined by a certain chemical composition. The characteristics of Jet A/A-1 are derived from petroleum going through modern refinery processes, e.g., distillation, hydrotreatment, catalytic reforming, etc. Specifications and tests have been developed to measure performance properties such as net heat of combustion, thermal stability, viscosity, distillation curve, freezing point, flash point, smoke point, density, lubricity, aromatic content, sulfur content, etc. (Hemighaus, et al., 2007). Over time, the property specifications have been reviewed and updated, testing improved, and new specifications added. The intent has been to make Jet A/A-1 the safest and most suitable possible fuel for aviation.

Aviation gas turbines are designed to operate on and utilize the properties of Jet A/A-1 (Heyne et al., 2021). Jet A/A-1 properties are tightly linked to the reliability and safety of aviation. For example, the flash point of Jet A/A-1 is such that a match will not ignite the fuel at room temperature (ASTM International, 2020). Yet gas turbines can ignite the fuel at conditions as cold as Fairbanks, Alaska, or as hot as Saudi Arabia, and can be re-lit in mid-flight at 30,000 feet.

The ASTM qualification process (ASTM D4054) has been adapted to enable synthesized fuel approvals (Rumizen, 2021). Thus far, all synthesized blended fuel has been required to be drop-in and meet every specification for petroleum-based Jet A/A-1 (ICAO, 2018), because it was not known what specific properties of the fuel were critical for operability and safety and which properties could be relaxed. An 8% minimum aromatics content was set to ensure compatibility for nitrile seals. Combustor performance includes factors such as cold weather ignition, altitude relight, lean blow-out characteristics, interactions with combustor acoustics and dynamics, flame stability, flame luminosity, heat release patterns, and so on. Safety and reliability in external components must consider such factors as cold fuel viscosity system performance, vapor pressure characteristics and impact on pump performance, cavitation potential, low lubricity, seal compatibility, thermal stability and tendency to varnish, icing characteristics, entrained water, biocide compatibility, flammability, and other criteria (Colket et al., 2016; Colket and Heyne, 2021).

Although jet fuel combustion has been studied for decades, unknowns remain. For example, critical factors for altitude relight are not well characterized: atomization is a complex interplay of fuel surface tension, viscosity, density, and air temperature and pressure; fuel vapor pressure, and molecular composition are also important (Peiffer et al., 2019; Boehm et al., 2021). Research, such as the National Jet Fuels Combustion Program (Colket et al., 2016; CAAFI R&D Team, 2019), has added to the understanding of the interaction of fuel chemical composition and physical properties with combustion. However, that understanding is not complete, and any uncertainty may impact safety.

Jet fuel is not only used for combustion in the aircraft. Fuel is used to exchange heat with the oil, to power fueldraulic actuators, and to lubricate (or at least not excessively wear) pumps (Heyne et al., 2021). Additionally, in legacy aircraft, the nitrile seals are sensitive to fuel composition and their performance might be impacted (Graham, et al., 2013). To be drop-in, the fuel must satisfy these functionalities as well.

The industry position is that safety for all past, present and future aircraft must be addressed in the specification of any fuel. For 100% synthesized fuels, new requirements may need to be added to the specification. For example, the NJFCP suggested several characteristics as potentially critical to the safety and operability of jet fuels, such as derived cetane number (Colket et al., 2016; Stachler et al., 2020; Boehm et al., 2021). These new

requirements need to be considered, researched and verified. Similarly, to better enable synthesized fuel cost-effectiveness, it may be desired to redefine or add other specifications and properties, which would require additional research and verification to insure 100% drop-in compatibility.

Without knowing the impact of a fuel not meeting all Jet A/A-1 characteristics, a proposed non-drop-in fuel must be limited to validated applications. A non-drop-in fuel requires separate handling, storage, and logistics, and must be compatible with that separate infrastructure (e.g., fueling trucks, hydrant system, tanks, etc.). It requires safety measures to eliminate any possible mistakes in fuel identity. It may require separate fittings, separate fuel tanks, unique identification procedures, and testing similar to procedures used for gasoline and diesel fuels at gas stations, with the potential for much more severe safety consequences if mistakes are made.

Thus, 100% synthesized fuels should be drop-in for all aviation applications, at least in the short- to mid-term. However, the specifications for Jet A/A-1 may be refined and expanded as additional learning is acquired.

APPROACHES TO ACHIEVE 100% SYNTHESIZED JET FUEL

Here are approaches to achieve 100% synthesized jet fuel that should be considered.

1. Replicate All Jet A/A-1 Properties in a Single Fuel. In 1999, Sasol developed Fischer-Tropsch (FT) fuels from coal, first as no more than a 50% blending component, then, with a process change to include aromatics to replicate all Jet A/A-1 properties, as a 100% fully synthesized jet fuel. Extensive testing, including long duration engine tests, ensured that all the required Jet A/A-1 performance characteristics were met. Similarly, there are current biomass-based pathways, some of which are FT processes, that replicate all Jet A/A-1 performance properties (MODUK, 2020).
2. Replicate All Jet A/A-1 Properties in a Blended Fuel. Current synthesized blending components must be combined with conventional Jet A/A-1 to meet all necessary performance properties including aromatic content. In the future, a synthesized blendstock with no aromatics could be combined with a synthesized blendstock with aromatic content to achieve a 100% synthesized that meets all required Jet A/A-1 properties. Conceivably, as many blending components as needed could be used to replicate the properties of Jet A/A-1.
3. Substitute for Aromatics or Reduce Aromatics Requirement. The requirement for aromatics is linked to the performance of nitrile seals in older engines: without the aromatics, the seals shrink and fuel leaks occur. Other molecules, such as cycloparaffins, can act like aromatics from seal performance perspective (Graham, et al., 2013). This potential is currently under evaluation. Additionally, the 8% lower limit for aromatics is known to be safe with margin (Heminghaus, et al., 2006). If 100% SAF with low or no aromatics is sought to reduce nvPM, the specification for aromatics could be reduced or removed, while retaining all other Jet A/A-1 performance properties. Research could identify substitute molecules and the true lower limit of aromatic content.
4. Remove the Requirement for Seal-Swelling Components (non-drop-in). Modern engines have replaced nitrile seals with better performing fluorocarbons and fluorosilicone seals. Engine and flight tests have been performed on "neat" SAFs (Applied Research Associates, 2016; Airbus, 2021; Palmer, 2021; Rolls-Royce, 2021). Thus, a fuel without aromatics, e.g. 100% paraffinic, that matches all other specifications for Jet A/A-1 could be considered for use in compatible aircraft. However, this fuel would not be "drop-in" for legacy aircraft and would face the reliability and safety concerns outlined previously.
5. Redefine Jet Fuel Requirements. It is possible that not all the current specifications for Jet A/A-1 are necessary for engine and aircraft performance. Changing, removing, or adding alternative requirements may make it easier to produce improved synthesized fuels from biological sources. Bacteria and yeast tend to produce very specific chemicals rather than a broad range of chemical components like petroleum-based Jet A/A-1. For example, the "Hydroprocessed Fermented Sugars to Synthetic Isoparaffins" process (ASTM D7566 A3, HFS-SIP) produces solely farnesene, a 15-carbon molecule (ASTM International, 2021), Extensive research and testing are needed to define specification modifications and assure the reliability and safety of fuels produced to the redefined specifications.

Currently, the first two options (100% synthesized fuels from a single or blended fuels) could be near term paths, while Options 3 and 5 (redefining jet fuel requirements based on further research) have future potential with sufficient research and learning. Option 4 (non-drop-in fuels) is not desirable since it would require significant, expensive changes to aircraft equipment and infrastructure.

Thus far, the ASTM D4054 specification process has been viewed from the perspective of comparison to a conventional fuel (Rumizen, 2021). A key question is whether and how this process could be changed to better enable 100% synthesized fuels. Does the ASTM specification process need to become more stringent to capture unknowns that have been ignored because they have been unknown for petroleum-based fuels? Or can it be simplified due to more physics and chemistry-based understanding? Recently an optional prescreening approach has been formalized that uses only a small quantity of fuel to perform analyses that help identify the suitability and potential gaps for a particular proposed fuel (CAAFI R&D Team, 2019). It may be possible to make other changes to make the process more effective and efficient while continuing to ensure the safety of aviation fuels.

The ASTM qualification process should be continuously reviewed and improved as additional learning with respect to 100% synthesized fuels and their properties is acquired, which in the longer term would enable modifications to jet fuel specifications needed for Options 3 and 5 above.

SUSTAINABILITY OF 100% SYNTHESIZED JET FUEL

To further refine the definition of a 100% synthesized aviation fuel to 100% *Sustainable* Aviation Fuel, any SAF needs to be produced in a way that demonstrably meets sustainability criteria to ensure environmental, social, and economic performance. Sustainability requirements are applied to synthesized aviation fuels separately from the technical, safety, and performance characteristics that qualify a fuel to be used in aviation under the ASTM specifications; therefore, a 100% synthesized fuel is not necessarily a 100% sustainable aviation fuel, even if it comes from a renewable feedstock. Nevertheless, the sustainability performance is critical to the value proposition of these fuels and must be ensured.

There are existing approaches to evaluate the environmental performance of SAF, including regulatory scheme compliance, such as qualification for the United States Renewable Fuel Standard (US Environmental Protection Agency, 2010) or California's Low Carbon Fuel Standard (State of California, 2020). The full sustainability (environmental, social, and economic) performance of SAF can be evaluated and assured through the use of voluntary sustainability certification schemes, such as those used for CORSIA qualification (ICAO, 2021b) or the European Union's Renewable Energy Directive (European Union, 2021). The certification approach assures sustainable production of SAF to the extent possible.

Currently, there is no consistent definition for the use of the term SAF. The aviation sector must continue to decide how to evaluate the sustainability of SAF, which sustainability factors to address, and whether the existing approaches for regulatory compliance and voluntary certification are sufficient to qualify fuels as sustainable. At a minimum, it is reasonable to expect that the aviation sector will call fuels SAF that meet the sustainability criteria agreed upon by ICAO for CORSIA (ICAO, 2021c), as these are clearly defined and can be used to meet existing emissions obligations. Some nations and some airlines or aviation groups may commit to greater sustainability requirements or specific requirements in isolation (e.g., the United States Grand Challenge defines SAF as having a 50% reduction in carbon intensity for SAF, whereas CORSIA requires a 10% reduction). A minimum standard for labeling fuels as SAF will reduce confusion and ensure that SAF achieve the sustainability performance on which their value proposition depends.

It should be noted that sustainability certification as currently implemented does not fully address important societal choices and tradeoffs that are beyond the scope of aviation, such as interactions among economies, competition/balance with other renewable energy approaches, how wastes should be credited as feedstocks, and how these considerations should be valued both locally and internationally. Previous studies have concluded that biofuels in particular may have issues of overall scalability and environmental impact if deployed at a global level as a primary fossil energy replacement solution (de Castro et al., 2014; Gomiero, 2015). These factors are not addressed by certification at the fuel/feedstock producer level. The choice of which sectors of the economy use bio-based fuels and the scale of their use are societal decisions to which the aviation sector can contribute.

DISCUSSION

While the ongoing ICAO Long Term Aspirational Goals (LTAG) exercise is considering technology horizons in aviation of 2050 and 2070 (ICAO, 2021d), action must be taken now, as the actions with the greatest impacts will take time to penetrate the global aviation market.

Considering the options presented herein, the definition and qualification process for Option 1—Replicate All Jet A/A-1 Properties in a Single Fuel—could be achievable within 2 years. This approach has already been pioneered by SASOL, and other fuels are following that pathway (DefStan 91-091). Option 2—Replicate All Jet A/A-1 Properties in a Blended Fuel—could follow closely, a year or two behind, since in essence, it is the pathway being followed for current blended SAFs. The ASTM Task Force AC598 (Standardization of Jet Fuel Fully Comprised of Synthesized Hydrocarbons) has begun work to consider the definition and qualification process for Options 1 and 2 (Polek, 2021); that process will need to take into account the challenges laid out in this paper.

Options 3 and 5 that would modify Jet A/A-1 properties require significant research and testing before the safety of either replacing or lowering the aromatics is assured, and any redefinition of, or addition to, current specifications or standards is made. Future research must include investigation of how fuel compositions interact with the operability, reliability and safety of aircraft and flight. Finally, since Option 4—Remove the Requirement for Seal-Swelling Components—leads to a non-drop-in fuel, it is not likely to be supported by industry.

AUTHOR CONTRIBUTIONS

The individual authors listed here were all engaged in the drafting, revision, and referencing of this mini-review based on individual and organizational experience and knowledge.

FUNDING

KL and PH participation was funded by the United States Federal Aviation Administration Office of Environment and Energy through agreement number 693KA9-20-N-00013 under the supervision of Nathan Brown. JH work was funded by United States Federal Aviation Administration Office of Environment and Energy through ASCENT, the FAA Center of Excellence for Alternative Jet Fuels and the Environment, Project 34 through FAA Award Number 13-C-AJFE-UD-024 under the supervision of Anna Oldani. Any opinions, findings, conclusions or recommendations expressed in this material are those of the authors and do not necessarily reflect the views of the FAA. Open access publication fees are provided by the FAA through the Volpe National Transportation Systems Center.

REFERENCES

Airbus (2021). An A350 Fuelled by 100% SAF Just Took off. Available at: https://www.airbus.com/newsroom/stories/A350-fuelled-by-100-percent-SAF-just-took-off.html (Accessed September 9, 2021).

Anuar, A., Undavalli, V. K., Khandelwal, B., and Blakey, S. (2021). Effect of Fuels, Aromatics and Preparation Methods on Seal Swell. *Aeronaut. J.* 125, 1542–1565. doi:10.1017/aer.2021.25

Applied Research Associates (2016). ARA's History-Making Sustainable Aviation Fuel (SAF) Technology. Available at: https://www.ara.com/products/readijet/ (Accessed September 9, 2021).

ASTM International (2020). *D1655-20d: Standard Specification for Aviation Turbine Fuels*. West Conshohocken, PA, USA: ASTM International.

ASTM International (2021). *D7566-20c: Standard Specification for Aviation Turbine Fuel Containing Synthesized Hydrocarbons*. West Conshohocken, PA, USA. doi:10.1520/D7566-20C

ATAG (2021). Waypoint 2050. Air Transport Action Group. Available at: https://aviationbenefits.org/environmental-efficiency/climate-action/waypoint-2050/.

Bell, D. C., Heyne, J. S., Won, S. H., and Dryer, F. L. (2018). "The Impact of Preferential Vaporization on Lean Blowout in a Referee Combustor at Figure of Merit Conditions," in Proceedings of the ASME 2018 Power Conference collocated with the ASME 2018 12th International Conference on Energy Sustainability and the ASME 2018 Nuclear Forum, Lake Buena Vista, FL, USA, June 24–28, 2018 (ASME). doi:10.1115/POWER2018-7432

Boehm, R. C., Colborn, J. G., and Heyne, J. S. (2021). Comparing Alternative Jet Fuel Dependencies between Combustors of Different Size and Mixing Approaches. *Front. Energ. Res.* 9, 701901. doi:10.3389/fenrg.2021.701901

Boeing (2021). Boeing Commits to Deliver Commercial Airplanes Ready to Fly on 100% Sustainable Fuels. Available at: https://boeing.mediaroom.com/2021-01-22-Boeing-Commits-to-Deliver-Commercial-Airplanes-Ready-to-Fly-on-100-Sustainable-Fuels (Accessed December 8, 2021).

CAAFI R&D Team (2019). Prescreening of Synthesized Hydrocarbons Intended for Candidates as Blending Components for Aviation Turbine Fuels (Aka Alternative Jet Fuels or AJF). Available at: https://www.caafi.org/tools/docs/CAAFI_RD_Prescreening_Guidance_Document_v1.0.pdf.

CAAFI (2021). About CAAFI. Available at: https://caafi.org/about/caafi.html.

Colket, M. B., Heyne, J., Rumizen, M., Edwards, J. T., Gupta, M., Roquemore, W. M., et al. (2016). An Overview of the National Jet Fuels Combustion Program. *AIAA J.*, 1087–1104. doi:10.2514/1.J055361

Colket, M., and Heyne, J. (2021). Fuel Effects on Operability of Aircraft Gas Turbine Combustors. *Prog. Astronautics Aeronautics*, 1–534. doi:10.2514/4.106040

Csonka, S. (2020). Aviation's Market Pull for SAF (Sustainable Aviation Fuel). Available at: https://www.caafi.org/focus_areas/docs/CAAFI_SAF_Market_Pull_from_Aviation.pdf (Accessed September 3, 2021).

de Castro, C., Carpintero, Ó., Frechoso, F., Mediavilla, M., and de Miguel, L. J. (2014). A Top-Down Approach to Assess Physical and Ecological Limits of Biofuels. *Energy* 64 (1), 506–512. doi:10.1016/j.energy.2013.10.049

Edwards, J. (2017). "Reference Jet Fuels for Combustion Testing," in 55th AIAA Aerospace Sciences Meeting, Grapevine, TX, January 9-13, 2017 (American Institute of Aeronautics and Astronautics). Available at: https://www.caafi.org/news/pdf/Edwards_AIAA-2017-0146_Reference_Jet_Fuels.pdf.

European Union (2021). Voluntary Schemes. Available at: https://ec.europa.eu/energy/topics/renewable-energy/biofuels/voluntary-schemes_en.

Fleming, G., and de Lepinay, I. (2019). Environmental Trends in Aviation to 2050. International Civil Aviation Organization (ICAO). Available at: https://www.icao.int/environmental-protection/Documents/EnvironmentalReports/2019/ENVReport2019_pg17-23.pdf.

Gomiero, T. (2015). Are Biofuels an Effective and Viable Energy Strategy for Industrialized Societies? A Reasoned Overview of Potentials and Limits. *Sustainability* 7 (7), 8491–8521. doi:10.3390/su7078491

Graham, J. L., Rahmes, T. F., Kay, M. C., Belières, J.-P., Kinder, J. D., Millett, S. A., et al. (2013). Impact of Alternative Jet Fuel and Fuel Blends on Non-Metallic Materials Used in Commercial Aircraft Fuel Systems. Available at: https://www.faa.gov/about/office_org/headquarters_offices/apl/research/aircraft_technology/cleen/reports/media/Boeing_Alt_Fuels_Final.pdf.

Hemighaus, G., Boval, T., Bacha, J., Barnes, F., Franklin, M., Gibbs, L., et al. (2007). *Aviation Fuels Technical Review*. San Ramon, CA: Chevron Products Company.

Heminghaus, G., Boval, T., Bosley, C., Organ, R., Lind, J., Brouette, R., et al. (2006). *Alternative Jet Fuels, Addendum 1 to Aviation Fuels Technical Review*. San Ramon, CA: Chevron Corporation.

Hepperle, M. (2012). "Electric Flight – Potential and Limitations," in AVT-209 Workshop on Energy Efficient Technologies and Concepts Operation, Lisbon, Portugal. Available at: https://www.sto.nato.int/publications/STO%20Meeting%20Proceedings/Forms/Meeting%20Proceedings%20Document%20Set/docsethomepage.aspx?ID=30995&FolderCTID=0x0120D5200078F9E87043356C409A0D30823AFA16F602008CF184CAB7588E468F5E9FA364E05BA5&List=7e2cc123-6186-4c30-8082-1ba072228ca7&RootFolder=%2Fpublications%2FSTO%20Meeting%20Proceedings%2FSTO%2DMP%2DAVT%2D209 (Accessed August 10, 2021).

Heyne, J., Rauch, B., Le Clercq, P., and Colket, M. (2021). Sustainable Aviation Fuel Prescreening Tools and Procedures. *Fuel* 290, 120004. doi:10.1016/j.fuel.2020.120004

IATA (2019). Aircraft Technology Roadmap to 2050. International AIr Transport Association (IATA). Available at: https://www.iata.org/contentassets/8d19e716636a47c184e7221c77563c93/technology20roadmap20to20205020no20foreword.pdf.

ICAO (2021a). Carbon Offsetting and Reduction Scheme for International Aviation (CORSIA). Montreal, Quebec, Canada. Available at: https://www.icao.int/environmental-protection/CORSIA/Pages/default.aspx.

ICAO (2021b). CORSIA Approved Sustainability Certification Schemes. Available at: https://www.icao.int/environmental-protection/CORSIA/Documents/ICAO%20document%2004%20-%20Approved%20SCSs.pdf.

ICAO (2021c). CORSIA Eligible Fuels. Available at: https://www.icao.int/environmental-protection/CORSIA/Pages/CORSIA-Eligible-Fuels.aspx.

ICAO (2021d). Feasibility of a Long Term Global Aspirational Goal for International Aviation. Available at: https://www.icao.int/environmental-protection/Pages/LTAG.aspx.

ICAO (2018). Sustainable Aviation Fuels Guide Version 2. Available at: https://www.icao.int/environmental-protection/Documents/Sustainable%20Aviation%20Fuels%20Guide_100519.pdf.

Lee, D. S., Fahey, D. W., Skowron, A., Allen, M. R., Burkhardt, U., Chen, Q., et al. (2021). The Contribution of Global Aviation to Anthropogenic Climate Forcing for 2000 to 2018. *Atmos. Environ.* 244, 117834. doi:10.1016/j.atmosenv.2020.117834

Malicier, V. (2021). *Fuel Suppliers Urge Governments to Impose SAF Blending Mandates*. Editor J. Fox (London, UK: S&P Global Platts).

McKinsey and Co (2020). Hydrogen-powered Aviation: A Fact-Based Study of Hydrogen Technology, Economics, and Climate Impact by 2050. Brussels: European Commission. Available at: https://www.fch.europa.eu/sites/default/files/FCH%20Docs/20200507_Hydrogen%20Powered%20Aviation%20report_FINAL%20web%20%28ID%208706035%29.pdf.

MODUK (2020). DEF STAN 91-091, Revision I12. MODUK - British Defense Standards (MODUK). Available at: https://www.academia.edu/28340693/Ministry_of_Defence_Defence_Standard_91_91.

Moore, R. H., Shook, M., Beyersdorf, A., Corr, C., Herndon, S., Knighton, W. B., et al. (2015). Influence of Jet Fuel Composition on Aircraft Engine Emissions: A Synthesis of Aerosol Emissions Data from the NASA APEX, AAFEX, and ACCESS Missions. *Energy Fuels* 29 (4), 2591–2600. doi:10.1021/ef502618w

Palmer, W. (2021). United Flies World's First Passenger Flight on 100% Sustainable Aviation Fuel Supplying One of its Engines. GE Future of Flight. Available at: https://www.ge.com/news/reports/united-flies-worlds-first-passenger-flight-on-100-sustainable-aviation-fuel-supplying-one.

Peiffer, E. E., Heyne, J. S., and Colket, M. (2019). Sustainable Aviation Fuels Approval Streamlining: Auxiliary Power Unit Lean Blowout Testing. *AIAA J.* 57 (11), 4854–4862. doi:10.2514/1.J058348

Polek, G. (2021). OEMs All in on SAF Development. AIN Online. Available at: https://www.ainonline.com/aviation-news/air-transport/2021-06-01/oems-all-saf-development.

Rolls-Royce (2021). Rolls-Royce Conducts First Tests of 100% Sustainable Aviation Fuel for Use in Business Jets. Available at: https://www.rolls-royce.com/https://www.rolls-royce.com/media/press-releases/2021/01-02-2021-business-aviation-rr-conducts-first-tests-of-100-precent-sustainable-aviation-fuel.aspx (Accessed September 9, 2021).

Rumizen, M. A. (2021). Qualification of Alternative Jet Fuels. *Front. Energ. Res.* 9, 760713. doi:10.3389/fenrg.2021.760713

Schäfer, A. W., Barrett, S. R. H., Doyme, K., Dray, L. M., Gnadt, A. R., Self, R., et al. (2019). Technological, Economic and Environmental Prospects of All-Electric Aircraft. *Nat. Energ.* 4, 160–166. doi:10.1038/s41560-018-0294-x

Stachler, R., Heyne, J., Stouffer, S., and Miller, J. (2020). Lean Blowoff in a Toroidal Jet-Stirred Reactor: Implications for Alternative Fuel Approval and Potential Mechanisms for Autoignition and Extinction. *Energy Fuels* 34 (5), 6306–6316. doi:10.1021/acs.energyfuels.9b01644

State of California (2020). *Low Carbon Fuel Standard Regulation*. Sacramento, CA, USA: State of California.

U.S. White House (2021). FACT SHEET: Biden Administration Advances the Future of Sustainable Fuels in American Aviation. Washington, DC, USA. Available at: https://www.whitehouse.gov/briefing-room/statements-releases/2021/09/09/fact-sheet-biden-administration-advances-the-future-of-sustainable-fuels-in-american-aviation/(Accessed December 07, 2021).

US Environmental Protection Agency (2010). 40 CFR Part 80, Subpart M. *Renewable Fuel Stnadard*. USA. Available at: https://www.epa.gov/renewable-fuel-standard-program/regulations-and-volume-standards-renewable-fuel-standards (Accessed August 10, 2021).

Voigt, C., Kleine, J., Sauer, D., Moore, R. H., Bräuer, T., Le Clercq, P., et al. (2021). Cleaner Burning Aviation Fuels Can Reduce Contrail Cloudiness. *Commun. Earth Environ.* 2 (114). doi:10.1038/s43247-021-00174-y

Won, S. H., Rock, N., Lim, S. J., Nates, S., Carpenter, D., Emerson, B., et al. (2019). Preferential Vaporization Impacts on Lean Blow-Out of Liquid Fueled Combustors. *Combustion and Flame* 205, 295–304. doi:10.1016/j.combustflame.2019.04.008

Zschocke, A., Scheuermann, S., and Ortner, J. (2012). High Biofuel Blends in Aviation (HBBA): ENER/C2/2012/420-1 Final Report. Available at: https://ec.europa.eu/energy/sites/ener/files/documents/final_report_for_publication.pdf.

Conflict of Interest: Author SK was employed by the company Pratt & Whitney. Author GA was employed by the Company General Electric. Author JE was employed by the company Boeing.

The remaining authors declare that the research was conducted in the absence of any commercial or financial relationships that could be construed as a potential conflict of interest.

Publisher's Note: All claims expressed in this article are solely those of the authors and do not necessarily represent those of their affiliated organizations, or those of the publisher, the editors, and the reviewers. Any product that may be evaluated in this article, or claim that may be made by its manufacturer, is not guaranteed or endorsed by the publisher.

frontiers in Energy Research

REVIEW
published: 24 January 2022
doi: 10.3389/fenrg.2021.771849

Social Science Applications in Sustainable Aviation Biofuels Research: Opportunities, Challenges, and Advancements

Brian J. Anderson[1], Daniel W. Mueller[2], Season A. Hoard[1,3], Christina M. Sanders[1] and Sanne A. M. Rijkhoff[4]*

[1]Division of Governmental Studies and Services, Washington State University, Pullman, WA, United States, [2]United States Coast Guard Academy, New London, CT, United States, [3]School of Politics, Philosophy and Public Affairs, Washington State University, Pullman, WA, United States, [4]Deparment of Social Sciences, Texas A&M University—Corpus Christi, Corpus Christi, TX, United States

Social science has an important role in aviation biofuels research, yet social science methods and approaches tend to be underdeveloped and under-utilized in the broader aviation biofuels literature and biofuels overall. Over the last 5 years, social science approaches in aviation biofuels research, particularly site-selection, have made several advances. Where early site-selection models either entirely excluded social science concepts or included only a few measurements using poor proxies, current models more accurately, and more comprehensively capture key social science concepts to better examine and predict project implementation success and long-term sustainability. Despite several studies published within the last 20 years noting the need for more empirical studies of social sustainability and improvement in incorporation of social criteria, progress has remained rather stagnant in several areas. To help move the field forward, we conduct a review of the current state of social science research in aviation biofuels with a focus on sustainability, site-selection, and public acceptance research, identifying key approaches, important developments, and research gaps and weaknesses of current approaches. While several review studies already exist, they tend to focus on a single area of biofuels such as public acceptance. By broadening our review to several areas, we are able to identify several common limitations across these areas that contribute to the continued underutilization of social science approaches in aviation biofuels. This includes the preference for practical and reliable indicators for social criteria that prioritize quantitative methods over other approaches. Based on these limitations, we make several recommendations to improve social science research in aviation biofuels, including ensuring that social scientists are key members of the research team, the adoption of a mixed-methods research designs that combines quantitative and qualitative approaches that better measure some criteria and local-level impacts, and adequate resources for social science research throughout biofuel development projects as these methods are often more time-consuming and costly to implement. We argue that implementing these recommendations in future aviation biofuel development projects will improve social

OPEN ACCESS

Edited by:
Mohammad Rehan, King Abdulaziz University, Saudi Arabia

Reviewed by:
Richa Arora, Punjab Agricultural University, India
Abdul-Sattar Nizami, Government College University, Lahore, Pakistan

***Correspondence:**
Brian J. Anderson
brian.anderson2@wsu.edu

Specialty section:
This article was submitted to Bioenergy and Biofuels, a section of the journal Frontiers in Energy Research

Received: *07 September 2021*
Accepted: *13 December 2021*
Published: *24 January 2022*

Citation:
Anderson BJ, Mueller DW, Hoard SA, Sanders CM and Rijkhoff SAM (2022) Social Science Applications in Sustainable Aviation Biofuels Research: Opportunities, Challenges, and Advancements. Front. Energy Res. 9:771849. doi: 10.3389/fenrg.2021.771849

science approaches utilized in aviation biofuels research and address a long-acknowledged gap in the field.

Keywords: aviation biofuel, social science, sustainability, social acceptance, modeling, methodology, research methods

1 INTRODUCTION

The social sciences have much to contribute to aviation biofuels development, the broader literature and research in sustainability, and expertise in the effective and appropriate use of social science research and methodology, such as survey design, implementation, and analysis. Despite this importance, social science research in the field continues to be undervalued, underdeveloped, underrepresented or, at times, ignored across the literature, especially in empirical studies. While there has been improvement in recent studies, inclusion of social science considerations in empirical sustainable aviation fuel research is still in its early stages. Social science aspects, when employed, can play an important role in helping assess potential for acceptance of biofuel-related projects (Marciano et al., 2014; Ahmad and Xu, 2019; Segreto et al., 2020), provide the opportunity to more fully assess community capacity to sustain biofuel facilities (See Martinkus et al., 2017; Rijkhoff et al., 2017; Martinkus et al., 2019; Mueller et al., 2020; Rijkhoff et al., 2021), and more fully understand the sustainability of biofuel supply chains (See Wang et al., 2017; Pashaei Kamali et al., 2018; Wang et al., 2019).

Despite these advancements, there are several limitations to the application of social science research and methodologies in biofuels development. Part of the issue is the preference for accessible and reliable quantitative measures, especially in frameworks that attempt to combine environmental, economic, and social sustainability criteria. As many important social sustainability criteria are not easily accessible without additional, often qualitative research, this preference leads to similar social criteria with questionable validity being employed. To be sure, social science has made important contributions in the field of biofuel development, but this work has much less prominence, less resources are committed to social aspects of biofuel development and sustainability, and ultimately, the consequence is that the understanding of social costs and benefits of biofuel development are lacking, especially at the local level.

As more public and private attention and funding is being devoted to aviation biofuels research globally, this is an ideal time to address social science research gaps in the field. To facilitate this process, a review of social science research was conducted in three broad areas of aviation biofuels research, sustainability, site-selection, and public acceptance. Social science research and methodologies clearly exist outside these three broad areas; however, much theoretical and empirical social science work in the field is focused on these aspects of aviation biofuels development; thus, addressing gaps in these areas has the potential to move the field forward significantly. While several good reviews of research in social sustainability, social criteria, and site-selection exist (See Vallance et al., 2011; Kurka and Blackwood 2013; Pashaei Kamali et al., 2018; Gnansounou and Alves 2019b), these studies focus on biofuels in general, or on one aspect of aviation biofuels development research, such as sustainability or site-selection, and do not attempt or only cursorily examine larger trends across different areas of the broader development literature. This broader focus allows for identification of common limitations and issues in the way social science research and methods are applied in aviation biofuels research and assertion of specific policy and practical recommendations to address these gaps and limitations. One of the best methods for improving social science research and outcomes is to ensure that every biofuel development project is required to have a social science research team that is staffed with actual social scientists, with a variety of methods backgrounds, that this team is equal to other counterparts in the project (as evidenced by at least one member being a Co-PI), and that the team is adequately funded to conduct long-term social science research at both the national, regional and local level throughout the duration of the project.

We also argue an important area for future improvement, no matter the area of research, is more truly mixed-methods research that combines quantitative and qualitative measures, especially at the local level. While we acknowledge that quantitative methods that combine social, economic and environmental criteria, especially in initial stages, are important, more resources need to be available in all stages of biofuel development to collect local level social measures through both quantitative and qualitative methods. Without this, the full impact of aviation biofuel development, and ultimately the sustainability of this development for current and future generations cannot be assessed.

This article is organized as follows. First, we provide an explanation of our review methodology, followed by a review of social sustainability, especially empirical social sustainability research focusing on appropriate social criteria, identifying current trends, and limitations. Next, we examine combined framework and models used in aviation biofuels research for site-selection and life-cycle social sustainability research. The literature on public acceptance of aviation biofuels is then discussed as well as ways to improve these studies through engagement with the broader biofuels acceptance literature. Lastly, based on shared limitations of social science research in empirical studies across these three broad areas, recommendations are provided for improvement of interdisciplinary research and engagement with the social sciences to more fully evaluate aviation biofuel development.

2 REVIEW METHODOLOGY

This review focuses on social science applications in aviation biofuels research with specific attention to empirical studies that

utilize social science methods and techniques, either wholly or in part. Our aim is to identify how social science has been incorporated into current and past empirical aviation biofuels research. This review is less concerned with conceptual issues and perspectives as many strong reviews, especially in sustainability, already address these issues, and makes empirical applications its central focus. As such, we identified three key areas in aviation biofuels research that constitute much of the social science empirical research currently being used in the field, sustainability, site-selection with a specific attention to combined frameworks and modeling, and public acceptance. The analytical focus on these areas allows us to capture and examine a wide variety of empirical studies across aviation biofuels, identify commonalities in how social science research and methodologies are currently applied, and highlight critical areas for improvement. Based on this, we make recommendations for strengthening social science applications in the future across a vast array of empirical studies, specifically in studies concerning aviation biofuel.

3 SUSTAINABILITY

An important concept in research on aviation biofuel is sustainability. However, it is often unclear what is meant precisely with this word, which leads to challenges of measuring sustainability and thus makes it difficult to provide evidence of said sustainability in projects. Generally, sustainability is viewed as a balance and trade-off between environmental sustainability, economic sustainability, and social sustainability. This three-pillar approach of sustainability has been conceptualized in several ways, among which interconnected pillars (Basiago 1995; Moldan et al., 2012), dimensions (Stirling, 1999; Mori and Christodoulou, 2012); components (Du and Jacobus, 2006; Zijp et al., 2015). Popular depictions of the model include venn diagrams, concentric circles, and pillars where sustainability is identified in the overlap between components or supported by the three separate pillars. This approach, while still prominent in the sustainability literature, has been criticized for being under-theorized and for over-simplified depictions that obfuscate the meaning of sustainability, leading to inconsistent operationalization, and hindering understanding of the overall concept (Thompson, 1995; Purvis et al., 2019).

This three-component approach also dominates the biofuels sustainability research, and variations of this approach are present in several public and private biofuel certification schemes. Among the three components, social sustainability is particularly difficult to define, and across sustainably literatures there are various interpretations of the concept. These definitions are often based, at least partially, upon the definition of sustainable development in the Brundtland Report, which defined sustainability as "development that meets the needs of the present without compromising the ability of future definitions to meet their own needs" (Brundtland, 1987, p. 40). As a whole, social sustainability conceptualization and operationalization tends to focus on social equality across several dimensions, including economic, gender, educational, health, and cultural equality (Moldan et al., 2012), but even this generalization oversimplifies the plethora of conceptual and empirical studies that attempt to examine social sustainability in different ways. This conceptual muddle leads to various typologies and dimensions for social sustainability that can contribute to further confusion (See Foladori 2005; Vallance et al., 2011; Åhman 2013). Put simply, the definition of social sustainability is still being developed and there is not one generally accepted definition or operationalization of this concept.

In their review of sustainability literature, Vallance et al. (2011) distinguish between three types of social sustainability: developmental social sustainability, bridge social sustainability, and maintenance social sustainability. Developmental social sustainability is rooted in the definition of development found in the previously mentioned Brundtland Report, and focuses on needs met through economic development, and tends to assume positive social outcomes from this development. According to the authors, "it captures the essence of a much larger construct that attempts to address both tangible and less tangible necessities for life which, in turn, was seen to depend on reviving growth; changing the quality of growth; meeting essential needs for jobs, food, energy, water, and sanitation…" (p. 343). This literature focuses on sustainability in addressing basic, physical needs (McKenzie, 2004; Dudziak 2007), and examining equity in access to services, education and other factors that threaten society in the long term (Campbell 1996; Partridge 2005). Bridge social sustainability is less anthropocentric and focuses on the needs of the biophysical environment, while maintaining social sustainability "speaks to traditions, practices, preferences and places people would like to see *maintained* (sustained) or improved" (Vallance et al., 2011, p. 345). These types of sustainability conflict cause confusion as the needs of the people (developmental) conflict with their desires (maintenance) and the needs of the environment (bridge) (Vallance et al., 2011). Additionally, conflict occurs when you examine whose needs are being met (as these needs are rarely met across groups of people), or whether maintenance of some resources actually harms other resources and groups.

While Vallance et al. (2011) framework is referenced in more studies, it is not the only framework or typology which tends to produce additional confusion. Åhman (2013) examines the many theoretical frameworks that exist in the social sustainability literature, including Vallance et al. (2011), and differentiates between several themes: basic needs and equity, education, quality of life, social capital, social cohesion, integration and diversity, sense of place development/ maintenance, and others. The author argues for a larger "polemic structure" based on similarities across the different frameworks and themes that helps us better understand the concept "as a construct entailing value statements and scientific methods as well as cultural, political, and economic positions" (p. 1163). Because the conceptualization of social sustainability is complex and contentious, it should be no surprise that social indicators are equally contentious; scientists in a variety of disciplines have debated appropriate indicators.

Similar to issues with conceptualization, the operationalization of social sustainability is problematic. In terms of empirical research, social sustainability receives much less attention than both the environmental and economic pillars in biofuel sustainability research (See Demirbas 2004; Cherubini et al., 2009; Acquaye et al., 2011; Clarens et al., 2011). In fact, several recent studies continue to examine sustainability without including social aspects or only focus on economic viability (See Diniz et al., 2018; Resurreccion et al., 2021). When social sustainability is included, it tends to focus on a developmental perspective and more specifically basic needs.

Additionally, while several key certification schemes include social sustainability aspects, the extent to which it is addressed and whether it is included in monitoring and reporting standards varies (Scarlet and Dallemand 2011; de Man and German, 2017). For instance, EU-RED (European Union's Renewable Directive 2009/28/EC) does not include social sustainability criteria, instead relegating aspects of social sustainability to biennial reporting mechanisms (See de Man and German 2017). Not only is this problematic from a theoretical standpoint, as one of the necessary pillars for overall sustainability is ignored or insufficiently examined, but the cumulative evidence from several biofuel-related projects illustrates that "costs and benefits are unevenly distributed within and between communities, with consequences for the ways in which social, economic, and environmental impacts are experienced" (Hodbod and Julia, 2013). As a result, only certain actors are better positioned to capitalize on biofuel production opportunities and poverty reduction in rural areas is not guaranteed with biofuel expansion (Hodbod and Julia, 2013). Correa et al. (2019) make several recommendations for implementing sustainable biofuel production systems and call for "rigorous assessments that integrate socioeconomic and environmental objectives at local, regional, and global scales". Despite these calls, local level analysis is still lacking.

Social sustainability has received more attention in the last 20 years; however, conceptual studies far outweigh empirical analysis in biofuels sustainability research (See Pashaei Kamali et al., 2018; Gnansounou and Alves 2019b). Among empirical studies, few have included social sustainability criteria in a broader attempt to identify appropriate indicators for biofuel sustainability evaluations, often using systematic literature reviews to identify potential indicators and expert surveys or stakeholder engagement to rank potential indicators according to their relevance (relevance of criteria to system sustainability), practicality (existence of measurements, data availability, data costs), reliability (reliability/reproducibility of available data), importance (importance of criteria for assessing sustainability of system), and other metrics (See Buchholz et al., 2009; Kurka and Blackwood 2013; Pashaei Kamali et al., 2018).

Surveys are increasingly used in aviation biofuels in a variety of ways, including but not limited to assessing public opinion and support, identifying sustainability criteria, evaluating the impact of noise on health of populations, and stakeholder engagement. While several technological developments have made surveys more accessible to researchers, limited prior experience with survey methodology can lead to surveys with questionable reliability, validity, and at times improper analysis and generalization. A good source for those interested in using survey methodology is Dillman et al. (2014) which covers design and implementation of phone, mail, and online surveys.

Studies ranking sustainability criteria have used both survey methodology and stakeholder engagement but conclusion drawn are problematic given their sample sizes, questions, and analysis. For instance, when social, environmental, and economic criteria were ranked together, social criteria were ranked lower across dimensions and often had the most disagreement across experts (Buchholz et al., 2009; Kurka and Blackwood 2013). Additionally, where several social criteria were ranked highly in relevance, especially local level factors such as standard of living, they often performed poorly in reliability, practicality, and importance. Social criteria were also rated significantly differently between industrialized and non-industrialized countries (Buchholz et al., 2009). In their recommendations, Buchholz et al. (2009) did not rule out any criteria, instead recommending more engagement to identify the top third criteria for assessment. In contrast, Kurka and Blackwood (2013), based on feedback from experts, narrowed their list to the following two social criteria: *regional job creation* (created jobs/kWh for plants and supply chains) and *regional food security* (the percentage of total productive land use change in favour of energy crop plantation).

It is concerning that Kurka and Blackwood chose to narrow the list of social criteria based on results of their survey of experts. First, Bussholz et al. (2009) had 46 global bioenergy experts respond to their survey while Kurka and Blackwood had only 13 total regional participants in their stakeholder forum. Both these sample sizes necessitate limited generalization and caution, and do not support making any preliminary decisions regarding these criteria. Additionally, these surveys used non-probability sampling, which makes sense given the sample size, which further limits any inferences to the larger population of biofuels experts. Both studies also provide limited background on their participants, stressing their expertise either regionally or globally in biofuels. Kurka and Blackwood (2013) do state they used non proportional quota sample to get a balance of participants from the following backgrounds: "local authorities, the regulative body, the business support agency, environmental protection, harvesting and supply, sawmilling, bioenergy production, agriculture, forestry, and waste management". Based on the information given, it is unlikely that social science experts were included in either study, or at least had very limited participation in ranking criteria. This would bias results of the ranking exercises as it is unclear that those with different backgrounds would have the expertise to effectively rank these criteria.

In their assessment of the literature, Pashaei Kamali et al. (2018) only included social criteria stating that the social dimension of sustainability is far less developed than environmental and economic dimensions. These authors argue that in order to assess social performance of biofuel supply chains, relevant social and governance issues must be identified, which should be done through case studies rather than attempting to create a static framework and indicators (see also Wang et al., 2017, Wang et al., 2019). Through a case-study of the sugarcane

biojet fuel supply chain in Brazil, these authors included biofuel sector experts' evaluations of social and governance issues found in a systematic literature review according to their relevance, practicality, reliability, importance, and simplicity. They found a high level of agreement between the literature review (factors examined by studies) and the sector experts, with the most practical factors included in more empirical studies. For instance, while human health and safety was identified as the most important and relevant issue, it was not rated as highly in practicality, reliability or simplicity, and was only included in one empirical study. In contrast, employment was rated most practical which may be why so many studies include it in social criteria metrics. The authors found that social cohesion and cultural diversity had the lowest rankings across all dimensions by experts and were addressed in no empirical studies. There was also a high-level of support for including human health and safety, labor rights, and social development in certification schemes for Brazil biojet fuel supply, but practicality and reliability hinder their inclusion and implementation which lead the authors to argue that "improvement in measurement and data collection of these issues should be pursued urgently" (Pashaei Kamali et al., 2018).

While the authors' focus on social criteria is laudable and much needed, it is important to note that this study has a relatively small sample size as well (39 valid responses) and the extent of participation of social scientists is unclear. The authors identified five "expert groups" among their sample: academia, consultancy, certification body, government, and non-profit. While some of their academic experts, consultancies, and non-profits may have social science expertise, this is not guaranteed and information to effectively evaluate whether this expertise is present is not provided. At a minimum, better background information needs to be provided in order to determine their ability to fully assess social factors. Studies examining social criteria need to include social science experts in the field. The higher percentage of "no opinion" responses for several social criteria suggest the participants did not have expertise to rank these options. Social science experts, particularly at a regional and local level, are necessary to fully assess these criteria and have better knowledge of what is currently available. These studies are essential for identifying criteria that can accurately assess sustainability and present the perfect opportunity to more fully engage social scientists in sustainability research. We also note some concerns with the questionnaire used that may impact how respondents answered questions. It is not always easy to obtain the survey questionnaire used in published research but access to the survey questionnaire is essential to fully evaluate the methodology and results. First, some questions utilized in the Pashaei Kamali et al. (2018) study may have potentially biased survey responses through question wording, such as using "more relevant" rather than rate the relevance of the following options. Second, some definitions provided may be unclear for some participants. Third, some factors ranked need more explanation to ensure they are interpreted by respondents the same way and in the way the researchers intended. Lastly, often the survey response options did not match the question and the scales should have been better balanced. For instance, for reliability, survey respondents were asked: "which issues do you consider reliable to in jet biofuel supply chain from ethanol? [*sic*]" Not only is question wording confusing, but the response options were actually *the least important, very unimportant, neither important nor unimportant, very important, the most important* and *I don't know*. It is curious that the authors chose not to include just *important* as a response option for a more balanced scale. In future iterations, a seven point Likert scale could be used for more nuanced analysis (although more respondents would be required). Based on the questionnaire we would make several revisions to the survey instrument for more reliable and valid results.

The importance of including social scientists to improve social sustainability research has been noted (see Vallance et al., 2011), yet adequate participation of social scientists seems to be lacking even in more recent studies. Several issues lead to the subjugation of social sustainability and social concerns with limited improvement in measurements used in most empirical studies. First, while the preference for both practical and reliable criteria is understandable in terms of ease of access, use, and comparability across cases, it also preferences quantitative data over other methods. This is problematic as data for many social issues, particularly at the local level, are not widely available and often qualitative. Reliability and practicality does not mean these are valid measurements of the concepts in question. The preference of practical and reliable criteria therefore not only ignores data that may better reflect these concerns and issues but can encourage empirical studies to leave social criteria out altogether. Ultimately, this leads to data driven studies instead of theory informed research.

Second, as noted, the preference for this convenient data can prevent accurate and reliable analysis of social concerns at a local level. Even studies conducting case-study analysis (e.g. Kurka and Blackwood 2013; Pashaei Kamali et al., 2018), do not effectively address these concerns of confusing levels of analysis as regional and local level concerns are not included. The use of national-level data can obfuscate the consequences of biofuel development at the local level. Unfortunately, the preference for reliable and practical quantitative measures encourages a lack of study at a more localized level, or at the very least, incomplete studies with limited quantitative data. Hodbod and Julia, (2013) reviewed the social sustainability analysis of supply chains and found a lack of studies at the local level. In fact, they argue that even studies that include sustainability experts tend to focus on national or even more often, on international effects. Lacking the inclusion of experts at the local level overlooks the detrimental effects of sustainable development at this level (Hodbod and Julia, 2013), which is a significant issue. Based on our evaluation of the methods utilized in these studies and the conclusion drawn, we would also recommend that social science experts with experience in survey methodology be included in this work. Not only should they be present in the review process for published studies but their experience in this field is necessary for improvement of these methods and the conclusion drawn.

While social indicators are often ignored or undervalued, there are at least some contributions to biofuel research that have

attempted to include social metrics in more holistic analyses. Much of this progress is occurring in combining social metrics in broader modeling. This approach still tends to rely on quantitative data and may not be able to perfectly capture local conditions in communities where biofuel supply chains are emerging, but it does indicate a genuine attempt by researchers to pay more attention to social metrics and include them when assessing the overall sustainability of a biofuel supply chain. In the next section, these contributions are explored.

4 COMBINED FRAMEWORKS AND MODELING

One important way the social sciences have contributed to aviation biofuels research is through the development of combined frameworks and modeling to assess sustainability of biofuel supply chains and biorefinery site selection. These approaches attempt to blend traditional indicators of success for biofuel supply chains, such as available feedstocks, infrastructure, economic factors, etc., with often overlooked social indicators that are just as important to determining the viability of these supply chains. Given that most of these attempts rely on quantitative data, the preference is to use quantitative indicators of social sustainability as well which is in conflict with the more appropriate qualitative approach of measuring social science sets. However, despite the combined modeling approach still cannot capture all important social data in a given community, it marks a significant departure from the total omission of social metrics in previous biofuel research.

One major approach utilizing social assets includes the life cycle sustainability assessment (LCSA or LCA), which is a tool designed to assess the environmental, economic, and social sustainability of a biofuel production chain by calculating the impact of the product from feedstock to end user (Fokaides and Christoforou 2016). LCSA has existed for several decades but has only recently been applied to biofuel production as biofuels emerge as an important tool in the fight against climate change. An early study by Markevičius et al. (2010) developed several metrics for sustainability popular in the literature at the time including 15 social metrics (out of 35 total). These include, for example, cultural acceptability within communities, working conditions, and food security for social metrics, among others. However, when the authors asked biofuel experts to rank the most important sustainability metrics in terms of their relevance, practicality, reliability, and importance to biofuel production, social metrics were consistently ranked low in all four attributes, reflecting the inattentiveness of biofuels experts to social sustainability metrics, and the lack of social science participation in these ranking studies.

Collotta et al. (2019) reviewed 60 LCSA studies that examined sustainability at various stages in the biofuel production chain and found that only a handful were attentive to social factors related to biofuel production, including social well-being, and social impacts to farmers and communities where biofuels are produced and refined. This study, completed almost 10 years after the research by Markevičius et al. (2010), reveals, as detailed earlier, that most research on biofuels ignores social factors, even though they are understood to be an equally important part of the three-pillar approach to sustainability. In fact, of the few studies that Collotta et al. (2019) determined to be focused on social factors, most only focused on economic impacts of biofuel production related to revenues, while the remainder explored more nuanced social perspectives, such as the role that social contexts and stakeholder values play in sustainability assessments (Ekener et al., 2018), and how socioeconomic contexts of the societies in which biofuels are produced can cause impacts of biofuel production to be positive in some communities and negative in others (Ekener-Petersen et al., 2014; Ribeiro and Quintanilla 2015). Another comprehensive study of biofuel LCSAs completed since 2008 supported the findings of Collotta et al. (2019), finding that while social indicators were examined in many analyses, of the over 100 analyses indexed, "the main [social] indicator used is employment, and in many analyses, this is the only indicator considered" (Visentin et al., 2020). This is in line with the previously mentioned study by Pashaei Kamali et al. (2018) which shows that within a decade, biofuel experts have made progress in recognizing the importance of social metrics. However, in practice, these metrics are still excluded due to issues with the practicality and ease of including them in quantitative models. Thus, social science is not only overlooked in the more general sustainability analyses in aviation biofuel research, but there is also still a significant lack of the use of proper metrics in the more specialized combined approach of for instance the life cycle sustainability assessments.

While it is clear that social factors of sustainability remain sidelined in the great bulk of biofuel LCSAs, these more nuanced approaches to sustainability assessments of biofuel supply chains remain important. By bringing attention to important social factors that can determine not only whether supply chains are economically viable, but also whether biofuel production can bring long-lasting positive social effects to the communities where production takes place, LCSAs have the potential to enhance our understanding of the viability of biofuel production. As noted by Lan et al. (2020), "the conflicts and relationships between stakeholders at varied scales and levels in [biofuel supply chains (BSC)] need a better understanding to support effective BSC design at an early stage". This suggests that a major challenge to the development of biofuel supply chains and the research associated with them is the dearth of social science research that assesses stakeholder relationship and other social factors associated with biofuel production. The analysis by Visentin et al. (2020) also reflects this, revealing that only a handful of the more than 100 LCSAs completed in the last decade or so focused on social factors like supplier relations or community involvement beyond merely employment.

The need for more social science research and the greater attention to social factors that the social sciences have brought to biofuel production chains have resulted in the creation of social life cycle assessments (SLCA), which are variations of life cycle assessments that attempt to include more social factors when assessing biofuel production. While these assessments would also be considered a form of LCSA, SLCAs emphasize the social

elements of sustainability in ways that LCSAs have ignored. International guidelines, developed by the United Nations Environmental Programme, for how to undertake SLCAs have been around for over a decade (UNEP, 2009). Since then, several studies have attempted to use SLCAs in the area of biofuel production, to great success. Gnansounou and Alves (2019b) note that SLCA is still a relatively new technique without standardization in tools and data. They also discuss biases that result from the information collected. However, it should be noted that social scientists are trained to deal with many of the issues they discussed showing the importance of including social scientists when attempting to include social aspects in these frameworks. Mattioda et al. (2020) also note that while SLCA is not standardized, it can be used across multiple different sectors to develop a much more holistic assessment of any production supply chain. The authors provide nine examples of SLCA being used in biofuel production, all of which pay special attention to how biofuels affect various stakeholders, workers in the biofuel industry, and community and societal effects of biofuel production (Mattioda et al., 2020). This focus helps bring more empirical attention to the question of social sustainability and is important for moving both conceptual and empirical work on social sustainability forward.

While SLCAs attempt to provide a more broad and holistic picture of a biofuel supply chain, from feedstock to end-user, many scholars have also narrowed in on specific stages of biofuel production, utilizing social science research to enhance our understanding of every step of the biofuel supply chain. One example of this is biorefinery site selection, a process that relies on numerous biogeophysical indicators to find the most optimal location to build a biorefinery. These indicators can include distance to feedstock supplies, the presence of nearby highway and railway infrastructure, and the economic viability of the biorefinery, among others. In site selection literature, the focus is often on long term accomplishments of industries, assuming that when the proper biogeophysical assets are present, a project will likely succeed. However, without taking social assets into account, a project might never get realized. By relying on biogeophysical indicators alone, a vital component in site selection is thus overlooked.

Some scholars have begun to focus on social factors: Santibañez-Aguilar et al. (2014) attempt to factor in the social impact of biorefineries by calculating the number of jobs generated by a facility, suggesting that more jobs would lead to positive social impacts in the community. Martinkus et al. (2014) go even further by developing a social asset factor that measures a community's capacity for collective action, suggesting that high social asset factor communities are better suited to complex projects like the construction of biorefineries. This approach reflects the Social Hotspot Database method described by Gnansounou and Alves (2019a) and Rijkhoff et al. (2017) further develop Martinkus et al. (2014) work by creating a social asset framework that includes social, creative, and human capital to assess community suitability for biofuel projects. In a later paper, Martinkus et al. (2017) further refine this capitals approach by building social, cultural, and human capital indicators into a decision support tool that also includes more traditional indicators for site selection, arguing that higher levels of these community traits would improve the implementation process of biorefineries, while ignoring them risks long-term success of biofuel production. Mueller et al. (2020) also attempt to use a capitals approach to biorefinery siting, using the Community Assets and Attributes Model (CAAM) to develop strategies for biofuel project leaders to approach and interact with communities in positive ways, further enhancing the chance of biorefinery success and viability. **Figure 1** provides a visual representation of the theoretical indicators feeding into calculation of the capitals contained in the CAAM model. Despite this progress, the focus is still on quantifiable measures of social assets, rather than combining that with the more appropriate qualitative approach.[1]

These areas of research in biofuel supply chains all indicate a potential for a robust social science presence in biofuel research, and the authors cited above reflect the need for even more social science scholars in the field. Unfortunately, many of the studies that attempt to incorporate social aspects do so only superficially "in a nonmethodological way" (Gnansounou and Alves 2019b). There are various potential methods for incorporating social aspects more methodically and reliably in aviation biofuels research but Gnansounou and Alves (2019b) criticize several approaches since they require more stakeholder engagement. For instance, they point out that SLCA is still lacking proper tools and data (p. 126). It is encouraging that researchers and biofuel project leaders understand that, in theory, social sustainability is just as important as economic and environmental sustainability, but unfortunate that they have, in practice, shied away from the inclusion of social metrics in biofuel research, largely due to the inconsistency of social metrics and the difficulty associated with measuring social traits. It is further discouraging that the preference for quantitative measures may cause researchers to shy away from methods that may more validly capture social sustainability due to the time and resources needed for these methods. However, aviation biofuel supply chain viability cannot simply incorporate only the traditional biogeophysical and economic factors that usually go into determining the success of biofuel production. If sustainability is the goal of these supply chains, then social sustainability must be considered, and that includes using the content expertise and methods—qualitative as well as quantitative—of social scientists to ascertain a more holistic vision of what a truly sustainable biofuel supply chain really looks like.

The complications and problems that come from severely under-developed social sustainability criteria will continue as long as the preference for uniform frameworks with easily obtainable data remains. While this preference is understandable, its dominance ensures that social sustainability will receive little empirical analysis or improvement. There is a need in the aviation biofuels

[1]We recommend Gnansounou and Alves (2019a), for an overview of current studies making use of integrated sustainability assessment (ISA) which is applied to biofuel and biofuel feedstock production options.

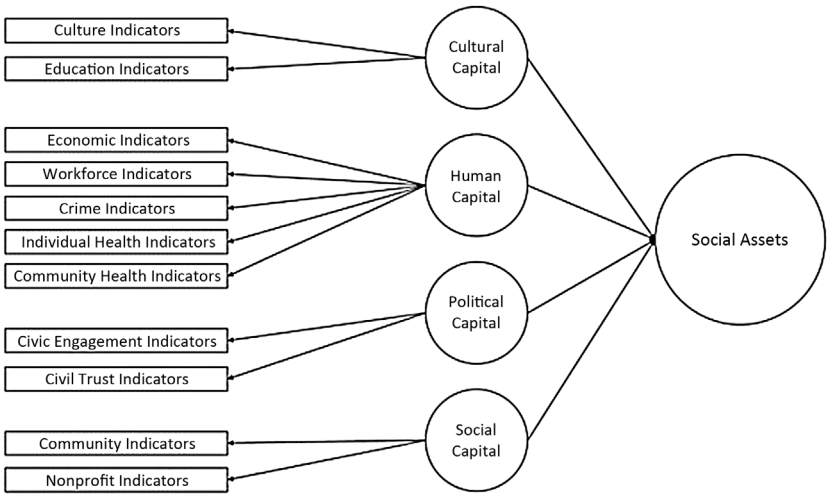

FIGURE 1 | Visualization of the community assets and attributes model. Note: Based on Mueller et al. (2020).

literature, and the broader biofuels literature, for more interdisciplinary research that includes social science research experts, particularly those with expertise in various social issues for the case in question. Additionally, while the dominance of quantitative methods in aviation biofuels research is understandable, more mixed-methods research that include qualitative methods would greatly benefit our understanding of sustainability overall and social sustainability in particular. We agree with Pashaei Kamali et al. (2018) that case study analysis is important for identifying social sustainability criteria, and mixed-method research could be especially beneficial for identifying sustainability issues on a case-by-case basis, and at a local level. This does not preclude trying to adopt a somewhat unified framework for social criteria, but these frameworks may be better developed through other methods, such as qualitative comparative analysis, rather than the methods typically utilized in the aviation biofuels literature.

An active area of social science research and concepts is the literature on public acceptance of biofuels which can be considered as an important component of the supply chain and sustainability. However, the application of these concepts and methods has been underwhelming in regard to aviation biofuels specifically. Fortunately, the larger literature provides guidance on how to improve analysis of public acceptance of aviation biofuels for future studies.

5 PUBLIC ACCEPTANCE OF BIOFUELS

Understanding public approval of aviation biofuels and the factors that make the public more (or less) supportive is an important part of social sustainability of aviation biofuel. Including public attitudes and perceptions helps to describe and explain various communities and cultures which potentially act as barriers to public support of biofuels. Moreover, the incorporation of public acceptance can make forecasting and estimating outcomes more culturally sensitive and accurate given that factors influencing public acceptance evolve over time (Sovacool 2014). Systematic reviews of the literature on public approval include mainly studies that examine public perceptions and acceptance of new technologies in the broad sense (e.g., Cohen et al., 2014; Sovacool 2014; Drews and van den Bergh 2016; Segeto et al., 2020). Specifically, research has shown that while there is strong support for transitions to renewable energy systems in the abstract (Bertsch et al., 2016), there are many examples of opposition to specific projects at the local level, two examples being Upreti and van der Horst (2004), and Jobert et al. (2007).

Case studies and several meta-analyses (Brohmann et al., 2007; Cohen et al., 2014; Segreto et al., 2020) include research of social acceptance of renewable energy systems, including wind farms, biomass energy generation, and others. However, researchers have lamented the scarcity of scientific studies on public attitudes toward, and acceptance of, biofuels in general, and sustainable aviation biofuels (SAFs) specifically (Filimonau and Högström 2017; Ahmad and Xu, 2019; Løkke et al., 2021). This is worrisome for proponents of SAF, for while there may be potent arguments for adoption of SAF to mitigate climate change, lack of social acceptance is a key barrier for sustainable implementation (see for example, Upreti and van der Horst 2004). While SAF acceptance research can fruitfully draw from the existing literature, SAF differs from most forms of sustainable energy systems in its need for feedstock production, and its connection to the aviation industry and its related benefits and risks. This is apparent when examining public support for aviation biofuels, where factors such as airline ticket price can affect support for a policy (for example, Lynch et al., 2017).

Related to the difficulties of the conceptualization of public acceptance is its operationalization. In a meta-analysis of the literature on energy scholarship, Sovacool (2014) finds that only roughly 12.6 percent of articles include "human centered" (sic) research methods. As mentioned in the discussion on

sustainability, the most often used methodological approach focuses on quantitative measures which lack precision and accuracy of the social concepts. While the social science inclusions in studies on public perceptions of SAF is both qualitative and quantitative, quantitative approaches are dominant. Specifically, surveys dominate these studies with fewer incorporating field research, focus groups, or interviews (p. 11). It should be noted that these surveys greatly vary in terms of sampling methods utilized, sample sizes, and the information provided to fully assess results. Some provide detailed information on sampling strategies, sample demographics, and operationalization and measurement for effective assessment of the methodology (See Dragojlovic and Einsiedel 2015; Spartz et al., 2015; Rice et al., 2020), while others may lack detailed information in one or more components (See Radics et al., 2016). Also, it can be difficult to access the survey questionnaire as most studies do not provide this information. While surveys have several benefits, sophisticated surveys, especially those using probability sampling, are costly even when conducting online surveys and may not appropriately measure the phenomena of interest. Jensen and Andersen (2013) specifically argue that in-depth, qualitative methods are important when examining perceptions of new technologies—in this case aviation biofuels—that may not be familiar to participants. Others have pointed out that due to the lack of prior research in this area, exploratory, qualitative methods are needed (Filimonau and Högström 2017). Despite these critiques, Løkke et al. (2021) found that the predominant method of measuring public opinion is still through surveys while employing in-depth qualitative interviews and focus groups are better able to address the complexity of the factors impacting acceptance of biofuels. This is supported by a Moula et al. (2017) study conducted in Finland. Conducting in person surveys, they noted that several respondents were concerned they did not have enough information on the topic and may answer incorrectly. This could impact response rates to surveys, lead to non-response bias, and ultimately shows that some aspects of public support and acceptance are difficult to capture through a survey instrument.

Given the lack of specific research on social approval in aviation biofuels, conceptualization, and operationalization of public acceptance is vital. However, scholars disagree and use various definitions. For instance, Ahmad and Xu, (2019) define public acceptance of biofuels as the willingness to use biofuels, while Bertsch et al. (2016) describe acceptance "as an active or passive approval of a certain technology/product or policy." Perhaps more useful, Wüstenhagen et al. (2007) provide a thorough overview of the conceptualization of social acceptance of renewable energy innovation. They conceptualize acceptance as having three categories or dimensions: socio-political acceptance (broad acceptance), community acceptance (acceptance of local projects and impacts), and market acceptance (or market adoption). This framework might be applicable to the discussion of social acceptance of SAF. **Table 1** illustrates the utility of the framework in categorizing studies examining different aspects of public acceptance of SAF. We show that current studies mainly focus on a single dimension of socio-political acceptance.

Most work has been done on the first of the three dimensions namely socio-political acceptance of SAF. Similar to the broader acceptance of renewable energy literature, there seems to be widespread support for biofuel use in the aviation industry in theoretical terms, but there are reservations when it comes to the practical implications. One way to operationalize the dimension of socio-political support for SAF is to use general attitudes towards the use of aviation biofuels or general support for biofuel policies. Lynch et al. (2017) operationalizing acceptance as support for specific national policies, found in their case study of the Netherlands, that the Dutch support the idea of using biofuels to achieve a more environmentally friendly aviation system. When it comes to using arable land and biomass for fuel instead of for the food industry, public concerns became clear.[2] Furthermore, the public indicated a lack of clarity on whether SAFs result in a reduction of greenhouse gas emissions and keeping the price of flying affordable (p. 136). Another study in Europe explored a more general or broad support for environmental policies in Sweden and found that only 18% of the population had negative attitudes towards a mandate for biofuel blending in the aviation industry (Larsson et al., 2020). Furthermore, Filimonau and Högström, (2017) used semi-structured interviews of tourists to examine perceptions of the use of SAF in the United Kingdom civil aviation sector. Like the studies above, they found that most were supportive of SAF generally. In other words, people seem to be generally open and supportive of environmental policies towards increasing sustainability but remain skeptical to its implementation.

The socio-political acceptance dimension thus seems to be in conflict with the community acceptance dimension from time to time. In social psychology this effect is known as not in my backyard, or NIMBY, which describes situations in which citizens generally agree with the policy initiatives but retract their support as soon as they find out that they might suffer negative consequences in their immediate neighborhood. This component of public acceptance of biofuel is relevant with regard to combined frameworks such as LCSA and specifically in studies on site selection. Apart from environmental advantages, sustainable aviation biofuel initiatives may bring economic benefits for a business, city, or country and locals may benefit from improved infrastructure and new jobs. Nevertheless, the public may oppose such initiatives with objections related to expected noise, traffic, and other individual costs. One of the main challenges to sustainable aviation biofuel is for external stakeholders to win the trust of

[2]It should be noted that the food price and land use concerns are largely associated with first- and second-generation biofuels that use crops such as corn or oil-based plants as feed stock. Third and fourth generation biofuels, produced by algae, would not have the same need for arable land (Hasan et al., 2021), but may have other tradeoffs that affect its viability. Third and fourth generation biofuels are relatively new developments, and research into public perceptions of these types of biofuels is lacking. Of course, it would be difficult to study perceptions of these more recent biofuels if people do not know how they are produced, and potential risks and benefits associated with this new technology.

TABLE 1 | Overview of operationalization of public acceptance of (aviation) biofuels.

Dimension of social acceptance	Technology	Operationalization of acceptance	Method	Example studies
Socio-political	Aviation biofuels	Support for national policies	Survey	Lynch et al. (2017), Larsson et al. (2020)
	Aviation biofuels	Attitudes toward use of aviation biofuels	Semi-structured interviews	Filimonau and Högström, (2017)
	Aviation biofuels	Willingness to fly with SAF	Online Survey	Ahmad and Xu, (2019)
	Biofuels	Risk/Benefit perceptions	Survey	Cacciatore et al. (2016)
Community	Renewable energy	Willingness to pay	Survey	Liu et al. (2013)
	Biomass energy plant	Support for establishment of local project	Survey, In-depth interviews, focus groups	Upreti and van der Horst (2004)
	Biorefineries	Risk/Benefit perceptions	Survey	Marciano et al. (2014)
Market	Biofuels	Willingness to purchase	Survey	Chaiyapa et al. (2021)
	Aviation biofuels	Drivers and Barriers	Interviews	Smith et al. (2017)
	Aviation biofuels	Outlook on adoption of aviation biofuels	Semi-structured interviews	Dodd et al. (2018)

Note: The listed dimensions of social acceptance are based on Wüstenhagen et al. (2007).

the public. These studies point to another way that socio-political acceptance of SAF has been operationalized namely as risk/benefit perceptions. Several studies have used perceptions of the risks and benefits of SAF as a proxy for acceptance. For example, Cacciatore et al. (2016) calculate a net risk/benefit variable as part of their study of the impact of partisanship on perceptions of biofuels. Their findings point to several factors that impact perceptions of benefits and risks of biofuels, including age, party identification, and media consumption (Cacciatore et al., 2016). While this study focused specifically on the impact of partisanship on risk/benefit perceptions of biofuels it did not then discuss how perceptions of risks and benefits impacts support for biofuels.

Scholarship about attitudes toward climate change, and sustainable energy, indicate they are driven by four key things: 1) sociodemographics; 2) underlying values and beliefs; 3) perceptions about climate change and the energy industry; and 4) short term cues, such as information from stakeholders or news media (see Drews and Van den Bergh 2016 for an overview). There have been some attempts at developing a framework for understanding the determinants of attitudes toward SAF. One approach follows the theory of planned behavior (Ajzen 1991) and argues that knowledge, perceived concerns, perceived benefits, and social trust predict attitudes toward sustainable aviation fuel (Ahmad and Xu, 2019). This framework has not been explored empirically, with only a small, descriptive pilot conducted to date. This again shows that research in the area of social acceptance of biofuels is under-developed. More broadly, other frameworks have been tested for understanding perceptions of biodiesel which include the four determinants mentioned previously but also add attitude toward technologies, past and intended behavior, and trust in key players (Amin et al., 2017). Utilizing participants in Malaysia, Amin et al. (2017) indicate that the most important predictors of attitudes toward biodiesel were perceptions of benefits and trust in key actors. It is useful to replicate these studies in other contexts: what impacts perceptions in Malaysia may not be as salient in the United States, for example. Additionally, there may be differences in the way these variables affect public acceptance when it comes to biodiesel compared to aviation biofuel.

Though studies using a qualitative approach in understanding and predicting SAF are limited, one important exception is the study by Filimonau and Högström, (2017) who used semi-structured interviews of tourists to examine perceptions of the use of SAF in the United Kingdom civil aviation sector. It was found that while most tourists are supportive of SAF generally, they lack knowledge of the environmental benefits of SAF use in the aviation industry (Filimonau and Högström 2017). Building on this, Filimonau et al. (2018) conducted a survey of 306 respondents in Poland. Results of this study suggest that knowledge of the application of biofuels in aviation is indeed lacking, leading to participants' concerns about the safety of the technology. In both studies, the authors conclude that knowledge of biofuels and SAF specifically should be promoted by governmental and non-governmental actors to promote adoption of the technology more widely. This recommendation is echoed by Kim et al. (2019) who suggest that increased public knowledge of aviation biofuels and its benefits may accelerate the transition from traditional fuel to SAF.

While increased knowledge is assumed to promote support, two studies (though focusing on biofuels generally and not SAF), show that increased knowledge was actually correlated with negative perceptions of biofuels (Cacciatore et al., 2016; Lanzini et al., 2016). Indeed, more studies have shown—perhaps unsurprisingly—that support for biofuels decreases when participants are primed with information about the potential for negative side effects of biofuel production (i.e., higher food prices, land use changes, etc.) (Jensen and Andersen 2013; Fung et al., 2014; Dragojlovic and Einsiedel 2015). This impact of new information can be moderated by partisanship, as demonstrated in a study looking at support for a biofuels tax credit in the United States (Goldfarb and Kriner 2021).

Political beliefs, especially given the context within the United States, are another potential determinant of attitudes toward SAF identified in the literature. In general, Democrats in the United States have more positive evaluations of biofuels and the policies that support them (Dragojlovic and Einsiedel 2014; Cacciatore et al., 2016; Goldfarb and Kriner 2021). Party affiliation has been shown to interact with perceptions of the risks and benefits, which in turn impacts support for biofuels (Fung et al., 2014). That is, Republicans and Democrats weigh benefits

and risks differently. As suggested by one study, this may be because individuals view media representations of biofuels through a partisan lens (Cacciatore et al., 2016). In summary, researchers have examined socio-political acceptance for SAF and have tried to explore the determinants of these general attitudes. From the few studies that have been conducted using predominantly quantitative approaches, there is some evidence to suggest that knowledge of biofuels, partisanship, and trust in key actors can impact acceptance of biofuels.

Though socio-political acceptance and community acceptance can be in conflict with one another, the latter has been widely studied in the broader renewable energy literature. For example, research has been conducted on the development of renewable energy sources in rural China (Liu et al., 2013), a biomass energy plant in the United Kingdom (Upreti and van der Horst 2004), or biorefineries in the north-east United States (Marciano et al., 2014). Multiple reviews of case studies and trends in social acceptance research of sustainable energy systems have been published (Brohmann et al., 2007; Segreto et al., 2020). These studies demonstrate the importance of context in understanding how to best approach implementation of renewable energy projects at the local level. In line with recommendations from social science, many utilize in-depth, qualitative methods. Still, the SAF acceptance literature has, to the best of our knowledge, not yet attempted to examine site-specific reasons for the success or failure of an SAF project or policy. While there may be parallels between acceptance of renewable energy projects generally and SAF projects specifically, the unique impacts of biofuels production (i.e., feedstock and processing) on local communities and economies clearly calls for focused and rigorous research in this area. There is thus a clear gap in the literature around SAF acceptance, that resembles the limitations in research on social sustainability in general and in aviation biofuel in particular.

The third and last dimension of the framework of social acceptance of renewable energy innovation as conceptualized by Wüstenhagen et al. (2007) is market acceptance and has been more frequently studied in the biofuels and SAF literature than socio-political and community acceptance. The overview by Løkke et al. (2021) shows that willingness to pay is one of the main measures of market acceptance. For example, Rice et al. (2020) found that participants are willing to pay more for sustainable aviation practices (including biofuels), but that willingness was moderated by ticket price, degree of greenhouse gas reduction, and gender. Similarly, Rains et al. (2017) found that participants were willing to pay more for airfare if the increase was due to adopting SAF. Market acceptance studies are also performed after the implementation of policies, for instance, after a biofuels policy in Vietnam failed due to lack of market uptake, residents of two cities were surveyed about their awareness of biofuels, motivations to use biofuels, and willingness to purchase (Chaiyapa et al., 2021). Yet other studies have focused on market acceptance from the perspectives of direct stakeholders instead of from the public perspective. Smith et al. (2017) looked at the acceptance and adoption of aviation biofuels among industry insiders and companies by conducting interviews with fuel supply chain stakeholders in the United States Pacific Northwest to explore barriers and opportunities for transitioning to SAF. Similarly, Dodd et al. (2018) reviewed attitudes from 58 aviation-related organizations in several countries to examine why transitions to SAF have stalled. Given the complexity of all dimensions of social acceptance, these studies are a step in the right direction, but much more research is needed.

To summarize, research into public acceptance of SAF is in its infancy compared to the state of the literature on other types of biofuels development. While drawing from literature on social acceptance of other renewable energy technologies can provide guidance, the unique aspects of SAF warrant focused research.

6 FINDINGS AND DISCUSSION

Despite calls to improve social sustainability research and better examine local level effects of aviation biofuel development, these areas remain under-developed, and under-researched. Social sustainability continues to be a conceptual muddle with confusion on definitions and appropriate criteria. In addition to conceptualization issues, social indicators used in empirical research to assess sustainability remain underwhelming with questionable validity despite their reliability and practicality. Moreover, the local level determinants and effects of aviation biofuels remains under researched and under-estimated.

This review of social science research in three broad areas of aviation biofuels research, sustainability, site-selection, and public acceptance, reveals common limitations that, if addressed, would improve research in the field overall. Despite the body of conceptual literature, sustainability, and more specifically social sustainability remain ill-defined. Many attempts to incorporate social sciences in aviation biofuel research fail to use accurate measures due to the lack of proper concepts. While combined frameworks and modeling provide better indicators for social sustainability and related social concerns, the focus is still on quantifying these determinants that are often primarily of qualitative nature. Similarly, studies incorporating public acceptance of sustainable energy do not fully understand what contributes to specific support. Findings suggest that while perceptions of sustainable aviation fuel (SAF) are generally positive, there is a lack of knowledge among the public on the application and benefits of SAF, especially for third and fourth generation biofuels. Future studies should include how perceptions, community acceptance, and market acceptance of SAF, are affected by political beliefs (Dragojlovic and Einsiedel 2014; Fung et al., 2014; Cacciatore et al., 2016), media representations (Delshad and Raymond 2013), increased knowledge, and other factors. Furthermore, while surveys are increasingly used in aviation biofuels, the surveys conducted thus far vary greatly in terms of sophistication and quality. The expense and time required to conduct a valid and reliable survey are often underestimated and this impacts conclusion that can be drawn. Several review studies, especially in public acceptance and support of aviation biofuels, have shown the growing prevalence of surveys but to our knowledge a review of survey methodology in the field has not been developed. A future study examining survey methodology in particular with a goal of improving current practice would be beneficial, especially as online surveys, online panels, and technology increases access to this method.

However, this does not mean surveys are always the appropriate method for gathering social data, especially in aviation biofuels research.

An important limitation in all three areas is the preference for quantitative methods and indicators, especially in mixed-methods frameworks, that prioritize accessible, and reliable measures without additional local research. Many of the social impacts of biofuel development do not lend themselves to easily quantifiable metrics and the preference for these types of indicators leads to, at best, an incomplete assessment, and at worst, invalid conclusions, and inaccurate predictions. This preference also contributes to inadequate research at the local level where biofuel development has the most impact. To be sure, broader assessments of sustainability criteria that include social criteria have received more attention in the last 10 years and this is an important and necessary development. However, focusing on quantitative methods and indicators is an important limitation of this research that must be addressed.

Truly mixed methods research that combines quantitative and qualitative assessment is needed and is severely lacking in aviation biofuels and the broader biofuel development literature. Mixed methods approaches that combine quantitative and qualitative methods are especially needed to address limitations of evaluations at the local level, and expand the indicators used to evaluate whether biofuel development is sustainable through a focus beyond "practical" indicators. Although we agree with Pashaei Kamali et al. (2018) that case-studies of social issues are important to determine appropriate social criteria to assess sustainability, these case studies must also focus on community-level impacts to avoid becoming too focused on the national or regional levels only.

7 PRACTICAL IMPLICATIONS OF THIS STUDY AND RECOMMENDATIONS

To facilitate better and more consistent application of social science approaches in not only aviation biofuels research and projects but the broader biofuels field, we recommend that certification schemes include social sustainability criteria and that these criteria be included in monitoring and reporting standards. While we acknowledge that quantitative metrics are often the focus of these standards, we recommend flexibility in the criteria reported and how the criteria are reported to better suit a particular case and better capture localized impacts of biofuel supply chains.

As current criteria are inadequate in terms of social sustainability, those conducting biofuel development and research projects should ensure that social sustainability and criteria are being adequately addressed. To help ensure inclusion of this important component, these projects should include a social science research team that is equal to the other interdisciplinary team components and at least one member of the social science team should serve as a Co-PI for the life of the project. Social science research should be adequately funded throughout the project with consideration for time, travel (especially for qualitative data collection), and project adaptability as researchers identify appropriate methods for data collection for a specific case. Social science team members should have a range of social science backgrounds and research training, including both qualitative and quantitative experience. Ensuring that some of these team members also have experience with the case(s) being examined is also recommended. If surveys will be utilized, social scientists with survey research backgrounds should be part of the development, implementation, and analysis phases, at least in an advisory role. As stakeholder engagement is crucial to the success of biofuel development projects, it is also recommended that members of the social science team help lead these aspects and have experience in different components of stakeholder engagement, including interviews, focus group, and survey methodologies.

Further, the approach employed to understand social impacts of biofuel development projects should be mixed-method, including both qualitative and quantitative methods as appropriate. This can include the use of secondary data collected by outside sources but should also include both qualitative and quantitative data collection as appropriate. Incorporating social science considerations should occur throughout the duration of the project, and should include metrics and goals at the local, regional, and national level. Furthermore, it is necessary to integrate a plan for adequately funded post-project evaluation components to monitor long term impacts, especially at the local level. The importance of research design and data collection flexibility is also important as these projects should be informed by not only current literature and projects in this area, but should also seek to develop appropriate metrics for their specific case.

This review indicates that significant strides have taken place in social sustainability and social science research in aviation biofuels over the last decade. We encourage scholars, practitioners, and funding organizations to include social science experts in current and future studies to ensure that sustainability, all aspects of it, is achieved in aviation biofuel initiatives. The recommendations provided can help ensure that social criteria are better addressed in the future and that social scientists have adequate support and prominence within a project to continue much needed work in the field.

AUTHOR CONTRIBUTIONS

SH, DM, and SR contributed to the conception of the study. BA, DM, SH, and CS wrote sections of the first draft of the article. All authors contributed to the article revision. SR provided **Figure 1** and prepared the final article for publication.

FUNDING

This research was funded by the U.S. Federal Aviation Administration Office of Environment and Energy through ASCENT, the FAA Center of Excellence for Alternative Jet Fuels and the Environment, project 001(A) through FAA Award Number 13-C-AJFE-WaSU-013 under the supervision of under the supervision of Dr. James Hileman and Nathan Brown. Any opinions, findings, conclusions or recommendations expressed in this material are those of the authors and do not necessarily reflect the views of the FAA.

REFERENCES

Acquaye, A. A., Wiedmann, T., Feng, K., Crawford, R. H., Barrett, J., Kuylenstierna, J., et al. (2011). Identification of 'Carbon Hot-Spots' and Quantification of GHG Intensities in the Biodiesel Supply Chain Using Hybrid LCA and Structural Path Analysis. *Environ. Sci. Technol.* 45 (6), 2471–2478. doi:10.1021/es103410q

Ahmad, S., and Xu, B. (2019). "Public Attitude towards Aviation Biofuels: A Pilot Study Findings," Phil Greening, and Jamal Ouenniche. in Proceedings of 11th International Conference on Applied Energy Vasteras, Sweden. Available at: http://www.energy-proceedings.org/wp-content/uploads/2020/03/958_Paper_0531091009.pdf.4

Åhman, H. (2013). Social Sustainability - Society at the Intersection of Development and Maintenance. *Local Environ.* 18 (10), 1153–1166. doi:10.1080/13549839.2013.788480

Amin, L., Hashim, H., Mahadi, Z., Ibrahim, M., and Ismail, K. (2017). Determinants of Stakeholders' Attitudes Towards Biodiesel. *Biotechnol. Biofuels.* 10 (1), 219. doi:10.1186/s13068-017-0908-8

Ajzen, I. (1991). The Theory of Planned Behavior. *Organizational Behavior and Human Decision Processes* 50 (02), 179–211.

Basiago, A. D. (1995). Methods of Defining 'sustainability'. *Sust. Dev.* 3 (3), 109–119. doi:10.1002/sd.3460030302

Benoît, C., and Bernard, M. United Nations Environment Programme, CIRAIG, and Processes and Services Interuniversity Research Centre for the Life Cycle of Products (2013). *Guidelines for Social Life Cycle Assessment of Products*. Paris, France: United Nations Environment Programme. Available at: https://www.deslibris.ca/ID/236529.

Bertsch, V., Hall, M., Weinhardt, C., and Fichtner, W. (2016). Public Acceptance and Preferences Related to Renewable Energy and Grid Expansion Policy: Empirical Insights for Germany. *Energy.* 114 (November), 465–477. doi:10.1016/j.energy.2016.08.022

Brundtland, G. (1987). Report of the World Commission on Environment and Development: Our Common Future. *United Nations General Assembly document A/42/427* https://sustainabledevelopment.un.org/content/documents/5987our-common-future.pdf (Accessed February 10, 1987), 1–300.

Buchholz, T., Luzadis, V. A., and Volk, T. A. (2009). Sustainability Criteria for Bioenergy Systems: Results from an Expert Survey. *J. Clean. Prod.* 17 (November), S86–S98. doi:10.1016/j.jclepro.2009.04.015

Cacciatore, M. A., Scheufele, D. A., Binder, A. R., and Shaw, B. R. (2016). Public Attitudes toward Biofuels: Effects of Knowledge, Political Partisanship, and Media Use. *Polit. Life Sci.* 31 (1/2), 36–51. doi:10.2990/31_1-2_36

Campbell, S. (1996). Green Cities, Growing Cities, Just Cities?: Urban Planning and the Contradictions of Sustainable Development. *J. Am. Plann. Assoc.* 62 (3), 296–312. doi:10.1080/01944369608975696

Chaiyapa, W., Nguyen, K. N., Ahmed, A., VuVu, Q. T. H., Bueno, M., Wang, Z., et al. (2021). Public Perception of Biofuel Usage in Vietnam. *Biofuels.* 12 (1), 21–33. doi:10.1080/17597269.2018.1442667

Clarens, A. F., NassauWhite, H., Resurreccion, E. P., White, M. A., and Colosi, L. M. (2011). Environmental Impacts of Algae-Derived Biodiesel and Bioelectricity for Transportation. *Environ. Sci. Technol.* 45 (17), 7554–7560. doi:10.1021/es200760n

Cohen, J. J., Reichl, J., and Schmidthaler, M. (2014). Re-Focussing Research Efforts on the Public Acceptance of Energy Infrastructure: A Critical Review. *Energy.* 76 (November), 4–9. doi:10.1016/j.energy.2013.12.056

Collotta, M., Champagne, P., Tomasoni, G., Alberti, M., Busi, L., and Mabee, W. (2019). Critical Indicators of Sustainability for Biofuels: An Analysis Through a Life Cycle Sustainabilty Assessment Perspective. *Renew. Sustainable Energ. Rev.* 115 (November), 109358. doi:10.1016/j.rser.2019.109358

Correa, D. F., Beyer, H. L., Joseph, E., Possingham, H. P., Thomas-Hall, S. R., and Schenk, P. M. (2019). Towards the Implementation of Sustainable Biofuel Production Systems. *Renew. Sustainable Energ. Rev.* 107 (June), 250–263. doi:10.1016/j.rser.2019.03.005

de Man, R., and German, L. (2017). Certifying the Sustainability of Biofuels: Promise and Reality. *Energy Policy* 109 (October), 871–883. doi:10.1016/j.enpol.2017.05.047

Delshad, A., and Raymond, L. (2013). Media Framing and Public Attitudes Toward Biofuels. *Rev. Pol. Res.* 30 (2), 190–210. doi:10.1111/ropr.12009

Dillman, D. A., Smyth, J. D., and Christian., L. M. (2014). *Internet, Phone, Mail, and Mixed-Mode Surveys: The Tailored Design Method*. Hoboken, New Jersey: John Wiley & Sons.

Diniz, A. P. M. M., Sargeant, R., and Millar., G. J. (2018). Stochastic Techno-Economic Analysis of the Production of Aviation Biofuel from Oilseeds. *Biotechnol. Biofuels.* 11 (1), 161. doi:10.1186/s13068-018-1158-0

Dodd, T., Orlitzky, M., and Nelson, T. (2018). What Stalls a Renewable Energy Industry? Industry Outlook of the Aviation Biofuels Industry in Australia, Germany, and the USA. *Energy Policy.* 123 (December), 92–103. doi:10.1016/j.enpol.2018.08.048

Dragojlovic, N., and Einsiedel, E. (2014). The Polarization of Public Opinion on Biofuels in North America: Key Drivers and Future Trends. *Biofuels.* 5 (3), 233–247. doi:10.1080/17597269.2014.913901

Dragojlovic, N., and Einsiedel, E. (2015). What Drives Public Acceptance of Second-Generation Biofuels? Evidence from Canada. *Biomass and Bioenergy.* 75 (April), 201–212. doi:10.1016/j.biombioe.2015.02.020

Drews, S., and van den Bergh, J. C. J. M. (2016). What Explains Public Support for Climate Policies? A Review of Empirical and Experimental Studies. *Clim. Pol.* 16 (7), 855–876. doi:10.1080/14693062.2015.1058240

Du Pisani, J. A., and Jacobus, A. (2006). Sustainable Development - Historical Roots of the Concept. *Environ. Sci.* 3 (2), 83–96. doi:10.1080/15693430600688831

Dudziak, E. A. (2007). Information Literacy and Lifelong Learning in Latin America: The Challenge to Build Social Sustainability. *Inf. Development.* 23 (1), 43–47. doi:10.1177/0266666907075630

Ekener, E., Hansson, J., Larsson, A., and Peck, P. (2018). Developing Life Cycle Sustainability Assessment Methodology by Applying Values-Based Sustainability Weighting - Tested on Biomass Based and Fossil Transportation Fuels. *J. Clean. Prod.* 181 (April), 337–351. doi:10.1016/j.jclepro.2018.01.211

Ekener-Petersen, E., Höglund, J., and Finnveden, G. (2014). Screening Potential Social Impacts of Fossil Fuels and Biofuels for Vehicles. *Energy Policy.* 73 (October), 416–426. doi:10.1016/j.enpol.2014.05.034

Filimonau, V., and Högström, M. (2017). The Attitudes of UK Tourists to the Use of Biofuels in Civil Aviation: An Exploratory Study. *J. Air Transport Management.* 63 (August), 84–94. doi:10.1016/j.jairtraman.2017.06.002

Filimonau, V., Mika, M., and Pawlusiński, R. (2018). Public Attitudes to Biofuel Use in Aviation: Evidence from an Emerging Tourist Market. *J. Clean. Prod.* 172 (January), 3102–3110. doi:10.1016/j.jclepro.2017.11.101

Fokaides, P. A., and Christoforou, E. (2016). "Life Cycle Sustainability Assessment of Biofuels," in *Handbook of Biofuels Production*. Editors R. Luque and K. Wilson. Second Edition (Clark: Woodhead Publishing), 41–60. doi:10.1016/B978-0-08-100455-5.00003-5

Foladori, G. (2005). Advances and Limits of Social Sustainability as an Evolving Concept. *Can. J. Development Studies/Revue canadienne d'études du développement.* 26 (3), 501–510. doi:10.1080/02255189.2005.9669070

Fung, T. K. F., Choi, D. H., Scheufele, D. A., and Shaw, B. R. (2014). Public Opinion about Biofuels: The Interplay between Party Identification and Risk/Benefit Perception. *Energy Policy.* 73 (October), 344–355. doi:10.1016/j.enpol.2014.05.016

Gnansounou, E., and Alves, C. M. (2019b). "Social Assessment of Biofuels," in Biofuels: Alternative Feedstocks and Conversion Processes for the Production of Liquid and Gaseous Biofuels (Academic Press), 123–139. doi:10.1016/b978-0-12-816856-1.00005-1

Gnansounou, E., and Alves, C. M. (2019a). "Integrated Sustainability Assessment of Biofuels," in Biofuels: Alternative Feedstocks and Conversion Processes for the Production of Liquid and Gaseous Biofuels (Academic Press), 197–214. doi:10.1016/b978-0-12-816856-1.00008-7

Goldfarb, J. L., and Kriner, D. L. (2021). U.S. Public Support for Biofuels Tax Credits: Cost Frames, Local Fuel Prices, and the Moderating Influence of Partisanship. *Energy Policy.* 149 (February), 112098. doi:10.1016/j.enpol.2020.112098

Hasan, M. A., Mamun, A. A., RahmanRahman, S. M., Malik, K., Al Amran, M. I. U., Khondaker, A. N., et al. (2021). Climate Change Mitigation Pathways for the Aviation Sector. *Sustainability.* 13 (7), 3656. doi:10.3390/su13073656

Brohmann, B., Feenstra, Y., Heiskanen, E., Hodson, M., Mourik, R., Raven, R., et al. (2007). Factors Influencing the Societal Acceptance of New Energy Technologies: Meta-Analysis of Recent European Projects in European

Roundtable on Sustainable Consumption and Production, Basel, Switzerland, June 20–22, 2007.

Hodbod, J., and Tomei, J. (2013). Demystifying the Social Impacts of Biofuels at Local Levels: Where Is the Evidence? *Geogr. Compass.* 7 (7), 478–488. doi:10.1111/gec3.12051

Jensen, M., and Andersen, A. H. (2013). Biofuels: A Contested Response to Climate Change. *Sustainability: Sci. Pract. Pol.* 9 (1), 42–56. doi:10.1080/15487733.2013.11908106

Jobert, A., Laborgne, P., and Mimler, S. (2007). Local Acceptance of Wind Energy: Factors of Success Identified in French and German Case Studies. *Energy Policy.* 35 (5), 2751–2760. doi:10.1016/j.enpol.2006.12.005

Kurka, T., and Blackwood, D. (2013). Participatory Selection of Sustainability Criteria and Indicators for Bioenergy Developments. *Renew. Sustainable Energ. Rev.* 24 (August), 92–102. doi:10.1016/j.rser.2013.03.062

Lan, K., Park, S., and Yao, Y. (2020). "Key Issue, Challenges, and Status Quo of Models for Biofuel Supply Chain Design," in *Biofuels for a More Sustainable Future*. Editors J. Ren, A. Scipioni, A. Manzardo, and H. Liang (Elsevier), 273–315. doi:10.1016/B978-0-12-815581-3.00010-5

Lanzini, P., Testa, F., and Iraldo, F. (2016). Factors Affecting Drivers' Willingness to Pay for Biofuels: the Case of Italy. *J. Clean. Prod.* 112 (January), 2684–2692. doi:10.1016/j.jclepro.2015.10.080

Larsson, J., Matti, S., and Nässén, J. (2020). Public Support for Aviation Policy Measures in Sweden. *Clim. Pol.* 20 (10), 1305–1321. doi:10.1080/14693062.2020.1759499

Liu, W., Wang, C., and Mol, A. P. J. (2013). Rural Public Acceptance of Renewable Energy Deployment: The Case of Shandong in China. *Appl. Energ.* 102 (February), 1187–1196. doi:10.1016/j.apenergy.2012.06.057

Løkke, S., Aramendia, E., and Malskær, J. (2021). A Review of Public Opinion on Liquid Biofuels in the EU: Current Knowledge and Future Challenges. *Biomass and Bioenergy.* 150 (July), 106094. doi:10.1016/j.biombioe.2021.106094

Lynch, D. H. J., Klaassen, P., and Broerse, J. E. W. (2017). Unraveling Dutch Citizens' Perceptions on the Bio-Based Economy: The Case of Bioplastics, Bio-Jetfuels and Small-Scale Bio-Refineries. *Ind. Crops Prod.* 106 (November), 130–137. doi:10.1016/j.indcrop.2016.10.035

Marciano, J. A., Lilieholm, R. J., Teisl, M. F., Leahy, J. E., and Neupane, B. (2014). Factors Affecting Public Support for Forest-Based Biorefineries: A Comparison of Mill Towns and the General Public in Maine, USA. *Energy Policy.* 75 (December), 301–311. doi:10.1016/j.enpol.2014.08.016

Markevičius, A., Katinas, V., Perednis, E., and Tamašauskienė, M. (2010). Trends and Sustainability Criteria of the Production and Use of Liquid Biofuels. *Renew. Sustainable Energ. Rev.* 14 (9), 3226–3231. doi:10.1016/j.rser.2010.07.015

Martinkus, N., Rijkhoff, S. A. M., Hoard, S. A., Shi, W., Smith, P., Gaffney, M., et al. (2017). Biorefinery Site Selection Using a Stepwise Biogeophysical and Social Analysis Approach. *Biomass and Bioenergy.* 97 (February), 139–148. doi:10.1016/j.biombioe.2016.12.022

Martinkus, N., Shi, W., Lovrich, N., Pierce, J., Smith, P., and Wolcott, M. (2014). Integrating Biogeophysical and Social Assets into Biomass-To-Biofuel Supply Chain Siting Decisions. *Biomass and Bioenergy.* 66 (July), 410–418. doi:10.1016/j.biombioe.2014.04.014

Martinkus, N., Latta, G., Rijkhoff, S. A. M., Mueller, D., Hoard, S. A., Sasatani, D., et al. (2019). A Multi-Criteria Decision Support tool for Biorefinery Siting: Using Economic, Environmental, and Social Metrics for a Refined Siting Analysis. *Biomass and Bioenergy.* 128, 105330. doi:10.1016/j.biombioe.2019.105330

Mattioda, R. A., Tavares, D. R., Casela, J. L., and Junior, O. C. (2020). "Social Life Cycle Assessment of Biofuel Production," in *Biofuels for a More Sustainable Future*. Editors J. Ren, A. Scipioni, A. Manzardo, and H. Liang (Elsevier), 255–271. doi:10.1016/B978-0-12-815581-3.00009-9

McKenzie, S. (2004). *"Social Sustainability: Towards Some Definitions." Hawke Research Institute Working Paper Series*. MagillSouth Australia: University of South Australia. Available at: http://www.hawkecentre.unisa.edu.au/institute/.

Moldan, B., Janoušková, S., and Hák, T. (2012). How to Understand and Measure Environmental Sustainability: Indicators and Targets. *Ecol. Indicators.* 17 (June), 4–13. doi:10.1016/j.ecolind.2011.04.033

Mori, K., and Christodoulou, A. (2012). Review of Sustainability Indices and Indicators: Towards a New City Sustainability Index (CSI). *Environ. Impact Assess. Rev.* 32 (1), 94–106. doi:10.1016/j.eiar.2011.06.001

Moula, M. M. E., Nyári, J., and Bartel, A. (2017). Public Acceptance of Biofuels in the Transport Sector in Finland. *Int. J. Sustainable Built Environ.* 6 (2), 434–441. doi:10.1016/j.ijsbe.2017.07.008

Mueller, D., Hoard, S., Roemer, K., Sanders, C., Rijkhoff, S. A. M., and Rijkhoff, M. (2020). Quantifying the Community Capitals Framework: Strategic Application of the Community Assets and Attributes Model. *Community Development.* 51 (5), 535–555. doi:10.1080/15575330.2020.1801785

Partridge, E. (2005). "Social Sustainability": A Useful Theoretical Framework? Ausralasian Political Science Association Annual Conference (Dunedin, New Zealand. Available at: https://www.academia.edu/3678834/Social_sustainability_a_useful_theoretical_framework.

Pashaei Kamali, F., Borges, J. A. R., Osseweijer, P., and Posada, J. A. (2018). Towards Social Sustainability: Screening Potential Social and Governance Issues for Biojet Fuel Supply Chains in Brazil. *Renew. Sustainable Energ. Rev.* 92 (September), 50–61. doi:10.1016/j.rser.2018.04.078

Purvis, B., Mao, Y., and Robinson, D. (2019). Three Pillars of Sustainability: In Search of Conceptual Origins. *Sustain. Sci.* 14 (3), 681–695. doi:10.1007/s11625-018-0627-5

Radics, R. I., Dasmohapatra, S., and Kelley, S. S. (2016). Public Perception of Bioenergy in North Carolina and Tennessee. *Energ Sustain. Soc.* 6 (1), 17. doi:10.1186/s13705-016-0081-0

Rains, T., Winter, S. R., Rice, S., Milner, M. N., Bledsaw, Z., and Anania, E. C. (2017). Biofuel and Commercial Aviation: Will Consumers Pay More for it? *Int. J. Sustainable Aviation.* 3 (3), 217. doi:10.1504/IJSA.2017.086846

Resurreccion, E. P., Roostaei, J., Martin, M. J., Maglinao, R. L., Zhang, Y., and Kumar, S. (2021). The Case for Camelina-Derived Aviation Biofuel: Sustainability Underpinnings from a Holistic Assessment Approach. *Ind. Crops Prod.* 170 (October), 113777. doi:10.1016/j.indcrop.2021.113777

Ribeiro, B. E., and Quintanilla, M. A. (2015). Transitions in Biofuel Technologies: An Appraisal of the Social Impacts of Cellulosic Ethanol Using the Delphi Method. *Technol. Forecast. Soc. Change.* 92 (March), 53–68. doi:10.1016/j.techfore.2014.11.006

Rice, C., Ragbir, N. K., Rice, S., and Barcia, G. (2020). Willingness to Pay for Sustainable Aviation Depends on Ticket Price, Greenhouse Gas Reductions and Gender. *Technology Soc.* 60 (February), 101224. doi:10.1016/j.techsoc.2019.101224

Rijkhoff, S. A. M., Hoard, S. A., Gaffney, M. J., and Smith, P. M. (2017). Communities Ready for Takeoff. *Polit. Life Sci.* 36 (1), 14–26. doi:10.1017/pls.2017.6

Rijkhoff, S. A. M., Martinkus, N., Roemer, K., Laninga, T. J., and Hoard, S. A. (2021). A Capitals Approach to Biorefinery Siting Using an Integrative Model in *Energy Impacts: A Multidisciplinary Exploration of North American Energy Development*, Editor J. B. Jacquet, J. H. Haggerty, and G. L. Theodori (Logan, UT: Social Ecology Press and Utah State University Press), 176–214.

Santibañez-Aguilar, J. E., González-Campos, J. B., Ponce-Ortega, J. M., Serna-González, M., El-Halwagi, M. M., Mahmoud, M., et al. (2014). Optimal Planning and Site Selection for Distributed Multiproduct Biorefineries Involving Economic, Environmental and Social Objectives. *J. Clean. Prod.* 65 (February), 270–294. doi:10.1016/j.jclepro.2013.08.004

Scarlat, N., and Dallemand, J.-F. (2011). Recent Developments of Biofuels/Bioenergy Sustainability Certification: A Global Overview. *Energy Policy.* 39 (3), 1630–1646. doi:10.1016/j.enpol.2010.12.039

Segreto, M., Principe, L., Desormeaux, A., Torre, M., Tomassetti, L., Tratzi, P., et al. (2020). Trends in Social Acceptance of Renewable Energy Across Europe-A Literature Review. *Int. J. Environ. Res. Public Health.* 17 (24), 9161. doi:10.3390/ijerph17249161

Smith, P. M., Gaffney, M. J., Shi, W., Hoard, S., Armendariz, I. I., and Mueller, D. W. (2017). Drivers and Barriers to the Adoption and Diffusion of Sustainable Jet Fuel (SJF) in the U.S. Pacific Northwest. *J. Air Transport Management.* 58 (January), 113–124. doi:10.1016/j.jairtraman.2016.10.004

Sovacool, B. K. (2014). What Are We Doing Here? Analyzing Fifteen Years of Energy Scholarship and Proposing a Social Science Research Agenda. *Energ. Res. Soc. Sci.* 1 (March), 1–29. doi:10.1016/j.erss.2014.02.003

Spartz, J. T., Rickenbach, M., and Shaw, B. R. (2015). Public Perceptions of Bioenergy and Land Use Change: Comparing Narrative Frames of Agriculture and Forestry. *Biomass and Bioenergy.* 75 (April), 1–10. doi:10.1016/j.biombioe.2015.01.026

Stirling, A. (1999). The Appraisal of Sustainability: Some Problems and Possible Responses. *Local Environ.* 4 (2), 111–135. doi:10.1080/13549839908725588

Thompson, P. B. (1995). *The Spirit of the Soil: Agriculture and Environmental Ethics*. London ; New York: Environmental Philosophies Series.

UNEP (2009). United Nations Environment Programme (2010), *UNAP Annual Report 2009: Seizing the Green Opportunity*. Available at: https://www.unep.org/resources/annual-report/unep-2009-annual-report (Accessed February, 2010).

Upreti, B. R., and van der Horst, D. (2004). National Renewable Energy Policy and Local Opposition in the UK: The Failed Development of a Biomass Electricity Plant. *Biomass and Bioenergy.* 26 (1), 61–69. doi:10.1016/S0961-9534(03)00099-0

Vallance, S., Perkins, H. C., and Dixon, J. E. (2011). What Is Social Sustainability? A Clarification of Concepts. *Geoforum.* 42 (3), 342–348. doi:10.1016/j.geoforum.2011.01.002

Visentin, C., Trentin, A. W. d. S., Braun, A. B., and Thomé, A. (2020). Life Cycle Sustainability Assessment: A Systematic Literature Review Through the Application Perspective, Indicators, and Methodologies. *J. Clean. Prod.* 270 (October), 122509. doi:10.1016/j.jclepro.2020.122509

Wang, Z., Osseweijer, P., and Duque, J. P. (2017). "Assessing Social Sustainability for Biofuel Supply Chains: The Case of Aviation Biofuel in Brazil," in IEEE Conference on Technologies for Sustainability (SusTech), 1–5. doi:10.1109/sustech.2017.8333474

Wang, Z., Pashaei Kamali, F., Osseweijer, P., and Posada, J. A. (2019). Socioeconomic Effects of Aviation Biofuel Production in Brazil: A Scenarios-Based Input-Output Analysis. *J. Clean. Prod.* 230, 1036–1050. doi:10.1016/j.jclepro.2019.05.145

Wüstenhagen, R., Wolsink, M., and Bürer, M. J. (2007). Social Acceptance of Renewable Energy Innovation: An Introduction to the Concept. *Energy Policy.* 35 (5), 2683–2691. doi:10.1016/j.enpol.2006.12.001

Zijp, M., Heijungs, R., van der Voet, E., van de Meent, D., Huijbregts, M., Hollander, A., et al. (2015). An Identification Key for Selecting Methods for Sustainability Assessments. *Sustainability.* 7 (3), 2490–2512. doi:10.3390/su7032490

Conflict of Interest: The authors declare that the research was conducted in the absence of any commercial or financial relationships that could be construed as a potential conflict of interest.

frontiers in Energy Research

ORIGINAL RESEARCH
published: 31 January 2022
doi: 10.3389/fenrg.2021.771697

Building Structure-Property Relationships of Cycloalkanes in Support of Their Use in Sustainable Aviation Fuels

Alexander Landera[1]*, *Ray P. Bambha*[1], *Naijia Hao*[2], *Sai Puneet Desai*[2], *Cameron M. Moore*[2], *Andrew D. Sutton*[2†] *and Anthe George*[1]

[1]Sandia National Laboratories, Livermore, CA, United States, [2]Los Alamos National Laboratory, Los Alamos, NM, United States

OPEN ACCESS

Edited by:
Zia Haq,
United States Department of Energy (DOE), United States

Reviewed by:
Halil Durak,
Yüzüncü Yıl University, Turkey
Johnathan Holladay,
LanzaTech, United States

***Correspondence:**
Alexander Landera
alande@sandia.gov

†Present address:
Andrew D. Sutton,
Oak Ridge National Laboratory, Oak Ridge, TN, United States

Specialty section:
This article was submitted to Bioenergy and Biofuels, a section of the journal Frontiers in Energy Research

Received: *06 September 2021*
Accepted: *24 December 2021*
Published: *31 January 2022*

Citation:
Landera A, Bambha RP, Hao N, Desai SP, Moore CM, Sutton AD and George A (2022) Building Structure-Property Relationships of Cycloalkanes in Support of Their Use in Sustainable Aviation Fuels. Front. Energy Res. 9:771697. doi: 10.3389/fenrg.2021.771697

In 2018 13.7 EJ of fuel were consumed by the global commercial aviation industry. Worldwide, demand will increase into the foreseeable future. Developing Sustainable Aviation Fuels (SAFs), with decreased CO_2 and soot emissions, will be pivotal to the on-going mitigation efforts against global warming. Minimizing aromatics in aviation fuel is desirable because of the high propensity of aromatics to produce soot during combustion. Because aromatics cause o-rings to swell, they are important for maintaining engine seals, and must be present in at least 8 vol% under ASTM-D7566. Recently, cycloalkanes have been shown to exhibit some o-ring swelling behavior, possibly making them an attractive substitute to decrease the aromatic content of aviation fuel. Cycloalkanes must meet specifications for a number of other physical properties to be compatible with jet fuel, and these properties can vary greatly with the cycloalkane chemical structure, making their selection difficult. Building a database of structure-property relationships (SPR) for cycloalkanes greatly facilitates their furthered inclusion into aviation fuels. The work presented in this paper develops SPRs by building a data set that includes physical properties important to the aviation industry. The physical properties considered are energy density, specific energy, melting point, density, flashpoint, the Hansen solubility parameter, and the yield sooting index (YSI). Further, our data set includes cycloalkanes drawn from the following structural groups: fused cycloalkanes, n-alkylcycloalkanes, branched cycloalkanes, multiple substituted cycloalkanes, and cycloalkanes with different ring sizes. In addition, a select number of cycloalkanes are blended into Jet-A fuel (POSF-10325) at 10 and 30 wt%. Comparison of neat and blended physical properties are presented. One major finding is that ring expanded systems, those with more than six carbons, have excellent potential for inclusion in SAFs. Our data also indicate that polysubstituted cycloalkanes have higher YSI values.

Keywords: structure-property relationship, jet fuel, cycloalkane, o-ring, physical properties

1 INTRODUCTION

In 2012 the aviation sector accounted for 11% of the world's transportation energy (International Energy Outlook, 2016). By 2040 global energy demand for aviation fuel is forecast to increase by 10.6 EJ. This increase is concerning because the continued combustion of petroleum fuel will emit more CO_2 into the atmosphere and with it comes larger effects from global warming. The fifth Assessment Report of the Intergovernmental Panel on Climate Change (IPCC), published in 2014, concluded that in 2010 aviation accounted for 10.62% of the global CO_2 emitted within the transportation sector (Sims et al., 2014). Although, CO_2 emissions from road transportation is increasing at a faster absolute pace, when viewed by percent CO_2 change, gains in the aviation sector are faster. Further, unlike other forms of travel, such as cars and trucks, there is no foreseeable path to electrify the aviation sector. Therefore, mitigation efforts are necessary to decarbonize the aviation industry. Sustainable Aviation Fuels (SAFs) are produced from renewable feedstocks and offer the potential of a lower carbon intensive alternative to current petroleum refined jet fuels. There are currently seven approved SAFs, which are approved as blends of 50% or lower by volume with conventional jet fuel: Fischer-Tropsch Synthetic Paraffinic Kerosene (FT-SPK), Hydroprocessed Esters and Fatty Acids Synthetic Paraffinic Kerosene (HEFA-SPK), Hydroprocessed Fermented Sugars to Synthetic Isoparaffins (HES-SIP), Fischer-Tropsch Synthetic Paraffinic Kerosene with Aromatics (FT-SPK/A), Alcohol to Jet Synthetic Paraffinic Kerosene (ATJ-SPK), Catalytic Hydrothermolysis Synthesized Kerosene (CH-SK), and Hydrocarbon-Hydroprocessed Esters and Fatty Acids (HC-HEFA-SPK) (ASTM D7566, 2015). SAF developed biofuels are attractive because they can significantly reduce CO_2 emissions over their life cycle and also decrease sooting and radiative forcing through the inhibition of contrail formation (Yang et al., 2019). A recent review highlighted these reductions by pointing out that many biojet fuels show large decreases in particulate matter ranging from 25 to 95% over conventional jet fuels (Yang et al., 2019).

Whilst SAFs can enable soot reduction from aromatics, a minimum quantity of aromatics are required in aviation fuel, according to ASTM-D7566, to ensure sufficient seal swelling in the aircraft and fuel circulation systems (ASTM D7566, 2015). The degree of fuel swelling is dependent on the material o-rings are made from and the type of aromatic molecules present in the fuel. Previous work with nitrile rubber shows that fuel swelling increases with the hydrogen bonding character, and the polarity of an aromatic molecule (Graham et al., 2006). In addition, lower molecular weight aromatics were found to increase o-ring swelling. Similar results were shown in acrylonitrile- butadiene o-rings, in which smaller, less hindered, aromatics were observed to cause o-ring swelling (Romanczyk et al., 2019). Cycloalkanes have also been shown to induce some o-ring swelling (Balster et al., 2008; Kosir et al., 2020). Recent research shows that cycloalkanes must be present in significant amounts to achieve a comparable amount of o-ring swelling to Jet-A. A recent study by Boeing shows that when "active cycloparaffins" are present in SPK fuels at 30 vol% an o-ring swelling behavior similar to a low aromatic Jet-A fuel is achieved (Graham et al., 2011). Other work has shown that at least 60% decalin was needed in order to swell nitrile o-rings to a level comparable to Jet A-1 (Liu and Wilson, 2012). It is apparent that, with respect to cycloalkanes, the type and amount of cycloalkanes is a crucial component in determining the degree of o-ring swelling observed. Jet-A (POSF-10325) is composed of on average 32 wt% total cycloalkanes (mono and bicyclic alkanes) (Holladay et al., 2020). If cycloalkanes are blended into Jet-A at 10 or 30 wt%, the cycloalkane content of a typical fuel increases from 32 wt% to 40 or 52 wt%, respectively. Depending on which cycloalkane is blended, this may yield sufficient o-ring swelling in at least some o-ring materials used in aviation. In addition to o-ring swelling behavior, SAFs must meet a number of criteria for physical properties. These criteria are part of the ASTM-D7566 testing protocol and are provided in **Table 1** (ASTM D7566, 2015). These specifications are based on operability, safety, and performance of the aircraft. Currently, information on the physical properties of a large range of cycloalkanes is limited. Moreover, the data that are available is distributed across a wide expanse of literature covering a large number of research areas. Researchers aiming to convert feedstocks into SAFs must have reliable estimates or measurements of the physical properties of cycloalkanes so that they can target fuels that meet specification.

TABLE 1 | Jet-A constraints and Median Jet-A values for the physical properties considered in this work. Jet-A constraints come from ASTM D7566, and median values come from the Petroleum Quality Information System, and consists of 770 data points.

Physical property	Constraint	Median value
Specific Energy, MJ/kg	>42.8	43.20
Energy Density, MJ/L	***	34.90
Density at 15°C, kg/m^3	775–840	810
Flashpoint, °C	>38C	46.39
Melting point, °C	<–40	–49.43

The chemical space occupied by cycloalkanes is large and experimental measurements of even a small fraction of this space is not tractable. Computational models have been shown to be fast, efficient, and accurate and can therefore cover a larger portion of this chemical space. Supplementing experimental measurements with predictions can enable the development of Structure-Property Relationships (SPRs) and trends deduced from these SPRs will allow researchers to better select new SAF targets for production. This paper attempts to deduce SPRs by predicting relevant physical properties. Data are obtained from many different sources and are supplemented with estimates from computational models. The physical properties considered in this paper are freezing point, physical density, specific energy, energy density, flashpoint, and Hansen solubility parameter (HSP). These are shown in **Table 1** along with the required values for a reference aviation fuel, Jet-A (As per ASTM D7566) (ASTM D7566, 2015). Cycloalkanes are split into different groups based on their structural features and the influence of those structural features on the physical properties are used to infer SPRs. In addition, data of blends with some

promising cycloalkanes are shown and discussed. When in this paper, minimums and maximums of Jet-A properties are referenced they are always in regards to the specifications of Jet-A properties as laid out in ASTM-D1655 (ASTM D1655, 2019). In addition, when reference is made to median Jet-A specific energy and energy density values these values are taken from 770 PQIS (Petroleum Quality Information System) data points (Defense Technical Information Center, 2013).

2 MATERIALS AND METHODS

When available, data from National Institute of Standards and Technology, NIST, or experimental data from the literature were used (Kazakov et al., 2002; Acree and Chickos, 2011; Bradley and Andrew, 2014). When data from the literature are used it is cited in the appropriate section, where it is used. However, many values used in generating SPRs are derived from computational models. These models are described below. The accuracy of each computational model is described in **Section 3**.

2.1 SAFT-γ-Mie

The SAFT-γ-Mie EoS is used to predict physical properties when no experimental or other more accurate method is unavailable. The SAFT-γ-Mie EoS attempts to accurately model the Helmhotz free energy (A), by decomposing A into different parts. A is obtained through the following equation:

$$A = A^{ideal} + A^{mono} + A^{chain} + A^{assoc} \tag{1}$$

where A^{ideal} is the Helmholtz free energy obtained through the ideal gas law, A^{mono} is the residual accounting for monomeric Mie segment interactions, A^{chain} is the residual accounting for molecule formation, and A^{assoc} is a term that accounts for association interactions. With each additional term in the expansion, a more realistic chemistry is obtained, and a more realistic representation of A is realized. An exact expression for A^{ideal} is known, and the other terms can be determined through group contribution theory perturbation theory or Wertheim's first-order perturbation theory (TPT1) (Barker and Henderson, 1967; Wertheim, 1984a; Wertheim, 1984b; Wertheim, 1986a; Wertheim, 1986b). Once A is known, physical properties can be determined using simple partial derivative relations i.e., such as Maxwell's equations.

2.2 Specific Energy, Energy Density, and Density

Using the coefficients of a balanced combustion reaction, the enthalpy of combustion can be calculated using a quantum chemistry composite method, such as, CBS-QB3 method (Montgomery et al., 2000). The energy required to vaporize the cycloalkane is accounted for by using the standard heat of vaporization, which is calculated using the SAFT-γ-Mie Equation of State (EoS). The enthalpy of combustion, once calculated, is then converted to the specific energy by using the molecular weight as a conversion factor. The energy density is calculated by multiplying the Specific Energy by the density of the target molecule at 25°C. The SAFT-γ-Mie EoS is used to calculate densities, and a description of the SAFT-γ-Mie EoS is provided above.

2.3 Flashpoint

The flashpoint of a pure molecule is calculated using an empirical equation that has been shown to be accurate for a wide range of compounds (Catoire and Naudet, 2004). The inputs to the flashpoint equation, **Eq. 2**, are the number of carbon atoms, the normal boiling point, and the standard heat of vaporization (Catoire and Naudet, 2004). This equation is accurate for flashpoints that are between −100 and 200°C, normal boiling points (NBP) that are between 250 and 650 K, standard enthalpies of vaporization ($\triangle H_{vap}(298.15)$) between 20 and 110 kJ mol^{-1}, and number of carbon atoms (C_{num}) between 1 and 21. NBP are obtained from the literature, when possible, but, if not possible, are calculated using the SAFT-γ-Mie EoS.

$$T_{fp} = \left(1.477 \times NBP^{0.79686} \times \triangle H_{vap}^{0.16845} \times C_{num}^{-0.05948}\right) - 278.15 \tag{2}$$

2.4 O-Ring Swelling *via* Hansen Solubility Parameters

O-ring swelling behavior of cycloalkanes were investigated by using the framework provided by Hansen (1967). The framework, called Hansen Solubility Parameters (HSP), relies on the ability to calculate a dispersion, polar, and hydrogen bonding term. These terms form the basis of a three coordinate system, often called Hansen space. Molecules can be plotted using this coordinate system, and the closer two molecules are on this space, the more alike they are. The framework provided by HSP allows for the determination of the likelihood of o-ring swelling. The more alike a cycloalkane is with a polymer, the more likely the cycloalkane can permeate through the polymer and cause o-ring swelling. Once the three HSP are known, the distance between two molecules (Ra) can be calculated as follows:

$$Ra^2 = 4(\delta_{d2} - \delta_{d1})^2 + \left(\delta_{p2} - \delta_{p1}\right)^2 + (\delta_{h2} - \delta_{h1})^2 \tag{3}$$

Each polymer also has an interaction radius (Ro) ascribed to it. For a cycloalkane and a polymer, if Ra/Ro is less than 1, the two molecules a alike, and o-ring swelling behavior is predicted to occur. If Ra/Ro is greater than 1, then the two molecules are not alike, and o-ring swelling is not predicted to occur. One important aspect of cycloalkanes is that they are not very polar, and they do not hydrogen bond with other hydrocarbon cycloalkanes. This simplifies **Eq. 3**, where now, only the first term is important. In this work, the dispersion term is calculated through the following equation:

$$\sqrt{\frac{H_{vap}}{V_m}} \tag{4}$$

where, H_{vap} is the standard enthalpy of vaporization, and V_m is the molar volume at 25°C.

2.5 Experimental Methodology

All chemicals and solvents were obtained from commercial sources and used as received unless otherwise specified. $NbOPO_4$ was heated to 100°C in a vacuum oven overnight prior to use. ^1H and ^{13}C NMR spectra were collected at room temperature on a Bruker AV400 MHz spectrometer, with chemical shifts referenced to the residual solvent signal. GC-MS analysis was carried out using an Agilent 7890 GC system equipped with an Agilent 5975 mass selective detector, a flame ionization detector (FID) and a Polyarc system. The Polyarc system is a catalytic microreactor that converts all organic compounds to methane after chromatographic separation and prior to detection.

Combustion calorimeter measurements were performed using an IKA C1 compact combustion calorimeter. Higher heating values were measured in triplicate using approximately 0.3 g sample and averaged. The lower heating values (reported as the specific energy) were calculated by subtracting the contribution due to hydrogen content from the higher heating value. Flash point was measured on an Ametek Miniflash FP flash point tester according to ASTM D6450 (ASTM D6450, 2021). In each run, around 1 ml of sample was injected into the sample cup and the heating rate was set to 5.5°C/min. Viscosity and density measurements were performed using an Anton Paar SVM 3001 according to ASTM D7042 (ASTM D7042, 2021) and ASTM D4052 (ASTM D4052, 2019). Freeze point (ASTM D5972) (ASTM D5972, 2016) and other cold flow properties such as cloud point (ASTM D5773) (ASTM D5773, 2021) and pour point (ASTM D5949) (ASTM D5949, 2016) were measured using Phase Technology PSA-70Xi-FP analyzer. Elemental analyses were performed by Atlantic Microlabs, Inc. (Norcross, GA, United States). Cyclohexane, cycloheptane, cyclooctane, cyclododecanone, cyclopentadecanone, (s)-(-)-limonene, and γ-terpinene were purchased from Sigma Aldrich. β-pinene and β-caryophyllene were purchased from Floraplex.

2.5.1 Synthesis of Cyclododecane

A 50 ml stainless-steel reactor was charged with cyclododecanone (2.00 g; 0.0109 mol), Ni/SiO_2-Al_2O_3 (20 wt%; 0.400 g), $NbOPO_4$ (50 wt%; 1.00 g), and hexane (12 ml). The reactor was sealed and pressurized with 300 psi H_2, flushing three times. The vessel was placed in a preheated aluminum block at 180°C and heated for 21 h with stirring. The reactor was cooled in a water bath until reaching room temperature and depressurized. An aliquot of the reaction mixture was filtered and analyzed by GC-MS, confirming complete consumption of cyclododecanone and formation of alkane products. The reaction mixture was filtered through a Celite plug into a vial containing ~1 g of $MgSO_4$ and the volatiles were removed under reduced pressure, yielding a white semi-solid (1.74 g; 0.0103 mol; 94% yield). ^1H NMR (400 MHz, $CDCl_3$): 1.35 ppm (singlet). ^{13}C NMR (100 MHz, $CDCl_3$): 23.84 ppm (singlet). GC-MS: m/z = 168.1 (retention time = 11.13 min).

2.5.2 Synthesis of Cyclopentadecane

A 50 ml stainless-steel reactor was charged with cyclopentadecanone (2.00 g; 0.009 mol), Ni/SiO_2-Al_2O_3 (20 wt %; 0.400 g), $NbOPO_4$ (50 wt%; 1.00 g), and hexane (12 ml). The reactor was sealed and pressurized with 300 psi H_2, flushing three times. The vessel was placed in a preheated aluminum block at 180°C and heated for 21 h with stirring. The reactor was cooled in a water bath until reaching room temperature and depressurized. An aliquot of the reaction mixture was filtered and analyzed by GC-MS, confirming complete consumption of cyclopentadecanone and formation of alkane products. The reaction mixture was filtered through a Celite plug into a vial containing ~1 g of $MgSO_4$ and the volatiles were removed under reduced pressure, yielding a white semi-solid (1.60 g; 0.0085 mol; 96% yield). ^1H NMR (400 MHz, $CDCl_3$): 1.33 ppm (singlet). ^{13}C NMR (100 MHz, $CDCl_3$): 27.03 ppm (singlet). GC-MS: m/z = 210.2 (retention time = 12.34 min).

2.5.3 Hydrogenation of Terpenes

The hydrogenation of terpenes was carried out in a 50 ml stainless-steel reactor. Typically, 5 g of terpene was placed in the reactor, which was purged with hydrogen gas three times. For β-pinene and β-caryophyllene, 10% Pd/C (10 wt%) was added to the reactant, while for (s)-(-)-limonene and γ-terpinene 5% Pt/C (10 wt%) was added to the reactant. The reactor was charged with 200 psi H_2, after H_2 was completely consumed, the reactor was re-charged with H_2 based on the calculated H_2 consumption required for complete hydrogenation of 5 g of a terpene. An aliquot of the reaction mixture was filtered and analyzed by GC-MS and NMR, confirming complete hydrogenation and formation of saturated products. The reaction mixture was filtered through a Celite plug into a vial, and the resulting products were used without further purification.

3 RESULTS AND DISCUSSION

The computational methods used to make predictions have been previously shown to yield accurate results. With respect to specific energy and energy density, the literature shows that the enthalpies calculated with the CBS-QB3 method have a RMSD (Root Mean Square Deviation) of 1.49 kcal mol^{-1} (Pokon et al., 2001). To understand how the accuracies of enthalpies translates to accurate specific energy and energy density the specific energy and energy density were calculated for a set of hydrocarbons. The absolute average deviation (AAD) was found by comparing the predicted values to measured values from the literature (Heyne, 2018). The AAD for specific energy and energy density were found to be 0.35 MJ/kg, and 0.51 MJ/L, respectively. This is in accord with the reproducibility quoted in the ASTM standard for specific energy, ASTM-D240, of 0.4 MJ/kg (ASTM D240, 2019). Results of this analysis are shown in **Supplementary Table S1**. Although there is a systematic underprediction in the specific energy using CBS-QB3 is accurate such that predictions of the specific energy fall within the error bars of experimentally determined values.

Part of the process of predicting the energy density involves predicting the physical density of the target molecule. The density of each target molecule is calculated using the SAFT-γ-Mie EoS.

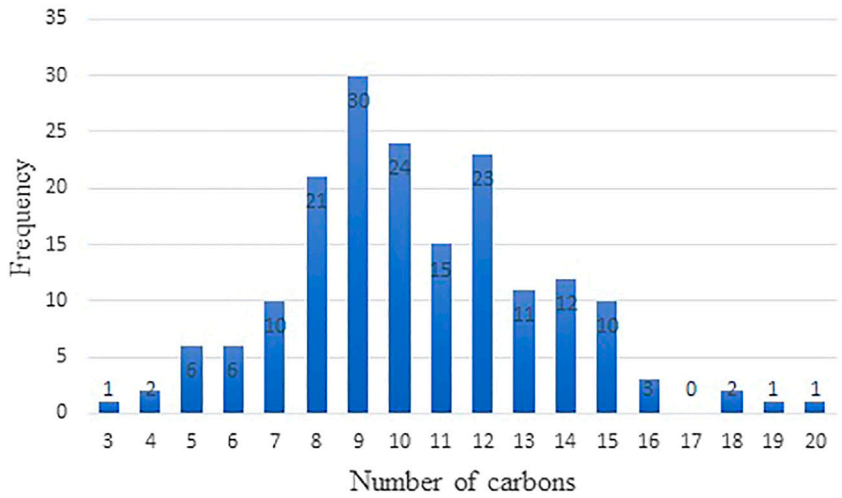

FIGURE 1 | Distribution of cycloalkanes in the database as a function of the number of carbons in the cycloalkane.

SAFT-γ-Mie consistently yields accurate densities throughout the full liquid range of simple and complex mixtures, and variants of it have been used for decades (Chapman et al., 1989; Gross and Sadowski, 2002; Abala et al., 2021). Additionally, in 2017 Perez et al. published a comparison study between different EoS approaches to evaluate predictions of VLE (Vapour-Liquid Equlibria), and density for pure and binary mixtures commonly found in carbon-capture sequestration work (Chapman et al., 1989). This study relied on 22,904, 26,479, and 31,928 measurements of VLE, binary mixture density, and single-phase density, respectively. Perez et al. (2017) concluded that SAFT EoSs methods for predicting density had accuracies better than 3.0% AAD% (Percent Absolute Average Deviation) for all chemical systems studied, and an average AAD% of 1.16. All data taken together, the SAFT EoS was superior to other EoS methods studied.

178 cycloalkane structures were examined in this study. **Figure 1** plots the number of cycloalkane structures in the database with the number of carbons in the structure. The maximum of the distribution occurs at a carbon number of 9, for which we have 30 structures. A second peak occurs with structures containing 12 carbon atoms. This distribution is lighter than the distribution of petroleum based jet fuels where molecular structures containing 9 to 16 carbon atoms is typical. The distribution found in **Figure 1** broadly represents components found in jet fuel (Corporan et al., 2011). Melting points given here were taken from published databases and the open literature (Acree and Chickos, 2011; Bradley and Andrew, 2014; Rosenkoetter et al., 2019; Muldoon and Harvey, 2020). Unfortunately, not every cycloalkane in the database has a melting point value. There are no accurate prediction tools available for melting point, and melting points were only taken from databases and the open literature. In the next few sub-sections basic SPR are shown which, together, start to reveal the relationship between structure and function that lead to good jet fuel performance.

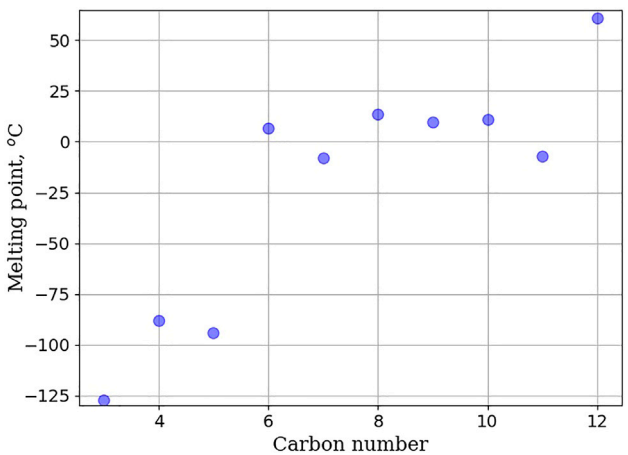

FIGURE 2 | Plot of melting point as a function of the number of carbons in the ring of the cycloalkane. Melting point of unsubstituted cycloalkanes do not increase linearly, but rather reach a plateau between cyclohexane and cyclodecane before increasing to 61°C.

3.1 Unsubstituted Cycloalkanes

Figure 2 shows the melting point of unsubstituted rings as a function of the number of carbon atoms in the ring. Rings larger than 5 carbon atoms fail to meet the melting point specification for Jet-A. Melting point does not increase monotonically but rather reaches a plateau between 6 and 10 carbon atoms, before decreasing slightly, and then increasing to a melting point of 61°C, for cyclododecane. Drotloff and Moller used DSC (Differential Scanning Calorimetry) to investigate the phase transition of large cycloalkane rings (Drotloff and Moller, 1987). They observed that melting point behavior is correlated to the amount of disorder in the liquid phase and that cycloalkanes with lower ring strain can adopt multiple, different conformations. The degree to which these conformations can be accessed influences the melting point.

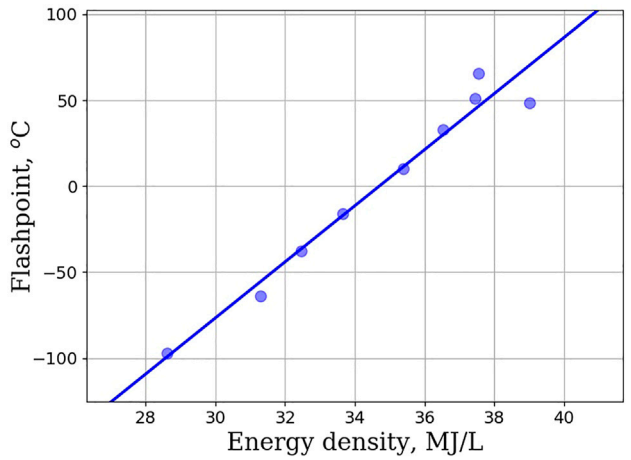

FIGURE 3 | Flashpoint (in degrees Celsius) as a function of energy density (in MJ/L for unsubstituted cycloalkanes. The linear trend suggests that ring size, flashpoint, and energy density are directly correlated.

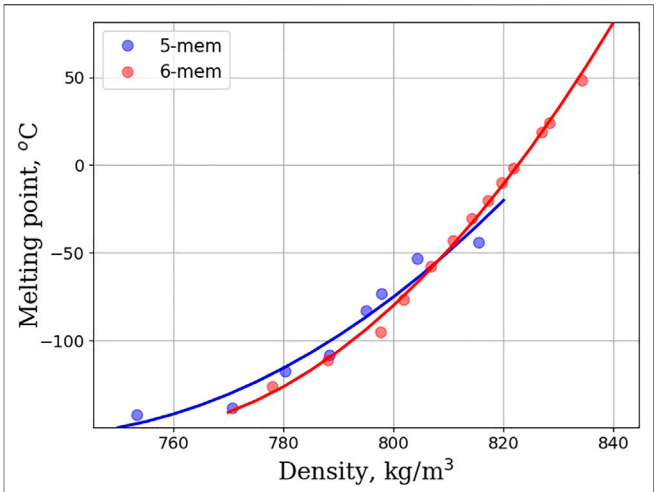

FIGURE 5 | Melting point (in degrees Celsius) as a function of density (in kg/m^3) for 5 and 6 membered rings within the monosubstituted linear cycloalkane group.

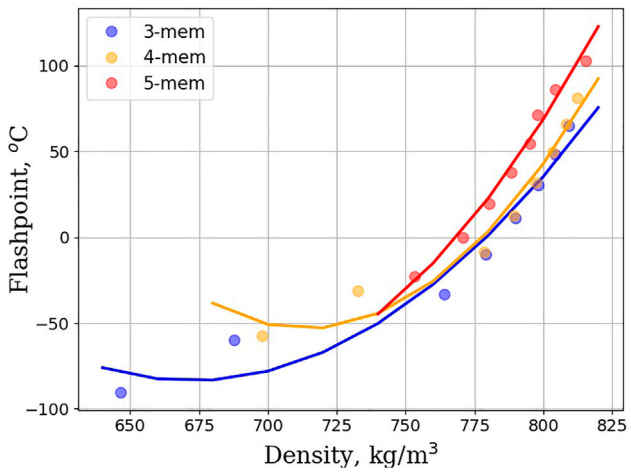

FIGURE 4 | Flashpoint (in degrees Celsius) as a function of density (in kg/m^3) for monosubstituted linear cycloalkanes. Data are shown for 3, 4, and 5 membered rings, and are fitted to a second order polynomial. Each curve is plotted, starting from methylcycloalkane, and increasing the size of the alkyl group by 1 carbon with each successive point.

Figure 3 shows the variation in flashpoint as a function of energy density. This relationship is mostly linear, with deviations occurring with larger ring sizes. The low energy density for small rings (cyclopropane and cyclobutane) is a byproduct of their much smaller densities. Conversely, their high specific energies are a results of their higher ring strain, which when broken releases more energy (Sirjean et al., 2006). The inference drawn from **Figure 3** is that as ring size increases benefits to flashpoint and energy density are obtained. Unsubstituted cycloalkanes can be used in the design of SAFs so long as they are included as blends or contain other structural features that can decrease their melting point. **Supplementary Tables S2–S5** shows experimental values for blending unsubstituted rings with Jet-A (POSF-10325) at 10 wt%. All blends meet the Jet-A specification for freeze point, viscosity, and specific energy. This is contrary to the neat cycloalkane physical properties where all of the cycloalkanes fail to meet the jet-A specification for melting point. In addition, pure solutions of cyclohexane, cycloheptane, and cyclooctane fail to meet jet-A specification for flashpoint. The data show that as modest (10 wt % blends), unsubstituted cycloalkanes can lead to acceptable jet-A fuels. Unfortunately, data for higher blends are not promising. **Supplementary Tables S6–S9** show experimental measurements for unsubstituted cycloalkanes blended into Jet-A (POSF-10325) at 30 wt%. 30 wt% blends fail to meet many of the Jet-A specifications. The cyclododecane blend fails to meet the freeze point specification, the cyclohexane and cycloheptane blend fail to meet the flashpoint requirement, and the cyclododecane and the cyclopentadecane blend fail to meet the viscosity requirement for Jet-A. All unsubstituted cycloalkanes studied fail to meet at least one of the requirements for Jet-A, and at 30 wt% blends, unsubstituted rings cannot be used.

3.2 Monosubstituted Linear Cycloalkane

An alternative route to meet Jet-A specification is to add alkyl substituents to unsubstituted cycloalkane rings. **Figure 4** shows the flashpoint vs. density plot for monosubstituted linear cycloalkanes. The homologous series of 3, 4, and 5 membered rings is depicted, and a clearly discernable trend is that as density increases so too does the flashpoint. Strikingly, the curves for 3, 4, and 5 membered rings are nearly overlapping, suggesting that ring size plays little to no role in this trend. **Figure 5** shows the density vs. melting point for the homologous series of 5 and 6 membered monosubstituted linear cycloalkanes. The literature shows that the orientational dependence, upon freezing, plays a large role in understanding the melting properties of monosubstituted linear cycloalkanes. Hasha and Huang

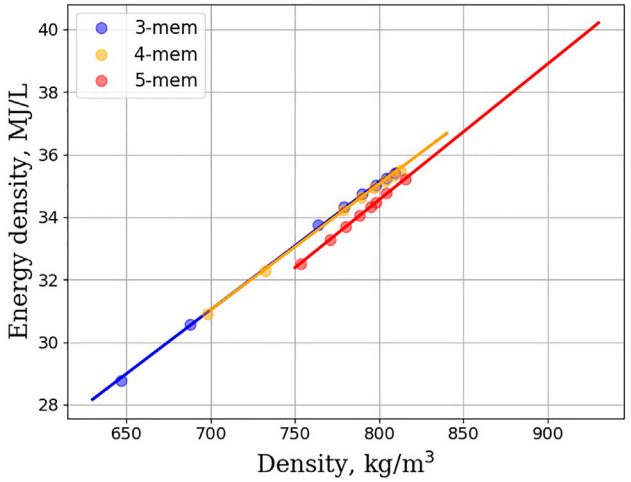

FIGURE 6 | Energy density (in MJ/L) as a function of density (in kg/m^3) for the homologous series of 3, 4, and 5 membered rings. The linear relationship suggests that the energy density and density are insensitive to the chemical structure of multisubstituted linear cycloalkanes. Data are fit to a linear equation.

observed a coupling between the rotational and translational motion of methylcyclohexane using NMR (Hasha and Huang, 1979). They postulated that this coupling plays a large role in the melting properties of methylcyclohexane. The crystal structure of methylcyclopentane was investigated and found to be oriented in an envelope conformation, with the methyl group adopting a pseudo-equitorial position (Bream et al., 2006). Upon freezing, the methylcyclopentanes adopt a zig-zag pattern with each other, with some methyl groups pointed diagonally upwards, and some pointed diagonally downwards. Finally, Milhet et al. used DSC to observe the melting behavior of n-alkyl cyclohexanes. Their observations revealed that melting temperature increases as chain length increases, but that odd carbon length chains behaved differently from even carbon length chains (Milhet et al., 2007). Adding an extra CH2 to an alkyl chain with an odd number of carbons increased the melting temperature more than if a CH2 was added to an alkyl chain length with an even number of carbons. This suggests that indeed orientational dependence does play a role, but that as alkyl chain length increases the number of orientations that can be adopted in a crystalline structure decreases, and solidification becomes easier. The plot in **Figure 5** captures this orientational dependence by plotting the density and shows that melting point increases as the linear alkane length increases. The linear relationship between density and energy density is shown in **Figure 6**. For all homologous series studied, the energy density is a linear function of the density and if large energy densities are desired, large densities are needed. The conclusions drawn from **Figures 4–6** are that density is an overriding factor in determining what role monosubstituted linear cycloalkanes can play in the generation of SAFs. Higher densities lead to higher energy densities, but at the expense of higher melting points, and trade-offs are required to ensure that existing fuel requirements are met. If a mixture of simple linear cycloalkanes were generated with densities at the top range of the jet-A specification (840 kg/m^3), such a mixture would likely fail to meet the jet-A specification for melting point. **Figure 6** indicates that it would have a melting point estimate of >50°C. In order to meet the melting point specification, it would need to have a density < ~810 kg/m^3.

3.3 Polysubstituted Linear Cycloalkane

Due to the structural complexity available in this group, there are no easily identifiable trends within the data however, all structures exceed the minimum Jet-A specification for specific energy of 42.8 MJ/kg. A few cycloalkanes in this group are notable in that they have specific energy in excess of 0.5% above the median Jet-A while achieving comparable energy density. These structures, and their properties are shown below in **Table 2**. A pattern that emerges from this data is that multiply substituted molecules with rings greater than 6 carbons are suitable cycloalkanes for the development of SAFs. These are suitable molecules, because they feature large densities and flashpoints while maintaining very low melting points. In addition, although viscosity is not covered in this work, there is evidence in the literature that they can have good viscosities (Rosenkoetter et al., 2019). A mixture of 1,4 and 1,5 dimethylcyclooctane was prepared using a [4 + 4] cycloaddition of isoprene catalyzed by an Iron catalyst (Rosenkoetter et al., 2019). Measured physical properties of this mixture show that its freezing point is <−78°C, and its viscosity at −20°C is 4.17 mm^2/s (Rosenkoetter et al., 2019). These values are well below the maximum value for Jet-A, as indicated in **Table 1**. The structural reasons for why polysubstituted ring expanded cycloalkanes have good cold flow properties is not known, but, as discussed previously, it may be related to greater flexibility conferred by the addition of multiple alkyl chains to the ring. Running quantum mechanics calculations on 1,4-dimethylcyclooctane, the lowest energy configuration is the crown configuration. This is different from the boat-chair conformation adopted by cyclooctane. Another pattern that emerges from the data is that cyclic structures which have di-methylated carbon atoms can have very good physical properties.

3.4 Monosubstituted and Polysubstituted Branched Cycloalkanes

The main biological route to branched cycloalkanes is through the MEP pathway. Using computational modeling the production of limonene in cyanobacteria was increased 100 fold (Wang et al., 2016). The computational modeling identified a bottleneck to the production of limonene, which once removed, allowed for increased limonene production. Through genetic engineering of *R. turuloides* researchers were able to achieve titers of α-bisabolene and 1,8-cineole of 2.6 and 1.4 g/L, a several fold increase over previously reported efforts (Kirby et al., 2021). Chemical routes reported in the literature are sparse and rely on reduction of a starting oxygenate. Starting from diacetone alcohol, a dehydration/diels alder process was developed, which when hydrogenated furnished a mixture of

TABLE 2 | Notable polysubstituted linear cycloalkanes structures.

Chemical name	SE, MJ/kg	ED, MJ/L	MP, °C	Density, kg/m^3	Flashpoint, °C
1,1-diethylcyclohexane	43.60	35.81	−54.4	828.60	49.20
1,2,3,4-tetramethylcyclohexane	43.26	35.4	−75	825.80	40.50
1,4-dimethylcyclooctane	43.82	36.22	−78	827.00	49.50
1,1,4-trimethylcycloheptane	43.56	34.83	***	807.60	42.50
1,1,5-trimethyl-2-pentylcyclohexane	43.46	35.00	<−75	812.60	***

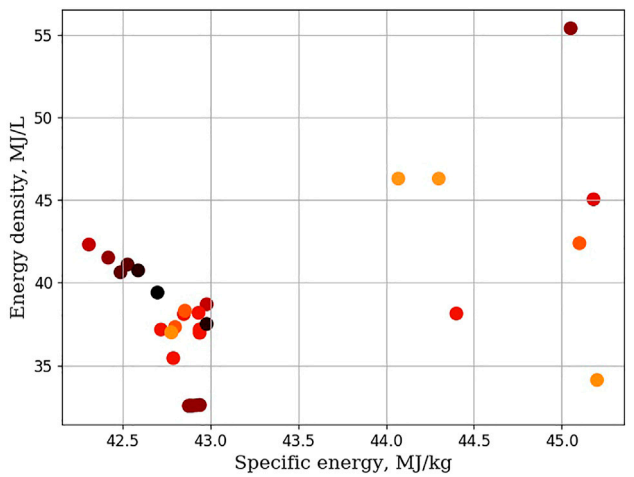

FIGURE 7 | SEED plot of the multicyclic cycloalkanes studied in this work. Specific energy is in MJ/kg, Energy density is in MJ/L, and the shading of each marker corresponds to molecular weight. Darker colors indicate higher molecular weights.

cyclopentanes. Branched cyclopentanes were a major fraction of the products formed, and the overall mixture has a freezing point of −56.6°C (Chen et al., 2016a). Starting from a lignocellulosic oxygenated by product, hydrodeoxygenation afforded a 12 C branched cycloalkane (Li et al., 2020). One important feature of branched cycloalkanes is their low melting points. In the database, constructed for this paper, isopropyl and isobutyl substitutions lead to melting points of at least 50°C below the jet-A specification. Tert-butyl linkages also have good melting points, but tert-butylcyclohexane's melting point of −41.2°C hovers just below the jet-A specification. No melting point data outside of 5 and 6 membered rings are available hence, a correlation between ring size and branching substituent is not possible. Of the branched cycloalkanes examined, specific energies increased by an average of 1.04%, and energy densities fell by an average of 1.73% over median jet-A values. The molecules with the highest specific energies were those with an isopropyl group. Most molecules with a tert-butyl group showed the largest decreases in energy density. Reasons for this include lower specific energies, but also lower physical densities.

Polysubstituted branched cycloalkanes do not show any benefit over monosubstituted branched cycloalkanes. Specific energies and energy densities calculated are commensurate with those calculated for monosubstituted branched cycloalkanes. Additionally, not a lot is known about the melting points of polysubstituted branched cycloalkanes. Further, because they have multiple substitution sites, they are likely to have higher YSI yields. Given the difficulty of producing polysubstituted branched cycloalkanes, it is unlikely that there will be benefits to including them in SAFs.

3.5 Multicyclic-Cycloalkanes

The SEED plot for molecules in the MC group are shown in **Figure 7**. Most multicyclic molecules are located within a band bounded between 42 and 43 MJ/kg, and 33 and 43 MJ/L. The remaining seven molecules are cis-carane, and a group of molecules that belong to a class of molecules called ladderanes. Further, there is no correlation between molecular weight and where a molecule falls in the SEED plot. This finding indicates that the type of carbon-carbon bond is important, and that low molecular weight, ring strained molecules can lead to elevated energy densities and specific energies. Focusing on decalins, in 2009, researchers using an ignition quality tester, IQT, determined that the cetane number of cis-decalin was significantly higher than trans-decalin (Hasha and Huang, 1979). Although cis-decalin does not have great physical properties for jet fuel, the authors suggested those physical properties may be improved by adding a single isoparaffin group to the cis-decalin core (Heyne et al., 2009). Also, in 2019 researchers upgraded cyclopentanone to a series of alkyl-decalins. The measured freezing point of the isomerization mixture was reported to be −23.45°C. In this work, several derivatives of cis-decalin were evaluated as possible candidates for inclusion into SAFs. **Table 3** lists these derivatives along with their physical properties. Cis-decalin has a measured energy density of 38.7 MJ/L. This is 10.8% higher than the median Jet-A value. However, its specific energy of 42.98 MJ/kg is 0.51% lower than the median Jet-A value. As a jet fuel component, its melting point of −38.8°C is slightly above the −40°C upper limit of the jet-A fuel specification, and has a low temperature viscosity, at −20°C, of 11.3 mm^2/s (see **Table 1**). In this work, a series of dimethyl cis-decalins have been evaluated. The physical properties of cis-decalin, and its derivatives, are tabulated in **Table 3**. Dimethyl cis-decalins have lower densities and thus lower energy density than cis-decalin. A 2016 paper outlined a conversion strategy, starting from cyclopentanol, which generated a mixture of C10 decalin and C15 polycycloalkanes. Measured physical properties of this mixture show that it has a melting point that is less than −110°C, and a density, measured at 20°C, of 876 kg/m^3 (Chen et al., 2016b). The clear suggestion here is that decalin mixtures can yield promising

TABLE 3 | Physical properties of cis-decalin and some dimethyl-decalins analyzed in this work.

Chemical name	Specific energy, MJ/kg	Energy density, MJ/L	Melting pt. °C	Density at 15°C kg/m^3
cis-decalin	42.98	38.70	-38.80	901.02
1,10-dimethyl-cis-decalin	42.90	32.56	***	***
1,2-dimethyl-cis-decalin	42.94	32.60	***	***
1,3-dimethyl-cis-decalin	42.88	32.55	***	***
1,4-dimethyl-cis-decalin	42.89	32.56	***	***
1,5-dimethyl-cis-decalin	42.88	32.55	***	***
1,6-dimethyl-cis-decalin	42.92	32.58	***	***
1,7-dimethyl-cis-decalin	42.88	32.55	***	***
1,8-dimethyl-cis-decalin	42.94	32.60	***	***

TABLE 4 | Physical properties of octahydropentalene and its derivatives analyzed in this work.

Chemical name	Specific energy, MJ/kg	Energy density, MJ/L	Density at 15°C kg/m^3
Octahydropentalene	42.78	37.00	873.50
methyl-octahydropentalene	42.86	38.31	902.67
ethyl-octahydropentalene	42.93	38.18	897.67
propyl-octahydropentalene	42.98	38.06	893.56
sec-butyl-octahydropentalene	42.95	37.95	891.47

physical properties. However, SAF generating process are unlikely to derive large benefits from the inclusion of dimethyl cis-decalins. Adding larger alkyl substituents, like an n-butyl substituent to cis-decalin recovers most of the density lost from alkylation of cis-decalin, but likely have melting points that are too high to be useful as SAF components. Of course, cis-decalin is not the only fused bicyclic compound available. Other bicyclic compounds, such as octahydropentalene (two fused cyclopentanes), and mixed cyclic fused molecules are also available. **Table 4** shows the physical properties for octahydropentalene and its derivatives. Octahydropentalenes show only modestly higher specific energy values but show elevated energy density. Additionally, they show densities that are too high to meet Jet-A requirements. Octahydropentalene's flashpoint is 20.7°C, 17.3°C below the Jet-A specification. It is likely that octahydropentalenes will require blending to meet the requirements for Jet-A fuel. Octahydropentalene can be chemically synthesized through a number of routes (Gunbas et al., 2005). Further, iodination and bromination can serve as sites for further derivatization by alkyl substitution (Gunbas et al., 2005). Other derivatizations are also possible (Kendhale et al., 2008). A biological pathways to octahydropentalene derivatives is available, starting from glycerol (Li et al., 2014). Some work has been reported on other fused rings containing 5 and 6 membered rings. Starting from aromatic aldehydes and methyl isobutyl ketone a pathway to the formation of octahydroindanes was reported (Muldoon and Harvey, 2020). The route yields a mixture that has a freezing point that hovers around the −40°C upper limit and features a density of 885 kg/m^3. The formation of a binary mixture of perhydrofluorene and dicyclohexamethane from aromatic building blocks, yielded a melting point of −40°C, and a density of 930 kg/m^3 (Muldoon and Harvey, 2020). A class of molecules called ladderanes consist of fused cyclobutanes. They can be prepared chemically in a variety of ways, and are natural products produced by planctomycetes. Anammox planctomycetes, which is the species responsible for producing ladderanes, plays an important part in the remediation of nitrogen-rich wastewater. **Table 5** shows the ladderane structures examined in this work, along with the measured and predicted physical properties. Ladderanes, even the simples bicyclic ladderane, possess remarkably high specific energy and energy density. An analysis from NIST reveals that the bicyclic ladderane possesses a viscosity of 0.77 mm^2/s at −13.15°C (Kazakov et al., 2002). It is likely therefore, that it meets the maximum viscosity of 8 mm^2/s at −20°C. Further, the density of the bicyclic ladderane at 15°C is 828.2 kg/m^3, below the maximum of 840 kg/m^3. When the bicyclic ladderane is alkylated, our work shows that the energy density increases while the specific energy remains elevated. This suggests that alkylation of ladderanes can serve as routes to improve physical properties.

Strained, multicyclic cycloalkanes are also possible. In the literature, these are often hydrogenated terpenes, and in this work, those which were studies, along with their physical properties, are tabulated in **Supplementary Table S13**. Cis-carane, pinane, and sabinane all have the same chemical formula (C10H18). Cis-Carane has higher specific energy and energy density values, and has a viscosity, measured at −40°C, of 6.83 mm^2/s, and a density, measured at 15°C, of 842 kg/m^3. Pinane has somewhat lower specific energy and energy density, compared to cis-carane, but still higher than the median value of Jet-A fuels. At −40°C, the viscosity of pinane is 11.23 mm^2/s, and has a freeze point of −53°C. Its flashpoint is 39.7°C.

Blends of hydrogenated terpenes can often be beneficial. Experimental measurements using 10 and 30 wt % of pinane,

TABLE 5 | Physical properties of ladderanes and their derivatives analyzed in this work.

Chemical name	Specific energy, MJ/kg	Energy density, MJ/L
Ladderane Sims et al. (2014)	44.60	42.30
Ladderane ASTM D756 (2015), syn	44.30	46.30
ladderane ASTM D7566 (2015), anti	44.07	46.30
dimethyl-ladderane Sims et al. (2014)	45.20	34.12
isopropyl-ladderane Sims et al. (2014)	45.10	42.39
diethyl-ladderane Sims et al. (2014)	45.18	45.05
dipropyl-ladderane Sims et al. (2014)	45.05	55.40

TABLE 6 | Hansen Solubility Parameters, average Ra/Ro, and standard deviations for the polymers and cycloalkane data set analyzed in this work. Standard deviations are very low, indicating that most cycloalkanes either exhibit o-ring swelling, or do not. HSP data taken from Accu Dyne Test.

Polymer material	δD	δP	δH	Average Ra/Ro	Std. dev.
Fluorocarbon	14.6	10	1.6	1.25	0.08
Silicon	13.8	5	1.2	0.53	0.09
Poly(acrylonitrile)	21.7	14.1	9.1	1.81	0.08
Poly(butadiene)	17.5	2.3	3.4	0.73	0.10
Acrylonitrile butadiene styrene (ABS)	17	5.7	6.8	0.97	0.03
Epoxies	19.2	10.9	9.6	1.40	0.05
Fluorinated ethylene polypropylene	19	4	3	1.78	0.28

carryophyllane, limonene, and p-menthane were carried out. Blends were generated using the POSF 10325 Jet-A fuel. **Supplementary Tables S10–S13** shows the neat physical properties of these hydrogenated terpenes, followed by their blended physical properties. The viscosity of pinane at −40°C is 12.256 mm^2/s, which is at the border of pass/fail. At 10 wt% blends with Jet-A, the viscosity is measured to be 8.94 mm^2/s, within the Jet-A specification. Carryophyllane fails to meet viscosity requirements for Jet-A. As a 10 wt% blend, it still fails to meet viscosity specification. Smaller blends are possible, but will dilute the elevated energy density and specific energy neat values of carryophyllane. Limonane and terpinane have neat properties that meet Jet-A specifications. As blends, low temperature viscosities increase, specific energies decrease, and flashpoints increase. In this scenario, a trade-off needs to be made between decreasing specific energy and increasing flashpoints.

3.6 O-Ring Swelling

O-ring swelling behavior was inspected by using the framework provided by Hansen Solubility Parameters (HSP). This framework allows for the identification of molecules with similar interactional forces. It is described in further detail in the methodology section. A number of polymer materials were analyzed, and the results of the analysis are shown in **Table 6**. HSPs were obtained from (Accu Dyne Test, 2021) Polymers which have a Ra/Ro that is less than 1 indicate that o-rings made out of that polymer will exhibit o-ring swelling behavior when exposed to cycloalkanes. Polymer materials with low polarity and hydrogen bonding terms, but a high dispersion term show the best promise for o-ring swelling behavior. All cycloalkanes studied indicate they will produce o-ring swelling in o-rings made from polybutadiene. Di methyl and tri methyl cyclohexanes and cyclopentanes show Ra/Ro values that were closest to 1, indicating that they may produce minimal amounts of o-ring swelling. Ra/Ro values were all significantly above 1 for o-rings made with polyacrylonitrile polymers, indicating that cycloalkanes are less likely to induce o-ring swelling in polyacrylonitrile than in polybutadiene. The best performing cycloalkanes were fused cycloalkanes. Octacyclopentalene (two five membered rings fused together), and decahydro-1H-cyclopenta[a]pentalene (three five membered rings fused together) were best performers. Research has indicated that disruption of the interaction of nitrile groups is important to inducing o-ring swelling. Although no definitive conclusions can be drawn, it appears that many of the cycloalkanes studied do not possess the ability to disrupt these interactions in acrylonitrile. O-ring swelling in acrylonitrile-butadiene-styrene polymers were also examined, by analyzing the results of HSP. Results indicate that cycloalkanes may produce some o-ring swelling in o-rings made from acrylonitrile-butadiene-styrene material. Ra/Ro values hover around 1. It is unclear which cycloalkanes may provide o-ring swelling. The standard deviation is small (0.03), and because of uncertainty it is difficult to ascertain which cycloalkanes may be considered best performers. Overall, what can be said of this analysis is that fused cycloalkanes tend to provide the best opportunities for o-ring swelling. This seems to be true regardless of the o-ring material. This does not mean that o-ring swelling is guaranteed, merely that fused cycloalkanes provide the best opportunity to induce sufficient o-ring swelling. Future experimental work may shed more light, but computational simulations may also aid in understanding the criteria necessary for cycloalkanes to induce o-ring swelling in different materials. Some of the molecules studied in this work have physical properties that are at least commensurate with those of Jet-A. As blends, these molecules offer the best

opportunities for providing adequate o-ring swelling while maintaining the physical properties of the blended fuel.

3.7 Sooting Propensity

Aromatics are well known to contribute substantially to soot production during combustion compared to most non-aromatic compounds found in conventional jet fuel (Aromatics perform an important seal-swelling function in jet fuel, and cyclic alkanes have been proposed as an alternative for aromatics to perform the seal-swelling function.). A number of indices have been developed to quantify the relative tendency of hydrocarbons to produce soot. One of the earliest indices, Smoke Point (SP), has been used since the 1930's (Woodrow, 1933), and the measurement involves observing a flame from a standard lamp and measuring the fuel consumption rate (Schalla and McDonald, 1953) or flame height at which visible smoking occurred with lower SPs intended to indicate a greater tendency to produce soot. Systematic measurements of different molecular classes revealed qualitative structure property relationships for SP (Hunt, 1953; Calcote and Manos, 1983) with the general trend in sooting tendency following the pattern: n-paraffins < iso-paraffins < cycloalkanes < alkenes < alkynes < benzenes < naphthalenes. The Threshold Sooting Index (TSI) index was subsequently developed to provide an approximate adjustment for variations in SP related to the quantity of air consumed during combustion, with TSI defined as aMW/SP+b where MW is the molecular weight of the fuel and a and b are constants assigned through measurements of standard compounds to put all TSI measurements on a common scale. Using TSI values the additional trend if increasing soot tendency with increasing carbon number could be seen within different classes of hydrocarbons. In order to improve the reproducibility and precision of sooting tendencies compared to TSI values researchers have subsequently developed other indices that do not rely on SP measurements including Yield Sooting Index (YSI) (McEnally and Pfefferle, 2007; YSI database v2, 2021), Micropyrolysis Index (MPI) (Crossley et al., 2008), and Fuel Equivalent Sooting Index (FESI) (Lemaire et al., 2015). Quantitative structure property relationships based on group contribution methods have been developed for YSI (Crossley et al., 2008; John et al., 2017; Lemaire et al., 2021) for predicting sooting tendencies of uncharacterized hydrocarbons on the basis of their chemical structure.

As a specific example we can look at YSI values, which are derived from the maximum volume-fraction of soot measured by laser induced incandescence along the centerline of a methane co-flow diffusion flames doped with small quantity a specific hydrocarbon. YSI values on the current unified scale (Das et al., 2018) are scaled to give a value of 30 for n-hexane and 100 for benzene. The current YSI database includes 16 cycloalkanes with species in four ring sizes: cyclopentane, cyclohexane, cycloheptane, and cyclooctane. For cycloalkanes with the same molecular weight, higher YSI values are measured for cycloalkanes with multiple substitutions compared to cycloalkanes with longer alkyl side chains. The highest YSI value for a cycloalkane in the database is 82.8 for 1,2,4-trimethylcyclohexane, and the lowest two are cyclohexane and cyclopentane at 42.7 and 39.4, respectively. By comparison, naphthalene has a value of 466.1. The trends in measured YSI values (YSI database v2, 2021) for different structural classes of cycloalkanes is shown in **Figure 8**.

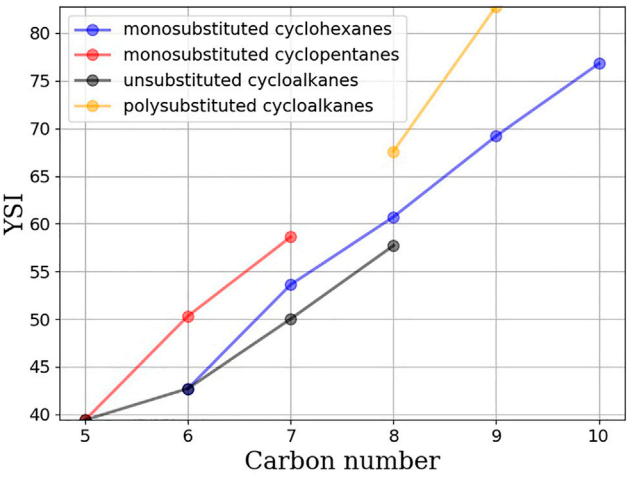

FIGURE 8 | YSI values for different classes of cycloalkanes.

In an effort to understand the potential of including cycloalkanes into SAFs, a database of cycloalkanes, and their physical properties was developed. This database contains 178 cycloalkane structures, and includes information on specific energy, energy density, liquid density, flashpoint, and HSP. From this database, SPRs were developed based on cycloalkane structural features. These structural features include ring size, monosubstituted linear substitutions, polysubstituted linear substitutions, monosubstituted branched substitutions, polysubstituted branched cycloalkanes, and multicyclic cycloalkanes. The SPR developed indicate that unsubstituted cycloalkanes are of limited usefulness for the production of SAFs, because of their high melting points. Experiments, blending unsubstituted cycloalkanes into Jet-A (POSF-10325), show that 10 wt% blends meet the specifications outlined by ASTM D1655, but 30 wt% blends do not. Linear alkyl substitutions can greatly decrease melting points, while maintaining suitably high specific energies and energy densities. In particular, polysubstituted linear, ring expanded cycloalkanes offer large benefits, in terms of exceptional melting points, and large specific energies and energy densities. However, due to their larger YSI values, careful consideration must be taken to avoid sooting issues. Branched substitutions can be beneficial to lowering melting point however, their specific energies and energy densities are only commensurate with median Jet-A values. Given the difficulty of generating (biologically or chemically) branched cycloalkenes, their inclusion into SAFs may be challenging. HSP show that fused cycloalkanes are consistently amongst the most likely cycloalkanes to provide o-ring swelling. For that reason, they should also be considered as possible jet-fuel cycloalkane candidates. Experimental measurements show that some fused cycloalkanes can meet jet-A standards, as specified by ASTM D-1655, especially as 10 and 30 wt% blends. However, not all fused cycloalkanes are good fuel component candidates.

Carryophyllane failed to meet Jet-A specifications, even at a modest 10 wt% blend into Jet-A (POSF-10325).

DATA AVAILABILITY STATEMENT

The raw data supporting the conclusion of this article will be made available by the authors, without undue reservation.

AUTHOR CONTRIBUTIONS

AL and RPB wrote manuscript. AL, RPB, SPD, and NH conducted research. CMM, ADS, and AG supervised research.

FUNDING

Fuel property prediction models, experimental measurements, and the work contained in this paper were funded by the U.S. Department of Energy (DOE) Office of Energy Efficiency and Renewable Energy, Bioenergy Technologies Office.

SUPPLEMENTARY MATERIAL

The Supplementary Material for this article can be found online at: https://www.frontiersin.org/articles/10.3389/fenrg.2021.771697/full#supplementary-material

REFERENCES

Abala, I., Lifi, M., Alaoui, F. E. M., Munoz-Rujas, N., Aguilar, F., and Montero, E. A. (2021). Density, Speed of Sound, Isentropi Compressibility, and Refractive index of Ternary Mixtures of Oxygenated Additives and Hydrocarbons (Dibutyl Ether + 1-Butanol + Toluene or Cyclohexane) in Fuels and Biofuels: Experimental Data and PC-SAFT Equation-Of-State Modeling. *J. Chem. Eng. Data* 66, 1406–1424. doi:10.1021/acs.jced.0c01025

Accu Dyne Test (2021). Surface Free Energy Components by Polar/Dispersion and Acid-Base Analyses; and Hansen Solubility Parameters for Various Polymers. Available from: https://www.accudynetest.com/polytable_02.html (cited July 11, 2021).

Acree, W. E., and Chickos, J. S., (2011). Phase Transition Enthalpy Measurements of Organic and Organometallic Compounds.

ASTM D1655 (2019). *Standard Specification for Aviation Turbine Fuels*. West Conshohocken, PA: ASTM International. www.astm.org.

ASTM D240 (2019). *Standard Test Method for Heat of Combustion of Liquid Hydrocarbon Fuels by Bomb Calorimeter*. West Conshohocken, PA: ASTM International. www.astm.org.

ASTM D4052 (2019). *Standard Test Method for Density, Relative Density, and API Gravity of Liquids by Digital Density Meter*. West Conshohocken, PA: ASTM International. www.astm.org.

ASTM D5773 (2021). *Standard Test Method for Cloud Point of Petroleum Products and Liquid Fuels (Constant Cooling Rate Method)*. West Conshohocken, PA: ASTM International. www.astm.org.

ASTM D5949 (2016). *Standard Test Method for Pour Point of Petroleum Products (Automatic Pressure Pulsing Method)*. West Conshohocken, PA: ASTM International. www.astm.org.

ASTM D5972 (2016). *Standard Test Method for Freezing Point of Aviation Fuels (Automatic Phase Transition Method)*. West Conshohocken, PA: ASTM International. www.astm.org.

ASTM D6450 (2021). *Standard Test Method for Flash Point by Continuously Closed Cup (CCCFP) Tester*. West Conshohocken, PA: ASTM International. www.astm.org.

ASTM D7042 (2021). *Standard Test Method for Dynamic Viscosity and Density of Liquids by Stabinger Viscometer (And the Calculation of Kinematic Viscsoity)*. West Conshohocken, PA: ASTM International. www.astm.org.

ASTM D7566 (2015). *Standard Specification for Aviation Turbine Fuel Containing Synthesized Hydrocarbons*. West Conshohocken, PA: ASTM International. www.astm.org.

Balster, L. M., Corporan, E., DeWitt, M. J., Edwards, T., Ervin, J. S., Graham, J. L., et al. (2008). Development of an Advanced, Thermally Stable, Coal-Based Jet Fuel. *Fuel Process. Technol.* 89, 364–378. doi:10.1016/j.fuproc.2007.11.018

Barker, J. A., and Henderson, D. (1967). Perturbation Theory and Equation of State for Fluids. II. A Successful Theory of Liquids. *J. Chem. Phys.* 47, 4714–4721. doi:10.1063/1.1701689

Bradley, J-C., and Andrew, L. (2014). *Open Melting point Dataset*. doi:10.6084/m9.figshare.1031638

Bream, R., Watkin, D., and Cowley, A. (2006). Acta Crystallographica Section. *Methylcyclopentane* E62, 1211–1212. doi:10.1107/S1600536806006003

Calcote, H. F., and Manos, D. M. (1983). Effect of Molecular Structure on Incipient Soot Formation. *Combust. Flame* 49, 289–304. doi:10.1016/0010-2180(83)90172-4

Catoire, L., and Naudet, V. (2004). A Unique Equation to Estimate Flashpoints of Selected Pure Liquids Application to the Correction of Probably Erroneous Flashpoint Values. *J. Phys. Chem. Ref. Data* 33, 1083–1111. doi:10.1063/1.1835321

Chapman, W. G., Gubbins, K. E., Jackson, G., and Radosz, M. (1989). SAFT: Equation-Of-State Solution Model for Associating Fluids. *Fluid Phase Equilib.* 52, 31–38. doi:10.1016/0378-3812(89)80308-5

Chen, F., Li, N., Li, S., Li, G., Wang, A., Cong, Y., et al. (2016). Synthesis of Jet Fuel Range Cycloalkanes with Diacetone Alcohol from Lignocellulose. *Green. Chem.* 18, 5751–5755. doi:10.1039/C6GC01497F

Chen, F., Li, N., Yang, X., Li, L., Li, G., Li, S., et al. (2016). Synthesis of High-Density Aviation Fuel with Cyclopentanol. *ACS. Sustain. Chem. Eng.* 4, 6160–6166. doi:10.1021/acssuschemeng.6b01678

Corporan, E., Edwards, T., Shafer, L., DeWitt, M. J., Klingshirn, C., Zabarnick, S., et al. (2011). Chemical, Thermal Stability, Seal Swell, and Emissions Studies of Alternative Jet Fuels. *Energy Fuels* 25, 955–966. doi:10.1021/ef101520v

Crossley, S. P., Alvarez, W. E., and Resasco, D. E. (2008). Novel Micropyrolysis index (MPI) to Estiamte the Sooting Tendency of Fuels. *Energy Fuels* 22, 2455–2464. doi:10.1021/ef800058y

Das, D. D., John, St. P., McEnally, C. S., Kim, S., and Pfefferle, L. D. (2018). Measuring and Predicting Sooting Tendencies of Oxygenates, Alkanes, Alkenes, Cycloalkanes, and Aromatics in a Unified Scale. *Combust. Flame* 190, 349–364. doi:10.1016/j.combustflame.2017.12.005

Defense Technical Information Center (2013). *Petroleum Quality Information System 2013 Annual Report*. Fort Belvoir: Diversified Enterprises.

Drotloff, H., and Moller, M. (1987). On the Phase Transition of Cycloalkanes. *Thermochim. Acta* 112, 57–62. doi:10.1016/0040-6031(87)88079-6

Graham, J. L., Rahmes, T. F., Kay, M. C., Belieres, J-P., Kinder, J. D., Millett, S. A., et al. (2011). Impact of Alternative Jet Fuel and Fuel Blends on Non-metallic Materials Used in Commercial Aircraft Fuel Systems. Federal Aviation Administration Report DOT/FAA/AEE/2014-10.

Graham, J. L., Striebich, R. C., Myers, K. J., Minus, D. K., and Harrison, W. E. (2006). Swelling of Nitrile Rubber by Selected Aromatics Blended in a Synthetic Jet Fuel. *Energy Fuels* 20, 759–765. doi:10.1021/ef050191x

Gross, J., and Sadowski, G. (2002). Application of the Perturbed-Chain SAFT Equation of State to Associating Systems. *Ind. Eng. Chem. Res.* 41, 5510–5515. doi:10.1021/ie010954d

Gunbas, D. D., Algi, F., Hokelek, T., Watson, W. H., and Balci, M. (2005). Functionalization of Saturated Hydrocarbons. High Temperature Bromination of Octahydropentalene Part 19. *Tetrahedron* 61, 11177–11183. doi:10.1016/j.tet.2005.09.019

Hansen, C. M. (1967). *The Three Dimensional Solubility Parameter and Solvent Diffusion Coefficient: Their Importance in Surface Coating Formulation*. Copenhagen: Danish Technical Press. Dissertation.

Hasha, J. J., and Huang, S. G. (1979). Self-diffusion and Viscosity of Methylcyclohexane in the Dense Liquid Region. *J. Chem. Phys.* 71, 3996–4000. doi:10.1063/1.438155

Heyne, J. (2018). Down-selected molecules, Dayton. Available at: https://docs.google.com/spreadsheets/d/1fnPldO1z6zrLixZUBe01mccWayGJG5jBv17HXgZzLYI/edit#gid=1784110097 (Accessed September, 2018).

Heyne, J. S., Boehman, A. L., and Kirby, S. (2009). Autoignition Studies of Trans- and Cis-Decalin in an Ignition Quality Tester (IQT) and the Development of a High thermal Stability Unifuel/Single Battlefiel Fuel. *Energy Fuels* 23, 5879–5885. doi:10.1021/ef900715m

Holladay, J., Abdullah, Z., and Heyne, J. (2020). Sustainable Aviation Fuel: Review of Technical Pathways. Available at: https://www.energy.gov/sites/prod/files/2020/09/f78/beto-sust-aviation-fuel-sep-2020.pdf (accessed December 16, 2021). doi:10.2172/1660415

Hunt, R. A. (1953). Relation of Smoke point to Molecular Structure. *Ind. Eng. Chem.* 45, 602–606. doi:10.1021/ie50519a039

International Energy Outlook (2016). Transportation Sector Energy Consumption. Available at: https://www.eia.gov/outlooks/ieo/pdf/transportation.pdf (accessed July 12, 2021).

John, St. P., Kairys, P. W., Das, D. D., McEnally, C. S., Pfefferle, L. D., Robichaud, D. J., et al. (2017). A Quantitative Model for the Prediction of Sooting Tendency from Molecular Structure. *Energy Fuels* 31, 9983–9990. doi:10.1021/acs.energyfuels.7b00616

Kazakov, A. F., Muzy, C. D., Chirico, R., Diky, V., and Frenkel, M., NIST/TRC Web Thermo Tables-Professional Edition NIST Standard Reference Subscription Database 3, NIST/TRC Web Thermo Tables-Professional Edition NIST Standard Reference Subscription Database 3. 2002.

Kendhale, A. M., Gonnade, R., Rajamohanan, P. R., and Sanjayan, G. J. (2008). A Rigid bicyclo[3.3.0]octane (Octahydropentalene): a Heavily Constrained Novel Aliphatic Template for Molecular Self-Assembly. *Tetrahedron Lett.* 49, 3056–3059. doi:10.1016/j.tetlet.2008.03.062

Kirby, J., Geiselman, G. M., Yaegashi, J., Kim, J., Zhuang, X., Tran-Gyamfi, M. B., et al. (2021). Further Engineering of R. Toruloides for the Production of Terpenes from Lignocellulosic Biomass. *Biotechnol. Biofuels* 14, 101. doi:10.1186/s13068-021-01950-w

Kosir, S., Heyne, J., and Graham, J. (2020). A Machine Learning Framework for Drop-In Volume Swell Characteristics of Sustainable Aviation Fuel. *Fuel* 274, 117832. doi:10.1016/j.fuel.2020.117832

Lemaire, R., Lapalme, D., and Seers, P. (2015). Analysis of the Sooting Propensity of C-4 and C-5 Oxygenates: Comparison of Sooting Indexes Issued from Laser-Based Experiments and Group Additivity Approaches. *Combust. Flame* 162, 3140–3155. doi:10.1016/j.combustflame.2015.03.018

Lemaire, R., Le Corre, G., and Nakouri, M. (2021). Predicting the Propensity to Soot of Hydrocarbons and Oxygenated Molecules by Means of Structural Group Contribution Factors Derived from the Processing of Unified Sooting Indexes. *Fuel* 302, 121104. doi:10.1016/j.fuel.2021.121104

Li, H., Jiang, W., Liang, W., Huang, J., Mo, Y., Ding, Y., et al. (2014). Induced marine Fungus Chondrostereum Sp. As a Means of Producing New Sesquiterpenoids Chondrosterins I and J by Using Glycerol as the Carbon Source. *Mar. Drugs* 12, 167–175. doi:10.3390/md12010167

Li, K., Zhou, F., Liu, X., Ma, H., Deng, J., Xu, G., et al. (2020). Hydrodeoxygenation of Lignocellulose-Derived Oxygenates to Diesel or Jet Fuel Range Alkanes under Mild Conditions. *Catal. Sci. Technol.* 10, 1151–1160. doi:10.1039/C9CY02367D

Liu, Y., and Wilson, C. W. (2012). Investigation into the Impact of N-Decane, Decalin, and Isoparaffinic Solvent on Elastomeric Sealing Materials. *Adv. Mech. Eng.* 4, 127430. doi:10.1155/2012/127430

McEnally, C. S., and Pfefferle, L. D. (2007). Improved Sooting Tendency Measurements for Aromatic Hydrocarbons and Their Implications for Naphthalene Formation Pathways. *Combust. Flame* 148, 210–222. doi:10.1016/j.combustflame.2006.11.003

Milhet, M., Pauly, J., Coutinho, J. A. P., and Daridon, J. (2007). Solid-Liquid Equilibria under High-Pressure of Eight Pure N-Alkylcyclohexanes. *J. Chem. Eng. Data* 52, 1250–1254. doi:10.1021/je600575r

Montgomery, J. A., Jr., Frisch, M. J., Ochterski, J. W., and Petersson, G. A. (2000). A Complete Basis Set Model Chemistry. VII. Use of the Minimum Population Localization Method. *J. Chem. Phys.* 112, 6532–6542. doi:10.1063/1.481224

Muldoon, J. A., and Harvey, B. G. (2020). Bio-Based Cycloalkanes: The Missing Link to High-Performance Sustainable Jet Fuels. *ChemSusChem* 13, 5777–5807. doi:10.1002/cssc.202001641

Perez, A. G., Coquelet, C., Paricaud, P., and Chapoy, A. (2017). Comparative Study of Vapour-Liquid Equilibrium and Density Modeling of Mixtures Reltated to Carbon Capture and Storage with the SRK, PR, PC-SAFT and SAFT-VR Mie Equations of State for Industrial Uses. *Fluid Phase Equilib.* 440, 19–35. doi:10.1016/j.fluid.2017.02.018

Pokon, E. K., Liptak, M. D., Feldgus, S., and Shields, G. C. (2001). Comparison of CBS-QB3, CBS-APNO, and G3 Predictions of Gas Phase Deprotonation Data. *J. Phys. Chem. A.* 105, 10483–10487. doi:10.1021/jp012920p

Romanczyk, M., Ramirez Velasco, J. H., Xu, L., VozkaDissanayake, P. P., Dissanayake, P., Wehde, K. E., et al. (2019). The Capability of Organic Compunds to Swell Acrylonitrile Butadiene O-Rings and Their Effects on O-Ring Mechanical Properties. *Fuel* 238, 483–492. doi:10.1016/j.fuel.2018.10.103

Rosenkoetter, K. E., Kennedy, C. R., Chirik, P. J., and Harvey, B. G. (2019). [4+4]-Cycloaddition of Isoprene for the Production of High-Performance Bio-Based Jet Fuel. *Green. Chem.* 21, 5616–5623. doi:10.1039/C9GC02404B

Schalla, R. L., and McDonald, G. E. (1953). Variation in Smoking Tendency Among Hydrocarbons of Low Molecular Weight. *Ind. Eng. Chem.* 45, 1497–1500. doi:10.1021/ie50523a038

Sims, R. E. H., Creutzig, F., Cruz-Nunez, X., D'Agosto, M., Dimitriu, D., Meza, M. J. F., et al. (2014). in *Transport in Climate Change 2014: Mitigation of Climate Change. Contribution of Working Group III to the Fifth Assesment Report of the Intergovernmental Panel on Climate Change*. Editors P.-M. R. Edenhofer O., Y. Sokona, E. Farahani, S. Kadner, K. Seyboth, A. Adler, et al. (Cambridge, United Kingdom and New York, NY, USA: Cambridge University Press).

Sirjean, B., Glaude, P. A., Ruiz-Lopez, M. F., and Fournet, R. (2006). Detailed Kinetic Study of the Ring Opening of Cycloalkanes by CBS-QB3 Calculations. *J. Phys. Chem. A.* 110, 12693–12704. doi:10.1021/jp0651081

Wang, X., Liu, W., Xin, C., Zheng, Y., Cheng, Y., Sun, S., et al. (2016). Enhanced Limonene Production in Cyanobacteria Reveals Photosynthesis Limitations. *Proc. Natl. Acad. Sci.* 113, 14225–14230. doi:10.1073/pnas.1613340113

Wertheim, M. S. (1984). Fluids with Highly Directional Attractive Forces. II. Thermodynamic Perturbation Theory and Integral Equations. *J. Statist. Phys.* 35, 35–47. doi:10.1007/bf01017363

Wertheim, M. S. (1984). Fluids with Highly Directional Attractive Forces. I. Statistical Thermodynamics. *J. Statist. Phys.* 35, 19–34. doi:10.1007/bf01017362

Wertheim, M. S. (1986a). Fluids with Highly Directional Attractive Forces. I. Multiple Attraction Sites. *J. Statist. Phys.* 42, 459–476. doi:10.1007/bf01127721

Wertheim, M. S. (1986b). Fluids with Highly Directional Attractive Forces. IV. Equilibrium Polymerization. *J. Statist. Phys.* 42, 477–492. doi:10.1007/bf01127722

Woodrow, W. A. (1933). *Second World Petroleum Congr.* 2 Proc. 732.

Yang, J., Xin, Z., He, Q., Corscadden, K., and Niu, H. (2019). An Overview on Performance Characteristics of Bio-Jet Fuels. *Fuel* 237, 916–936. doi:10.1016/j.fuel.2018.10.079

Ysi database v2 (2021). Yield Sooting Index Database Volume 2: Sooting Tendencies of a Wide Range of Fuel Compounds on a Unified Scale. Available from: https://dataverse.harvard.edu/dataset/xhtml?persistentId=10.7910/DVN/7HGFT8 (Cited July 31, 2021).

Author's Disclaimer: Sandia National Laboratories is a multimission laboratory managed and operated by National Technology & Engineering Solutions of Sandia, LLC, a wholly owned subsidiary of Honeywell International Inc., for the U.S. Department of Energy's National Nuclear Security Administration under contract DE-NA0003525. This paper describes objective technical results and analysis. Any subjective views or opinions that might be expressed in the paper do not necessarily represent the views of the U.S. Department of Energy or the United States Government.

Conflict of Interest: The authors declare that the research was conducted in the absence of any commercial or financial relationships that could be construed as a potential conflict of interest.

Publisher's Note: All claims expressed in this article are solely those of the authors and do not necessarily represent those of their affiliated organizations, or those of the publisher, the editors and the reviewers. Any product that may be evaluated in this article, or claim that may be made by its manufacturer, is not guaranteed or endorsed by the publisher.

frontiers in Energy Research

ORIGINAL RESEARCH
published: 07 March 2022
doi: 10.3389/fenrg.2022.830236

Understanding the Compositional Effects of SAFs on Combustion Intermediates

M. Mehl[1]*, *M. Pelucchi*[1] and *P. Osswald*[2]

[1]CRECK Modeling Laboratory, Department of Chemistry, Materials and Chemical Engineering "G. Natta", Politecnico di Milano, Milano, Italy, [2]German Aerospace Center (DLR), Institute of Combustion Technology, Stuttgart, Germany

This work analyses, experimentally and numerically, the combustion behavior of three aviation fuels: a standard Jet A-1, a high aromatic content fuel, and an isoparaffinic Alcohol to Jet (ATJ) fuel. The goal is to demonstrate the ability of a chemical kinetic model to capture the chemistry underlying the combustion behavior of a wide range of jet fuels, starting from compositional information. Real fuels containing up to hundreds of components are modeled as surrogates containing less than 10 components, which represent the chemical functionalities of the real fuel. By using an in-house numerical optimizer, the fuel components and their relative quantities are selected, and a semi-detailed kinetic model (containing about 450 species) is used to simulate the formation of the main oxidation products and reaction intermediates. Calculations are compared with species profiles measured in a laminar flow reactor to validate the model and provide insights into the reactivity of the fuels. Finally, starting from the results, general observations on the strengths and limits of the approach are provided, highlighting areas where further investigations are required.

Keywords: chemical kinetics, flow reactor, renewable fuels, combustion modeling, surrogates

OPEN ACCESS

Edited by:
Michael P. Wolcott, Washington State University, United States

Reviewed by:
Joshua Heyne, University of Dayton, United States
Atmadeep Bhattacharya, Aalto University, Finland

***Correspondence:**
M. Mehl
marco.mehl@polimi.it

Specialty section:
This article was submitted to Bioenergy and Biofuels, a section of the journal Frontiers in Energy Research

Received: *06 December 2021*
Accepted: *01 February 2022*
Published: *07 March 2022*

Citation:
Mehl M, Pelucchi M and Osswald P (2022) Understanding the Compositional Effects of SAFs on Combustion Intermediates. Front. Energy Res. 10:830236. doi: 10.3389/fenrg.2022.830236

1 INTRODUCTION

Hard-to-decarbonize sectors, such as aviation, require mid-to long-term solutions to meet climate change mitigation targets. According to the recent reports emerging from the 2050 Waypoint project (Aviationbenefits, 2021), an Air Transport Action Group initiative, the greatest opportunity for decarbonizing the aviation sector comes from an aggressive transition to sustainable aviation fuels (SAFs): Hydroprocessed Esters and Fatty Acids (HEFA), Fisher Tropsch, Alcohol to Jet (ATJ), and Power to Liquid (PtL) fuels. The diversity of resources from which SAFs can be produced, will unavoidably expand the chemical complexity of future fuels.

For this reason, programs such as JETSCREEN (European Commission, 2022) have been supported by the EU to effectively tackle the critical process of fuel optimization, qualification and approval. The final goal is to provide tools that, by means of experimental tests and accurate models, will be capable of assessing a priori the compatibility of new SAFs (and mixtures of SAFs and traditional fuels) with existing infrastructures (i.e., engines, fuel system). In this framework, a key step is the capability of correctly predicting relevant combustion properties such as auto-ignition propensity, laminar flame speed and pollutants emissions (e.g., soot) starting from compositional information. The development of detailed chemical kinetic models serves the goal of predicting fuel behavior ahead of possible experimental campaigns for any new candidate fuel or fuel component that might be of interest in the area of SAFs.

TABLE 1 | Mass composition (%mass), H/C ratio, average molecular weight and density of the three fuels.

Composition	A1	B1	C1
normal paraffins	19.2	0	10.1
iso-paraffins	30.7	99.9	15
monocyclic paraffins	21.8	0.1	16.4
polycyclic paraffins	8	0	33.8
mono aromatics	15.5	0	1.9
naphto aromatics	2.9	0	2.9
di-aromatics	1.8	0	19.9
H/C	1.94	2.152	1.718
MW [kg/kmol]	150	180	182
Density [kg/m3]	786.8	756.4	858.1

Specifically, when a novel fuel mixture emerges, simpler multicomponent fuel surrogates are developed by means of optimization algorithms that take into account compositional data (e.g., GCxGC data) and other target properties such as viscosity, density, distillation curve, heat of combustion, H/C ratio, smoke point, *etc.* In the context of kinetic modeling, such surrogates are typically composed of 3–10 compounds, which, mixed together, allow to match the properties of the fuel under investigation. For each of these components a dedicated kinetic subset (i.e., a network of elementary chemical reactions) is developed to model its combustion properties (e.g., ignition delay times, laminar flame speed, intermediate and by-products formation). Such models are validated by means of comparisons with experimental data available in literature for pure components and their blends in 0-D or 1-D laminar reactors and flames, where the chemical kinetic effects are entirely, or at least significantly, decoupled from heat and mass transfer phenomena. Validated kinetic models can then be used to perform targeted parametric analysis to unravel temperature, pressure and composition dependency of the combustion characteristics in such simple systems. Furthermore, skeletal model reduction can be used to bring down the size of such models, making them applicable to large scale (2-D or 3-D) fluid dynamic simulation of real, or close-to-real, systems. This approach can speed up the fuel screening process and support the optimization of combustion devices, favoring the full market implementation of SAFs. Indeed, even by exercising the model on simple systems, it is possible to draw relevant conclusions about the ignitability of mixtures, their burning velocities, their soot propensity and blending behavior.

On these premises, this work analyzes, experimentally and numerically, the combustion behavior of three aviation fuels: a standard Jet A-1 (A1), an isoparaffinic Alcohol to Jet fuel (B1), and a high aromatic fuel (C1). The standard jet fuel, formulated in a previous study (Pelucchi et al., 2021), is used as a reference, while the renewable ATJ fuel (derived from iso-butanol) and the high aromatic content fuel, present extreme compositional features: the ATJ is almost entirely constituted by a single highly-branched iso-alkane, while the high aromatic fuel contains unusually high fractions of mono- and di-aromatics. Compositional information and global composition indexes such as H/C ratio and average molecular weight for the three fuels are reported in **Table 1**.

While other literature works discuss the development and validation of fuel surrogates and models for specific fuels (Dooley et al., 2010; Kim et al., 2014; Liu et al., 2019; Prak et al., 2022), this paper focuses on the methodological aspects involved in the definition of general models aiming at capturing fundamental aspects of the fuel chemistry. In this work, combustion chemistry models for three highly diverse fuels are obtained by coupling a single comprehensive kinetic mechanism and a surrogate formulation approach incorporating compositional information. The fuel models are then validated against well-characterized kinetic data from the DLR flow reactor. The final goal is to demonstrate how the workflow here presented allows capturing the speciation profiles of a broad range of fuels with high accuracy and enables the analysis of the relative behavior of the fuels on a more fundamental level. The rationale is that reaction intermediates are strictly related to the composition of the active radical pool that controls fuel oxidation and ultimately determines global combustion characteristics such as auto-ignition, flame behavior and soot formation. This successful validation, therefore, represents an important step towards predictive models for new candidate fuels able to predict features of practical interest such as burning velocity, emissions (Saffaripour et al., 2014; Pelucchi et al., 2021), high altitude relight (Martinos et al., 2021), and lean blow off (Yi et al., 2009; Rock et al., 2021).

2 PREDICTIVE MODELS FOR SAFS: METHODS

2.1 Experimental Facility and Procedures

The first step towards the development of validated models for the combustion of jet fuels is the experimental evaluation of their oxidative behavior in well-characterized conditions. To achieve this goal, species profiles for selected fuels have been measured by DLR in a high-temperature flow reactor coupled to a molecular beam mass (MBMS) spectrometer. This set up allows for in-depth investigation of relevant combustion chemistry features by identifying simultaneously multiple intermediates and, therefore, reaction channels controlling the formation of products (Oßwald and Köhler, 2015). The species profiles measured provide useful validation data for the development of detailed chemical kinetic model, enabling the assessment of the impact of fuel composition on emissions in technical combustors. **Figure 1** provides an overview of the experimental apparatus. Since a comprehensive literature was recently produced on this specific experimental setup (Köhler et al., 2018; Bierkandt et al., 2019; Chu et al., 2019), only a brief description is given here.

The system can be divided into two segments: a high-temperature laminar flow reactor including gas supply and a vaporizer system, and a molecular beam mass spectrometry (MBMS) time-of-flight detection (TOF) system. The reactor exit is positioned to the sampling nozzle of the MBMS-TOF system and gas is sampled directly from the reactor outlet and transferred to the high-vacuum detection system.

The reactor features a ceramic tube (total length of 1,497 mm); a laminar flow of highly diluted (> 99% Ar) mixture is fed into the

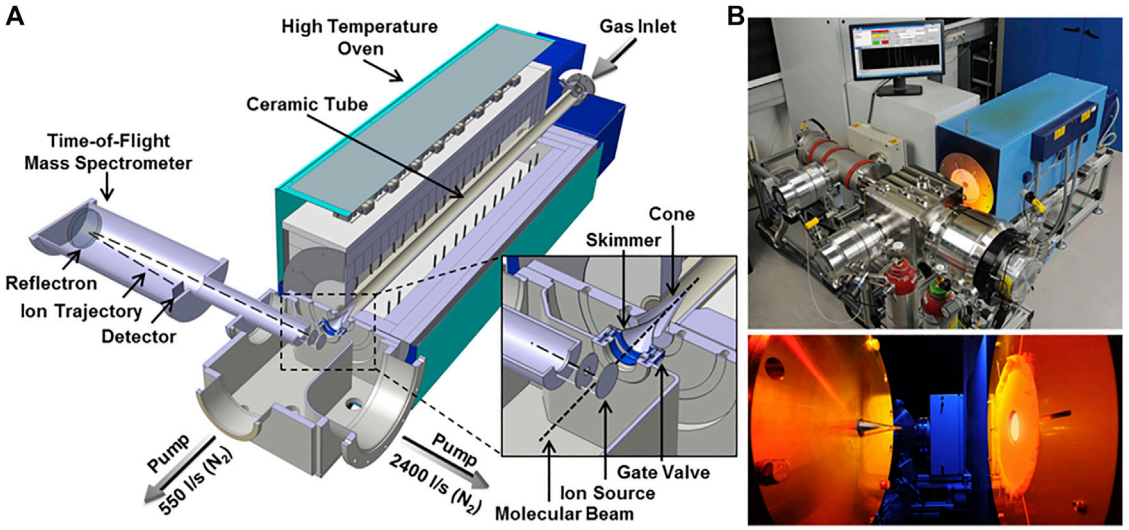

FIGURE 1 | Schematic DLR high-temperature flow reactor and photographs from (Oßwald and Köhler, 2015). The zoomed cutout shows a detailed view of the sampling interface and the ion source. Note that the high-temperature oven is mounted on moveable rails and sampling is performed inside the tube at ambient pressure.

TABLE 2 | Inlet conditions and H-content. 17.64 g/min Ar diluent added at all conditions.

Fuel		A1	B1	C1
Hydrogen	[wt-%]	14.022	15.275	12.689
Uncertainty (SD)	[wt-%]	0.024	0.003	0.026
Fuel	[mg/min]	31.16	31.62	30.69
O_2 lean	[mg/min]	132.6	137.1	127.9
O_2 rich	[mg/min]	88.4	91.4	85.2

reactor. The high dilution suppresses significant volumetric heat release allowing a better control on the temperature profile in the reactor. The relatively large inner diameter (40 mm) allows minimizing boundary effects. A commercial setup (Bronkhorst, CEM) is used in the mixture preparation section to vaporize the fuel. All input streams are metered in high precision (accuracy ±0.5%) by Coriolis mass flow meters. The high dilution of the system also guarantees the complete evaporation of the fuels, whose partial pressures are maintained below100 Pa.

Operating conditions are designed to yield constant carbon flow at slightly rich (Φ = 1.2) and lean (Φ = 0.8) conditions, respectively. Oxygen concentration is adjusted according to the desired stoichiometry. The exact stoichiometry was determined by measuring the hydrogen content of the fuels using low resolution pulsed NMR (ASTM D7171). The heteroatoms content is assumed to be negligible. The obtained H-content is summarized in **Table 2** with the respective inlet flow conditions.

Homogeneous flow conditions are obtained by feeding the premixed gases through a tempered flange equipped with a porous bronze plug. The reaction segment is 1,000 mm long, and is contained in customized high-temperature oven (Gero, Type HTRH 40-1,000), capable of reaching temperatures up to 1900 K. Samples taken at the reactor exit are transferred to high vacuum (10^{-6} mbar) by a two-stage differential pumping system. The rapid expansion quenches chemical reactions immediately by lowering temperatures and concentrations, effectively "freezing" the composition. Detection is carried out using an electron impact (EI) time-of-flight (TOF) mass spectrometer (Kaesdorf, mass resolution R = 3,000). This system is able to determine the elemental composition of combustion intermediates within a C/H/O system. Soft electron energies are applied (10.6 eV) to avoid species fragmentation during the ionization process. Additionally, a quadrupole mass spectrometer is positioned in the ionization chamber (off beam) and operated at a higher electron energy (70 eV) to track major species contemporarily to the MBMS-TOF measurements. Details on the experimental setup, including a schematic and its instrumentation, may be found in previous publications (Oßwald and Köhler, 2015; Köhler et al., 2018).

A monotonically decreasing temperature ramp (−200 K/h) is applied to the oven and all measurements are performed maintaining a constant inlet mass flow. A temperature window spanning from 600 to 1200 K was scanned, covering all regimes between the absence of reactions to full conversion and thermal equilibrium. The flow regime is laminar for all the temperature conditions, but previous studies demonstrated how this system can be successfully simulated treating the system as one-dimensional, adopting a predefined axial temperature profile derived from the experiments and the plug flow hypothesis for kinetic calculations (Oßwald and Köhler, 2015; Kathrotia et al., 2017). Temperature profiles along the reactor axis were measured during the temperature ramps, providing the necessary boundary condition for the kinetic model.

The quantitative evaluation of the species was performed adopting well established techniques (Herrmann et al., 2013; Schenk et al., 2013; Oßwald and Köhler, 2015) performing

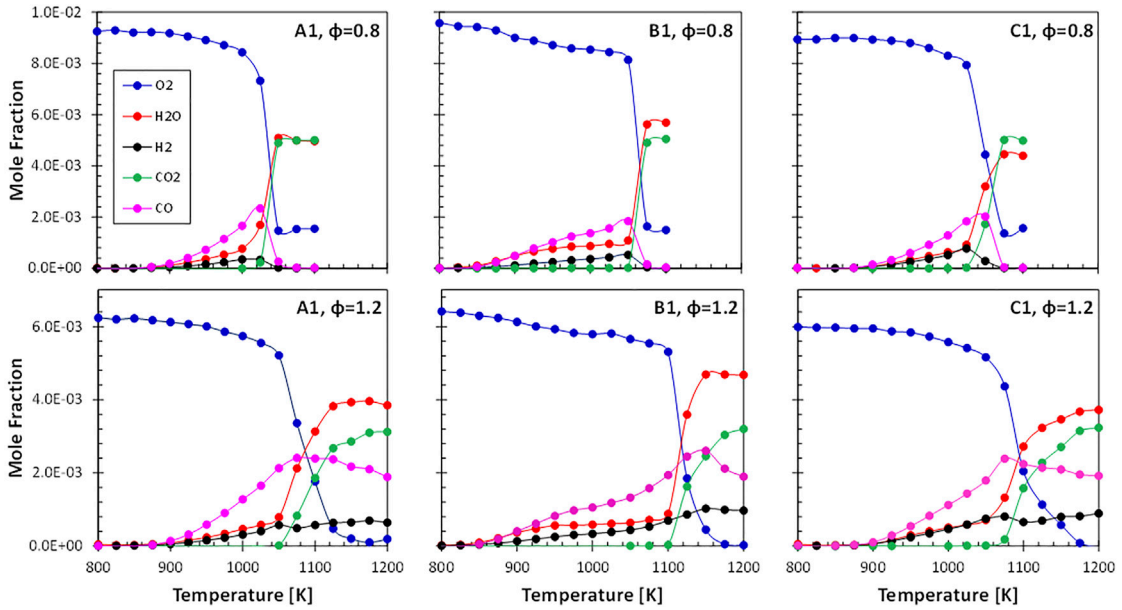

FIGURE 2 | Major species profiles measured in the DLR high-temperature flow reactor.

direct binary (species/Ar) calibration measurements or estimating the ionization cross section based on the RICS (Relative Ionization Cross Section) method. Calibration by direct cold gas measurements was performed for most species. The estimation procedure (RICS) was applied for all radicals, as well as for C_2H_2O, C_7H_8, C_8H_6, C_8H_8, C_9H_8, $C_{12}H_8$, $C_{12}H_{10}$, $C_{13}H_{10}$, and $C_{14}H_{10}$. Note that species predominantly showing a fuel-like behavior (i.e., maximum concentration at low temperature) are calibrated internally using the respective fuel composition determined by two dimensional gas chromatography (GCxGC) obtained by IFPEN.

For the three fuels, more than 500 quantitative species profiles could be obtained at two equivalence ratio conditions. Results are obtained as a function of the oven temperature. Further details about the experimental set-up and additional data are available in (Oßwald et al., 2021). **Figure 2** summarizes the major species (product and reactants) for all initial compositions.

A similar global reaction behavior was observed for all fuels with moderate temperature shifts across the fuels. The highly-branched paraffinic ATJ (B1) fuel is shifted to slightly higher temperatures, indicating a longer total ignition delay time. **Figure 3** summarizes some selected soot precursor intermediate species: benzene C_6H_6, indene C_9H_8, naphthalene $C_{10}H_8$, and anthracene $C_{14}H_{10}$. Note that naphthalene is also contained in the real fuel, therefore starting with a non-zero concentration. For these species a clear correlation with the fuel composition can be drawn. As can be expected, soot precursor species are more abundant in fuels with higher aromatic content (or low hydrogen content). Hydrogen content is considered to be a useful indicator for sooting propensity at technical combustors' conditions such as jet engines (Schripp et al., 2018).

2.2 Kinetic Modeling of Real Fuels

Describing the chemistry controlling the combustion of a real fuel in terms of its fundamental kinetic processes is a daunting task: typically, real fuels are mixtures of hundreds of components whose exact chemical structure is often unknown. Moreover, the full combustion of each fuel component is the result of tens, hundreds, if not thousands of elementary reactions whose rate needs to be determined. Finally, suitable solvers are needed to effectively compute the ODE (Ordinary Differential Equation) and DAE (Differential Algebraic Equation) systems describing the chemical evolution of the system. The following sections detail the approaches and the different steps used to obtain an accurate and predictive model able to represent the chemistry involved in the combustion of jet fuels of practical interest.

2.2.1 The Kinetic Model

Detailed kinetic models attempt to identify all the important reaction pathways controlling the combustion of fuel components, and to assign to each elementary step temperature and pressure dependent reaction rates (i.e., the larger is the molecule, the higher is the number of reactions involved in its oxidation). Thermodynamic properties are used to define rate constants of backward reactions for reversible elementary steps. The two main challenges a kinetic model has to address are: i) the identification of the relevant reaction intermediates (whose number dictates the number of equations required to calculate the composition of the system), and ii) the determination of the thousands of reaction rate parameters it includes, together with thermodynamic properties of each species.

Because of the complexity of detailed kinetic models and of the computational burden associated with their use, reduced models

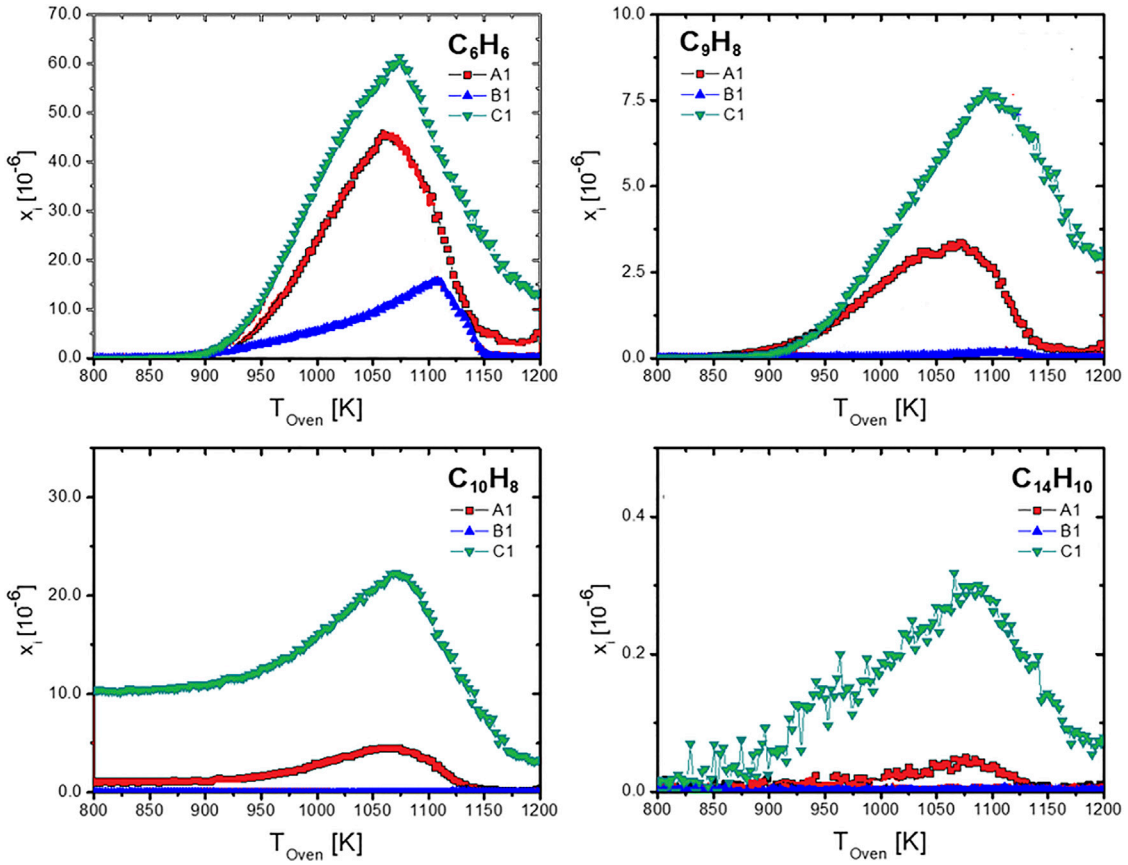

FIGURE 3 | Soot precursor species measured at rich conditions (Φ = 1.2).

including a smaller number of intermediates and global reactions are generally preferred for practical calculations and combustors' design. The model proposed by the CRECK Modelling Lab of Politecnico di Milano attempts to couple the fundamentals of detailed chemical kinetic models and the practicality of reduced models, by limiting the number of species (and therefore of reactions) through isomer lumping (Ranzi et al., 2001).

By doing so, it is possible to simulate the fundamental processes controlling combustion and by-products formation of complex mixtures of large molecules with a relatively low number of species (few 100s), reducing considerably the computational cost of simulations and easing the interpretation of relevant chemical pathways. The CRECK model (which is meant to be general and applicable to a wide window of operating conditions) can be further reduced for computational fluid-dynamic applications based on the specific windows of compositions and thermodynamic conditions of interest (e.g., T, p, φ).

The other main challenge is the determination of reaction rates. While an extensive corpus of experimental and fundamental work exists on the reaction rates of small hydrocarbons (1-2 carbon atoms), most of the reactions involved in the oxidation of heavier molecules cannot be easily measured or calculated using quantum-chemical approaches. To overcome this issue, a systematic approach based on modularity, hierarchy and self-consistency is used in the construction of models for large fuel molecules.

The model is built hierarchically from light to heavy fuel species starting from a reaction mechanism core which describes the oxidation and pyrolysis of small gas-phase hydrocarbons. The current version of the CRECK model (Pejpichestakul et al., 2019) adopts the Aramco 2.0 (Metcalfe et al., 2013), (Burke et al., 2015) as its core. The core, which includes species up to three carbon atoms in size (C3), provides the basis for additional modules including larger molecules (Ranzi et al., 2012; Ranzi et al., 2014). At high temperature, the first step in the oxidation of large hydrocarbons is their decomposition to smaller fragments. Reactions involving C3 hydrocarbons or lower are subsets of the oxidation mechanisms of larger species which form them by fragmentation. By expanding the model towards heavier fuels, it is possible to describe the oxidation of larger molecules through the addition of blocks of reactions, which are built and validated starting from the core and moving up. Jet fuels include components with a number of carbons in the C7-C16 range and their kinetic models require the determination of a large number of parameters to quantify the reaction rates involved. From a micro-kinetic standpoint, the primary oxidation steps controlling combustion show strong similarities within a certain family of fuel components (paraffins, olefins, aromatics,

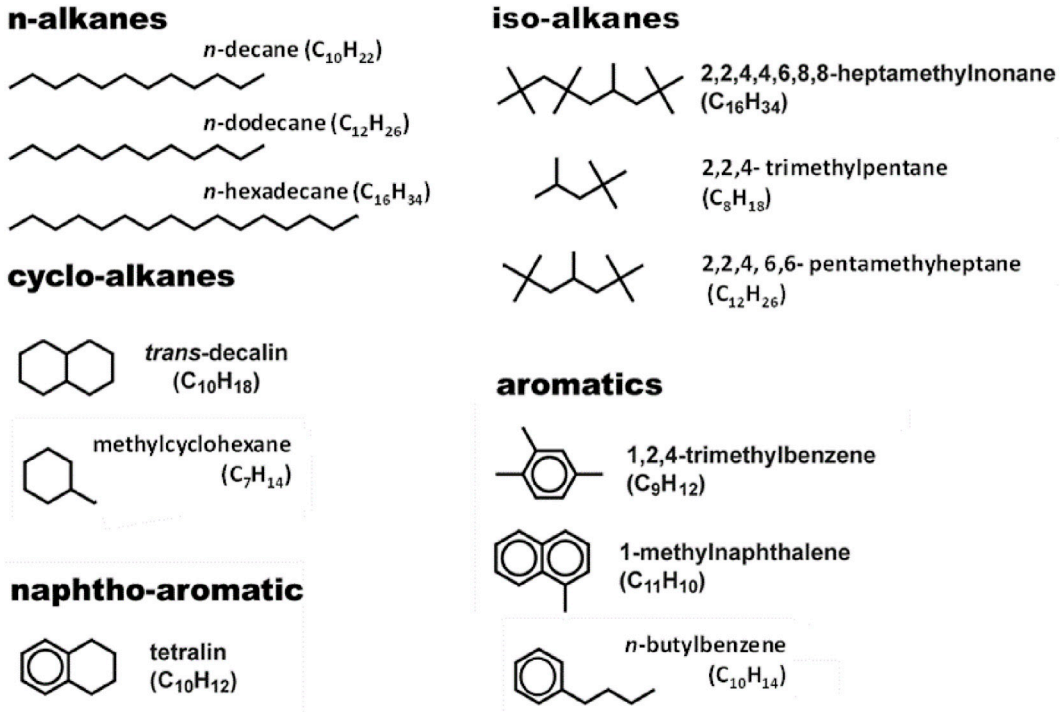

FIGURE 4 | Palette of candidate components for the formulation of modelling oriented surrogates.

TABLE 3 | Mass composition (%mass) of the three jet fuel surrogates proposed in this work.

Composition	A1	B1	C1
n-dodecane	23.1		
iso-dodecane	25.4	87.1	9.0
iso-cetane	12.3	12.9	22.5
methylcyclohexane	14.0		20.1
decalin	9.4		29.2
tri-methylbenzene	13.9		1.7
methylnaphthalene	1.9		17.6
H/C	1.96	2.161	1.77
MW [kg/kmol]	147.1	175.6	141.6
Density [kg/m3]	787	745.3	843

naphthenes, etc.). For this reason, using analogy rules, it is possible to estimate reaction rates for molecules that have not been studied before. Adhering to principles of hierarchy, modularity, and self-consistency among reaction classes built on structural similarities, the CRECK team developed models for many components relevant to mid-distillates' combustion. Among these, based on the compositional analysis provided by IFPEN, a set of components representative of the ones detected in the real fuels were selected (e.g., C12 n- and iso-alkanes, decalin, butylbenzene, butylcyclohexane, etc.).

The CRECK kinetic model covers both high (T > 1000 K) and low temperature (T = 500-1000K) reactions. High-temperature reactions are relevant to flame conditions and pollutant formation, while the low-temperature reactions (600–900 K) are required to predict the auto-ignition propensity of the fuel. At high pressure, low-temperature reactions become more important and they should be included in a comprehensive model to guarantee accurate predictions, particularly when transients are simulated.

Thermodynamic properties for all the species in the model have been adopted from the active thermochemical tables (Ruscic, 2015), from the online repository compiled by Burcat (Burcat and Ruscic, 2005), or determined based on group additivity methods. The final kinetic model includes about 460 species and 14,000 reactions, although, depending on the components and the operating window of interest, it is possible to reduce the size of the model for specific applications by removing non-relevant kinetic modules.

2.2.2 Surrogate Formulation

While the detailed composition of a full-blend fuel is rarely fully resolved, simpler analytical techniques allow to determine the breakdown into families of compounds, or their H/C ratio. Two dimensional gas chromatography (GCxGC) allows for a much more refined analysis, detecting both the family and the molecular weight distribution of the components.

Because of compositional complexity and lack of accurate information, it is not feasible to simulate the chemical behavior of a fuel reproducing its exact composition, especially when a detailed kinetic modelling approach is sought. In this case, modelers often adopt the surrogate approach: a simpler mixture (<10 components) matching a set of target properties of the real fuel is selected and used to represent the real fuel

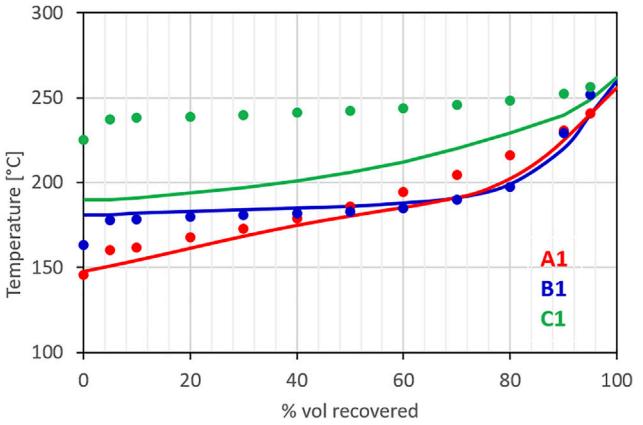

FIGURE 5 | Measured distillation curves of the three fuels considered in the model (symbols) and calculated equilibrium distillation curves of their surrogates.

(Dooley et al., 2010; Kim et al., 2014; Prak et al., 2022). The selection of the surrogate can be performed "manually" by an expert user or, especially when many targets and fuel components are to be included, using an optimization tool.

In this work a hybrid approach has been selected, where the fuel palette used in the optimization is "manually" selected and, following the numerical optimization, minor variations are introduced to account for finer details relevant to the fuel composition (e.g., small amounts of a specific family of components that can play a role in the pollutant formation processes).

The first step in surrogate formulation is the definition of the palette of components to be included in the optimization. Since our goal is to generate a kinetic model for jet fuels, it is important to choose fuel components for which a reliable kinetic model exists (or can be easily built) and, ideally, has already been extensively validated. **Figure 4** shows the set of components currently adopted for the fuel surrogate palette.

In the context of this project, POLIMI developed a fuel surrogate optimization tool. The optimization of the composition of a fuel surrogate is a multi-target multidimensional problem. The number of targets to be matched can be in the order of the 10s, while the dimensionality is equal to the number of components included in the palette minus one, with multiple solutions. Different optimization strategies have been proposed in literature for this type of problems (machine learning and genetic algorithms are among them) (Kim and Violi, 2022; Yu et al., 2022). The optimizer used in this work exploits the optimization package available in Matlab and is inspired by a previous literature work by Narayanaswamy et al. (Narayanaswamy and Pepiot, 2018). Different optimization algorithms are available within the tool developed at CRECK, including local optimization and a genetic algorithm.

The optimization targets available at this stage are DCN, H/C ratio, distribution within the different family of components, average molecular weight, threshold sooting index, density, distillation curve, and liquid viscosity. More targets will be added in future works to accommodate all the properties deemed important for the scopes of SAFs design, optimization and approval.

Based on this optimization process, surrogates were formulated for fuels A1 and C1. Fuel B1 is a synthetic fuel with a well-defined composition: the GCxGC data provided by IFPEN clearly identified iso-alkanes as the only components and, based on the process involved in its production and the compositional information available, it is possible to infer that these iso-alkanes are strongly branched oligomers of iso-C4 units. The GCxGC indicates that a C12 iso-paraffin is the main component and a surrogate based on iso-dodecane and iso-cetane was selected accordingly. **Table 3** summarizes the composition of the three surrogates.

Figure 5 compares the distillation curves measured for the three jet fuels using the ASTM D86 standard method against the distillation curve calculated for the surrogates using a standard equilibrium approach for ideal mixtures (i.e., a linear combination of partial pressures calculated using the Antoine coefficients from (Yaws, 2005)). The distillation curve calculated for the surrogate of fuel A1 matches with good approximation the experimental one targeted in the surrogate optimization process. Similarly, the calculated distillation curve for the surrogate of fuel B1, which was formulated directly from the compositional information provided by IFPEN, agrees very well with the measurements. The distillation curve for fuel C1, as anticipated, shows greater deviations. Because of the lack of fuel components suitable to reproduce both the distillation curve and the H/C ratio, priority was given to the H/C ratio, a fundamental chemical property. Future works will add new components to the surrogate palette to overcome the current limitation. In particular, based on the GCxGC analysis, the need for higher molecular weight alkyl-cycloparaffins emerged. The surrogate for fuel C1, still, results to be the least volatile among the three fuels, reproducing, at least qualitatively, the relative behavior of the fuels.

3 RESULTS

The flow reactor data collected at DLR have been simulated using OpenSmoke++ (Cuoci et al., 2015). Calculations allowed to estimate the gas composition at the exit of the reactor for temperatures between 800 and 1150 K (nominal temperature) at two equivalence ratios (φ = 0.8 and 1.2). Not all the measured species can be directly compared with the experiments, as the surrogates mimic the composition of the real fuel by targeting the moieties it contains, and not the actual fuel component concentrations. A clear example comes from naphthalene, which can be both a secondary product formed during combustion and a fuel component. For this reason, in the following comparisons, we focus mostly on the smaller species that are formed during the decomposition and oxidation of the initial fuel and that may have an impact on the following soot and NOx formation processes. However, because of the relevance of polycyclic species to the formation of PAHs, naphthalene concentration profiles are shown for all the fuels.

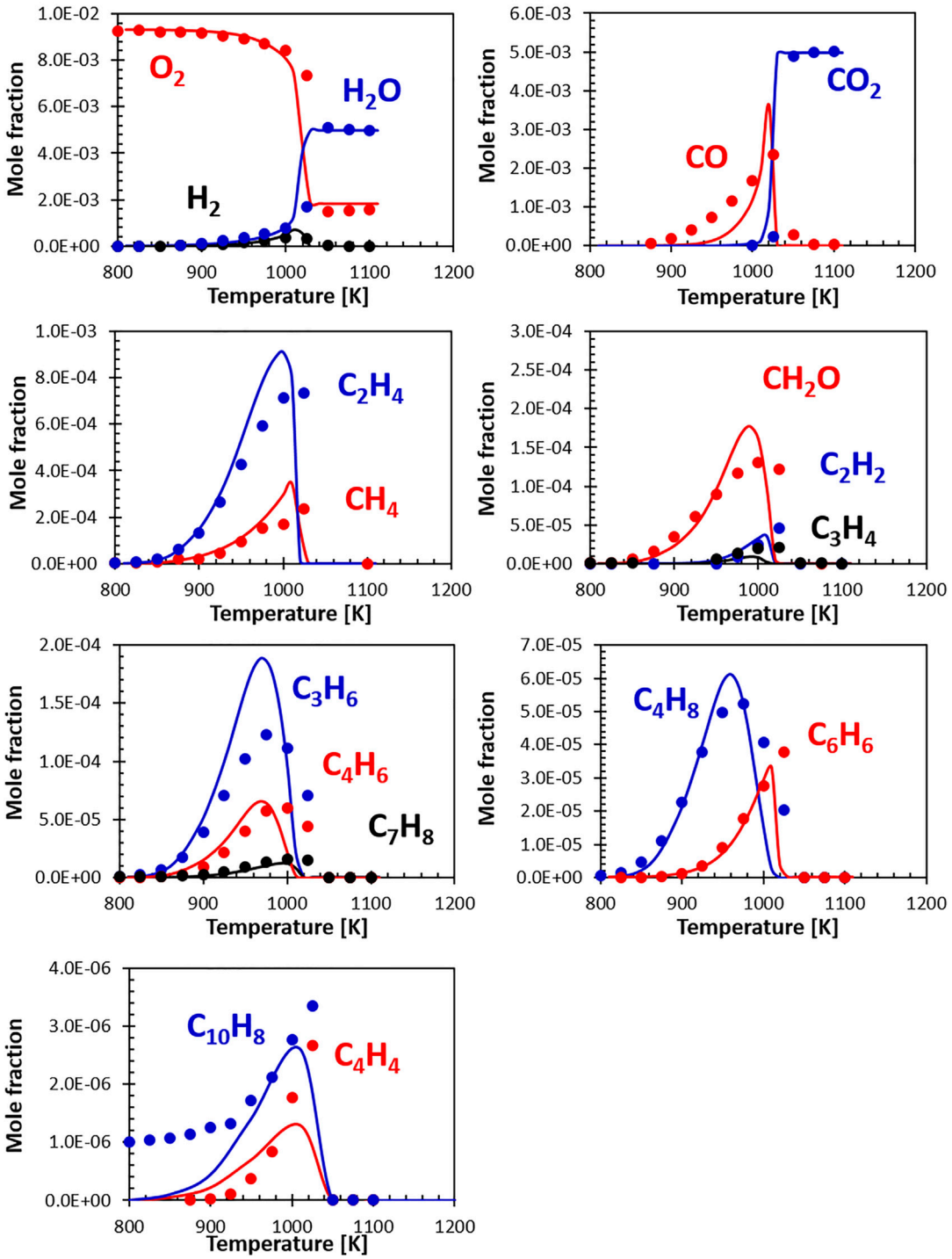

FIGURE 6 | Comparison between measured (symbols) and calculated (lines) species profiles in the DLR flow reactor: Fuel A1, Φ = 0.8. Series are labeled using matching colors.

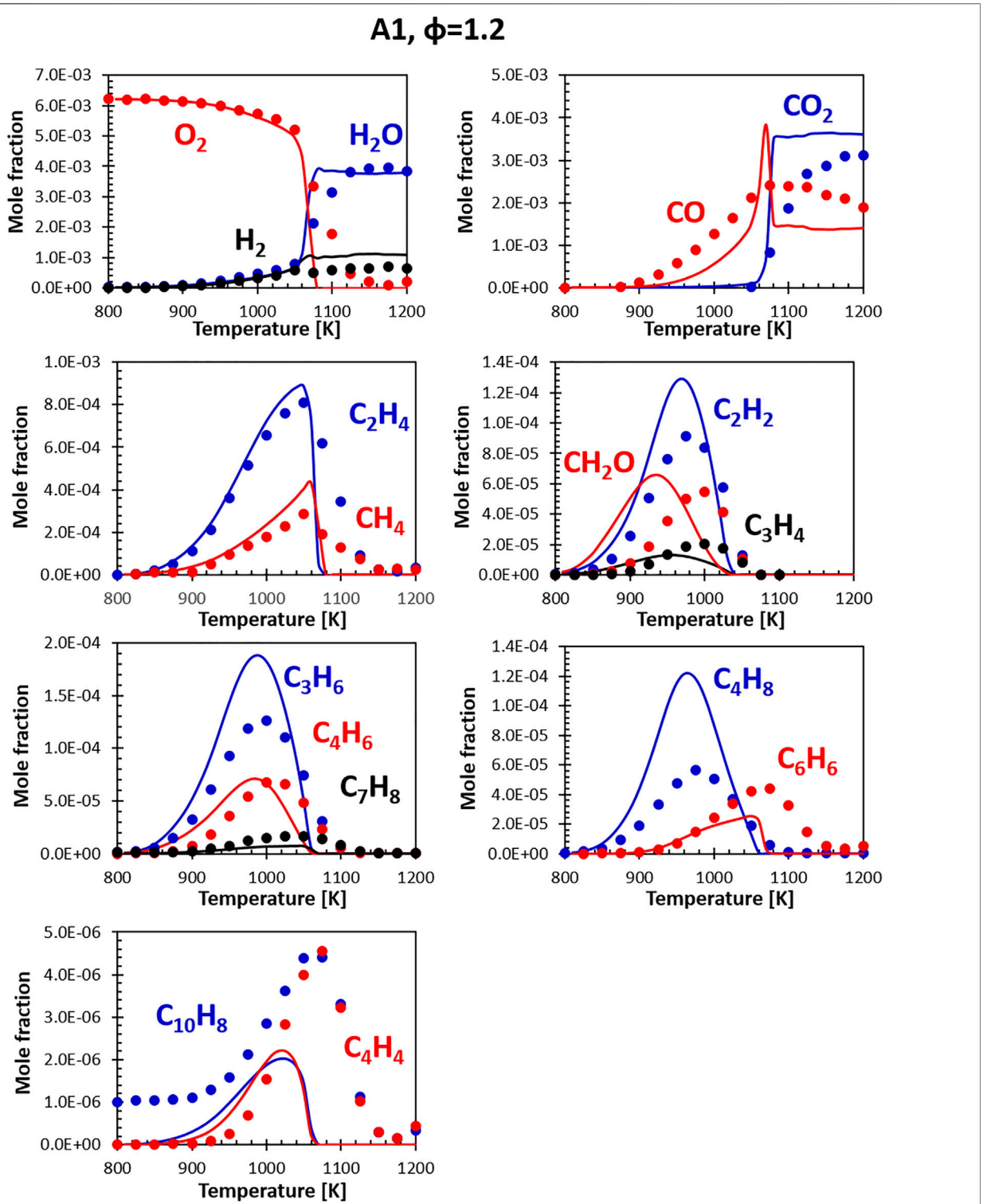

FIGURE 7 | Comparison between measured (symbols) and calculated (lines) species profiles in the DLR flow reactor: Fuel A1, Φ = 1.2. Series are labeled using matching colors.

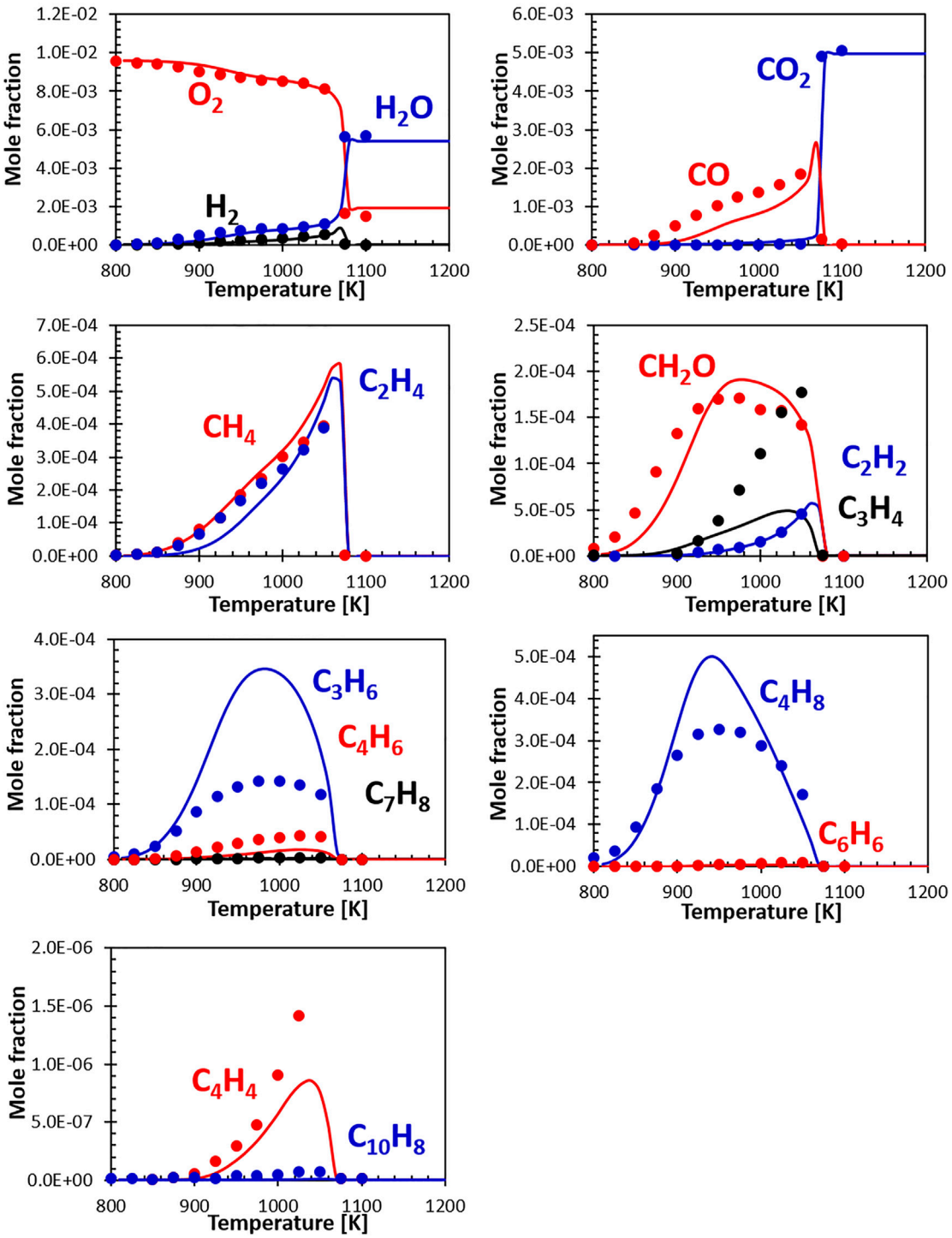

FIGURE 8 | Comparison between measured (symbols) and calculated (lines) species profiles in the DLR flow reactor: Fuel B1, Φ = 0.8. Series are labeled using matching colors.

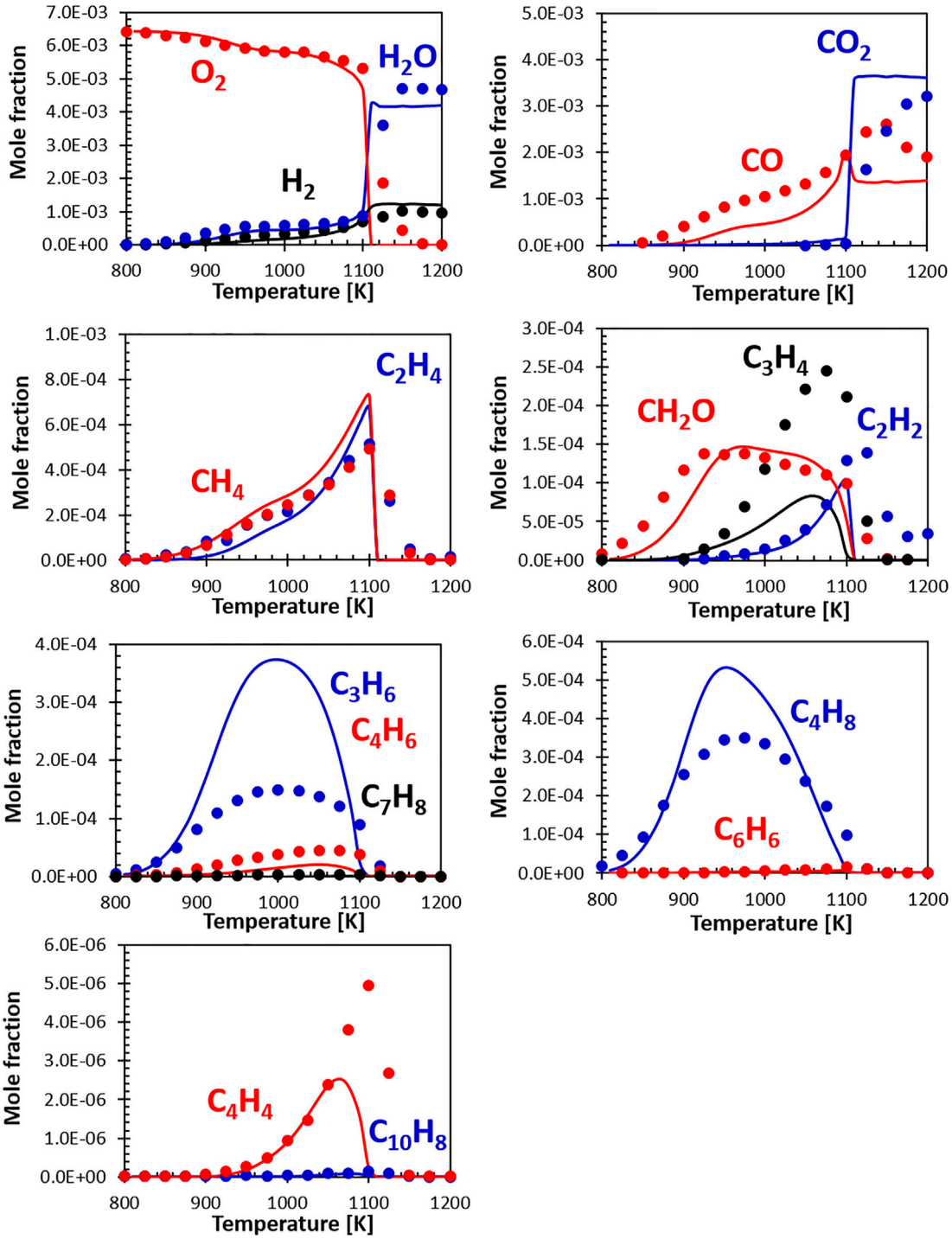

FIGURE 9 | Comparison between measured (symbols) and calculated (lines) species profiles in the DLR flow reactor: Fuel B1, Φ = 1.2. Series are labeled using matching colors.

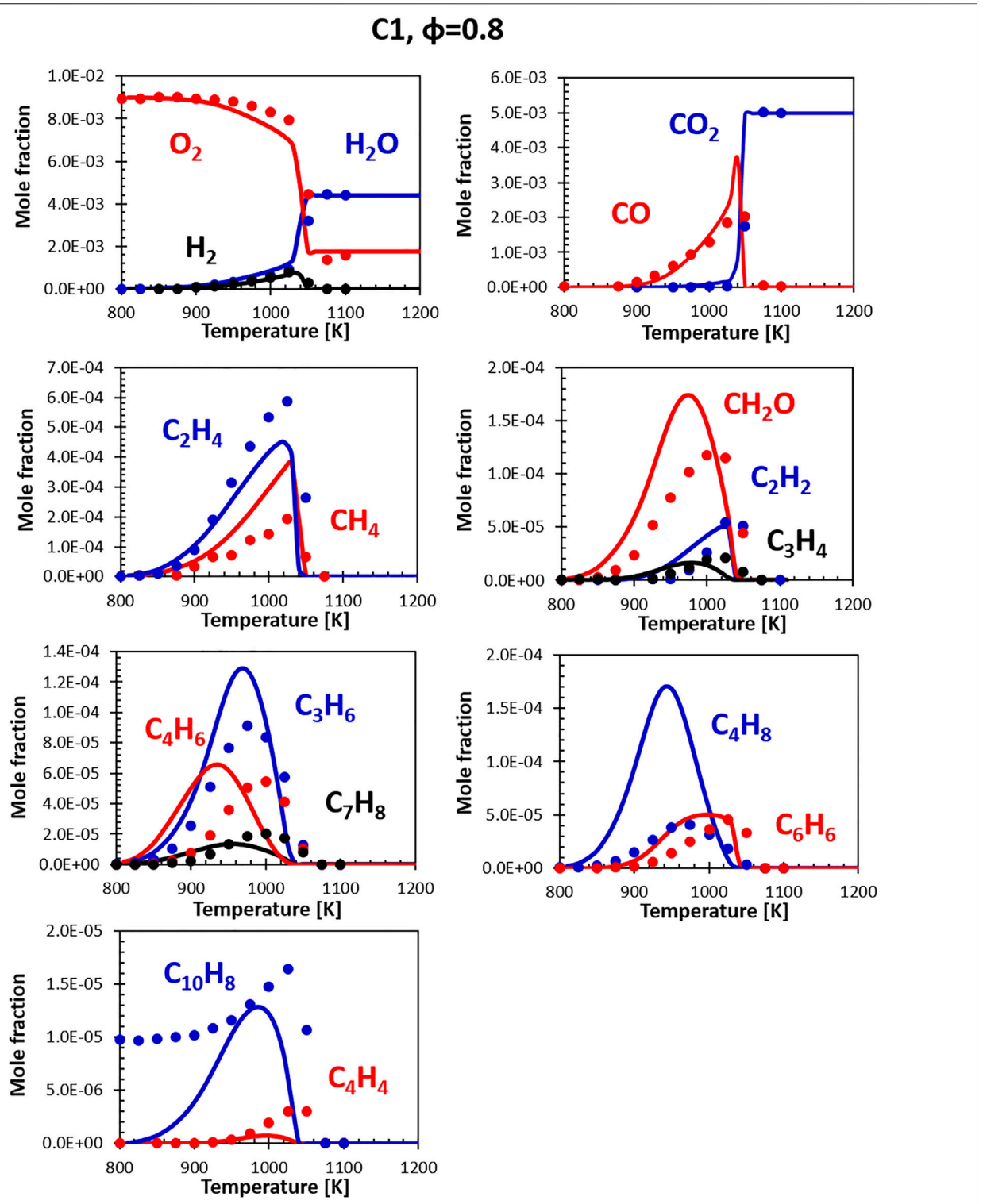

FIGURE 10 | Comparison between measured (symbols) and calculated (lines) species profiles in the DLR flow reactor: Fuel C1, Φ = 0.8. Series are labeled using matching colors.

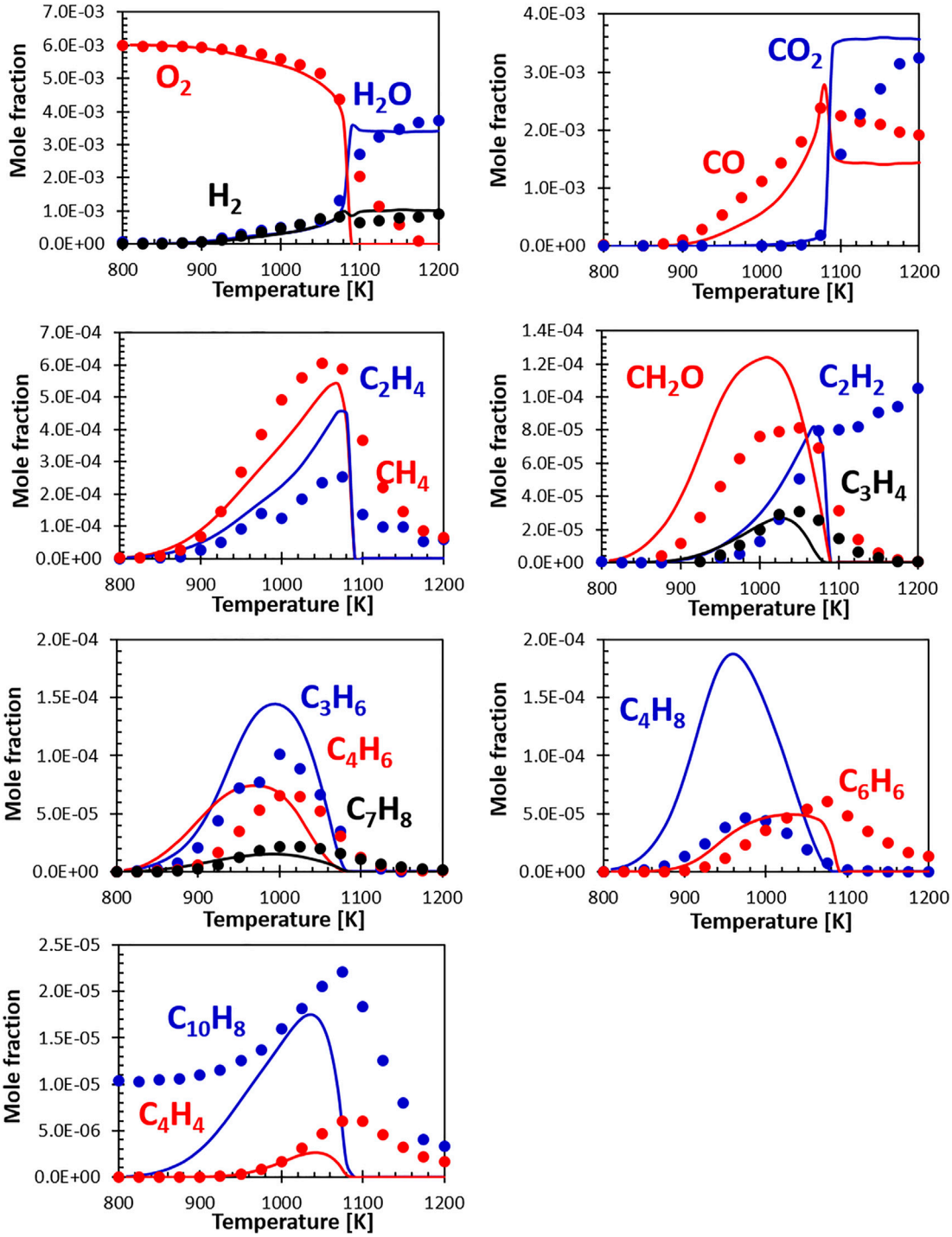

FIGURE 11 | Comparison between measured (symbols) and calculated (lines) species profiles in the DLR flow reactor: Fuel C1, Φ = 1.2. Series are labeled using matching colors.

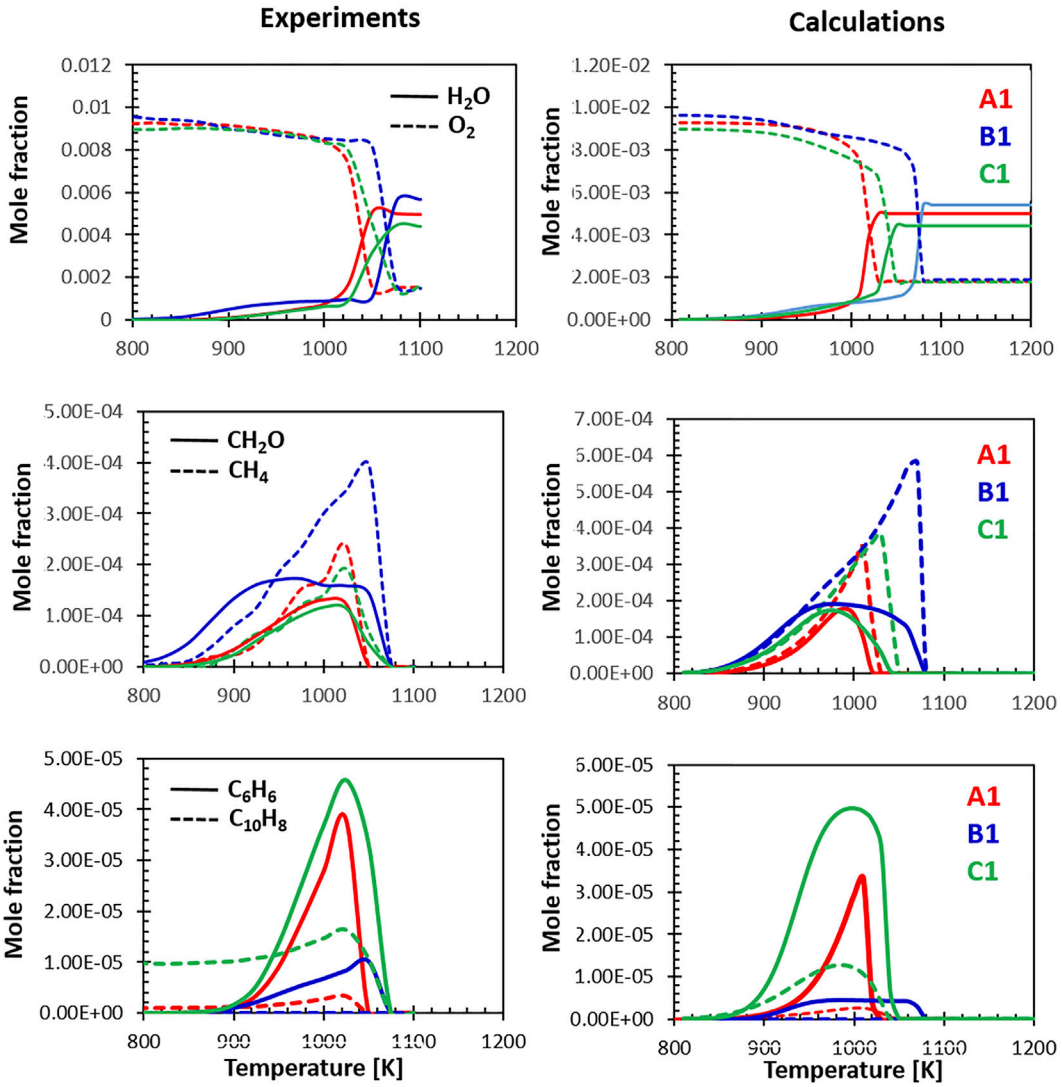

FIGURE 12 | Relative selectivity of the three fuels towards their oxidation intermediates at Φ = 0.8, experiments **(A)** and calculations **(B)**.

3.1 Fuel A1 (JET A-1)

Figures 6, **7** show the comparisons between calculations and experiments for Jet fuel A-1 (i.e., the standard jet fuel). The fuel model (constituted by the combination of the surrogate and the relative kinetic model) correctly reproduces the profiles of the major products, the consumption of the oxidizer (O_2) and the formation of the final combustion products. H_2O and CO_2 are well captured, while small discrepancies are observed for H_2 and CO. The peak in H_2 concentration is measured at about 1020 K; the model accurately predicts its rate of formation, but has a slight delay in the onset of its consumption. The CO peak is reproduced correctly, although its shape is somewhat sharper. This could be partially related to the simplified approach adopted in the simulation of the flow reactor, which neglects the axial and radial inhomogeneity that may be present in the real device.

The agreement with minor species (ethylene, acetylene and other unsaturated species) is generally satisfactory. A systematic deviation is the over-prediction of C_4H_8 formation compensated by an under-prediction in C_4H_4 concentration. As mentioned, a direct comparison for $C_{10}H_8$ experimental and model profiles is not possible, as the real fuel already contains some naphthalene, not present in the surrogate (the representative species adopted to match the di-aromatics content in the surrogates is α-methyl-naphthalene). Despite the difference in the initial concentration, the model captures the timing of naphthalene formation and its consumption. The entity of naphthalene formation (i.e., the delta between the initial value and the peak value) is still well reproduced. The overall agreement at lean conditions is generally satisfactory.

At rich conditions (**Figure 7**) the model/experiment comparisons show similar features. However, it appears that the model presents more abrupt variations in the concentrations of some species, even though the peaks are

generally captured correctly. The experimental and modeling results are, however, comparable to the ones obtained for other fuels previously tested on the same rig and simulations performed using other kinetic models. These deviations appear to be somewhat systematic for the stoichiometry condition here considered (φ = 1.2). More fuel-rich conditions seem to be captured by most models significantly better. Further analysis will focus on understanding if these discrepancies are the results of deviations from the plug flow reactor hypothesis used in the simulations or actual deficiencies in the model.

3.2 Fuel B1

Figures 8, **9** show the comparisons between calculations and experiments for Jet fuel B1 (ATJ). When compared with the other two fuels, fuel B1 shows an earlier onset of the reactivity. This shows in the form of an early initial drop in the oxygen concentration associated with the formation of formaldehyde. It should be noted that B1 fuel was simulated using a two component surrogate formulated from compositional information only, and the chemical composition of the fuel used in the experiment matches almost perfectly the composition of the surrogate. Fuel simplicity eases the surrogate formulation step, leaving all the weight of the discrepancies on the kinetic mechanism. As the B1 mixture is composed largely of iso-dodecane, the simulation results are strongly dependent on how accurate its model is. The CRECK mechanism for iso-dodecane has been developed applying the analogy rules introduced in **Section 2.2.1**, using the mechanism of iso-octane (a widely studied fuel sharing strong structural similarities) as reference for the reaction rates. Unfortunately, experimental data available for the validation of the iso-dodecane kinetic model are still somewhat limited, and no speciation data were available at the time of the model formulation. Future works will focus on the refinement of the iso-dodecane model, also including data from Gutzman et al. (Guzman et al., 2019).

Despite the limited validation, the agreement with the flow reactor data obtained for this fuel is comparable with what seen for the A1 fuel, confirming, at least in this instance, that reasonably accurate models can be built starting from the fundamentals even in the absence of extensive validation data. Notably, both the experiments and the simulations show that this fuel produces a very limited amount of soot precursors (e.g., C_6H_6, $C_{10}H_8$) even at slightly rich conditions.

3.3 Fuel C1

Figures 10, **11** show the comparisons between calculations and experiments for the C1 fuel (the high aromatic content fuel). The agreement with the experimental data is satisfactory also in this case, even though the same issues that plague fuel A1 at rich conditions can be observed. The presence of naphthalene in the fuel (not in the surrogate) is particularly evident here, but the $C_{10}H_8$ peak ends up being relatively close to the experimental one and the consumption temperature is well captured.

3.4 Relative Behavior of the Three Fuels

The last set of comparisons shown in **Figure 12** focuses on the relative behavior of the three fuels at lean conditions. The model captures very well the differences in reactivity highlighted by the drop in the O_2 concentration and the sharp rise in water. Fuel B1 appears to be the most refractory to high temperature oxidation at the conditions of the flow reactor. The high aromatic content fuel is the second least reactive and, compared with the other fuels, produces a lower amount of water, compatibly with his lower H/C ratio. In terms of oxidation products, fuel B1 oxidation starts at lower temperature with an early formation of CH_2O. The shape and magnitude of the CH_4 and CH_2O peaks are captured correctly by the model, which also hints at their earlier formation.

Finally, the last row of **Figure 12** highlights the relative formation of C_6H_6 and $C_{10}H_8$ measured by the experiments and predicted by the model. Beside the initial amount of naphthalene present in the fuel, the model does a good job at reproducing the relative concentrations. Fuel B1 produces only very limited amounts of benzene and naphthalene, while the high aromatic fuel, as expected, is the most prone to the formation of aromatic rings. These results could be correlated to the sooting tendencies of the three fuels as the formation of mono- and, later, di-aromatics is the first step along the growth of larger PAHs and soot. The ability of the model to capture the differences in reactivity and the relative selectivity to products reinforces the idea that, in future analyses, a modeling grounded approach based on composition-based surrogates and detailed kinetics can be used to predict the combustion behavior of novel fuels, assisting the certification process of fuel candidates.

4 CONCLUSION

This paper describes the procedures used to characterize the reactivity of three representative jet fuels from the fuel palette selected by the JETSCREEN program. A standard Jet fuel, an ATJ fuel and a high aromatic content fuel were investigated experimentally and numerically in a flow reactor at temperatures in the 800-1150K range and two fuel air ratios (Φ = 0.8 and 1.2) at atmospheric pressure. Semi-detailed models reproducing the oxidation mechanism of the fuels were developed by coupling the CRECK chemical kinetic model and a customized numerical tool for the formulation of fuel surrogates. Comparisons of the experimental data collected by DLR were used to validate the model and support the analysis of the combustion behavior.

From the numerical and experimental results it is possible to conclude that the general modeling framework can capture major combustion characteristics of the real fuels and reproduce with good accuracy the selectivity towards different intermediates during the oxidation of the real fuels. It is evident that the fuel with the highest aromatic content has a significantly greater tendency to form soot precursors, while the ATJ fuel (B1) has the least one. The high temperature reactivity of the ATJ is also reduced

compared to a traditional Jet A-1 (A1). The intermediate species peaks for the ATJ extend to higher temperatures compared to the ones of the two fossil-based fuels (A1 and C1). Moreover, fuel B1 (ATJ) also presents an earlier onset of the oxygen (and fuel) consumption, associated with the formation of formaldehyde.

From a modelling perspective, it emerged that more validation is needed for some of the compounds used in the surrogate palette, particularly for the aromatic and naphthenic fractions. Recently published data may also offer the opportunity for improving the current iso-dodecane model. Because of the entanglements introduced when considering complex mixtures, these experiments are not generally suitable for the validation of specific submodels, although it is fair to conclude that some systematic discrepancies may be related to deficiencies in the kinetic model. The simulations consistently underestimate the formation of C_4H_8 in favor of more dehydrogenated species (C_4H_4), pointing to inaccuracies in the oxidation and pyrolysis of small species. This mechanism may influence soot growth phenomena, since strongly unsaturated linear species are prone to condensation reactions leading to PAHs.

Moreover, for fuels with similarities to the high aromatic fuel C1, more components (high molecular weight ones, in particular) may be needed to capture both the chemical and physical properties of the target fuel (e.g., its distillation curve). While n-alkanes have been extensively studied in well-characterized reacting systems (e.g., flow reactor, jet-stirred reactors, shock-tubes), data for high molecular weight alkyl-aromatics and alkyl-cycloalkanes are more scarce, as their low volatility, combined with their slower reactivity, makes their probing more challenging. In the absence of data, models can only be constructed based on similarity rules, as described in the kinetic model section, leading to higher uncertainties. Therefore, further research will have to locate the optimum between uncertainties in the surrogate formulations and in the kinetic model of the components it contains.

DATA AVAILABILITY STATEMENT

The raw data supporting the conclusions of this article will be made available by the authors, without undue reservation.

AUTHOR CONTRIBUTIONS

Experimental work by PO, Modelling activity by MM and MP.

FUNDING

This work was performed in the context of JetSCREEN, a project funded from the European Union's Horizon 2020 research and innovation program under agreement No. 723525.

REFERENCES

Aviationbenefits (2021). Waypoint 2050. Available at: https://aviationbenefits.org/environmental-efficiency/climate-action/waypoint-2050/ (Accessed Jan 14, 2022).

Bierkandt, T., Oßwald, P., Schripp, T., and Köhler, M. (2019). Experimental Investigation of Soot Oxidation under Well-Controlled Conditions in a High-Temperature Flow Reactor. *Combustion Sci. Tech.* 191, 1499–1519. doi:10.1080/00102202.2018.1554651

Burcat, A., and Ruscic, B. (2005). *Third Millenium Ideal Gas and Condensed Phase Thermochemical Database for Combustion (With Update from Active Thermochemical Tables).* Lemont: Argonne National Laboratory. doi:10.2172/925269

Burke, S. M., Burke, U., Mc Donagh, R., Mathieu, O., Osorio, I., Keesee, C., et al. (2015). An Experimental and Modeling Study of Propene Oxidation. Part 2: Ignition Delay Time and Flame Speed Measurements. *Combustion and Flame* 162 (2), 296–314. doi:10.1016/J.COMBUSTFLAME.2014.07.032

Chu, T.-C., Buras, Z. J., Oßwald, P., Liu, M., Goldman, M. J., and Green, W. H. (2019). Modeling of Aromatics Formation in Fuel-Rich Methane Oxy-Combustion with an Automatically Generated Pressure-dependent Mechanism. *Phys. Chem. Chem. Phys.* 21 (2), 813–832. doi:10.1039/C8CP06097E

Cuoci, A., Frassoldati, A., Faravelli, T., and Ranzi, E. (2015). OpenSMOKE++: An Object-Oriented Framework for the Numerical Modeling of Reactive Systems with Detailed Kinetic Mechanisms. *Comp. Phys. Commun.* 192, 237–264. doi:10.1016/J.CPC.2015.02.014

Dooley, S., Won, S. H., Chaos, M., Heyne, J., Ju, Y., Dryer, F. L., et al. (2010). A Jet Fuel Surrogate Formulated by Real Fuel Properties. *Combustion and Flame* 157 (12), 2333–2339. doi:10.1016/j.combustflame.2010.07.001

European Commission (2022). JET Fuel SCREENing and Optimization | JETSCREEN Project | Fact Sheet | H2020 | CORDIS | European Commission. Available at: https://cordis.europa.eu/project/id/723525 (Accessed Jan 14, 2022).

Guzman, J., Kukkadapu, G., Brezinsky, K., and Westbrook, C. (2019). Experimental and Modeling Study of the Pyrolysis and Oxidation of an Iso-Paraffinic Alcohol-To-Jet Fuel. *Combustion and Flame* 201, 57–64. doi:10.1016/j.combustflame.2018.12.013

Herrmann, F., Oßwald, P., and Kohse-Höinghaus, K. (2013). Mass Spectrometric Investigation of the Low-Temperature Dimethyl Ether Oxidation in an Atmospheric Pressure Laminar Flow Reactor. *Proc. Combustion Inst.* 34 (1), 771–778. doi:10.1016/J.PROCI.2012.06.136

Kathrotia, T., Naumann, C., Oßwald, P., Köhler, M., and Riedel, U. (2017). Kinetics of Ethylene Glycol: The First Validated Reaction Scheme and First Measurements of Ignition Delay Times and Speciation Data. *Combustion and Flame* 179, 172–184. doi:10.1016/J.COMBUSTFLAME.2017.01.018

Kim, D., Martz, J., and Violi, A. (2014). A Surrogate for Emulating the Physical and Chemical Properties of Conventional Jet Fuel. *Combustion and Flame* 161 (6), 1489–1498. doi:10.1016/j.combustflame.2013.12.015

Kim, D., and Violi, A. (2022). Uncertainty-based Weight Determination for Surrogate Optimization. *Combustion and Flame* 237, 111850. doi:10.1016/j.combustflame.2021.111850

Köhler, M., Oßwald, P., Krueger, D., and Whitside, R. (2018). Combustion Chemistry of Fuels: Quantitative Speciation Data Obtained from an Atmospheric High-Temperature Flow Reactor with Coupled Molecular-Beam Mass Spectrometer. *JoVE* 132, 56965. doi:10.3791/56965

Liu, Y.-X., Richter, S., Naumann, C., Braun-Unkhoff, M., and Tian, Z.-Y. (2019). Combustion Study of a Surrogate Jet Fuel. *Combustion and Flame* 202, 252–261. doi:10.1016/j.combustflame.2019.01.022

Prak, D. J. l., Simms, G. R., Dickerson, T., McDaniel, A., and Cowart, J. S. (2022). Formulation of 7-Component Surrogate Mixtures for Military Jet Fuel and Testing in Diesel Engine. *ACS Omega* 7, 2275–2285. doi:10.1021/acsomega.1c05904

Martinos, A.-D., Zarzalis, N., and Harth, S.-R. (2021). "Analysis of Ignition Processes at Combustors for Aero Engines at High Altitude Conditions with and without Effusion Cooling," in Proceedings of ASME Turbo Expo 2020

Turbomachinery Technical Conference and Exposition GT2020, September 21-25, 2020. doi:10.1115/GT2020-16173

Metcalfe, W. K., Burke, S. M., Ahmed, S. S., and Curran, H. J. (2013). A Hierarchical and Comparative Kinetic Modeling Study of C1 − C2 Hydrocarbon and Oxygenated Fuels. *Int. J. Chem. Kinet.* 45 (10), 638–675. doi:10.1002/kin.20802

Narayanaswamy, K., and Pepiot, P. (2018). Simulation-driven Formulation of Transportation Fuel Surrogates. *Combustion Theor. Model.* 22 (5), 883–897. doi:10.1080/13647830.2018.1464210

Oßwald, P., and Köhler, M. (2015). An Atmospheric Pressure High-Temperature Laminar Flow Reactor for Investigation of Combustion and Related Gas Phase Reaction Systems. *Rev. Scientific Instr.* 86 (10), 105109. doi:10.1063/1.4932608

Oßwald, P., Zinsmeister, J., Kathrotia, T., Alves-Fortunato, M., Burger, V., van der Westhuizen, R., et al. (2021). Combustion Kinetics of Alternative Jet Fuels, Part-I: Experimental Flow Reactor Study. *Fuel* 302, 120735. doi:10.1016/j.fuel.2021.120735

Pejpichestakul, W., Ranzi, E., Pelucchi, M., Frassoldati, A., Cuoci, A., Parente, A., et al. (2019). Examination of a Soot Model in Premixed Laminar Flames at Fuel-Rich Conditions. *Proc. Combustion Inst.* 37 (1), 1013–1021. doi:10.1016/J.PROCI.2018.06.104

Pelucchi, M., Oßwald, P., Pejpichestakul, W., Frassoldati, A., and Mehl, M. (2021). On the Combustion and Sooting Behavior of Standard and Hydro-Treated Jet Fuels: An Experimental and Modeling Study on the Compositional Effects. *Proc. Combustion Inst.* 38 (1), 523–532. doi:10.1016/j.proci.2020.06.353

Ranzi, E., Dente, M., Goldaniga, A., Bozzano, G., and Faravelli, T. (2001). Lumping Procedures in Detailed Kinetic Modeling of Gasification, Pyrolysis, Partial Oxidation and Combustion of Hydrocarbon Mixtures. *Prog. Energ. Combustion Sci.* 27 (1), 99–139. doi:10.1016/S0360-1285(00)00013-7

Ranzi, E., Frassoldati, A., Grana, R., Cuoci, A., Faravelli, T., Kelley, A. P., et al. (2012). Hierarchical and Comparative Kinetic Modeling of Laminar Flame Speeds of Hydrocarbon and Oxygenated Fuels. *Prog. Energ. Combustion Sci.* 38 (4), 468–501. doi:10.1016/J.PECS.2012.03.004

Ranzi, E., Frassoldati, A., Stagni, A., Pelucchi, M., Cuoci, A., and Faravelli, T. (2014). Reduced Kinetic Schemes of Complex Reaction Systems: Fossil and Biomass-Derived Transportation Fuels. *Int. J. Chem. Kinet.* 46 (9), 512–542. doi:10.1002/kin.20867

Rock, N., Stouffer, S., Hendershott, T., Heyne, J., Blunck, D., Zheng, L., et al. (2021). "Lean Blowout Studies," in *Fuel Effects on Operability of Aircraft Gas Turbine Combustors* (Reston: American Institute of Aeronautics and Astronautics, Inc.), 143–196. doi:10.2514/5.9781624106040.0143.0196

Ruscic, B. (2015). Active Thermochemical Tables: Sequential Bond Dissociation Enthalpies of Methane, Ethane, and Methanol and the Related Thermochemistry. *J. Phys. Chem. A.* 119 (28), 7810–7837. doi:10.1021/acs.jpca.5b01346

Saffaripour, M., Veshkini, A., Kholghy, M., and Thomson, M. J. (2014). Experimental Investigation and Detailed Modeling of Soot Aggregate Formation and Size Distribution in Laminar Coflow Diffusion Flames of Jet A-1, a Synthetic Kerosene, and N-Decane. *Combustion and Flame* 161 (3), 848–863. doi:10.1016/j.combustflame.2013.10.016

Schenk, M., Leon, L., Moshammer, K., Oßwald, P., Zeuch, T., Seidel, L., et al. (2013). Detailed Mass Spectrometric and Modeling Study of Isomeric Butene Flames. *Combustion and Flame* 160 (3), 487–503. doi:10.1016/J.COMBUSTFLAME.2012.10.023

Schripp, T., Anderson, B., Crosbie, E. C., Moore, R. H., Herrmann, F., Oßwald, P., et al. (2018). Impact of Alternative Jet Fuels on Engine Exhaust Composition during the 2015 ECLIF Ground-Based Measurements Campaign. *Environ. Sci. Technol.* 52 (8), 4969–4978. doi:10.1021/acs.est.7b06244

Yaws, C. L. (2005). *The Yaws Handbook of Vapor Pressure : Antoine Coefficients*. Amsterdam: Elsevier.

Yi, T., Gutmark, E. J., and Walker, B. K. (2009). Stability and Control of Lean Blowout in Chemical Kinetics-Controlled Combustion Systems. *Combustion Sci. Tech.* 181 (2), 226–244. doi:10.1080/00102200802424559

Yu, Z., Wei, S., Wu, C., Wu, L., Sun, L., and Zhang, Z. (2022). Development and Verification of RP-3 Aviation Kerosene Surrogate Fuel Models Using a Genetic Algorithm. *Fuel* 312, 122853. doi:10.1016/j.fuel.2021.122853

Conflict of Interest: The authors declare that the research was conducted in the absence of any commercial or financial relationships that could be construed as a potential conflict of interest.

frontiers in Energy Research

ORIGINAL RESEARCH
published: 09 March 2022
doi: 10.3389/fenrg.2022.749738

Economic Impacts of the U.S. Renewable Fuel Standard: An *Ex-Post* Evaluation

Farzad Taheripour[1]*, *Harry Baumes*[2] *and Wallace E. Tyner*[1]

[1]Department of Agricultural Economics, Purdue University, West Lafayette, IN, United States, [2]National Center for Food and Agriculture Policy, Washington, DC, United Sates

This paper examines the extent to which biofuel production has been driven over time by the U.S. Renewable Fuel Standard (RFS) and the extent to which it was driven by non-RFS policies and market forces. While the RFS has played a critical role in providing a secure environment to produce and use more biofuels, at least in the 2000s, it was not the only factor that encouraged the biofuel industry to grow. While the existing literature has successfully identified the key drivers of the growth in biofuels, it basically has failed to properly quantify the impacts and contributions of each of these drivers separately. This paper develops short- and long-run economic analyses, using Partial Equilibrium (PE) and Computable General Equilibrium (CGE) models, to differentiate the economic impacts of the RFS from other drivers that have helped biofuels to grow. Results show: 1) the bulk of the ethanol production prior to 2012 was driven by what was happening in the national and global markets for energy and agricultural commodities and by the federal and sometimes state incentives for biofuel production; 2) the medium-to long-run price impacts of biofuel production were not large; 3) due to biofuel production, regardless of the drivers, real crop prices have increased between 1.1 and 5.5% in 2004–11 with only one-tenth of the price increases were assigned to the RFS, 4) for 2011–16, the long-run price impacts of biofuels were less than the time period of 2004–11, as in the second period biofuel production increased at much slower rate; 5) biofuel production, regardless of the drivers, has increased the US annual farm incomes by $8.3 billion between 2004–11 with an extra additional annual income of $2.3 billion between 2011–2016; 6) the modeling practices provided in this paper assign 28% of the expansion in farm incomes of the period of 2004–2011 and 100% of the extra additional incomes of the period of 2011–16 to the RFS.

Keywords: renewable fuel standard, biofuels, food and crop prices, economic impacts, partial and general equilibrium

OPEN ACCESS

Edited by:
Kristin C. Lewis,
Volpe National Transportation Systems Center, United States

Reviewed by:
Gal Hochman,
Rutgers, The State University of New Jersey, United States
Matthew Langholtz,
Oak Ridge National Laboratory (DOE), United States

***Correspondence:**
Farzad Taheripour
tfarzad@purdue.edu

Specialty section:
This article was submitted to Sustainable Energy Systems and Policies, a section of the journal Frontiers in Energy Research

Received: *06 August 2021*
Accepted: *03 February 2022*
Published: *09 March 2022*

Citation:
Taheripour F, Baumes H and Tyner WE (2022) Economic Impacts of the U.S. Renewable Fuel Standard: An Ex-Post Evaluation. Front. Energy Res. 10:749738. doi: 10.3389/fenrg.2022.749738

INTRODUCTION

When a government imposes a regulation, it usually indicates that policy makers believe that the market would not produce the socially desired outcome. The U.S. Renewable Fuel Standard (RFS) is a good example of such a regulation. Congress believed that markets would not produce the "desired" amounts of renewable fuels, so it established requirements for minimum levels of use of different kinds of renewable fuels, providing biofuels access to the fuels market. However, it is not always the case that the mandate becomes binding if market conditions change. It is possible that with

unforeseen changes in market conditions, a biofuel would be produced and/or used due to market forces, at least to some extent. This paper examines the extent to which biofuel production has been driven through time primarily by the RFS, and the extent to which it was driven by market changes unforeseen at the time of RFS passage.

The original RFS was enacted by Congress in 2005 (U.S. Congress, 2005). It was amended in 2007, and the revised and current RFS is sometimes referred to as RFS2 (U.S. Congress, 2007). However, in this paper, we will refer to it as RFS. The major objectives of the RFS were 1) to provide a source of increased incomes and employment in rural areas, 2) to increase US energy security, and 3) to reduce greenhouse gas (GHG) emissions (Tyner, 2012). However, prior to the enactment of the RFS, there was other legislation related to ethanol, which is summarized by Tyner (2008). The National Energy Conservation Policy Act (U.S. Congress, 1978) was essentially the first piece of renewable energy legislation and established an excise tax exemption for ethanol of $0.40/gal.[1] This tax incentive was converted to a Volumetric ethanol Excise Tax Credit (VEETC) in the American Jobs Creation Act of 2004 (U.S. Congress, 2004). The government support continued in some form through 2011 and varied between $0.40 and $0.60/gal. of ethanol. The use of government incentives and the RFS were the two main policy instruments aimed at helping to establish and grow the ethanol industry to accomplish the three aforementioned goals. However, as described in this paper, there were many other factors that helped drive biofuel industry to grow since 1980.

Determining the economic impacts of the RFS is a complicated task. Part of the complication is the questions of attribution. For example, some of the early literature tended to blame the RFS for all increases in commodity prices. However, over time it has become abundantly clear that many factors have been involved in the evolution of commodity and food prices, with the RFS and biofuel production in general being only one.

The **Supplementary Material** (SM) of this paper provides a comprehensive literature review and data analysis to highlight the major debates in this area and review the historical trends in the key variables that sketch the interactions between the RFS and markets for energy and agriculture products. The SM divides the historical analyses into five periods that are characterized by different drivers, as shown in **Supplementary Table S1**.

The first period is 1980–2004. The only ethanol incentive during this period was the ethanol tax exemption, varied from 40 to 60 cents (Tyner, 2008). However, the Clean Air Act Amendments of 1990 also provided some demand for ethanol as a source of oxygen in gasoline (U.S. Congress, 1990). Prior to 2004, the price of crude oil was relatively low ranging from $10 to $33 per barrel (**Supplementary Figure S2**) and the price of corn was also usually low ranging from $1.4 to $4.4 per bushel (**Supplementary Figure S3**). Between 1983 and 2005, prior to enactment of RFS, the annual growth rate of demand for ethanol was about 9.5% (Tyner, 2008; Hertel et al., 2010) due to favorable market conditions such as low corn price, ethanol tax exemption, and demand for ethanol as an oxygen additive.

The second period is 2004–2008. Lots of things were changing during this period. The first RFS was passed in 2005, but it was not really binding in this period, except for 2008. A mandate is considered to be binding if it results in changes in production from what the market would have produced absent the mandate. In the case of the RFS, an indication of the extent to which the RFS is binding can be the price of Renewable Identification Numbers (RINs). If RINs prices are very low, it means the RFS is not playing a major role in determining production levels (Abbott, 2014). The ethanol RIN price was usually lower than five cents per gallon in this period, confirming a non-binding mandate. In this period the wholesale gasoline price sharply increased from $1.05 per gallon in January 2004 to $3.35 per gallon in July 2008 (**Supplementary Figure S7**). The ban on the use of Methyl Tertiary-Butyl Ether (MTBE), a toxic gasoline additive, has been passed in June 2006. This significantly increased demand for ethanol as a cheap and non-toxic substitute for MTBE, which helped ethanol industry to grow faster. In this period, ethanol production grew at a substantial 24% annual rate.

In this period commodity, and food prices generally increased. Various papers have studied the key drivers of commodity and food price increases that occurred in this time period (a few examples are: Delgado, 2008; Henderson, 2008; Trostle, 2008; and many more). Abbott et al. (2008) have reviewed many of these papers and concluded that the commodity and food price increases had three main sets of drivers for this time period: global changes in production and consumption of key commodities; the depreciation of the US dollar (exchange rate); and growth in production of biofuels.

The third period is 2008–2009. The great global recession began in this period. Many of the key drivers that had operated in the period leading up to 2008 went into reverse. Crude oil and gasoline prices plummeted (see **Supplementary Figures S6, S7**). With reduced global incomes, demand for most commodities and their prices fell. With declining gasoline prices, the price of ethanol followed. However, ethanol production remained strong because corn price fell along with or even further than ethanol prices. Though the recession was quite deep, commodity prices generally began a rebound in 2009. Throughout this period, ethanol RIN prices remained low suggesting again that the RFS was not binding in this period.

The fourth period is 2010–2011. Commodity prices again rose in this period, with crude oil topping $100 per barrel. During this period, some of the key drivers from earlier periods remained, but there were also new drivers (Abbott et al., 2011). Poor harvests in several parts of the world were more important in 2011 than in 2008 leading to higher agricultural commodity prices. Leading up to 2011 there was also a significant change in Chinese policy with respect to soybean imports. With persistent demands for corn for biofuels and China for soybeans, overall price elasticity became more inelastic, which led to higher prices and more price volatility. Ethanol and corn prices rose together in 2010–11. Blend wall concerns began to appear in 2011 (Tyner and Viteri, 2010; Abbott, 2014), but ethanol exports increased

[1]The form and amount of the government support has changed over the years.

substantially over that period (see **Supplementary Figure S9**). As shown in **Supplementary Figure S11**, RIN prices for ethanol continued at low levels, indicating that the RFS still was not binding for ethanol. However, RIN priced for biodiesel surged, indicating a binding RFS for this biofuel (see **Supplementary Figure S11**).

Another development that began around 2009 was that ethanol prices moved below gasoline prices (**Supplementary Figure S7**) and appeared poised to remain low for some time. Many refiners saw this as an opportunity to reduce refining costs by producing lower-cost 84 octane gasoline out of the refinery and blending with 10 percent ethanol to yield an 87-octane blend at the pump. In fact, ethanol prices did remain below gasoline for years to come, and that change increased the market demand for ethanol as an octane additive. In other words, ethanol became more a standard part of the gasoline refining system. Ethanol has higher value as a fuel additive (oxygen and octane) than as a fuel extender, but this value is difficult to capture in economic models. However, in a recent *FarmDoc Daily* post, Scott Irwin quantified the added value ethanol provides as an octane enhancer (Irwin, 2019).

The fifth period is 2011–2016. In this period production of ethanol did not grow as before due to changes in market force. In 2012, the US experienced a major drought which led to a high corn price and negative ethanol margins according to the iowa State ethanol Profitability model and as illustrated in **Supplementary Figure S10** (Agricultural Marketing Resource Center, 2019). As a consequence, ethanol production and exports declined (**Supplementary Figures S1, S9**).

During this period the gasoline consumption did not grow as it was expected due to two main factors. First, the great recession of 2008–09 led to a large drop in gasoline consumption, and consumption growth did not pick up for a considerable amount of time. Second, the US enacted more stringent fuel economy standards, which meant consumers could drive more miles with less fuel. High oil and gasoline prices also encouraged consumers to purchase more fuel-efficient vehicles and perhaps to drive slightly less. Due to these changes, the gasoline market moved towards the historical definition of the blend wall, the 10% maximum ethanol content (Tyner W. et al., 2010; Tyner W. E. et al., 2010; Tyner, and Viteri, 2010). Because of the decline in gasoline consumption, not enough ethanol could be blended at the historical 10% maximum ethanol content to achieve the implied RFS targets starting in 2013 (see Section 1.5 of the MS for details).

As mentioned before, prior to 2011, ethanol was basically in demand as a fuel extender and an octane additive. This changed after 2011 and a portion of ethanol was consumed as a substitute for gasoline to meet the RFS requirements, along with providing a source of octane. Since 2011, as the total consumption of ethanol moved towards the historical 10% maximum ethanol content (that was allowed in non-flex-fuel vehicles), demand for ethanol did not grow due to market forces enough to meet the minimum RFS requirement, and that led to higher RINs prices. Starting in 2013, the market observed major increases in the corn ethanol RIN values, as shown in **Supplementary Figure S11**. Starting in 2013 ethanol RIN prices moved up to biodiesel RIN prices and essentially followed biodiesel until recently as shown in **Supplementary Figure S11**. The RFS and historical 10% blend rate became the limiting factor until 2016. Due to the nested structure of the RFS, biodiesel and other advanced RINs could be used to satisfy the part of the conventional fuel (ethanol) requirement (adjusted and implied by the EPA) that could not be done with ethanol. Korting et al. argue that in addition to the RFS nested structure, the joint gasoline and diesel compliance base is also important (Korting et al., 2019).

Another important change in energy markets that occurred during this time period and negatively affected profitability of ethanol is the shale oil boom (Taheripour et al., 2014), which led to a 57% increase in US crude oil production between 2011 and 2016 (**Supplementary Figure S12**). This remarkable increase in US production helped push world crude oil prices lower as shown in **Supplementary Figure S2**, (for details see Section 1.5 of the SM).

In addition to dividing the literature and data analysis into the periods mentioned above, the SM also discusses other papers that provide a somewhat different take on the RFS such as one by Abbott (2014). It also covers other important papers that examine the time varying relationship between biofuels and commodity and food prices.

USDA has published some important papers on the food-fuel issue (Trostle, 2008; Trostle et al., 2011). There have been many econometric studies of the relationships among prices of crude oil, gasoline, ethanol, corn, and other commodities (Zhang et al., 2010; Wright, 2011; Chiou-Wei et al., 2019; Filip et al., 2019). Filip et al. (2019) have provided a review of much of the econometric literature. In addition, these authors used a comprehensive data set covering many commodities and other variables and concluded that: 1) ethanol did not affect agricultural commodity prices prior to the 2008 food crisis; 2) during the food crisis periods about 15 percent of the variance in corn prices was due to ethanol and 5 percent of other commodities; 3) after the food crisis, ethanol contributed about 10 percent of the variability in agricultural commodity prices; 4) biofuels did not serve as a leading source of high commodity prices. Finally, Filip et al. (2019) have asserted that their results serve as an "ex-post correction" of the previous results suggesting dramatic effects of biofuels on commodity and food prices. It is important to note that these authors have not separated impacts of the RFS from other market factors driving biofuels. It is just an analysis of the impacts and commodity price linkages due to biofuels regardless of whether the biofuels were driven by market forces or the RFS or some combination. For further discussion on the price impact of RFS see Sections 1.6 and 1.7 of the SM.

The main take-away from the literature review and analyses provided in the SM is that most of the analyses that have been done to date do not distinguish between market drivers of ethanol production growth and the RFS as a driver. In the 1980s and 1990s, ethanol tax incentives and the Clean Air Act Amendments of 1990, which established reformulated gasoline, were the key policies enabling establishment and relatively slow growth of the industry during a period of low crude oil prices. In the years 2004–08, there was a substantial run-up in crude oil prices that pulled ethanol into the market. The crude oil price increase and

the 2006 MTBE ban were the key drivers in capacity additions. Ethanol margins were strong in 2005–07, which provided strong incentives to add capacity. Of course, the added ethanol production increased demand for corn and was part of the reason for the corn and other commodity price increases. Filip et al. (2019) have estimated that biofuels may have been responsible for about 15 percent of the rise in corn prices. But that was biofuels production induced primarily by market forces, and the ethanol tax incentive. Price correlations continued strong through the recession and the second commodity price surge in 2011. The 2012 drought reduced US corn production, and higher prices sent ethanol margins negative and led to a temporary drop in ethanol production. The short-run impact of biofuels on commodity prices may have been more important in late 2008 and early 2009. Since 2013 RIN prices increased rapidly due to constraints on the growth of ethanol consumption, as the market moved towards the 10% historical blend rate. Ethanol exports started a growing trend in 2013 that continued until 2019, when this research has been developed.

The literature review and analyses provided in the MS confirm that biofuels production being driven mainly by market forces and government support for ethanol, which ended in 2011. Prior to this year, the RFS provided an incentive to get capacity built and also generated a safety net for biofuels to grow, but it was not binding in the markets except for a few months in 2008–09. Since 2011, the RFS in combination with constraints on the growth of ethanol consumption drove the markets for biofuels. Finally, the recent econometric evidence suggests that biofuels were not the main driver of commodity price increases, (for detail see the SM).

A crucial question to ask given our conclusions on the role of markets in driving biofuels growth is How it would have been different if all these market changes had not occurred. In other words, what if crude oil price had not surged, MTBE had not been banned, ethanol did not get integrated into the fuel system becoming a fuel additive instead of a fuel extender, etc.? The answer is clearly that the RFS would have played a much greater role. So, in a sense, the RFS has been the backstop, but by circumstance, it was overpowered by tax incentives and market forces through 2011. Another important comparison is between what happened over this period for ethanol compared with biodiesel and cellulosic biofuels. For both biodiesel and cellulosic biofuels, the original mandated levels have not been implemented in practice and frequently revised over time. Hence, the RFS has not reached its original goals for these biofuels. However, after the waivers, the RFS was still clearly an important driver of production and consumption. RIN prices were always relatively high, and the RFS was always binding. Clearly, the market changes that benefitted ethanol did not work as much in favor of these other biofuels.

While the existing literature indicates that the RFS has played a critical role in providing a secure environment to produce and use more biofuels, to the best of our knowledge, no major effort has been made to isolate the economic impacts of this policy for other factors that helped the biofuel industry to grow. While, in general, the existing literature has successfully identified the key drivers of the growth in biofuels, it basically has failed to properly quantify the impacts and contributions of each of these drivers separately. This paper takes primary steps to fill this knowledge gap. Following an extensive literature review, it develops short- and long-run economic analyses, using Partial Equilibrium (PE) and Computable General Equilibrium (CGE) models, to differentiate the economic impacts of the RFS from other drivers that have helped biofuels to grow. Unlike the existing PE and CGE modeling efforts that typically provided *ex ante* economic analyses for biofuels, this paper follows Taheripour et al. (2019) and develops a new approach that uses actual observations for the time period 2004–16 to construct ex-post historical baselines and counterfactual simulations to achieve the goals of this research. The existing literature has addressed the economic impacts of biofuel production and policy from different perspectives including but not limited to: welfare gains and loses; demand for and supply of transportation fuels; fuel prices; food and commodity prices; and contributions to agricultural resource utilization. This paper concentrates on the last two topics of this list and provides new important and critical insights in these areas. It is important to note that the immediate price impacts of the RFS (e.g., monthly price impacts) could provide important insights on immediate price responses. However, our partial and general equilibrium modeling frameworks are not suitable for this type of analyses.

The literature review, data analysis, and modeling practices provided in this paper shows that: 1) while the RFS has played a critical role in providing a secure environment to produce and use more biofuels, at least in the 2000s, it was not the only factor that encouraged the biofuel industry to grow; 2) since 2011, the RFS in combination with constraints on the growth of ethanol consumption drove the markets for biofuels; 3) the medium-to long-run price impacts of biofuel production were noticeable, while the RFS had minor impacts on crops and food prices; 4) over time, biofuel production and policy made major contributions to the agricultural sector to utilize its resources more efficiently and that significantly improved farm incomes in the US; 5) biofuel production, regardless of the drivers, has increased the US annual farm incomes by $8.3 billion between 2004–11 with an extra additional annual income of $2.3 billion between 2011–2016; 6) the modeling practices provided in this paper assign 28% of the expansion in farm incomes of the period of 2004–2011 and 100% of the extra additional incomes of the period of 2011–16 to the RFS; and finally, the RFS as a backup policy has provided a secure environment for biofuel producers and that reduced policy uncertainties, which facilitated capacity generation and investment in biofuel industry in 2000s.

The rest of this paper is organized into three sections. First, we explain the approach we will use in this analysis. After that we will present the quantitative results of our model simulations and relate them to the literature and data discussions. The last section covers the conclusions.

MATERIALS AND METHODS

To assess the annual, short-run, and long-run price impacts of the US RFS, in this research, we make use of both a Computable General Equilibrium (CGE) model and a Partial Equilibrium (PE)

model. Each modeling approach has advantages and disadvantages, and we use each model relying on its unique strengths and fit for the question(s) being asked. In general, GTAP-BIO is used for the global and longer-term analysis, whereas the PE model is used for specific analysis of the US agricultural and liquid fuel sectors to capture finer and shorter-term impacts. The combination of the two modeling frameworks permits us to analyze and evaluate all the important issues related to biofuels, RFS, and commodity and food prices. We use the models iteratively in the analysis to gain the advantages of both approaches.

Computable General Equilibrium Model

To accomplish the goals of this paper, we will use a well-known global CGE model: GTAP-BIO. This model is an advanced version of the standard GTAP model. The standard model is fully described in Hertel (1997). GTAP-BIO extends the capabilities of the standard model to develop economic and land use analyses related to the environmental, agricultural, energy, trade, and biofuel policies and actions. This model has been improved over time and used in various applications (Taheripour and Tyner, 2011; Beckman et al., 2012; Taheripour and Tyner, 2013; Taheripour and Tyner, 2014; Taheripour et al., 2016b; Brookes et al., 2017; Taheripour and Tyner, 2018; Yao et al., 2018). Taheripour et al. (2017b) described the background of this model and Taheripour et al. (2017a) developed the latest version of this model.

This model traces production, consumption, and trade of all goods and services (aggregated into various categories) at the global scale. Unlike the standard model, GTAP-BIO disaggregates oil crops, vegetable oils, and meals into several categories including: soybeans, rapeseed, palm oil fruit, other oil seeds, soy oil, rapeseed oil, palm oil, other oils and fats, soy meal, rapeseed meal, palm kernel meal, and other meals. In addition to the standard commodities and services, this model integrates the production and consumption of biofuels (e.g., corn ethanol, sugarcane ethanol, and biodiesel) and their by-products (DDGS and meals). Therefore, unlike the standard GTAP model, the enhanced model takes into account the use of commodity feedstocks for food and fuel and the competition or trade-offs between those and other market uses. In addition, it traces land use (and changes in land prices) across the world at the level of Agro-Ecological Zone (AEZ). The latest version of this model handles intensification in crop production due to technological progress, multi-cropping, and conversion of unused cropland to crop production. Finally, the parameters of this model were calibrated to recent observations. This model traces the inter-relationships among crop, livestock, feed, and food sectors and links them with biofuels sectors and accounts for upstream and downstream linkages among these sectors and other economic activities. This model also considers resource constraints and technological progress. Hence, it provides a comprehensive framework to assess the price impacts of biofuel production and policies. While the GTAP-BIO model produces global outputs, for the purposes of this analysis, we focus on the US impacts.

Partial Equilibrium Model

The CGE analyses developed in this paper provide comprehensive and overall medium-to long-run analyses of the price impacts of the US RFS and do not include short-run and annual price changes induced by the RFS or other factors. The literature is rich with explanations of key drivers of price changes that may not be included in medium-to long-term models. A good example is the series of Farm Foundation papers that explain how the drivers of commodity and food price changes over the period 2008–2011 (Abbott et al., 2008; Abbott et al., 2009; Abbott et al., 2011). To provide short-run and annual analyses we will use an improved version of an Agricultural Energy Partial Equilibrium (AEPE) model which was developed by Taheripour and Tyner and used in several publications (Tyner and Taheripour, 2008; Tyner W. et al., 2010; Taheripour et al., 2016a) to examine interactions between agricultural and energy markets and evaluate the consequences of changes in biofuel policies. The improved version of the model covers crude oil, gasoline, corn ethanol, biodiesel, corn, soybeans, and feed (e.g., DDGS and meals) markets. The model is for the US economy. It distinguishes demand for corn and soybeans in their alternative uses (food, feed, biofuels, and exports) and traces changes in agricultural subsidies and biofuel policies.

The AEPE model uses a base year data set and short-run demand and supply elasticities for the (commodity) markets included in the model, and long-run and short-run shift factors in demand and supply of each market and determines their new equilibriums over time. The long-run and short-run shift factors are exogenous to this model. The long-run shift factors (e.g., population, income growth, and growth in demand for livestock products) help the model to adjust overtime. The short run shift factors represent annual exogenous changes (e.g., reductions in crop yields due to a drought). We have used this model for the time period 2004 to 2016 to better characterize short-run changes in the agricultural and fuel markets over this period. Some of the shift factors are directly observable, while others may not be directly observable. For example, historical data represent annual fluctuations in crop yields or changes in ethanol incentives are directly observable. The PE model takes into account these shift factors through its exogenous variables. For unobservable shift factors (e.g., shift factors in the demand of energy or shifts in foreign demand for corn), we will rely on the

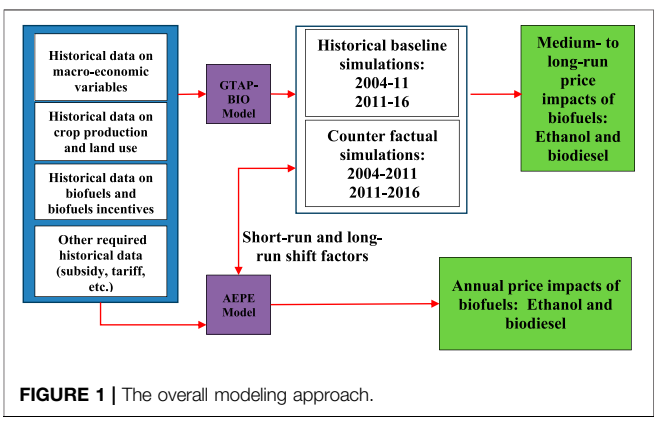

FIGURE 1 | The overall modeling approach.

outputs of the GTAP-BIO model and other observations as discussed later in this paper.

Overall Modeling Approach

In essence, we use the AEPE model to provide more detailed results for the US than is possible from a global CGE model. The combination of the CGE and PE models and their results enables us to respond to most the goals of this project. **Figure 1** represents our modeling approach and the links between the CGE and PE models. The CGE model results are used to assess the medium-to long-run price impacts of biofuels. The PE model assesses the annual and short-term price impacts of biofuels, including corn ethanol and soybean biodiesel. This figure shows interactive links between the CGE and PE models through the shift factors.

Examined Experiments

As described above, the main goal of this research is to answer the following important questions:

1) To what extent the RFS alone has affected commodity and food prices,
2) To what extent the expansion in US biofuel production has affected commodity and food prices, regardless of the causes,
3) To what extent the RFS alone has contributed to agricultural resource utilization,
4) To what extent the expansion in US biofuel production has contributed to agricultural resource utilization, regardless of the causes.

To answer these questions, we developed historical simulations and counterfactual experiments using the CGE and PE models. Essentially, we modeled what happened in the agricultural and energy sectors due to all causal factors. Then, we removed the RFS to determine what the impact of the RFS had been isolated from all the other market drivers of changes in these markets. Then, we removed biofuels production increases to determine what had been the impact of biofuels (whether driven by the RFS or other factors). In each case, the difference between the simulated historic baseline and the experiment gives us the impacts on prices, production, etc., due to the one factor that was being altered. The historical simulations capture and represent changes in economic variables as happened in the real world. The counterfactual experiments repeat the baseline simulations under alternative assumptions to capture the RFS/biofuel impacts from the impacts of other drivers. In what follows we describe the baselines and counterfactual experiments, first for the CGE approach and then for the PE method.

Computable General Equilibrium Baselines and Counterfactual Experiments

During the time period of 2004–2016, crop and food prices followed increasing trends until 2012 and then traced downward paths or remained relatively flat in the US. One can observe a similar pattern globally as well. Given this observation, since one goal of this research is to determine the impacts of the RFS on crop and food prices, we split the CGE analyses into two distinct time segments of 2004–2011 and 2011–2016 to better understand the differences between the price determining forces of these time periods. Therefore, for each of these time slices we developed several historical and counterfactual experiments.

Historical Baselines: A historical baseline in a typical static CGE analysis captures and represents changes in the global economy for a given observed time period, say 2004–11 or 2011–2016 in our analysis. To construct a historical baseline using a static CGE model, we exogenously shock the model for a given set of variables (including macroeconomic and policy variables) and allow the model to determine changes in the production, consumption, and trade for all goods and services (including crops and food items) and also prices by region[2]. A baseline simulation usually takes into account technological progress in production of goods and services as well. Changes in Total Factor Productivity (TFP) and improvements in productivities of the primary and intermediate inputs usually represent technological progress.

To construct the historical baseline for each time period we closely followed the approach used by Yao et al. (2018). These authors developed a static historical baseline for the time period of 2004–2011 for a different application. Following these authors, in constructing the historical baseline for each time period, we exogenously shocked the model for the regional observed changes in population, gross domestic product (GDP), capital formation, labor force, managed land, biofuel production and policy, and agricultural and trade policies. We then allow the model to determine changes in the production, consumption, and trade for all goods and services (including crops and food items) and also prices by region. Given these exogenous shocks, the model determines TFP by country[3]. Given that technological progress in agriculture is a key driver of crop prices, we use observed changes in crop supplies to determine the rate of technological progress in crop sectors[4]. As mentioned in the literature review section, there were major shifts in crop demands between 2004 and 2016. Hence, in addition to the changes in crop yields, some demand shifters were introduced in the simulation processes for crop demands. Finally, the crude oil industry has changed significantly over the period 2004 to 2016. Since GTAP cannot capture these changes endogenously, we added proper shifters

[2]Yao et al. (2018) have followed this approach and developed a static historical baseline for the time period of 2004–11 for a different application. For details see the appendix of the paper.

[3]The standard GTAP model endogenously determines GDP for given changes in primary factors of production and TFP. In the baseline simulation we shock the model for the observed changes in GDP and primary factors of production. This allows us to alter the model closure to determine TFP for the given changes in GDP and primary factors of production. This is a standard approach for estimating TFP by country using a CGE model.

[4]The Standard GTAP model uses production functions to determine crop supplies. The production function of each crop determines supply of that crop for given inputs (including intermediate and primary inputs) and rates of unbiased and biased technological progress. The rate of unbiased technological progress for each crop acts as a shift factor in the supply function of that crop. In our baseline simulation we will ask the model to determine these crop specific shift factors for the observed changes in crop supplies.

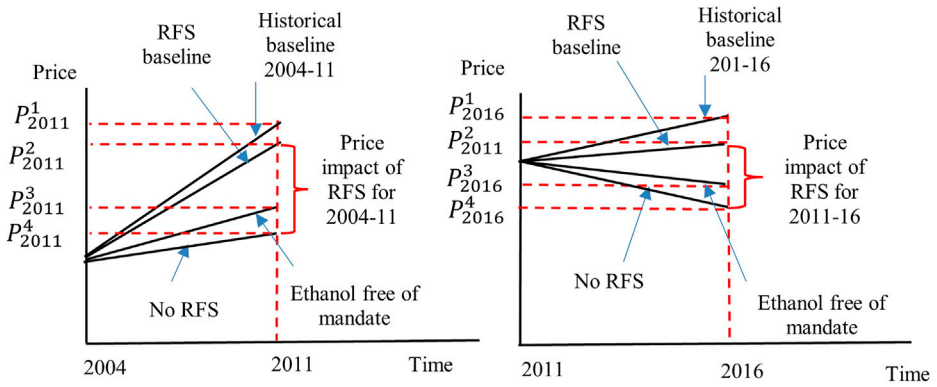

FIGURE 2 | A schematic representation of historical baselines and counterfactual experiments including: FRS *Baselines*, *ethanol free of mandate*, and *no RFS*. The left panel represents 2004–11 and the right panel 2011–16. The vertical axis shows the price of a representative product. P^1, P^2, P^3, and P^4 indicate the projected prices of this product for the *historical baselines*, RFS *Baseline*, *ethanol free of mandate*, and *No RFS* experiments, respectively.

(shocks) to capture major changes in the oil market exogenously. Finally, as mentioned in the next section we obtained data from credible sources including but not limited to the World Bank, Food and Agricultural Organization of the United Nations (FAO), Organization for Economic Cooperation and Development (OECD), and USDA to calculate the implemented shocks for the baseline construction process of each time period.

To isolate the impacts (e.g., price impact) of the RFS from all other drivers that may affect production of biofuels we developed the following counterfactual experiments:

RFS Baseline: The historical baseline, among all drivers, captures the impacts of biofuel production on commodity and food prices. However, a portion of ethanol produced in the US was not used domestically. In 2011 and 2016 the US net export of ethanol was about one billion gallons and 1.1 billion gallons. Given that the RFS targets domestic consumption of ethanol, we eliminated the impacts of trade of ethanol from the historical baseline of each time period. In this experiment we freeze trade of ethanol to remain at its initial levels in the base year for each time slice. The difference between this experiment and the historical baseline captures the trade impacts of biofuels.

Counterfactual I- ethanol free of Mandate: This experiment repeats the *RFS baseline* while removing the restriction on ethanol consumption and allows market forces to determine ethanol consumption. For each time period, the difference between the RFS baseline and this counterfactual experiment represents the impacts of RFS for conventional ethanol.

Counterfactual II-No RFS: This experiment repeats the *RFS baseline* while removing the restriction on consumption of both ethanol and biodiesel and allows market forces to determine consumption of these biofuels. The difference between *RFS baseline* and this counterfactual experiment represents the impacts of RFS for both ethanol and biodiesel.

Figure 2 provides a schematic picture for these counterfactual experiments and their relationships with the historical baseline for each time period of 2004–11 (left panel) and 2011–16 (right panel). Consider the left panel of this figure, which represents the historical and counterfactual simulations with the solid black lines. The vertical axis shows the price of a representative product. For example, P^2_{2011} and P^4_{2011} indicate the projected price of this product in 2011 for the *RFS baseline* and *No RFS* cases, respectively. The difference between these two prices represents the impact of RFS on the price of the representative product for the time period of 2004–11.

Counterfactual III- No Expansion in ethanol: This experiment repeats the historical baseline, while it freezes production of ethanol at its base year level for each time period. The difference between this experiment and the *historical baseline* captures the impacts of expansion in ethanol production.

Counterfactual IV- No Expansion in Biofuels: This experiment repeats the historical baseline, while it freezes production of ethanol and biodiesel at their base year levels for each time period. The difference between this experiment and the *historical baseline* captures the impacts of expansions in ethanol and biodiesel.

Figure 3 provides a schematic picture for the last two counterfactual experiments and their relationships with the historical baseline for each time period of 2004–11 (left panel) and 2011–16 (right panel). Consider the left panel of this figure which represents the historical and counterfactual simulations with the solid black lines. The vertical axis shows the price of a representative product for each experiment. For example, P^1_{2011} and P^6_{2011} show the price of this product in 2011 for the *historical baseline* and *No expansion in biofuels* cases, respectively. The difference between these two prices represents the impacts of the expansion in biofuel production on the price of the representative product for the time period of 2004–11.

For the PE simulations we followed the same principle as well. First, we developed a baseline to replicate annual changes in the US markets for gasoline, ethanol, biodiesel, corn, and soybeans and their trade. To accomplish this task, we first calibrated the model to represent actual observations for 2015. We then run the model annually for a set of exogenous variables (e.g., crude oil price, ethanol trade, and targets for biofuel production) and tuning parameters to trace annual changes that occurred in

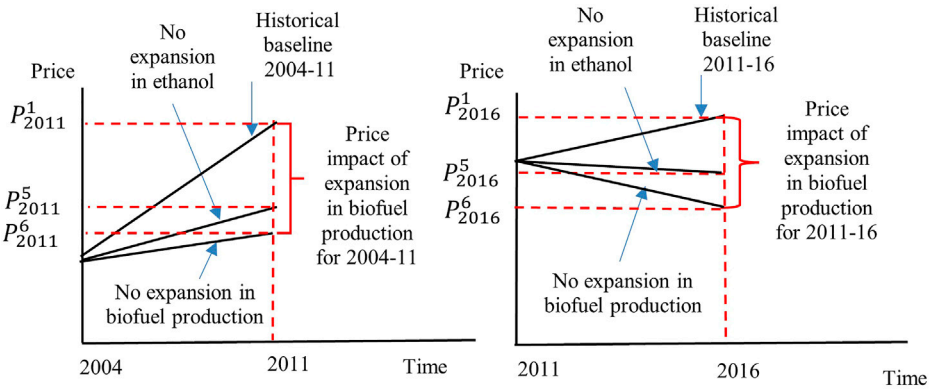

FIGURE 3 | A schematic representation of historical baselines and counterfactual experiments including: *No expansion in ethanol* and *No expansion in biofuels*. The left panel represents 2004–11 and the right panel illustrates 2011–16. The vertical axis shows the price of a representative product. P^1, P^5, and P^6 show the projected prices of this product for the *historical baselines*, *No expansion in ethanol* and *No expansion* in biofuels, respectively.

the energy and agricultural markets. Then for each year we developed a counterfactual experiment to evaluate changes in the energy and commodity markets without targeting ethanol production. Hence, for the PE model we have only two cases: A *historical annual baseline* and a *market counterfactual* case which does not target production of ethanol. This counterfactual is in line with the CGE *counterfactual I*.

Shift Factors and Collected Data

The shift factors were determined using an iterative approach between the CGE and PE models and model parameters. We first run the CGE model for 2004–11 and 2011–16 with no shift factors. We learned that for both time periods the model needs shift factors to accurately represent crude oil markets. Using actual observations, we defined shift factors to replicate changes in the crude oil price exogenously. The shift factors indeed capture changes in the global market for crude oil that economic models fail to capture. One example is production of crude oil from shale resources in the US, which altered the global market for this product. When we ran the PE model for annual changes, we found demand shifters are required to properly capture the observed changes in this variable. First, there was the recession, which caused a major downward shift in gasoline demand. Then, the fuel economy standards began to take hold, which also caused a downward shift in gasoline demand. In fact, US gasoline demand did not catch up with the 2007 level until 2016. We developed shifters to represent these exogenous changes in gasoline demand. These shifters developed for the PE model also helped us to calibrate shifters in the gasoline market for the GE model.

In modeling the annual changes in the US markets for corn and soybeans, it became apparent that there were some exogenous shifts in international trade that could not be captured in the standard model and its imbedded parameters. The best example is the very large increase in Chinese imports of soybeans, which was mainly due to policy changes that are not captured in the model. To take care of these changes we included demand shifters to represent changes in the global demand for these products.

To support simulations, data on macro variables including GDP, population, labor force, investment, and GDP deflator were collected from the World Bank data base. A summary of macro variables is presented in **Supplementary Table S3**.

The GTAP database has data on crop production and harvested area by crop for 2004 and 2011. We prepared the same data for 2016 using data from the Food and Agricultural Organization (FAO) of the United Nations. **Supplementary Table S4** provides a summary of crop production and harvested area for the US and the rest of the world for 2004, 2011, and 2016. While the model traces all crop categories included in the data bases, for this table we aggregated crops into three main categories including coarse grains (covering all coarse grains except sorghum), soybeans, and all other crops. Sorghum is included in the other category. The category of coarse grains basically represents corn. In addition to these data items, we collected a wide range of monthly and annual data on crop prices; prices of crude oil, gasoline, and ethanol; trade of agricultural products; etc. to support our analyses and/or to be use in our simulations or to be compared to our results.

RESULTS

Computable General Equilibrium Model Results

As mentioned, we developed a historical baseline and several counterfactual experiments for each time period of 2004–11 and 2011–16. In this section we highlight the following results for each time period:

1) Impacts of removing RFS only for corn ethanol: The difference between the results of *RFS* baseline and *ethanol free of mandate*,
2) Impacts of removing RFS for corn ethanol and biodiesel: The difference between the results of *RFS baseline* and *No RFS*,

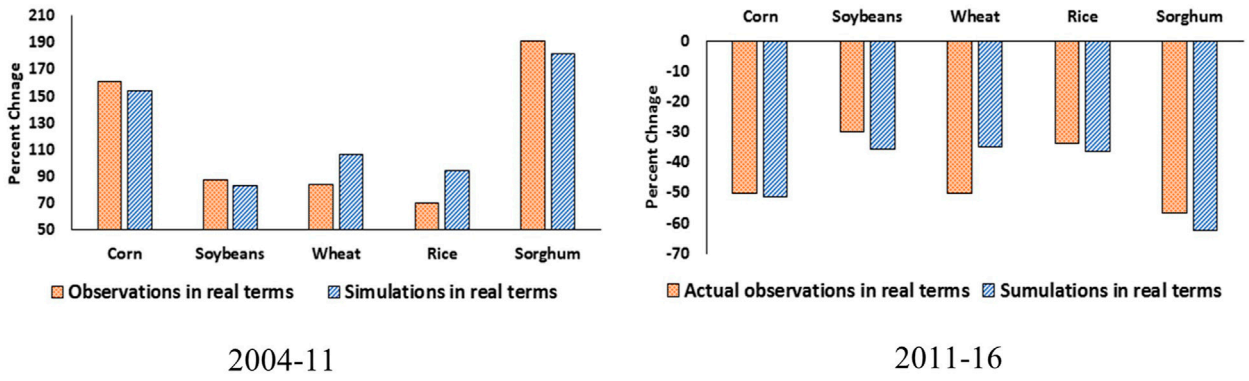

FIGURE 4 | Observed and simulated percent change in real crop prices for time periods of 2004–11 (left panel) and 2011–16 (right panel) The GDP price deflator is used to convert nominal prices to real prices.

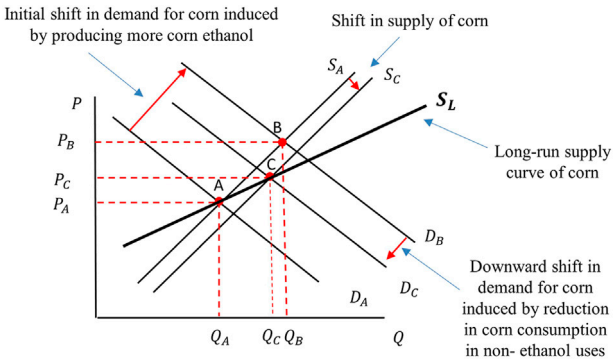

FIGURE 5 | Short-run and long-run changes in corn market. This figure was designed to explain difference between the short- and long-run supply elasticities. The demand and supply curves and their shifts are all hypothetical. **Box 1** shows numerical estimates.

3) Impacts of no expansion in corn ethanol: The difference between the results of *Historical baseline* and *No expansion in ethanol,*
4) Impacts of no expansion in biofuels: The difference between the results of *Historical baseline* and *No expansion in biofuels.*

Before presenting the results of these experiments, as a measure of validation, we compare the results of the historical simulations on the US crop prices for the time periods of 2004–11 and 2011–16 with their corresponding actual observations in **Figure 4**. This figure represents changes in crop prices in real terms. Given that GTAP represents real prices, the GDP price deflator is used to convert nominal observed prices to real prices. The left panel of this figure shows that crop prices have increased sharply between 2004 and 2011. This panel also shows that the model projections are in general very close to the actual observations. For this time period, there were somewhat greater differences between the actual observations and model simulations for wheat and rice. The right panel of **Figure 5** shows that, unlike the first time period, crop prices have declined largely during the time period of 2011–16. This panel also shows that the model projections are in general very close to the actual observations. For this time period, there was only somewhat greater difference between the actual observation and model simulation for wheat. Hence, in general, the model projections for changes in crop prices are fairly in line with actual observations.

Results for 2004–2011 Time Period

The mandated level of ethanol for 2011 is 12.6 BG. When we remove this mandate, the market determines consumption of ethanol, and it falls to about 12 BG in 2011. This means that the RFS on ethanol basically boosts consumption of ethanol by about 0.6 BG at the end of the first time period. This can be considered as an additional gradual increase in ethanol consumption by 0.6 BG over the period of 2004–2011. This projection is consistent with findings of the existing literature that non-RFS drivers including higher crude oil prices, tax incentives, added demand for oxygen and octane, and banning consumption of MTBE pave the way for ethanol industry to grow during this time period. In the PE section results, we will explain that in each year of this period, in general, the RFS was not binding except for short periods in 2008 and 2011.

The removal of biodiesel mandate drops consumption of ethanol furthermore by 0.1 BG (from 0.6 BG to 0.7 BG) in 2011. Interactions between livestock, biofuel, and crop industries induced by changes in relative prices cause this tiny reduction. Removing biodiesel mandate reduces production of oilseed meals (by-products of biodiesel) used by the livestock industry. The reduction in meal availability increases production costs of the livestock industry. In response, this industry mainly produces less. This reduction weakens demand for animal feeds (in particular corn and DDGS). This has two opposite effects on profitability of the ethanol industry. The reduction in demand for DDGS drops its price and negatively affects profitability of corn ethanol. On the other hand, fewer demand for corn (as animal feed) reduces corn price which increases profitability of corn ethanol. The net of these two effects combined with changes in the relative prices of gasoline and ethanol, not in favor of ethanol,

TABLE 1 | Percentage change in crop outputs under alternative examined counterfactual experiments for 2004–2011.

Description	Removing mandate of corn ethanol	Removing mandates of corn ethanol and biodiesel	No expansion in corn ethanol	No expansion in biofuels
Coarse grains	–1.2	–1.4	–20.8	–20.8
Soybeans	0.2	–1.6	3.2	0.1
Wheat	0.1	0.6	2.4	3.0
Rice	0.0	0.2	0.7	1.0
Sorghum	0.0	0.0	0.6	0.6
Rapeseed	0.2	–12.4[a]	5.6	–11.0[a]
Other oilseeds	0.1	-4.3	1.8	–3.6
Sugar crops	0.0	0.1	0.4	0.4
Other crops	0.1	0.0	1.0	0.8

[a]*Large percentage changes for rapeseed are due to very small quantities in the base year.*

TABLE 2 | Percentage change in real commodity prices under alternative counterfactual experiments for 2004–2011.

Description	Removing mandate of corn ethanol	Removing mandates of corn ethanol and biodiesel	No expansion in corn ethanol	No expansion in biofuels
Coarse grains	–0.3	–0.6	–5.3	–5.5
Soybeans	–0.1	–0.7	–1.6	–2.5
Wheat	–0.1	–0.2	–0.9	–1.1
Rice	–0.1	–0.2	–1.0	–1.2
Sorghum	–0.1	–0.2	–0.9	–1.1
Rapeseed	–0.1	–3.2	–1.3	–5.0
Other oilseeds	–0.1	–0.8	–0.9	–1.8
Sugar crops	–0.2	–0.5	–3.6	–4.0
Other crops	–0.1	–0.4	–1.7	–2.0

drops profitability of corn ethanol. This drops ethanol consumption by the tiny amount of 0.1 BG. Note that other factors such as changes in trade of crops and livestock products are also marginally contribute to this observation. These analyses suggest that the biodiesel mandate may have had a minor positive impact on corn ethanol expansion in this time period.

We now analyze the impacts of RFS on commodity outputs and prices. First consider the impacts on commodity outputs presented in the first two numerical columns of **Table 1**. The first numerical column is for removing ethanol mandate, and the second one is for removing both ethanol and biodiesel mandates. The results show if there was no mandate on ethanol, farmers within the US produce less coarse grains (basically corn) by 1.2% and slightly more of other crops. When we remove both mandates on ethanol and biodiesel, outputs of coarse grains, soybeans, rapeseed, and other oilseeds drop by 1.4, 1.6, 12.4, and 4.3% while outputs of all other crop categories grow slightly. From these results we can conclude, ignoring the contributions of non-RFS factors, the impact of RFS on crop production was very small. However, it encouraged farmers to produce more corn and oilseeds. Later in this section we discuss the overall impacts of biofuel production due to all drivers that encouraged biofuel production.

Regarding the commodity price impacts of RFS, consider the first two numerical columns of **Table 2**. The first numerical column is for removing ethanol mandate and the second one is for removing both ethanol and biodiesel mandates. The results show minor impacts in each case and for each crop category. For example, removing ethanol mandate lowers the price of coarse grains and soybeans by 0.3 and 0.1%. When we remove both mandates then these prices fall by 0.6 and 0.7%. The price impacts are also small for all other crop categories.

Now consider the overall impacts of biofuel production due to all drivers that encouraged producing more biofuels. The impacts on commodity outputs are presented in the last two columns of **Table 1**. The results show that if there was no expansion in ethanol farmers produce less coarse grains (basically corn) by 20.8% and more of all other crops. With no expansion in ethanol and no expansion in biodiesel, regardless of the drivers, outputs of coarse grains, rapeseed, and other oilseeds drop by 20.8, 11, and 3.6% while outputs of all other crop categories grow slightly. From these results we can conclude that biofuel production encouraged farmers to shift to produce more coarse grains (corn) and oilseeds. The impact for corn was large for the first time period. This is consistent with actual objections that confirm changes in the mix of crops produced in the first time period in favor of corn.

Regarding the commodity price impacts of biofuel production consider the last two columns of **Table 2**. The results show a reduction of 5.3% in the price of coarse grains with no expansion in corn ethanol. The price of coarse grains declines by 5.5% with no expansion in corn ethanol and no expansion in biodiesel.

Results of the CGE modeling practice for the first time period indicate that, in general, the RFS had minor impacts on crop prices. However, the price impacts of the expansion in biofuels were noticeable. For example, our analysis indicates that if there was no expansion in corn ethanol in this time period, supply of corn was lower by 20.8% and price of corn was lower by 5.3%. That means that the expansion in corn ethanol in this time period caused a 20.8% increase in supply of corn ethanol with 5.3% increase in the price of this commodity. A 20.8% increase in supply for 5.3% increase in price represents a relatively elastic supply of corn. In what follows we further explain this outcome.

Consider **Figure 5**, which demonstrates schematic short-run and long-run analyses for corn market. At the status quo, the market operates at point A, with corn price of P_A and quantity of Q_A. The initial supply and demand curves are presented by S_A and D_A, respectively. An increase in corn ethanol, in the short-run shifts the demand for corn to D_B. With the initial supply curve (S_A) and the new demand (D_B) one may think that the market would move to point B with the higher price of P_B and production of Q_B. However, that would not happen in the real world as market mediated responses begin to act. First, the demand for corn in non-ethanol uses will drop due to higher prices, and that shifts the overall demand for corn downward to D_C. Then the supply of corn will increase over time in response to higher corn prices. Therefore, the supply curve of corn shifts to S_C. With these changes, the market moves to a new equilibrium at point C with supply of Q_C and price of P_C. Clearly, the price of P_C is considerably lower than the price P_B. **Figure 5** clearly indicates that, in long-run, the economy moves from point A to C on its long-run supply curve (the bold and back curve of $\mathbf{S_L}$), not on the short-run supply curve of S_A. From **Figure 5**, one can see that the short run supply curves of S_A and S_C are both less elastic than the long-run supply curve of $\mathbf{S_L}$. In fact, the long-run market mediated responses spread out the price impacts of ethanol production from one crop (i.e., corn) to all crops and by that they mitigate the price impacts for corn. As shown in **Tables 5**, **6**, under all cases, production of corn ethanol affects supplies for all crop categories and their prices. Of course, the extent and intensity of changes vary by crop.

We now explain the implications for food prices. Of course, changes in commodity prices do not translate directly to changes in food prices. When the ethanol RFS or both ethanol and biodiesel requirements were removed, the food price index fell by 0.04%. In other words, the RFS was responsible for only tiny changes in the overall food price index. When ethanol expansion was not permitted, the food price index dropped 0.21%, and when both ethanol and biodiesel expansion was prohibited, the drop was 0.25%. Biofuels did have some small impact on food prices, but not the RFS.

The other important factor to consider is changes in farm income. Farm incomes include the value added generated by crop producers (all king of crops), livestock producers (dairy, ruminant, and non-ruminant farms) and forestry. Value added measures payments to the primary inputs such as land, labor, and capital. The quantity of each primary input times its rental rate represents the value added of that input. For example, value added of labor in corn production equals number of labors (all kinds including management) times the average wage. The GTAP data base includes information on all elements of value added by sectors. The GTP-BIO model traces changes in value added by sector and by the type of primary input. For example, a reduction in mandate on corn ethanol could reduce both area of corn land and the rent rate of land used in corm production. The model determines these changes endogenously. These are shown for the time period 2004–2011 **Table 3**. First consider the impacts on farmers who produce crops. Removing ethanol mandates decreases incomes of farmers by $461.6 million and removing both mandates on corn ethanol and biodiesel lowers farmers' incomes by $1,299.6 million for the period of 2004–11. These figures confirm that the RFS had positive impacts on farmer's incomes. **Table 3** also indicates that removing the expansion in corn ethanol drops the farmers' incomes by $6,923.8 million. The drop in incomes increases to $8,010.6 million with no expansion of either ethanol or biodiesel. These figures confirm that biofuel production had significant favorable impacts on farmers' incomes during the first time period.

The last row of **Table 3** shows the overall impacts on incomes of the agricultural sectors, including incomes of crop and livestock producers plus incomes of the forestry sector. This row shows slightly larger impacts (in absolute terms) compared with the first row. That confirms that agricultural activities in general gained from the RFS and also biofuel producers. The additional farm incomes are attributed to two factors: 1) slightly higher crop prices and higher land rents induced by biofuel production and 2) retaining and allocating agricultural resources (say land) in higher valued activities. Compared to the baseline, with no expansion in biofuels, nearly 2,563 thousand hectares (6.3 million acres) of the US cropland would go out of production in the time period of 2004–11. The model assigns 16% of these areas to the RFS. In the absence of biofuel production and policy, agricultural production activities would have provided fewer employment opportunities resulted in idled agriculture production capacity and unused resources across rural areas.

Results for 2011–2016 Time Period

Conditions were quite different for the 2011–16 period than for the 2004–11 period. The earlier period was one of rapid growth in ethanol production driven primarily by increasing crude oil prices, the ethanol tax incentives, and changes in the use of ethanol as a source of oxygen and octane in blended fuels. The government's ethanol support ended in 2011. Ethanol's role in the gasoline fuel system as an important source of oxygen and octane had been established and continued through the second period and to today. In addition, in the second time period the price of crude oil declined sharply and that caused a sharp reduction in the price of conventional gasoline and a faster reduction in biofuel prices. These factors drove down profitability of ethanol production in the second time period significantly. On the other hand, the RFS targets for the first generation of biofuels (in particular for conventional ethanol) approached their higher required values.

Finally, it is important to take into account that the rate of ethanol blended with gasoline has increased rapidly from about

TABLE 3 | Changes in farm income with and without the RFS and biofuel changes for 2004–2011 (Million USD).

Description	Removing mandate of corn ethanol	Removing mandates of corn ethanol and biodiesel	No expansion in corn ethanol	No expansion in biofuels
Crop sectors	–461.6	–1,299.6	–6,923.8	–8,010.6
Overall agriculture	–478.9	–1,371.0	–7,143.3	–8,313.1

2.5% in 2004 to nearly 9.6% in 2011 and then continued to increase slowly to 10%. That suggests that in the second time period demand for ethanol basically continued to grow slowly to meet the adjusted down RFS quantities determined and set by the EPA, perhaps based on the traditional 10% maximum ethanol content. As mentioned before, in response to the observed high RIN prices, which could reflect constraints on the growth in consumption of ethanol, the EPA adjusted down the original enacted RFS targets for 2014–2016. The effective mandated level of ethanol for 2016 was 14.3 BG[5]. When we remove this level of mandate, the market forces drop the consumption of ethanol to 12.5 BG. This means that the RFS on ethanol basically boosts consumption of ethanol by about 1.8 BG for the second time period. This means that the mandate on corn ethanol was more important in the second time period. In the PE section results, we will explain annual contributions of the RFS to consumption of ethanol.

The removal of biodiesel mandate eliminates a portion of the reduction in ethanol consumption by 0.3 BG. Hence, removing both ethanol and biodiesel mandates drops consumption of ethanol by 1.5 BG. This means removing biodiesel mandate increases ethanol consumption for the period 2011–16. In this period the removal of biodiesel mandate drops consumption of this biofuel by a relatively a large quantity of 1.2 BG, which confirms that the RFS is very effective in 2011–16. Similar to the case of 2004–11, removing biodiesel mandate reduces production of oilseed meals (by-products of biodiesel) used by the livestock industry. The reduction in meal availability increases production costs of the livestock industry. However, for the time period of 2011–16, due to a stronger demand for meat products, the livestock industry instead of cutting supply uses other feeds including other feed crops and DDGS to replace the missing meals. The higher demand for DDGS plus a lower corn price due to conversion of cropland from oilseeds to corn improve profitability of corn ethanol. This leads to an increase in corn ethanol supply and consumption by about 0.3 billion gallons.

We now analyze the impacts of RFS on commodity outputs and prices. First, we consider the impacts on commodity outputs presented in the first two numerical columns of **Table 4**. The first numerical column is for removing the ethanol mandate, and the second one is for removing both ethanol and biodiesel mandates. The results show if there was no mandate on ethanol, farmers would produce 2% less coarse grains (basically corn) and slightly more of other crops. This percent reduction in absolute terms is larger than the corresponding figure for the first time period. One needs to take into account the fact that the base of consumption in the second time period is also larger than the base of consumption in the first time period[6]. When we remove both mandates on ethanol and biodiesel, outputs of coarse grains drop by 1.6% and again supplies of other crops increase slightly.

For the period of 2011–16, unlike the first period of 2004–11, removing the expansion in corn ethanol alone (or jointly with biodiesel) has much smaller impacts on crop supplies. Compare the last two columns of **Table 4** and with their corresponding columns of **Table 1**. In the second time period, production of corn ethanol did not grow substantially. It only changed from 13.9 BG in 2011 to 15.4 BG in 2016, an increase of 1.5 BG.

Regarding the commodity price impacts of RFS in the second time period, consider the first two numerical columns of **Table 5**. The first numerical column is for removing the ethanol mandate and the second one is for removing both ethanol and biodiesel mandates. Similar to the first time period, the results show that in the second time period the price impacts of removing the RFS requirements (for only corn ethanol or both biofuels) are small, less than 1%. Nonetheless, the RFS price impacts are larger in the second time period. Unlike the first time period, the RFS was the key driver of the expansion in biofuels in the second time period. Note that, unlike the first time period, removing the expansion in corn ethanol alone (or jointly with biodiesel) in the second time period has no large impacts on crop prices, compare the last two columns of **Tables 2**, **5**. That is because, as mentioned before, in the second time period production of corn ethanol did not grow that much.

Finally, we present changes in farm incomes for the time period of 2011–16. **Table 6** shows these changes. The first row of this table indicates that, for this time period, removing ethanol mandates drops incomes of farmers by $2,062.2 million, and removing both mandates on corn ethanol and biodiesel drops farmers' incomes by $2,454.8 million. These figures confirm that the RFS had positive and important impacts on farmer's incomes in 2011–2016. Table 10 also indicates that removing the expansion in corn ethanol drops the farmers' incomes by $1,652.2 million. The drop in incomes increases to $2,281.2 million with no expansion of either ethanol or biodiesel. These figures confirm that biofuel production had significant impacts on farmers' incomes during the second time period as well. The

[5]This was indeed very close to 10% of gasoline consumption in this year.

[6]Note that for the first time period, the comparison is for supplies of corn with and without mandate in 2011. For the second time period, the comparison is for supplies of corn with and without mandate in 2016.

TABLE 4 | Percentage change in crop outputs under alternative examined counterfactual experiments for 2011–2016.

Description	Removing mandate of corn ethanol	Removing mandates of corn ethanol and biodiesel	No expansion in corn ethanol	No expansion in biofuels
Coarse grains	–2.0	–1.6	–1.6	–1.6
Soybeans	1.1	0.3	0.9	0.5
Wheat	0.8	0.4	0.6	0.3
Rice	1.1	1.2	0.9	1.1
Sorghum	0.0	0.5	0.0	0.4
Rapeseed	1.9	1.5	1.5	1.6
Other oilseeds	1.0	0.5	0.8	0.7
Sugar crops	0.6	0.5	0.6	0.6
Other crops	0.4	0.3	0.3	0.3

TABLE 5 | Percentage change in real commodity prices under alternative counterfactual experiments for 2011–2016.

Description	Removing mandate of corn ethanol	Removing mandates of corn ethanol and biodiesel	No expansion in corn ethanol	No expansion in biofuels
Coarse grains	–0.9	–0.9	–0.7	–0.8
Soybeans	–0.3	–0.5	–0.2	–0.4
Wheat	–0.1	–0.1	–0.1	–0.1
Rice	–0.2	–0.3	–0.2	–0.3
Sorghum	–0.6	–0.6	–0.4	–0.5
Rapeseed	–0.2	–0.5	–0.2	–0.4
Other oilseeds	–0.2	–0.5	–0.2	–0.3
Sugar crops	–0.7	–0.8	–0.5	–0.7
Other crops	–0.3	–0.4	–0.3	–0.3

TABLE 6 | Changes in farm income with and without the RFS and biofuel changes for 2011–16 (Million USD).

Description	Removing mandate of corn ethanol	Removing mandates of corn ethanol and biodiesel	No expansion in corn ethanol	No expansion in biofuels
Crop sectors	–2,062.2	–2,454.8	–1,652.2	–2,281.2
Overall agriculture	–2,040.6	–2,414.2	–1,635.9	–2,222.6

BOX 1 | Long-run analysis versus short-run analysis

In presenting the results for the first time period we explained why a large change in supply of corn in the long-run induces a relatively moderate change in the corn price (see **Figure 5** and its corresponding analysis). We showed that the long-run supply of corn is more elastic than its short-run supply. That analysis applies to the second time period as well. For example, removing the ethanol mandate alone reduces supply of corn ethanol by 1.5 BG which causes a reduction in supply of coarse grains (basically corn) by 2%, and that leads to 0.9% reduction in the price. This represents a relatively elastic long-run supply curve. Here we show that in the short-run when demand and supply functions operate with lower elasticities, and markets have limited capacities to respond to the economic shocks, the price impacts could be larger.

To depict the short-run impacts, we repeated the experiment that drops the mandates for ethanol and biodiesel with an inelastic supply for corn, lower substitution between corn and DDGs, and a lower trade elasticity for corn. With these short-term elasticities, the drop in the price of coarse grains changed from -0.9% to -6.7%. We then kept the low trade elasticity and the low substitution between corn and DDGS and allowed the supply of corn to respond. In this case the price of corn changed by -2.7%.

last row of **Table 6** shows the overall impacts on incomes of agricultural sectors, including incomes of crop and livestock producers plus incomes of the forestry sector. This row shows slightly different impacts (in absolute terms) compared with the first row.

Compared to the baseline, with no expansion in biofuels, about 77 thousand hectares (160 thousand acres) of the US cropland would go out of production in the time period of 2011–16. The model assigns 100% of these areas to the RFS. Similar to the first time period, in the absence of biofuel production and policy, agricultural production activities would have provided fewer employment opportunities resulted in idled agriculture production capacity and unused resources across rural areas.

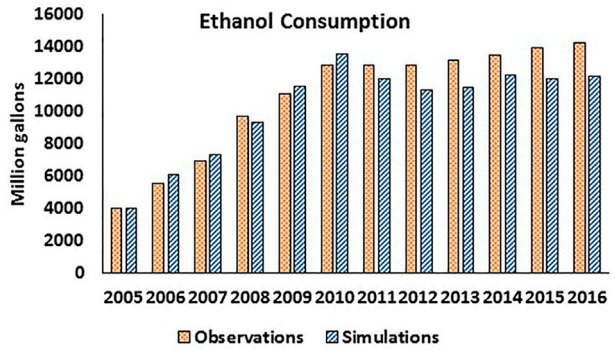

FIGURE 6 | Actual and simulated market results for ethanol consumption 2005–16.

Partial Equilibrium Model Results

The partial equilibrium model described above (AEPE) was used to simulate the annual changes from 2005 to 2016. The model was calibrated to 2005. For the simulations, corn and soybean yields were targeted as in the CGE model. Total area of corn and soybeans (not individually) was also targeted. So, the model allocates land between corn and soybeans. Throughout the period, crude oil price was exogenous as explained above. The net trade of ethanol is exogenous in the PE model. The gasoline consumption was tuned to actual values via shifters. By using demand shifters, we attempted to capture drivers like the 2006 MTBE substitution and the later use of ethanol as an octane additive for blended gasoline. Of course, we also captured the 2012 drought and other agricultural commodity supply and demand changes due to changes in world market conditions. Following the CGE approach, we first developed a historical baseline. However, unlike the CGE work, the PE baseline covers annual changes for each year from 2005 to 2016. Then we made market based annual simulations that only take into account market forces to determine production and consumption of ethanol. Finally, it is important to note that, unlike the CGE model, the PE model uses nominal prices. Hence, the prices presented below are nominal values.

In what follows we present the results for the market-based simulations and compare them with actual observations. We begin with consumption of ethanol. The actual observations and simulated market-based results for ethanol consumption are presented in **Figure 6**. This figure indicates that prior to 2011 the market-based projections for ethanol consumption were usually slightly larger than their real-world observations, with one exception in 2008. That suggests a non-binding RFS prior to 2011, except for 2008. Since 2011 the market-based projections for ethanol consumption were smaller than their real-world observations. That means the RFS pushed up consumption of ethanol in these years. For example, in 2016 the actual consumption of ethanol was 14.3 BG with a market-based

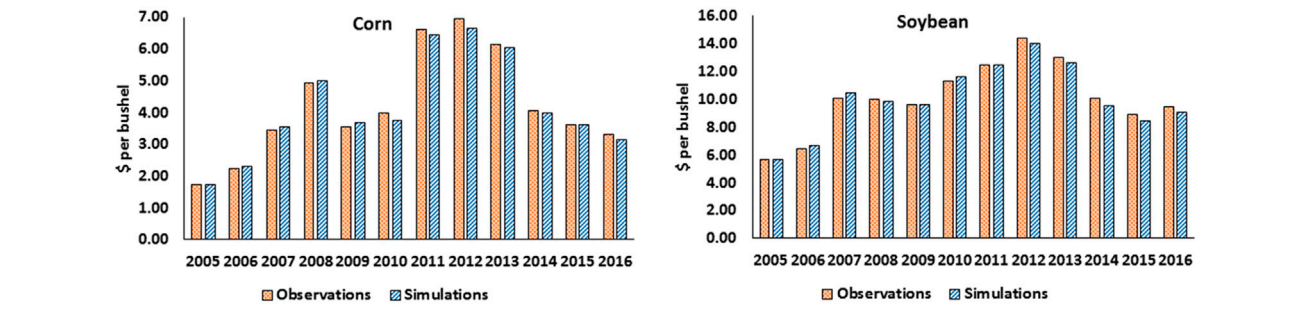

FIGURE 7 | Observed and simulated market results for corn and soybean nominal prices 2005–16.

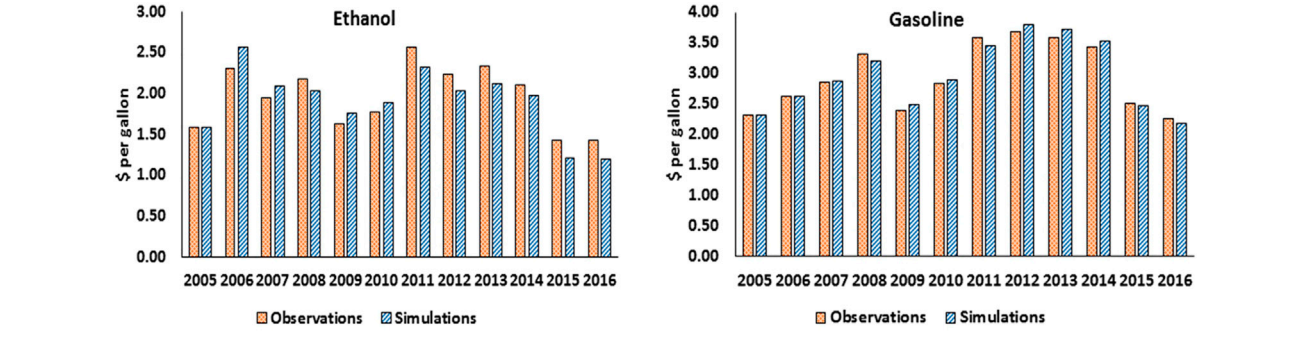

FIGURE 8 | Observed and simulated market results for ethanol and gasoline nominal prices 2005–16.

projection of 12.1 BG. This means that in this particular year the RFS increased consumption of ethanol by about 2.1 BG. This is the largest contribution of RFS to ethanol consumption over our study period. These results are consistent with our CGE findings.

The actual observations and simulated market-based results for corn and soybean prices are presented in **Figure 7**. This figure shows that, in general, the actual observations and market-based projections are similar with some noticeable exceptions. For example, in 2016 the actual corn price was $3.33 per bushel with a market-based projection of $3.16 per bushel, 5% lower than the actual observation. From 2005 to 2009 the market-based projections for the price of corn were higher than the baseline, and then the reverse occurred.

The actual observations and simulated market-based results for ethanol and gasoline prices are presented in **Figure 8**. This figure shows that, from 2005 to 2010 the market-based projections for ethanol price are higher than the actual observations, except in 2008. Then from 2011 the reverse has happened. For example, the actual ethanol price in 2016 was $1.43 per gallon with a market-based projection of $1.20 per gallon. Hence one can conclude that since 2011 the RFS has positively affected the price of ethanol.

CONCLUSION

Determining the economic impacts of the RFS is a complicated task. Part of the complication is the questions of attribution. For example, some of the early literature tended to blame the RFS for all increases in commodity prices. However, over time it has become abundantly clear that many factors have been involved in the evolution of commodity and food prices, with the RFS and biofuel production in general being only one. The purpose of this study is to determine the extent to which commodity and food prices were driven by the RFS and to what extent they were driven by biofuels regardless of what caused the level of biofuels production.

This study first examines the literature and data on what was actually happening in agricultural and energy markets over the relevant period. From the data presentation and literature review alone, it became clear that the bulk of the ethanol production prior to 2012 was driven by what was happening in the national and global markets for energy and agricultural commodities and by the federal and sometimes state incentives for biofuel production. This conclusion is supported by examining the data, by the conclusions of the recent literature, and by the fact that until 2012 the RINs prices were very low, indicating that the non-RFS policies and market forces (demand for ethanol as a fuel extender, demand for ethanol as an additive, and MTBE ban) helped biofuels to grow, while the RFS provided a safety net for the whole biofuel industry to invest and expand its production capacity by requiring minimum levels of biofuels use.

We provided long-run CGE analyses for two time periods: 2004–2011 and 2011–2016. Our results confirm that, in general, the long-run price impacts of biofuel production were not large. Due to biofuel production, regardless of the drivers, crop prices (adjusted to inflation) have increased between 1.1% (for wheat) and 5.5% (for the category of coarse grains) in the first time period (i.e., 2004–11). The model determines the contributions of RFS to the price increases due to biofuel production. For example, as shown in **Table 1**, the model results indicate that the price of coarse grains drops by 5.5% with no expansion in biofuels compared to baseline. On the other hand, the price of coarse grains drops by 0.6% with no mandates compare to the corresponding baseline. Therefore, only one-tenth of the 5.5% increase in the price of coarse grains is related to the RFS impacts. For the second time period (i.e., 2011–16) the long-run price impacts of biofuels were less than the first time period, as in this period biofuel production has increased slowly. Due to biofuel production, crop prices have increased by less than 1% in the second time period. However, unlike the first time period, the RFS was the main driver of these changes. Finally, in both time periods, the long-run effects of biofuel production and policy on food prices were negligible for both time periods.

The long-run CGE results indicate that biofuel production and policy made major contributions to the agricultural sector in both time periods, while they only affected the commodity prices moderately. Biofuel production, regardless of the drivers, has increased the US annual farm incomes by $8.3 billion and $2.3 billion at constant prices in the first and second time periods, respectively. Hence, with no biofuels, the US annual farm income would drop by an estimated $10.6 billion, ignoring the changes since 2016. The model assigns 28% of the expansion in farm incomes of the first time period to the RFS. The corresponding figure for the second time period is 100%. This means that, the additional gains in farm incomes were entirely due to the RFS in the second time period. As explained with details in the results section, for the second time period (2011–2016), when we remove mandates the uses of biofuels decline almost to their initial levels in 2011 or even lower for the cases of biodiesel. Hence, the reduction in farm incomes caused by the removal of mandates is entirely due to the RFS effect in the second time period.

The PE analyses indicate that prior to 2011 the market-based projections for annual consumption of ethanol are usually smaller than their real-world observations, with one exception in 2008. That suggests a binding RFS in this year. Since 2011 the market-based projections for annual ethanol consumption are smaller than their real-world observations. That means the RFS pushed up consumption of ethanol in these years. The RFS has increased the demand for ethanol by 7–14% between 2011 and 2016. For example, in 2016 the actual consumption of ethanol was 14.3 BG with a market-based projection of 12.1 BG. This means that in this particular year the RFS increased consumption of ethanol by about 2.1 BG. The impact of RFS on the price of corn in this year was about 5%.

Prior to 2011, ethanol was basically in demand as a fuel extender and an octane additive. This has changed after this year and a portion of ethanol was consumed as a source of octane and as a substitute for gasoline to meet the RFS requirements. Since 2011 as the total consumption of ethanol moved towards the historical 10% maximum ethanol content (that was allowed in non-flex-fuel vehicles), demand for gasoline, and hence, ethanol did not grow enough and that raised the RINs prices. This could change in the future considering that E15 has been approved for

use in 2001 and newer vehicles since 2011 and flex-fuel vehicles using E85. The USDA's 2015 Biofuels Infrastructure Partnership, in combination with private-sector resources, has helped improve market access for higher blends of ethanol. The more recent evidence confirms that the consumption of ethanol has passed the historical 10% bend rate and demand for E15 and E85 is growing since 2016. Since our analyses end in 2016, this paper does not cover these new developments.

There is clearly a difference in impacts of the RFS and biofuels production due to market forces. One of the main contributions of this research is to demonstrate that biofuels production growth that is often attributed to the RFS is actually due to energy and agricultural market conditions and key drivers. We have identified and characterized these drivers and shown that the market drivers have been the main contributor to biofuels growth, in particular through 2011. In a sense, this means that biofuels' contribution to commodity price increases is really no different from fructose corn syrup, increased feed demands, or other market demands. Indeed, they all affect commodity price through the same mechanism. To understand what has happened to agricultural markets over the past 2 decades, it is absolutely critical to include in the analysis all the global and national demand and supply factors in both energy and agricultural markets, and we have done that.

An interesting question to ask given our conclusions on the role of markets in driving biofuels growth is how it would have been different if all these market changes had not occurred. In other words, what if crude oil price had not surged, MTBE had not been banned, ethanol did not get integrated into the fuel system becoming a fuel additive instead of a fuel extender, etc.? The answer is clearly that the RFS would have played a much greater role. So, in a sense, the RFS has been the backstop, but by circumstance, it was overpowered by tax incentives and market forces prior to 2011.

Another interesting comparison is between what happened over this period for ethanol compared with biodiesel and cellulosic biofuels. For both biodiesel and cellulosic biofuels, the original mandated levels have not been implemented in practice and frequently revised over time. Hence, the RFS has not reached its original goals for these biofuels. However, after the waivers, the RFS was still clearly an important driver of production and consumption. RIN prices were always relatively high, and the RFS was always binding for biodiesel and cellulosic ethanol. Clearly, the market changes that benefitted ethanol did not work as much in favor of these other biofuels.

These findings could help policy makers to define the goals of the RFS beyond the year of 2022, as this policy only specified targets for consumption of biofuels until 2022. In defining the future goals of this policy, it is important to evaluate the potential new sources of demand for biofuels. While demand for biofuels in road transportation may not grow significantly in future, the use of biofuels in aviation industry could play an important role in defining the future goals for the RFS. The International Civil Aviation Organization (ICAO) of the United Nations has defined the Carbon Offsetting and Reduction Scheme for International Aviation (CORSIA) to reduce Greenhouse Gas (GHG) emissions. Sustainable Aviation Fuels (SAFs) will play an important role in achieving the goal of this scheme (Zhao et al., 2021; Prussi et al., 2021: in press). An explicit recognition of these biofuels by the RFS will help the biofuel industry to operate in a secure environment in future.

DATA AVAILABILITY STATEMENT

The original contributions presented in the study are included in the article/**Supplementary Material**, further inquiries can be directed to the corresponding author.

AUTHOR CONTRIBUTIONS

Conceptualization: FT, WT, HB; Methodology FT, WT; Data Assembly: FT; Simulations: FT; Formal Analysis: FT, WT, HB; Original Draft: WT, FT; Final Draft: FT, HB. Virtualizations: FT; Supervision: FT, WT.

FUNDING

This study received financial support from: National Corn Growers Association and the Renewable Fuels Association.

ACKNOWLEDGMENTS

The content of this manuscript has been partly presented at the following conferences: 23rd Annual Conference on Global Economic Analysis, June 2019, Virtual; Agricultural and Applied Economics Association Meeting, July 2019, Virtual; and European Association of Agricultural Economics Meeting, July 2021, Virtual.

SUPPLEMENTARY MATERIAL

The Supplementary Material for this article can be found online at: https://www.frontiersin.org/articles/10.3389/fenrg.2022.749738/full#supplementary-material

REFERENCES

Abbott, P. (2014). "Biofuels, Binding Constraints, and Agricultural Commodity price Volatility," in *The Ecnomics of Food Volatility*. Editors J. Chavas, D. Hummels, and B. D. Wright (Chicago, Illinois, USA: University of Chicago Press), 91–134.

Abbott, P., Hurt, C., and Tyner, W. E. (2011). What's Driving Food Prices in 2011?, in Issue Report 2011, Farm Foundation. Issue Report. Avialble at: What's Driving Food Prices in 2011? (repec.Org).

Abbott, P., Hurt, C., and Tyner, W. E. (2009). *What's Driving Food Prices? Farm Foundation, Issue Report. Available at: What's Driving Food Prices? March 2009 Update (repec.Org)*.

Abbott, P., Hurt, C., and Tyner, W. E. (2008). *What's Driving Food Prices? Farm Foundation, Issue Report, Available at: What's Driving Food Prices? (repec.Org)*.

Agricultural Marketing Resource Center (2019). *Ethanol Profitability*. Ames, Iowa: Agricultural Marketing Resource Center, Iowa State University. Available at: http://www.agmrc.org/renewable_energy/.

Beckman, J., Hertel, T., Taheripour, F., and Tyner, W. (2012). Structural Change in the Biofuels Era. *Eur. Rev. Agric. Econ.* 39 (1), 137–156. doi:10.1093/erae/jbr041

Brookes, G., Taheripour, F., and Tyner, W. E. (2017). The Contribution of Glyphosate to Agriculture and Potential Impact of Restrictions on Use at the Global Level. *GM Crops & Food* 8 (4), 216–228. doi:10.1080/21645698.2017.1390637

Chiou-Wei, S.-Z., Chen, S.-H., and Zhu, Z. (2019). Energy and Agricultural Commodity Markets Interaction: An Analysis of Crude Oil, Natural Gas, Corn, Soybean, and Ethanol Prices. *Energ. J.* 40 (2), 265–296. doi:10.5547/01956574.40.2.schi

Delgado, C. (2008). *Food Policy Implications of Longer-Run Price Rise*. Washington, D.C., USA: Agriculture and Rural Development Department. World Bank.

Filip, O., Janda, K., KristoufekZilberman, L. D., and Zilberman, D. (2019). Food versus Fuel: An Updated and Expanded Evidence. *Energ. Econ.* 82, 152–166. doi:10.1016/j.eneco.2017.10.033

Henderson, J. (2008). *What Is Driving Food Price Inflation?* Kansas City, Missouri, USA: Federal Reserve Bank of Kansas City.

Hertel, T. W. (1997). *Global Trade Analysis: Modeling and Applications*. New York: Cambridge University Press.

Hertel, T. W., Tyner, W. E., and Birur, D. K. (2010). The Global Impacts of Biofuel Mandates. *Energ. J.* 30 (1), 75–100.

Irwin, S. (2019). *Revisiting the Value of Ethanol in E10 Gasoline Blends*. Illinois: University of Illinois. Farmdoc daily (9):60, Available at: https://farmdocdaily.illinois.edu/2019/04/revisiting-the-value-of-ethanol-in-e10-gasoline-blends.html.

Korting, C., Gorter, H., and Just, D. R. (2019). Who Will Pay for Increasing Biofuel Mandates? Incidence of the Renewable Fuel Standard Given a Binding Blend Wall. *Am. J. Agric. Econ.* 101 (2), 492–506. doi:10.1093/ajae/aay047

Prussi, M., Lee, U., Wang, M., Malina, R., Valin, V., Taheripour, F., et al. (2021). CORSIA: The First Internationally Adopted Approach to Calculate Life-Cycle GHG Emissions for Aviation Fuels. *Renew. Sustain. Energ. Rev.*

Taheripour, F., Zhao, X., and Tyner, W. E. (2017b). The Impact of Considering Land Intensification and Updated Data on Biofuels Land Use Change and Emissions Estimates. *Biotechnol. Biofuels* 10 (191), 191. doi:10.1186/s13068-017-0877-y

Taheripour, F., Cui, H., and Tyner, W. E. (2017a). "An Exploration of Agricultural Land Use Change at the Intensive and Extensive Margins: Implications for Biofuels Induced Land Use Change," in *Bioenergy and Land Use Change, American Geophysical Union*. Editors Z. Qin, U. Mishra, and A. Hastings. (Hoboken, NJ, USA: Wiley)

Taheripour, F., Fiegel, J., and Tyner, W. (2016a). Development of Corn Stover Biofuel: Impacts on Corn and Soybean Markets and Crop Rotation. *Sustain. Agric. Res.* 5 (1), 1–9.

Taheripour, F., Hertel, T. W., and Ramankutty, N. (2019). Market-mediated Responses Confound Policies to Limit Deforestation from Oil palm Expansion in Malaysia and Indonesia. *Proc. Natl. Acad. Sci. USA* 116 (38), 19193–19199. doi:10.1073/pnas.1903476116

Taheripour, F., Mahaffey, H., and Tyner, W. E. (2016b). Evaluation of Economic, Land Use, and Land Use Emission Impacts of Substituting Non-GMO Crops for GMO in the United States. *AgBioForum* 19 (2), 156–172.

Taheripour, F., and Tyner, W. (2013). Biofuels and Land Use Change: Applying Recent Evidence to Model Estimates. *Appl. Sci.* 3, 14–38. doi:10.3390/app3010014

Taheripour, F., and Tyner, W. E. (2018). Impacts of Possible Chinese Protection on US Soybeans and Other Agricultural Commodities. *Quarter* 2.

Taheripour, F., and Tyner, W. E. (2011). *Introducing First and Second Generation Biofuels into GTAP Data Base Version 7 in GTAP. Research Memorandum No 21*. West Lafayette, IN, USA: Purdue University.

Taheripour, F., and Tyner, W. E. (2014). Corn Oil Biofuel Land Use Change Emission Impacts: Sharing Emission Savings between Ethanol and Biodiesel. *Biofuels* 5 (4), 353–364. doi:10.1080/17597269.2014.977582

Taheripour, F., Tyner, W. E., and Sarica, K. (2014). "Shale Gas Boom, Trade and Environmental Policies: Global Economic and Environmental Analyses in a Multidisciplinary Modeling Framework (2014)," in *Issues in Environmental Science and Technology, Vol. 39 Fracking*. Editors R. E. Hester and R. Harrison (Cambridge, UK: Royal Society of Chemistry).

Trostle, R. (2008). Global Agricultural Supply and Demand: Factors Contributing to the Recent Increase in Food Commodity Prices." Economic Research Service. *United State. Department Agric.* May 2008.

Trostle, R., Marti, D., Rosen, S., and Westcott, P. (2011). *Why Have Food Commodity Prices Risen Again?* Washington, D.C., USA: U.S. Department of Agriculture Economic Research Service, WRS-1103.

Tyner, W. E. (2012). Biofuels and Agriculture: a Past Perspective and Uncertain Future. *Int. J. Sustain. Develop. World Ecol.* 19, 389–394. doi:10.1080/13504509.2012.691432

Tyner, W. E., Dooley, F., and Viteri, D. (2010a). Alternative Pathways for Fulfilling the RFS Mandate. *Am. J. Agric. Econ.* 2010 (5), 92. doi:10.1093/ajae/aaq117

Tyner, W. E., Taheripour, F., and Perkis, D. (2010b). Comparison of Fixed versus Variable Biofuels Incentives. *Energy Policy* 38 (10), 5530–5540. doi:10.1016/j.enpol.2010.04.052

Tyner, W. E., and Taheripour, F. (2008). Policy Options for Integrated Energy and Agricultural Markets*. *Rev. Agric. Econ.* 30 (3), 387–396. doi:10.1111/j.1467-9353.2008.00412.x

Tyner, W. E. (2008). The US Ethanol and Biofuels Boom: Its Origins, Current Status, and Future Prospects. *BioScience* 58 (7), 646–653. doi:10.1641/b580718

Tyner, W. E., and Viteri, D. (2010). Policy Update: Implications of Blending Limits on the US Ethanol and Biofuels Markets. *Biofuels* 1 (2), 251–253. doi:10.4155/bfs.09.24

U.S. Congress (2004). *American Jobs Creation Act of 2004, Public Law 108-357, 108th Congress*. Washing D.C: U.S. Congress.

U.S. Congress (1990). *Clean Air Act of 1990, Public Law 101–549*. Washing D.C: U.S. Congress.

U.S. Congress (2007). *Energy Independence and Security Act of 2007, in H.R. 6, 110 Congress, 1st Session*. Washing D.C: U.S. Congress.

U.S. Congress (2005). *Energy Policy Act of 2005, Public Law 109-58. 2005*. Washing D.C: U.S. Congress.

U.S. Congress (1978). *National Energy Conservation Policy Act, Public Law 95-619, 95th Congress (1977-78), H.R. 5037*. Washing D.C: U.S. Congress.

Wright, B. D. (2011). *Biofuels and Food Security: Time to Consider Safety Valves?* Washington D.C: International Food and Agricultural Trade Policy Council IPC.

Yao, G., Hertel, T. W., and Taheripour, F. (2018). Economic Drivers of Telecoupling and Terrestrial Carbon Fluxes in the Global Soybean Complex. *Glob. Environ. Change* 50, 190–200. doi:10.1016/j.gloenvcha.2018.04.005

Zhang, Z., Lohr, L., Escalante, C., and Wetzstein, M. (2010). Food versus Fuel: What Do Prices Tell Us? *Energy Policy* 38 (1), 445–451. doi:10.1016/j.enpol.2009.09.034

Zhao, X., Taheripour, F., Malina, R., Staple, M., and Tyner, W. (2021). Estimating Induced Land Use Change Emissions for Sustainable Aviation Biofuel Pathways. *Sci. Total Environ.* 779, 146238. doi:10.1016/j.scitotenv.2021.146238

Conflict of Interest: The authors declare that the research was conducted in the absence of any commercial or financial relationships that could be construed as a potential conflict of interest.

Publisher's Note: All claims expressed in this article are solely those of the authors and do not necessarily represent those of their affiliated organizations, or those of the publisher, the editors and the reviewers. Any product that may be evaluated in this article, or claim that may be made by its manufacturer, is not guaranteed or endorsed by the publisher.

frontiers in Energy Research

ORIGINAL RESEARCH
published: 10 March 2022
doi: 10.3389/fenrg.2022.828789

Cumulative Impact of Federal and State Policy on Minimum Selling Price of Sustainable Aviation Fuel

Kristin L. Brandt[1]*, *Lina Martinez-Valencia*[2] *and Michael P. Wolcott*[1]

[1]*Composite Materials and Engineering Center, Washington State University, Pullman, WA, United States,* [2]*Biological Systems Engineering Department, Washington State University, Pullman, WA, United States*

With jet fuel consumption projected to more than double by 2050, dramatic expansion of sustainable aviation fuel (SAF) use will be essential to meeting the aviation industry goal of achieving carbon neutrality in the same time frame. However, to date, the SAF price has, in part, been responsible for the lack of widespread adoption signaling the need for strong and stable policy. Multiple pathways have been developed and received ASTM approval to convert a variety of feedstocks into SAF, each with strengths and weaknesses that vary with conversion technology, feedstock, and production location. To assist researchers and governments in understanding the role of policy on fuel pricing, a set of harmonized, techno-economic analyses (TEAs) were developed to assess three ASTM-qualified production pathways: hydroprocessed esters and fatty acids (HEFAs), alcohol to jet (ATJ), and Fischer–Tropsch (FT), with multiple feedstock options. These decision support tools were used to assess the minimum selling price (MSP) for fuel distillates. Both mature (*n*th) plants and first of a kind (pioneer plants) were assessed using TEAs. Existing and proposed U.S. incentives, at both the federal and state levels, were integrated into the tools to determine the impact on the MSP. Considering the existing federal policies, analysis indicated that HEFAs could achieve a SAF price that would be competitive to conventional fuels when using waste lipid feedstocks, making this the most viable near-term option. However, this feedstock for HEFAs is limited and unlikely to support the production of large quantities of SAF. After stacking federal and state programs, SAF produced using FT with municipal solid waste (MSW) has the lowest MSP, although FT forest residuals, FT agricultural residues, ATJ corn ethanol, and HEFAs using second crop oilseeds all approach the historical range of traditional jet fuel prices for *n*th plants. Pioneer plants are viable for only ATJ corn ethanol; however, FT-MSW is approaching price parity.

Keywords: policy, sustainable aviation fuel, techno-economic analysis, hydroprocessed esters and fatty acids, alcohol to jet, Fischer–Tropsch

OPEN ACCESS

Edited by:
Sgouris Sgouridis,
Dubai Electricity and Water Authority, United Arab Emirates

Reviewed by:
Christopher Michael Saffron, Michigan State University, United States
Arnaldo Walter, State University of Campinas, Brazil

***Correspondence:**
Kristin L. Brandt
kristin.brandt@wsu.edu

Specialty section:
This article was submitted to Sustainable Energy Systems and Policies, a section of the journal Frontiers in Energy Research

Received: *04 December 2021*
Accepted: *31 January 2022*
Published: *10 March 2022*

Citation:
Brandt KL, Martinez-Valencia L and Wolcott MP (2022) Cumulative Impact of Federal and State Policy on Minimum Selling Price of Sustainable Aviation Fuel. Front. Energy Res. 10:828789. doi: 10.3389/fenrg.2022.828789

1 INTRODUCTION

In an effort to reduce the climate impact of aviation, the Air Transport Action Group (ATAG), the International Air Transportation Association (IATA), Airlines for America (A4A), and the U.S. government have recently announced an updated goal of achieving net-zero carbon emissions by 2050. This time frame also coincides with a predicted doubling of global aviation fuel demand (Holladay et al., 2020; Airlines for America, 2021; Air Transportation Action Group (ATAG), 2021;

Federal Aviation Administration, 2021; International Air Transportation Association (IATA), 2021). Simultaneously, the International Civil Aviation Organization (ICAO) is instituting the Carbon Offsetting and Reduction Scheme for International Aviation (CORSIA) to reach carbon neutral growth at 2019 emissions levels from 2021 through 2035 (International Civil Aviation Organization (ICAO), 2020; Petsonk, 2020). Although U.S. airlines are introducing operations and technologies that decrease fuel burn, these actions are insufficient to meet targets (A4A 2020). Instead, a suite of actions will likely be needed to meet the carbon reduction goals, with widespread use of sustainable aviation fuel (SAF) being essential. Drop-in SAF that does not require modifications of aircraft or infrastructure presents an opportunity to make significant progress toward the emission reduction goals in the near term using existing aircraft fleets. Major U.S. airlines are working with governmental agencies to reach the net-zero carbon emissions goal by 2050, pledging to support the production of 3 billion gallons of SAF for U.S. consumption by 2030 (Airlines for America, 2021) as outlined by the U.S. SAF Grand Challenge (Federal Aviation Administration, 2021).

Since 2009, seven conversion and two co-processing pathways have received ASTM D7566 qualification with additional methodologies currently in the qualification process. However, of these methods, only three are approaching commercial production. With over a decade of approval and certification, the worldwide SAF use is only 0.01% of the aviation fuel consumed (Air Transportation Action Group (ATAG), 2020). The low production volume is likely a result of SAF's high minimum selling price (MSP) caused by sizable capital costs, high risk of the unproven technologies, the high cost to gain certification for a new fuel pathway, and a current policy that favors road transportation over aviation (Ghatala, 2020; Dodd and Yengin, 2021). However, European countries are issuing mandates that will soon require large quantities of SAF, some as high as 30% in 2030 (Finland and Sweden) (Royal Netherlands Aerospace Center (NLR) and Amsterdam Economics (SEO), 2021). In the United States, the policy support is under consideration by Congress, and commitment by federal agencies to a SAF Grand Challenge will support U.S. SAF production expansion (The White House, 2021) Although mandates and policy support will begin moving SAF production forward, high prices will continue to impede progress. In 2019, fuel costs were nearly a quarter of global airline operating costs, making price parity imperative for long-term success (International Air Transportation Association (IATA), 2019).

The ability for SAF to meet price parity with conventional jet fuel is well understood to be a challenge (de Jong et al., 2015; Chao et al., 2019; Holladay et al., 2020; Airlines for America, 2021; Dodd and Yengin, 2021) and thought to be required for large-scale CO_2 abatement in the aviation industry. While conventional jet fuel is valued exclusively on the energy content required to power the flight, SAF is required to meet these standards while also providing the environmental services to reduce the greenhouse gas emissions compared to conventional fuels (Martinez-Valencia et al., 2021). Government policies and corporate sustainability programs will be vital to aid the technological innovations needed to close the price gap between conventional and sustainable fuels (Moriarty et al., 2021; Wang et al., 2021).

The objective of this study is to utilize a set of harmonized techno-economic analyses (TEAs) to assess the impact of existing and proposed U.S. clean fuel and carbon reduction programs on the minimum selling price and capital investment requirements of three SAF pathways currently under commercialization. Specifically, this analysis aims to quantify the impact of pathways, feedstocks, and plant maturity on MSP. The suite of analyses also demonstrates the effect of multiple policy incentive scenarios combined with technology maturity, and fuel carbon intensity score (CI) on SAF MSP.

2 TECHNO-ECONOMIC ANALYSIS

Three SAF conversion pathways are considered in this analysis because of their role in the emerging U.S. biofuel landscape. Hydroprocessed esters and fatty acids (HEFAs) are used in the World Energy SAF facility (World Energy, 2021), and nearly two billion liters (L) of annual renewable diesel production in the United States. This volume is predicted to roughly quadruple with planned expansions and proposed new facilities and facilities already under construction (Pavlenko et al., 2019; Doliente et al., 2020; Bryan, 2021). Although the Fischer–Tropsch (FT) and alcohol to jet (ATJ) pathways are not yet fully commercialized, both technologies have facilities under construction in the United States. Red Rock Biofuels and Fulcrum BioEnergy plan to use FT to make liquid fuels or liquid fuel intermediates, while LanzaJet is currently constructing an ATJ facility (Fulcum Bioenergy, 2021; LanzaJet, 2021; Red Rocks Biofuel, 2021). Additional details on each pathway are provided in **Supplementary Information S1**.

While proprietary knowledge of processes for individual companies would be required to accurately predict economic results, generic modeling of the processes through public literature can provide valuable information regarding the relative cost performance and capital requirements of various processes. To achieve this goal, generic, open-source excel-based TEA models for the aforementioned pathways utilizing the applicable feedstock were established to generate comparative analyses. These TEAs were harmonized to assure a common set of financial assumptions, capital and operating expenditures where applicable, financial calculations, and non-SAF fuel pricing for greenfield facilities (Brandt et al., 2021a; Brandt et al., 2021b; Brandt et al., 2021c). This approach allows comparisons between technology and feedstock combinations, called "conversion pathways" in this work. Economic variables are detailed in the spreadsheet models (Brandt et al., 2021a; Brandt et al., 2021b; Brandt et al., 2021c), with a partial list provided in **Table 1**. The deterministic models were constructed using ratio factors to estimate outside battery limit (OSBL) costs from inside battery limit (ISBL) equipment costs (Peters et al., 2003). This method uses factors to estimate the typical costs of OSBL infrastructure based on historical data, has an estimated accuracy of ±20–30%,

TABLE 1 | Condensed list of baseline economic variables used in all models (Brandt et al., 2020).

Variable	Baseline value
U.S. cost year	2017
Corporate tax rate	17.3%
Working capital	20% of annual OPEX
Real discount rate	10%
Inflation	2%
Equity	30%
Loan term, rate	10 years, 8%
Depreciation schedule, duration	Double decline balance to straight line, 7 years

and has been implemented often for biofuels in the existing literature (Humbird et al., 2011; Davis et al., 2015; de Jong et al., 2015; Geleynse et al., 2018; Brandt et al., 2020; Eswaran et al., 2021; Tanzil et al., 2021). Details of the methodology can be found in Peters et al. (2003) and Brandt et al. (2020).

The FT process converts syngas into an FT wax that is subsequently cracked and distilled. The model is structured to utilize various feedstocks for the required syngas. The preprocessing costs for forest residues, agricultural residuals, and municipal solid waste (MSW) to be used in gasification are included in the feedstock costs (Brandt and Wolcott, 2021; International Civil Aviation Organization (ICAO), 2021). In addition, two gaseous CO_2 feedstocks [from direct air capture (DAC) and flue gas] that are subsequently converted to CO *via* power-to-liquid technologies are considered. Flue gas represents CO_2 directly collected from industrial emissions, for example, at an ethanol production facility (Bains et al., 2017). In direct air capture, CO_2 is extracted from the atmosphere. No additional processing is needed for feedstocks in the ATJ process where corn ethanol or second-generation (2G) cellulosic ethanol is assumed to be purchased as the feedstock. HEFA feedstocks include fats, oils, and grease (FOGs) that are assumed to be 75% animal tallow and 25% used cooking oil (Port of Seattle and Washington State University, 2020). Second-crop oilseeds are oilseeds that are cultivated on an existing farmland during a season where the land is normally left fallow. Baseline feedstock costs are listed in **Table 2**, with the understanding that these values can be controlling in the final fuel price (Tao et al., 2014; Davis et al., 2015; de Jong et al., 2015; Bann et al., 2017; Geleynse et al., 2018; Brandt et al., 2020; Doliente et al., 2020). The impact of baseline feedstock cost on SAF MSP is included in International Civil Aviation Organization (ICAO), 2021.

In this study, two options for plant maturity are included: *n*th and pioneer plants. An *n*th plant is a technologically mature facility that is a replica of other successful facilities and is assumed to operate at a large scale. A pioneer plant is a first or near-first of its kind facility and is traditionally smaller than mature plants (**Table 2**) (International Civil Aviation Organization (ICAO), 2021). The small scale of a pioneer facility increases capital costs per liter of fuel and impedes the start-up ramp. Increased capital costs were modeled using cost growth factors. The production ramp for initial plant performance was calculated, and an assumed 20% per year increase was applied until full capacity was attained (Merrow et al., 1981; de Jong et al., 2015). The smaller pioneer facilities are assumed to have the same total distillate output across conversion pathways. However, this is not realistic for *n*th plants. Three FT feedstocks, MSW, agricultural residuals, and forest residues, are limited by the quantity of feedstock that can practically be aggregated at a single location (**Table 2**).

The baseline yield, feedstock price, and facility scales were selected as mid-range values from the literature (Brandt et al., 2021a; Brandt et al., 2021b; Brandt et al., 2021c). Changing these values impacts the MSP for each scenario discussed. Details on these trends, found using adaptations of the utilized models, are presented in International Civil Aviation Organization (ICAO), 2021. Increased yield decreased feedstock price, and the economies of scale for larger facilities help reduce the computed MSP.

TABLE 2 | Conversion pathways with feedstock price and scale for both *n*th and pioneer scale facilities.

Technology	Feedstock	Feedstock price ($/t)	*n*th plant total distillate (million L/yr)	Pioneer plant total distillate (million L/yr)
FT[a]	MSW	30	500	100
FT[a]	Agricultural residuals	110	300	100
FT[a]	Forest residues	125	400	100
FT	DAC CO_2	300	1,000	100
FT	flue gas CO_2	50	1,000	100
ATJ	Corn ethanol	472	1,000	100
ATJ	2G ethanol	1,524	1,000	100
HEFA	FOGs	580	1,000	100
HEFA	Vegetable oil	810	1,000	100
HEFA	Second-crop oilseed	701	1,000	100

[a]*Feedstock prices are preprocessed.*

2.1 Sustainable Fuel Programs

The purpose of many existing and proposed government programs is to either account for the environmental benefits afforded by sustainable fuels or provide economic support to this new industry. Additional programs exist that encourage the development and deployment of SAF. Understanding the financial impact of these various policy efforts is vital to differentiating the cost of the energy production for these fuels and the environmental services that they provide. Incenting domestic fuel production, decreasing the CI of liquid fuels, and securing rural jobs are a few examples of policy objectives for these programs. Additional details related to conversion pathway CI score are included in **Supplementary Information S2**.

Understanding the complexity and interactions of fuels, pathways, feedstocks, processing variables, and the environmental services provided by these fuels allows for a better understanding of financial viability. This is completed by considering the revenues of both the fuel sales and various government programs available for sustainable products. The impact of stacking the applicable incentives while balancing the process and feedstock costs required to qualify allows for the comparison of both fuel and environmental services revenues (Airlines for America, 2021; Wang et al., 2021). Policy support might be an effective method to incentivize SAF production in the United States, as demonstrated in renewable diesel production where the stacking of existing federal and state programs has been reported to generate enough income to cover production costs (Stratas Advisors, 2020).

2.1.1 Federal Sustainable Fuels Programs

The Renewable Fuel Standard (RFS) establishes a marketplace for the sale and purchase of renewable identification numbers (RINs) for compliance of fuel blenders to meet renewable volume obligations. This existing federal standard was designed to assist the United States in meeting long-term energy security and environmental goals by increasing the renewable fuel use through 2022. To qualify for RINs, a producer is required to meet a threshold greenhouse gas (GHG) emissions reduction. The value of a RIN is determined from the combination of production technology, feedstock, and fuel type produced (Environmental Protection Agency (EPA), 2021a). RIN values are tied to classifications, among which the producer chooses the highest value option. For example, a D3 RIN, generated for cellulosic biofuels, is often worth more than a D4, D5, or D6 RIN generated for biomass-based diesel, advanced biofuels including diesel from vegetable oil, and renewable ethanol, respectively (Environmental Protection Agency (EPA), 2021a; Environmental Protection Agency (EPA), 2021b).

A variety of existing and proposed blender's tax credits (BTCs) exist to reduce the tax burden of a fuel blender. In the existing biomass-based BTC, the blender earns the credit as tax-free income once their tax burden has been erased (U.S. Department of Energy, 2021a; U.S. Department of Energy, 2021b). The biodiesel mixture excise tax credit, commonly called the diesel BTC, is \$0.26/L BTC for biodiesel, agri-diesel, and renewable diesel. It does not have a lifecycle GHG reduction threshold or fuel use requirements. The alternative fuel excise tax credit, or gasoline blender's tax credit, provides \$0.13/L for various distillates without a CI reduction requirement (U.S. Department of Energy, 2021a). In May 2021, a proposed BTC for SAF was introduced in the Sustainable Skies Act. The bill includes an incentive of \$0.40/L for SAF, with a minimum of 50% GHG emission reduction. The incentive value ramps up linearly to a maximum value of \$0.53/L for SAF with 100% or greater GHG emission reduction and is proposed to be paid through 2031 (Schneider, 2021).

2.1.2 State Sustainable Fuel Programs

Selected states have created programs to encourage the production and use of sustainable fuels. The first such program is California's low-carbon fuel standard (LCFS), which pays energy producers based on the tCO_2e/MJ avoided (California Air Resources Board (CARB), 2021). Each producer's CI is tracked with the producer being paid a premium per unit of fuel based on the quantity of the avoided carbon emissions. This model encourages continuous reductions in CI scores while also rewarding small CI changes. Similar programs have been implemented in Oregon (Oregon Department of Environmental Quality, 2021) and voted into law in Washington State (Department of Ecology, 2021).

2.1.3 Capital Grants

Investors in the alternative fuels industry weigh the massive capital requirements and the relatively immature technology against the probability of the industry succeeding. Incentives can be used to lower financial risks, which may persuade more investors to finance projects. Capital grants have been used to lower the investment requirements for biofuel plants in the United States. In 2014, Red Rock Biofuels was awarded \$70 million as part of the United States Defense Production Act Title III Advanced Drop-in Biofuels project in the second phase. This followed \$4.1 million from the first phase for engineering, for a total of nearly \$75 million (Renewable Energy Focus.com, 2014). The same Department of Defense funding granted \$70 million to Fulcrum BioEnergy for their MSW to fuel facility in Nevada (Reid, 2014). Fulcrum BioEnergy was also granted \$4.7 million as funds in phase 1 of this project for engineering, bringing the total grant to \$74.7 million (Schill, 2013).

2.2 Economic Impact of Federal and State Programs

To assess the relative impact of various federal and local programs on the minimum selling price and capital investment of SAF, a variety of incentive options were incorporated into harmonized TEA models. The programs modeled for all conversion pathways were categorized as 1) existing federal (EF), 2) proposed federal, 3) state, or 4) capital grants. The EF programs included the diesel BTC, the gasoline BTC, and RINs. The values used for various RINs were chosen as the median of the values from 2014 through 2020 (Environmental Protection Agency (EPA), 2021b). The

sole proposed federal program was the federal SAF BTC. The California LCFS represented the state program modeled in the TEAs. We note that the LCFS values are similar to those in the Oregon CFP. After the demand in states with local incentives is met, fuel will have to be sold in markets supported by only federal incentives. Each incentive has specifications that must be met and are detailed with the calculations used to estimate the incentive value in **Supplementary Material S2**. For pioneer plants, $75 million capital grants were added to determine if these facilities could be de-risked enough to incent investment.

The BTC is paid to the blender of the fuel, which can be the producer or another company. Both the existing gasoline and diesel BTC require an unspecified amount of petroleum fuel to be added to the neat biofuel, a practice termed "splash blending," which allows producers to blend without buying large quantities of petroleum diesel or the capital required for large tank farms. Given this common practice, we assume that producers are also the blender of record for diesel, gasoline, naphtha, and propane products. However, it is not apparent that splash blending would be permitted in the SAF BTC, thereby restricting producer-based blending only to large petroleum refiners. When SAF is produced and certified to meet ASTM 7566, the SAF is then blended with conventional fuels at a predetermined limit to meet ASTM 1655. As the ASTM standard is currently written, splash-blending does not meet the neat or blended SAF standards. While this could be addressed through future changes to the ASTM standards, we assume here that splash-blending of SAF is not permitted. The uncertainty surrounding blending by an SAF producer is addressed by analyzing this incentive in two ways. The first scenario assumes that the producer receives the entire incentive to reduce taxes and then as tax-free income. The second scenario assumes that the producer will receive a portion of the incentive, a variable that will be analyzed at multiple values, as taxable income. We speculate that with low volumes of and increasing demand for SAF, the producer will recover a large portion of the incentive. In all of these scenarios, we assume that the BTCs are available for the first 10 years of a facility's 20-year production life, as is currently represented in the proposed bill.

As a means of comparison, the computed MSP for SAF is benchmarked against the mean, maximum, and minimum annual wholesale petroleum jet fuel price from 2011 through 2020 (Energy Information Administration (EIA), 2021b). MSP values calculated with incentives include incentives for all eligible liquid fuels. While the RFS does not currently include FT with either DAC or flue gas as feedstocks, for the purpose of this analysis, we assume that this conversion pathway would be eligible for advanced biofuel, D5 RINs. For determining the CI score for fuels produced with DAC and flue gas, we assumed that only renewable electricity and green hydrogen were used.

The U.S. EPA has not defined a pathway to convert ethanol RINs to RINs for other distillates or a method to not issue RINs for ethanol that is used as an intermediate in manufacturing other fuels. To address this in the ATJ pathway, it was assumed that the ethanol purchased to produce fuels is produced at the SAF facility, and the ethanol price paid is a transfer cost equal to the cost of production.

3 RESULTS

The following subsections present the SAF MSP ($/L) for the different technologies and feedstocks. The baseline corresponds only to the MSP of the fuel's energy content. Policies and programs are included for existing and proposed federal programs, state programs, and capital grants for comparison to the baseline. The figures include the wholesale petroleum jet fuel price from 2011 to 2020 for reference.

3.1 No Policy Support

MSP values were determined for both *n*th and pioneer plants without considering revenues from various government programs (**Table 3**). The *n*th plant MSP values are the baseline values to which all comparisons are made unless stated otherwise. Pioneer values for HEFA facilities were not included because the technology is sufficiently advanced to be assumed as mature (de Jong et al., 2015). However, for all other processes, MSP values from the pioneer plant were significantly

TABLE 3 | Total distillate production and MSP for *n*th and pioneer plants for each conversion pathway using baseline assumptions, which do not include incentives.

Technology	Feedstock	*n*th plant		Pioneer plant	
		Total distillate (million L/yr)	MSP ($/L)	Total distillate (million L/yr)	MSP ($/L)
FT	MSW	500	1.0	100	1.7
FT	Agricultural residuals	300	2.0	100	3.2
FT	Forest residues	400	1.7	100	2.7
FT	DAC CO_2	1,000	3.7	100	4.0
FT	flue gas CO_2	1,000	2.8	100	3.1
ATJ	Corn ethanol	1,000	0.8	100	1.0
ATJ	2G ethanol	1,000	2.3	100	2.5
HEFA	FOGs	1,000	0.8	NA	NA
HEFA	Vegetable oil	1,000	1.1	NA	NA
HEFA	Second-crop oilseed	1,000	0.9	NA	NA

higher than *n*th plant due to smaller plant scale and higher technology uncertainties.

HEFA viability is controlled by the availability of low-cost feedstock, a controlling variable in MSP for this lower capital pathway. For the ATJ SAF using 2G ethanol as the feedstock, the MSP is much higher if the feedstock is corn ethanol. It is understood that the price of 2G ethanol will likely drop over time as it becomes more widely available, which will reduce the SAF MSP. This expected price drop will be combined with a more significant GHG reduction for 2G ethanol, increasing some incentive values. FT processes are not mature, and high capital costs limit the ability of this pathway without very low-cost feedstock, for example, MSW. MSW, agricultural residuals, and forest residuals differ on the distillates yield (Brandt et al., 2021b), and all require preprocessed feedstocks that increase the resulting fuel MSP. However, the additional revenues of recyclable separation assist in reducing MSW feedstock costs.

3.2 Existing and Proposed Federal Programs

Calculated values of the existing and proposed federal incentives for each conversion pathway are listed in **Table 4**. The RIN type and thus RIN value are a function of the conversion pathway and meeting a minimum CI reduction, based on RFS legislation. Both the gasoline and diesel BTC do not have specific CI targets, making this a low-effort policy to earn. The lower gasoline and diesel BTC incentive values for MSW reflect a reduction taken for the non-biogenic portion of the feedstock.

The decrease in MSP from EF and the proposed SAF BTC varies with the conversion pathway. The decline is controlled by the estimated value of each incentive, the tax qualifications of the policy revenues, capital intensity of the pathway, the cost of the feedstock selected, and the scale of non-feedstock operating costs (**Figures 1**–**3**). The small decrease in SAF MSP for vegetable oil (**Figure 1**) results from the diesel and gasoline BTCs that do not specify CI reduction thresholds. This conversion pathway does not meet the proposed CI criteria for the proposed SAF BTC, so no benefit is realized. Both FOGs and second-crop oilseed oil meet the criteria to get RINs having more significant incentives that result in bigger MSP drops. The ability to stack program benefits combined with lower feedstock cost makes fuels produced from both of these feedstocks a more financially attractive alternative than vegetable oil. Although a competitive price can be obtained with existing and proposed federal programs, the availability of FOGs and the nascent practice of second cropping limit industry deployment using only HEFA.

SAF produced using FT has prices above the wholesale petroleum price range from 2011 to 2020 without any program support, regardless of the feedstock selected. However, the lowest cost feedstock, MSW, may be able to overcome the high capital costs with existing federal programs. Forest residues become a possible feedstock if the existing federal programs are combined with the proposed SAF BTC. The smaller facility scale for agricultural residuals hinders this feedstock choice. Although DAC and flue gas both have low CI scores (**Supplementary Information S2**), the overwhelming operating and capital costs will need substantially more significant support to attain MSP value similar to other SAF conversion pathways (**Figure 2**).

Using corn ethanol to manufacture SAF is attractive both from fuel cost and feedstock availability positions. However, the low CI improvement and RIN classification mean that the policy support for monetizing environmental services is low. However, for 2G ethanol to be a realistic feedstock, the ethanol cost will have to decrease, even with stacking of the existing and proposed federal programs (**Figure 3**).

The introduction of incentives and their respective constraints have the ability to reorder the economic viability of conversion pathways not from the value of fuel product but from the environmental services that sustainable fuels provide. Prospective producers will look at profitability with and without policy support and weigh the stability of the expected support when selecting a conversion and feedstock pathways.

3.2.1 Variations to the Proposed SAF BTC

The proposed SAF BTC could be implemented in a variety of manners, which will influence the impact of the proposed legislation on SAF production. As this legislation stands, the value reduces the blender's tax liability to zero before becoming a tax-free income stream. Companies that can purchase or rent tank farms as well as purchase large quantities of petroleum jet fuel will likely blend SAF to be eligible for the entire proposed SAF BTC. However, this approach is likely cost-prohibitive for

TABLE 4 | Value of federal incentives for technologies and feedstocks modeled using CORSIA CI scores. RINs listed are for SAF.

Technology	Feedstock	RIN type	RIN ($/L)	Gas BTC ($/L)	Diesel BTC ($/L)	SAF BTC ($/L)
FT	MSW	D3	0.67	0.11	0.22	0.38
FT	Agricultural residuals	D3	0.67	0.13	0.26	0.51
FT	Forest residues	D3	0.67	0.13	0.26	0.50
FT	DAC CO_2	D5	0.23	0.13	0.26	0.50
FT	flue gas CO_2	D5	0.23	0.13	0.26	0.50
ATJ	Corn ethanol	D6	0.20	0.13	0.26	0.00
ATJ	2G ethanol	D3	0.67	0.13	0.26	0.44
HEFA	FOGs	D4	0.23	0.13	0.26	0.47
HEFA	Vegetable oil	-[a]	0.00	0.13	0.26	0.00
HEFA	Second-crop oilseed	D4	0.23	0.13	0.26	0.49

[a]*Vegetable oil does not meet 50% GHG reduction with assumed CI score.*

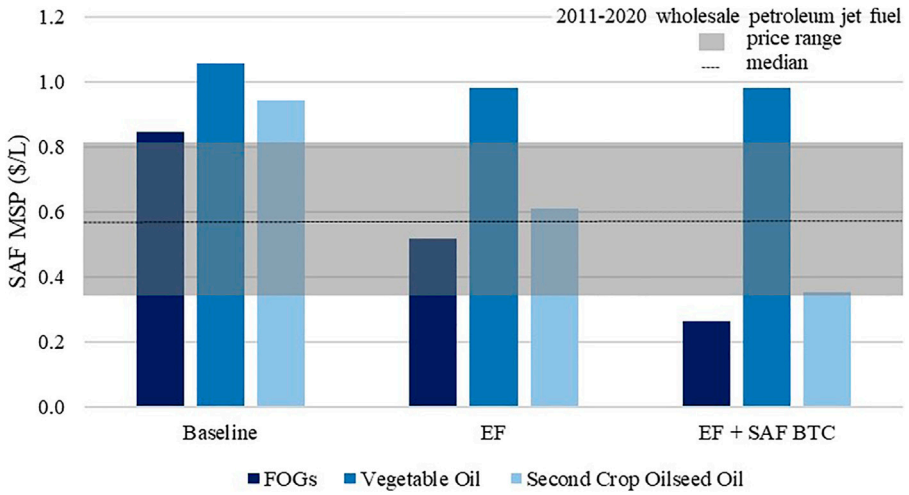

FIGURE 1 | Impact of EF and proposed SAF BTC on MSP for three feedstocks using the HEFA process.

smaller organizations. To quantify the impact of sharing the value of the SAF BTC with a producer, three scenarios were analyzed for a subset of the feedstocks using the FT pathway with approved feedstocks. In each scenario, the value of the BTC passed to the producer ranges from 70 to 90% and is considered taxable income (**Figure 4**). Predictably, the SAF MSP increases when more of the incentive is kept by the blender. The increase in MSP is $0.11/L between the 100% tax-free and 70% taxable scenarios. The decreased value does not change the financial viability for fuels produced with either MSW or agricultural residues. MSW is viable without the SAF BTC, and the proposed SAF BTC value is not enough to reduce the agricultural residue MSP to a value within the 2011–2020 wholesale petroleum jet fuel price range. However, the MSP drops into the range of petroleum jet fuel for forest residues for only the producer as the blender scenario.

Monetizing the environmental benefits of SAF appears to be an effective means of increasing the financial viability of production. However, the effective duration of the government program impacts both the MSP and the likelihood of investment (Ghatala, 2020). To understand the impact that uncertainty in government programs may have on the MSP of SAF, the SAF BTC was modeled with a 20-, 10-, 5-, and 2-year life span for FT processes. As expected, maintaining the program for the effective plant life has the largest impact on MSP, especially for marginally competitive feedstocks like forest residuals (**Figure 5**). Given the minimal MSP improvement for short duration program, investors may likely not even consider it in building a facility.

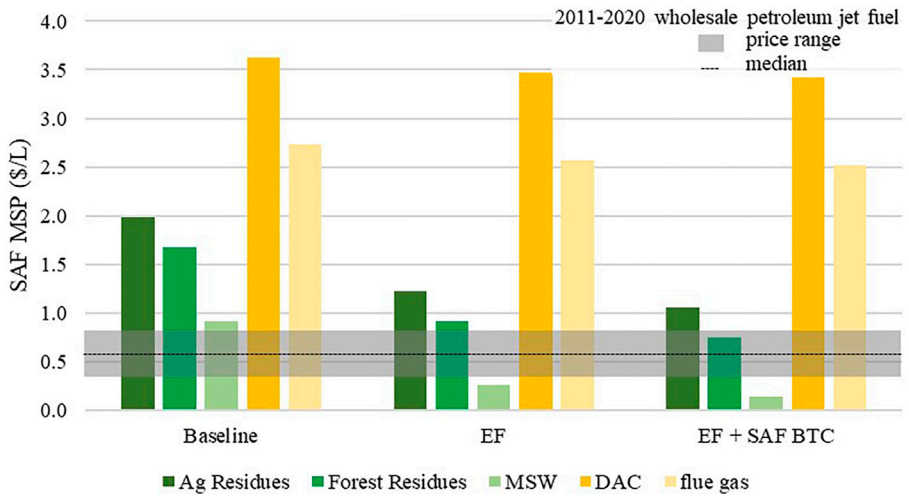

FIGURE 2 | Impact of EF and proposed SAF BTC on MSP for five feedstocks using the FT process.

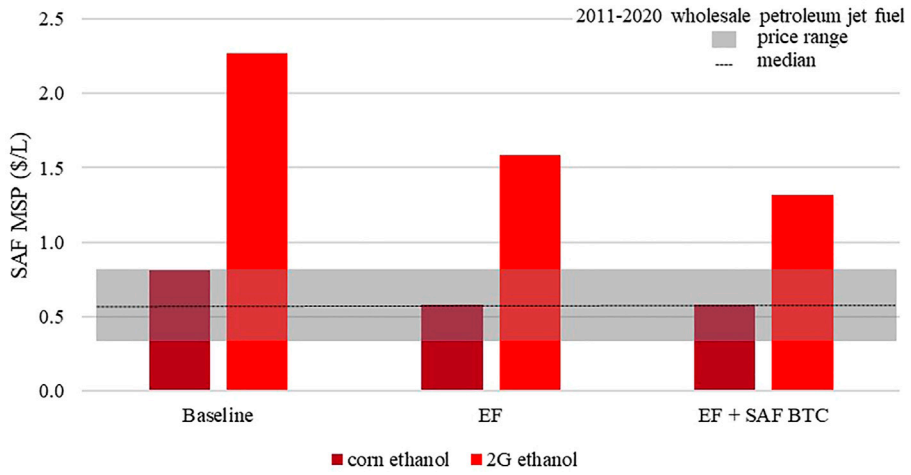

FIGURE 3 | Impact of EF and proposed SAF BTC on MSP for two feedstocks using the ATJ process.

Currently, road fuel production is incentivized over SAF (Pavlenko et al., 2019). In the United States, this is most evident through the diesel BTC. In addition, SAF generally requires additional hydrogen, energy, and operating time to crack FT waxes or lipids to the lower SAF molecular weights. While some amount of middle distillate representing the SAF cut is produced in these processes, the breadth of the diesel standard allows this cut to be sold in diesel with little effect on diesel quality. Without the passage of the Sustainable Skies Act, it is unlikely that biofuel producers will choose to produce SAF at any significant quantity. Diesel currently earns a BTC of $0.26/L, regardless of CI reduction. The proposed SAF BTC value is higher at $0.40–0.53/L but requires a minimum CI reduction of 50% to be met.

To overcome the financial impetus of simply selling the SAF cut with the diesel, SAF programs need to be more favorable. Using FT with MSW as an example, **Figure 6** shows the total 20-years revenue as the sum of fuel sales and policy support, for three distillate cut options and two policy scenarios: EF and EF plus SAF BTC. In these scenarios, we assume that the SAF price is equal to the mean petroleum jet fuel price from 2011 to 2020 (Energy Information Administration (EIA), 2021b). In addition, the three distillate cuts examined were 0:80:20, 40:40:20, and 50:30:20 for the assumed jet:diesel: naphtha volume fractions. This analysis was completed using the simplifying assumption that no additional equipment or operating costs are needed to complete the distillate slate change.

The results depicted in **Figure 6** illustrate that without the SAF BTC, selling only diesel is more financially attractive than a combination of diesel and SAF. This point is evidenced by the fact that for all scenarios, the total revenue is greater when a producer sells only diesel with only EF policies. However, with the addition of the SAF BTC, although revenues from fuel sales might

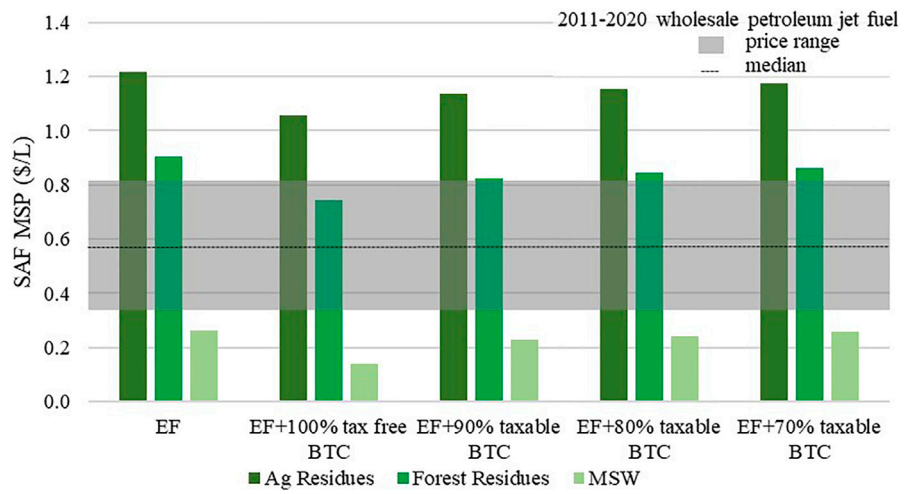

FIGURE 4 | Scenarios illustrating the impact of SAF BTC implementation variables.

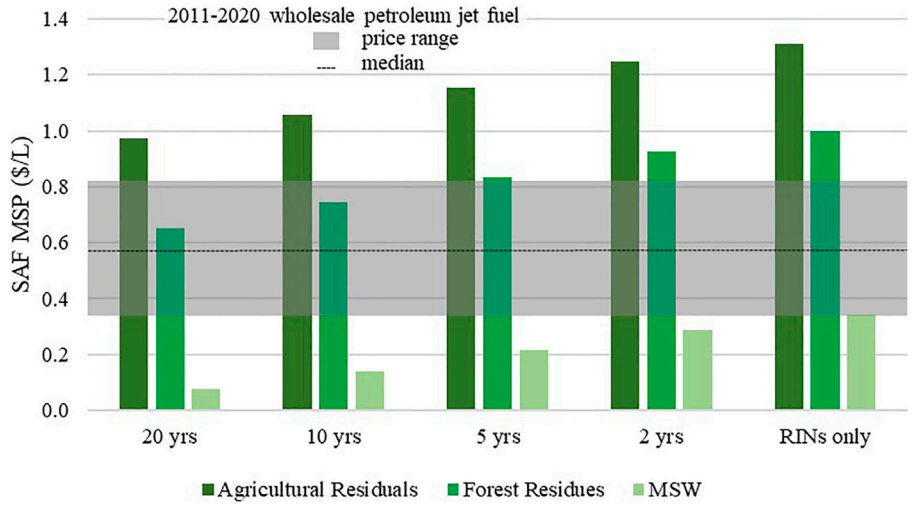

FIGURE 5 | SAF MSP values with RINs and four BTC durations.

decrease, the total revenue, including policy support, is maximized.

3.3 State Programs

Localized state-level incentives can be stacked with federal incentives to lower estimated MSP values further. Here, we use the LCFS incentives to demonstrate this impact. Localized incentives reduce MSP values appreciably, even into negative MSP values, but are inherently limited to the fuel volumes used in the applicable region (**Table 5**). After stacking the LCFS program credits with existing and proposed federal programs, seven conversion pathways drop into the 2011–2020 wholesale petroleum jet fuel price range (**Table 5**). Three conversion pathways result in negative MSP values. Negative MSP values demonstrate that higher returns could be realized by producers than is assumed in the baseline model scenarios. States with programs that can be stacked with the federal policy will provide the most lucrative market. In 2019, California used 16.9 billion L of petroleum jet fuel, with close to 17% of the total U.S. consumption (Energy Information Administration (EIA), 2021a). If half of this fuel volume is replaced with SAF, 8.4 billion L will be needed to saturate the California market. When the volumes for both Oregon and Washington are included at the same addition rate, an additional 2 billion L/yr is required. The U.S. potential for SAF production from FOGs has been estimated to be approximately 3 billion L/yr, well short of the 10.4 billion L west coast demand (Skaggs et al., 2018; Wolff et al., 2020). Although second-crop oilseeds are a possible feedstock, it will take time to ramp up production. With the HEFA feedstock

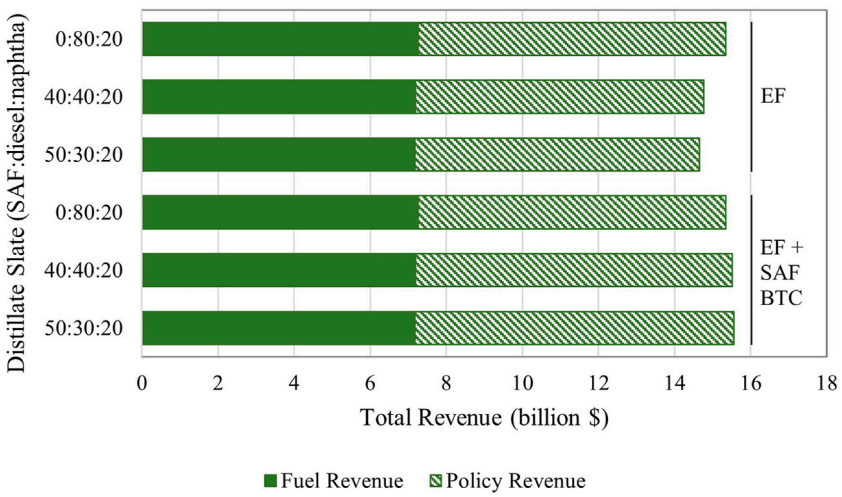

FIGURE 6 | Total, fuel, and policy revenues for three distillate cut scenarios with either EF or EF plus SAF BTC policy support.

TABLE 5 | Value of LCFS incentives for technologies and feedstocks modeled using CORSIA CI scores. SAF MSP values were calculated, including RINs, diesel, gasoline, and SAF BTC, in addition to LCFS.

Technology	Feedstock	LCFS ($/L)	SAF MSP ($/L)
FT	MSW	0.33	−0.21
FT	Agricultural residuals	0.43	0.62
FT	Forest residues	0.43	0.30
FT	DAC CO_2	0.42	3.29
FT	flue gas CO_2	0.42	2.39
ATJ	Corn ethanol	0.12	0.45
ATJ	2G ethanol	0.31	1.02
HEFA	FOGs	0.36	−0.06
HEFA	Vegetable oil	0.13	0.85
HEFA	Second-crop oilseed	0.40	−0.01

limitations, the volume of SAF demand in the west coast states may allow technology and feedstocks to be de-risked for the earliest entrants. However, this may be prevented or delayed if HEFA SAF floods the market from existing domestic and foreign renewable diesel facilities.

3.4 Capital Grants

The combination of existing and proposed federal programs with state programs shift predicted MSP values to levels that appear financially attractive for *n*th plants (**Table 5**). However, the MSP values associated with pioneer plants are much higher (**Table 3**). One of the programs available for pioneer plants that are used to encourage new SAF facilities is capital grants. The impact of these grants depends on both the capital intensity of a conversion pathway and the relative level of operating costs. These grants are not intended for mature technology, and although pioneer plants are more expensive per volume of fuel produced, the total capital investment (TCI) can be significantly lower than that of a mature plant because of the smaller scale. To quantify the potential impact of this incentive class, a $75 million capital grant was added to the baseline pioneer plant analyses for the FT and ATJ technologies. The absolute drop in MSP is $0.09/L across all feedstocks for FT and ATJ, although the percentage drop in MSP values varies (**Figure 7**). For ATJ, the percentage drop in TCI is much more than that for the FT facilities. The drop in TCI de-risks a new technology facility, even if the MSP does not drop significantly and may lead to investment. None of the pioneer technology conversion pathways reach the comparative petroleum jet fuel price range with only a capital grant.

The cost reductions in **Figure 7** increase with the addition of the three BTC incentives, RINs and LCFS, but only for fuels with emission reductions that meet the requirements. To illustrate the effect of each incentive on MSP, FT-MSW and FT-forest residues MSP are shown in **Figure 8** and **Figure 9**, respectively. For a scenario with a pioneer FT-MSW facility, the combination of a $75 million capital grant, three BTC incentives, RINs, and LCFS, the SAF MSP approaches, but does not enter the traditional jet price range. Despite the stacking of incentives, the SAF MSP for forest residues is still twice the highest value in the price band for the petroleum jet fuel. However, if FT-MSW is successful, some of the learnings will apply to FT forest residues, and capital costs for the first plants could drop. This FT conversion pathway is the closest to price parity for a pioneer plant, which clarifies that a suite of incentives will be needed to aid in the maturation of this technology. Corn ethanol is cost-competitive for a pioneer plant with the stacking of policy support; however, the CI reduction is low.

4 CONCLUSION

SAF is a critical product to meet local, national, and global GHG reduction targets. Policy support that monetizes the environmental benefits is vital to deploying new technologies and production capacity. The incorporation of the SAF BTC in the United States, combined with existing federal and state programs, is needed to encourage producers to add SAF into

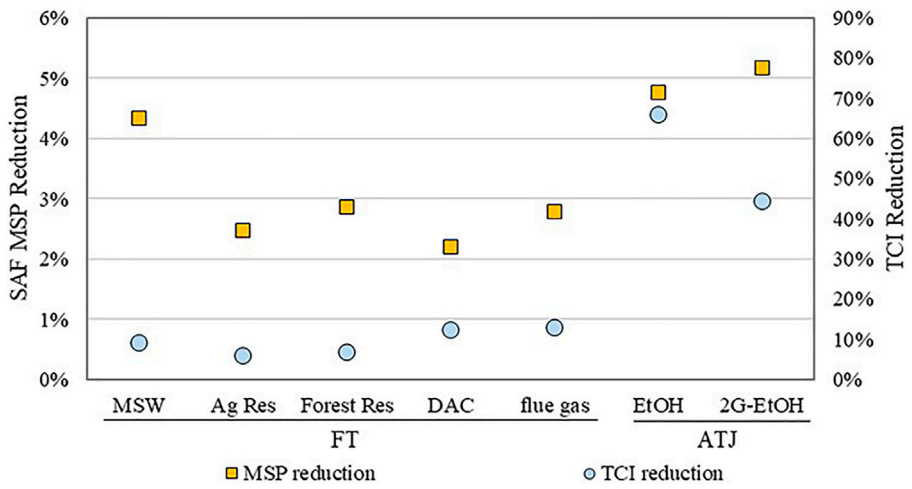

FIGURE 7 | Percent reduction of baseline MSP and TCI for pioneer plants with a $75 million capital grant.

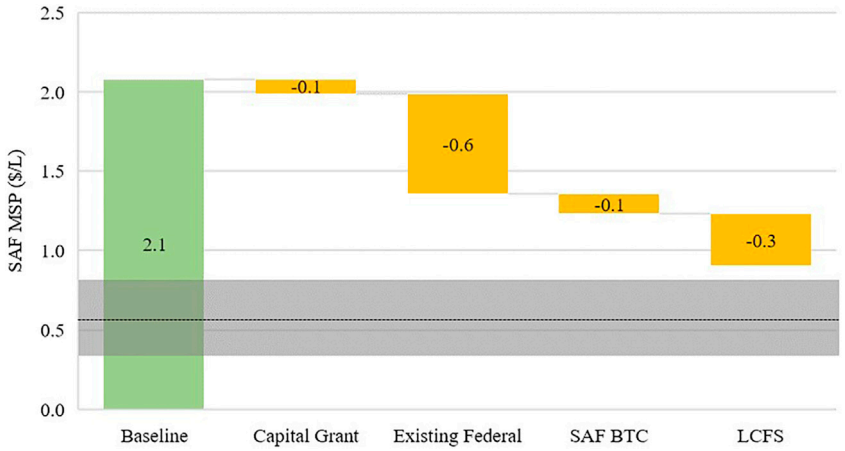

FIGURE 8 | Progressive impact of incentives on FT-MSW SAF MSP for pioneer plants.

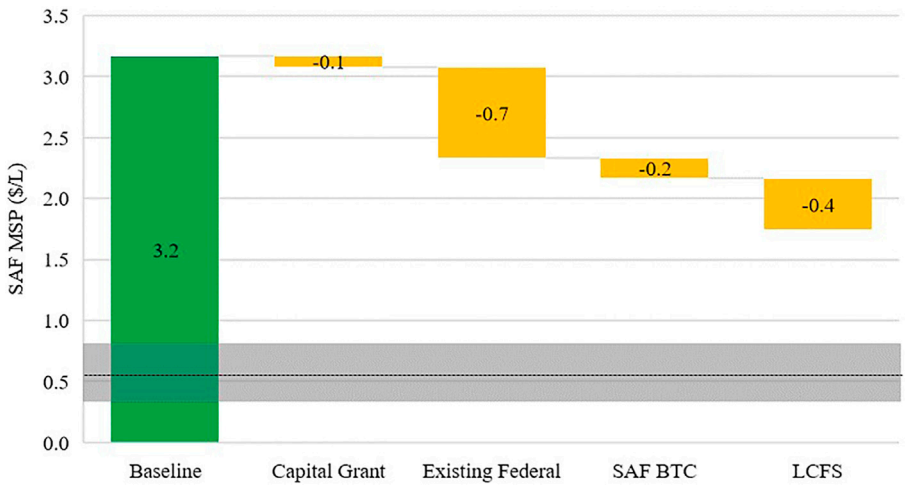

FIGURE 9 | Progressive impact of incentives on FT forest residues SAF MSP for pioneer plants.

their product slate. Without the addition of the SAF BTC, producers are unlikely to sell SAF outside of offtake requirements as it generates lower revenues than diesel. Programs that correlate the monetary value with CI value favor conversion pathways with lower CI values, which in turn selectively lower MSP values for fuels that yield the most environmental services (e.g., CO_{2e} reductions). This can change the rank order of the economic feasibility of conversion pathways, making the lowest CI fuels more profitable. ATJ-corn ethanol has the lowest MSP, tied with HEFA-FOGs without incentives. However, ATJ corn drops to fifth with the addition of incentives because of the relatively high CI score assigned to this feedstock, while HEFA-FOGs drop to the second place behind FT-MSW. The differential payment schedule of the proposed SAF BTC, the value of RIN classifications, and the state programs help steer production toward pathways with the lowest CI score.

Program values are volatile in value and duration. The impact of duration of each program should be studied further, looking at set end dates and the possibility of legislation that assures a facility of a set number of years from the end of construction. Future work should also analyze changes in program credit values. Between 2014 and 2020, if the selected RIN values were the minimum or maximum annual value, the MSP for FT-MSW or FT forest residues will change by ±$0.30/L–$0.40/L. The scale of this change is even more pronounced for LCFS, with changes as great as $0.75/L. The CI scores used in this study are general values that will change with specific processes and locations and will impact the value of the SAF BTC and LCFS. A stochastic analysis of existing and proposed incentive values is a crucial next step to understanding the potential impact of incentives on the production and sale of SAF. Stacking of policies and programs is

necessary to encourage the development of a robust SAF market, especially for pioneer technology.

DATA AVAILABILITY STATEMENT

The original contributions presented in the study are included in the article/**Supplementary Material**, further inquiries can be directed to the corresponding author.

AUTHOR CONTRIBUTIONS

The study described in this work was designed by KB and MW and the data was largely compiled by KB and LM-V. The analysis was completed by KB. KB wrote the draft manuscript that was reviewed by MW and LM-V.

FUNDING

This research was funded by the U.S. Federal Aviation Administration Office of Environment and Energy through ASCENT, the FAA Center of Excellence for Alternative Jet Fuels, and the Environment, project 001A through FAA Award Number 13C-AJFE-WaSU-16 under the supervision of Nathan Brown. Any opinions, findings, conclusion, or recommendations expressed in this material are those of the authors and do not necessarily reflect the views of the FAA. LM-V is very thankful to the Fulbright-Colciencias Scholarship program for financial support of her studies and living expenses in the United States.

ACKNOWLEDGMENTS

The authors would like to acknowledge the discussions and clarifications provided by Glenn Johnston, Alex Menotti, and John Plaza. Their expertise helped shape the scenarios analyzed.

SUPPLEMENTARY MATERIAL

The Supplementary Material for this article can be found online at: https://www.frontiersin.org/articles/10.3389/fenrg.2022.828789/full#supplementary-material

REFERENCES

Air Transportation Action Group (2021). Aviation Industry Adopts 2050 Net-Zero Carbon Goal. Available at: https://www.atag.org/component/news/?view=pressrelease&id=125 (Accessed October 28, 2021).

Air Transportation Action Group (2020). Waypoint 2050. Available at: https://aviationbenefits.org/media/167187/w2050_full.pdf.

Airlines for America (2021). *U.S. Airlines Announce 3-Billion-Gallon Sustainable Aviation Fuel Production Goal*. Washington, DC: News Updat.

Bains, P., Psarras, P., and Wilcox, J. (2017). CO 2 Capture from the Industry Sector. *Prog. Energ. Combustion Sci.* 63, 146–172. doi:10.1016/j.pecs.2017.07.001

Bann, S. J., Malina, R., Staples, M. D., Suresh, P., Pearlson, M., Tyner, W. E., et al. (2017). The Costs of Production of Alternative Jet Fuel: A Harmonized Stochastic Assessment. *Bioresour. Tech.* 227, 179–187. doi:10.1016/j.biortech.2016.12.032

Brandt, K., Geleynse, S., Martinez-Valencia, L., Zhang, X., Garcia-Perez, M., and Wolcott, M. P. (2021a). Alcohol to Jet Techno-Economic Analysis. doi:10.7273/000001461

Brandt, K. L., Wooley, R. J., Geleynse, S. C., Gao, J., Zhu, J., Cavalieri, R. P., et al. (2020). Impact of Co-product Selection on Techno-economic Analyses of Alternative Jet Fuel Produced with forest Harvest Residuals. *Biofuels, Bioprod. Bioref.* 14, 764–775. doi:10.1002/bbb.2111

Brandt, K., Tanzil, A. H., Martinez-Valencia, L., Garcia-Perez, M., and Wolcott, M. P. (2021b). Fischer Tropsch Techno-Economic Analysis. doi:10.7273/000001459

Brandt, K., Tanzil, A. H., Martinez-Valencia, L., Garcia-Perez, M., and Wolcott, M. P. (2021c). Hydroprocessed Esters and Fatty Acids Techno-Economic Analysis. doi:10.7273/000001460

Brandt, K., and Wolcott, M. P. (2021). Fischer Tropsch Feedstock Pre-processing Techno-Economic Analysis. doi:10.7273/000001463

Bryan, T. (2021). Renewable Diesel's Rising Tide. *Biodiesel Mag.* Available at: http://www.biodieselmagazine.com/articles/2517318/renewable-diesels-rising-tide (Accessed August 25, 2021).

California Air Resources Board (2021). Data Dashboard. Available at: https://ww3.arb.ca.gov/fuels/lcfs/dashboard/dashboard.htm (Accessed July 14, 2021).

Chao, H., Agusdinata, D. B., DeLaurentis, D., and Stechel, E. B. (2019). Carbon Offsetting and Reduction Scheme with Sustainable Aviation Fuel Options: Fleet-Level Carbon Emissions Impacts for U.S. Airlines. *Transportation Res. D: Transport Environ.* 75, 42–56. doi:10.1016/j.trd.2019.08.015

Davis, R., Tao, L., Scarlata, C., Tan, E. C. D., Ross, J., Lukas, J., et al. (2015). *Process Design and Economics for the Conversion of Lignocellulosic Biomass to Hydrocarbons: Dilute-Acid and Enzymatic Deconstruction of Biomass to Sugars and Catalytic Conversion of Sugar to Hydrocarbons*. Golden, CO, United States: NREL. Available at: https://web.archive.org/web/20200623200535id_/https://www.nrel.gov/docs/fy15osti/62498.pdf.

de Jong, S., Hoefnagels, R., Faaij, A., Slade, R., Mawhood, R., and Junginger, M. (2015). The Feasibility of Short-Term Production Strategies for Renewable Jet Fuels - a Comprehensive Techno-Economic Comparison. *Biofuels, Bioprod. Bioref.* 9, 778–800. doi:10.1002/bbb.1613

Department of Ecology, S. of W (2021). Clean Fuel Stadard. *Reducing Greenh. Gases*. Available at: https://ecology.wa.gov/Air-Climate/Climate-change/Reducing-greenhouse-gases/Clean-Fuel-Standard (Accessed December 1, 2021).

Dodd, T., and Yengin, D. (2021). Deadlock in Sustainable Aviation Fuels: A Multi-Case Analysis of agency. *Transportation Res. Part D: Transport Environ.* 94, 102799. doi:10.1016/j.trd.2021.102799

Doliente, S. S., Narayan, A., Tapia, J. F. D., Samsatli, N. J., Zhao, Y., and Samsatli, S. (2020). Bio-aviation Fuel: A Comprehensive Review and Analysis of the Supply Chain Components. *Front. Energ. Res.* 8, 38. doi:10.3389/fenrg.2020.00110

Energy Information Administration (2021a). Table F1: Jet Fuel Consumption, price and Expenditure Estimates, 2019U.S. States, State Profile Energy Estim. Available at: https://www.eia.gov/state/seds/data.php?incfile=/state/seds/sep_fuel/html/fuel_jf.html&sid=CA (Accessed October 14, 2021).

Energy Information Administration (2021b). U.S. Kerosene-type Jet Fuel Wholesale/Resale Price by Refiners. *Pet. Other Liq.* Available at: https://www.eia.gov/dnav/pet/hist/LeafHandler.ashx?n=PET&s=EMA_EPJK_PWG_NUS_DPG&f=M (Accessed September 28, 2021).

Environmental Protection Agency (2021a). Approved Pathways for Renewable Fuel. *Renew. Fuel Stand. Progr.* Available at: https://www.epa.gov/renewable-fuel-standard-program/approved-pathways-renewable-fuel (Accessed July 14, 2021).

Environmental Protection Agency (2021b). Renewable Fuel Standard Program. Available at: https://www.epa.gov/renewable-fuel-standard-program (Accessed July 14, 2021).

Eswaran, S., Subramaniam, S., Geleynse, S., Brandt, K., Wolcott, M., and Zhang, X. (2021). Techno-economic Analysis of Catalytic Hydrothermolysis Pathway for Jet Fuel Production. *Renew. Sust. Energ. Rev.* 151, 111516. doi:10.1016/j.rser.2021.111516

Federal Aviation Administration (2021). Aviation Climate Action Plan. *Sustainability*. Available at: https://www.faa.gov/sustainability/aviation-climate-action-plan (Accessed March 12, 2021).

Fulcum Bioenergy (2021). Our Process. *Technology*. Available at: https://fulcrum-bioenergy.com/technology/our-process/ (Accessed August 25, 2021).

Geleynse, S., Brandt, K., Garcia-Perez, M., Wolcott, M., and Zhang, X. (2018). The Alcohol-To-Jet Conversion Pathway for Drop-In Biofuels: Techno-Economic Evaluation. *ChemSusChem* 11, 3728–3741. doi:10.1002/cssc.201801690

Ghatala, F. (2020). *Sustainable Aviation Fuel Policy in the United States: A Pracmatic Way Forward*. Washington D.C. Available at: https://www.atlanticcouncil.org/wp-content/uploads/2020/04/AC_SAF_0420_v8.pdf.

Holladay, J., Abdullah, Z., and Heyne, J. (2020). Sustainable Aviation Fuel, Review of Technical Pathways. Available at: https://www.energy.gov/sites/prod/files/2020/09/f78/beto-sust-aviation-fuel-sep-2020.pdf.doi:10.2172/1660415

Humbird, D., Davis, R., Tao, L., Kinchin, C., Hsu, D., Aden, A., et al. (2011). *Process Design and Economics for Biochemical Conversion of Lignocellulosic Biomass to Ethanol: Dilute-Acid Pretreatment and Enzymatic Hydrolysis of Corn Stover*. United States: Golden, CO. doi:10.2172/1013269

International Air Transportation Association (2019). Fuel Fact Sheet. Available at: https://www.iata.org/contentassets/25e5377cf53c4e48bbaa49d252f3ab03/fact-sheet-fuel.pdf.

International Air Transportation Association (2021). Net-Zero Carbon Emissions by 2050. *2021 Press. Releases*. Available at: https://www.iata.org/en/pressroom/2021-releases/2021-10-04-03/ (Accessed May 6, 2021).

International Civil Aviation Organization (2020). Carbon Offsetting and Reduction Scheme for International Aviation (CORSIA). Available at: https://www.icao.int/environmental-protection/CORSIA/Documents/CORSIA_FAQs_December 2020_final.pdf.

International Civil Aviation Organization (2021). SAF Rules of Thumb. *Environ. Prot*. Available at: https://www.icao.int/environmental-protection/Pages/SAF_RULESOFTHUMB.aspx (Accessed November 9, 2021).

LanzaJet (2021). Georgia - Freedom Pines Fuels. *Where We Oper*. Available at: https://www.lanzajet.com/where-we-operate/#georgia (Accessed August 25, 2021).

Martinez-Valencia, L., Garcia-Perez, M., and Wolcott, M. P. (2021). Supply Chain Configuration of Sustainable Aviation Fuel: Review, Challenges, and Pathways for Including Environmental and Social Benefits. *Renew. Sust. Energ. Rev.* 152, 111680. doi:10.1016/j.rser.2021.111680

Merrow, E. W., Phillips, K., and Myers, C. W. (1981). *Understanding Cost Growth and Performance Shortfalls in Pioneer Process Plants*. Santa Monica, CA: RAND Corporation PP - Santa Monica, CA. Available at: https://www.rand.org/pubs/reports/R2569.html.

Moriarty, K., Milbrandt, A., and Tao, L. (2021). *Port Authority of New York and New Jersey Sustainable Aviation Fuel Logistics and Production Study*. United States. doi:10.2172/1827314Port Authority of New York and New Jersey Sustainable Aviation Fuel Logistics and Production Study

Oregon Department of Environmental Quality (2021). Clean Fuel Program Overview. *Oreg. Clean Fuels Progr*. Available at: https://www.oregon.gov/deq/ghgp/cfp/Pages/CFP-Overview.aspx (Accessed July 14, 2021).

Pavlenko, N., Searle, S., and Christen, A. (2019). The Cost of Dupporting Alternative Jet Fuels in the European Union. Available at: https://theicct.org/sites/default/files/publications/Alternative_jet_fuels_cost_EU_20190320.pdf.

Peters, M. S., Timmerhaus, K. D., and West, R. E. (2003). *Plant Design and Economics for Chemical Engineers*. 5 th. New York, NY: McGraw-Hill.

Petsonk, A. (2020). *ICAO Council Bows to Aviation Industry Request to Rewrite First Three Years of Climate Program Rules*. Press release Arch. Washington, DC: Environmental Defense Fund. Available at: https://www.edf.org/media/icao-council-bows-aviation-industry-request-rewrite-first-three-years-climate-program-rules (Accessed October 28, 2021).

Port of Seattle; Washington State University (2020). Potential Northwest Regional Feedstock and Production of Sustainable Aviation Fuel. *Seattle*. Available at: https://www.portseattle.org/sites/default/files/2020-08/PofSeattleWSU2019updated_appendix.pdf.

Red Rocks Biofuel (2021). Technology. Available at: https://www.redrockbio.com/ (Accessed August 25, 2021).

Reid, H. (2014). *Reid Announces $70 Million for Dulcrum BioEnergy. 2*. Available at: https://fulcrum-bioenergy.com/documents/2014-09-19ReidAnnouncesDoDGranttoFulcrumBioEnergy.pdf.

Renewable Energy Focus.com (2014). Red Rock Biofuel Wins $70 Million Grabt for Biomass Project. *Renew. Energ. Focus*. Available at: http://www.renewableenergyfocus.com/view/40077/red-rock-biofuels-wins-70-million-grant-for-biomass-project/.

Royal Netherlands Aeroespace Centre, and Amsterdam Economics (2021). Destination 2050: A Route to Net Zero European Aviation. Available at: https://www.destination2050.eu/wp-content/uploads/2021/02/Destination2050_Report.pdf.

Schill, S. R. (2013). Fulcrum Lands Phase 1 Defense grant for MSW-To-Jet Fuel Plant. *Ethanol Prod. Mag*. Available at: http://ethanolproducer.com/articles/9906/fulcrum-lands-phase-1-defense-grant-for-msw-to-jet-fuel-plant.

Schneider, B. S. (2021). *Sustainable Skies Act*. Washington D.C. House of Representatives. Available at: https://www.congress.gov/117/bills/hr3440/BILLS-117hr3440ih.pdf.

Skaggs, R. L., Coleman, A. M., Seiple, T. E., and Milbrandt, A. R. (2018). Waste-to-Energy Biofuel Production Potential for Selected Feedstocks in the Conterminous United States. *Renew. Sust. Energ. Rev.* 82, 2640–2651. doi:10.1016/j.rser.2017.09.107

Stratas Advisors (2020). Overcapacity Looms as More and More US Refiners Enter Renewable Diesel Market. *Insight*, 6. Available at: https://stratasadvisors.com/Insights/2020/06112020LCFS-RD-Investment (Accessed August 25, 2021).

Tanzil, A. H., Brandt, K., Wolcott, M., Zhang, X., and Garcia-Perez, M. (2021). Strategic Assessment of Sustainable Aviation Fuel Production Technologies: Yield Improvement and Cost Reduction Opportunities. *Biomass and Bioenergy* 145, 105942. doi:10.1016/j.biombioe.2020.105942

Tao, L., Tan, E. C. D., McCormick, R., Zhang, M., Aden, A., He, X., et al. (2014). Techno-economic Analysis and Life-cycle Assessment of Cellulosic Isobutanol and Comparison with Cellulosic Ethanol and N-butanol. *Biofuels, Bioprod. Bioref.* 8, 30–48. doi:10.1002/bbb.1431

The White House (2021). FACT SHEET: Biden Administration Advances the Future of Sustainable Fuels in American Aviation. *Statements and Releases*. Available at: https://www.whitehouse.gov/briefing-room/statements-releases/2021/09/09/fact-sheet-biden-administration-advances-the-future-of-sustainable-fuels-in-american-aviation/ (Accessed December 3, 2021).

U.S. Department of Energy (2021a). Alternative Fuel Excise Tax Credit. *Altern. Fuels Data Cent.* Available at: https://afdc.energy.gov/laws/319 (Accessed October 14, 2021).

U.S. Department of Energy (2021b). Biodiesel Laws and Incentives. *Altern. Fuels Data Cent.* Available at: https://afdc.energy.gov/fuels/laws/BIOD?state=US (Accessed July 22, 2021).

Wang, Z. J., Staples, M. D., Tyner, W. E., Zhao, X., Malina, R., Olcay, H., et al. (2021). Quantitative Policy Analysis for Sustainable Aviation Fuel Production Technologies. *Front. Energ. Res.* 9, 10. doi:10.3389/fenrg.2021.751722

Wolff, C., Soubly, K., Delasalle, F., and Pinnel, L. (2020). *Join Policy Proposal to Accelerate the Development of Sustainable Aviation Fuels in Europe*. Geneva, Switzerland. Available at: https://www3.weforum.org/docs/WEF_CST_Policy_European_Commission_SAF_2020.pdf.

World Energy (2021). The Future of Aviation. *Products*. Available at: https://www.worldenergy.net/products/sustainable-aviation-fuel-saf/ (Accessed October 20, 2021).

Author Disclaimer: The views and opinions expressed in this article are those of the authors and do not necessarily reflect the official policy or position of any corporation and any agency of the U.S. government.

Conflict of Interest: The authors declare that the research was conducted in the absence of any commercial or financial relationships that could be construed as a potential conflict of interest.

Publisher's Note: All claims expressed in this article are solely those of the authors and do not necessarily represent those of their affiliated organizations, or those of the publisher, the editors, and the reviewers. Any product that may be evaluated in this article, or claim that may be made by its manufacturer, is not guaranteed or endorsed by the publisher.

frontiers in Energy Research

ORIGINAL RESEARCH
published: 10 March 2022
doi: 10.3389/fenrg.2022.771325

Advanced Fuel Property Data Platform: Overview and Potential Applications

Simon Blakey[1,2]*, *Bastian Rauch*[3], *Anna Oldani*[4,5] *and Tonghun Lee*[4]

[1]Department of Mechanical Engineering, University of Birmingham, Birmingham, United Kingdom, [2]Department of Mechanical Engineering, University of Sheffield, Sheffield, United Kingdom, [3]DLR, German Aerospace Center, Institute of Combustion Technology, Cologne, Germany, [4]Department of Mechanical Science and Engineering, University of Illinois at Urbana-Champaign, Champaign, IL, United States, [5]Current affiliation, Federal Aviation Administration, Washington, D.C., United States

OPEN ACCESS

Edited by:
Michael P. Wolcott,
Washington State University,
United States

Reviewed by:
Richard Herbert Moore,
Langley Research Center, National Aeronautics and Space Administration (NASA), United States
Jonathan Lloyd Male,
Pacific Northwest National Laboratory (DOE), United States

***Correspondence:**
Simon Blakey
s.g.blakey@bham.ac.uk

Specialty section:
This article was submitted to Bioenergy and Biofuels, a section of the journal Frontiers in Energy Research

Received: 06 September 2021
Accepted: 28 January 2022
Published: 10 March 2022

Citation:
Blakey S, Rauch B, Oldani A and Lee T (2022) Advanced Fuel Property Data Platform: Overview and Potential Applications. Front. Energy Res. 10:771325. doi: 10.3389/fenrg.2022.771325

This report outlines the establishment of distributed databases for management and integration of current and future aviation fuels. Aviation fuel property and performance data has been gathered for many years in public and company specific fuel surveys. These surveys are suitable for use as overall quality control information and for monitoring changes and trends in the fuels in used for flight. In recent years, significant data has been generated for alternative fuels as part of the due diligence of their approval for use through ASTM D4054, including those outside of the specification. Recently, this data, along with fundamental chemistry data has led to the creation of the Fast Track route for fuels approval when the fuel is constrained to a necessarily narrowly defined composition. The data behind these developments are often stored in a disparate, unindexed way, resulting in their underutilisation for a range of research, engineering design, specification, and in service quality control applications. To make the best use of this data, we present a scalable, Json based format for the storing of fuels data. This concept has been proposed by the Horizon 2020 Jet Fuel SCREENing and Optimization (JETSCREEN) project in conjunction with the Center of Excellence for Alternative Jet Fuels and Environment (ASCENT) programme. We have worked collaboratively to develop a joint database which currently contains data from around 30,000 conventional and 400 alternative fuels/fuel blends from a range of European and United States of America (U.S.) lead research programmes and data sources. This database can be used for a variety of purposes, both in conjunction with, or in isolation of commercially sensitive data with a greater degree of restriction. We present a number of test cases for how we see this model for data storage could be used for the benefit of all. We invite further suggestions as to how this approach could be used and welcome opportunities to work with the wider fuels community to develop this idea further.

Keywords: aviation fuel, alternative fuels, fuels approval, database, fuel properties

INTRODUCTION

The civil aviation sector has spent much of the last 60 years optimizing the design of aircraft and engines to reduce fuel consumption, lower CO_2, noise and NO_x emissions. The sector has had significant success in this undertaking, however during this period the composition and properties of aviation fuel have been treated as a bought in commodity, and have essentially remained unchanged. This has meant that the sector has been optimizing changes to the fuel systems in aircraft and ground handling hardware around a range of average, or for specific properties, the worst case fuels available.

These conventional fuels, coming from sources identified in **Section 4** of the DEFSTAN 91-091 (Ministry of Defence 2016) and Section 6.11 of the ASTM D 1655 (ASTM International 2020) are: "Aviation turbine fuel, except as otherwise specified in this specification, shall consist predominantly of refined hydrocarbons derived from conventional sources including crude oil, natural gas liquid condensates, heavy oil, shale oil, and oil sands." These fuel types are seen as those suitable for gas turbine powered aviation and as long as these sources produced fuel which met the specification, they were permitted to be used, regardless of the actual hydrocarbon chemical composition and performance properties of the fuel. In addition to the hydrocarbons, the specification places requirements on the cleanliness of the fuels and the concentrations of hetroatomic species, metal and water content. These fuel sources have not significantly changed since the beginnings of the jet age, and as such is the "Jet A-1 everybody knows," based on accumulated experience. This means that much of the risk in the use of these fuels is mitigated through the use of this experience and trusted, standardized specification measurements used in the above standards, and the standards represent a batch certification of the fuel as safe for flight.

Throughout this period, fuel user groups have carried out surveys of fuel quality based around the available fuel property data as part of the Jet A-1 specifications, and this data has been reported in regional and global fuels surveys. Key examples are those carried out by the United Kingdom MoD (later the Energy Institute) (Energy Institute and QinetiQ 2014) and the Petroleum Quality Information Service (PQIS) annual reports (The Defense Energy Suppor 2009), amongst others, which report the variability of fuel in use currently. This data is limited, in the extent that it reports the specification performance of the fuel to the above standards without detailed information of the chemical composition of the fuel. As the PQIS survey includes a wider range of fuels for applications outside of aviation, it also contains additional data such as H/C ratios and Cetane index results. These survey reports are supported by the beyond specification information provided by the CRC world fuels survey (Hadaller and Johnson, 2006). And the CRC Aviation Fuel Handbook (Coordinating Research Council 1983), which is a valuable and commonly used reference within the industry, despite it representing Jet A-1 fuel by a single line, as shown as shown in **Figure 1** along with the range of fuels within fuel surveys (Coordinating Research Council 2014). These combined data are invaluable in assessing what fuel is being flown on at the present time and also in keeping track of the longer term trends in fuel quality over time. The information captured in these reports is of great importance to the sector, however, it is often contained in paper based reports, or the electronic equivalent (such as pdf files), which limits its usefulness to the sector as a tool to assess the "fit" of any alternative fuel, or indeed any conventional fuel from a novel source.

During a brief period at the beginning of the 1980's and a more sustained manner since the early 2000's an increasing range of alternative fuels have been proposed which, following thorough testing, have been demonstrated to be technically suitable for use in civil aviation, and approved for use through the ASTM D4054 process (ASTM 2020). These fuels include Sustainable Aviation Fuels (SAFs) which are produced from sustainable sources. Importantly the sustainability criteria for SAF are not assessed in the D4054 process, which is exclusively a technical suitability assessment. These fuels have been assessed in a far more technically rigorous way than those fuels derived from fossil sources highlighted above. The D4054 is a robust process, and one which follows a strict management of change in the expansion of fuel sources away from the "Jet A-1 everybody knows." Unfortunately, at present, much of this technical information is stored in reports and files in a way which makes the data very hard to access and use. As such there is a risk that this valuable information is not being used to accelerate the screening of any future candidate fuel, or in the assessment of engine and airframe performance with modified fuel properties.

METHODOLOGY

Common Philosophy

The Horizon 2020 Jet Fuel SCREENing and Optimization (JETSCREEN) (Rauch 2020) and Center of Excellence for Alternative Jet Fuels and Environment (ASCENT) (altjetfuels 2015) projects had both independently proposed methods for increasing the usefulness of this information through a common data schema, an online source for data respectively. The projects identified an opportunity through the publically funded work to share data. As part of this opportunity, it was necessary to develop a common philosophy for the storage and use of data. This paper details this common philosophy and goes on to present some examples of usage in the hope that future discussions develop these ideas further.

The overarching concept of the JETSCREEN database project is to make available the public data generated in previous research activities and in the current JETSCREEN project, in a form that is human readable and can therefore be used to produce statistical and comparative analysis of any candidate fuel. It is envisaged that this assessment can streamline some of the early screening processes of the D4504 process for fuel approval, as captured by the "Tier Zero" or "Tier Alpha" concepts presented by JETSCREEN and the FAA (Heyne et al., 2021). This dataset will start with the chemical hydrocarbon composition of the fuel, using a method such as GCxGC to identify the molecular families of molecules present in the fuel, the specification properties and fit for purpose data required for approval, but will go onto include

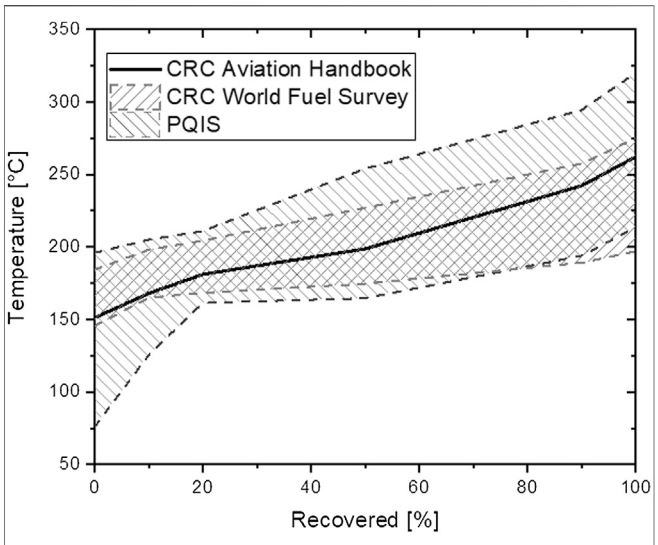

FIGURE 1 | Comparison of CRC Aviation Fuel Handbook typical Jet A-1 distillation vs range of data from CRC World Fuel Survey and PQIS.

more diverse data on a fuel's behavior during the course of the JETSCREEN project. Importantly, where data already exists in the public domain, a candidate fuel can be compared to the fuels already in use, those approved, and importantly those not approved and help to develop structure-property relationships for molecules in jet fuel.

Where possible, the database will provide information which can be used to develop and validate statistical, empirical and fundamental models linking the chemical and compositional details of a fuel to its specification and performance properties. Importantly, it should also be possible to use the models developed through this process to predict compositional information based on desired performance properties. This is an active area of research and many sources of data and analysis studies have been made using available fuel property data (Dryer et al., 2014; Moses 2017; Heyne et al., 2019; Heyne et al., 2022) amongst many others.

As such the database proposed can provide a single knowledge base of fuels which are in use today, have been through the approvals process and those from the research community where data is available. This approach will provide significant gearing for the use of this data in the assessment and screening of candidate fuels in the future particularly if the users can determine the quality control on the uploaded data, an oversight role that the authors currently perform for their respective databases. In the preparation of this work, it became clear that the database could have significant uses beyond fuel pre-screening and should be of interest to the wider aviation fuels community as a resource for conducting any fuel related monitoring and development studies. This schema provides a structure for open science and the sharing of data which encourages advancement and the rapid adoption of new technologies in the field of fuel properties by promotes diverse, just and sustainable outcomes for all stakeholders (Grahe et al., 2020).

Data Schema

The sharing of data is limited to that data which is available in the public domain. Clearly, many datasets are private and not available for sharing, however if they share a common file storage schema or format, the results of these datasets may be rapidly integrated to provide the user a more statistically significant set of fuels data within individual organizations. The current joint database between JETSCREEN and FAA is based on such a common storage schema, where non-proprietary data is shared through a common cloud server as shown in **Figure 2**. Both JETSCREEN and FAA can access this server automatically to upload and download data through an hourly or daily sync process.

Shared data is stored using a mongo DB database structure using a common standard JavaScript Object Notation (.json) format. This formatting is beneficial as it is an unstructured method for storing data and can incorporate a high degree of flexibility whilst providing a standard, human readable format which can also be easily interpreted by computer code. A live schema for fuel data storage is maintained by the JETSCREEN consortium at the following URL: https://github.com/JETSCREEN-h2020/FuelDatabase/wiki/JETSCREEN-Schema-philosophy.

The schema of a database is the organization of data i.e. how a database or the data exchange file is constructed. At this URL, the organization of fuel data in the form of a JSON file is described. The structure presented here is version 2.0 of the data schema.

The data schema is a living document and will grow and mature with the projects and its use. As such, the current documentation will not be listed in this paper, however, links to a github site which provides access to the latest version will be embedded into the document. An example of the current schema is shown in **Figure 3**.

The basic schema of fuel data is divided into three parts:

(1) A Header section: with metadata about the fuel and authors. (https://github.com/JETSCREEN-h2020/FuelDatabase/wiki/Header).
(2) Composition section: example aromatics, contaminants etc (https://github.com/JETSCREEN-h2020/FuelDatabase/wiki/Composition).
(3) Properties section: like acidity, distillation, flash point, etc (https://github.com/JETSCREEN-h2020/FuelDatabase/wiki/Properties).
    - Use issues

(1) Conventions.
    - https://github.com/JETSCREEN-h2020/FuelDatabase/wiki/Convention

(2) Data quality.
    - https://github.com/JETSCREEN-h2020/FuelDatabase/wiki/Data-Quality

Data Sources

The principle sources of published data used in this dataset are a combination of survey results of conventional fuels in service today, research reports and publications on alternative fuels. The major drawback of the fuels survey results is that they contain

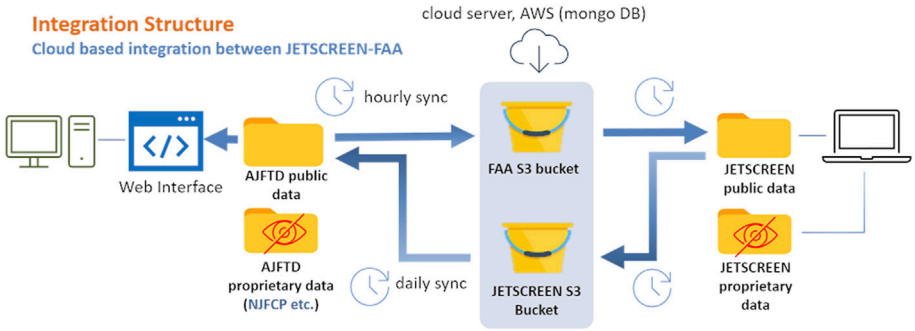

FIGURE 2 | Overview of database integration between JETSCREEN and FAA


```
,,
"property": {
    "acidity_total": [
        {
            "test_method": "D3242",
            "unit": "mg KOH/g",
            "value": 0.001
        }
    ],
    "distillation": [
        {
            "test_method": "D86",
            "volume_evaporated_unit": "%",
            "volume_evaporated_value": 0.0,
            "unit": "C",
            "value": 147.9
        },
        {
            "test_method": "D86",
            "volume_evaporated_unit": "%",
            "volume_evaporated_value": 10.0,
            "unit": "C",
            "value": 163.7
        },
        {
```


FIGURE 3 | Excerpt of the standardised fuel property schema showing the formatted structure of the data recorded including fuel meta data.

little or no information regarding the chemical composition of the fuel. There are many thousands of unique fuels across these published data sources which can be integrated into a common database and, their inclusion gives the database and any user an understanding of in service fuel quality. This is significantly more valuable than an understanding based on a single baseline fuel and its associated performance properties. Importantly, this data should be stored on file as specific properties of a single fuel, and not as statistical averages of fuel properties.

The AJFTD contains a vast library of information relevant to the alternative jet fuel industry and is accessible via https://www.altjetfuels.illinois.edu/. While its main feature is its library of over 25,000 different samples of domestic and internationally sourced fuels, other data categories available include documents on chemical kinetics mechanisms, aviation emissions, relevant publications and literature, and experimental testing results. Alternative fuels from all Annexes of the ASTM D7566 specification are represented in the database. The fuel data represents a variety of manufacturers, and all data was acquired from five main sources: Metron Aviation, the National Jet Fuel Combustion Program (NJFCP), Air Force Research Laboratory (AFRL), Naval Air Systems Command (NAVAIR), and the European program JETSCREEN.

Table 1 below outlines a sampling of fuels from AFRL, available on the AJFTD website. This table demonstrates the breadth of fuel types available to users, from a wide range of fuel types to a variety of fuel manufacturers. The selected property and composition categories included in the table are included to exemplify the potential range and variability of fuel properties and compositions observed between different fuels, variability which in some cases spans a large range of acceptable property or composition limits as outlined by ASTM D7566 standards. This kind of variability underlines the usefulness of a centralized, extensive database in elucidating the degree of the aviation fuel industry's heterogeneity, especially considering how ongoing development of new certification pathways will inevitably increase diversity in this arena.

Fuel data is often difficult to obtain from manufacturers due to policies protecting proprietary information. This leads to data gaps in the database. Fuel samples from the most recent Annexes to D7566 are not as well represented as older ones. Additionally, the acquisition of fuel data from a variety of sources inevitably leads to data sparsity and inconsistencies in data categories among different fuel samples. Critical next steps for the online database include ongoing database integration with international programs, interception of fuel samples from domestic airport supply chains, re-organization of the database structure to optimize navigation capability and interactive features, and the incorporation of data analysis tools like machine learning algorithms. These improvements will better equip the website for user adoption.

The well-established example of the risk associated with using average data rather than individual fuel data is the calculation of dynamic viscosity from the average density and kinematic viscosity of a fuel data set and the average dynamic viscosity from the individual densities and kinematic viscosities of all fuels in the dataset, as shown in **Table 2**. Although the average dynamic viscosities calculated by two methods are similar, the value calculated from the individual densities and kinematic viscosities also contains standard deviation

TABLE 1 | Examples fuels available on AJFTD website.

Fuel Type	POSF/AJFTD Name	Manufacturer	Aromatic Content [%vol]	Density [kg/m^3]
JP8	4751	N/A[a]	19.2	804
Jet A	10325	Shell	17.4	803
FT	5642	Sasol	0.7	762
FT	7629	Sasol	1.9	760
HEFA	5480	Syntroleum	0.6	762
SIP BLEND	50% SIP	N/A[a]	8.4	793
ATJ-SKA	ATJ-SKA	N/A	19.4	786
ATJ	7695	Gevo	0.0	760
ATJ BLEND	7700	Gevo	9.2	782
CH-SK	CH-Kerosene	N/A[a]	19.7	805
HC-HEFA	13784	IHI	0.0	782

[a]*Entries marked "N/A" denote information not available on the database.*

TABLE 2 | Example of error introduced by calculations based on average values from property databases.

	Calculated from individual densities and kinematic viscosities of all fuels in the dataset (Ns/m^2)	Calculated from average density and kinematic viscosity (Ns/m^2)
Minimum	0.001011	n/a
Maximum	0.002353	n/a
Standard Deviation	0.000236	n/a
Average Dynamic Viscosity	0.001426	0.001425

information which is missing in the conventional approach. This greater detail is important for a number of stakeholders and like **Figure 1**, reinforces the view that it is misleading to using average values for fuel properties. Engineers using these properties for their work should take into account the statistical information such as standard deviation calculated from a database of these properties.

The growing volume of data on the performance of alternative fuels provided through the research literature, D4054 reports and aviation fuels research projects such as JETSCREEN and the U.S. National Jet Fuel Combustion Program (NJFCP) (Colket and Heyne 2021) are more useful for the stated goals of the database, as they contain detailed compositional information as well as specification and performance data. However such data is much more sparse. Current estimations are that there are around 150–180 fuels with sufficient data from these programmes to be included at the start of this exercise. Included within these studies are a number of conventional fuels for which this additional analysis has been conducted, including GCxGC data and fit for purpose testing fuel specification properties, as well as fundamental combustion properties (Oßwald et al., 2021). This smaller sub-set of research fuels is very useful in bridging the gap between the larger, more statistically useful conventional fuel surveys and the more detailed datasets from research into fuel performance.

It is hoped that this schema can be adopted in future programmes and surveys so that fuel composition, specification and performance data can be presented in a truly interoperable way to integrate into existing and future tools and workflows. This level of adoption would greatly increase the usefulness of any fuel property data generated. In the following sections, several usage cases for this database are presented. It is fully envisaged that these usage cases can be expanded upon significantly by individual users with particular fuel data requirements.

APPLICATION

Screening and Safety

In line with the original objectives of JETSCREEN, the fuels stored in the fuels database can be used to compare the specification and performance properties of a new candidate fuel with the fuels present in the database, offering a rapid comparison with existing fuels and presenting the data in a graphically simple representation, easily understandable by the user. This is a method to assist the acceleration through the early stages of pre-screening and assist fuel producers with access to fuel property data [xi]. **Figure 4** shows a comparison of a 100% HEFA fuel from the E.U. project 308,807: Initiative Towards sustAinable Kerosene for Aviation (ITAKA), as represented by the individual data points for each property, the fuels used in the United Kingdom in 2014 (as represented by the whisker plots, showing the minimum, 1st quartile, mean, 3rd quartile and maximum value for each property) and the conventional fuel specification, in this case DEFSTAN 91-091 (dashed lines). It is clear that the candidate fuel would not comply with this specification as it is above the 50% blend limit, and is shown here for example as some of the properties of the fuel do fit within the specification without blending. This clearly shows the areas where the candidate fuel is within the specification (indicated by a green colour), with the

ITAKA HEFA fuel

Fuel specification	Min	Max	Fuel Sample
Colour			30
Acidity (mg KOH/g)	0	0.015	0.002
Aromatics IP 156 (%vol)	0	25	1.8
Sulphur (%mass)	0	0.3	0.018
Mercaptan (%mass)	0	0.003	0
IBP (degC)			148.8
10% (degC)		205	169.8
50% (degC)			198.7
90% (degC)			235.1
FBP (degC)		300	251.9
Flash point (degC)	38		41.5
Density @15degC (kg/m3)	775	840	759.6
Freezing point (degC)		-47	-59
Viscosity @-20degC (cSt)	0	8	3.885
Smoke point (mm)	5		50
Naphthalenes (%vol) if SP > 25mm		3	0
Specific Energy (MJ/kg)	42.8		44.023
Existent Gum (mg/100 ml)		7	1
MSEP	85		99

Survey data from EI - The Quality of Aviation Fuel Available in the Untied Kingdom Annual Survey 2014

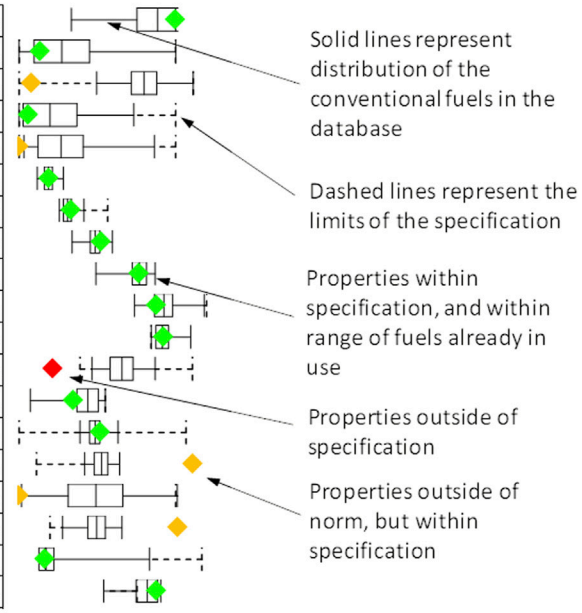

FIGURE 4 | Example comparison of candidate novel fuel to conventional fuels database and DEFSTAN 91-091 specification limits: Highlighting areas of concern for any fuel approval.

Hydrocarbon group	Fuel Sample (%m/m)
n-P	19.48
i-P	71.35
N	6.58
Di-N	0.08
mAr	1.91
NmAr	0.59

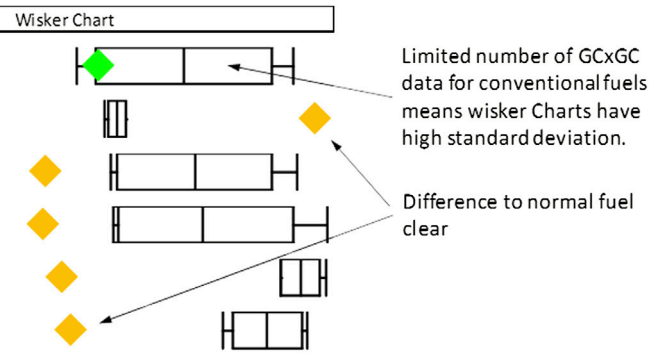

FIGURE 5 | Example comparison of candidate novel fuel to limited conventional fuels CGxCG database: Highlighting areas of concern for any fuel approval.

specification but outside the norm for conventional fuels (indicated in orange) and where the specific property is outside the specification, (indicated in red). For this candidate fuel, it is immediately obvious that the only real spec failing would be the density of the fuel. This is due to the low levels of aromatics present in the ITAKA product. Although the other specification properties are still within the specification, they are well outside of the norm–specifically, low aromatics, low sulfur, high smoke point and high calorific value. In many respects, this understanding is implicit for the fuels experts of the aviation sector. However, as the number of fuel producers increases with the various feedstocks proposed to produce aviation fuel from unconventional sources, it is necessary to communicate the particular requirements of the aviation specifications to an increasingly wider audience. For such information sharing, simply understood graphics such as the whisker comparison plots, and a traffic light colour scheme are essential.

Also **Figure 5** shows a comparison of the GCxGC composition of the fuel compared with the limited range of conventional fuels already in the database. This comparison also shows clearly where the ITAKA fuel is outside of the norm. Importantly, as there are

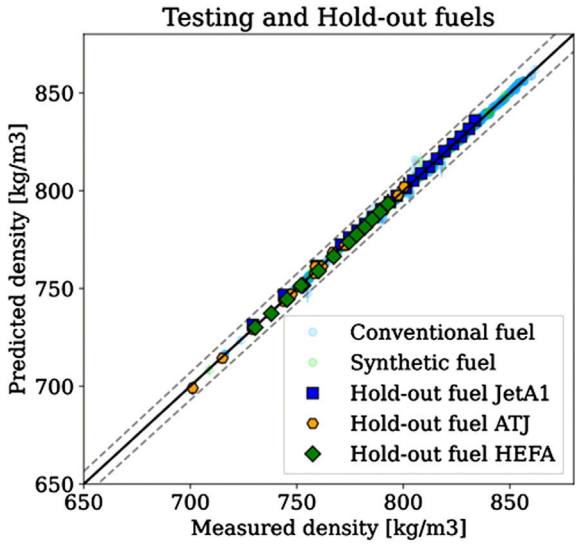

FIGURE 6 | Unity plot displaying the predictive capability of machine learning models for synthetic fuels compared with data from the fuels database (Hall et al., 2021).

no specification limits for a GCxGC composition, therefore there are no returned red data points.

Both **Figure 4** and **Figure 5** can be used to consider the maximum acceptable blending ratio of SAF with conventional fuels, indicating that for most properties, there would be a large variation in acceptable blend depending on the conventional blendstock specification results DEFSTAN 91-091 for specification limits.

Engineering and Science

It is envisaged that as the uptake of SAF increases, the usefulness of such fuels data will increase as there will be a slow drift in fuel specification properties over time as greater volumes of SAF are blended with conventional fuels. In order for this process to be properly monitored and controlled, availability of specific fuel by fuel data will be required in order to exploit the largest benefit from the SAF.

In addition, a common fuel schema and database could allow a quicker identification of specific fuel properties if further investigations are required into following a fuel related system or component failure in the supply system or on-board.

Access to larger datasets of specification and further fit for purpose properties of fuels in a common format would greatly enhance the ability of engineers and scientists to perform analysis of fuel behaviour and performance, increasing the understanding of the link between fuel composition and fuel performance.

This would also facilitate the development and validation of statistical and more fundamental models of fuel properties adding to the chemo-informatics tools which are being developed to assist in the early screening of candidate fuels for the approvals process. This can also be used to enhance the development and production of alternative fuels, particularly in using these developed tools to point towards optimum fuel compositions for performance in flight.

The statistical analysis and feature detection for aircraft related fuel properties can facilitate the design of aircraft components impacted by the fuel performance. As optimisation of the engine and airframe continue further, the fuel systems are likely to become increasingly sensitive to changes in fuel composition. Therefore access to fuels data which are easily integrated into design tools would improve the workflows of the design process.

This dataset is already in use within the JETSCREEN project to develop and validate machine-learning and other tools to predict important fuel specifications and performance characteristics as shown by the example in **Figure 6**, showing the prediction of fuel density from the GCxGC compositional results alone for a wide range of different aviation fuels (Hall et al., 2021). The term hold-out is used to indicate data used for assessing the machine learning model after the training step has been completed. Furthermore, as considerable amount of data is available for conventional and synthetic fuels, the predictive capability (accuracy, prediction uncertainty and model reliability) of models can be assess systematically over the potential application domain.

Figure 7 shows a comparison of a range of fuels from the ASCENT database, looking for correlations between fuel compositions and emissions performance. This shows the suggestion of correlations between Smoke Point and DCN, but more significantly between Smoke Point and H/C ratio. Such correlations can be made for any select group of fuels, and efforts are being made to adapt machine learning techniques for both understanding of correlation between various properties and also using this relation to impute missing property data of fuels.

For integration of advanced ML strategies, an effort is being made to convert much of the property data to a CSV format. In the future, analysis of the data using advanced techniques will also be available for download directly from the website using a similar format. The presentation of fuel data in a universal format will allow the information to be read by multiple software using an appropriate script to create tailored, reproducible output for specific user needs.

System Operations

As a consequence of improved access to specific fuels data, there are possibilities in terms of improving the quality control and tracking of fuels in use: through the processing and production of the fuel, through the supply chain and to its end use. The fuel data is currently transferred through the system using the quality assurance certificates, which then need to be manually integrated into fuel surveys or modelling tools. If the data were stored in a common electronic schema or format and processed into a quality document at the point of need, it would increase the flexibility of this data.

The availability of this data in an interoperable format will be of benefit for both airports and airlines. It will simplify the gathering of evidence to demonstrate the safe usage of SAF with detailed supply information. It is hoped that this will build trust between producers, suppliers and consumers. Finally, the common electronic schema for fuels data

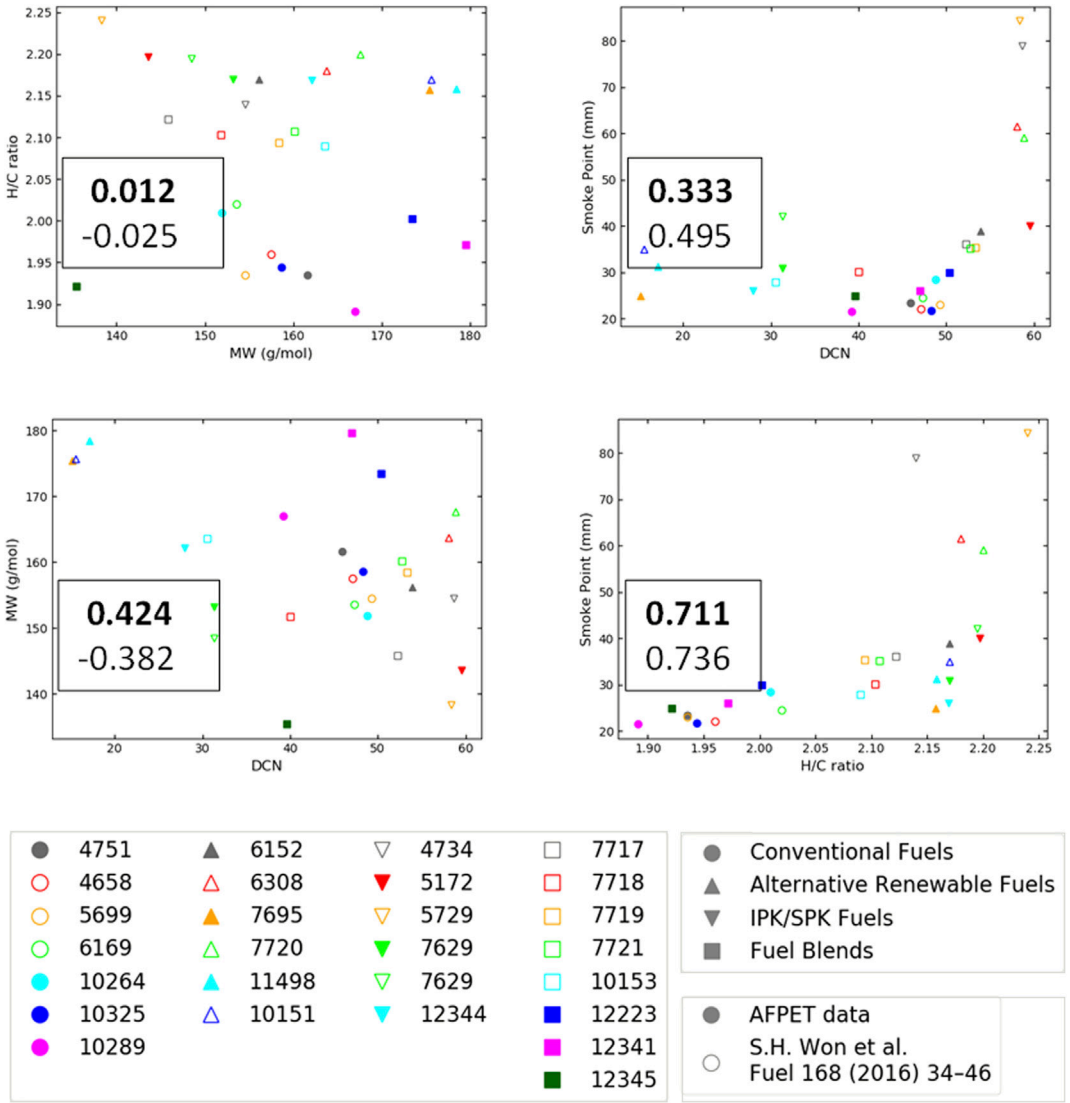

FIGURE 7 | Searching for correlations of fuel properties to emissions performance linking to specific fuel compositional families (indicating the R^2 correlation coefficient: bold type set indicates solid data points, regular type set indicates hollow data points), clockwise from top left, molecular weight vs hydrogen/carbon ratio, DCN vs smoke point, smoke point vs H/C ratio and DCN vs molecular weight.

throughout the supply chain will expand the availability of operational data and increase systems optimisation across the industry.

For just the fuel specification properties, the size of the required .json file is around 5 kB, which grows significantly if beyond specification fuel composition and performance properties are considered. Unfortunately this is larger than the data which can be stored within a QR code (3 kB), however key fuel properties could be stored within a QR code for a specific batch of fuel along with a hyperlink to a complete fuel .json file which could be considered a digital twin of the fuel, travelling through the fuel system. This type of fuel information would be of great usefulness for the community in the future. As it would facilitate effective fuel blending (especially for high blending ratios) and informing the airline operator and pilots about the actual fuel in use.

Figure 8 shows the analysis of results from the METRON program in the U.S. (https://altjetfuels.illinois.edu/), which was a survey of fuels from the U.S. domestic airports as part of the ASCENT program. **Figure 8** shows the change in fuel properties with location, the trend in aromatics level across a single year as well as longer term trends at individual locations for specific fuel properties. For these results, it is clear that the overall average aromatic content is slightly less than 16%, which when blended at 50% with HEFA SAF would give a value to just satisfy the 8% minimum aromatic content requirement since aromatics content

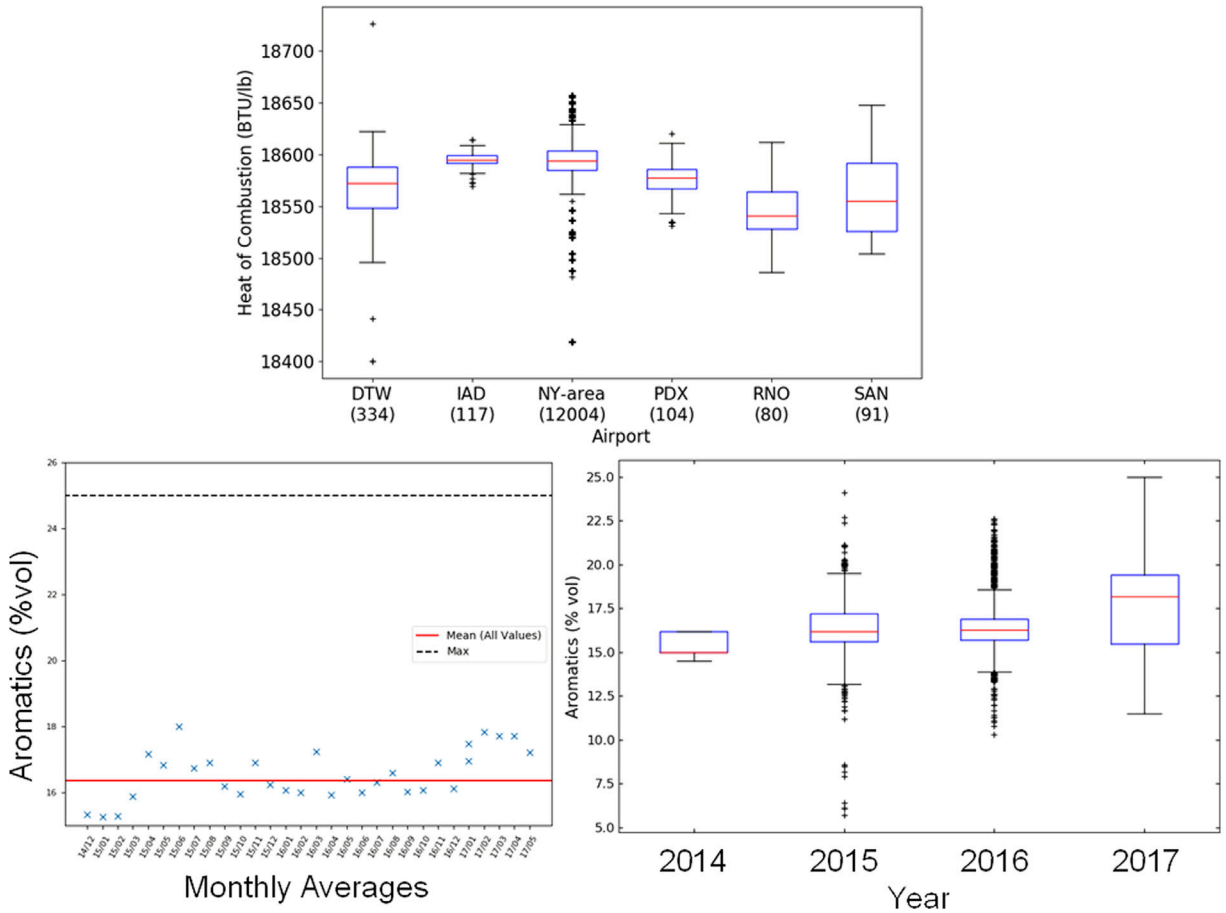

FIGURE 8 | Collated data from the U.S. Domestic Airport data sampling program, METRON–change in fuel properties by airport, over time (single year) and long term trends.

requirement since aromatic content shows linear blending properties.

This does also suggest that if sufficient volumes of SAF are available for higher than 50% blending, then higher blend ratios of SAF could be achievable for higher aromatic conventional fuels whilst still complying with the minimum aromatic content of 8%. This fuel would currently be out of the specification limits, whilst still complying with the fuel normal behaviour as suggested in **Figure 4**. With the currently available data and operational processes, it is most likely that fuel suppliers will be more conservative than this maximum blending ratio–for example, a 30:70 blend would ensure that the fuel always meets the specification, accounting for variability in the conventional fuel aromatic content assuming no information regarding the actual aromatic of the conventional fuel is available. If more knowledge of specific fuel composition were to be more readily available, say as part of the fuel supply then such a decision could be justified in the future. In order to reduce any risks associated with reaching the limits of the specification for this fuel property a more complete understanding of the aromatic components of the fuel is required. The composition of the aromatic portion of the fuel will also impact the fuel performance and is an area of current and future research.

DISCUSSION

The availability of specific fuel data is increasingly important in the current climate for aviation fuels. A significant amount of data is already available and is currently of a low level of utilisation due to the formatting of the data which lowers its impact. This is particularly the case for the data of fuel surveys which unfortunately means that it is possible for fuel related decisions are made without full knowledge of the current range of fuels in used in service and an over reliance on "average" fuel properties. This can be addressed by the methods presented in the current paper and this is presented with some usage cases.

In the future there is likely to be a further need for fuel specific data which can be provided by a Digital Twin of the fuel as it travels through the fuel system. For example, more detailed knowledge of the exact density, aromatic content and calorific volume of fuel uploaded onto aircraft can remove the need for calculating conservative estimates of fuel requirements for particular flight missions. This operational change could result in a reduction in fuel burn and consequently CO_2 emission during flight as well as

improved understanding of fuel impact on emissions and non-CO_2 impacts on a specific flight mission (Voigt et al., 2021). As the levels of SAF increase, it will become important for ascribing environmental impact from particular flights ultimately as part of the ICAO Carbon Offsetting and Reduction Scheme for International Aviation (CORSIA). Indirect changes in the CO_2 emissions of flight such as the example cited above due to the fuel properties will need to be taken into account to avoid the unnecessary consumption of aviation fuels.

Currently the CORSIA certification model does not have any fuel type specification details. Although this is perhaps not envisaged for the early stages of CORSIA, it is something that will be needed for the full monitoring and control of environmental impact as the levels of SAF increase. In addition, the non-CO_2 impact of the uptake of SAF will need to be properly accounted for.

This schema system is intended to be as flexible as possible for integration into an unstructured database for carrying out queries and searches of the database. The database can be extended to include fuel production information, where publically available, and specifically for environmental impact, the life cycle assessment performance of particular fuel production processes.

The reliability any conclusions drawn from the use of such databases is a function of the quality of information provided in the fuel database .json files. Much of the data is built on the fuel specification results of D1655 and DEFSTAN -091 91 for which experimental methods are standardised and whilst may not be as accurate as research methods for determining fuel properties, they are consistent and can be used for comparison across very large datasets. A positive case in point is the distillation standard D86, which is a simple distillation process which has known short comings, but is very repeatable across fuel laboratories and facilities. A less positive case would be the Smoke Point results, which have been shown to be highly stratified by the fidelity of the experimental set up in D1322, and influenced by the 25 mm cut off for the requirement of Naphthalene testing.

Nonetheless, the inclusion of performance data from fit for purpose or in service testing would be more susceptible to repeatability issues across different laboratories. Due to the unstructured nature of the .json format, it would be possible to ascribe meta data to any fuel property indicating a level of confidence in the recorded data. This would be essential to allow the data to be treated with an appropriate level of confidence.

There is an increasing desire to track individual fuels through the supply system particularly in terms of ensuring quality control as the fuel passes through the system. Having access to the specific fuel digital twin as well as the specification information of the fuels in the supply system at the same time would allow the assessment of any cross contamination or blending issues in a much more flexible and scalable manner than with previous systems.

In the current state of the databases, the overseers of information quality are the authors of this manuscript. As this database develops further, one approach would be for the data to be overseen by an independent body similar to those that already host fuel property data. Alternatively, the data could be maintained using a Block Chain approach, removing the need for a single central authority. Through the approaches the authors are making to share data across servers, the database is approaching the position of a leger of "blocks" of data across many servers which should ensure data integrity. However, careful consideration needs to be given to this step, were it to be taken.

CONCLUSION

The concept of a shared data schema allows fuels data to be far more flexible in the future. A feature that is important for a developing multi stakeholder fuel and SAF industry. This paper presents an interoperable and scalable method for the sharing of such data. This work initially was focused on supporting the early stages of fuel pre-screening, however it has quickly become apparent that the system proposed could make fuel by fuel data available to be utilised for a wide range of usage cases.

A graphical visualisation method to simplify the complex data in the fuel specifications into a format that can be easily interpreted by eye is presented, and can be used for communication of a range of otherwise complex comparisons between specific fuels and the average and specification limits of performance.

The supporting material provided with this paper provide an initial toolset for users to develop their own datasets and the authors would be encouraged by feedback or suggestions as to how the usage set could be expanded in the future.

It would be recommended that future publicly funded fuels research programmes adopt the schema for the recording of their fuels data as part of their data management plans. This will ensure the interoperability of data in future.

The next steps in developing this approach are sharing a common schema and establishing a platform for data sharing along with a protocol for the addition of similar databases in the future. There is significant demand for a public dataset particularly for SAF which the JETSCREEN and ASCENT projects will both be releasing in their own programmes. It is important to not to lose the benefit of conventional fuels data. The monitoring of the impact of the uptake of SAF is also an important process the database approach can support.

DATA AVAILABILITY STATEMENT

The raw data supporting the conclusions of this article will be made available by the authors, without undue reservation.

AUTHOR CONTRIBUTIONS

SB, TL, BR and AO contributed to conception and design of the study. SB, TL and BR organized the databases. SB, BR and AO performed the statistical analysis. SB wrote the first draft of the manuscript. SB, TL, BR, and AO wrote sections of the manuscript. All authors contributed to manuscript revision, read, and approved the submitted version.

FUNDING

The research presented in this paper has been performed in the framework of the JETSCREEN project (JET fuel SCREENING and optimization) and has received funding from the European Union Horizon 2020 Programme under grant agreement n°723525. This research was also funded by the U.S. Federal Aviation Administration Office of Environment and Energy through ASCENT, the FAA Center of Excellence for Alternative Jet Fuels and the Environment, project 033 through FAA Award Number 13-C-AFJE-UI-015 under the supervision of Cecilia Shaw. Any opinions, findings, conclusions or recommendations expressed in this material are those of the authors and do not necessarily reflect the views of the FAA.

REFERENCES

altjetfuels (2015). Federal Aviation Administration National Alternative Jet Fuels Test Database. Available at: https://altjetfuels.illinois.edu/.

ASTM (2020). *D4054-20c, Standard Practice for Evaluation of New Aviation Turbine Fuels and Fuel Additives*. West Conshohocken, PA: ASTM International.

ASTM International (2020). *D1655-20a, Standard Specification for Aviation Turbine Fuels*. West Conshohocken, PA: ASTM International.

Colket, M., and Heyne, J. (2021). *Fuel Effects on Operability of Aircraft Gas Turbine Combustors*. Reston: AIAA. doi:10.2514/4.106040

Coordinating Research Council (1983). *Handbook of Aviation Fuels Properties*. Alpharetta, GA: CRC.

Coordinating Research Council (2014). *Coordinating Research Council Inc.* ALPHARETTA, GA 30022, Report No. 663, Aviation Fuel Properties Handbook 4th Ed.

Dryer, F. L., Jahangirian, S., Dooley, S., Won, S. H., Heyne, J., Iyer, V. R., et al. (2014). Emulating the Combustion Behavior of Real Jet Aviation Fuels by Surrogate Mixtures of Hydrocarbon Fluid Blends: Implications for Science and Engineering. *Energy Fuels* 28 (No. 5), 3474–3485. doi:10.1021/ef500284x

Energy Institute; QinetiQ (2014). *The Quality of Aviation Fuel Available in the United Kingdom Annual Survey 2014*. London: Energy Institute.

Grahe, J. E., Cuccolo, K., Leighton, D. C., and Cramblet Alvarez, L. D. (2020). Open Science Promotes Diverse, Just, and Sustainable Research and Educational Outcomes. *Psychol. Learn. Teach.* 19 (1), 5–20. doi:10.1177/1475725719869164

Hadaller, O. J., and Johnson, J. M. (2006). *Coordinating Research Council Inc.* ALPHARETTA, GA 30022, Report No. 647, World Fuel Sampling Program.

Hall, C., Rauch, B., Bauder, U., Le Clercq, P., and Aigner, M. (2021). Predictive Capability Assessment of Probabilistic Machine Learning Models for Density Prediction of Conventional and Synthetic Jet Fuels. *Energy Fuels* 35, 2520–2530. doi:10.1021/acs.energyfuels.0c03779

Heyne, J., Bell, D., Feldhausen, J., Yang, Z., and Boehm, R. (2022). Towards Fuel Composition and Properties from Two-Dimensional Gas Chromatography with Flame Ionization and Vacuum Ultraviolet Spectroscopy. *Fuel* 312, 122709. doi:10.1016/j.fuel.2021.122709

Heyne, J., Opacich, K., Peiffer, E., and Colket, M. (2019). "The Effect of Chemical and Physical Fuel Properties on the Approval and Evaluation of Alternative Jet Fuels," in 11th U.S.National Combustion Meeting, Pasadena, CA, March 24-27, 2009.

Heyne, J., Rauch, B., Le Clercq, P., and Colket, M. (2021). Sustainable Aviation Fuel Prescreening Tools and Procedures. *Fuel* 290, 120004. doi:10.1016/j.fuel.2020.120004

Ministry of Defence (2016). *Defence Standard 91-091, Turbine Fuel, Aviation Kerosine Type, Jet A-1, NATO Code: F-35; Joint Service*. AVTUR (9).

Moses, C. (2017). *AFRL-RQ-WP-TR-2017-0091, Delivery Order 0006: Airbreathing Propulsion Fuels and Energy Exploratory Research and Development (APFEERD), Subtask: Review of Bulk Physical Properties of Synthesized Hydrocarbon: Kerosenes and Blends*.

Oßwald, P., Zinsmeister, J., Kathrotia, T., Alves-Fortunato, M., Burger, V., van der Westhuizen, R., et al. (2021). Combustion Kinetics of Alternative Jet Fuels, Part-I: Experimental Flow Reactor Study. *Fuel* 302, 120735. doi:10.1016/j.fuel.2021.120735

Rauch, B. (2020). JETSCREEN: JET Fuel SCREENing and Optimization 2020. Available at: https://cordis.europa.eu/project/id/723525.

The Defense Energy Support Center (2009). *Petroleum Quality Information System Annual Report 2008*. Fort Belvoir: The Defense Energy Support Center.

Voigt, C., Kleine, J., Sauer, D., Moore, R. H., Bräuer, T., Le Clercq, P., et al. (2021). Cleaner Burning Aviation Fuels Can Reduce Contrail Cloudiness. *Commun. Earth Environ.* 2, 114. doi:10.1038/s43247-021-00174-y

Conflict of Interest: The authors declare that the research was conducted in the absence of any commercial or financial relationships that could be construed as a potential conflict of interest.

Publisher's Note: All claims expressed in this article are solely those of the authors and do not necessarily represent those of their affiliated organizations, or those of the publisher, the editors and the reviewers. Any product that may be evaluated in this article, or claim that may be made by its manufacturer, is not guaranteed or endorsed by the publisher.

frontiers | Frontiers in Energy Research

ORIGINAL RESEARCH
published: 13 April 2022
doi: 10.3389/fenrg.2022.837883

Modeling Yield, Biogenic Emissions, and Carbon Sequestration in Southeastern Cropping Systems With Winter Carinata

John L. Field[1,2], Yao Zhang[2], Ernie Marx[2], Kenneth J. Boote[3], Mark Easter[2†], Sheeja George[4], Nahal Hoghooghi[5], Glenn Johnston[6], Farhad Hossain Masum[7], Michael J. Mulvaney[8], Keith Paustian[2,9], Ramdeo Seepaul[4], Amy Swan[2], Steve Williams[2], David Wright[4] and Puneet Dwivedi[7]*

[1]Bioresource Science & Engineering Group, Environmental Sciences Division, Oak Ridge National Laboratory, Oak Ridge, TN, United States, [2]Natural Resource Ecology Laboratory, Colorado State University, Fort Collins, CO, United States, [3]Department of Agricultural and Biological Engineering, University of Florida, Gainesville, FL, United States, [4]North Florida Research and Education Center, University of Florida, Quincy, FL, United States, [5]School of Environmental, Civil, Agricultural, and Mechanical Engineering, University of Georgia, Athens, GA, United States, [6]Nuseed, West Sacramento, CA, United States, [7]Warnell School of Forestry and Natural Resources, University of Georgia, Athens, GA, United States, [8]Department of Plant and Soil Sciences, Mississippi State University, Starkville, MS, United States, [9]Department of Soil and Crop Sciences, Colorado State University, Fort Collins, CO, United States

Sustainable aviation fuel (SAF) production from lipids is a technologically mature approach for replacing conventional fossil fuel use in the aviation sector, and there is increasing demand for such feedstocks. The oilseed *Brassica carinata* (known as Ethiopian mustard or simply carinata) is a promising SAF feedstock that can be grown as a supplemental cash crop over the winter fallow season of various annual crop rotations in the Southeast US, avoiding land use changes and potentially achieving some of the soil carbon sequestration and ecosystem service benefits of winter cover crops. However, carinata may require more intensive management than traditional cover crops, potentially leading to additional soil greenhouse gas (GHG) emissions through increased carbon losses from soil tillage and nitrous oxide (N_2O) emissions from nitrogen fertilizer application. In this work, the 2017 version of the process-based DayCent ecosystem model was used to establish initial expectations for the total regional SAF production potential and associated soil GHG emissions when carinata is integrated as a winter crop into the existing crop rotations across its current suitability range in southern Alabama, southern Georgia, and northern Florida. Using data from academic and industry carinata field trials in the region, DayCent was calibrated to reproduce carinata yield, nitrogen response, harvest index, and biomass carbon-to-nitrogen ratio. The resulting model was then used to simulate the integration of carinata every third winter across all 2.1 Mha of actively cultivated cropland in the study area. The model predicted regional average yields of 2.9–3.0 Mg carinata seed per hectare depending on crop management assumptions. That results in the production of more than two million Mg of carinata seed annually across the study area, enough to supply approximately one billion liters of SAF. Conventional management of carinata led to only modest increases in soil carbon storage that were largely offset by additional N_2O emissions. Climate-smart management via adopting no-till carinata

OPEN ACCESS

Edited by:
Zia Haq,
United States Department of Energy (DOE), United States

Reviewed by:
Sheikh Adil Edrisi,
Thapar Institute of Engineering & Technology, India
Burton C. English,
The University of Tennessee, United States

***Correspondence:**
John L. Field
john.L.field@gmail.com

†Present Address:
Mark Easter,
Indigo Agriculture, Boston, MA, United States

Specialty section:
This article was submitted to Bioenergy and Biofuels, a section of the journal Frontiers in Energy Research

Received: *17 December 2021*
Accepted: *04 March 2022*
Published: *13 April 2022*

Citation:
Field JL, Zhang Y, Marx E, Boote KJ, Easter M, George S, Hoghooghi N, Johnston G, Masum FH, Mulvaney MJ, Paustian K, Seepaul R, Swan A, Williams S, Wright D and Dwivedi P (2022) Modeling Yield, Biogenic Emissions, and Carbon Sequestration in Southeastern Cropping Systems With Winter Carinata. Front. Energy Res. 10:837883. doi: 10.3389/fenrg.2022.837883

establishment or using poultry litter as a nitrogen source resulted in a substantial net soil GHG sink (0.23–0.31 Mg CO_2e ha^{-1} y^{-1}, or 0.24–0.32 Mg CO_2e per Mg of seed produced) at the farms where carinata is cultivated.

Keywords: carinata, winter oilseed, soil carbon, ecosystem modeling, Daycent model, sustainable aviation fuel, life cycle assessment, climate-smart agriculture

INTRODUCTION

Of the different measures proposed to reduce fossil fuel use in aviation, shipping, and long-haul transport, biofuels are seen as one of the most technologically mature and cost-effective approaches (Fulton et al., 2015; Davis et al., 2018). Many decarbonization scenarios project a significant role for advanced liquid biofuels, working in conjunction with demand management and other low-carbon fuel alternatives (Williams et al., 2021). Sustainable aviation fuels (SAF) are the central element of many aviation sector decarbonization plans, which anticipate a substantial build-out of biofuel production facilities (Chiaramonti, 2019). Most SAF production today involves converting waste oils from the food sector to hydrogenated esters and fatty acids (HEFA), the cheapest and most technologically mature SAF production pathway (O'Malley et al., 2021). Waste oil supplies are limited, but the cultivation of purpose-grown oilseed crops offers an alternative more scalable feedstock option (Zemanek et al., 2020; O'Malley et al., 2021).

In addition to the transportation sector, urgent measures are also needed to reduce emissions from the agricultural sector consistent with climate stabilization targets (Clark et al., 2020). Priorities include increasing soil organic carbon (SOC) storage and reducing emissions of nitrous oxide (N_2O) associated with nitrogen (N) fertilizer use (Paustian et al., 2016; Rockström et al., 2016; Minasny et al., 2017). Winter cover crops are a means to improve both SOC levels and N management. Replacing winter fallow periods with vegetation cover may contribute to increased annual net primary production and soil carbon. Meta-analyses report SOC increase rates of 0.2–0.6 Mg C ha^{-1} y^{-1} from the addition of cover crops, with the largest SOC benefits observed under non-legume cover crops in temperate climates and on fine-textured soils (Poeplau and Don, 2015; Abdalla et al., 2019; Jian et al., 2020; McClelland et al., 2021). Winter cover crops can also immobilize soil mineral N and potentially improve system N use efficiency through reduced nitrate leaching (Tonitto et al., 2006; Abdalla et al., 2019), though cover crop effects on N_2O vary depending on how residues are managed and whether legume species are included (Muhammad et al., 2019).

Winter oilseed cash crops present an opportunity for temporal intensification to produce SAF feedstock without displacing existing summer crop production or requiring land use change (Heaton et al., 2013), while potentially achieving some of the same soil health benefits as winter cover cropping. Options for oilseed cultivation include pennycress integrated into corn–soybean rotations in the US Corn Belt (Markel et al., 2018; Cubins et al., 2019) and camelina integrated into winter wheat–fallow rotations in the Great Plains (Resurreccion et al., 2021). In the relatively mild climate of the Southeast US, *Brassica carinata* can achieve greater yields than other oilseed species. Carinata seed contains a large proportion (~40% by mass) of high-quality oil that is readily converted to SAF with existing technologies (George et al., 2021). The carinata seed meal remaining after oil extraction is protein-rich and has value as animal feed (Schulmeister et al., 2019b; Schulmeister et al., 2019a; Schulmeister et al., 2021). Carinata stems, leaves, and roots remain in the field after seed harvest, where they can contribute to SOC. The Southeast Partnership for Advanced Renewables from Carinata (SPARC) is a public–private partnership funded by the US Department of Agriculture to advance carinata for these multiple applications, in collaboration with relevant stakeholders (George et al., 2021).

As with the introduction of any new crop, much is unknown regarding the best management practices, likely yields, environmental consequences, and financial outcomes of growing carinata in the Southeast. While there have been limited measurements of SOC, N_2O, and other soil GHGs for carinata grown as a summer crop in the cooler and drier climate of the Northern Great Plains (Li et al., 2019; Bhattarai et al., 2021), the authors are aware of no comparable soil GHG measurements for carinata grown as a winter cover crop in the Southeast. Furthermore, best management practices are still being developed, and it is unknown to what extent the agronomy of this winter cash crop can be optimized to simultaneously achieve both high yields as well as the environmental and soil health benefits expected of a cover crop. While cover-cropping generally increases SOC levels, carinata may require additional tillage operations for establishment (Iboyi et al., 2021) that could undermine this effect due to soil disturbance and SOC destabilization (Bailey et al., 2019). Similarly, economically viable carinata seed production requires the application of substantial amounts of N fertilizer during the winter (Seepaul et al., 2019a; Bashyal et al., 2021) which may increase N_2O emissions (Crutzen et al., 2008; Roth et al., 2015).

This work used a process-based ecosystem model to estimate carinata productivity and net soil GHG sink performance when carinata is integrated into annual crop rotations within a sub-region of the Southeast US. The model was calibrated and validated against data from carinata field trials in the region. The analysis assumed that carinata would be cultivated once every third winter (to limit disease and pest issues; Seepaul et al., 2019b) across all annual cropland in the region. In addition to a conventional carinata management scenario involving intensive field preparation and synthetic N fertilizer application, two alternative climate-smart management scenarios were also considered. This assessment focused on the biophysical dimensions of carinata production and local soil GHG

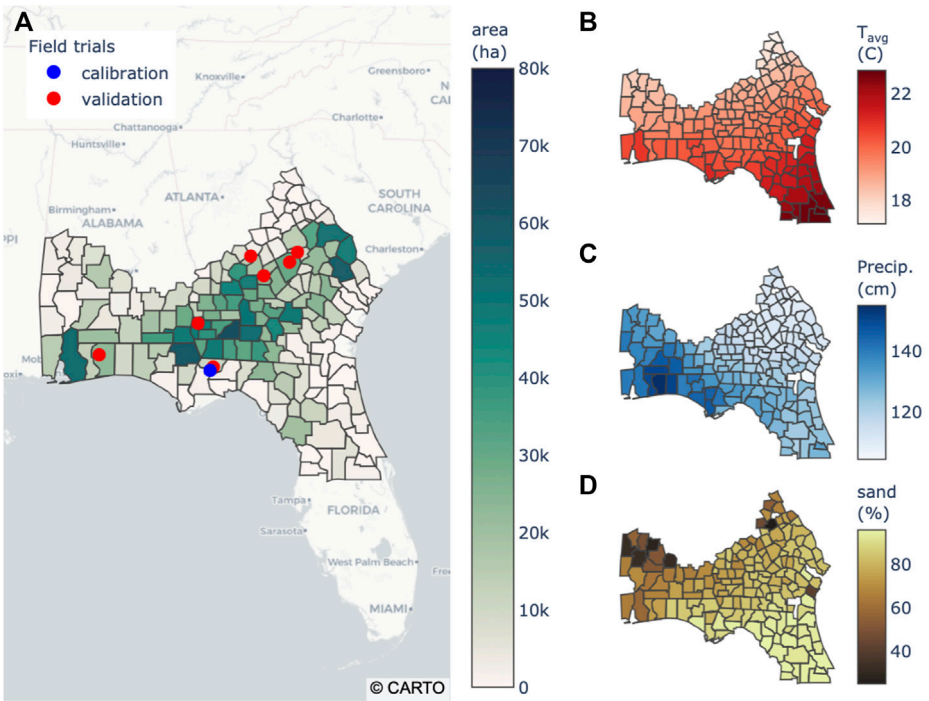

FIGURE 1 | Study area characteristics based on spatial data inputs used with the DayCent model. **(A)** Cultivated cropland area as per NLCD, with locations of carinata trials used for calibration (blue marker) and validation (red markers). **(B)** Average air temperature and **(C)** annual total precipitation as per NARR. **(D)** Average sand content of the surface soil layer as per SSURGO, considering cropland areas only.

emissions. Other supply chain sustainability considerations such as upstream emissions from fertilizer production and the alternate fate of poultry litter are left for future consequential life-cycle assessment studies.

MATERIALS AND METHODS

Study Area

This analysis considered the integration of winter-grown carinata within existing agricultural rotations across a sub-region of the Southeastern US covering southern Alabama, southern Georgia, and northern Florida (**Figure 1**). These study area boundaries were selected based on prior analysis of weather and soil suitability for existing commercial carinata varieties (Alam and Dwivedi, 2019). The LANDSAT-derived 2016 Land Cover database (NLCD) (Homer et al., 2020) was used to identify cultivated cropland in this study area. Four counties around the periphery of the study area (Franklin County in Florida and Camden, Lincoln, and McIntosh Counties in Georgia) contained no cultivated cropland and were excluded from further analysis. The remaining 163 counties included 2.34 Mha of cultivated cropland as per NLCD, distributed as shown in **Figure 1A**. The majority of the cultivated cropland in this study area falls within the Southern Coastal Plain Major Land Resource Area (MLRA 133A), an area of deep, loamy Utisols, Entisols, and Incepticols (USDA NRCS, 2006). Other MLRAs included in the study area were the Alabama and Mississippi Blackland Prairie (135A); the Carolina and Georgia Sand Hills (137); the Eastern Gulf Coast (152A), Atlantic Coast (153A), and Southern Florida (155) Flatwoods; and the North-Central (138) and South-Central (154) Florida Ridge. Cultivated cropland in these areas supports various rotations of soybean, cotton, corn, wheat, and peanut. The remainder of the study area is dominated by woody wetlands and evergreen forest (Boryan et al., 2011).

This region has a humid subtropical climate as per the Köppen Climate Classification system. Average annual air temperature varies from 17 to 23°C across a north–south gradient (**Figure 1B**), and average annual precipitation varies from 105 cm in eastern Georgia to more than 150 cm at the Alabama Gulf Coast (**Figure 1C**), as computed using data from the North American Regional Reanalysis (NARR; Mesinger et al., 2006). Surface soil textures cover a wide range as computed from the Soil Survey Geographic (SSURGO) database (Ernstrom and Lytle, 1993), from moderate-texture soils in the northern part of the study area to extremely coarse (>90% sand) soils in central Florida (**Figure 1D**).

Ecosystem Model Calibration

The DayCent ecosystem model was used to predict carinata seed yields and soil GHG effects in the region. DayCent is a process-based model that simulates carbon, N, and water cycling in natural and agricultural ecosystems on a daily timestep as a function of soils, climate, and management (Del Grosso et al., 2002). DayCent has previously been used to model a variety of other oilseed crops including canola (He et al., 2021), sunflower

TABLE 1 | Field data sources used for DayCent model calibration and validation.

Site	Season(s)	Data Types	Use
Quincy, FL	2015/16	Yield response to N fertilizer rates Tissue C:N ratios Root:shoot ratios	Calibration
Quincy, FL	2017/18 2018/19	Seed and biomass yield	Validation
Jay, FL	2017/18 2018/19	Yield response to N fertilizer rates	Validation
Hawkinsville, GA	2017/18	Average seed yield	Validation
Dublin, GA	2017/18	Average seed yield	Validation
Wrightsville, GA	2016/17	Average seed yield	Validation
Blakely, GA	2017/18	Average seed yield	Validation
Byron, GA	2016/17	Average seed yield	Validation

(Gryze et al., 2010), and soybean (Zhang et al., 2020a). It has also been used extensively in bioenergy assessments to predict energy crop yields and associated changes in SOC storage and N_2O emissions (Field et al., 2018). DayCent estimates of crop production are sensitive to growing-season temperatures, as well as water and N stresses that reflect the balance of multiple input and loss mechanisms in addition to water and N movement vertically through the soil profile (Qian et al., 2019). These simulations utilized the DDcentEVI version of DayCent from May 2017.

Field data on carinata performance were collected by academic and industry collaborators at a variety of sites across the study area, as illustrated in **Figure 1A** and summarized in **Table 1**. Initial model calibration was based on data from plot-scale field trials conducted at the University of Florida North Florida Research and Education Center in Quincy, Florida over the winter of 2015/2016 (Seepaul et al., 2019a). The experimental site featured coarse-textured soil with 82% sand content. Carinata was grown as a winter crop following a fallow summer (i.e., outside of a standard regional crop rotation) under a range of N fertilizer application rates (0, 45, 90, and 135 kg N ha^{-1} y^{-1}). This trial produced data on seed yield after mechanical harvest, harvest index, root:shoot ratio, and C:N ratio of aboveground biomass at the time of harvest, which were used for DayCent calibration. The study featured a randomized complete block design with four replications, and the average results across all four replications were used for model calibration purposes.

A generalized carinata crop was created within DayCent by calibrating individual crop parameters manually with an iterative method for best fit against the calibration dataset, in a process similar to that described by Del Grosso et al. (2011) and Field et al. (2016). Carinata is photoperiod-sensitive, so crop phenology (i.e., emergence and physiological maturity) was set based on fixed calendar dates rather than as a function of growing degree day accumulation. Physiological maturity was set to occur on May 6 based on the average date observed in the field trials at Quincy FL and Jay FL listed in **Table 1**, plus additional trials at Quincy and in Shorter, Alabama. The 2017 version of DayCent does not explicitly represent the dynamics of annual crop physiological maturation and senescence, so crop growth was terminated on the physiological maturity date. Calibration results against the various measurements from the 2015/16 Quincy field trials are shown in **Supplementary Figure S1**. The calibrated model was generally able to reproduce key observations from the field trial, though with some tendency to under-estimate seed yield and aboveground biomass C:N ratios under lower N rates.

Following model calibration, seed yield data from multiple subsequent carinata field trials were used for independent model validation. Plot-scale, machine-harvested carinata yield data was collected during the 2017/2018 and 2018/2019 winter seasons under a single N fertilizer treatment at Quincy, Florida, and under a range of N application rates at the University of Florida West Florida Research and Education Center in Jay, Florida (Bashyal et al., 2021; Boote et al., 2021). Other aspects of the experimental design were consistent with the 2015/2016 Quincy experiment. In addition, the project commercial partner Agrisoma, Inc. (later acquired by Nuseed) provided field-scale yield data from trials conducted at five farms in Georgia, listed in **Table 1** using the name of the nearest town to preserve landowner anonymity.

No measurements of SOC change or N_2O emissions under carinata within the study area were available for model calibration or validation purposes at the time of this study.

Management Scenarios

Existing cropping patterns in this region include corn, cotton, peanut, soybean, wheat, and sorghum grown in various rotations. Research is ongoing to develop early maturing carinata varieties and determine their best integration into existing rotations to relieve disease and pest cycles while minimizing any delay in summer crop planting (Seepaul et al., 2019b; George et al., 2021). This study considered the integration of carinata into annual crop rotations across all cultivated cropland in the study area. For simplicity, all cropland is modeled as being under a 3-year cotton–cotton–peanut rotation. Carinata should be grown only once every 3 years to minimize pest and disease issues (Seepaul et al., 2019b), so this analysis considered the integration of a single winter carinata crop over the winter between the two cotton summer crops (with the remaining two winters left fallow). These simulations are meant to be broadly representative of carinata integration into a range of existing crop rotations practiced across this region.

Within that modified rotation, a conventional carinata management scenario was considered involving tilled field preparation and synthetic fertilizer use, as well as two "climate-smart" management scenarios that could lead to improved soil GHG outcomes. The management scenarios draw heavily from the experience of agronomic field trials supported by the SPARC project (George et al., 2021) and its predecessors (Seepaul et al., 2019a). In both cases, the new rotation with carinata was evaluated against the continued business-as-usual cotton–cotton–peanut rotation with winter fallow.

Conventional Management Scenario

The conventional management scenario included conventional tillage practices for field preparation and synthetic fertilizer application to meet the N needs of the carinata crop. Field preparation was simulated as two moderately heavy disking

TABLE 2 | Summary of regional-scale simulation results for different carinata management scenarios. All soil GHG values are evaluated relative to the continued business-as-usual cotton–cotton–peanut reference rotation.

	Conventional Management	Climate-Smart Management: No-Till	Climate-Smart Management: Poultry Litter
Field Preparation	2 disk passes Seed drill	Herbicide burn-down Seed drill	2 disk passes Seed drill
N source	90 kg N ha^{-1} y^{-1} UAN-32	90 kg N ha^{-1} y^{-1} UAN-32	2 Mg litter ha^{-1} y^{-1} 40 kg N ha^{-1} y^{-1} UAN-32
Annual seed production (Mt y^{-1})	2.03	1.97	1.99
Average seed yield rate (Mg ha^{-1})	2.96	2.88	2.91
SOC change rate (Mg C ha^{-1} y^{-1})	0.028	0.093	0.088
SOC emissions (Mg CO_2e ha^{-1} y^{-1})	–0.104	–0.340	–0.323
Direct N_2O emissions (Mg CO_2e ha^{-1} y^{-1})	0.053	0.028	0.075
Indirect N_2O emissions (Mg CO_2e ha^{-1} y^{-1})	0.008	0.003	0.015
CH_4 emissions (Mg CO_2e ha^{-1} y^{-1})	–0.001	0.000	–0.001
Net GHG_{soil} emissions (Mg CO_2e ha^{-1} y^{-1})	–0.043	–0.308	–0.234

steps (DayCent CULT H events), and carinata was planted in mid-November with a seed drill. A total of 90 kg N ha^{-1} fertilizer was applied in the form of UAN-32 in a split application, with 20 kg N ha^{-1} applied at the time of planting and the remainder applied in mid-February. This rate is slightly lower than the economic optimum rate estimated for carinata in this region (103 kg N ha^{-1}; Seepaul et al., 2020) to maximize the soil GHG and ecosystem service benefits of the crop. Carinata was simulated as reaching physiological maturity on May 6, and it was assumed that harvest would occur in late May following a 3-week dry-down period, and the following summer crop planted immediately afterward.

Climate-Smart Management Scenarios

In addition to the conventional management scenario, two alternative climate-smart management scenarios (Paustian et al., 2016) designed to improve the soil GHG balance of carinata production were considered, as highlighted in **Table 2**. The first scenario assumed no-till establishment of carinata in which the disking of the conventional management scenario is replaced with an herbicide "burn-down" step, followed by drilling of carinata seed into the stubble of the last crop. Initial agronomic field trials suggest this may be a viable establishment method in this region (Iboyi et al., 2021). DayCent simulates a number of potential feedbacks on crop productivity from the no-till establishment, including delayed germination from a surface litter mulching effect, and reduced rates of soil N mineralization.

The second climate-smart management scenario assumed that poultry litter is applied as an N-rich soil amendment and incorporated into the soil during disking, reducing the need for synthetic N fertilizer application (George et al., 2021). Data on poultry litter organic carbon (C_{org}) and N concentrations were gathered from literature studies where both values were explicitly reported so that litter C:N ratios could be calculated (Das et al., 2002; Sharpley et al., 2009; Lynch et al., 2013; Rogeri et al., 2016; Ashworth et al., 2020), as summarized in **Supplementary Table S1**. Based on this analysis, a poultry litter organic amendment was parameterized with a C:N ratio of 7.3 and assuming that only half of total litter N content is plant-available in the first year after application (Gaskin et al., 2013). In this climate-smart scenario approximately half of the carinata N requirement is met through application and incorporation of 2.0 Mg ha^{-1} poultry litter at the time of crop establishment, and an additional 40 kg N ha^{-1} is applied in the form of UAN-32 in mid-February.

Specifying and Executing Simulations

Specifying DayCent Simulations

DayCent is a one-dimensional model, and multiple point simulations must be run to capture the heterogeneity in soils, climate, and land use history across the study area (Field et al., 2016). DayCent simulation requires input data on soil texture throughout the soil profile, as well as representative daily air temperature and precipitation totals. These inputs were derived via a GIS intersect of the NLCD land cover, SSURGO soil, and Precipitation-elevation Regressions on Independent Slopes Model (PRISM; Daly et al., 1994) weather data layers. The principal soil component was used as representative of each SSURGO soil map unit. PRISM data is available on a 4 km grid, though a 3 × 3 nearest neighbor re-sampling (to a new effective grid size of 12 km) was performed to limit the number of simulations required. The simulations used 38 years of historic PRISM weather data (1981–2018) to represent past and future weather variability in this region.

Every unique combination of SSURGO soil component and re-sampled PRISM weather grid cell occurring on NLCD cultivated cropland represents a unique DayCent 'strata' requiring individual simulation. A total of 30,720 individual strata were identified in the study area. The density of strata was generally highest in counties with the greatest cropland area, as shown in **Supplementary Figure S2**.

Model Initialization and Batch Simulations

Model initialization was performed to estimate initial soil carbon and N levels in various model pools based on pre-cultivation land cover and region-specific dates of historic European settlement and associated cropping practices, aligned with the DayCent procedures used for the EPA Inventory of U.S. Greenhouse Gas Emissions and Sinks and farm-level GHG emissions accounting tools (Paustian et al., 2018; US EPA, 2020a). Next, 6 decades of cotton–cotton–peanut rotation was simulated on all

cropland in the study area, so that soil carbon pools could approach new equilibrium values reflecting that management. Following that, a reference case of continued business-as-usual cotton–cotton–peanut rotation was simulated for 30 years into the future (starting in the year 2020), re-using historic PRISM weather data. In addition, carinata integration under each of the three different carinata management scenarios was also simulated for the future period. Each of these four forward scenarios was simulated for each DayCent strata (a total of 11.1 million new simulation-years) via batch execution on the Colorado State University Natural Resource Ecology Laboratory computing cluster.

Post-Processing and Analysis

Post-Processing Carinata Yield and Soil Greenhouse Gas Emissions

DayCent model output for each strata was converted to per-area carinata seed yield rates and the various components of the soil GHG balance. DayCent reports crop yield in carbon units (g C m^{-2}), and this was converted to per-area yield of field-dry seed at 8% moisture content (Mg seed ha^{-1}) assuming a seed carbon concentration of 45% (the same assumptions utilized during model calibration and validation). Total annual production per county was calculated by multiplying the carinata yield rate calculated for each stratum by the area of NLCD cultivated cropland covered by that stratum, summing those results across each county, and then dividing by three to reflect that the crop is only cultivated once every 3 years.

The soil GHG emissions balance associated with carinata production was calculated from a variety of raw DayCent model outputs including total SOC (simulated to a depth of 20 cm), the emissions rate of N in the form of N_2O from soil nitrification and denitrification processes, the loss rates of N via volatilization and nitrate leaching, and the soil oxidation rate of methane (CH_4). The rates of annual SOC change (Mg C ha^{-1} y^{-1}), direct N_2O emissions from nitrification and denitrification, and soil oxidation of CH_4 were extracted directly from DayCent model output and averaged across the full length of the 30-years forward simulation. Indirect emissions of N_2O were estimated based on the average DayCent-simulated annual rates of N volatilization and leaching, using the indirect N_2O emissions factors recommended by the Intergovernmental Panel on Climate Change (IPCC) guidelines (Eggleston et al., 2006).

The average rates of SOC change, direct and indirect N_2O emissions, and soil oxidation of CH_4 under the business-as-usual reference rotation were then subtracted from the average rates calculated in each carinata scenario, to identify the relative changes attributable to carinata cultivation. Rates of soil carbon change were translated to a net flux of CO_2 into or out of the soil profile, and N_2O and CH_4 fluxes were translated into CO_2-equivalent terms based on their 100-year global warming potential as per IPCC guidelines (Stocker et al., 2014). The total net soil GHG balance of carinata production was calculated as the sum of these CO_2-equivalent emissions from SOC change (with SOC loss producing a positive emission to the atmosphere and SOC gain producing a negative emission from the atmosphere), direct and indirect N_2O emissions, and soil CH_4 oxidation (with increased oxidation producing a negative emission from the atmosphere). Finally, direct N_2O emissions rates were compared to the total additional (synthetic and organic) N inputs for carinata production, to calculate N_2O-N emissions factors comparable to those used in IPCC emissions accounting (Eggleston et al., 2006).

Cropland Area Correction

The DayCent spatial modeling workflow required a remotely sensed land cover product like NLCD to identify specific cropland locations so that the underlying soils could be accurately represented. However, remotely-sensed land use products can differ significantly from one another, and from survey-based land-use estimates, in terms of the total cropland area quantified in each county (Johnson, 2013). The USDA Census of Agriculture (CoA; https://www.nass.usda.gov/AgCensus/) is generally considered the most accurate estimate of US cropland extent (Maxwell et al., 2008; Lark et al., 2020). Previous studies have shown that county cropland areas reported by NLCD and CoA agree well in agriculture-heavy areas of the US Corn Belt (Maxwell et al., 2008), but diverge significantly in regions with smaller farm size and lower agricultural land extent (Maxwell et al., 2008; Goslee, 2011), as is the case in the Southeast US.

To most accurately represent the true annual cropland extent in this region, DayCent results were re-scaled against the annual cropland area in each county as per the 2017 CoA. Actively utilized annual cropland was estimated from the sum of the "harvested", "failed", and "summer fallow" cropland sub-categories within CoA, avoiding areas classified as idle cropland or cropland–pasture (which are included in the top-level census "cropland" category, but are generally not representative of active annual crop rotations) (US EPA, 2018; Lark et al., 2020). **Supplementary Figure S3** shows how the remotely-sensed NLCD product tends to over-estimate cropland area relative to CoA in the relatively crop-dense center of the study area, but underestimate it elsewhere. This re-scaling procedure revised the total cropland extent in the study area downward by 12% (from 2.34 Mha down to 2.05 Mha) and reduced the estimate of total regional carinata seed production by a similar amount. This procedure assumed that NLCD provides an unbiased estimate of which soils within a given county are cropped, i.e., there is minimal correlation between NLCD classification errors and underlying soil type.

Results in the Context of Sustainable Aviation Fuel Production

Simulated carinata seed yields and soil GHG emissions results were also interpreted in the context of SAF production. Total regional carinata–SAF production potential was calculated based on a prior estimate of 524 L of SAF yield per Mg of carinata seed from a HEFA conversion process (Alam and Dwivedi, 2019). Based on that conversion yield, and assuming an SAF energy density of 30.8 MJ per liter, soil GHG results were also expressed in terms of their potential contribution to the GHG footprint of carinata-derived SAF, i.e., in units of g CO_2e (MJ fuel)$^{-1}$. Such calculations must reflect that carinata seed crushing produces both carinata oil and a seed meal co-product (with value as a

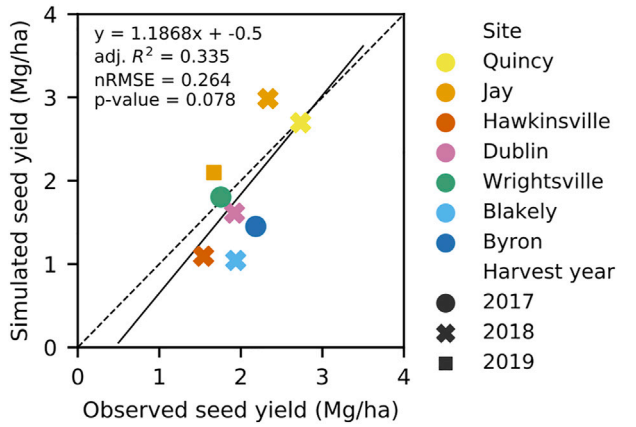

FIGURE 2 | DayCent model validation results, using field observations described in **Table 1**.

high-protein animal feed supplement), and that converting carinata oil to SAF via a HEFA process also yields propane and naphtha fuel fractions. Thus, SAF constitutes only 32% of the total mass, 62% of the total market value, and 49% of the total energy content of all products derived from carinata seed (Alam et al., 2021), and it should only be allocated a comparable amount of the total environmental burdens and benefits of carinata production.

RESULTS

Model Validation

Figure 2 shows the results of validating the DayCent carinata model against an independent set of carinata seed yield data as described in **Table 1**. Only results for 90 kg N ha^{-1} fertilizer treatments are included, to focus on the model's ability to capture site-to-site and year-to-year variability. The calibrated DayCent model was able to reproduce approximately 1/3 of the variability in carinata yield observed across site–years, with a normalized root mean square error of 0.26. Additional validation results that include the full range of N treatments at the Jay, FL field trial site are shown in **Supplementary Figure S4**.

Regional Seed Yield

Simulated yields were similar across all three carinata management scenarios. Representative results for the conventional carinata management scenario are shown in **Figure 3**. The average simulated carinata seed yield across the study area was 2.96 Mg ha^{-1} in that scenario, with maximum county-averaged values of approximately 3.2 Mg ha^{-1} achieved in southwestern Georgia (**Figure 3A**). The simulated yield was lower and more variable from year-to-year (**Supplementary Figure S5**) on the sandy soils of central Florida, likely attributable to N stress driven by nitrate leaching.

Figure 3B shows average annual seed production in each county when carinata was integrated every third year into existing rotations across all actively utilized annual cropland. Annual production of more than 40,000 Mg was achieved in multiple counties across Georgia, as well as counties on the Alabama Gulf Coast and Florida Panhandle with high yields and relatively large amounts of cropland (**Supplementary Figure S3B**). Total regional carinata seed production is summarized in **Table 2** for the three different carinata management scenarios. This total production was relatively constant over the management scenarios analyzed, at approximately 2.0 million tonnes (Mt).

Soil Carbon

Figure 4 shows illustrative soil carbon results under the climate-smart no-till scenario for four randomly selected DayCent simulation strata (0.01% of the total), with the underlying soil surface texture indicated by color. In general, finer-textured soils with high clay and silt content were associated with higher overall SOC levels, and larger differences between the business-as-usual reference rotation (solid lines) and the carinata scenarios (in this case, the climate-smart no-till scenario; dashed lines). In DayCent, soil microbial carbon use efficiency is controlled by soil texture; finer-textured soils with high clay and silt content have lower respiration losses and stabilize more SOC per unit of carbon input. The jaggedness in the SOC lines was due to inter-annual variability in temperature and precipitation, which affect both simulated plant productivity (i.e., carbon inputs to the soil) and heterotrophic respiration rates (carbon losses from the soil).

These simulations suggest that carinata integration would lead to soil carbon increases at average regional rates of 0.028, 0.093, and 0.088 Mg C ha^{-1} y^{-1} under the conventional, no-till, and poultry litter

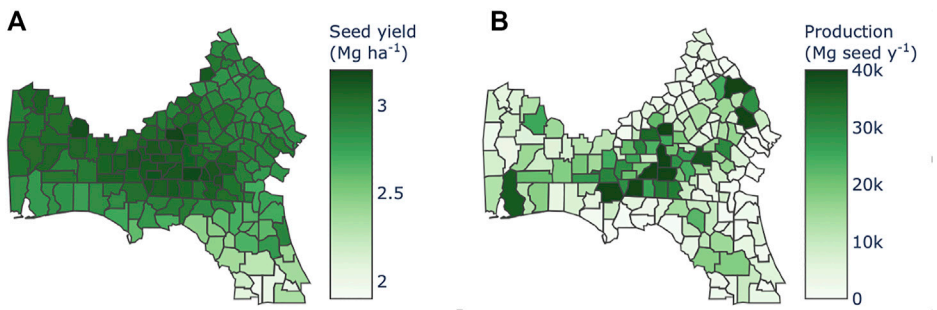

FIGURE 3 | DayCent-simulated **(A)** carinata seed yield rates, and **(B)** corresponding annual seed production per county when carinata is integrated every third year into existing rotations across all active annual cropland, under the conventional carinata management scenario.

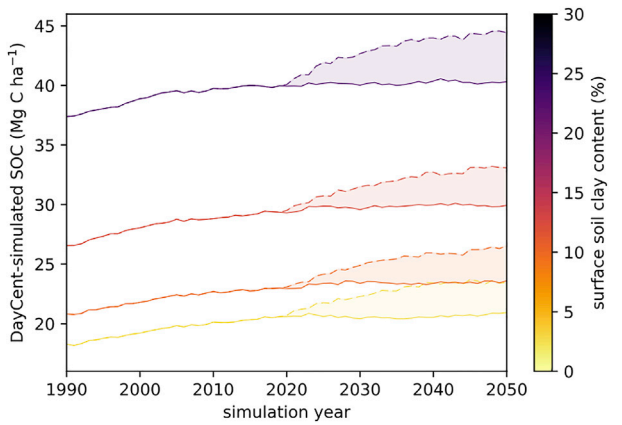

FIGURE 4 | Representative soil carbon modeling results for the climate-smart no-till establishment scenario, showing four randomly selected simulation strata. The solid lines show SOC trends under the business-as-usual cotton–cotton–peanut reference rotation for each stratum, with the underlying soil texture indicated by color. Carinata integration starts in 2020 and results in an increasing SOC trend (dashed lines).

management scenario, respectively (**Table 2**). These rates are relatively low compared to the 0.2–0.6 Mg C ha^{-1} y^{-1} quantified in meta-analyses of winter cover crops. The lower rates simulated here are likely attributable to the assumption that carinata is grown only once every 3 years (compared to annual use of cover crops). Additionally, DayCent predicts higher rates of soil microbial activity in warm, wet climates and lower soil microbe carbon efficiency on sandy soils, which would all contribute to reduced soil organic carbon stabilization in this particular region (**Figures 1B–D**). SOC increase rates were lowest in the sandy soils of central Florida, and highest in the relatively fine-textured soils in the northwestern and northeastern edges of the study area (**Figures 5A–C**). This effect is consistent with a recent meta-analysis that found the highest rates of SOC sequestration under winter cover crops in temperate climates and on fine-textured soils (Jian et al., 2020). These simulated regional SOC increase rates are equivalent to a soil CO_2 sink (i.e., a negative emission) of 0.10–0.34 Mg CO_2 ha^{-1} y^{-1} (**Table 2**).

N_2O and Net Soil Greenhouse Gas Balance

Nitrous oxide emissions are often expressed in terms of emissions factors describing the fraction of applied N that is emitted in the form of N_2O-N. DayCent predicted that 0.01–0.5% of N applied

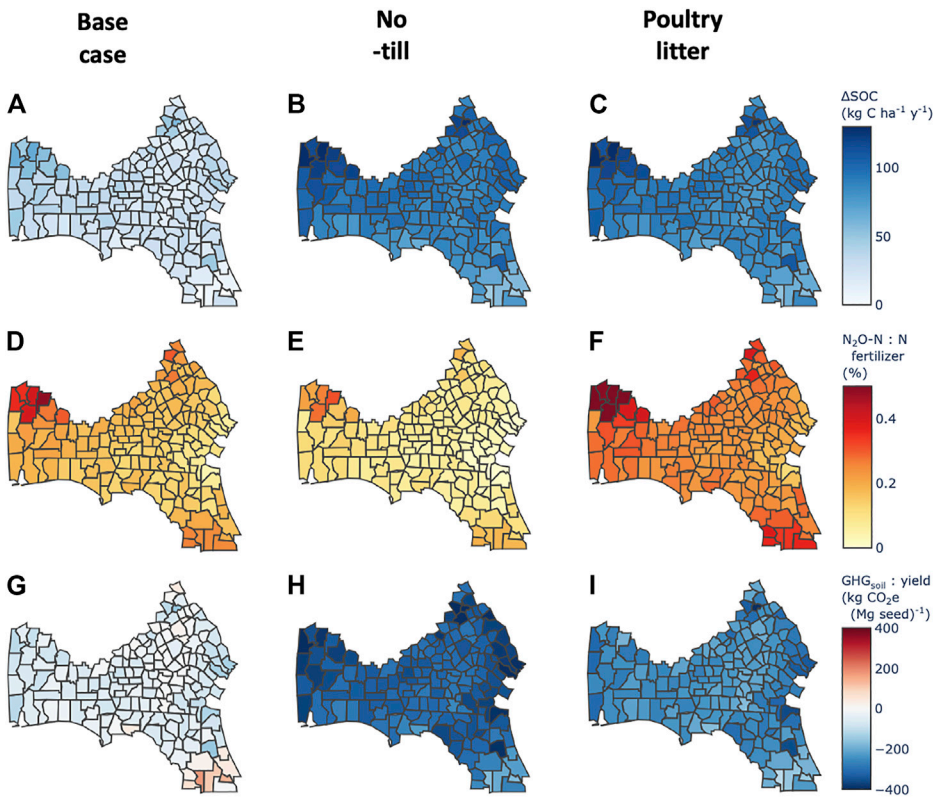

FIGURE 5 | DayCent-simulated soil GHG fluxes under different carinata cultivation scenarios, relative to the continued business-as-usual reference rotation. **(A–C)** increase in soil organic carbon storage. **(D–F)** The fraction of new N applications lost in the form of direct nitrous oxide emissions. **(G–I)** The net soil GHG footprint of carinata seed production, which reflects the sum of positive CO_2-equivalent emissions from additional N_2O production, plus negative CO_2-equivalent emissions associated with an increased soil sink of carbon and CH_4.

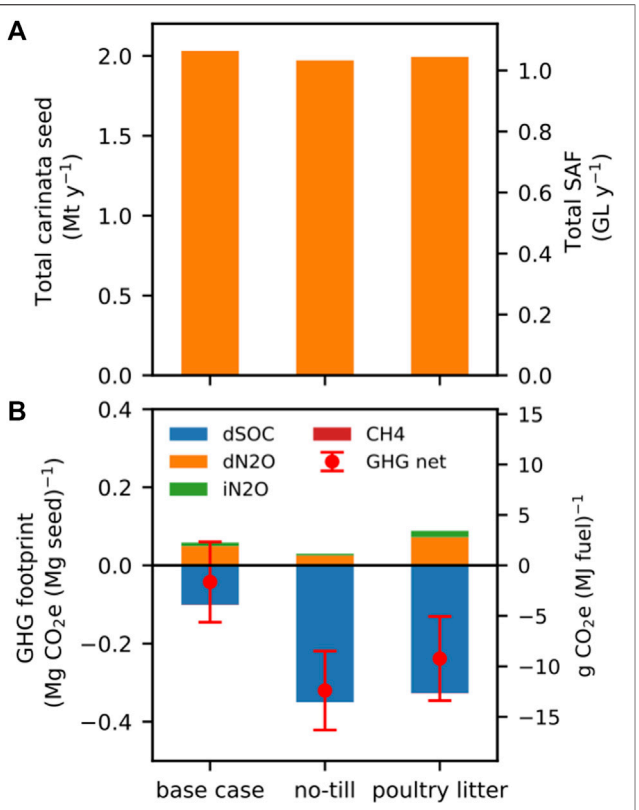

FIGURE 6 | Performance of different carinata management scenarios in terms of **(A)** total annual seed yield and associated SAF potential from the study region, and **(B)** the associated soil GHG footprint per Mg of seed production, also expressed in units of global warming intensity (g CO_2e (MJ fuel)$^{-1}$) for the resulting carinata–SAF. Red error bars denote ±2SD of field-to-field variability. These results focus on the local soil GHG balance only; neither upstream emissions from nitrogen production and farm operations nor the alternate fate of poultry litter are included.

in the form of UAN-32 or poultry litter would be lost as direct N_2O emissions from soil nitrification and denitrification processes (**Figures 5D–F**). This range falls largely below the IPCC default emissions factor range of 0.3–3% (Eggleston et al., 2006). This is likely a function of the coarse-textured soils in this region, which limits water-filled pore space and associated anoxic denitrification losses. The highest simulated N_2O-N emissions factors occurred on the relatively fine-textured soils in the northwestern and northeastern edges of the study area and fall within the 0.3–3% IPCC default range. Average regional direct N_2O emissions in CO_2-equivalent units were 0.05–0.08 Mg CO_2e ha^{-1} y^{-1} (**Table 2**). These new N_2O emissions offset about half of the CO_2-equivalent SOC sink in the conventional management scenario, but only 8% of the SOC sink in the climate-smart no-till management scenario.

Simulated indirect N_2O emissions rates and changes in soil CH_4 oxidation rates were very small in comparison (**Table 2**), so the total soil GHG balance (GHG_{soil}) of carinata production was dominated by the SOC and direct N_2O terms. **Figures 5G–I** shows regional patterns in the GHG_{soil} footprint of carinata seed production (i.e., GHG_{soil}/annual seed yield). In the climate-smart management scenarios, the CO_2-equivalent SOC sink exceeded N_2O emissions across the entire study area, such that carinata seed production was always associated with a net soil GHG sink. In contrast, the SOC sink was relatively weak in the conventional management scenario, so many individual counties were approximately soil GHG-neutral or even a small net GHG source (e.g., counties in central Florida; **Figure 5G**).

Total Regional Seed and Sustainable Aviation Fuel Production

Total regional carinata SAF production potential was insensitive to the different management scenarios investigated. Cultivating carinata once every 3 years across the 2.05 Mha of active annual cropland in the study area would yield 1.97–2.03 Mt of carinata seed annually, enough feedstock to produce 1.03–1.06 billion liters (GL) of SAF (**Figure 6A**). However, the soil GHG footprint of carinata production is much more sensitive to management (**Figure 6B**). The net soil GHG balance was approximately neutral in the conventional management scenario, with a modest net SOC sink largely offset by new N_2O emissions. The error bars in **Figure 6B** denote two standard deviations of field-to-field variability (i.e., the variability in different DayCent strata simulations), showing that farm-level soil GHG outcomes would range from a small net GHG source to a moderate net GHG sink. In contrast, the climate-smart management scenarios resulted in substantial and consistent net soil GHG sinks of 0.23–0.31 Mg CO_2e ha^{-1} y^{-1}. Since each hectare of land yields approximately 3 Mg of carinata seed when it is cultivated once every 3 years, this soil GHG sink is equivalent to 0.24–0.32 Mg CO_2e per Mg of carinata seed produced.

These soil GHG emissions results can also be expressed on the basis of SAF produced, for illustrative purposes. Using market-based allocation, 62% of the soil GHG benefits of carinata seed production should be allocated to SAF (with the remaining 38% allocated across the various other co-products derived from that seed). The soil GHG sinks in the climate-smart management scenarios correspond to a 9.2–12.4 g CO_2e MJ^{-1} reduction in the overall GHG footprint of the resulting SAF. For comparison, that is equivalent to 10.4–13.9% of the GHG footprint of conventional aviation fuel (89 g CO_2e MJ^{-1}; Prussi et al., 2021). While this calculation helps to illustrate the magnitude of the soil GHG benefits in relation to the amount of SAF produced, note that it stops short of a full life-cycle accounting for upstream emissions associated with fertilizer production and spreading, the alternate fate of poultry litter, and more formal displacement method coproduct crediting.

DISCUSSION

Carinata has been previously investigated as a feedstock for SAF or other biofuel production when grown as a summer

crop integrated into existing winter wheat–fallow rotations in the US Great Plains (Bhattarai et al., 2021), or on marginal lands in the semi-arid climates of the Mediterranean Region (Cardone et al., 2003; Montemurro et al., 2016) and elsewhere (Hagos et al., 2020). This study suggests that winter carinata cultivation can contribute to the sustainable intensification of existing annual cropping systems in the Southeast US, producing a valuable SAF feedstock while simultaneously improving soil organic matter levels on the farm. Integrating carinata every third year into existing annual crop rotations across the ~2 Mha of active annual cropland in this region (1.5% of total US cropland) results in enough feedstock to produce approximately one billion liters of SAF. This is complementary to other winter oilseeds such as pennycress that are more suitable in other climates (Markel et al., 2018; Cubins et al., 2019). All of the scenarios studied are expected to result in a net sink of soil GHG at the regional scale, and climate-smart management introduces a significant negative emissions term within the life cycle of carinata-derived SAF fuel. This effect would persist over the first several decades of production before soil carbon levels come to equilibrium at a higher level under the new management.

This study should be viewed as a first exploratory estimate of carinata production potential and soil GHG impacts in this region, though it is based on a limited amount of field data. The DayCent yield modeling has reasonable fidelity for this exercise (**Figure 2**), though it lacks the granularity necessary to reliably inform individual farmer management decisions. In particular, there is limited long-term data on the susceptibility of carinata to frost damage and no measurements of changes in SOC levels or N_2O emissions under carinata available from this region for model validation purposes. Additionally, there are reasons for caution when estimating regional resource potentials using models that have been developed all or in part using data from small-scale plot trials. It has been suggested that yields measured in small-scale trials should be interpreted as representing "the highest potential range rather than an expected near-future performance at commercial level" (Mola-Yudego et al., 2015). However, all of the plot trials analyzed here were machine-harvested (eliminating that as a potential source of bias), and the final calibrated DayCent model under-estimates yield for four of the five larger field-scale trials (Hawkinsville, Dublin, Blakely, and Byron; **Figure 2**), so there is no evidence of potential scale-related bias in the regional projections at this time.

There are a number of other limitations to the modeling approach used here. The DayCent model focuses only on SOC dynamics in the surface layer of soil (to 20 cm depth). While there is a well-established SOC benefit from replacing winter fallow periods with crops, tillage effects on SOC are found to be smaller and much more uncertain when evaluated across the full depth of the soil profile (Ogle et al., 2019), and thus DayCent and many other process-based ecosystem models may over-estimate SOC differences between different tillage practices. In addition, the version of DayCent used for this analysis does not endogenously represent crop phenology, which likely limits the model performance observed in the independent validation (**Figure 2**). The model simulates a reduced rate of plant growth on cold days, but it does not represent plant mortality from frost damage in photoperiod-sensitive crops. While this study area was selected to minimize frost risk (Alam and Dwivedi, 2019), and the effects of frost can be mitigated using best management practices (Mulvaney et al., 2018; Seepaul et al., 2019b), this model limitation may still result in some overestimation of the production potential from this region. A newer version of DayCent that dynamically predicts crop phenology stages, explicitly simulates leaf area index, and represents crop mortality from frost is under testing (Zhang et al., 2018; Zhang et al., 2020b), but was not readily available at the time of this study.

Identifying the agricultural land base across the Southeast US on which winter oilseed crops might ultimately be viable is also challenging. Carinata requires careful integration into existing cropping systems so that its spring maturation and harvest do not clash with the planting of the subsequent summer cash crop (Nóia Júnior et al., 2022). Winter carinata can probably be grown before sorghum or soybean summer crops, but chemical desiccants may be required to expedite carinata harvest (Seepaul et al., 2018) before crops such as cotton and peanut that require relatively early spring planting to reach full maturity. This is an active area of research, though this study assumes the viability of the cotton–carinata–cotton–peanut rotation *a priori*. For simplicity, the current analysis treats all annual cropland in the region as being managed under a cotton–cotton–peanut rotation. Future work could use the USDA Cropland Data Layer (CDL) (Boryan et al., 2011) to identify specific crop rotations in the region, and more selectively model carinata integration into only the most viable rotations. However, like the NLCD used in this assessment, CDL also shows some divergence with CoA cropland area statistics (Lark et al., 2017), particularly in areas outside the agriculturally-dense Corn Belt (Larsen et al., 2015).

Finally, this study assesses the biophysical impacts of winter carinata cultivation but does not include a full life-cycle assessment. This modeling focuses on soil GHG emissions (the dominant source from the US agricultural sector; US EPA, 2020b) but ignores emissions from farm energy use and inputs such as nitrogen fertilizer. The climate-smart management scenarios include quantification of the local soil carbon benefits of poultry litter application, though the full environmental impacts of that practice depend on the alternative uses of that litter (Beausang et al., 2020). There are a variety of environmental issues associated with the indiscriminate surface application of poultry litter in agricultural fields (Bolan et al., 2010), and thus soil incorporation of poultry litter in carinata systems is likely an environmentally preferable disposal option. However, the resulting soil C sequestration may not be additional (i.e., it might have occurred anyways during business-as-usual

management of poultry litter waste), so these poultry litter results should be interpreted as an estimate of local sequestration potential rather than a broad impact assessment meant to inform policy (Plevin et al., 2014). The yield and soil GHG data presented here can be used as an input to life-cycle assessment studies (e.g., Alam et al., 2021) for a more holistic view of the sustainability of carinata–SAF.

CONCLUSION

There is 2.05 Mha of active annual cropland across the region of southern Alabama, southern Georgia, and northern Florida suitable for growing current varieties of carinata as a winter cash crop with low frost risk. This modeling study estimates an average carinata seed yield of 2.9–3.0 Mg ha^{-1} across this study region, depending on crop management practices. Integrating carinata into existing annual crop rotations once every third winter would produce 2.0 Mt of carinata seed annually, which could be converted to over one billion liters of SAF, smaller fractions of other hydrocarbons, and a high-protein seed meal with value as a feed supplement.

The soil carbon and GHG emissions associated with carinata production are highly sensitive to management assumptions. Establishing carinata with conventional tillage and applying synthetic nitrogen fertilizer results in modest soil carbon gains (0.028 Mg C ha^{-1} y^{-1}), the climate benefit of which is largely offset by new N_2O emissions. In contrast, climate-smart management with no-till carinata establishment or using poultry litter as a synthetic N substitute results in more substantial soil carbon sinks at the farms where carinata is cultivated (0.093 and 0.088 Mg C ha^{-1} y^{-1}, respectively), and a net negative total soil GHG footprint of cultivation (–0.308 and –0.234 Mg CO_2e ha^{-1} y^{-1}, respectively). This is equivalent to –0.24 to –0.32 Mg CO_2e per Mg of carinata seed produced, or a 9.2–12.4 g CO_2e MJ^{-1} reduction in the GHG footprint of the resulting carinata-derived SAF using market-based allocation. These results can be incorporated into full life-cycle assessment studies that consider the energy and material inputs to the rest of the carinata–SAF supply chain, e.g., Alam et al. (2021).

The potential for carinata scale-up in this region depends on minimizing frost damage and fitting well within existing crop rotations. Carinata breeding efforts are currently working towards more frost-tolerant and earlier-maturing varieties that can be harvested before interfering with the planting of the next summer crop in the rotation. There are also management options that can limit vulnerability to damage during frost events, and speed up drying (Seepaul et al., 2018). This study suggests that carinata cultivation can create a net soil GHG sink, leading to a modest reduction in the life-cycle GHG footprint of carinata–SAF, and improvements in soil organic matter levels. These results support carinata as a potential win–win–win for generating SAF feedstocks, creating new farm revenue streams, and improving soil quality in the Southeast US.

DATA AVAILABILITY STATEMENT

Data and code supporting the conclusion of this article are available at https://doi.org/10.6084/m9.figshare.19372454. Additional modeling resources supporting the conclusion of this article will be made available by the authors, without undue reservation.

AUTHOR CONTRIBUTIONS

JF conducted the modeling analysis and produced the first draft of the paper. GJ, MJM and RS provided field trial data and developed the crop management scenarios. KB scaled the plant-level yield data observed in field trials to per-hectare yields for modeling purposes. YZ, ME, AS and SW performed the initial model calibration, and YZ performed subsequent model validation. NH, GJ, MJM, RS and PD contributed to the development of baseline crop rotation assumptions. MFHM contributed to land use analysis. KP, SG and DW contributed to funding acquisition and project management. PD also contributed to research management. All authors contributed to the final editing of the paper.

FUNDING

This work was supported by U.S. Department of Agriculture National Institute of Food and Agriculture (USDA/NIFA) through the Southeast Partnership for Advanced Renewables from Carinata (SPARC; award number 2016-11231), through USDA/NIFA award number 2017-67019-26,327, and through ORNL Laboratory Directed Research and Development Project #10681.

ACKNOWLEDGMENTS

We thank Jeff Kent for his advice on modeling specific tillage practices in DayCent, and Tyler Lark and Seth Spawn for their advice on cropland area corrections.

SUPPLEMENTARY MATERIAL

The Supplementary Material for this article can be found online at: https://www.frontiersin.org/articles/10.3389/fenrg.2022.837883/full#supplementary-material

REFERENCES

Abdalla, M., Hastings, A., Cheng, K., Yue, Q., Chadwick, D., Espenberg, M., et al. (2019). A Critical Review of the Impacts of Cover Crops on Nitrogen Leaching, Net Greenhouse Gas Balance and Crop Productivity. *Glob. Change Biol.* 25, 2530–2543. doi:10.1111/gcb.14644

Alam, A., and Dwivedi, P. (2019). Modeling Site Suitability and Production Potential of Carinata-Based Sustainable Jet Fuel in the southeastern United States. *J. Clean. Prod.* 239, 117817. doi:10.1016/j.jclepro.2019.117817

Alam, A., Masum, M. F. H., and Dwivedi, P. (2021). Break-even price and Carbon Emissions of Carinata-based Sustainable Aviation Fuel Production in the Southeastern United States. *GCB Bioenergy* 13, 1800–1813. doi:10.1111/gcbb.12888

Ashworth, A. J., Chastain, J. P., and Moore, P. A. (2020). "Nutrient Characteristics of Poultry Manure and Litter," in *Animal Manure* (Madison, WI: John Wiley & Sons), 63–87. Available at: http://acsess.onlinelibrary.wiley.com/doi/abs/10.2134/asaspecpub67.c5 (Accessed February 15, 2021). doi:10.2134/asaspecpub67.c5

Bailey, V. L., Pries, C. H., and Lajtha, K. (2019). What Do We Know about Soil Carbon Destabilization? *Environ. Res. Lett.* 14, 083004. doi:10.1088/1748-9326/ab2c11

Bashyal, M., Mulvaney, M. J., Lee, D., Wilson, C., Iboyi, J. E., Leon, R. G., et al. (2021). Brassica Carinata Biomass, Yield, and Seed Chemical Composition Response to Nitrogen Rates and Timing on Southern Coastal Plain Soils in the United States. *GCB Bioenergy* 13, 1275–1289. doi:10.1111/gcbb.12846

Beausang, C., McDonnell, K., and Murphy, F. (2020). Anaerobic Digestion of Poultry Litter - A Consequential Life Cycle Assessment. *Sci. Total Environ.* 735, 139494. doi:10.1016/j.scitotenv.2020.139494

Bhattarai, D., Abagandura, G. O., Nleya, T., and Kumar, S. (2021). Responses of Soil Surface Greenhouse Gas Emissions to Nitrogen and Sulfur Fertilizer Rates to Brassica Carinata Grown as a Bio-jet Fuel. *GCB Bioenergy* 13, 627–639. doi:10.1111/gcbb.12784

Bolan, N. S., Szogi, A. A., Chuasavathi, T., Seshadri, B., Rothrock, M. J., and Panneerselvam, P. (2010). Uses and Management of Poultry Litter. *World's Poult. Sci. J.* 66, 673–698. doi:10.1017/s0043933910000656

Boote, K. J., Seepaul, R., Mulvaney, M. J., Hagan, A. K., Bashyal, M., George, S., et al. (2021). Adapting the CROPGRO Model to Simulate Growth and Production of Brassica Carinata , a Bio-fuel Crop. *GCB Bioenergy* 13, 1134–1148. doi:10.1111/gcbb.12838

Boryan, C., Yang, Z., Mueller, R., and Craig, M. (2011). Monitoring US Agriculture: the US Department of Agriculture, National Agricultural Statistics Service, Cropland Data Layer Program. *Geocarto Int.* 26, 341–358. doi:10.1080/10106049.2011.562309

Cardone, M., Mazzoncini, M., Menini, S., Rocco, V., Senatore, A., Seggiani, M., et al. (2003). Brassica Carinata as an Alternative Oil Crop for the Production of Biodiesel in Italy: Agronomic Evaluation, Fuel Production by Transesterification and Characterization. *Biomass and Bioenergy* 25, 623–636. doi:10.1016/s0961-9534(03)00058-8

Chiaramonti, D. (2019). Sustainable Aviation Fuels: the challenge of Decarbonization. *Energ. Proced.* 158, 1202–1207. doi:10.1016/j.egypro.2019.01.308

Clark, M. A., Domingo, N. G. G., Colgan, K., Thakrar, S. K., Tilman, D., Lynch, J., et al. (2020). Global Food System Emissions Could Preclude Achieving the 1.5° and 2°C Climate Change Targets. *Science* 370, 705–708. doi:10.1126/science.aba7357

Crutzen, P. J., Mosier, A. R., Smith, K. A., and Winiwarter, W. (2008). N2O Release from Agro-Biofuel Production Negates Global Warming Reduction by Replacing Fossil Fuels. *Atmos. Chem. Phys.* 8, 389–395. doi:10.5194/acp-8-389-2008

Cubins, J. A., Wells, M. S., Frels, K., Ott, M. A., Forcella, F., Johnson, G. A., et al. (2019). Management of Pennycress as a winter Annual Cash Cover Crop. A Review. *Agron. Sustain. Dev.* 39, 46. doi:10.1007/s13593-019-0592-0

Daly, C., Neilson, R. P., and Phillips, D. L. (1994). A Statistical-Topographic Model for Mapping Climatological Precipitation over Mountainous Terrain. *J. Appl. Meteorol.* 33, 140–158. doi:10.1175/1520-0450(1994)033<0140:astmfm>2.0.co;2

Das, K. C., Minkara, M. Y., Melear, N. D., and Tollner, E. W. (2002). Effect of Poultry Litter Amendment on Hatchery Waste Composting. *J. Appl. Poult. Res.* 11, 282–290. doi:10.1093/japr/11.3.282

Davis, S. J., Lewis, N. S., Shaner, M., Aggarwal, S., Arent, D., Azevedo, I. L., et al. (2018). Net-zero Emissions Energy Systems. *Science* 360, eaas9793. doi:10.1126/science.aas9793

Del Grosso, S. J., Parton, W. J., Keough, C. A., and Reyes-Fox, M. (2011). "Special Features of the DayCent Modeling Package and Additional Procedures for Parameterization, Calibration, Validation, and Applications," in *Advances in Agricultural Systems Modeling Methods of Introducing System Models into Agricultural Research*. Editors L. R. Ahuja and L. Ma (Madison, WI: American Society of Agronomy, Crop Science Society of America, Soil Science Society of America), 155–176. Available at: https://dl.sciencesocieties.org/publications/books/abstracts/advancesinagric/methodsofintrod/155 (Accessed February 3, 2014).

Del Grosso, S., Ojima, D., Parton, W., Mosier, A., Peterson, G., and Schimel, D. (2002). Simulated Effects of Dryland Cropping Intensification on Soil Organic Matter and Greenhouse Gas Exchanges Using the DAYCENT Ecosystem Model. *Environ. Pollut.* 116, S75–S83. doi:10.1016/s0269-7491(01)00260-3

Ernstrom, D. J., and Lytle, D. (1993). Enhanced Soils Information Systems from Advances in Computer Technology. *Geoderma* 60, 327–341. doi:10.1016/0016-7061(93)90034-i

Field, J. L., Evans, S. G., Marx, E., Easter, M., Adler, P. R., Dinh, T., et al. (2018). High-resolution Techno-Ecological Modelling of a Bioenergy Landscape to Identify Climate Mitigation Opportunities in Cellulosic Ethanol Production. *Nat. Energ.* 3, 211–219. doi:10.1038/s41560-018-0088-1

Field, J. L., Marx, E., Easter, M., Adler, P. R., and Paustian, K. (2016). Ecosystem Model Parameterization and Adaptation for Sustainable Cellulosic Biofuel Landscape Design. *GCB Bioenergy* 8, 1106–1123. doi:10.1111/gcbb.12316

Fulton, L. M., Lynd, L. R., Körner, A., Greene, N., and Tonachel, L. R. (2015). The Need for Biofuels as Part of a Low Carbon Energy Future. *Biofuels, Bioprod. Bioref.* 9, 476–483. doi:10.1002/bbb.1559

Gaskin, J. W., Harris, G. H., Franzluebbers, A., and Andrae, J. (2013). *Poultry Litter Application on Pastures and Hayfields*. Athens, GA: The University of Georgia Cooperative Extension.

George, S., Seepaul, R., Geller, D., Dwivedi, P., DiLorenzo, N., Altman, R., et al. (2021). A Regional Inter-disciplinary Partnership Focusing on the Development of a Carinata-centered Bioeconomy. *GCB Bioenergy* 13, 1018–1029. doi:10.1111/gcbb.12828

Goslee, S. C. (2011). National Land-Cover Data and Census of Agriculture Estimates of Agricultural Land-Use Area Differ in the Northeastern United States. *Photogramm Eng. Remote Sensing* 77, 141–147. doi:10.14358/pers.77.2.141

Gryze, S. D., Wolf, A., Kaffka, S. R., Mitchell, J., Rolston, D. E., Temple, S. R., et al. (2010). Simulating Greenhouse Gas Budgets of Four California Cropping Systems under Conventional and Alternative Management. *Ecol. Appl.* 20, 1805–1819. doi:10.1890/09-0772.1

Hagos, R., Shaibu, A. S., Zhang, L., Cai, X., Liang, J., Wu, J., et al. (2020). Ethiopian Mustard (Brassica Carinata A. Braun) as an Alternative Energy Source and Sustainable Crop. *Sustainability* 12, 7492. doi:10.3390/su12187492

He, W., Grant, B. B., Jing, Q., Lemke, R., St. Luce, M., Jiang, R., et al. (2021). Measuring and Modeling Soil Carbon Sequestration under Diverse Cropping Systems in the Semiarid Prairies of Western Canada. *J. Clean. Prod.* 328, 129614. doi:10.1016/j.jclepro.2021.129614

Heaton, E. A., Schulte, L. A., Berti, M., Langeveld, H., Zegada-Lizarazu, W., Parrish, D., et al. (2013). Managing a Second-Generation Crop Portfolio through Sustainable Intensification: Examples from the USA and the EU. *Biofuels, Bioprod. Bioref* 7, 702–714. doi:10.1002/bbb.1429

Homer, C., Dewitz, J., Jin, S., Xian, G., Costello, C., Danielson, P., et al. (2020). Conterminous United States Land Cover Change Patterns 2001-2016 from the 2016 National Land Cover Database. *ISPRS J. Photogrammetry Remote Sensing* 162, 184–199. doi:10.1016/j.isprsjprs.2020.02.019

H. S. Eggleston, L. Buendia, K. Miwa, T. Ngara, and K. Tanabe (Editors) (2006). *Agriculture, Forestry and Other Land Use," in 2006 IPCC Guidelines for National Greenhouse Gas Inventories* (Japan: Institute for Global Environmental Strategies IGES), 4.

Iboyi, J. E., Mulvaney, M. J., Balkcom, K. S., Seepaul, R., Bashyal, M., Perondi, D., et al. (2021). Tillage System and Seeding Rate Effects on the Performance of Brassica Carinata. *GCB Bioenergy* 13, 600–617. doi:10.1111/gcbb.12809

Jian, J., Du, X., Reiter, M. S., and Stewart, R. D. (2020). A Meta-Analysis of Global Cropland Soil Carbon Changes Due to Cover Cropping. *Soil Biol. Biochem.* 143, 107735. doi:10.1016/j.soilbio.2020.107735

Johnson, D. M. (2013). A 2010 Map Estimate of Annually Tilled Cropland within the Conterminous United States. *Agric. Syst.* 114, 95–105. doi:10.1016/j.agsy.2012.08.004

Lark, T. J., Mueller, R. M., Johnson, D. M., and Gibbs, H. K. (2017). Measuring Land-Use and Land-Cover Change Using the U.S. Department of Agriculture's Cropland Data Layer: Cautions and Recommendations. *Int. J. Appl. Earth Observation Geoinformation* 62, 224–235. doi:10.1016/j.jag.2017.06.007

Lark, T. J., Spawn, S. A., Bougie, M., and Gibbs, H. K. (2020). Cropland Expansion in the United States Produces Marginal Yields at High Costs to Wildlife. *Nat. Commun.* 11, 4295. doi:10.1038/s41467-020-18045-z

Larsen, A. E., Hendrickson, B. T., Dedeic, N., and MacDonald, A. J. (2015). Taken as a Given: Evaluating the Accuracy of Remotely Sensed Crop Data in the USA. *Agric. Syst.* 141, 121–125. doi:10.1016/j.agsy.2015.10.008

Li, N., Kumar, P., Lai, L., Abagandura, G. O., Kumar, S., Nleya, T., et al. (2019). Response of Soil Greenhouse Gas Fluxes and Soil Properties to Nitrogen Fertilizer Rates under Camelina and Carinata Nonfood Oilseed Crops. *Bioenerg. Res.* 12, 524–535. doi:10.1007/s12155-019-09987-4

Lynch, D., Henihan, A. M., Bowen, B., Lynch, D., McDonnell, K., Kwapinski, W., et al. (2013). Utilisation of Poultry Litter as an Energy Feedstock. *Biomass and Bioenergy* 49, 197–204. doi:10.1016/j.biombioe.2012.12.009

Markel, E., English, B. C., Hellwinckel, C., Menard, R. J., et al.United States. Federal Aviation Administration; Center of Excellence for Alternative Jet Fuels and Environment (2018). Potential for Pennycress to Support a Renewable Jet Fuel Industry. Available at: https://rosap.ntl.bts.gov/view/dot/57458 (Accessed November 5, 2021).

Maxwell, S. K., Wood, E. C., and Janus, A. (2008). Comparison of the USGS 2001 NLCD to the 2002 USDA Census of Agriculture for the Upper Midwest United States. *Agric. Ecosyst. Environ.* 127, 141–145. doi:10.1016/j.agee.2008.03.012

McClelland, S. C., Paustian, K., and Schipanski, M. E. (2021). Management of Cover Crops in Temperate Climates Influences Soil Organic Carbon Stocks: a Meta-Analysis. *Ecol. Appl.* 31, e02278. doi:10.1002/eap.2278

Mesinger, F., DiMego, G., Kalnay, E., Mitchell, K., Shafran, P. C., Ebisuzaki, W., et al. (2006). North American Regional Reanalysis. *Bull. Amer. Meteorol. Soc.* 87, 343–360. doi:10.1175/bams-87-3-343

Minasny, B., Malone, B. P., McBratney, A. B., Angers, D. A., Arrouays, D., Chambers, A., et al. (2017). Soil Carbon 4 Per Mille. *Geoderma* 292, 59–86. doi:10.1016/j.geoderma.2017.01.002

Mola-Yudego, B., Díaz-Yáñez, O., and Dimitriou, I. (2015). How Much Yield Should We Expect from Fast-Growing Plantations for Energy? Divergences between Experiments and Commercial Willow Plantations. *Bioenerg. Res.* 8, 1769–1777. doi:10.1007/s12155-015-9630-1

Montemurro, F., Diacono, M., Scarcella, M., D'Andrea, L., Boari, F., Santino, A., et al. (2016). Agronomic Performance for Biodiesel Production Potential of Brassica Carinata A. Braun in Mediterranean Marginal Areas. *Ital. J. Agron.* 10, 57–64. doi:10.4081/ija.2016.684

Muhammad, I., Sainju, U. M., Zhao, F., Khan, A., Ghimire, R., Fu, X., et al. (2019). Regulation of Soil CO2 and N2O Emissions by Cover Crops: A Meta-Analysis. *Soil Tillage Res.* 192, 103–112. doi:10.1016/j.still.2019.04.020

Mulvaney, M. J., Seepaul, R., Small, I. M., Wright, D. L., Paula-Moraes, S. V., Crozier, C., et al. (2018). Frost Damage of Carinata Grown in the Southeastern US: SS-AGR-420/ag420, 5/2018. *EDIS* 2018. Available at: https://journals.flvc.org/edis/article/view/105892 (Accessed February 26, 2022), 5. doi:10.32473/edis-ag420-2018

Nóia Júnior, R. de. S., Fraisse, C. W., Bashyal, M., Mulvaney, M. J., Seepaul, R., Zientarski Karrei, M. A., et al. (2022). Brassica Carinata as an Off-Season Crop in the southeastern USA: Determining Optimum Sowing Dates Based on Climate Risks and Potential Effects on Summer Crop Yield. *Agric. Syst.* 196, 103344. doi:10.1016/j.agsy.2021.103344

Ogle, S. M., Alsaker, C., Baldock, J., Bernoux, M., Breidt, F. J., McConkey, B., et al. (2019). Climate and Soil Characteristics Determine where No-Till Management Can Store Carbon in Soils and Mitigate Greenhouse Gas Emissions. *Sci. Rep.* 9, 11665. doi:10.1038/s41598-019-47861-7

O'Malley, J., Pavlenko, N., and Searle, S. (2021). *Estimating Sustainable Aviation Fuel Feedstock Availability to Meet Growing European Union Demand*. Washington, DC: International Council on Clean Transportation.

Paustian, K., Easter, M., Brown, K., Chambers, A., Eve, M., Huber, A., et al. (2018). Field- and Farm-Scale Assessment of Soil Greenhouse Gas Mitigation Using COMET-Farm. *Precision Conservation: Geospatial Tech. Agric. Nat. Resour. Conservation Agron. Monogr.* 59, 341–359. Available at: http://dl.sciencesocieties.org/publications/books/abstracts/agronomymonogra/agronmonogr59/agronmonogr59.2013.0033 (Accessed May 15, 2019). doi:10.2134/agronmonogr59.c16

Paustian, K., Lehmann, J., Ogle, S., Reay, D., Robertson, G. P., and Smith, P. (2016). Climate-smart Soils. *Nature* 532, 49–57. doi:10.1038/nature17174

Plevin, R. J., Delucchi, M. A., and Creutzig, F. (2014). Using Attributional Life Cycle Assessment to Estimate Climate-Change Mitigation Benefits Misleads Policy Makers. *J. Ind. Ecol.* 18, 73–83. doi:10.1111/jiec.12074

Poeplau, C., and Don, A. (2015). Carbon Sequestration in Agricultural Soils via Cultivation of Cover Crops - A Meta-Analysis. *Agric. Ecosyst. Environ.* 200, 33–41. doi:10.1016/j.agee.2014.10.024

Prussi, M., Lee, U., Wang, M., Malina, R., Valin, H., Taheripour, F., et al. (2021). CORSIA: The First Internationally Adopted Approach to Calculate Life-Cycle GHG Emissions for Aviation Fuels. *Renew. Sustain. Energ. Rev.* 150, 111398. doi:10.1016/j.rser.2021.111398

Qian, B., Zhang, X., Smith, W., Grant, B., Jing, Q., Cannon, A. J., et al. (2019). Climate Change Impacts on Canadian Yields of spring Wheat, Canola and maize for Global Warming Levels of 1.5°C, 2.0°C, 2.5°C and 3.0°C. *Environ. Res. Lett.* 14, 074005. doi:10.1088/1748-9326/ab17fb

Resurreccion, E. P., Roostaei, J., Martin, M. J., Maglinao, R. L., Zhang, Y., and Kumar, S. (2021). The Case for Camelina-Derived Aviation Biofuel: Sustainability Underpinnings from a Holistic Assessment Approach. *Ind. Crops Prod.* 170, 113777. doi:10.1016/j.indcrop.2021.113777

Rockström, J., Schellnhuber, H. J., Hoskins, B., Ramanathan, V., Schlosser, P., Brasseur, G. P., et al. (2016). The World's Biggest Gamble. *Earth's Future* 4, 465–470. doi:10.1002/2016EF000392

Rogeri, D. A., Ernani, P. R., Mantovani, A., and Lourenço, K. S. (2016). Composition of Poultry Litter in Southern Brazil. *Revista Brasileira de Ciência Do Solo* 40. Available at: http://www.scielo.br/scielo.php?script=sci_abstract&pid=S0100-06832016000100525&lng=en&nrm=iso&tlng=en (Accessed February 15, 2021).

Roth, B., Finnan, J. M., Jones, M. B., Burke, J. I., and Williams, M. L. (2015). Are the Benefits of Yield Responses to Nitrogen Fertilizer Application in the Bioenergy cropMiscanthus × Giganteusoffset by Increased Soil Emissions of Nitrous Oxide? *GCB Bioenergy* 7, 145–152. doi:10.1111/gcbb.12125

Schulmeister, T. M., Ruiz-Moreno, M., Silva, G. M., Garcia-Ascolani, M., Ciriaco, F. M., Henry, D. D., et al. (2021). Characterization of Dietary Protein in Brassica Carinata Meal when Used as a Protein Supplement for Beef Cattle Consuming a Forage-Based Diet. *J. Anim. Sci.* 99, skaa383. doi:10.1093/jas/skaa383

Schulmeister, T. M., Ruiz-Moreno, M., Silva, G. M., Garcia-Ascolani, M., Ciriaco, F. M., Henry, D. D., et al. (2019b). Evaluation ofBrassica Carinatameal on Ruminant Metabolism and Apparent Total Tract Digestibility of Nutrients in Beef Steers1,2. *J. Anim. Sci.* 97, 1325–1334. doi:10.1093/jas/skz009

Schulmeister, T. M., Ruiz-Moreno, M., Silva, G. M., Garcia-Ascolani, M., Ciriaco, F. M., Henry, D. D., et al. (2019a). Evaluation of Brassica Carinata Meal as a Protein Supplement for Growing Beef Heifers1,2. *J. Anim. Sci.* 97, 4334–4340. doi:10.1093/jas/skz280

Seepaul, R., Marois, J., Small, I., George, S., and Wright, D. L. (2018). Optimizing Swathing and Chemical Desiccant Timing to Accelerate Winter Carinata Maturation. *Agron.j.* 110, 1379–1389. doi:10.2134/agronj2017.08.0496

Seepaul, R., Marois, J., Small, I. M., George, S., and Wright, D. L. (2019a). Carinata Dry Matter Accumulation and Nutrient Uptake Responses to Nitrogen Fertilization. *Agron.j.* 111, 2038–2046. doi:10.2134/agronj2018.10.0678

Seepaul, R., Mulvaney, M. J., Small, I. M., George, S., and Wright, D. L. (2020). Carinata Growth, Yield, and Chemical Composition Responses to Nitrogen Fertilizer Management. *Agron.j.* 112, 5249–5263. doi:10.1002/agj2.20416

Seepaul, R., Small, I. M., Mulvaney, M. J., George, S., Leon, R. G., Paula-Moraes, S. V., et al. (2019b). *Carinata, the Sustainable Crop for a Bio-Based Economy:*

2018-2019 Production Recommendations for the Southeastern United States. Gainesville, FL: University of Florida/IFAS Extension, Agronomy Department.

Sharpley, A., Slaton, N., Tabler, T., VanDevender, K., Daniels, M., Jones, F., et al. (2009). *Nutrient Analysis of Poultry Litter*. Fayetteville, AR: University of Arkansas Cooperative Extension Service.

Stocker, T. F., Qin, D., Plattner, G.-K., Tignor, M. M., Allen, S. K., Boschung, J., et al. (2014). Climate Change 2013: The Physical Science Basis. Contribution of Working Group I to the Fifth Assessment Report of IPCC the Intergovernmental Panel on Climate Change. Available at: https://www.ipcc.ch/report/ar5/wg1/ (Accessed December 2, 2021).

Tonitto, C., David, M. B., and Drinkwater, L. E. (2006). Replacing Bare Fallows with Cover Crops in Fertilizer-Intensive Cropping Systems: A Meta-Analysis of Crop Yield and N Dynamics. *Agric. Ecosyst. Environ.* 112, 58–72. doi:10.1016/j.agee.2005.07.003

US EPA (2020a). "ANNEX 3 Methodological Descriptions for Additional Source or Sink Categories," in *Inventory of U.S. Greenhouse Gas Emissions and Sinks: 1990-2018* (Washington, DC: U.S. Environmental Protection Agency), 318. Available at: https://www.epa.gov/ghgemissions/inventory-us-greenhouse-gas-emissions-and-sinks-1990-2018 (Accessed May 18, 2020).

US EPA (2018). *Biofuels and the Environment: The Second Triennial Report to Congress*. Washington, DC: US Environmental Protection Agency.

US EPA (2020b). *Inventory of U.S. Greenhouse Gas Emissions and Sinks: 1990-2018*. Washington, DC: US Environmental Protection Agency. Available at: https://www.epa.gov/ghgemissions/inventory-us-greenhouse-gas-emissions-and-sinks-1990-2018 (Accessed May 18, 2020).

USDA NRCS (2006). *Land Resource Regions (LRR) and Major Land Resource Areas (MLRA) of the United States, the Caribbean, and the Pacific Basin*. Washington, DC: U.S. Department of Agriculture

Williams, J. H., Jones, R. A., Haley, B., Kwok, G., Hargreaves, J., Farbes, J., et al. (2021). Carbon-Neutral Pathways for the United States. *AGU Adv.* 2, e2020AV000284. doi:10.1029/2020av000284

Zemanek, D., Champagne, P., and Mabee, W. (2020). Review of Life-cycle Greenhouse-gas Emissions Assessments of Hydroprocessed Renewable Fuel (HEFA) from Oilseeds. *Biofuels, Bioprod. Bioref.* 14, 935–949. doi:10.1002/bbb.2125

Zhang, Y., Gurung, R., Marx, E., Williams, S., Ogle, S. M., and Paustian, K. (2020a). DayCent Model Predictions of NPP and Grain Yields for Agricultural Lands in the Contiguous U.S. *J. Geophys. Res. Biogeosci.* 125. Available at: https://onlinelibrary.wiley.com/doi/abs/10.1029/2020JG005750 (Accessed August 20, 2020).

Zhang, Y., Marx, E., Williams, S., Gurung, R., Ogle, S., Horton, R., et al. (2020b). Adaptation in U.S. Corn Belt Increases Resistance to Soil Carbon Loss with Climate Change. *Sci. Rep.* 10, 13799. doi:10.1038/s41598-020-70819-z

Zhang, Y., Suyker, A., and Paustian, K. (2018). Improved Crop Canopy and Water Balance Dynamics for Agroecosystem Modeling Using DayCent. *Agron.j.* 110, 511–524. doi:10.2134/agronj2017.06.0328

Conflict of Interest: GJ was employed by Nuseed, West Sacramento, CA, United States.

The remaining authors declare that the research was conducted in the absence of any commercial or financial relationships that could be construed as a potential conflict of interest.

Publisher's Note: All claims expressed in this article are solely those of the authors and do not necessarily represent those of their affiliated organizations, or those of the publisher, the editors and the reviewers. Any product that may be evaluated in this article, or claim that may be made by its manufacturer, is not guaranteed or endorsed by the publisher.

frontiers | Frontiers in Energy Research

ORIGINAL RESEARCH
published: 18 May 2022
doi: 10.3389/fenrg.2022.780795

The Economic Impact of a Renewable Biofuels/Energy Industry Supply Chain Using the Renewable Energy Economic Analysis Layers Modeling System

Burton C. English[*†‡], *R. Jamey Menard*[†‡] *and Bradly Wilson*[†‡]

Institute of Agriculture, Department of Agricultural and Resource Economics, University of Tennessee, Knoxville, TN, United States

OPEN ACCESS

Edited by:
William Goldner, United States Department of Agriculture (USDA), United States

Reviewed by:
Damjan Gojko Vučurović, University of Novi Sad, Serbia
Johnathan Holladay, LanzaTech, United States

***Correspondence:**
Burton C. English
benglish@utk.edu

[†]*These authors have contributed equally to this work and share first authorship*

[‡]*These authors have contributed equally to this work and share senior authorship*

Specialty section:
This article was submitted to Bioenergy and Biofuels, a section of the journal Frontiers in Energy Research

Received: *21 September 2021*
Accepted: *28 February 2022*
Published: *18 May 2022*

Citation:
English BC, Menard RJ and Wilson B (2022) The Economic Impact of a Renewable Biofuels/Energy Industry Supply Chain Using the Renewable Energy Economic Analysis Layers Modeling System. Front. Energy Res. 10:780795. doi: 10.3389/fenrg.2022.780795

The University of Tennessee's (UT) Department of Agricultural and Resource Economics models supply chains for both liquid and electricity generating technologies currently in use and/or forthcoming for the bio/renewable energy industry using the input–output model IMPLAN®. The approach for ethanol, biodiesel, and other liquid fuels includes the establishment and production of the feedstock, transportation of the feedstock to the plant gate, and the one-time investment as well as annual operating of the facility that converts the feedstock to a biofuel. This modeling approach may also include the preprocessing and storage of feedstocks at depots. Labor/salary requirements and renewable identification number (RIN) values and credits attributable to the conversion facility, along with land-use changes for growing the feedstock are also included in the supply chain analyses. The investment and annual operating of renewable energy technologies for electricity generation for wind, solar, and digesters are modeled as well. Recent modeling emphasis has centered on the supply chain for liquid fuels using the Bureau of Economic Analysis's 179 economic trading areas as modeling regions. These various data layers necessary to estimate the economic impact are contained in UT's renewable energy economic analysis layers (REEAL) modeling system. This analysis provides an example scenario to demonstrate REEAL's modeling capabilities. The conversion technology modeled is a gasification Fischer–Tropsch biorefinery with feedstock input of 495,000 metric tons per year of forest residue transported to a logging road that is less than one mile in distance. The biorefinery is expected to produce sustainable aviation fuel (SAF), diesel, and naphtha. An estimated one million tons of forest residue are required at fifty percent moisture content. Based on a technical economic assessment (TEA) developed by the Aviation Sustainability Center (ASCENT) and the quantity of hardwood residues available in the Central Appalachian region, three biorefineries could be sited each utilizing 495,000 dry metric tons per year. Each biorefinery could produce 47.5 million liters of SAF, 40.3 million liters of diesel, and 23.6 million liters of naphtha. Annual gross revenues for fuel required for the biorefineries to break even are estimated at $193.7 million per biorefinery. Break-even plant gate fuel prices when

assuming RINs and 12.2 percent return on investment are $1.12 per liter for SAF, $1.15 per liter for diesel, and $0.97 per liter for naphtha. Based on IMPLAN, an input–output model, and an investment of $1.7 billion, the estimated economic annual impact to the Central Appalachian region if the three biorefineries are sited is over a half a billion dollars. Leakages occur as investment dollars leaving the region based on the regions local purchase coefficients (i.e., LPPs), which totals $500 million. This results in an estimated $2.67 billion in economic activity with a multiplier of 1.7, or for every million dollars spent, an additional $0.7 million in economic activity is generated in the regional economy. Gross regional product is estimated at $1.28 billion and employment of nearly 1,200 jobs are created during the construction period of the biorefineries, which results in $700 million in labor income with multiplier effects. Economic activity for the feedstock operations (harvesting and chipping) is estimated at slightly more than $16.8 million resulting in an additional $30 million in the economic impact. The stumpage and additional profit occurring from the harvest of the forest residues result in $40 million directly into the pockets of the resource and logging operation owners. Their subsequent expenditures resulted in a total economic activity increase of $71.4 million. These operations result in creating an estimated 103 direct jobs for a total of 195 with multiplier effects. Direct feedstock transportation expenditures of more than $36.7 million provide an estimated increase in economic activity of almost $68 million accounting for the multiplier effects.

Keywords: biorefinery, economic impact, sustainable aviation fuel, SAF, input–output, spatial simulation, Central Appalachia

INTRODUCTION

Economic impact analysis (EIA) is one methodology used to evaluate the impact of a policy, program, or project on the economy to a specified region. EIA is a useful analysis tool for decision-making, providing a measure of strategic goal achievement that complements the analysis of efficiency (benefit-cost) and financial feasibility. EIA provides information on the effects of events on a regional economy. Typically, the impact is measured using several indicators that include changes in business or economic activity, employment (jobs), gross regional product (GRP), and tax collections as a result of attracting a new industry to a region.

Frequently, national-, state-, and/or county-level actions are proposed to provide incentives for attracting an industry. To evaluate the potential benefits of such actions, information on changes in community welfare is sought. EIA is an important tool to assist in this decision-making providing information on not only the economic impact to input supplying industries but also the impact from the investment and annual operations of the new industry and potential job creations.

The costs of an energy policy can be determined, but the benefits generated by that policy may be difficult to estimate or very limited in what is considered. An accounting of costs is required, but the costs do not reflect how the policy will affect a state, region, or community. Not including all benefits will impact decision-making and "can prevent environmental, energy, and/or economic policy makers from capturing all the potential gains associated with pursuing energy efficiency and renewable energy policies" (Environmental Protection Agency, 2010).

Input–output analysis provides a framework for use in EIA. This method of analysis has been used since 1930s, first introduced by Wassily Leontief (Lonergan and Cocklin, 1985). Input–output (I-O) analysis, which is based on the interdependence of the different economic sectors and households that exist in a regional economy, quantifies the total economic effects of a change in the demand for a given product or service and captures relationships and interdependencies within the region of interest (Baumol, 2000). The model uses industry interdependence formed by production functions. The production functions reflect regional interdependence and are determined through transactions or purchases sectors make during production of goods and services. These relationships project change that might occur because of a demand change for inputs. Input–output modeling evaluates the initial shock of the event and its ripple effects through the economy. The event in this analysis is the creation of a "new" industry—production of sustainable aviation fuel (SAF) in Central Appalachia.

Analysis requires information on proposed transactions from the "new" industry that might occur or be lost. What that "new" industry looks like, its supply chains, what products are produced, and what impact the industry may have on existing transactions are all questions requiring information. The transactions occurring once (e.g., investment) need to be separated from the transactions occurring yearly. Some transactions will have a positive effect whereas others a negative on the region's economy.

This information can be both expensive and quite extensive as well as proprietary to obtain. Yet, quick and accurate information

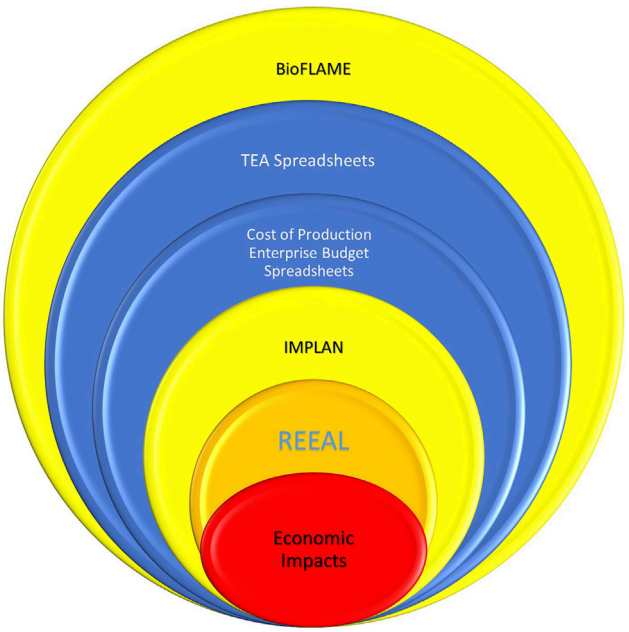

FIGURE 1 | Renewable energy economic analysis layers (REEAL) modeling system and its components.

is required. The University of Tennessee's (UT) Department of Agricultural and Resource Economics has reviewed and identified supply chain information on renewable energy technologies such as electricity generation via wind, solar, geothermal, and biopower as well as biofuel generation through pyrolysis, gasification, hydro-processed esters and fatty acids (HEFAs), and other technologies. This inventory of technologies and supply chain components has been incorporated into the renewable energy economic analysis layers (REEAL) modeling system (**Figure 1**). While renewable technologies such as the generation of electricity via wind, solar, and digesters have been conducted in the past, recent modeling emphasis has centered on the supply chain for liquid fuels (English et al., 2006; De La Torre Ugarte, 2007; English et al., 2009a; English et al., 2009b; English et al., 2009c; English et al., 2009d; Lambert et al., 2016; Markel et al., 2019).

The location of these "new" industries via spatial analysis is required for decision makers. Providing regional analysis via using the Bureau of Economic Analysis's (BEA) 179 economic trading areas provides a template for regional modeling (**Figure 2**). BEAs represent centers of economic activity, recognize both metropolitan and micropolitan statistical areas, and provide information on changes in economic and population growth in the United States (Johnson and Kort, 2004).

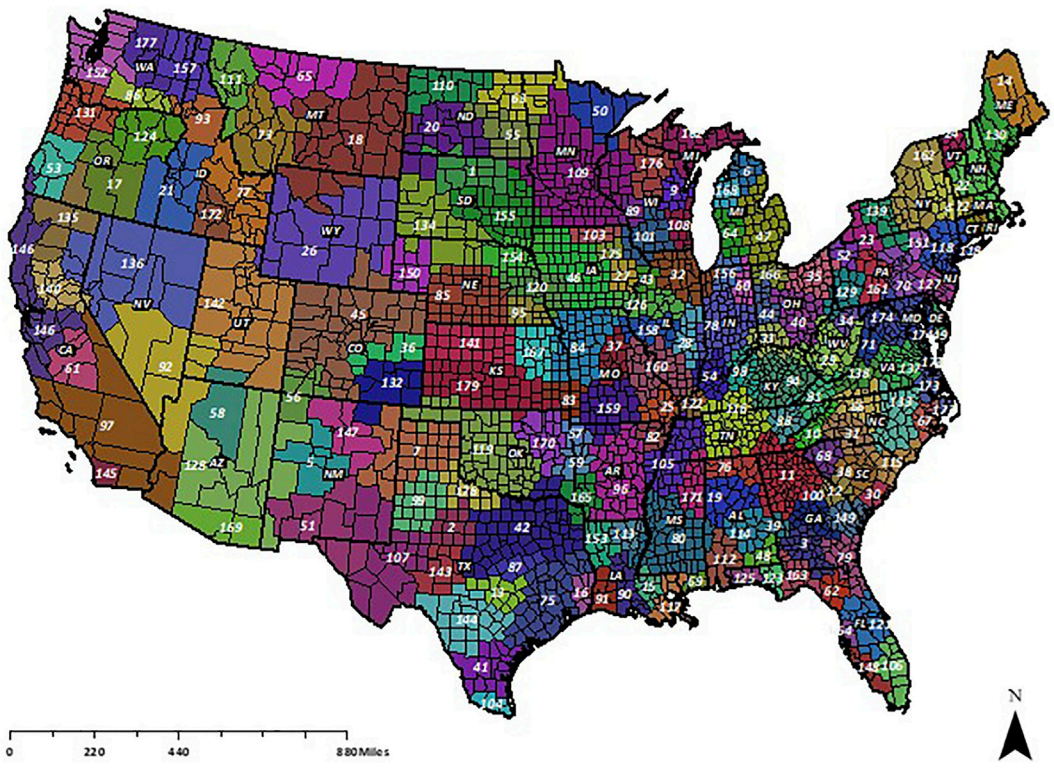

FIGURE 2 | Bureau of Economic Analysis's economic areas for input–output analysis modeling.

One existing I-O modeling system and its inherent databases for regional estimates of the economic impact occurring in a potential renewable biofuels supply chain is the IMPLAN® (IMPLAN Group LLC, 2018). The IMPLAN's data support system provides an annual quantitative description of each U.S. county's economic activity, which can be aggregated to multicounty economic regions. Thus, within REEAL, the economic impact is evaluated at a BEA region using multicounty-level aggregated data. From this information, regional purchase coefficients are generated to determine the leakage (purchases outside the study region) that occurs as inputs are purchased. These coefficients define where (within or outside the region) purchases are made and the proportion of goods or services used to meet intermediate or final demand that is supplied within the region of interest (Ralston, Hastings, and Brucker, 1986). Transactions occurring outside the study region (coined a "leakage" in I-O analysis) are not considered for regional economic activity. For larger events, for example, a regional model representing multiple BEAs, a larger regional or national analysis is conducted in addition to the BEA analysis. The difference in the impact between those estimated for each BEA and those estimated by the national analysis provide information on the impact of those leakages to the multiple BEA areas or the nation.

The siting or location of the technology (for example, biofuel conversion) can be specified or simulated. In this article, the location is simulated using a spatial GIS model, BioFLAME (Biofuels Facility Location Analysis Modeling Endeavor), which provides information on where the conversion technologies, feedstock, and transportation routes might be located. This spatial analytical tool is based on current infrastructure, costs, and land use (Graham, English, and Noon, 2000; He-Lambert, English, Menard, and Lambert, 2016; Sharma, Birrell, and Miguez, 2017; He-Lambert et al., 2018; Markel, English, Hellwinckel, and Menard, 2019). These models typically minimize cost of feedstock to identify potential locations. The conversion technologies modeled in REEAL provide information on what purchases are required, their infrastructure requirements, and the costs of conversion.

The supply chain in this analysis for sustainable aviation fuel and other coproduct fuels includes both downstream and upstream effects, more specifically, the establishment and production of the feedstock and the transportation of the feedstock to the plant gate and fuel from the biorefinery along with the one-time investment plus annual operating costs of the biorefinery that converts the feedstock to a biofuel. Other supply chain components may also include the preprocessing and storage of feedstocks on the "farm" or at depots. Labor/salary needs for these activities, the economic impact of renewable identification number (RIN) values and credits attributable to the conversion facility, and land-use changes for growing the feedstock are also included in this analysis. A discussion of REEAL's components, along with an analysis example using the model, is provided.

The example provides estimates of the economic impact resulting from SAF biorefineries located in a depressed region of the United States—Central Appalachia. The feedstock available to the industry is forest residues. The technology available to convert those residues to SAF and other biofuels is based on a greenfield gasification Fischer–Tropsch technology (Brandt et al., 2021).

METHODOLOGY

Multiple information sources are used to develop REEAL. Engineering techno-economic assessment (TEA) spreadsheet tools or cost of production enterprise budgets are used to provide cost information. The TEAs represent conversion technologies for either preprocessing the feedstock or fuel conversion. The enterprise budgets provide information on feedstock and transportation. Information is also derived from the 179 I-O models developed using IMPLAN. These models incorporate the information from the spreadsheet to develop an estimate of economic impact resulting from the establishment of the technology or feedstock being investigated. The spatial land use model, BioFLAME, provides information on the extent of the impact. For each supply region that comes into solution, information on feedstock quantity, cost, miles transported, and the cost of that transportation is estimated. Adding these two cost categories provides information on break-even delivered cost to the biorefinery. Since I-O models are linear in nature, the analysis is conducted for a single conversion facility. If two or more conversion facilities locate in a particular BEA, then the economic impact increases by that factor. **Table 1** indicates the current technology information available from the spreadsheets in REEAL. Also included are the general impact relating primarily to reduced expenditures because of changes in land use and increased expenditures because of changes in proprietor income and the sale of RINs.

The initial step in the development of the event is to specify the supply chain, which consists of feedstock production/maintenance/harvest, preprocessing, conversion, and distribution of products. Once defined, the scale of the preprocessing and conversion components is required, along with the type of needed feedstock—agricultural residues, forest residues, dedicated energy crops, and/or oilseeds, and the pathway, which defines the conversion technology along with some of the potential incentives that are available. In the following example, the economic impact is estimated for converting forest residues in Central Appalachia via a gasification Fischer–Tropsch (GFT) biorefinery with a feedstock input of 495,000 dry metric tons per year (1,500 metric tons per day) to demonstrate REEAL's modeling capabilities. The supply chain consists of transporting the feedstock to a forest landing, chipping, transporting the feedstock to the biorefinery, and feedstock conversion.

Cost of Feedstock Production

Feedstock costs are derived from several sources: 1) the Billion-Ton study (U.S. Department of Energy, 2016); 2) an agricultural and forest model POLYSYS (Policy Analysis Systems Model) (English, et al., 2006; Hellwinckel, 2019); 3) ForSEAM (Forest Sustainable and Economic Analysis Model) (English et al., 2006); and 4) crop enterprise spreadsheets developed at the University of

TABLE 1 | Conversion and renewable energy technologies, feedstocks, and land-use changes incorporated into the renewable energy economic analysis layers modeling system.

Renewable power and fuel technologies	
1 Alcohol-to-jet	2 Gasification and Fischer–Tropsch w/microreactor
3 Biodiesel	4 Horizontal axis wind
5 Bio-jet *via* Virent's BioForming	6 Hydro-treated esters and fatty acids (HEFAs)
7 Co-firing	8 Land fill
9 Digesters (dairy and swine)	10 Photovoltaic
11 Direct sugar hydrocarbon (DSHC)	12 Pyrolysis
13 Direct wood fired	14 Solvent extraction
15 Enzymatic (cellulosic ethanol)	16 Stoker boiler
17 Gasification	18 Utility photovoltaic
19 Gasification and Fischer-Tropsch	—
Preprocessing technologies	
1 Bailing	2 Pyrolysis depot
3 High-moisture pelleting	4 Solvent extraction
5 Oil crush	—
Potential feedstocks	
1 Algae	2 Pennycress
3 Camelina	4 Rye
5 Carinata	6 Short-rotation woody crops
7 Corn	8 Soybeans
9 Corn stover	10 Switchgrass
11 Forest residues	12 Triticale
13 Municipal solid waste	—
Potential land use changes	—
1 Cotton	2 Hay
3 Grains	4 Oilseeds
Transportation	—
1 Bales	2 Logs
3 Liquid biomass	**4 Wood chips/pellets**
5 Liquid fuel	—

Note: The example for this analysis uses the technologies in bold*. No preprocessing technologies are required since a no depot supply chain is assumed. Any preprocessing required occurs at the biorefinery.*

Tennessee for switchgrass, short-rotation poplar, and oilseed crops such as carinata, camelina, and pennycress. The POLYSYS database provides information on selected agricultural residues such as corn stover and wheat straw as well as additional dedicated energy crops that include *Miscanthus*, energy cane, and short-rotation tree species such as willow, sweetgum, and sycamore. For perennial dedicated energy herbaceous and tree crops, an establishment cost is estimated and treated as an investment in the development of the feedstock. All the crops have maintenance and harvest/collection costs. **Table 2** contains information on these costs for each of the feedstocks.

Techno-Economic Assessment Spreadsheets–Conversion and Preprocessing

ASCENT TEAs contain information on pre-specified engineering technology information on investment in the facility as well as its operation costs. The TEAs provide inputs needed, the conversion technologies output, along with information on capital expenditures (CAPEX) and operating expenditures (OPEX) (Brandt, Tanzil, Garcia-Perez, and Wolcott, 2021). Currently, ASCENT TEAs include alcohol-to-jet, gasification/Fischer–Tropsch, HEFA, gasification with microreactor, and pyrolysis. The ASCENT baseline spreadsheets calculate a break-even value for the coproducts produced assuming a 12.2 percent return on investment, and the net present value equals zero. These baseline spreadsheets have a specified throughput and feedstock that the user can change. The baseline is used to estimate the impact with an average feedstock cost. The scenarios use alternative feedstocks and capacity when compared to the baseline. This analysis uses the gasification/Fischer–Tropsch TEA in its analysis.

To meet the specification requirements of the conversion facility, preprocessing of biomass feedstock is often required. Preprocessing is either performed at the conversion facility, a depot, or in the field. Depot preprocessing spreadsheets are incorporated in REEAL for conventional and high-moisture pelleting (pellets), chipping at landing (chips), pyrolysis (oil), and crushing (oil).

BioFLAME

BioFLAME is a large-scale, multiregional optimization model that determines the least-cost locations of biofuel facilities supplying aviation fuel to airports, or other demanders, and the attendant changes in land use, given the location of the feedstock. In other words, BioFLAME determines which BEAs the biorefinery will be sited. It is currently calibrated for the southeastern US but is capable of being calibrated for other

TABLE 2 | Summary of the basic costs of feedstock production.

Item	Type	Activity	Base direct value (2018$)	Assumption used to determine the base direct value
Algae	Investment	Establishment	$450,252,407	37.5 US tons/acre/yr (based on 5,000 wetted acres)
Algae	Annual operating	Feedstock maintenance and harvest	$72,023,735	37.5 US tons/acre/yr (based on 5,000 wetted acres)
Camelina	Annual operating	Feedstock maintenance and harvest	$15,280,635	Based on 100,000 acres
Carinata	Annual operating	Feedstock maintenance and harvest	$17,902,526	Based on 100,000 acres
Wood chips	Annual operating	Harvest and Preprocessing	$1,000,000	Based on Billion-Ton cost estimates
Chipping	**Annual operating**	**Stumpage and preprocessing into chips at landing**	**$650,000**	**Based on Billion-Ton cost estimates**
Forest residue labor during harvest and preprocessing	**Annual operating**	**Labor involved in harvest**	**$350,000**	**Based on Billion-Ton cost estimates**
Harvesting logs	Annual operating	Feedstock harvest	$1,000,000	Based on Billion-Ton cost estimates
Pennycress	Annual operating	Feedstock maintenance and harvest	$10,210,129	Based on 100,000 acres
Rye	Annual operating	Feedstock maintenance and harvest	$27,335,984	Based on 100,000 acres
Switchgrass	Investment	Establishment	$37,143,544	Based on 100,000 acres
Switch harvest	Annual operating	Feedstock harvest	$32,729,572	Based on 100,000 acres
Switchgrass maintenance	Annual operating	Feedstock maintenance	$15,994,957	Based on 100,000 acres
Switchgrass storage	Annual operating	Feedstock storage	$14,387,330	Based on 100,000 acres
Triticale	Annual operating	Feedstock maintenance and harvest	$33,910,050	Based on 100,000 acres
Transportation	**Annual operating**	**Mode-truck**	**$10,000,000**	**See Table 3 for additional information**

Note: The example for this analysis uses the technologies in bold*. No preprocessing technologies are required since a no depot supply chain is assumed. Any preprocessing required occurs at the biorefinery.*

regions. BioFLAME determines the least-cost potential feedstock draw areas and possible direct land-use changes. BioFLAME operates on GIS architecture and consists of geospatial layers used to identify refinery locations (i.e., road networks and transmission lines, etc.). Information supplied includes site suitability, feedstock availability, delivered feedstock costs, transportation emissions, direct land use change, potential supply, and transportation costs. Road networks, transmission lines, and other geospatial layers are used to identify candidate refinery locations. BioFLAME provides estimates for:

- the cost-minimizing locations where feedstock would be sourced to supply a biorefinery,
- the annual cost of procuring and transporting feedstock, and
- the number of facilities a region can support.

BioFLAME has two sets of identifier nodes. The initial set is the supply regions. These regions take the form of hexagons and contain 5 square miles of area (**Figure 3**). The potential quantity of feedstock by type is estimated for each supply region and is assumed to be located at the centroid. The United States is divided into these hexagons, and in the Southeast, there are approximately 1.3 million supply units. Transportation is defined from the centroid of each supply region to the nearest road and then to each supply region in the model. The second set of nodes is the potential sites for conversion of the feedstock. These nodes can serve as preprocessing or conversion nodes and are known as candidate nodes. Currently, the model relies on available industrial park locations that meet the infrastructure needs of the facility being sited. In areas where this information is not known, towns with a population of 10,000 or more serve as candidate nodes. Each hexagon is assigned to a county, state, and BEA.

The solution of BioFLAME provides information on the origin of the feedstock, the destination of the feedstock, the type of feedstock, the quantity delivered, area, the costs of the feedstock (establishment, maintenance, harvesting/collection, and transportation), previous land use, and miles traveled. *Ex post* analysis projects change in transportation emissions and soil erosion, if cropland is involved. Embedded in BioFLAME is a transportation sector. The transportation sector contains the U.S. detailed streets TIGER 2000-based dataset enhanced by the Environmental Science Research Institute (ESRI) and Tele Atlas (ESRI, 2006). Transportation is primarily by truck originating from the farm gate or forest landing to a depot or

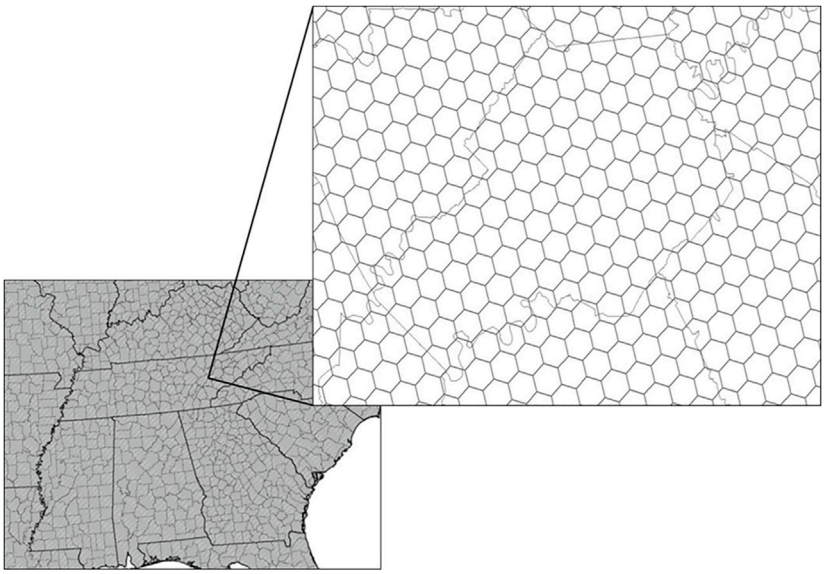

FIGURE 3 | BioFLAME's supply regions.

TABLE 3 | Trucking cost of biomass feedstock ($/unit-km) (2017$).

Feedstock	Capital cost	Weight/load	Distance	Transportation cost	Transportation cost
—	$	MT	km	$/dry MT	$/dry MT-km
Wood chips	137,901	21.74	48.28	$10.13	$0.21
Logs	—	—	—	—	—
Switchgrass	120,000	14.17	48.28	$15.26	$0.32
Corn/soyabeans	110,500	26.54	48.28	$6.14	$0.13
—	—	Liters	—	$/L	$/L-km
Vegetable oil/SAF	131,325	23,659	48.28	$0.01	0.00022

Semi-truck with walking floor trailer (wood chips), semi-truck + log trailer, semi-truck + flatbed trailer (switchgrass), semi-truck + grain trailer (corn/soybeans), and semi-truck + tanker trailer (vegetable oil/SAF).

biorefinery. In BioFLAME, the gross vehicle weight rating is a constraint on the load assumed at 36.3 MT. To arrive at a $ per MT-km cost estimate, a trip distance is assumed, along with a weight load (**Table 3**). In total, four different feedstock transportation types are estimated as follows: 1 forest residue and short-rotation trees in the form of chips, 2 traditional forest products in the form of logs, 3 herbaceous material in the form of bales, and 4. oil seeds and corn. In addition, a tanker truck cost carrying pyrolysis oil or final liquid fuel product is estimated. The cost estimates are based on the dry matter content of the material being trucked from field to initial destination−−depot or biorefinery. In this analysis, depots are not assumed, and feedstocks enter the biorefinery in the form of chips.

Mileage is determined from the center of the supply node to each of the other supply nodes. The shortest distance and road types between supply nodes are determined and used in estimating distance and speed. Trailer types and possible payloads for those trailers are predetermined and depend on the feedstock. For instance, if bales of herbaceous feedstock are hauled with a large truck, you cannot have a 24 MT load, and the density of the feedstock will not allow it. The capacity of the trailer is 36 large round bales, 24 rectangular bales, or 13 condensed/wrapped bales. The trailer carries 13 tons in round bales, 16 tons in rectangular bales, or 26 tons in wrapped bales. A dry matter loss during transportation is two percent (Kumar and Sokhansanj, 2007; Larson et al., 2010). The quantity of green tons identified by BioFLAME in each supply region is divided by the weight per load to determine the number of trucks required to bring the material from supply node to the biorefinery or preprocessing depot. A similar calculation is made when delivering intermediate or final products to their destinations. Emissions of the additional truck traffic are available based on the EPA's Motor Vehicle Emission Simulator (MOVES) model (EPA, 2010) once BioFLAME is solved.

IMPLAN

IMPLAN® (Version 3.0 using 2018 data) output from the model provides descriptive measures of the economy including total industry output (economic activity or the value of all sales), employment, labor income, value-added, and state/local taxes for

546 industries based on the U.S. Department of Census's North American Industry Classification System (NAICS) in each BEA (U.S. Department of Census, 2021)[1] Data are aggregated to BEA economic areas and then converted to BEA input–output models to measure changes in economic activity (Johnson and Kort, 2004).

Each BEA IMPLAN model can also provide estimates of multiplier-based impacts (for example, how siting a conversion facility will impact the rest of the BEA economy). In analysis of the impacts of the supply chain activities, the indirect multiplier effect (i.e., the impact on the supply chain part of the economy in this case) is also included. Multipliers operate on the assumption that as consumers and institutions increase expenditures, demand increases for products made by local industries that in turn make new purchases from other local industries and so forth. Stated another way, the multipliers in the model will measure the response of the entire BEA economy to a set of changes in production for liquid and/or electric technologies currently in use and/or forthcoming for the bio/renewable energy industry. The analysis uses the IMPLAN's local purchase percentage (LPP) option, which affects the direct impact value applied to the multipliers in each BEA. Instead of a 100 percent direct expenditure value (i.e., electricity, water, construction, manufacturing, and waste management) applied to the BEA multipliers, the value which reflects the BEA's purchases is used. The analysis is achieved by using analysis-by-parts (ABP) methodology (Clouse, 2021) by supply chain stages. ABP is conducted by splitting the payments for inputs into the industries that receive them and then impact those industries. The total impact is the aggregation of all the parts over all stages of the supply chain. Each part represents an industry that provides input into the industry under consideration. In addition, labor impacts and the impact of changes in proprietor income are also included.

TABLE 4 | Location of potential forest residues in the BEAs supplying feedstock to the biorefineries.

BEA region	Quantity of forest residues
—	(Dry metric tons)
10	210,099
29	169,049
31	143,357
33	57,321
40	31,722
66	311,735
68	106,112
81	139,296
88	195,450
94	301,786
116	11,933
138	163,245
Total	1,841,106

Source: Adapted from ForSEAM output.

TABLE 5 | Quantity of forest residues supplied by BEA.

BEA	Surry	McDowell	Morgan	Total
—		Dry metric tons		
10	28,353	181,687	0	210,041
29	6,594	142	129,489	136,225
31	31,800	111,485	0	143,285
33	0	0	57,305	57,305
40	0	0	25,963	25,963
66	286,382	7,509	0	293,891
68	0	105,810	0	105,810
81	7,737	77,667	27,670	113,074
88	0	10,148	2,750	12,897
94	0	0	251,022	251,022
138	133,728	0	0	133,728
Total	494,595	494,446	494,199	1,483,239

THE EXAMPLE

The economic impact is estimated for converting forest residue in Central Appalachia *via* a gasification Fischer–Tropsch (GFT) biorefinery with a feedstock input of 495,000 dry metric tons per year (1,500 metric tons per day) to demonstrate REEAL's modeling capabilities. The supply chain consists of moving the feedstock to a forest landing, chipping, transporting the feedstock to the biorefinery, and converting the feedstock into the product. In this example, the model is not including costs resulting from the movement of the product to the final user to determine the location of the biorefineries.

Feedstock Availability

The amount of forest residues available each year is defined by ForSEAM (He-Lambert et al., 2016). The hardwood residues are located primarily in eastern KY, Western NC, and western VA (**Table 4**). Within the region, there are an estimated 1.84 million dry metric tons of forest residues available annually for use in the bioeconomy. These residues are within one mile of a road as indicated by the Forest Inventory Assessment Data. Other assumptions are consistent with the 2016 Billion-Ton studies medium demand for wood products. Both BEA 66 (located in North Carolina and Virginia) and BEA 94 (located in Kentucky and West Virginia) have over 300,000 dry metric tons each. If this is examined by state, North Carolina, Kentucky, Virginia, and Tennessee each are projected to have more than 250,000 dry metric tons of hardwood logging residues each year within the study area.

BioFLAME Results

Analysis by BioFLAME indicates that enough feedstock is available within the supply area to supply the three

[1]Total industry output is defined as the annual dollar value of goods and services that an industry produces. Employment represents total waged and salaried employees as well as self-employed jobs in a region, for the both full- and part-time workers. Labor income consists of employee compensation and proprietor income. Total value added is defined as all income to workers paid by employers (employee compensation); self-employed income (proprietor income); interests, rents, royalties, dividends, and profit payments; and excise and sales taxes paid by individuals to businesses. State/local taxes are comprised of sales tax, property taxes, motor vehicle license taxes, and other taxes.

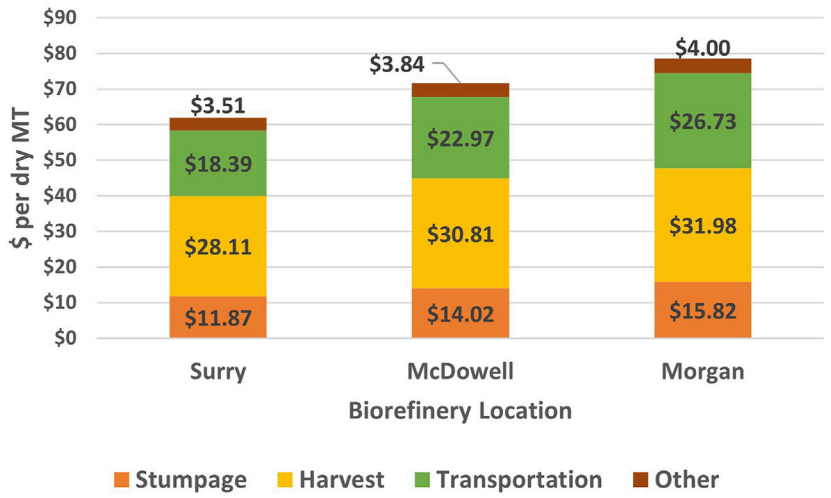

FIGURE 4 | Per dry metric ton costs of delivered feedstocks for each of the biorefineries.

biorefineries (**Table 5**) sited in Morgan County, Kentucky (BEA 94), and Surry and McDowell counties in North Carolina (BEA 31 and 61, respectively) (**Figure 4**). The cost of the feedstock delivered to the three biorefineries is $104.8 million or about $71/MT (**Table 6**). This total cost contains costs for the following cost categories: 1. stumpage (~20 percent), 2. harvest and chipping (~43 percent), 3. ownership or proprietor income (~5 percent), and 4. transportation (32 percent) (**Figure 5**). Transportation of the feedstocks costs about $33.7 million or about $22.70 per dry metric ton (**Table 7**). Stumpage costs are estimated at about $13.90 per dry metric ton with harvest and chipping cost estimated at $30.30 per dry metric ton.

TABLE 6 | Cost of the delivered forest residues supplied by BEA.

BEA	Surry	McDowell	Morgan	Total
—		Dollars		
10	$1,931,650	$11,176,174	$0	$13,107,824
29	$458,346	$13,276	$9,874,489	$10,346,111
31	$2,187,282	$8,572,349	$0	$10,759,631
33	$0	$0	$4,631,618	$4,631,618
40	$0	$0	$1,806,965	$1,806,965
66	$16,828,598	$636,397	$0	$17,464,995
68	$0	$7,236,837	$0	$7,236,837
81	$523,149	$6,855,219	$2,538,341	$9,916,710
88	$0	$934,287	$266,171	$1,200,458
94	$0	$0	$19,691,631	$19,691,631
138	$8,672,131	$0	$0	$8,672,131
Total	$30,601,157	$35,424,538	$38,809,216	$104,834,911

Biorefinery Transactions and Output

The biorefinery information used in this analysis data originates from a TEA greenfield gasification Fischer–Tropsch facility spreadsheet with the scale and feedstock costs modified to match the example presented in this article[2]. The facility requires inputs other than feedstock, so those sectors are also impacted. The initial values/assumptions reflect the original development for the United States. The spreadsheet model, once values are changed, calculates the manufacturer's selling price (MSP) values for all products. Production incentives used in the analysis include RIN values for fuel pathway L given a fuel code of D7 (cellulosic diesel). The prices for fuel code D7 are not available from the EPA's website, so a D3 (ethanol made from cellulosic material) price series from 2015–2020 is used to establish the estimated RIN value. This value is multiplied by the equivalent value (EV) factor of 1.7 (e-Code of the Federal Regulations (CFR), 2021). The average value of a RIN based on weekly verified observations over December 2019 through August 2020 is 0.32 per liter ranging from $0.13 to $0.47 per liter. When adjusted using the EV factor, the estimated RIN value used in the analysis is $0.55 per liter of advanced fuel (**Table 8**). The output in liters of sustainable aviation fuel and diesel produced by the biorefineries is obtained from the biorefinery TEA spreadsheet. Naphtha does not have RIN value in this analysis[3]. Annual production for one biorefinery is 47.5 million liters for SAF,

[2]Most of the ASCENT TEA conversion facility spreadsheets are developed at Washington State University (WSU). These spreadsheets contain information on a prespecified technology on investment in the facility as well as operations. Currently, these TEAs provide an input sheet and an output sheet, along with information on CAPEX and OPEX (Brandt et al., 2021). The ASCENT technologies available are a portion of the TEAs that have been created and include alcohol-tojet, gasification/Fischer–Tropsch, and HEFA. Since ASCENT technologies focus on SAF, other TEAs are also incorporated into REEAL that focus on the production of other liquid fuels. The ASCENT baseline spreadsheets calculate a minimum selling price for the fuel products produced assuming that a 12.2 percent return on investment is required. These baseline spreadsheets have a specified throughput and cost of feedstock that the user can change.

[3]Naphtha in not identified as a fuel in approved pathway L. Naphtha is identified as a fuel in several other pathways. These pathways have either a D5 or a D7 fuel code. Had either the D5 or D7 price been used, the estimated selling price required to allow the facility to break even would have decreased.

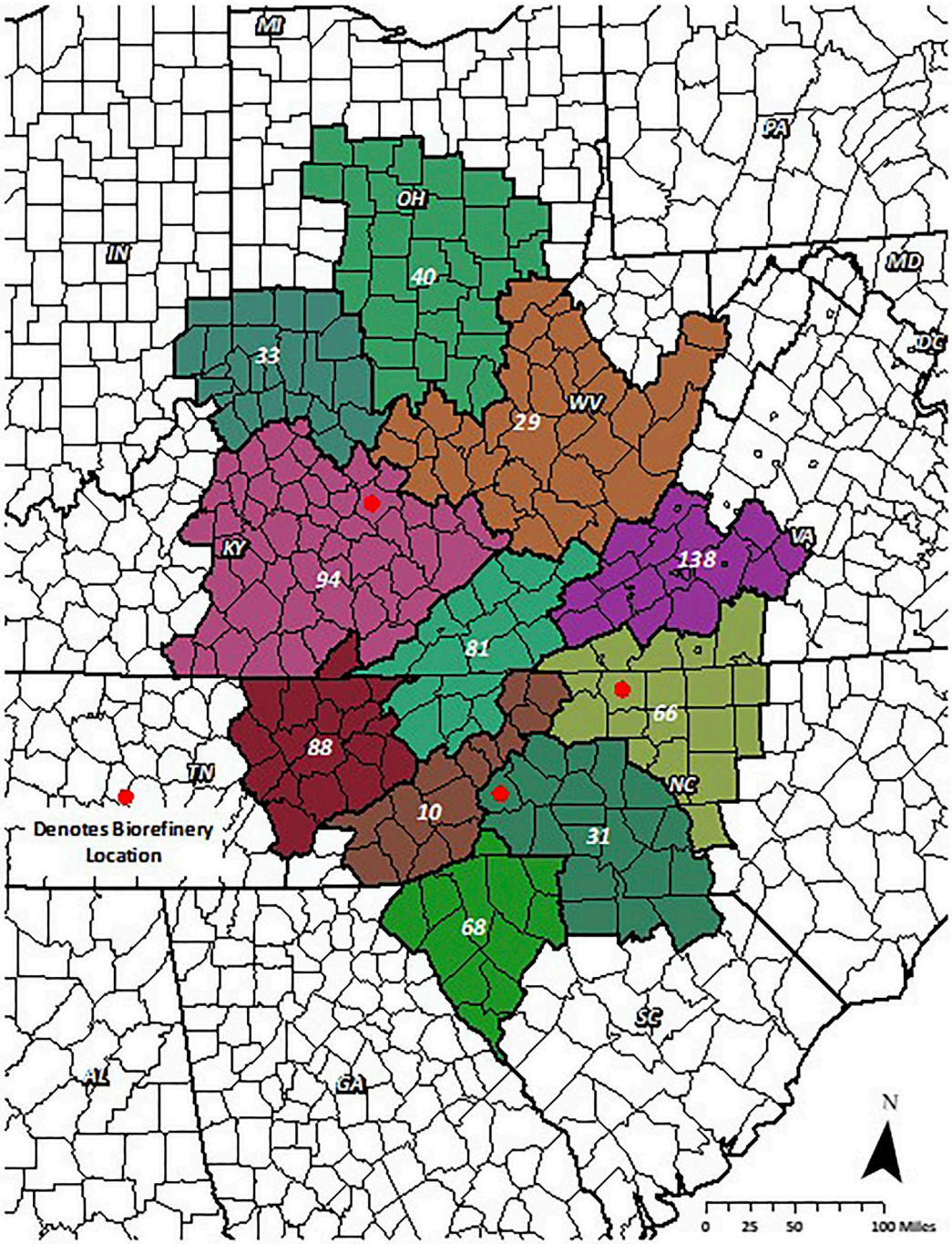

FIGURE 5 | Location of the Central Appalachia feedstock draw areas by Bureau of Economic Analysis regions for the gasification and Fischer–Tropsch biorefineries.

40.3 million liters for diesel, and 23.6 million liters for naphtha. Both SAF and diesel qualify for RINs. The biorefinery break-even prices required to satisfy investors are estimated at $1.28, $1.32, and $1.13 per liter for SAF, diesel, and naphtha, respectively, for the first biorefinery and $1.37, $1.40, and $1.19, respectively, for the third. The cost differences reflect the changes in feedstock costs delivered to the biorefinery.

Capital Costs

The original TEA was developed based on an annual feedstock throughput of 348.5 thousand metric tons with investment costs of $444.6 million (Brandt, Tanzil, Garcia-Perez, and Wolcott, 2021). The designed biorefinery used in this analysis has feedstock throughput of 495 thousand metric tons with an investment cost of $563.6 million (**Table 9**).

TABLE 7 | Cost to transport forest residues to biorefineries by BEA.

	Biorefinery location			
BEA	**Surry**	**McDowell**	**Morgan**	**Total**
—		Dollars		
10	$724,479	$2,647,502	—	$3,371,982
29	$247,278	$8,592	$3,939,965	$4,195,834
31	$701,480	$2,666,905	—	$3,368,385
33	—	—	$1,443,105	$1,443,105
40	—	—	$857,280	$857,280
66	$3,974,040	$248,162	—	$4,222,202
68	—	$2,541,242	—	$2,541,242
81	$257,215	$2,870,891	$1,111,652	$4,239,759
88	—	$375,016	$154,227	$529,242
94	—	—	$5,701,953	$5,701,953
138	$3,189,990	—	—	$3,189,990
Total	$9,094,482	$11,358,309	$13,208,182	$33,660,973

TABLE 8 | RIN values increased by the equivalent value BTU adjustment over the last 9 Months, i.e., December 2019 to August 2020.

	D3	**D4**	**D5**	**D6**
—		$ per liter		
Average	0.547	0.225	0.221	0.092
Maximum	0.808	0.292	0.292	0.207
Minimum	0.229	0.139	0.153	0.004

Adapted from the United States Environmental Protection Agency (EPA), RIN Trades and Price Information, accessed 10/6/2020 at https://www.epa.gov/fuels-registration-reporting-and-compliance-help/rin-trades-and-price-information.

TABLE 9 | Summary of capital investment and annual operating costs for the gasification and Fischer–Tropsch conversion facility.

Expenditure type	**Million 2017$**
Capital investment	—
Gasification	$76.8
Syngas cleaning	$9.3
Fuel synthesis	$18.2
Hydroprocessing	$8.4
Air separation	$8.8
Total direct equipment cost (TDEC)	121.5
Total direct cost (TDC)	$388.7
Fixed capital investment (FCI)	$541.7
Working capital (WC)	$8.4
Total capital investment (TCI)	$563.6
Annual operating (non-feedstock)	
Forest residuals	$35.1
Catalytic cost	$9.1
Gasification, FT synthesis, and power	24.0
Salaries (45 employees) (not including benefits)	$2.7
Fixed operating costs[a]	$47.7
Total operating expenditures	$118.6

[a]*Includes property insurance, local taxes, maintenance and repairs, and overhead.*

The capital costs for the biorefinery include equipment cost, installation of equipment, and working capital required. The equipment costs for gasification ($76.8 million), syngas cleaning ($9.3 million), fuel synthesis ($27.5 million), hydro-processing ($15.5 million), and air separation ($8.8 million) are multiplied by a ratio factor of 4.46 to determine the fixed capital investment for a facility using mature technology ($605.5 million)[4]. Working capital is equal to an additional $14.5 million. The information from the original spreadsheet with a biorefinery throughput equal to 348.5 thousand metric tons was placed into IMPLAN for each BEA in the conterminous United States. Using analysis-byparts (Lucas, 2020), the economic impact resulting from this investment was estimated. The factors were developed based on the investment ratio, actual investment over original investment estimate (563.6/348.5). Therefore, in each BEA that a biorefinery was located, a factor of 1.78 is used to estimate the economic impact of a larger facility and then the original.

Operating Costs

Operating hours are estimated at 7,884 h per year. Delivered equipment costs are delineated as gasification, syngas cleaning, fuel synthesis, hydro-processing, and air separation and comprise $121.5 (2017$) million of the total capital investments. The remaining costs are based on ratio factors and/or percentages based on information from the plant design and assumptions made for the construction of chemical-based facilities (i.e., total direct cost (3.20), fixed capital investment (4.46), and working capital (20 percent of yearly operating)).

Each biorefinery produces 47.5 mm L/year of sustainable aviation fuel, 40.3 mm L/year of diesel, and 23.6 mm L/year of naphtha. The total feedstock cost delivered to the biorefineries is estimated at $35.1 million (**Table 4**). An estimated 1.5 million metric tons of dry forest residue are required. However, they are not dried when transported from the field to the biorefinery. Fifty percent moisture content is assumed. Average per ton-mile distance from field to biorefinery is 107 km. The trucks are hauling 18.15 metric tons of chips and 107 km on average. Working 330 days/year and 16 h/day, 31 trucks must be emptied every hour or one truck every 2 min. If they have a longer trailer and can haul 20.4 metric tons of chips, then they need to unload 27–28 trucks per hour. Total feedstock costs arriving at the biorefinery in chipped form average $70.66 per metric ton and include a stumpage fee, harvest and chipping cost, ownership payment, and transportation.

Operating Revenues

Required gross revenues containing a ROI (return on investment) of 12.2% for each of the biorefineries are estimated at $193.7 million from fuel, if $47 million is generated from RINs assuming a RIN price of $0.55 with an energy value (EV) factor of 1.7 for

[4]Mature technology or "nth" plant is assumed for the biorefinery as compared to a "pioneer" facility. The pioneer facility would likely not be as large and therefore would not incorporate economies of scale that potentially exist. In addition, the other aspects of the supply chain are mature. The technologies used to grow, maintain, and harvest the feedstocks, in addition to transporting those feedstocks, are mature or "proven" technologies compared to pioneer technology. Changes in all steps of the supply chain are likely to be different than those modeled.

TABLE 10 | Factors used to estimate the economic impact from feedstock harvest and delivery to the biorefineries by BEA.

BEA	Wood harvest	Harvest salaries	Stumpage	Other income	Transportation
10	4.06	2.18	2.71	0.78	0.34
29	2.55	1.37	1.74	0.49	0.42
31	3.01	1.62	2.17	0.58	0.34
33	1.26	0.68	1.01	0.24	0.14
40	0.40	0.22	0.26	0.08	0.09
66	5.53	2.98	3.67	1.06	0.42
68	1.98	1.06	1.27	0.38	0.25
81	2.29	1.24	1.71	0.44	0.42
88	0.27	0.15	0.20	0.05	0.05
94	5.54	2.98	4.40	1.07	0.57
138	2.32	1.25	1.47	0.45	0.32

sustainable aviation fuels and diesel. Break-even plant gate fuel price when assuming RINs and a 12.2% on investment are $1.12 per liter for sustainable aviation fuel, $1.15 per liter for diesel, and $0.97 per liter for naphtha. If the output generated from the biorefinery is sold at prices reflected at refineries, then prices reflect the market price and not the price required for sustainable operations.

Generating the Factors

Each stage along the supply chain has a spreadsheet generated for a specific technology, value, and/or size. For instance, the impact for a change in proprietor income is estimated using a million-dollar expenditure within the economy for the proprietor income sector. Transactions resulting from transportation are estimated assuming that they occur from the point of origin and are equal to ten million dollars. A 348.5-thousand-ton biorefinery is assumed and the impact for that sized biorefinery is assumed in the spreadsheets representing that technology. The feedstock transactions are broken into stumpage (proprietor income), harvest costs including chipping, and a small amount for profit. Reestablishment is not assumed, and therefore the costs are not included though these costs would be allocated to a traditional logging operation that leaves the residues behind. The factors are estimated using estimated transactions divided by the direct transactions assumed by the spreadsheet. For instance, if a particular BEA has an estimated eight million dollars in transportation transactions, the factor would equal 0.8 for that BEA. **Table 10** contains the factors used to estimate the economic impact for the collection/harvest and delivery of feedstock to the biorefinery. Once at the biorefinery, the factors are based on plant capacity and compared to the expenditures of the modeled facility having a capacity of 348,500 metric tons of feedstock per year. These factors for investment, operating, and salaries are 1.268, 1.325, and 1.271, respectively, for BEAs 10, 66, and 94, the BEA's where the biorefineries are located.

Economic Impact

Based on the IMPLAN-estimated economic impact, the annual economic impact on the Central Appalachian region, if three biorefineries are established, is over half a billion dollars ($537 million per year) based on an investment of $1.69 billion. The investment results in $2.67 billion in economic activity and the multiplier of 1.71. In other words, for every additional million dollars spent, an additional $0.71 million in economic activity is generated in the regional economy (**Table 11**). The gross regional product is estimated at $1.28 billion from the investment and nearly 200 million each year in annual operating. Each biorefinery employs 47 individuals, but the reverberation of the biorefineries economic activity throughout the BEA regions supports nearly 1,200 jobs because of regional transactions stemming from biorefinery operations.

The feedstock operations also add economic activity to the region. Slightly more than $16.8 million was spent in the harvest and chipping operations (**Table 12**). This expenditure resulted in an additional $30 million in the economic impact. The stumpage and additional profit occurring from the harvest of the forest residues resulted in $40 million directly into the pockets of the resource and logging operation owners. Their subsequent expenditures resulted in a total economic activity increase of $71.4 million. These operations resulted in creating an estimated 103 jobs directly and a total of 195 jobs. Slightly more than $36.7 million was spent on feedstock transportation resulting in increased economic activity of almost $68 million. The economic activity generated includes the costs of operations, any profit generated, and equipment repair and depreciation along with the multiplier effects that occur after these transactions occur.

DISCUSSION

Based on ASCENT's GFT conversion techno-economic analysis for sustainable aviation fuel and BioFLAME to simulate the location and transportation of feedstock, this static modeling approach indicates that the biorefinery would need to sell their sustainable aviation fuel at $1.68 to $1.76 per liter, if a required rate of investment is 12.2%. If the hardwood feedstock qualified for RINs, using the average RIN value over December 2019–August 2020 time frame, this break-even price would be reduced to $1.21 to $1.26 per liter assuming a D3 RIN price of $0.32 per liter and an EV factor of 1.7. The economic analysis demonstrates, using GFT technology, to be feasible, the airlines will need to purchase the fuel at a price higher than current levels of aviation fuel or additional subsidies will be required in order to incentivize production. It is estimated that if incentivized, the increase in supply chain expenditures would lead to an annual

TABLE 11 | Total economic activity generated from the three biorefineries.

Item causing the impact	Multiplier	Direct	Total
—	—	Million $	
Biorefinery (one time investment)	1.68	$1,589.5	$2,671.9
Biorefinery (annual)	1.70	$216.5	$368.3
Feedstock operations (annual)	1.80	$93.8	$169.2
Total from operations	1.73	$310.3	$537.5
Employment generated from investment	1.64	11,265	18,429
Employment generated from annual operations	3.76	561.0	2,108.2

increase of $600 million through direct expenditures and $1.06 billion after the multiplier effect occurs. In addition, the investment in three biorefineries of $1.7 billion leads to a regional impact of $2.06 billion. The analysis assumes that no additional investment will be required in the logging industry or the transportation industry.

The economic impact in the Central Appalachian region is rather large and given the demise in coal production, could be the new economic engine for the region. The payroll will likely increase by $45 million per year. In 2017, 19 counties within the Central Appalachian region had some of the highest unemployment rates in Appalachia ranging from 8 to 15.7 percent (Appalachian Regional Commission, 2019), whereas the U.S. average during that time period was 4.4 percent. The adoption of this industry will result in additional jobs for the region likely to reduce poverty and out-migration. Families will benefit from the increased economic development as their standard of living increases.

The limitation of input–output models and, certainly a limitation in this analysis, is that the assumptions used are static. They represent a snapshot of the economy at a point in time. Significant change in the demand for inputs might encourage growth of other supporting industries in the region. This change would affect the EIA results. In addition, input–output models are linear, and doubling the output does not change the production function used to determine transactions. Cottage industries that exist may become more efficient as they scale up. Finally, they may overestimate the impact on employment. As suggested by EPA, this occurs since the model does not have resource constraints or substitution effects (Environmental Protection Agency, 2010).

The analysis assumes that mature technology exists to estimate the economic benefits of the biorefineries. The investment, feedstock harvest and delivery, and the operating costs are the estimates. They are not known with certainty. While the technology has been shown to be feasible at the bench scale, a commercial plant has not been constructed yet. Actual costs and economic impacts will likely differ as a result. In addition, the analysis does not include risk except in the assumption that the investment requires a 12.2 percent return. As indicated by Trejo-Pech et al. (2021), this return might not be acceptable.

TABLE 12 | Economic activity generated by the three biorefinery industry.

Item causing the impact	Multiplier	Direct	Total
—	—	Million $	
Biorefineries			
Investment:	—	—	—
Economic activity	1.68	$1,589.5	$2,671.9
Gross regional product	1.76	$725.5	$1,277.5
Employment (jobs)	1.64	11,265	18,429
Annual operations:	—	—	—
Economic activity excluding salaries	1.68	$198.8	$333.2
Salary	1.98	$17.7	$35.2
Annual economic activity generated	—	$216.5	$368.3
Gross regional product	1.61	$128.6	$206.6
Feedstock operations			
Annual operations:	—	—	—
Feedstock to landing:	—	—	—
Economic activity excluding salaries	1.79	$11.1	$19.9
Salary	1.76	$5.7	$10.1
Resource and logging operation owners	—	$40.2	$71.4
Annual economic activity generated	1.78	$57.1	$101.3
Gross regional product	1.55	$12.7	$19.8
Feedstock transportation:	—	—	—
Economic activity	1.85	$36.7	$67.8
Gross regional product	1.80	$20.3	$36.5

DATA AVAILABILITY STATEMENT

The raw data supporting the conclusion of this article will be made available by the authors, without undue reservation.

AUTHOR CONTRIBUTIONS

All authors listed have made a substantial, direct, and intellectual contribution to the work and approved it for publication.

FUNDING

This work was funded in part by the U.S. Federal Aviation Administration (FAA) Office of Environment and Energy as a part of ASCENT Project 1 under FAA Award Number: 13-C-AJFEUTENN-Amd 13. Funding also was provided by the USDA through Hatch Project TN000444. Any opinions, findings, and conclusions or recommendations expressed in this article are those of the authors and do not necessarily reflect the views of the FAA or other ASCENT-sponsored organizations.

ACKNOWLEDGMENTS

The authors would like to thank Nathan Brown (FAA), Anna Oldani (FAA), and Jim Hileman (FAA) for providing the means to develop the modeling system and Tim Rials (UT) for inviting us to provide feedstock information to ASCENT.

REFERENCES

Appalachian Regional Commission (2019). Unemployment Rates in Appalachia, 2017. Baumol, William, 2000. "Leontief's Great Leap Forward," Economic Systems Research https://www.arc.gov/map/unemployment-rates-in-appalachia-2017/(Accessed September 20, 2021).

Baumol, W. (2000). Leontief's Great Leap Forward: Beyond Quesnay, Marx, and von Bortkiewicz. *Econ. Syst. Res.* 12, 1. doi:10.1080/095353100500056624 1-152

Brandt, K., Tanzil, A. H., Garcia-Perez, M., and Wolcott, M. (2021). GFT_CAEP-v6.xlsm, Excel Notebook. February 4, 2021 email.

Clouse, D. (2021). ABP: Introduction to Analysis-By-Parts. Available at: https://implanhelp.zendesk.com/hc/en-us/articles/360013968053-ABP-Introduction-to-Analysis-By-Parts (Accessed September 21, 2021).

De La Torre Ugarte, D., English, B. C., and Jensen, K. (2007). Sixty Billion Gallons by 2030: Economic and Agricultural Impacts of Ethanol and Biodiesel Expansion. *Am. J. Agric. Econ.* 89, 1290–1295. doi:10.1111/j.1467-8276.2007.01099.x

e-Code of the Federal Regulations (CFR) (2021). § 80.1426 How Are RINs Generated and Assigned to Batches of Renewable Fuel? Available at: https://www.ecfr.gov/current/title-40/chapter-I/subchapter-C/part-80/subpart-M/section-80.1426 (Last accessed September 21, 2021).

English, B. C., Ugarte, D. G. D. L. T., Walsh, M. E., Hellwinkel, C., and Menard, J. (2006). Economic Competitiveness of Bioenergy Production and Effects on Agriculture of the Southern Region. *J. Agric. Appl. Econ.* 38, 389–402. doi:10.1017/S1074070800022434

English, B., de la Torre Ugarte, D., Jensen, K., Hellwinckel, C., Menard, J., Wilson, B., et al. (2006). 25% Renewable Energy for the United States by 2025: Agricultural and Economic Impacts. Accessed at https://ag.tennessee.edu/arec/Documents/AIMAGPubs/BioEnergy/25x25RenewableEnergyAgEcon Impacts.pdf.

English, B., Jensen, K., Menard, J., and de la Torre Ugarte, D. (2009a). Projected Impacts of Federal Renewable Portfolio Standards on the Colorado Economy. Accessed at https://ag.tennessee.edu/arec/Documents/AIMAGPubs/BioEnergy/ColoradoStudyDocument.pdf.

English, B., Jensen, K., Menard, J., and de la Torre Ugarte, D. (2009b). Projected Impacts of Federal Renewable Portfolio Standards on the Florida Economy. Accessed at https://ag.tennessee.edu/arec/Documents/AIMAGPubs/BioEnergy/FloridaStudyDocument.pdf.

English, B., Jensen, K., Menard, J., and de la Torre Ugarte, D. (2009c). Projected Impacts of Federal Renewable Portfolio Standards on the Kansas Economy. Accessed at https://ag.tennessee.edu/arec/Documents/AIMAGPubs/BioEnergy/KansasStudyDocument.pdf.

English, B., Jensen, K., Menard, J., and de la Torre Ugarte, D. (2009d). Projected Impacts of Federal Renewable Portfolio Standards on the North Carolina Economy. Accessed at https://ag.tennessee.edu/arec/Documents/AIMAGPubs/BioEnergy/NCStudyDocument.pdf.

Environmental Protection Agency (EPA) (2010). Motor Vehicle Emission Simulator (MOVES3), User Guide for MOVES2010a. Available at: https://nepis.epa.gov/Exe/ZyPDF.cgi?Dockey=P1008EU8.pdf (Accessed September 21, 2021).

Environmental Science Research Institute (2006). U.S. Detailed Streets. Available at: https://www.lib.ncsu.edu/gis/esridm/2006/usa/streets.html (Accessed August 21, 2016).

Graham, R. L., English, B. C., and Noon, C. E. (2000). A Geographic Information System-Based Modeling System for Evaluating the Cost of Delivered Energy Crop Feedstock. *Biomass and Bioenergy* 18, 309–329. doi:10.1016/s0961-9534(99)00098-7

He, L., English, B. C., Menard, R. J., and Lambert, D. M. (2016). Regional Woody Biomass Supply and Economic Impacts from Harvesting in the Southern U.S. *Energ. Econ.* 60, 151–161. doi:10.1016/j.eneco.2016.09.007

He-Lambert, L., English, B. C., Lambert, D. M., Shylo, O., Larson, J. A., Yu, T. E., et al. (2018). Determining a Geographic High Resolution Supply Chain Network for a Large Scale Biofuel Industry. *Appl. Energ.* 218, 266–281. doi:10.1016/j.apenergy.2018.02.162

Hellwinckel, C. (2019). Spatial Interpolation of Crop Budgets. Documentation of POLYSYS Regional Budget Estimation. University of Tennessee. Agricultural Policy Analysis Center. Available at: https://arec.tennessee.edu/wp-content/uploads/sites/17/2021/03/POLYSYS_documentation_3_budgeting_database.pdf (Accessed September 21, 2021).

IMPLAN Group LLC (2018) IMPLAN System (2018 Data and V. 3 Software), Available at: Economic Impact Analysis for Planning | IMPLAN [Accessed September 21, 2021].

Johnson, K. P., and Kort, J. R. (2004). 2004 Redefinition of the BEA Economic Areas. Available at: https://apps.bea.gov/scb/pdf/2004/11November/1104Econ-Areas.pdf ([Last accessed September 21, 2021).

Kumar, A., and Sokhansanj, S. (2007). Switchgrass (Panicum Vigratum, L.) Delivery to a Biorefinery Using Integrated Biomass Supply Analysis and Logistics (IBSAL) Model. *Bioresour. Techn.* 98 (5), 1033–1044. doi:10.1016/j.biortech.2006.04.027

Lambert, D. M., English, B. C., Menard, R. J., and Wilson, B. (2016). Regional Economic Impacts of Biochemical and Pyrolysis Biofuel Production in the Southeastern US: A Systems Modeling Approach. *As* 07, 407–419. doi:10.4236/as.2016.76042

U.S. Department of Energy, M. H. Langholtz, B. J. Stokes, and L. M. Eaton (2016). in *2016 Billion-Ton Report: Advancing Domestic Resources for a Thriving Bioeconomy, Volume 1: Economic Availability of Feedstocks* (Oak Ridge, TN: Oak Ridge National Laboratory), 448. (Leads), ORNL/TM-2016/160. Accessed at: http://energy.gov/eere/bioenergy/2016-billion-ton-report. doi:10.2172/1271651

Larson, J. A., Yu, T. H., English, B. C., Mooney, D. F., and Wang, C. (2010). Cost Evaluation of Alternative Switchgrass Producing, Harvesting, Storing, and Transporting Systems and Their Logistics in the Southeastern USA. *Agric. Finance Rev.* 70 (2), 184–200. doi:10.1108/00021461011064950

Lonergan, S. C., and Cocklin, C. (1985). Use of Input-Output Analysis in Environmental Planning. *J. Environ. Manage.* 20, 2. U.S. Department of Energy, Office of Scientific and Technical Information, Accessed at https://www.osti.gov/biblio/5390971.

Lucas, M. (2020). IMPLAN Online: The Basics of Analysis-By-Parts. Available at: https://support.implan.com/hc/en-us/articles/360000814393-IMPLAN-Online-The-Basics-of-Analysis-By-Parts.

Markel, E., English, B. C., Hellwinckel, C. M., and Menard, R. J. (2019). Potential for Pennycress to Support a Renewable Jet Fuel Industry. *SciEnvironm* 1, 121. Available at: https://www.hendun.org/viewJournal/RAS211-177/Potential-for-Pennycress-to-Support-a-Renewable-Jet-Fuel-Industry.

Ralston, S. N., Hastings, S. E., and Brucker, S. M. (1986). Improving Regional I-O Models: Evidence against Uniform Regional purchase Coefficients across Rows. *Ann. Reg. Sci.* 20, 65–80. doi:10.1007/BF01283624

Sharma, B., Birrell, S., and Miguez, F. E. (2017). Spatial Modeling Framework for Bioethanol Plant Siting and Biofuel Production Potential in the U.S. *Appl. Energ.* 191, 75–86. doi:10.1016/j.apenergy.2017.01.015

Trejo-Pech, C. O., Larson, J. A., English, B. C., and Yu, T. E. (2021). Biofuel Discount Rates and Stochastic Techno-Economic Analysis for a Prospective Pennycress (Thlaspi Arvense L.) Sustainable Aviation Fuel Supply Chain. *Front. Energ. Res.* 9. URL=https://Frontiers | Biofuel Discount Rates and Stochastic Techno-Economic Analysis for a Prospective Pennycress (Thlaspi arvense L.) Sustainable Aviation Fuel Supply Chain | Energy Research (frontiersin.org). doi:10.3389/fenrg.2021.770479

U.S. Department of Census (2021). North American Industry Classification System. Available at: https://www.census.gov/naics/(Accessed September 21, 2021).

Conflict of Interest: The authors declare that the research was conducted in the absence of any commercial or financial relationships that could be construed as a potential conflict of interest.

Publisher's Note: All claims expressed in this article are solely those of the authors and do not necessarily represent those of their affiliated organizations, or those of the publisher, the editors, and the reviewers. Any product that may be evaluated in this article, or claim that may be made by its manufacturer, is not guaranteed or endorsed by the publisher.

frontiers | Frontiers in Energy Research

REVIEW
published: 24 June 2022
doi: 10.3389/fenrg.2022.793776

From Farm to Flight: CoverCress as a Low Carbon Intensity Cash Cover Crop for Sustainable Aviation Fuel Production. A Review of Progress Towards Commercialization

Winthrop B. Phippen[1]*, *Rob Rhykerd*[2], *John C. Sedbrook*[3,4], *Cristine Handel*[4] and *Steve Csonka*[5]

[1]School of Agriculture, Western Illinois University, Macomb, IL, United States, [2]Department of Agriculture, Illinois State University, Normal, IL, United States, [3]School of Biological Sciences, Illinois State University, Normal, IL, United States, [4]CoverCress Inc., St. Louis, MO, United States, [5]Commercial Aviation Alternative Fuels Initiative, Cincinnati, OH, United States

OPEN ACCESS

Edited by:
Season Hoard,
Washington State University,
United States

Reviewed by:
May M. Wu,
Argonne National Laboratory (DOE),
United States
Johnathan Holladay,
LanzaTech, United States
Jonathan Lloyd Male,
Pacific Northwest National Laboratory
(DOE), United States

***Correspondence:**
Winthrop B. Phippen
wb-phippen@wiu.edu

Specialty section:
This article was submitted to
Bioenergy and Biofuels,
a section of the journal
Frontiers in Energy Research

Received: 12 October 2021
Accepted: 02 June 2022
Published: 24 June 2022

Citation:
Phippen WB, Rhykerd R,
Sedbrook JC, Handel C and Csonka S
(2022) From Farm to Flight:
CoverCress as a Low Carbon Intensity
Cash Cover Crop for Sustainable
Aviation Fuel Production. A Review of
Progress Towards Commercialization.
Front. Energy Res. 10:793776.
doi: 10.3389/fenrg.2022.793776

Thlaspi arvense L. (Field Pennycress; pennycress) is being converted into a winter-annual oilseed crop that confers cover crop benefits when grown throughout the 12 million-hectares U.S. Midwest. To ensure a fit with downstream market demand, conversion involves not only improvements in yield and maturity through traditional breeding, but also improvements in the composition of the oil and protein through gene editing tools. The conversion process is similar to the path taken to convert rapeseed into Canola. In the case of field pennycress, the converted product that is suitable as a rotational crop is called CoverCress™ as marketed by CoverCress Inc. or golden pennycress if marketed by others. Off-season integration of a CoverCress crop into existing corn and soybean hectares would extend the growing season on established croplands and avoid displacement of food crops or ecosystems while yielding up to 1 billion liters of seed oil annually by 2030, with the potential to grow to 8 billion liters from production in the U.S. Midwest alone. The aviation sector is committed to carbon-neutral growth and reducing emissions of its global market, which in 2019 approached 122 billion liters of consumption in the U.S. and 454 billion liters globally. The oil derived from a CoverCress crop is ideally suited as a new bioenergy feedstock for the production of drop-in Sustainable Aviation Fuel (SAF), renewable diesel, biodiesel and other value-added coproducts. Through a combination of breeding and genomics-enabled mutagenesis approaches, considerable progress has been made in genetically improving yield and other agronomic traits. With USDA-NIFA funding and continued public and private investments, improvements to CoverCress germplasm and agronomic practices suggest that field-scale production can surpass 1,680 kg ha^{-1} (1,500 lb ac^{-1}) in the near term. At current commodity prices, economic modeling predicts this level of production can be profitable across the entire supply chain. Two-thirds of the grain value is in oil converted to fuels and chemicals, and the other one-third is in the meal used as an animal feed, industrial applications, and potential plant-based protein products. In addition to strengthening rural communities by providing income to producers and agribusinesses, cultivating a CoverCress crop

potentially offers a myriad of ecosystem services. The most notable service is water quality protection through reduced nutrient leaching and reduced soil erosion. Biodiversity enhancement by supporting pollinators' health is also a benefit. While the efforts described herein are focused on the U.S., cultivation of a CoverCress crop will likely have a broader application to regions around the world with similar agronomic and environmental conditions.

Keywords: bioenergy, *Thlaspi arvense*, cover crop, low-carbon fuel, public-private partnership, carbon intensity, sustainable aviation fuel

INTRODUCTION

A reliable, sustainable, and secure biofuels industry in the U.S. requires a diverse portfolio of feedstocks that can be utilized across multiple energy platforms. This includes dedicated industrial crops for production of lipids which can be efficiently converted to drop-in fuels using both proven and emerging technologies. According to the National Oilseed Processing Association (NOPA), companies are investing in oilseed-to-biofuels processing facilities across the U.S. Cargill, Bunge, and ADM are leading the industry in conversion of soy oil, distillers corn oil, and other diverse soft oilseeds for the biodiesel and renewable diesel markets. Additionally, the Commercial Aviation Alternative Fuels Initiative (CAAFI) is monitoring the efforts of multiple companies who have communicated their intent to install over 45.4 billion liters of additional lipid hydro-processing facilities over the next 5 years. However, the limited domestic availability of diverse oilseed feedstocks may hinder such development. To address the demand for lipid feedstocks for sustainable aviation and other biofuels, the authors are working to convert pennycress (*Thlaspi arvense* L., Field pennycress) into a new oilseed crop to be grown as a winter-annual industrial crop throughout the U.S. Midwest Corn Belt. While the primary near-term goal is to commercialize converted pennycress as a feedstock for renewable diesel, there is a longer-term goal to also commercialize converted pennycress as a feedstock for sustainable aviation fuel. To reach this longer-term goal, there are many steps along the path to commercialization from 'farm to flight'.

In 2019, the authors were awarded a $10 million grant to fund the IPREFER (Integrated Pennycress Research Enabling Farm and Energy Resilience; www.iprefercap.org/) Project as part of the USDA-NIFA Coordinated Agriculture Projects focused on Sustainable Agricultural Systems. This project has the singular goal of removing production bottlenecks to commercialize converted pennycress by 2022. The IPREFER team consists of academic collaborators from Illinois State University, Ohio State University, University of Minnesota, University of Wisconsin, Southern Illinois University, and Western Illinois University in addition to researchers from the USDA-ARS North Central Soil Conservation Research Lab and the Agricultural Utilization Research Institute in Minnesota. The private partner developing and commercializing a converted form of pennycress is CoverCress Inc. (CCI) in St. Louis, MO.

To ensure a fit with downstream market demand, the conversion of pennycress involves not only improvements in yield and maturity through traditional breeding but also improvements in the composition of the oil and protein through gene editing tools. The conversion process is similar to the path taken to convert rapeseed into Canola. In the case of field pennycress, the converted product that is suitable as a rotational crop is called CoverCress™ as marketed by CCI or golden pennycress if marketed by others. This integrated team of researchers has diverse expertise to deliver advances in pennycress germplasm, gene editing techniques, crop management, harvest efficiency, and post-harvest handling and processing of CoverCress seeds.[1]

Agronomic studies are conducted on environmentally-diverse test plots located in four Midwestern states (IL, MN, OH, WI). Economic, social, and environmental data generation helps guide research and development directions as well as inform community dissemination through leveraged extension and education components. Results of the agronomic work are integrated into the evaluation of fuel and byproduct production with the goal of economic sustainability for the entire supply chain. These efforts are coupled with techno-economic analyses of the entire energy-crop value chain as well as development of decision-making tools applicable throughout the Midwest region. Outreach is focused on regional producers and agricultural industries along with 4-H, undergraduate and graduate students, and the general public. Through these integrated approaches, the new CoverCress crop is successfully progressing along the path to commercialization as evidenced to date by industry partner CCI who will be delivering CoverCress seed to contracted growers for fall 2022 planting.

IMPORTANCE TO AVIATION INDUSTRY

The anthropogenic greenhouse gases (GHGs) contributed by the transportation sector are significant. The U.S. Energy Information Administration indicates the commercial aviation market is responsible for up to 13% of such transportation GHG emissions (U.S. Energy Information Administration, 2020b), i.e., generating less than 3% of all manmade CO_2 production.

[1]Reference to the term CoverCress seed or crop implies inclusion of golden pennycress seed or crop marketed by companies other than CoverCress Inc.

However, demand for commercial air travel continues to grow, with expected, sustained average annual traffic growth rates of from 3%–5%, with strong demand coming from developing regions. Depending on traffic growth and new aircraft (with improved efficiency driven by new technology incorporation) assimilation rates, the current global aviation CO_2 emissions have the potential to increase to 200%–300% of today's levels by 2050. The civil aviation industry recognizes the pressure of such emissions growth with respect to societal demands to reduce GHGs and has made multiple voluntary commitments to do so. Aviation is the first industrial sector to make a significant commitment to near-term carbon-neutral growth, from 2020 onward, and making a long-term (2050) commitment on physical net carbon reductions of −50% from 2005 levels. In early 2021, U.S. airline members of Airlines for America updated their goals and committed to 2030 SAF usage levels, and to net-zero carbon by 2050 (Airlines for America, 2020). On 04 October 2021, the International Air Transport Association (IATA) announced an agreement from their member airlines, worldwide, to commit to net zero carbon by 2050 (IATA Net Zero, 2022). The announcement outlines significant targets for SAF production and use as required to meet the goal, as well as calling on the International Civil Aviation Organization (ICAO) to develop by 2022 a long-term goal for SAF than can be promulgated under the Carbon Offsetting and Reduction Scheme (CORSIA). All these goals will rely on the use of sustainable aviation fuels (SAF) that are able to demonstrate significant net lifecycle reductions in CO_2 emissions (low Carbon Intensity (CI) scores) versus use of petroleum-based jet fuel.

CORSIA was established by ICAO as a framework of standards concerning the assessment and adoption of SAF that demonstrate reduction of CO_2 emissions in international aviation. As of September 2021, the United States and 106 other countries have committed to participate in the first voluntary phase of CORSIA from 2021–2026, covering >77% of all international aviation activity. All ICAO member states will participate in the second phase from 2027–2035 representing >90% of all international activity, even with CORSIA allowed exceptions. A CORSIA approved SAF is a renewable or waste-derived fuel that meets the sustainability criteria of CORSIA (ICAO CORSIA, 2022).

The Biden administration, on 9 September 2021 held a Sustainable Aviation Summit where they announced a SAF Grand Challenge entailing government agencies working together to develop a comprehensive strategy for scaling up new technologies to produce SAF on a commercial scale. Goals of the Challenge include a nearer term goal of producing 1.63 billion liters per year by 2030 (or about 10% of U.S. demand) and ultimately supplying sufficient SAF to meet 100% of U.S. aviation fuel demand by 2050 (159 billion liters per year) (The White House, 2021a; Energy, 2021). U.S. airlines simultaneously announced their intent to utilize such fuel volumes. There has also been legislation proposed in the U.S. House and Senate to foster the development of SAF with incentives including the Clean Skies Act and Sustainable Aviation Fuels Act, a primary tenet of which is the implementation of a Blender's Tax Credit for the production of SAF meeting certain CI scoring. Legislative efforts are also being pursued around the world to either incentivize or mandate the use of SAF, including in the European Union, United Kingdom, and Canada.

Due to U.S. production only occurring at two facilities (World Energy's Paramount, California, USA, facility, and Gevo's facility in Silsbee, Texas, USA), SAF has been in regular commercial use since 2016 in limited volumes. In 2020, the Environmental Protection Agency reported U.S. SAF usage (volumes complying with the U.S. Renewable Fuels Standard) of 21 million liters which falls short of the civil aviation demand (U.S. Environmental Protection Agency, 2021d). However, additional SAF production facilities are in development worldwide with the Air Transport Action Group of the International Air Transport Association reporting airline industry SAF offtake commitments of more than 12 billion liters at the end of September 2021 (GreenAir News, 2021), with additional deals being announced on a frequent basis.

Low carbon feedstocks therefore are gaining prominence in the effort to develop SAF and meet industry targets and commitments. Concerns regarding food-versus-fuel conflicts and other unintended consequences of first-generation biofuels have driven bioenergy research towards developing novel feedstocks that minimize competition with food-crop production. Bioenergy feedstocks can be sustainably produced through 'sustainable intensification' or, extensification, which is the targeted use of underutilized land or biomass residues or the intensification of conventional crop rotations (Heaton et al., 2013). Among such crop rotations, purpose-grown oilseeds hold promise for meeting the regulatory specifications of SAF and other renewable fuels. Specifically, the use of lipid feedstock as a source of renewable liquid fuels is particularly significant because they can easily be converted to produce drop-in fuels that have been tested successfully in commercial and military operations and are market-ready.

The aviation industry has qualified the use of two thermochemical conversion processes to convert fats, oils, and greases (FOG) to synthetic jet fuel, as well as allowing FOG to be co-processed with petroleum in existing refineries (see ASTM D7566 and D1655 specifications respectively). Additional efforts are underway to: evaluate four additional conversion processes for FOG; expand the possibility for refinery co-processing; and, allow select FOG conversion processes to be used as fully drop-in fuels with no blending requirements.

FOG include waste greases, animal fats, municipal waste and sludge, algae, food processing oils, and purpose grown oil-bearing seeds and nuts. Several industrial oilseed crops fit the criteria of no direct land-use change (Shi et al., 2019) due to being non-food crops and non-land displacing especially since these are suited for winter production in most regions.

Winter oilseeds, like CoverCress seed, are "second generation" feedstocks that are also an example of temporal intensification in which feedstock crops are integrated into the fallow seasons of existing rotations and avoids the direct and indirect land-use change impacts associated with agricultural intensification (Fargione et al., 2008) or displacement of existing crop production (Searchinger et al., 2008), respectively. They also

provide a means of achieving the ecosystem service benefits of cover cropping, such as erosion control and reduced nutrient leaching, with a net profit to producers rather than at a significant cost (Plastina et al., 2018). Winter oilseeds are known to be effective in various rotations to break disease and pest cycles, recycle nutrients in the soil, reduce nutrient leaching, and reduce or eliminate weed problems (Seepaul et al., 2016; Shi et al., 2019). Biomass returned to the soil with only the seed being harvested is a major differentiating factor between non-food oilseed crops and other first generation (starches and sugars) or certain second generation (cellulosic and lignocellulosic) crops. This results in maximum sequestration of carbon and return of nutrients to the soil for the following crops (Seepaul et al., 2019).

WHY PENNYCRESS?

Pennycress is an oilseed-producing member of the Brassicaceae family, closely related to rapeseed, canola, carinata, and camelina (Best and Mcintyre, 1975; Warwick et al., 2010; Franzke et al., 2011). Containing 30%–32% oil with a fatty acid profile that allows for easy conversion to biofuels meeting the U.S. Renewable Fuels Standard, pennycress can help fill the demand for SAF (Moser et al., 2009; Moser, 2012). Pennycress is unique in that it has a small non-repetitive diploid genome (Dorn et al., 2013; Dorn et al., 2015; McGinn et al., 2018) and can be easily genetically manipulated (Sedbrook et al., 2014; Chopra et al., 2018; McGinn et al., 2018; Chopra et al., 2020), akin to its well-known model relative *Arabidopsis thaliana*. Extremely winter hardy with high oilseed yields and a short life cycle, pennycress can be integrated into the fallow period of existing cropping systems in the U.S. Midwest as a profitable winter cover crop (Phippen and Phippen, 2012; Fan et al., 2013; Johnson et al., 2015; Jordan et al., 2016; Johnson et al., 2017; Ott et al., 2018). For example, pennycress, as converted to CoverCress, can be planted following corn or soybean in late summer/early fall. Early-maturing pennycress varieties can be harvested in mid-May to June in time to plant full-season summer crops which allows producers to produce two cash crops on the same land in 1 year.

As a protective living cover during the offseason in the Midwest, a pennycress crop, such as CoverCress, provides numerous ecosystem services. Ecosystem benefits include nutrient retention, increased pollinator health, and biodiversity (Malakoff, 1998; Eberle et al., 2015). The deadzone in the Gulf of Mexico, which is the second largest deadzone in the world, has been attributed to nitrogen inputs from agriculture in Minnesota, Iowa, Illinois, Indiana, and Ohio (Malakoff, 1998; Scavia, and Donnelly, 2007; David et al., 2010). Both surface and subsurface drainage modifications bypass traditional mitigation efforts (Baker and Johnson, 1981; Baker et al., 2008). Nutrients losses from agricultural fields can be reduced, in part, with the implementation of reduced fertilizer application rates in combination with optimized spatial and temporal applications (Roth et al., 2018; Wang and Weil, 2018). However, producers are reluctant to reduce nitrogen application due to perceived risk to corn yields. Moreover, tile drainage bypasses traditional best management practices. Cover crops, like pennycress, provide a remedy in that they sequester nutrients before reaching tiles (Lemke et al., 2011; Jarecki et al., 2018).

A pennycress crop may serve as a nectar and pollen source as early as late April in central Minnesota and earlier in more southern states (Sindelar et al., 2017). No other agronomic crops, aside from winter camelina (a companion oilseed of pennycress), have the ability to flower so early and en masse as a pennycress crop in the U.S. Midwest region, particularly in its converted form as a CoverCress crop. Pennycress fields can flower for 3–4 weeks during which they produce abundant quantities of pollen and nectar (Eberle et al., 2015; Thom et al., 2018). Pennycress flowers are visited frequently by a wide range of insects, including native bees (Eberle et al., 2015; Groeneveld and Klein, 2015; Thomas et al., 2017; Thom et al., 2018). If early, reliable, and extensive floral resources were available in the U.S. Midwest, local honey production would increase, and overall colony health would improve. It is also hypothesized that health and vigor of early-emerging native pollinators would increase with access to fields of spring-flowering pennycress.

Field trials in Illinois and Minnesota have demonstrated that a pennycress crop has a minimal impact on yields of soybean crops following pennycress (Phippen and Phippen, 2012; Johnson et al., 2015; Ott et al., 2018). A pennycress crop, particularly in its converted form as a CoverCress crop, is not invasive, and producers who have grown the crop multiple years in commercial fields attest that it is not a problem weed. Since the same equipment used to manage conventional crops can be used with a pennycress crop (e.g., the same combines used to harvest soybean are used to harvest pennycress), minimal new farm equipment is required. Therefore, a CoverCress crop fits into existing crop rotations resulting in higher total seed yields (two cash crops in 1 year) without requiring new land commitments.

A CoverCress crop is unique among winter cover crops in that it can generate income as an oilseed crop thereby providing incentive for adoption by producers and stakeholders. Off-season integration of a CoverCress crop into existing corn and soybean hectares would extend the growing season on established croplands while avoiding displacement of food crops. At current commodity prices, our economic modeling informed by producers, industry partners, investors, and other stakeholders predicts the modest production increases enabled by the IPREFER project will make a CoverCress crop profitable across the entire supply chain.

HOW HAVE RESEARCHERS IMPROVED PENNYCRESS FOR COMMERCIALIZATION AS COVERCRESS?

Researchers have developed varieties with low seed coat fiber content and low erucic acid seed oil that produce seed meal and oil equivalent to that of canola (Chopra et al., 2018; Chopra et al., 2020). After less than a decade of selection and breeding,

CoverCress lines yield over 1,680 kg ha^{-1} (1,500 lb ac^{-1}) of seed with newer varieties approaching 2,241 kg ha^{-1} (2,000 lb ac^{-1}). Wild pennycress stands have been reported to produce seed yields as high as 2,246 kg ha^{-1} (Mitich, 1996) which equates to 646 L (170 gal) of oil and 1,460 kg of seed meal per ha (1,302 lb ac^{-1}). Given the success of their breeding, gene editing, and agronomic program, CCI believes 2,465 kg ha^{-1} (2,200 lb ac^{-1}) can be attained commercially in a CoverCress crop in the near term through marker-assisted breeding in combination with gene editing and improvements to agronomic practices. At 2,200 kg ha^{-1} (2,000 lb ac^{-1}), a CoverCress crop planted on half of the rotational hectares of the U.S. Midwest Corn Belt would produce 5 billion liters (1.1 billion gal) of oil and 7 million metric tons (MT) of edible seed meal annually.

In addition to rapid advances in breeding, CCI researchers have identified and validated pennycress mutations that confer agronomic trait improvements necessary for commercial launch. These mutations were generated using both classical mutagenesis and Clustered Regularly Interspaced Short Palindromic Repeats (CRISPR)-Cas9 gene editing approaches. Trait improvements include: absence of erucic acid in seed oil (*fae1* mutation produces edible oil equivalent to canola oil and well-suited for biodiesel and SAF generation), reduced seed glucosinolate content (e.g., *aop2* mutation makes the seed meal highly palatable as an animal feed), reduced seed coat fiber (e.g., *ttg1*, *tt8*, or *tt2* mutations individually reduce seed coat fiber content thereby improving the nutritional value of the CoverCress meal), increased seed oil from 25%–30% to 30%–34%, and reduced seed pod shatter (*ind* partial loss-of-function mutations reduce preharvest seed loss) (Chopra et al., 2018; McGinn et al., 2018). As of 2021, researchers have combined these genetic improvements into elite breeding lines and are currently conducting field trials across multiple locations throughout the central U.S. Midwest region as well as commercial seed inventory production for a planned commercial launch of CoverCress in the fall of 2022.

To support our efforts in securing CoverCress as a newly converted pennycress crop, the U.S. Department of Energy Biological and Environmental Research (DOE-BER) program funded in 2020 the $13 million Integrated Pennycress Resilience Project (IPReP; www.pennycressresilience.org/) focused on interrogating natural and induced genetic variation in pennycress to improve abiotic stress tolerance. As a winter annual, pennycress/CoverCress undergoes a plethora of environmental challenges including drought in the fall, freeze-thaw cycles throughout the winter, and water logging and heat waves in the spring. These environmental challenges are becoming more frequent and severe with climate change (IPCC, 2021), hence the need to introduce genetics into future generations of the crop to confer improved resilience. IPReP involves interdisciplinary teams from public universities, non-profit institutions and U.S. DOE labs who are employing eco-evolutionary computational genomics along with traditional mutagenesis and CRISPR genome editing approaches to identify key genetic variants that confer superior abiotic stress resilience.

COVERCRESS COMMERCIALIZATION EFFORTS

During the initial years of converting pennycress, it became apparent breeding varieties with consistent seed yields across years would be essential for commercialization. CCI (previously known as Arvegenix) was founded in 2013 and started with a structured plant-breeding program including a broad germplasm base, detailed crossing and testing programs, and the goal to convert pennycress into CoverCress following a path similar to the one taken for converting rapeseed into canola (Bell, 1982) (**Figure 1**). CoverCress grain will initially be marketed as a feed ingredient in the production of broiler chickens and in its whole grain form at a 2%–4% inclusion rate in the feed ration. As CCI scales hectares and CoverCress grain production increases, CoverCress grain (following completion of product development efforts) will go to crush and the extracted oil will be used in renewable fuel production and the extracted meal as livestock feed, using all carbon components produced.

The transition from whole grain feed to a crush ready product with the extracted oil for fuel will occur when economies of scale are met. This will occur when sufficient volumes of seed reached, product development efforts are completed, and processing facilities are improved to handle diversified feedstocks including CoverCress grain that has been specifically produced under an offtake agreement with Bunge that was announced in the spring of 2022. As part of a recently announced partnership between Bunge and Chevron, Bunge and CCI entered into a product offtake agreement whereby Bunge will purchase and process CoverCress grain. Also as a part of that announced partnership, Bunge will begin modifying and improving the current processing facilities to handle new feedstocks. Bunge's U.S. soybean processing plants in Destrehan, Louisiana, and Cairo, Illinois, will be a part of the joint venture with Chevron contributing approximately $600 million in cash (Bunge, 2022). Plans include approximately doubling the combined capacity of these facilities from 7,000 MT per day by the end of 2024 (Bunge, 2022). Under the agreements, Bunge will operate the facilities; Chevron will have purchase rights for the oil to use as a renewable feedstock to manufacture transportation fuels with lower lifecycle carbon intensity (Bunge, 2022). The CCI and Bunge offtake agreement is an integral part of the Bunge and Chevron joint venture (Lane, 2022).

Breeding and Gene Editing

CCI's current CoverCress product offering is a gene edited "golden seed" variety converted from pennycress having low fiber content in the seed meal for improved animal feeding and low erucic acid which produces healthier oil characteristics. Another striking improvement has been in seed germination. Wild pennycress varieties have a characteristically high initial dormancy rate, with first year germination of only 30%–50%. With mutations in the *tt8* gene, the seed coat is thinner, has a golden color, and seed exhibits dramatically improved germination rates to greater than 95% for freshly harvested seed. The improved germination has substantially increased yield by allowing for a more reliable and consistent stand establishment in the fall which leads to an earlier harvest in

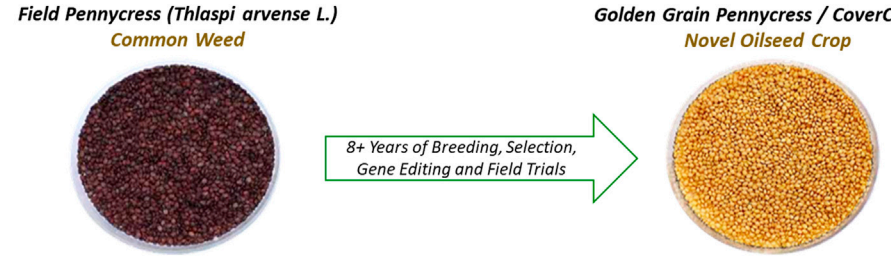

Oil	~25-30% Total Oil >35% of Oil = Long Chain, Unhealthy Erucic Acid	→	~30-34% Total Oil ZERO Long Chain, Unhealthy Erucic Acid
Fiber	Thick, Dark Seed Coat (Black) Low germ rate (~30%-50%)/high dormancy	→	Thin, Transparent Seed Coat (Golden) Immediate germ rate (>95%)/no dormancy
Agronomic	560-1,345 kg/ha yield Early June maturity	→	1,681-,2241 kg/ha yield Mid-May maturity (5 to 10 days earlier)
Meal	>40% ADF Fiber in meal/25% in seed ~25% Crude protein	→	~20% ADF Fiber in meal/14% in seed ~30% Crude Protein

FIGURE 1 | Breeding efforts to improve pennycress to address seed yield and new markets.

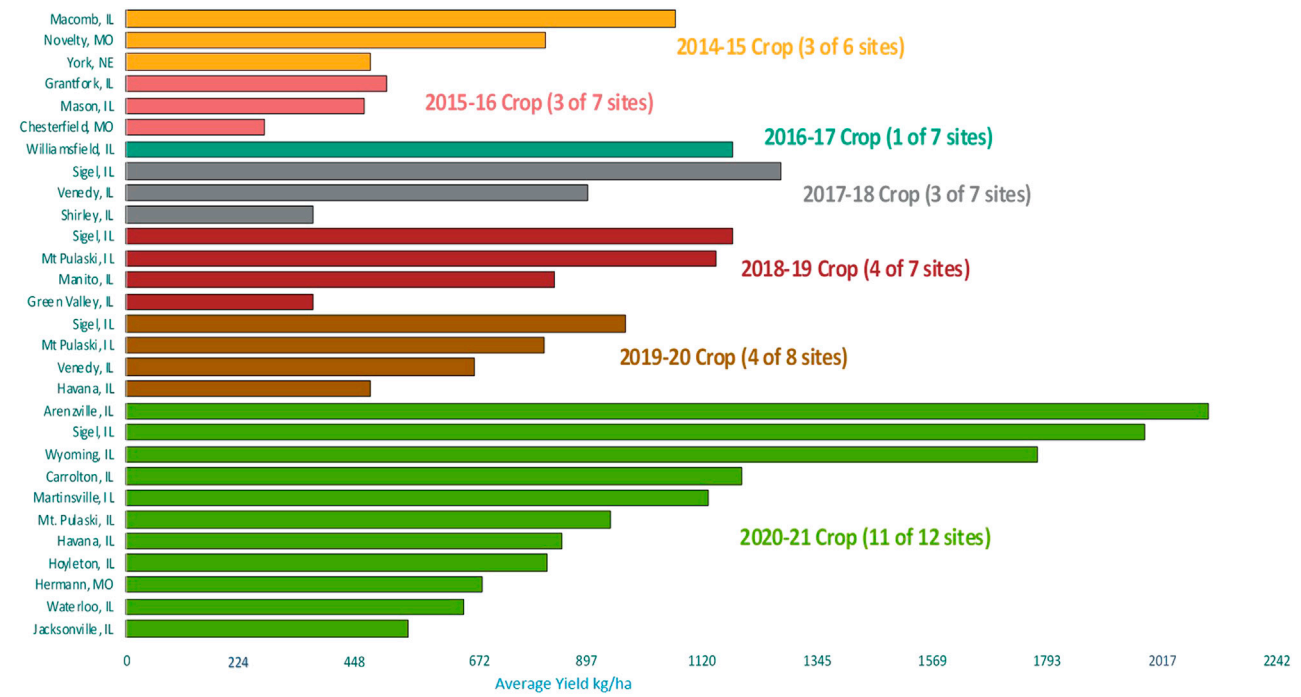

FIGURE 2 | Multi-year and multi-location yield data demonstrating significant seed yield increases of CoverCress™ through traditional plant breeding and gene-editing.

the spring (**Figure 2**). Reducing seed dormancy also alleviates weediness due to the seeds germinating when planted instead of lingering in the soil. By increasing the crude protein content in the seed meal from 25% to 30%, value is added as a livestock feed. CCI, along with the parallel work at IPREFER institutions, is working together through plant breeding, gene editing, and agronomy programs to continuously improve the current products for higher yields and added positive traits. Traits currently in the development pipeline include reduced glucosinolates and herbicide tolerance.

Seed Increase and Supply Chain

The first commercial CoverCress product was developed in 2019. This led to foundation-seed-expansion efforts in the 2020–21 season and commercial seed production in the 2021–2022 season. As expansion efforts continue, the details on the immediate

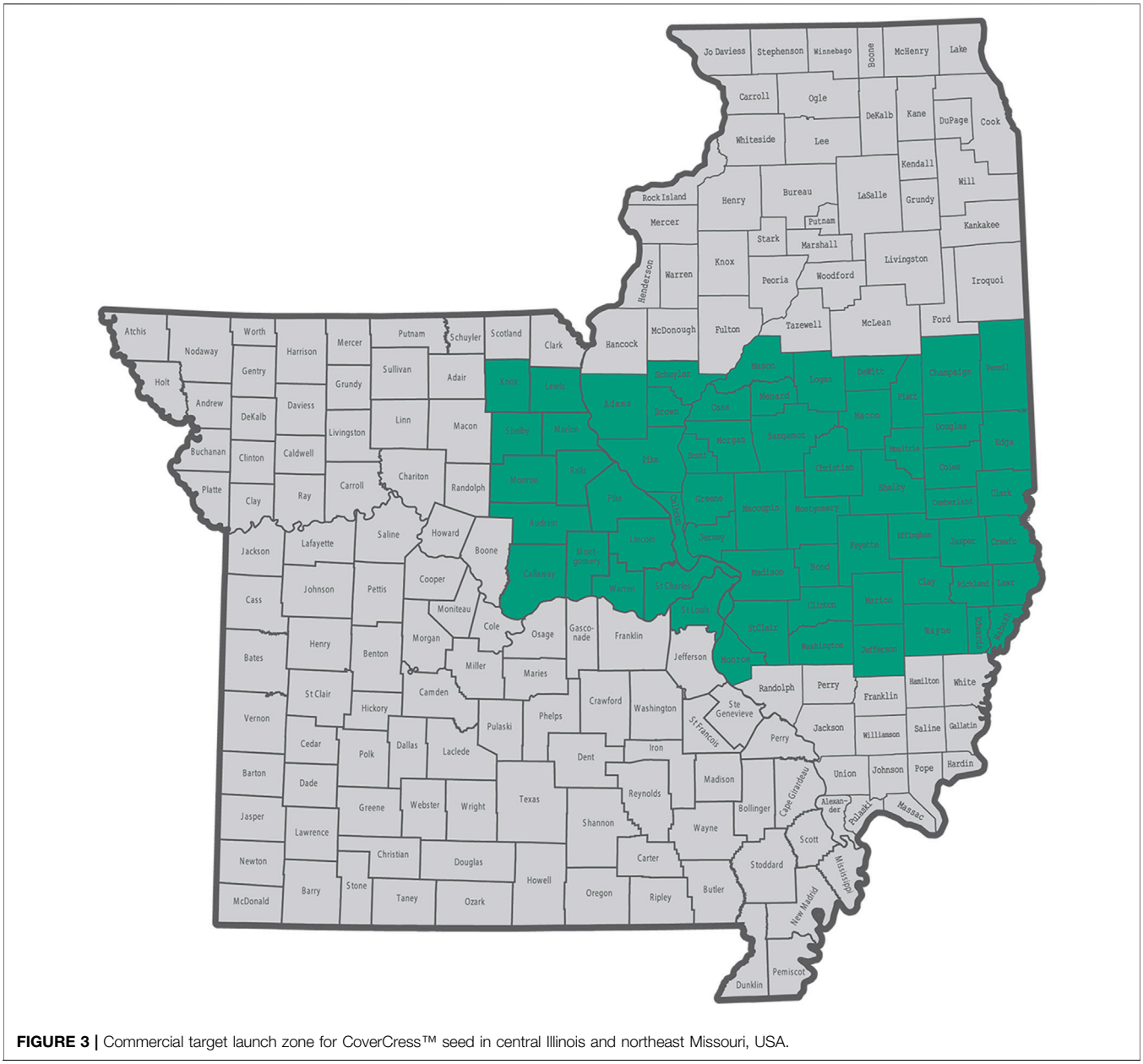

FIGURE 3 | Commercial target launch zone for CoverCress™ seed in central Illinois and northeast Missouri, USA.

supply chain for grain handling becomes paramount. One hectare of commercial seed production can produce the seed for 48 ha (121 acres), assuming a yield of 1,681 kg ha^{-1} (1,500 lb ac^{-1}) and a seeding rate of 5.6 kg ha^{-1} (5 lb ac^{-1}).

Ideal foundation-seed-expansion production ground is a relatively flat topography, relatively weed free or free of certain weed types, where no HPPD (4-Hydroxyphenylpyruvate dioxygenase inhibitor) herbicide was applied in the spring/summer before CoverCress seeding. Fields are observed throughout the season for weeds and CoverCress stand establishment. To ensure high quality seed and purity, a very clean combine optimized for small oilseeds is used for harvest.

The main supply chain components are: contract grower production (plant/cultivate/harvest/deliver), transportation to local seed handlers, grain cleaning/drying and storage, and seed delivery to end-product users. After an initial period of expansion (i.e., during the period when CoverCress grain is marketed in its whole grain form for inclusion in broiler feed) and final product development to achieve the low glucosinolate trait, the grain will also go to crush (for oil excrescence and meal production), with the initial customer being Bunge under the aforementioned offtake agreement. The oil and meal will be delivered to subsequent product producers. Harvesting CoverCress grain could use one of three likely models: 1) individual producers harvesting their fields; 2) one producer harvesting for each farm cluster (simplifying out-of-season machinery use); or 3) hired custom harvest. It is likely that a combination of the three models will be employed, especially in the first 5–10 years as hectares increase and the best option is determined.

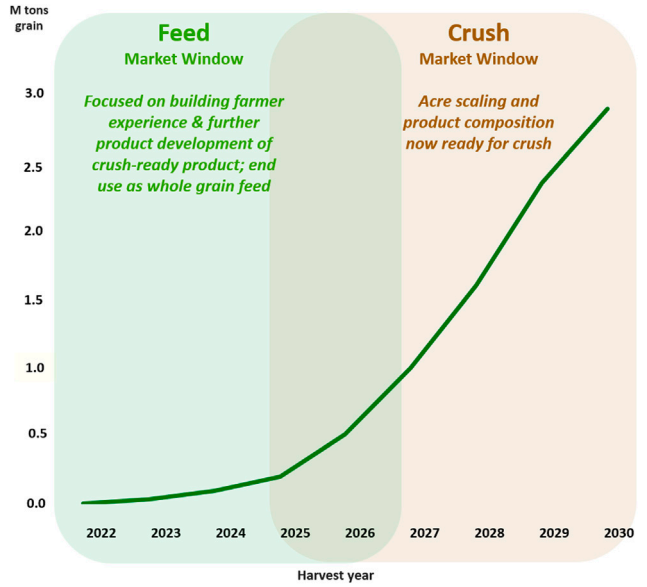

FIGURE 4 | CoverCress commercialization forecast in M tons of harvested grain.

Grain cleaning efforts show that a single additional sieving process after harvest at the seed handler will provide adequately clean grain when seed is harvested with properly adjusted combines. Forced-air grain drying at ambient temperature works well for CoverCress grain, and a moisture level of ~10%–12% which is adequate for storage is achieved in a couple of days (when the grain is harvested at ~18% moisture). While CoverCress grain can be stored in standard bins by grain handlers, customization of the bin flooring is required due to the small seed size. Flat storage with movement of grain via bucket loaders is also a viable option.

Launch Area

The initial launch area considered by CCI is south central Illinois and portions of Missouri (**Figure 3**). The initial launch is slated for 4,046 ha (10,000 ac) to be planted in fall 2022 with expected expansion to 20,234 ha (50,000 ac) in fall 2023. As producers become more interested about contracting for CoverCress grain production and expansion of hectares increase, CCI will expand its geography to include Iowa, Indiana and Ohio. The commercialization model depicted in **Figure 4** mainly considered farmer adoption for increased hectares along with the development of new CoverCress varieties having improved yields as well as earlier maturity (shorter cycle) allowing for expansion of where the crop can be planted.

CoverCress seed is an important part of the broad solution to produce low carbon intensity fuels which are critical to reducing global warming. Because crush facilities for plant-based oil extraction and fuel production from these oils use well-established processes, CoverCress seed oil can be added rapidly to the fuel feedstock markets. As shown by Frank et al. (2021), time is a critical component in the fight against climate change. Well established processes can make the final impact more relevant due to the time it will take to fully implement lower carbon alternatives to our way of life.

HOW DOES COVERCRESS FIT INTO THE LOW CARBON BIOECONOMY?

In the United States, approximately 80% of the total energy consumed is supplied from fossil fuels (U.S. Energy Information Administration, 2020a). The U.S. ranks second globally in GHG emissions, contributing approximately 15% of the total amount released annually (U.S. Environmental Protection Agency, 2021a). The U.S. Energy Independence and Security Act of 2007 mandates an increase in renewable transportation fuels to 136 metric liters by 2022 (Fan et al., 2013; U.S. Environmental Protection Agency, 2021b), but progress in fuel production beyond ethanol and biodiesel has been rather limited versus expectations included in the Act. Recently, President Biden signed an executive order to reduce emissions across federal operations which calls for a 65% reduction in emissions by 2030 and net-zero emissions by 2050 (The White House, 2021b). A few states have imposed their own programs to reduce GHG emissions. One of the most ambitious programs to reduce GHG emissions is the California Low Carbon Fuel Standard (LCFS), which requires oil refineries and distributors to reduce GHG emissions by replacing petroleum-based fuels with renewable fuels used for transportation. The program considers a full life cycle analysis of the fuel, which includes carbon emissions during production and consumption of the fuel. The program is designed to encourage the adoption of low carbon and renewable fuel alternatives which in turn will reduce the carbon intensity of transportation fuels by 20 percent by 2030 (California Air Resource Board, 2021a). An LCFS program also exists in Oregon, modelled closely after the California model, and a Clean Fuel Program was also created in Washington in 2021. This sets the stage for LCFS incentives to draw renewable fuel production and deliveries to west coast markets, irrespective of their area of production. These LCFS programs are designed to provide the greatest reward to those producing biofuels with the lowest CI scores. These programs are designed to provide incentives that are aligned with the desired behavior of producing fuels with increasingly less carbon intensive. This strategy further promotes transitions among alternative fuels.

CI scores measure the amount of carbon dioxide equivalent ($C0_{2e}$), by weight, emitted per unit of energy consumed for a given fuel (e.g. grams (g) of CO_2e MJ^{-1}). Fuel derived from biological sources, such as plants which pulled their carbon content from the atmosphere, have much lower CI scores than petroleum-based fuels. Renewable fuels with lower CI scores than petroleum-based fuels will aid with climate and environmental protection and promote the transition from a fossil fuel-based economy towards a sustainable biobased or bioeconomy having sustainable economic growth.

In California, the beginnings of a biobased economy are well underway. Businesses that produce biofuel with CI scores lower than the target value for the year can earn an LCFS credit which

can be sold to a company whose fuel production process generates excessive carbon emissions. The credit price of carbon for the week of 15 November 2021 traded at \$179.36 MT^{-1} with a volume of 618,108 MT traded for a total value of \$110,862,192 (California Air Resources Board, 2021b). From 2011 to 2018, the LCFS program removed 38 million MT of CO_2 emissions and saw a 74% increase in renewable fuel use. In 2018, the total value of credit transactions was approximately \$2 billion (California Air Resources Board, 2021b).

Reported CI scores for producing petroleum-based diesel and jet fuel are 91.66 and 89.37 g CO_2e MJ^{-1}, respectively (California Air Resource Board, 2021c). By comparison, the CI score for biodiesel and renewable jet fuels has been reported at 35.4 and 36.4 g CO_2e MJ^{-1}, respectively (U.S. Environmental Protection Agency, 2021c). CI scores for a fuel can vary based upon inputs (petroleum-based or plant-based oil), production efficiencies, and for plant-based renewable fuels, from how the crop was grown. Growing biofuel crops following best management practices that minimize GHG production will lower CI scores of the fuel produced. Such best management practices include adopting conservation tillage practices, including winter cover crops, and optimizing fertilizer inputs to increase yields while limiting GHG emissions such as CO_2 and N_2O. Paustian et al. (2019) describes how conservation tillage practices can reduce C losses from soil while improved crop rotations and the inclusion of winter cover crops can add C to soils with the potential of sequestering 4–5 Gt CO_2 per year globally for 2–3 decades.

As conservation practices are introduced on cropland, carbon sequestration in soil typically follows a sigmoidal curve, eventually reaching a new equilibrium concentration. It has been estimated that soil may be able to sequester 5%–15% of global fossil fuel emissions (Lal, 2004). Carefully managing fertilizer applications are essential because higher fertilizer rates can stimulate microbial activity that will release more GHG from soil, increasing the crops CI score. A study by Field et al. (2018) found that by optimizing soil cultivation and N fertilizer application on switchgrass used as a feedstock to produce cellulosic ethanol, GHG emissions were reduced by up to 22 g CO_2e MJ^{-1} of energy produced compared to conventional gasoline.

The CoverCress product shows great potential as an oilseed crop because it can produce renewable fuels such as biodiesel, renewable diesel, and SAF and may be suitable to grow on approximately 12 million hectares in the Midwest typically left winter fallow. A preliminary life cycle analysis by CCI has reported a CI score of 30.23 g CO_2e MJ^{-1} for biodiesel production (CoverCress, 2019), although biodiesel produced from fatty acid methyl esters will have a lower carbon intensity than hydrotreated oils used to make jet fuel (Moser, 2012). In addition, CCI conducted an Induced Land Use Changes (ILUC) study through Purdue University using the GTAP-BIO model used by the California Air Resources Board (CARB). This ILUC study examined the effects of a limited stock of 757 million liters (200 million gallons) of biodiesel produced from CoverCress as a second crop with the level of biodiesel produced from pennycress generating an ILUC value of −30.6 g CO_2e MJ^{-1} on average. Fan et al. (2013) conducted a life cycle assessment comparing pennycress to petroleum to synthesize biodiesel and renewable jet fuel. The study evaluated pennycress as a winter annual in the U.S. Midwest, grown between corn harvested in the fall and soybean planted in the spring. The study concluded that using pennycress to produce biodiesel and renewable jet fuel reduced GHG emissions by up to 85% and 63% respectively, compared to producing petroleum-based fuels. It was further concluded that growing pennycress between corn and soybean did not compete with food crops for land, nor did pennycress cause a yield reduction from the subsequent soybean crop (Fan et al., 2013).

While in the past, producers have been incurring unrecoverable costs in adopting cover crops, there appears to be progress on clearing this hurdle to CoverCress commercialization. Thompson et al. reviewed the 2017 U.S. Census of Agriculture and reported that cover crops had been adopted on only 11% of farms, and just 4% of cropland acres, in Illinois, Indiana, and Iowa (2021). They further highlighted the reluctance of producers to plant cover crops is evident in that more than half of cover crop adopters planted less than 20 ha (50 ac) of cover crops (Thompson et al., 2021). However, in more recent surveys, producers are expressing an interest in growing a CoverCress crop. A survey conducted by Zhou et al. (2021) evaluated the willingness of producers to grow CoverCress as an energy feedstock. Results showed that approximately 58% of producers surveyed were interested in growing a CoverCress crop if it was profitable; and among those interested, 54.4% would accept the farmgate price of \$0.28 kg^{-1}. They further concluded a profit of \$179 ha^{-1} could be achieved from an average harvest of 1,600 kg ha^{-1} (1,427 lb ac^{-1}) sold at \$0.28 kg^{-1} (\$0.62 lb^{-1}). This would generate a gross income of \$448 ha^{-1} (\$988 ac^{-1}) and assumed a production cost of \$269 ha^{-1} (\$665 ac^{-1}) (Zhou et al., 2021).

CONCLUSION

In order to substantially reduce GHG emissions of commercial aviation and meet the SAF Grand Challenge, a second-generation of biofuels is needed to develop feedstocks that minimize competition with food-crop production. As an extremely hardy winter cover crop with high oilseed yields and a low CI score, a CoverCress crop helps to fulfill this need. The efforts of IPREFER and its constituent university teams, as well as those of CCI in varietal and product development, supply chain strategies, and rapid growth in commercialization hectares have positioned CoverCress as new rotational crops to become a source of renewable fuels such as renewable diesel, SAF and biodiesel. As commercial farm production of the CoverCress crop begins in the fall 2022, converted pennycress is well on its way from "farm-to-flight" as it becomes a commercial low carbon intensity cash cover crop for sustainable aviation fuel. IPREFER, in close partnership with CCI, will be working a multifaceted research,

education, and outreach approach over the next 3 years to remove the remaining hurdles for broad producer and stakeholder adoption.

AUTHOR CONTRIBUTIONS

WP, RR, JS, CH, and SC contributed to conception and design of the manuscript. WP organized the first draft of the manuscript. WP, RR, JS, CH, and SC wrote sections of the manuscript. All authors contributed to manuscript revision, read, and approved the submitted version.

FUNDING

In addition to research funding provided by Western Illinois University, Illinois State University, and CoverCress Inc., this material is based upon work that is supported by the National Institute of Food and Agriculture, U.S. Department of Agriculture, under award numbers 2014-67009-22305, 2018-67009-27374, and 2019-67009-29004 and the Agriculture and Food Research Initiative Competitive Grant No. 2019-69012-29851. Portions of this research are also supported by the U.S. Department of Energy, Office of Science, Office of Biological and Environmental Research, Genomic Science Program grant no. DE-SC0021286.

REFERENCES

Airlines for America (2020). Airlines Fly Green. Available at: https://www.airlines.org/airlines-fly-green/(Accessed Oct 3, 2021).

Baker, J. L., David, M. B., Lemke, A. M., and Jaynes, D. B. (2008). "Understanding Nutrient Fate and Transport, Including the Importance of Hydrology in Determining Field Losses, and Potential Implications for Management Systems to Reduce Those Losses," in *Final Report Gulf Hypoxia and Local Water Quality Concerns Workshop*. Upper Mississippi River Sub-basin Hypoxia Nutrient Committee editor (St. Joseph, Michigan, USA: American Society of Agricultural and Biological Engineers), 1–17.

Baker, J. L., and Johnson, H. P. (1981). Nitrate-Nitrogen in Tile Drainage as Affected by Fertilization. *J. Environ. Qual.* 10, 519–522. doi:10.2134/jeq1981.00472425001000040020x

Bell, J. M. (1982). From Rapeseed to Canola: A Brief History of Research for Superior Meal and Edible Oil. *Poult. Sci.* 61, 613–622. doi:10.3382/ps.0610613

Best, K. F., and Mcintyre, G. I. (1975). The Biology of Canadian Weeds: 9. *Thlaspi Arvense* L. *Can. J. Plant Sci.* 55, 279–292. doi:10.4141/cjps75-039

Bunge (2022). *Bunge and CoverCress Inc. Announce Partnership to Meet Growing Demand for Renewable Fuel Feedstocks*. Missouri, USA: Bunge. Available at: https://bunge.com/news/bunge-and-covercress-inc-announce-commercial-partnership-meet-growing-demand-renewable-fuel.

California Air Resource Board (2021c). *Low Carbon Fuel Standard*. Sacramento, CA, USA. Available at: https://ww2.arb.ca.gov/sites/default/files/2020-05/basics-notes.pdf (Accessed May 23, 2022).

California Air Resources Board (2021a). Low Carbon Fuel Standard. Available at: https://ww2.arb.ca.gov/our-work/programs/low-carbon-fuel-standard (Accessed May 23, 2022).

California Air Resources Board (2021b). Weekly LCFS Credit Transfer Activity Reports. Available at: https://ww3.arb.ca.gov/fuels/lcfs/credit/lrtweeklycreditreports.htm (Accessed May 23, 2022).

Chopra, R., Johnson, E. B., Daniels, E., McGinn, M., Dorn, K. M., Esfahanian, M., et al. (2018). Translational Genomics Using *Arabidopsis* as a Model Enables the Characterization of Pennycress Genes through Forward and Reverse Genetics. *Plant J.* 96 (6), 1093–1105. doi:10.1111/tpj.14147

Chopra, R., Johnson, E. B., Emenecker, R., Cahoon, E. B., Lyons, J., Kliebenstein, D. J., et al. (2020). Identification and Stacking of Crucial Traits Required for the Domestication of Pennycress. *Nat. Food* 1, 84–91. doi:10.1038/s43016-019-0007-z

CoverCress (2019). *1st Cash Cover Crop for the Midwest*. St. Louis, MI, USA. Available at: https://caafi.org/resources/pdf/CoverCress_Handel_12_05_2019.pdf (Accessed May 23, 2022).

David, M. B., Drinkwater, L. E., and McIsaac, G. F. (2010). Sources of Nitrate Yields in the Mississippi River Basin. *J. Environ. Qual.* 39, 1657–1667. doi:10.2134/jeq2010.0115

Dorn, K. M., Fankhauser, J. D., Wyse, D. L., and Marks, M. D. (2015). A Draft Genome of Field Pennycress (*Thlaspi Arvense*) Provides Tools for the Domestication of a New Winter Biofuel Crop. *DNA Res.* 22, 121–131. doi:10.1093/dnares/dsu045

Dorn, K. M., Fankhauser, J. D., Wyse, D. L., and Marks, M. D. (2013). De Novo assembly of the Pennycress (*Thlaspi Arvense*) Transcriptome Provides Tools for the Development of a Winter Cover Crop and Biodiesel Feedstock. *Plant J.* 75, 1028–1038. doi:10.1111/tpj.12267

Eberle, C. A., Thom, M. D., Nemec, K. T., Forcella, F., Lundgren, J. G., Gesch, R. W., et al. (2015). Using Pennycress, Camelina, and Canola Cash Cover Crops to Provision Pollinators. *Industrial Crops Prod.* 75, 20–25. doi:10.1016/j.indcrop.2015.06.026

Energy (2021). Sustainable Aviation Fuel Grand Challenge. Available at: https://www.energy.gov/eere/bioenergy/sustainable-aviation-fuel-grand-challenge (Accessed May 23, 2022).

Fan, J., Shonnard, D. R., Kalnes, T. N., Johnsen, P. B., and Rao, S. (2013). A Life Cycle Assessment of Pennycress (*Thlaspi Arvense* L.) -derived Jet Fuel and Diesel. *Biomass Bioenergy* 55, 87–100. doi:10.1016/j.biombioe.2012.12.040

Fargione, J., Hill, J., Tilman, D., Polasky, S., and Hawthorne, P. (2008). Land Clearing and the Biofuel Carbon Debt. *Science* 319 (5867), 1235–1238. doi:10.1126/science.1152747

Field, J. L., Evans, S. G., Marx, E., Easter, M., Adler, P. R., Dinh, T., et al. (2018). High-resolution Techno-Ecological Modelling of a Bioenergy Landscape to Identify Climate Mitigation Opportunities in Cellulosic Ethanol Production. *Nat. Energy* 3, 211–219. doi:10.1038/s41560-018-0088-1

Frank, J., Brown, T., Haverly, M., Slade, D., and Malmsheimer, R. (2021). Quantifying the Comparative Value of Carbon Abatement Scenarios over Different Investment Timing Scenarios. *Fuel Commun.* 8, 100017. doi:10.1016/j.jfueco.2021.100017

Franzke, A., Lysak, M. A., Al-Shehbaz, I. A., Koch, M. A., and Mummenhoff, K. (2011). Cabbage Family Affairs: The Evolutionary History of Brassicaceae. *Trends Plant Sci.* 16, 108–116. doi:10.1016/j.tplants.2010.11.005

GreenAir News (2021). Aviation Industry Looks to ICAO for Leadership on Delivering a Global Long-Term Goal to Reduce Emissions. Available at: https://www.greenairnews.com/?p=1769 (Accessed May 23, 2022).

Groeneveld, J. H., and Klein, A. M. (2015). Pennycress-corn Double-Cropping Increases Ground Beetle Diversity. *Biomass Bioenergy* 77, 16–25. doi:10.1016/j.biombioe.2015.03.018

Heaton, E. A., Schulte, L. A., Berti, M., Langeveld, H., Zegada-Lizarazu, W., Parrish, D., et al. (2013). Managing a Second-Generation Crop Portfolio through Sustainable Intensification: Examples from the USA and the EU. *Biofuels, Bioprod. Bioref* 7 (6), 702–714. doi:10.1002/bbb.1429

IATA Net Zero (2022). IATA Net-Zero Carbon Emissions by 2050. Available at: https://www.iata.org/en/pressroom/2021-releases/2021-10-04-03/(Accessed May 23, 2022).

ICAO CORSIA (2022). ICAO CORSIA Eligible Fuels. Available at: https://www.icao.int/environmental-protection/CORSIA/Pages/CORSIA-Eligible-Fuels.aspx (Accessed May 23, 2022).

IPCC (2021). *Sixth Assessment Report of the United Nations Intergovernmental Panel on Climate Change*. Geneva: IPCC. Available at: https://www.ipcc.ch/ (Accessed May 23, 2022).

Jarecki, M., Grant, B., Smith, W., Deen, B., Drury, C., VanderZaag, A., et al. (2018). Long-term Trends in Corn Yields and Soil Carbon under Diversified Crop Rotations. *J. Environ. Qual.* 47, 635–643. doi:10.2134/jeq2017.08.0317

Johnson, G. A., Kantar, M. B., Betts, K. J., and Wyse, D. L. (2015). Field Pennycress Production and Weed Control in a Double Crop System with Soybean in Minnesota. *Agron. J.* 107, 532–540. doi:10.2134/agronj14.0292

Johnson, G. A., Wells, M. S., Anderson, K., Gesch, R. W., Forcella, F., and Wyse, D. L. (2017). Yield Tradeoffs and Nitrogen between Pennycress, Camelina, and Soybean in Relay- and Double-Crop Systems. *Agron. J.* 109, 2128–2135. doi:10.2134/agronj2017.02.0065

Jordan, N. R., Dorn, K., Runck, B., Ewing, P., Williams, A., Anderson, K. A., et al. (2016). Sustainable Commercialization of New Crops for the Agricultural Bioeconomy. *Elem. Sci. Anthropocene* 4, 000081. doi:10.12952/journal.elementa.000081

Lal, R. (2004). Soil Carbon Sequestration Impacts on Global Climate Change and Food Security. *Science* 304, 1623–1627. doi:10.1126/science.1097396

Lane, J. (2022). *Bunge, CoverCress, Chevron Taking Us into the Future and into the Past.* Florida, USA: The Digest. Available at: https://www.biofuelsdigest.com/bdigest/2022/05/09/bunge-covercress-chevron-taking-us-into-the-future-and-into-the-past/.

Lemke, A. M., Kirkham, K. G., Lindenbaum, T. T., Herbert, M. E., Tear, T. H., Perry, W. L., et al. (2011). Evaluating Agricultural Best Management Practices in Tile-Drained Subwatersheds of the Mackinaw River, Illinois. *J. Environ. Qual.* 40, 1215–1228. doi:10.2134/jeq2010.0119

Malakoff, D. (1998). Death by Suffocation in the Gulf of Mexico. *Science* 281, 190–192. doi:10.1126/science.281.5374.190

McGinn, M., Phippen, W. B., Chopra, R., Bansal, S., Jarvis, B. A., Phippen, M. E., et al. (2018). Molecular Tools Enabling Pennycress (*Thlaspi Arvense*) as a Model Plant and Oilseed Cash Cover Crop. *Plant Biotechnol. J.* 17 (4), 776–788. doi:10.1111/pbi.13014

Mitich, L. W. (1996). Field Pennycress (*Thlaspi Arvense* L.) -The Stinkweed. *Weed Technol.* 10, 675–678. doi:10.1017/S0890037X00040604

Moser, B. R. (2012). Biodiesel from Alternative Oilseed Feedstocks: Camelina and Field Pennycress. *Biofuels* 3, 193–209. doi:10.4155/bfs.12.6

Moser, B. R., Knothe, G., Vaughn, S. F., and Isbell, T. A. (2009). Production and Evaluation of Biodiesel from Field Pennycress (*Thlaspi Arvense* L.) Oil. *Energy fuels.* 23, 4149–4155. doi:10.1021/ef900337g

Ott, M. A., Eberle, C. A., Thom, M. D., Archer, D. W., Forcella, F., Gesch, R. W., et al. (2019). Economics and Agronomics of Relay-Cropping Pennycress and Camelina with Soybean in Minnesota. *Agron. J.* 111, 1281–1292. doi:10.2134/agronj2018.04.0277

Paustian, K., Larson, E., Kent, J., Marx, E., and Swan, A. (2019). Soil C Sequestration as a Biological Negative Emission Strategy. *Front. Clim.* 1, 8. doi:10.3389/fclim.2019.00008

Phippen, W. B., and Phippen, M. E. (2012). Soybean Seed Yield and Quality as a Response to Field Pennycress Residue. *Crop Sci.* 52, 2767–2773. doi:10.2135/cropsci2012.03.0192

Plastina, A., Liu, F., Sawadgo, W., Miguez, F. E., Carlson, S., and Marcillo, G. (2018). Annual Net Returns to Cover Crops in Iowa. *J. Appl. Farm Econ.* 2 (2), 19–36. doi:10.7771/2331-9151.1030

Roth, R. T., Ruffatti, M. D., O'Rourke, P. D., and Armstrong, S. D. (2018). A Cost Analysis Approach to Valuing Cover Crop Environmental and Nitrogen Cycling Benefits: A Central Illinois on Farm Case Study. *Agric. Syst.* 159, 69–77. doi:10.1016/j.agsy.2017.10.007

Scavia, D., and Donnelly, K. A. (2007). Reassessing Hypoxia Forecasts for the Gulf of Mexico. *Environ. Sci. Technol.* 41 (23), 8111–8117. doi:10.1021/es0714235

Searchinger, T., Heimlich, R., Houghton, R. A., Dong, F., Elobeid, A., Fabiosa, J., et al. (2008). Use of U.S. Croplands for Biofuels Increases Greenhouse Gases through Emissions from Land-Use Change. *Science* 319 (5867), 1238–1240. doi:10.1126/science.1151861

Sedbrook, J. C., Phippen, W. B., and Marks, M. D. (2014). New Approaches to Facilitate Rapid Domestication of a Wild Plant to an Oilseed Crop: Example Pennycress (*Thlaspi Arvense* L.). *Plant Sci.* 227, 122–132. doi:10.1016/j.plantsci.2014.07.008

Seepaul, R., George, S., and Wright, D. L. (2016). Comparative Response of Brassica Carinata and B. Napus Vegetative Growth, Development and Photosynthesis to Nitrogen Nutrition. *Industrial Crops Prod.* 94, 872–883. doi:10.1016/j.indcrop.2016.09.054

Seepaul, R., Marois, J., Small, I. M., George, S., and Wright, D. L. (2019). Carinata Dry Matter Accumulation and Nutrient Uptake Responses to Nitrogen Fertilization. *Agron. J.* 111 (4), 2038–2046. doi:10.2134/agronj2018.10.0678

Shi, R., Archer, D. W., Pokharel, K., Pearlson, M. N., Lewis, K. C., Ukaew, S., et al. (2019). Analysis of Renewable Jet from Oilseed Feedstocks Replacing Fallow in the U.S. Northern Great Plains. *ACS Sustain. Chem. Eng.* 7, 18753–18764. doi:10.1021/acssuschemeng.9b02150

Sindelar, A. J., Schmer, M. R., Gesch, R. W., Forcella, F., Eberle, C. A., Thom, M. D., et al. (2017). Winter Oilseed Production for Biofuel in the US Corn Belt: Opportunities and Limitations. *GCB Bioenergy* 9, 508–524. doi:10.1111/gcbb.12297

The White House (2021b). Executive Order on Catalyzing Clean Energy Industries and Jobs through Federal Sustainability. Available at: https://www.whitehouse.gov/briefing-room/presidential-actions/2021/12/08/executive-order-on-catalyzing-clean-energy-industries-and-jobs-through-federal-sustainability/(Accessed May 23, 2022).

The White House (2021a). FACT SHEET: President Biden's Leaders Summit on Climate. Available at: https://www.whitehouse.gov/briefing-room/statements-releases/2021/04/23/fact-sheet-president-bidens-leaders-summit-on-climate/(Accessed May 23, 2022).

Thom, M. D., Eberle, C. A., Forcella, F., Gesch, R., and Weyers, S. (2018). Specialty Oilseed Crops Provide an Abundant Source of Pollen for Pollinators and Beneficial Insects. *J. Appl. Entomol.* 142, 211–222. doi:10.1111/jen.12401

Thomas, J. B., Hampton, M. E., Dorn, K. M., Marks, D. M., and Carter, C. J. (2017). The Pennycress (*Thlaspi Arvense* L.) Nectary: Structural and Transcriptomic Characterization. *BMC Plant Biol.* 17, 201. doi:10.1186/s12870-017-1146-8

Thompson, N. M., Reeling, C. J., Fleckenstein, M. R., Prokopy, L. S., and Armstrong, S. D. (2021). Examining Intensity of Conservation Practice Adoption: Evidence from Cover Crop Use on U.S. Midwest Farms. *Food Policy* 101, 102054. doi:10.1016/j.foodpol.2021.102054

U.S. Energy Information Administration (2020b). *July 2020, Monthly Energy Review*. Washington, DC, USA. Available at: https://www.eia.gov/totalenergy/data/monthly/pdf/mer.pdf (Accessed May 23, 2022).

U.S. Energy Information Administration (2020a). *Primary Energy Overview*. Washington, DC, USA. Available at: https://www.eia.gov/totalenergy/data/monthly/pdf/sec1_3.pdf (Accessed May 23, 2022).

U.S. Environmental Protection Agency (2021a). Global Greenhouse Gas Emissions Data. Available at: https://www.epa.gov/ghgemissions/global-greenhouse-gas-emissions-data#Country (Accessed May 23, 2022).

U.S. Environmental Protection Agency (2021c). Lifecycle Greenhouse Gas Results. Available at: https://www.epa.gov/fuels-registration-reporting-and-compliance-help/lifecycle-greenhouse-gas-results (Accessed May 23, 2022).

U.S. Environmental Protection Agency (2021b). Renewable Fuel Standard Program: Regulations and Volume Standards for Renewable Fuel Standards. Available at: https://www.epa.gov/renewable-fuel-standard-program/regulations-and-volume-standards-renewable-fuel-standards (Accessed May 23, 2022).

U.S. Environmental Protection Agency (2021d). RINs Generated Transactions. Available at: https://www.epa.gov/fuels-registration-reporting-and-compliance-help/rins-generated-transactions (Accessed May 23, 2022).

Wang, F., and Weil, R. R. (2018). The Form and Vertical Distribution of Soil Nitrogen as Affected by Forage Radish Cover Crop and Residual Side-Dressed N Fertilizer. *Soil Sci.* 183, 22–33. doi:10.1097/SS.0000000000000224

Warwick, S. I., Mummenhoff, K., Sauder, C. A., Koch, M. A., and Al-Shehbaz, I. A. (2010). Closing the Gaps: Phylogenetic Relationships in the Brassicaceae Based on DNA Sequence Data of Nuclear Ribosomal ITS Region. *Plant Syst. Evol.* 285, 209–232. doi:10.1007/s00606-010-0271-8

Zhou, X. V., Jensen, K. L., Larson, J. A., and English, B. C. (2021). Farmer Interest in and Willingness to Grow Pennycress as an Energy Feedstock. *Energies* 14, 2066. doi:10.3390/en14082066

Conflict of Interest: Author CH was employed by the company CoverCress Inc. Author SC was employed by the sponsors of the Commercial Aviation Alternative Fuels Initiative, a public-private-partnership. Illinois State University (JS) has entered licensing agreements with CoverCress, Inc. for use of pennycress mutants. Author JS has stock in CoverCress, Inc.

The remaining authors declare that the research was conducted in the absence of any commercial or financial relationships that could be construed as a potential conflict of interest.

Publisher's Note: All claims expressed in this article are solely those of the authors and do not necessarily represent those of their affiliated organizations, or those of the publisher, the editors and the reviewers. Any product that may be evaluated in this article, or claim that may be made by its manufacturer, is not guaranteed or endorsed by the publisher.

Advantages of publishing in Frontiers

OPEN ACCESS
Articles are free to read for greatest visibility and readership

FAST PUBLICATION
Around 90 days from submission to decision

HIGH QUALITY PEER-REVIEW
Rigorous, collaborative, and constructive peer-review

TRANSPARENT PEER-REVIEW
Editors and reviewers acknowledged by name on published articles

Frontiers
Avenue du Tribunal-Fédéral 34
1005 Lausanne | Switzerland

Visit us: www.frontiersin.org
Contact us: frontiersin.org/about/contact

REPRODUCIBILITY OF RESEARCH
Support open data and methods to enhance research reproducibility

DIGITAL PUBLISHING
Articles designed for optimal readership across devices

FOLLOW US
@frontiersin

IMPACT METRICS
Advanced article metrics track visibility across digital media

EXTENSIVE PROMOTION
Marketing and promotion of impactful research

LOOP RESEARCH NETWORK
Our network increases your article's readership